

Kraus
and
Carver

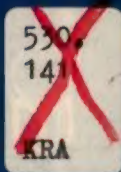
ELECTROMAGNETICS

SECOND EDITION

Kraus and Carver

ELECTROMAGNETICS

SECOND
EDITION



McGRAW-HILL
KOGAKUSHYA

INTERNATIONAL STUDENT EDITION

SYMBOLS, PREFIXES, AND ABBREVIATIONS

See Appendixes A-1 (Units) and A-2 (constants and conversions) for more detailed information

A	ampere
\AA	angstrom = 10^{-10}
A	vector potential, Wb m^{-1}
A, a	area, m^2
AR	axial ratio
AU	astronomical unit
a	atto = 10^{-18}
\hat{a}	unit vector
B, B	magnetic flux density, $\text{T} = \text{Wb m}^{-2}$
B	susceptance, \mathcal{U}
B	susceptance/unit length, $\mathcal{U} \text{ m}^{-1}$
BWFN	beam width, first nulls
C	coulomb
C	capacitance, F
C	capacitance/unit length, $F \text{ m}^{-1}$
C, c	a constant, c = velocity of light
cc	cubic centimeter
$^{\circ}\text{C}$	degree Celcius
D, D	electric flux density, C m^{-2}
d	distance, m
deg	degree, angle
dB	decibel = $10 \log(P_2/P_1)$
dBi	decibels over isotropic
dl	element of length (scalar), m
dl	element of length (vector), m
ds	element of surface (scalar), m^2
ds	element of surface (vector), m^2
dv	element of volume (scalar), m^3
E, E	electric field intensity, V m^{-1}
emf	electromotive force, V
e	electric charge, C
F	farad
F, F	force, N
f	femto = 10^{-15}
f	force per volume, N m^{-3}
f	frequency, Hz
fu	flux unit
G	giga = 10^9
G	conductance, \mathcal{U}
G	conductance/unit length, $\mathcal{U} \text{ m}^{-1}$
g	gram
H	henry
H, H	magnetic field, A m^{-1}
HPBW	half-power beam width
Hz	hertz = 1 cycle per second
I, I, i	current, A
J	joule
J, J	current density, A m^{-2}
K	kelvin

K, K	sheet-current density, A m^{-1}
K, k	a constant
k	kilo = 10^3
kg	kilogram
L	inductance, H
L, L	inductance/unit length, H m^{-1}
l, L	length (scalar), m
l	length (vector), m
LCP	left circularly polarized
LEP	left elliptically polarized
In	natural logarithm (base e)
log	common logarithm (base 10)
M	mega = 10^6
M, M	magnetization, A m^{-1}
M	polarization state = $M(\epsilon, \tau)$
m, m	magnetic (dipole) moment, A m^2
m	meter
m	milli = 10^{-3}
min	minute
N	newton
N, n	number (integer)
Np	neper
n	nano = 10^{-9}
\hat{n}	unit vector normal to a surface
P, P	polarization of dielectric, C m^{-2}
p	electric dipole moment, C m^{-3}
P	polarization state = $P(\gamma, \delta)$
P	power, W
P	power per solid angle, W rad^{-2}
P_h	power pattern, dimensionless
\mathcal{P}	permeance, H
\mathcal{P}	radiation pressure, N m^{-2}
p	pico = 10^{-12}
Q, q	charge, C
R	resistance, Ω
R	resistance/unit length, $\Omega \text{ m}^{-1}$
\mathcal{R}	reluctance, H^{-1}
RCP	right circular polarization
REP	right elliptical polarization
r	revolution
r	radius, m; also coordinate direction
\hat{r}	unit vector in r direction
rad	radian
rad ²	square radian = steradian = sr
S, S	Poynting vector, W m^{-2}
S	resistivity, $\Omega \text{ m}$
S, s	distance, m; also surface area, m^2
s	second (of time)
sr	steradian = square radian = rad ²

T	tesla = Wb m^{-2}
T	tera = 10^{12}
T	torque, N m
t	time, s
U	magnetostatic potential, A
V	volt
V	voltage (also emf), V
\mathcal{U}	emf (electromotive force), V
v	velocity, m s^{-1}
W	watt
W	energy, J
Wb	weber = 10^4 gauss
w	energy density, J m^{-3}
X	reactance, Ω
X	reactance/unit length, $\Omega \text{ m}^{-1}$
\hat{x}	unit vector in x direction
x	coordinate direction
Y	admittance, Ω
Y	admittance/unit length, $\Omega \text{ m}^{-1}$
\hat{y}	unit vector in y direction
y	coordinate direction
Z	impedance, Ω
Z	impedance/unit length, $\Omega \text{ m}^{-1}$
Z_c	intrinsic impedance, conductor, Ω per square
Z_d	intrinsic impedance, dielectric, Ω per square
Z_L	load impedance, Ω
Z_{yz}	transverse impedance, rectangular waveguide, Ω
Z_{ϕ}	transverse impedance, cylindrical waveguide, Ω
Z_0	intrinsic impedance, space, Ω per square
Z_0	characteristic impedance, transmission line, Ω
\hat{z}	unit vector in z direction
z	coordinate direction, also red shift
α	(alpha) angle (deg or rad)
β	(beta) angle, deg or rad; also phase
	constant = $2\pi/\lambda$
γ	(gamma) angle, deg or rad
δ	(delta) angle, deg or rad
ϵ	(epsilon) permittivity, F m^{-1}
ϵ_0	permittivity of vacuum, F m^{-1}
$\tilde{\epsilon}$	(epsilon) tensor permittivity, F m^{-1}
η	(eta) index of refraction
θ	(theta) angle, deg or rad
$\hat{\theta}$	(theta) unit vector in θ direction
κ	(kappa)
Λ	(capital lambda) flux linkage, Wb turn
λ	(lambda) wavelength, m
μ	(mu) permeability, H m^{-1}
μ_0	permeability of vacuum, H m^{-1}
μ	(mu) mobility, $\text{m}^2 \text{ s}^{-1} \text{ V}^{-1}$
μ	(mu) micro = 10^{-6}
ν	(nu)
ξ	(xi)
π	(pi) = 3.14
ρ	(rho) electric charge density, C m^{-3} ; also mass density, kg m^{-3}
ρ	reflection coefficient, dimensionless
ρ_s	surface charge density, C m^{-2}
ρ_L	linear charge density, C m^{-1}
σ	(sigma) conductivity, $\Omega \text{ m}^{-1}$
τ	(tau) tilt angle, polarization ellipse, deg or rad
τ	transmission coefficient, deg or rad
ϕ	(phi) angle, deg or rad
Φ	(phi) unit vector in ϕ direction
χ	(chi) susceptibility, dimensionless
ψ	(psi) angle, deg or rad
ψ_m	magnetic flux, Wb
Ω	(capital omega) ohm
Ω	(capital omega) solid angle, sr or deg ²
\mathcal{O}	(upsidedown capital omega) mho ($\mathcal{O} = 1/\Omega = S$, siemens)
ω	(omega) angular frequency (= $2\pi f$), rad s^{-1}

McGRAW-HILL ELECTRICAL AND ELECTRONIC ENGINEERING SERIES

FREDERICK EMMONS TERMAN, Consulting Editor

W. W. HARMAN, J. G. TRUXAL, AND R. A. ROHRER, Associate Consulting Editors

ANGELAKOS AND EVERHART: Microwave Communications

ANGELO: Electronic Circuits

ANGELO: Electronics: BJTs, FETs, and Microcircuits

ASELTINE: Transform Method in Linear System Analysis

ATWATER: Introduction to Microwave Theory

BEOLOVE, SCHACHTER, and SCHILLING: Digital and Analog Systems, Circuits, and Devices: An Introduction

BENNETT: Introduction to Signal Transmission

BERANEK: Acoustics

BRACEWELL: The Fourier Transform and Its Application

BRENNER AND JAVID: Analysis of Electric Circuits

CARLSON: Communication Systems: An Introduction to Signals and Noise in Electrical Communication

CHEN: The Analysis of Linear Systems

CHEN: Linear Network Design and Synthesis

CHIRLIAN: Analysis and Design of Electronic Circuits

CHIRLIAN: Basic Network Theory

CHIRLIAN: Electronic Circuits: Physical Principles, Analysis, and Design

CHIRLIAN AND ZEMANIAN: Electronics

CLEMENT AND JOHNSON: Electrical Engineering Science

CUNNINGHAM: Introduction to Nonlinear Analysis

D'AZZO AND HOUPIS: Feedback Control System Analysis and Synthesis

ELGERD: Control Systems Theory

ELGERD: Electric Energy Systems Theory: An Introduction

EVELEIGH: Adaptive Control and Optimization Techniques

EVELEIGH: Introduction to Control Systems Design

FEINSTEIN: Foundations of Information Theory

FITZGERALD, HIGGINBOTHAM, and GRABEL: Basic Electrical Engineering

FITZGERALD, KINGSLEY, and KUSKO: Electric Machinery

FRANK: Electrical Measurement Analysis

FRIEDLAND, WING, and ASH: Principles of Linear Networks

GEHMILICH and HAMMOND: Electromechanical Systems

GHAUSI: Principles and Design of Linear Active Circuits

GHOSE: Microwave Circuit Theory and Analysis

GLASFORD: Fundamentals of Television Engineering

GREINER: Semiconductor Devices and Applications

HAMMOND and GEHLICH: Electrical Engineering

HANCOCK: An Introduction to the Principles of Communication Theory

HARMAN: Fundamentals of Electronic Motion

HARMAN: Principles of the Statistical Theory of Communication

HARMAN and LYTHE: Electrical and Mechanical Networks

HAYASHI: Nonlinear Oscillations in Physical Systems

HAYT: Engineering Electromagnetics

HAYT and KEMMERLY: Engineering Circuit Analysis

HILL: Electronics in Engineering

JAVID and BROWN: Field Analysis and Electromagnetics

JOHNSON: Transmission Lines and Networks

KOENIG, TOKAD, and KESAVAN: Analysis of Discrete Physical Systems

KRAUS: Antennas

KRAUS and CARVER: Electromagnetics

KUH and PEDERSON: Principles of Circuit Synthesis

KUO: Linear Networks and Systems

LEDLEY: Digital Computer and Control Engineering

LEPAGE: Complex Variables and the Laplace Transform for Engineering

LEPAGE and SEELEY: General Network Analysis

LEVI and PANZER: Electromechanical Power Conversion

LEY, LUTZ, and REHBERG: Linear Circuit Analysis

LINVILL and GIBBONS: Transistors and Active Circuits

LITTAUER: Pulse Electronics

LYNCH and TRUXAL: Introductory System Analysis

LYNCH and TRUXAL: Principles of Electronic Instrumentation

LYNCH and TRUXAL: Signals and Systems in Electrical Engineering

MCCLUSKEY: Introduction to the Theory of Switching Circuits

MANNING: Electrical Circuits

MEISEL: Principles of Electromechanical-energy Conversion

MILLMAN and HALKIAS: Electronic Devices and Circuits

MILLMAN and HALKIAS: Integrated Electronics: Analog and Digital Circuits and Systems

MILLMAN and TAUB: Pulse, Digital, and Switching Waveforms

MINORSKY: Theory of Nonlinear Control Systems

MISHKIN and BRAUN: Adaptive Control Systems

MOORE: Travelling-wave Engineering

MURDOCH: Network Theory

OBERMAN: Disciplines in Combinational and Sequential Circuit Design

PETTIT and MCWHORTER: Electronic Amplifier Circuits

PETTIT and MCWHORTER: Electronic Switching, Timing, and Pulse Circuits

REZA: An Introduction to Information Theory

REZA and SEELEY: Modern Network Analysis

RUSTON and BORDOGNA: Electric Networks: Functions, Filters, Analysis

RYDER: Engineering Electronics

SCHILLING and BELOVE: Electronic Circuits: Discrete and Integrated

SCHWARTZ: Information Transmission, Modulation, and Noise

SCHWARTZ and FRIEDLAND: Linear Systems

SEELEY: Electromechanical Energy Conversion

SEIFERT and STEEG: Control Systems Engineering

SHOOMAN: Probabilistic Reliability: An Engineering Approach

SISKIND: Direct-current Machinery

SKILLING: Electric Transmission Lines

STEVENSON: Elements of Power System Analysis

STEWART: Fundamentals of Signal Theory

STRAUSS: Wave Generation and Shaping

SU: Active Network Synthesis

TAUB and SCHILLING: Principles of Communication Systems

TERMAN: Electronic and Radio Engineering

TERMAN and PETTIT: Electronic Measurements

THALER and PASTEL: Analysis and Design of Nonlinear Feedback Control Systems

TOU: Digital and Sampled-data Control Systems

TOU: Modern Control Theory

TRUXAL: Automatic Feedback Control System Synthesis

TUTTLE: Electric Networks: Analysis and Synthesis

VALDES: The Physical Theory of Transistors

WEEKS: Antenna Engineering

WEINBERG: Network Analysis and Synthesis

Whistling swan family with father, right, and mother, center, both equipped with migration transmitter and wrap-around dipole antenna. Juvenile swan or cygnet is at left. The units radiate pulses of 1-mW peak power at 222 MHz and have a 100-km operating range with four months of service life. The units were developed to study flight pattern, flight altitude, air temperature, heart rate, and body-core temperature during migrations. These magnificent 10-kg (22-lb) birds make 14,000-km round trips each year between Chesapeake Bay and Alaska. Typically they fly in formation for distances of 1000 km at altitudes of 3 km in nonstop flights lasting 10 hours (average speed 100 km/h). The tracking aircraft following such a flight must land twice to refuel. The transmitter, including batteries, weighs only 90 g (3 oz) and is secured to the upper middle back by four teflon straps which go under the wings and around the body. A flexible wire dipole antenna runs part way along two of the straps. The system does not interfere with the swan's activities in flight or on the water, and is almost invisible beneath the feathers. In the photograph the transmitter cases have been retouched for clarity and the location of the dipoles is indicated by dashed lines. The swan at the right also has a large plastic neck band for visual identification. The asymmetrical mounting of the dipole antenna results in vertically polarized radiation when the swan is on the water, and in horizontally polarized radiation when in flight. A change from vertical to horizontal polarization alerts the monitoring station that the swan has become airborne. (*Photograph by John W. Hamblen, Applied Physics Laboratory, Johns Hopkins University. See W. A. Good and J. W. Hamblen, APL Technical Digest, vol. 10, no. 2, pp. 2-10, Nov.-Dec. 1970.*)



McGRAW-HILL
KOGAKUSHYA, LTD.

Tokyo
Auckland
Düsseldorf
Johannesburg
London
Mexico
New Delhi
Panama
São paulo
Singapore
Sydney

INTERNATIONAL STUDENT EDITION

JOHN D. KRAUS

Taine G. McDougal Professor of Electrical
Engineering and Astronomy
Director, Radio Observatory
The Ohio State University

KEITH R. CARVER

Associate Professor of Electrical Engineering
Senior Engineer, Physical Science Laboratory
New Mexico State University

ELECTROMAGNETICS
SECOND EDITION

**McGRAW-HILL
KOGAKUSHYA, LTD.**

Tokyo
Auckland
Düsseldorf
Johannesburg
London
Mexico
New Delhi
Panama
São paulo
Singapore
Sydney

INTERNATIONAL STUDENT EDITION

JOHN D. KRAUS

*Taine G. McDougal Professor of Electrical
Engineering and Astronomy
Director, Radio Observatory
The Ohio State University*

KEITH R. CARVER

*Associate Professor of Electrical Engineering
Senior Engineer, Physical Science Laboratory
New Mexico State University*

ELECTROMAGNETICS
SECOND EDITION

ACCESSION No.		112864	
CLASS No.			
S30.141		KRA	
		31 MAY 1978	
G/S	N	CATEGORY	
	✓	NORMAL	

OTHER McGRAW-HILL BOOK COMPANY BOOKS BY JOHN D. KRAUS

Antennas 1950
 Radio Astronomy 1966

Library of Congress Cataloging in Publication Data

Kraus, John Daniel, 1910–
 Electromagnetics.

(McGraw-Hill electrical and electronic engineering
 series)

Bibliography: p.

1. Electromagnetic theory. I. Carver, Keith R.,
 1940– joint author. II. Title.
 QC661.K72 1973 530.1'41 72-13520
 ISBN 0-07-035396-4 ✓

ELECTROMAGNETICS

INTERNATIONAL STUDENT EDITION

Exclusive rights by McGraw-Hill Kogakusha, Ltd., for
 manufacture and export. This book cannot be re-exported
 from the country to which it is consigned by McGraw-Hill.

III

Copyright © 1973 by McGraw-Hill, Inc. All rights reserved.
 Copyright 1953 by McGraw-Hill, Inc. All rights reserved.
 No part of this publication may be reproduced, stored in a
 retrieval system, or transmitted, in any form or by any
 means, electronic, mechanical, photocopying, recording,
 or otherwise, without the prior written permission of
 the publisher.

CONTENTS

Preface	xvii
1 Introduction	1
<i>1-1 Electromagnetics Defined</i>	
<i>1-2 Dimensions and Units</i>	
<i>1-3 Fundamental and Secondary Units</i>	
<i>1-4 How to Read the Symbols and Notation</i>	
<i>1-5 Equation Numbering</i>	
<i>1-6 Dimensional Analysis</i>	
<i>1-7 Thumbnail Electromagnetics</i>	
<i>1-8 SPEMP Chart</i>	
2 The Static Electric Field: Part 1	12
<i>2-1 Introduction</i>	
<i>2-2 The Force between Point Charges and Coulomb's Law</i>	
<i>2-3 Idealness and Staticness</i>	
<i>2-4 Electric Field Intensity</i>	
<i>2-5 Positiveness, Right-handedness, and Outwardness</i>	

- 2-6 The Electric Field of Several Point Charges and the Principle of Superposition of Fields
- 2-7 The Electric Scalar Potential
- 2-8 The Electric Scalar Potential as a Line Integral of the Electric Field
- 2-9 Relation of Electric Field Lines and Equipotential Contours; Orthogonality
- 2-10 Field of Two Equal Point Charges of Opposite Signs and of Same Sign
- 2-11 Charge Density and Continuous Distributions of Charge
- 2-12 Electric Potential of Charge Distributions and the Principle of Superposition of Potential
- 2-13 The Electric Field as the Gradient of the Electric Potential
- 2-14 Gradient in Rectangular Coordinates
- 2-15 The Electric Dipole and Electric-dipole Moment
- 2-16 Electric Flux
- 2-17 Electric Flux over a Closed Surface; Gauss' Law
- 2-18 Single Shell of Charge
- 2-19 Conductors and Induced Charges
- 2-20 Conducting Shell
- 2-21 Capacitors and Capacitance
- 2-22 Boundary Relations at a Conducting Surface
Problems

3 The Static Electric Field: Part 2

56

- 3-1 Introduction
- 3-2 Homogeneity, Linearity, and Isotropy
- 3-3 Dielectrics and Permittivity
- 3-4 The Electric Field in a Dielectric
- 3-5 Polarization
- 3-6 Artificial Dielectrics
- 3-7 Boundary Relations
- 3-8 Table of Boundary Relations
- 3-9 Parallel-plate Capacitor
- 3-10 Dielectric Strength
- 3-11 Energy in a Capacitor
- 3-12 Energy Density in a Static Electric Field
- 3-13 Fields of Simple Charge Configurations
- 3-14 Field Distributions
- 3-15 Field of a Finite Line of Charge
- 3-16 Field of an Infinite Line of Charge

3-17	Infinite Cylinder of Charge
3-18	Infinite Coaxial Transmission Line
3-19	Two Infinite Lines of Charge
3-20	Infinite Two-wire Transmission Line
3-21	Infinite Single-wire Transmission Line
3-22	Graphical Mapping of Static Electric Fields; Field Cells
3-23	Divergence of the Flux Density \mathbf{D}
3-24	Maxwell's Divergence Equation
3-25	Divergence Theorem
3-26	Divergence of \mathbf{D} and \mathbf{P} in a Capacitor
3-27	The Laplacian Operator; Poisson's and Laplace's Equations
	Problems

4	The Steady Electric Current	109
----------	------------------------------------	------------

4-1	Introduction
4-2	Conductors and Insulators
4-3	The Electric Current
4-4	Resistance and Ohm's Law
4-5	Power Relations and Joule's Law
4-6	The Electric Circuit
4-7	Resistivity and Conductivity
4-8	Table of Conductivities
4-9	Current Density and Ohm's Law at a Point
4-10	Kirchhoff's Voltage Law and the Difference between Potential and Emf
4-11	Tubes of Current
4-12	Kirchhoff's Current Law
4-13	Divergence of \mathbf{J} and Continuity Relations for Current
4-14	Current and Field at a Conductor-Insulator Boundary
4-15	Current and Field at a Conductor-Conductor Boundary
4-16	Current Mapping and the Resistance of Simple Geometries; Conductor Cells
4-17	Laplace's Equation for Conducting Media
	Problems

5	The Static Magnetic Field of Steady Electric Currents	140
----------	--	------------

5-1	Introduction; Effect of a Current on a Magnet
5-2	Effect of a Magnet on a Current-carrying Wire
5-3	The Magnetic Field of a Current-carrying Element; The Biot-Savart Law

- 5-4 The Magnetic Field of an Infinite Linear Conductor
- 5-5 The Force between Two Parallel Linear Conductors; Definition of the Ampere
- 5-6 The Magnetic Field of a Current-carrying Loop
- 5-7 Magnetic Flux ψ_m and Magnetic Flux Density \mathbf{B}
- 5-8 Magnetic Flux over a Closed Surface
- 5-9 Magnetic Field Relations in Vector Notation
- 5-10 Torque on a Loop; Magnetic Moment
- 5-11 The Solenoid
- 5-12 Inductors and Inductance
- 5-13 Inductance of Simple Geometries
- 5-14 Ampère's Law and \mathbf{H}
- 5-15 Ampère's Law Applied to a Conducting Medium and Maxwell's Equation
- 5-16 Magnetostatic Potential U and Mmf F
- 5-17 Field Cells and Permeability
- 5-18 Energy in an Inductor
- 5-19 Energy Density in a Static Magnetic Field
- 5-20 Magnetic Poles
- 5-21 Curl
- 5-22 Maxwell's First Curl Equation
- 5-23 Summary of Operations Involving ∇
- 5-24 A Comparison of Divergence and Curl
- 5-25 The Vector Potential
- 5-26 A Comparison of Static Electric and Magnetic Fields
- Problems

6 The Static Magnetic Field of Ferromagnetic Materials

198

- 6-1 Introduction
- 6-2 Bar Magnets and Magnetic Poles
- 6-3 Magnetic Materials
- 6-4 Relative Permeability
- 6-5 Magnetic Dipoles and Magnetization
- 6-6 Uniformly Magnetized Rod and Equivalent Air-filled Solenoid
- 6-7 The Magnetic Vectors \mathbf{B} , \mathbf{H} , and \mathbf{M}
- 6-8 Boundary Relations
- 6-9 Table of Boundary Relations for Magnetic Fields
- 6-10 Ferromagnetism
- 6-11 Magnetization Curves

- 6-12 Hysteresis**
- 6-13 Energy in a Magnet**
- 6-14 Permanent Magnets**
- 6-15 Table of Permanent Magnetic Materials**
- 6-16 Demagnetization**
- 6-17 The Magnetic Circuit; Reluctance and Permeance**
- 6-18 Magnetic Field Mapping; Magnetic Field Cells**
- 6-19 Comparison of Field Maps in Electric, Magnetic, and Current Cases**
- 6-20 Gapless Circuit**
- 6-21 Magnetic Circuit with Air Gap**
- 6-22 Magnetic Gap Force**
- 6-23 Permanent Magnet with Gap**
- 6-24 Comparison of Electric and Magnetic Relations Involving Polarization and Magnetization**
- Problems**

7 Laplace's and Poisson's Equations and Boundary-value Problems 262

- 7-1 Introduction**
- 7-2 Solution of Laplace's Equation in Rectangular Coordinates**
- 7-3 Example 1: The Parallel-plate Capacitor**
- 7-4 Uniqueness**
- 7-5 Point-by-point, or Iterative, Method**
- 7-6 Example 2: The Infinite Square Trough**
- 7-7 Example 3: Square Trough with Different Potential on Each Side**
- 7-8 Digital-computer Solution**
- 7-9 Analog-computer Solution**
- 7-10 Example 4: Conducting Sheet between Two Conducting Planes**
- 7-11 Solution of Laplace's Equation in Cylindrical and Spherical Coordinates**
- 7-12 Example 5: Coaxial Line**
- 7-13 Poisson's Equation**
- 7-14 Example 6: Parallel-plate Capacitor with Space Charge**
- 7-15 The Theory of Images**
- 7-16 Example 7: Charged Cylindrical Conductor over an Infinite Metallic Ground Plane**
- 7-17 Example 8: Current-carrying Conductor over Infinite Metallic Ground Plane**
- Problems**

8 Time-changing Electric and Magnetic Fields	305
8-1 Introduction	
8-2 Faraday's Law	
8-3 Maxwell's Equation from Faraday's Law: Integral Form	
8-4 Moving Conductor in a Magnetic Field	
8-5 General Case of Induction	
8-6 Examples of Induction	
8-7 Stokes' Theorem	
8-8 Maxwell's Equation from Faraday's Law: Differential Form	
8-9 Mutual Inductance and Self-inductance	
8-10 The Transformer	
8-11 Alternating-current Behavior of Ferromagnetic Materials	
8-12 Eddy Currents	
8-13 Displacement Current	
8-14 Maxwell's Equation from Ampère's Law: Complete Expression	
8-15 Dielectric Hysteresis	
8-16 Boundary Relations	
8-17 General Field Relations	
8-18 Comparison of Electric and Magnetic Field Relations	
Problems	
9 The Relation between Field and Circuit Theory; Maxwell's Equations	348
9-1 Introduction	
9-2 Applications of Circuit and Field Theory	
9-3 The Series Circuit; Comparison of Field and Circuit Theory	
9-4 Maxwell's Equations as Generalizations of Circuit Equations	
9-5 Maxwell's Equations in Free Space	
9-6 Maxwell's Equations for Harmonically Varying Fields	
9-7 Tables of Maxwell's Equations	
Problems	
10 Plane Waves in Dielectric and Conducting Media	363
10-1 Introduction	
10-2 Plane Waves and the Wave Equation	
10-3 Solutions of the Wave Equation	
10-4 Table of Solutions of the Wave Equation	
10-5 Phase Velocity	
10-6 Index of Refraction	
10-7 Group Velocity	

- 10-8 Impedance of Dielectric Media**
- 10-9 Impedance of Transmission-line Cell**
- 10-10 Two Plane Waves Traveling in Opposite Directions; Standing Waves**
- 10-11 Energy Relations in a Traveling Wave**
- 10-12 The Poynting Vector**
- 10-13 Energy Relations in a Standing Wave**
- 10-14 Conductors and Dielectrics**
- 10-15 Wave Equation for Conducting Media**
- 10-16 Depth of Penetration**
- 10-17 Relaxation Time**
- 10-18 Impedance of Conducting Media**
- 10-19 The Poynting Vector in Conducting Media**
- 10-20 Circuit Application of the Poynting Vector**
- 10-21 General Development of the Wave Equation**
- Problems**

11 Wave Polarization**426**

- 11-1 Introduction**
- 11-2 Linear, Elliptical, and Circular Polarization**
- 11-3 Poynting Vector for Elliptically or Circularly Polarized Waves**
- 11-4 The Polarization Ellipse and the Poincaré Sphere**
- 11-5 Partial Polarization and the Stokes Parameters**
- 11-6 Cross Field**
- Problems**

12 Wave Reflection, Refraction, and Diffraction**445**

- 12-1 Introduction**
- 12-2 Plane Wave, Normal Incidence**
- 12-3 The Terminated Wave**
- 12-4 Linearly Polarized Plane Wave, Oblique Incidence**
- 12-5 Elliptically Polarized Plane Wave, Oblique Incidence**
- 12-6 Huygens' Principle and Physical Optics**
- 12-7 Geometrical-optics Concepts**
- 12-8 Scattering from a Conducting Strip**
- 12-9 Geometrical Theory of Diffraction**
- Problems**

13 Transmission Lines, Waveguides, and Resonators**482**

- 13-1 Introduction**

13-2	Coaxial, Two-wire, and Infinite-plane Transmission Lines	
13-3	The Infinite Uniform Transmission Line	
13-4	Comparison of Circuit and Field Quantities	
13-5	Characteristic-impedance Determinations	
13-6	The Terminated Uniform Transmission Line	
13-7	Transmission-line Charts	
13-8	$\lambda/4$ Transformer	
13-9	Transformer Bandwidth	
13-10	Wave Reflections on a $\lambda/4$ Transformer	
13-11	Further Time-domain Studies of $\lambda/4$ Transformer	
13-12	Power Flow on a Transmission Line	
13-13	Circuits, Lines, and Guides: A Comparison	
13-14	TE Mode Wave in the Infinite-parallel-plane Transmission Line	
13-15	The Hollow Rectangular Waveguide	
13-16	The Hollow Circular Cylindrical Waveguide	
13-17	Hollow Waveguides of Other Cross Section	
13-18	Attenuation at Frequencies Less than Cutoff	
13-19	Attenuation at Frequencies Greater than Cutoff	
13-20	Waveguide Devices	
13-21	Waveguide Iris Theory	
13-22	Intrinsic, Characteristic, and Wave Impedances	
13-23	Waves Traveling to a Plane Boundary	
13-24	Open Waveguides	
13-25	Cavity Resonators	
	Problems	
14	Antennas and Radiation	601
14-1	Introduction	
14-2	Retarded Potentials	
14-3	The Short Dipole Antenna	
14-4	Radiation Resistance of a Short Dipole	
14-5	Directivity, Gain, and Effective Aperture	
14-6	Array Theory	
14-6.1	Two Isotropic Point Sources	
14-6.2	Pattern Multiplication	
14-6.3	Binomial Array	
14-6.4	Array with n Sources of Equal Amplitude and Spacing	
14-6.5	Array with n Sources of Equal Amplitude and Spacing: Broadside Case	

14-6.6	Array with n Sources of Equal Amplitude and Spacing: End-fire Case	
14-6.7	Graphical Representation of Phasor Addition of Fields	
14-6.8	Simple Two-element Interferometer	
14-7	Continuous Aperture Distribution	
14-8	Fourier Transform Relations between the Far-field Pattern and the Aperture Distribution	
14-9	Linear Antennas	
14-10	Fields of $\lambda/2$ Dipole Antenna	
14-11	Traveling-wave Antennas	
14-12	The Small Loop Antenna	
14-13	The Small Helical Antenna	
14-14	The Helical-beam Antenna	
14-15	Beam Width and Directivity of Arrays	
14-16	Scanning Arrays	
14-17	Frequency-independent Antennas	
14-18	Reciprocity	
14-19	Self and Mutual Impedance and Arrays of Dipoles	
14-20	Reflector and Lens Antennas	
14-20.1	Infinite-flat-sheet Reflector	
14-20.2	Finite-flat-sheet Reflector	
14-20.3	Thin Reflectors and Directors	
14-20.4	Corner Reflectors	
14-20.5	Parabolic Reflectors and Lens Antennas	
14-20.6	Some Comments on Corner Reflectors vs. Parabolic Reflectors	
14-21	Slot and Complementary Antennas	
14-22	Horn Antennas	
14-23	Aperture Concept	
14-24	Coherence	
14-25	Friis Formula and Radar Equation	
14-26	Radio Telescopes, Noise Power, and Antenna Temperature	
14-27	Rotating Bar Magnet as a Very-low-frequency Radiator (Pulsar)	
14-28	Antennas for Polarization Measurements	
	Problems	
15	Particles and Plasmas	716
15-1	Introduction	
15-2	Charged Particle in a Static Electric Field	

15-3	Charged Particle in a Static Magnetic Field	
15-4	The Cathode-ray Tube	
15-5	The Cyclotron	
15-6	The Mass Spectrograph	
15-7	Table of Charge and Mass for Common Particles	
15-8	Plane Waves in an Ionized Medium in the Presence of a Magnetic Field	
15-9	Faraday Rotation	
15-10	Magnetohydrodynamic Waves	
	Problems	
16	Moving Systems and Space-Time	749
16-1	Introduction	
16-2	Simultaneity	
16-3	Space-Time Concept	
16-4	Coordinate Transformation	
16-5	Invariance in Space-Time	
16-6	Four-dimensional Field Formulation	
16-7	Fields of a Moving System	
16-8	Maxwell's Stress Tensor	
	Problems	
Appendix A	Units, Constants, and a Few Mathematical Relations	785
A-1	Units	
A-2	Constants and Conversions	
A-3	Trigonometric Relations	
A-4	Hyperbolic Relations	
A-5	Logarithmic Relations	
A-6	Approximation Formulas for Small Quantities	
A-7	Series	
A-8	Solution of Quadratic Equation	
A-9	Vector Identities	
A-10	Recurrence Relations for Bessel Functions	
A-11	Coordinate Diagrams	
Appendix B	Bibliography	801
Appendix C	Answers to Starred Problems	803
Index		813

PREFACE

The wide and continued use of the first edition of *Electromagnetics*, including a foreign translation, has given us the incentive to prepare a second edition. Many users have told us of features they wish to have retained in a new edition. But new advances and changes in emphasis and teaching methods have made the addition of new material and revision of the old desirable. The aim of the book, as before, is to present the basic elements of electromagnetic theory for an introductory fields course. The topics have been selected from a wide variety of subjects, but these have been chosen to illustrate important concepts without becoming encyclopedic. As prerequisites the student is assumed to have a knowledge of introductory physics and mathematics through differential and integral calculus. Also a course in vector analysis is essential either beforehand or concurrently.

The introduction (Chap. 1) includes sections on units and dimensions, dimensional analysis and two teaching aids: Thumbnail Electromagnetics and SPEMP chart. Modernized metric (SI) units and nomenclature are used throughout the book. The five chapters (2 to 6) on static electric and magnetic fields and steady currents form the foundation of field theory. Three chapters (7 to 9) discuss boundary-value problems, time-changing fields, and the relation of field and circuit theory, culminating in Maxwell's equations. Problem solutions by a variety of methods including analytical,

graphical, and computer (both digital and analog) are discussed. Chapters 10 to 12 cover waves in dielectric and conducting media, wave polarization and wave reflection, refraction, and diffraction. Treatments using both physical optics (wavefront) and geometrical optics (ray-path) methods are included. Chapters 13 and 14 explain transmission lines, waveguides, resonators, antennas, and radiation. New sections in these chapters include such topics as bandwidth, time-domain reflectometry, aperture concepts, array theory, radar equation, antenna temperature and radio telescopes. Chapters 15 and 16 treat particles, plasmas, moving systems, and space-time (or relativity). Topics in these chapters include particles in static electric and magnetic fields, wave propagation in a magnetized plasma, Faraday rotation, magnetohydrodynamic (MHD) waves, the space-time concept, fields of a moving system, and radiation pressure. It is shown that there is no such thing as a pure electric or magnetic field which retains its identity for all observers. With the increasing emphasis on outer space and systems in relative motion, these ideas are of fundamental importance. Appendix A contains tables of important constants, equations, and formulas. There is also a very complete tabulation of units and their equivalents. Appendix B is a brief bibliography, and Appendix C gives answers to the starred problems. There is a complete listing of symbols inside the front cover and some frequently used vector relations inside the back cover.

Almost half of the illustrations are new. The problem sets, which are completely revised and expanded, are an important feature of the new edition. Many extend or supplement the text. Among the wide variety of problems included are many which pertain to modern real-world engineering situations, e.g., problems involving a study of engineering feasibility and/or the design of an operational device. Some of these have multiple or indefinite solutions (few real-world problems have exact answers). Such problems can be used for class discussion or term papers. There are also many problems of the more conventional type, yielding definite numerical answers with all gradations of difficulty. A considerable number of problems are arranged for solution by computers. Answers are given to one-half of the problems. There is much to be gained by becoming familiar with the problems, whether one intends to solve them or not. Many topics are included which are not discussed elsewhere in the book and some very interesting and thought-provoking ideas are presented. We recommend "problem reading for pleasure."

The worked examples, numbering about 100, are valuable instructional aids. These examples are of great assistance in understanding the theory and how to apply it to practical situations.

The book is designed to provide flexibility for course needs in introductory field theory. There is adequate material for a one-year course. The material is also well adapted for shorter courses. For example, a short course can cover the first six, seven, eight, nine or ten chapters either completely or with the omission of all or

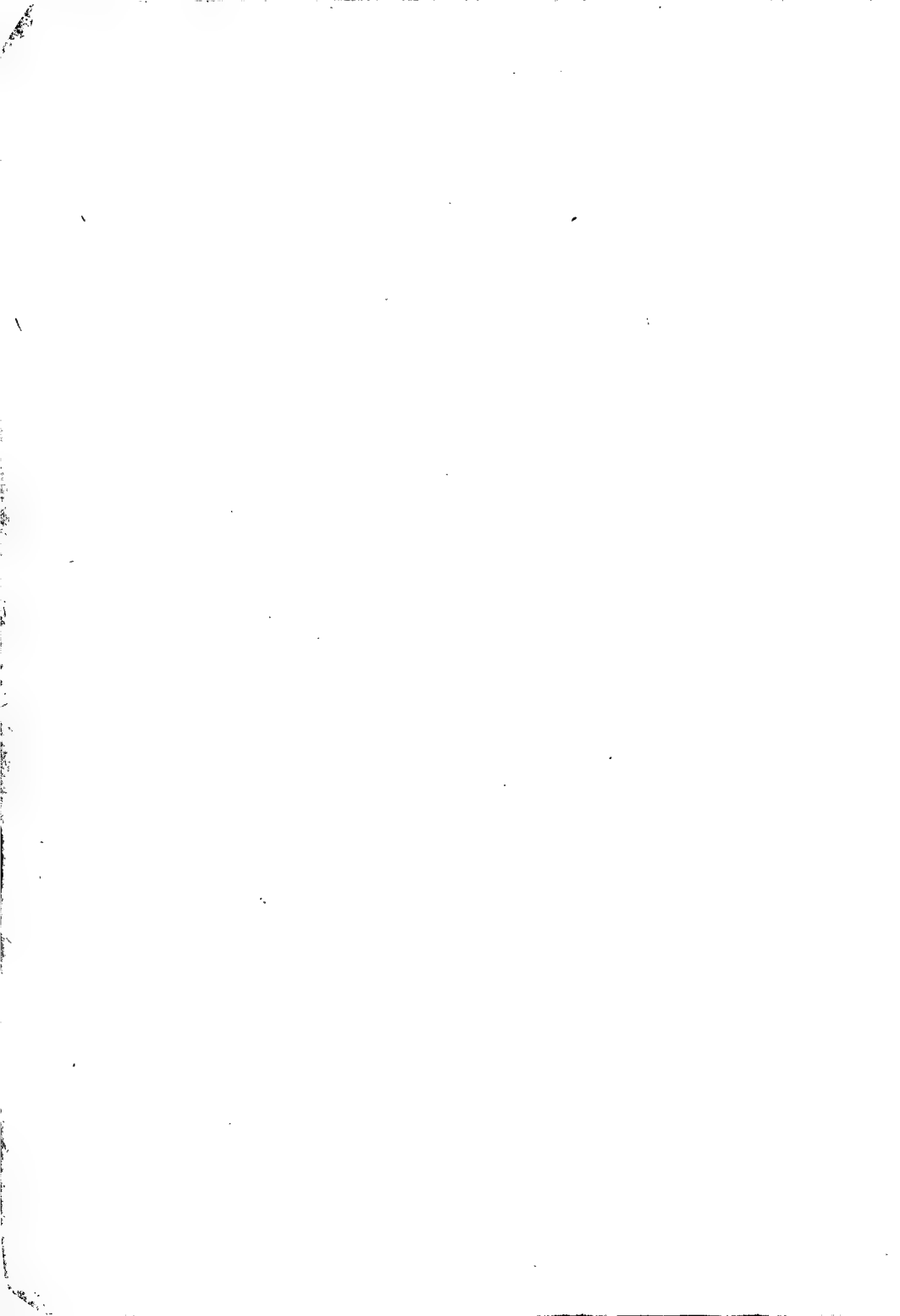
part of the following sections: 3-14 through 3-22; 4-14; 4-15; 4-16; 5-25, 5-26; 6-12 through 6-24; 7-10 through 7-17; 10-10; and 10-13 through 10-21. Another option for a short course is to omit all or most of these sections but to include parts of Chaps. 13 to 16; for example, Secs. 13-1 through 13-6 (transmission lines); 14-1, 14-2, 14-5, 14-6, and 14-7 (antenna aperture and array theory); 15-2 and 15-3 (charged particles); and 16-2 (simultaneity). Still other options are possible. Antennas are remarkable in that they can interface between a circuit and space, and some familiarity with them is desirable even in a short fields course. The antenna sections (14-1, 14-2, 14-5, 14-6, and 14-7), indicated above, use nothing more advanced than phasor addition.

Although great care has been exercised, some errors in the text or figures are inevitable. Anyone finding them will do us a great service by writing us so that they can be corrected in subsequent printings.

We are grateful to many teachers and a generation of students who have used the first edition and have generously supplied us with comments and suggestions. Professor Charles F. Fell, University of Nevada, made many recommendations and is responsible for the definitions of idealness, staticness, etc., used in Secs. 2-3 and 2-5. Professor Clarence W. Schultz, University of Connecticut, offered numerous suggestions and supplied the method used with Fig. 6-6 for developing the relation between B , H , and M . We are much indebted to Professors Chen-To Tai, University of Michigan, and John N. Cooper, Navy Post Graduate School; and Professors Louis L. Bailin, John D. Cowan, Jr.; Daniel B. Hodge, Hsien Ching Ko, Curt A. Levis, Edward M. Kennaugh, Robert G. Kouyoumjian, William H. Peake, Leon Peters, Jr., Jack H. Richmond, and Thomas A. Seliga of The Ohio State University. The suggestions by several anonymous reviewers chosen by the publisher were also most useful.

Finally, one of us (J. D. K.), expresses his sincere appreciation to his wife, Alice, for her assistance on the manuscript and for her patience and encouragement during the years of its preparation.

JOHN D. KRAUS
KEITH R. CARVER



INTRODUCTION

1-1 ELECTROMAGNETICS DEFINED

Electromagnetics embraces electricity, magnetism, electric fields, magnetic fields, and electromagnetic waves. In circuit theory the emphasis is on the voltage at a pair of terminals and the current through a conductor, but in electromagnetics the emphasis is on the space between conductors and the electric and magnetic fields in this space. The field approach of electromagnetics is essential for an understanding of waveguides, antennas, waves in space, and particle-field interactions. Electromagnetics also provides a basic insight into the operation and characteristics of such basic circuit elements as capacitors, inductors, and resistors. The title of this book could have been "Electric and Magnetic Fields," "Fields and Waves," or "Electromagnetic Theory and Applications." All this and more is meant by the word *Electromagnetics*, which was used as the title for the first edition of this book (1953) and is used again as the title for this edition.

1-2 DIMENSIONS AND UNITS

Lord Kelvin is reported to have said: When you can measure what you are speaking about and express it in numbers you know something about it; but when you cannot measure it, when you cannot express it in numbers your knowledge is of a meagre and unsatisfactory kind; it may be the beginning of knowledge but you have scarcely progressed in your thoughts to the stage of science whatever the matter may be.

To this it might be added that before we can measure something, we must define its dimensions and provide some standard, or reference unit, in terms of which the quantity can be expressed numerically.

A *dimension* defines some physical characteristic. For example, length, mass, time, velocity, and force are dimensions. The dimensions of length, mass, time, electric current, temperature, and luminous intensity are considered as the *fundamental dimensions* since other dimensions can be defined in terms of these six. This choice is arbitrary but convenient. Let the letters L , M , T , I , \mathcal{T} , and \mathcal{I} represent the dimensions of length, mass, time, electric current, temperature, and luminous intensity. Other dimensions are then secondary dimensions. For example, area is a secondary dimension which can be expressed in terms of the fundamental dimension of length squared (L^2). As other examples, the fundamental dimensions of velocity are L/T and of force are ML/T^2 .

A *unit* is a standard or reference by which a dimension can be expressed numerically. Thus, the meter is a unit in terms of which the dimension of length can be expressed, and the kilogram is a unit in terms of which the dimension of mass can be expressed. For example, the length (dimension) of a steel rod might be 2 meters and its mass (dimension) 5 kilograms.

1-3 FUNDAMENTAL AND SECONDARY UNITS

The units for the fundamental dimensions are called the *fundamental or base units*. In this book the International System of Units, abbreviated SI, is used.[†] In this system the *meter*, *kilogram*, *second*, *ampere*, *kelvin*, and *candela* are the base units for the six fundamental dimensions of length, mass, time, electric current, temperature, and luminous intensity. The definitions for these fundamental units are:

Meter (m) Length equal to 1,650, 763.73 wavelengths in vacuum corresponding to the $2p_{10}-5d_5$ transition of krypton 86.

[†] The International System of Units is the modernized version of the metric system. The abbreviation SI is from the French name Système Internationale d'Unités. For the complete official description of the system see U.S. Natl. Bur. Stand. Spec. Pub. 330, 1971.

Kilogram (kg) Equal to mass of international prototype kilogram, a platinum-iridium mass preserved at Sèvres, France. This standard kilogram is the only artifact among the SI base units.

Second (s) Equal to duration of 9,192,631,770 periods of radiation corresponding to the transition between two hyperfine levels of the ground state of cesium 133. The second was formerly defined as 1/86,400 part of a mean solar day. The earth's rotation rate is gradually slowing down, but the atomic (cesium-133) transition is much more constant and is now the standard. The two standards differ by about 1 second per year.

Ampere (A) Electric current which if flowing in two infinitely long parallel wires in vacuum separated by 1 meter produces a force of 200 nanonewtons per meter of length ($200 \text{ nN m}^{-1} = 2 \times 10^{-7} \text{ N m}^{-1}$).

Kelvin (K) Temperature equal to 1/273.16 of the triple point of water (or triple point of water equals 273.16 kelvins).†

Candela (cd) Luminous intensity equal to that of 1/600,000 square meter of a perfect radiator at the temperature of freezing platinum.

The units for other dimensions are called *secondary*, or *derived*, units and are based on these fundamental units (see Table 2, Sec. A-1, in Appendix A).

The material in this book deals almost exclusively‡ with the four fundamental dimensions *length*, *mass*, *time*, and *electric current* (dimensional symbols *L*, *M*, *T*, *I*). The four fundamental units for these dimensions are the basis of what was formerly called the meter-kilogram-second-ampere (mksa) system, now a subsystem of the SI.

The complete SI involves not only units but also other recommendations, one of which is that multiples and submultiples of the SI units be stated in steps of 10^3 or 10^{-3} . Thus, the kilometer ($1 \text{ km} = 10^3 \text{ m}$) and the millimeter ($1 \text{ mm} = 10^{-3} \text{ m}$) are preferred units of length, but the centimeter ($= 10^{-2} \text{ m}$) is not. For example, the proper SI designation for the width of motion-picture film is 35 mm, not 3.5 cm. For a list of the preferred units see Appendix A, Sec. A-1, Table 1.

In this book *rationalized* SI units are used. The rationalized system has the advantage that the factor 4π does not appear in Maxwell's equations although it does appear in certain other relations. A complete table of units in this system is given as Table 2, Sec. A-1, in Appendix A. The table lists dimensions or quantities alphabetically under each of the following headings: Fundamental, Mechanical, Electrical, and Magnetic. For each quantity the mathematical symbol (as used in equations), description, SI unit and abbreviation, equivalent units, and fundamental dimensions are listed.

† Note that the symbol for degree is not used with kelvins. Thus, the boiling temperature of water is 373 kelvins (373 K), not 373°K. However, the degree sign is retained with degrees Celsius.

‡ A couple of equations involve temperature. None involve luminous intensity.

It is suggested that as each new quantity and unit is discussed the student refer to the table and, in particular, become familiar with the fundamental dimensions for the quantity.

1-4 HOW TO READ THE SYMBOLS AND NOTATION

In this book *quantities* or *dimensions*, which are scalars, like charge Q , mass M , or resistance R , are always in italics. Quantities which may be vectors or scalars are boldface as vectors and italics as scalars, e.g., electric field \mathbf{E} (vector) or $E (= |\mathbf{E}|)$ (scalar). Unit vectors are always boldface with a hat (circumflex) over the letter like $\hat{\mathbf{x}}$ or $\hat{\mathbf{t}}$.[†] A dot over the symbol indicates explicitly that the quantity is harmonically time-varying (a phasor). Thus, $\dot{\mathbf{E}}$ is a space vector and time phasor (vector-phasor), but \dot{E}_x is a scalar-phasor ($\dot{E} = \hat{\mathbf{x}}\dot{E}_x$; $\dot{E}_x = E_1 e^{j\omega t}$).

Units are in roman type, i.e., *not* italic; for example, H for henry, s for second, or A for ampere.[‡] The abbreviation for a unit is capitalized if the unit is derived from a proper name; otherwise it is lowercase (small letter). Thus, we have C for coulomb but m for meter. Note that when the unit is written out, it is always lowercase even though derived from a proper name. Prefixes for units are also roman, like n in nC for nanocoulomb or M in MW for megawatt. See Table 1, Sec. A-1, in Appendix A for complete lists of prefixes.

EXAMPLE 1

$$\mathbf{D} = \hat{\mathbf{x}}200 \text{ pC m}^{-2}$$

means that the electric flux density \mathbf{D} is a vector in the positive x direction with a magnitude of 200 picocoulombs per square meter ($= 2 \times 10^{-10}$ coulombs per square meter).

EXAMPLE 2

$$V = 10 \text{ V}$$

means that the voltage V equals 10 volts. Distinguish carefully between V (italics) for voltage and V (roman) for volts.

[†] In the few places in the book where tensors appear they are indicated by a boldface letter with a bar over it like $\bar{\mathbf{F}}$. In longhand notation a vector may be indicated by a bar over the letter and a tensor by two bars.

[‡] In longhand notation no distinction is usually made between quantities (italics) and units (roman). However, it can be done by placing a bar under the letter to indicate italics or writing the letter with a distinct slant.

EXAMPLE 3

$$S = 4 \text{ W m}^{-2} \text{ Hz}^{-1}$$

means that the flux density S (a scalar) equals 4 watts per square meter per hertz. This can also be written $S = 4 \text{ W/m}^2/\text{Hz}$ or $4 \text{ W}/(\text{m}^2 \text{ Hz})$, but the form $\text{W m}^{-2} \text{ Hz}^{-1}$ is more direct and less ambiguous.

Note that for conciseness, prefixes are used where appropriate instead of exponents. Thus, the velocity of light would be given as $c = 300 \text{ Mm s}^{-1}$ (300 megameters per second) and *not* $3 \times 10^8 \text{ m s}^{-1}$. However, in solving a problem the exponential form ($3 \times 10^8 \text{ m s}^{-1}$) would be used.

The modernized metric (SI) units and the conventions used herein combine to give a concise, exact, and unambiguous notation, and if the reader is attentive to the details, he will find it has both elegance and beauty.

1-5 EQUATION NUMBERING

Important equations and those referred to in the text are numbered consecutively beginning with each section. When reference is made to an equation in a different section its number is preceded by the chapter and section number. Thus, (14-15-3) refers to Chap. 14, Sec. 15, Eq. (3). A reference to this same equation within Sec. 15 of Chap. 14 would read simply (3). Note that chapter and section numbers are printed at the top of each page.

1-6 DIMENSIONAL ANALYSIS

It is a necessary condition for correctness that every equation be balanced dimensionally. For example, consider the hypothetical formula

$$\frac{M}{L} = DA$$

where M = mass

L = length

D = density (mass per unit volume)

A = area

The dimensional symbols for the left side are M/L , the same as those used. The dimensional symbols for the right side are

$$\frac{M}{L^3} L^2 = \frac{M}{L}$$

Therefore, both sides of this equation have the dimensions of mass per length, and the equation is balanced dimensionally. This is not a guarantee that the equation is correct; i.e., it is not a *sufficient* condition for correctness. It is, however, a *necessary* condition for correctness, and it is frequently helpful to analyze equations in this way to determine whether or not they are dimensionally balanced.

Such *dimensional analysis* is also useful for determining what the dimensions of a quantity are. For example, to find the dimensions of force, we make use of Newton's second law that

$$\text{Force} = \text{mass} \times \text{acceleration}$$

Since acceleration has the dimensions of length per time squared, the dimensions of force are

$$\frac{\text{Mass} \times \text{length}}{\text{Time}^2}$$

or in dimensional symbols

$$\text{Force} = \frac{ML}{T^2}$$

1-7 THUMBNAIL ELECTROMAGNETICS

Here are the basic equations of electromagnetic theory as covered in the book. Ultimately the student should be able to recognize each equation, be able to picture the physical circumstances surrounding its development, know the dimensions (and units) in which it is expressed, and know how to apply it. For example, (31) should be recognized as Ampère's law, which equates the magnetic field \mathbf{H} integrated around a closed contour or loop to the current through the loop (or integral of the current density over a surface bounded by the loop). A diagram should be drawn, as in Fig. 1-1. Units should be stated and the application to a simple problem outlined.

The student is urged to refer frequently to these equations while studying the book and as he progresses to check each one he feels he understands. These equations will also be useful as a brief course outline or reference while preparing for tests or examinations.

$$(1) \quad \mathbf{F} = \hat{\mathbf{r}} \frac{Q_1 Q_2}{4\pi\epsilon_0 r^2} \quad (2) \quad \mathbf{E} = \frac{\mathbf{F}}{Q_2} = \hat{\mathbf{r}} \frac{Q_1}{4\pi\epsilon_0 r^2} \quad (3) \quad d\mathbf{F} = (\mathbf{I} \times \mathbf{B}) dl$$

$$(4) \quad \mathbf{B} = \frac{\mathbf{F}}{Q_m^2}$$

$$(5) \quad \mathbf{E} = -\nabla V \quad (6) \quad V = - \int \mathbf{E} \cdot d\mathbf{l} \quad (7) \quad \mathbf{B} = \nabla \times \mathbf{A} \quad (8) \quad d\mathbf{B} = \frac{\mu_0}{4\pi} \frac{\mathbf{I} \times \hat{\mathbf{r}}}{r^2} dl$$

$$(9) \quad \mathbf{E} = -\nabla V - \frac{\partial \mathbf{A}}{\partial t} \quad (10) \quad V = \frac{Q}{4\pi\epsilon_0 r} \quad (11) \quad \mathbf{B} = \frac{\mu_0}{4\pi} \iiint \frac{\mathbf{J} \times \hat{\mathbf{r}}}{r^2} dv$$

$$(12) \quad \mathbf{A} = \frac{\mu_0}{4\pi} \iiint \frac{\mathbf{J}}{r} dv$$

$$(13) \quad V = \frac{1}{4\pi\epsilon_0} \left(\sum_1^N \frac{Q_n}{r_n} + \int \frac{\rho_L}{r} dl + \iint \frac{\rho_s}{r} ds + \iiint \frac{\rho}{r} dv \right) \quad (14) \quad NI = \oint \mathbf{H} \cdot d\mathbf{l}$$

$$(15) \quad dB = \frac{\mu_0 I}{4\pi r^2} dl \sin \theta$$

$$(16) \quad V = \frac{1}{4\pi\epsilon_0} Ql \frac{1}{r^2} \cos \theta \quad (17) \quad \mathbf{D} = \epsilon \mathbf{E} \quad (18) \quad \mathbf{B} = \mu \mathbf{H} \quad (19) \quad \mathbf{J} = \sigma \mathbf{E}$$

$$(20) \quad Q = \iint \mathbf{D} \cdot d\mathbf{s} = \iiint \rho dv \quad (21) \quad \nabla \cdot \mathbf{D} = \rho \quad (22) \quad \psi_m = \iint \mathbf{B} \cdot d\mathbf{s}$$

$$(23) \quad \iint \mathbf{B} \cdot d\mathbf{s} = 0$$

$$(24) \quad \nabla^2 V = 0 \quad (25) \quad \nabla^2 V = -\frac{\rho}{\epsilon} \quad (26) \quad \iint \mathbf{J} \cdot d\mathbf{s} = 0 \quad (27) \quad \nabla \cdot \mathbf{B} = 0$$

$$(28) \quad C = \frac{\epsilon A}{l} \quad (29) \quad IA = Q_m l \quad (30) \quad \nabla \cdot \mathbf{J} = 0$$

$$(31) \quad I = \oint \mathbf{H} \cdot d\mathbf{l} = \iint \mathbf{J} \cdot d\mathbf{s}$$

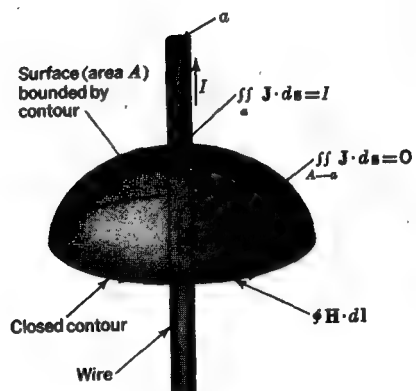


FIGURE 1-1
Illustrating Ampère's law (31).

- (32) $R = \frac{1}{G} = \frac{Sl}{A} = \frac{l}{\sigma A}$ (33) $\mathcal{R} = \frac{1}{\mathcal{P}} = \frac{l}{\mu A}$ (34) $\nabla \times \mathbf{H} = \mathbf{J}$
- (35) $\nabla \cdot \mathbf{A} = 0$
- (36) $E_{t1} = E_{t2}$ (37) $D_{n1} - D_{n2} = \rho_s$ (38) $B_{n1} = B_{n2}$ (39) $H_{t1} = H_{t2}$
- (40) $\mathbf{D} = \epsilon_0 \mathbf{E} + \mathbf{P}$ (41) $\mathbf{B} = \mu_0(\mathbf{H} + \mathbf{M})$ (42) $\mathbf{B} = \nabla \times \mathbf{A}$
- (43) $\mathbf{H} \times \mathbf{H} = \mathbf{K}$
- (44) $\frac{C}{d} = \epsilon$ (45) $\frac{L}{d} = \mu$ (46) $L = \frac{d\Lambda}{dI} = \frac{\Lambda}{I}$ (47) $L = \frac{\mu N^2 A}{l}$
- (48) $H = \frac{NI}{l} = K$
- (49) $w_e = \frac{1}{2}\epsilon E^2$ (50) $W_e = \frac{1}{2}CV^2$ (51) $w_m = \frac{1}{2}\mu H^2$ (52) $W_m = \frac{1}{2}LI^2$
- (53) $\mathcal{U} = -\frac{d\Lambda}{dt}$ (54) $\mathcal{U} = \oint \mathbf{E} \cdot d\mathbf{l} = -\frac{d}{dt} \iint \mathbf{B} \cdot d\mathbf{s} = -\iint \frac{\partial \mathbf{B}}{\partial t} \cdot d\mathbf{s}$
- (55) $B = \frac{\mu I}{2\pi R}$
- (56) $I = \oint \mathbf{H} \cdot d\mathbf{l} = \iint \left(\mathbf{J} + \frac{\partial \mathbf{D}}{\partial t} \right) \cdot d\mathbf{s}$ (57) $\nabla \times \mathbf{E} = -\frac{\partial \mathbf{B}}{\partial t}$ (58) $v = \frac{1}{\sqrt{\mu\epsilon}}$
- (59) $\nabla \times \mathbf{H} = \mathbf{J} + \frac{\partial \mathbf{D}}{\partial t}$ (60) $\mathcal{U} = \oint (\mathbf{v} \times \mathbf{B}) \cdot d\mathbf{l} - \iint \frac{\partial \mathbf{B}}{\partial t} \cdot d\mathbf{s}$
- (61) $\text{VSWR} = \frac{E_0 + E_1}{E_0 - E_1}$
- (62) $\mathbf{S} = \mathbf{E} \times \mathbf{H}$ (63) $\dot{\mathbf{S}} = \frac{1}{2}(\mathbf{E} \times \mathbf{H}^*)$ (64) $S_{av} = \frac{1}{2} \operatorname{Re}(\mathbf{E} \times \mathbf{H}^*)$
- (65) $W = VI$
- (66) $W_{av} = \frac{1}{2} \operatorname{Re} VI^*$ (67) $E = E_0 \sin(\omega t \pm \beta x)$ (68) $\nabla \cdot \mathbf{J} = -\frac{\partial \rho}{\partial t}$
- (69) $|Z_c| = \sqrt{\frac{\mu\omega}{\sigma}}$ (70) $\eta = \sqrt{\epsilon_r}$ (71) $\nabla \times \nabla \times \mathbf{E} - \gamma^2 \mathbf{E} = 0$
- (72) $V = \cos \frac{MM_a}{2}$ (73) $W = \frac{1}{2}A_e S(1 + d \cos MM_a)$
- (74) $d = \sqrt{s_1^2 + s_2^2 + s_3^2}$
- (75) $I = \frac{\langle E_1^2 \rangle + \langle E_2^2 \rangle}{Z}$ (76) $Q = \frac{\langle E_1^2 \rangle - \langle E_2^2 \rangle}{Z}$
- (77) $U = \frac{2}{Z} \langle E_1 E_2 \cos \delta \rangle$ (78) $V = S \langle \sin 2\epsilon \rangle$

$$(79) \quad \frac{d^2V}{dx^2} - ZYV = 0 \quad (80) \quad Z = \sqrt{\frac{L}{C}} \quad (81) \quad \frac{G}{C} = \frac{R}{L} \quad (82) \quad v = \frac{1}{\sqrt{LC}}$$

$$(83) \quad v = \frac{\omega}{\beta} = \frac{v_0}{\sqrt{1 - (\lambda_0/\lambda_{oc})^2}} \quad (84) \quad Z = \frac{Z_d}{\sqrt{1 - (\lambda_0/\lambda_{oc})^2}} \quad (85) \quad \lambda_{oc} = \frac{2\pi r_0}{k_{nr}}$$

$$(86) \quad \gamma = \sqrt{\left(\frac{n\pi}{y_1}\right)^2 + \left(\frac{m\pi}{z_1}\right)^2} - \omega^2 \mu \epsilon \quad (87) \quad E_\theta = 60\pi I_0 \frac{l}{\lambda} \frac{1}{r} j e^{j(\omega t - \theta r)} \sin \theta$$

$$(88) \quad Z_d = \frac{E}{H} = \sqrt{\frac{\mu}{\epsilon}} \quad (89) \quad Z = \frac{V}{I} = \frac{\oint \mathbf{E} \cdot d\mathbf{l}}{\oint \mathbf{H} \cdot d\mathbf{l}} \quad (90) \quad Z_{yz} = \frac{E_y}{H_z}$$

$$(91) \quad Q = \frac{2\pi}{T} \frac{P}{-dP/dt} \quad (92) \quad P = \iint \mathbf{S}_{av} \cdot d\mathbf{s} \quad (93) \quad \Omega_A = \oint P_n(\theta, \phi) d\Omega$$

$$(94) \quad D = \frac{4\pi}{\Omega_A} = 4\pi \frac{A_e}{\lambda^2} = \frac{P_{max}}{P_{av}} \quad (95) \quad \lambda^2 = A_e \Omega_A \quad (96) \quad D \approx \frac{4\pi}{\theta \phi} = \frac{41253}{\theta^0 \phi^0}$$

$$(97) \quad E = E_0(1 + e^{j\psi} + e^{j2\psi} + e^{j3\psi} + \dots + e^{j(n-1)\psi}) = E_0 \frac{\sin(n\psi/2)}{\sin(\psi/2)} \underbrace{\Big/}_{(n-1)} \frac{\psi}{2}$$

$$(98) \quad E_\theta = \int E(y) \exp(j\beta y \cos \theta) dy \quad (99) \quad E_0 = \frac{A_0 E_a}{2r_0 \lambda} \quad (100) \quad \text{HPBW} = \frac{1}{L/\lambda}$$

$$(101) \quad L = \frac{2\pi}{\lambda_0} \int \eta \, dl \quad (102) \quad Z_s = \frac{Z_0^2}{4Z_d} \quad (103) \quad \epsilon_{ap} = \frac{A_e}{A_p} = \frac{E_{av}^2}{(E^2)_{av}}$$

$$(104) \quad w = kT \quad (105) \quad S = \frac{2w}{A_e} = \frac{2kT_A}{A_e} \quad (106) \quad \frac{P_r}{P_t} = \frac{A_{er} A_{et}}{r^2 \lambda^2}$$

$$(107) \quad T_{min} = \frac{T_{sys}}{\sqrt{\Delta f} t} \quad (108) \quad \frac{P_r}{P_t} = \frac{A^2 \sigma}{4\pi \lambda^2 r^4} \quad (109) \quad I = JA = \rho v A$$

$$(110) \quad F = evB \quad (111) \quad \mathbf{F} = m\mathbf{a} = m \frac{d\mathbf{v}}{dt} \quad (112) \quad \mathbf{F} = e\mathbf{E} = e(\mathbf{v} \times \mathbf{B})$$

$$(113) \quad W = eV$$

$$(114) \quad v = \sqrt{\frac{2eV}{m}} \quad (115) \quad \omega^2 = \frac{Ne^2}{\epsilon_0 m} \quad (116) \quad n = \sqrt{1 - \left(\frac{\omega_0}{\omega}\right)^2} \quad (117) \quad v = \frac{B_0}{\sqrt{\mu\rho}}$$

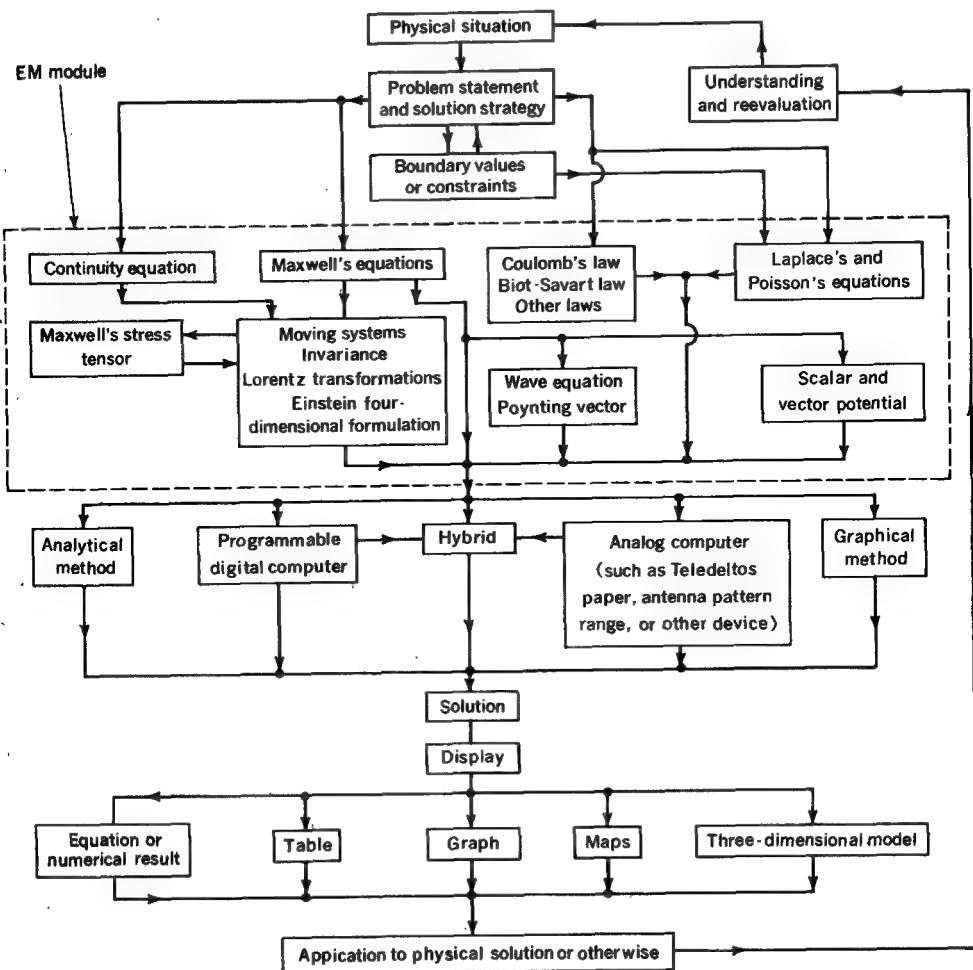
$$(118) \quad \frac{d\mathbf{v}}{dt} = \mathbf{G} + \frac{1}{\rho} (\mathbf{J} \times \mathbf{B} - \nabla p) \quad (119) \quad \frac{l'}{l} = \frac{\sqrt{1 + (v/c)^2}}{\sqrt{1 - (v/c)^2}}$$

$$(120) \quad \frac{\partial \mathbf{G}_{mn}}{\partial x_n} = \mathbf{J}_m \quad (121) \quad \frac{\partial \mathbf{F}_{mn}}{\partial x_n} = 0 \quad (122) \quad \frac{\partial \mathbf{J}_m}{\partial x_m} = 0 \quad (123) \quad \frac{\partial V_m}{\partial x_m} = 0$$

$$(124) \quad E'_\perp = \gamma |E_\perp + (v \times B)| \quad (125) \quad B'_\perp = \gamma \left| B_\perp - \left(\frac{1}{c^2} v \times E \right) \right|$$

$$(126) \quad \nabla \cdot J = 0 \quad (127) \quad F = \nabla \cdot T_{mn}$$

SPEMP CHART
Solution Paths for Electromagnetic Problems



1-8 SPEMP CHART

In the preceding section the fundamental equations of electromagnetic theory are presented. In applying these equations to a problem a path is followed in order to achieve a solution and display the results. A choice of methods and displays is usually available. The SPEMP chart shows Solution Paths for Electromagnetic Problems. As the student progresses through the book, he should refer to this chart, which will clarify the steps and procedures. Note that the part related to electromagnetic (EM) theory is contained within the dashed line (EM module) while the part outside (analogous to the "main frame") is general and can be used for any discipline if an appropriate module is substituted.

PROBLEMS

- * 1-1 Give (a) the dimensional description, (b) the dimensional formulas in terms of the symbols M , L , T , and I , and (c) the SI units for each of the following:

$$\frac{dl}{dt} \quad \text{where } l = \text{length and } t = \text{time}$$

$$\int F dl \quad \text{where } F = \text{force}$$

$$\frac{dl}{dx}$$

- * 1-2 Give the information requested in Prob. 1-1 for each of the following:

$$\iiint \rho dv \quad V \quad E \quad \int \mathbf{E} \cdot d\mathbf{l} \quad \frac{1}{4\pi\epsilon_0} \quad \frac{Q^2}{4\pi\epsilon_0 r^2} \quad J \quad BIl$$

* Answers to starred problems are given in Appendix C.

2

THE STATIC ELECTRIC FIELD: PART 1

2-1 INTRODUCTION

In this chapter the basic relations for static electric fields in free space are discussed. They include Coulomb's law and the force per charge, Gauss' law and the electric flux, and the superposition of fields. The equivalence of the electric field to the gradient of the electric potential and of the electric potential to the line integral of the electric field are explained. The orthogonality of field lines and equipotential contours is pointed out. Shells of charge and capacitance are also considered. Also mentioned are the simplifying concepts of staticness and idealness and the conventions of positiveness, right-handedness, and outwardness.

2-2 THE FORCE BETWEEN POINT CHARGES AND COULOMB'S LAW

A group of charged particles, i.e., atoms or electrons, occupies a finite† volume. Even a single electron has a finite size. However, it is often convenient to regard a

† By "finite" is meant "not infinitesimal."

small, concentrated region of charged particles as a *point charge*. This assumption leads to no appreciable error provided the size of the volume occupied by the charged particles is small compared with the other distances involved.

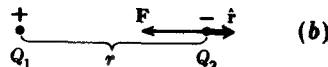
The basic experiment of electrostatics was first reported by Coulomb in 1785,[†] using small charged bodies which may be regarded as point charges. The results of this experiment are given by *Coulomb's law*, which states that the force F between two point charges Q_1 and Q_2 is proportional to the product of the charges and inversely proportional to the square of the distance r between them, i.e.,

$$F = k \frac{Q_1 Q_2}{r^2} \quad (\text{N}) \quad (1)$$

where k is a constant of proportionality. Because of the inverse-square effect of distance this law is said to be an inverse-square law. The force is in the direction of the line connecting the charges. As suggested in Fig. 2-1a, the force is outward (repulsive force) if the two charges are of the same sign, but, as suggested in Fig. 2-1b, the force is inward (attractive force) if the two charges are of opposite sign.



FIGURE 2-1

(a) Two point charges of same sign and
(b) opposite sign.

In the International System the constant of proportionality is given by

$$k = \frac{1}{4\pi\epsilon}$$

where ϵ is the permittivity[‡] of the medium in which the charges are situated. By dimensional analysis of (1) we find that ϵ has the dimensions of capacitance[§] per length, or in dimensional symbols $T^4 I^2 / M L^3$. The SI unit for permittivity is the farad per meter ($F \text{ m}^{-1}$). The permittivity of vacuum is

$$\epsilon_0 = 8.85 \times 10^{-12} \text{ F m}^{-1} = 8.85 \text{ pF m}^{-1}$$

$$\approx \frac{1}{36\pi} \times 10^{-9} \text{ F m}^{-1} = \frac{1}{36\pi} \text{ nF m}^{-1}$$

[†] Charles A. de Coulomb, *History Royal Acad. Sci. (France)*, 1785, pp. 569 and 579.

[‡] Also called the *dielectric constant*.

[§] For a discussion of capacitance see Sec. 2-24. See also Sec. 3-22 on the field-cell capacitor.

The permittivity of air is substantially the same as for vacuum. In this chapter it is assumed that the medium is air or vacuum, and so to be more explicit the permittivity ϵ could be written ϵ_0 throughout. However, the same equations apply to a medium of infinite extent provided the medium is isotropic, homogeneous, and linear. The general situation of material media for which $\epsilon \neq \epsilon_0$ is discussed further in Chap. 3.

Force is a vector; i.e., it has both magnitude and direction. Rewriting (1) as a vector equation and also substituting the value of k , we have

$$\boxed{\mathbf{F} = \hat{\mathbf{r}} \frac{Q_1 Q_2}{4\pi\epsilon r^2}} \quad (2)$$

where \mathbf{F} = force, N†

$\hat{\mathbf{r}}$ = unit vector (see Fig. 2-1) pointing in direction of line joining the charges
(thus, $\mathbf{F} = \hat{\mathbf{r}}F$)

Q_1 = charge 1, C

Q_2 = charge 2, C

ϵ = permittivity of medium, F m⁻¹

r = distance between point charges, m

This is the complete vector expression for Coulomb's law stated in rationalized SI units. To demonstrate the application of this law let us consider the following problems.

EXAMPLE 1 A negative point charge of $1 \mu\text{C}$ is situated in air at the origin of a rectangular coordinate system. A second negative point charge of $100 \mu\text{C}$ is situated on the positive x axis at the distance of 500 mm from the origin. What is the force on the second charge?

SOLUTION By Coulomb's law the force

$$\begin{aligned}\mathbf{F} &= \hat{\mathbf{x}} \frac{(-10^{-6})(-10^{-4})}{(4\pi \times 0.5^2)(10^{-9}/36\pi)} \\ &= + 23.6 \text{ N}\end{aligned}$$

That is, there is a force of 3.6 N (0.8 lb) in the positive x direction on the second charge.

EXAMPLE 2 Two point charges of 1 C each and of the same sign are placed 1 mm apart in air. What is the magnitude of the repulsive force?

† One newton equals the force required to accelerate 1 kg 1 m s⁻².

SOLUTION From Coulomb's law the force is

$$F = \frac{1 \times 1}{4\pi\epsilon_0 \times 10^{-6}} = 9 \times 10^{15} \text{ N}$$

≈ weight of 9.2×10^{11} metric tons

≈ weight of 10^{12} U.S. tons

This force is sufficient to lift millions of Empire State buildings, or roughly all the buildings in the United States simultaneously. [Note that the force N at the earth's surface due to gravity equals the mass (kg) times 9.8 m s^{-2} .]

2-3 IDEALNESS AND STATICNESS

The concept of a point charge employed in Sec. 2-2 is an idealization. In many situations discussed in science and technology *idealness* is invoked in this manner in order to simplify the problem.

In Chaps. 2 and 3 it is important to note that it is the *static* electric field which is discussed. The implication here is that all charges and objects are at rest with respect to one another. This is also something of an idealization but one which is useful in developing the basic concepts of field theory. In later chapters the situation under conditions of motion will be treated.

2-4 ELECTRIC FIELD INTENSITY E

Consider a positive electric point charge Q_1 placed rigidly at the origin of a polar coordinate system. If another positive point charge Q_2 is brought into the vicinity of Q_1 , it is acted upon by a force. This force is directed radially outward and becomes greater as Q_2 approaches Q_1 . It may be said that Q_1 has a field around it where forces may act. The nature of this field is suggested by the vector diagram of Fig. 2-2, the length of the vector being proportional to the force at the point (at center of vector).

Dividing (2-2-2) by Q_2 puts the equation in the dimensional form of force per charge, i.e.,

$$\frac{F}{Q_2} = \frac{\text{force}}{\text{charge}}$$

which has the dimensional symbols

$$\frac{ML}{T^2 Q} = \frac{ML}{T^3 I}$$

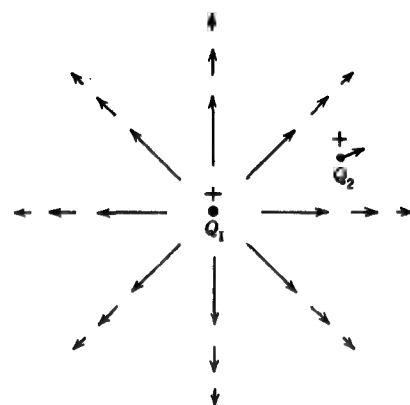


FIGURE 2-2

Point charge Q_1 with vectors indicating magnitude and direction of associated electric field.

If Q_2 is a *positive test charge*, the resulting *force per unit charge* is defined as the *electric field intensity*[†] E . Thus,

$$E = \frac{F}{Q_2} = k \frac{Q_1}{4\pi\epsilon r^2} \quad (1)$$

where Q_2 = positive test charge.

The SI unit of electric field intensity is the newton per coulomb ($N C^{-1}$). As will appear after the discussion of electric potential (Sec. 2-7), an equivalent unit for the electric field intensity is the volt per meter ($V m^{-1}$).

According to (1), the point charge Q_1 is surrounded by an *electric field* of intensity E which is proportional to Q_1 and is inversely proportional to r^2 . The electric field intensity E is a vector having the same direction as the force F but differing in dimensions and in numerical magnitude.

It is not implied by (1) that the positive test charge has a value of 1 C. It may have any convenient value since the ratio of the force (newtons) to the test charge (coulombs) is independent of the size of the charge provided the test charge does not disturb the field being measured. As noted in Example 2 above, 1 C represents a much larger charge than is ordinarily encountered in static problems. Thus, if we attempted to use a test charge of 1 C, we would tend to disturb the charges whose field we seek to measure. Therefore, it is necessary to use small test charges; in fact, the test charge should be small enough to ensure that it does not appreciably disturb the charge configuration whose field is to be measured.

[†] Also called the *electric field strength*.

If the test charge is made small enough, it may be regarded as of infinitesimal size, so that the ultimate value of the electric field intensity at a point becomes the force ΔF on a positive test charge ΔQ divided by the charge (ΔQ) with the limit taken as the charge approaches zero; i.e.,

$$\mathbf{E} = \lim_{\Delta Q \rightarrow 0} \frac{\Delta \mathbf{F}}{\Delta Q} \quad (2)$$

Actually the smallest available test charge is an electron. Since this is a finite charge, it follows that \mathbf{E} cannot be measured with unlimited accuracy. Although this is of importance in atomic problems, it need not concern us in the large-scale, or macroscopic, problems treated in this book. In practice, \mathbf{E} would be measured with a small but finite test charge, and if this charge is small enough, \mathbf{E} would differ inappreciably from that measured with an infinitesimal or vanishingly small test charge as implied in (2).

EXAMPLE A negative point charge 10 nC is situated in air at the origin of a rectangular coordinate system. What is the electric field intensity at a point on the positive x axis 3 m from the origin?

SOLUTION By (1) the field intensity is given by

$$\begin{aligned} \mathbf{E} &= -\hat{x} \frac{10^{-8}}{(4\pi \times 3^2)(10^{-9}/36\pi)} \\ &= -\hat{x} 10 \quad \text{N C}^{-1} \text{ (or V m}^{-1}\text{)} \end{aligned}$$

That is, the electric field intensity is 10 N C^{-1} (or 10 V m^{-1}) and is in the negative x direction.

2-5 POSITIVENESS, RIGHT-HANDEDNESS, AND OUTWARDNESS

It will be convenient at the outset to adopt several conventions.

- 1 It is convenient to define the electric field, as in Sec. 2-4, in terms of *positive* charge. Thus, the electric field at any point is in the direction of the force on a *positive* test charge placed at that point.
- 2 It is convenient to standardize on right-handed coordinate systems. For example, the rectangular coordinate system in Fig. 2-3a is *right-handed* since turning the *positive* x axis into the *positive* y axis and proceeding the direction of a *right-handed* screw, we move in the *positive* z direction. This set of coordinate axes may accordingly be termed a *positive set*. The rectangular coordinate system in Fig. 2-3b is *left-handed* since turning the *positive* x axis into the *positive*

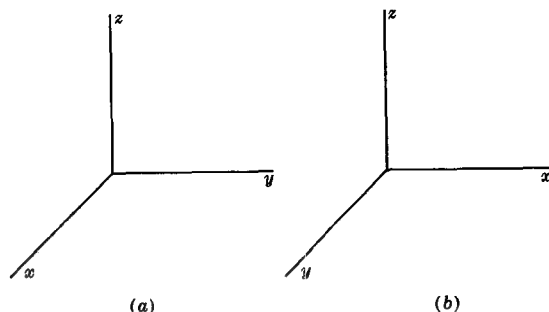


FIGURE 2-3

(a) Right-handed and (b) left-handed coordinate systems.

y axis, we must proceed like a left-handed screw to move in the positive *z* direction.

- 3 It is a consequence of the positiveness convention that the electric field around a positive charge is *outward* (see Fig. 2-2). A further consequence is that we take the *positive* direction of the normal at any point on a closed surface as the *outward* normal. Thus, applying Gauss' law (Sec. 2-17), we shall note that the integral of the *normal* component of the outward electric flux density over a closed surface yields the *positive* charge enclosed.

The concept of positiveness is inherent in our definitions and, as discussed above, is also associated with the definitions of right-handedness and outwardness.

2-6 THE ELECTRIC FIELD OF SEVERAL POINT CHARGES AND THE PRINCIPLE OF SUPERPOSITION OF FIELDS

Since the electric field of a point charge is a linear function of the value of the charge, it follows that the fields of more than one point charge are linearly superposable by vector addition. As a generalization, this fact may be stated as the *principle of superposition* applied to electric fields as follows:

The total or resultant field at a point is the vector sum of the individual component fields at the point.

Thus, referring to Fig. 2-4, the field intensity of the point charge Q_1 at the point P is \mathbf{E}_1 and of the point charge Q_2 is \mathbf{E}_2 . The total field at P due to both point charges is the vector sum of \mathbf{E}_1 and \mathbf{E}_2 , or \mathbf{E} , as indicated in the figure.

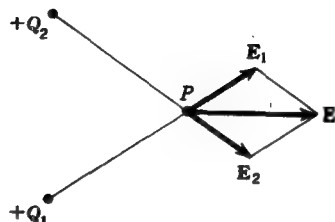


FIGURE 2-4

Vector addition of fields due to two equal point charges of the same sign to give resultant, or total field \mathbf{E} .

EXAMPLE A positive point charge of 1 nC is situated in air at the origin ($x = 0, y = 0$), and a negative point charge of -2×10^{-9} C is situated on the y axis 1 m from the origin ($x = 0, y = 1$), as shown in Fig. 2-5. Find the total electric field intensity at the point P on the x axis 2 m from the origin ($x = 2, y = 0$).

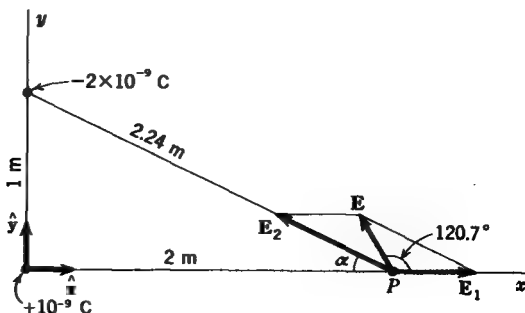


FIGURE 2-5

Vector addition of fields due to two unequal point charges of opposite sign to give resultant, or total field \mathbf{E} .

SOLUTION The vector value of the electric field \mathbf{E}_1 due to the charge at $(0, 0)$ is, from (2-4-1),

$$\begin{aligned}\mathbf{E}_1 &= \hat{\mathbf{x}} \frac{10^{-9}}{(4\pi \times 2^2)(10^{-9}/36\pi)} \\ &= \hat{\mathbf{x}} 2.25 \text{ N C}^{-1}\end{aligned}$$

The magnitude of the field \mathbf{E}_2 due to the charge at $(0, 1)$ is

$$\begin{aligned}\mathbf{E}_2 &= \frac{-2 \times 10^{-9}}{(4\pi \times 2.24^2)(10^{-9}/36\pi)} \\ &= -3.59 \text{ N C}^{-1}\end{aligned}$$

The vector value of \mathbf{E}_2 is given by

$$\begin{aligned}\mathbf{E}_2 &= -\hat{x}3.59 \cos \alpha + \hat{y}3.59 \sin \alpha \\ &= -\hat{x}3.58 \frac{2}{2.24} + \hat{y}3.59 \frac{1}{2.24} \\ &= -\hat{x}3.2 + \hat{y}1.6 \text{ N C}^{-1}\end{aligned}$$

where \hat{x} = unit vector in x direction

\hat{y} = unit vector in y direction.

The total vector field \mathbf{E} can be obtained by graphical vector addition of \mathbf{E}_1 and \mathbf{E}_2 or analytically as follows:

$$\mathbf{E} = \hat{x}(2.25 - 3.2) + \hat{y}1.6$$

or in both rectangular and polar forms

$$\mathbf{E} = -\hat{x}0.95 + \hat{y}1.6 = 1.86/\underline{120.7^\circ} \text{ N C}^{-1}$$

2-7 THE ELECTRIC SCALAR POTENTIAL

Consider two points, x_1 and x_2 , situated in a uniform electric field \mathbf{E} parallel to the x direction. Let a *positive* test charge at x_2 be moved in the negative x direction to x_1 as in Fig. 2-6. The field exerts a force on the charge so that it requires work to move the charge against the force. The amount of work per unit charge is equal to the force per unit charge (or field intensity \mathbf{E}) times the distance through which the charge is moved. Thus,

$$E(x_2 - x_1) = \text{work per unit charge} \quad (\text{joules/coulomb, J C}^{-1}) \quad (1)$$

The dimensions are

$$\frac{\text{Force}}{\text{Charge}} \times \text{length} = \frac{\text{work}}{\text{charge}}$$

$$\text{or} \quad \frac{ML}{T^2} \frac{L}{Q} = \frac{ML^2}{T^3 I}$$

In SI units the relation is

$$\frac{\text{Newtons}}{\text{Coulomb}} \times \text{meters} = \frac{\text{joules}}{\text{coulomb}}$$

The dimensions of work per charge are those of potential. In our example (Fig. 2-6), the work or energy per unit charge required to transport the test charge from x_2 to x_1 is called the difference in *electric potential*[†] of the points x_2 and x_1 . The point x_1 has the higher potential since it requires work to reach it from point x_2 . Thus, moving from x_2 to x_1 (opposite to \mathbf{E}), we experience a *rise* in potential. The unit

[†] Potential, in general, is a measure of energy per some kind of unit quantity. For example, the difference in gravitational potential at sea level and 100 m above sea level is equal to the work required to raise a 1-kg mass from sea level to a height of 100 m against the earth's gravitational field. Potential is a scalar quantity, i.e., it has magnitude but no direction.

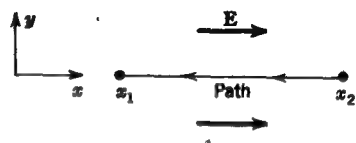


FIGURE 2-6
Linear path in uniform electric field.

of electric potential V is the volt (V) and is equal to 1 J C^{-1} . Hence, electric potential is expressible either in joules per coulomb or in volts.

$$\frac{\text{Newtons}}{\text{Coulomb}} \times \text{meters} = \frac{\text{joules}}{\text{coulomb}} = \text{volts}$$

Dividing by meters, we obtain

$$\frac{\text{Newtons}}{\text{Coulomb}} = \frac{\text{volts}}{\text{meter}} = \text{electric field intensity}$$

Thus, the electric field intensity E is expressible in either newtons per coulomb or in volts per meter.

EXAMPLE Let the uniform electric field in Fig. 2-6 have an intensity E of 10 V m^{-1} . If the distance $x_2 - x_1$ is 100 mm , what is the potential difference of the two points?

SOLUTION From (1) the electric potential is given by

$$V = 10 \times 0.1 = 1 \text{ V}$$

That is, the potential of x_1 is 1 V higher than the potential of x_2 .

Consider next the case of a nonuniform field such as exists in the vicinity of the positive point charge Q (Fig. 2-7). The electric field E is radial and is inversely proportional to the square of the distance r from the charge Q . The energy per coulomb required to move a *positive* test charge from r_2 to r_1 along a radial path equals the potential difference, or rise, V_{21} between the points. This is given by

$$V_{21} = \int_{r_2}^{r_1} dV = - \int_{r_2}^{r_1} E dr \quad (\text{V})$$

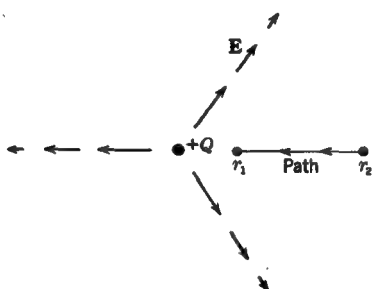


FIGURE 2-7
Linear path in nonuniform electric field.

The negative sign takes into account the fact that the motion from r_2 to r_1 is opposite to the direction of the field. Substituting the value of E from (2-4-1) yields

$$\begin{aligned} V_{21} &= V_1 - V_2 = - \int_{r_2}^{r_1} \frac{Q}{4\pi\epsilon r^2} dr \\ &= - \frac{Q}{4\pi\epsilon} \int_{r_2}^{r_1} \frac{dr}{r^2} = \frac{Q}{4\pi\epsilon} \left(\frac{1}{r_1} - \frac{1}{r_2} \right) \end{aligned} \quad (2)$$

where V_1 = potential at point r_1

V_2 = potential at point r_2

The potential difference in (2) is positive since work must be expended to move the positive test charge from r_2 to r_1 against the field. However, if the motion is from r_1 to r_2 , the field does work on the charge and there is a fall in potential (negative potential difference).

If the point r_2 (Fig. 2-7) is removed to infinity, we can arbitrarily define it to be at zero potential. Thus, (2) becomes

$$V_1 = \frac{Q}{4\pi\epsilon r_1} \quad (V) \quad (3)$$

This potential is called the *absolute potential* of the point r_1 due to the charge Q . It is inversely proportional to the distance from Q to the point r_1 and is, by definition, the work per coulomb required to bring a positive test charge from infinity to the point r_1 .

2-8 THE ELECTRIC SCALAR POTENTIAL AS A LINE INTEGRAL OF THE ELECTRIC FIELD

In Sec. 2-7 the test charge is moved via the shortest path between two points. Actually, the path followed is immaterial since the potential difference is determined solely by the difference in potential of the two end points of the path. Thus, referring to Fig. 2-7, the potential at the point r_1 with respect to the potential at r_2 is said to be *single-valued*; i.e., it can have only one value regardless of the path taken from r_2 to r_1 . When the path of the test charge is not parallel to \mathbf{E} but at an angle θ , as in Fig. 2-8, the potential difference V_{21} between the points x_2 and x_1 is equal to the path length $x_2 - x_1$ multiplied by the component of \mathbf{E} parallel to it. Thus, $V_{21} = (x_2 - x_1)E \cos \theta$.

If the test charge is moved perpendicular to the direction of the field ($\theta = 90^\circ$), no work is performed and hence this path is said to be an *equipotential* line. It is an important property of fields that equipotential and field lines are orthogonal.

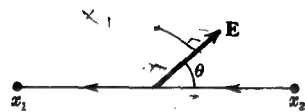


FIGURE 2-8
Linear path in uniform electric field at angle θ .

Let us consider next the case where the path of the test charge is curved. Then the potential difference between the end points of the path is given by the product of the infinitesimal element of path length dl and the component of \mathbf{E} parallel to it, integrated over the length of the path from a to b . For the path in the uniform field \mathbf{E} in Fig. 2-9, the infinitesimal potential rise dV between the ends of the path element dl is given by

$$dV = -E \cos \theta \, dl = -\mathbf{E} \cdot d\mathbf{l} \quad (1)$$

where θ is the angle between the path element and the field. A potential rise (positive potential difference dV) requires that the component of the motion parallel to \mathbf{E} be opposed to the field. Hence the negative sign in (1). By integrating (1) between the points a and b we obtain the potential rise V_{ab} between the points a and b . Thus,

$$V_{ab} = \int_a^b dV = V_b - V_a = - \int_a^b E \cos \theta \, dl = - \int_a^b \mathbf{E} \cdot d\mathbf{l} \quad (2)$$

Referring to the zigzag path in Fig. 2-9, we note that contributions to the work occur only when the path has a component parallel to \mathbf{E} . Hence, the work in going from a to b is the sum of the work increments along the zigzag-path elements parallel to \mathbf{E} ($\theta = 180^\circ$) taken in the limit as the increments approach zero with no work contribution from the zigzag-path elements perpendicular to \mathbf{E} ($\theta = 90^\circ$).

The integral involving dl in (2) is called a *line integral*. Hence, the potential rise between a and b equals the line integral of \mathbf{E} along the curved path from a to b . As written in (2), the result can be expressed either in scalar form (with $\cos \theta$) or in vector form as a scalar or dot product,

EXAMPLE 1 In Fig. 2-9 let \mathbf{E} be everywhere in the $+x$ direction and equal to 10 V m^{-1} (a uniform field). Let $x_1 = 1 \text{ m}$. Find V_{ab} .

SOLUTION From (2)

$$V_{ab} = - \int_a^b E \cos \theta \, dl = - \int_{x_1}^0 E \, dx = Ex_1 = +10 \text{ V}$$

Consider now the situation where the path of the test charge is curved and the electric field is nonuniform. Let the nonuniform field be produced by a point charge $+Q$ as in Fig. 2-10. The field intensity due to a point charge is given by (2-4-1).

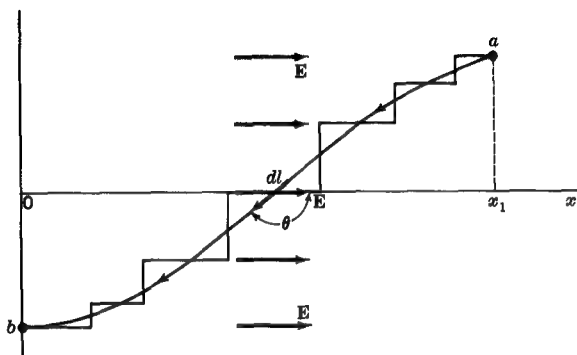


FIGURE 2-9
Curved path in a uniform electric field.

Substituting this in (2) and also putting $dr = \cos \theta dl$, where dr is an infinitesimal element of radial distance, gives

$$V_{ab} = -\frac{Q}{4\pi\epsilon_0} \int_{r=a}^{r=b} \frac{dr}{r^2} = \frac{Q}{4\pi\epsilon_0} \left(\frac{1}{b} - \frac{1}{a} \right) \quad (\text{V}) \quad (3)$$

Putting $b = r_1$ and $a = r_2$ makes this result identical with (2-7-1), where the path is along a radial line.

EXAMPLE 2 Let the positive charge Q , Fig. 2-10, be equal to 223 pC. Also let $a = 400$ mm and $b = 100$ mm. The medium is air. Find the absolute potential V_a at a , the absolute potential V_b at b , and the potential rise V_{ab} .

SOLUTION

$$V_a = \frac{Q}{4\pi\epsilon_0 a} \approx 5 \text{ V}$$

$$V_b = \frac{Q}{4\pi\epsilon_0 b} \approx 20 \text{ V}$$

$$V_{ab} = V_b - V_a \approx 15 \text{ V}$$

The work to move a test charge along an equipotential contour or surface is zero ($\theta = 90^\circ$). The maximum amount of work per unit distance is performed by moving normal to an equipotential surface. This coincides with the direction of the field.

The work to transport a test charge around any *closed path* in a static field is zero since the path starts and ends at the same point. Thus, the upper and lower limits of the integrals in (2) become the same, and the result is zero. A property of the

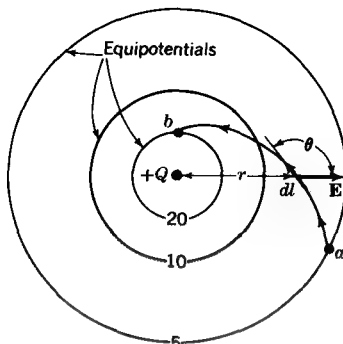


FIGURE 2-10
Curved path in a nonuniform electric field.

static electric field is, then, that the *line integral of this field around a closed path is zero*. It follows that the potential difference between any two points is independent of the path.

2-9 RELATION OF ELECTRIC FIELD LINES AND EQUIPOTENTIAL CONTOURS; ORTHOGONALITY

A field line indicates the direction of the force on a positive test charge introduced into the field. If the test charge is released, it moves in the direction of the field line.

In a uniform field, the field lines are parallel, as in Fig. 2-11. A single field line gives no information about the intensity of the field. It indicates only the direction. However, by measuring the work per coulomb required to move a positive test charge

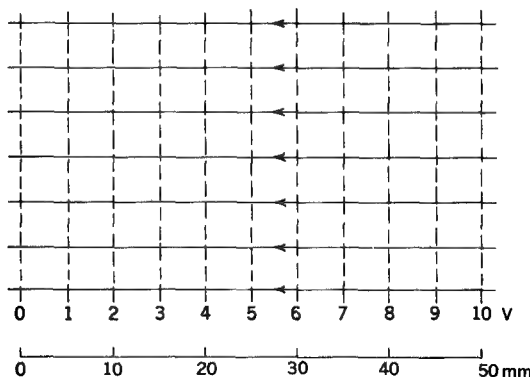


FIGURE 2-11
Field lines (solid) and equipotential lines (dashed) of a uniform electric field.

along a field line the potential differences along the line can be determined. The larger the potential difference between two points a unit distance apart, the stronger the field. In a uniform field the potential difference per unit length is constant, so that the equipotential lines (which are orthogonal to the field lines) are equally spaced. In the example of Fig. 2-11, the electric field intensity is 0.2 V mm^{-1} , so that the equipotential contours at 1-V intervals are parallel lines spaced 5 mm apart. One of the lines is arbitrarily taken as having a zero potential so that the potentials shown are relative to this line.

Consider now the case of a nonuniform field such as exists in the vicinity of the positive point charge Q in Fig. 2-12. If a positive test charge is released in this field, it moves radially away from Q , so that the field lines are radial. The field intensity varies inversely as the square of the distance. In Fig. 2-12 this is suggested by the fact that the field lines become more widely separated as the distance from Q increases. The absolute potential is inversely proportional to the distance from Q . If $Q = 10 \text{ pC}$, the equipotential contours for 20, 10, 5, and 3 V are then as shown by the concentric circles in Fig. 2-12.

 It is to be noted that a potential rise is always in the opposite direction to \mathbf{E} .

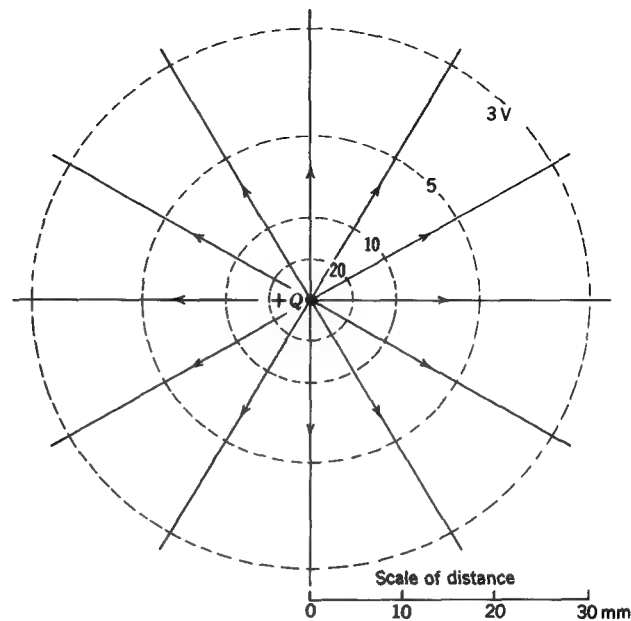


FIGURE 2-12
Field lines (solid) and equipotential lines (dashed) of a nonuniform electric field.

2-10 FIELD OF TWO EQUAL POINT CHARGES OF OPPOSITE SIGNS AND OF SAME SIGN

The electric field at a point P due to two point charges $+Q$ and $-Q$ is equal to the vector sum of the fields at P due to each of the charges alone. This is illustrated in Fig. 2-13. The potential V at P is equal to the algebraic sum of the potentials at P due to each charge alone.

A map of the field lines (solid) and equipotential contours (dashed) is shown in Fig. 2-13 for point charges $+Q$ and $-Q$ separated by 127 mm. The equipotential contours are given in volts for $Q = 140 \text{ pC}$. The charge configuration in Fig. 2-13 constitutes an electric dipole with a charge separation of 127 mm.

In contrast to the above let us consider two equal point charges of the same sign (positive) as in Fig. 2-14. A map of the field lines (solid) and equipotential contours (dashed) is shown for a charge separation of 127 mm. The equipotential contours are given in volts for $Q = 140 \text{ pC}$. The only difference between the charge configuration of Fig. 2-14 and that in Fig. 2-13 is that the lower charge is positive.

Near each charge the effect of the other charge is small, and the equipotentials are circles like those around an isolated point charge. For intermediate distances the equipotentials have the shapes shown in Fig. 2-14. Of particular interest is the figure-eight-shaped equipotential ($V = 39.5 \text{ V}$) that crosses itself at the point P , where $E = 0$. This point is called a singular point. At such a point, field and equipotential lines are not perpendicular.

Note that in three dimensions the (dashed) equipotential lines are surfaces generated by rotating Figs. 2-13 and 2-14 about the (vertical) axis through the charges.

2-11 CHARGE DENSITY AND CONTINUOUS DISTRIBUTIONS OF CHARGE

The electric *charge density* ρ is equal to the total charge Q in a volume v divided by the volume. Thus,

$$\boxed{\rho = \frac{Q}{v}} \quad (1)$$

Electric charge density has the dimensions of charge per unit volume, or in dimensional symbols Q/L^3 . The SI unit of charge density is the *coulomb per cubic meter* ($C \text{ m}^{-3}$).

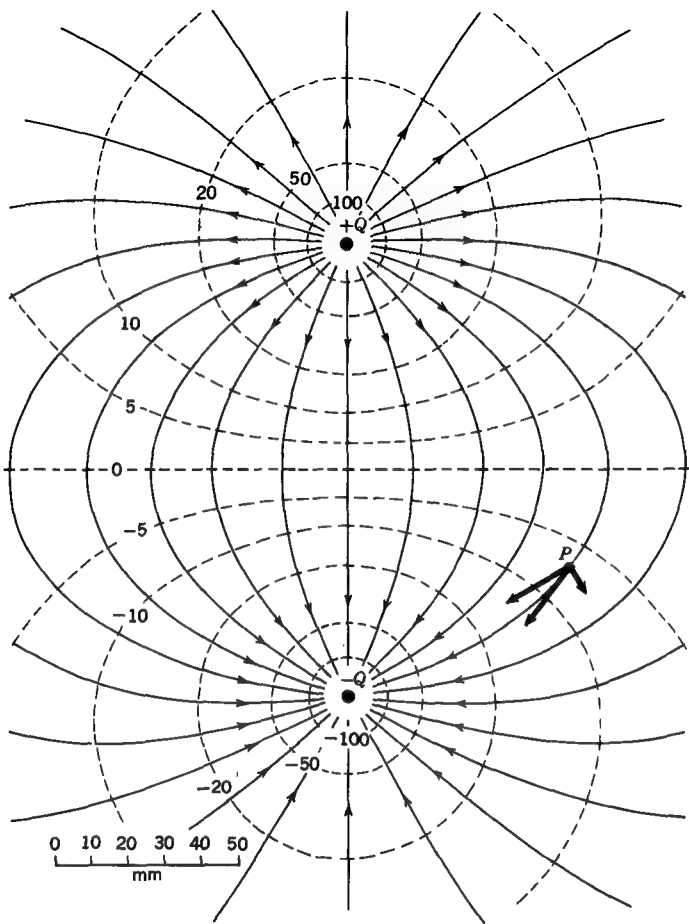


FIGURE 2-13

Electric field and potential variation around an electric dipole consisting of a positive and negative charge of 140 pC separated by 127 mm. The solid lines are field lines, and the dashed lines are equipotential contours, with their potential level indicated in volts.

By assuming that electric charge can be continuously distributed throughout a region we can also define the value of the charge density ρ at a point P as the charge ΔQ in a small volume element Δv divided by the volume, with the limit of this ratio taken as the volume shrinks to zero around the point P . In symbols,

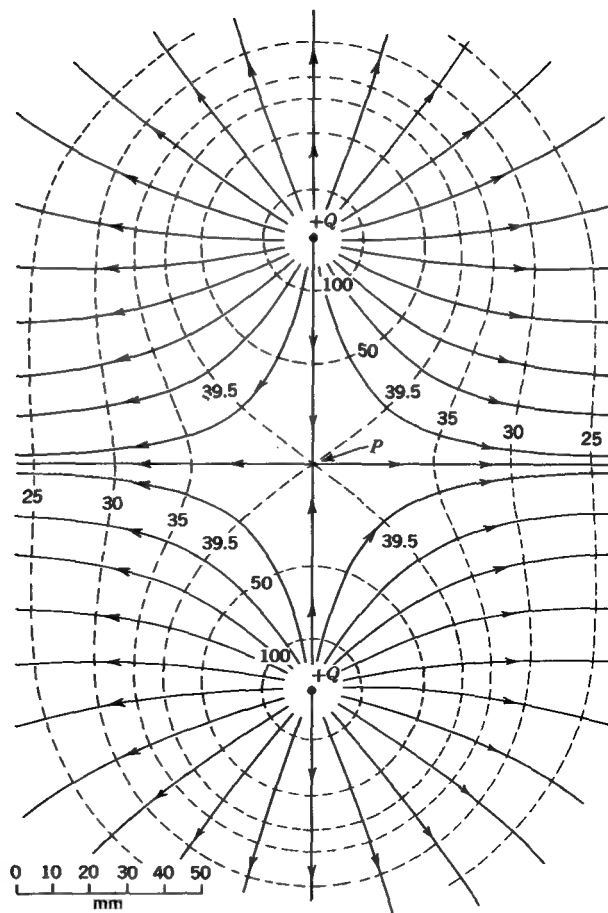


FIGURE 2-14

Electric field and potential variation around two equal positive charges of 140 pC separated by 127 mm. The solid lines are field lines, and the dashed lines are equipotential contours, with their potential level indicated in volts.

$$\rho = \lim_{\Delta v \rightarrow 0} \frac{\Delta Q}{\Delta v} \quad (2)$$

This gives the value of ρ at a point and hence defines ρ as a point function.

It will be convenient to use this definition of ρ , but it is to be noted that it is based on the assumption that the electric charge is continuously distributed. Actually electric charge is not continuously distributed but is associated with discrete particles

(electrons or atoms) separated by finite atomic distances. Nevertheless, the assumption of a continuous charge distribution (an idealization) leads to no appreciable error provided the region contains many atoms or electrons and the distances involved are large compared with atomic dimensions. The assumption of continuous charge distribution can be applied to the large-scale, or macroscopic, problems treated in this book but would not be applicable to problems on atomic structure, where the non-continuous nature of the charge distribution must be taken into account.

The charge density ρ , discussed above, is sometimes called a *volume charge density* to distinguish it from surface charge density and linear charge density. The *surface charge density* ρ_s gives the charge per unit area (coulombs per square meter, $C\ m^{-2}$) at a point on a continuous surface distribution of charge. The *linear charge density* ρ_L gives the charge per unit length (coulombs per meter, $C\ m^{-1}$) at a point on a continuous line distribution of charge. Both ρ_s and ρ_L are point functions which can be defined as in (2), with a surface or line element substituted for the volume element.

2-12 ELECTRIC POTENTIAL OF CHARGE DISTRIBUTIONS AND THE PRINCIPLE OF SUPERPOSITION OF POTENTIAL

Since the electric scalar potential due to a single point charge is a linear function of the value of its charge, it follows that the potentials of more than one point charge are linearly superposable by scalar (algebraic) addition. As a generalization, this fact may be stated as the *Principle of Superposition* applied to electric potential† as follows:

The total electric potential at a point is the algebraic sum of the individual component potentials at the point.

Thus, if only the three point charges Q_1 , Q_2 , and Q_3 are present in Fig. 2-15, the total electric potential (work per unit charge) at the point P is given by

$$V_p = \frac{1}{4\pi\epsilon} \left(\frac{Q_1}{r_1} + \frac{Q_2}{r_2} + \frac{Q_3}{r_3} \right) \quad (1)$$

where r_1 = distance from Q_1 to P

r_2 = distance from Q_2 to P

r_3 = distance from Q_3 to P

This can also be expressed with a summation sign. Thus,

$$V_p = \frac{1}{4\pi\epsilon} \sum_{n=1}^3 \frac{Q_n}{r_n} \quad (2)$$

† Although electric *scalar* potential is implied, the word *scalar* will usually be omitted for brevity.

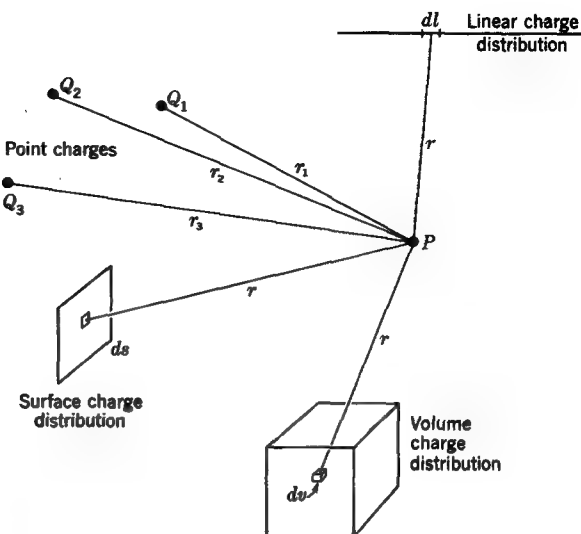


FIGURE 2-15

Electric potential at P is the algebraic sum of the potentials due to the point, line, surface, and volume distributions of charge.

If the charge is not concentrated at a point but is distributed along a line as in Fig. 2-15, the potential at P due to this linear charge distribution is

$$V_L = \frac{1}{4\pi\epsilon} \int \frac{\rho_L}{r} dl \quad (V) \quad (3)$$

where ρ_L = linear charge density, $C m^{-1}$

dl = element of length of line, m

The integration is carried out over the entire line of charge.

When the charge is distributed over a surface, as in Fig. 2-15, the potential at P caused by this surface charge distribution is

$$V_s = \frac{1}{4\pi\epsilon} \iint \frac{\rho_s}{r} ds \quad (V) \quad (4)$$

where ρ_s = surface charge density, $C m^{-2}$

ds = element of surface, m^2

The integration is carried out over the entire surface of charge.

For a volume charge distribution, as in Fig. 2-15,

$$V_v = \frac{1}{4\pi\epsilon} \iiint \frac{\rho}{r} dv \quad (\text{V}) \quad (5)$$

where ρ = (volume) charge density, $C m^{-3}$

dv = element of volume, m^3

The integration is taken throughout the volume containing charge.

If the point charges, the line charge distribution, the surface charge distribution, and the volume charge distribution of Fig. 2-15 are all present simultaneously, the total electric potential at the point P due to all of these distributions is by the superposition principle the algebraic sum of the individual component potentials. Thus,

$$V = V_p + V_L + V_s + V_v \quad (6)$$

or

$$V = \frac{1}{4\pi\epsilon} \left(\sum_1^N \frac{Q_n}{r_n} + \int \frac{\rho_L}{r} dl + \iint \frac{\rho_s}{r} ds + \iiint \frac{\rho}{r} dv \right) \quad (7)$$

We may also write (7) as

$$V = \sum_1^N Q_n G_n + \int \rho_L G dl + \iint \rho_s G ds + \iiint \rho G dv \quad (8)$$

where $G = 1/4\pi\epsilon r$.

G is the electrostatic Green's function and is equal to the potential for a 1-C point charge.

EXAMPLE As shown in Fig. 2-16 a square that is 1 m on a side in air has a point charge $Q_1 = +1 \text{ pC}$ at the upper right corner, a point charge $Q_2 = -10 \text{ pC}$ at the lower right corner, and a line distribution of charge of uniform density $\rho_L = +10 \text{ pC m}^{-1}$ along the left edge. Find the potential at the point P at the center of the square.

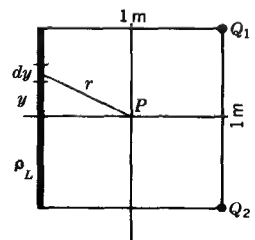


FIGURE 2-16
Line and point charges for example illustrating superposition of electric potential.

SOLUTION The potential at P due to the point charges is

$$V_p = \frac{1}{4\pi\epsilon_0} \left(\frac{10^{-12}}{0.707} - \frac{10^{-11}}{0.707} \right) = -0.115 \text{ V}$$

The potential at P caused by the line distribution of charge is

$$V_L = \frac{1}{4\pi\epsilon_0} \int_{y=-0.5}^{y=0.5} \frac{10^{-11}}{\sqrt{0.5^2 + y^2}} dy = +0.158 \text{ V}$$

The total potential at P is then

$$V = V_p + V_L = +43 \text{ mV}$$

The principle of superposition stated for the special cases of potential in this section and for fields in Sec. 2-6 can be applied, in general, to any quantity which is linearly related to its cause. The electric fields or potentials at a point are linear functions of the charge producing them and hence are superposable (by vector addition for fields and scalar addition for potential).

2-13 THE ELECTRIC FIELD AS THE GRADIENT OF THE ELECTRIC POTENTIAL

The potential rise between two points along an electric field line is a measure of the *gradient* of the potential in the same way that the elevation rise between two points on a slope is a measure of the gradient of the slope. More specifically the gradient of the potential at a point is defined as the potential rise ΔV across an element of length Δl *along a field line* divided by Δl , with the limit of this ratio taken as Δl approaches zero. Thus,

$$\text{Gradient of } V = \lim_{\Delta l \rightarrow 0} \frac{\Delta V}{\Delta l} = \frac{dV}{dl} \quad (1)$$

More completely, the gradient of V is a vector whose direction is along a field line with magnitude as given in (1). Since a potential *rise* occurs when moving *against* the electric field (see Sec. 2-8), the direction of the gradient is opposite to that of the field. Thus,

$$\text{Gradient of } V = -\mathbf{E}$$

In more symbolic notation we can write

$\text{Gradient of } V = \text{grad } V = \nabla V = -\mathbf{E}$

(2)

where $\text{grad } V$ stands for the gradient of V . As will be discussed in the next section, the gradient of V can also be expressed with the operator del, or nabla, ∇ , as ∇V .

2-14 GRADIENT IN RECTANGULAR COORDINATES

In this section a relation for gradient will be developed in rectangular coordinates. To do this, consider the electric potential distribution of Fig. 2-17. The work per coulomb to bring a positive test charge to the point P (at origin of coordinates) is 104 V. This is the absolute potential V at P . The potential elsewhere is a function of both x and y , and its variation is indicated by the equipotential contours. The field is uniform. Thus, the contours are straight, parallel, and equally spaced. There is no variation with respect to z (normal to page). At P the electric field is as indicated by the vector \mathbf{E} , perpendicular to the equipotential line.

Consider now the change in potential along an infinitesimal element of path length in the x direction ($y = \text{constant}$). Then

$$-\frac{\partial V}{\partial x} = E \cos \alpha = E_x$$

where α = angle between \mathbf{E} and x axis

E_x = component of \mathbf{E} in x direction

Likewise, for an infinitesimal element of path length in the y direction,

$$-\frac{\partial V}{\partial y} = E \cos \beta = E_y$$

where β = angle between \mathbf{E} and y axis

E_y = component of \mathbf{E} in y direction

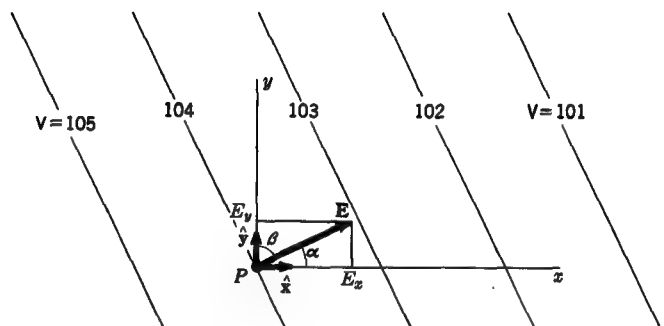


FIGURE 2-17
Potential distribution with electric field \mathbf{E} at a point P .

By the principle of superposition the total field \mathbf{E} at the point P is the vector sum of the component fields at the point. Hence,

$$\mathbf{E} = \hat{\mathbf{x}} E_x + \hat{\mathbf{y}} E_y = -\left(\hat{\mathbf{x}} \frac{\partial V}{\partial x} + \hat{\mathbf{y}} \frac{\partial V}{\partial y}\right) = -\operatorname{grad} V = -\nabla V$$

Thus, the gradient in this rectangular two-dimensional case is equal to the x and y derivatives of the potential added vectorially.

EXAMPLE Suppose that in Fig. 2-17 the potential decreases by 2 V m^{-1} in the x direction and by 1 V m^{-1} in the y direction. Find the electric field \mathbf{E} .

SOLUTION

$$\operatorname{grad} V = -\hat{\mathbf{x}} 2 - \hat{\mathbf{y}} 1$$

and

$$\mathbf{E} = -\operatorname{grad} V = \hat{\mathbf{x}} 2 + \hat{\mathbf{y}} 1 = 2.24/26.6^\circ \text{ V m}^{-1}$$

Therefore, \mathbf{E} has a magnitude of 2.24 V m^{-1} and is directed at an angle of 26.6° with respect to the positive x axis ($\alpha = 26.6^\circ$).

The two-dimensional case discussed above can readily be extended to three dimensions. Thus, as shown in Fig. 2-18, there are field components at the origin in the three coordinate directions as follows:

$$\hat{\mathbf{x}} E_x = \hat{\mathbf{x}} E \cos \alpha = -\hat{\mathbf{x}} \frac{\partial V}{\partial x}$$

$$\hat{\mathbf{y}} E_y = \hat{\mathbf{y}} E \cos \beta = -\hat{\mathbf{y}} \frac{\partial V}{\partial y}$$

$$\hat{\mathbf{z}} E_z = \hat{\mathbf{z}} E \cos \gamma = -\hat{\mathbf{z}} \frac{\partial V}{\partial z}$$

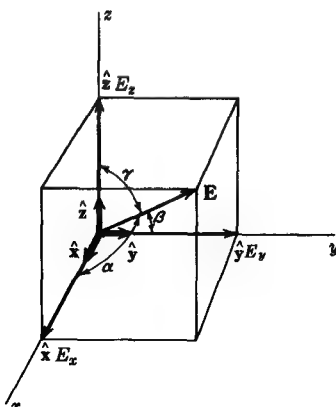


FIGURE 2-18
Components of electric field in rectangular coordinates.

By the principle of superposition the total field \mathbf{E} at the origin is the vector sum of the component fields, or

$$\mathbf{E} = - \left(\hat{x} \frac{\partial V}{\partial x} + \hat{y} \frac{\partial V}{\partial y} + \hat{z} \frac{\partial V}{\partial z} \right) \quad (1)$$

where the relation in the parentheses is the complete expression in rectangular coordinates for the gradient of V . It is often convenient to consider that this expression is the product of V and the operator del (∇). Thus, in rectangular coordinates

$$\nabla = \hat{x} \frac{\partial}{\partial x} + \hat{y} \frac{\partial}{\partial y} + \hat{z} \frac{\partial}{\partial z} \quad (2)$$

The quantity ∇ is a vector operator. It is meaningless until applied. Taking the product of ∇ and V yields the gradient of V . That is,

$$\nabla V = \hat{x} \frac{\partial V}{\partial x} + \hat{y} \frac{\partial V}{\partial y} + \hat{z} \frac{\partial V}{\partial z} = \text{grad } V = -\mathbf{E} \quad (3)$$

Expressions for the gradient in other coordinate systems are given inside the back cover.

2-15 THE ELECTRIC DIPOLE AND ELECTRIC-DIPOLE MOMENT

The combination of two equal point charges of opposite sign separated by a small distance is called an *electric dipole*, and the product Ql is called the *electric-dipole moment*. If the two charges were superposed, the resultant field would be zero. However, when the two charges are separated by even a small distance l , there is a finite resultant field (see Fig. 2-13).

By regarding the separation between the charges as a vector \mathbf{l} , pointing from the negative to the positive charge as in Fig. 2-19, the dipole moment can be expressed as a vector $Q\mathbf{l}$ with the magnitude Ql and the direction of \mathbf{l} .

Referring to Fig. 2-19, the potential of the positive charge at a point P is

$$V_1 = \frac{Q}{4\pi\epsilon r_1}$$

The potential of the negative charge at P is

$$V_2 = \frac{-Q}{4\pi\epsilon r_2}$$

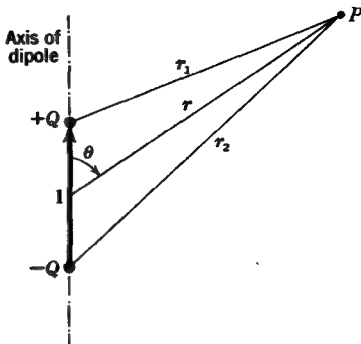


FIGURE 2-19
Electric dipole.

The total potential V at P is then

$$V = V_1 + V_2 = \frac{Q}{4\pi\epsilon} \left(\frac{1}{r_1} - \frac{1}{r_2} \right)$$

If the point P is at a large distance compared with the separation l , so that the radial lines r_1 , r , and r_2 are essentially parallel, we have very nearly that

$$r_1 = r - \frac{l}{2} \cos \theta \quad \text{and} \quad r_2 = r + \frac{l}{2} \cos \theta$$

where r = distance from center of dipole to point P

θ = angle between axis of dipole and r

Hence, the potential V at a distance r from an electric dipole is

$$V = \frac{Ql \cos \theta}{4\pi\epsilon r^2} \quad (\text{V})$$

(1)

where it is assumed that r is much greater than l ($r \gg l$) so that terms in l^2 can be neglected compared with those in r^2 .

It is instructive to consider (1) as the product of four factors involving the dipole moment, the angle, the distance, and a constant characteristic of the system of units employed. Thus,

$$V = Q I \cos \theta \frac{1}{r^2} \frac{1}{4\pi\epsilon} \quad (2)$$

Dipole	Angle	Distance	Constant
moment	factor	factor	

Expressions for the potential and also the electric field of dipoles (and quadrupoles and higher-order configurations) always contain these four kinds of factors.

To find the electric field of the dipole of Fig. 2-19 it is convenient to make use of the gradient discussed in the preceding section. Thus, let us take the gradient of the potential given by (1), obtaining†

$$\mathbf{E} = -\hat{\mathbf{r}} \frac{\partial V}{\partial r} - \hat{\theta} \frac{1}{r} \frac{\partial V}{\partial \theta} = \hat{\mathbf{r}} \frac{Ql \cos \theta}{2\pi\epsilon r^3} + \hat{\theta} \frac{Ql \sin \theta}{4\pi\epsilon r^3} \quad (3)$$

where $\hat{\mathbf{r}}$ = unit vector in r direction (see Fig. 2-20)

$\hat{\theta}$ = unit vector in θ direction

l = separation of dipole charges Q

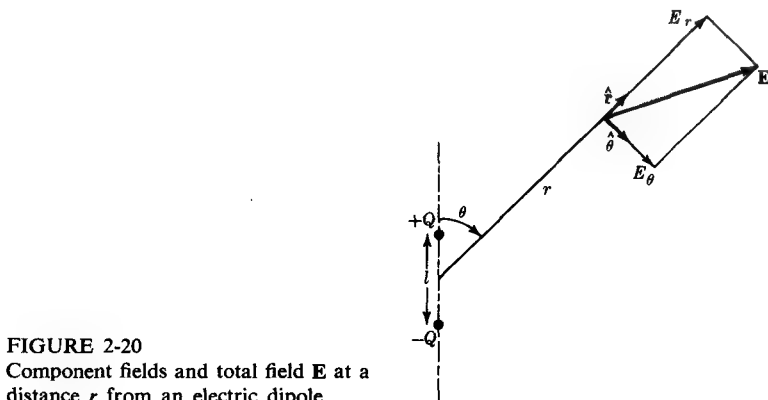


FIGURE 2-20
Component fields and total field \mathbf{E} at a distance r from an electric dipole.

According to (3), the electric field has two components, as shown in Fig. 2-20, one in the r direction (E_r) and one in the θ direction (E_θ). Thus

$$\mathbf{E} = \hat{\mathbf{r}} E_r + \hat{\theta} E_\theta \quad (4)$$

or $E_r = \frac{Ql \cos \theta}{2\pi\epsilon r^3}$ and $E_\theta = \frac{Ql \sin \theta}{4\pi\epsilon r^3}$ (V m⁻¹) (5)

In these equations the restriction applies that $r \gg l$.

By a similar procedure to that followed above it is possible to obtain the potential and field relations for more complex charge configurations, e.g., the quadrupole or octopole shown in Fig. 2-21 (see Probs. 2-15 and 2-16). The potential and field variations with distance for these configurations are listed in Table 2-1, along with the distance factors for a dipole and a single charge. We note that the higher the order

† See inside back cover for gradient in spherical coordinates.

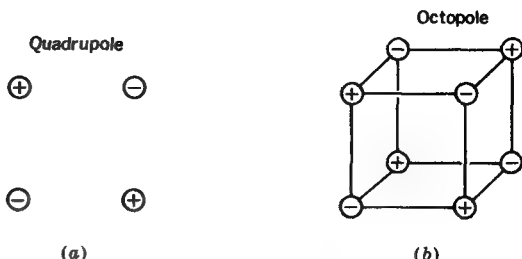


FIGURE 2-21

Charge configuration (a) for a quadrupole and (b) for an octopole.

of the charge configuration the more rapidly the potential or field falls off with distance. We also note that for any given configuration the field falls off more rapidly than the potential.

Table 2-1 DISTANCE FACTOR OF ELECTRIC POTENTIAL AND ELECTRIC FIELD FOR DIFFERENT CHARGE CONFIGURATIONS

Configuration	Electric potential V	Electric field E
Single charge	r^{-1}	r^{-2}
Dipole	r^{-2}	r^{-3}
Quadrupole	r^{-3}	r^{-4}
Octopole	r^{-4}	r^{-5}

2-16 ELECTRIC FLUX

Referring to Fig. 2-22, imagine that the two point charges $+Q$ and $-Q$ are connected by tubes of electric flux or chargelike flow between them. The electric flux ψ through any tube is a constant given by

$$\psi = DA \quad (\text{C})$$

where D = average flux density, C m^{-2}

A = cross-sectional area of tube, m^{-2}

More generally we have

$$\psi = \iint \mathbf{D} \cdot d\mathbf{s} = \iint D_n ds \quad (\text{C}) \quad (1)$$

(60°)
(60°)
(60°)

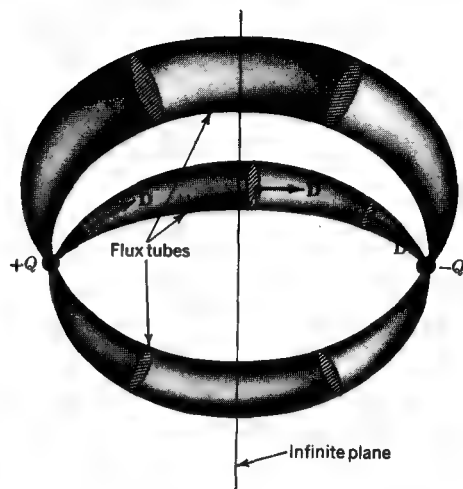


FIGURE 2-22

Electric field between two point charges of opposite sign with flux tubes joining them. The tubes follow the electric field lines. Each tube has a constant amount of flux.

This relation states that the electric flux through any surface equals the integral of the flux density over the surface. In Fig. 2-22 ψ is constant along any tube. If all space is filled with flux tubes connecting $+Q$ and $-Q$, the total flux through all the tubes passing through the infinite plane separating the charges is equal to Q . Likewise integrating \mathbf{D} over the infinite plane yields Q , or

$$\psi = \iint_{\text{infinite plane}} \mathbf{D} \cdot d\mathbf{s} = Q \quad (\text{C}) \quad (2)$$

Consider next the electric field around a single isolated positive point charge Q as in Fig. 2-23†. This is given by

$$\mathbf{E} = k \frac{Q}{4\pi r^2} \quad \text{or} \quad \epsilon \mathbf{E} = k \frac{Q}{4\pi r^2}$$

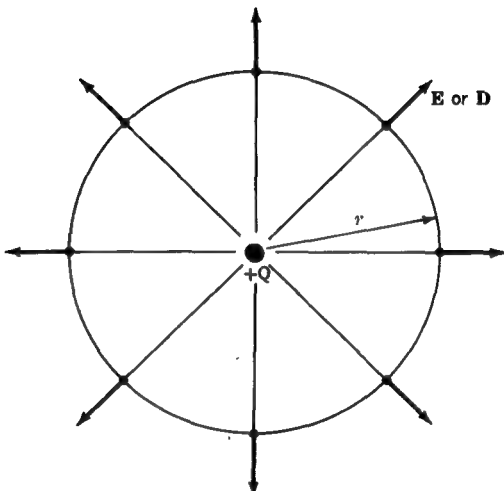
The second equation has the dimensions of charge per unit area, or electric flux density. It follows that

$$\mathbf{D} = k \frac{Q}{4\pi r^2} \quad (3)$$

or

$$\boxed{\mathbf{D} = \epsilon \mathbf{E}} \quad (4)$$

† We imagine that the field lines end on an equal negative charge distributed over the inside of a sphere at infinity.

**FIGURE 2-23**

Electric field of an isolated positive point charge Q . The flux density D at a radius r is the same as the surface charge density on the sphere if Q were uniformly distributed over the sphere.

where \mathbf{D} = electric flux density, $C\ m^{-2}$

ϵ = permittivity of medium, $F\ m^{-1}$

\mathbf{E} = electric field intensity, $V\ m^{-1}$

According to (4), the flux density and field intensity are vectors with the same direction. This is true for all isotropic media, i.e., media whose properties do not depend on direction.

Since $4\pi r^2$ equals the area of a sphere of radius r , it follows that the magnitude of \mathbf{D} at the radius r is identical with the surface charge density which would occur if the charge Q were distributed uniformly over a sphere of radius r instead of concentrated at the center (see Fig. 2-23).

2-17 ELECTRIC FLUX OVER A CLOSED SURFACE; GAUSS' LAW

Referring to Fig. 2-24, let a positive point charge Q be situated at the center of an imaginary sphere of radius r . The infinitesimal amount of electric flux through the surface element $d\mathbf{s}$ is given by

$$d\psi = \mathbf{D} \cdot d\mathbf{s}$$

Integrating this over the sphere of radius r then gives the total flux through the sphere

$$\psi = \iint \mathbf{D} \cdot d\mathbf{s} \quad (1)$$

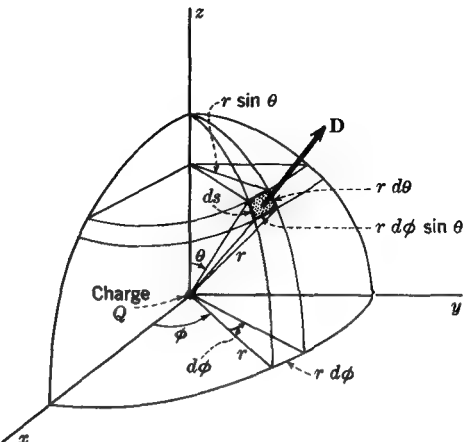


FIGURE 2-24
Point charge Q at origin of spherical coordinate system.

We note that \mathbf{D} is everywhere normal to the sphere, so that

$$\mathbf{D} \cdot d\mathbf{s} = D ds$$

where $D = |\mathbf{D}|$ = scalar magnitude of the vector \mathbf{D}

$ds = |d\mathbf{s}|$ = scalar magnitude of the vector $d\mathbf{s}$

From (1) and (2-16-3)

$$\psi = \iint \frac{Q}{4\pi r^2} ds \quad (2)$$

From Fig. 2-24 $ds = (r d\theta)(r d\phi \sin \theta) = r^2 \sin \theta d\theta d\phi$, and the solid angle $d\Omega$ subtended by the spherical element of surface area ds is $ds/r^2 = d\Omega = \sin \theta d\theta d\phi$; therefore

$$\begin{aligned} \psi &= \frac{Q}{4\pi} \iint d\Omega = \frac{Q}{4\pi} \int_0^{2\pi} \int_0^\pi \sin \theta d\theta d\phi \\ &= \frac{Q}{4\pi} [-\cos \theta]_0^\pi \int_0^{2\pi} d\phi = \frac{Q}{4\pi} \times 2 \times 2\pi = Q \end{aligned} \quad (3)$$

Thus, the total electric flux over the sphere (obtained by integrating the normal component of the flux density \mathbf{D} over the sphere) is equal to the charge Q enclosed by the sphere. We could have obtained the result in this case more simply by multiplying $D = Q/4\pi r^2$ by the area of the sphere ($4\pi r^2$). However, the above development serves to illustrate a more general procedure which can also be applied to cases where \mathbf{D} is not constant as a function of angle.

The result in the above example is a statement of Gauss' law for a special case. A general statement of Gauss' law† for electric fields is:

The surface integral of the normal component of the electric flux density \mathbf{D} over any closed surface equals the charge enclosed.

Thus, in symbols

$$\iint D \cos \theta \, ds = \iint \mathbf{D} \cdot d\mathbf{s} = Q \quad (\text{C}) \quad (4)$$

where Q is the total or net charge enclosed. This charge may also be expressed as the volume integral of the charge density ρ , so that

$$\iint \mathbf{D} \cdot d\mathbf{s} = \iiint \rho \, dv = Q \quad (5)$$

where the surface integration is carried out over a closed surface and the volume integration throughout the region enclosed. An alternative notation is

$$\oint_s \mathbf{D} \cdot d\mathbf{s} = \oint_v \rho \, dv = Q \quad (6)$$

where \oint_s = double, or surface, integral over closed surface

\oint_v = triple, or volume, integral throughout region enclosed

Gauss' law is the basic theorem of electrostatics. It is a necessary consequence of the inverse-square law (Coulomb's law). Thus, if \mathbf{D} for a point charge did not vary as $1/r^2$, the total flux over a surface enclosing it would not equal the charge.

To illustrate Gauss' law, several situations will be analyzed with its aid in the following sections.

2-18 SINGLE SHELL OF CHARGE

Referring to Fig. 2-25a, suppose that a positive charge Q is uniformly distributed over an imaginary spherical shell of radius r_1 . The medium is air. Applying Gauss' law by integrating \mathbf{D} over a spherical surface (radius $r_1 - dr$) just inside the shell of charge, we have

$$\epsilon \oint_s \mathbf{E} \cdot d\mathbf{s} = 0 \quad (1)$$

since the charge enclosed is zero. It follows from symmetry that \mathbf{E} inside the shell

† Propounded by Karl Friedrich Gauss in 1813.

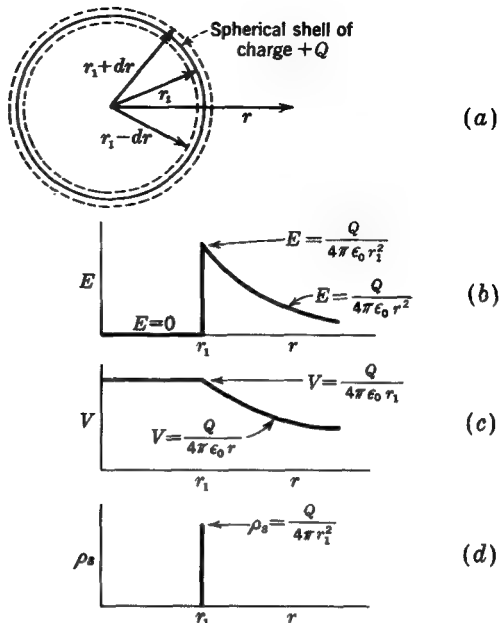


FIGURE 2-25

Uniformly charged spherical shell with graphs showing variation of electric field intensity E , electric potential V , and surface charge density ρ_s as a function of radial distance r .

is zero. Applying Gauss' law to a spherical shell (radius $r_1 + dr$) just outside the shell of charge, we have, neglecting infinitesimals,

$$\epsilon_0 \oint_s \mathbf{E} \cdot d\mathbf{s} = \epsilon_0 E 4\pi r_1^2 = Q \quad (2)$$

or

$$E = \frac{Q}{4\pi\epsilon_0 r_1^2} \quad (3)$$

This value of field intensity is identical with that at a radius r_1 from a point charge Q . We can therefore conclude that the field outside the shell of charge is the same as if the charge Q were concentrated at the center. Summarizing, the field everywhere due to a spherical shell of charge is

$$\mathbf{E} = 0 \text{ inside} \quad r \leq r_1 \quad (4)$$

$$\mathbf{E} = \frac{Q}{4\pi\epsilon_0 r^2} \text{ outside} \quad r \geq r_1 \quad (5)$$

The variation of \mathbf{E} as a function of r is illustrated by Fig. 2-25b.[†]

[†] Note that a point charge at the origin gives an infinite \mathbf{E} as $r \rightarrow 0$ but a surface charge of finite area at a radius r_1 gives a finite \mathbf{E} as $r \rightarrow r_1$. This is because the volume charge density ρ of a point charge is infinite, whereas the surface charge density ρ_s of the shell of charge is finite. In the present case $\rho_s = Q/4\pi r_1^2$.

The absolute potential at a radius r outside the shell is given by

$$V = - \int_{\infty}^r \mathbf{E} \cdot d\mathbf{r} \quad (6)$$

Introducing the value of \mathbf{E} from (5),

$$V = - \frac{Q}{4\pi\epsilon_0} \int_{\infty}^r \frac{dr}{r^2} = \frac{Q}{4\pi\epsilon_0 r} \quad (\text{Vm}^{-1}) \quad (7)$$

At the shell, where $r = r_1$, we have

$$V = \frac{Q}{4\pi\epsilon_0 r_1} \quad (8)$$

Since \mathbf{E} inside the shell is zero, it requires no work to move a test charge inside and therefore the potential is constant, being equal to the value at the shell. Summarizing, the electric potential everywhere due to a spherical shell of charge of radius r_1 is

$$V = \frac{Q}{4\pi\epsilon_0 r_1} \text{ inside} \quad r \leq r_1 \quad (9)$$

$$V = \frac{Q}{4\pi\epsilon_0 r} \text{ outside} \quad r \geq r_1 \quad (10)$$

The variation of V as a function of r is illustrated by Fig. 2-25c. The variation of the surface charge density ρ_s is shown by Fig. 2-25d. The surface density is zero everywhere except at $r = r_1$, where it has the value $Q/4\pi r_1^2$, as indicated by the vertical line, or spike.

It is to be noted that the potential is continuous, both (9) and (10) being equal at the shell ($r = r_1$). However, the electric field is discontinuous, jumping abruptly from zero just inside the shell to a value $Q/4\pi\epsilon_0 r_1^2$ just outside the shell. This results from the assumption that the shell of charge has zero thickness.

2-19 CONDUCTORS AND INDUCED CHARGES

A conductor can conduct, or convey, electric charge. In static situations a conductor may be defined as a medium in which the electric field is always zero. It follows that all parts of a conductor must be at the same potential. Metals such as copper, brass, aluminum, and silver are examples of conductors.

When a metallic conductor is brought into an electric field, different parts of the conductor would assume different potentials were it not for the fact that electrons flow in the conductor until a surface charge distribution is built up that reduces the total field in the conductor to zero.[†] This surface charge distribution is said to consist

[†] The electrons in the outermost shell of the atoms of a conductor are so loosely held that they migrate readily from atom to atom under the influence of an electric field.

of *induced charges*. The field in which the conductor is placed may be called the *applied field* \mathbf{E}_a , while the field produced by the surface charge distribution may be called the *induced field* \mathbf{E}_i . The sum of the applied and induced fields yields a total field in the conductor equal to zero. Although the total field inside the conductor is zero after the static situation has been reached, the total field is not zero while the induced charges are in motion, i.e., while currents are flowing.

To summarize, under static conditions the electric field in a conductor is zero, and its potential is a constant. Charge may reside on the surface of the conductor, and, in general, the surface charge density need not be constant.

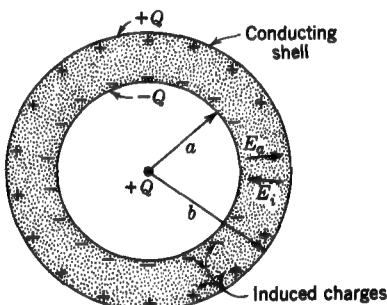


FIGURE 2-26
Conducting shell of wall thickness $b - a$
with point charge Q at center.

2-20 CONDUCTING SHELL

An initially uncharged conducting shell of inner radius a and outer radius b (wall thickness $b - a$) is shown in cross section in Fig. 2-26. Let a point charge $+Q$ be placed at the center of the shell. This might be done by introducing the charge through a hole in the shell which is plugged after the charge is inside.[†] The point charge has a radial electric field. Let this be called the applied field \mathbf{E}_a . For the total field \mathbf{E} in the conducting wall to be zero requires an induced field \mathbf{E}_i inside the wall such that

$$\mathbf{E}_a + \mathbf{E}_i = \mathbf{E} = 0 \quad (1)$$

or

$$\mathbf{E}_i = -\mathbf{E}_a \quad (2)$$

The induced field \mathbf{E}_i is produced by a distribution of induced negative charges on the inner shell wall and induced positive charges on the outer shell wall, as suggested in Fig. 2-26. Let us apply Gauss' law to this situation to determine quantitatively the magnitude of these induced charges.

[†] This is an idealized version of an experiment first performed by Faraday, using an ice pail.

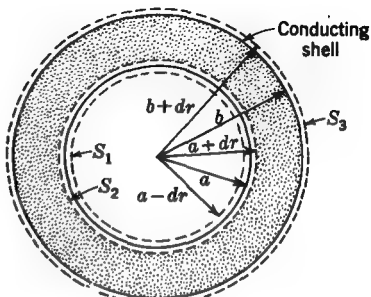


FIGURE 2-27
Conducting shell of wall thickness $b - a$
with surfaces of integration.

Suppose that an imaginary sphere designated S_1 with a radius $a - dr$ is situated just inside the inner wall of the shell as in Fig. 2-27. By Gauss' law the surface integral of the normal component of \mathbf{D} over this sphere must equal $+Q$. That is,

$$\oint_{S_1} \mathbf{D} \cdot d\mathbf{s} = +Q \quad (3)$$

Applying Gauss' law to the sphere S_2 of radius $a + dr$ just inside the conductor, we have, since the total field \mathbf{E} in the conductor is zero,

$$\oint_{S_2} \mathbf{D} \cdot d\mathbf{s} = \epsilon \oint_{S_2} \mathbf{E} \cdot d\mathbf{s} = 0 \quad (4)$$

Thus, the total charge inside the sphere S_2 must be zero. It follows that a charge $-Q$ is situated on the inner surface of the shell wall. Since the shell was originally uncharged, this negative charge $-Q$, produced by a migration of electrons to the inner surface, must leave a deficiency of electrons, or positive charge Q , on the outer surface of the shell. It is assumed that the surface charges reside in an infinitesimally thin layer.

Applying Gauss' law to the sphere S_3 of radius $b + dr$ just outside the outer surface of the shell, we then have

$$\oint_{S_3} \mathbf{D} \cdot d\mathbf{s} = +Q \quad (5)$$

To summarize, the charge $+Q$ at the center of the shell induces an exactly equal but negative charge $-Q$ on the inner surface of the shell, and this in turn results in an equal positive charge ($+Q$) distributed over the outer surface of the shell. The flux tubes originating on $+Q$ at the center end on the equal negative charge on the inside of the shell. There is no total field and no flux in the shell wall. Outside the shell the flux tubes continue from the charge $+Q$ on the outer surface as though no shell were present. The variation of the component fields E_a (applied) and E_r

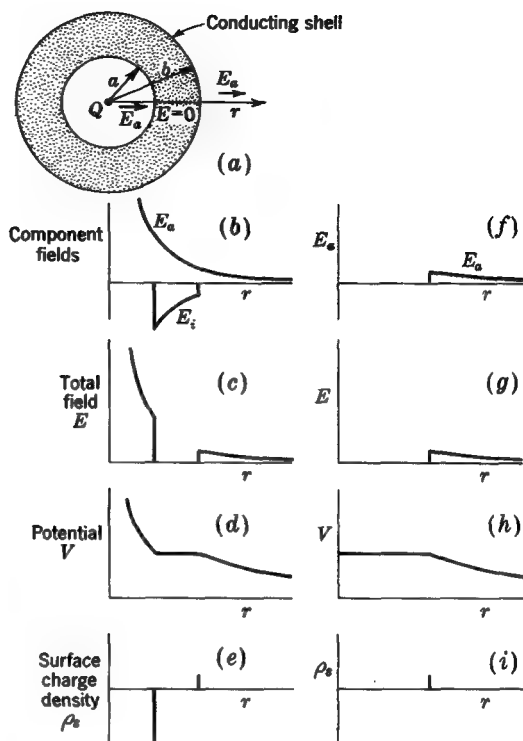


FIGURE 2-28

Conducting shell of wall thickness b — a with graphs showing variation of applied field E_a , induced field E_i , total field E , potential V , surface charge density ρ_s with charge Q at center (b, c, d , and e) and with charge only on outside of shell (f, g, h , and i).

(induced) as a function of r is illustrated by Fig. 2-28b. The variation of the total field \mathbf{E} is shown in Fig. 2-28c.

If a conducting wire is connected from the inner surface of the shell to the charge $+Q$ at the center, electrons will flow and reduce the charge at the center and on the inner surface to zero. However, the charge $+Q$ remains on the outer surface of the shell. This results in an applied field only external to the shell ($r \geq b$) and of the same value as before. There is no induced field whatsoever. Thus, the total field is identical with the applied field and is zero for $r \leq b$ as shown by Fig. 2-28f and g. This final result might have been achieved more simply in the first place by applying the charge $+Q$ to the outside of the originally uncharged conducting sphere.

The variation of V and ρ_s as a function of r when the charge $+Q$ is at the center of the sphere is indicated in Fig. 2-28d and e, while the variation when the charge is only on the outside of the shell is shown by Fig. 2-28h and i.

2-21 CAPACITORS AND CAPACITANCE

A *capacitor*[†] is an electrical device consisting of two conductors separated by an insulating or dielectric medium.

By definition the *capacitance* of a capacitor is the ratio of the charge on one of its conductors to the potential difference between them. Thus, the capacitance C of a capacitor is

$$\frac{Q}{V} = C \quad (1)$$

where Q = charge on one conductor

V = potential difference of conductors

Dimensionally (1) is

$$\frac{\text{Charge}}{\text{Potential}} = \frac{\text{charge}}{\text{energy/charge}} = \frac{\text{charge}^2}{\text{energy}} = \text{capacitance}$$

or in dimensional symbols

$$\frac{Q^2}{ML^2/T^2} = \frac{I^2 T^4}{ML^2}$$

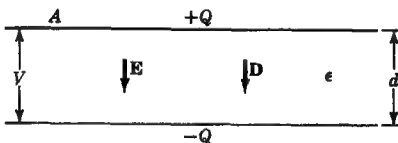
The SI unit of capacitance is the *farad* (F). Thus, 1 C V^{-1} equals 1 F, or

$$\frac{\text{Coulombs}}{\text{Volt}} = \text{Farads}$$

In other words, a capacitor that can store 1 C charge with a potential difference of 1 V has a capacitance of 1 F. Since a capacitor of 1 F capacitance is much larger than is ordinarily used in practice, microfarads (μF) and picofarads (pF) are commonly used.

FIGURE 2-29

Parallel-plate capacitor with voltage difference V and plate charge Q . The area of each plate is A , and the plate separation is d .



EXAMPLE A *parallel-plate capacitor* consists of two flat metal sheets of area A separated by distance d , as shown in cross section in Fig. 2-29. If the medium has a permittivity ϵ , find the capacitance.

[†] Formerly called a *condenser*.

SOLUTION If a voltage V is applied between the plates, we have

$$V = Ed \quad (\text{V})$$

where E is the electric field between the plates. The charge on one plate is given by

$$Q = DA \quad (\text{C})$$

where D is the flux density between the plates. But $D = \epsilon E$; so $Q = \epsilon EA$, and the capacitance is

$$C = \frac{Q}{V} = \frac{\epsilon EA}{Ed} = \frac{\epsilon A}{d} \quad (\text{F})$$

Thus the capacitance is proportional to the permittivity ϵ , and the plate area A and is inversely proportional to the plate-separation distance d . It was assumed that the field was uniform between the plates and zero outside (no fringing). Actually any fringing effects will be small if the plates are large compared to d .

2-22 BOUNDARY RELATIONS AT A CONDUCTING SURFACE

Referring to Fig. 2-30, let a thin imaginary volume element be constructed at the surface of a conductor. The medium outside the conductor may, for example, be air. The volume element is half in the conductor and half in air. The volume element has an area A parallel to the conductor surface but has an infinitesimal thickness dl normal to the surface. According to Gauss' law, the normal component of the flux

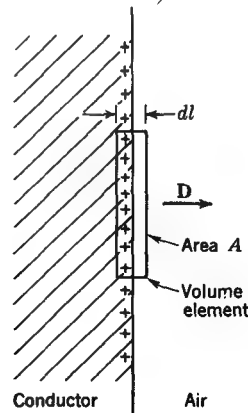


FIGURE 2-30
Conductor-air boundary with cross section through small volume element half in the conductor and half in air.

density \mathbf{D} over the volume element must equal the total charge Q enclosed. Thus, if ρ_s is the surface charge density, we have

$$\oint_s \mathbf{D} \cdot d\mathbf{s} = Q = \rho_s A \quad (1)$$

Now \mathbf{D} in the conductor is zero, and so the integral reduces to the normal component D_n of the flux density in air multiplied by the area A . Hence

$$D_n A = \rho_s A$$

or

$$D_n = \rho_s \quad (2)$$

This important boundary relation states that the normal component of the flux density \mathbf{D} at a conducting surface equals the surface charge density. Both D_n and ρ_s have the dimensions of charge per area and are expressed in coulombs per square meter ($C m^{-2}$).

If a thin conducting sheet is introduced normal to an electric field, surface charges are induced on the sheet so that the original field external to the sheet is undisturbed. The value of the induced surface charge density ρ_s is, by (2), equal to the flux density D at the sheet. Hence, one can interpret the flux density D at a point as equal to the charge density ρ_s which would appear on a thin conducting sheet introduced normal to \mathbf{D} at the point. Referring, for example, to the thin conducting sheet normal to the field in Fig. 2-31, the relation of \mathbf{D} and ρ_s is as follows:

On left side: $\mathbf{D} = -\hat{n}\rho_s$

On right side: $\mathbf{D} = +\hat{n}\rho_s$

where \hat{n} is the unit vector normal to the surface. Thus \mathbf{D} is normally inward on the left side and normally outward on the right. The magnitude of the flux density on each side is equal to the charge density ρ_s .

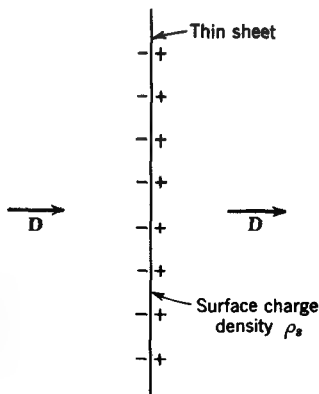


FIGURE 2-31

Thin conducting sheet placed normal to field has an induced surface charge density ρ_s equal to the flux density D of the field at the sheet. The surface charge densities on the two sides of the sheet are equal in magnitude but opposite in sign.

PROBLEMS

Note: $\epsilon = \epsilon_0$ everywhere.

- ★ 2-1 Find the force \mathbf{F} on a positive point charge of 100 pC at a distance 100 mm from a positive point charge of 10 nC.
- ★ 2-2 A positive point charge of 10 pC is located at $x = 0, y = 100$ mm and another such charge at $x = 0, y = -200$ mm. Find the magnitude and direction of the force \mathbf{F} on a positive point charge of 10 nC at $x = 300$ mm, $y = 0$.
- ★ 2-3 Find the electric field intensity \mathbf{E} and the absolute potential V at a distance 100 mm from a positive point charge of 10 nC.
- ★ 2-4 Two positive point charges of 1 C each are separated by $2a$. At the point halfway between find the electric field \mathbf{E} (magnitude and direction) and electric potential V .
- 2-5 A positive point charge of 1 C and a negative point charge of 1 C are separated by $2a$. At the point halfway between find the electric field \mathbf{E} (magnitude and direction) and the electric potential V .
- 2-6 A point charge of $-1.6 \mu\text{C}$ is at the origin, and positive point charges of $1 \mu\text{C}$ are 3 m in the $+y$ and $-y$ directions. At a point 4 m from the origin in the x direction find the electric field \mathbf{E} (magnitude and direction) and electric potential V .
- ★ 2-7 A charge of $+3$ nC is at the point $x = 0, y = 2$ m, and a charge of -1 nC is at the point $x = 0, y = -2$ m. Find the electric field \mathbf{E} (magnitude and direction) and the electric potential V at the point $x = 0, y = -1$ m.
- ★ 2-8 Find the unit normal to the plane $3x + 4y + 5z = 10$.
- 2-9 A potential distribution is given by $V = 6x + 3$ V. What is the expression for \mathbf{E} ? What is its vector value (magnitude and direction) at the point (0,0) and at (10,0), that is, $x = 0, y = 0$ and $x = 10, y = 0$?
- ★ 2-10 A potential distribution is given by $V = 3y^{1/2}$ V. What is the expression for \mathbf{E} ? What is its vector value (magnitude and direction) at the points (0,0), (4,0), and (0,4)?
- ★ 2-11 A potential distribution is given by $V = 7y^2 + 12x$ V. What is the expression for \mathbf{E} ? What is its vector value (magnitude and direction) at points (0,0), (5,0), (0,3), and (5,3)?
- 2-12 A potential distribution is given by $V = 5/(x^3 + y + z^3)$ V. What is the expression for \mathbf{E} ? What is its vector value at the points (0,0,4) and (5,4,3)?
- 2-13 A potential distribution is given by $V = kr^{1/2} \sin \theta$. Find \mathbf{E} .
- ★ 2-14 Two small-diameter 10-g dielectric balls can slide freely on a vertical plastic thread. Each ball carries a negative charge of $1 \mu\text{C}$. (a) Find the separation if the lower ball is restrained from moving. (b) What is the dipole moment?
- 2-15 (a) Show that at a large distance from a quadrupole (as in Fig. 2-21a) the potential is given by

$$V = \frac{Ql^2 \sin \theta \cos \theta}{2\pi\epsilon_0 r^3}$$

* Answers to starred problems are given in Appendix C.

where Q = individual charge

l = spacing between charges

r = radial distance

θ = angle from x or y axis to radial line (quadrupole oriented as in Fig. 2-21a)

(b) Find the electric field \mathbf{E} .

2-16 As an extension of Prob. 2-15 find the potential V and electric field \mathbf{E} at a large distance r from an octopole as in Fig. 2-21b.

2-17 A charge of $+2Q$ is located at the point $x = 0, y = 1$ and a charge $+Q$ at the point $x = 0, y = -1$. Find the point for which $E = 0$.

2-18 A charge of $+2Q$ is located at the point $x = 0, y = 1$ and a charge $-Q$ at the point $x = 0, y = -1$. Find the line in the xy plane for which $V = 0$. Draw a graph.

2-19 A dipole in a uniform field experiences no translational force. However, it does experience a torque tending to align the dipole axis with the field. Show that for a dipole of moment ql in a uniform field \mathbf{E} this torque is $q/E \sin \theta$, where θ is the angle between the dipole axis and the field.

* 2-20 A positive charge of 10 nC is uniformly distributed throughout a spherical volume of radius $R = 100 \text{ mm}$. (a) Find \mathbf{E} and V everywhere. (b) Draw a graph of E and V as a function of radius from the center of the sphere to a radius of 400 mm .

2-21 A sphere of radius R has a charge-density function $\rho = kr^2$. Find \mathbf{E} and V inside and outside the sphere. Note that four answers are required.

2-22 A shell of thickness $r_2 - r_1$ has a charge-density function $\rho = kr$. (a) Find \mathbf{E} and V for all values of r . Note that six answers are required. (b) Draw a graph of E and V as a function of r to a distance $3r_2$.

2-23 Show that the vectors $\mathbf{A} = \hat{x} + 4\hat{y} + 3\hat{z}$ and $\mathbf{B} = 4\hat{x} + 2\hat{y} - 4\hat{z}$ are perpendicular.

2-24 Find $\mathbf{A} \cdot \mathbf{B}$ where $\mathbf{A} = 3\hat{x} + 2\hat{y} + \hat{z}$ and \mathbf{B} is a unit vector in the \mathbf{r} direction at $\theta = 45^\circ$ and $\phi = 30^\circ$.

* 2-25 If $\mathbf{E} = \hat{x}x + \hat{y}y + \hat{z}z$, find the total electric flux over a sphere of radius R .

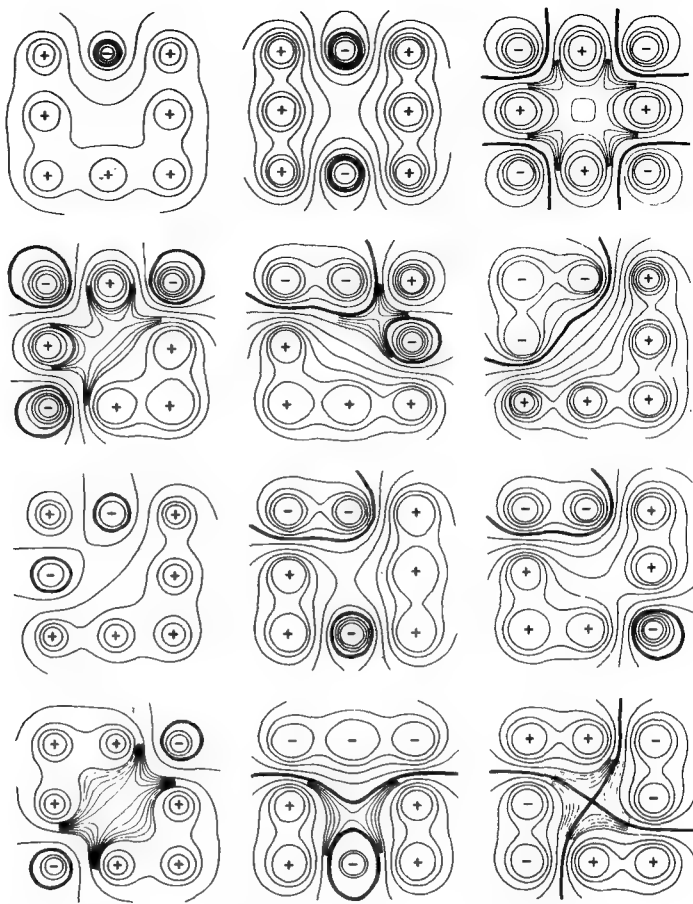
2-26 Point charges are situated as follows: 10 nC at $x = 0, y = 0$, 20 nC at $x = 3, y = 0 \text{ m}$; and -30 nC at $x = 0, y = 4 \text{ m}$. (a) Find V , \mathbf{E} , and \mathbf{D} at $x = 3, y = 4 \text{ m}$. Give units. (b) What is the total electric flux over spheres of radius 1, 3.5, and 5 m?

2-27 A cubical volume of side length $2l$ has a uniform charge density ρ . Find the integral of the normal \mathbf{D} over one face ($-l \leq x \leq l; -l \leq y \leq l$).

2-28 Using Gauss' law, find the total electric charge inside a cubical volume 1 m on a side situated in the positive octant with three edges coincident with the x, y, z axes and one corner at the origin if the electric flux density \mathbf{D} is given by (a) $\mathbf{D} = \hat{x}(x+3)$ and (b) $\mathbf{D} = \hat{y}(y^2+4)$.

* 2-29 Using Gauss' law, find the total electric charge inside a cubical volume 2 m on a side situated in the positive octant with three edges coincident with the x, y, z axes and one corner at the origin if the electric flux density \mathbf{D} is given by (a) $\mathbf{D} = \hat{x}2x^2$; (b) $\mathbf{D} = \hat{xyz}$; (c) $\mathbf{D} = \hat{x}(x+3) + \hat{y}(y+4) + \hat{z}(z+5)$; (d) $\mathbf{D} = \hat{x}xyz + \hat{y}x^2y^2z^2 + \hat{z}x^3y^3z^3$.

2-30 Eight equal positive or negative point charges are located at points (x, y) of $(100, 100), (100, 250), (100, 400), (250, 100), (250, 400), (400, 100), (400, 250)$, and $(400, 400) \text{ mm}$. Using a computer program and one of the charge configurations of Fig. P2-30 (or other

**FIGURE P2-30**

Computer-generated potential contour maps for 12 different configurations of 8 charges of the same magnitude with signs as indicated. The heavy line is the zero-potential contour.

combinations), obtain a computer-plotted contour map of the area $0 \leq x \leq 500$, $0 \leq y \leq 500$ mm and label all contours with the proper potential (voltage). The actual map can be drawn to some convenient size smaller than 500 by 500 mm by applying a scale factor. All charges are $\pm \frac{1}{2}$ nC, so that the potential at any point is

$$V = \frac{1}{4\pi\epsilon_0} \sum \frac{Q}{r} = \sum \frac{1}{r} \quad (\text{V})$$

Make the contour interval 1 or 2 V. In Fig. P2-30 contours are shown only at 5- or 10-V intervals except in interesting regions, where the interval is 1 V. The heavy lines in Fig. P2-30 are the zero-potential contours.

2-31 Referring to the potential contour map of Prob. 2-30, determine the field \mathbf{E} at the points (50,50), (50,450), (150,150), (150,350), (200,200), (200,300), (250,250), (300,200), (300,300), (350,150), (350,350), (450,50), and (450,450) mm by noting the contour orientation and interval (∇V) and also by the vector addition of the field contributions from each of the eight charges. Compare the values of \mathbf{E} obtained as the gradient of V from the map and by vector addition of the field contributions from the individual charges. Add arrows of appropriate length and orientation on the map to indicate the value of the field \mathbf{E} at the above points.

2-32 Complete the map of Prob. 2-30 by drawing the electric field lines (with arrows) as in Figs. 2-13 and 2-14. Note that this is not a two-dimensional problem (V varies perpendicular to page), so that an area bounded by V and \mathbf{E} lines for a constant voltage increment will not form curvilinear squares over the entire map (see Sec. 3-22).

2-33 If the mass of the earth were uniformly distributed in a thin spherical shell of the same radius as the earth, show that the gravitational field outside would be unchanged but inside would be zero.

* **2-34** (a) What electric charge would be required on the earth and the moon to balance their gravitational attraction if the charges were in the same ratio as the masses? Take the mass of the earth as 6×10^{24} kg, of the moon as 7×10^{22} kg, and their separation as 400 Mm. The gravitational constant in the analog to Coulomb's law is 6.7×10^{-11} N m² kg⁻². (b) If the charges were of opposite sign what is the dipole moment?

2-35 An isolated metal sphere has a radius R . Find its capacitance.

2-36 The earth is surrounded by an ionized shell, or ionosphere. If it is assumed to be equivalent to a conducting shell at a height of 500 km, what is the capacitance of the earth-shell combination?

2-37 Show that Gauss' law depends on the inverse-square law, that is, $E \propto 1/r^2$ for a point charge.

* **2-38** Two concentric shells have radii r_1 and r_2 . Charge $+Q_1$ is uniformly distributed over the shell of radius r_1 , and charge $+Q_2$ is uniformly distributed over the shell of radius r_2 . Apply Gauss' law to find (a) the field \mathbf{E} everywhere and (b) the potential V everywhere.

2-39 What is the capacitance of the earth? Take the earth's radius as 6.4 Mm.

* **2-40** A thin-walled metal sphere of 10 liters capacity is filled with nitrogen at atmospheric pressure. If one electron is removed from each molecule of the gas (and removed to a large distance from the sphere) find the potential of the sphere. The medium outside the sphere is air. Take the density of the nitrogen gas as 3×10^{22} molecules per liter.

2-41 Two concentric spherical metal shells have radii r_1 and r_2 . Find their capacitance. The shell thickness is negligible.

2-42 Describe how electrostatic fields are employed in the operation of a xerographic machine. See, for example, A. D. Moore, Electrostatics, *Sci. Am.*, 226: 47 (March 1972).

3

THE STATIC ELECTRIC FIELD: PART 2

3-1 INTRODUCTION

This chapter extends the theory introduced in Chap. 2 to include material media. The conditions of homogeneity, linearity, and isotropy are pointed out. The influence of a dielectric medium on field distributions is discussed, and the concepts of electrostatic energy and energy density are introduced. The fields of several charge distributions are found. Introduction of the divergence concept leads to Maxwell's divergence equation in \mathbf{D} , which is then applied to the parallel-plate capacitor.

3-2 HOMOGENEITY, LINEARITY, AND ISOTROPY

A medium is *homogeneous* if its physical characteristics (mass density, molecular structure, etc.) do not vary from point to point. If the medium is not homogeneous, it may be described as inhomogeneous, nonhomogeneous, or heterogeneous.

A medium is *linear* with respect to an electrostatic field if the flux density \mathbf{D} is proportional to the electric field intensity \mathbf{E} . This is the case in free space, where $\mathbf{D} = \epsilon_0 \mathbf{E}$. Here the factor ϵ_0 , or permittivity, is a constant. In material media the permittivity ϵ may not always be constant. If it is not, the material is said to be nonlinear.

An *isotropic* material is one whose properties are independent of direction. Generally, materials whose molecular structure is randomly oriented will be isotropic. However, crystalline media or certain plasmas may have directional characteristics. Such materials are said to be nonisotropic or anisotropic.

In this book concepts are usually developed first for the case where the medium is *homogeneous*, *linear*, and *isotropic*.[†] Later the ideas may be extended to cases where one or more of these restrictions no longer hold.

3-3 DIELECTRICS AND PERMITTIVITY

In a *conductor* the outer electrons of an atom are easily detached and migrate readily from atom to atom under the influence of an electric field. In a *dielectric*, on the other hand, the electrons are so well bound or held near their equilibrium positions that they cannot be detached by the application of ordinary electric fields. Hence, an electric field produces no migration of charge in a dielectric, and, in general, this property makes dielectrics act as good insulators. Paraffin, glass, and mica are examples of dielectrics.

An important characteristic of a dielectric is its *permittivity*[‡] ϵ . Since the permittivity of a dielectric is always greater than the permittivity of vacuum, it is often convenient to use the relative permittivity ϵ_r of the dielectric, i.e., the ratio of its permittivity to that of vacuum. Thus

$$\boxed{\epsilon_r = \frac{\epsilon}{\epsilon_0}} \quad (1)$$

where ϵ_r = relative permittivity of dielectric

ϵ = permittivity of dielectric

ϵ_0 = permittivity of vacuum = 8.85 pF m^{-1}

Whereas ϵ or ϵ_0 is expressed in farads per meter (F m^{-1}), the relative permittivity ϵ_r is a dimensionless ratio.

The relative permittivity is the value ordinarily given in tables. The relative permittivity of a few media is shown in Table 3-1, where the values are for static (or low-frequency) fields and, except for vacuum or air, are approximate. Note that ϵ_r for air is so close to unity that for most problems we can consider air equivalent to vacuum.

[†] Dielectrics of this type are sometimes designated *Class A dielectrics*.

[‡] Also called the *dielectric constant*. However, the permittivity is not always a constant, as one might be led to infer by this term (see Chap. 8).

Table 3-1 PERMITTIVITIES OF DIELECTRIC MEDIA†

Medium	Relative permittivity ϵ_r
Vacuum	1‡
Air (atmospheric pressure)	1.0006
Styrofoam	1.03
Paraffin	2.1
Plywood	2.1
Polystyrene	2.7
Amber	3.0
Rubber	3
Plexiglas	3.4
Dry sandy soil	3.4
Nylon (solid)	3.8
Sulfur	4
Quartz	5
Bakelite	5
Formica	6
Lead glass	6
Mica	6
Marble	8
Flint glass	10
Ammonia (liquid)	22
Glycerin	50
Water (distilled)	81
Rutile (TiO_2)	89-173§
Barium titanate ($BaTiO_3$)	1,200
Barium strontium titanate ($2BaTiO_3 : 1SrTiO_3$)	10,000¶
Barium titanate zirconate ($4BaTiO_3 : 1BaZrO_3$)	13,000††
Barium titanate stannate ($9BaTiO_3 : 1BaSnO_3$)	20,000††

† For a comprehensive tabulation of permittivities, see A. R. Von Hippel, "Dielectric Materials and Applications," pp. 301-370, The M.I.T. Press, Cambridge, Mass., 1954.

‡ By definition.

§ Crystals, in general, are nonisotropic; i.e., their properties vary with direction. Rutile is an example of such a nonisotropic crystalline substance. Its relative permittivity depends on the direction of the applied electric field with relation to the crystal axes, being 89 when the field is perpendicular to a certain crystal axis and 173 when the field is parallel to this axis. For an aggregation of randomly oriented rutile crystals $\epsilon_r = 114$. All crystals, except those of the cubic system, are nonisotropic to electric fields; i.e., their properties vary with direction. Thus, the permittivity of many other crystalline substances may vary with direction. However, in many cases the difference is slight. For example, a quartz crystal has a relative permittivity of 4.7 in one direction and 5.1 at right angles. The average value is 4.9. The nearest integer is 5, and this is the value given in the table.

|| The permittivity of these titanates is highly temperature-sensitive. The above values are for 25°C. See, for example, E. Wainer, High Titania Dielectrics, *Trans. Electrochem. Soc.*, **89** (1946).

†† K. W. Plessner and R. West, High-permittivity Ceramics for Capacitors, in J. B. Birks and J. H. Schulman (eds.), "Progress in Dielectrics," vol. 2, John Wiley & Sons, Inc., New York, 1960.

3-4 THE ELECTRIC FIELD IN A DIELECTRIC

In free space, the electric field is defined as force per unit charge. This implies that the electric field in free space is a *measurable quantity*. However, to measure the electric field inside a dielectric or other material medium may be very difficult or impractical. But, if we confine our attention to the external effects of the dielectric, such internal measurements become unnecessary provided a theory can be formulated for the behavior of the dielectric which produces agreement with external measurements. Thus, a distinction should be made between an electric field as a *measurable quantity* (as in free space) and an electric field as a *theoretical quantity* (as in a dielectric).† In this chapter a theory for the electrostatic field in a dielectric is developed and then related to the external field by means of boundary conditions.

$$E = \frac{F}{Q}$$

3-5 POLARIZATION

Although there is no migration of charge when a dielectric is placed in an electric field, there does occur a slight displacement of the electrons with respect to their nuclei so that individual atoms behave like very small, or *atomic, dipoles*.‡ When these atomic dipoles are present, the dielectric is said to be *polarized* or to be in a state of *polarization*. When the field is removed and the atoms return to their normal, or unpolarized, state, the dipoles disappear.§

In the above simple picture an atom of a dielectric material is represented by an electric dipole, i.e., a positive point charge representing the nucleus and a negative point charge representing the electronic charge, the two charges being separated by a small distance. The electrons revolve in orbits around the nucleus and act like a negatively charged cloud surrounding the nucleus. When the atom is unpolarized, the cloud surrounds the nucleus symmetrically, as in Fig. 3-1a, and the dipole moment is zero (the equivalent positive and negative point charges have zero displacement). Under the influence of an electric field the electron cloud becomes slightly displaced or asymmetrical, as in Fig. 3-1b, and the atom is polarized. According to our simple picture, the atom may then be represented by the equivalent point-charge dipole of Fig. 3-1c (dipole moment = Ql).

† The Teaching of Electricity and Magnetism at the College Level (Report of the Coulomb's Law Committee of the American Association of Physics Teachers), *Am. J. Phys.*, 18 (1):5 (January 1950).

‡ The dipoles may also be of molecular size. In a liquid the molecules are free to turn when a field is applied, and this may result in a relatively large permittivity. Water is an example.

§ When polarization in a dielectric persists in the absence of an applied electric field, the substance is permanently polarized and is called an *electret*. A strained piezoelectric crystal is an example of an electret.

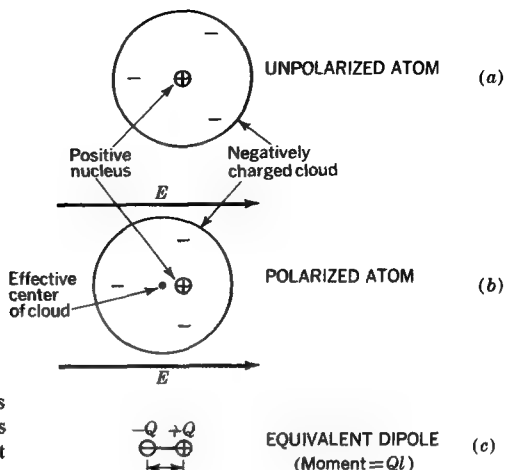


FIGURE 3-1

Unpolarized atom as in (a) becomes polarized as in (b) when electric field is applied. Equivalent dipole is shown at (c).

Consider the dielectric slab of permittivity ϵ in Fig. 3-2a situated in vacuum. Let a uniform field E be applied normal to the slab. This polarizes the dielectric, i.e., induces atomic dipoles throughout the slab. In the interior the positive and negative charges of adjacent dipoles annul each other's effects. The net result of the polarization is to produce a layer of negative charge on one surface of the slab and a layer of positive charge on the other, as suggested in Fig. 3-2a.

The effect of the atomic dipoles can be described by the polarization P or dipole moment per unit volume. Thus,

$$P = \frac{p}{v} = \frac{QL}{v} \quad (1)$$

where $p = QL$ is the net dipole moment in the volume v . For example, consider the rectangular volume of surface area A and thickness L ($v = AL$) in Fig. 3-2a. For this volume

$$P = \frac{p}{v} = \frac{QL}{AL} = \frac{Q}{A} = \rho_{sp} \quad (2)$$

where ρ_{sp} is the surface charge density of polarization charge appearing on the slab faces. Thus, P has the dimensions of charge per area, the same as D .

The value of P in (2) is an average for the volume v . To define the meaning of P at a point, it is convenient to assume that a dielectric in an electric field has a continuous distribution of infinitesimal dipoles, i.e., a continuous polarization, whereas the dipoles actually are discrete polarized atoms. The assumption of a continuous

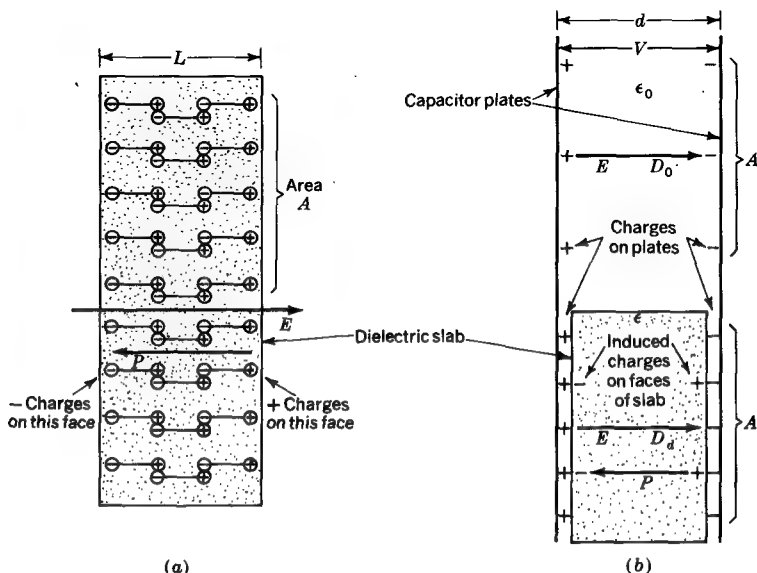


FIGURE 3-2

(a) Dielectric slab in uniform electric field. (b) Parallel-plate capacitor with dielectric slab in lower part.

distribution leads to no appreciable error provided that we restrict our attention to volumes containing many atoms or dipoles, i.e., to macroscopic regions. Assuming now a continuously polarized dielectric, the value of P at a point can be defined as the net dipole moment p of a small volume Δv divided by the volume, with the limit taken as Δv shrinks to zero around the point. Thus,

$$P = \lim_{\Delta v \rightarrow 0} \frac{p}{\Delta v} \quad (3)$$

Consider now a uniform electric field in a parallel-plate capacitor with plates separated by a distance d , as in the cross-sectional view of Fig. 3-2b. There is a voltage V between the plates so that the electric field $E = V/d$ everywhere. The medium in the upper part of the capacitor is vacuum (or air) with permittivity ϵ_0 . The lower part is filled with a dielectric of permittivity ϵ . The dielectric completely fills the space between the plates, but in Fig. 3-2b there is a gap in order to show the charges on the plates.

In the upper part of the capacitor (Fig. 3-2b) we have

$$D_0 = \epsilon_0 E \quad (4)$$

where D_0 = electric flux density in vacuum (or air-filled) part of capacitor, $C\ m^{-2}$
 ϵ_0 = permittivity of vacuum = $8.85\ pF\ m^{-1}$
 $E = V/d$ = electric field intensity, $V\ m^{-1}$

In the lower, dielectric-filled part of the capacitor the electric field polarizes the dielectric causing a surface charge density ρ_{sp} to appear on both faces of the dielectric slab. These bound charges induce free charges of opposite sign on the capacitor plates (compare upper and lower parts of Fig. 3-2b). As a result the free-charge surface density on the plates is increased by ρ_{sp} . Therefore, in the dielectric we have

$$D_d = \epsilon_0 E + \rho_{sp} \quad (5)$$

but from (2) $\rho_{sp} = P$, and so

$$D_d = \epsilon_0 E + P \quad (6)$$

where D_d = electric flux density in dielectric, $C\ m^{-2}$
 ϵ_0 = permittivity of vacuum = $8.85\ pF\ m^{-1}$
 E = electric field intensity, $V\ m^{-1}$
 P = polarization (of dielectric), $C\ m^{-2}$

Equation (6) implies the presence of dielectric (because of the P term), and so the subscript to D is redundant. Therefore, (6) can be written

$$\boxed{\mathbf{D} = \epsilon_0 \mathbf{E} + \mathbf{P}} \quad (7)$$

Although developed for the special case of a parallel-plate capacitor, (7) is a (vector) relation which applies in general.

In the dielectric we can also write

$$D = D_d = \epsilon E \quad (8)$$

where ϵ is the permittivity of the dielectric material in farads per meter. Equating (6) and (8) gives

$$\epsilon E = \epsilon_0 E + P \quad (9)$$

or

$$\boxed{\epsilon = \epsilon_0 + \frac{P}{E}} \quad \text{or} \quad \boxed{\frac{P}{E} = \epsilon - \epsilon_0} \quad (10)$$

The ratio P/E is also sometimes written

$$\frac{P}{E} = \chi \epsilon_0 \quad (11)$$

where χ is the electric susceptibility (dimensionless). Comparing (10) and (11) gives

$$\chi = \epsilon_r - 1 \quad (12)$$

Thus, the susceptibility $\chi = 0$ for vacuum, for which $\epsilon_r = 1$.

EXAMPLE Find the relative permittivity ϵ_r and polarization P for the dielectric slab of Fig. 3-2b. Assume each plus or minus sign represents 1 nC m^{-2} and $A = 1 \text{ m}^2$.

SOLUTION

$$\epsilon_r = \frac{\epsilon}{\epsilon_0} = \frac{\epsilon E}{\epsilon_0 E} = \frac{D_d}{D_0} = \frac{5}{3} \quad (\text{dimensionless})$$

By inspection of Fig. 3-2b we can write

$$P = \rho_{sp} = 2 \text{ nC m}^{-2}$$

This result can also be obtained as follows. From (6)

$$P = D_d - \epsilon_0 E$$

Therefore,

$$P = 5 - 3 = 2 \text{ nC m}^{-2}$$

the same as before.

In isotropic media \mathbf{P} and \mathbf{E} are in the same direction, so that their quotient is a scalar and hence ϵ is a scalar. In nonisotropic media, such as crystals, \mathbf{P} and \mathbf{E} are, *in general*, not in the same direction, so that ϵ is no longer a scalar (see Chap. 15). Thus, $\mathbf{D} = \epsilon_0 \mathbf{E} + \mathbf{P}$ is a general relation, while $\mathbf{D} = \epsilon \mathbf{E}$ is a more concise expression, which, however, has a simple significance only for isotropic media or certain special cases in nonisotropic media.

3-6 ARTIFICIAL DIELECTRICS

Certain of the properties of a dielectric material may be simulated with *artificial dielectrics*, which were developed as a material for lenses for focusing short-wavelength radio waves.[†] Whereas the true dielectric consists of atomic or molecular particles of microscopic size, the artificial dielectric consists of discrete metal particles of macroscopic size. For example, the artificial dielectric may consist of a large number of

[†] W. E. Kock, Metallic Delay Lens, *Bell Syst. Tech. J.*, 27: 58-82 (January 1948). See also discussion in J. D. Kraus, "Antennas," p. 390, McGraw-Hill Book Company, New York, 1950.

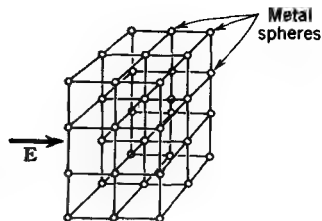


FIGURE 3-3
Slab of artificial dielectric consisting of metal spheres in lattice arrangement.

metal spheres, as in Fig. 3-3, arranged in a three-dimensional, or lattice, structure which simulates the arrangement of the atoms of a true dielectric *but on a much larger scale.*†

The permittivity of an artificial dielectric made of metal spheres will now be calculated. This calculation is approximate but provides a good illustration of the significance of polarization and its application in a practical problem. Let a uniform electric field E be applied, as in Fig. 3-3, to a slab of artificial dielectric consisting of many metal spheres. The field E induces charges on the individual spheres as suggested in Fig. 3-4a. Thus, the spheres become analogous to the polarized atoms of a true dielectric, and each sphere may be represented by an equivalent dipole of charge q and length l , as in Fig. 3-4b. The polarization P of the artificial dielectric is, by (3-5-1), equal to the net dipole moment per unit volume, or

$$P = Nql \quad (1)$$

where N = number of spheres per unit volume, m^{-3}

ql = dipole moment of individual sphere, C m

From (3-5-10) the permittivity is given by

$$\epsilon = \epsilon_0 + \frac{P}{E} \quad (2)$$

Introducing the value of P from (1) into (2), we have

$$\epsilon = \epsilon_0 + \frac{Nql}{E} \quad (3)$$

According to (3), the permittivity of the artificial dielectric can be determined if the number of spheres per unit volume and the dipole moment of one sphere per unit applied field are known. Proceeding now to find the dipole moment of one sphere

† If the spheres are hollow (or if metal disks or strips are used), the artificial dielectric slab may be much lighter in weight than the corresponding slab of true dielectric. This is a principal advantage of the artificial-dielectric material.

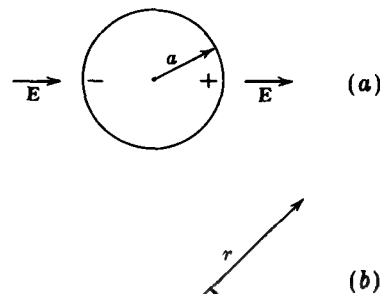


FIGURE 3-4

(a) Individual sphere of artificial dielectric and (b) equivalent dipole.

it is assumed that each sphere is in a uniform field. This neglects the interaction of spheres, but this is negligible provided the sphere radius is small compared with the spacing between spheres.

The potential V_0 at a point in a uniform field is given by

$$V_0 = - \int_0^r E \cos \theta \, dr = -Er \cos \theta \quad (4)$$

where r = radial distance from origin (taken at center of dipole)

θ = angle between field direction or axis of dipole and radial line (see Fig. 3-4b)
According to (4), $V_0 = 0$ at all points in a plane through the origin and normal to \mathbf{E} . Equation (4) gives the potential at a point in a uniform field. Assuming that $r \gg l$, the potential V_d of a dipole in air is, from (2-15-1),

$$V_d = \frac{ql \cos \theta}{4\pi\epsilon_0 r^2} \quad (5)$$

The total potential V is, by superposition, the sum of (4) and (5) or

$$V = V_0 + V_d = -Er \cos \theta + \frac{ql \cos \theta}{4\pi\epsilon_0 r^2} \quad (6)$$

The metal sphere has only induced charges on its surface (equal amounts of positive and negative charge), so that its potential is zero. Thus, for $r = a$, (6) reduces to

$$0 = -Ea \cos \theta + \frac{ql \cos \theta}{4\pi\epsilon_0 a^2} \quad (7)$$

Solving for ql/E , we have

$$\frac{ql}{E} = 4\pi\epsilon_0 a^3 \quad (8)$$

Introducing (8) into (3) we obtain $\epsilon = \epsilon_0 + 4\pi\epsilon_0 Na^3$, or

$$\epsilon_r = 1 + 4\pi Na^3 \quad (9)$$

where ϵ = permittivity of artificial dielectric

ϵ_r = relative permittivity of artificial dielectric

N = number of spheres per unit volume

a = radius of sphere

Both the unit volume and the radius are expressed in the same unit of length.

Since the volume v of the sphere is $4\pi a^3/3$, (9) can also be written

$$\epsilon_r = 1 + 3vN \quad (10)$$

where N = number of spheres per unit volume

v = volume of sphere (in same units as unit volume)

Thus, the permittivity of the artificial dielectric depends on both the number of spheres per unit volume and the size of the spheres.

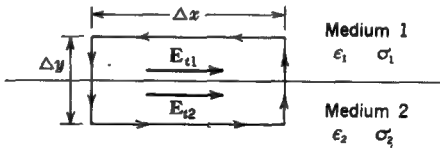
3-7 BOUNDARY RELATIONS

In a single medium the electric field is continuous. That is, the field, if not constant, changes only by an infinitesimal amount in an infinitesimal distance. However, at the boundary between two different media the electric field may change abruptly both in magnitude and direction. It is of great importance in many problems to know the relations of the fields at such boundaries. These boundary relations are discussed in this section.

It is convenient to analyze the boundary problem in two parts, considering first the relation between the fields *tangent* to the boundary and second the fields *normal* to the boundary.

Taking up first the relation of the fields tangent to the boundary, let two dielectric media of permittivities ϵ_1 and ϵ_2 be separated by a plane boundary as in Fig. 3-5. It is assumed that both media are perfect insulators, i.e., the conductivities† σ_1 and σ_2 of the two media are zero. Consider a rectangular path, half in each medium, of

FIGURE 3-5
The tangential electric field is continuous across a boundary.



† For discussion of conductivity see Sec. 4-7.

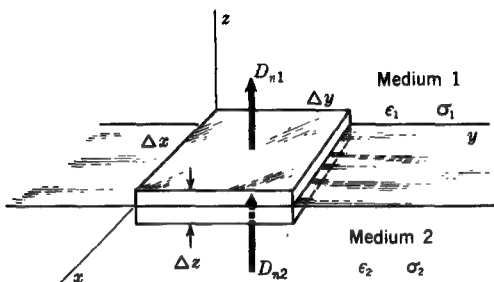


FIGURE 3-6

The normal component of the flux density is continuous across a charge-free boundary.

length Δx parallel to the boundary and of length Δy normal to the boundary. Let the average electric field intensity tangent to the boundary in medium 1 be E_{t1} and the average field intensity tangent to the boundary in medium 2 be E_{t2} . The work per unit charge required to transport a positive test charge around this closed path is the line integral of \mathbf{E} around the path ($\oint \mathbf{E} \cdot d\mathbf{l}$). By making the path length Δy approach zero the work along the segments of the path normal to the boundary is zero even though a finite electric field may exist normal to the boundary. The line integral of \mathbf{E} around the rectangle in the direction of the arrows is then

$$E_{t1} \Delta x - E_{t2} \Delta x = 0 \quad (1)$$

or

$$E_{t1} = E_{t2} \quad (2)$$

According to (2) the tangential components of the electric field are the same on both sides of a boundary between two dielectrics. In other words, the tangential electric field is continuous across such a boundary.

If medium 2 is a conductor ($\sigma_2 \neq 0$), the field E_{t2} in medium 2 must be zero under static conditions and hence (2) reduces to

$$E_{t1} = 0 \quad (3)$$

According to (3), the tangential electric field at a dielectric-conductor boundary is zero.[†]

Turning our attention next to the fields normal to the boundary, consider two dielectric media of permittivities ϵ_1 and ϵ_2 separated by the xy plane as shown in Fig. 3-6. It is assumed that both media are perfect insulators ($\sigma_1 = \sigma_2 = 0$). Suppose

[†]This assumes that no currents are flowing. If currents are present, \mathbf{E} in the conductor is not zero, unless the conductivity is infinite, and (2) applies rather than (3). In Chap. 8 the relations of (2) and (3) are extended to include time-changing fields, and it is shown that the relation $E_{t1} = E_{t2}$ of (2) holds with static or changing fields for the boundary between any two media of permittivities, permeabilities, and conductivities $\epsilon_1, \mu_1, \sigma_1$ and $\epsilon_2, \mu_2, \sigma_2$. Furthermore, for changing fields the relation $E_{t1} = 0$ of (3) is restricted to the case where the conductivity of medium 2 is infinite ($\sigma_2 = \infty$). This follows from the fact that a time-changing electric field in a conductor is zero only if the conductivity is infinite.

that an imaginary box is constructed, half in each medium, of area $\Delta x \Delta y$ and height Δz . Let D_{n1} be the average flux density normal to the top of the box in medium 1 and D_{n2} the average flux density normal to the bottom of the box in medium 2. D_{n1} is an outward normal (positive), while D_{n2} is an inward normal (negative). By Gauss' law the electric flux or surface integral of the normal component of \mathbf{D} over a closed surface equals the charge enclosed. By making the height of the box Δz approach zero the contribution of the sides to the surface integral is zero. The total flux over the box is then due entirely to flux over the top and bottom surfaces. If the average surface charge density on the boundary is ρ_s , we have on applying Gauss' law

$$D_{n1} \Delta x \Delta y - D_{n2} \Delta x \Delta y = \rho_s \Delta x \Delta y$$

or

$$\boxed{D_{n1} - D_{n2} = \rho_s} \quad (4)$$

According to (4) the normal component of the flux density changes at a charged boundary between two dielectrics by an amount equal to the surface charge density. This is usually zero at a dielectric-dielectric boundary unless charge has been placed there by mechanical means, as by rubbing.

If the boundary is free from charge, $\rho_s = 0$ and (4) reduces to

$$D_{n1} = D_{n2} \quad (5)$$

According to (5), the normal component of the flux density is continuous across the charge-free boundary between two dielectrics.

If medium 2 is a conductor, $D_{n2} = 0$ and (4) reduces to

$$D_{n1} = \rho_s \quad (6)$$

According to (6), the normal component of the flux density at a dielectric-conductor boundary is equal to the surface charge density on the conductor.†

It is important to note that ρ_s in these relations refers to actual electric charge separated by finite distances from equal quantities of opposite charge and *not* to surface charge ρ_{sp} due to polarization. The polarization surface charge is produced by atomic dipoles having equal and opposite charges separated by what is assumed to be an infinitesimal distance. It is not permissible to separate the positive and negative charges of such a dipole by a surface of integration, and hence the volume must always contain an integral (whole) number of dipoles and, therefore, zero net charge. Only when the positive and negative charges are separated by a macroscopic distance (as on the opposite surfaces of a conducting sheet) can we separate

† In Chap. 8 it is pointed out that the relation $D_{n1} - D_{n2} = \rho_s$ of (4) and $D_{n1} = D_{n2}$ of (5) hold with static or time-changing fields for *any* two media of permittivities, permeabilities, and conductivities $\epsilon_1, \mu_1, \sigma_1$ and $\epsilon_2, \mu_2, \sigma_2$.

them by a surface of integration. This emphasizes a fundamental difference between the polarization, or so-called "bound" charge, on a dielectric surface and the true charge on a conductor surface. In a similar way the boundary relation for polarization is

$$P_{n1} - P_{n2} = -\rho_{sp} \quad (7)$$

If medium 2 is free space,

$$P_{n1} = -\rho_{sp} \quad (8)$$

Equations (6) and (8) are written more generally as

$$\mathbf{D} \cdot \hat{\mathbf{n}} = \rho_s \quad \text{and} \quad -\mathbf{P} \cdot \hat{\mathbf{n}} = \rho_{sp} \quad (9)$$

The minus sign in the polarization relation results from the fact that with positive polarization charge at a dielectric surface the polarization is directed *inward* while the surface normal is directed *outward* (see Sec. 2-5).

EXAMPLE 1 *Boundary between two dielectrics.* Let two isotropic dielectric media 1 and 2 be separated by a charge-free plane boundary as in Fig. 3-7. Let the permittivities be ϵ_1 and ϵ_2 , and let the conductivities $\sigma_1 = \sigma_2 = 0$. Referring to Fig. 3-7, the problem is to find the relation between the angles α_1 and α_2 of a static field line or flux tube which traverses the boundary. For example, given α_1 , to find α_2 .

SOLUTION Let

D_1 = magnitude of \mathbf{D} in medium 1

D_2 = magnitude of \mathbf{D} in medium 2

E_1 = magnitude of \mathbf{E} in medium 1

E_2 = magnitude of \mathbf{E} in medium 2

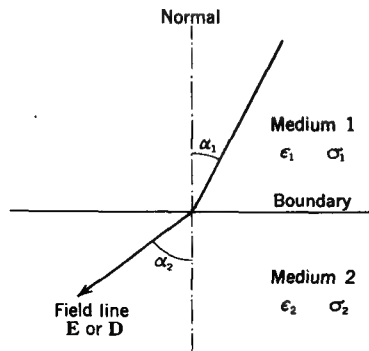


FIGURE 3-7
Boundary between two dielectric media showing change in direction of field line.

In an isotropic medium, **D** and **E** have the same direction. According to the boundary relations,

$$\underline{D_{n1} = D_{n2}} \quad \text{and} \quad \underline{E_{t1} = E_{t2}} \quad (10)$$

Referring to Fig. 3-7,

$$D_{n1} = D_1 \cos \alpha_1 \quad \text{and} \quad D_{n2} = D_2 \cos \alpha_2 \quad (11)$$

$$\text{while} \quad E_{t1} = E_1 \sin \alpha_1 \quad \text{and} \quad E_{t2} = E_2 \sin \alpha_2 \quad (12)$$

Substituting (11) and (12) into (10) and dividing the resulting equations yields

$$\frac{D_1 \cos \alpha_1}{E_1 \sin \alpha_1} = \frac{D_2 \cos \alpha_2}{E_2 \sin \alpha_2} \quad (13)$$

But $D_1 = \epsilon_1 E_1$, and $D_2 = \epsilon_2 E_2$, so that (13) becomes

$$\frac{\tan \alpha_1}{\tan \alpha_2} = \frac{\epsilon_1}{\epsilon_2} = \frac{\epsilon_{r1} \epsilon_0}{\epsilon_{r2} \epsilon_0} = \frac{\epsilon_{r1}}{\epsilon_{r2}} \quad (14)$$

where ϵ_{r1} = relative permittivity of medium 1

ϵ_{r2} = relative permittivity of medium 2

ϵ_0 = permittivity of vacuum

Suppose, for example, that medium 1 is air ($\epsilon_{r1} = 1$), while medium 2 is a slab of sulfur ($\epsilon_{r2} = 4$). Then when $\alpha_1 = 30^\circ$, the angle α_2 in medium 2 is 66.6° .

EXAMPLE 2 *Boundary between a conductor and a dielectric.* Suppose that medium 2 in Fig. 3-7 is a conductor. Find α_1 .

SOLUTION Since medium 2 is a conductor, $D_2 = E_2 = 0$ under static conditions. According to the boundary relations,

$$D_{n1} = \rho_s \quad \text{or} \quad E_{t1} = \frac{\rho_s}{\epsilon_1}$$

and

$$E_{t1} = 0$$

Therefore

$$\alpha_1 = \tan^{-1} \frac{E_{t1}}{E_{n1}} = \tan^{-1} 0 = 0$$

It follows that a static electric field line or flux tube at a dielectric-conductor boundary is always perpendicular to the conductor surface (when no currents are present). This fact is of fundamental importance in field mapping (see Sec. 3-22).

3-8 TABLE OF BOUNDARY RELATIONS

Table 3-2 summarizes the boundary relations for static fields developed in the preceding section.

Table 3-2 BOUNDARY RELATIONS FOR STATIC ELECTRIC FIELDS†

Field component	Boundary relation	Condition
Tangential	$E_{t1} = E_{t2}$ (1)	Any two media
Tangential	$E_{t1} = 0$ (2)	Medium 1 is a dielectric; medium 2 is a conductor
Normal	$D_{n1} - D_{n2} = \rho_s$ (3)	Any two media with charge at boundary
Normal	$D_{n1} = D_{n2}$ (4)	Any two media with no charge at boundary
Normal	$D_{n1} = \rho_s$ (5)	Medium 1 is a dielectric; medium 2 is a conductor with surface charge

† Relations (1), (3), and (4) apply in the presence of currents and also for time-varying fields (Chap. 8). The other relations, (2) and (5), also apply for time-changing situations provided $\sigma_2 = \infty$.

3-9 PARALLEL-PLATE CAPACITOR

Consider the parallel-plate capacitor shown in Fig. 3-8. From Sec. 2-21 we have

$$C = \frac{\epsilon A}{l} \quad (1)$$

where ϵ = permittivity of medium between capacitor plates, $F\ m^{-1}$

A = area of plates, m^2

l = separation of plates, m



FIGURE 3-8
Parallel-plate capacitor.

Introducing the relative permittivity ϵ_r and the value of ϵ_0 , we obtain for the capacitance of the parallel-plate capacitor

$$C = 8.85 \frac{A\epsilon_r}{l} \quad (\text{pF}) \quad (2)$$

where ϵ_r is the relative permittivity of the medium between the plates.

EXAMPLE A parallel-plate capacitor consists of two square metal plates 500 mm on a side and separated by 10 mm. A slab of sulfur ($\epsilon_r = 4$) 6 mm thick is placed on the lower plate, as indicated in Fig. 3-9a. This leaves an air gap 4 mm thick between the sulfur slab and the upper plate. Find the capacitance of the capacitor. Neglect fringing of the field at the edges of the capacitor.

SOLUTION Imagine that a thin metal foil is placed on the upper surface of the sulfur slab. The foil is not connected to either plate. Since the foil is normal to E (and assuming that it is of negligible thickness) the field in the capacitor is undisturbed. The capacitor may now be regarded as two capacitors in series, an air capacitor of 4 mm plate spacing and capacitance C_a , and a sulfur-filled capacitor of 6 mm plate spacing and capacitance C_s , as suggested in Fig. 3-9b. The capacitance of the air capacitor is, from (4),

$$C_a = \frac{8.85 A \epsilon_r}{l} = \frac{8.85 \times 0.5^2 \times 1}{0.004} = 553 \text{ pF}$$

The capacitance of the sulfur-filled capacitor is

$$C_s = \frac{8.85 \times 0.5^2 \times 4}{0.006} = 1,475 \text{ pF}$$

The total capacitance of two capacitors in parallel is the sum of the individual capacitances. However, the total capacitance of two capacitors in series, as here, is the reciprocal of the sum of the reciprocals of the individual capacitances. Thus, the total capacitance C is given by

$$\frac{1}{C} = \frac{1}{C_a} + \frac{1}{C_s}$$

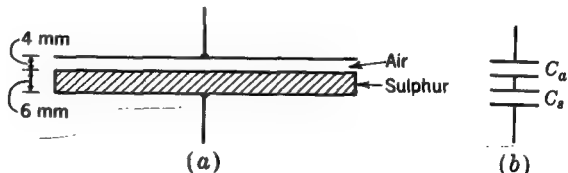


FIGURE 3-9
(a) Parallel-plate capacitor with sulfur slab and air gap and **(b)** equivalent series capacitor.

or

$$C = \frac{C_a C_s}{C_a + C_s} = \frac{553 \times 1,475}{553 + 1,475} = 402 \text{ pF}$$

3-10 DIELECTRIC STRENGTH

The field intensity E in a dielectric cannot be increased indefinitely. If a certain value is exceeded, sparking occurs and the dielectric is said to break down.[†] The maximum field intensity that a dielectric can sustain without breakdown is called its *dielectric strength*.

In the design of capacitors it is important to know the maximum potential difference that can be applied before breakdown occurs. For a given plate spacing this breakdown is proportional to the dielectric strength of the medium between the plates. The radius of curvature of the edge of the capacitor plate is another factor, since this curvature largely determines the maximum field intensity that occurs for a given potential difference (see Sec. 3-23).

Many capacitors have air as the dielectric. These types have the advantage that if breakdown occurs, the capacitor is not permanently damaged. For applications requiring large capacitance or small physical size or both, other dielectrics are employed. The dielectric strengths of a number of common dielectric materials are listed in Table 3-3. The dielectric strengths are for a uniform field, and the materials are arranged in order of increasing strength.

Table 3-3

Material	Dielectric strength MV m ⁻¹
Air (atmospheric pressure)	3
Oil (mineral)	15
Paper (impregnated)	15
Polystyrene	20
Rubber (hard)	21
Bakelite	25
Glass (plate)	30
Paraffin	30
Quartz (fused)	30
Mica	200

[†] As E is gradually increased, sparking occurs in air almost immediately when a critical value of field is exceeded if the field is uniform (E everywhere parallel), but a glowing, or corona, discharge may occur first if the field is nonuniform (diverging) with sparkover following as E is increased further.

3-11 ENERGY IN A CAPACITOR

It requires work to charge a capacitor. Hence energy is stored by a charged capacitor.

To determine the magnitude of this energy, consider a capacitor of capacitance C charged to a potential difference V between the two conductors. Then from (2-21-1)

$$q = CV \quad (1)$$

where q is the charge on each conductor. Potential is work per charge. In terms of infinitesimals it is the infinitesimal work dW per infinitesimal charge dq . That is,

$$V = \frac{dW}{dq} \quad (2)$$

Introducing the value of V from (2) in (1) we have

$$dW = \frac{q}{C} dq \quad (3)$$

If the charging process starts from a zero charge and continues until a final charge Q is delivered, the total work W is the integral of (3), or

$$W = \frac{1}{C} \int_0^Q q dq = \frac{1}{2} \frac{Q^2}{C} \quad (4)$$

This is the energy stored in the capacitor. By (2-21-1) this relation can be variously expressed as

$$W = \frac{1}{2} \frac{Q^2}{C} = \frac{1}{2} CV^2 = \frac{1}{2} QV \quad (5)$$

where W = energy, J

C = capacitance, F

V = potential difference, V

Q = charge on one conductor, C

3-12 ENERGY DENSITY IN A STATIC ELECTRIC FIELD

Consider the parallel-plate capacitor of capacitance C shown in Fig. 3-10. When it is charged to a potential difference V between the plates, the energy stored is

$$W = \frac{1}{2} CV^2 = \frac{1}{2} QV \quad (1)$$

The question may now be asked: In what part of the capacitor is the energy stored? The answer is: The energy is stored in the electric field *between* the plates.

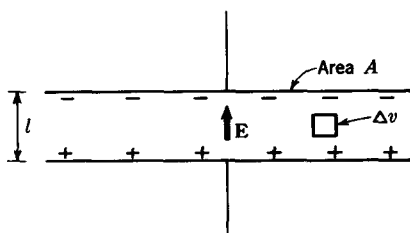


FIGURE 3-10
Energy is stored in the electric field between the capacitor plates.

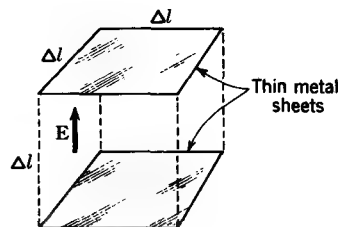


FIGURE 3-11
Small cubical volume of capacitance $\epsilon \Delta l$.

To demonstrate this, let us proceed as follows. Consider the small cubical volume $\Delta v (= \Delta l^3)$ between the plates as indicated in Fig. 3-10. This volume is shown to a larger scale in Fig. 3-11. The length of each side is Δl , and the top and bottom faces (of area Δl^2) are parallel to the capacitor plates (normal to the field E). If thin sheets of metal foil are placed coincident with the top and bottom faces of the volume, the field will be undisturbed provided the sheets are sufficiently thin. The volume Δv now constitutes a small capacitor of capacitance

$$\Delta C = \frac{\epsilon \Delta l^2}{\Delta l} = \epsilon \Delta l \quad (2)$$

The potential difference ΔV of the thin sheets is given by

$$\Delta V = E \Delta l \quad (3)$$

Now the energy ΔW stored in the volume Δv is, from (3-11-5),

$$\Delta W = \frac{1}{2} \Delta C \Delta V^2 \quad (4)$$

Substituting (2) for ΔC and (3) for ΔV in (4), we have

$$\Delta W = \frac{1}{2} \epsilon E^2 \Delta v \quad (5)$$

Dividing (5) by Δv and taking the limit of the ratio $\Delta W/\Delta v$ as Δv approaches zero, we obtain the energy per volume, or *energy density*, w at the point around which Δv shrinks to zero. Thus†

$w = \lim_{\Delta v \rightarrow 0} \frac{\Delta W}{\Delta v} = \frac{1}{2} \epsilon E^2 \quad (\text{J m}^{-3}) \quad (7)$

† For the more general case of a nonisotropic medium in which D and E may not be in the same direction,

$$w = \frac{1}{2} D \cdot E \quad (6)$$

Now the total energy W stored by the capacitor of Fig. 3-10 will be given by the integral of the energy density w over the entire region in which the electric field \mathbf{E} has a value;

$$W = \int_v w \, dv = \frac{1}{2} \int_v \epsilon E^2 \, dv \quad (8)$$

where the integration is taken throughout the region between the plates. For simplicity it is assumed that the field is uniform between the plates and that there is no fringing of the field at the edges of the capacitor. Thus, evaluating (8),

$$W = \frac{1}{2} \epsilon E^2 A l = \frac{1}{2} DAEl = \frac{1}{2} QV \quad (J) \quad (9)$$

where A = area of one capacitor plate, m^2

l = spacing between capacitor plates, m

This result, obtained by integrating the energy density throughout the volume between the plates of the capacitor, is identical with the relation given by (3-11-5).

3-13 FIELDS OF SIMPLE CHARGE CONFIGURATIONS

In many problems it is desirable to know the distribution of the electric field and the associated potential. For example, if the field intensity exceeds the breakdown value for the dielectric medium, sparking, or corona, can occur. From a knowledge of the field distribution, the charge surface density on conductors bounding the field and the capacitance between them can also be determined.

In the following sections the field and potential distributions for a number of simple geometric forms are discussed. The field and potential distributions around point charges, charged spheres, line charges, and charged cylinders are considered first. The field and potential distributions of these configurations can be expressed by relatively simple equations. The extension of these relations by the method of images to situations involving large conducting sheets or ground planes is then considered. Finally, the field and potential distributions for some conductor configurations which are not easily treated mathematically are found by a simple graphical method known as *field mapping*. Many field problems are conveniently solved by the use of computers; such methods are discussed in Chap. 7.

3-14 FIELD DISTRIBUTIONS

Field and potential distributions may be presented in various ways. For example, a graph of the variation of the magnitude of the electric field E and of the electric potential V along a reference line may give the desired information. This is illustrated

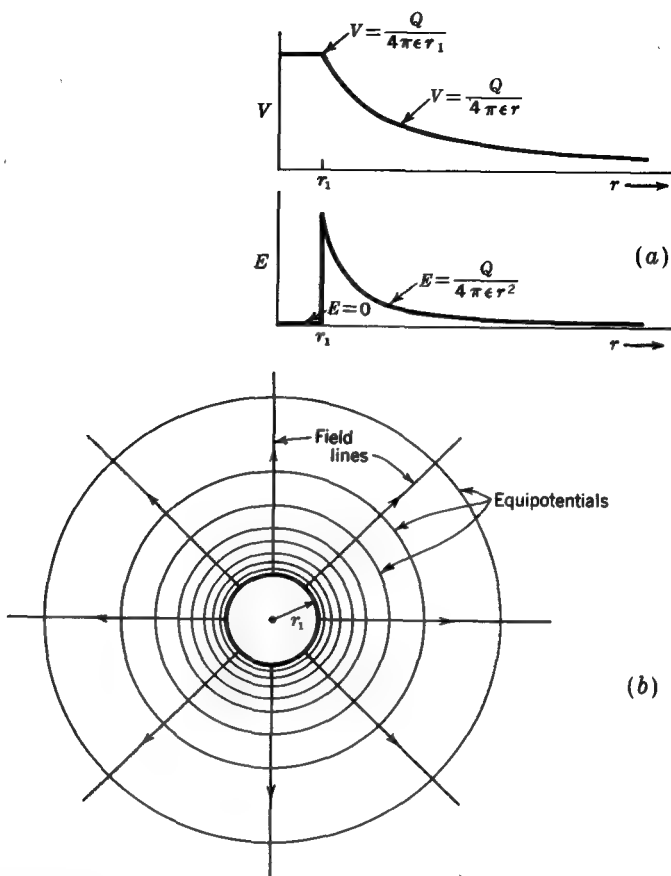


FIGURE 3-12
Variation of electric field E and potential V of an isolated charged conducting sphere of radius r_1 .

by the curves for E and V in Fig. 3-12a for the field and potential along a radial line extending from the center of a charged conducting sphere of radius r_1 . Or the field and potential distributions may be indicated by a contour map, or graph, as in Fig. 3-12b. In this map the radial lines indicate the direction of the electric field, while the circular contours are equipotential lines. In this diagram the potential difference between contours is a constant.

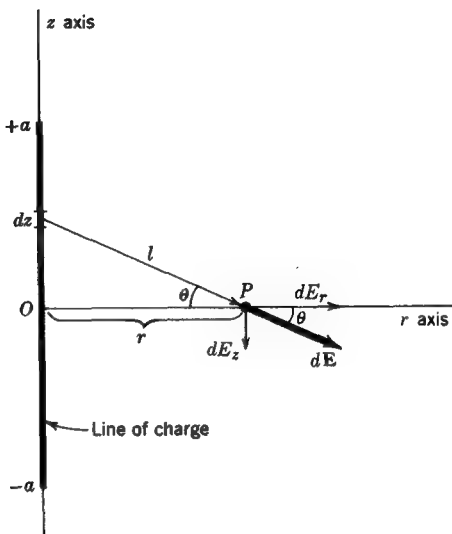


FIGURE 3-13
Thin line of charge of length $2a$.

3-15 FIELD OF A FINITE LINE OF CHARGE

Consider now the field produced by a thin line of electric charge. Let a positive charge Q be distributed uniformly as an infinitesimally thin line of length $2a$ with center at the origin, as in Fig. 3-13. The linear charge density ρ_L (charge per unit length) is then

$$\rho_L = \frac{Q}{2a} \quad (1)$$

where ρ_L is in coulombs per meter when Q is in coulombs and a is in meters.

At the point P on the r axis, the infinitesimal electric field $d\mathbf{E}$ due to an infinitesimal length of wire dz is the same as from a point charge of magnitude $\rho_L dz$. Thus,

$$d\mathbf{E} = \mathbf{l} \frac{\rho_L dz}{4\pi\epsilon_0 l^2} \quad (2)$$

where $l = \sqrt{r^2 + z^2}$

\mathbf{l} = unit vector in direction of l

Since the z axis in Fig. 3-13 is an axis of symmetry, the field has only z and r components. These are

$$dE_r = dE \cos \theta = dE \frac{r}{l} \quad (3)$$

and

$$dE_z = dE \sin \theta = dE \frac{z}{l} \quad (4)$$

The resultant or total r component E_r of the field at a point on the r axis is obtained by integrating (3) over the entire line of charge. That is,

$$E_r = \frac{\rho_L r}{4\pi\epsilon} \int_{-a}^{+a} \frac{dz}{l^3} = \frac{\rho_L r}{4\pi\epsilon} \int_{-a}^{+a} \frac{dz}{\sqrt{(r^2 + z^2)^3}}$$

and

$$E_r = \frac{\rho_L a}{2\pi\epsilon r \sqrt{r^2 + a^2}} \quad (5)$$

By symmetry the resultant z component E_z of the field at a point on the r axis is zero. Hence the total field \mathbf{E} at points along the r axis is radial and is given by

$$|\mathbf{E}| = E_r = \frac{\rho_L a}{2\pi\epsilon r \sqrt{r^2 + a^2}} \quad (6)$$

This relation gives the field as a function of r at points on the r axis for a *finite* line of charge of length $2a$ and uniform charge density ρ_L .

3-16 FIELD OF AN INFINITE LINE OF CHARGE

Consider that the line of charge in Fig. 3-13 extends to infinity in both positive and negative z directions. By dividing the numerator and denominator of (3-15-6) by a and letting a become infinite the electric field intensity due to an *infinite line of positive charge* is found to be

$$|\mathbf{E}| = E_r = \frac{\rho_L}{2\pi\epsilon r} \quad (1)$$

The potential difference V_{21} between two points at radial distances r_2 and r_1 from the infinite line of charge is then the work per unit charge required to transport a positive test charge from r_2 to r_1 . Assume that $r_2 > r_1$. This potential difference

is given by the line integral of E_r from r_2 to r_1 , the potential at r_1 being higher than at r_2 if the line of charge is positive. Thus

$$V_{21} = - \int_{r_2}^{r_1} E_r dr = \frac{\rho_L}{2\pi\epsilon} \int_{r_1}^{r_2} \frac{dr}{r}$$

or

$$V_{21} = \frac{\rho_L}{2\pi\epsilon} \ln r \Big|_{r_1}^{r_2} = \frac{\rho_L}{2\pi\epsilon} \ln \frac{r_2}{r_1} \quad (2)\dagger$$

3-17 INFINITE CYLINDER OF CHARGE

If the charge is distributed uniformly along a cylinder of radius r_1 instead of concentrated along an infinitesimally thin line, the field external to the cylinder is given by (3-16-1) for $r \geq r_1$. Inside the cylinder, $\mathbf{E} = 0$.

The potential difference between the cylinder and points outside the cylinder is given by (3-16-2), where $r_2 > r_1$ and ρ_L is the charge per unit length of the cylinder. Inside the cylinder the potential is the same as the potential at the surface ($r = r_1$).

3-18 INFINITE COAXIAL TRANSMISSION LINE

A coaxial transmission line consists of two conductors arranged coaxially, as shown by the cross section of Fig. 3-14a. This is a common type of transmission line, and much can be learned about its properties from a consideration of its behavior under static conditions. Let a fixed potential difference be applied between the inner and

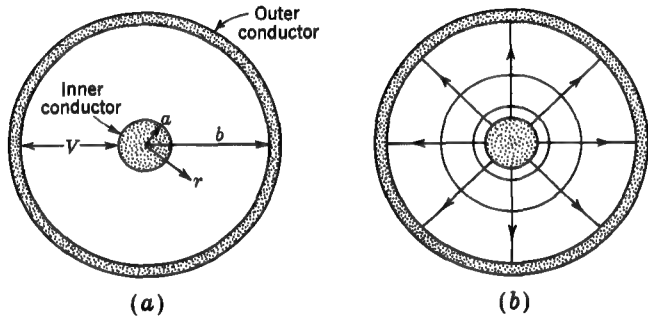


FIGURE 3-14
Coaxial transmission line.

[†] If we put $r = r_1$, then $V = 0$ at $r = r_2$. That is, the surface for which $r = r_2$ becomes a reference surface with respect to which the potential values are measured.

outer conductors of an infinitely long coaxial line so that the charge Q per unit length l of one line is ρ_L . The field is confined to the space between the two conductors. The field lines are radial, and the equipotential lines are concentric circles, as indicated in Fig. 3-14b. The magnitude of the field at a radius r is given by (3-16-1), where $a \leq r \leq b$, and where ρ_L is the charge per unit length on the inner conductor. The potential difference V between the conductors is, from (3-16-2),

$$V = \frac{\rho_L}{2\pi\epsilon} \ln \frac{b}{a} \quad (1)$$

Since capacitance is given by the ratio of charge to potential, $C = Q/V$. Dividing by length l , we have $C/l = (Q/l)/V$. The ratio Q/l equals the linear charge density ρ_L (C m^{-1}). Hence, the capacitance per unit length C/l of the coaxial line is

$$\frac{C}{l} = \frac{\rho_L}{V} = \frac{2\pi\epsilon}{\ln(b/a)} \quad (\text{F m}^{-1}) \quad (2)$$

where ϵ is the permittivity of the medium between conductors.

Since $\epsilon = \epsilon_0 \epsilon_r$, where $\epsilon_0 = 8.85 \text{ pF m}^{-1}$, (2) can be expressed more conveniently as

$$\frac{C}{l} = \frac{55.6\epsilon_r}{\ln(b/a)} = \frac{24.2\epsilon_r}{\log(b/a)} \quad (\text{pF m}^{-1}) \quad (3)$$

where ϵ_r = relative permittivity of medium between conductors

b = inside radius of outer conductor

a = radius of inner conductor (in same units as b)

3-19 TWO INFINITE LINES OF CHARGE

Let two infinite parallel lines of charge be separated by a distance $2s$ as in Fig. 3-15. Assume that the linear charge density of the two lines is equal but of opposite sign. The resultant electric field \mathbf{E} at a point P , distant r_1 from the negative line and r_2 from the positive line, is then the vector sum of the field of each line taken alone.

Let the origin of the coordinates in Fig. 3-15 be the reference for potential. Imagine that only the positively charged line is present. Then, from (3-16-2) the potential difference between P and the origin is

$$V_+ = \frac{\rho_L}{2\pi\epsilon} \ln \frac{s}{r_2} \quad (1)$$

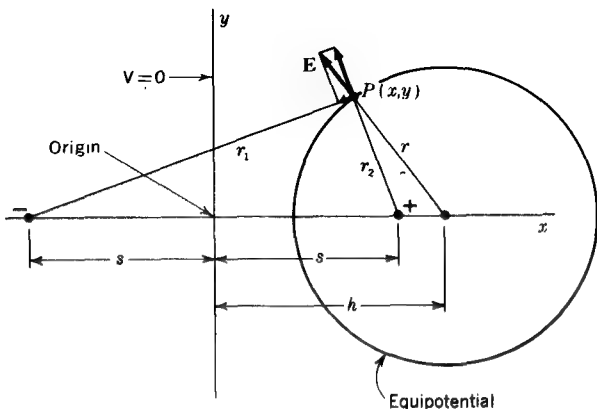


FIGURE 3-15
Two infinite lines of charge separated by a distance $2s$.

Similarly for the negatively charged line

$$V_- = -\frac{\rho_L}{2\pi\epsilon} \ln \frac{s}{r_1} \quad (2)$$

With both lines present the total potential difference V between P and the origin is the algebraic sum of (1) and (2), or

$$V = V_+ + V_- = \frac{\rho_L}{2\pi\epsilon} \ln \frac{r_1}{r_2} \quad (3)$$

If V in (3) is a constant, (3) is the equation of an equipotential line. The form of the equipotential line will be more apparent if (3) is transformed in the following manner. From (3)

$$\ln \frac{r_1}{r_2} = \frac{2\pi\epsilon V}{\rho_L} \quad (4)$$

and

$$\frac{r_1}{r_2} = e^{2\pi\epsilon V/\rho_L} \quad (5)$$

Since $2\pi\epsilon V/\rho_L$ is a constant for any equipotential line, the right side of (5) is a constant K . Thus

$$e^{2\pi\epsilon V/\rho_L} = K \quad \text{and} \quad r_1 = Kr_2 \quad (6)$$

The coordinates of the point P in Fig. 3-15 are (x, y) , so that $r_1 = \sqrt{(s+x)^2 + y^2}$ and $r_2 = \sqrt{(s-x)^2 + y^2}$. Substituting these values of r_1 and r_2 in (6), squaring, and rearranging yields

$$x^2 - 2xs \frac{K^2 + 1}{K^2 - 1} + s^2 + y^2 = 0 \quad (7)$$

Adding $s^2(K^2 + 1)^2/(K^2 - 1)^2$ to both sides of (7) to complete the square on the left side, we have

$$\left(x - s \frac{K^2 + 1}{K^2 - 1}\right)^2 + y^2 = \left(\frac{2Ks}{K^2 - 1}\right)^2 \quad (8)$$

This is the equation of a circle having the form

$$(x - h)^2 + y^2 = r^2 \quad (9)$$

where x, y = coordinates of point on circle

h = x coordinate of center of circle

r = radius of circle

Comparing (8) and (9), it follows that the equipotential curve passing through the point (x, y) is a circle of radius

$$r = \frac{2Ks}{K^2 - 1} \quad (10)$$

with its center on the x axis at a distance from the origin

$$h = s \frac{K^2 + 1}{K^2 - 1} \quad (11)$$

An equipotential line of radius r with center at $(h, 0)$ is shown in Fig. 3-15. As K increases, corresponding to larger equipotentials, r approaches zero and h approaches s , so that the equipotentials are smaller circles with their centers more nearly at the line of charge. This is illustrated by the additional equipotential circles in Fig. 3-16. The potential is zero along the y axis. That is, $V = 0$ at $x = 0$. Thus, the plane $x = 0$ is the reference plane for potential.

Field lines are also shown in Fig. 3-16. These are everywhere orthogonal to the potential circles and also are circles with their centers on the y axis.

3-20 INFINITE TWO-WIRE TRANSMISSION LINE

The discussion of two infinite lines of charge in the previous section is easily extended to the case of an infinite line consisting of two parallel cylindrical conductors or wires. This is a type of transmission line commonly used in practice, and much can be learned

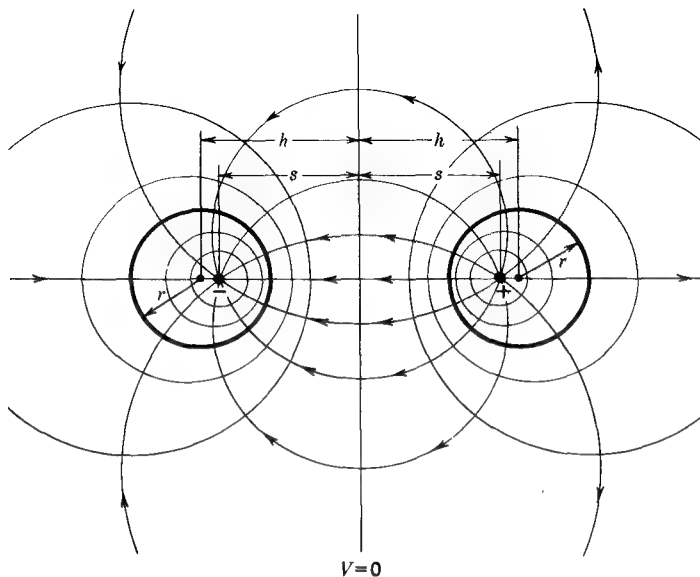


FIGURE 3-16

Field and equipotential lines around two infinite parallel lines of charge or around an infinite two-conductor transmission line.

about its properties from a consideration of its behavior under static conditions. Let a fixed potential difference be applied between the conductors so that the charge per unit length of each conductor is ρ_L .

The surface of the wire is an equipotential surface, and therefore an equipotential circle in Fig. 3-16 will coincide with the wire surface. Thus, the heavy circles of radius r and center-to-center spacing $2h$ can represent the two wires. The field and potential distributions external to the wire surfaces are the same as if the field were produced by two infinitesimally thin lines of charge with a spacing of $2s$. The field inside the wires is, of course, zero, and the potential is the same as on the surface. The charge is not uniformly distributed on the wire surface but has higher density on the adjacent sides of the conductors.

The potential difference V_c between one of the conductors and a point midway between them is, from (3-19-3) and (3-19-6),

$$V_c = \frac{\rho_L}{2\pi\epsilon} \ln K \quad (1)$$

The value of K can be expressed in terms of the radius r and half the center-to-center spacing h by eliminating s from (3-19-10) and (3-19-11) and solving for K , obtaining

$$K = \frac{h}{r} + \sqrt{\frac{h^2}{r^2} - 1} \quad (2)$$

The potential difference V_{2c} between the two conductors is then

$$V_{2c} = \frac{\rho_L}{\pi\epsilon} \ln\left(\frac{h}{r} + \sqrt{\frac{h^2}{r^2} - 1}\right) \quad (3)$$

To find the *capacitance per unit length*, C/l , of the two-conductor line we take the ratio of the charge per unit length on one conductor to the difference of potential between the conductors, i.e.,

$$\boxed{\frac{C}{l} = \frac{\rho_L}{V_{2c}} = \frac{12.1\epsilon_r}{\log[(h/r) + \sqrt{(h/r)^2 - 1}]}} \quad (\text{pF m}^{-1}) \quad (4)$$

where ϵ_r = relative permittivity of the medium surrounding the conductors, dimensionless

h = half center-to-center-spacing

r = conductor radius (same units as h)

3-21 INFINITE SINGLE-WIRE TRANSMISSION LINE

A single-wire transmission line with ground return is another form sometimes used. Let the conductor radius be r and the height of the center of the conductor above ground be h . Assume that the conductor has a positive charge ρ_L per unit length and that the ground is at zero potential.

The field and potential distribution of this type of line is readily found by the *theory of images*.† Thus, if the ground is removed and an identical conductor with charge $-\rho_L$ per unit length placed as far below ground level as the other conductor is above, the situation is the same as for a two-conductor line (Fig. 3-16). The conductor which replaces the ground is called the *image* of the upper conductor. The field and potential distribution for the single conductor line is then as illustrated by Fig. 3-17.

The difference in potential between the single conductor and the ground is as given by (3-20-1) or by one-half of (3-20-3). The capacitance per unit length C/l is twice the value given by (3-20-4), or

$$\frac{C}{l} = \frac{24.2\epsilon_r}{\log[(h/r) + \sqrt{(h/r)^2 - 1}]} \quad (\text{pF m}^{-1}) \quad (1)$$

† The theory of images is discussed more fully in Sec. 7-15.

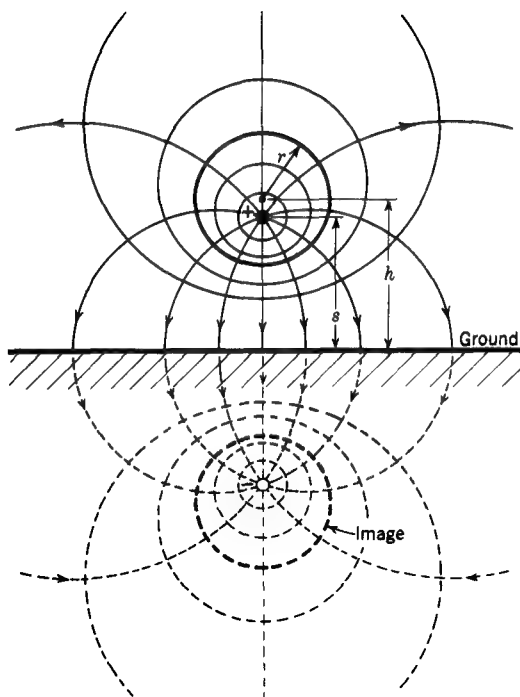


FIGURE 3-17
Conductor over a metallic ground plane.

3-22 GRAPHICAL MAPPING OF STATIC ELECTRIC FIELDS; FIELD CELLS

Not all conductor configurations can be treated mathematically as readily as those above. Other methods are discussed in Chap. 7. However, for two-dimensional problems† a very effective *graphical-field-mapping*‡ method is applicable. Some experience in graphical field mapping is valuable because it is based on and emphasizes such important fundamental properties of static electric fields as the following:

- 1 Field and potential lines intersect at right angles.§
- 2 The surface of a conductor is an equipotential surface.
- 3 The field meets a conducting surface normally.
- 4 In a uniform field, the potential varies linearly with distance.

† By a two-dimensional problem is meant one in which the conductor configuration can be shown by a single cross section, all cross sections parallel to it being the same.

‡ A. D. Moore, "Fundamentals of Electrical Design," McGraw-Hill Book Company, New York, 1927.

§ Except at singular points, as at point P in Fig. 2-14.

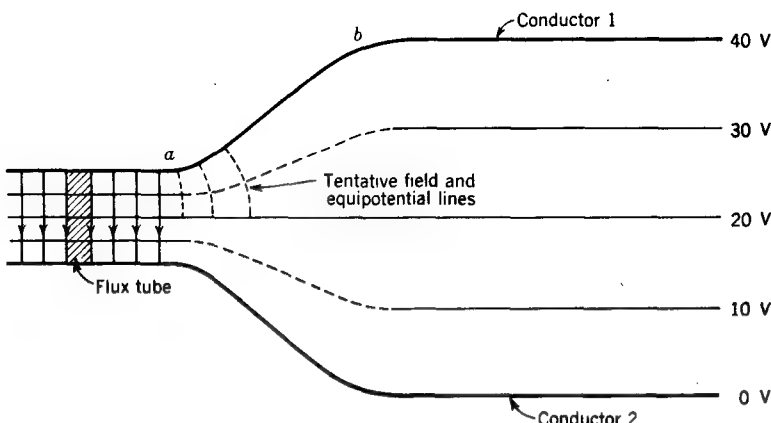


FIGURE 3-18
Cross section of two sheet conductors with partially completed field map.

- 5 A flux tube is parallel to the field,[†] and the electric flux is constant over any cross section of a flux tube.
- 6 A tube of flux originates on a positive charge and ends on an equal negative charge.

Graphical field mapping will be introduced with the aid of an example. Consider two charged sheet conductors 1 and 2 as shown in cross section in Fig. 3-18. The sheets extend infinitely far to the left and right and also normal to the page. This is a two-dimensional problem, all cross sections parallel to the page being the same. Therefore, the field and potential distribution everywhere between the sheets will be known if it can be found for a two-dimensional cross section such as shown in Fig. 3-18. Let the potential difference between the conductors be 40 V, with the upper conductor positive and the lower conductor at zero potential. To the left of *a* and to the right of *b* the field is uniform, so that equipotential surfaces 10 V apart are equally spaced as indicated, the conductor surfaces being equipotentials at 0 and 40 V. Between *a* and *b* the conductor spacing changes, and the equipotentials may be drawn tentatively as shown by the dashed lines.

The next step in the mapping procedure is to draw field lines from conductor 1 to conductor 2 in the uniform field region to the left of *a* with the spacing equal to that between the equipotentials. In this way the region is divided into squares. Each square is the end surface of a rectangular volume, or cell, of depth *d* into the page. A stack, or series, of squares bounded by the same field lines represents the sidewall

[†] The sidewalls of a flux tube are field lines.

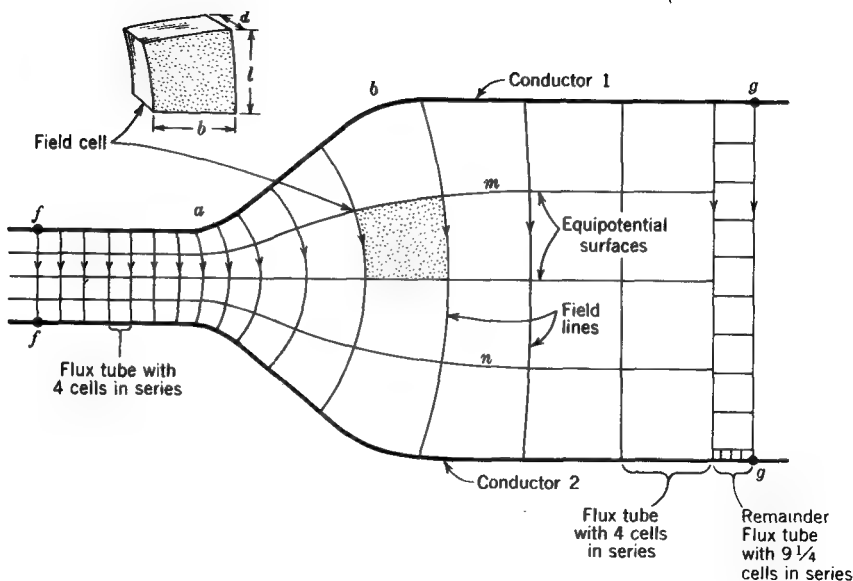


FIGURE 3-19

Cross section of two sheet conductors with completed field map. Inset shows three-dimensional view of a field cell.

of a rectangular flux tube extending between the positive charge on one conductor to the negative charge on the other. The field map is next extended to the right by drawing *field lines as nearly normal to the equipotentials as possible*, with the field lines spaced so that the areas formed are as nearly square as possible. After one or two revisions of the tentative equipotentials between a and b and also of the field lines, it should be possible to remap the region to the right of a so that field and equipotential lines are everywhere orthogonal and the areas between the lines are all *squares* or *curvilinear squares*. The completed field map is shown in Fig. 3-19.

By a *curvilinear square* is meant *an area that tends to yield true squares as it is subdivided into smaller and smaller areas by successive halving of the equipotential interval and the flux per tube*. A partially subdivided curvilinear square is illustrated in Fig. 3-20.

A field map, such as shown in Fig. 3-19, divides the field into many squares each of which represents a side of a *field cell*. These field cells have a depth d (into the page) as suggested by the three-dimensional view of the typical field cell in Fig. 3-19. The cell has a length l (parallel to the field) and a width b . The sidewalls of a field cell are the walls of a flux tube (parallel to the field), while the top and bottom coincide

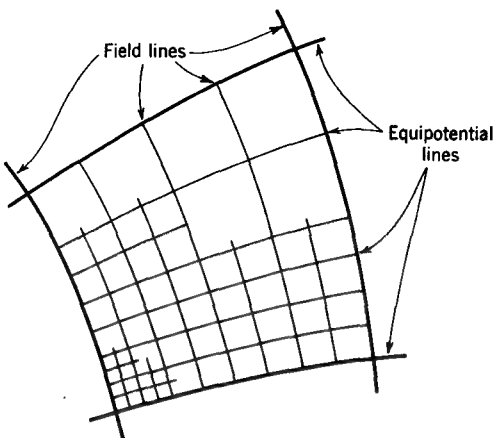


FIGURE 3-20
Partially subdivided curvilinear square.

with equipotential surfaces. As curvilinear cells are subdivided into smaller cells, their end areas tend to become true squares. The subdivided cells are always of depth d (into the page), the same as the larger cells. Thus, a *field cell*, or simply a *cell*, may be defined as a *curvilinear square volume*.

If thin sheets of metal foil are applied to the equipotential surfaces of a field cell, we have a *field-cell capacitor*. The capacitance C of a parallel-plate capacitor is

$$C = \frac{\epsilon A}{l} \quad (1)$$

where ϵ = permittivity of medium

A = area of plates

l = spacing of plates

Applying this relation to a field-cell capacitor with a square end ($b = l$), we have for the capacitance C_0 of the field cell

$$C_0 = \frac{\epsilon b d}{l} = \epsilon d \quad (2)$$

Dividing by d , we obtain the capacitance per unit depth of a field cell as

$$\frac{C_0}{d} = \epsilon$$

(3)

where ϵ is the permittivity of the medium in farads per meter.

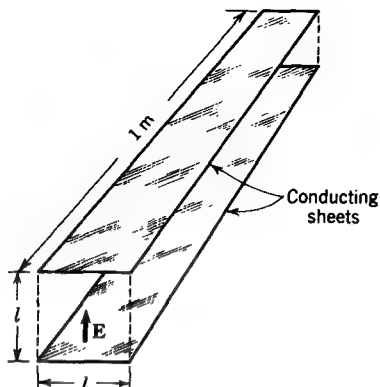


FIGURE 3-21

A field-cell capacitor has a capacitance per unit depth equal to the permittivity ϵ of the medium. For air ($\epsilon = \epsilon_0$) the capacitance of the capacitor shown is 8.85 pF.

Thus, the significance of the value of ϵ is that it is the capacitance per unit depth of a field-cell capacitor. For example, a field-cell capacitor of unit depth in a medium of air (or vacuum) has a capacitance of 8.85 pF. Such a capacitor is illustrated in Fig. 3-21.[†]

Any field cell can be subdivided into smaller square-ended cells with as many cells in parallel as in series. Hence the capacitance[‡] per unit depth of *any* field cell, large or small, exactly square or curvilinear is equal to ϵ .

In a field map, such as in Fig. 3-19, most of the area is divided into "regular" cells with four in series for each flux tube. These cells all have the same potential difference across them (10 V). Hence these cells may be defined as *cells of the same kind*. The remaining area of the map consists of a fractional, or remainder, flux tube. This tube is also divided into cells. These cells are of two kinds, both different from those in the rest of the map. One kind of cell in the remainder flux tube has about 4.3 V across it and the other kind about 1 V across it. There are nine 4.3-V cells and four 1-V cells.

Any field cell has the same capacitance per unit depth. Many additional properties are common to *field cells of the same kind*. These cells of the same kind have the same potential differences across them. In uniform fields the areas of the ends of those cells are the same, but in nonuniform fields the areas will not be the same.

[†] The capacitance of an isolated capacitor such as shown in Fig. 3-21 is somewhat greater than 8.85 pF because of fringing of the field. However, a field cell represents only a portion of a more extensive field, and its sides are parallel to the field (no fringing).

[‡] It is understood that this capacitance is that which would be obtained if the *field cell* were made into a *field-cell capacitor* by placing thin sheets of metal foil coincident with its equipotential surfaces (if no conductor is already present).

Since the capacitance per unit depth of any cell of the same kind is the same, it follows that the electric flux through any cell of the same kind is the same ($Q/d = VC/d$). Thus, the 10-V cells in Fig. 3-19 have a flux of 10ϵ C/unit depth, while the 4.3- and 1-V cells have 4.3ϵ and ϵ C/unit depth, respectively.

Now the average flux density D at the equipotential surface of a field cell is given by

$$D = \frac{Q}{bd} = \rho_s \quad (\text{C m}^{-2}) \quad (4)$$

where Q = total charge on foil at equipotential surface of field cell = total flux ψ through cell, C

b = width of cell, m

d = depth of cell, m

ρ_s = average surface charge density on foil at equipotential surface, C m^{-2}

Hence, the average flux density is inversely proportional to the field-cell or flux-tube width. Also the average surface charge density ρ_s at a conducting surface is inversely proportional to the width of the field cell or flux tube at the surface. For example, the spacing of conductors 1 and 2 to the right of b in Fig. 3-19 is 4 times that to the left of a ; so in the uniform field region to the left of a the surface charge density ρ_s is 4 times the value of ρ_s in the uniform field region to the right of b . The surface charge density is even smaller than to the right of b in the region of concave conductor curvature near b and somewhat larger than to the left of a in the region of convex conductor curvature near a .

Since $E = D/\epsilon$, the field intensity is also inversely proportional to the cell width, or length ($E = V/l$). Furthermore, the energy $W (= \frac{1}{2}QV)$ stored in any cell of the same kind is the same. It follows that the average energy density w is inversely proportional to the area of the end of the cell ($= bl$ for a square-ended cell). For example, the energy density in the uniform field region to the left of a in Fig. 3-19 is 16 times the energy density in the uniform field region to the right of b .

To summarize, the properties of an accurate electric field map† are as follows:

- 1 The capacitance of any field cell is the same.
- 2 The capacitance C_0 per unit depth of any field cell is equal to the permittivity ϵ of the medium.
- 3 The potential difference across any field cell of the same kind is the same.
- 4 The flux ψ through any field cell of the same kind is the same.
- 5 The flux ψ over any cross section of a flux tube is the same.
- 6 The average flux density D in any cell of the same kind is inversely proportional to the width of the cell or flux tube.

† In a single medium of uniform permittivity.

- 7 The average charge density ρ_s at the conducting boundary of any cell of the same kind is inversely proportional to the width of the cell at the boundary.
- 8 The average field intensity E in any cell of the same kind is inversely proportional to the cell width.
- 9 The energy stored in any cell of the same kind is the same.
- 10 The average energy density w in any cell of the same kind is inversely proportional to the area of the end of the cell. (This is the area that appears in the field map.)

In order to test the accuracy of a field map, and hence the accuracy with which the above properties hold for a particular map, the curvilinear squares of the map can be further subdivided by halving the equipotential interval and halving the flux per tube, as in Fig. 3-20. If the smaller regions so produced tend to become more nearly true squares, the field is accurately mapped. However, if the regions tend to become rectangles, the map is inaccurate and another attempt should be made. Also field and equipotential lines should intersect orthogonally. It is especially important that this rule be observed at all stages of making a field map. Often it is better to erase and begin again than to try to revise an inaccurate map. *In graphical field mapping an eraser is as important as a pencil.*

With analog and digital computers and methods discussed in Chap. 7, a process equivalent to graphical field mapping is carried out. With the digital computer, iteration is continued until no further change occurs in the map. Experience in graphical field mapping is a valuable prelude to computer mapping.

EXAMPLE Referring to Fig. 3-19, let the conductor separation at ff' be 10 mm and at gg' be 40 mm, and let the conductors have a depth (into the page) of 200 mm. If the conductors end at ff' and gg' , and if fringing of the field is neglected, find the capacitance C of the resulting capacitor. The medium in the capacitor is air.

SOLUTION The method of solution will be to evaluate the series-parallel combination of capacitors formed by the individual cells.

Each cell has a capacitance

$$C_0 = \epsilon_0 d = 8.85 \times 0.2 = 1.77 \text{ pF}$$

The capacitance between the ends of each flux tube with 4 cells in series is then

$$\frac{1.77}{4} = 0.443 \text{ pF}$$

The capacitance between the ends of the remainder flux tube with 9.25 cells in series is

$$\frac{1.77}{9.25} = 0.191 \text{ pF}$$

There are fifteen 4-cell tubes and one remainder (9.25-cell) tube. Hence the total capacitance C between ff and gg is the sum of the capacitances of all the flux tubes, or

$$C = (15 \times 0.443) + 0.191 = 6.83 \text{ pF}$$

The above calculation is somewhat simplified if each cell is arbitrarily assigned a capacitance of unity. On this basis the total capacitance in arbitrary units is given by

$$\frac{15}{4} + \frac{1}{9.25} = 3.86 \text{ units}$$

and the total actual capacitance C is the product of this result and the actual capacitance of a cell, or

$$C = 3.86 \times (8.85 \times 0.2) = 6.83 \text{ pF}$$

Yet another method of calculation is to use the relation that the total capacitance C is given by

$$C = \frac{N}{n} C_0 \quad (5)$$

where N = number of cells (or flux tubes) in parallel

n = number of cells in series

C_0 = capacitance of one cell

and where all cells are of the same kind. Thus in the above example, counting in terms of the 10-V cells, we have

$$C = \frac{15.43}{4} \times (8.85 \times 0.2) = 6.83 \text{ pF}$$

Note that if we had wanted the capacitance of a capacitor with conductors coinciding with the equipotentials m and n (Fig. 3-19) and of 200 mm depth, the cells in series would be reduced to two and the capacitance doubled. In this way the capacitance of any conductor configuration conforming to the equipotential surfaces of a field map can be easily calculated.

3-23 DIVERGENCE OF THE FLUX DENSITY \mathbf{D}

In Sec. 2-17 Gauss' law is applied to surfaces enclosing finite volumes, and it is shown that the normal component of the flux density \mathbf{D} integrated over a closed surface equals the electric charge enclosed. By an extension of this relation to surfaces enclosing infinitesimal volumes we are led to a useful relation called *divergence*.

Let Δv be a small but finite volume. If we assume a uniform charge density throughout the volume, the charge ΔQ enclosed is the product of the volume charge

density ρ and the volume Δv . By Gauss' law the charge enclosed is also equal to the integral of the normal component D_n of the flux density over the surface of the volume Δv . Thus,

$$\oint_s D_n ds = \Delta Q = \rho \Delta v \quad (1)$$

and

$$\frac{\oint_s D_n ds}{\Delta v} = \rho \quad (2)$$

If the charge density is not uniform throughout Δv , we may take the limit of (2) as Δv shrinks to zero, obtaining the charge density ρ at the point around which Δv collapses. The limit of (2) as Δv approaches zero is called the divergence of \mathbf{D} , written $\operatorname{div} \mathbf{D}$ or $\nabla \cdot \mathbf{D}$. Hence

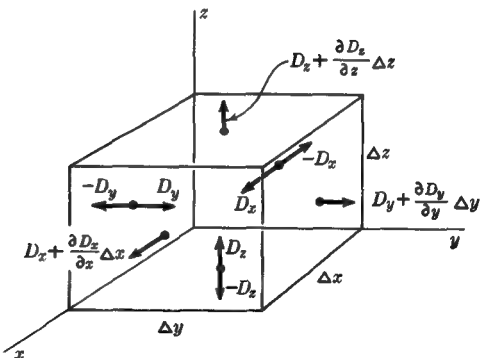
$$\lim_{\Delta v \rightarrow 0} \frac{\oint_s D_n ds}{\Delta v} = \operatorname{div} \mathbf{D} = \rho \quad (\text{C m}^{-3}) \quad (3)$$

Whereas the integral of the normal component of \mathbf{D} over a finite volume yields the *free charge* enclosed, the divergence of \mathbf{D} gives the *free charge density at a point*. If the charge is zero at a point, it follows that the charge density is zero and also that the divergence of \mathbf{D} is zero at that point. It is important to note that the divergence of \mathbf{D} is a scalar point function.

Let us now discuss divergence in a more formal way, developing it as a differential expression. A small volume $\Delta x \Delta y \Delta z = \Delta v$ is placed in an electric field with flux density \mathbf{D} , having components D_x , D_y , and D_z in the three coordinate directions as shown in Fig. 3-22. The total flux density \mathbf{D} is related to its components by

$$\mathbf{D} = \hat{x} D_x + \hat{y} D_y + \hat{z} D_z \quad (4)$$

FIGURE 3-22
Construction used to develop differential expression for divergence of \mathbf{D} .



The normal outward component of \mathbf{D} at the back face is $-D_x$ since the field is directed inward. If the field changes between the back and front faces, the normal component of \mathbf{D} at the front face can, by Taylor's theorem, be represented by an infinite series,

$$D_x + \frac{\partial D_x}{\partial x} \frac{\Delta x}{1} + \frac{\partial^2 D_x}{\partial x^2} \frac{\Delta x^2}{2!} + \frac{\partial^3 D_x}{\partial x^3} \frac{\Delta x^3}{3!} + \dots \quad (5)$$

When Δx is very small, the square and higher-order terms may be neglected, so that at the front face we have for the normal component of \mathbf{D}

$$D_x + \frac{\partial D_x}{\partial x} \Delta x \quad (6)$$

In like manner the normal component of \mathbf{D} at the left side face is $-D_y$, and at the right side face is

$$D_y + \frac{\partial D_y}{\partial y} \Delta y \quad (7)$$

Similarly at the bottom face it is $-D_z$ and at the top face is

$$D_z + \frac{\partial D_z}{\partial z} \Delta z \quad (8)$$

The outward flux of \mathbf{D} over the back face is

$$-D_x \Delta y \Delta z \quad (9)$$

and over the front face is

$$\left(D_x + \frac{\partial D_x}{\partial x} \Delta x \right) \Delta y \Delta z \quad (10)$$

Adding up the outward flux of \mathbf{D} over the entire volume, we obtain for the total flux

$$\begin{aligned} \Delta\psi = & \left(-D_x + D_x + \frac{\partial D_x}{\partial x} \Delta x \right) \Delta y \Delta z \\ & + \left(-D_y + D_y + \frac{\partial D_y}{\partial y} \Delta y \right) \Delta x \Delta z + \left(-D_z + D_z + \frac{\partial D_z}{\partial z} \Delta z \right) \Delta x \Delta y \end{aligned} \quad (11)$$

which simplifies to

$$\Delta\psi = \left(\frac{\partial D_x}{\partial x} + \frac{\partial D_y}{\partial y} + \frac{\partial D_z}{\partial z} \right) \Delta x \Delta y \Delta z \quad (12)$$

From Gauss' law we know that the total electric flux over the surface of the volume (or integral of the normal component of \mathbf{D} over the surface of the volume) is equal to

the charge enclosed. The charge enclosed is also equal to the integral of the charge density ρ over the volume. Therefore

$$\Delta\psi = \oint_s D_n ds = \left(\frac{\partial D_x}{\partial x} + \frac{\partial D_y}{\partial y} + \frac{\partial D_z}{\partial z} \right) \Delta v = \oint_v \rho dv \quad (13)$$

Dividing by Δv and taking the limit as Δv approaches zero, we obtain the divergence of \mathbf{D} . Thus,

$$\lim_{\Delta v \rightarrow 0} \frac{\oint_s D_n ds}{\Delta v} = \frac{\partial D_x}{\partial x} + \frac{\partial D_y}{\partial y} + \frac{\partial D_z}{\partial z} = \rho \quad (14)$$

and

$$\text{div } \mathbf{D} = \frac{\partial D_x}{\partial x} + \frac{\partial D_y}{\partial y} + \frac{\partial D_z}{\partial z} = \rho \quad (15)$$

The center member of (15) is a differential relation for the divergence of \mathbf{D} expressed in rectangular coordinates. The divergence of \mathbf{D} can also be written as the scalar, or dot product of the operator ∇ and \mathbf{D} . That is,

$$\text{div } \mathbf{D} = \nabla \cdot \mathbf{D} \quad (16)$$

This is readily seen by expanding (16) into the expressions for ∇ and \mathbf{D} . Then

$$\nabla \cdot \mathbf{D} = \underbrace{\left(\hat{x} \frac{\partial}{\partial x} + \hat{y} \frac{\partial}{\partial y} + \hat{z} \frac{\partial}{\partial z} \right)}_{\nabla} \cdot \underbrace{\left(\hat{x} D_x + \hat{y} D_y + \hat{z} D_z \right)}_{\mathbf{D}} \quad (17)$$

Performing the multiplication indicated in (17) gives nine dot-product terms as follows:

$$\begin{aligned} \nabla \cdot \mathbf{D} &= \hat{x} \cdot \hat{x} \frac{\partial D_x}{\partial x} + \hat{y} \cdot \hat{x} \frac{\partial D_x}{\partial y} + \hat{z} \cdot \hat{x} \frac{\partial D_x}{\partial z} + \hat{x} \cdot \hat{y} \frac{\partial D_y}{\partial x} + \hat{y} \cdot \hat{y} \frac{\partial D_y}{\partial y} \\ &\quad + \hat{z} \cdot \hat{y} \frac{\partial D_y}{\partial z} + \hat{x} \cdot \hat{z} \frac{\partial D_z}{\partial x} + \hat{y} \cdot \hat{z} \frac{\partial D_z}{\partial y} + \hat{z} \cdot \hat{z} \frac{\partial D_z}{\partial z} \end{aligned} \quad (18)$$

The dot product of a unit vector on itself is unity, but the dot product of a vector with another vector at right angles is zero. Accordingly, six of the nine dot products in (18) vanish, but the three involving $\hat{x} \cdot \hat{x}$, $\hat{y} \cdot \hat{y}$, and $\hat{z} \cdot \hat{z}$ do not, and the product indicated by (17) becomes

$$\nabla \cdot \mathbf{D} = \frac{\partial D_x}{\partial x} + \frac{\partial D_y}{\partial y} + \frac{\partial D_z}{\partial z} \quad (19)$$

The dot product of the operator ∇ with a vector function is the divergence of the vector. The quantity $\nabla \cdot$ may be considered as a *divergence operator*. Thus the

divergence operator applied to a vector function yields a scalar function. For example, $\nabla \cdot \mathbf{D}$ (divergence of \mathbf{D}) is given in rectangular coordinates by the right side of (19) and is a scalar, being equal to the charge density ρ .

If \mathbf{D} is known everywhere, taking the divergence of \mathbf{D} enables us to find the sources (positive charge regions) and sinks (negative charge regions) responsible for the electric flux, and, hence, for \mathbf{D} .

3-24 MAXWELL'S DIVERGENCE EQUATION

The relation (3-23-15) that

$$\boxed{\nabla \cdot \mathbf{D} = \rho} \quad (1)$$

was developed by an application of Gauss' law to an infinitesimal volume. It is the fundamental differential relation for static electric fields. This relation is one of a set of four differential relations known as *Maxwell's equations*. The other three are developed in later chapters.

In a region free from charge, $\rho = 0$, and

$$\nabla \cdot \mathbf{D} = 0 \quad (2)$$

EXAMPLE As a simple nonelectrical example of divergence consider that a long hollow cylinder is filled with air under pressure. If the cover over one end of the cylinder is removed quickly, the air rushes out. It is apparent that the velocity of the air will be greatest near the open end of the cylinder, as suggested by the arrows representing the velocity vector \mathbf{v} in Fig. 3-23a. Suppose that the flow of air is free from turbulence, so that \mathbf{v} has only an x component. Let us assume that the velocity v in the cylinder is independent of y but is directly proportional to x , as indicated by

$$|\mathbf{v}| = v_x = Kx \quad (3)$$

where K is a constant of proportionality. The question is: What is the divergence of \mathbf{v} in the cylinder?

SOLUTION Apply the divergence operator to (3), giving

$$\nabla \cdot \mathbf{v} = \frac{\partial v_x}{\partial x} = K \quad (4)$$

Hence, the divergence of \mathbf{v} is equal to the constant K .

A velocity field can be represented graphically by lines showing the direction of \mathbf{v} with the density of the lines indicating the magnitude of \mathbf{v} . The velocity field in the cylinder

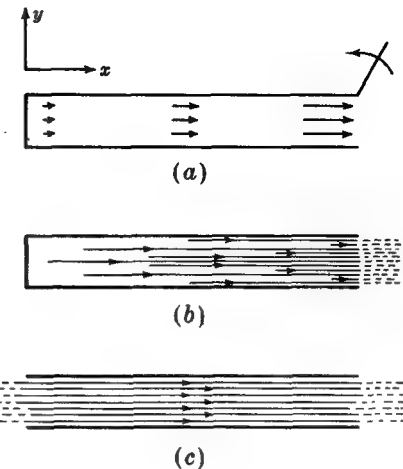


FIGURE 3-23

The velocity \mathbf{v} of air rushing from a tube has divergence (a) and (b). When air flows with uniform velocity through a tube open at both ends, as at (c), the divergence of \mathbf{v} is zero.

represented in this way is illustrated in Fig. 3-23b. We note that \mathbf{v} lines originate, i.e., have their source, throughout the cylinder, the number increasing with x . This indicates that \mathbf{v} increases as a function of x . This situation is concisely expressed by $\operatorname{div} \mathbf{v} = K$. That is, the divergence of \mathbf{v} has a constant value K throughout the cylinder, and this tells us that, assuming (3) to be correct, the source of the velocity field provided by the expanding air is uniformly distributed throughout the cylinder.

If, on the other hand, both ends of the cylinder are open and air passes through with the same velocity everywhere, v_x equals a constant and the divergence of \mathbf{v} is zero in the cylinder. In this case, the source of the velocity field must be somewhere external to the cylinder, and the velocity field diagram would be as shown in Fig. 3-23c.

If more lines enter a small volume† than leave it or more leave it than enter, the field has divergence. If the same number enter as leave the volume, the field has a zero divergence.

3-25 DIVERGENCE THEOREM

From Gauss' law (2-17-6) we have

$$\oint_s \mathbf{D} \cdot d\mathbf{s} = \oint_v \rho dv \quad (1)$$

where \mathbf{D} is integrated over the surface s and ρ is integrated throughout the volume v enclosed by s .

† In the limit an infinitesimal volume.

From (3-24-1) let us introduce $\nabla \cdot \mathbf{D}$ for ρ in (1), obtaining

$$\oint_s \mathbf{D} \cdot d\mathbf{s} = \oint_v \nabla \cdot \mathbf{D} dv \quad (2)$$

The relation stated in (2) is the *divergence theorem* as applied to the flux density \mathbf{D} , or *Gauss' theorem* (as distinguished from Gauss' law). This relation holds not only for \mathbf{D} , as in (2), but also for any vector function. In words, the divergence theorem states that *the integral of the normal component of a vector function over a closed surface s equals the integral of the divergence of that vector throughout the volume v enclosed by the surface s.*

3-26 DIVERGENCE OF D AND P IN A CAPACITOR

As further illustrations of the significance of divergence let us consider the charged parallel-plate capacitor of Fig. 3-24. A slab of paraffin fills the space between the plates except for the small air gaps. True charge of surface density ρ_s is present on the surface of the plates. Polarization charge of surface density ρ_{sp} is present on the surface of the paraffin.

According to (3) of Table 3-2, the relation of \mathbf{D} at a boundary is given by

$$D_{n1} - D_{n2} = \rho_s \quad (1)$$

where D_{n1} = flux density in air gap

D_{n2} = flux density in conducting plate = 0

ρ_s = true surface charge density

Suppose that the true charge ρ_s is distributed *uniformly* throughout a thin layer of thickness Δx , as suggested in Fig. 3-24. Then the total change ΔD_n in flux density from one side of the layer to the other is given by

$$D_{n1} - D_{n2} = \Delta D_n = \Delta D_x \quad (2)$$

But when Δx is small,

$$\Delta D_x = \frac{dD_x}{dx} \Delta x \quad (3)$$

Therefore, (1) becomes

$$\frac{dD_x}{dx} = \frac{\rho_s}{\Delta x} = \rho \quad (4)$$

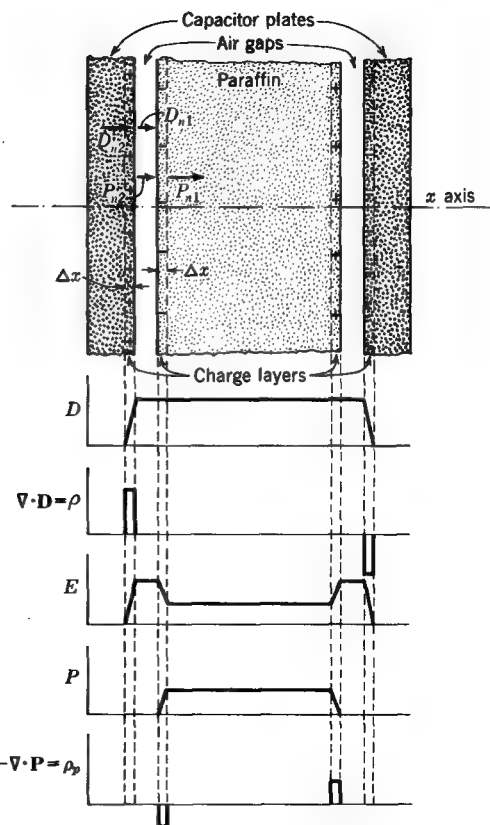


FIGURE 3-24

Cross section through parallel-plate capacitor with paraffin slab showing the variation of the flux density D , charge density ρ , electric field E , polarization P , and polarization charge density ρ_p along axis between the plates. The thickness Δx of the charge layers is greatly exaggerated.

where ρ is the volume charge density in the charge layer. Since \mathbf{D} has only an x component, $dD_x/dx = \text{div } \mathbf{D}$. Thus,

$$\frac{dD_x}{dx} = \nabla \cdot \mathbf{D} = \rho \quad (5)$$

Hence the change of \mathbf{D} with distance (in the charge layer) equals the divergence of \mathbf{D} and also the volume charge density. It follows that if the charge layer is infinitesimally thin ($\Delta x \rightarrow 0$), then $\nabla \cdot \mathbf{D}$ and ρ approach infinity. However, it is more reasonable to consider that the charge layer is of small but finite thickness, so that although $\nabla \cdot \mathbf{D}$ and ρ may be large, they are not infinite. The variation of \mathbf{D} and $\nabla \cdot \mathbf{D}$ along the x axis of the capacitor is shown graphically in Fig. 3-24.

At the paraffin surface \mathbf{D} is constant, but both \mathbf{E} and \mathbf{P} change. From (3-5-7)

$$\mathbf{P} = \mathbf{D} - \epsilon_0 \mathbf{E} \quad (6)$$

Now the change in polarization \mathbf{P} is equal to the surface charge density ρ_{sp} due to polarization. Thus, from (3-7-7),

$$P_{n1} - P_{n2} = -\rho_{sp} \quad (7)$$

where P_{n1} = polarization in paraffin

P_{n2} = polarization in air gap ≈ 0

ρ_{sp} = polarization surface-charge density

Assume that the polarization surface charge is uniformly distributed throughout a thin layer of thickness Δx at the paraffin surface, as suggested in Fig. 3-24. Then the total change ΔP_x in polarization from one side of the layer to the other is given by

$$P_{n1} - P_{n2} = \Delta P_x = \Delta P_x \quad (8)$$

But when Δx is small,

$$\Delta P_x = \frac{dP_x}{dx} \Delta x \quad (9)$$

Therefore, (7) becomes

$$\frac{dP_x}{dx} = -\frac{\rho_{sp}}{\Delta x} = -\rho_p \quad (10)$$

where ρ_p is the volume density of polarization charge in the layer at the paraffin surface in coulombs per cubic meter. Polarization charge differs from true charge ρ in that it cannot be isolated, whereas true charge can. In this sense it is a fictitious charge. Since \mathbf{P} has only an x component, which is a function only of x , $dP_x/dx = \text{div } \mathbf{P}$. Thus,

$$\frac{dP_x}{dx} = \boxed{\nabla \cdot \mathbf{P} = -\rho_p} \quad (11)$$

If the polarization distribution is uniform, $\nabla \cdot \mathbf{P} = 0$. Hence the change of \mathbf{P} with distance (in the charge layer) equals the divergence of \mathbf{P} and also the volume density ρ_p of polarization charge. The assumption of a polarization charge layer that is of small but finite thickness results in a value of $\nabla \cdot \mathbf{P}$ that may be large but not infinite.

The divergence of \mathbf{D} yields the sources of the \mathbf{D} field (true charge), while the divergence of \mathbf{P} yields the sources of the polarization field.

The variation of \mathbf{E} , \mathbf{P} , and $-\nabla \cdot \mathbf{P}$ along the x axis of the capacitor is illustrated graphically in Fig. 3-24.

It may be shown that the potential V_p in an unbounded volume due to a polarization distribution is given by

$$V_p = -\frac{1}{4\pi\epsilon_0} \int \frac{\mathbf{V} \cdot \mathbf{P}}{r} dv \quad (12)$$

Thus, when both true charge and polarization are present and the distribution of both are fixed, the total potential V_T in the unbounded volume is

$$V_T = \frac{1}{4\pi\epsilon_0} \int_v \frac{\rho}{r} dv - \frac{1}{4\pi\epsilon_0} \int_v \frac{\nabla \cdot \mathbf{P}}{r} dv$$

or

$$V_T = \boxed{\frac{1}{4\pi\epsilon_0} \int_v \frac{\rho - \nabla \cdot \mathbf{P}}{r} dv}$$

(13)

where ρ = true volume charge density, $C m^{-3}$

\mathbf{P} = polarization, $C m^{-2}$

ϵ_0 = permittivity of vacuum = 8.85 pF m^{-1}

r = distance from volume element containing charge or polarization to point at which V_T is to be calculated, m

The volume integration is taken over all regions containing charge or polarization.

The field intensity \mathbf{E} is then

$$\mathbf{E} = -\nabla V_T \quad (14)$$

Whereas (2-12-5) applies to a single homogeneous dielectric medium of permittivity ϵ , (13) is more general since it can be applied also to space with several different dielectric media, i.e., a nonhomogeneous medium. For the case of a single homogeneous medium, (2-12-5) and (13) are equivalent.

3-27 THE LAPLACIAN OPERATOR; POISSON'S AND LAPLACE'S EQUATIONS

As an extension of the divergence operator we are led to the laplacian (la-plah-si-an) operator. From (3-24-1)

$$\nabla \cdot \mathbf{D} = \rho \quad (1)$$

Since $\mathbf{D} = \epsilon \mathbf{E}$ and $\mathbf{E} = -\nabla V$, we have

$$\mathbf{D} = -\epsilon \nabla V \quad (2)$$

Introducing (2) in (1) gives

$$\nabla \cdot \nabla V = -\frac{\rho}{\epsilon} \quad (3)$$

This is *Poisson's* (pwas'-awns) *equation*. The double operator (divergence of the gradient) is also written as ∇^2 (del squared) and is called the *laplacian operator*. Thus Poisson's equation can be written

$$\boxed{\nabla^2 V = -\frac{\rho}{\epsilon}} \quad (4)$$

If $\rho = 0$, (4) reduces to

$$\boxed{\nabla^2 V = 0} \quad (5)$$

which is known as *Laplace's equation*.

In rectangular coordinates

$$\nabla^2 V = \frac{\partial^2 V}{\partial x^2} + \frac{\partial^2 V}{\partial y^2} + \frac{\partial^2 V}{\partial z^2} \quad (6)$$

The static potential distribution for any conductor configuration can be determined if a solution to Laplace's equation can be found which also satisfies the boundary conditions. This is discussed in Chap. 7.

PROBLEMS

- ★ 3-1 A plane slab of dielectric ($\epsilon_r = 5$) is placed normal to a uniform field with a flux density D of 1 C m^{-2} . If the slab occupies a volume of 0.1 m^3 and is uniformly polarized, what are (a) the polarization in the slab and (b) the total dipole moment of the slab?
- ★ 3-2 A flat slab of sulfur ($\epsilon_r = 4$) is placed normal to a uniform field. If the polarization-surface-charge density ρ_{ss} on the slab surfaces is 0.5 C m^{-2} , what are (a) polarization in the slab, (b) flux density in the slab, (c) flux density outside the slab (in air), (d) field intensity in slab, and (e) field intensity outside the slab (in air)?
- ★ 3-3 The left half of a horizontal parallel-plate capacitor is filled with a dielectric of permittivity ϵ while the right half is air-filled. The plate separation is 10 mm, and there is 100 V potential difference between the plates. Find E , D , and P in both halves. $\epsilon = 3\epsilon_0$.
- ★ 3-4 A horizontal parallel-plate capacitor has a 10-mm plate separation and a 100-V potential difference. There is a dielectric of permittivity ϵ and thickness 5 mm on the lower plate. The space above is air-filled. (a) Find E , D , and P in the air space and in the dielectric. (b) Find V as a function of the distance between the plates. $\epsilon = 3\epsilon_0$.
- ★ 3-5 Two cavities are cut in a dielectric medium ($\epsilon_r = 5$) of large extent. Cavity 1 is a thin disk-shaped cavity with flat faces perpendicular to the direction of D in the dielectric. Cavity 2 is a long needle-shaped cavity with its axis parallel to D . The cavities are filled with air. If $D = 10 \text{ nC m}^{-2}$, what is the magnitude of E at (a) the center of cavity 1 and (b) the center of cavity 2?

* Answers to starred problems are given in Appendix C.

* 3-6 A parallel-plate capacitor is 1 m square and has a plate separation of 1 mm. The space between the plates is filled with a dielectric ($\epsilon_r = 25$). If 1 kV potential difference is applied to the plates, find the force in newtons squeezing the plates together.

3-7 The electric field E in air above a slab of dielectric ($\epsilon_r = 5$) is at an angle of 30° with respect to a normal to the plane surface of the slab. What is the angle between E and the normal inside the slab?

3-8 Three plane dielectric slabs of equal thickness with $\epsilon_r = 2, 3$, and 4 are sandwiched together. If E in air is at an angle of 30° with respect to a normal to the plane surface of the $\epsilon_r = 2$ slab, find the angle of E with respect to the normal inside the slabs. Draw a figure showing the path of the E line through the sandwich.

3-9 What is the magnitude of E , D , and P 400 mm from a point charge of 1 nC in an infinite medium (a) of air and (b) of a dielectric with $\epsilon_r = 9$?

* 3-10 What is ϵ_r for an artificial dielectric made of a uniform cubical lattice of metal spheres in air if the spheres are 30 mm in diameter and spaced uniformly 60 mm between centers in the x , y , and z directions?

3-11 Show that the maximum possible ϵ_r for an artificial dielectric of metal spheres arranged in a uniform cubical lattice in air is 2.57. It is assumed that there is no interaction between spheres and that they are almost touching.

* 3-12 A horizontal parallel-plate capacitor of area A has a plate separation d and a potential difference V . A dielectric slab of relative permittivity ϵ_r and thickness t is placed midway between the plates [air space above and below the slab of thickness $(d-t)/2$]. Find E , D , and P in the slab and air spaces. Neglect fringing.

3-13 A parallel-plate capacitor of area A is filled with a dielectric of permittivity $\epsilon = \epsilon_0[1 + (\epsilon_r y/d)]$, where $y = 0$ at one plate and $y = d$ at the other plate. Neglect fringing. (a) Find E , D , P , and V as a function of distance y between the plates. (b) Make a graph showing the variation of ϵ , E , D , P , and V as a function of y . (c) Find the capacitance. (d) Find the polarization-volume-charge density ρ_p as a function of y and the polarization-surface-charge density ρ_{sp} at $y = 0$ and $y = d$. (e) Make a graph of ρ_p vs. y .

3-14 Repeat Prob. 3-13 for the case where the plate at $y = 0$ remains in contact with the slab but the other plate is moved to a distance $y = 2d$ with the space between $y = d$ and $y = 2d$ air-filled.

3-15 Design an electrostatic press for applying pressures of 1 N mm^{-2} to 1-m-square plywood sheets 10 mm thick (see Prob. 3-6).

* 3-16 A parallel-plate capacitor is 200 by 200 mm with 10 mm plate separation. The medium is air. Neglect fringing. Find the capacitance if a sheet of powdered rutile (take $\epsilon_r = 114$) is placed between the plates under the following conditions: (a) sheet 1 mm thick (remaining 9 mm is air), (b) sheet 2 mm thick, (c) sheet 4 mm thick, (d) sheet 6 mm thick, (e) sheet 8 mm thick, (f) sheet 10 mm thick (g) Draw a graph of the capacitance vs. sheet thickness.

3-17 (a) If 100 V is applied to the capacitor of Prob. 3-16, calculate the energy stored for the six conditions listed. (b) Find the energy density in the dielectric and in the air space for the six conditions.

3-18 What volume of capacitor would be required to store 1 kW hr of energy? This is the amount of energy which can be stored in a typical automobile storage battery.

3-19 What is the maximum voltage to which an isolated metal sphere can be charged if the sphere is 300 mm in diameter and situated in air? Take the dielectric strength of air as 3 MV m^{-1} .

* **3-20** A parallel-plate air capacitor is charged to 1,000 V, the potential source disconnected, and the plates separated to twice their original spacing. (a) What is the energy stored in the two cases? (b) Account for the difference in energies.

3-21 Relate Prob. 3-20 to the voltage buildup in a storm cloud in a rising air current.

3-22 The permittivity of the dielectric in a parallel-plate capacitor is a function of the distance y between the plates ($y = 0$ at one plate and $y = y_1$ at the other plate) as given by $\epsilon = \epsilon_0 e^y$. Find the capacitance.

3-23 A charge Q is uniformly distributed in a circular ring of radius r_1 . Find E and V at the center of the ring.

* **3-24** A charge Q is uniformly distributed in a square ring of side length l . Find E and V at the center of the ring.

3-25 A charge Q is uniformly distributed in a half-circular ring of radius r_1 . Find E and V at the origin.

* **3-26** A charge Q is uniformly distributed along a line of length l situated coincident with the x axis with one end at the origin and the other end at $x = l$. Find V at a point x_1 on the x axis where $x_1 > l$.

3-27 Repeat Prob. 3-26 for the case where the linear charge density varies as x^2 .

3-28 Map the field lines and equipotential contours of a coaxial transmission line consisting of a circular inner conductor of diameter d symmetrically located inside an outer conductor of square cross section with an inner side dimension of $3d$. Note that thanks to symmetry only one octant (45° sector) need be mapped.

3-29 Referring to Prob. 3-28, (a) what is the capacitance per meter length of the line? (b) If 100 V is applied to the line, what is the potential of a point midway between the inner conductor and a corner?

3-30 If 100 V is applied to the plates of the capacitor of Fig. P3-30, find E at the points A and $B(r = 10 \text{ mm})$.

3-31 If 100 V is applied to the asymmetrical coaxial transmission line of Fig. P3-31,

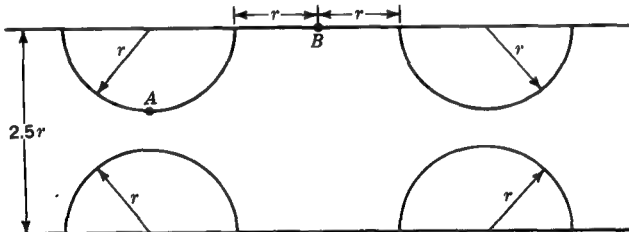


FIGURE P3-30

Parallel-plate capacitor with metal half-cylinders attached.

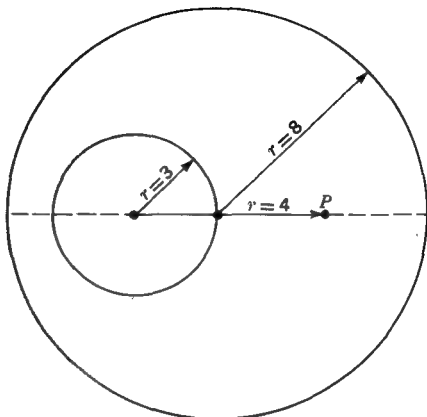


FIGURE P3-31
Cross section of asymmetrical coaxial transmission line.

find V at the point P . The potential of the outer conductor is zero.

3-32 What is the ratio of the capacitance per unit depth of capacitor A to capacitor B shown in Fig. P3-32? Neglect fringing.

- ★ 3-33 A coaxial transmission line consists of an inner conductor of diameter d situated symmetrically inside a triangular outer conductor of equilateral cross section with inner side lengths all equal to $3d$. (a) Map the field lines and equipotential contours. (b) What is the ratio of surface charge density at the center point of a side of the outer conductor to that at a point on the side midway from the center to a corner? (c) If 100 V is applied to the line, what is the potential at a point midway from the inner conductor to a corner? The outer conductor is at zero potential. (d) What is the capacitance per unit length?
- ★ 3-34 A high-voltage conductor is brought through a grounded metal panel by means of the double concentric capacitor bushing shown in Fig. P3-34. The medium is air (dielectric strength 3 MV m^{-1}). Neglect fringing and thickness of sleeves. (a) Find the outer sleeve length L which equalizes the voltage across each space. (b) Find L which results in the same value of maximum field in each space. (c) What is the maximum working voltage for each condition? (d) If the inner sleeve (200 mm long) were removed, what would be the maximum working voltage? (e) If the number of concentric sleeves is increased in number so that

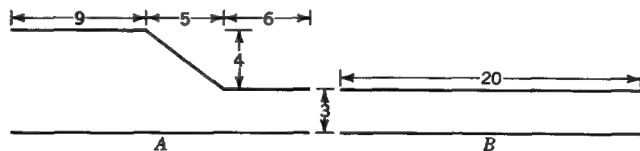


FIGURE P3-32
Cross section of two capacitors.

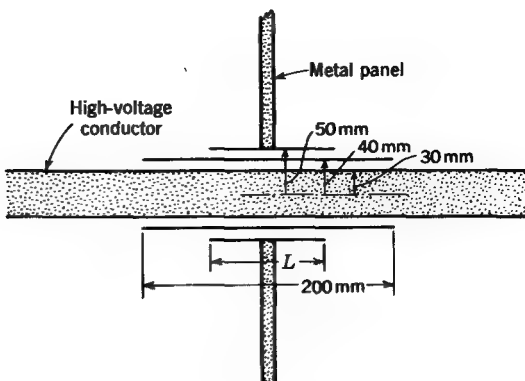


FIGURE P3-34
Concentric capacitor bushing.

the spacing between sleeves becomes smaller, what is the ultimate working voltage? (f) Draw graphs of E vs. radius for the conditions in parts (a), (b), (d), and (e).

3-35 A charge Q is uniformly distributed in a thin circular ring of radius r_1 . Derive expressions for E and V as a function of radius r (a) in the plane of the ring and (b) perpendicular to the plane of the ring along its axis. (c) Draw graphs of E and V for both cases to a distance of $4r_1$.

3-36 A charge Q is uniformly distributed over a plane square area of side length L . (a) Derive expressions for E and V as a function of distance normal to the center of the area. (b) Draw graphs of E and V to a distance of $5L$.

3-37 Repeat Prob. 3-36 for the case where the charge has a cosine distribution, i.e., the charge density is a maximum at the center of the area and tapers as a cosine function to zero at the edges.

3-38 Map the field lines and equipotential contours for the following situations: (a) Two point charges $+Q$ and $+2Q$ separated by a distance d . (b) Two point charges $+Q$ and $-2Q$ separated by a distance d . (c) Four point charges of equal magnitude forming a quadrupole as in Fig. 2-21a. (d) Four equal point charges arranged as in Fig. 2-21a but all of the same sign. (e) An infinite array of equal positive and negative point charges arranged in a uniform rectangular grid. Adjacent charges are of opposite sign. Use a computer with machine or cathode-ray-tube plotter. (f) Repeat (e) for a uniform hexagonal grid. Note that (e) and (f) are but two of many configuration which can give interesting displays with a computer.

* 3-39 Find the divergence of the following vector functions:

$$(a) \mathbf{F} = \hat{\mathbf{x}} \sin az + \hat{\mathbf{y}} \cos ax + \hat{\mathbf{z}} y \quad (b) \mathbf{G} = \hat{\mathbf{x}} \cos ay + \hat{\mathbf{y}} x - \hat{\mathbf{z}} \sin az$$

$$3-40 \text{ Show that } \nabla \cdot \mathbf{P} = (\epsilon_r - 1)\epsilon_0 \nabla \cdot \mathbf{E}.$$

3-41 A sphere of radius r_1 has a uniform charge density ρ . (a) Find D and $\nabla \cdot D$ as a function of radius. (b) Make a graph of D and $\nabla \cdot D$ to a radius of $3r_1$.

3-42 Repeat Prob. 3-41 for the case where the charge density $\rho = kr$, where k = constant.

3-43 Show that the total capacitance of n unequal capacitors is (a) more than the capacitance of the largest when they are connected in parallel and (b) less than the capacitance of the smallest when they are connected in series.

* **3-44** Find the divergence of the following vector functions:

- (a) $\mathbf{A} = \hat{x}3x + \hat{y}4y^3 + \hat{z}5z^2$
- (b) $\mathbf{B} = \hat{x}2xy^2z - \hat{y}3xz + \hat{z}4x^2y^3$
- (c) $\mathbf{C} = \hat{x}2 + \hat{y}7x^2y^2z^2 - \hat{z}z^{-1}$
- (d) $\mathbf{D} = \hat{x}y + \hat{y}z + \hat{z}xy$
- (e) $\mathbf{E} = \hat{x}\sin\phi + \hat{y}\cos\phi + \hat{z}z^2$
- (f) $\mathbf{F} = \hat{x}2r^{1/2} - \hat{y}\sin\phi\cos\phi + \hat{z}\tan\phi$
- (g) $\mathbf{G} = \hat{x}r^{-1} + \hat{y}\sin\theta\sin\phi - \hat{z}\sin\theta\sin\phi$
- (h) $\mathbf{H} = \hat{x}z + \hat{y}\cos\theta\sin\phi + \hat{z}r^{1/2}$

3-45 Find the gradient and laplacian of the following scalar functions:

- (a) $U = \frac{1}{x^2 + y^2}$
- (b) $U = x^3y^2z$
- (c) $V = \frac{1}{r}$ (cylindrical coordinates)
- (d) $V = \frac{1}{r}$ (spherical coordinates)
- (e) $V = \frac{1}{e^r}$ (cylindrical coordinates)
- (f) $V = \frac{1}{e^r}$ (spherical coordinates)
- (g) $W = x^2 - yz$
- (h) $W = xy + xz$

3-46 Problems 2-28 and 2-29 were to be solved by integrating \mathbf{D} over the surface of the cubical volume ($\oint \mathbf{D} \cdot d\mathbf{s} = Q$). Now solve Probs. 2-28 and 2-29 by first taking the divergence of \mathbf{D} and integrating this result over the volume of the cube ($\iiint \nabla \cdot \mathbf{D} dv = \iiint \rho dv = Q$).

3-47 A parabolic line of charge with vertex at the origin and focus at $x = 1$ m extends 3 m in both $+y$ and $-y$ directions. If $\rho_L = 1$ nC m $^{-1}$, find V and E at the focus. An approximate solution can be obtained by dividing the parabolic-line charge into segments and adding their contributions.

3-48 Repeat Prob. 3-47 for the case where the parabolic line of charge extends only from $y = 0$ to $y = +3$ m.

* **3-49** A point charge $+Q$ is situated at the center of a dielectric sphere of permittivity ϵ and radius R . (a) Find V and E in the dielectric and in the air outside. (b) Determine the surface charge density required on the surface of the sphere to maintain the same field inside the sphere but reduce the field outside to zero.

3-50 A typical 12-V automobile lead acid storage battery can store 1 kW hr of energy. (a) What is the smallest practical volume in which 1 kW hr of energy can be stored in electrostatic form? (b) What is the ratio of this volume to that of the storage battery?

THE STEADY ELECTRIC CURRENT

4-1 INTRODUCTION

Electric charge in motion constitutes an *electric current*. In metallic conductors the charge is carried by electrons. In liquid conductors (electrolytes) the charge is carried by ions, both positive and negative. In semiconductors the charge is carried by electrons and holes, the holes behaving like positive charges (see Sec. 4-7).

In this chapter the important relations governing the behavior of steady electric currents in conductors are discussed.[†]

The fields associated with steady currents are constant with time and hence are static fields. In Chaps. 2 and 3 the discussion was almost entirely concerned with static fields having all associated charges stationary, i.e., with no currents present. In this chapter the fields are also static, but steady direct currents may be present.

[†] Specifically, a *steady direct current* is meant. This should not be confused with a *steady-state current*, which may imply a time-changing current that repeats itself periodically.

4-2 CONDUCTORS AND INSULATORS

In some metals, like silver and copper, there is but one electron in the outermost occupied shell of the atom. This electron is so loosely held that it migrates easily from atom to atom when an electric field is applied. Materials that permit such electron motion are called *conductors*. Silver and copper are examples of good conductors, their resistance to electronic motion being relatively slight. Not all good conductors have only one electron in the outermost occupied shell. Some have two, and a few, such as aluminum, three. However, in all conductors these electrons are loosely bound and can migrate readily from atom to atom. Such electrons are often called *true charges*.

In other substances, however, the electrons may be so firmly held near their normal position that they cannot be liberated by the application of ordinary fields.[†] These materials are called *dielectrics* or *insulators*. Although a field applied to an insulator may produce no migration of charge, it can produce a polarization of the insulator, or dielectric (Sec. 3-5), i.e., a displacement of the electrons with respect to their equilibrium positions. The charges of an insulator are often called *bound* or *polarization charges* in contrast to the free, or true, charges of a conducting material.

Certain other materials with properties intermediate between conductors and insulators are called *semiconductors*. Under some conditions such a substance may act like an insulator but with the application of heat or sufficient field may become a fair conductor.

4-3 THE ELECTRIC CURRENT

When an isolated conducting object is introduced into an electric field, charges migrate (currents flow) until a surface charge distribution has been built up that reduces the total field in the conductor to zero. If, however, the conducting object is not isolated and the applied field is maintained, current will continue to flow in the conductor.

For example, consider an infinitely long conductor, such as a metal wire, in a uniform field \mathbf{E} as in Fig. 4-1. The field \mathbf{E} in the conductor is not zero if current is flowing. Rather, \mathbf{E} is the same inside and outside the conductor. This follows from the boundary relation (1) of Table 3-2 that the tangential component of the electric field is continuous across a boundary. The field causes the electrons in the conductor to migrate parallel to the field. Since the electrons are negatively charged, they move in a sense opposite to the field direction. If there are n electrons per meter of length of the conductor and their average velocity is $v \text{ m s}^{-1}$, then the total charge per second

[†] However, they may be torn off by mechanical means such as rubbing.

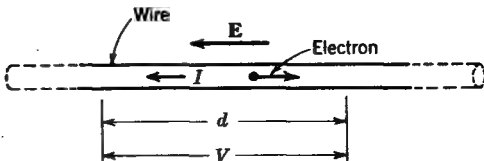


FIGURE 4-1
Infinite conductor in uniform field.

passing a fixed point on the wire is nqv , where q is the charge of each electron. The electric current I in the wire is then defined as

$$I = -nqv \quad (1)$$

The electric current is, by definition, taken to be in the opposite direction to the electron motion. Hence the negative sign in (1). Electric current has the dimensions of current, or in dimensional symbols $I (= Q/T)$. The SI unit of current is the ampere (A). Thus,

$$\text{Amperes} = \frac{\text{coulombs}}{\text{second}}$$

That is, a current of 1 A is produced by charge flowing by a fixed point at the rate of 1 C s^{-1} .

4-4 RESISTANCE AND OHM'S LAW

In 1826 Georg Simon Ohm experimentally determined the relations between the voltage V over a length of conductor and the current I through the conductor in terms of a parameter characteristic of the wire (see Fig. 4-1). This parameter, called the resistance R , is defined as the ratio of the voltage V to the current I . Thus,

$$R = \frac{V}{I} \quad \text{or} \quad V = IR \quad (1)$$

The latter form is the usual statement of *Ohm's law*, which states that *the potential difference or voltage V between the ends of a conductor is equal to the product of its resistance R and the current I* .

It is assumed that R is independent of I ; that is, R is a constant. Conversely, such a resistance is said to obey Ohm's law. There exist circuit elements, however, such as rectifiers, whose resistance is not a constant. Such elements are said to be *nonlinear*, and a V -vs.- I diagram is required to display their behavior. Nevertheless, the resistance of the nonlinear element is still defined by $R = V/I$, but R is not independent of I and the resistance does not obey Ohm's law.

Resistance has the dimensions of potential divided by current or, in dimensional symbols, ML^2/IT^3 . The SI unit of resistance is the ohm (Ω). Thus

$$\frac{\text{Volts}}{\text{Ampere}} = \text{ohms}$$

That is, the resistance of a conductor is 1 Ω if a current of 1 A flows when a potential difference of 1 V is applied between the ends of the conductor.

4-5 POWER RELATIONS AND JOULE'S LAW

Referring again to Fig. 4-1, the potential difference or voltage V across the length d of the conductor is equal to the work per unit charge (current \times time) required to move a charge through the distance d . Multiplying by the current I yields the work per unit time, or power P . Thus,

$$\frac{\text{Work}}{\text{Current} \times \text{time}} \times \text{current} = \frac{\text{work}}{\text{time}} = \text{power}$$

or

$$VI = P \quad (1)$$

This is the power dissipated in the length d of the conductor. The SI unit of power is the watt (W). Hence,

$$\text{Volts} \times \text{amperes} = \text{watts} \quad (\text{W})$$

or in dimensional symbols

$$\frac{ML^2}{IT^3} I = \frac{ML^2}{T^3}$$

Introducing the value of V from Ohm's law (4-4-1) into (1) yields

$$P = I^2 R \quad (2)$$

Thus, the work or energy dissipated per unit time in the conductor is given by the product of its resistance R and the square of the current I . This energy appears as heat in the conductor.

The energy W dissipated in the conductor in a time T is then

$$W = PT = I^2 RT \quad (3)$$

where W = energy, J

P = power, W

I = current, A

R = resistance, Ω

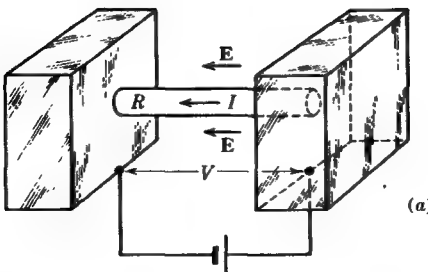
T = time, s

This relation is known as *Joule's law*. It is assumed that P is constant over the time T . If it is not constant, $I^2 R$ is integrated over the time interval T .

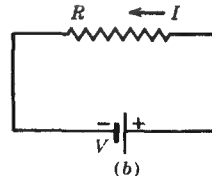
4-6 THE ELECTRIC CIRCUIT

The discussion in the preceding sections concerns an infinitely long conductor along which a field E is applied (Fig. 4-1). Consider now a cylindrical conductor of finite length d as in Fig. 4-2a between two large conducting blocks of negligible resistance maintained at a constant potential difference V by a battery. This produces a uniform field E along the conductor. This field is given by $E = V/d$. As long as this field is maintained in the conductor, current flows that has a value

$$I = \frac{V}{R} = \frac{Ed}{R}$$

(a)



(b)

FIGURE 4-2

(a) Cylindrical conductor of length d between end blocks, and (b) schematic diagram.

Assuming that the resistance of the wires connected to the battery is negligible compared with R , the potential difference V is equal to the voltage appearing across the terminals of the battery. The arrangement of Fig. 4-2a may then be represented by the schematic diagram of Fig. 4-2b.

This is a diagram of a closed *electric circuit* of the most elementary form consisting of a *resistor* of resistance R and a battery of voltage V .

4-7 RESISTIVITY AND CONDUCTIVITY

The resistance of a conductor depends not only on the type of material of which the conductor is made but also on its shape and size. To facilitate comparisons between different types of substances, it is convenient to define a quantity which is characteristic only of the substance. The *resistivity* S is such a quantity. The resistivity of a material is numerically equal to the resistance of a homogeneous unit cube of the material with a uniform current distribution. This condition may be produced by clamping the cube between two heavy blocks of negligible resistance, as in Fig. 4-3. With a current I through the cube, the resistivity S of the material is given by $S = V/I$, where V is the potential between the blocks.

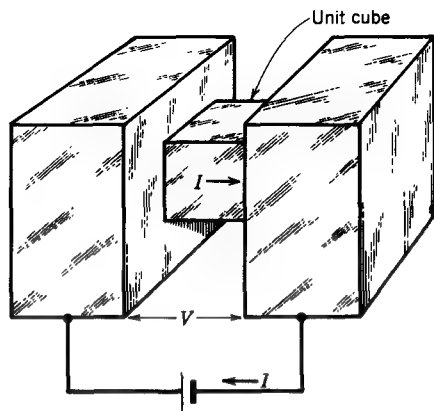


FIGURE 4-3
Unit cube between end blocks.

In SI units, this measurement is in ohms for a cube of material 1 m on a side. If two cubes are placed in series between the blocks, the resistance measured is $2S$, while if two cubes are placed in parallel, the resistance is $\frac{1}{2}S$. It follows that the resistance R of a rectangular block of length l and cross section a , as in Fig. 4-4, is

$$R = \frac{Sl}{a} \quad \text{or} \quad S = \frac{Ra}{l} \quad (1)$$



FIGURE 4-4
Block of conducting material.

where S is the resistivity of the block material. From (1) resistivity has the dimensions

$$\frac{\text{Resistance} \times \text{area}}{\text{Length}} = \text{resistance} \times \text{length}$$

Thus, resistivity has the dimensions of resistance times length and in SI units is expressed in ohm-meters ($\Omega \text{ m}$).

The resistivity is a function of the temperature. In metallic conductors it varies nearly linearly with absolute temperature. Over a considerable temperature range from a reference or base temperature T_0 the resistivity S is given approximately by

$$S = S_0[1 + \alpha(T - T_0)]$$

where T = temperature of material, $^{\circ}\text{C}$

T_0 = reference temperature (usually 20°C)

S_0 = resistivity at temperature T_0 , $\Omega \text{ m}$

α = temperature coefficient of resistivity, numerical units $^{\circ}\text{C}^{-1}$

EXAMPLE For copper the resistivity S_0 at 20°C is $17.7 \text{ n}\Omega \text{ m}$ and the corresponding coefficient $\alpha = 0.0038^{\circ}\text{C}^{-1}$. Find the resistivity at 30°C .

SOLUTION The resistivity S at a temperature T is

$$S = 1.77 \times 10^{-8}[1 + 0.0038(T - 20)] \quad (\Omega \text{ m})$$

At a temperature of 30°C ,

$$S = 1.77 \times 10^{-8}[1 + 0.0038(10)] = 18.4 \text{ n}\Omega \text{ m}$$

This is an increase of nearly 4 percent over the resistivity at 20°C .

At temperatures near absolute zero ($T = 0 \text{ K}^{\dagger}$ or -273°C) some metals become superconducting, an effect first observed by H. Kamerlingh Onnes in 1911. The resistivity drops to zero, and the magnetic field is expelled, so that $B = 0$. The transition is very abrupt. Niobium (also called columbium) becomes superconducting at 9.2 K , aluminum at 1.2 K , but copper and gold are not superconducting, at least not at temperatures down to 0.05 K . Some intermetallic compounds like $\text{Nb}_3(\text{Al-Ge})$ become superconducting at the relatively high temperature of about 21 K . If materials

[†] The SI unit for absolute temperature is the kelvin (K) (see Sec. 1-3).

are developed which become superconducting at 25 K or more, a technological revolution will occur since this will permit use of superconductors cooled by relatively inexpensive liquid hydrogen (boiling temperature 20.4 K).†

The reciprocal of resistance R is *conductance* G . That is, $G = 1/R$. Since resistance is expressed in ohms, conductance is expressed in reciprocal ohms. A reciprocal ohm is called a *mho* (ohm spelled backward); conductance is given in mhos, and the SI symbol is an upsidedown capital omega (Ω).

The reciprocal of resistivity S is *conductivity* σ . That is,

$$\sigma = \frac{1}{S} = \frac{l}{Ra} \quad (1a)$$

Although the resistivity is convenient in certain applications, it is often more convenient to deal with its reciprocal, the conductivity, e.g., where parallel circuits are involved. Since resistivity is expressed in ohm-meters, the conductivity is expressed in mhos per meter ($\Omega \text{ m}^{-1}$).

The resistance R of a rectangular block, as in Fig. 4-4, of material of conductivity σ is

$$R = \frac{l}{\sigma a} \quad (\text{ohms, } \Omega) \quad (2)$$

or the conductance G of the block is

$$G = \frac{1}{R} = \frac{\sigma a}{l} \quad (\text{mhos, } \Omega) \quad (3)$$

where σ = conductivity of block material, $\Omega \text{ m}^{-1}$

a = cross-sectional area of block, m^2

l = length of block, m

A semiconductor contains *electrons* and *holes* (vacant spaces in the semiconductor lattice). The electrons move opposite to E , but the holes move with E , like positive charges. From $J = \sigma E$ the conductivity may be expressed.

$$\sigma = \frac{J}{E} = \rho \frac{v}{E} = \rho \mu \quad (4)$$

where ρ is the electron (or hole) charge density, in coulombs per cubic meter. The quantity μ is the drift velocity v of the electron (or hole) per unit field E and is called the *mobility* ($\text{m}^2 \text{ s}^{-1} \text{ V}^{-1}$). The mobility of electrons and holes is different. Hence, we may write for the conductivity of a semiconductor

† B. T. Matthias, The Search for High-temperature Superconductors, *Phys. Today*, 24: 23–28 (August 1971).

$$\boxed{\sigma = \rho_e \mu_e + \rho_h \mu_h \quad (\text{V m}^{-1})} \quad (5)$$

where ρ_e = charge density of electrons, C m^{-3}

μ_e = mobility of electrons, $\text{m}^2 \text{s}^{-1} \text{V}^{-1}$

ρ_h = charge density of holes, C m^{-3}

μ_h = mobility of holes, $\text{m}^2 \text{s}^{-1} \text{V}^{-1}$

4-8 TABLE OF CONDUCTIVITIES

The conductivities σ_0 of some common materials are listed in Table 4-1 for a temperature of 20°C and for a superconductor at temperatures below 21 K.

Table 4-1 TABLE OF CONDUCTIVITIES

Substance	Type	Conductivity, V m^{-1}
Quartz, fused	Insulator	$\sim 10^{-17}$
Ceresin wax	Insulator	$\sim 10^{-17}$
Sulfur	Insulator	$\sim 10^{-15}$
Mica	Insulator	$\sim 10^{-15}$
Paraffin	Insulator	$\sim 10^{-15}$
Rubber, hard	Insulator	$\sim 10^{-15}$
Glass	Insulator	$\sim 10^{-12}$
Bakelite	Insulator	$\sim 10^{-9}$
Distilled water	Insulator	$\sim 10^{-4}$
Seawater	Conductor	~ 4
Tellurium	Conductor	$\sim 5 \times 10^2$
Carbon	Conductor	$\sim 3 \times 10^4$
Graphite	Conductor	$\sim 10^5$
Cast iron	Conductor	$\sim 10^6$
Mercury	Conductor	10^6
Nichrome	Conductor	10^6
Constantan	Conductor	2×10^6
Silicon steel	Conductor	2×10^6
German silver	Conductor	3×10^6
Lead	Conductor	5×10^6
Tin	Conductor	9×10^6
Phosphor bronze	Conductor	10^7
Brass	Conductor	1.1×10^7
Zinc	Conductor	1.7×10^7
Tungsten	Conductor	1.8×10^7
Duralumin	Conductor	3×10^7
Aluminum, hard-drawn	Conductor	3.5×10^7
Gold	Conductor	4.1×10^7
Copper	Conductor	5.7×10^7
Silver	Conductor	6.1×10^7
$\text{Nb}_3(\text{Al-Ge})$	Super-conductor	$\sim \infty$

4-9 CURRENT DENSITY AND OHM'S LAW AT A POINT

If the current is distributed uniformly throughout the cross section of a wire, the *current density* J is uniform and is given by the total current I divided by the cross-sectional area a of the wire. That is,

$$J = \frac{I}{a} \quad \checkmark \quad (1)$$

Current density has the dimensions of current per area and in SI units is expressed in amperes per square meter ($A\ m^{-2}$).

If the current is not uniformly distributed, (1) gives the average current density. However, it is often of interest to consider the current density at a point. This is defined as the current ΔI through a small area Δs divided by Δs , with the limit of this ratio taken as Δs approaches zero. Hence, the current density at a point is given by

$$\mathbf{J} = \lim_{\Delta s \rightarrow 0} \frac{\Delta I}{\Delta s} \quad (2)$$

It is assumed that the surface Δs is normal to the current direction. The current density \mathbf{J} is a vector point function having a magnitude equal to the current density at the point and the direction of the current at the point.

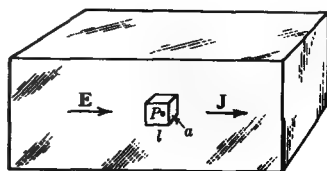
Consider now a block of conducting material as indicated in Fig. 4-5. Let a small imaginary rectangular cell of length l and cross section a be constructed around a point P in the interior of the block with a normal to \mathbf{J} as indicated. Then on applying Ohm's law to this cell we have $V = IR$, where V is the potential difference between the ends of the cell. But $V = El$ and $I = Ja$; so $El = JaR$ and

$$J = \frac{l}{aR} E \quad (3)$$

By making the cell enclosing P as small as we wish, this relation can be made to apply at the point P , and we can write

$$\boxed{\mathbf{J} = \sigma \mathbf{E}} \quad \checkmark \quad (4)$$

FIGURE 4-5
Block of conducting material with small
imaginary cell enclosing the point P .



Equation (4) is *Ohm's law at a point* and relates the current density \mathbf{J} at a point to the total field \mathbf{E} at the point and the conductivity σ of the material. In the above discussion it is assumed that the conducting material is homogeneous (same material throughout), isotropic (resistance between opposite faces of a cube independent of the pair chosen), and linear (resistance independent of current).

4-10 KIRCHHOFF'S VOLTAGE LAW AND THE DIFFERENCE BETWEEN POTENTIAL AND EMF

Consider the simple electric circuit shown by the schematic diagram in Fig. 4-6. The circuit consists of a resistor R_o and the battery. The current is I at all points in the circuit. At any point in the conducting material of the circuit we have from Ohm's law at a point that $\mathbf{J}/\sigma = \mathbf{E}$, where \mathbf{E} is the total field at the point.

In general the total field \mathbf{E} may be due not only to static charges but also to other causes such as the chemical action in a battery. To indicate this explicitly, we write

$$\mathbf{E} = \mathbf{E}_c + \mathbf{E}_e \quad (1)$$

where \mathbf{E}_c = static electric field due to charges; the subscript c is to indicate explicitly that the field is due to *charges*

\mathbf{E}_e = electric field generated by other causes as by a battery; the subscript e is to indicate explicitly that it is an *emf-producing* field

Whereas \mathbf{E}_c is derivable as the gradient of a scalar potential due to charges ($\mathbf{E}_c = -\nabla V$), this is not the case for \mathbf{E}_e . Substituting (1) in (4-9-4), writing $\mathbf{J} = I/a$, where a is the cross-sectional area of the conductor, and noting the value of σ from (4-7-2), we have

$$\frac{\mathbf{J}}{\sigma} = I \frac{R}{l} = \mathbf{E}_c + \mathbf{E}_e \quad (2)$$

where R/l is the resistance per unit length in ohms per meter. This applies at any point in the circuit. Integrating around the complete circuit gives

$$\oint \mathbf{E}_c \cdot d\mathbf{l} + \oint \mathbf{E}_e \cdot d\mathbf{l} = I \oint \frac{R}{l} dl \quad (3)$$

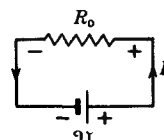


FIGURE 4-6
Series circuit of battery and external resistance.

The first term is zero; i.e., the line integral of a field due to charges is zero around a closed circuit (see Sec. 2-8, last paragraph). However, the second term involving the line integral of \mathbf{E}_e around the circuit is not zero but is equal to a voltage called the total *electromotive force*, or *emf*,† \mathcal{U}_T of the circuit. The field \mathbf{E}_e is produced, in the present example, by chemical action in the battery. If it were absent, no current would flow since an electric field \mathbf{E}_c due to charges is not able to maintain a steady current. The right-hand side of (3) equals the total IR drop around the circuit. Hence (3) becomes

$$\mathcal{U}_T = IR_T \quad (4)$$

where R_T is the total resistance of the circuit (equals R_0 if the internal resistance of the battery is zero).

In general, for a closed circuit containing many resistors and sources of emf,

$$\sum \mathcal{U} = I \sum R \quad (5)$$

This is *Kirchhoff's voltage law*. In words it states that *the algebraic sum of the emfs around a closed circuit equals the algebraic sum of the ohmic or IR drops around the circuit*.‡ Kirchhoff's voltage law applies not only to an isolated electric circuit as in Fig. 4-6 but to any single mesh (closed path) of a network.

To distinguish emf from the scalar potential V , the symbol \mathcal{U} (script V) is used for emf. Both V and \mathcal{U} are expressed in volts, so that either may be referred to as a voltage if one does not wish to make a distinction between potential and emf.

It is to be noted that the scalar potential V is equal to the line integral of the static field \mathbf{E}_c , while the emf \mathcal{U} equals the line integral of \mathbf{E}_e . Thus, between any two points a and b ,§

$$V_{ab} = V_b - V_a = - \int_a^b \mathbf{E}_c \cdot d\mathbf{l} \quad (6)$$

and

$$\mathcal{U}_{ab} = \int_a^b \mathbf{E}_e \cdot d\mathbf{l} \quad (7)$$

In (6) V_{ab} is independent of the path of integration between a and b , but \mathcal{U}_{ab} , in (7), is not.

† Also called *electromotance*.

‡ In time-varying situations, where the circuit dimensions are small compared with the wavelength, Kirchhoff's law is modified: The algebraic sum of the *instantaneous* emfs around a closed circuit equals the algebraic sum of the *instantaneous* ohmic drops around the circuit.

§ An open-circuited battery (no current flowing) has a terminal potential difference V equal to its emf \mathcal{U} . The potential V is as given by (6). As explained in the examples that follow, \mathbf{E}_c and \mathbf{E}_e have opposite directions in the battery. Therefore, in order that $V_{ab} = \mathcal{U}_{ab}$ for an open-circuited battery, (7) has no negative sign.

For closed paths, $\oint \mathbf{E}_c \cdot d\mathbf{l} = 0$ and $\oint \mathbf{E}_e \cdot d\mathbf{l} = \mathcal{U}_T$, where \mathcal{U}_T is the total emf around the circuit.

EXAMPLE Let the circuit of Fig. 4-6 be redrawn as in Fig. 4-7a. The battery has an internal resistance R_1 , and it will be convenient in this example to assume that the field \mathbf{E}_e in the battery is uniform between the terminals (*c* and *d*). The point *b* (or *c*) is taken arbitrarily to be at zero potential. The resistor has a uniform resistance R_0 , and the wires connecting the resistor and the battery are assumed to have infinite conductivity ($\sigma = \infty$). Hence, in the wire, $\mathbf{E}_c = 0$. The field \mathbf{E}_e has a value only in the battery, being zero elsewhere. Find the variation of the potential V around the circuit.

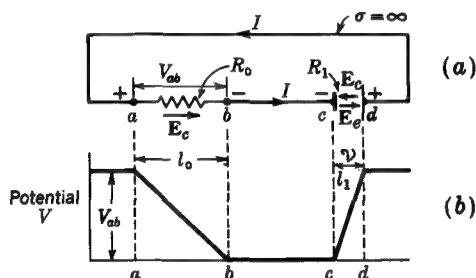


FIGURE 4-7

(a) Series circuit of battery and external resistance with (b) graph showing variation of potential around circuit.

SOLUTION By Kirchhoff's voltage law the sum of the emfs around the circuit equals the sum of the IR drops. Thus

$$\mathcal{U} = IR_0 + IR_1$$

or

$$I = \frac{\mathcal{U}}{R_0 + R_1}$$

In the resistor $\mathbf{E}_e = 0$, but \mathbf{E}_c has a value (as discussed in connection with Fig. 4-2). Applying Ohm's law (4-9-4) to the resistor (between *a* and *b*), we have

$$\mathbf{E}_c = \frac{\mathbf{J}}{\sigma_0} = I \frac{R_0}{l_0}$$

where σ_0 = conductivity of resistor material (assumed uniform)

l_0 = distance from *a* to *b*

Integrating from *a* to *b* yields

$$\int_a^b \mathbf{E}_c \cdot d\mathbf{l} = I \frac{R_0}{l_0} \int_a^b dl$$

or

$$V_{ab} = -IR_0$$

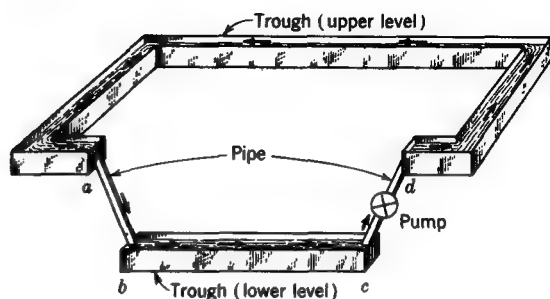


FIGURE 4-8
Hydraulic analog for electric circuit of Fig. 4-7.

where V_{ab} is the potential difference between a and b . Since point a is connected to d and b to c with perfectly conducting wires, $V_{cd} = -V_{ab}$, where V_{cd} is the potential difference appearing across the terminals of the battery. Therefore, we have

$$\mathcal{U} = V_{cd} + IR_1$$

or

$$V_{cd} = \mathcal{U} - IR_1$$

Thus, the potential difference appearing between the terminals of the battery is equal to the emf \mathcal{U} of the battery minus the drop IR_1 due to the internal resistance of the battery. The variation of the potential V around the circuit is as indicated in Fig. 4-7b.

It is instructive to compare the electric circuits of the above examples with the analogous hydraulic systems. Thus, a hydraulic system analogous to the circuit of the above example (Fig. 4-7) is shown in Fig. 4-8. Between b and c there is an open horizontal trough at what may be called a lower level, corresponding to the ground potential in Fig. 4-7. Between c and d there is a pump which raises the water or other liquid against the gravitational field in the same manner as the battery in Fig. 4-7 raises positive charge against the static electric field E_c . Thus, the water in the upper trough has a higher potential energy than the water in the lower trough in the same way as the charge in the wire between d and a in the electric circuit of Fig. 4-7 is at a higher potential than the charge in the wire from b to c . From d to a the water moves in a horizontal frictionless trough at an upper level corresponding to the perfectly conducting wire between these points in Fig. 4-7. From a to b the water falls through a pipe to the lower level and in so doing gives up the energy it acquired in being pumped to the upper level. The pipe offers resistance to the flow of water, and the energy given up by the water appears as heat. This energy is analogous to that appearing as heat in the resistor of Fig. 4-7 owing to charge falling in potential from a to b . In this analogy the pump does work, raising the water against the gravitational field in

the same manner as the chemical action in the battery does work per unit charge (against the electrostatic field \mathbf{E}_e and internal resistance R_1) equal to the emf of the battery.

In a single-cell battery with two electrodes the field \mathbf{E}_e is largely confined to a thin layer at the surface between the electrode and the electrolyte and is zero in the electrolyte between the two electrodes. Thus, the potential variation assumed in the preceding example is not representative of an actual two-electrode cell although it could be approached if each battery consisted of a large number of cells of small emf connected in series between c and d in Fig. 4-7.

4-11 TUBES OF CURRENT

In Chap. 2 we discussed tubes of flux. Let us now consider an analogous concept, namely, that of *tubes of current*. A tapered section of a long conductor is shown in Fig. 4-9. Let all the space in the conductor be filled with current tubes. Each tube is everywhere parallel to the current direction and hence, from the relation $\mathbf{J} = \sigma\mathbf{E}$, is also parallel to the electric field. Since no current passes through the wall of a current tube, the total current I_0 through any cross section of a tube is a constant. Thus

$$I_0 = \iint_a \mathbf{J} \cdot d\mathbf{s} = \text{constant} \quad (1)$$

where \mathbf{J} = current density, A m^{-2}

a = cross section of tube (over which \mathbf{J} is integrated), m^2

If \mathbf{J} is constant over the cross section and normal to it, then $I_0 = Ja$ or, referring to the current tube of rectangular cross section in Fig. 4-9,

$$I_0 = Jbd$$

where b and d are the tube cross-sectional dimensions (see Fig. 4-9).

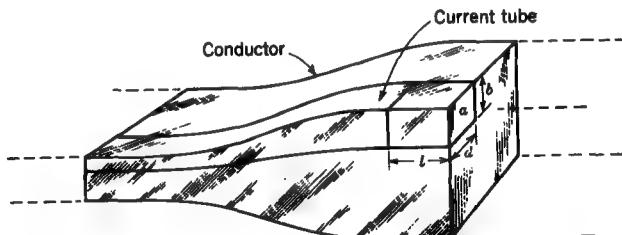


FIGURE 4-9
Tapered section of a long conductor showing current tube.

If all of the conductor is divided up into current tubes, each with the same current I_0 , the total current I through the conductor is $I = I_0 n$, where n is the number of current tubes.

Surfaces normal to the direction of the current (or field) are equipotential surfaces. The potential difference V between two equipotential surfaces separated by a distance l is by Ohm's law equal to the current I_0 in a current tube times the resistance R of a section of tube of length l . Thus, $V = I_0 R$. If the current density is uniform (field uniform), the resistance R is, from (4-7-2), given by

$$R = \frac{l}{\sigma a} \quad (\Omega) \quad (2)$$

where l = length of tube section, m

σ = conductivity of conducting medium, S m^{-1}

a = cross-sectional area of tube, m^2

4-12 KIRCHHOFF'S CURRENT LAW

Whereas flux tubes in a static electric field begin and end on electric charge and hence are *discontinuous*, the tubes of a steady current form closed circuits on themselves and hence are *continuous*. To describe this continuous nature of steady currents, it is said that the current is *solenoidal*. That is, it has no sources or sinks (ending places) as do the flux tubes, which start and end on electric charges in a static electric field. As a consequence as much current must flow into a volume as leaves it. Thus, in general, the integral of the normal component of the current density \mathbf{J} over a closed surface s must equal zero, or

$$\oint_s \mathbf{J} \cdot d\mathbf{s} = 0$$

(1)

This relation is for steady currents and applies to any volume. For example, the volume may be entirely inside a conducting medium, or it may be only partially filled with conductors. The conductors may form a network inside the volume, or they may meet at a point. As an illustration of this latter case, the surface S in Fig. 4-10 encloses a volume that contains five conductors meeting at a junction point P . Taking the current flowing away from the junction as positive and the current flowing toward the junction as negative, we have from (1) that

$$I_1 - I_2 - I_3 + I_4 - I_5 = 0$$

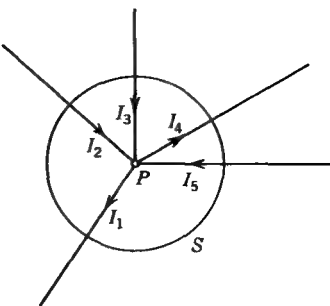


FIGURE 4-10
Junction point of several conductors.

In other words, *the algebraic sum of the currents at a junction is zero*. This is Kirchhoff's current law, which can be expressed in general by the relation

$$\boxed{\sum I = 0} \quad (2)$$

4-13 DIVERGENCE OF J AND CONTINUITY RELATIONS FOR CURRENT

Consider the small volume element Δv shown in Fig. 4-11 located inside a conducting medium. The current density \mathbf{J} is a vector having the direction of the current flow. In general, it has three rectangular components that vary with position. The development here is formally the same as for \mathbf{D} in Sec. 3-23 and yields

$$\boxed{\nabla \cdot \mathbf{J} = 0} \quad (1)$$

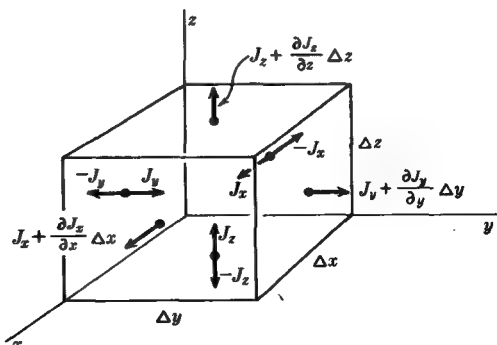


FIGURE 4-11
Construction used to develop differential expression for divergence of \mathbf{J} .

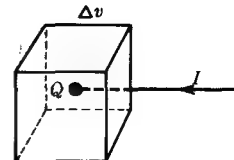


FIGURE 4-12
Construction for the continuity relation between current and charge.

This is a point relation. It states that steady currents have no sources or sinks. Any vector function whose divergence is everywhere zero is said to be solenoidal.

Equation (4-12-1) is an *integral* relation involving \mathbf{J} for a finite region. Equation (1) is a *differential* relation involving \mathbf{J} at a point. Both equations are expressions of the continuous nature of \mathbf{J} . Both are statements of Kirchhoff's current law.

Let us digress briefly to consider the situation if the current is not steady as assumed above. Then (4-12-1) does not necessarily hold, and the difference between the total current flowing out of and into a volume must equal the rate of change of electric charge inside the volume. Specifically, a *net* flow of current *out* of the volume (positive current flow) must equal the *negative* rate of change of charge with time (rate of decrease of charge). Now the total charge in the volume Δv of Fig. 4-11 is $\rho \Delta v$, where ρ is the average charge density. Therefore

$$\oint_s \mathbf{J} \cdot d\mathbf{s} = -\frac{\partial \rho}{\partial t} \Delta v \quad (2)$$

Dividing by Δv and taking the limit as Δv approaches zero, we obtain

$$\nabla \cdot \mathbf{J} = -\frac{\partial \rho}{\partial t} \quad (3)$$

This is the general *continuity relation*[†] between current density \mathbf{J} and the charge density ρ at a point. For steady currents $\partial \rho / \partial t = 0$ and (3) reduces to (1).

Consider now the situation shown in Fig. 4-12, where a wire carrying a current I terminates inside a small volume Δv . Applying (2) to this situation, the integral of \mathbf{J} over the volume yields the net current entering or leaving the volume. Assuming that I is entering the volume, we have

$$\oint \mathbf{J} \cdot d\mathbf{s} = -I \quad (4)$$

Since $\rho \Delta v$ equals the total charge Q inside the volume,

$$\frac{\partial \rho}{\partial t} \Delta v = \frac{dQ}{dt} \quad (5)$$

[†] Also called the equation of *conservation of charge*.

Substituting (4) and (5) in (2) yields

$$I = \frac{dQ}{dt} \quad (6)$$

This is the continuity relation between the current and charge in a wire.

4-14 CURRENT AND FIELD AT A CONDUCTOR-INSULATOR BOUNDARY

The relation between the current density J and the electric field intensity E in a conductor is $J = \sigma E$. Consider now the situation at a conductor-insulator boundary as in Fig. 4-13. Assuming that the conductivity of the insulator is zero, $J = 0$ in the insulator. At the boundary, current in the conductor must flow tangentially to the boundary surface. Thus, on the conductor side of the boundary we have

$$E_t = \frac{J_t}{\sigma} \quad (1)$$

where E_t = component of electric field tangential to boundary = $|E|$

J_t = component of current density tangential to boundary = $|J|$

σ = conductivity of conducting medium

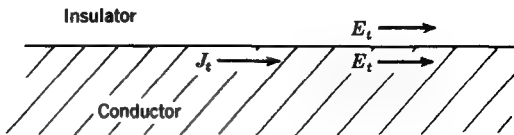


FIGURE 4-13
Insulator-conductor boundary.

By the continuity of the tangential electric field at a boundary, the tangential field on the insulator side of the boundary is also E_t .

When current flows, a conductor of finite conductivity is not an equipotential body as it is in the static case with no currents present. For example, the potential varies along a current-carrying wire with uniform current density as suggested in Fig. 4-14. The arrows indicate the field and current directions, while the transverse

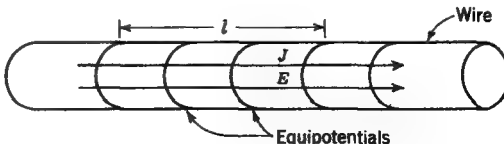


FIGURE 4-14
Section of long wire.

lines are equipotentials. Since \mathbf{E} is uniform, the potential difference V of two points separated by a distance l along the wire is El . This potential difference is also equal to the IR drop, that is, $V = IR$, where I is the current in the wire and R is the resistance of a length l of the wire. The field is the same both inside and outside the wire and is entirely tangential (and parallel to the axis of the wire).

If superimposed on this situation there is a static electric charge distribution at the boundary surface due to the proximity of other conductors at a different potential, a component of the electric field E_n normal to the conductor-insulator boundary also is present on the insulator side of the boundary. The total field in the insulator is then the vector sum of the normal component E_n and the tangential component E_t . In the conductor, $E_n = 0$, and the field is entirely tangential to the boundary. For instance, consider the longitudinal cross section shown in Fig. 4-15 through a part of a long coaxial cable. Current flows to the right in the inner conductor and returns through the outer conductor. The field in the conductor is entirely tangential (and parallel to the axis of the cable) and is indicated by E_t . Since the conductivity of the conductor is large, this field is relatively weak, as suggested by the short arrows for E_t . In the insulating space between the inner and outer conductors there may exist a relatively strong field due to the voltage applied at the end of the cable. This field is a static electric field. It is entirely normal to the surfaces and is indicated by E_n . It is relatively strong, as suggested by the long arrows for E_n . At a point P at the surface of the inner conductor (Fig. 4-15) the total field \mathbf{E} is then the sum of the two components E_n and E_t , added vectorially as in Fig. 4-16. If the conductivity of the metal in the cable is high, E_t may be so small that \mathbf{E} is substantially normal to the surface and equal to E_n . However, the size of E_t has been exaggerated in Fig. 4-16

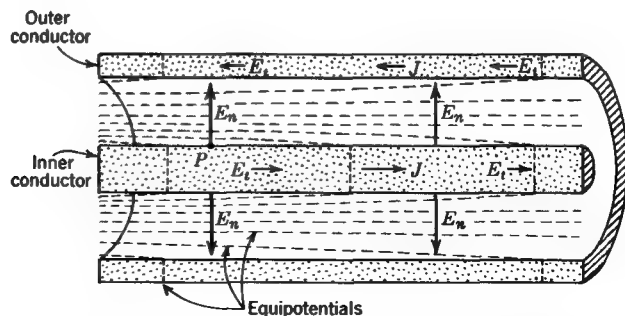


FIGURE 4-15

Longitudinal cross section of coaxial transmission line. Equipotentials are shown by the dashed lines. The arrows indicate the direction of the normal and tangential field components, E_n and E_t , and the current density J .

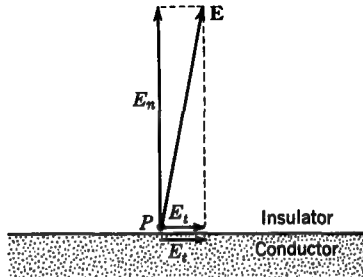


FIGURE 4-16

Total field E at insulator-conductor boundary (point P in Fig. 4-15) resolved into normal and tangential components. The tangential component E_t is due to the current in the conductor ($= J_t/\sigma$) while the normal component E_n is due to the surface charge induced by the voltage between the inner and outer conductors.

in order to show the slant of the total field more clearly. The shape of the total field lines across the entire insulating space between the inner and outer conductors is suggested in Fig. 4-17, with the slant of the field at the conductors greatly exaggerated. Equipotential surfaces are indicated by the dashed lines.

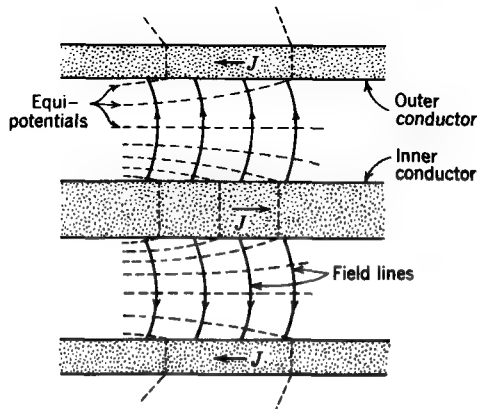


FIGURE 4-17

Longitudinal cross section of coaxial transmission line showing equipotentials (dashed) and total field lines (solid).

4-15 CURRENT AND FIELD AT A CONDUCTOR-CONDUCTOR BOUNDARY

*Consider the conductor-conductor boundary shown in Fig. 4-18 between two media of constants σ_1, ϵ_1 and σ_2, ϵ_2 . In general, the direction of the current changes in flowing from one medium to the other.

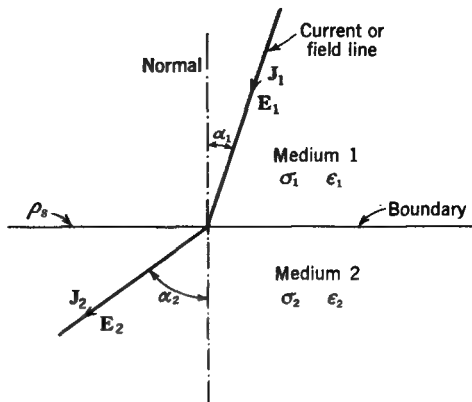


FIGURE 4-18

Boundary between two different conducting media showing change in direction of current or field line.

For steady currents we have the boundary relation

$$J_{n1} = J_{n2} \quad (1)$$

where J_{n1} = component of current density normal to boundary in medium 1

J_{n2} = component of current density normal to boundary in medium 2

From relation (1) of Table 3-2 we also have

$$E_{t1} = E_{t2} \quad (2)$$

where E_{t1} = component of field tangent to boundary in medium 1

E_{t2} = component of field tangent to boundary in medium 2

It follows that

$$\frac{J_{t1}}{\sigma_1} = \frac{J_{t2}}{\sigma_2} \quad (3)$$

where J_{t1} = component of current density tangent to boundary in medium 1

J_{t2} = component of current density tangent to boundary in medium 2

Dividing (3) by (1) gives

$$\frac{J_{t1}}{\sigma_1 J_{n1}} = \frac{J_{t2}}{\sigma_2 J_{n2}} \quad (4)$$

or

$$\frac{\tan \alpha_1}{\tan \alpha_2} = \frac{\sigma_1}{\sigma_2} \quad (5)$$

where α_1 and α_2 are as shown in Fig. 4-18. This relation is similar to Snell's law of refraction (see Chap. 12).

4-16 CURRENT MAPPING AND THE RESISTANCE OF SIMPLE GEOMETRIES; CONDUCTOR CELLS

If the current density is uniform throughout a conductor, its resistance is easily calculated from its dimensions and conductivity. For example, consider the homogeneous rectangular bar of conductivity σ shown in Fig. 4-19. It has $l' = 1$ m, $b' = 400$ mm, and $d = 400$ mm. If the end faces of the bar are clamped against high-conductivity blocks, as in Fig. 4-3, the field and current density throughout the bar will be uniform. The resistance R of the bar is

$$R = \frac{l'}{\sigma b'} = \frac{1}{0.16\sigma} \quad (\Omega) \quad (1)$$

where σ is the conductivity of the bar in mhos per meter.

The resistance of the bar can also be calculated by dividing the side of the bar into square areas each representing the end surface of a *conductor cell*. The sides of the cells are equipotentials. The top and bottom surfaces of the cell are parallel to the current direction. The resistance R_0 of such a cell is given by

$$R_0 = \frac{l}{\sigma d} = \frac{1}{\sigma d} = \frac{S}{d} \quad (1a)$$

where S is the resistivity of the bar material. Hence the product of R_0 and the depth d equals the resistivity S of the bar material, or

$$R_0 d = S \quad (2)$$

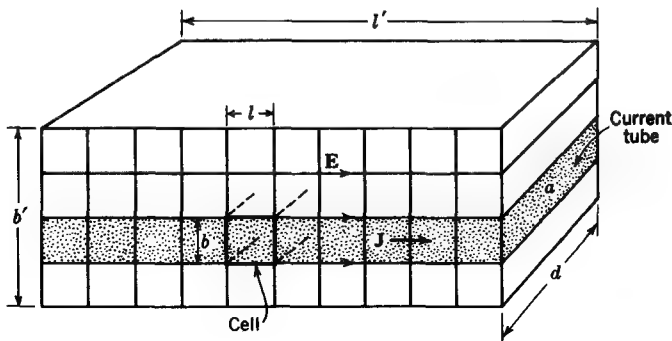


FIGURE 4-19
Conductor divided into current tubes. Vertical lines are equipotentials.

Taking the reciprocal of (2) yields

$$\boxed{\frac{G_0}{d} = \sigma} \quad (3)$$

That is, the conductance per unit depth of a conductor cell is equal to the conductivity of the medium. Referring to Fig. 4-19, let the conductance of each cell equal 1 Ω . Then the total conductance of the bar is

$$\frac{\text{Number of cells (or current tubes) in parallel}}{\text{Number of cells in series}} = \frac{4}{10}$$

From (3) the conductance per unit depth of a conductor cell is σ , so that the actual conductance G_0 of a cell of bar material is given by

$$G_0 = d\sigma = 0.4\sigma \quad (4)$$

The total conductance of the bar is then

$$G = \frac{4}{10}G_0 = \frac{4}{10}0.4\sigma = 0.16\sigma \quad (5)$$

The total resistance is the reciprocal, or

$$R = \frac{1}{0.16\sigma} = 6.25S \quad (6)$$

The method of calculating the resistance or conductance of the bar by means of evaluating the series-parallel combination of conductor cells is more general than the method used in arriving at (1) since it can be applied not only to uniform current distributions (as here) but also to the more general situation where the current distribution is nonuniform. In a nonuniform distribution the sides of many or all of the conductor cells will be curvilinear squares. Their area and arrangement may be determined by graphical current-mapping techniques that are like the field-mapping procedures discussed in Sec. 3-22.

Graphical current-mapping techniques can be applied to any two-dimensional problem, i.e., to a conductor whose shape can be described by a single cross section with all other cross sections parallel to this one being identical to it. Current mapping is actually electric field mapping *in a conducting medium* since the current and the field have the same direction in isotropic media ($J = \sigma E$).

The following fundamental properties are useful in current mapping:

- 1 Current lines and equipotentials intersect at right angles.
- 2 Current flows tangentially to an insulating boundary.
- 3 The total current through any cross section of a continuous current tube is a constant.
- 4 In a uniform current distribution the potential varies linearly with distance.
- 5 Current tubes are continuous.

With these properties in mind one divides a conductor cross section into current tubes and then by equipotentials into *conductor cells* with sides that are squares or curvilinear squares, using the same trial-and-error method described in Sec. 3-22 in connection with field mapping in an insulating medium.

In calculating the conductance of a conductor with a nonuniform current distribution a *current map* is first made, as discussed above. The conductance G is then given by

$$G = \frac{N}{n} G_0 \quad (6)$$

where N = number of cells (or current tubes) in parallel

n = number of cells in series = number of cells per tube

G_0 = conductance of each cell as given by (4)

The accuracy of the conductance (or its reciprocal, the resistance) depends primarily on the accuracy with which the curvilinear squares are mapped.

EXAMPLE A homogeneous rectangular bar of conductivity σ has the dimensions shown in Fig. 4-20a. This bar is identical with the one of Fig. 4-19 except that two cuts have been made across the full width of the bar, as indicated. Find the resistance of the bar when its ends are clamped between high-conductivity blocks as in Fig. 4-3.

SOLUTION A longitudinal cross section of the bar is drawn to scale and a current map made with the result shown in Fig. 4-20b.[†] A portion of one quadrant has been further subdivided to test the accuracy of the curvilinear squares. From (4) or (1a) the resistance R_0 of one conductor cell is $R_0 = 1/0.4\sigma$ (Ω). There are 13 cells in series in a tube, and there are 4 tubes in parallel. Hence, from (6) the resistance R of the bar is

$$R = \frac{13R_0}{4} = \frac{13}{1.6\sigma} = 8.1S \quad (\Omega)$$

Thus, comparing this result with (5) for the uniform bar, the slots in the bar produce an increase of 30 percent in its resistance.

4-17 LAPLACE'S EQUATION FOR CONDUCTING MEDIA

For steady currents $\nabla \cdot \mathbf{J} = 0$, but $\mathbf{J} = \sigma \mathbf{E}$; so $\sigma \nabla \cdot \mathbf{E} = 0$. Recalling that $\mathbf{E} = -\nabla V$, we get $\sigma \nabla \cdot (\nabla V) = 0$ or

$\nabla^2 V = 0$

(1)

[†] Although the entire cross section of the bar has been mapped, the symmetry is such that a map of only one quadrant is required.

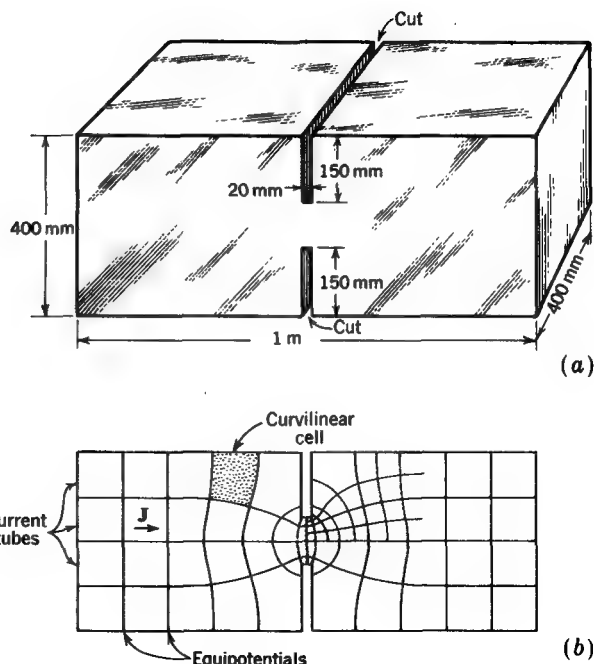


FIGURE 4-20

(a) Conducting bar with notch and (b) current map. Resistance of bar equals ratio of cells in series to cells in parallel multiplied by the resistance of each cell.

This is Laplace's equation. It was derived previously in Sec. 3-27 for static electric fields, and since it also applies here, it follows that problems involving distributions of steady currents in conducting media can be handled in the same way as problems involving static field distributions in insulating media. If we have a conductor with an unknown current distribution, and if a solution to Laplace's equation can be found that also satisfies the boundary conditions, we can obtain the potential and current distribution in the conductor. If this is not possible, we can nevertheless find the approximate potential and current distribution in two-dimensional problems by graphical current mapping as discussed in Sec. 4-16. From a knowledge of the current distribution we can determine the resistance, the maximum current density, and other items of practical importance for a given conductor configuration.

In conducting media, current tubes and the conductivity σ are analogous to the flux tubes and permittivity ϵ in insulating media. Thus in conducting media we have

$$J = \sigma E \quad (\text{A m}^{-2}) \quad (2)$$

while in insulating media we have

$$D = \epsilon E \quad (\text{C m}^{-2}) \quad (3)$$

It is also to be noted that in a conducting medium the *conductance per unit depth* of a conductor cell equals the conductivity of the medium, or

$$\frac{G_0}{d} = \sigma \quad (\Omega \text{ m}^{-1}) \quad (4)$$

where d is the depth of the cell (see Fig. 4-19), while in an insulating medium the capacitance per unit depth of a dielectric field cell equals the permittivity ϵ of the medium, or

$$\frac{C_0}{d} = \epsilon \quad (\text{F m}^{-1}) \quad (5)$$

For a static electric field in a dielectric medium of permittivity ϵ there are no currents, but there is a flux density $D = \epsilon E$. For a static electric field in a conducting medium of conductivity σ there is current of density $J = \sigma E$. Since both fields obey Laplace's equation, a solution in the conductor situation is also a solution for the analogous dielectric situation, and vice versa. For example, if the medium between conductors 1 and 2 in Fig. 3-19 is a conductor of conductivity σ , the conductance per unit depth between ff and gg is given by

$$\frac{G}{d} = \frac{15.43}{4} \sigma = 3.86\sigma \quad (\Omega \text{ m}^{-1})$$

A further discussion of Laplace's equation is given in Chap. 7.

PROBLEMS

- * 4-1 A copper bar 20 by 80 mm in cross section by 2 m in length has 50 mV applied between its ends. Find the following quantities and give units in each case: (a) resistance R of the bar, (b) conductance G of the bar, (c) current I , (d) current density J , (e) electric field E , (f) power loss P in the bar, (g) power loss per unit volume, (h) energy loss W per hour, (i) drift velocity v of electrons. Take $T = 20^\circ\text{C}$ and $\rho = 2\text{GC m}^{-3}$.
- 4-2 Repeat Prob. 4-1 for $T = 100^\circ\text{C}$.
- * 4-3 If $J = 3yz \text{ A m}^{-2}$, find the current I through a square 2 m on a side with one corner at the origin and other corners at $(0,2,0)$, $(0,0,2)$, and $(0,2,2)$.
- * 4-4 A 20-mm-thick L-shaped copper block has the dimensions shown in Fig. P4-4. At 20°C find the resistance R and conductance G (a) between faces 1 and 2, (b) between sides 3 and 4, and (c) between front and back surfaces (parallel to page). (d) If 1 mV is applied between faces 1 and 2, find the current density J and electric field E at the points P_1 and P_2 . The point P_1 is 10 percent of the distance along the diagonal from the inside corner, and P_2

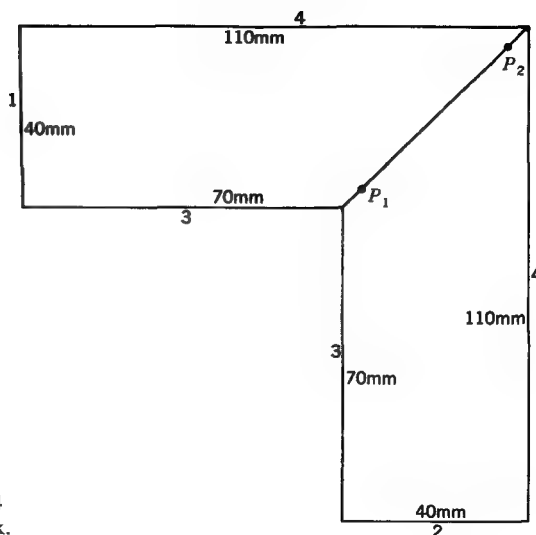


FIGURE P4-4
L-shaped block.

is 10 percent of the distance from the outside corner. (e) What is the ratio of the current density J at P_1 to that at P_2 ?

- * 4-5 If the L-shaped block of Fig. P4-4 is cut along the diagonal at the bend and one half turned over, the two halves can be joined to form a straight bar 20 by 40 mm in cross section by 180 mm long. (a) What is the resistance between the ends of this bar? (b) What is the ratio of the resistance between the faces 1 and 2 of the L-shaped bar [part (a) of Prob. 4-4] and the resistance of the straight bar [part (a) of this problem]? (c) Why is this ratio not unity?

- * 4-6 Two aluminum bars 20 by 20 mm in cross section by 100 mm long are joined by being overlapped 20 mm. At 20°C (a) what is the resistance between the ends of this combination (field map required)? (b) What is the resistance of a continuous bar 20 by 20 mm in cross section by 180 mm long [same length as overlapped bars in (a)]? (c) What is the resistance of a continuous bar 20 by 20 mm in cross section by 200 mm long [same length as two bars of (a) placed end to end]? (d) Why is resistance in (a) greater than in (b) but less than in (c)?

- 4-7 (a) A resistance R_0 and three batteries are connected in series as shown in Fig. P4-7. For the first battery the emf $\mathcal{U}_1 = 1.5$ V and the electrolyte or internal resistance $R_1 = 1 \Omega$, for the second battery the emf $\mathcal{U}_2 = 2$ V and the internal resistance $R_2 = 0$, and for the third battery the emf $\mathcal{U}_3 = 3$ V and the internal resistance $R_3 = 1 \Omega$. The first two batteries have single cells, while the third has three cells in series, each cell of 1 V emf and $\frac{1}{3} \Omega$ internal resistance. Assume that half the total emf of a cell occurs at each electrode, and

* Answers to starred problems are given in Appendix C.

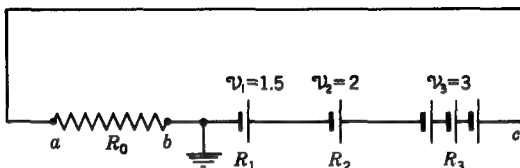


FIGURE P4-7
Series circuit.

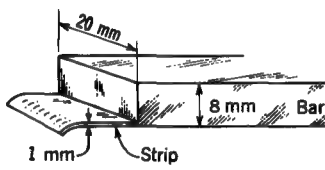
assume that all connections between cells have negligible resistance. Draw a graph such as in Fig. 4-7, showing the variation of potential with position between points *a* and *c* when $R_0 = 4.5 \Omega$ and also when $R_0 = 0$. Take $V = 0$ at the point *b*. (b) Referring to the circuit of Fig. P4-7, let the emfs be as indicated, and let $R_1 = 1.5 \Omega$, $R_2 = 2 \Omega$, and $R_3 = 3 \Omega$. Draw a graph of the variation of potential with position when $R_0 = 6.5 \Omega$ and also when $R_0 = 0$.

* 4-8 Four wires meet at a common junction point. The current in wires 1 and 2 is 5 A each and flowing away from the junction, while the current in wire 3 is 6 A flowing toward the junction. What are the current magnitude and direction in the fourth wire?

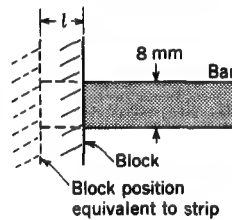
* 4-9 A nichrome bar 40 by 40 mm in cross section by 100 mm long has a hole through it which is symmetrically situated at the center of a long side. The hole is 30 mm in diameter. At 20°C (a) what is the resistance between the ends of the bar? (b) What is the resistance of a solid bar (without hole)? (c) What is the length of a solid bar having the same resistance as in (a)?

4-10 A bar and strip are connected as shown in Fig. P4-10a. The bar has finite conductivity, while the strip conductivity is assumed to be infinite. If the end of the bar is clamped against a large, infinitely conducting block as in Fig. P4-10b instead of connected to the strip as in Fig. P4-10a, determine by what length l the bar would need to be lengthened for its resistance to be the same as when connected to the strip.

4-11 Why is the resistance of the bar of Fig. P4-10 larger when it is connected to the strip than when contact is made with the block?



(a)



(b)

FIGURE P4-10
Bar and strip.

4-12 Deduce the relation $\nabla \cdot \mathbf{J} = 0$ by applying the divergence theorem to

$$\oint_s \mathbf{J} \cdot d\mathbf{s} = 0$$

4-13 Show that the definition of current given by Eq. (4-3-1) leads to the continuity relation $I = dQ/dt$, where Q = positive charge.

4-14 Demonstrate that the source of the emf energizing the coaxial line of Fig. 4-17 is at the left end by showing that if the source were at the right end, the field lines would be bowed in the opposite direction.

4-15 Show that at a conductor-conductor boundary $\sigma_1/\sigma_2 = E_{n2}/E_{n1} = J_{t1}/J_{t2}$.

* 4-16 (a) A wire 2 mm in diameter has a resistance of 1Ω per 100 m. A current of 10 A is flowing in the wire. What is the electric field E in the wire? (b) If a uniform static surface charge of 8 pC m^{-2} is applied to the wire, what is the electric field E (magnitude and direction) just outside the surface of the wire? The medium outside the wire is air.

4-17 The current direction at the flat boundary surface between two media makes an angle of 45° with respect to the surface in medium 1. What is the angle between the current direction and the surface in medium 2? The constants for the media are $\sigma = 1 \text{ MU m}^{-1}$ and $\epsilon = \epsilon_0$ in medium 1 and $\sigma = 1 \text{ k}\Omega \text{ m}^{-1}$ and $\epsilon = 3\epsilon_0$ in medium 2.

4-18 If the current density J in medium 1 is 20 A m^{-2} , what is the surface charge density at the boundary in Prob. 4-17?

* 4-19 Two long parallel zinc-plated iron pipelines have a spacing of 4 m between centers. The pipes are half buried in the ground as indicated in Fig. P4-19. The diameter of the pipes is 500 mm . The conductivity of the ground (sandy soil) is $100 \mu\Omega \text{ m}^{-1}$. Without drawing a field map, find the resistance between the two pipes per meter of length. Hint: Note the analogy between this situation and the static electric field between two parallel cylindrical conductors.

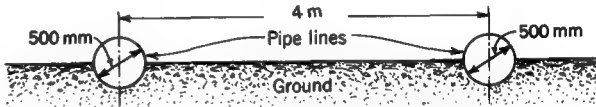


FIGURE P4-19
Pipelines half buried in the ground.

* 4-20 A flat washer of thickness t has an inner radius r_1 and outer radius r_2 . If the conductivity is σ , determine the resistance (a) between the inner and outer edges, (b) between the flat surfaces, and (c) around the washer (same as resistance between the edges of an infinitesimally thick saw cut through one radius of the washer).

4-21 For an applied emf \mathcal{U} determine the current density J as a function of radius for cases (a) and (c) of Prob. 4-20.

4-22 A flat washer of thickness t has an inner radius r_1 and a square outer edge of side length $l = 3r_1$. If the conductivity is σ , determine the resistance (a) between inner and outer edges, (b) between the flat surfaces, and (c) around the washer (same as resistance between the edges of an infinitesimally thick saw cut through one radius of the washer).

4-23 In general, a surface charge is present on the boundary between two conductors (conductivities σ_1 and σ_2 and permittivities ϵ_1 and ϵ_2 , respectively) across which current is flowing. Show that the surface charge density ρ_s is given by

$$\rho_s = J_n \left(\frac{\epsilon_1}{\sigma_1} - \frac{\epsilon_2}{\sigma_2} \right)$$

where J_n is the normal component of current density.

* 4-24 (a) At 30°C, intrinsic semiconductor germanium has an electron mobility of 0.4 and hole mobility of $0.2 \text{ m}^2 \text{s}^{-1} \text{V}^{-1}$. If the electron and hole charge densities are both 4 C m^{-3} , find the conductivity of the material. (b) If an electric field of 10 V m^{-1} is applied find the velocity of the electrons and of the holes.

4-25 Find the current in a wire of 1 mm^2 cross section with an applied field of 0.1 V m^{-1} (a) if the wire is of germanium with properties as in Prob. 4-24 and (b) if the wire is of copper with conductivity of $57 \text{ M}\Omega \text{ m}^{-1}$. (c) If the electron mobility for copper is $0.003 \text{ m}^2 \text{s}^{-1} \text{V}^{-1}$, what is the charge density for the copper wire? (d) Compare the electron drift velocities and charge densities for the two wires.

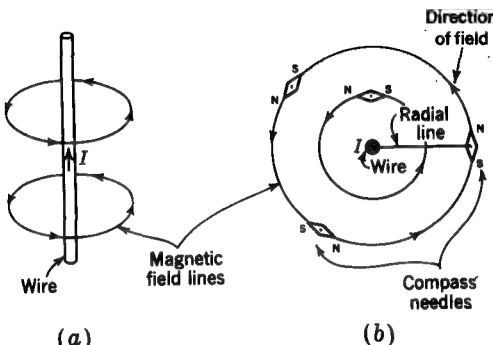
5

THE STATIC MAGNETIC FIELD OF STEADY ELECTRIC CURRENTS

5-1 INTRODUCTION; EFFECT OF A CURRENT ON A MAGNET

A static electric charge has an electric field, as discussed in Chaps. 2 and 3. An electric current, on the other hand, possesses a magnetic field. For instance, a wire carrying a current I has a magnetic field surrounding it, as suggested in Fig. 5-1a. When this field is explored with a pivoted magnet or compass needle, the magnetic field produces an *aligning force* or *torque* on the needle such that the needle always orients itself normal to a radial line originating at the center of the wire. This orientation is parallel to the magnetic field. If one moves in the direction of the needle, it is found that the magnetic field forms *closed circular loops* around the wire.

The direction of the magnetic field is taken to be the direction indicated as "north" (N) by the compass needle, as in Fig. 5-1b. The relation of the magnetic field direction to the current direction can be easily remembered by means of the *right-hand rule*. With the thumb pointing in the direction of the current, as in Fig. 5-2, the fingers of the right hand encircling the wire point in the direction of the magnetic field or lines of magnetic flux.

**FIGURE 5-1**

(a) Magnetic field around wire carrying a current. (b) Cross section perpendicular to the wire. The current is flowing out of the page.

5-2 EFFECT OF A MAGNET ON A CURRENT-CARRYING WIRE

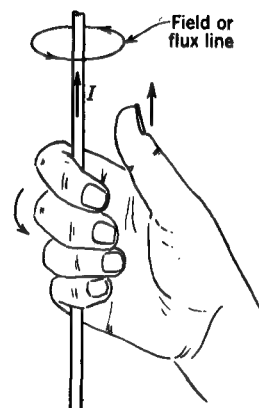
Consider the uniform magnetic field between the poles of a permanent magnet as in Fig. 5-3.† A compass needle may be used to explore this field as suggested. If a straight conductor with current I is placed in the field, it will be acted on by a force

$$F = BIL \quad \text{or} \quad F = LIB \quad (\text{N}) \quad (1)$$

where L = length of conductor in magnetic field, m

I = current in conductor, A

B = factor involving the magnetic field

**FIGURE 5-2**

Right-hand rule relating direction of field or flux lines (fingers) to direction of current I (thumb).

† Due to fringing effects the field will not be uniform at the edges. However, if the pole cross section is large compared to the gap spacing, the effects will be small.

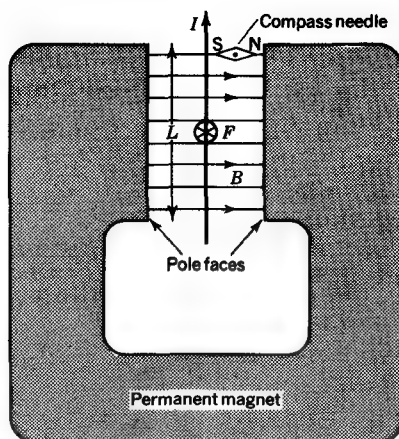


FIGURE 5-3

Linear conductor of length L and current I in uniform magnetic field between pole pieces of a magnet. There is a force on the conductor normal to the page (inward).

In Fig. 5-3, the force is in a direction perpendicular to the page (inward). From (1)

$$B = \frac{F}{IL} = \frac{\text{force}}{\text{current moment}} \quad (\text{N A}^{-1} \text{ m}^{-1} \text{ or T}) \quad (2)$$

Thus, B can be described as a *force per current moment*. However, as will be discussed later, it is customary to call it the *magnetic flux density*. The unit is the weber per square meter (Wb m^{-2}), or tesla (T) ($1 \text{ Wb m}^{-2} = 1 \text{ T}$).

In Fig. 5-3, I , B , and F are mutually perpendicular. If I is not perpendicular to B , we find that F is a function of ϕ (see Fig. 5-4). In general, for any elemental current element

$$dF = BI dl \sin \phi \quad (3)$$

This equation and $F = BIL$ are the basic *motor equations*.

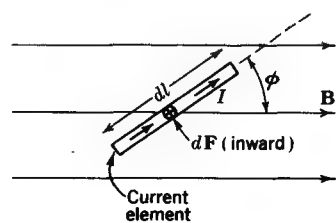


FIGURE 5-4

The force on a current element is normal to the plane containing the element and B .

5-3 THE MAGNETIC FIELD OF A CURRENT-CARRYING ELEMENT; THE BIOT-SAVART LAW

Let the aligning *torque* on an arbitrarily small perfectly mounted magnetic needle be used to measure the field B produced by an incremental current-carrying element of length Δl , as in Fig. 5-5. From these measurements we find (for $r \gg \Delta l$) that the incremental B is a function of I , Δl , r , and θ , as given by

$$\Delta B = k \frac{I \Delta l \sin \theta}{r^2} \quad (1)$$

where k is a constant of proportionality given by

$$k = \frac{\mu}{4\pi} \quad (2)$$

where μ is the *permeability* of the medium. By dimensional analysis of (1) we find that μ has the dimensions of flux per current divided by length. It will be shown in Sec. 5-12 that inductance has the dimensions of flux per current. Therefore permeability has the dimensions of inductance divided by length. The SI unit for

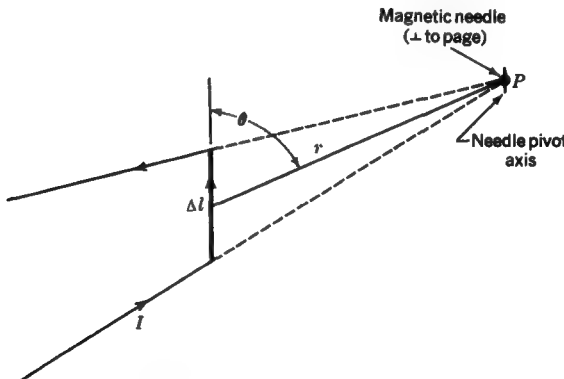


FIGURE 5-5

Arrangement for measuring B produced by short current-carrying element Δl as a function of radius r , angle θ , current I , and length Δl . B is determined by measuring the aligning torque on an arbitrarily small magnetic needle (normal to page) at P . The wires supplying current to the element Δl are always arranged so that they are radial with respect to P , and thus they do not affect B at P .

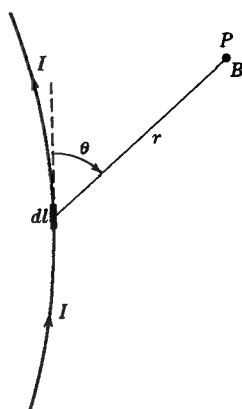


FIGURE 5-6
Construction for calculating flux density B at a point P due to a current I in a long conductor.

permeability is the henry per meter.[†] The permeability of vacuum is

$$\mu_0 = 4\pi \times 10^{-7} \text{ H m}^{-1} = 400\pi \text{ nH m}^{-1}$$

Introducing (2) in (1) and writing infinitesimals instead of incrementals, we obtain the more fundamental relation

$$dB = \frac{\mu}{4\pi} \frac{I dl \sin \theta}{r^2} \quad (3)$$

The direction of dB is normal to the page (inward at P).

In case we wish to know B at a point P , as in Fig. 5-6, due to a current I in a long, straight or curved conductor contained in the plane of the page, we assume that the conductor is made up of elements or segments of infinitesimal length dl connected in series. The total flux density B at the point P is then the sum of the contributions from all these elements and is expressed by the integral of (3). Thus

$$B = \frac{\mu I}{4\pi} \int \frac{\sin \theta}{r^2} dl \quad (4)$$

[†] Recall that permittivity ϵ has the dimensions of *capacitance* per length and is expressed in farads per meter. Note that

$$\frac{1/4\pi\epsilon_0}{\mu_0/4\pi} = \frac{1}{\mu_0\epsilon_0} = c^2$$

where c is the velocity of light or radio waves equal to 300 Mm s^{-1} .

where B = flux density at P , $\text{N A}^{-1} \text{ m}^{-1}$ or T

μ = permeability of medium, H m^{-1}

I = current in conductor, A

dl = length of current element, m

r = distance from element to P , m

θ = angle measured clockwise from positive direction of current along dl to direction of radius vector r extending from dl to P

The integration is carried out over the length of the conductor. Equations (3) and (4) are statements of the *Biot-Savart law*.

5-4 THE MAGNETIC FIELD OF AN INFINITE LINEAR CONDUCTOR

The magnetic field or flux density B at a radius R from a thin linear conductor of infinite length with a current I can be obtained from (5-3-4).

The geometry is shown in Fig. 5-7. With the current I as indicated, \mathbf{B} at the right of the wire is into the page. This is according to the right-hand rule. Since $dl \sin \theta = r d\theta$ and $R = r \sin \theta$, (5-3-4) in this case becomes

$$B = \frac{\mu I}{4\pi R} \int_0^\pi \frac{1}{r} d\theta = \frac{\mu I}{4\pi R} \int_0^\pi \sin \theta d\theta$$

where the integration is between the angles $\theta = 0$ and $\theta = \pi$, that is, over the entire length of an infinite wire. Integrating gives

$$B = \frac{\mu I}{4\pi R} [-\cos \theta]_0^\pi = \frac{\mu I}{4\pi R} 2$$

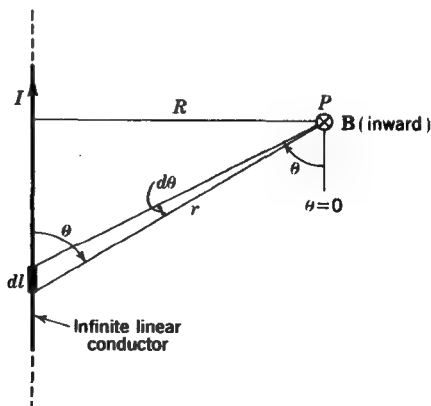


FIGURE 5-7

Construction for finding flux density B near a long straight wire.

or

$$B = \frac{\mu I}{2\pi R} \quad (1)$$

where B = flux density, $\text{N A}^{-1} \text{ m}^{-1}$ or T

μ = permeability of medium, H m^{-1}

I = current in conductor, A

R = radial distance, m

5-5 THE FORCE BETWEEN TWO PARALLEL LINEAR CONDUCTORS; DEFINITION OF THE AMPERE

Consider a length l of two long parallel linear conductors in air spaced a distance R as in Fig. 5-8. Assume that conductor 1 carries a current I and conductor 2 a current I' in the opposite direction. The flux lines due to conductor 1 are into the page at conductor 2. It follows that there is a force to the right on conductor 2 and a force to the left on conductor 1. That is, the conductors are repelled. If the currents were in the same direction, the forces would be reversed and the conductors would be attracted.

The magnitude F of the force on a length l of conductor 2 is

$$F = I' B \int_0^l dl = I' B l \quad (1)$$

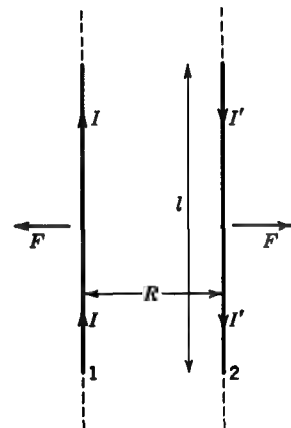


FIGURE 5-8
Force between two long parallel conductors in air.

where I' = current in conductor 2

B = flux density at conductor 2 produced by current I in conductor 1

Introducing the value of B from (5-4-1) gives

$$F = \frac{\mu_0 II'}{2\pi R} l \quad (2)$$

where F = force on length l of conductor 2, N

I = current in conductor 1, A

I' = current in conductor 2, A

R = separation of conductors, m

μ_0 = permeability of vacuum or air = 400π nH m⁻¹

Since (2) is symmetrical in I and I' , the force on a length l of conductor 1 is of the same magnitude as the force F on conductor 2.

Dividing (2) by l yields the *force per unit length* on either conductor as

$$\boxed{\frac{F}{l} = \frac{\mu_0 II'}{2\pi R}} \quad (3)$$

If $I' = I$, and introducing the value for μ_0 ,

$$F = 2 \times 10^{-7} \frac{I^2 l}{R} \quad (\text{N}) \quad (4)$$

If $l = R = 1$ m and $F = 2 \times 10^{-7}$ N, then $I = 1$ A. This measurement is used to define the ampere in the SI system (see Sec. 1-3).

5-6 THE MAGNETIC FIELD OF A CURRENT-CARRYING LOOP

Let the loop be in the xy plane with its center at the origin, as in Fig. 5-9, so that the z axis coincides with the loop axis. The loop has a radius R and current I . At the point P on the loop axis the contribution dB produced by an element of length dl of the loop is, from (5-3-3),

$$dB = \frac{\mu I dl \sin \theta}{4\pi r^2} \quad (1)$$

where θ is the angle between dl and the radius vector of length r . It is assumed that the loop is in a medium of uniform permeability μ . The direction of dB is normal to the radius vector of length r , that is, at an angle ξ with respect to the loop or z axis.

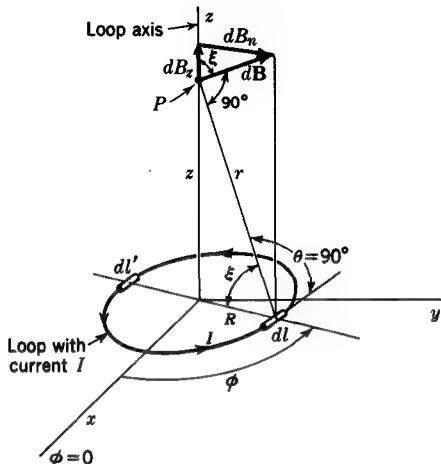


FIGURE 5-9
Construction for finding flux density B
on axis of current loop.

The component dB_z in the direction of the z axis is given by

$$dB_z = dB \cos \xi = dB \frac{R}{r} \quad (2)$$

From Fig. 5-9 we note that $\theta = 90^\circ$, $dl = R d\phi$, and $r = \sqrt{R^2 + z^2}$. Introducing these values into (1) and substituting this value for dB in (2), we have

$$dB_z = \frac{\mu I R^2}{4\pi(R^2 + z^2)^{3/2}} d\phi \quad (3)$$

The total flux density B_z in the z direction is then the integral of (3) around the entire loop. The element dl also produces a component of dB_n normal to the axis of the loop. Integrating this component for all elements around the loop yields zero because of symmetry. Hence, B_z equals the total flux density B at the point P as given by

$$B = B_z = \frac{\mu I R^2}{4\pi(R^2 + z^2)^{3/2}} \int_0^{2\pi} d\phi = \frac{\mu I R^2}{2(R^2 + z^2)^{3/2}} \quad (4)$$

At the center of the loop, $z = 0$, and

$$B = \frac{\mu I}{2R} \quad (5)$$

where B = flux density at center of loop, $\text{N A}^{-1} \text{ m}^{-1}$ or T

μ = permeability of medium, H m^{-1}

I = current in loop, A

R = radius of loop, m

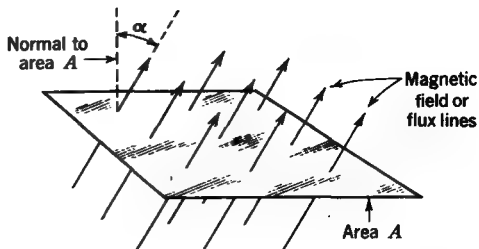


FIGURE 5-10
Flux lines and area A .

5-7 MAGNETIC FLUX ψ_m AND MAGNETIC FLUX DENSITY B

The magnetic field quantity B introduced above as a force per current moment can also be regarded as a *magnetic flux density*, and this term is in more common use. Thus, we describe B as the magnetic flux per unit area or

$$B = \frac{\psi_m}{A} \quad (1)$$

In (1) it is assumed that the magnetic field lines are perpendicular to A . More generally we have (see Fig. 5-10)

$$\psi_m = BA \cos \alpha \quad (2)$$

where ψ_m = magnetic flux through area A

B = magnitude of magnetic flux density B

α = angle between normal to area A and direction of B

Dimensionally

$$\psi_m = \frac{\text{force}}{\text{current moment}} \times \text{area}$$

or in dimensional symbols

$$\frac{ML}{T^2} \frac{L^2}{IL} = \frac{ML^2}{IT^2}$$

The SI unit of magnetic flux ψ_m is the weber (Wb). The unit of magnetic flux density B is the weber per square meter (Wb m^{-2}) or tesla (T) (dimensional symbols M/IT^2).

If B is not uniform over an area, the simple product (2) must be replaced by a surface integral, so that, in general, we have

$$\psi_m = \iint B \cos \alpha \, ds \quad (3)$$

where ds = element of surface area

B = magnitude of \mathbf{B}

α = angle between normal to ds and direction of \mathbf{B}

Equation (3) can also be written as a scalar or dot product. Thus,

$$\psi_m = \iint \mathbf{B} \cdot d\mathbf{s} \quad (4)$$

where ψ_m = magnetic flux, Wb

\mathbf{B} = magnetic flux density, Wb m⁻² or T or N A⁻¹ m⁻¹

$d\mathbf{s}$ = vector with direction normal to surface element ds and magnitude equal to area of ds , m²

5-8 MAGNETIC FLUX OVER A CLOSED SURFACE

The flux tubes of a static electric field originate and end on electric charges. On the other hand, tubes of magnetic flux are continuous; i.e., they have no sources or sinks. This is a fundamental difference between static electric and magnetic fields. To describe this continuous nature of magnetic flux tubes it is said that the flux density \mathbf{B} is *solenoidal*. Since it is continuous, as many magnetic flux tubes must enter a volume as leave it. Hence, when (5-7-4) is carried out over a *closed* surface, the result must be zero, or

$$\oint_s \mathbf{B} \cdot d\mathbf{s} = 0 \quad (1)\dagger$$

This relation may be regarded as Gauss' law applied to magnetic fields [compare with (2-17-6) for electric fields].

It follows that the divergence of \mathbf{B} equals zero. That is,

$$\nabla \cdot \mathbf{B} = 0 \quad (2)$$

Both (1) and (2) are expressions of the continuous nature of \mathbf{B} , (1) being the relation for a finite volume and (2) the relation at a point. Equation (2) is one of Maxwell's equations (in differential form). The same equation in integral form is given by (1).

[†] The symbol \oint_s indicates an integral over a closed surface.

5-9 MAGNETIC FIELD RELATIONS IN VECTOR NOTATION

A linear current-carrying conductor placed in a uniform magnetic field experiences a force F on a length L of conductor that is given, from (5-2-3), by

$$F = IB \sin \phi \int_0^L dl = IBL \sin \phi \quad (1)$$

where F = force, N

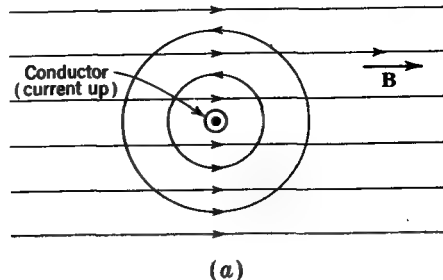
I = current in conductor, A

B = flux density of field, T

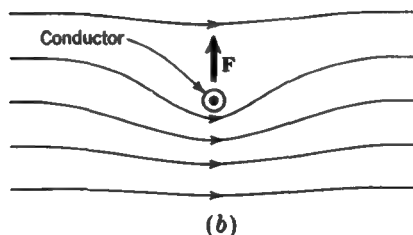
L = length of conductor, m

ϕ = angle between I and B

Equation (1) is a scalar equation and relates only the magnitudes of the quantities involved. The force F is perpendicular to both I and B . For example, let the conductor be normal to a uniform magnetic field of flux density B as in Fig. 5-11a. If the current in the conductor is flowing out of the page, it produces flux lines, as indicated, so that the flux density is increased below the wire and weakened above. The resulting force is therefore upward, as suggested in Fig. 5-11b.



(a)



(b)

FIGURE 5-11
Force F on current-carrying conductor
in uniform magnetic field.

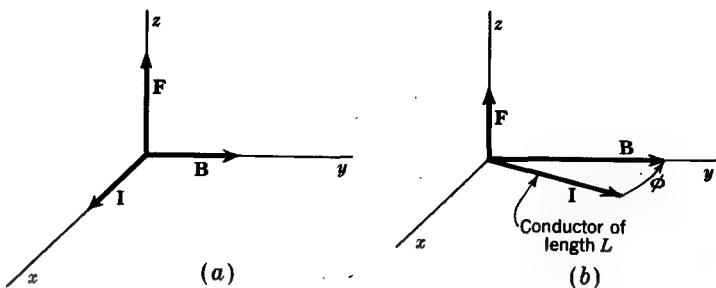


FIGURE 5-12
Relation between current direction \mathbf{I} , field direction \mathbf{B} , and force \mathbf{F} .

Relating the directions to the coordinate axes as in Fig. 5-12a, we have \mathbf{F} in the positive z direction when \mathbf{I} is in the positive x direction and \mathbf{B} in the positive y direction. If the direction of \mathbf{I} is not perpendicular to the direction of \mathbf{B} but is as shown in Fig. 5-12b, the force \mathbf{F} is still in the positive z direction with a magnitude given by (1), where ϕ equals the angle measured from the positive direction of \mathbf{I} to the positive direction of \mathbf{B} (counterclockwise in Fig. 5-12b). With ϕ measured in this way, the force \mathbf{F} is in the positive z direction if $\sin \phi$ is positive.

A more concise method of expressing the relation is by means of the *vector, or cross product*.

The cross product of two vectors is defined as a third vector whose magnitude is equal to the product of the vector magnitudes and the sine of the angle between them. The direction of the third vector is perpendicular to the plane of the two vectors and in such a sense that the three vectors form a right-handed set.

Using the vector product, we can state the relation as

$$\mathbf{F} = (\mathbf{I} \times \mathbf{B})L \quad (2)$$

For an elemental length of conductor this becomes†

$$d\mathbf{F} = (\mathbf{I} \times \mathbf{B}) dl \quad (4)$$

where $d\mathbf{F}$ = vector indicating magnitude and direction of force on element of conductor, \mathbf{N}

\mathbf{I} = vector indicating magnitude and direction of current in conductor, \mathbf{A}

dl = length of conductor, m

\mathbf{B} = vector indicating magnitude and direction of the flux density, \mathbf{T}

† For a volume distribution of current we have

$$d\mathbf{F} = (\mathbf{J} \times \mathbf{B}) dv \quad (3)$$

where $d\mathbf{F}$ is the force on the volume element dv at which the current density is \mathbf{J} .

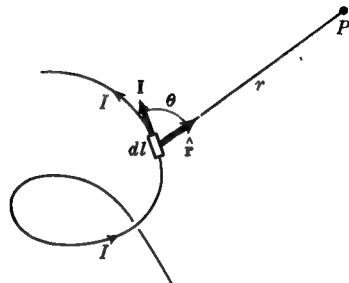


FIGURE 5-13
Relation for finding \mathbf{B} at a point P due
to a current I in a conductor of any shape.

Equation (4) combines in one expression the relations between both the magnitudes and the directions of the quantities involved, whereas (1) related only the magnitudes.

Equation (5-3-4) gives the magnitude of \mathbf{B} at a point as produced by a current I in a straight or curved conductor contained in a single plane. A more general relation applying to a conducting wire of any shape, as in Fig. 5-13, can be stated with the aid of the vector product:

$$\boxed{\mathbf{B} = \frac{\mu}{4\pi} \int \frac{\mathbf{I} \times \hat{\mathbf{r}}}{r^2} dl} \quad (5)$$

where \mathbf{B} = flux density at P , T

μ = permeability of medium, H m⁻¹

\mathbf{I} = current in conductor (vector pointing in positive direction of current at element dl), A

$\hat{\mathbf{r}}$ = unit vector pointing from element dl to point P , dimensionless

r = distance from dl to P , m

dl = infinitesimal element of length of conductor, m

The integration in (5) is carried out over the length of conductor under consideration.

If the current is distributed throughout a volume, the flux density \mathbf{B} is given by

$$\boxed{\mathbf{B} = \frac{\mu}{4\pi} \iiint \frac{\mathbf{J} \times \hat{\mathbf{r}}}{r^2} dv} \quad (6)$$

where \mathbf{J} is the current density in a volume element dv at a distance r . Equations (4), (5), and (6) are basic magnetic field relations.

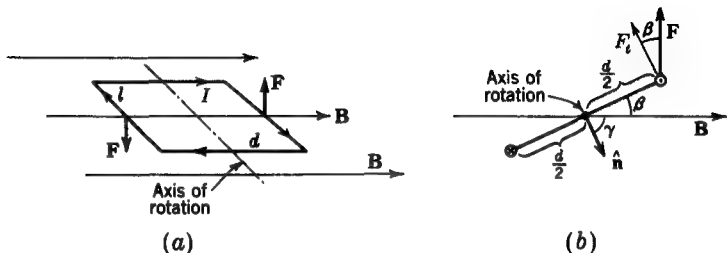


FIGURE 5-14
Rectangular loop in field of uniform flux density \mathbf{B} .

5-10 TORQUE ON A LOOP; MAGNETIC MOMENT

When a current loop is placed parallel to a magnetic field, forces act on the loop that tend to rotate it. The tangential force times the radial distance at which it acts is called the *torque*, or mechanical moment, on the loop. Torque (or mechanical moment) has the dimensions of force times distance and is expressed in newton-meters (N m).

Consider the rectangular loop shown in Fig. 5-14a with sides of length l and d situated in a magnetic field of uniform flux density \mathbf{B} . The loop has a steady current I . According to (5-9-4), the force on any element of the loop is

$$d\mathbf{F} = (\mathbf{I} \times \mathbf{B}) dl \quad (1)$$

If the plane of the loop is at an angle β with respect to \mathbf{B} , as indicated in the cross-sectional view of Fig. 5-14b, the tangential force is

$$F_t = |\mathbf{F}| \cos \beta = IB \cos \beta \int_0^l dl = IBl \cos \beta \quad (2)$$

The total torque on the loop is then

$$T = 2F_t \frac{d}{2} = IBld \cos \beta \quad (3)$$

But ld equals the area A of the loop; so

$$T = IAB \cos \beta \quad (4)$$

According to (4), the torque is proportional to the current in the loop, to its area, and to the flux density of the field in which the loop is situated.

The product IA in (4) has the dimensions of current times area and is the *magnetic moment* of the loop. Its dimensional symbols are IL^2 , and it is expressed in

amperes times square meters (A m^2). Let us designate magnetic moment by the letter m . Then† $m = IA$, and $T = mB \cos \beta$, or

$$T = mB \sin \gamma \quad (5)$$

where γ is the angle between the normal to the plane of the loop and the direction of \mathbf{B} (see Fig. 5-14b). If the loop has N turns, the magnetic moment $m = NIA$.

If the magnetic moment is regarded as a vector \mathbf{m} with direction $\hat{\mathbf{n}}$ normal to the plane of the loop and with its positive sense determined by the right-hand rule (fingers in direction of current, thumb in direction of $\hat{\mathbf{n}}$), the torque relation of (5) can be expressed in a more general form using the vector product. Thus

$$\boxed{\mathbf{T} = \mathbf{m} \times \mathbf{B}} \quad (6)$$

where \mathbf{T} = torque on loop, N m

$\mathbf{m} = \hat{\mathbf{n}}m = \hat{\mathbf{n}}IA$ = magnetic moment of loop, A m^2

\mathbf{B} = flux density of field in which loop is situated, \mathbf{T}

The torque \mathbf{T} is considered to be a vector coinciding with the axis of rotation of the loop as given by $\mathbf{m} \times \mathbf{B}$. The direction of the torque on the loop is obtained by turning \mathbf{m} into \mathbf{B} .

5-11 THE SOLENOID

A helical coil, or solenoid, is often used to produce a magnetic field. Let us calculate the flux density for such a coil.

Let the coil consist of N turns of thin wire carrying a current I . The coil has a length l and radius R (Fig. 5-15a). The spacing between turns is small compared with the radius R of the coil. A cross section through the solenoid is shown in Fig. 5-15b. If the spacing between turns is sufficiently small, or if the wire is replaced by a thin conducting strip of width l/N and with negligible spacing between turns as in Fig. 5-15c, one may consider that the current in the coil produces a current sheet with a linear current density $K = NI/l (\text{A m}^{-1})$. This is equivalent to a single turn of a conducting sheet, as in Fig. 5-15d, with total current $NI (=KI)$.

To find the flux density B at the center of the solenoid, let a section of the coil of length dx , as in Fig. 5-15c, be regarded as a single-turn loop with a current equal to

$$K dx = \frac{NI}{l} dx \quad (1)$$

† Although the loop in Fig. 5-14 has a rectangular area, the relation $m = IA$ applies regardless of the shape of the loop area.

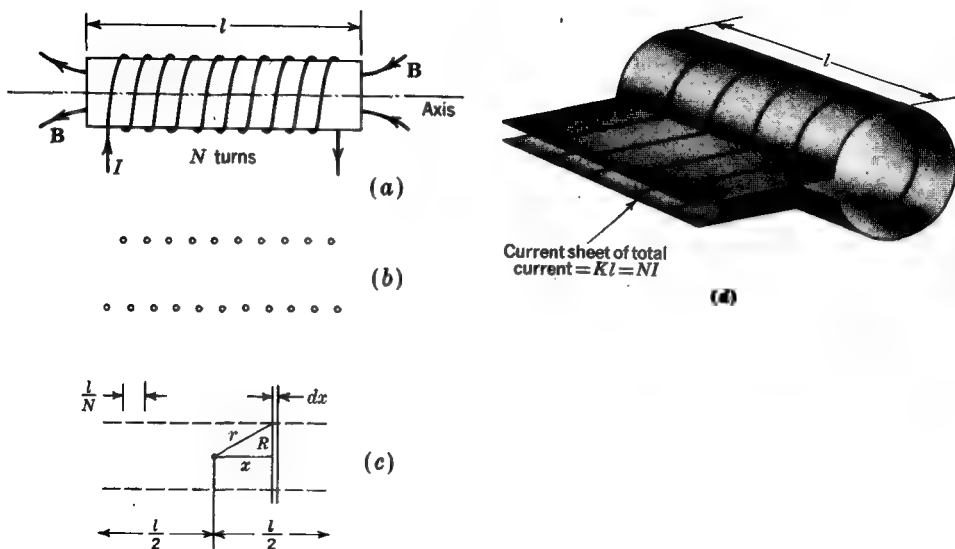


FIGURE 5-15.
(a) Solenoidal coil, (b) cross section, (c) coil with strips and (d) equivalent current sheet.

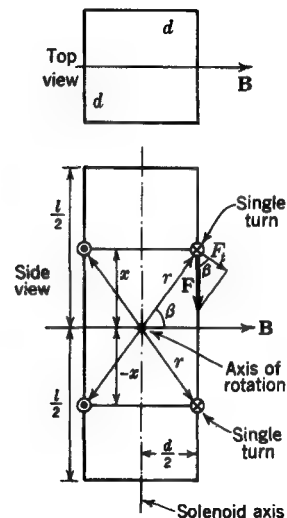


FIGURE 5-16
Solenoid in field of uniform flux density B .

From (5-6-4) the flux density dB at the center of the solenoid due to this loop of length dx at a distance x from the center is

$$dB = \frac{\mu N I R^2}{2l(R^2 + x^2)^{3/2}} dx \quad (2)$$

The total flux density B at the center of this coil is then equal to this expression integrated over the length of the coil. That is,

$$B = \frac{\mu N I R^2}{2l} \int_{-l/2}^{+l/2} \frac{dx}{(R^2 + x^2)^{3/2}} \quad (3)$$

Performing the integration gives

$$B = \frac{\mu N I}{\sqrt{4R^2 + l^2}} \quad (4)$$

If the length of the solenoid is much greater than its radius ($l \gg R$), (4) reduces to

$$B = \frac{\mu N I}{l} = \mu K \quad \text{and} \quad \frac{NI}{l} = K \quad (5)$$

where B = flux density, T

μ = permeability of medium, H m⁻¹

N = number of turns on solenoid, dimensionless

I = current through solenoid, A

l = length of solenoid, m

K = sheet current density, A m⁻¹

Equations (4) and (5) give the flux density at the center of the solenoid. By changing the limits of integration in (3) to 0 and l we obtain the flux density at one end of the coil (on the axis) as

$$B = \frac{\mu N I}{2\sqrt{R^2 + l^2}} \quad (6)$$

For $l \gg R$ this reduces to

$$B = \frac{\mu N I}{2l} = \frac{1}{2}\mu K \quad (7)$$

which is one-half the value at the center of the coil as given by (5).

Let us now calculate the maximum torque tending to rotate a solenoid placed in a magnetic field of uniform flux density. The torque is maximum when the solenoid axis is normal to the direction of B , as in Fig. 5-16. The axis of rotation is at the

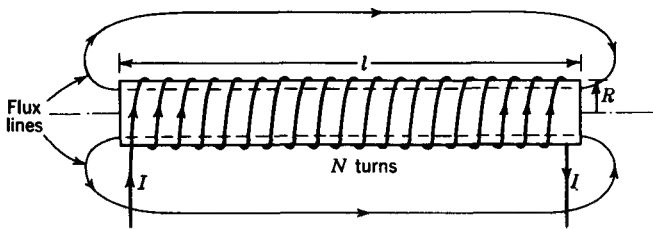


FIGURE 5-17
Solenoid and magnetic flux lines.

center of the solenoid. Assuming that the solenoid is of square cross section, the tangential force F_t on a single straight segment of 1 turn is given by

$$F_t = IBd \cos \beta \quad (8)$$

The net torque due to 2 turns, one at a distance x above the center of the solenoid and another at an equal distance below, is then $T = 4IBrd \cos \beta$. But $\cos \beta = d/2r$; so

$$T = 2Id^2B = 2IAB \quad (9)$$

where $A = d^2$ is the area of the solenoid. This torque is independent of the distance of the turns from the center of the solenoid. Hence, the total torque on the solenoid is equal to Eq. (9) times $N/2$, where N is the number of turns. This is the maximum torque T_m . That is,

$$T_m = NIAB = m'B \quad (10)$$

where $m' = NIA$ is the magnetic moment of the solenoid.

5-12 INDUCTORS AND INDUCTANCE

An inductor† is a device for storing energy in a magnetic field. It may be regarded as the magnetic counterpart of a capacitor, which stores energy in an electric field. As examples, loops, coils, and solenoids are inductors.

The magnetic lines produced by a current in a solenoidal coil form closed loops, as suggested in Fig. 5-17. Each line that passes through the entire solenoid as in the figure links the current N times. If all the lines link all the turns, the total *magnetic*

† An *inductor* is sometimes called an *inductance*. However, it is usual practice to refer to a coil or solenoid as an inductor. This makes for uniform usage when we speak, for example, of an *inductor* of 1 H *inductance*, a *capacitor* of 1 μF *capacitance*, or a *resistor* of 1 Ω *resistance*.

flux linkage Λ (capital lambda) of the coil is equal to the total magnetic flux ψ_m through the coil times the number of turns, or

$$\text{Flux linkage} = \Lambda = N\psi_m \quad (\text{Wb turns})$$

By definition the *inductance* L is the ratio of the total magnetic flux linkage to the current I through the inductor, or

$$L = \frac{N\psi_m}{I} = \frac{\Lambda}{I} \quad (1)$$

This definition is satisfactory for a medium with a constant permeability, such as air. As discussed in Chap. 6, however, the permeability of ferrous media is not constant, and in this case the inductance is defined as the ratio of the infinitesimal change in flux linkage to the infinitesimal change in current producing it, or

$$L = \frac{d\Lambda}{dI} \quad (2)$$

Inductance has the dimensions of magnetic flux (linkage) divided by current. The unit of inductance is the *henry* (H). Thus,

$$\text{Henrys} = \frac{\text{webers}}{\text{ampere}}$$

The dimensional symbols for inductance are ML^2/I^2T^2 .

5-13 INDUCTANCE OF SIMPLE GEOMETRIES

The inductance of many inductors can be readily calculated from their geometry. As examples, expressions for the inductance of a long solenoid, a toroid, a coaxial line, and a two-wire line will be derived in this section.

In Sec. 5-11 it was shown that the flux density B at the end of a long solenoid is less than at the center. This is caused by flux leakage near the ends of the solenoid. However, this leakage is mostly confined to a short distance at the ends of the solenoid, so that if the solenoid is very long, one may, to a good approximation, take B constant over the entire interior of the solenoid and equal to its value at the center (5-11-5). The total flux linkage of a long solenoid is then

$$\Lambda = N\psi_m = NBA = \frac{\mu N^2 IA}{l} \quad (1)$$

Thus, the inductance of a long solenoid (see Fig. 5-17) is

$$L = \frac{\Lambda}{I} = \frac{\mu N^2 A}{l} \quad (2)$$

where L = inductance of solenoid, H

Λ = flux linkage, Wb turns

I = current through solenoid, A

μ = permeability of medium, H m⁻¹

N = number of turns on solenoid, dimensionless

A = cross-sectional area of solenoid, m²

l = length of solenoid, m

EXAMPLE Calculate the inductance of a solenoid of 2,000 turns wound uniformly over a length of 500 mm on a cylindrical paper tube 40 mm in diameter. The medium is air ($\mu = \mu_0$)

SOLUTION From (2) the inductance of the solenoid is

$$L = \frac{4\pi \times 10^{-7} \times 4 \times 10^6 \times \pi \times 4 \times 10^{-4}}{0.5} = 12.6 \text{ mH}$$

If a long solenoid is bent into a circle and closed on itself, a toroidal coil, or toroid, is obtained. When the toroid has a uniform winding of many turns, the magnetic lines of flux are almost entirely confined to the interior of the winding, B being substantially zero outside. If the ratio R/r (see Fig. 5-18) is large, one may calculate B as though the toroid were straightened out into a solenoid. Thus, the flux linkage is

$$\Lambda = N\psi_m = NBA = N \frac{\mu NI}{2\pi R} \pi r^2 = \frac{\mu N^2 I \pi r^2}{2\pi R} = \frac{\mu N^2 r^2}{2R} \quad (3)$$

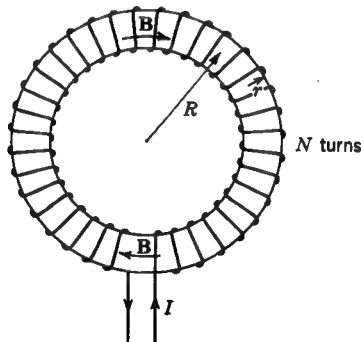


FIGURE 5-18
Toroid.

The inductance of the toroid is then

$$L = \frac{\Lambda}{I} = \frac{\mu N^2 r^2}{2R} \quad (4)$$

where L = inductance of toroid, H

μ = permeability (uniform and constant) of medium inside coil, H m⁻¹

N = number of turns of toroid, dimensionless

r = radius of coil (see Fig. 5-18), m

R = radius of toroid, m

Consider next a coaxial transmission line constructed of conducting cylinders of radius a and b , as in Fig. 5-19. The current on the inner conductor is I . The return current on the outer conductor is of the same magnitude. The flux density B at any radius r is the same as at this radius from a long straight conductor with the same current, or

$$B(\text{at } r) = \frac{\mu I}{2\pi r} \quad (5)$$

The total flux linkage for a length d of line is then d times the integral of (5) from the inner to the outer conductor, or

$$\Lambda = d \int_a^b B dr = \frac{d\mu I}{2\pi} \int_a^b \frac{dr}{r} = \frac{d\mu I}{2\pi} \ln \frac{b}{a} \quad (6)$$

Hence, the inductance of a length d of the coaxial line is

$$L = \frac{\Lambda}{I} = \frac{\mu d}{2\pi} \ln \frac{b}{a} \quad (\text{H}) \quad (7)$$

or the inductance per unit length (L/d) for the coaxial line is given by

$$\frac{L}{d} = \frac{\mu}{2\pi} \ln \frac{b}{a} \quad (\text{H m}^{-1}) \quad (8)$$

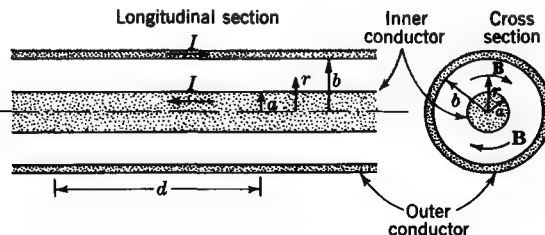


FIGURE 5-19
Coaxial transmission line.

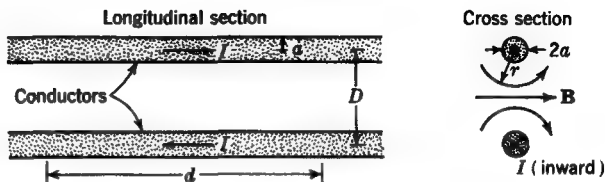


FIGURE 5-20
Two-wire transmission line.

where μ = permeability (uniform and constant) of medium inside coaxial line, H m^{-1}

b = inside radius of outer conductor

a = outside radius of inner conductor (in same units as b)

It is assumed that the currents are confined to the radii a and b . This is effectively the case when the walls of the conductors are thin.

Evaluating (8) for an air-filled line ($\mu = \mu_0$), we have

$$\boxed{\frac{L}{d} = 0.2 \ln \frac{b}{a} = 0.46 \log \frac{b}{a}} \quad (\mu\text{H m}^{-1}) \quad (9)$$

Let us consider finally a two-wire transmission line as illustrated in Fig. 5-20. The conductor radius is a , and the spacing between centers is D . At any radius r from one of the conductors the flux density B due to that conductor is given by (5). The total flux linkage due to both conductors for a length d of line is then d times twice the integral of (5) from a to D , or

$$\Lambda = 2d \int_a^D B dr = \frac{\mu Id}{\pi} \int_a^D \frac{dr}{r} = \frac{\mu Id}{\pi} \ln \frac{D}{a} \quad (10)$$

Hence, the inductance of a length d of the two-conductor line is

$$L = \frac{\Lambda}{I} = \frac{\mu d}{\pi} \ln \frac{D}{a} \quad (11)$$

or the inductance per unit length of line (L/d) is given by

$$\boxed{\frac{L}{d} = \frac{\mu}{\pi} \ln \frac{D}{a} \quad (\text{H m}^{-1})} \quad (12)$$

where μ = permeability (uniform and constant) of medium, H m^{-1}

D = spacing between centers of conductors

a = radius of conductors (in same units as D)

It is assumed that the current is confined to a radius a . This is effectively the case when the walls of the conductors are thin.

Evaluating (12) for a medium of air ($\mu = \mu_0$), we have

$$\frac{L}{d} = 0.4 \ln \frac{D}{a} = 0.92 \log \frac{D}{a} \quad (\mu\text{H m}^{-1}) \quad (13)$$

5-14 AMPÈRE'S LAW AND H

According to (5-4-1), the flux density B at a distance R from a long straight conductor (Fig. 5-21) is given by

$$B = \frac{\mu I}{2\pi R} \quad (1)$$

where μ = permeability of medium, H m^{-1}

I = current in wire, A

If \mathbf{B} is now integrated around a path of radius R enclosing the wire once, we have

$$\oint \mathbf{B} \cdot d\mathbf{l} = \frac{\mu I}{2\pi R} \oint dl = \frac{\mu I}{2\pi R} 2\pi R = \mu I \quad (2)$$

or

$$\oint \mathbf{B} \cdot d\mathbf{l} = \mu I \quad (3)$$

Relation (3) holds not only in the example considered but also in all cases where the integration is over a singly closed path. Equation (3) may be made independent of the medium by introducing the vector \mathbf{H} defined as follows:

$$\boxed{\mathbf{H} = \frac{\mathbf{B}}{\mu}} \quad (4)$$

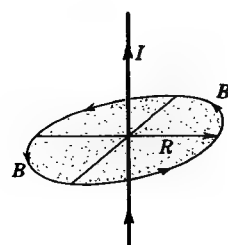


FIGURE 5-21
Relation of flux density B to current I .

According to (4), \mathbf{H} and \mathbf{B} are vectors having the same direction. This is true for all isotropic media.

The quantity \mathbf{H} is called the magnetic field \mathbf{H} , the vector \mathbf{H} , or simply \mathbf{H} . It has the dimensions of

$$\frac{\text{Flux density}}{\text{Permeability}} = \frac{\text{current}}{\text{length}}$$

The dimensional symbols for \mathbf{H} are I/L . In SI units \mathbf{H} is expressed in

$$\frac{\text{Webers/meter}^2}{\text{Webers/ampere-meter}} = \frac{\text{amperes}}{\text{meter}}$$

Introducing (4) into (3) yields

$$\oint \mathbf{H} \cdot d\mathbf{l} = I$$

(5)

where \mathbf{H} = magnetic field, A m^{-1}

$d\mathbf{l}$ = infinitesimal element of path length, m

I = current enclosed, A

This relation is known as *Ampère's law*. In words it states that *the line integral of \mathbf{H} around a single closed path is equal to the current enclosed*.

In the case of a single wire the integration always yields the current I in the wire regardless of the path of integration provided only that the wire is completely enclosed by the path. As illustrations, integration around the two paths at (a) and (b) in Fig. 5-22 yields I , while integration around the paths at (c) and (d) yields zero since these paths do not enclose the wire.

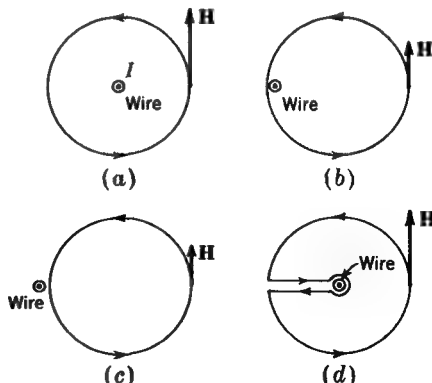


FIGURE 5-22

Line integral of \mathbf{H} around closed paths equals current in wire when paths enclose the wire (a) and (b) but is zero when the paths do not enclose the wire (c) and (d).

EXAMPLE 1 The magnitude of \mathbf{H} at a radius of 1 m from a long linear conductor is 1 A m^{-1} . Find the current in the wire.

SOLUTION According to (5), the current in the wire is given by

$$I = \oint \mathbf{H} \cdot d\mathbf{l} = H \times 2\pi R = 2\pi A$$

EXAMPLE 2 A solid cylindrical conductor of radius R has a uniform current density. Derive expressions for H both inside and outside the conductor. Plot the variation of H as a function of radial distance from the center of the wire.

SOLUTION See Fig. 5-23a. Outside the wire ($r \geq R$)

$$H = \frac{I}{2\pi r} \quad (6)$$

Inside the wire the value of H at a radius r is determined solely by the current inside the radius r . Thus, inside the wire ($r \leq R$)

$$H = \frac{I'}{2\pi r} \quad (7)$$

where $I' = I(r/R)^2$ is the current inside radius r . Therefore, inside the wire

$$H = \frac{I}{2\pi R^2} r \quad (8)$$

At the surface of the wire $r = R$, and (8) equals (6). A graph of the variation of H with r is presented in Fig. 5-23b.

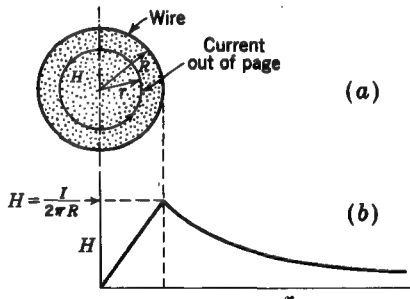


FIGURE 5-23
 H inside and outside current-carrying wire (Example 2).

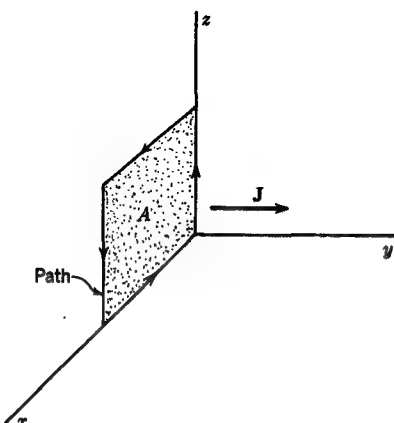


FIGURE 5-24
Rectangular path in medium with
current density J .

5-15 AMPÈRE'S LAW APPLIED TO A CONDUCTING MEDIUM AND MAXWELL'S EQUATION

Ampère's law as discussed in the preceding section may be applied to the more general situation of a path inside a conducting medium. Thus, suppose that the origin of the coordinates in Fig. 5-24 is situated inside a conducting medium of large extent. Let the current density in the medium be J (amperes per square meter) in the positive y direction as shown. According to Ampère's law, the line integral of \mathbf{H} around the rectangular path enclosing the area A (Fig. 5-24) is equal to the current enclosed. In this case, the current I enclosed by the path is given by the integral of the normal component of J over the surface A , or

$$\oint \mathbf{H} \cdot d\mathbf{l} = \iint_A J \cdot d\mathbf{s} = I \quad (1)$$

This expression is a generalization of Ampère's law and constitutes one of Maxwell's equations in integral form.

5-16 MAGNETOSTATIC POTENTIAL U AND MMF F

The line integral of the static electric field \mathbf{E}_c around a closed path is zero.[†] That is,

$$\oint \mathbf{E}_c \cdot d\mathbf{l} = 0 \quad (1)$$

[†] The symbol \mathbf{E}_c indicates explicitly a static electric field as produced by electric charges, as distinguished from an emf-generating field \mathbf{E}_e , as, for example, in a battery. In Chaps. 2 and 3 only \mathbf{E}_c fields were considered, and so for simplicity no subscript was used, it being understood in those chapters that \mathbf{E} means \mathbf{E}_c .

Fields of this type are called *lamellar* and can be derived from a related scalar potential function. Thus, \mathbf{E}_c , which is due to charges, is derivable as the negative gradient of a scalar potential V , or

$$\mathbf{E}_c = -\nabla V \quad (2)$$

Between any two points along a path in the field we have

$$\int_1^2 \mathbf{E}_c \cdot d\mathbf{l} = V_1 - V_2 \quad (3)$$

Although the static magnetic field is not lamellar (since magnetic flux lines form closed loops), it can be treated like a lamellar field if paths of integration are entirely outside current regions and do not enclose any current. Thus, *when no current is enclosed*,

$$\oint \mathbf{H} \cdot d\mathbf{l} = 0 \quad (4)$$

Under this condition, \mathbf{H} can then be derived from a scalar magnetic potential function (or magnetostatic potential) U . That is,[†]

$$\mathbf{H} = -\nabla U \quad (5)$$

Between any two points along a path in the field we have

$$\int_1^2 \mathbf{H} \cdot d\mathbf{l} = U_1 - U_2 \quad (6)$$

The scalar potential U has the dimensions of

$$\frac{\text{Current}}{\text{Distance}} \times \text{distance} = \text{current}$$

Hence, U is expressed in amperes.

Returning now to a further consideration of electric fields, we have learned in Sec. 4-10 that if emfs exist in a path of integration,

$$\oint \mathbf{E} \cdot d\mathbf{l} = \mathcal{U} \quad (7)$$

where \mathbf{E} = total field, V m^{-1}

\mathcal{U} = total emf around path, V

[†] Since $\nabla \cdot \mathbf{D} = 0$ in charge-free regions, we obtain Laplace's equation $\nabla^2 V = 0$. In a magnetic field we always have $\nabla \cdot \mathbf{B} = 0$; so if no current is enclosed, we may write Laplace's equation in the magnetostatic potential as $\nabla^2 U = 0$.

In a magnetic field we may write an analogous relation, based on Ampère's law, that *when current is enclosed* by a path of integration,

$$\oint \mathbf{H} \cdot d\mathbf{l} = I = F \quad (\text{A}) \quad (8)$$

where the quantity F , called the *magnetomotance* or *magnetomotive force* (mmf), is equal to the current enclosed. If the path of integration in (8) encloses a number of turns of wire each with a current I in the same direction, (8) may be written

$$\boxed{\oint \mathbf{H} \cdot d\mathbf{l} = NI = F \quad (\text{A turns})} \quad (9)$$

where N = number of turns of wire enclosed, dimensionless

I = current in each turn, A

The product NI is expressed in *ampere-turns*, and the mmf in this case has the same units.

The above relations for electric and magnetic fields are summarized in Table 5-1.

When the integration is restricted to current-free regions and to paths that are not closed, the potential U and mmf F are the same. The requirement that the path not link the current can be met by introducing a hypothetical barrier surface in the magnetic field through which the path is not allowed to pass. For example, imagine

Table 5-1 COMPARISON OF ELECTRIC AND MAGNETIC FIELD RELATIONS

Relation	Electrostatic fields	Magnetostatic fields
Closed path	$\oint \mathbf{E}_e \cdot d\mathbf{l} = 0$	$\oint \mathbf{H} \cdot d\mathbf{l} = 0$; no current enclosed (Fig. 5-25)
Gradient of scalar potential	$\mathbf{E}_e = -\nabla V \quad (\text{V m}^{-1})$	$\mathbf{H} = -\nabla U \quad (\text{A m}^{-1})$; in current-free region
Integral between two points	$\int_1^2 \mathbf{E}_e \cdot d\mathbf{l} = V_1 - V_2 \quad (\text{V})$	$\int_1^2 \mathbf{H} \cdot d\mathbf{l} = U_1 - U_2 \quad (\text{A})$; path avoids all currents
Closed path	$\oint \mathbf{E} \cdot d\mathbf{l} = \nabla U \quad (\text{V})$	$\oint \mathbf{H} \cdot d\mathbf{l} = I = F \quad (\text{A})$; path encloses current (Fig. 5-26a) or $\oint \mathbf{H} \cdot d\mathbf{l} = NI = F \quad (\text{A turns})$; path encloses current N times (Fig. 5-26b)

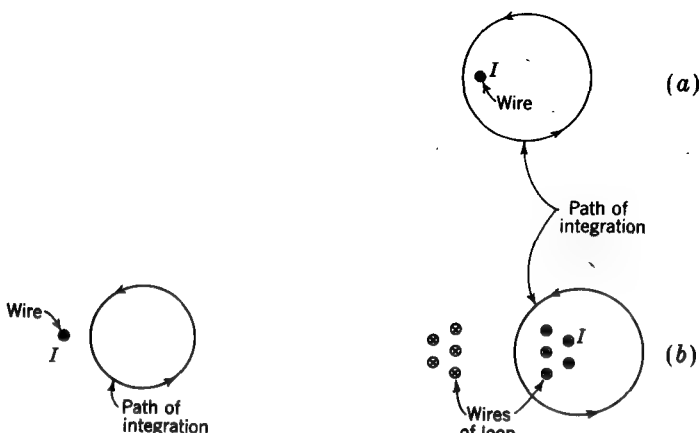


FIGURE 5-25
Path of integration enclosing no current (see Table 5-1).

FIGURE 5-26
(a) Path of integration enclosing current I .
(b) Cross section through 5-turn loop showing path linking the 5 turns (see Table 5-1).

that a long conductor normal to the page as in Fig. 5-27 carries a current I . Let a barrier surface be constructed that extends from the wire an infinite distance to the left, as suggested in the figure. Now the integral of \mathbf{H} from points 1 to 2 yields the current I provided 2 and 1 are separated by an infinitesimal distance. Thus

$$\int_1^2 \mathbf{H} \cdot d\mathbf{l} = U_1 - U_2 = I \quad (\text{A})$$

The requirement of (4) is still satisfied since the line integral of \mathbf{H} around the closed path 1231 that avoids crossing the barrier is zero. That is,

$$\oint_{1231} \mathbf{H} \cdot d\mathbf{l} = 0 \quad (\text{11})$$

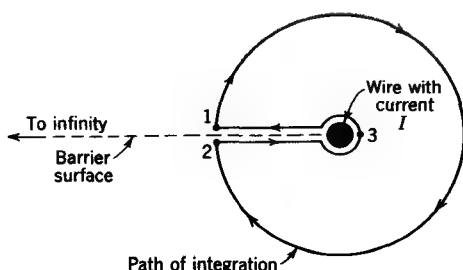


FIGURE 5-27
Conductor and barrier surface.

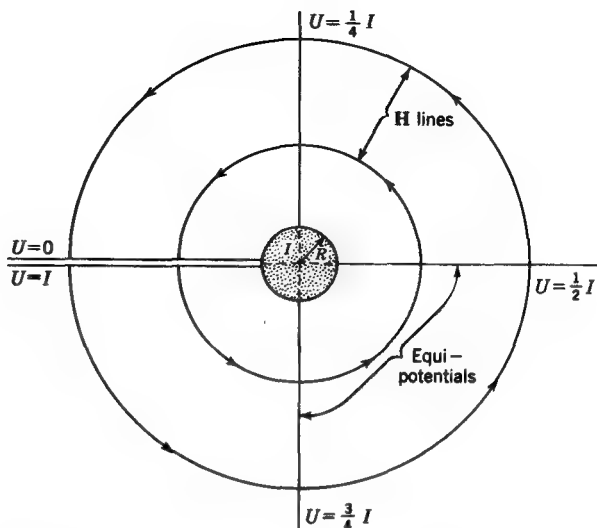


FIGURE 5-28

Current-carrying wire showing magnetic equipotentials (radial) and field lines (circles).

Both U and F are scalar functions. The potential U is independent of the path of integration; that is, U is a single-valued function of position. This follows from the fact that the path of integration never completely encloses the current and is restricted to current-free regions. If a current-carrying wire is encircled more than once by the path of integration (multiple linking), the result is called the mmf F . It is multiple-valued since its magnitude depends on the number of times the path encircles the wire. Hence F is not, in general, independent of the path of integration.

In Fig. 5-27 the barrier surface represents a magnetic equipotential plane. If point 1 is taken arbitrarily as zero potential, then the potential of point 2 on the other side of the barrier is I . Hence, we may construct two surfaces as in Fig. 5-28, one with $U = 0$ and the other $U = I$. Other equipotential surfaces are also drawn in Fig. 5-28 for $U = I/4$, $U = I/2$, and $U = 3I/4$. The equipotential surfaces are everywhere normal to \mathbf{H} and extend from the surface of the wire to infinity. They do not extend into the interior of the wire.

5-17 FIELD CELLS AND PERMEABILITY

Consider a transmission line of two flat parallel conducting strips as in Fig. 5-29a. The strips have a width w and a separation l . Each strip carries a current I . The transmission line is shown in cross section in Fig. 5-29b. The field between the strips

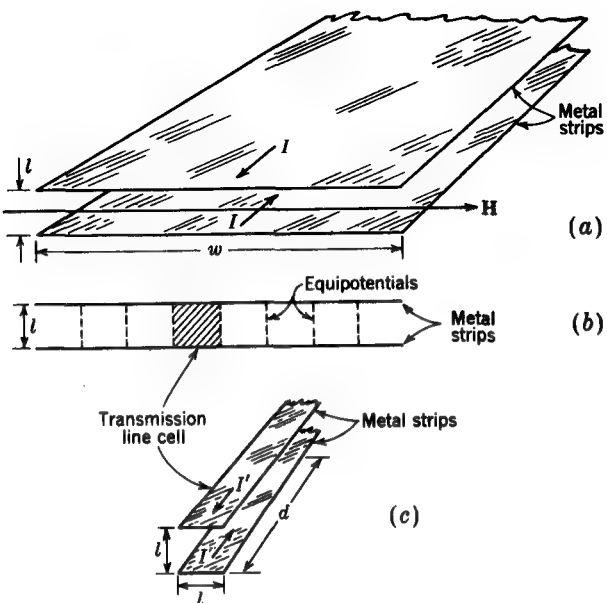


FIGURE 5-29

Parallel-strip transmission line (a) in perspective and (b) in cross section. (c) Magnetic field cell (or transmission-line cell) with strips of width equal to spacing.

is uniform, except near the open sides. If equipotentials are drawn in the uniform field region with a spacing equal to the separation l of the line, we may regard the line as being composed of a number of *field-cell transmission lines* (or *transmission-line cells*) arranged in parallel. Each transmission-line cell has a square cross section, as in Fig. 5-29c.

The current in each strip of a line cell is $I' = (l/w)I$ where I is the current in the entire line. Thus, across one cell $Hl = I'$. Now the total flux linkage per length d of line is given by $\Lambda = Bld$. The inductance of this length of line is then

$$L_0 = \frac{\Lambda}{I'} = \frac{Bld}{Hl} = \mu d \quad (1)$$

or the inductance per unit length is

$$\boxed{\frac{L_0}{d} = \mu} \quad (2)$$

For air $\mu = \mu_0 = 400\pi \text{ nH m}^{-1}$, so that a field-cell transmission line with air as the medium has an inductance per unit length of $400\pi \text{ nH m}^{-1}$, or $1.26 \mu\text{H m}^{-1}$.

Thus, the permeability μ of a medium may be interpreted as the inductance per unit length of a transmission-line cell filled with this medium.

EXAMPLE Using the field-cell concept, calculate the inductance and also capacitance per unit length of the coaxial transmission line shown in cross section in Fig. 5-30. The line is air-filled.

SOLUTION The inductance per unit length of the coaxial line is given by

$$\frac{L}{d} = \frac{1}{n} \frac{L_0}{d} = \frac{\mu_0}{n} \quad (\text{H m}^{-1}) \quad (3)$$

where L_0/d = inductance per unit length of transmission-line cell

n = number of line cells in parallel

μ_0 = permeability of air = $1.26 \mu\text{H m}^{-1}$

Dividing the space between the coaxial conductors into curvilinear squares, we obtain 9.15 line cells in parallel. Thus

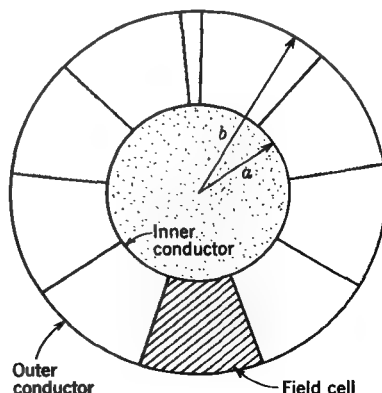
$$\frac{L}{d} = \frac{1.26}{9.15} = 0.138 \mu\text{H m}^{-1}$$

As a check, we note that the radius of the outer conductor is twice the radius of the inner so that from (5-13-9) we get

$$\frac{L}{d} = 0.46 \log 2 = 0.138 \mu\text{H m}^{-1}$$

which is the same result as obtained above.

FIGURE 5-30
Coaxial transmission line divided into
9.15 field-cell lines in parallel.



The capacitance per unit length of the coaxial line of Fig. 5-30 is given by

$$\frac{C}{d} = n \frac{C_0}{d} = n\epsilon_0 \quad (\text{F m}^{-1}) \quad (4)$$

where C_0/d = capacitance per unit length of line cell (same as capacitance per unit length of field-cell capacitor; see Sec. 3-22)

n = number of line cells in parallel

ϵ_0 = permittivity of air = 8.85 pF m^{-1}

Thus

$$\frac{C}{d} = 9.15 \times 8.85 = 81 \text{ pF m}^{-1}$$

Using the relation of (3-18-3),

$$\frac{C}{d} = \frac{24.2}{\log 2} = 81 \text{ pF m}^{-1}$$

which is the same as obtained by the cell method.

5-18 ENERGY IN AN INDUCTOR

An inductor stores energy, as may be demonstrated with the aid of the circuit of Fig. 5-31. With the switch s closed the lamp is lighted. When the switch is opened, the lamp increases momentarily in brilliance because the magnetic energy stored in the magnetic field of the inductance induces a current as the field collapses. The (magnetic) energy delivered to the lamp is

$$W_m = \int P dt = \int VI dt \quad (\text{J}) \quad (1)$$

From circuit theory the voltage across the inductor is given by $V = L dI/dt$; so

$$W_m = L \int I dI = \frac{1}{2} LI^2 \quad (\text{J}) \quad (2)$$

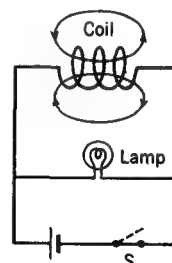


FIGURE 5-31
Circuit for demonstrating energy storage
in a magnetic field.

Thus, the magnetic energy has the dimensions of inductance times current squared. Since $L = \Lambda/I$, the energy stored can be variously expressed as

$$W_m = \frac{1}{2}LI^2 = \frac{1}{2}\Lambda I = \frac{1}{2} \frac{\Lambda^2}{L} \quad (3)$$

where W_m = energy stored, J

L = inductance of inductor, H

I = current through inductor, A

Λ = flux linkage, Wb turns

5-19 ENERGY DENSITY IN A STATIC MAGNETIC FIELD

The energy possessed by an inductor is stored in its magnetic field. Let us find the density of this energy as a function of the flux density B . Consider a small unit cube of side length Δl and volume $\Delta v = \Delta l^3$ situated in a magnetic field as in Fig. 5-32a. Let thin metal sheets be placed on the top and bottom surfaces of the cube, each with a current ΔI as indicated. Also let all the surrounding space be filled with such cubes, as suggested by the cross section of Fig. 5-32b. The directions of the current flow on the sheets are indicated by the circles with a dot (current out of page) and circles with a cross (current into page).

Each cube can be regarded as a magnetic field-cell transmission line of length (into page) of Δl . Each cell has an inductance $\Delta L = \mu \Delta l$. The field H is related to the current ΔI by $H \Delta l = \Delta I$. The energy stored in each cell is, from (5-18-3),

$$\Delta W_m = \frac{1}{2}\Delta L \Delta I^2 \quad (\text{J})$$

It follows that

$$\Delta W_m = \frac{1}{2}\mu H^2 \Delta l^3 = \frac{1}{2}\mu H^2 \Delta v \quad (1)$$

Dividing (1) by Δv and taking the limit of the ratio $\Delta W_m/\Delta v$ as Δv approaches zero, we obtain the energy per volume, or *energy density*, w_m of the magnetic field at the point around which the cell of volume Δv shrinks to zero. Thus

$$w_m = \lim_{\Delta v \rightarrow 0} \frac{\Delta W}{\Delta v} = \frac{1}{2}\mu H^2 \quad (2)$$

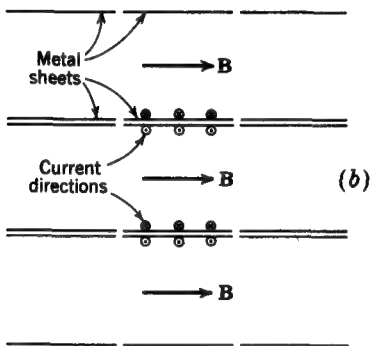
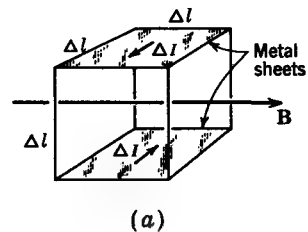


FIGURE 5-32

(a) Small cubical volume in a magnetic field. (b) Cross section through region filled with many such cubes.

5-20 MAGNETIC POLES

A bar magnet can be represented by two magnetic poles of pole strength Q_m separated by a distance l resulting in a dipole moment $Q_m l$. Since the poles of a magnet cannot be separated (see Chap. 6), an isolated magnetic pole is not physically realizable. This contrasts with electric charges (positive and negative), which can be separated. Nevertheless, an isolated magnetic pole is a convenient fiction and will be utilized in the next section to illustrate the concept of curl. We write for the force on the pole

$$\mathbf{F} = \mathbf{B} Q_m \quad \text{or} \quad \mathbf{B} = \frac{\mathbf{F}}{Q_m} \quad (1)$$

where Q_m is the pole strength in ampere meters.

5-21 CURL

Equation (5-14-3) relates the line integral of \mathbf{B} around a *finite closed path*, or *loop*, to μI , where I is the *current* enclosed by the loop. Let us regard the line integral of \mathbf{B} as the work per unit pole required to move an isolated magnetic pole around the closed path.

Although relations involving finite paths are useful in circuit theory, it is frequently desirable in field theory to be able to relate quantities *at a point* in space. Curl is such a point relation and can be regarded as an extension of Ampère's law so that it applies at a point.

Consider a small plane area Δs in a conducting medium with a current ΔI flowing through the area and normal to it. The meaning of the curl of \mathbf{B} may then be expressed as follows: *The magnitude of the curl of \mathbf{B} is equal to the ratio of the work per unit magnetic pole (carried around the boundary of the area) to the area Δs as Δs approaches zero. Further, the curl of \mathbf{B} is a vector with a direction normal to the plane of the area.* Thus, the magnitude of the curl of \mathbf{B} is given by

$$\lim_{\Delta s \rightarrow 0} \frac{\oint \mathbf{B} \cdot d\mathbf{l}}{\Delta s} = \lim_{\Delta s \rightarrow 0} \mu \frac{\Delta I}{\Delta s} = \mu J \quad (1)$$

where J = current density = $\Delta I/\Delta s$ as $\Delta s \rightarrow 0$

ΔI = current through area Δs

The direction of the curl of \mathbf{B} is normal to the area Δs .

Equation (1) gives the total curl of \mathbf{B} if \mathbf{J} is normal to the plane of the loop. If \mathbf{J} is not normal to the plane of the loop, (1) gives only one component of the total curl expression, which will be developed in the following paragraphs.

Suppose that the rectangular coordinate system shown in Fig. 5-33 is situated inside a conducting medium of large extent. Let the current density in the medium be \mathbf{J} and the component of the current density in the x direction J_x . The total current ΔI through the small area $\Delta y \Delta z$ (Fig. 5-33) is then

$$J_x \Delta y \Delta z = \Delta I \quad (2)$$

This current produces a magnetic field. Let the flux density along edge 1 of the area at the y axis be B_y and the flux density along edge 4 at the z axis be B_z . If the field is not uniform, its value at edges 2 and 3 may be expressed to a first approximation (see Fig. 5-33) by

$$B_z + \frac{\partial B_z}{\partial y} \Delta y \quad \text{and} \quad B_y + \frac{\partial B_y}{\partial z} \Delta z \quad (3)$$

Consider now the work performed per unit magnetic pole carried around the periphery of the area. The total work is equal to the sum of the increments of work along each of the four edges. Each increment of work equals the force per unit pole (\mathbf{B}) multiplied by the distance the unit pole moves. The total work will be calculated per unit magnetic pole moved around the path in a counterclockwise direction, as shown in Fig. 5-33. This is the positive direction around the path since a right-

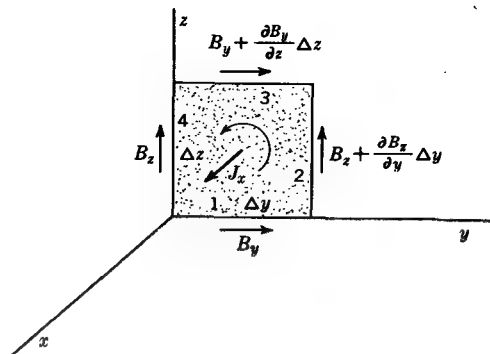


FIGURE 5-33
Construction for finding x component of
curl of \mathbf{B} .

handed screw rotated in this direction will advance in the positive x direction. The work to move the unit pole along edge 1 is $B_y \Delta y$ and along edge 2 is

$$\left(B_z + \frac{\partial B_z}{\partial y} \Delta y \right) \Delta z$$

The work along edge 3 is

$$- \left(B_y + \frac{\partial B_y}{\partial z} \Delta z \right) \Delta y$$

the minus sign indicating that the motion is against the field. The work along edge 4 is $-B_z \Delta z$. The total work equals the sum of these four increments, and this is equal to μ times the total current through the area as given by (2). Thus,

$$\oint \mathbf{B} \cdot d\mathbf{l} = B_y \Delta y + B_z \Delta z + \frac{\partial B_z}{\partial y} \Delta y \Delta z - B_y \Delta y - \frac{\partial B_y}{\partial z} \Delta y \Delta z - B_z \Delta z = \mu J_x \Delta y \Delta z \quad (4)$$

from which

$$\oint \mathbf{B} \cdot d\mathbf{l} = \left(\frac{\partial B_z}{\partial y} - \frac{\partial B_y}{\partial z} \right) \Delta y \Delta z = \mu J_x \Delta y \Delta z \quad (5)$$

Dividing by the area $\Delta y \Delta z$ and taking the limit of the ratio

$$\frac{\text{Work done around periphery of area}}{\text{Area}}$$

as the area approaches zero, we obtain by definition the curl of \mathbf{B} . In this instance it is the x component of the curl of \mathbf{B} , written $\text{curl}_x \mathbf{B}$. Therefore, we have

$$\lim_{\Delta y \Delta z \rightarrow 0} \frac{\oint \mathbf{B} \cdot d\mathbf{l}}{\Delta y \Delta z} = \frac{\partial B_z}{\partial y} - \frac{\partial B_y}{\partial z} = \mu J_x = \text{curl}_x \mathbf{B} \quad (6)$$

Equation (6) is the complete differential expression for $\text{curl } \mathbf{B}$ if the current flows only in the x direction. However, if the current also has components flowing in the y and z directions, $\text{curl } \mathbf{B}$ also has components in these directions. Deriving them in an identical manner to that above and adding them vectorially, we obtain the complete expression for the curl

$$\text{curl } \mathbf{B} = \hat{x} \left(\frac{\partial B_z}{\partial y} - \frac{\partial B_y}{\partial z} \right) + \hat{y} \left(\frac{\partial B_x}{\partial z} - \frac{\partial B_z}{\partial x} \right) + \hat{z} \left(\frac{\partial B_y}{\partial x} - \frac{\partial B_x}{\partial y} \right) \quad (7)$$

This is equal to the vector sum of the current-density components, or

$$\text{curl } \mathbf{B} = \mu (\hat{x} J_x + \hat{y} J_y + \hat{z} J_z) = \mu \mathbf{J} \quad (8)$$

Dividing by μ , we have

$$\text{curl } \mathbf{H} = \mathbf{J} \quad (9)$$

$\text{Curl } \mathbf{H}$ is conveniently expressed in vector notation as the cross product of the operator del (∇) and \mathbf{H} , that is,

$$\begin{aligned} \nabla &= \hat{x} \frac{\partial}{\partial x} + \hat{y} \frac{\partial}{\partial y} + \hat{z} \frac{\partial}{\partial z} \\ \mathbf{H} &= \hat{x} H_x + \hat{y} H_y + \hat{z} H_z \end{aligned} \quad (10)$$

which yields

$$\begin{aligned} \nabla \times \mathbf{H} &= \hat{x} \left(\frac{\partial H_z}{\partial y} - \frac{\partial H_y}{\partial z} \right) + \hat{y} \left(\frac{\partial H_x}{\partial z} - \frac{\partial H_z}{\partial x} \right) + \hat{z} \left(\frac{\partial H_y}{\partial x} - \frac{\partial H_x}{\partial y} \right) \\ &= \hat{x} J_x + \hat{y} J_y + \hat{z} J_z = \mathbf{J} \end{aligned} \quad (11)$$

or

$$\boxed{\nabla \times \mathbf{H} = \mathbf{J}} \quad (12)$$

$\nabla \times \mathbf{H}$ can also be conveniently expressed in determinant form as

$$\nabla \times \mathbf{H} = \begin{vmatrix} \hat{x} & \hat{y} & \hat{z} \\ \frac{\partial}{\partial x} & \frac{\partial}{\partial y} & \frac{\partial}{\partial z} \\ H_x & H_y & H_z \end{vmatrix} \quad (13)$$

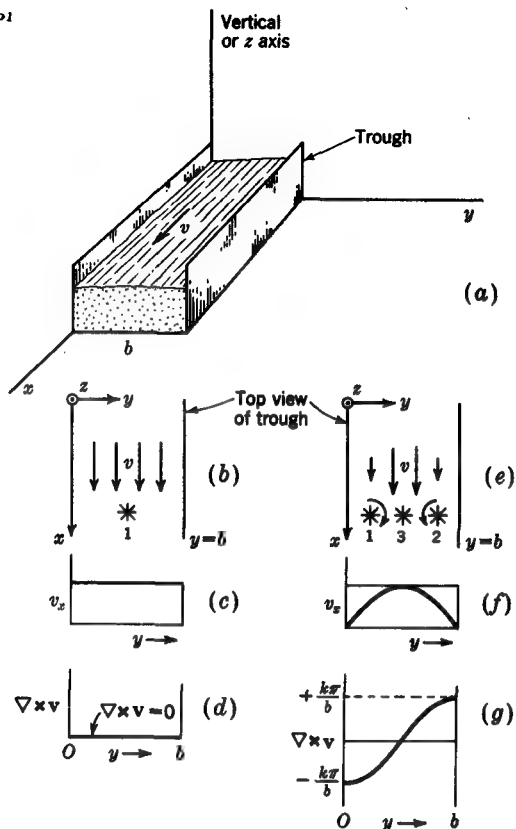


FIGURE 5-34
Water trough for Example 1.

The curl of a quantity is a point function. Therefore, according to (12), $\nabla \times \mathbf{H}$ has a nonzero value only at points where the current density \mathbf{J} is not zero. At a point inside a wire carrying a steady current, $\nabla \times \mathbf{H}$ equals the current density \mathbf{J} at the point, but at a point outside the wire $\nabla \times \mathbf{H} = 0$.

EXAMPLE 1 A rectangular trough carries water in the x direction. A section of the trough is shown in Fig. 5-34a, the vertical direction coinciding with the z axis. The width of the trough is b . Find the curl of the velocity v of the water for two assumed conditions. (a) The velocity is everywhere uniform and equal to a constant, i.e.,

$$\mathbf{v} = \hat{\mathbf{x}}K \quad (14)$$

where \hat{x} = unit vector in positive x direction, dimensionless

$$K = \text{a constant, m s}^{-1}$$

A top view of the trough is shown in Fig. 5-34b with the positive x direction downward. The fact that the velocity v is constant is suggested by the arrows of uniform length and also by the graph of v_x as a function of y in Fig. 5-34c.

(b) The velocity varies from zero at the edges of the trough to a maximum at the center, the quantitative variation being given by

$$\mathbf{v} = \hat{x}K \sin \frac{\pi y}{b} \quad (15)$$

where K = a constant, m s^{-1}

b = width of trough, m

The sinusoidal variation of v is suggested by the arrows in the top view of the trough in Fig. 5-34e and also by the graph of v_x as a function of y in Fig. 5-34f.

SOLUTION (a) Equation (14) can be reexpressed

$$\mathbf{v} = \hat{x}v_x \quad (16)$$

where v_x is the component of velocity in x direction. Thus $v_x = K$. The curl of \mathbf{v} has two terms involving v_x , namely, $\partial v_x / \partial z$ and $\partial v_x / \partial y$. Since v_x is a constant, both terms are zero and hence $\nabla \times \mathbf{v} = 0$ everywhere in the trough (see Fig. 5-34d).

(b) Equation (15) can be reexpressed $\mathbf{v} = \hat{x}v_x$. Thus

$$v_x = K \sin \frac{\pi y}{b} \quad (17)$$

Since v_x is not a function of z , the derivative $\partial v_x / \partial z = 0$. However, v_x is a function of y so that

$$\frac{\partial v_x}{\partial y} = \frac{K\pi}{b} \cos \frac{\pi y}{b} \quad (18)$$

and we have for the curl of \mathbf{v}

$$\nabla \times \mathbf{v} = -\hat{z} \frac{K\pi}{b} \cos \frac{\pi y}{b} \quad (19)$$

where \hat{z} is the unit vector in the positive z direction; i.e., at the left of the center of the trough the curl of \mathbf{v} is in the negative z direction (downward in Fig. 5-34a), while to the right of the center it is in the positive z direction. The variation of the curl of \mathbf{v} across the trough is presented graphically in Fig. 5-34g.

A physical interpretation of the curl of \mathbf{v} in the above example can be obtained with the aid of the curl-meter, or paddle-wheel, device† of Fig. 5-35. If this device is inserted with its shaft vertical into the trough with the assumed sinusoidal variation

† H. H. Skilling, "Fundamentals of Electric Waves," 2d ed., p. 24, John Wiley & Sons, Inc., New York, 1948.

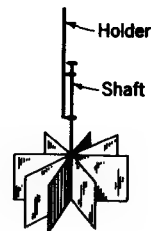


FIGURE 5-35
Paddle wheel for measuring curl.

for the velocity of the water [part (b) of Example 1], it spins clockwise when it is at the left of the center of the trough (position 1 in Fig. 5-34e) and counterclockwise when it is at the right of the center of the trough (position 2 in Fig. 5-34e), corresponding to negative and positive values of curl. At the center of the trough (position 3 in Fig. 5-34e) the curl meter does not rotate since the forces on the paddles are balanced. This corresponds to the curl of \mathbf{v} being zero. The rate of rotation of the paddle-wheel shaft is proportional to the curl of \mathbf{v} at the point where it is inserted. Thus, it rotates fastest near the edges of the trough. At any point the rate of rotation is also a maximum with the shaft vertical (rather than inclined to the vertical), indicating that $\nabla \times \mathbf{v}$ is in the z direction. It is assumed that the paddle wheel is small enough to avoid affecting the flow appreciably and to indicate closely the conditions at a point.

If the curl meter with shaft vertical is inserted in water with uniform velocity, as assumed in part (a) of Example 1, it will not rotate (curl \mathbf{v} equals zero).

EXAMPLE 2 Consider a current-carrying conductor of radius R as shown in cross section in Fig. 5-36a. The current is uniformly distributed so that the current density \mathbf{J} is a constant. Taking the axis of the wire in the z direction,

$$\mathbf{J} = \hat{\mathbf{z}} J = \hat{\mathbf{z}} \frac{I}{\pi R^2} \quad (\text{A m}^{-2}) \quad (20)$$

where I is the total current in the conductor in amperes. Find the curl of \mathbf{H} both inside and outside the wire.

SOLUTION The variation of H as a function of radius was worked out for this case in Example 2 of Sec. 5-14. The variation found for H is shown in the graph of Fig. 5-36b. Since \mathbf{H} is entirely in the θ direction, we have

$$\mathbf{H} = \hat{\theta} H_\theta \quad (21)$$

where

$$H_\theta = \begin{cases} \frac{I}{2\pi r} & \text{outside conductor} \\ \frac{I}{2\pi R^2} r & \text{inside conductor} \end{cases}$$

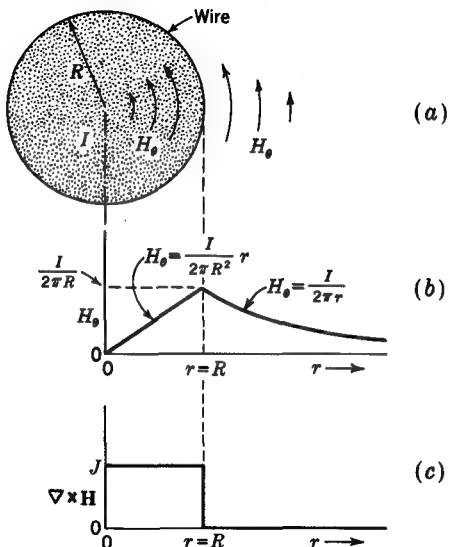


FIGURE 5-36
Conducting wire (Example 2).

Using the expression for curl in cylindrical coordinates (see inside back cover), we have

$$\nabla \times \mathbf{H} = 0 \quad \text{outside conductor} \quad (22)$$

$$\nabla \times \mathbf{H} = \hat{z} \frac{I}{\pi R^2} = \mathbf{J} \quad \text{inside conductor} \quad (23)$$

Hence, the curl of \mathbf{H} has a value only where there is current, being a constant in the conductor and zero outside (see Fig. 5-36c).

5-22 MAXWELL'S FIRST CURL EQUATION

The relation derived from Ampère's law in Sec. 5-21 that

$$\nabla \times \mathbf{H} = \mathbf{J} \quad (1)\dagger$$

is one of Maxwell's equations. Equation (1) is a differential expression and relates the field \mathbf{H} to the current density \mathbf{J} at a point. The corresponding expression in integral form, as given by (5-15-1), relates \mathbf{H} around a finite closed path to the total current passing through the area enclosed.

[†] Equation (1) is a special form of the more general relation given in (8-14-4). The more general equation has an additional term involving the displacement current density. However, a displacement current is present only for time-changing fields so that for steady fields, as considered here, (8-14-4) reduces to (1).

Thus far, we have encountered three of Maxwell's four equations applying at a point. They are $\nabla \cdot \mathbf{D} = \rho$, $\nabla \cdot \mathbf{B} = 0$, and (1). The fourth relation, (8-8-2), is also an equation involving curl, so that (1) may be referred to as Maxwell's first curl equation and (8-8-2) as the second.

5-23 SUMMARY OF OPERATIONS INVOLVING ∇

We have discussed four operations involving the operator ∇ (del), namely, the gradient, divergence, laplacian, and curl. Although the laplacian can be resolved into the divergence of the gradient ($\nabla^2 f = \nabla \cdot \nabla f$), this operation is of such importance as to warrant listing it separately. These operators with their differential equivalents in rectangular coordinates are listed below with f representing a scalar function and \mathbf{F} a vector function.

$$\text{Gradient: } \nabla f = \mathbf{grad} f = \hat{x} \frac{\partial f}{\partial x} + \hat{y} \frac{\partial f}{\partial y} + \hat{z} \frac{\partial f}{\partial z} \quad (1)$$

Gradient operates on a scalar function to yield a vector function.

$$\text{Divergence: } \operatorname{div} \mathbf{F} = \nabla \cdot \mathbf{F} = \frac{\partial F_x}{\partial x} + \frac{\partial F_y}{\partial y} + \frac{\partial F_z}{\partial z} \quad (2)$$

Divergence operates on a vector function to yield a scalar function.

$$\text{Laplacian: } \operatorname{div}(\nabla f) = \nabla \cdot (\nabla f) = \nabla^2 f = \frac{\partial^2 f}{\partial x^2} + \frac{\partial^2 f}{\partial y^2} + \frac{\partial^2 f}{\partial z^2} \quad (3)$$

The laplacian operates on a scalar function to yield another scalar function.[†]

$$\text{Curl: } \operatorname{curl} \mathbf{F} = \nabla \times \mathbf{F} = \hat{x} \left(\frac{\partial F_z}{\partial y} - \frac{\partial F_y}{\partial z} \right) + \hat{y} \left(\frac{\partial F_x}{\partial z} - \frac{\partial F_z}{\partial x} \right) + \hat{z} \left(\frac{\partial F_y}{\partial x} - \frac{\partial F_x}{\partial y} \right) \quad (4)$$

Curl operates on a vector function to yield another vector function.

[†] In rectangular coordinates it is also possible to interpret the laplacian of a vector function as the vector sum of the laplacians of the three scalar components of the vector. Thus

$$\nabla^2 \mathbf{F} = \hat{x} \nabla^2 F_x + \hat{y} \nabla^2 F_y + \hat{z} \nabla^2 F_z$$

However, in no other coordinate system is this simple interpretation possible.

5-24 A COMPARISON OF DIVERGENCE AND CURL

Whereas divergence operates on a vector function to yield a scalar function, curl operates on a vector function to yield a vector function. There is another important difference. Referring to the differential relation for the divergence in (5-23-2), we note that the differentiation with respect to x is on the x component of the field, the differentiation with respect to y is on the y component, etc. Therefore, to have divergence the field must vary in magnitude along a line having the same direction as the field.[†]

Referring to the relation for curl in (5-23-4), we note, on the other hand, that the differentiation with respect to x is on the y and z components of the field, the differentiation with respect to y is on the x and z components, etc. Therefore, to have curl the field must vary in magnitude along a line normal to the direction of the field.[‡]

This comparison is illustrated in Fig. 5-37. The field at (a) is everywhere in the y direction. It has no variation in the x or z directions but varies in magnitude as a function of y . Therefore this field has divergence but no curl. The field at (b) is also everywhere in the y direction. It has no variation in the x and y directions but does vary in magnitude as a function of z . Therefore, this field has curl but no divergence.

Let us now discuss the significance of operations involving ∇ twice. First consider the divergence of the curl of a vector function; i.e.,

$$\nabla \cdot (\nabla \times \mathbf{F}) \quad (1)$$

where \mathbf{F} is any vector function given in rectangular coordinates by

$$\mathbf{F} = \hat{x}F_x + \hat{y}F_y + \hat{z}F_z$$

If we first take the curl of \mathbf{F} , we obtain another vector. Next taking the divergence of this vector, the result is identically zero. Thus

$$\nabla \cdot (\nabla \times \mathbf{F}) \equiv 0 \quad (2)$$

In words (2) states that *the divergence of the curl of a vector function is zero*. As a corollary we may say that if the divergence of a vector function is zero, then it must be the curl of some other vector function.

[†] This is a necessary but not a sufficient condition that a vector field have divergence. For example, the \mathbf{D} field due to a point charge is radial and varies as $1/r^2$ but has no divergence except at the charge. If, however, the field is *everywhere* in the y direction, as in Fig. 5-37a, and varies only as a function of y , then this field does have divergence.

[‡] This is a necessary but not a sufficient condition that a vector field have curl. For example, the \mathbf{H} field outside of a long wire varies in magnitude as $1/r$ and has a direction normal to the radius vector; yet \mathbf{H} has no curl in this region. If, however, the field is *everywhere* in the y direction, as in Fig. 5-37b, and varies only as a function of z , then this field does have curl.

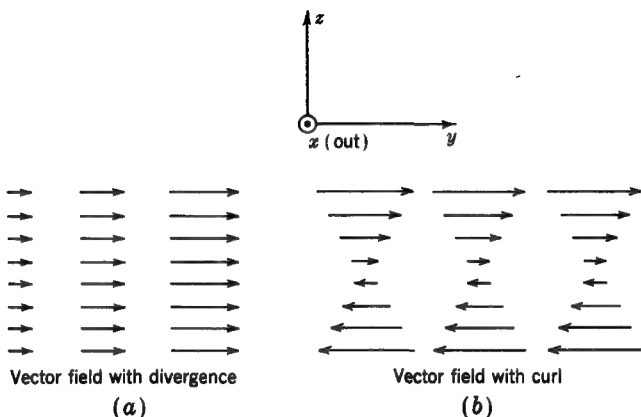


FIGURE 5-37
Examples of fields with divergence and with curl.

For example, the divergence of \mathbf{B} is always zero everywhere; i.e.,

$$\nabla \cdot \mathbf{B} = 0 \quad (3)$$

Therefore, \mathbf{B} can be expressed as the curl of some other vector function. Let us designate this other vector function by \mathbf{A} . Then

$$\mathbf{B} = \nabla \times \mathbf{A} \quad (4)$$

The function **A** in (4) is called the *vector potential* and is discussed in more detail in the next section.

Let us consider another operation involving ∇ twice, namely, the curl of the gradient of a scalar function f . That is,

$$\nabla \times (\nabla f) = 0 \quad (5)$$

Taking first the gradient of f and then the curl of the resulting vector function, the result is found to be identically zero. Thus

$$\nabla \times (\nabla f) \equiv 0 \quad (6)$$

In words (6) states that *the curl of the gradient of a scalar function is zero*. As a corollary, any vector function which is the gradient of some scalar function has no curl.

For example, we recall from (2-13-2) that the static electric field due to charges E_c is derivable as the gradient of a scalar potential V . Thus

$$\mathbf{E}_c = -\nabla V \quad (7)$$

It follows, therefore, that the curl of \mathbf{E}_c is zero, or

$$\nabla \times \mathbf{E}_c = 0 \quad (8)$$

If a vector field has no curl, it is said that the field is *lamellar*. Thus the electric field \mathbf{E}_c is lamellar. The flux tubes of such fields are discontinuous. They originate on positive charges (as sources) and terminate on negative charges (as sinks). On the other hand, if a vector field has no divergence such as \mathbf{B} , it is said that the field is *solenoidal*. Its flux tubes are continuous, having no sources or sinks.

Finally, it is important to note that from $\nabla \cdot \mathbf{D} = \rho$, the divergence of \mathbf{D} finds the sources (ρ) of the electric field, and from $\nabla \times \mathbf{H} = \mathbf{J}$ the curl of \mathbf{H} finds the sources (\mathbf{J}) of the magnetic field.

5-25 THE VECTOR POTENTIAL

According to (5-9-6), the magnetic flux density \mathbf{B} at a point P produced by a current distribution, as in Fig. 5-38, is given by

$$\mathbf{B} = \frac{\mu}{4\pi} \iiint \frac{\mathbf{J} \times \hat{\mathbf{r}}}{r^2} dv \quad (1)$$

where \mathbf{B} = flux density, T

μ = permeability of medium (uniform), H m⁻¹

\mathbf{J} = current density at volume element, A m⁻²

$\hat{\mathbf{r}}$ = unit vector in direction of radius vector r , dimensionless

r = radius vector from volume element to point P , m

dv = volume element, m³

Carrying out the integration over the entire volume occupied by the current-carrying conductor gives the total flux density \mathbf{B} at P due to the current.

In Sec. 5-24 we noted that since the divergence of \mathbf{B} is always zero, it should be possible to express \mathbf{B} as the curl of some other vector. Thus from (5-24-4) we can write

$$\mathbf{B} = \nabla \times \mathbf{A} \quad (2)$$

where \mathbf{A} is called a *vector potential* since it is a potential function that is also a vector.† If we also make

$$\nabla \cdot \mathbf{A} = 0 \quad (3)$$

† The potential function V from which the electric field \mathbf{E}_c can be derived (by the relation $\mathbf{E}_c = -\nabla V$) is a scalar quantity, and hence V is a *scalar potential*.

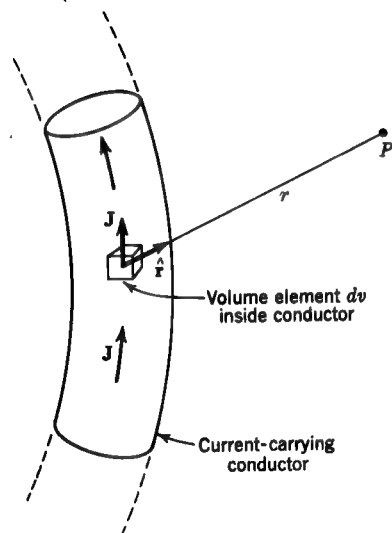


FIGURE 5-38
Construction for finding flux density \mathbf{B} at P . \mathbf{B} is into the page at P .

\mathbf{A} is completely defined. Taking the curl of (2) yields

$$\nabla \times \nabla \times \mathbf{A} = \nabla \times \mathbf{B} = \mu \mathbf{J} \quad (4)$$

By the vector identity for the curl of the curl of a vector (see Appendix A, Sec. A-9) equation (4) becomes

$$\nabla(\nabla \cdot \mathbf{A}) - \nabla^2 \mathbf{A} = \mu \mathbf{J} \quad (5)$$

Introducing the condition of (3), this reduces to

$$\nabla^2 \mathbf{A} = -\mu \mathbf{J} \quad (6)$$

or in terms of the three rectangular components of \mathbf{A} and \mathbf{J}

$$\hat{x}\nabla^2 A_x + \hat{y}\nabla^2 A_y + \hat{z}\nabla^2 A_z = -\mu(\hat{x}J_x + \hat{y}J_y + \hat{z}J_z) \quad (7)$$

Equation (7) is the vector sum of three scalar equations. Hence,

$$\begin{aligned} \nabla^2 A_x &= -\mu J_x \\ \nabla^2 A_y &= -\mu J_y \\ \nabla^2 A_z &= -\mu J_z \end{aligned} \quad (8)$$

Each of these relations has the same form as Poisson's equation. Therefore solutions to the three equations of (8) are

$$\begin{aligned} A_x &= \frac{\mu}{4\pi} \iiint \frac{J_x}{r} dv \\ A_y &= \frac{\mu}{4\pi} \iiint \frac{J_y}{r} dv \\ A_z &= \frac{\mu}{4\pi} \iiint \frac{J_z}{r} dv \end{aligned} \quad (9)$$

Taking the vector sum of the components for \mathbf{A} in (9) gives

$$\boxed{\mathbf{A} = \frac{\mu}{4\pi} \iiint \frac{\mathbf{J}}{r} dv} \quad (10)$$

According to (10), the vector potential \mathbf{A} at a point due to a current distribution is equal to the ratio \mathbf{J}/r integrated over the volume occupied by the current distribution, where \mathbf{J} is the current density at each volume element dv and r is the distance from each volume element to the point P , where \mathbf{A} is being evaluated (see Fig. 5-38). If the current distribution is known, \mathbf{A} can be found. Knowing \mathbf{A} at a point, the flux density \mathbf{B} at that point is then obtained by taking the curl of \mathbf{A} as in (2).

From (2) we note that \mathbf{A} has the dimensions of

$$\text{Magnetic flux density} \times \text{distance} = \frac{\text{magnetic flux}}{\text{distance}} = \frac{\text{force}}{\text{current}}$$

Hence, the vector potential \mathbf{A} can be expressed in webers per meter or newtons per ampere. The dimensional symbols for \mathbf{A} are ML/IT^2 .

EXAMPLE Consider a short copper wire of length l and a cross-sectional area a situated in air coincident with the z axis at the origin, as shown in Fig. 5-39. The current density \mathbf{J} is in the positive z direction. Assume the hypothetical situation that \mathbf{J} is uniform throughout the wire and constant with respect to time. Find the magnetic flux density \mathbf{B} everywhere at a large distance from the wire, using the vector potential to obtain the solution.

SOLUTION The vector potential \mathbf{A} at any point P produced by the wire is given by (10), where the ratio \mathbf{J}/r is integrated throughout the volume occupied by the wire. Since we wish to find \mathbf{B} only at a large distance r from the wire, it suffices to find \mathbf{A} at a large distance. Specifically the distance r should be large compared with the length of the wire ($r \gg l$). Then, at any point P the distance r to different parts of the wire can be considered constant and (10) written as

$$\mathbf{A} = \frac{\mu_0}{4\pi r} \iiint \mathbf{J} dv \quad (11)$$

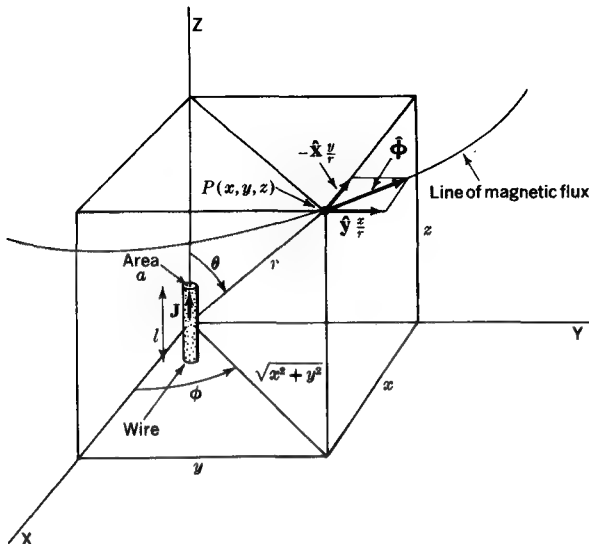


FIGURE 5-39

Construction for finding the vector potential \mathbf{A} and flux density \mathbf{B} due to a short current-carrying wire.

Now \mathbf{J} is everywhere in the z direction and also is uniform. Thus $\mathbf{J} = \hat{\mathbf{z}} J_z$, and

$$\iiint \mathbf{J} dv = \hat{\mathbf{z}} \int_{-l/2}^{l/2} \iint \mathbf{J}_z ds dl = \hat{\mathbf{z}} \int_{-l/2}^{l/2} I dl \quad (12)$$

where $I = J_z a$ is the current in the wire. Completing the integration in (12) and substituting this result in (11), we obtain

$$\mathbf{A} = \hat{\mathbf{z}} \frac{\mu_0 I l}{4\pi r} = \hat{\mathbf{z}} A_z \quad (13)$$

where \mathbf{A} = vector potential at distance r from wire, Wb m^{-1}

$\hat{\mathbf{z}}$ = unit vector in positive z direction, dimensionless

μ_0 = permeability of air = $400\pi \text{ nH m}^{-1}$

I = current in wire, A

l = length of wire, m

r = distance from wire, m

Equation (13) gives the vector potential \mathbf{A} at a large distance from the wire. It is everywhere in the positive z direction as indicated by the unit vector $\hat{\mathbf{z}}$ and is inversely proportional to the distance r from the wire. It is not a function of angle (ϕ or θ in Fig. 5-39).

Having found the vector potential \mathbf{A} , we obtain the flux density \mathbf{B} by taking the curl of \mathbf{A} . In rectangular components the curl of \mathbf{A} is given by

$$\nabla \times \mathbf{A} = \hat{\mathbf{x}} \left(\frac{\partial A_x}{\partial y} - \frac{\partial A_y}{\partial z} \right) + \hat{\mathbf{y}} \left(\frac{\partial A_x}{\partial z} - \frac{\partial A_z}{\partial x} \right) + \hat{\mathbf{z}} \left(\frac{\partial A_y}{\partial x} - \frac{\partial A_z}{\partial y} \right) \quad (14)$$

Since \mathbf{A} has only a z component, (14) reduces to

$$\nabla \times \mathbf{A} = \hat{\mathbf{x}} \frac{\partial A_z}{\partial y} - \hat{\mathbf{y}} \frac{\partial A_z}{\partial x} \quad (15)$$

Now $r = \sqrt{x^2 + y^2 + z^2}$. Therefore

$$\frac{\partial A_z}{\partial y} = \frac{\mu_0 I l}{4\pi} \frac{\partial}{\partial y} (x^2 + y^2 + z^2)^{-1/2} = -\frac{\mu_0 I l}{4\pi r^3} y \quad (16)$$

and $\frac{\partial A_z}{\partial x} = \frac{\mu_0 I l}{4\pi} \frac{\partial}{\partial x} (x^2 + y^2 + z^2)^{-1/2} = -\frac{\mu_0 I l}{4\pi r^3} x \quad (17)$

Introducing these relations in (15) and noting the geometry in Fig. 5-39, we have

$$\nabla \times \mathbf{A} = \frac{\mu_0 I l}{4\pi r^2} \left(-\hat{\mathbf{x}} \frac{y}{r} + \hat{\mathbf{y}} \frac{x}{r} \right) = \hat{\mathbf{z}} \frac{\mu_0 I l}{4\pi r^2} \frac{\sqrt{x^2 + y^2}}{r} \quad (18)$$

or $\mathbf{B} = \nabla \times \mathbf{A} = \hat{\mathbf{z}} \frac{\mu_0 I l \sin \theta}{4\pi r^2} \quad (19)$

where \mathbf{B} = magnetic flux density at distance r and angle θ , T

$\hat{\mathbf{z}}$ = unit vector in ϕ direction (see Fig. 5-39), dimensionless

θ = angle between axis of wire and radius vector r , dimensionless

μ_0 = permeability of air = 400π nH m $^{-1}$

I = current in wire, A

l = length of wire, m

r = distance from wire to point where \mathbf{B} is being evaluated, m

According to (19), the flux density \mathbf{B} produced by the wire is everywhere in the ϕ direction. That is, the lines of magnetic flux form closed circles concentric with the z axis. The planes of the circles are parallel to the xy plane. One such line of magnetic flux at a distance r from the origin is indicated in Fig. 5-39. According to (19), \mathbf{B} is also proportional to $\sin \theta$ and inversely proportional to r^2 .

Although the result of (19) could have been written down almost directly from (1), without using the vector potential explicitly, the above example serves to illustrate the manner in which the vector potential can be applied. Employing the vector potential in the above example is analogous to using a 10-ton steam hammer to crack a walnut. However, on many problems of a more difficult nature the vector potential is indispensable.

5-26 A COMPARISON OF STATIC ELECTRIC AND MAGNETIC FIELDS

It is instructive to compare electric and magnetic fields and to note both their differences and their similarities. A partial comparison is given in Table 5-2 involving relations developed in the preceding chapters for static fields. A comparison of relations for nonstatic fields is given in Sec. 8-18.

Table 5-2 A COMPARISON OF STATIC ELECTRIC AND MAGNETIC FIELD EQUATIONS

Description of equation	Electric fields	Magnetic fields
Force	$\mathbf{F} = Q\mathbf{E}$	$d\mathbf{F} = (\mathbf{I} \times \mathbf{B}) dl$ $\mathbf{F} = Q_m \mathbf{B}$
Basic relations for lamellar and solenoidal fields	$\nabla \times \mathbf{E}_c = 0$ [†]	$\nabla \cdot \mathbf{B} = 0$
Derivation from scalar or vector potential	$\mathbf{E}_c = -\nabla V$ $V = \frac{1}{4\pi\epsilon_0} \int_v \frac{\rho}{r} dv$	$\mathbf{B} = \nabla \times \mathbf{A}$ $\mathbf{A} = \frac{\mu_0}{4\pi} \int_v \frac{\mathbf{J}}{r} dv$
Constitutive relations	$\mathbf{D} = \epsilon \mathbf{E}$	$\mathbf{B} = \mu \mathbf{H}$
Source of electric and magnetic fields	$\nabla \cdot \mathbf{D} = \rho$	$\nabla \times \mathbf{H} = \mathbf{J}$
Energy density	$w_e = \frac{1}{2}\epsilon E^2 = \frac{1}{2}ED$	$w_m = \frac{1}{2}\mu H^2 = \frac{1}{2}BH$
Capacitance and inductance	$C = \frac{Q}{V}$	$L = \frac{\Lambda}{I}$
Capacitance and inductance per unit length of a cell	$\frac{C}{d} = \epsilon$	$\frac{L}{d} = \mu$
Closed path of integration	$\oint \mathbf{E} \cdot d\mathbf{l} = \mathbf{0}$ $\oint \mathbf{E}_c \cdot d\mathbf{l} = 0$	$\oint \mathbf{H} \cdot d\mathbf{l} = \mathbf{F} = NI$ $\oint \mathbf{H} \cdot d\mathbf{l} = 0 \quad \text{no current enclosed}$
Derivation from scalar potentials	$\mathbf{E}_c = -\nabla V$	$\mathbf{H} = -\nabla U \quad \text{in current-free region}$

[†] \mathbf{E}_c is the static electric field intensity (due to charges). \mathbf{E} (without subscript) implies that emf-producing fields (not due to charges) may also be present.

PROBLEMS ($\mu = \mu_0$ everywhere)

- * 5-1 Two long parallel linear conductors carry 100 A. If the conductors are separated by 20 mm, what is the force per meter of length on a conductor if the currents flow (a) in opposite directions and (b) in the same direction?
- * 5-2 A long linear conductor with current of 10 A is coincident with the z axis. The current flows in the $+z$ direction. If $\mathbf{B} = \hat{x}3 + \hat{y}4$ T, find the vector value of the force \mathbf{F} per meter length of conductor.
- 5-3 Show that (5-9-4) can also be written $d\mathbf{F} = -(\mathbf{B} \times \mathbf{I}) dl$.
- * 5-4 A square wire loop 2 m on a side is situated with edges coincident with the positive x and y axes and one corner at the origin. A long straight wire with 50 A flowing in the $+x$ direction is situated in the xy plane and is parallel to the x axis at a distance of 1 m (straight wire crosses loop without touching it). If the loop current is 20 A flowing clockwise, as viewed from the $+z$ direction, find the vector value of the force on the loop.
- * 5-5 (a) If $\mathbf{B} = 2k \sin(\pi x/2) \sin(\pi y/2)$ T, find the total magnetic flux over a square area 2 m on a side with edges coincident with the positive x and y axes and one corner at the origin. (b) If $\mathbf{B} = 2k/r$ T, what is the magnetic flux through a circle of radius r_0 ?
- 5-6 A thin linear conductor of length l carrying a current I is coincident with the y axis. The medium surrounding the conductor is air. One end of the conductor is at a distance y_1 from the origin and the other end at a distance y_2 . Show that the flux density due to the conductor at a point on the x axis at a distance x_1 from the origin is

$$B = \frac{\mu_0 I}{4\pi x_1} \left(\frac{y_2}{\sqrt{x_1^2 + y_2^2}} - \frac{y_1}{\sqrt{x_1^2 + y_1^2}} \right)$$

Note that if the center of the conductor coincides with the origin ($-y_1 = y_2$), and if $x_1 \gg l$, the expression reduces to $B = \mu_0 Il/4\pi x_1^2$.

- * 5-7 A uniform cylindrical coil, or solenoid, of 2,000 turns is 600 mm long and 60 mm in diameter. If the coil carries a current of 15 mA, find the flux density (a) at the center of the coil, (b) on the axis at one end of the coil, (c) on the axis halfway between the center and end of the coil.

5-8 Calculate and plot a graph of B as function of position along the axis of the solenoid of Prob. 5-7 from the center of the solenoid to a distance of 100 mm beyond one end.

- 5-9 Show that the flux density at a point P on the axis of a uniform solenoid is given by

$$B = \mu_0 \frac{NI}{l} \left(1 - \frac{\Omega_1 + \Omega_2}{4\pi} \right)$$

where Ω_1 = solid angle subtended from point P by left end of solenoid ($= 2\pi$ if P is at left end of solenoid)

Ω_2 = solid angle subtended from point P by right end of solenoid ($= 2\pi$ if P is at right end of solenoid)

Note that at the center of a long slender solenoid $\Omega_1 = \Omega_2 \ll 4\pi$ so that $B = \mu_0 NI/l = \mu_0 K$.

* Answers to starred problems are given in Appendix C.

* 5-10 A solenoid 300 mm long and 15 mm in diameter has a uniform winding of 2,500 turns. If the solenoid is placed in a uniform field of 4 T flux density and a current of 2 A is passed through the solenoid winding, what is (a) maximum force on solenoid, (b) maximum torque on solenoid, and (c) magnetic moment of solenoid?

* 5-11 A uniformly wound solenoid of 5,000 turns is 1 m long by 15 mm in diameter. If the current $I = 2$ A, what is (a) the flux density B , (b) magnetic field H , and (c) magnetic energy density w_m at the center of the solenoid? (d) What is the equivalent sheet current density K , (e) the total magnetic energy W_m , and (f) the inductance L ?

5-12 A conducting washer of thickness t has an inner radius r_1 and outer radius r_2 . Find the flux density B as a function of radius r if a current I flows (a) between inner and outer edges, (b) between the flat surfaces, and (c) around the washer (circular loop current).

* 5-13 Find the magnetic flux density B at the center of a square wire loop 2 m on a side carrying a current of 3A.

* 5-14 An infinite wire of parabolic shape carries a current I . Find the magnetic flux density B at the focus.

5-15 An infinite wire of hyperbolic shape carries a current I . Find the magnetic flux density B at the foci.

5-16 Show that the magnetic flux density at a focus of an elliptically shaped loop of wire with current I is given by

$$B = \frac{\mu_0 I}{2\pi r} \left(1 - \sqrt{1 - e^2} \right) \left(\frac{\pi}{e} + \frac{\sqrt{1 - e^2}}{e^2} G \right) \quad (\text{T})$$

where $e = b/a = 1/\text{axial ratio}$

b = semiminor axis

a = semimajor axis

$r = a - \text{distance to focus from center of ellipse}$

and $G = 2\sqrt{2} + \gamma \ln \frac{(2 + \sqrt{2})\gamma + (\sqrt{2} + 1)}{(2 + \sqrt{2})\gamma - (\sqrt{2} + 1)} + 2\sqrt{\gamma^2 - 1} \sin^{-1} \frac{1}{\sqrt{2\gamma^2 - 1}}$

where

$$\gamma = \frac{1}{\sqrt{1 - e^2}}$$

* 5-17 (a) What is the maximum torque on a square loop of 200 turns in a field of uniform flux density $B = 4$ T? The loop is 150 mm on a side and carries a current of 8 A. (b) What is the magnetic moment of the loop?

* 5-18 What is the maximum torque on a small coil of magnetic moment 10^{-3} A m $^{-2}$ situated near the center of a long air-filled solenoid of 1,500 turns per meter with a current of 2 A?

5-19 Referring to Fig. P5-19, show that the force between the two current elements situated in air is given by

$$d\mathbf{F} = \frac{\mu_0 I_2 dl_2 I_1 dl_1}{4\pi r^2} \hat{a}_1 \times (\hat{a}_2 \times \hat{r}) \quad (1)$$

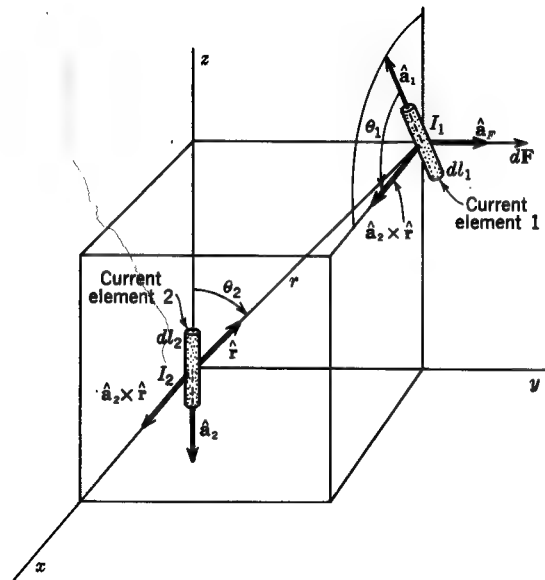


FIGURE P5-19
Geometry of short current-carrying elements for finding force between them.

where $d\mathbf{F}$ = force on element 1 due to current I_2 in element 2, N

μ_0 = permeability of air, H m^{-1}

dl_1, dl_2 = lengths of current elements 1 and 2, respectively, m

I_1, I_2 = currents in elements 1 and 2, respectively, A

r = distance between elements, m

$\hat{\mathbf{a}}_1$ = unit vector in direction of current I_1 in element 1, dimensionless

$\hat{\mathbf{a}}_2$ = unit vector in direction of current I_2 in element 2, dimensionless

$\hat{\mathbf{f}}$ = unit vector in radial direction (from element 2 to 1), dimensionless

Show further that $d\mathbf{F} = \hat{\mathbf{a}}_r d\mathbf{F}$, where $d\mathbf{F}$ is given by

$$d\mathbf{F} = |d\mathbf{F}| = \frac{\mu_0 I_2 dl_2 I_1 dl_1 \sin \theta_2 \sin \theta_1}{4\pi r^2}$$

where θ_2 = angle between $\hat{\mathbf{a}}_2$ and $\hat{\mathbf{f}}$ (see Fig. P5-19)

θ_1 = angle between $\hat{\mathbf{a}}_1$ and $\hat{\mathbf{a}}_2 \times \hat{\mathbf{f}}$

and

$$\hat{\mathbf{a}}_r = \frac{\hat{\mathbf{a}}_1 \times (\hat{\mathbf{a}}_2 \times \hat{\mathbf{f}})}{\sin \theta_2 \sin \theta_1}$$

where $\hat{\mathbf{a}}_r$ is the unit vector in the direction of force $d\mathbf{F}$.

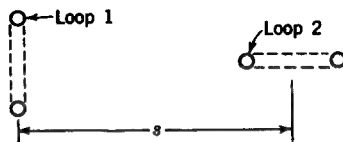


FIGURE P5-20
Geometry of loops for finding torque.

It is noted that these equations give the force on element 1 due to the presence of element 2 but not vice versa. That is, they are not symmetrical with respect to elements 1 and 2. However, with two closed circuits the force, as given by an integral of (1), is the same for both circuits. Thus, in the case of actual circuits Newton's third law, that to every action there is an equal (and opposite) reaction, is satisfied.

5-20 Two loops are arranged as shown in cross section in Fig. P5-20. If the separation s is large compared with the size of the loops, show that the torque T on loop 2 due to loop 1 is given by

$$T = \frac{\mu_0}{2\pi} \frac{mm'}{s^3}$$

where m = magnetic moment of loop 1

m' = magnetic moment of loop 2

5-21 Calculate the inductance of a uniform, 5,000-turn solenoidal coil 500 mm long and of 10 mm radius. The medium is air.

* 5-22 Calculate the inductance of an air-filled toroidal coil of $1,000 \text{ mm}^2$ cross-sectional area with a mean radius of 500 mm. The toroid has a uniform winding of 10,000 turns.

5-23 Two identical 100-turn circular coils 1 m in radius have their axes coincident and are spaced 1 m apart, forming a *Helmholtz pair*. Both carry 10 A in the same sense. Calculate and plot the variation of H along the axis of the coils from the center of one coil to the center of the other. Also calculate and plot the variation of H , along the axis of a single 100-turn coil 1 m in radius, due to a current I in the coil. Let the single coil be situated halfway between the coils of the Helmholtz pair and with its axis coincident with the axis of the pair. Also let I have such a value that H at the center of the single coil is the same as H from the Helmholtz pair at this point. Assume that the coils have negligible cross-sectional area so that each may be represented by a thin single-turn loop.

5-24 The field map for a coaxial transmission line with asymmetrically located inner conductor is shown in Fig. P5-24. If there is 10 V between the conductors and the sheet-current density K at the point P_1 is 2 A m^{-1} , use the map to find (a) the electric field E at P_2 , (b) E at P_3 , (c) the magnetic field H at P_2 , (d) H at P_3 , (e) capacitance per unit length of line, (f) inductance per unit length of line, (g) electric flux density D at P_2 , (h) D at P_3 , (i) magnetic flux density B at P_2 , (j) B at P_3 , (k) electric energy density w_e at P_2 , (l) w_e at P_3 , (m) magnetic energy density w_m at P_2 , (n) w_m at P_3 , (o) charge Q per unit length of line, (p) magnetic flux ψ_m per unit length of line, and (q) total current I .

5-25 If the transmission line of Prob. 5-24 is filled with a conductor of uniform conductivity σ and 1 A flows between the inner and outer conductor per unit length of line,

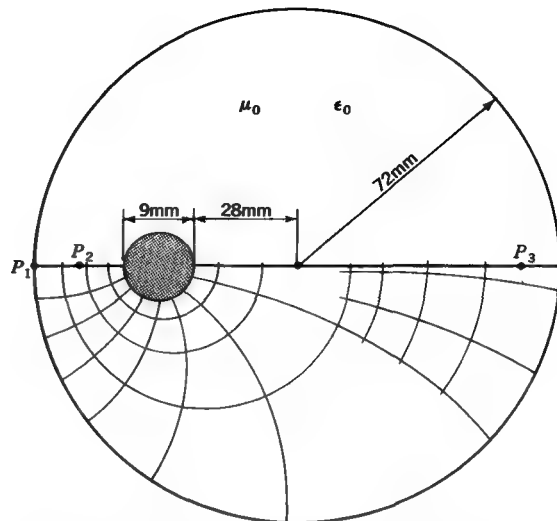


FIGURE P5-24
Coaxial line with asymmetrically located inner conductor.

find (a) current density J at P_2 , (b) J at P_3 , (c) shunt resistance R per unit length of line, and (d) shunt conductance G per unit length of line. It is assumed that the transmission-line conductors have infinite conductivity.

5-26 A transmission line consists of two long thin parallel conductors that carry currents of 10 A in opposite directions. The conductors are spaced a distance $2s$ apart. Draw a field map for a plane normal to the wires. Show both H lines and lines of equal magnetic potential. Indicate the value of potential for each equipotential line. Let the line joining the wires be arbitrarily taken to have zero potential. (Compare this map with Fig. 3-16 for two parallel lines of charge spaced a distance $2s$.)

★ 5-27 A long straight tubular conductor of circular cross section with an outside diameter of 50 mm and wall thickness of 5 mm carries a direct current of 50 A . Find H (a) just inside the wall of the tube, (b) just outside the wall of the tube, and (c) at a point in the tube halfway between the inner and outer surfaces.

5-28 (a) Prove that $\nabla \cdot (\nabla \times \mathbf{F}) = 0$, where $\mathbf{F} = \hat{x}F_x + \hat{y}F_y + \hat{z}F_z$. (b) Prove that $\nabla \times (\nabla f) = 0$, where f is a scalar function. (c) $\nabla \times \mathbf{H} = \mathbf{J}$ for steady currents. Show that $\nabla \cdot \mathbf{J} = 0$. (d) $\mathbf{E}_e = -\nabla V$ for static fields. Show that $\nabla \times \mathbf{E}_e = 0$. (e) Given that $\mathbf{B} = \nabla \times \mathbf{A}$, show that $\nabla \cdot \mathbf{B} = 0$.

5-29 (a) Deduce Maxwell's curl equation from Ampère's law and apply it to find the total current I through a square area 2 m on a side with edges coinciding with the positive x and y axes and one corner at the origin for a field $\mathbf{H} = \hat{x}2y^2 \text{ A m}^{-1}$. (b) Repeat for $\mathbf{H} = \hat{z}3x^2y \text{ A m}^{-1}$.

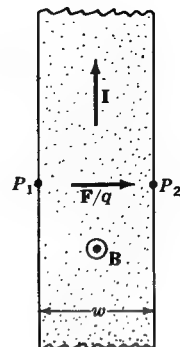


FIGURE P5-34
Conducting strip in magnetic field for determination of Hall effect voltage.

5-30 (a) Using the vector potential and its curl, deduce the magnetic flux density \mathbf{B} at a distance of 2 m normal to a short current element of length L with current of 10 mA.
 (b) Find \mathbf{B} for the situation in (a) using the Biot-Savart law.

5-31 Show that the field $\mathbf{F} = \hat{\mathbf{x}}y + \hat{\mathbf{y}}x$ has zero curl.

* **5-32** If $\mathbf{F} = \hat{\mathbf{x}}x^2 + \hat{\mathbf{y}}2yz - \hat{\mathbf{z}}x^2$, find $\nabla \times \mathbf{F}$ and the path of $\nabla \times \mathbf{F}$.

5-33 If $\mathbf{F} = \hat{\mathbf{x}}2x + \hat{\mathbf{y}}4xy^2z$, (a) find the curl of the curl of \mathbf{F} ; (b) evaluate this result at the point (2,2,2); (c) repeat (a) and (b) using $\nabla(\nabla \cdot \mathbf{F}) - \nabla^2\mathbf{F}$.

5-34 (a) When a current I flows as shown (Fig. P5-34) in a flat conducting strip with magnetic field \mathbf{B} normal to the strip, there is a force per unit charge to the right. Thus,

$$\mathbf{F} = (\mathbf{I} \times \mathbf{B})l = I(l \times \mathbf{B}) = \frac{Q}{t} l \times \mathbf{B} = Q(v \times \mathbf{B}) \quad \text{or} \quad \frac{\mathbf{F}}{Q} = v \times \mathbf{B}$$

If there are equal numbers of positive and negative charge carriers, the points P_1 and P_2 develop no potential difference. In metals the carriers are negative charges (electrons), and P_2 becomes negative with respect to P_1 . This is the *Hall effect*. Show that the emf developed between P_1 and P_2 is given by $\mathcal{U} = IB/nqd$, where n is the number of electrons per cubic meter in the metal, q is the electron charge, and d is the thickness of the strip. (b) If $I = 50 \text{ A}$, $B = 2 \text{ T}$, $w = 25 \text{ mm}$, and $d = 0.5 \text{ mm}$, find the Hall voltage between P_1 and P_2 for a copper strip. Take $n = 8.4 \times 10^{28} \text{ m}^{-3}$ for copper. (c) Why does the width w of the strip not appear in the above equation for the Hall voltage?

5-35 A transmission line consists of two parallel 10-mm-diameter conductors separated (on centers) by 500 mm. If there is a potential difference $V = 100 \text{ kV}$ between the conductors, is there a line current I which results in a balance between the electric and magnetic forces acting on the wires? If so, what is its value?

6

THE STATIC MAGNETIC FIELD OF FERROMAGNETIC MATERIALS

6-1 INTRODUCTION

Magnetic fields are present around a current-carrying conductor. They also exist around a magnetized object such as an iron bar magnet. The field of the iron bar is not produced by current circuits of the type considered in Chap. 5, but currents are the cause. In the bar the currents flow in circuits of atomically small dimensions. In contrast to these *microscopic* circuits, the circuits considered in Chap. 5 are of *macroscopic* size.

An electron revolving in its orbit around the nucleus of an atom forms a tiny electric current loop. Since a current loop has a magnetic field and all atoms have revolving electrons, we might suppose that all substances would exhibit magnetic effects. However, such effects are very weak in most materials. Nevertheless there is a group of substances, including iron, nickel, and cobalt, in which magnetic effects are very strong. These substances are called *ferromagnetic materials*. Both the orbital motion and the electron spin (or rotation of the electron around its own axis) contribute to the magnetic effect, the spin being particularly important. This electron, or charge, motion is equivalent in its effect to a tiny current loop, which

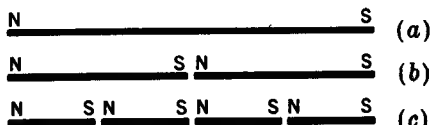


FIGURE 6-1

New poles appear at each point of division of a bar magnet.

acts as a miniature magnet or magnetic dipole. Although the effect of each atomic current loop is very small, the combined effect of billions of them in an iron bar results in a strong magnetic field around the bar.

6-2 BAR MAGNETS AND MAGNETIC POLES

If an iron bar magnet is freely suspended, it will turn in the earth's magnetic field so that one end points north. This end is called the *north-seeking pole* of the magnet or simply its *north pole*. The other end of the magnet has a pole of opposite polarity called a *south pole*. It is often convenient to call a north pole a *positive pole* and a south pole a *negative pole*.

All magnetized bodies have both a north and a south pole. They cannot be isolated. For example, consider the long magnetized iron rod of Fig. 6-1a. This rod has a north pole at one end and a south pole at the other. If the rod is cut in half, new poles appear, as in Fig. 6-1b, so that there are two magnets. If each of these is cut in half, we obtain four magnets, as in Fig. 6-1c, each with a north and a south pole. The reason for this is that the ultimate source of ferromagnetism is an atomic current circuit which acts like a tiny magnet with a north and a south pole. Therefore, even if the cutting process could be continued to atomic dimensions and a single iron atom isolated, it would still have a north and a south pole.

The fact that magnetic poles cannot be isolated, whereas electric charges can, is an important point of difference between electric charges and magnetic poles.

6-3 MAGNETIC MATERIALS

All materials show some magnetic effects. With the exception of the ferromagnetic group these effects are weak.

Depending on their magnetic behavior, substances can be classified as *diamagnetic*, *paramagnetic*, or *ferromagnetic*. In diamagnetic materials the magnetization (see Sec. 6-7) is opposed to the applied field, while in paramagnetic materials the magnetization is in the same direction as the field. The materials in both groups, however, show only weak magnetic effects. Materials in the ferromagnetic group, on the other

hand, show very strong magnetic effects. The magnetization is in the same direction as the field, the same as for paramagnetic materials. Most of this chapter deals with the magnetic fields of the ferromagnetic materials.

A number of substances are classified in Table 6-1 according to their magnetic behavior. Many substances show such weak magnetic effects that they are called *nonmagnetic*. However, vacuum is the only truly nonmagnetic medium.

6-4 RELATIVE PERMEABILITY

In dealing with many media, it is often convenient to speak of the relative permeability μ_r , defined as

$$\boxed{\mu_r = \frac{\mu}{\mu_0}} \quad (1)$$

where μ_r = relative permeability, dimensionless

μ = permeability, H m^{-1}

μ_0 = permeability of vacuum = $400 \pi \text{ nH m}^{-1}$

It is to be noted that the relative permeability is a dimensionless ratio.

The relative permeability of vacuum or free space is unity by definition. The relative permeability of diamagnetic substances is slightly less than 1, while for paramagnetic substances it is slightly greater than 1. The relative permeability of the ferromagnetic materials is generally much greater than 1 and in some special alloys may be as large as 1 million.

The relative permeability of diamagnetic and paramagnetic substances is relatively constant and independent of the applied field, much as the relative permittivity of dielectric substances is independent of the applied electric field intensity. However, the relative permeability of ferromagnetic materials varies over a wide range for different applied fields. It also depends on the previous history of the specimen (see Hysteresis, Sec. 6-12). However, the *maximum* relative permeability is a relatively definite quantity for a particular ferromagnetic material although in different materials the maximum may occur at different values of the applied field. This subject is considered in more detail in Sec. 6-11.

In Table 6-1, the relative permeabilities μ_r are listed for a number of substances. The substances are arranged in order of increasing permeability, and they are also classified as to group type. The value given for the ferromagnetic materials is the maximum relative permeability.

Table 6-1

Substance	Group type	Relative permeability μ_r
Bismuth	Diamagnetic	0.99983
Silver	Diamagnetic	0.99998
Lead	Diamagnetic	0.999983
Copper	Diamagnetic	0.999991
Water	Diamagnetic	0.999991
Vacuum	Nonmagnetic	1†
Air	Paramagnetic	1.0000004
Aluminum	Paramagnetic	1.00002
Palladium	Paramagnetic	1.0008
2-81 Permalloy powder (2 Mo, 81 Ni)‡	Ferromagnetic	130
Cobalt	Ferromagnetic	250
Nickel	Ferromagnetic	600
Ferrox cube 3 (Mn-Zn-ferrite powder)	Ferromagnetic	1,500
Mild steel (0.2 C)	Ferromagnetic	2,000
Iron (0.2 impurity)	Ferromagnetic	5,000
Silicon iron (4 Si)	Ferromagnetic	7,000
78 Permalloy (78.5 Ni)	Ferromagnetic	100,000
Mumetal (75Ni, 5Cu, 2Cr)	Ferromagnetic	100,000
Purified iron (0.05 impurity)	Ferromagnetic	200,000
Superalloy (5 Mo, 79 Ni)§	Ferromagnetic	1,000,000

† By definition.

‡ Percentage composition. Remainder is iron and impurities.

§ Used in transformer applications with continuous tape-wound (gapless) cores.

6-5 MAGNETIC Dipoles AND MAGNETIZATION

A loop of area A with current I has a magnetic moment of IA . The fields at a large distance from this loop are identical with those of a bar magnet of dipole moment $Q_m l$, where Q_m is the magnetic pole strength and l is the pole separation, provided the magnetic moment of the bar is equal to that of the loop (see Fig. 6-2). Thus,†

$$Q_m l = IA \quad (1)$$

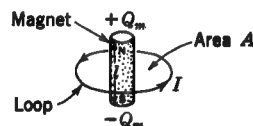


FIGURE 6-2
Bar magnet of moment $Q_m l$ and equivalent current loop of moment IA .

† This equivalence may be shown from the fact that a current loop in a field B has a maximum torque $T = LAB$ [from (5-10-4)] while for a bar magnet the maximum torque $T = Q_m l B$. It follows that for equal torques the moments must be equal.

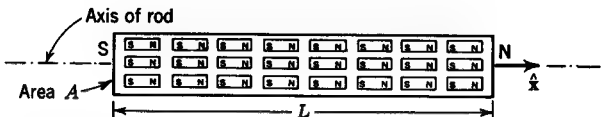


FIGURE 6-3
Uniformly magnetized rod with elemental magnetic dipoles.

It was Ampère's theory that the pronounced magnetic effects of an iron bar occur when large numbers of atomic-sized magnets associated with the iron atoms are oriented in the same direction so that their effects are additive. The precise nature of the tiny magnets is not important if we confine our attention to regions containing large numbers of them. Thus, they may be regarded as tiny magnets or as miniature current loops. In either case, it is sufficient to describe them by their magnetic moment, which can be expressed either as $Q_m l$ or as IA .

Consider the long iron rod shown in cross section in Fig. 6-3. Assume that all the atomic magnets are uniformly distributed throughout the rod and are oriented in the same direction, as suggested in the figure. This state of affairs may be described as one of *uniform* magnetization. The effect of the atomic magnets (or magnetic dipoles) can be conveniently described by a quantity called the *magnetization* M , which is defined as the magnetic-dipole moment per unit volume.[†] Thus

$$M = \frac{m}{v} = \frac{Q_m l}{v} = \frac{IA}{v} \quad (2)$$

where $m = Q_m l$ is the net magnetic (dipole) moment in volume v .

Magnetization has the dimensions of both magnetic-dipole moment per volume and of magnetic pole strength per area ($IL^2/L^3 = I/L$). It is expressed in amperes per meter (A m^{-1}).

The value of M in (2) is an average for the volume v . To define M at a point, it is convenient to assume that the iron rod has a continuous distribution of infinitesimal magnetic dipoles, i.e., a continuous magnetization, whereas the dipoles actually are of discrete, finite size. Nevertheless, the assumption of continuous magnetization leads to no appreciable error provided that we restrict our attention to volumes containing many magnetic dipoles. Then, assuming continuous magnetization, the value of M at a point can be defined as the net dipole moment m of a small volume Δv divided by the volume with the limit taken as Δv shrinks to zero around the point.

[†] The magnetization M is analogous to the electric polarization P (Sec. 3-5).

Thus

$$M = \lim_{\Delta v \rightarrow 0} \frac{m}{\Delta v} \quad (\text{A m}^{-1}) \quad (3)$$

If M is known as a function of position in a nonuniformly magnetized rod, the total magnetic moment of the rod is given by

$$m = \int_v M dv \quad (\text{A m}^2) \quad (4)$$

where the integration is carried out over the volume of the rod.

EXAMPLE If the long uniformly magnetized rod of Fig. 6-3 has N' elemental magnetic dipoles of moment Δm , find the magnetization of the bar.

SOLUTION From (2) the magnetization is

$$M = \frac{N'}{v} \Delta m = N'' \Delta m$$

where M = magnetization, A m^{-1}

$N'' = N'/v$ = elemental dipoles per unit volume, number m^{-3}

In this case the magnetization M is both an average value and also the value anywhere in the rod since the magnetization is assumed uniform.

6-6 UNIFORMLY MAGNETIZED ROD AND EQUIVALENT AIR-FILLED SOLENOID

Consider that a long bar magnet consists of miniature current loops as in Fig. 6-4, one in place of each tiny bar magnet of Fig. 6-3, with the moment IA of each loop equal to the moment $Q_m l$ of each magnet. Assuming that there are n loops in a single cross section of the rod (as in the end view in Fig. 6-4), we have

$$nA' = A \quad (1)$$

where A' = area of elemental loop

A = cross-sectional area of rod

Further, let us assume that there are N such sets of loops in the length of the rod (see the side view in Fig. 6-4). Then

$$nN = N' \quad (2)$$

where n = number of loops in a cross section of rod

N = number of such sets of loops

N' = total number of loops in rod

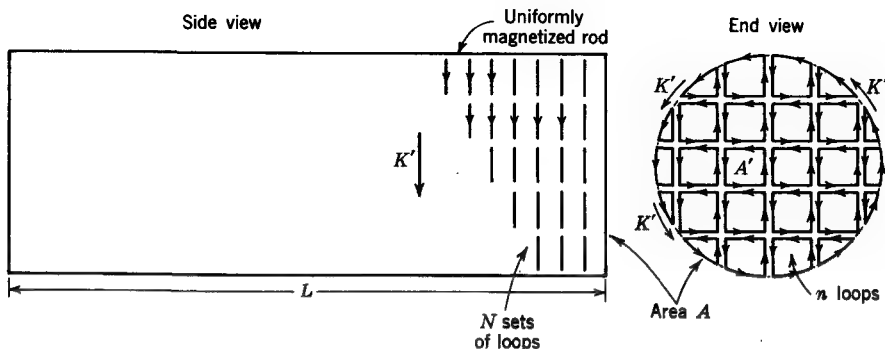


FIGURE 6-4
Uniformly magnetized rod with elemental current loops.

It follows that the magnetization M of the rod is given by

$$M = \frac{m}{v} = \frac{N'IA'}{LA} = \frac{NI}{L} \frac{nA'}{A} = \frac{NI}{L} = K' \quad (3)$$

where K' = equivalent sheet current density on outside surface of rod, A m^{-1}
 L = length of rod, m

Referring to the end view of the rod in Fig. 6-4, it is to be noted that there are equal and oppositely directed currents wherever loops are adjacent, so that the currents have no net effect with the exception of the currents at the periphery of the rod. As a result there is the equivalent of a current sheet flowing around the rod, as suggested in Figs. 6-4 and 6-5a. This sheet has a linear current density K' (A m^{-1}). Although the sets of current loops are shown for clarity in Fig. 6-4 with a large spacing, the actual spacing is of atomic dimensions, so that macroscopically we can assume that the current sheet is continuous.

This type of a current sheet is effectively what we also have in the case of a solenoid with many turns of fine wire, as in Fig. 6-5b (see also Fig. 5-15 and in particular Fig. 5-15d). The actual sheet-current density K for the solenoid is

$$K = \frac{NI}{L} \quad (\text{A m}^{-1}) \quad (4)$$

where N = number of turns in solenoid, dimensionless

I = current through each turn, A

L = length of solenoid, m

The sheet-current density K is expressed in amperes per meter.

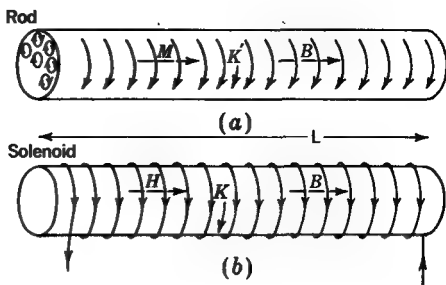


FIGURE 6-5
(a) Uniformly magnetized rod and (b)
equivalent solenoid.

If the solenoid of Fig. 6-5b is the same length and diameter as the rod of Fig. 6-5a, and if $K = K'$, the solenoid is the magnetic equivalent of the rod. In air $B = \mu_0 H$; and noting (5-11-5), we have at the center of the solenoid that

$$B = \mu_0 \frac{NI}{L} = \mu_0 K = \mu_0 H \quad (T) \quad (5)$$

At the center of the rod

$$B = \mu_0 K' = \mu_0 M \quad (T) \quad (6)$$

From (5) we have $H = K$, and from (6) we have $M = K'$. These are scalar relations. Vectorially we note that \mathbf{H} is perpendicular to \mathbf{K} and \mathbf{M} is perpendicular to \mathbf{K}' . The more general vector relations are

$$\mathbf{K} = \hat{\mathbf{n}} \times \mathbf{H} \quad \text{and} \quad \mathbf{K}' = \mathbf{M} \times \hat{\mathbf{n}} \quad (7)$$

where $\hat{\mathbf{n}}$ is the unit vector normal to the plane containing the field vectors.

6-7 THE MAGNETIC VECTORS, \mathbf{B} , \mathbf{H} , AND \mathbf{M}

Consider an air-filled toroid of area A and radius R with N_0 turns, as in Fig. 6-6. From (5-13-3)

$$B_0 = \mu_0 \frac{N_0 I}{2\pi R} \quad (1)$$

But from (6-6-5) $N_0 I / 2\pi R = K$, the sheet-current density. Hence,

$$B_0 = \mu_0 K = \mu_0 H \quad (2)$$

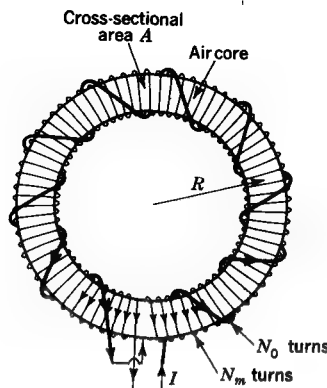


FIGURE 6-6

Toroid with N_0 turns of coarse winding (producing B_0) and N_m turns of fine winding (producing B_m).

If the same winding were placed on an iron ring of the same area and radius, the value of B would increase. Imagine now that in place of an iron ring we have the same air-filled toroid of Fig. 6-6 but with the ring's effect replaced by another toroidal winding of N_m turns. The magnetic field from this winding is

$$B_m = \mu_0 \frac{N_m I}{2\pi R} \quad (3)$$

But $N_m I / 2\pi R = K'$, the equivalent sheet-current density. Hence, from (6-6-6)

$$B_m = \mu_0 K' = \mu_0 M \quad (4)$$

It follows that the total B is given by

$$B = B_0 + B_m = \mu_0(H + M) \quad (5)$$

or

$$\boxed{\mathbf{B} = \mu_0(\mathbf{H} + \mathbf{M})} \quad (6)$$

where \mathbf{B} = magnetic flux density, T

\mathbf{H} = magnetic field, $A\ m^{-1}$

\mathbf{M} = magnetization, $A\ m^{-1}$

Although developed for the special case of a toroid, (6) is a (vector) relation which applies in general. Dividing by H gives

$$\boxed{\mu = \mu_0 \left(1 + \frac{M}{H}\right)} \quad (7)$$

Dividing by the permeability μ_0 gives

$$\mu_r = 1 + \frac{M}{H} \quad \text{or} . \quad \frac{M}{H} = \mu_r - 1 \quad (8)$$

The ratio M/H is also sometimes written

$$\frac{M}{H} = \chi_m \quad (9)$$

where χ_m is the magnetic susceptibility (dimensionless). Comparing (8) and (9), we have

$$\chi_m = \mu_r - 1 \quad (10)$$

Thus, the magnetic susceptibility $\chi_m = 0$ for vacuum, for which $\mu_r = 1$.

In isotropic media \mathbf{M} and \mathbf{H} are in the same direction, so that their quotient is a scalar and hence μ is a scalar. In nonisotropic media, such as crystals, \mathbf{M} and \mathbf{H} are, in general, not in the same direction, and μ is not a scalar (see Chap. 15). Hence, $\mathbf{B} = \mu_0(\mathbf{H} + \mathbf{M})$ is a general relation, while $\mathbf{B} = \mu\mathbf{H}$ is a more concise expression, which, however, has a simple significance only for isotropic media or certain special cases in nonisotropic media.

A single iron crystal is nonisotropic, but most iron specimens consist of an aggregate of numerous crystals oriented at random, so that macroscopically such specimens may be treated as though they were isotropic. In such cases $\mathbf{B} = \mu\mathbf{H}$ can be applied as a strictly macroscopic, or large-scale, relation.

Since $\nabla \cdot \mathbf{B} = 0$, we have, on taking the divergence of (6),

$$\boxed{\nabla \cdot \mathbf{H} = -\nabla \cdot \mathbf{M} \quad (\text{A m}^{-2})} \quad (11)$$

If the divergence of a vector field is not zero, the field has a source, or place of origin. We recall from the polarized dielectric case (Sec. 3-26) that $\nabla \cdot \mathbf{P} = -\rho_p$, which indicates that the polarization field originates on the polarization charge (of apparent volume density ρ_p) at the dielectric surface. In an analogous manner, (11) indicates that the \mathbf{H} field originates where the magnetization field \mathbf{M} ends and that the \mathbf{H} field ends where the \mathbf{M} field originates. This occurs at the ends of the rod in Fig. 6-3.

The locations where $\nabla \cdot \mathbf{H}$ (or $\nabla \cdot \mathbf{M}$) is not zero may be regarded as the locations of the magnetic poles of a magnetized object. Thus the poles of a uniformly magnetized rod, as in Fig. 6-3, are at the end faces of the rod.†

† In ordinary magnets with flat ends the magnetization tends to be nonuniform near the edges. Entirely uniform magnetization is possible in spherically or elliptically shaped magnetic objects. However, the assumption of uniform magnetization is a good approximation for a long homogeneous rod magnet, since the magnetization is nearly uniform over all of the rod except near the edges at the ends of the rod. In actual magnets with flat ends the effective separation between the pole centers is slightly less than the physical length of the magnet.

Taking the curl of (6), we have

$$\nabla \times \mathbf{B} = \mu_0(\nabla \times \mathbf{H}) + \mu_0(\nabla \times \mathbf{M}) \quad (12)$$

or

$$\nabla \times \mathbf{B} = \mu_0 \mathbf{J} + \mu_0(\nabla \times \mathbf{M}) \quad (13)$$

Where there is no magnetization, (13) reduces to $\nabla \times \mathbf{B} = \mu_0 \mathbf{J}$, as in (5-21-8). The curl of \mathbf{M} has the dimensions of current density (ampères per square meter) and represents the equivalent current of density $\mathbf{J}' (\text{A m}^{-2})$ flowing, for example, in a very thin layer around the cylindrical surface of a uniformly magnetized rod. The linear current density for this sheet is $K' = J' \Delta x (\text{A m}^{-1})$, where Δx is the thickness of the layer of current of average density J' . Thus (13) becomes

$$\nabla \times \mathbf{B} = \mu_0(\mathbf{J} + \mathbf{J}') \quad (14)$$

where \mathbf{J} = actual current density, as in current-carrying wire, A m^{-2}

\mathbf{J}' = equivalent current density, as at the surface of magnetized bar, A m^{-2}

The flux density \mathbf{B} is always the result of a current or its equivalent. For example, the magnitude of \mathbf{B} at the center of a long slender iron rod surrounded by a long solenoid is, from (6-6-5) and (6-6-6),

$$\mathbf{B} = \mu_0(K + K') \quad (\text{T}) \quad (15)$$

where K = sheet-current density due to solenoid current, A m^{-1}

K' = equivalent sheet-current density due to magnetization of rod, A m^{-1}

In many cases we can conveniently express \mathbf{B} directly in terms of the currents producing it, as in (15). In general, we can also express \mathbf{B} in terms of the vector potential \mathbf{A} , which in turn is related to the currents. Thus

$$\mathbf{B} = \nabla \times \mathbf{A} \quad (16)$$

If both conduction currents and magnetization are present,

$$\mathbf{A} = \frac{\mu_0}{4\pi} \int \frac{\mathbf{J} + \mathbf{J}'}{r} dv \quad (17)$$

where

$$\mathbf{J} = \nabla \times \mathbf{H} \quad \text{and} \quad \mathbf{J}' = \nabla \times \mathbf{M} \quad (\text{A m}^{-2})$$

EXAMPLE 1 Referring to Fig. 6-7a, a toroidal coil has a radius R and a cross-sectional area $A = \pi r^2$. The coil has a very narrow gap, as shown in the gap detail in Fig. 6-8a. The coil is made of many turns N of fine insulated wire with a current I . Draw graphs showing the variation of \mathbf{B} , \mathbf{M} , \mathbf{H} , and μ along the line of radius R at the gap (centerline of coil).

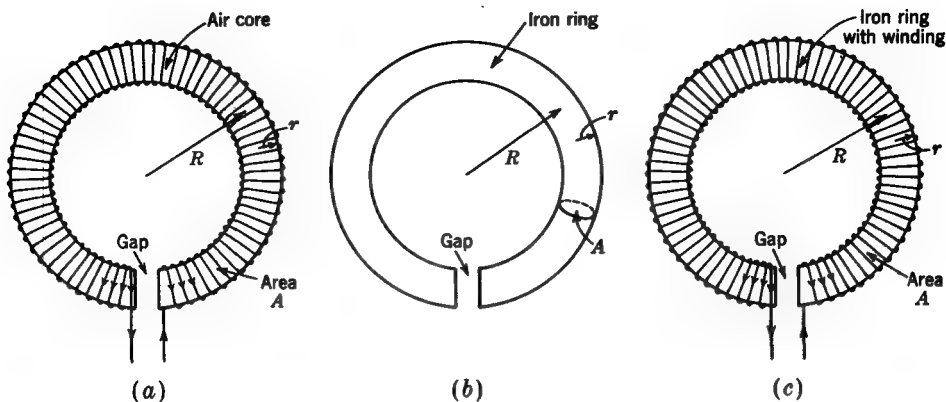


FIGURE 6-7

(a) Toroidal coil with gap. (b) Permanently magnetized iron ring with gap. (c) Iron-cored toroidal coil with gap.

SOLUTION Neglecting the small effect of the narrow gap, \mathbf{B} is substantially uniform around the inside of the entire toroid. Since $R \gg r$, its magnitude is, from (5-11-5), given approximately by

$$B = \frac{\mu_0 NI}{2\pi R} = \mu_0 K \quad (\text{T}) \quad (18)$$

where K is the magnitude of the linear sheet-current density in amperes per meter. A graph of the magnitude B along the centerline of the coil at the gap is shown in Fig. 6-8b.

No ferromagnetic material is present, so that the magnetization is negligible and $\mathbf{M} = 0$, as indicated in Fig. 6-8c. It follows that $\nabla \cdot \mathbf{M} = 0$ and also $\nabla \cdot \mathbf{H} = 0$.

Since $M = 0$, we have

$$H = \frac{B}{\mu_0} = \frac{\mu_0 K}{\mu_0} = K = \frac{NI}{2\pi R} \quad (\text{A m}^{-1}) \quad (19)$$

Therefore, the magnitude of \mathbf{H} is constant and equal to the sheet-current density K of the coil winding, as indicated in Fig. 6-8d. The permeability everywhere is μ_0 (Fig. 6-8e).

It is to be noted that \mathbf{B} is continuous and that in this case \mathbf{H} is also continuous since there is no ferromagnetic material present. Both \mathbf{B} and \mathbf{H} have the same direction everywhere in this case.

EXAMPLE 2 Consider now that the toroidal coil of Example 1 is replaced by an iron ring of the same size and also with a gap of the same dimensions, as suggested in Figs. 6-7b and

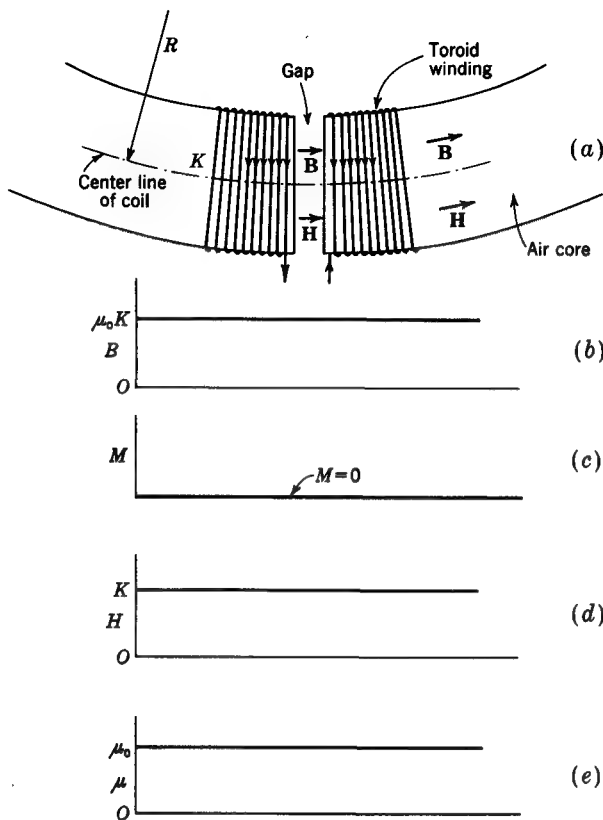


FIGURE 6-8

Magnitudes of magnetic quantities along the coil centerline at the gap in a toroid (see Fig. 6-7a) (Example 1).

6-9a. Assume that the ring has a uniform permanent magnetization M that is equal in magnitude to K for the toroid in Example 1. Draw graphs showing the variation of B , M , H , μ , and $\nabla \cdot \mathbf{H}$ along the centerline of the ring at the gap.

SOLUTION The ring has a north pole at the left side of the gap and a south pole at the right side. Neglecting the small effect of the narrow gap, B is substantially uniform around the interior of the entire ring and also across the gap. It is due entirely to the equivalent sheet-current density K' on the surface of the ring. From (6-6-3), $K' = M$. Thus

$$B = \mu_0 M = \mu_0 K' \quad (T) \quad (20)$$

where M and K' are, according to the stated conditions, equal to K for the solenoid in Example 1. Hence, B is the same in both examples. Its value at the gap is illustrated in Fig. 6-9b.

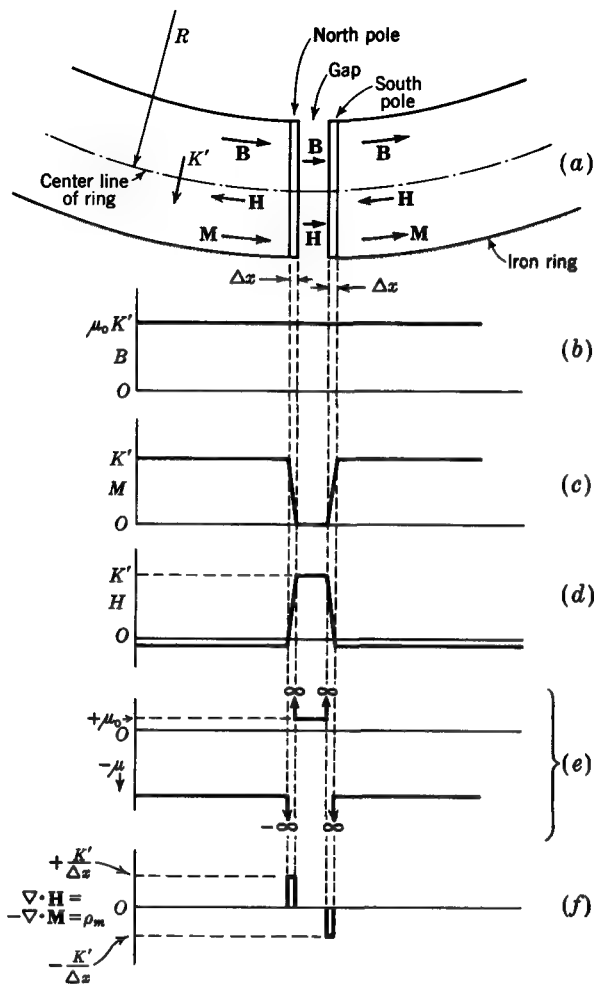


FIGURE 6-9

Variation of magnetic quantities along the centerline at the gap in a permanently magnetized iron ring (see Fig. 6-7b) (Example 2).

In the ring, $M = K'$, but outside the ring and in the gap $M = 0$. Suppose that the change in M from zero to K' at the gap occurs over a short distance Δx rather than as a square step function. The graph for M is then as shown in Fig. 6-9c.

Outside the ring and in the gap $M = 0$; so

$$H = \frac{B}{\mu_0} = K' \quad (\text{A m}^{-1})$$

Inside the ring

$$H = \frac{B}{\mu_0} - M \quad (\text{A m}^{-1}) \quad (21)$$

or approximately $H = K' - K' = 0$. The exact value of H is not zero† but is small and negative. The variation of H across the gap is illustrated in Fig. 6-9d.

From (6-7-7) the permeability in the ring is large and negative because H is small compared with M and is negative. In the air gap $\mu = \mu_0$. The variation of μ across the gap is suggested in Fig. 6-9e.

According to (6-7-11), the divergence of \mathbf{H} equals the negative divergence of \mathbf{M} , and this equals the apparent pole volume density ρ_m in the ring on both sides of the gap. Thus

$$\nabla \cdot \mathbf{H} = -\nabla \cdot \mathbf{M} = \rho_m \quad (\text{A m m}^{-3}) \quad (22)$$

This is zero everywhere except at the layers of assumed thickness Δx at the gap. Assuming that \mathbf{M} changes linearly in magnitude over this thickness, and assuming also that Δx is very small compared with the cross-sectional diameter $2r$ of the ring, we have on the centerline

$$\nabla \cdot \mathbf{M} = \frac{dM_x}{dx} = \frac{\mp K'}{\Delta x} = -\rho_m \quad (23)$$

$$\text{or} \quad \nabla \cdot \mathbf{H} = \frac{\pm K'}{\Delta x} = \rho_m \quad (24)$$

where the upper sign in front of K' applies if M decreases and H increases in proceeding across Δx in a positive direction (from left to right). The variation of $\nabla \cdot \mathbf{H}$ along the centerline is illustrated in Fig. 6-9f. Hence the pole volume density ρ_m has a value only in the layers of assumed thickness Δx at the sides of the gap. This locates the poles of the ring magnet at the sides of the gap, and for this reason the iron surfaces of the gap are called *pole faces*.

Since K' in this example equals K in Example 1, \mathbf{B} and \mathbf{H} in the gap have identical values in both examples. In the gap, the directions of \mathbf{B} and \mathbf{H} are the same. In the iron ring, \mathbf{B} is the same as in the toroid of Example 1, but \mathbf{H} is smaller and in the opposite direction. An \mathbf{H} direction opposite to that of \mathbf{B} is characteristic of conditions *inside* a permanent magnet.

EXAMPLE 3 Suppose now that the iron ring of the previous example has wound over it the toroidal coil of Example 1 with the gap in the toroid coinciding with the gap in the ring, as shown in Fig. 6-7c and in the gap detail of Fig. 6-10a. The combination constitutes an iron-cored toroid as contrasted with the air-cored toroid of Example 1. Let the sheet current density for the toroid winding be K as in the first example. Further, let the *induced* magnetization added to the *permanent* magnetization in the ring yield a *total* uniform magnetization (permanent and induced) that is equal in magnitude to $4K$. Draw graphs showing the variation of \mathbf{B} , \mathbf{M} , \mathbf{H} , μ , and $\nabla \cdot \mathbf{H}$ along the centerline of the ring at the gap.

† The above analysis is approximate since it neglects the effect of the gap. See Sec. 6-23.

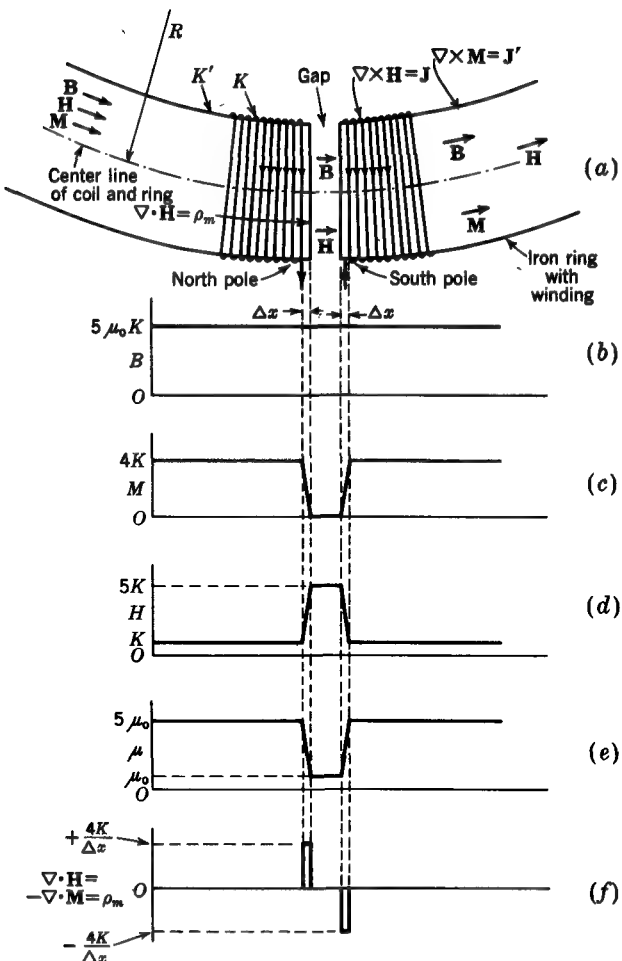


FIGURE 6-10

Variation of magnetic quantities along coil centerline at the gap in an iron-cored toroid (see Fig. 6-7c) (Example 3).

SOLUTION In this case the total magnetization is $M = K' = 4K$. Neglecting the small effect of the narrow gap, the flux density is substantially uniform around the inside of the ring and across the gap. It is given (see Fig. 6-10b) by

$$B = \mu_0(K + K') = 5\mu_0 K \quad (\text{T}) \quad (25)$$

In the ring $M = 4K$, and in the gap $M = 0$, as shown in Fig. 6-10c. It is again assumed that M changes linearly over a short distance Δx at the pole faces.

In the gap

$$H = \frac{B}{\mu_0} = 5K \quad (26)$$

In the ring

$$H = \frac{B}{\mu_0} - M \quad (27)$$

and so we have very nearly that $H = 5K - 4K = K$. The variation of H across the gap is depicted in Fig. 6-10d. In the gap $\mu = \mu_0$. In the ring (see Fig. 6-10e)

$$\mu = \mu_0 \left(1 + \frac{M}{H}\right) = \mu_0 \left(1 + \frac{4K}{K}\right) = 5\mu_0 \quad (28)$$

The divergence of \mathbf{H} or pole volume density ρ_m is given by the negative of the divergence of \mathbf{M} . This has a value of $\pm 4K/\Delta x$ over the assumed pole thickness Δx at the pole faces. This is illustrated in Fig. 6-10f. The fact that $\nabla \cdot \mathbf{H} = \rho_m$ at the pole faces is also indicated in Fig. 6-10a. Elsewhere $\nabla \cdot \mathbf{H} = 0$.

In this example, \mathbf{B} and \mathbf{H} have the same direction both in the gap and in the ring. In the ring, however, \mathbf{H} is weaker than in the gap.

In this example, the toroid has a sheet-current density of K (A m^{-1}), and the ring has an equivalent sheet-current density around its curved surface of $K' = 4K$ (A m^{-1}). Inside a wire of the toroidal coil $\nabla \times \mathbf{H} = \mathbf{J}$ (A m^{-2}) as suggested in Fig. 6-10a. Elsewhere $\nabla \times \mathbf{H} = 0$. At the curved surface of the ring $\nabla \times \mathbf{M} = \mathbf{J}'$ (A m^{-2}). Elsewhere $\nabla \times \mathbf{M} = 0$.

In the last two examples involving ferromagnetic material it is to be noted that the magnetization, or \mathbf{M} , lines originate, or have their source, on a south (negative) pole and end on, or have as a sink, a north (positive) pole. The \mathbf{H} lines, on the other hand, originate, as in Example 2, on a north pole and end on a south pole. Thus, $\nabla \cdot \mathbf{H}$ has a positive value at a north pole, while $\nabla \cdot \mathbf{M}$ has a positive value at a south pole.

As a final example let us compare the fields around a solenoid and the equivalent permanently magnetized rod.

EXAMPLE 4 A long uniform solenoid, as in Fig. 6-11a, is situated in air and has NI ampere-turns and a length l . A permanently magnetized iron rod (Fig. 6-11e) has the same dimensions as the solenoid, and has a uniform magnetization M equal to NI/l for the solenoid. Draw graphs showing the variation of \mathbf{B} , \mathbf{M} , and \mathbf{H} along the axes of the solenoid and the rod. Also sketch the configuration of the fields for the two cases.

SOLUTION Since the rod and solenoid have the same dimensions and $M = K' = K = NI/l$, the two are magnetically equivalent. The \mathbf{B} fields for both are the same every-

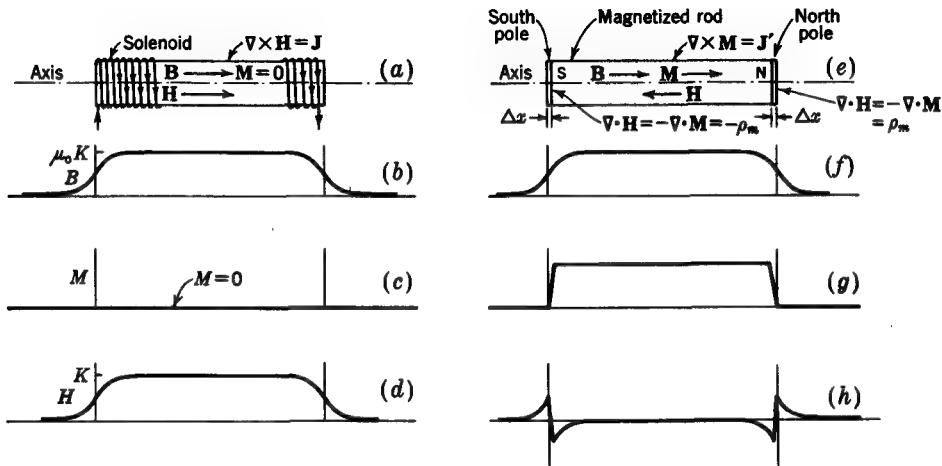


FIGURE 6-11
Solenoid and equivalent magnetized rod showing fields along axis (Example 4).

where, and the \mathbf{H} fields for both are the same outside the solenoid and rod. Assuming that the solenoid is long compared with its diameter, the flux density at the center is nearly given by

$$B = \mu_0 \frac{NI}{l} = \mu_0 K \quad (29)$$

At the ends of the solenoid

$$B = \frac{1}{2}\mu_0 K \quad (30)$$

The magnitude of \mathbf{B} at other locations along the solenoid axis can be obtained from (5-11-3) with a suitable change in limits. The variation of \mathbf{B} along the solenoid axis is shown graphically in Fig. 6-11b. The variation along the rod axis is the same (Fig. 6-11f).

For the solenoid case, $M = 0$ everywhere (Fig. 6-11c). In the rod the magnetization M is assumed to be uniform, as in Fig. 6-11g.

For the solenoid case, $\mathbf{H} = \mathbf{B}/\mu_0$ everywhere, so that $H = K$ at the center and $H = \frac{1}{2}K$ at the ends. The variation of H along the solenoid axis is shown in Fig. 6-11d. Outside the rod, H is the same as for the solenoid. Inside the rod $H = (B/\mu_0) - M$, so that the variation is as suggested in Fig. 6-11h. It is assumed that M changes from 0 to K over a short distance Δx at the ends of the rod. The direction of \mathbf{H} in the rod is opposite to that for \mathbf{B} .

Inside the wires of the solenoid winding, $\nabla \times \mathbf{H} = \mathbf{J}$, as indicated in Fig. 6-11a. On the cylindrical surface of the rod, $\nabla \times \mathbf{M} = \mathbf{J}'$, as suggested in Fig. 6-11e. In the solenoid case, $\nabla \cdot \mathbf{B} = 0$ and $\nabla \cdot \mathbf{H} = 0$ everywhere. In the rod case, $\nabla \cdot \mathbf{B} = 0$ everywhere, but $\nabla \cdot \mathbf{H} = -\nabla \cdot \mathbf{M} = \rho_m$ at the end faces of the rod.

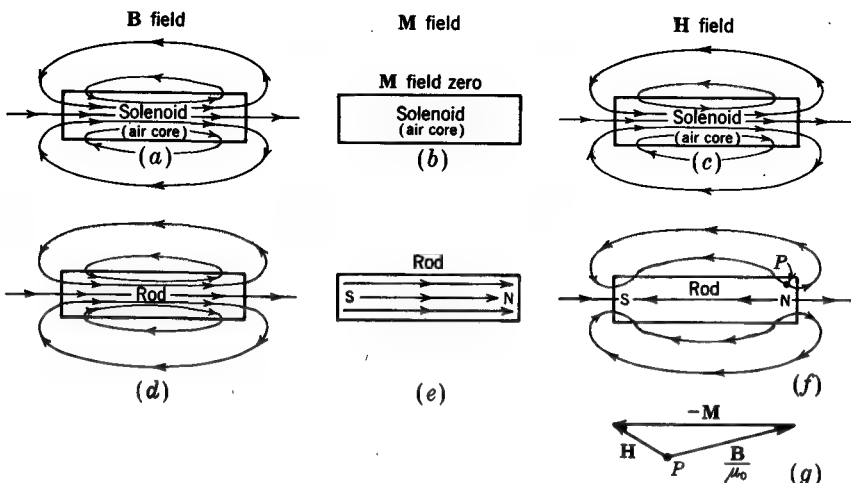


FIGURE 6-12

Fields of solenoid and equivalent permanently magnetized rod. The **B** fields are the same for both solenoid and rod [see (a) and (d)]. The **M** field is zero everywhere except inside the rod [see (b) and (e)]. The **H** fields are the same outside both solenoid and rod but are different inside [see (c) and (f)].

The **B**, **M**, and **H** fields for the two cases are sketched in Fig. 6-12. It is to be noted that inside the rod **H** is directed from the north pole to the south pole. Since **M** and **B** have, in general, different directions in the rod, μ loses its simple scalar significance in this case. Here **H** can be obtained by vector addition, using (6-7-6). As an example, **H** at the point *P* in Fig. 6-12*f* is obtained by the vector addition of \mathbf{B}/μ_0 and $-\mathbf{M}$ as in Fig. 6-12*g*.

Although the magnetization is based on the actual magnetization phenomenon, it is often simpler and more convenient to ignore the mechanism of the phenomenon and use the permeability μ to describe the characteristics of the magnetic medium. This is particularly true where μ can be treated as a scalar. In this case μ is determined experimentally from a sample of the material. However, since μ is not a constant for ferromagnetic materials but a function of **H** and also the previous history of the sample, the methods for dealing with ferromagnetic materials require special consideration (see Sec. 6-10 and following sections).

6-8 BOUNDARY RELATIONS

In a single medium the magnetic field is continuous. That is, the field, if not constant, changes only by an infinitesimal amount in an infinitesimal distance. However, at the boundary between two different media, the magnetic field may change abruptly both in magnitude and direction.

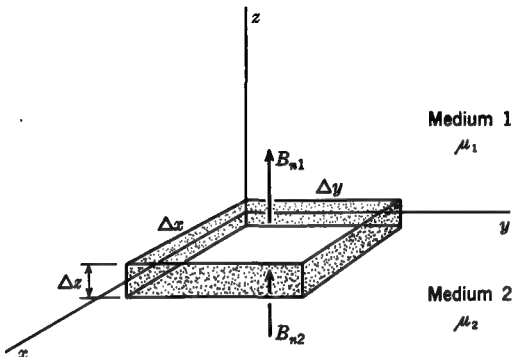


FIGURE 6-13
Construction for developing continuity relation for normal component of \mathbf{B} .

It is convenient to analyze the boundary problem in two parts, considering separately the relation of fields *normal* to the boundary and *tangent* to the boundary.

Taking up first the relation of fields normal to the boundary, consider two media of permeabilities μ_1 and μ_2 separated by the xy plane, as shown in Fig. 6-13. Suppose that an imaginary box is constructed, half in each medium, of area $\Delta x \Delta y$ and height Δz . Let B_{n1} be the average component of \mathbf{B} normal to the top of the box in medium 1 and B_{n2} the average component of \mathbf{B} normal to the bottom of the box in medium 2. B_{n1} is an outward normal (positive), while B_{n2} is an inward normal (negative). By Gauss' law for magnetic fields (5-8-1), the total magnetic flux over a closed surface is zero. In other words, the integral of the outward normal components of \mathbf{B} over a closed surface is zero. By making the height Δz of the box approach zero, the contribution of the sides of the box to the surface integral becomes zero even though there may be finite components of \mathbf{B} normal to the sides. Therefore the surface integral reduces to $B_{n1} \Delta x \Delta y - B_{n2} \Delta x \Delta y = 0$ or

$$\boxed{B_{n1} = B_{n2}} \quad (1)$$

According to (1), the *normal component of the flux density \mathbf{B} is continuous across the boundary between two media*.

Turning now to the relation for magnetic fields tangent to the boundary, let two media of permeabilities μ_1 and μ_2 be separated by a plane boundary, as in Fig. 6-14. Consider a rectangular path, half in each medium, of length Δx parallel to the boundary and of length Δy normal to the boundary. Let the average value of \mathbf{H} tangent to the boundary in medium 1 be H_{t1} and the average value of \mathbf{H} tangent to the boundary in medium 2 be H_{t2} . According to (5-14-5), the integral of \mathbf{H} around a closed path equals the current I enclosed. By making the path length Δy approach

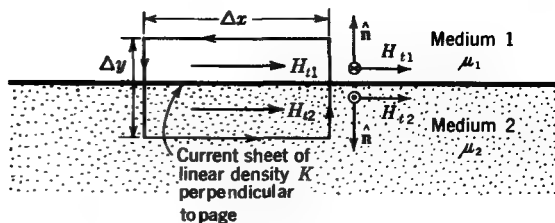


FIGURE 6-14

Construction for developing continuity relation for tangential component of \mathbf{H} .

zero, the contribution of these segments of the path becomes zero even though a finite field may exist normal to the boundary. The line integral then reduces to $H_{t1} \Delta x - H_{t2} \Delta x = I$ or

$$H_{t1} - H_{t2} = \frac{I}{\Delta x} = K \quad (\text{A m}^{-1}) \quad (2)$$

where K is the linear density of any current flowing in an infinitesimally thin sheet at the surface.[†]

According to (2), *the change in the tangential component of \mathbf{H} across a boundary is equal in magnitude to the sheet-current density K on the boundary.* It is to be noted that K is normal to \mathbf{H} ; that is, the direction of the current sheet in Fig. 6-14 is normal to the page. This is expressed by the vector relation

$$\hat{\mathbf{n}} \times \mathbf{H} = \mathbf{K} \quad (3)$$

where $\hat{\mathbf{n}}$ = unit vector normal to boundary, dimensionless

\mathbf{H} = change in magnetic field across boundary, A m^{-1}

\mathbf{K} = sheet-current density at boundary, A m^{-1}

If the field below the boundary is zero ($H_{t2} = 0$), (3) indicates that the current \mathbf{K} related to H_{t1} will be into the page in Fig. 6-14, while if the field above the boundary is zero ($H_{t1} = 0$), the current \mathbf{K} related to H_{t2} will be out of the page.

If $K = 0$, then

$$H_{t1} = H_{t2} \quad (4)$$

[†] If J is the current density in amperes per square meter in a thin sheet of thickness $\Delta y'$, then K is defined by

$$K = J \Delta y' \quad (\text{A m}^{-1})$$

where $J \rightarrow \infty$ as $\Delta y' \rightarrow 0$.

According to (4), the tangential components of \mathbf{H} are continuous across the boundary between two media provided the boundary has no current sheet.

If medium 1 is a nonconductor, and if $H_{t2} = 0$,

$$H_{t1} = K_2 \quad (5)$$

where K_2 is the sheet-current density in amperes per meter in medium 2 at the boundary (into the page in Fig. 6-14). When medium 1 is air and medium 2 is a conductor, (5) is approximated at high frequencies because the skin effect restricts the current in the conductor to a very thin layer at its surface (see Chap. 10).

EXAMPLE 1 Consider a plane boundary between two media of permeability μ_1 and μ_2 , as in Fig. 6-15. Find the relation between the angles α_1 and α_2 . Assume that the media are isotropic with \mathbf{B} and \mathbf{H} in the same direction.

SOLUTION From the boundary relations,

$$B_{n1} = B_{n2} \quad \text{and} \quad H_{t1} = H_{t2} \quad (6)$$

From Fig. 6-15,

$$B_{n1} = B_1 \cos \alpha_1 \quad \text{and} \quad B_{n2} = B_2 \cos \alpha_2 \quad (7)$$

$$H_{t1} = H_1 \sin \alpha_1 \quad \text{and} \quad H_{t2} = H_2 \sin \alpha_2 \quad (8)$$

where B_1 = magnitude of \mathbf{B} in medium 1

B_2 = magnitude of \mathbf{B} in medium 2

H_1 = magnitude of \mathbf{H} in medium 1

H_2 = magnitude of \mathbf{H} in medium 2

Substituting (7) and (8) into (6) and dividing yields

$$\frac{\tan \alpha_1}{\tan \alpha_2} = \frac{\mu_1}{\mu_2} = \frac{\mu_{r1}}{\mu_{r2}} \quad (9)$$

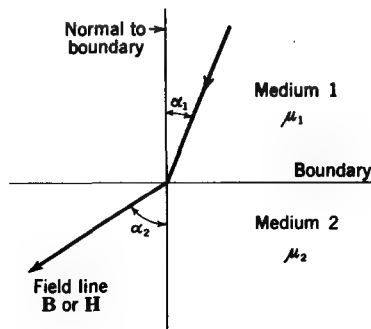


FIGURE 6-15

Boundary between two media of different permeability showing change in direction of magnetic field line.

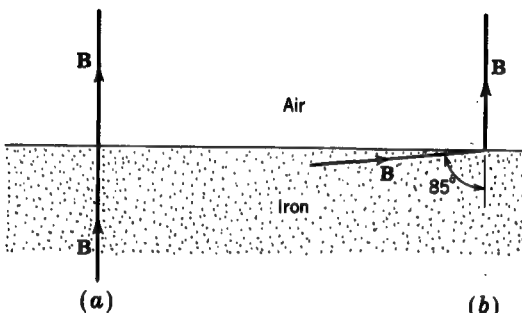


FIGURE 6-16
B lines at air-iron boundary.

where μ_{r1} = relative permeability of medium 1, dimensionless

μ_{r2} = relative permeability of medium 2, dimensionless

Equation (9) gives the relation between the angles α_1 and α_2 for **B** and **H** lines at the boundary between two media.[†]

EXAMPLE 2 Referring to Fig. 6-16, let medium 1 be air ($\mu_r = 1$) and medium 2 be soft iron with a relative permeability of 7,000. (a) If **B** in the iron is incident normal on the boundary ($\alpha_2 = 0$), find α_1 . (b) If **B** in the iron is nearly tangent to the surface at an angle $\alpha_2 = 85^\circ$, find α_1 .

SOLUTION (a) From (9)

$$\tan \alpha_1 = \frac{\mu_{r1}}{\mu_{r2}} \tan \alpha_2 = \frac{1}{7,000} \tan \alpha_2 \quad (10)$$

When $\alpha_2 = 0$, $\alpha_1 = 0$, so that the **B** line in air is also normal to the boundary (see Fig. 6-16a).

(b) When $\alpha_2 = 85^\circ$, we have, from (10), that $\tan \alpha_1 = 0.0016$, or $\alpha_1 = 0.1^\circ$. Thus, the direction of **B** in air is almost normal to the boundary (within 0.1°) even though its direction in the iron is nearly tangent to the boundary (within 5°) (see Fig. 6-16b). Accordingly, for many practical purposes the *direction of B or H in air or other medium of low relative permeability may be taken as normal to the boundary of a medium having a high relative permeability*. This property is reminiscent of the one for **E** or **D** at the boundary of a conductor.

[†] This relation applies only if **B** and **H** have the same direction (μ a scalar). In the absence of magnetization, as in air, **B** and **H** have the same direction. When magnetization is present, as in a soft-iron electromagnet, **B** and **H** also tend to have the same direction. However, this is *not* the situation in a permanent magnet.

6-9 TABLE OF BOUNDARY RELATIONS FOR MAGNETIC FIELDS

Table 6-2 summarizes the boundary relations for magnetic fields developed in Sec. 6-8.

Table 6-2 BOUNDARY RELATIONS FOR MAGNETIC FIELDS†

Field component	Boundary relation	Condition
Normal	$B_{n1} = B_{n2}$ (1)	Any two media
Normal	$\mu_{r1}H_{n1} = \mu_{r2}H_{n2}$ (2)	Any two media
Tangential	$H_{t1} - H_{t2} = K$ $\hat{n} \times \mathbf{H} = \mathbf{K}$ (3) (3a)	Any two media with current sheet of infinitesimal thickness at boundary
Tangential	$H_{t1} = H_{t2}$ (4)	Any two media with no current sheet at boundary
Tangential	$H_{t1} = K_2$ (5)	$H_{t2} = 0$; also medium 2 has a current sheet of infinitesimal thickness at boundary; H_{t1} and K_2 are normal to each other

† These relations apply for both static and time-varying fields (see Chap. 8).

6-10 FERROMAGNETISM

Although magnetic effects in most substances are weak, the group of substances known as ferromagnetic materials exhibits strong magnetic effects. The permeability of these materials is not a constant but is a function both of the applied field and of the previous magnetic history of the specimen. In view of the variable nature of the permeability of ferromagnetic materials, special consideration of their properties is needed.

In ferromagnetic substances the magnetic effects are produced by the motion of the electrons of the individual atoms. The net effect is to make an atom of a ferromagnetic substance act like a miniature bar magnet. In a ferromagnetic substance such as iron these atomic magnets over a region of many atoms tend to orient themselves parallel to each other, with north poles pointing one way. This region is called a magnetic *domain* and is spontaneously magnetized. The size of a domain depends on conditions but usually contains millions of atoms. In some substances the shape appears to be like a long, slender rod with a transverse dimension of microscopic size but lengths of the order of a millimeter or so. Thus, a domain acts like a small, but not atomically small, bar magnet.

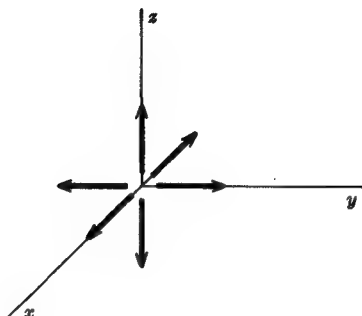


FIGURE 6-17
Six directions of easy magnetization in
an iron crystal.

In an unmagnetized iron crystal the domains are parallel to the direction of easy magnetization, but since as many have north poles pointing one way as the other, the external field of the crystal is zero. In an iron crystal there are six directions of easy magnetization. That is, there is a positive and negative direction along each of the three mutually perpendicular crystal axes (Fig. 6-17). Therefore the polarity of the domains in an unmagnetized iron crystal may be as suggested by the highly schematic diagram of Fig. 6-18a. A single N represents a domain with a north pole pointing out of the page and a single S a domain with a south pole pointing out of the page. If the crystal is placed in a magnetic field parallel to one of the directions of easy magnetization, the domains with polarity opposing or perpendicular to the field become unstable and a few of them may rotate so that they have the same direction as the field. With further increase of the field more domains change over, each as an individual unit, until when all the domains are in the same direction, *magnetic saturation* is reached, as suggested by Fig. 6-18b. The crystal is then magnetized to a maximum extent. If the majority of the domains retain their directions after the applied field is removed, the specimen is said to be *permanently magnetized*. Heat and mechanical shock tend to return the crystal to the original unmagnetized state. In fact, if the temperature is raised sufficiently high, the domains themselves are demagnetized and the ferromagnetism disappears. This is called the *Curie point* (about 770°C for iron).

Magnetization which appears only in the presence of an applied field may be spoken of as *induced magnetization*, as distinguished from *permanent magnetization*, which is present in the absence of an applied field.

6-11 MAGNETIZATION CURVES

The permeability μ of a substance is given by

$$\mu = \frac{B}{H} = \mu_0 \mu_r$$

(a)

N	S	N ← S	S → N
N ↑ S	S ↓ N	N ↑ S	S ↓ N
S → N	N ← S	S	N
N	S	S ↓ N	N ↑ S

(b)

S → N	S → N	S → N	S → N
S → N	S → N	S → N	S → N
S → N	S → N	S → N	S → N
S → N	S → N	S → N	S → N

Applied magnetic field

FIGURE 6-18

(a) Domain polarity in an unmagnetized iron crystal. Arrows indicate direction of magnetization. A single N represents a domain with a north pole pointing out of the page; a single S represents a domain with a south pole pointing out of the page. (b) Condition after crystal is saturated by a magnetic field directed to the right.

where B = magnitude of flux density, T

H = magnitude of field \mathbf{H} , A m⁻¹

μ_0 = permeability of vacuum = 400π nH m⁻¹

μ_r = relative permeability of substance, dimensionless

The permeability μ or the ratio B/H is not a constant for ferromagnetic materials. Therefore, to illustrate the relation of B to H , a graph showing B (ordinate) as a function of H (abscissa) is used. The line or curve showing B as a function of H on such a BH chart is called a *magnetization curve*. It is to be noted that μ is not the slope of the curve, which is given by dB/dH , but is equal to the ratio B/H .

To measure a magnetization curve for an iron sample, a thin, closed ring may be cut from the sample. A uniform primary winding is placed over the ring, forming an iron-cored toroid, as in Fig. 6-19. If the number of ampere-turns in the toroid is NI , the value of H applied to the ring is

$$H = \frac{NI}{l} \quad (\text{A turns m}^{-1})$$

where $l = 2\pi R$ and R is the mean radius of the ring or toroid. This value of H applied to the ring may be called the *magnetizing force*. Hence, in general, H is

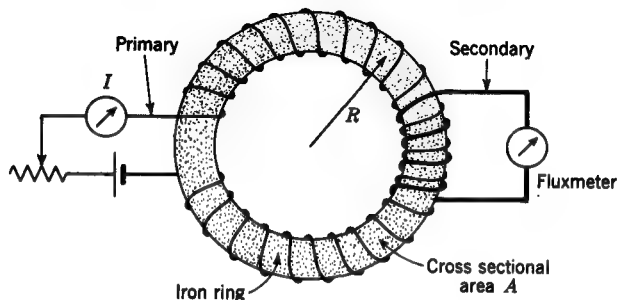


FIGURE 6-19
Rowland ring method of obtaining magnetization curve.

sometimes called by this name. The flux density B in the ring may be regarded as the result of the applied field H and is measured by placing another (secondary) coil over the ring, as in Fig. 6-19, and connecting it to a fluxmeter.[†] For a given change in H , produced by changing the toroid current I , there is a change in magnetic flux ψ_m through the ring. Both H and B are substantially uniform in the ring and negligible outside. Therefore the change in flux $\psi_m = BA$, where A is the cross-sectional area of the ring, and the resulting change in the flux density B in the ring is given by $B = \psi_m/A$ where ψ_m is measured by the fluxmeter. This ring method of measuring magnetization curves was used by Rowland in 1873.

A typical magnetization curve for a ferromagnetic material is shown by the solid curve in Fig. 6-20a. The specimen in this case was initially unmagnetized, and the change was noted in B as H was increased from 0. By way of comparison, four dashed lines are also shown in Fig. 6-20a, corresponding to constant relative permeabilities μ_r of 1, 10, 100, and 1,000. The relative permeability at any point on the magnetization curve is given by

$$\mu_r = \frac{B}{\mu_0 H} = 7.9 \times 10^5 \frac{B}{H} \quad (\text{dimensionless})$$

where B = ordinate of the point, T

H = abscissa of the point, A m⁻¹

A graph of the relative permeability μ_r as a function of the applied field H , corresponding to the magnetization curve in Fig. 6-20a, is presented in Fig. 6-20b. The maximum relative permeability, and therefore the *maximum permeability*, is at the point on the magnetization curve with the largest ratio of B to H . This is designated "max μ ";

[†] The *fluxmeter* operates on the emf induced in the secondary when the magnetic flux through it changes.

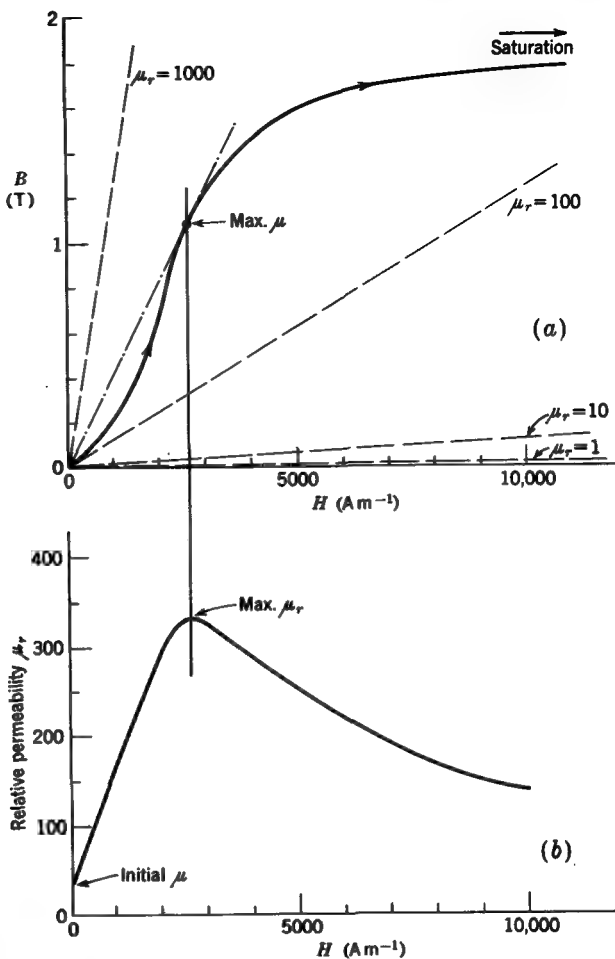


FIGURE 6-20

(a) Typical magnetization curve and (b) corresponding relation of relative permeability to applied field H .

it occurs at the point of tangency with the straight line of steepest slope that passes through the origin and also intersects the magnetization curve (dash-dot line in Fig. 6-20a).

The magnetization curve for air or vacuum would be given by the dashed line for $\mu_r = 1$ (almost coincident with the H axis) in Fig. 6-20a. The difference in the

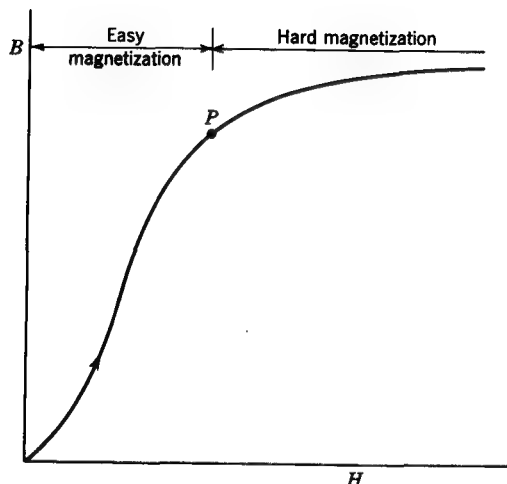


FIGURE 6-21
Regions of easy and hard magnetization
of initial-magnetization curve.

ordinate B between the magnetization curve of the ferromagnetic sample and the ordinate at the same H value on the $\mu_r = 1$ line is equal to the magnetization M of the ferromagnetic material times μ_0 .

The magnetization curve shown in Fig. 6-20a is an *initial-magnetization curve*. That is, the material is completely demagnetized before the field H is applied. As H is increased, the value of B rises rapidly at first and then more slowly. At sufficiently high values of H the curve tends to become flat, as suggested by Fig. 6-20a. This condition is called *magnetic saturation*.

The magnetization curve starting at the origin has a finite slope giving an *initial permeability*. Therefore the relative-permeability curve in Fig. 6-20b starts with a finite permeability for infinitesimal fields.

The initial-magnetization curve may be divided into two sections: (1) the steep section and (2) the flat section, the point P of division being on the upper bend of the curve (Fig. 6-21). The steep section corresponds to the condition of *easy magnetization*, while the flat section corresponds to the condition of difficult, or *hard magnetization*.

Ordinarily a piece of iron consists not of a single crystal but of an aggregate of small crystal fragments with axes oriented at random. The situation in a small piece of iron may be represented schematically as in Fig. 6-22. Here a number of crystal fragments are shown, each with a number of magnetic domains, represented in most cases by a small square. The boundaries between crystal fragments are indicated by the heavy lines, and domain boundaries by the light lines, which also indicate the direction of the crystal axes. In Fig. 6-22a, not only is the piece of iron unmagnetized,

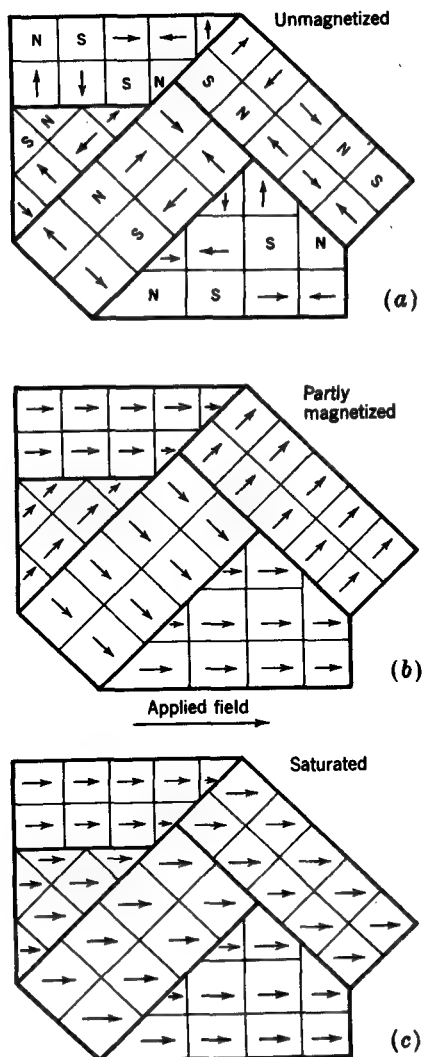


FIGURE 6-22

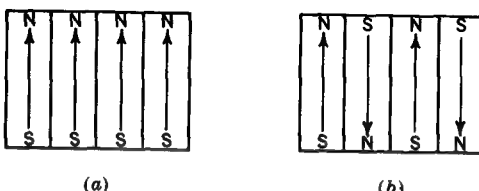
Successive stages of magnetization of a polycrystalline specimen with increasing field. Arrows indicate direction of magnetization of domains. An N represents a domain with a north pole pointing out of the page; an S represents a domain with a south pole pointing out of the page.

but also the individual crystal fragments are unmagnetized. The domains in each crystal are magnetized along the directions of easy magnetization, i.e., along the three crystal axes. However, the polarity of adjacent domains is opposite, so that the total magnetization of each crystal is negligible.

With the application of a magnetic field H in the direction indicated by the arrow (Fig. 6-22) some domains with polarities opposed to or perpendicular to the

FIGURE 6-23

Total energy is reduced when domains go from (a) aligned condition to (b) oppositely oriented condition.



applied field become unstable and rotate quickly to another direction of easy magnetization in the same direction as the field, or more nearly so. These changes take place on the steep (easy) part of the magnetization curve. The result, after all domains have changed over, is as suggested in Fig. 6-22b. This condition corresponds roughly to that at the point *P* on the magnetization curve (Fig. 6-21).

With further increase in the applied field, the direction of magnetization of the domains not already parallel to the field is rotated gradually toward the direction of *H*. This increase in magnetization is more difficult, and very high fields may be required to reach saturation, where all domains are magnetized parallel to the field, as indicated in Fig. 6-22c. This accounts for the flatness of the upper (hard) part of the magnetization curve.

The tendency of adjacent magnetic domains to be oppositely magnetized can be understood from energy considerations. Thus, when adjacent domains are oriented the same, as in Fig. 6-23a, the total energy is increased. When all domains are oppositely oriented, as in Fig. 6-23b, the energy is decreased. The situation can be illustrated by performing an experiment with two bar magnets arranged to slide easily on a rod. Let both magnets be placed side by side and oriented the same, as in Fig. 6-24a. If the left magnet is held but the right magnet is released, it will move to the right, as in Fig. 6-24b, since the adjacent like poles repel. As the right magnet moves farther away, it will rotate on the rod to the position shown in Fig. 6-24c. The opposite poles now attract, and the right magnet moves back to the left until it comes to rest

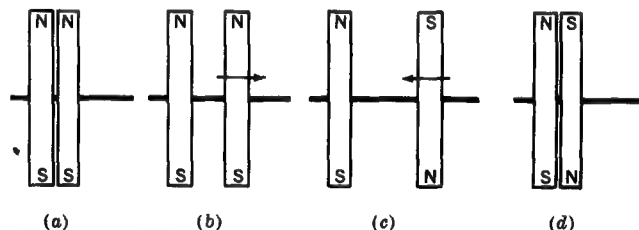


FIGURE 6-24

Experiment with 2 bar magnets illustrates the decrease in total energy.

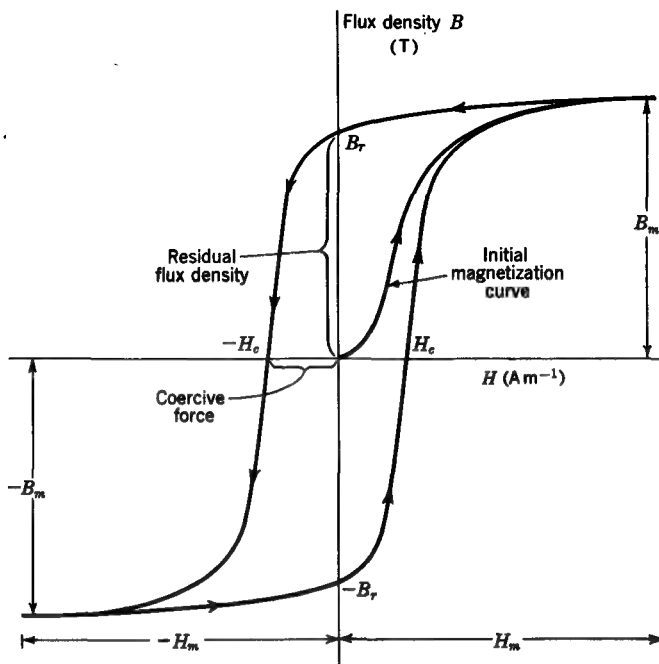


FIGURE 6-25
Hysteresis loop.

against the left magnet, as in Fig. 6-24d. The pair of magnets now has less energy than at the start (Fig. 6-24a). The decrease in total energy accounts for the work done by the right magnet in moving away, rotating, and moving back.

6-12 HYSTERESIS

If the field applied to a specimen is increased to saturation and is then decreased, the flux density B decreases, but not as rapidly as it increased along the initial-magnetization curve. Thus, when H reaches zero, there is a *residual density*, or *remanence*, B_r (Fig. 6-25).

In order to reduce B to zero, a negative field $-H_c$ must be applied (Fig. 6-25).† This is called the *coercive force*. As H is further increased in the negative direction, the specimen becomes magnetized with the opposite polarity, the magnetization at

† By reversing the battery polarity (Fig. 6-19).

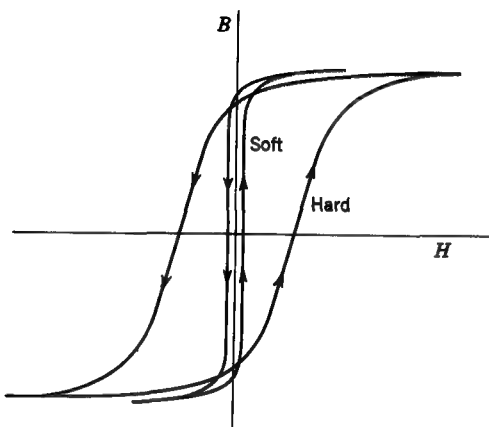


FIGURE 6-26
Hysteresis loops for soft and hard magnetic materials.

first being easy and then hard as saturation is approached. Bringing the field to zero again leaves a residual magnetization or flux density $-B_r$, and to reduce B to zero a coercive force $+H_c$ must be applied. With further increase in field, the specimen again becomes saturated with the original polarity.

The phenomenon which causes B to lag behind H , so that the magnetization curve for increasing and decreasing fields is not the same, is called *hysteresis*, and the loop traced out by the magnetization curve is called a *hysteresis loop* (Fig. 6-25). If the substance is carried to saturation at both ends of the magnetization curve, the loop is called the *saturation, or major, hysteresis loop*. The residual flux density B_r on the saturation loop is called the *retentivity*,† and the coercive force H_c on this loop is called the *coercivity*. Thus, the retentivity of a substance is the maximum value which the residual flux density can attain and the coercivity the maximum value which the coercive force can attain. For a given specimen no points can be reached on the BH diagram outside the saturation hysteresis loop, but any point inside can.

In soft, or easily magnetized, materials the hysteresis loop is thin, as suggested in Fig. 6-26, with a small area enclosed. By way of comparison, the hysteresis loop of a hard magnetic material is also shown, the area enclosed in this case being greater.

Turning our attention to the permeability μ , consider the hysteresis loop of Fig. 6-27a. The corresponding graph of μ as a function of H is as shown in Fig. 6-27b. At $H = 0$, it is apparent that μ becomes infinite. On the other hand, when

† The term retentivity is also sometimes used to mean the ratio of the residual flux density B_r to the maximum flux density B_m .

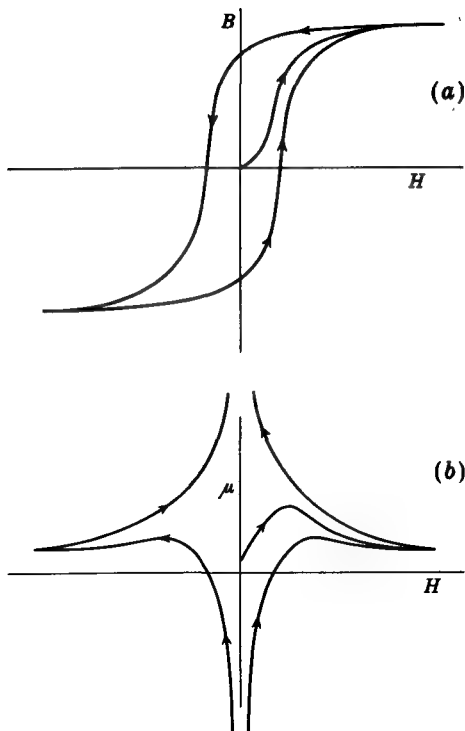


FIGURE 6-27
(a) Hysteresis loop. (b) Corresponding permeability curve.

$B = 0$, $\mu = 0$. Under such conditions, the permeability μ becomes meaningless. Therefore the use of μ must be confined to situations where it has significance, e.g., the initial magnetization curve. It is to be noted that the term maximum permeability signifies specifically the maximum permeability for an initial-magnetization curve and not for a hysteresis loop or other type of magnetization curve.

Another type of magnetization curve for which μ has a definite meaning is the *normal magnetization curve*. This curve is the locus of the tips of a series of hysteresis loops, obtained by cycling the field H over successively smaller ranges. Thus, as shown in Fig. 6-28, the field is changed slowly over the range $\pm H_1$, obtaining the saturation hysteresis loop. The field is next cycled slowly several times over a range $\pm H_2$, obtaining after a few reversals a repeatable hysteresis loop of smaller size. This process is repeated for successively smaller ranges in H , obtaining a series of loops of decreasing size. The curve passing through the tips of these loops is the *normal magnetization curve* (Fig. 6-28). This curve is useful since it is reproducible and is characteristic of the particular type of ferromagnetic material. The normal magnetization curve is actually very similar in shape to the initial-magnetization curve.

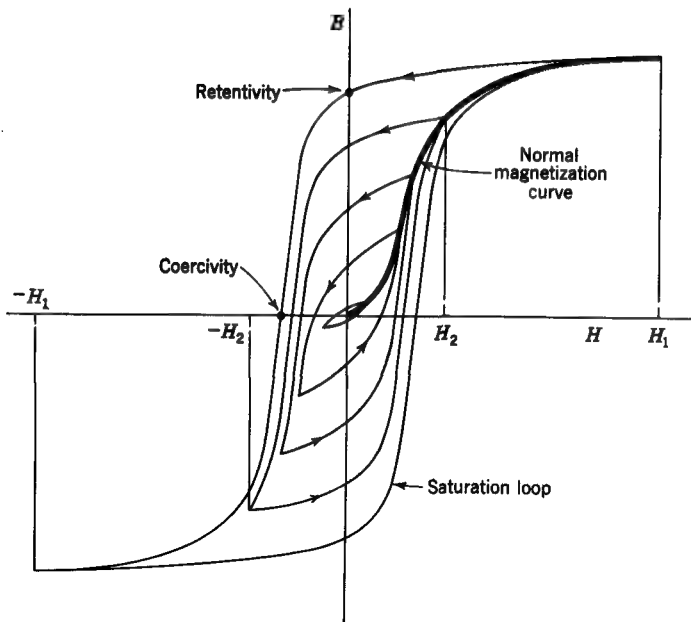


FIGURE 6-28
Normal magnetization curve with relation to hysteresis loops.

6-13 ENERGY IN A MAGNET

A specimen of iron with residual magnetization contains energy since work has been performed in magnetizing it. The magnetic energy w_m per unit volume of a specimen brought to saturation from an originally unmagnetized condition is given by the integral of the initial-magnetization curve expressed (see Table 5-2) by†

$$w_m = \int_0^B H dB \quad (\text{J m}^{-3}) \quad (1)$$

The dimensional relation for (1) is

$$\frac{I}{L} \frac{M}{IT^2} = \frac{M}{LT^2}$$

† Integrating yields $w_m = \frac{1}{2}\mu H^2$, as in Table 5-2.

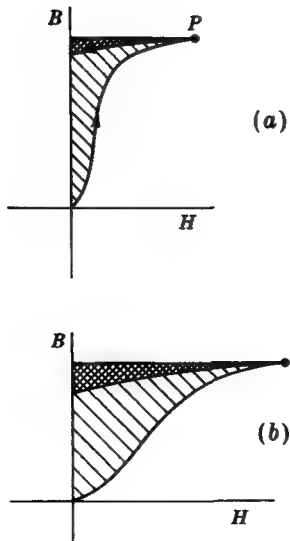


FIGURE 6-29
Energy density areas for (a) soft and
(b) hard magnetic materials.

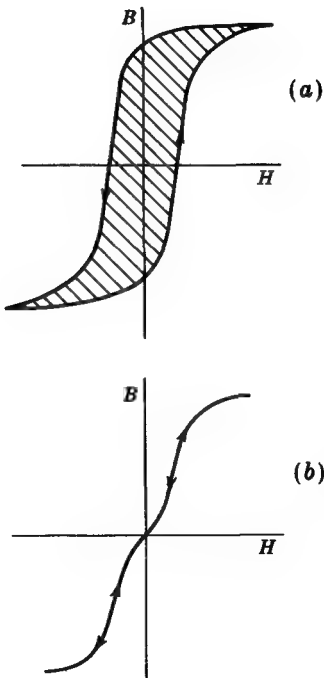


FIGURE 6-30
Energy lost in magnetization cycle is
proportional to area enclosed by hys-
teresis loop.

where M/LT^2 has the dimensions of energy density, which is expressed in joules per cubic meter. Thus, the area between the curve and the B axis is a measure of the energy density. This is indicated in Fig. 6-29a for an easily magnetized (magnetically soft) substance which has been carried to the point *P* in the magnetization process. A magnetically hard substance takes more work to magnetize, as indicated by the larger shaded area in Fig. 6-29b. On bringing H to zero some energy is released, as indicated by the crosshatched areas in Fig. 6-29.

If H is increased and decreased, so that the magnetization of a specimen repeatedly traces out a hysteresis loop, as in Fig. 6-30a, the area enclosed by this loop represents the energy per unit volume expended in the magnetization-demagnetization process in one complete cycle. In general the specimen retains some energy in stored magnetic form at any point in the cycle. However, in going once around the hysteresis loop and back to this point, at which the energy will again be the same, energy

proportional to the area of the loop is lost. This energy is expended in stressing the crystal fragments of the specimen and appears as heat. If no hysteresis were present and the initial-magnetization curve were retraced, the area of the loop would be zero (Fig. 6-30b). The magnetization-demagnetization process could then be accomplished with no loss of energy as heat in the specimen, assuming that eddy currents (see Sec. 8-12) are negligible.

6-14 PERMANENT MAGNETS

In many applications permanent magnets play an important part. In dealing with permanent magnets the section of the hysteresis loop in the second quadrant of the BH diagram is of particular interest. If the loop is a saturation or major hysteresis loop, the section in the second quadrant is called the *demagnetization curve* (Fig. 6-31a). This curve is a characteristic curve for a given magnetic material. The intercept of the curve with the B axis is the maximum possible residual flux density

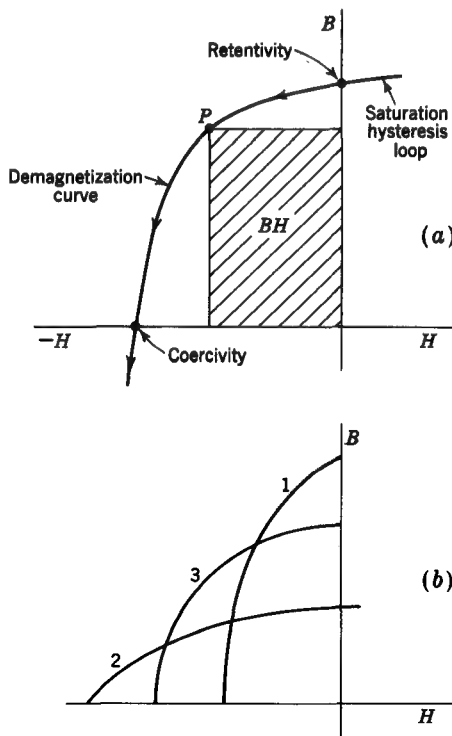


FIGURE 6-31
Demagnetization curves. (B is positive and H is negative.)

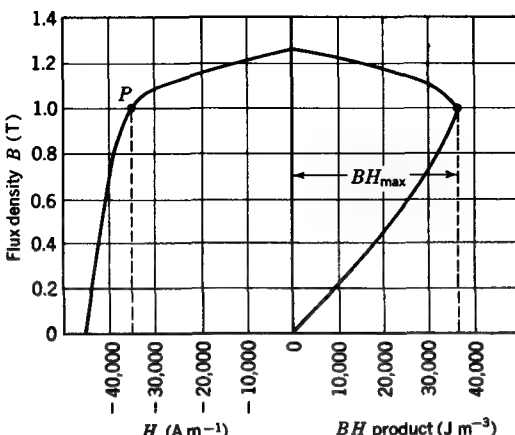


FIGURE 6-32
Demagnetization and BH product curves for Alnico 5.

B_r , or the retentivity, for the material, and the intercept with the H axis is the maximum coercive force, or the coercivity. It is usually desirable that permanent-magnet materials have a high retentivity, but it is also important that the coercivity be large so that the magnet will not be easily demagnetized.

In Fig. 6-31b, three demagnetization curves are shown. Curve 1 represents a material having a high retentivity but low coercivity, while curve 2 represents a material which is just the reverse; i.e., it has a low retentivity and high coercivity. Curve 3 represents a material which is a compromise between the other two, having relatively high retentivity and coercivity.

The maximum BH product, abbreviated BH_{\max} , is also a quantity of importance for a permanent magnet. In fact, it is probably the best single figure of merit, or criterion, for judging the quality of a permanent magnet material. Referring to Fig. 6-31b, it is apparent that BH_{\max} is greater for curve 3 than for either curves 1 or 2. The maximum BH product for a substance indicates the maximum energy density (in joules per cubic meter) stored in the magnet. A magnet at BH_{\max} delivers a given flux with a minimum of magnetic material.

Since the product BH has the dimensions of energy density, it is sometimes called the *energy product* and its maximum value the *maximum energy product*. The product BH for any point P on the demagnetization curve is proportional to the area of the shaded rectangle, as shown in Fig. 6-31a.

Figure 6-32 shows the demagnetization curve for Alnico 5, one of the best permanent-magnet materials, which is an alloy containing iron, cobalt, nickel, aluminum, and copper. A curve showing the BH product is also presented. The

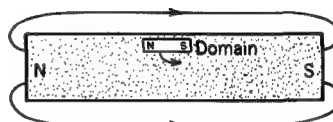
maximum BH product is about $36,000 \text{ J m}^{-3}$ and occurs at a flux density of about 1 T (see point *P*).

A discussion of the operating point of permanent magnets is given in Sec. 6-23.

6-15 TABLE OF PERMANENT MAGNETIC MATERIALS

Representative materials for permanent magnets are given in Table 6-3. The materials are listed in the order of increasing maximum BH product. Magnets of cobalt, copper, iron, and either cerium or samarium have been cast with coercivities of over 2 MA m^{-1} .

FIGURE 6-33
Demagnetization effect of bar-magnet field.



6-16 DEMAGNETIZATION

A bar of ferromagnetic material that has a residual flux density tends to become demagnetized spontaneously. The phenomenon is illustrated by Fig. 6-33, which shows a bar magnetized so that a north pole is at the left and a south pole at the right. The orientation of a single domain is indicated, and it is evident that the external field of

Table 6-3 PERMANENT MAGNETIC MATERIALS

Material†	Retentivity, T	Coercivity, A m^{-1}	$BH_{\max},$ J m^{-3}
Chrome steel (98 Fe, 0.9 Cr, 0.6 C, 0.4 Mn)	1.0	4,000	1,600
Oxide (57 Fe, 28 O, 15 Co)	0.2	72,000	4,800
Alnico 12 (33 Fe, 35 Co, 18Ni, 8Ti, 6Al)	0.6	76,000	12,000
Alnico 2 (55 Fe, 12 Co, 17 Ni, 10 Al, 6 Cu)	0.7	44,800	13,600
Alnico 5 (Alcomax) (51 Fe, 24 Co, 14 Ni, 8 Al, 3 Cu)	1.25	44,000	36,000
Platinum cobalt (77 Pt, 23 Co)	0.6	290,000	52,000

† Compositions in percent.

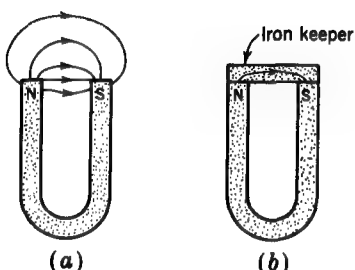


FIGURE 6-34
U-shaped magnet with and without keeper.

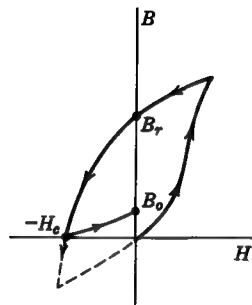


FIGURE 6-35
Partial hysteresis loop.

the bar magnet opposes this domain and, hence, will tend to turn it, or reverse its polarity, thereby partially demagnetizing the bar. The tendency for this demagnetization is reduced if the magnet is in the form of a U, as in Fig. 6-34a, since in this case there is but little demagnetizing field along the side of the magnet. The demagnetizing effect can be still further reduced by means of a soft-iron *keeper* placed across the poles, as in Fig. 6-34b.

The process of removing the permanent magnetization of a specimen so that the residual flux density is zero under conditions of zero H field is called *demagnetization* or *deperming*. It is evident that B can be reduced to zero by the application of the coercive force H_c , but on removing this field the residual flux density will rise to some value B_0 , as suggested in Fig. 6-35. Although it might be possible to end up at $B = 0$ and $H = 0$ by increasing $-H$ to slightly more than the coercive force and then decreasing it to zero, as suggested by the dashed lines, the process requires an accurate knowledge of B and H and the hysteresis loop.

A longer but more simply applied method is called *demagnetization* or *deperming by reversals*. In this method, $\pm H$ is brought to a smaller maximum amplitude on each reversal so that eventually the specimen is left in a demagnetized state at zero field, as suggested by Fig. 6-36. Although such a demagnetization procedure can be completely carried out in a matter of seconds with a small magnetic specimen such as a watch (using ac fields), many seconds or even minutes may be required for each reversal for large magnetic objects because of the slow decay of the induced eddy currents and the reluctance of the domains to change polarity. The matter of eddy currents is discussed further in Sec. 8-12.

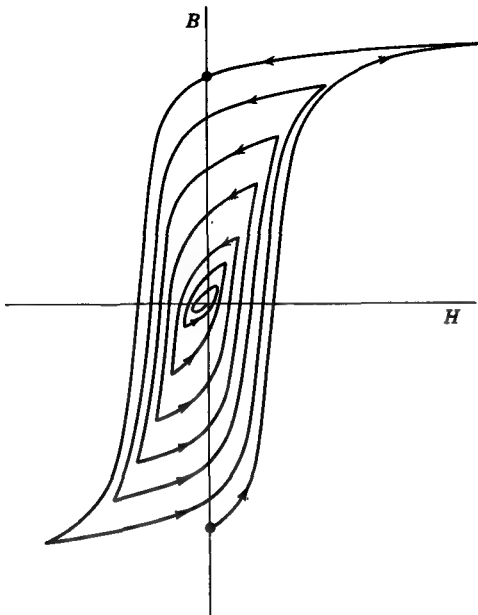


FIGURE 6-36
Demagnetization by reversals.

6-17 THE MAGNETIC CIRCUIT; RELUCTANCE AND PERMEANCE

An electric circuit forms a closed path or circuit through which the current flows. Magnetic flux tubes are continuous and form closed paths. Hence, by analogy, we may consider that a single flux tube is a *magnetic circuit*. Or all the flux tubes of a magnetic circuit, taken in parallel, may be considered as a magnetic circuit.

Consider first an electric circuit carrying a current I . By Kirchhoff's law the total emf in the circuit is equal to the total IR drop. Thus

$$\mathcal{U}_T = IR_T \quad (1)$$

where \mathcal{U}_T = total emf, V

R_T = total resistance, Ω

From (1) the total resistance is

$$R_T = \frac{\mathcal{U}_T}{I} \quad (2)$$

Consider now a magnetic circuit. Corresponding to the resistance of an electric circuit as given by (2), we may, by analogy, define a quantity for the magnetic circuit called the *reluctance* \mathcal{R} . Thus

$$\mathcal{R}_T = \frac{F_T}{\psi_m} \quad (3)$$

where \mathcal{R}_T = total reluctance of magnetic circuit

F_T = total mmf of magnetic circuit, A

ψ_m = flux through magnetic circuit, Wb

In general, the total flux ψ_m in a magnetic circuit is given by

$$\psi_m = \iint \mathbf{B} \cdot d\mathbf{s} \quad (\text{Wb}) \quad (4)$$

where \mathbf{B} = flux density, T

$d\mathbf{s}$ = element of surface, m²

The integration is carried out over the cross-sectional area of the flux tube or tubes that constitute the circuit. If \mathbf{B} is uniform over the entire cross section, $\psi_m = BA$, where A is the cross-sectional area of the circuit in square meters.

Reluctance has the dimensions of current per magnetic flux, or in dimensional symbols

$$I \frac{T^2 I}{ML^2} = \frac{T^2 I^2}{ML^2}$$

The relation $T^2 I^2 / ML^2$ has the dimensions of the reciprocal of inductance. Thus the unit for reluctance is the *reciprocal henry* (H^{-1}).

The reciprocal of reluctance \mathcal{R} is called the *permeance* \mathcal{P} , which is expressed in henrys. Hence, from (3),

$$\mathcal{P}_T = \frac{1}{\mathcal{R}_T} = \frac{\psi_m}{F_T} \quad (5)$$

where \mathcal{P}_T is the total permeance of the circuit in henrys.

The total mmf of a magnetic circuit is equal to the line integral of \mathbf{H} around the complete circuit, and this in turn is equal to the ampere-turns enclosed. Therefore, (3) becomes

$$\mathcal{R}_T = \frac{1}{\mathcal{P}_T} = \frac{F_T}{\psi_m} = \frac{\oint \mathbf{H} \cdot d\mathbf{l}}{\psi_m} = \frac{NI}{\psi_m} \quad (H^{-1}) \quad (6)$$

where NI is the ampere-turns enclosed.

The above discussion concerns the total reluctance of a circuit. Let us consider next the reluctance of a portion of a magnetic circuit. In an electric circuit, the resistance R between two points having no emfs between them is given by

$$R = \frac{V}{I} \quad (\Omega) \quad (7)$$

where V = potential difference between the points, V

I = current in circuit, A

In the analogous magnetic case, the reluctance \mathcal{R} between two points in a magnetic circuit is given by

$$\mathcal{R} = \frac{U}{\psi_m} \quad (H^{-1}) \quad (8)$$

where U is the magnetic potential difference between the points in amperes. From (5-16-6) for U and (4) for ψ_m we have

$$\mathcal{R} = \frac{\int_1^2 \mathbf{H} \cdot d\mathbf{l}}{\iint \mathbf{B} \cdot d\mathbf{s}} \quad (9)$$

where \mathbf{H} is integrated between the two points (1 and 2) between which we wish to find the magnetic potential difference U .

When the circuit has a uniform cross section of area A and the field is uniform, (9) reduces to

$$\mathcal{R} = \frac{Hl}{BA} = \frac{l}{\mu A} \quad (H^{-1}) \quad (10)$$

where \mathcal{R} = reluctance between points 1 and 2, H^{-1}

l = distance between points 1 and 2, m

A = cross-sectional area of magnetic circuit, m^2

μ = permeability of medium comprising the circuit, $H m^{-1}$

The permeance \mathcal{P} between the points 1 and 2 is given by

$$\mathcal{P} = \frac{1}{\mathcal{R}} = \frac{\mu A}{l} \quad (H)$$

(11)

Reluctances in series are additive in the same way that resistances in series are additive. For reluctances in parallel the reciprocal of the total reluctance is equal to the sum of the reciprocals of the individual reluctances. For reluctances in parallel it is usually more convenient to use permeance, the total permeance being equal to the sum of the individual permeances.

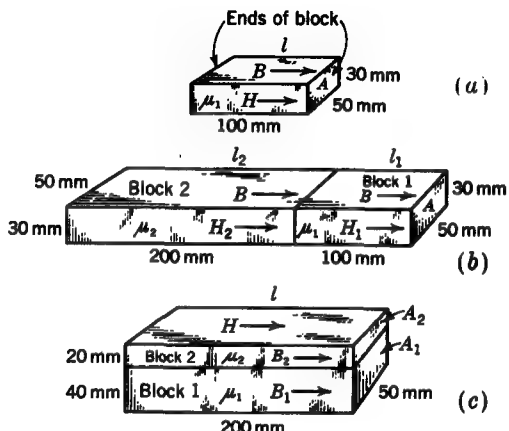


FIGURE 6-37
Rectangular iron blocks.

EXAMPLE 1 Find the reluctance and permeance between the ends of the rectangular block of iron shown in Fig. 6-37a, assuming that B is uniform throughout the block and normal to the ends. The permeability of the block is uniform and has a value $\mu_1 = 500\mu_0$, where μ_0 is the permeability of vacuum.

SOLUTION The reluctance of the block is, from (10),

$$\mathcal{R} = \frac{l}{\mu A} = \frac{0.1}{500 \times 4\pi \times 10^{-7} \times 15 \times 10^{-4}} = 1.06 \times 10^5 \text{ H}^{-1}$$

The permeance \mathcal{P} is the reciprocal of \mathcal{R} ; so

$$\mathcal{P} = \frac{1}{1.06 \times 10^5} = 9.4 \text{ } \mu\text{H}$$

EXAMPLE 2 Find the total reluctance and permeance between the ends of the *series-connected* rectangular iron blocks shown in Fig. 6-37b, assuming that B is uniform throughout the blocks and normal to the ends. The permeability of each block is uniform, the value in block 1 being $\mu_1 = 500\mu_0$ and in block 2, $\mu_2 = 2,000\mu_0$.

SOLUTION The reluctance \mathcal{R}_1 of block 1 is given in Example 1. The reluctance of block 2 is

$$\mathcal{R}_2 = \frac{l_2}{\mu_2 A} = \frac{0.2}{2,000 \times 4\pi \times 10^{-7} \times 15 \times 10^{-4}} = 0.53 \times 10^5 \text{ H}^{-1}$$

The total reluctance \mathcal{R}_T equals the sum of the individual reluctances; so

$$\mathcal{R}_T = \mathcal{R}_1 + \mathcal{R}_2 = (1.06 + 0.53) \times 10^5 = 1.59 \times 10^5 \text{ H}^{-1}$$

The total permeance

$$\mathcal{P}_T = \frac{1}{\mathcal{R}_T} = \frac{1}{1.59 \times 10^5} = 6.3 \mu\text{H}$$

EXAMPLE 3 Find the total reluctance and permeance between the ends of the *parallel-connected* rectangular iron blocks shown in Fig. 6-37c, assuming that B is uniform in each block and normal to the ends. The permeability of each block is uniform, the value in block 1 being $\mu_1 = 500\mu_0$ and in block 2 being $\mu_2 = 2,000\mu_0$.

SOLUTION Since the blocks are in parallel, it is more convenient to calculate the total permeance first. The permeance \mathcal{P}_1 of block 1 is

$$\mathcal{P}_1 = \frac{\mu_1 A_1}{l} = \frac{500 \times 4\pi \times 10^{-7} \times 20 \times 10^{-4}}{0.2} = 6.28 \mu\text{H}$$

The permeance of block 2 is

$$\mathcal{P}_2 = \frac{\mu_2 A_2}{l} = \frac{2,000 \times 4\pi \times 10^{-7} \times 10 \times 10^{-4}}{0.2} = 12.6 \mu\text{H}$$

The total permeance equals the sum of the individual permeances; so

$$\mathcal{P}_T = \mathcal{P}_1 + \mathcal{P}_2 = (6.28 + 12.6) \times 10^{-6} = 18.9 \mu\text{H}$$

The total reluctance is then given by

$$\mathcal{R}_T = \frac{1}{\mathcal{P}_T} = \frac{1}{1.89 \times 10^{-5}} = 5.3 \times 10^4 \text{ H}^{-1}$$

6-18 MAGNETIC FIELD MAPPING; MAGNETIC FIELD CELLS

The examples in the preceding section illustrate how the reluctance or permeance may be found for sections of a magnetic circuit that have a uniform cross section and uniform field. In two-dimensional problems where the field and cross section are nonuniform the magnetic field configuration, and consequently the reluctance or permeance, can also be found provided the permeability may be considered constant. Graphical field-mapping techniques such as are employed in Secs. 3-22 and 4-16 are applicable to such situations.

The following basic properties are useful in magnetic field mapping:

- 1 The field (\mathbf{H} or \mathbf{B}) lines and the magnetic potential (U) lines intersect at right angles.

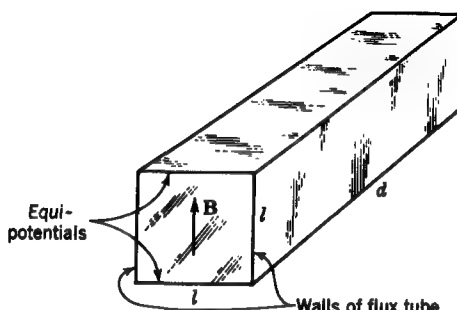


FIGURE 6-38
Magnetic field cell.

- 2 At the boundary between air and iron (or other high-permeability medium) the field lines on the air side of the boundary are substantially perpendicular to the boundary surface.
- 3 The boundary between air and iron (or other high-permeability medium) may be regarded as an equipotential with respect to the air side of the boundary but not, in general, with respect to the iron side.
- 4 In a uniform field the potential varies linearly with distance.
- 5 A magnetic flux tube is parallel to the field, and the magnetic flux over any cross section of the tube is a constant.
- 6 Magnetic flux tubes are continuous.

With these properties in mind a two-dimensional magnetic field can be divided into magnetic flux tubes and then by equipotentials into *magnetic field cells* with sides that are squares or curvilinear squares, using the trial-and-error method described in Sec. 3-22 in connection with electric field mapping.

A *magnetic field cell* is bounded on two sides by equipotential surfaces and on two others by the sidewalls of a flux tube. For instance, the sides of the magnetic field cell in Fig. 6-38 are the walls of a flux tube, while the top and bottom surfaces are equipotentials. The field is parallel to the sides and normal to the top and bottom surfaces. The permeance of a magnetic field cell, as measured between the equipotential surfaces, is, from (6-17-11),

$$\mathcal{P}_0 = \frac{\mu A}{l} = \frac{\mu ld}{l} = \mu d \quad (\text{H}) \quad (1)$$

and the permeance per unit depth is

$$\frac{\mathcal{P}_0}{d} = \mu \quad (\text{H m}^{-1})$$

(2)

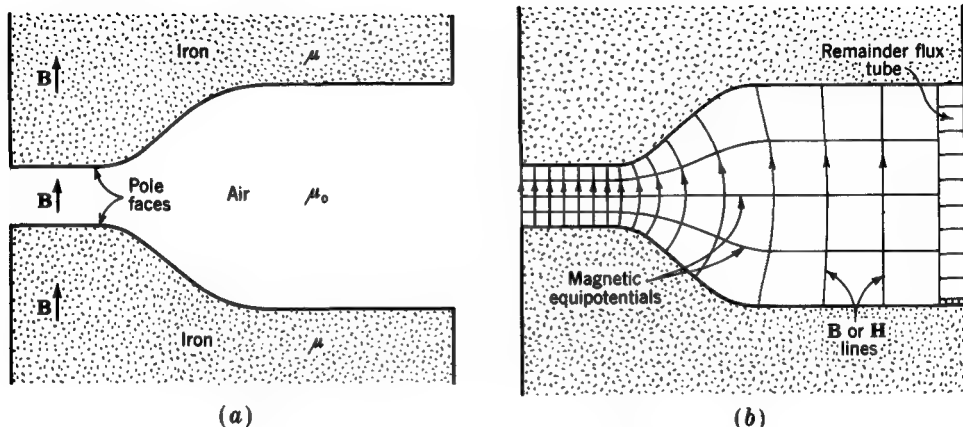


FIGURE 6-39
Magnetic field in air gap (Example 1).

where μ is the permeability of the cell medium in henrys per meter. Thus, the value of μ for a medium is equal to the permeance per unit depth of a magnetic field cell of that medium. For example, a magnetic field cell in air has a permeance per unit depth of $400\pi \text{ nH m}^{-1}$, or $1.26 \mu\text{H m}^{-1}$. Thus, if d in Fig. 6-38 equals 1 m and the medium is air, the permeance of the cell is $1.26 \mu\text{H}$.

Any field cell can be subdivided into smaller square-ended cells with as many cells in parallel as in series. Hence the permeance per unit depth of *any* field cell, large or small, exactly square or curvilinear, is equal to μ .

All cells with the same flux through them may be defined as *magnetic field cells of the same kind*. It follows that the magnetic potential difference across all cells of the same kind is the same.

To illustrate some of the principles of magnetic field mapping, let us consider three examples involving three variations of a two-dimensional problem.

EXAMPLE 1 A magnetic circuit has an air gap of nonuniform separation, as suggested in Fig. 6-39a. The iron has a uniform depth d into the page of 1 m. The geometry of the gap is identical with the region between ff' and gg' in the capacitor of Fig. 3-19. Find the permeance of the air gap, neglecting fringing of the field.

SOLUTION It may be assumed that the iron permeability is much greater than μ_0 , so that the field lines in the gap will be perpendicular to the air-iron boundary and this boundary can be treated as a magnetic equipotential. Since the geometry of the gap is the

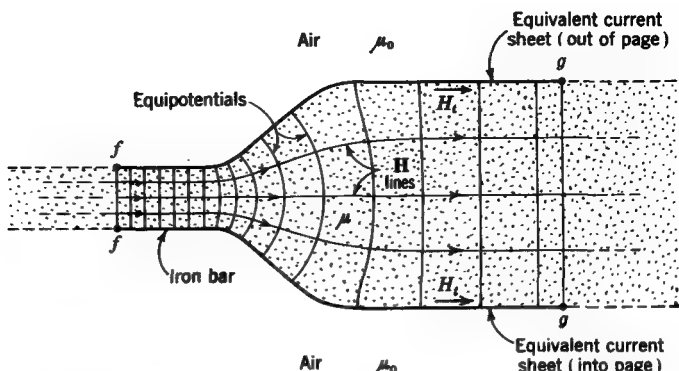


FIGURE 6-40
Iron bar of nonuniform cross section with internal field (Example 2).

same as that for the capacitor in Fig. 3-19, the field map in Fig. 3-19 may also serve in the present case, noting that the field lines here are B or H lines and the equipotentials are surfaces of equal magnetic potential U , as shown in Fig. 6-39b.

With the exception of the cells in the remainder flux tube, all the field cells are of the same kind, and the permeance of the air gap is given in terms of cells of the same kind by

$$\mathcal{P} = \frac{N}{n} \mathcal{P}_0 \quad (3)$$

where N = number of field cells (or flux tubes) in parallel, dimensionless

n = number of field cells in series, dimensionless

\mathcal{P}_0 = permeance of one cell, H

The remainder flux tube has $9\frac{1}{2}$ cells in series, while the other flux tubes have 4. Hence the remainder tube is $4/9\frac{1}{2} = 0.43$ of the width of a full tube, and $N = 15 + 0.43 = 15.43$. The total permeance of the gap is then $\mathcal{P}_T = (15.43/4)\mathcal{P}_0 = 3.86\mathcal{P}_0$. Since the depth of each cell is 1 m, the permeance of one cell is $\mathcal{P}_0 = \mu_0 d = 1.26 \times 1 = 1.26 \mu\text{H}$ and the total permeance is

$$\mathcal{P}_T = 3.86 \times 1.26 = 4.86 \mu\text{H}$$

It is assumed in this example that there is no fringing of the field. For an actual gap there would be fringing at the edges, and the actual permeance of the gap would be somewhat larger than given above.

EXAMPLE 2 Let the problem of the above example be modified to that shown in Fig. 6-40. Here the gap of the first example is replaced by iron and the iron poles by air. The iron may be regarded as part of a magnetic circuit of iron extending further to the left and to

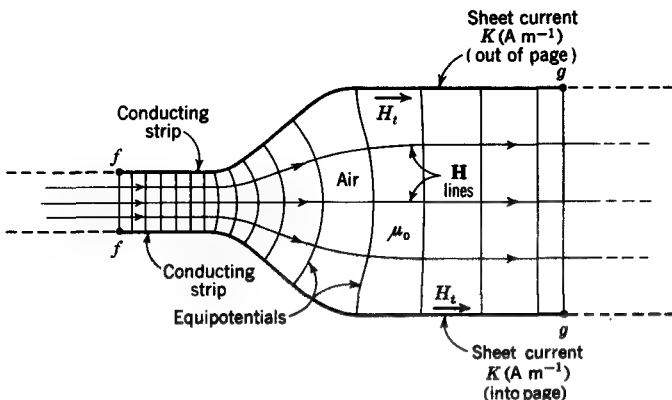


FIGURE 6-41
Cross section of strip transmission line (Example 3).

the right as suggested by the dashed lines in Fig. 6-40. The iron extends to a depth of 1 m normal to the page, with the cross section at any depth identical to that in Fig. 6-40. Assume that the iron has a uniform permeability μ which is much larger than μ_0 . Find the permeance between the surfaces indicated by the dash-dot lines ff and gg .

SOLUTION The field map for this problem is the same as for Example 1 (Fig. 6-39b) except that the field and equipotential lines are interchanged, as shown in Fig. 6-40. It is assumed that μ is so much greater than μ_0 that in the iron the H field at the air-iron boundary is substantially parallel to the boundary as indicated by the map. The total permeance between ff and gg is, from (3), $\mathcal{P} = (4/15.43)\mathcal{P}_0 = 0.259 \times \mu \times 1 = 0.259 \times 1.26\mu_r = 0.326\mu_r$, μH , where μ_r is the relative permeability of iron.

EXAMPLE 3 Let the problem of the preceding example be modified to that of a two-strip transmission line having the same cross section as the gap of Example 1 and the iron circuit of Example 2. As shown in Fig. 6-41, the two conducting strips extend normal to the page with a sheet of steady current flowing outward on the upper strip and an equal current flowing inward on the lower strip. The medium in which the strips are located is air. Neglect edge effects. Find the inductance of a 1-m length of the line.

SOLUTION Neglecting edge effects,[†] the field map between the strips is identical with that for the iron circuit in Fig. 6-40.

[†] If the conducting strips are extended an infinite distance to the left and right, as suggested by the dashed lines in Fig. 6-41, the field configuration is precisely as indicated. The field between the strips is produced by the currents on the strips. In Example 2 the field in the iron may be regarded as due to an equivalent current sheet at the surfaces of the iron bar normal to the page (Fig. 6-40).

If each cell in the map is regarded as a strip transmission line with sheet currents along its upper and lower surfaces, the inductance L_0 for a length d of 1 m of the single-cell line (normal to the page in Fig. 6-41) is, from (5-17-2), given by

$$L_0 = \mu_0 d = 1.26 \mu\text{H}$$

The total inductance L_T of a 1-m length of the line is then

$$L_T = \frac{4}{15.43} \times 1.26 = 0.326 \mu\text{H}$$

6-19 COMPARISON OF FIELD MAPS IN ELECTRIC, MAGNETIC, AND CURRENT CASES

Graphical field mapping was discussed in Sec. 3-22 for electric fields, in Sec. 4-16 for currents in conductors, and in Sec. 6-18 for magnetic fields. The technique is similar in all these cases. Of particular significance is the fact that a field map for a certain two-dimensional geometry can be applied to numerous problems having this geometry. An illustration of this was provided by the three examples in Sec. 6-18, in which the field map of Fig. 3-19 for a capacitor yielded the solution for the permeance of the volume with the field applied both transversely and longitudinally. The map also gave the inductance of a conducting-strip transmission line.

The same map can, in addition, supply the value of the conductance of a conducting bar with the current flowing transversely and with the current flowing longitudinally. The same map can also be applied to heat- and fluid-flow problems.

To summarize, sketches are given in Fig. 6-42, showing six different problems of the same geometry for which solutions are supplied by one field map. The actual map is shown in Fig. 6-42a, being omitted in the other sketches. The geometry of the problems is that of the capacitor of Fig. 3-19, which was also used in the problems of Figs. 6-39 to 6-41.

In Fig. 6-42a the map represents the electric field in a capacitor with the field transverse. In Fig. 6-42b the map represents the electric field in a conducting bar with current flowing transversely, while in Fig. 6-42c the current flows longitudinally. In Fig. 6-42d the map represents the magnetic field in the air gap between two iron pole faces, while in Fig. 6-42e it represents the magnetic field in an iron bar with the field applied longitudinally. In Fig. 6-42f the map represents the field between two conducting strips acting as a transmission line with current flowing normal to the page. For each case the capacitance, conductance, permeance, or inductance per unit depth (normal to the page) is given, as appropriate for the particular problem. Fringing of the field is neglected in all cases.

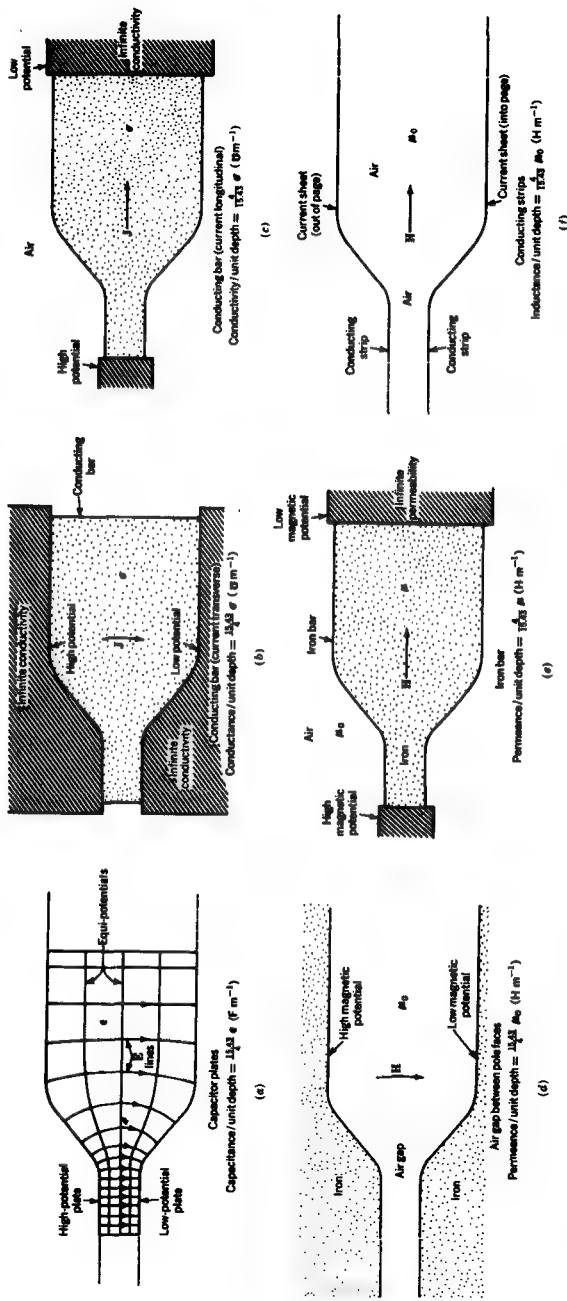


FIGURE 6-42
Application of one field map to six situations.

It is also of interest to compare the significance of the cells (square or curvilinear) of the field maps for the different problems we have considered. Thus, *the capacitance per unit depth of an electric field cell equals the permittivity ϵ of the medium; the conductance per unit depth of a conductor cell equals the conductivity σ of the medium; the permeance per unit depth of a magnetic field cell equals the permeability μ of the medium; and the inductance per unit length of a transmission-line cell equals the permeability μ of the medium.* These relationships are summarized in the last column of Table 6-4. This table also has columns headed Flow lines, Flow tubes, and Equi-potentials. Under Flow lines are listed the quantities having the direction of flow lines and under Flow tubes the quantities equal to the total flux through a tube.

Table 6-4 IMPORTANT FIELD-MAP QUANTITIES

Field	Flow lines	Flow tubes	Equi-potentials	Value of cell (per unit depth)
Electric	D or E	Electric flux ψ	V (V)	Permittivity ϵ ($F m^{-1}$)
Current	J or E	Current I	V (V)	Conductivity (Ωm^{-1})
Magnetic	B or H	Magnetic flux ψ_m	U (A)	Permeability μ ($H m^{-1}$)
Heat	Temperature gradient	Heat per time	Temperature	Thermal conductivity
Fluid flow (non-turbulent; incompressible)	Velocity	Mass per time	Velocity potential	Density

EXAMPLE Apply the above analogies to find the capacitance of an air capacitor by a resistance measurement.

SOLUTION The capacitor plates are immersed in a large tank filled with a liquid of uniform conductivity σ , and the dc resistance R is measured between the plates.

In general, the conductance G of a certain geometry is given by

$$G = \sigma d \frac{N}{n} \quad (1)$$

where N = number of cells in parallel

n = number of cells in series

d = depth of cells

An actual capacitor with the same geometry has the same field configuration (compare Fig. 6-42a and b); so the capacitance

$$C = \epsilon_0 d \frac{N}{n} \quad (2)$$

where N and n are the same as in (1). Hence, on dividing (2) by (1),

$$C = \frac{\epsilon_0}{\sigma} G = \frac{\epsilon_0}{\sigma R} \quad (3)$$

where C = capacitance of actual capacitor, F

ϵ_0 = permittivity of air = 8.85 pF m^{-1}

σ = conductivity of liquid, S m^{-1}

$R = 1/G$ = measured resistance, Ω

Thus when σ is known (it can be measured with a rectangular volume), the capacitance of an air capacitor can be obtained from (3) by a resistance measurement.

6-20 GAPLESS CIRCUIT

Consider the magnetic circuit of a closed ring of iron of uniform cross section A and mean length l . Suppose that a coil of insulated wire is wound uniformly around the ring and that we wish to know how large the product NI of the number of turns and the current must be to produce a flux density B in the ring.

The coil on the ring in Fig. 6-43a forms a toroid. In the toroid we have, from (5-11-5),

$$B = \frac{\mu NI}{l} = \frac{\mu NI}{2\pi R} \quad (\text{T}) \quad (1)$$

where μ = permeability (assumed uniform) of medium inside of toroid, H m^{-1}

N = number of turns, dimensionless

I = current, A

l = mean length of toroid, m

R = mean radius of toroid, m

Dividing by μ , we have $NI = Hl$ ampere-turns. If a certain flux density B is desired in the ring, the corresponding H value is taken from a BH curve for the ring material and the required number of ampere-turns calculated from $NI = Hl$.

EXAMPLE 1 An iron ring has a cross-sectional area $A = 1,000 \text{ mm}^2$ and a mean length $l = 600 \text{ mm}$. Find the number of ampere-turns required to produce a flux density $B = 1 \text{ T}$. From a BH curve for the iron, $H = 1,000 \text{ A m}^{-1}$ at $B = 1 \text{ T}$.

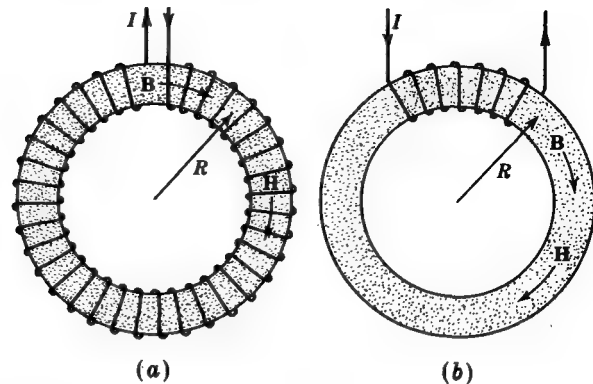


FIGURE 6-43
Closed iron ring (a) with uniform winding and (b) with concentrated winding.

SOLUTION From $NI = HI$

$$NI = 1,000 \times 0.6 = 600 \text{ A turns}$$

The coil could be 100 turns with a current of 6 A or 1,000 turns with 600 mA. The coil may be uniformly distributed around the ring, as in Fig. 6-43a, or concentrated in a small sector, as in Fig. 6-43b.

The required number of ampere-turns can also be found by calculating the reluctance of the ring circuit, as illustrated by the following example.

EXAMPLE 2 Find the number of ampere-turns required for the ring of Example 1 for $B = 1 \text{ T}$ by first evaluating the reluctance of the ring.

SOLUTION From (6-17-6)

$$\mathcal{R} = \frac{\oint \mathbf{H} \cdot d\mathbf{l}}{BA} \quad (2)$$

We also have $\oint \mathbf{H} \cdot d\mathbf{l} = HI = NI$. It follows that $NI = \mathcal{R}BA$, where

$$\mathcal{R} = \frac{l}{\mu A} \quad (3)$$

Since $H = 1,000 \text{ A m}^{-1}$ when $B = 1 \text{ T}$,

$$\mu = \frac{B}{H} = \frac{1}{1,000} = 1 \text{ mH m}^{-1} \quad (4)$$

It is to be noted that the relative permeability for this case is

$$\mu_r = \frac{B}{\mu_0 H} = \frac{10^{-3}}{4\pi \times 10^{-7}} = 795 \quad (5)$$

Introducing (4) in (3) and also the value of l and A gives the reluctance of the ring as

$$\mathcal{R} = \frac{0.6}{10^{-3} \times 10^{-3}} = 6 \times 10^5 \text{ H}^{-1} \quad (6)$$

Hence, the required number of ampere-turns is

$$NI = \mathcal{R}BA = 6 \times 10^5 \times 1 \times 10^{-3} = 600$$

as obtained in Example 1.

6-21 MAGNETIC CIRCUIT WITH AIR GAP

Let a narrow air gap of thickness g be cut in the iron ring of Sec. 6-20, as shown in Fig. 6-44a. The gap detail is presented in Fig. 6-44b. By the continuity of the normal component of B the flux density in the gap is the same as in the iron if fringing is neglected. Neglecting the fringing involves but little error where the gap is narrow, as assumed here. The field H_g in the gap is then $H_g = B/\mu_0$, while the field H_i in the iron is

$$H_i = \frac{B}{\mu} = \frac{B}{\mu_r \mu_0} = \frac{H_g}{\mu_r} \quad (1)$$

from which

$$\frac{H_g}{H_i} = \mu_r \quad (2)$$

The number of ampere-turns required to produce a certain flux density B in a magnetic circuit with gap, as in Fig. 6-44a, is a problem for which the solution can be obtained directly. For instance, according to (5-16-9), the line integral of H once around the magnetic circuit equals the total mmf F , or ampere-turns enclosed. That is,

$$\oint \mathbf{H} \cdot d\mathbf{l} = F = NI \quad (3)$$

EXAMPLE Let the iron ring of Fig. 6-44 have a cross-sectional area $A = 1,000 \text{ mm}^2$, an air gap of width $g = 2 \text{ mm}$, and a mean length $l = 2\pi R = 600 \text{ mm}$, including the air gap. Find the number of ampere-turns required to produce a flux density $B = 1 \text{ T}$.

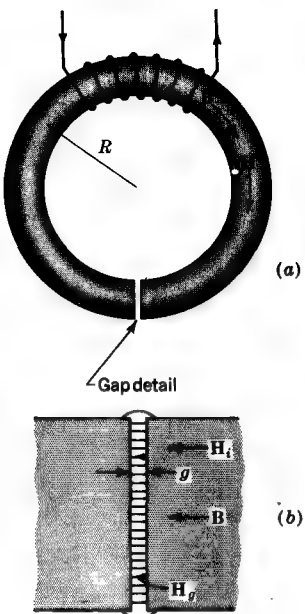


FIGURE 6-44
Iron ring with air gap.

SOLUTION We have

$$NI = \oint \mathbf{H} \cdot d\mathbf{l} = H_i(l - g) + H_g g \quad (4)$$

where $H_i = H$ field in iron

$H_g = H$ field in gap

From a BH curve for the iron, $H_i = 1,000 \text{ A m}^{-1}$, and from (2) we know H_g in terms of H_i . Hence (4) becomes

$$NI = H_i[(l - g) + \mu_r g] \quad (5)$$

where $\mu_r = 795$ is the relative permeability of the iron ring at $B = 1 \text{ T}$. Therefore,

$$NI = 1,000[(0.6 - 0.002) + 795 \times 0.002] = 2,188 \text{ A turns}$$

The introduction of the narrow air gap makes it necessary to increase the ampere-turns from 600 to 2,188 to maintain the flux density at 1 T.

The problem can also be solved by calculating the total reluctance of the magnetic circuit. Thus, from (4) we have

$$NI = \frac{\mu A}{\mu_0 A} H_i(l - g) + \frac{\mu_0 A}{\mu_0 A} H_g g \quad (6)$$

and

$$NI = BA(\mathcal{R}_i + \mathcal{R}_g) \quad (7)$$

where $\mathcal{R}_i = (I - g)/\mu A$ = reluctance of iron part of circuit

$\mathcal{R}_g = g/\mu_0 A$ = reluctance of air gap

6-22 MAGNETIC GAP FORCE

Referring to Fig. 6-44, the effect of the magnetic field is to exert forces which tend to close the air gap. That is, the magnetic poles of opposite polarity at the sides of the gap are attracted to each other. Forces produced by magnetic fields find application in numerous electromechanical devices. In this section an expression for the force between magnetic pole pieces is developed.

The density of energy stored in a magnetic field is

$$w_m = \frac{1}{2} \frac{B^2}{\mu} \quad (\text{J m}^{-3}) \quad (1)$$

If the gap is small, we may assume a uniform field in the air gap. The total energy W_m stored in the gap is then

$$W_m = w_m Ag = \frac{B^2 Ag}{2\mu_0} \quad (\text{J}) \quad (2)$$

where A = area of gap, m^2

g = width of gap, m

Suppose now that the iron ring in Fig. 6-44 is perfectly flexible, so that the gap must be held open by a force F as in Fig. 6-45. If the force is increased so as to increase the gap by an infinitesimal amount dg while at the same time the current through the coil is increased to maintain the flux density B constant, the energy stored in the gap is increased by the infinitesimal amount

$$dW_m = \frac{B^2 A}{2\mu_0} dg \quad (3)$$

Equation (3) has the dimensions of energy. But energy may also be expressed as force times distance, which in this case is $F dg$, where F is the attractive force between the poles. It is equal in magnitude to the force required to hold them apart. Thus

$$F dg = \frac{B^2 A}{2\mu_0} dg$$

or

$$F = \frac{B^2 A}{2\mu_0} \quad (4)$$

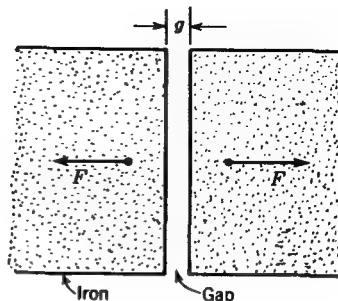


FIGURE 6-45
Forces at air gap.

where F = attractive force, N

B = flux density, T

A = area of gap, m

μ_0 = permeability of air = $400\pi \text{ nH m}^{-1}$

Dividing by the gap area A yields the pressure P . That is,

$$P = \frac{F}{A} = \frac{B^2}{2\mu_0} \quad (\text{N m}^{-2}) \quad (5)$$

6-23 PERMANENT MAGNET WITH GAP

Suppose first that a closed iron ring is magnetized to saturation with a uniform toroidal coil wound on the ring. When the coil is removed, the flux density in the iron is equal to the retentivity (see Fig. 6-47). If, however, the system has an air gap, as in Fig. 6-46, the flux density has a smaller value as given by a point P which lies somewhere on the demagnetization curve (Fig. 6-47) (see also Sec. 6-14). Further information is needed to locate this point. This may be obtained as follows. The line integral of \mathbf{H} once around a magnetic circuit is $\oint \mathbf{H} \cdot d\mathbf{l} = NI$. Since $NI = 0$,

$$\oint \mathbf{H} \cdot d\mathbf{l} = H_i(l - g) + H_g g = 0$$

or

$$H_i(l - g) = -H_g g \quad (1)$$

where $H_i = H$ field in the iron

$l = 2\pi R$ = total length of magnetic circuit (including gap)

g = width of gap

$H_g = H$ field in gap

Thus H_i and H_g are in opposite directions, as indicated in Fig. 6-46. If leakage is

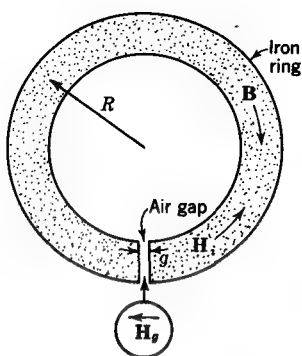


FIGURE 6-46
Permanently magnetized ring with air gap.

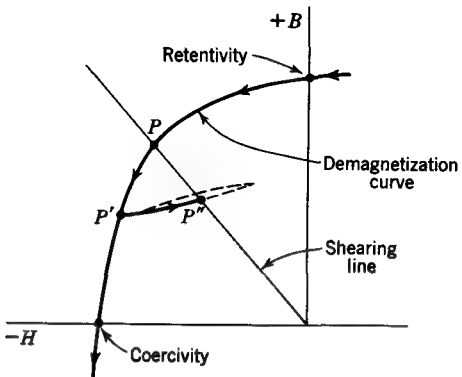


FIGURE 6-47
Demagnetization curves for permanent magnet.

neglected, B is uniform around the circuit. Multiplying (1) by μ_0 and solving for the ratio B/H_i , or the permeability of the iron, we obtain

$$\frac{B}{H_i} = -\mu_0 \frac{l-g}{g} \quad (2)$$

This ratio of the flux density B to the field H_i in the iron gives the slope of a line called the *shearing line*, as shown in Fig. 6-47. The intersection of this line with the demagnetization curve determines the position of the iron on the magnetization curve (point P). This location is a function of the ratio of the iron path length ($l-g$) to the gap length g .

In most permanent-magnet applications, where it is desired that B remain relatively constant, a moderate demagnetizing field is applied to the iron, moving the position of the iron to P' (Fig. 6-47). On removing the field, the iron moves to the point P'' on the shearing line. The ring magnet is now said to be *stabilized*, and when fields less than about the difference of H between points P' and P'' are applied to the ring and then removed, the iron will always return to approximately point P'' . Under these conditions the iron moves along a minor hysteresis loop, as suggested by the dashed lines in Fig. 6-47.

6-24 COMPARISON OF ELECTRIC AND MAGNETIC RELATIONS INVOLVING POLARIZATION AND MAGNETIZATION

It is interesting to compare the magnetic relations where magnetization M is present with the corresponding electric relations where polarization P is present (see Chap. 3). This is done in Table 6-5.

Table 6-5 COMPARISON OF EQUATIONS INVOLVING POLARIZATION P AND MAGNETIZATION M

Description of equation	Electric case	Magnetic case
Dipole-moment relations	$P = \frac{p}{v} = \frac{Ql}{v}$	$M = \frac{m}{v} = \frac{Q_m l}{v}$
Flux density	$\mathbf{D} = \epsilon_0 \mathbf{E} + \mathbf{P}$	$\mathbf{B} = \mu_0(\mathbf{H} + \mathbf{M})$
Permittivity and permeability	$\epsilon = \epsilon_0 + \frac{P}{E}$	$\mu = \mu_0 \left(1 + \frac{M}{H}\right)$
Relative permittivity and permeability	$\epsilon_r = 1 + \frac{P}{\epsilon_0 E}$	$\mu_r = 1 + \frac{M}{H}$
Susceptibilities	$\chi = \epsilon_r - 1$	$\chi_m = \mu_r - 1$
Relation to polarization charge density and to equivalent current density	$\nabla \cdot \mathbf{P} = \rho_p$	$\nabla \times \mathbf{M} = \mathbf{J}'$
Poisson's equations	$\nabla^2 V = -\frac{\rho}{\epsilon}$	$\nabla^2 U = \nabla \cdot \mathbf{M} = -\nabla \cdot \mathbf{H}$
Scalar and vector potentials	$V = \frac{1}{4\pi\epsilon_0} \int_v \frac{\rho - \nabla \cdot \mathbf{P}}{r} dv$	$\mathbf{A} = \frac{\mu_0}{4\pi} \int_v \frac{\mathbf{J} + \nabla \times \mathbf{M}}{r} dv$

* Answers to starred problems are given in Appendix C.

PROBLEMS

- * 6-1 A magnetized needle of 20 A m^2 magnetic moment is situated in a uniform magnetic field of $50 \mu\text{T}$ flux density. Find the maximum torque on the needle.
- 6-2 A magnetized needle of 30 A m^2 magnetic moment is situated with its center at the origin in a magnetic field of flux density $\mathbf{B} = \gamma B_o$. If a short bar magnet of moment $Q_m l$ is placed coincident with the x axis at a large distance x_0 from the origin, find the angle θ between the needle and the y axis assuming that the needle pivots freely around its center point.
- * 6-3 A uniformly magnetized bar with a volume of 0.01 m^3 has a magnetic moment of 500 A m^2 . If the flux density $B = 50 \text{ mT}$ in the bar, what is the value of H in the bar?
- 6-4 A bar magnet in a *uniform* magnetic field is acted on only by a torque, there being no translational force on the magnet. In a *nonuniform* field, there is a net translational force. Find the maximum value of this force on a uniformly magnetized bar magnet 5 mm long with a magnetic moment of 2 A m^2 situated 100 mm from one pole of a very long slender bar magnet having a pole strength of 500 A m .

- * 6-5 Two cavities are cut in a ferromagnetic medium ($\mu_r = 200$) of large extent. Cavity 1 is a thin disk-shaped cavity with flat faces perpendicular to the direction of \mathbf{B} in the ferromagnetic medium. Cavity 2 is a long needle-shaped cavity with its axis parallel to \mathbf{B} . The cavities are filled with air. If $B = 2 \text{ T}$, what is the magnitude of \mathbf{H} at (a) the center of cavity 1 and (b) the center of cavity 2?

- 6-6 Two long straight parallel conductors separated by a distance d carry a current I in opposite directions. Find the force per unit length of conductor if (a) the medium is air and (b) the medium everywhere has a relative permeability $\mu_r = 200$.

- 6-7 Two ferromagnetic media are separated by a plane boundary. Medium 1 has a relative permeability $\mu_r = 200$ and medium 2 a relative permeability $\mu_r = 1,500$. If the magnetic field direction in medium 2 is at an angle of 10° with respect to the surface, find the angle between the field direction and the surface in medium 1.

- * 6-8 A bar magnet with 10 A m^2 magnetic moment is brought 500 mm from a compass needle. What is the maximum angular deviation of the needle which the magnet can produce? Take the horizontal component of the earth's field as 1 mT.

- 6-9 Design a magnetic levitation system to raise 1,000 kg at the earth's surface by 5 mm using (a) permanent magnets and (b) electromagnets.

- * 6-10 A steel pipeline runs east-west at a constant depth below a flat ground. The undisturbed earth's magnetic field in the region has a dip of 70° (angle of \mathbf{B} from horizontal) and a declination of 0° (angle of \mathbf{B} from north). Locate the pipe and its depth if the following dip measurements are obtained with the dip needle 1 m above the ground:

Meters south of reference mark	0	2	4	6	8	10	12	14	16
Dip angle, deg	71	75	77	74	70	65	62	66	69

- * 6-11 A rectangular iron bar has a length x_1 and a cross-sectional area A . The permeability is a function of x and is given by

$$\mu = \mu_0 + \frac{\mu_1 - \mu_0}{x_1} x$$

Find the permeance of the bar.

- 6-12 A small bar magnet with magnetic moment of 50 A m^2 is situated parallel to a very long straight wire with current of 50 A. If the bar magnet is 500 mm from the wire, find the torque on the bar magnet.

- 6-13 A flat sheet of linear current density K separates two media with magnetic flux densities $B_1 = 5 \text{ mT}$ and $B_2 = 20 \text{ mT}$ in opposite directions parallel to the sheet. The relative permeabilities are $\mu_{r1} = 50$ and $\mu_{r2} = 100$. What is K ?

- 6-14 Show that at the center of a long uniformly magnetized bar of uniform cross-sectional area A that $|H| \approx 2MA/\pi l^2$, where M = magnetization and l = length of bar.

- 6-15 Show that the permeability at the center of a long permanently magnetized rod of uniform magnetization is given by $\mu_0[1 - (\pi l^2/2A)]$, where l = length of rod and A = cross-sectional area of rod.

6-16 A copper conductor of 50 mm radius is enclosed by a concentric iron tube of inner radius 100 mm and outer radius 150 mm. (a) If the current in the conductor is 200 A, find B and H at radii of 25, 50, 100, 125, 150, and 200 mm. Assume that the current density in the conductor is uniform and that $\mu_r = 400$ in the iron tube. (b) Sketch the variation of B and H as a function of radius from 0 to 250 mm.

6-17 Show that the flux density from a bar magnet is given by

$$B_\theta = \frac{\mu_0 Q_m l \sin \theta}{4\pi r^3} \quad \text{and} \quad B_r = \frac{\mu_0 Q_m l \cos \theta}{2\pi r^3}$$

where $Q_m l$ = dipole moment

θ = angle between bar axis and radius vector of length r

It is assumed that $r \gg l$.

6-18 Show that the flux density from a single-turn wire loop is given by

$$B_\theta = \frac{\mu_0 I A \sin \theta}{4\pi r^3} \quad \text{and} \quad B_r = \frac{\mu_0 I A \cos \theta}{2\pi r^3}$$

where I = current

A = area

IA = magnetic moment

θ = angle between axis of loop and radius vector of length r

It is assumed that r is much greater than the diameter of the loop.

6-19 A small bar magnet is situated in air at a distance d from the plane surface of a medium of large extent and permeability μ . The bar axis makes an angle θ with respect to a perpendicular to the surface. If the dipole moment of the bar magnet is $Q_m l$, find the force and torque on the bar magnet due to the magnetization induced in the medium of permeability μ .

* **6-20** A magnetized rod 10 mm in diameter and 30 mm long has a uniform magnetization of $1,200 \text{ A m}^{-1}$. Find the magnetic moment of the bar.

* **6-21** A uniformly magnetized rod 25 mm in diameter and 75 mm long has a magnetic moment of 12 kA m^2 . Find the equivalent sheet-current density at the surface of the rod.

6-22 Demonstrate that the force between two small bar magnets varies as the inverse fourth power of their separation and is independent of their relative orientation.

6-23(a) Assuming that the demagnetization curve of a certain ferromagnetic material is a straight line, what is the maximum BH product if the retentivity is 1 T and the coercivity is 20 kA m^{-1} ? (b) Prove that this is the maximum value.

6-24 According to Lord Rayleigh, the bottom part of the normal magnetization curve is given by $B = \mu_i H + aH^2$, where μ_i is the initial permeability (at $H = 0, B = 0$) and a is a constant. Assume that this relation applies to the initial-magnetization curve of an iron specimen. What is the expression for the energy density in the iron after the field is raised from $H = 0$ to $H = H_1$? Assume that the specimen is initially unmagnetized.

* **6-25** An iron ring has a uniform cross-sectional area of 150 mm^2 and a mean radius of 200 mm. The ring is continuous except for an air gap 1 mm wide. Find the number of ampere-turns required on the ring to produce a flux density $B = 0.5 \text{ T}$ in the air gap. Neglect fringing. When $B = 0.5 \text{ T}$ in the iron, $\mu_r = 250$.

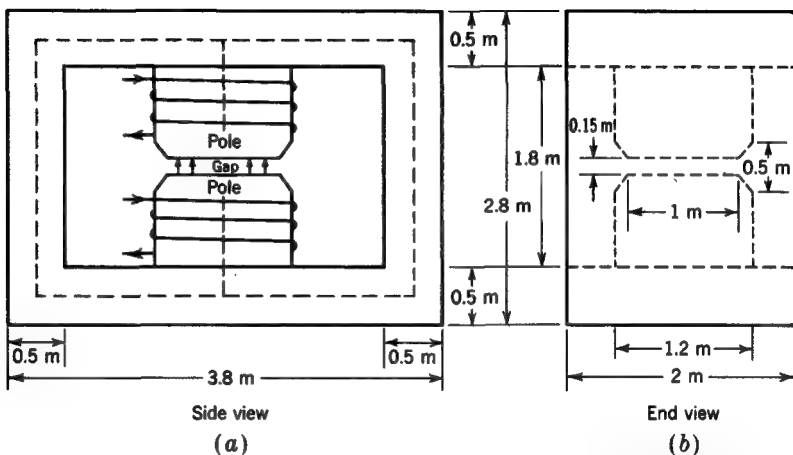


FIGURE P6-29
Cyclotron magnet.

6-26 A ring has a cross-sectional area of 200 mm^2 and a mean path length of 350 mm. Two-thirds of the length of the ring is composed of ferrite ($\mu_r = 1,000$) and the remaining one-third of mild steel ($\mu_r = 2,000$). Find the total magnetic flux in the ring if it is wound with a coil of 750 turns carrying 100 mA. Consider that the two butt joints between the ferrite and steel sections are equivalent to an air gap of $100 \mu\text{m}$.

* 6-27 Find the reluctance and permeance between the ends of an iron bar having the dimensions (a) shown in Fig. 4-20 assuming $\mu_r = 3,000$, (b) shown in Fig. P4-4 assuming $\mu_r = 5,000$.

6-28 (a) How much greater is the reluctance of the block of Fig. 4-20 compared to a uniform rectangular block without the notches assuming the same μ_r in both cases? (b) How much greater is the reluctance of the block of Fig. P4-4 compared to a uniform rectangular block obtained by cutting the one in Fig. P4-4 along the diagonal at the bend, turning one half over, and joining both halves to form a gapless straight bar?

6-29 A cyclotron magnet has the dimensions shown in Fig. P6-29. The pole pieces are cylindrical with tapered ends. The diameter of the gap is 1 m, and the gap spacing is 150 mm. How many ampere-turns are required in each of the two windings shown to produce a flux density of 1 T in the air gap? Assume that the magnet is made of iron with $\mu_r = 2,000$ and that there is no fringing at the gap. Neglect leakage along the magnet structure. As a further simplification take the effective length of sections as the length measured along the centerline (dashed line in Fig. P6-29a). Take the diameter of the tapered section of the poles as the average diameter.

* 6-30 An electromagnet consists of a U-shaped iron yoke and iron bar, as shown in Fig. P6-30. A thin copper sheet on the top of the bar prevents iron-to-iron contact between

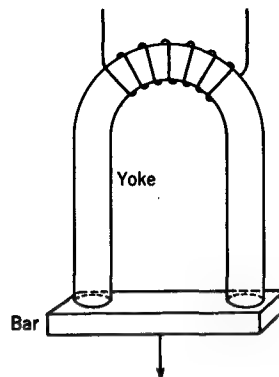


FIGURE P6-30
U-shaped electromagnet.

bar and yoke. If the magnetic flux through the circuit is 15 mWb and the yoke-bar contact area is 0.015 m^2 per pole, what is the weight which the yoke will support (including the weight of the bar)? Neglect fringing.

6-31 (a) If the contact area of the electromagnet of Prob. 6-30 is reduced to 0.005 m^2 by means of tapered sections on the yoke, what is the weight which the yoke will support? Assume that the total flux is the same as before and neglect fringing. (b) In practice what prevents the attractive force from increasing indefinitely as the contact area is reduced?

6-32 What is the contact pressure (a) in Prob. 6-30 and (b) in Prob. 6-31a?

* 6-33 An iron ring magnet of 0.02 m^2 cross-sectional area and 300 mm radius has a 1-mm air gap and a winding of 1,200 turns. If the current through the coil is 6 A, what is the force tending to close the gap? Take $\mu_r = 1,000$ for the iron and neglect fringing.

6-34 Show that the permeability of a permanent magnet with air gap can be expressed by $\mu = -\mu_0(\mathcal{P}_g/\mathcal{P})$, where μ_0 = permeability of air, \mathcal{P}_g = permeance of air gap, and \mathcal{P} = permeance of empty space occupied by the magnet.

6-35 A long conducting tube of negligible wall thickness carries a longitudinal current of uniform sheet density $K = I/2\pi R$, where I = total current and R = radius of tube. Find H (a) inside the tube ($r < R$), (b) at $r = R$, and (c) outside the tube ($r > R$). (d) What boundary relation is satisfied at $r = R$?

6-36 For many purposes the magnetic field of the earth at ionospheric heights or above may be regarded as if it were produced by a short magnetic dipole (or small current loop) situated at the center of the earth with $\mu = \mu_0$ everywhere (except within the dipole). If the horizontal component of \mathbf{B} at the earth's surface is $20 \mu\text{T}$ at a point where the dip angle of the field (angle from horizontal) is 72° , (a) find the magnetic moment required for the dipole (or loop) at the center of the earth. Take the earth's radius as 6.37 Mm. (b) Using this model, calculate B at a distance of 40 Mm above the earth's surface in the equatorial and polar directions.

7

LAPLACE'S AND POISSON'S EQUATIONS AND BOUNDARY-VALUE PROBLEMS

7-1 INTRODUCTION

In this chapter we shall consider a number of electrostatic field problems. In the first examples space is free of charge ($\rho = 0$), and we seek solutions to Laplace's equation† ($\nabla^2 V = 0$) which satisfy the boundary conditions. In a later example space charge is present, and a solution to Poisson's equation ($\nabla^2 V = -\rho/\epsilon$) is obtained. Because of the important part that boundary conditions play, these problems are often called *boundary-value problems*.

The solution of a boundary-value problem is usually facilitated if it is set up in a coordinate system in which the boundaries can be specified in a simple manner. For instance, a problem involving a rectangular object may be most readily handled with rectangular coordinates, a cylindrical object by cylindrical coordinates, an elliptical object by elliptical-hyperbolic coordinates, etc. The boundaries in many practical problems cannot be simply expressed in any coordinate system, and often in such cases resort must be made to other methods such as graphical, point-by-point, computer, or experimental methods. Thus, the field maps obtained in Secs. 3-22, 4-16, and 6-18 are all solutions of Laplace's equation.

† See Sec. 3-27.

7-2 SOLUTION OF LAPLACE'S EQUATION IN RECTANGULAR COORDINATES

In rectangular coordinates Laplace's equation ($\nabla^2 V = 0$) becomes

$$\frac{\partial^2 V}{\partial x^2} + \frac{\partial^2 V}{\partial y^2} + \frac{\partial^2 V}{\partial z^2} = 0 \quad (1)$$

Let us assume that V can be expressed as the product of three functions X , Y , and Z , or

$$V = XYZ \quad (2)$$

where X = function of x only

Y = function of y only

Z = function of z only

Substituting (2) into (1) we get

$$YZ \frac{d^2 X}{dx^2} + XZ \frac{d^2 Y}{dy^2} + XY \frac{d^2 Z}{dz^2} = 0 \quad (3)$$

Dividing by XYZ separates the variables, and so we have

$$\frac{1}{X} \frac{d^2 X}{dx^2} + \frac{1}{Y} \frac{d^2 Y}{dy^2} + \frac{1}{Z} \frac{d^2 Z}{dz^2} = 0 \quad (4)$$

Since the sum of the three terms on the left-hand side is a constant ($= 0$) and each variable is independent, each term must equal a constant. That is, we may write

$$\frac{1}{X} \frac{d^2 X}{dx^2} = a_1^2 \quad (5)$$

or $\frac{d^2 X}{dx^2} = a_1^2 X \quad (6)$

and similarly $\frac{d^2 Y}{dy^2} = a_2^2 Y \quad (7)$

and $\frac{d^2 Z}{dz^2} = a_3^2 Z \quad (8)$

where $a_1^2 + a_2^2 + a_3^2 = 0 \quad (9)$

The problem now is to find a solution for each of the three variables separately. Hence, the procedure we have been following is often referred to as the *method of separation of variables*.

A solution of (6) is

$$X = C_1 e^{a_1 x} + C_2 e^{-a_1 x} \quad (10)$$

where C_1 and C_2 are arbitrary constants that must be evaluated from the boundary conditions. Either term in (10) is a solution, or the sum is a solution, as may be verified by substituting the solution in (6).

It follows that a general solution of (1) is

$$V = (C_1 e^{a_1 x} + C_2 e^{-a_1 x})(C_3 e^{a_2 y} + C_4 e^{-a_2 y})(C_5 e^{a_3 z} + C_6 e^{-a_3 z})$$

where C_1 , C_2 , etc., are constants. Thus, solutions may take the form of exponential, trigonometric, or hyperbolic functions.

7-3 EXAMPLE 1: THE PARALLEL-PLATE CAPACITOR

Consider a parallel-plate capacitor as shown in cross section in Fig. 7-1a. The plates are infinite in extent and are separated by a distance x_1 . The left-hand plate is at zero potential and the right-hand plate at potential V_1 . Let us apply Laplace's equation to find the potential distribution between the plates.

There is no variation in potential in the y and z directions, so that the problem is one-dimensional and Laplace's equation ($\nabla^2 V = 0$) reduces to

$$\frac{d^2 V}{dx^2} = 0$$

(1)

For the second derivative of V with respect to x to be zero the first derivative must be equal to a constant. Thus, we have

$$\frac{dV}{dx} = C_1 \quad (2)$$

or

$$dV = C_1 dx \quad (3)$$

Integrating (3), we write

$$\int dV = C_1 \int dx$$

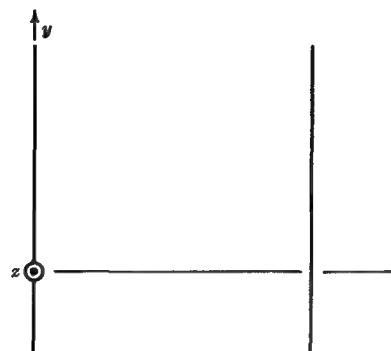
or

$$V = C_1 x + C_2 \quad (4)$$

The boundary conditions are

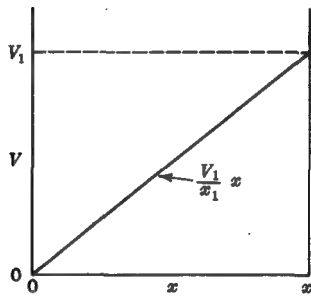
$$(1) \quad V = 0 \quad \text{at } x = 0$$

$$(2) \quad V = V_1 \quad \text{at } x = x_1$$



(a)

$$\begin{aligned}V &= 0 \\x &= 0 \\V &= V_1 \\x &= x_1\end{aligned}$$



(b)

FIGURE 7-1

(a) Parallel-plate capacitor and (b) potential variation.

From the first boundary condition (4) becomes

$$0 = 0 + C_2 \quad (5)$$

Hence, $C_2 = 0$. From the second boundary condition (4) becomes

$$V_1 = C_1 x_1 \quad (6)$$

so that

$$C_1 = \frac{V_1}{x_1} \quad (7)$$

Introducing the values for C_1 and C_2 from (7) and (5) into (4), we see that the solution for the potential between the capacitor plates is

$$V = \frac{V_1}{x_1} x \quad (\text{V}) \quad (8)$$

Thus, the variation of V between the plates is a linear function of x , as illustrated in Fig. 7-1b.

This result could have been anticipated since we would expect a uniform electric field \mathbf{E} between the plates with magnitude

$$E = \frac{V_1}{x_1} \quad (\text{V m}^{-1}) \quad (9)$$

with the potential at any point given by

$$V = Ex \quad (10)$$

The constant C_1 is thus equal to the electric field between the plates. Ordinarily we would not have resorted to Laplace's equation to solve this simple problem, but its application here serves to illustrate the procedures involved in applying Laplace's equation while using a minimum of mathematics.

7-4 UNIQUENESS

If a function V satisfies Laplace's equation ($\nabla^2 V = 0$) and the boundary conditions, it is a *unique solution*; i.e., it is the only possible solution. No other function will satisfy these requirements.[†]

Let us reexamine the solution (7-3-8) for the parallel-plate capacitor with respect to its uniqueness. It satisfies the boundary conditions, and it also satisfies Laplace's equation, as can be confirmed by substituting (7-3-8) into (7-3-1) and performing the indicated differentiation. The solution is $V_1 = C_1 x$, where $C_1 = V_1/x_1$. A function of the form $V = C_1 x + C_2$ will also satisfy Laplace's equation but will require different boundary conditions, that is, $V = C_2$ at $x = 0$ and $V = V_1 + C_2$ at $x = x_1$.

Let us try a function of the form $V = C_1 x^2$. This function can satisfy the same boundary conditions as $V = C_1 x$, but it does not satisfy Laplace's equation since substituting it in (7-3-1) gives a nonzero result ($d^2 V/dx^2 = 2C_1$). It is apparent that any

[†] A graphically obtained or computer-generated field map of a two-dimensional problem is likewise a unique solution.

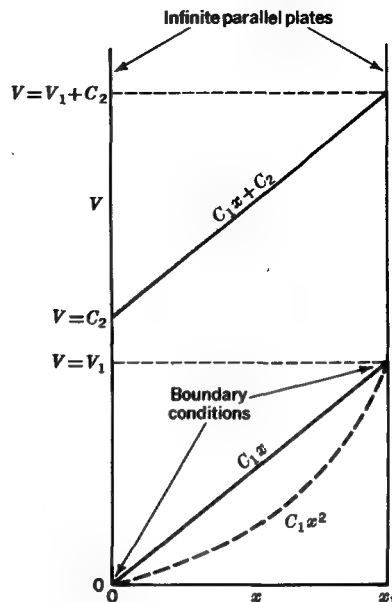


FIGURE 7-2

The potential variation C_1x satisfies Laplace's equation and the boundary conditions; $C_1x + C_2$ satisfies Laplace's equation but not the boundary conditions (unless $C_2 = 0$); while C_1x^2 satisfies the boundary conditions but not Laplace's equation.

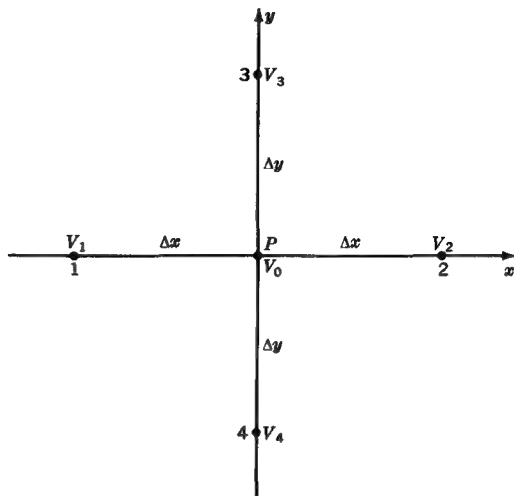
power of x other than unity will not be a solution. The various functions we have discussed are shown graphically in Fig. 7-2. Many different functions might be tried as solutions, but none except $V = (V_1/x_1)x$ satisfies Laplace's equation and the boundary conditions. *It is the unique solution.*

More elegant and rigorous proofs of uniqueness are available, but the above discussion illustrates the general approach, which involves a demonstration that solutions other than the unique one do not satisfy both Laplace's equation and the boundary conditions.

7-5 POINT-BY-POINT, OR ITERATIVE, METHOD

In this section a point-by-point method of solving Laplace's equation is discussed. The method is approximate, but by using sufficient points and by iteration, or repetitive application, the solution can be made as accurate as desired.†

† J. B. Scarborough, "Numerical Mathematical Analysis," 6th ed., pp. 391-422, Johns Hopkins Press, Baltimore, Md., 1966.

**FIGURE 7-3**

Construction to find potential at point P with respect to four surrounding points.

The basic step is to find a solution of Laplace's equation at a point by noting the slope of the second derivative of the potential V in orthogonal directions around the point. In rectangular coordinates Laplace's equation is given by

$$\frac{\partial^2 V}{\partial x^2} + \frac{\partial^2 V}{\partial y^2} + \frac{\partial^2 V}{\partial z^2} = 0 \quad (1)$$

If the potential variation is independent of z , the problem reduces to a two-dimensional one and (1) simplifies to

$$\frac{\partial^2 V}{\partial x^2} + \frac{\partial^2 V}{\partial y^2} = 0 \quad (2)$$

The first term in (2) is the second partial derivative of V with respect to x , that is, the rate of change of the rate of change of V with respect to x .† Similarly, the second term is the rate of change of the rate of change of V with respect to y . The sum of these two terms must be zero.

Consider a two-dimensional potential distribution around a point P , as in Fig. 7-3. Let the potential at P be equal to V_0 and at the four surrounding points be V_1 , V_2 , V_3 , and V_4 , as shown. Now $(V_2 - V_0)/\Delta x$ is the slope of V between points 2 and P . This is approximately equal to $\partial V/\partial x$ (becomes exact as $\Delta x \rightarrow 0$). Also $(V_0 - V_1)/\Delta x$ is the slope of V between points P and 1. The difference of these slopes

† Or since $\partial V/\partial x = -E$, $\partial^2 V/\partial x^2$ is equivalent to the negative of the rate of change of E with respect to x .

(per distance increment Δx) is approximately equal to $\partial^2 V / \partial x^2$. Hence, as discussed in the preceding paragraph, the significance of Laplace's equation is that the difference in slopes of V in the x direction and the difference of the slopes in the y direction must be equal and opposite in sign. Thus, we have

$$\frac{\partial(\partial V / \partial x)}{\partial x} = - \frac{\partial(\partial V / \partial y)}{\partial y} \quad (3)$$

or

$$\frac{[(V_2 - V_0)/\Delta x] - [(V_0 - V_1)/\Delta x]}{\Delta x} \approx - \frac{[(V_3 - V_0)/\Delta y] - [(V_0 - V_4)/\Delta y]}{\Delta y} \quad (4)$$

Letting $\Delta x = \Delta y$, we have

$$V_1 + V_2 + V_3 + V_4 - 4V_0 \approx 0 \quad (5)$$

and $V_0 \approx \frac{1}{4}(V_1 + V_2 + V_3 + V_4) \quad (6)$

If we know the potential at points 1, 2, 3, and 4, then according to Laplace's equation, the potential at the point P is as given by (6). In other words, the potential at P is the *average* of the potentials at the four neighboring points.[†]

7-6 EXAMPLE 2: THE INFINITE SQUARE TROUGH

To illustrate the point-by-point method consider the infinitely long square trough of sheet metal shown in cross section in Fig. 7-4a. The sides and bottom of the trough are at zero potential. A cover, separated by small gaps from the trough, is at a potential of 40 V. Let us use the point-by-point method to obtain the potential distribution. First, we find the potential at the center of the trough from (7-5-6) as

$$\frac{40 + 0 + 0 + 0}{4} = 10 \text{ V}$$

Next, we find the potential at the center of the four quadrants of the trough. For this we rotate the xy axes 45° and take the potential at the cover-trough gap as 20 V (average of 40 V and 0). Again from (7-5-6) we have

$$\frac{20 + 40 + 0 + 10}{4} = 17.5 \text{ V}$$

[†] In a three-dimensional problem we would use six surrounding points (four as shown in Fig. 7-3 plus one a distance Δz from P into the page and one a distance Δz from P out of the page; $\Delta z = \Delta x = \Delta y$) and the potential at P would be given by

$$V_0 = \frac{1}{6}(V_1 + V_2 + V_3 + V_4 + V_5 + V_6)$$

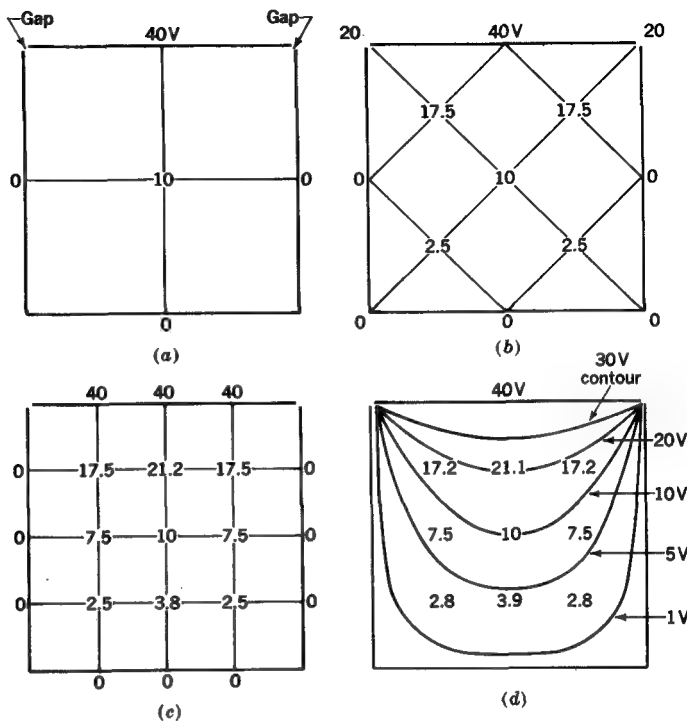


FIGURE 7-4

Application of point-by-point method to determine potential at nine points inside an infinite square trough.

for the upper and left and right quadrants, as in Fig. 7-4b, and

$$\frac{0 + 10 + 0 + 0}{4} = 2.5 \text{ V}$$

for the lower left and right quadrants. Next, we can find V at four more points, with voltages as shown in Fig. 7-4c (xy axes returned to usual orientation).

The procedure is now repeated starting at the upper left, obtaining

$$\frac{40 + 21.2 + 7.5 + 0}{4} = 17.2 \text{ V}$$

This new value of V is now used to recalculate the potential at the adjacent point to the right as

$$\frac{40 + 17.2 + 10 + 17.2}{4} = 21.1 \text{ V}$$

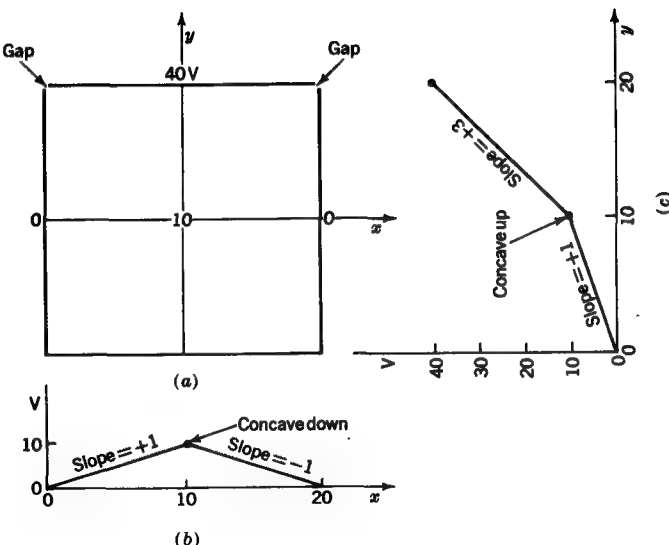


FIGURE 7-5

(a) Infinite square trough. (b) Slope or gradient of potential in x -direction. (c) Slope or gradient of potential in y -direction.

See Fig. 7-4d.[†] All points are recalculated in this way proceeding left to right and top to bottom over and over again until the values no longer change. This gives the most accurate solution to Laplace's equation we can get by this method with the number of points used. A still more accurate solution can be obtained by using a larger number of points (subdividing the area of the trough with a finer grid). As the distance between points (Δx or Δy) approaches zero, the solution can be made to approach an exact one. This method is well adapted for very accurate calculations using digital computers. However, manual calculations with relatively coarse grids can often provide solutions of sufficient accuracy for many purposes. Thus, a determination, as above, of the potential at nine points in this trough example is sufficient for drawing the potential contours as in Fig. 7-4d.

Referring to the first step (determination of V at the center of the trough), let us reexamine the problem. Using the center point and four neighboring points, as in Fig. 7-5a, we get the slopes of the potential in the x and y directions as shown in Fig. 7-5b and c. (We assume $\Delta x = \Delta y = 10$ units.) Thus, $\Delta V/\Delta x = 10/10 = \pm 1$, and

[†] In practice it is convenient to tabulate the voltage obtained in each iteration in column format at each grid point so that a running record is kept. When the voltages stabilize, the iteration can stop.

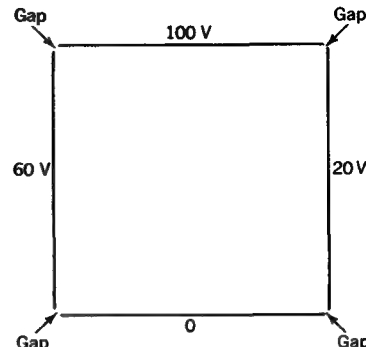


FIGURE 7-6
Infinite square trough with different potentials on each side.

$\Delta V / \Delta y = 10/10 = 1$ or $30/10 = 3$. Laplace's equation is satisfied since the difference of the slopes in the x direction equals the negative of the difference of the slopes in the y direction.[†] Thus,

$$+1 - (-1) = 2$$

and

$$+1 - (+3) = -2$$

We note in this problem that if the slope change is concave downward in one coordinate, it must be concave upward in the other coordinate (see Fig. 7-5b and c).

7-7 EXAMPLE 3: SQUARE TROUGH WITH DIFFERENT POTENTIAL ON EACH SIDE

Consider an infinitely long square trough of sheet metal as shown in cross section in Fig. 7-6. The four sides have small gaps between them, and they have individual potentials of 100, 60, 20, and 0 V, as indicated. Let us use the point-by-point method with a 9×9 grid of 81 points to obtain the potential distribution. There are 32 points on the four sides, where potentials are determined as part of the boundary conditions, and 49 ($= 7 \times 7$) points in the interior space, whose potentials must be determined by the point-by-point method. A manually obtained solution is shown in Fig. 7-7 with potential contours and field lines drawn in.

[†] Note that in the one-dimensional case the difference in slopes in one coordinate direction must be zero; that is, V must vary linearly with distance as in the parallel-plate-capacitor example (Sec. 7-3). In the three-dimensional case all one can say is that the *sum* of the slope differences in the three orthogonal coordinate directions must be zero.

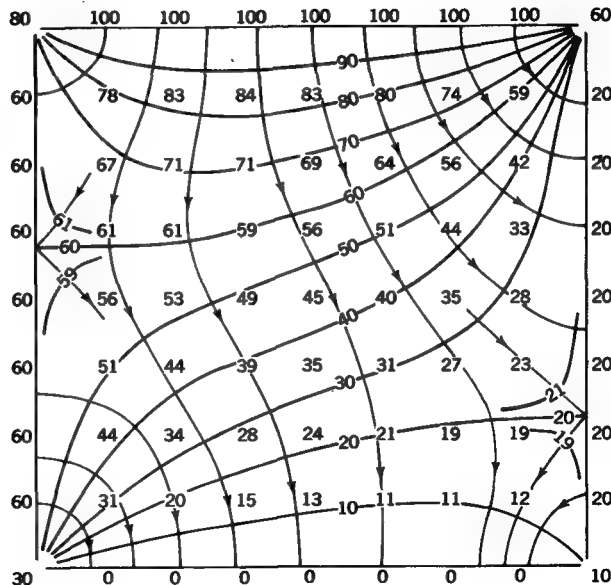


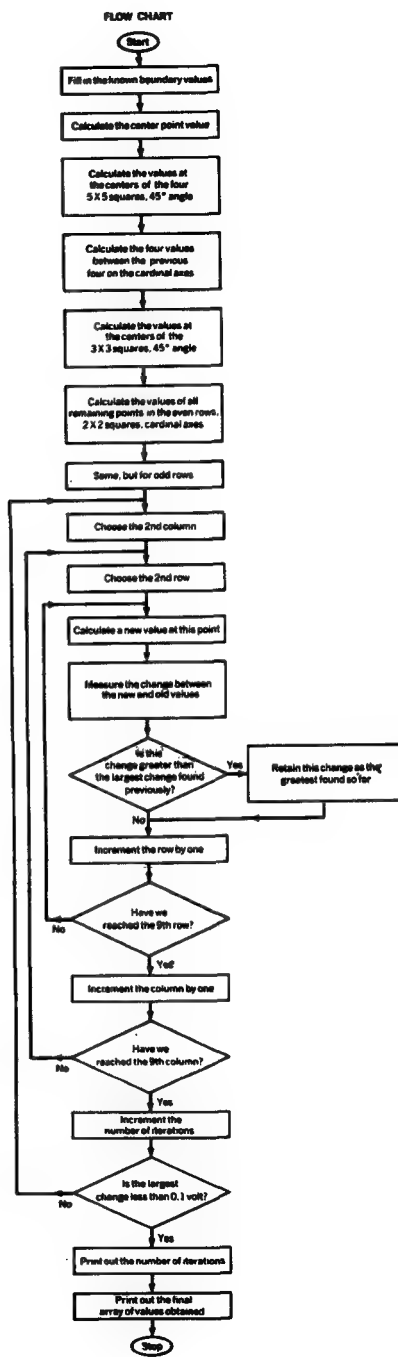
FIGURE 7-7

Solution of configuration of Fig. 7-6 using point-by-point method and 49 interior points. Potential contours (heavy) and field lines (light and with arrows) are also shown.

7-8 DIGITAL-COMPUTER SOLUTION

The method discussed in the preceding section is an iterative technique. For greater accuracy many more points and more iterations are required. The digital computer is ideally suited for making such computations. An algorithm can be developed for systematic computation of the averages involved in the relaxation method [see (7-5-6)]. Having developed a suitable algorithm, one constructs a flow chart, which is a map of the strategy to be pursued, and from the flow chart a series of program statements is written. This is the computer program. To demonstrate the method, a flow chart and a Fortran IV program† are given for the square trough with different potential on each side (Example 3). A grid of only 7×7 interior points is used (as in Fig. 7-7) in order to simplify plotting and to make a direct comparison with Fig. 7-7 possible.

[†] This flow chart and program were written by Dr. Robert S. Dixon, Ohio State University Radio Observatory.



Fortran IV Program

```

C PROGRAM TO CALCULATE ELECTRIC POTENTIAL BY THE ITERATION METHOD.
C COMMON Z(9,9)
C DIMENSION Z(9,9)
C THE DESIRED POINTS LIE ON A 9 X 9 SQUARE GRID IN THE FIRST QUADRANT.
C I.E. - Z(1,1) IS IN THE LOWER LEFT CORNER.
C DATA ITERAT/0/
C FILL IN THE KNOWN VALUES ON THE BOUNDARIES.
DO 1 J=2,8
Z(1,J)=60.
1 Z(9,J)=20.
DO 2 I=2,8
Z(I,1)=0.
2 Z(1,9)=100.
Z(1,1)=30.
Z(1,9)=80.
Z(9,9)=60.
Z(9,1)=10.
C CALCULATE THE CENTER VALUE, CASE 0, 9 X 9 SQUARE.
Z(5,5)=AVERAG(5,5,0,4)
C CALCULATE THE SURROUNDING POINTS, CASE 1, 5 X 5 SQUARES.
Z(3,7)=AVERAG(3,7,1,2)
Z(7,7)=AVERAG(7,7,1,2)
Z(7,3)=AVERAG(7,3,1,2)
Z(3,3)=AVERAG(3,3,1,2)
C CALCULATE 4 SURROUNDING POINTS, CASE 0, 3 X 3 SQUARES.
Z(3,5)=AVERAG(3,5,0,2)
Z(5,7)=AVERAG(5,7,0,2)
Z(7,5)=AVERAG(7,5,0,2)
Z(5,3)=AVERAG(5,3,0,2)
C NOW GO TO THE 3 X 3 SQUARES, CASE 1.
DO 3 IROW=2,8
DO 3 ICOL=2,8,2
3 Z(ICOL,IROW)=AVERAG(ICOL,IROW,1,1)
C NEXT THE IN-BETWEEN 2 X 2 SQUARES IN THE EVEN NUMBERED ROWS, CASE 0.
DO 4 IROW=2,8,2
DO 4 ICOL=3,7,2
4 Z(ICOL,IROW)=AVERAG(ICOL,IROW,0,1)
C THEN THE IN-BETWEEN 2 X 2 SQUARES IN THE ODD NUMBERED ROWS, CASE 0.
DO 5 IROW=3,7,2
DO 5 ICOL=2,8,2
5 Z(ICOL,IROW)=AVERAG(ICOL,IROW,0,1)
C AT THIS POINT, ALL POINTS HAVE BEEN GIVEN AN INITIAL VALUE.
C SO WE START ITERATING ALONG UNTIL THE VALUES STOP CHANGING.
C WE DO ONE COMPLETE ITERATION AT A TIME, THEN CHECK TO SEE IF THE LARGEST
C CHANGE IS LESS THAN 0.1 VOLT. CASE 0.
B DO 6 I=2,8
DO 6 J=2,8
6 Z(I,J)=AVERAG(I,J,0,1)
C MOVE THE NEW VALUES BACK TO THE ORIGINAL ARRAY, AND FIND THE LARGEST
C DIFFERENCE.
DIFF2=0.
DO 7 I=2,8
DO 7 J=2,8
7 DIFF1=Z(I,J)-Z(I,J)
IF(DIFF1.GT.DIFF2)DIFF2=DIFF1
Z(I,J)=Z(I,J)
C TEST FOR DIFFERENCE, REITERATE AS NECESSARY.
C KEEP COUNT OF THE NUMBER OF ITERATIONS.
ITERAT=ITERAT+1
IF(DIFF2.GT.0.1)GO TO 8
C WRITE OUT THE Z ARRAY AND THE NUMBER OF ITERATIONS.
WRITE(6,11)
WRITE(6,12)ITERAT
12 FORMAT(' SOLUTION OBTAINED AFTER ',I5,' ITERATIONS.',//)
11 FORMAT(1H1)
J=10
DO 10 K=1,9
J=J-1
10 WRITE(6,9) (Z(I,J),I=1,9)
9 FORMAT(1X,9(3X,F5.1)//)
C GO HOME.
CALL EXIT
STOP
END

C A FUNCTION TO COMPUTE THE AVERAGE OF FOUR POINTS, CENTERED AT
C SUBSCRIPT (I,J), SPACED "ISPACE" POINTS AWAY.
C IF ICASE=0, THE 4 POINTS ARE IN THE CARDINAL DIRECTIONS FROM THE
C CENTER.
C IF ICASE=1, THE 4 POINTS ARE IN THE 45 DEGREE DIRECTIONS FROM THE
C CENTER.
FUNCTION AVERAG(I,J,ICASE,ISPACE)
COMMON Z(9,9)
AVERAG=0.25*(Z(I-ISPACE,J-ICASE-ISPACE)
X +Z(I-ISPACE*ICASE,J+ISPACE)
X +Z(I+ISPACE,J+ISPACE*ICASE)
X +Z(I+ISPACE*ICASE,J-ISPACE))
RETURN
END

```

The computer-calculated voltages should be printed directly in a square 7×7 grid. The contours can be drawn manually or by an automatic computer-controlled plotter.

It is instructive to compare the times required using the manual and computer techniques. Thus, the manually constructed graph (as in Fig. 7-7) can be produced in an hour or two, although this time can be considerably reduced with the aid of a vest-pocket or desk-top micro- or minicomputer. The programmable digital computer will do the computations required in seconds, but automatic plotting may require minutes. However, many hours may be required to construct the flow chart and write the program statements, and it takes additional time before the program is ready to run on the computer. The advantages of the programmable computer is that once a program has been successfully executed, large numbers of similar problems (as for other boundary voltages in Fig. 7-7) can be solved very quickly. Furthermore, if more detail is desired for all or part of the map, this is readily obtained.

7-9 ANALOG-COMPUTER SOLUTION

In an analog computer the problem is simulated in analog form. Thus, in the solution of an electromagnetic field problem we can use the analogy between Laplace's equation and Kirchhoff's current law. Hence, to determine the potential V of the point P at the center of the trough of Example 2, we connect four resistors of resistance R as shown in Fig. 7-8a. According to Kirchhoff's current law at a point (Sec. 4-12), the sum of the currents at a junction is zero, or

$$I_1 + I_2 + I_3 + I_4 = 0 \quad (1)$$

From Ohm's law $I_1 = (V_1 - V)/R$, $I_2 = (V_2 - V)/R$, etc.; so we have

$$\frac{V_1 - V}{R} + \frac{V_2 - V}{R} + \frac{V_3 - V}{R} + \frac{V_4 - V}{R} = 0 \quad (2)$$

or

$$V_1 + V_2 + V_3 + V_4 - 4V = 0 \quad (3)$$

and

$$V = \frac{1}{4}(V_1 + V_2 + V_3 + V_4) \quad (4)$$

which is the same result we obtained by applying Laplace's equation. Hence, Kirchhoff's current law at a point and Laplace's equation must be equivalent. This is readily seen since Kirchhoff's current law from (4-13-1) can be expressed as

$$\nabla \cdot \mathbf{J} = 0 \quad (5)$$

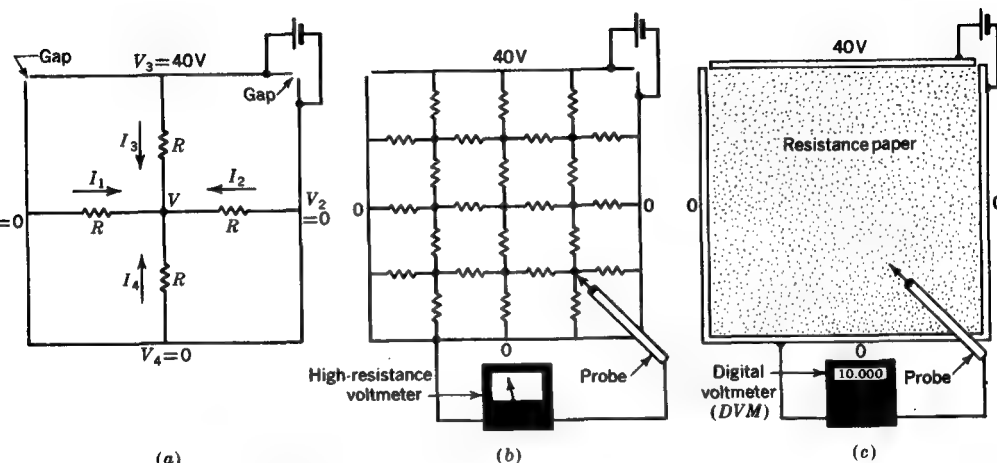


FIGURE 7-8

(a) Application of circuit analysis to determination of potential at center of infinite square trough. (b) Experimental measurement of potential at nine points inside trough and (c) at any point using resistance paper and digital voltmeter (DVM).

But $\mathbf{J} = \sigma \mathbf{E}$ and $\mathbf{E} = -\nabla V$, and so we have

$$\nabla \cdot \mathbf{J} = \sigma \nabla \cdot \mathbf{E} = \sigma \nabla^2 V = 0 \quad (6)$$

or

$$\nabla^2 V = 0 \quad (7)$$

which is Laplace's equation.

If the grid is made finer by using more resistors and junction points, the potential distribution can be determined more accurately. An experimental arrangement for doing this using a high-resistance voltmeter is shown in Fig. 7-8b. An even more practical and very accurate method is to use the equivalent of an infinite grid of points, namely, a sheet of uniform-resistance paper such as Teledeltos paper. The outline of the trough is drawn on the resistance paper with silver (conducting) paint, a battery connected as in Fig. 7-8c, and the potential contours traced out with a high-resistance voltmeter and probe as suggested.

To facilitate the measurements a digital voltmeter (DVM) can be employed. For example, with 40 V applied as in Fig. 7-8c and equipotential contours desired at 5-V intervals, the probe is moved until 5.000 appears on the readout, the point is marked, and then more points at this value are found, next progressing to 10.000 on the readout, etc.

We have discussed analytical, graphical, digital-computer, and analog-computer procedures for solving Laplace's equation. Each method has its advantages and disadvantages. In solving a particular problem one should consider all facets of the various techniques and then select the one best suited for the particular problem.

7-10 EXAMPLE 4: CONDUCTING SHEET BETWEEN TWO CONDUCTING PLANES

Referring to Fig. 7-9, two infinite parallel conducting plates are spaced a distance a . An infinitely long conducting strip is placed between the plates and normal to them, as shown in the figure.

The width of the strip is only very slightly less than the spacing between the plates. The strip is insulated from the plates. Let the two plates be connected together and a constant potential V be applied between the plates and the conducting strip. The medium between the plates is air. Suppose that the plates are at zero potential and that the strip is at a positive potential of 1 V ($V = 1\text{V}$). The problem is to find the potential distribution in the region M between the plates to the right of the strip, as indicated in the cross section of Fig. 7-9b.†

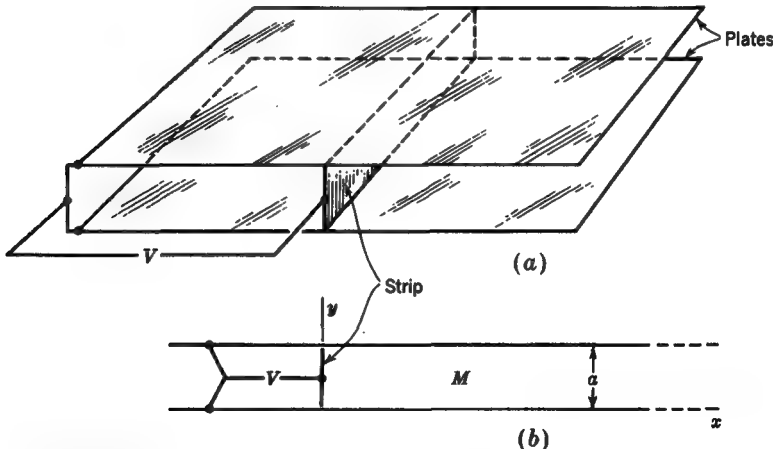


FIGURE 7-9

Infinite conducting strip between two infinite parallel conducting plates (a) in perspective view and (b) in cross section.

† This problem is similar to that for the square trough of Example 2 (Sec. 7-6) except that here the trough is not closed at the bottom (sides infinitely long). Also in the present problem the trough has been turned on its side.

It is possible to find the potential distribution by solving Laplace's equation ($\nabla^2 V = 0$) subject to the boundary conditions. It is most convenient to handle this problem in rectangular coordinates, the relation of the conductor boundaries to the coordinate axes being as in Fig. 7-10a. Expanding Laplace's equation in the two rectangular coordinates of the problem (x and y), we have

$$\frac{\partial^2 V}{\partial x^2} + \frac{\partial^2 V}{\partial y^2} = 0 \quad (1)$$

This differential equation is the most general way of expressing the variation of potential with respect to x and y . It is a partial differential equation of the second order and first degree. However, this equation does not tell us anything about the particular potential distribution in the problem. For this we must obtain a solution of the differential equation which is appropriate to the boundary conditions of the problem. These *boundary conditions* are

$$(1) \quad V = 0 \quad \text{at } \begin{cases} y = 0 \\ 0 \leq x \leq \infty \end{cases}$$

$$(2) \quad V = 0 \quad \text{at } \begin{cases} y = a \\ 0 \leq x \leq \infty \end{cases}$$

$$(3) \quad V = 1 \quad \text{at } \begin{cases} x = 0 \\ 0 \leq y \leq a \end{cases}$$

$$(4) \quad V = 0 \quad \text{at } \begin{cases} x = \infty \\ 0 \leq y \leq a \end{cases}$$

Proceeding now to find a solution of (1) by the method of separation of variables, let us assume that a solution for V can be expressed as

$$V = XY \quad (2)$$

where X = function of x alone

Y = function of y alone

Substituting (2) into (1) and dividing by XY , we have

$$\frac{1}{X} \frac{d^2 X}{dx^2} + \frac{1}{Y} \frac{d^2 Y}{dy^2} = 0 \quad (3)$$

In (3) the variables are separated. Since X and Y are independent and the sum of the two terms is a constant (zero), each term alone must equal a constant. Thus, we can write

$$\frac{1}{X} \frac{d^2 X}{dx^2} = k^2 \quad (4)$$

$$\text{and} \quad \frac{1}{Y} \frac{d^2 Y}{dy^2} = -k^2 \quad (5)$$

where k equals a constant and $k^2 - k^2 = 0$.

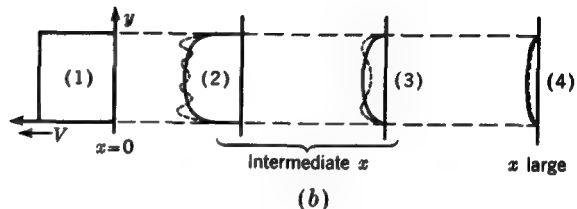
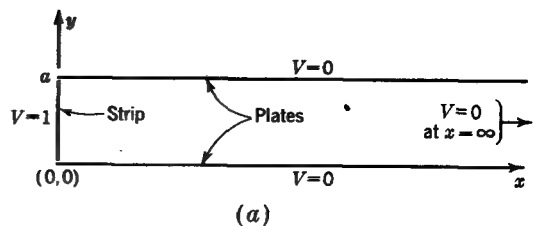


FIGURE 7-10

(a) Boundary conditions for potential-distribution problem of Fig. 7-9. (b) Potential variation between plates as obtained from solution of Laplace's equation at different distances (x) from the strip.

These equations may be rearranged to the form

$$\frac{d^2 X}{dx^2} - k^2 X = 0 \quad (6)$$

and

$$\frac{d^2 Y}{dy^2} + k^2 Y = 0 \quad (7)$$

Thus, the second-order partial differential equation of (1) has been reduced to two second-order ordinary differential equations, each involving but one variable. These equations, (6) and (7), have the solutions

$$X = C_1 e^{kx} + C_2 e^{-kx} \quad (8)$$

and

$$Y = C_3 e^{jky} + C_4 e^{-jky} \quad (9)$$

One may readily confirm that these are solutions by substituting them into (6) and (7), in each case obtaining an identity. Introducing (8) and (9) into (2) yields the general solution

$$V = C_1 C_3 e^{kx} e^{jky} + C_2 C_3 e^{-kx} e^{jky} + C_1 C_4 e^{kx} e^{-jky} + C_2 C_4 e^{-kx} e^{-jky} \quad (10)$$

which reduces to

$$V = C'_1 e^{k(x \pm jy)} + C'_2 e^{-k(x \pm jy)} \quad (11)$$

where $C'_1 = C_1 C_3$ or $C_1 C_4$ and $C'_2 = C_2 C_3$ or $C_2 C_4$, depending on which sign is chosen in $x \pm jy$.

Because of boundary condition (4) ($V = 0$ at $x = \infty$), $C'_1 = 0$, so that only the second term of (11) applies in our problem.† Also, using de Moivre's theorem, (11) then becomes

$$V = C'_2 e^{-kx} (\cos ky \pm j \sin ky) \quad (12)$$

To satisfy boundary condition (1) ($V = 0$ at $y = 0$) we should retain only the imaginary part of (12). That is,

$$V = C'_2 e^{-kx} \sin ky \quad (13)$$

This is a particular solution of Laplace's equation appropriate to our problem. It indicates that the potential V falls off exponentially with x and also that it varies as a sine function of y . To satisfy boundary condition (2) ($V = 0$ at $y = a$) requires that

$$k = \frac{n\pi}{a} \quad (14)$$

where n is a positive integer (1, 2, 3, ...). Introducing (14) into (13) yields

$$V = C'_2 e^{-n\pi x/a} \sin \frac{n\pi y}{a} \quad (15)$$

All the boundary conditions are now satisfied except for condition (3) ($V = 1$ at $x = 0$), that is, $V = 1$ at $x = 0$ for all values of y between 0 and a . Obviously (15) does not satisfy this requirement, and hence a more general solution is required. A more general solution can be obtained by taking the sum of expressions like (15) for different integral values of n . We then have

$$V = C_1 e^{-\pi x/a} \sin \frac{\pi y}{a} + C_2 e^{-2\pi x/a} \sin \frac{2\pi y}{a} + C_3 e^{-3\pi x/a} \sin \frac{3\pi y}{a} + \dots \quad (16)$$

where C_1 , C_2 , etc., are new constants.

Equation (16) can be expressed more concisely by

$$V = \sum_{n=1}^{\infty} C_n e^{-n\pi x/a} \sin \frac{n\pi y}{a} \quad (17)$$

† If we were interested in the potential distribution to the left instead of to the right of the strip (Fig. 7-9), the boundary condition is $V = 0$ at $x = -\infty$ so that $C'_2 = 0$.

The solution for V given by (16) or (17) is still incomplete since the coefficients C_1, C_2 , etc., are not evaluated. To find their values we impose boundary condition (3) ($V = 1$ at $x = 0$), so that (16) reduces to

$$1 = C_1 \sin \frac{\pi y}{a} + C_2 \sin \frac{2\pi y}{a} + C_3 \sin \frac{3\pi y}{a} + \dots \quad (18)$$

Now by the Fourier sine expansion,

$$f(by) = a_1 \sin by + a_2 \sin 2by + a_3 \sin 3by + \dots + a_n \sin nby \quad (19)$$

where

$$a_n = \frac{2}{\pi} \int_0^{\pi} f(by) \sin nby \, d(by)$$

It follows that for $f(by) = 1$

$$a_n = \begin{cases} \frac{4}{n\pi} & \text{for } n \text{ odd} \\ 0 & \text{for } n \text{ even} \end{cases}$$

Therefore, for $f(by) = 1$, (19) reduces to

$$1 = \frac{4}{\pi} (\sin by + \frac{1}{3} \sin 3by + \frac{1}{5} \sin 5by + \dots) \quad (20)$$

Comparing (20) with (18), it follows that

$$C_1 = \frac{4}{\pi}, C_2 = 0, C_3 = \frac{4}{3\pi}, C_4 = 0, C_5 = \frac{4}{5\pi}, \text{etc.} \quad \text{and} \quad b = \frac{\pi}{a}$$

Introducing these constants into (16), we have

$$V = \frac{4}{\pi} e^{-\pi x/a} \sin \frac{\pi y}{a} + \frac{4}{3\pi} e^{-3\pi x/a} \sin \frac{3\pi y}{a} + \frac{4}{5\pi} e^{-5\pi x/a} \sin \frac{5\pi y}{a} + \dots \quad (21)$$

This is the complete solution of Laplace's equation for the potential V appropriate to the boundary conditions of the problem. It gives the potential V as a function of position between the plates and to the right of the strip (Fig. 7-9).

Although an infinite number of terms is required for an exact representation of the potential distribution as a function of x and y , an approximate solution of practical value can be obtained with a finite number of terms. Each term attenuates at a different rate. Since the higher terms fall off more rapidly with x , only a few terms are

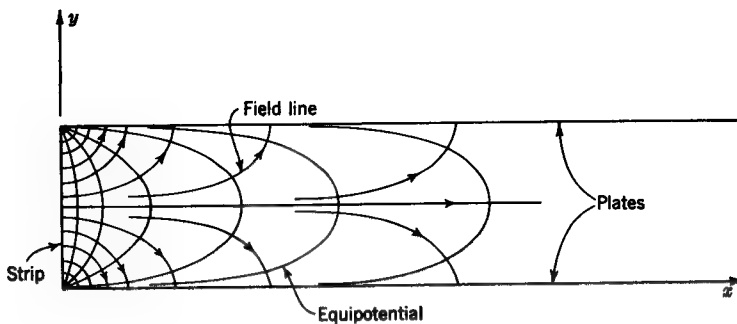


FIGURE 7-11
Electric field lines (with arrows) and equipotentials in space between conducting plates.

needed to give a good approximation except where x is small. That is, convergence is rapid at large x . Thus, when x is very large, the distribution is nearly equal to $\sin(\pi y/a)$, since the contribution of the harmonics higher than the first may be neglected. At $x = 0$, $V = 1$ for all values of y between 0 and a . The variation of V as a function of y at $x = 0$ and at a large value of x is shown at (1) and (4) in Fig. 7-10b. The distributions at two intermediate values of x are presented at (2) and (3). The actual distribution is shown by the solid curves, the dashed curves giving the approximate distribution as obtained by four terms ($n = 1, 3, 5, 7$) of the series at (2) and by two terms ($n = 1$ and 3) at (3). It is apparent that as x decreases, the effect of the higher terms becomes more important.

The potential distribution can also be presented by means of equipotential contours with orthogonal field lines, as suggested in Fig. 7-11. It is apparent that graphical, digital-computer, and analog-computer methods could have been used instead of the above analytical method to obtain an engineering solution for the potential distribution.

7-11 SOLUTION OF LAPLACE'S EQUATION IN CYLINDRICAL AND SPHERICAL COORDINATES

Laplace's equation in cylindrical coordinates (r, ϕ, z) (see Fig. A-1 and inside back cover) is

$$\frac{\partial^2 V}{\partial r^2} + \frac{1}{r} \frac{\partial V}{\partial r} + \frac{1}{r^2} \frac{\partial^2 V}{\partial \phi^2} + \frac{\partial^2 V}{\partial z^2} = 0 \quad (1)$$

Using the method of separation of variables (as illustrated in Sec. 7-2 for rectangular coordinates) a solution is

$$V = V_0(C_1 e^{kz} + C_2 e^{-kz})(C_3 \cos n\phi + C_4 \sin n\phi)[C_5 J_n(kr) + C_6 N_n(kr)] \quad (2)$$

where n = integer, dimensionless

$J_n(kr)$ = Bessel function of first kind and of order n , with argument kr , dimensionless

$N_n(kr)$ = Bessel function of second kind and of order n (also called a Neumann function), with argument kr , dimensionless

k = constant, m^{-1}

V_0 = constant, V

C_1, C_2 , etc. = constants, dimensionless

Laplace's equation in spherical coordinates (r, θ, ϕ) (see Fig. A-1 and inside back cover) is

$$\frac{\partial^2 V}{\partial r^2} + \frac{1}{r^2} \frac{\partial^2 V}{\partial \theta^2} + \frac{1}{r^2 \sin^2 \theta} \frac{\partial^2 V}{\partial \phi^2} + \frac{2}{r} \frac{\partial V}{\partial r} + \frac{\cot \theta}{r^2} \frac{\partial V}{\partial \theta} = 0 \quad (3)$$

Using the method of separation of variables, we find that a solution is

$$V = V_0(C_1 r^n + C_2 r^{-(n+1)})(C_3 \cos m\phi + C_4 \sin m\phi)[C_5 P_n^m(\cos \theta) + C_6 Q_n^m(\cos \theta)] \quad (4)$$

where n, m = integers, dimensionless

$P_n^m(\cos \theta)$ = associated Legendre function (solid zonal harmonic) of the first kind, dimensionless

$Q_n^m(\cos \theta)$ = associated Legendre function (solid zonal harmonic) of the second kind, dimensionless

C_1, C_2 , etc. = constants, dimensionless

V_0 = constant, V

The numerical calculations involved in solutions like (2) and (4) are conveniently carried out with a digital computer especially if subroutines are stored for needed functions such as $J_n(kr)$ or $P_n^m(\cos \theta)$.

7-12 EXAMPLE 5: COAXIAL LINE

Consider the section of coaxial transmission line shown in Fig. 7-12a. One end (at the origin) is short-circuited, and the other end is open. The radius of the inner conductor is a , and the inside radius of the outer conductor is b . The conductivity of the inner

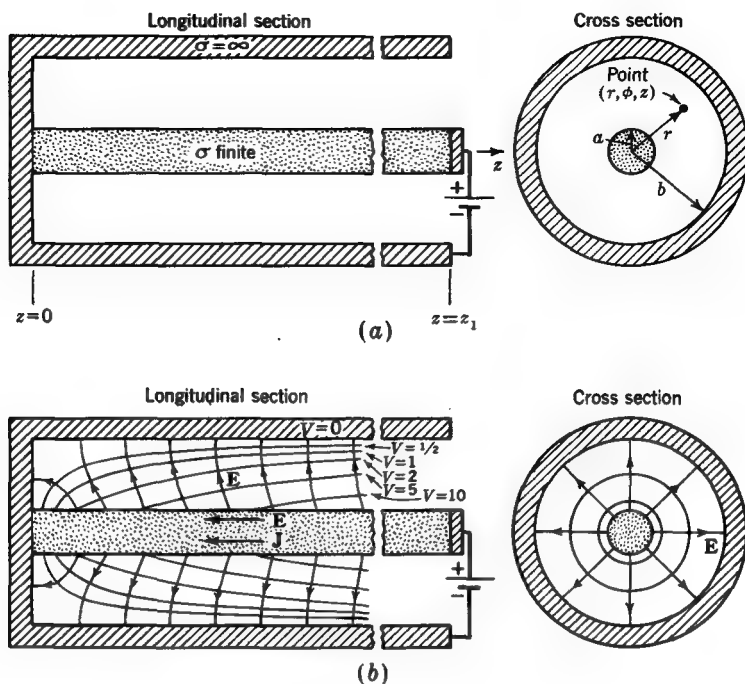


FIGURE 7-12
 (a) Section of coaxial transmission line. (b) Field distribution showing field lines (with arrows) and equipotentials.

conductor is finite, but the conductivity of the outer conductor and of the short-circuiting disk is assumed to be infinite. A constant voltage V_1 is applied between the inner and outer conductor at the open end of the line. The length z_1 of the line is long compared with its radius ($z_1 \gg b$). The problem is to find the potential V everywhere inside the line, except near the open end.

The *boundary conditions* for this problem are

$$(1) \quad V = 0 \quad \text{at } z = 0 \\ \text{at } a \leq r \leq b$$

$$(2) \quad V = 0 \quad \text{at } r = b \\ \text{at } 0 \leq z \leq z_1$$

$$(3) \quad V = V_1 \quad \text{at } z = z_1 \\ \text{at } r = a$$

There is also the condition that at any distance z from the origin the electric field inside the inner conductor and also along its surface ($r = a$) is given by

$$\frac{\partial V}{\partial z} = \frac{V_1}{z_1} \quad (1)$$

from which we have on integration that

$$V = \frac{V_1}{z_1} z \quad (2)$$

At $z = z_1$, (2) reduces to the third boundary condition above.

We wish to find a solution of Laplace's equation ($\nabla^2 V = 0$) that satisfies the boundary conditions. By symmetry V is independent of ϕ ; so expanding Laplace's equation in the other two cylindrical coordinates of the problem (r and z), we have†

$$\frac{\partial^2 V}{\partial r^2} + \frac{1}{r} \frac{\partial V}{\partial r} + \frac{\partial^2 V}{\partial z^2} = 0 \quad (3)$$

Using the method of separation of variables, let

$$\frac{V}{V_0} = RZ \quad (4)$$

where R = function only of r

Z = function only of z

V_0 = constant, V

Introducing (4) into (3) and dividing by RZ yields

$$\frac{1}{R} \frac{d^2 R}{dr^2} + \frac{1}{rR} \frac{dR}{dr} + \frac{1}{Z} \frac{d^2 Z}{dz^2} = 0 \quad (5)$$

The last term is a function only of z . Thus we can write

$$\frac{d^2 Z}{dz^2} = a_z^2 Z \quad (6)$$

where a_z = a constant. From (1) it follows that since V_1/z_1 is a constant the second derivative in (6) must be zero and hence a_z must be zero. A solution of (6) for $a_z = 0$ is

$$Z = C_1 z + C_2 \quad (7)$$

† Although V is dependent only on r and z , this problem is not two-dimensional in the sense that the problem of Example 5 is two-dimensional. Here the potential distribution for a longitudinal plane through the axis differs from the distribution for all planes parallel to it.

The last term of (5) may now be set equal to zero, so that the equation reduces to

$$r \frac{d^2 R}{dr^2} + \frac{dR}{dr} = 0 \quad (8)$$

A solution is

$$R = C_3 \ln r + C_4 \quad (9)$$

Introducing (9) for R and (7) for Z in (4) gives the solution for the potential

$$\frac{V}{V_0} = (C_1 z + C_2)(C_3 \ln r + C_4) \quad (10)$$

or $\frac{V}{V_0} = C_5 z \ln r + C_6 z + C_7 \ln r + C_8 \quad (11)$

where C_5 , C_6 , etc., are new constants. To evaluate these constants, we introduce the boundary conditions. When condition (1) ($V = 0$ at $z = 0$) is introduced, (11) becomes

$$0 = C_7 \ln r + C_8 \quad (12)$$

For (12) to be satisfied for all values of r requires that $C_7 = C_8 = 0$. Thus our solution reduces to

$$\frac{V}{V_0} = C_5 z \ln r + C_6 z \quad (13)$$

Introducing now boundary condition (2) ($V = 0$ at $r = b$), we have

$$0 = C_5 z \ln b + C_6 z \quad (14)$$

From boundary condition (3) ($V = V_1$ at $z = z_1$ and $r = a$) we get

$$\frac{V_1}{V_0} = C_5 z_1 \ln a + C_6 z_1 \quad (15)$$

From (14) and (15) we find that

$$C_5 = \frac{V_1}{V_0 z_1 \ln(a/b)} \quad \text{and} \quad C_6 = -\frac{V_1 \ln b}{V_0 z_1 \ln(a/b)}$$

When the values for these constants are introduced into (13) the complete solution for the problem is

$$V = V_1 \frac{z}{z_1} \frac{\ln(b/r)}{\ln(b/a)} \quad (16)$$

This solution satisfies Laplace's equation and the boundary conditions and hence must represent the potential distribution at all points between the inner and outer

conductors ($a \leq r \leq b$) except near the open end. This potential distribution is portrayed in Fig. 7-12b, the relative potential being indicated for the equipotential lines. Electric field lines (with arrows) are also shown, being normal to the equipotentials.

It is interesting to note in Fig. 7-12b that although the field lines are normal to the perfectly conducting surfaces (outer conductor and short-circuiting disk), they are not normal to the finitely conducting inner conductor. The current and field direction in the inner conductor is to the left ($-z$ direction). Comparison of Fig. 7-12b should be made with Figs. 4-15 and 4-17. In Figs. 4-15 and 4-17 both inner and outer conductors are assumed to have finite conductivity.

7-13 POISSON'S EQUATION

In the preceding sections, the volume charge density ρ was assumed to be zero. We now consider Poisson's equation (see Sec. 3-27), which applies to problems involving space charge ($\rho \neq 0$). Poisson's equation is

$$\boxed{\nabla^2 V = -\frac{\rho}{\epsilon}} \quad (1)$$

where V = potential, V

ρ = volume free-charge density, $C m^{-3}$

ϵ = permittivity of medium, $F m^{-1}$

Poisson's equation is a second-order inhomogeneous differential equation which applies at a point. From the theory of differential equations, it must have a solution of the following form:

$$V = \text{particular solution} + \text{complementary solution}$$

The particular solution must satisfy the inhomogeneous equation (1) whereas the complementary solution (which contains two linearly independent solution terms) must satisfy the homogeneous equation, i.e., Laplace's equation. In the first five examples of this chapter the volume charge density was zero, and the solution of Laplace's equation was the complementary solution. In Example 6 of Sec. 7-14, the volume charge density is not zero, and a particular solution is found.

In rectangular coordinates, (1) becomes

$$\boxed{\frac{\partial^2 V}{\partial x^2} + \frac{\partial^2 V}{\partial y^2} + \frac{\partial^2 V}{\partial z^2} = -\frac{\rho}{\epsilon}} \quad (2)$$

If V is independent of y and z , (2) becomes

$$\frac{d^2V}{dx^2} = -\frac{\rho}{\epsilon} \quad (3)$$

7-14 EXAMPLE 6: PARALLEL-PLATE CAPACITOR WITH SPACE CHARGE†

Consider the parallel-plate capacitor shown in Fig. 7-13a with potential difference V_1 applied between the plates as indicated. If the left-hand plate is coated with suitable material and both plates enclosed in a glass envelope and evacuated, an electron current passes between the plates when the left-hand plate is heated. This arrangement is called a *diode* or *two-element vacuum tube*. The left-hand plate or emitter is the *cathode*, and the right-hand plate or collector is the *anode*. Let us solve for the potential variation between the plates subject to the applied boundary conditions. Since there is electric charge between the plates, we must use Poisson's equation.

Let the cathode be held at potential $V = 0$ and a positive voltage $V = V_1$ be applied to the anode. When the cathode is heated, electrons are emitted, so that there is a volume charge density $\rho(x)$ between the plates.

From (7-13-3), Poisson's equation for this case is

$$\frac{d^2V}{dx^2} = -\frac{\rho}{\epsilon_0}$$

(1)

The solution to this differential equation must satisfy the two *boundary conditions*

$$(1) \quad V = 0 \quad \text{at } x = 0$$

$$(2) \quad V = V_1 \quad \text{at } x = x_1$$

In addition it is assumed that emitted electrons experience a repulsive force from other electrons already between the plates and are barely able to escape from the cathode (initial velocity zero). The result of this space-charge limitation is that the electric field $E (=dV/dx)$ is zero at $x = 0$. This can be expressed as a third *boundary condition*

$$(3) \quad E = -\frac{dV}{dx} = 0 \quad \text{at } x = 0$$

† K. R. Spangenberg, "Vacuum Tubes," p. 170, McGraw-Hill Book Company, New York, 1948.

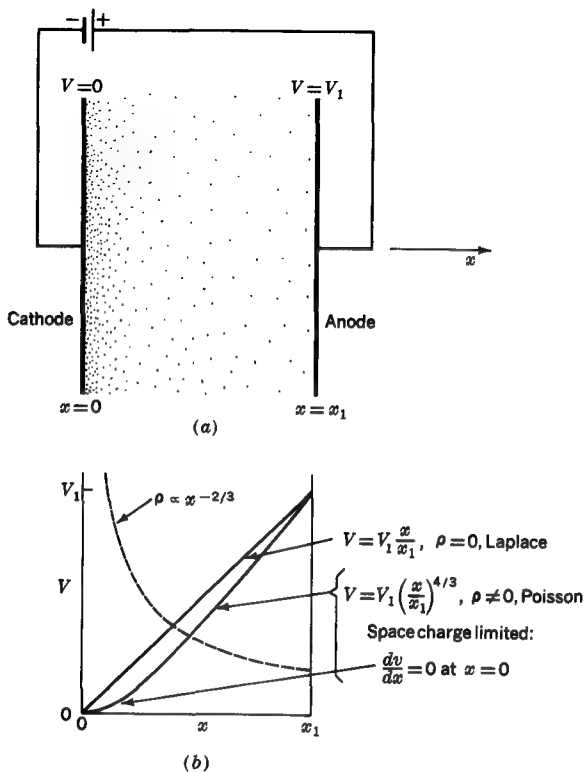


FIGURE 7-13
(a) Parallel-plate diode with space charge. (b) Potential and charge distribution.

As discussed in Chap. 15, we can equate the kinetic energy of an electron to the energy it acquires from the field, i.e.,

$$\frac{1}{2}mv^2 = eV \quad (2)$$

where m and e are the mass and charge of the electron, respectively (see Table 15-1). It is assumed in (2) that the initial velocity of the electron is zero.

The electrons in motion constitute a steady current of density

$$J = \rho v \quad (\text{A m}^{-2}) \quad (3)$$

Solving for v from (2) and substituting into (3) gives

$$\rho = J \sqrt{\frac{m}{2eV}} \quad (4)$$

Substituting (4) into Poisson's equation (1) yields

$$\frac{d^2V}{dx^2} = \frac{J}{\epsilon_0} \sqrt{\frac{m}{2eV}} \quad (5)$$

Multiplying by $2dV/dx$ and integrating, we have

$$\left(\frac{dV}{dx}\right)^2 = \frac{4J}{\epsilon_0} \sqrt{\frac{m}{2eV}} + C_1 \quad (6)$$

where C_1 is a constant. Applying the boundary conditions (1) and (3), we get

$$0 = 0 + C_1 \quad (7)$$

Hence, $C_1 = 0$. Integrating again gives

$$\frac{4}{3}V^{3/4} = 2 \sqrt{\frac{J}{\epsilon_0}} \sqrt{\frac{m}{2e}} x + C_2 \quad (8)$$

where C_2 is a constant. From the boundary condition (1)

$$0 = 0 + C_2 \quad (9)$$

Hence, $C_2 = 0$. Solving for V from (8) we have†

$$V = \left(\frac{3}{2} \sqrt{\frac{J}{\epsilon_0}} \sqrt{\frac{m}{2e}} \right)^{4/3} x^{4/3} \quad (10)$$

From boundary condition (2) this becomes

$$V_1 = \left(\frac{3}{2} \sqrt{\frac{J}{\epsilon_0}} \sqrt{\frac{m}{2e}} \right)^{4/3} x_1^{4/3} \quad (11)$$

Dividing (10) by (11) yields

$$V = V_1 \left(\frac{x}{x_1} \right)^{4/3}$$

(12)

which is the unique solution to Poisson's equation satisfying the three boundary conditions. This variation of V between the plates is shown by the lower solid curve in Fig. 7-13b. Note that the slope dV/dx is zero at $x = 0$ as a result of the space-charge limitation [boundary condition (3)]. For comparison the upper solid (straight) line gives the potential variation in the absence of space charge (solution of Laplace's

† Equation (10) is the particular solution to Poisson's equation. The complementary solution is zero for this problem.

equation, see Fig. 7-1). The difference between solutions is in the exponent for the ratio x/x_1 , which is unity for the solution to Laplace's equation and $4/3$ for the solution to Poisson's equation. Solving (11) for J gives

$$J = \frac{4}{9} \epsilon_0 \sqrt{\frac{2e}{m}} \frac{1}{x_1^{3/2}} V_1^{3/2} \quad (13)$$

This three-halves power-voltage relation for the diode current is the *Child-Langmuir space-charge law*.† Substituting (10) into (4), we can solve for the charge-density variation, obtaining

$$\rho \propto x^{-2/3} \quad (14)$$

This variation is as suggested by the dashed curve in Fig. 7-13b. (See Prob. 7-43 for a semiconductor junction example.)

7-15 THE THEORY OF IMAGES

Consider an arbitrary distribution of charge in space, with a known equipotential surface such as the $V = 10$ V surface of the dipole shown in Fig. 7-14a (same as Fig. 2-13). Confining our attention to the volume v bounded by the $V = 10$ surface, it follows by superposition that the potential V inside v is a result of charges both interior to and exterior to the volume. If we now remove the charge exterior to v , V inside will remain unchanged if an equivalent surface charge distribution is placed on the surface, as suggested in Fig. 7-14b. In effect, the lower charge of the dipole ($-Q$) has been spread over the $V = 10$ contour surface.

It follows that the converse of this argument holds. If we start out with some known potential at any point in a volume v bounded by a charged surface, that potential can also be produced by an equivalent charge distribution exterior to v , the charge distribution on the surface now being removed. The charges exterior to v are called *image charges*, as previously discussed in Sec. 3-21. The examples of the following sections illustrate the theory of images.

In Fig. 7-14 the $-Q$ charge is the image of the $+Q$ charge with respect to the $V = 10$ surface, or for that matter to any of the equivalent potential surfaces. Thus, for example, if the $V = 0$ surface is chosen, we have the case of a charge over a flat plane. A charged cylindrical conductor over a flat plane is discussed in the next section.

† D. C. Child, Discharge from Hot CaO, *Phys. Rev.*, 32: 492–511 (May 1911); I. Langmuir, The Effect of Space Charge and Residual Gases on Thermionic Currents in High Vacuums, *Phys. Rev.*, (2) 2: 450–486 (December 1913).

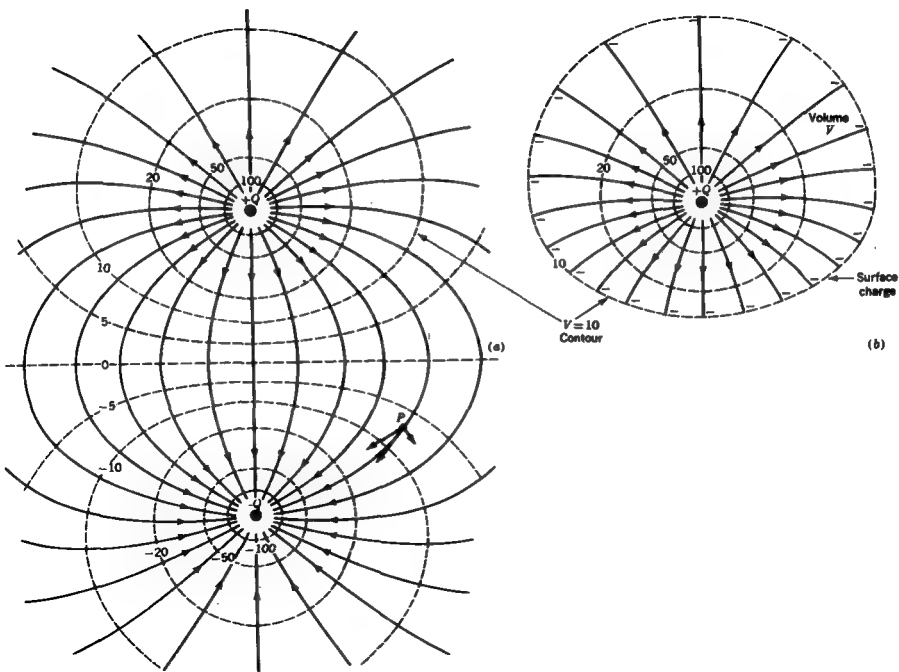


FIGURE 7-14

(a) Field and potential distribution of an electric dipole. (b) Distribution inside $V = 10$ contour remains unchanged when an equivalent surface charge is placed on the contour and the lower charge of the dipole is removed. Field inside contour is same as in (a), but field outside is zero.

7-16 EXAMPLE 7: CHARGED CYLINDRICAL CONDUCTOR OVER AN INFINITE METALLIC GROUND PLANE

Consider a long thin uniformly charged cylindrical conductor at a distance s from an infinite metallic ground plane, as in Fig. 7-15a. From the theory of images this configuration is equivalent to the upper half of Fig. 7-15b, where we have two identical parallel conductors of opposite charge separated by a distance $2s$.

It is instructive to examine first the two-conductor system. The behavior of the electric field of these two conductors can be found by superimposing the electric fields due to either conductor alone. This procedure gives the electric field as the vector superposition of the two components. (An alternative method, discussed in Sec. 2-13, is to find the scalar electrostatic potential V as the scalar superposition of

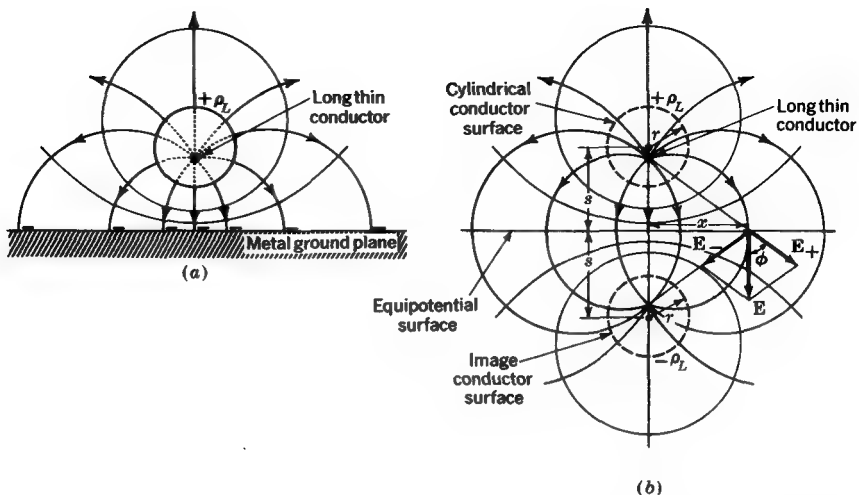


FIGURE 7-15

(a) Field of conductor over a ground plane. (b) Field of two oppositely charged conductors. Field above flat equipotential surface is same as in (a).

the potential due to each conductor alone. Then the electric field is found as the negative gradient of V .) The electric field lines due to either conductor alone would point radially outward from the conductor. Thus, on the equipotential surface equidistant from the two conductors, a simple graphical addition at any point shows that the resultant electric field is directed downward, as suggested in Fig. 7-15b. Thus, since E is orthogonal to the surface, it must be an equipotential surface.[†]

According to the previously developed image theory, the fields above the surface will remain unchanged if we remove the lower conductor and place a surface charge distribution on the surface. This surface charge is

$$\rho_s = D_n = -\epsilon_0 E_n \quad (1)$$

Consider first the case where both conductors are thin lines of charge. The electric field from the positively charged conductor is E_+ , and the electric field from the negatively charged conductor is E_- . If each line charge is now replaced by a cylindrical conductor of radius r , positioned so that its surface (shown dashed in

[†] Therefore, without formally solving for all equipotential surfaces, we already know from symmetry considerations where one such surface is.

Fig. 7-15b) coincides with an equipotential surface, the field outside the cylindrical conductors will be undisturbed. From (3-16-1) and Fig. 3-15,

$$|\mathbf{E}_+| = \frac{\rho_L}{2\pi\epsilon_0\sqrt{s^2 + x^2}} = |\mathbf{E}_-| \quad (2)$$

As shown in Fig. 7-15b, the normal component of the electric field can be found from superposition as

$$E_n = 2 \cos \phi |\mathbf{E}_+| = 2 \cos \phi \frac{\rho_L}{2\pi\epsilon_0\sqrt{s^2 + x^2}} \quad (3)$$

But since $\cos \phi = s/\sqrt{s^2 + x^2}$, (3) becomes

$$E_n = \frac{\rho_L}{\pi\epsilon_0} \frac{s}{s^2 + x^2} \quad (4)$$

Thus, substituting (4) into (1) gives

$$\rho_s = - \frac{\rho_L}{\pi} \frac{s}{s^2 + x^2} \quad (\text{C m}^{-2}) \quad (5)$$

Equation (5) indicates that the equivalent surface density of charge on the equipotential surface is strongest at the point of closest approach to the upper conductor, that is, at $x = 0$.

If we now imagine that a large, thin, perfectly conducting flat plane is slipped in along the equipotential surface, the field lines will be undisturbed since they are already normal to this metallic sheet, thus satisfying the boundary conditions. Since the field lines have not been disturbed, it follows from the preceding discussion that a charge distribution according to (5) will be set up on this conducting ground plane. Thus, the field above the ground plane is identical to the field of the conductor and its image without the ground plane.

7-17 EXAMPLE 8: CURRENT-CARRYING CONDUCTOR OVER INFINITE METALLIC GROUND PLANE

Up to this point, the discussion of images has been limited to distributions of static charges. Consider now a filamentary conductor in air carrying a current I parallel to, and at a height s above, a metallic ground plane, as shown in Fig. 7-16a. By convention, the current I flowing to the right is identified with the motion of positive charges to the right, the charges having a velocity v , that is,

$$I = \rho_L v \quad (\text{A}) \quad (1)$$

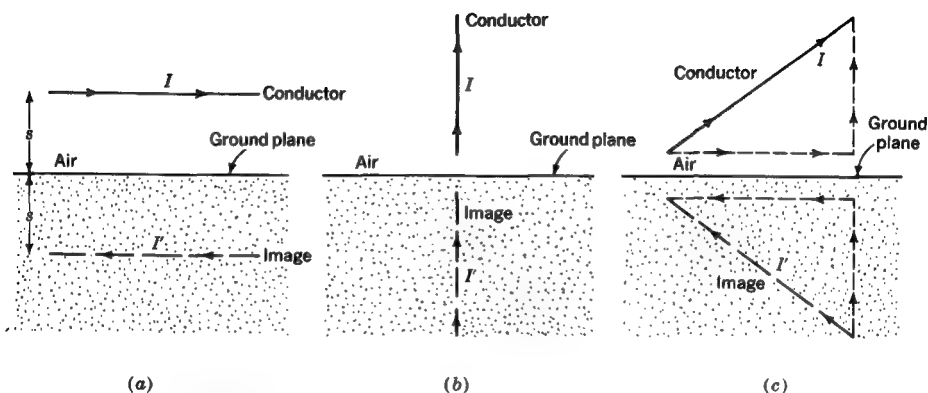


FIGURE 7-16

Image of a horizontal, vertical, and slant current-carrying conductor over a ground plane.

where ρ_L is the charge per unit length of conductor. The motion of *positive* charge to the right is imaged by the motion of *negative* charge to the right. This is equivalent to the motion of positive charge to the left. Hence, the current I will have an image current I' below the ground plane, equal in magnitude but flowing in the opposite direction, as suggested in Fig. 7-16a, i.e.,

$$I' = -\rho_L v = -I \quad (\text{A}) \quad (2)$$

Next consider a filamentary conductor carrying a current I perpendicular to a metallic ground plane, as shown in Fig. 7-16b. Using similar reasoning, it can be seen that this filamentary conductor has a vertical image conductor carrying current in the same same direction, as shown. The image of a conductor making an arbitrary angle with a metallic ground plane can be found by resolving it into vertical and horizontal components, as shown in Fig. 7-16c.

PROBLEMS

- * 7-1 A strip transmission line is shown in cross section in Fig. P7-1. It consists of a strip conductor supported by a medium of $\mu_r = 1$ and $\epsilon_r = 100$ on a large flat conductor or ground plane. If 10 V is applied between the conductors, find (a) the electric field E , (b) the electric flux density D , and (c) the capacitance per unit length C/l (use geometry). (d) Draw a curvilinear square field map (neglect fringing) and (e) use a count of the series and parallel squares of the map in (d) for comparison with (c). Give units for all results.

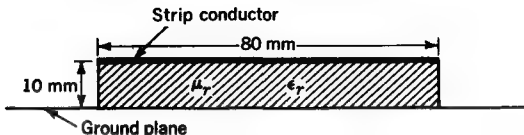


FIGURE P7-1
Strip transmission line.

- * 7-2 A cylindrical coaxial transmission line is shown in cross section in Fig. P7-2. The medium filling the line is air. If 10 V is applied between the conductors and the total current is 10 mA, find (a) electric field E at P_1 and P_2 , (b) electric flux density D at P_1 and P_2 , (c) magnetic flux density B at P_1 and P_2 , (d) magnetic field H at P_1 and P_2 , (e) exact capacitance per unit length, C/l , (f) exact inductance per unit length L/l , (g) total electric flux per unit length Q/l , and (h) total magnetic flux per unit length ψ_m/l . (i) Draw a curvilinear square map (both V and E lines) with equipotential contours at 2, 4, 6, and 8 V, and (j) use a count of the series and parallel squares of the map of (i) for comparison with the exact capacitance and inductance values of (e) and (f). Give units for all results.

7-3 An elliptical coaxial transmission line is shown in cross section in Fig. P7-3. The medium filling the line has $\mu_r = 50$ and $\epsilon_r = 60$. If 2 V is applied between conductors and the total current is 5 mA, find (a) E , D , B , and H at points P_1 , P_2 , P_3 , and P_4 (16 values), (b) capacitance per unit length C/l and inductance per unit length L/l , and (c) total electric and magnetic flux per unit length (Q/l and ψ_m/l). Give units for all results. (d) Draw a curvilinear square field map. The field map may be obtained by graphical or experimental (Teledeltos paper) methods and the answers to the other parts deduced from the map. Or an exact solution may be obtained, in which case a count of the series and parallel squares on the map should be made for comparison.

- * 7-4 A transmission line consists of a square trough with insulated cover, as shown in cross section in Fig. P7-4. The sides and bottom of the trough are 100 mm, and the cover

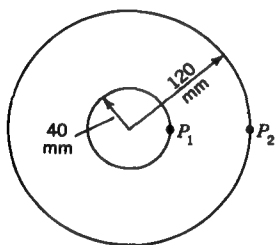


FIGURE P7-2
Cylindrical coaxial transmission line.

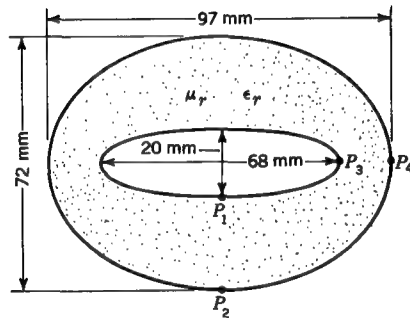


FIGURE P7-3
Elliptical coaxial transmission line.

* Answers to starred problems are given in Appendix C.

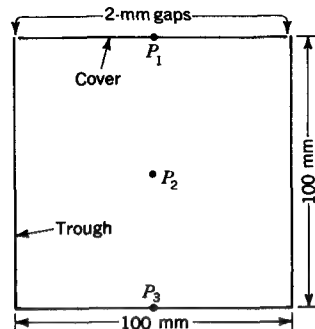


FIGURE P7-4
Square-trough transmission line.

is separated by 2-mm gaps from the trough. The sides and bottom of the trough are at zero potential, and the cover is at 10 V. The total current is 1 A. (a) If the medium is air, find E , D , B , and H at points P_1 , P_2 , and P_3 along the center line of the trough (point P_2 is at the center of the trough). (b) Draw a curvilinear square map with equipotential contours at 1-V intervals. (c) What is the capacitance per unit length?

7-5 Show that if $\Delta x \neq \Delta y$ in Fig. 7-3 the potential V_0 at the center point is given by

$$V_0 = \frac{V_1}{2 \left[1 + \left(\frac{\Delta x}{\Delta y} \right)^2 \right]} + \frac{V_2}{2 \left[1 + \left(\frac{\Delta x}{\Delta y} \right)^2 \right]} + \frac{V_3}{2 \left[1 + \left(\frac{\Delta y}{\Delta x} \right)^2 \right]} + \frac{V_4}{2 \left[1 + \left(\frac{\Delta y}{\Delta x} \right)^2 \right]}$$

7-6 Show that if all length values in Fig. 7-3 are unequal the potential V_0 at 0 (point P) in Fig. 7-3 is given by

$$V_0 = \frac{V_1}{(1+a)\left(1+\frac{b}{c}\right)} + \frac{V_2}{(1+a^{-1})\left(1+\frac{b}{c}\right)} + \frac{V_3}{(1+c)\left(1+\frac{d}{b}\right)} + \frac{V_4}{(1+c^{-1})\left(1+\frac{d}{b}\right)}$$

where $a = \Delta x_1 / \Delta x_2$

$b = \Delta x_1 / \Delta x_2$

$c = \Delta y_3 / \Delta y_4$

$d = \Delta y_3 / \Delta y_4$

Δx_1 = distance from point P at 0 to 1

Δx_2 = distance 0 to 2

Δy_3 = distance 0 to 3 and so forth

7-7 A long rectangular metal trough with insulated cover is shown in cross section in Fig. P7-7. The trough is at zero potential, and the cover is at potential V . Show that the potential at any point (x, y) inside is given by

$$V = \sum_{n \text{ odd}} \frac{4V_1 \sin \frac{n\pi}{x_1} x \sinh \frac{n\pi}{x_1} y}{n\pi \sinh \frac{n\pi y_1}{x_1}}$$

7-8 If the dimensions of the rectangular trough of Prob. 7-7 are $x_1 = 160$ mm, $y_1 = 240$ mm, with 4-mm gaps between the cover and sides of the trough, and the lid potential is 40 V, determine the potential distribution inside by means of (a) point-by-point manual method with 4×6 mesh, (b) point-by-point method using a digital computer with 20×30 mesh (or larger number), (c) resistance (Teledeltos) paper method, and (d) exact analytical solution. (e) Compare the four methods, in particular at points 20, 40, 60, 80, and 100 mm along a bisector from a lower corner, as indicated in Fig. P7-7. Discuss accuracy and reasons for differences. (f) Draw the equipotential contours for $V = 1.25, 2.5, 5, 10, 15, 20, 25, 30$, and 35 V based on one or more of the four methods. (g) Complete the map of (f) by drawing in E lines so as to form curvilinear squares.

7-9 A long triangular trough with insulated cover is shown in cross section in Fig. P7-9. All sides are equal. The trough is at zero potential, and the cover is at 8 V. (a) Determine the potential distribution inside by any of the methods mentioned in Prob. 7-8. (b) Draw a curvilinear square map with equipotential contours at 1-V intervals.

7-10 A long half-cylindrical trough with insulated cover is shown in cross section in Fig. P7-10. The trough is at zero potential, and the cover is at 8 V. (a) Determine the potential distribution inside by any of the methods mentioned in Prob. 7-8. (b) Draw a curvilinear square map with equipotential contours at 1-V intervals.

* 7-11 (a) What sheet-current distribution on the surface of a sphere will provide a uniform magnetic field inside? $\mu = \mu_0$ everywhere. (b) How should the turns of a winding be arranged on the sphere to produce this result?

* 7-12 A steady electric surface current given by $K = \phi k_0 \sin \theta$ exists on the surface of a sphere of radius R . k_0 is a constant, and $\mu = \mu_0$ everywhere. The magnetic flux density set up by the current is given by $B = 2C_1$ for $r < R$ and $B = (C_2/r^3)(2 - k^3 \cos \theta)$ for $r > R$. Find C_1 and C_2 .

7-13 A long thin linear conductor carrying a current I extends along the plane boundary between two media, air and iron. Assuming that the permeability of the iron is uniform, show that the magnetic field H in air at a radius r from the conductor is $H_0 = \mu I/[(\mu + \mu_0)\pi r]$ while in the iron at a radius r from the conductor it is given by $H_i = \mu_0 I/[(\mu + \mu_0)\pi r]$.

7-14 A long square trough is shown in cross section in Fig. P7-14. The sides and top and bottom are separated by small gaps. The sides are at zero potential, and the top is at 40 V. Determine the potential distribution inside and draw a curvilinear square map if the bottom is (a) at 40 V, (b) -40 V, and (c) 20 V. Any of the methods mentioned in Prob. 7-8 may be used. Compare with Fig. 7-7.

7-15 A conducting rectangular trough with electrode is shown in cross section in Fig. P7-15. If the trough is at zero potential, find the required shape of the electrode at potential V_1 such that the potential in the trough below the electrode is of the form $V = C \sin kx \sinh ky$. Reduce the equation for the electrode to its simplest form and construct an accurate graph of the trough and electrode for the case $x_1 = y_1$.

* 7-16 (a) Find the potential distribution between two infinite metal cones as shown in cutaway view in Fig. P7-16. The potential of the outer cone is zero and of the inner cone is V_1 . The half-angle of the inner cone is θ_i and of the outer cone is θ_o . (b) Find the

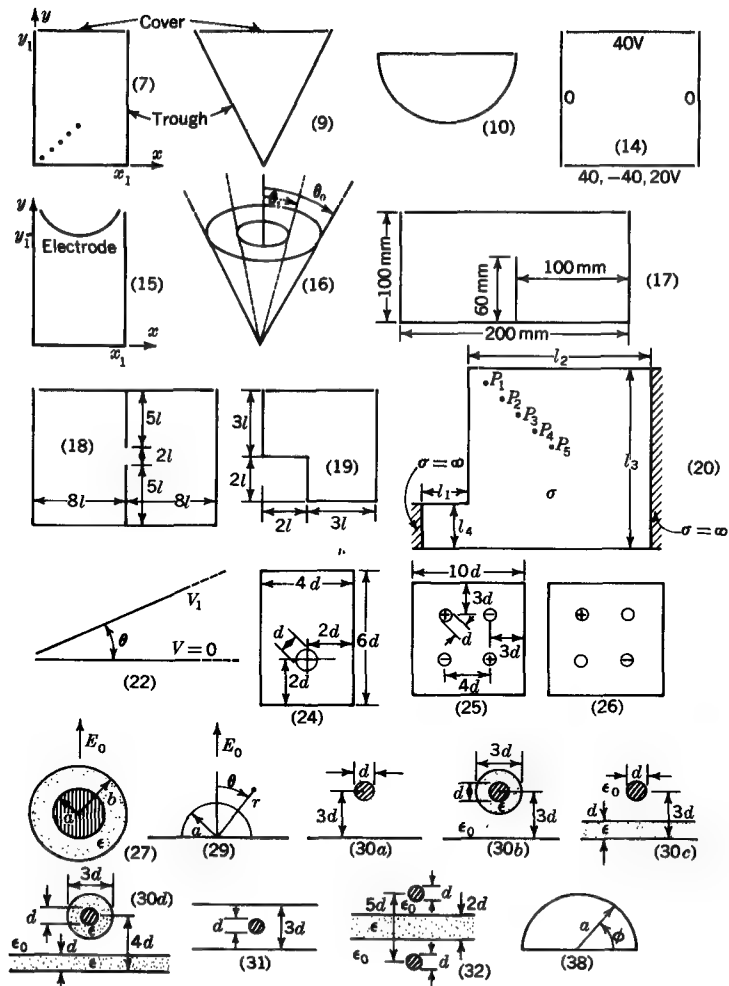


FIGURE P7-7 to P7-38

The problem to which each sketch relates is indicated by the number in parentheses.

potential distribution between a single cone at potential V_1 and a flat metal sheet at zero potential. This is a special case of (a) for which the outer cone half-angle $\theta_0 = 90^\circ$.

7-17 A long metal trough with insulated cover is shown in cross section in Fig. P7-17. The trough has a central partition. The trough and partition are at zero potential, and the cover is at 8 V. (a) Determine the potential distribution inside. Any of the methods mentioned in Prob. 7-8 may be used. (b) Draw a curvilinear square map with equipotential contours at 1-V intervals.

7-18 Repeat Prob. 7-17 for the long metal trough with partition and insulated cover and fin shown in cross section in Fig. P7-18.

7-19 Repeat Prob. 7-17 for the irregular trough with insulated cover shown in cross section in Fig. P7-19.

7-20 A rectangular conducting block of thickness $t = 25$ mm has left and right sides butted against media of perfect conductivity ($\sigma = \infty$), as indicated in Fig. P7-20. The dimensions are $l_1 = 20$ mm, $l_2 = 80$ mm, $l_3 = 80$ mm, and $l_4 = 20$ mm. If the block conductivity $\sigma = 10 \Omega^{-1} m^{-1}$, find (a) the resistance of the block and (b) the current density J at the points P_1, P_2, P_3, P_4 , and P_5 at 10-mm intervals along the bisector of the corner if 100 mV is applied between the ends of the block.

7-21 Repeat Prob. 7-20 for the case where $l_1 = 60$ mm and $l_2 = 240$ mm. If the total current is the same, find J at the five points (P_1, P_2 , etc.) and compare with values in Prob. 7-20.

★ 7-22 Determine the potential distribution V between two infinite flat metal sheets meeting at an angle θ , as shown in cross section in Fig. P7-22. The left edges of the sheets are separated by an infinitesimal gap. The lower sheet is at zero potential, and the upper sheet is at potential V_1 .

★ 7-23 A metal sphere of radius r_1 and charge Q is enclosed by a dielectric shell of relative permittivity ϵ_r , inner radius r_2 ($r_2 > r_1$), and outer radius r_3 . If the medium elsewhere is air, find the potential distribution as a function of radius r .

7-24 A coaxial transmission line consists of a rectangular outer conductor and a cylindrical inner conductor, as shown in cross section in Fig. P7-24. If the potential difference between conductors is 8 V, (a) determine the potential distribution inside and (b) draw a curvilinear square map with equipotential contours at 1-V intervals. Any of the methods mentioned in Prob. 7-8 may be used. The medium is air.

7-25 A transmission line consists of four cylindrical conductors, two at a potential of +8 V and two at a potential of -8 V, enclosed in a grounded conductor of square cross section, as shown in Fig. P7-25. (a) Determine the potential distribution and (b) draw a curvilinear square map with equipotential contours at 1-V intervals. The medium is air.

7-26 Repeat Prob. 7-25 for the case where two of the conductors are at zero potential (grounded) while the other two are at +8 and -8 V, as suggested in Fig. P7-26.

★ 7-27 A conducting wire of radius a is situated in air in an originally uniform field E_0 perpendicular to the wire. The wire has an insulating coating of radius b and permittivity ϵ , as shown in Fig. P7-27. Find the potential V_0 everywhere outside the insulating coating and the potential V_1 everywhere inside the insulating coating.

7-28 The electric field is uniform and equal to E_0 and is normal to one side of an infinite plane conducting sheet. The field is zero on the other side. If a slot of width s is cut in the sheet, show that the surface charge density on the E_0 side is

$$\rho_s = \frac{\epsilon_0 E_0}{2} \left\{ 1 + \frac{u}{[u^2 - (s/2)^2]^{1/2}} \right\}$$

and on the side where the field was originally zero is given by

$$\rho_s = \frac{\epsilon_0 E_0}{2} \left\{ 1 - \frac{u}{[u^2 - (s/2)^2]^{1/2}} \right\}$$

where u is the distance from the center of the slot.

- * 7-29 A conducting hemisphere of radius a is placed on a flat conducting sheet of infinite extent, as shown in Fig. P7-29. Before the hemisphere was introduced, the electric field everywhere above the sheet was normal to it and equal to E_0 . The medium is air, and the sheet and hemisphere are at zero potential. (a) Find V as a function of r and θ everywhere above the sheet and hemisphere. (b) Find the surface charge density at all points on the sheet and hemisphere. (c) Plot a graph of the surface charge density on the hemisphere and along the flat sheet to a distance of $5a$.

7-30 Determine the potential distribution and draw a curvilinear square map for a transmission line consisting of (a) cylindrical conductor of diameter d placed $3d$ above an infinite metal ground plane as in Fig. P7-30a, (b) insulated cylindrical conductor, as in Fig. P7-30b, (c) cylindrical conductor above a metal ground plane with dielectric slab, as in Fig. P7-30c, and (d) insulated cylindrical conductor above metal sheet with dielectric slab, as in Fig. P7-30d.

7-31 Determine the potential distribution and draw a curvilinear square map for a transmission line consisting of a cylindrical inner conductor situated midway between two grounded infinite metal sheets, as in Fig. P7-31.

7-32 Determine the potential distribution and draw a curvilinear square map for a transmission line consisting of two cylindrical conductors with an infinite dielectric slab of permittivity ϵ midway between them, as in Fig. P7-32.

7-33 A long cylindrical wire of radius a is situated at a distance d from its center to two flat conducting sheets of infinite extent which intersect to form a square corner. The wire runs parallel to the corner. If the sheets are grounded and the wire is at a potential V_1 , (a) find the potential V everywhere in the corner. (b) Draw a curvilinear square map for the case where $d = 10a$. (c) Find the surface charge density ρ_s along the sheets for the situation in (b) and plot a graph of ρ_s to a distance of $5d$ from the corner.

- * 7-34. A thin conducting spherical shell of radius r_1 is cut into two hemispheres separated by a very small air gap. If one hemisphere is at a potential V_1 and the other at a potential V_2 , find the potential everywhere (a) outside the sphere and (b) inside the sphere.

- * 7-35 A slot of width s is cut in an infinite horizontal flat conducting sheet. Before the slot was cut, the electric field above the sheet was everywhere vertical and equal to E_0 , while below the sheet the field was zero. At what distance below the center of the slot is the potential V equal to (a) $0.1E_0 s$, (b) $0.01E_0 s$, and (c) $0.001E_0 s$?

7-36 A transmission line consists of two thin conducting strips 100 mm wide and separated by 20 mm. The medium is air. (a) Use a conformal transformation to find the exact potential and field distribution in and around the transmission line and draw a curvilinear square map. (b) Use an experimental (Teledeltos paper) method to obtain a curvilinear square map. For this make the strips 1 or 2 mm thick. [In part (a) zero thickness is assumed.] (c) Compare results and discuss reasons for differences.

7-37 The electric field E in the uniform field region between the horizontal plates of a large parallel-plate air capacitor is 10 kV m^{-1} . Find E at a point in the fringing field halfway between the plates and at a horizontal distance from the edges of the plates of (a) d , (b) $10d$, and (c) $100d$, where d is the plate spacing. Assume that the plates have zero thickness.

7-38 A half-cylindrical metal tube of radius a , shown in cross section in Fig. P7-38, is at zero potential. If a metal plate at a potential V_1 is placed across one end of the tube but not in contact with it, show that the potential inside the tube at a large distance z from the plate is of the form

$$V = Ce^{-(R_{11}/a)z} \sin \phi J_1\left(\frac{R_{11}}{a} r\right)$$

where $C = \text{constant}$

J_1 = first-order Bessel function

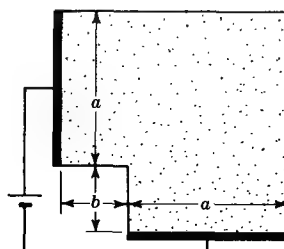
R_{11} = first root of $J_1 (= 3.832)$

Assume that the tube is infinitely long.

7-39 Develop a computer program so that the potential distribution for problems like 7-7 to 7-10, 7-14, 7-17 to 7-20, etc., will appear on a cathode-ray oscilloscope screen for conductor configurations outlined on the screen by a light pen or "magic pencil." For changes in the conductor configuration note the changes in the potential distribution.

7-40 (a) Prepare a curvilinear square map of a conductor of uniform thickness with right-angle bend connected as in Fig. P7-40. The map may be constructed by experimental (Teledeltos paper), iterative, or graphical methods. Take $a = 3b$. (b) From the map find the resistance of the configuration in terms of the sheet resistance per square (resistance of a square of the sample of the conductor of the same thickness). (c) Compare the result of (b) with that given by Chawla's formula [B. R. Chawla, Proc. IEEE, 60:151 (January 1972)].

FIGURE P7-40
Conductor with right-angle bend.



7-41 Use the point-by-point (iterative) method to map the electric field in a symmetrical coaxial transmission line consisting of a square outer conductor and a square inner conductor of one third the size.

* 7-42 In a one-dimensional device the charge density $\rho = \rho_0(x/x_1)$. If $E = 0$ at $x = 0$ and $V = 0$ at $x = x_1$, find V .

7-43 A *semiconductor* rod extending in the x direction has a constant cross section A with a *junction* at $x = 0$. If the charge density on both sides of the junction is given by $\rho = \rho_0 x(x^2 + x_1^2)^{-3/2}$ find (a) the voltage V as a function of x and (b) the capacitance of the junction between the points $x = \pm 100 x_1$. Take $E = 0$ at large x and $V = 0$ at $x = 0$. (c) Plot graphs of ρ , E , and V versus x to $x = \pm 10 x_1$.

TIME-CHANGING ELECTRIC AND MAGNETIC FIELDS

8-1 INTRODUCTION

In the preceding chapters the principles of static electric and magnetic fields have been considered. In this chapter electric and magnetic fields that change with time are discussed, and a number of new relations and concepts are introduced. Some of the more important of these are (1) *Faraday's law*, which gives the emf induced in a closed circuit due to a change of magnetic flux linking it; (2) a relation giving the emf induced in a conductor moving in a magnetic field; (3) *Maxwell's displacement current*, which represents an extension of the current concept to include charge-free space, (4) the equivalent conductivity of a dielectric, and (5) an extension of the boundary relations developed in earlier chapters to include time-varying situations.

8-2 FARADAY'S LAW

In Chap. 5 we observed that a current-carrying conductor produces a magnetic field. About 1831 Michael Faraday in London and Joseph Henry in Albany found independently that the reverse effect is also possible. That is, a magnetic field can produce

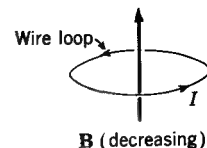


FIGURE 8-1
Relation between decreasing flux density
 \mathbf{B} and induced current I in loop.

a current in a closed circuit but with the important qualification that the magnetic flux linking the circuit must be changing.

Consider, for example, the closed wire loop in Fig. 8-1. A magnetic field with flux density \mathbf{B} is normal to the plane of the loop. If \mathbf{B} is directed upward and *decreasing* in magnitude, a current I flows in the wire in the direction indicated.[†] It is said that the current is *induced* by the magnetic field. The relation between the direction of \mathbf{B} and I is given by the right-hand rule (Fig. 5-2). This is for the case where \mathbf{B} is *decreasing* in magnitude. If \mathbf{B} is directed upward as before but is *increasing* in magnitude, the direction of the induced current is opposite.

When the applied flux density \mathbf{B} is decreasing in magnitude, the current induced in the loop is in such a direction as to produce a field which tends to increase \mathbf{B} (Fig. 8-2a). On the other hand, when \mathbf{B} is increasing, the current induced in the loop is in such a direction as to produce a field opposing \mathbf{B} (Fig. 8-2b). Thus *the induced current in the loop is always in such a direction as to produce flux opposing the change in \mathbf{B}* (Lenz's law).

The changing magnetic field produces an electric field \mathbf{E}_e . Integrating this field around the loop yields an emf \mathcal{U} . That is,

$$\mathcal{U} = \oint \mathbf{E}_e \cdot d\mathbf{l} \quad (1)$$

When the loop is open-circuited, as in Fig. 8-3a, this emf appears between the terminals.

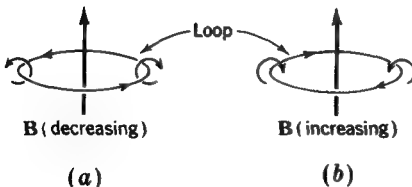
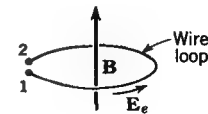


FIGURE 8-2
Induced currents for decreasing and
increasing flux density \mathbf{B} .

FIGURE 8-3
Single-turn loop.



[†] The direction is that of the conventional current, which is opposite to the direction of motion of the electron current.

The electric field \mathbf{E}_e should be distinguished from an electric field \mathbf{E}_c due to charges. Whereas \mathbf{E}_c can be described as the gradient of an electric potential V , that is, $\mathbf{E}_c = -\nabla V$, the field \mathbf{E}_e cannot. The electric field \mathbf{E}_e may be regarded as an *emf-producing field*. This type of field can result from the chemical action in a battery as discussed in Sec. 4-10. It also results, as we see here, from a changing magnetic field.

The electric potential V is a single-valued function of position. That is, a point P in an electric field \mathbf{E}_c due to charges has a single potential value V with respect to some reference point P' , such as infinity or the ground. This value of V given by

$$V = - \int_{P'}^P \mathbf{E}_c \cdot d\mathbf{l} \quad (2)$$

is independent of the path by which \mathbf{E}_c is integrated from P' to P . However, the emf \mathfrak{U} is not a single-valued function. That is, the emf \mathfrak{U} between two points 1 and 2 as given by

$$\mathfrak{U} = \int_1^2 \mathbf{E}_e \cdot d\mathbf{l} \quad (3)$$

does depend on the path by which \mathbf{E}_e is integrated from 1 to 2. For example, if the terminals 1 and 2 of the wire loop in Fig. 8-3 are infinitesimally close together, the emf \mathfrak{U} between them as obtained by integrating \mathbf{E}_e from 1 to 2 around the loop is equal to the line integral of \mathbf{E}_e around the closed loop. But if \mathbf{E}_e is integrated from 1 to 2 directly across the gap, the resulting emf is negligible.

The quantitative relation between the emf induced in a closed loop and the magnetic field producing the emf is given by *Faraday's law*.† According to this law, *the total emf induced in a closed circuit is equal to the time rate of decrease of the total magnetic flux linking the circuit*. Thus, in symbols,

$$\mathfrak{U} = - \frac{d\psi_m}{dt} \quad (4)$$

where \mathfrak{U} = total emf, V

ψ_m = total flux, Wb

t = time, s

The negative sign indicates that the emf and current directions are positive (the right-hand rule relates positive directions) with respect to the direction of the field when the

† Michael Faraday, "Experimental Researches in Electricity," B. Quaritch, London, 1839. Equation (4) is also sometimes referred to as Neumann's law.

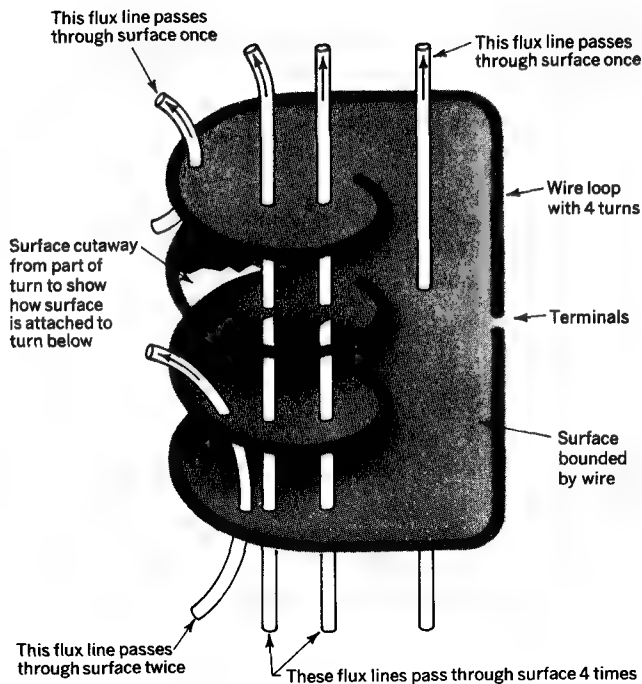


FIGURE 8-4

Circuit with 4-turn coil. The wire loop forms the boundary of a single continuous surface. Part of the surface of 1 turn has been cut away to show how the surface is bounded by the turn below.

field, and hence the flux, is *decreasing* with time.[†] This situation is indicated in Fig. 8-2a.

The total flux through a circuit is equal to the normal component of the flux density \mathbf{B} over the surface bounded by the circuit. That is, the total magnetic flux is given by

$$\psi_m = \iint \mathbf{B} \cdot d\mathbf{s} \quad (5)$$

[†] With loops of N turns where each turn links the same amount of flux one can also write $\Delta = N\psi_m$, where Δ = total flux linkage and ψ_m = flux linked by each turn. Thus, (4) becomes

$$\Delta U = -N \frac{d\psi_m}{dt} = -\frac{d\Delta}{dt} \quad (4a)$$

The surface over which the integration is carried out is the surface bounded by the periphery of the circuit, as in Fig. 8-4. Equation (5) applies to a closed single-conductor circuit of any number of turns or loops. It is important to note that *any closed circuit with any number of turns forms the boundary of a single surface* (see Fig. 8-4) and $\iint \mathbf{B} \cdot d\mathbf{s}$ over this surface yields the total flux. Thus, integrating \mathbf{B} over the surface in Fig. 8-4 yields all the flux. Lines of flux passing through the surface only once are integrated once, but those linking all 4 turns are integrated 4 times since they pass through the surface 4 times. Substituting (5) in (4) leads to†

$$\mathcal{U} = - \frac{d}{dt} \int_s \mathbf{B} \cdot d\mathbf{s} \quad (6)$$

where \mathcal{U} = induced emf, V

\mathbf{B} = flux density, T

$d\mathbf{s}$ = surface element, m^2

t = time, s

When the loop or closed circuit is stationary or fixed, (6) reduces to

$$\mathcal{U} = - \int_s \frac{\partial \mathbf{B}}{\partial t} \cdot d\mathbf{s} \quad (7)$$

This form of Faraday's law gives the induced emf due specifically to a time rate of change of \mathbf{B} for a loop or circuit that is fixed with respect to the observer. This is sometimes called the *transformer induction equation*.

8-3 MAXWELL'S EQUATION FROM FARADAY'S LAW: INTEGRAL FORM

From (8-2-1) and (8-2-7) we have‡

$$\mathcal{U} = \oint \mathbf{E} \cdot d\mathbf{l} = - \int_s \frac{\partial \mathbf{B}}{\partial t} \cdot d\mathbf{s} \quad (1)$$

where \mathcal{U} = induced emf, V

$\mathbf{E} = \mathbf{E}_e$ = emf-producing electric field, V m^{-1}

$d\mathbf{l}$ = element of path, m

\mathbf{B} = flux density, T

$d\mathbf{s}$ = element of area, m^2

t = time, s

† The symbol \int_s indicates a double or surface integral (\iint) over a surface s .

‡ To simplify the notation, the symbol \mathbf{E}_e will be used only where it is desirable to indicate explicitly that the field is an emf-producing type. Since here the integral of the electric field is an emf \mathcal{U} , it is obvious that \mathbf{E} is emf-producing and to be explicit could be written \mathbf{E}_e . The same situation applies in (8-4-2).

This relation is referred to as *Maxwell's equation as derived from Faraday's law*. It appears in (1) in its integral form. The corresponding differential relation is given in Sec. 8-8.

According to (1), the line integral of the electric field around a fixed closed circuit is equal to the normal component of the time rate of decrease of the flux density \mathbf{B} integrated over a surface bounded by the circuit. Both are also equal to the total emf \mathcal{U} induced in the circuit.

8-4 MOVING CONDUCTOR IN A MAGNETIC FIELD

As discussed in Sec. 15-3, the force \mathbf{F} on a particle of electric charge e moving with a velocity \mathbf{v} in a magnetic field of flux density \mathbf{B} is

$$\mathbf{F} = e\mathbf{v} \times \mathbf{B} \quad (\text{N}) \quad (1)$$

Suppose that the charged particle is situated in a wire moving with a velocity \mathbf{v} through a magnetic field of flux density \mathbf{B} , as suggested in Fig. 8-5. Dividing (1) by e , we obtain the force per charge or electric field intensity \mathbf{E} ,† or

$$\mathbf{E} = \frac{\mathbf{F}}{e} = \mathbf{v} \times \mathbf{B} \quad (\text{V m}^{-1}) \quad (2)$$

The magnitude of \mathbf{E} is given by $E = vB \sin \theta$, where θ is the angle between \mathbf{v} and \mathbf{B} (Fig. 8-6). The electric field \mathbf{E} is of the emf-producing type and is normal to the plane containing \mathbf{v} and \mathbf{B} . For example, in Fig. 8-5, \mathbf{v} is in the positive y direction, and \mathbf{B} is in the positive z direction. Hence, crossing \mathbf{v} into \mathbf{B} yields \mathbf{E} in the positive x direction or along the wire.‡ The emf \mathcal{U} induced between two points 1 and 2 on the wire (Fig. 8-5) is then

$$\mathcal{U} = \int_2^1 \mathbf{E} \cdot d\mathbf{l} = \int (\mathbf{v} \times \mathbf{B}) \cdot d\mathbf{l} \quad (\text{V}) \quad (3)$$

where \mathcal{U} = emf induced over a length l of wire, V

\mathbf{E} = electric field, V m^{-1}

$d\mathbf{l}$ = element of length of wire, m

\mathbf{v} = velocity of wire, m s^{-1}

\mathbf{B} = flux density of magnetic field, T

† Properly the \mathbf{E} (or \mathbf{E}_e) for this motional case should be primed (as in Sec. 16-7) or otherwise distinguished from the \mathbf{E} for the stationary case, but for simplicity here no distinction is made.

‡ It is assumed that the conductivity of the wire is finite so that the component of \mathbf{E} tangent to the wire need not be zero.

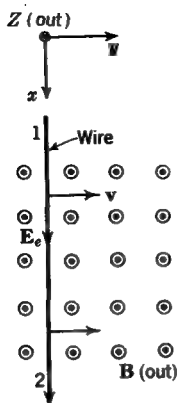


FIGURE 8-5
An emf is induced in a wire moving across a magnetic field.

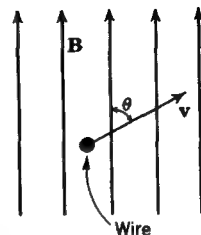


FIGURE 8-6
Relation between direction of motion of wire and direction of \mathbf{B} .

For a straight wire where v , B , and the wire are mutually perpendicular, B is uniform, and v is the same for all parts of the wire; (3) reduces to

$$\mathcal{U} = El = vBl \quad (V) \quad (4)$$

where l is the length of the wire in meters.

Equations (3) and (4) are *motional-induction or flux-cutting laws* giving the emf induced in a conductor moving with respect to the observer in a magnetic field. Equation (3) is the more general form, while (4) applies to the special case where the directions of the wire, its motion, and the magnetic field are all mutually perpendicular. It is also assumed in (4) that all parts of the wire have the same value of v and that B is uniform.

The relations may be used to find the emf induced in any part of a circuit due to its motion through a magnetic field. They also can be applied to find the total emf induced in a closed circuit that is moved or deformed in a magnetic field that does not change with time. For a closed circuit (3) becomes

$$\mathcal{U} = \oint \mathbf{E} \cdot d\mathbf{l} = \oint (\mathbf{v} \times \mathbf{B}) \cdot d\mathbf{l} \quad (5)$$

where \mathcal{U} is the total emf induced in the circuit.

8-5 GENERAL CASE OF INDUCTION

Equation (8-3-1) gives the emf induced in a closed circuit due to the time rate of change of \mathbf{B} (transformer induction). Equation (8-4-5) gives the emf induced in a closed circuit due to its motion. When both kinds of changes are occurring simultaneously,

i.e., when \mathbf{B} changes with time and the circuit is also in motion, the total emf induced is equal to the sum of the emfs given by (8-3-1) and (8-4-5), or†

$$\mathcal{U} = \oint (\mathbf{v} \times \mathbf{B}) \cdot d\mathbf{l} - \int_s \frac{\partial \mathbf{B}}{\partial t} \cdot d\mathbf{s} \quad (1)$$

The first term of the right-hand member gives the emf induced by the motion, while the second term gives the emf induced by the time change in \mathbf{B} . The line integral in the first term is taken around the entire circuit, while the surface integral in the second term is taken over the entire surface bounded by the circuit.

Equation (1) is a general relation and gives the correct value of total induced emf in all cases. For the special case of motion only, $\partial \mathbf{B} / \partial t = 0$, and (1) reduces to

$$\mathcal{U} = \oint (\mathbf{v} \times \mathbf{B}) \cdot d\mathbf{l} \quad (2)$$

For the special case of time change of flux density only, $\mathbf{v} = 0$, and (1) reduces to

$$\mathcal{U} = - \int_s \frac{\partial \mathbf{B}}{\partial t} \cdot d\mathbf{s} \quad (3)$$

To summarize, the induction relations are

$$(I) \quad \mathcal{U} = \oint (\mathbf{v} \times \mathbf{B}) \cdot d\mathbf{l} - \int_s \frac{\partial \mathbf{B}}{\partial t} \cdot d\mathbf{s} \quad \text{general case}$$

$$(II) \quad \mathcal{U} = \oint (\mathbf{v} \times \mathbf{B}) \cdot d\mathbf{l} \quad \text{motion only (motional induction)}$$

$$(III) \quad \mathcal{U} = - \int_s \frac{\partial \mathbf{B}}{\partial t} \cdot d\mathbf{s} \quad \mathbf{B} \text{ change only (transformer induction)}$$

8-6 EXAMPLES OF INDUCTION

In this section seven examples are given in which the total emf induced in a closed circuit (total induction) is calculated. The general relation (I) gives the correct result in all cases. In some cases (motion only or time change only) (II) or (III) alone is sufficient.

† A general development of (1) is given in Chap. 16 [see (16-7-32)]. Equation (1) can also be derived from (8-2-6) by means of the Helmholtz formula. See C-T Tai On the Presentation of Maxwell's Theory, Proc. IEEE, 60: 936-945 (August 1972). Note that (8-2-6) involves a *total* derivative and that to evaluate it one must resolve it into two terms, as in (1), using the Helmholtz formula.

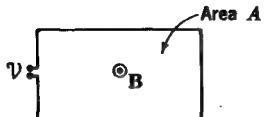


FIGURE 8-7
Fixed loop of area *A* (for Example 1).

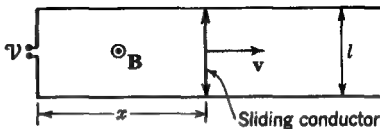


FIGURE 8-8
Sliding conductor for increasing loop area
(for Examples 2 and 3).

EXAMPLE 1 Consider the fixed rectangular loop of area *A* shown in Fig. 8-7. The flux density **B** is normal to the plane of the loop (outward in Fig. 8-7) and is uniform over the area of the loop. However, the magnitude of **B** varies harmonically with respect to time as given by

$$B = B_0 \cos \omega t \quad (1)$$

where B_0 = maximum amplitude of B , T

ω = radian frequency ($= 2\pi f$, where f = frequency), rad s⁻¹

t = time, s

Find the total emf induced in the loop.

SOLUTION This is a pure case of **B** change only, there being no motion. Hence, from (III), the total emf induced in the loop is

$$\mathcal{U} = - \int_s \frac{\partial \mathbf{B}}{\partial t} \cdot d\mathbf{s} = A\omega B_0 \sin \omega t \quad (\text{V}) \quad (2)$$

This emf appears at the terminals of the loop (Fig. 8-7). Since the velocity $v = 0$, the emf calculated by (II) is zero and by (I) is identical with that in (2).

EXAMPLE 2 Consider the rectangular loop shown in Fig. 8-8. The width *l* of the loop is constant, but its length *x* is increased uniformly with time by moving the sliding conductor at a uniform velocity v . The flux density **B** is everywhere the same (normal to the plane of the loop) and is constant with respect to time. Find the total emf induced in the loop.

SOLUTION This is a pure case of motion only, the flux density **B** being constant. Hence, from (II),

$$\mathcal{U} = \oint (\mathbf{v} \times \mathbf{B}) \cdot d\mathbf{l} = vBl \quad (\text{V}) \quad (3)$$

The entire emf in this case is induced in the moving conductor of length *l*. Since $\partial B / \partial t = 0$, the emf by (III) is zero and by (I) is identical with (3).

EXAMPLE 3 Consider again the same loop with sliding conductor discussed in the preceding example (Fig. 8-8). The flux density **B** is normal to the plane of the loop and is

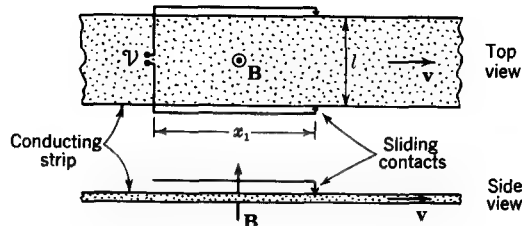


FIGURE 8-9

Fixed loop with sliding strip (for Examples 4 and 5).

uniform everywhere. The sliding conductor moves with a uniform velocity v . These conditions are the same as in the preceding example. However, in this case let the magnitude of the flux density B vary harmonically with time as given by

$$B = B_0 \cos \omega t \quad (4)$$

Find the total emf induced in the loop.

SOLUTION This is a case involving both motion and a time-changing B . The emf \mathcal{U}_m due to the motion is given, from (II), by

$$\mathcal{U}_m = \oint (\mathbf{v} \times \mathbf{B}) \cdot d\mathbf{l} = vBl = vIB_0 \cos \omega t \quad (5)$$

The emf \mathcal{U}_t , due to a time-changing B is, from (III),

$$\mathcal{U}_t = - \int_s \frac{\partial \mathbf{B}}{\partial t} \cdot ds = \omega xlB_0 \sin \omega t \quad (6)$$

According to (I) the total emf \mathcal{U} is the sum of the emfs of (5) and (6), or

$$\begin{aligned} \mathcal{U} &= \oint (\mathbf{v} \times \mathbf{B}) \cdot d\mathbf{l} - \int_s \frac{\partial \mathbf{B}}{\partial t} \cdot ds \\ &= vB_0 l \cos \omega t + \omega xB_0 l \sin \omega t \\ &= B_0 l \sqrt{v^2 + (\omega x)^2} \sin(\omega t + \delta) \end{aligned} \quad (7)$$

where $\delta = \tan^{-1}(\mathbf{v}/\omega x)$

x = instantaneous length of loop

EXAMPLE 4 The circuit for a rectangular loop of width l and length x_1 is completed by sliding contacts through a thin conducting strip, as suggested in Fig. 8-9. The loop is stationary, but the strip moves longitudinally with a uniform velocity v . The magnetic flux density B is normal to the strip and the plane of the loop. It is constant with respect to time and is uniform everywhere. The width of the strip is l , the same as for the loop, although for clarity the loop is shown with a slightly greater width in Fig. 8-9. Find the total emf induced in the circuit.

SOLUTION This is another case of motion only. Therefore from (II) the total emf is given by

$$\mathcal{U} = \oint (\mathbf{v} \times \mathbf{B}) \cdot d\mathbf{l} = vBl \quad (8)$$

The entire emf in this case is induced in the moving strip and appears at the terminals. Since $\partial B / \partial t = 0$, the emf by (III) is zero and by (I) is identical with (8). A variation of the arrangement of Example 4 is provided by the Faraday disk generator (see Prob. 8-11).

EXAMPLE 5 Consider now the same loop and strip as in the preceding example (Fig. 8-9), but let the magnitude of the flux density vary harmonically with time as given by

$$B = B_0 \cos \omega t \quad (9)$$

Find the total emf induced in the circuit.

SOLUTION This case involves both motion and a time-changing B . From (II) the emf \mathcal{U}_m due to the motion is

$$\mathcal{U}_m = \oint (\mathbf{v} \times \mathbf{B}) \cdot d\mathbf{l} = vBl = vB_0 l \cos \omega t \quad (10)$$

From (III) the emf \mathcal{U}_t due to a time-changing B is†

$$\mathcal{U}_t = - \int_s \frac{\partial \mathbf{B}}{\partial t} \cdot d\mathbf{s} = \omega x_1 B_0 l \sin \omega t \quad (11)$$

According to (I), the total emf \mathcal{U} is the sum of (10) and (11), or

$$\begin{aligned} \mathcal{U} &= \mathcal{U}_m + \mathcal{U}_t = vB_0 l \cos \omega t + \omega x_1 B_0 l \sin \omega t \\ &= B_0 l \sqrt{v^2 + (\omega x_1)^2} \sin(\omega t + \delta) \end{aligned} \quad (12)$$

where $\delta = \tan^{-1}(v/\omega x_1)$.

EXAMPLE 6 Consider next a rotating rectangular loop in a steady magnetic field as in Fig. 8-10a. The loop rotates with a uniform angular velocity ω radians per second. This arrangement represents a simple ac generator, the induced emf appearing at terminals connected to the slip rings. If the radius of the loop is R and its length l , find the total emf induced.

SOLUTION Since this is a case of motion only, the total emf can be obtained from (II). Referring to Fig. 8-10b, it is given by

$$\mathcal{U} = \oint (\mathbf{v} \times \mathbf{B}) \cdot d\mathbf{l} = 2vBl \sin \theta \quad (13)$$

† At low frequencies the effect of eddy currents in the strip can be neglected. The effect of eddy currents will be even less if the strip is very thin and its conductivity poor.

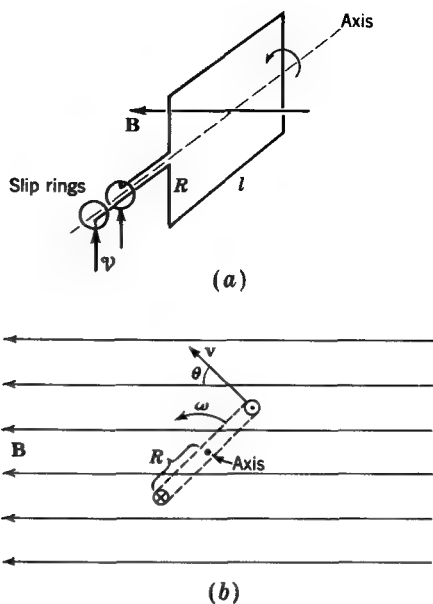


FIGURE 8-10
AC generator (for Examples 6 and 7):
(a) perspective view; (b) cross section
perpendicular to axis.

Since $\theta = \omega t$, we have

$$\mathcal{U} = 2\omega Rl/B \sin \omega t \quad (14)$$

The factor 2 is necessary because there are two conductors of length l moving through the field, the emfs in both aiding. Since $2Rl = A$, the area of the loop, (14) reduces to

$$\mathcal{U} = \omega BA \sin \omega t \quad (15)$$

Since $\partial B / \partial t = 0$, the emf calculated by (III) is zero. Hence from (I) the emf is as given by (14) or (15).

EXAMPLE 7 Consider finally the same rotating loop as in the preceding example with the modification that B varies with time as given by $B = B_0 \sin \omega t$ (ω same as rotation angular velocity). When $t = 0$, $B = 0$ and $\theta = 0$ (Fig. 8-10b). Find the total emf induced.

SOLUTION This case involves both motion and a time-changing B . From (II) the emf \mathcal{U}_m due to the motion is

$$\mathcal{U}_m = 2\omega RlB_0 \sin^2 \omega t = \omega RlB_0 - \omega RlB_0 \cos 2\omega t \quad (16)$$

From (III) the emf \mathcal{U}_t , due to a time-changing B is

$$\mathcal{U}_t = -2\omega RlB_0 \cos^2 \omega t = -\omega RlB_0 - \omega RlB_0 \cos 2\omega t \quad (17)$$

From (I) the total emf \mathcal{U} is given by the sum of (16) and (17), or

$$\mathcal{U} = \mathcal{U}_m + \mathcal{U}_t = -2\omega RIB_0 \cos 2\omega t \quad (18)$$

The emf in this example is at twice the rotation, or magnetic field, frequency. It is to be noted that the emf calculated from either (II) or (III) alone contains a dc component. In adding the emfs of (II) and (III) the dc component cancels, yielding the correct total emf given by (18).

8-7 STOKES' THEOREM

In Sec. 8-3 Maxwell's equation from Faraday's law is stated in integral form. This equation may be transformed from an integral to a differential form by means of Stokes' theorem, which is developed in this section and applied to Maxwell's equation in Sec. 8-8.

Consider a square of area Δs in the xy plane as in Fig. 8-11. Let the electric field \mathbf{E} have components E_x and E_y as shown. The work per coulomb required to move a charge around the perimeter of the square is given by the line integral of \mathbf{E} around the perimeter. This work equals the total emf around the perimeter. That is,

$$\mathcal{U} = \oint \mathbf{E} \cdot d\mathbf{l} \quad (1)$$

Dividing by the area Δs and taking the limit of this ratio as Δs approaches zero yields the curl of \mathbf{E} normal to Δs at the point around which Δs shrinks to zero (see Sec. 5-22). Thus

$$\lim_{\Delta s \rightarrow 0} \frac{\oint \mathbf{E} \cdot d\mathbf{l}}{\Delta s} = (\nabla \times \mathbf{E})_n \quad (2)$$

where $(\nabla \times \mathbf{E})_n$ is the component of the curl of \mathbf{E} normal to the area Δs .

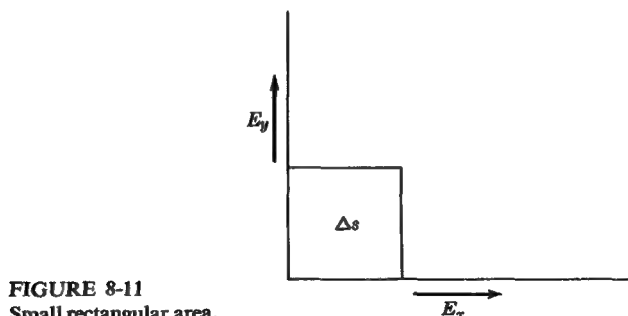


FIGURE 8-11
Small rectangular area.

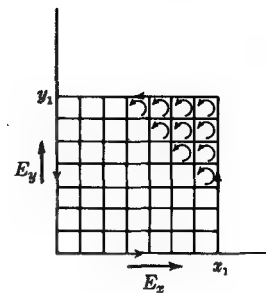


FIGURE 8-12
Illustration for Stokes' theorem.

Consider now a surface of area x_1y_1 as shown in Fig. 8-12. Let the area be divided into infinitesimal areas as suggested. From (2) the work per coulomb to carry a charge around an infinitesimal loop divided by its area is equal to the curl of \mathbf{E} at the point. If the curl of \mathbf{E} is integrated over the entire area x_1y_1 , all contributions to the total work cancel except for the work along the periphery of the area x_1y_1 .

The situation here is analogous to that of a single current loop with current I , Fig. 8-13a, whose effect is the same as a mesh of current loops, each with a current I , as suggested in Fig. 8-13b. It is assumed that the adjacent sides of the small loops are very close together. Since the currents in adjacent sides are oppositely directed, their fields cancel. The only currents whose effects are not canceled are those along the periphery of the area of radius R .

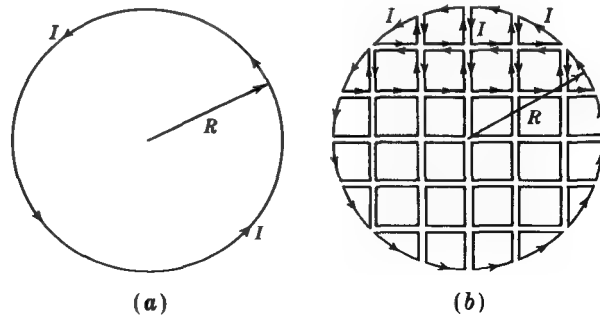


FIGURE 8-13
(a) Single current loop and (b) equivalent mesh of small current loops.

Returning now to the area x_1y_1 in Fig. 8-12, the integral of the normal component of the curl over the area x_1y_1 must equal the line integral of \mathbf{E} around the periphery of the area. That is,

$$\oint \mathbf{E} \cdot d\mathbf{l} = \int_s (\nabla \times \mathbf{E}) \cdot d\mathbf{s} \quad (3)$$

Dimensionally (3) is of the form

$$\frac{\text{Force}}{\text{Charge}} \times \text{distance} = \frac{\text{work/charge}}{\text{area}} \times \text{area}$$

Since force \times distance = work, (3) is balanced dimensionally. In (3) it is understood that if the curl of \mathbf{E} is integrated over an area s , the line integral of \mathbf{E} is taken around the periphery of the same area s . That is,

$$\oint_{\text{periphery of } s} \mathbf{E} \cdot d\mathbf{l} = \int_{\text{surface of } s} (\nabla \times \mathbf{E}) \cdot d\mathbf{s} \quad (4)$$

The relation expressed by (3) or (4) is called *Stokes' theorem* as applied to electric fields. In general, Stokes' theorem states that *the line integral of a vector function around a closed contour C is equal to the integral of the normal component of the curl of that vector function over any surface having the contour C as its bounding edge.*

8-8 MAXWELL'S EQUATION FROM FARADAY'S LAW: DIFFERENTIAL FORM

By means of Stokes' theorem (8-7-4) let us substitute the surface integral of the curl of \mathbf{E} for the line integral of \mathbf{E} in (8-3-1). That is,

$$\iint (\nabla \times \mathbf{E}) \cdot d\mathbf{s} = - \iint \frac{\partial \mathbf{B}}{\partial t} \cdot d\mathbf{s} \quad (1)$$

Since $d\mathbf{s}$ in (1) applies to any surface element, it is arbitrary and therefore the integrands in (1) are equal. Thus

$$\nabla \times \mathbf{E} = - \frac{\partial \mathbf{B}}{\partial t} \quad (2)$$

This is Maxwell's equation, in differential form, as derived from Faraday's law. The integral form of the equation was given in (8-3-1).

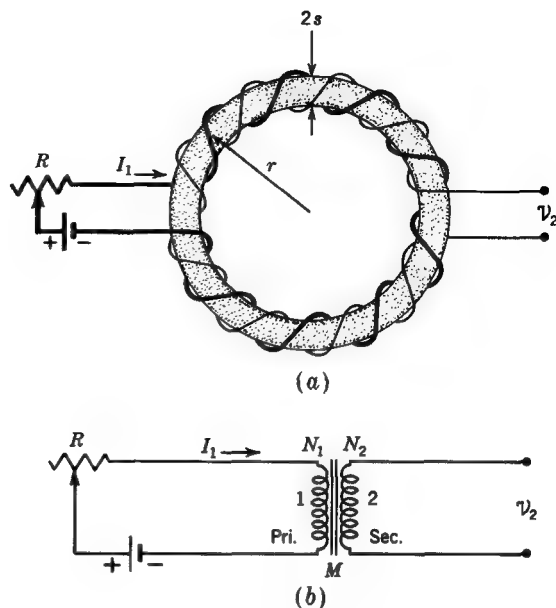


FIGURE 8-14
Toroidal coil with two windings.

8-9 MUTUAL INDUCTANCE AND SELF-INDUCTANCE

Consider that two uniform toroidal coils are interwound as in Fig. 8-14a. Coil 1 of N_1 turns is indicated by a heavy wire and coil 2 of N_2 turns by a fine wire. There is no electrical connection between the coils. The ring-shaped form on which the coils are wound is assumed to have a constant permeability μ . Coil 1 will be called the *primary winding* and coil 2 the *secondary*. A schematic diagram of the arrangement is shown in Fig. 8-14b.

If the primary current I_1 is constant in value, the emf v_2 appearing at the terminals of the secondary coil is zero, since the flux ψ_{m1} produced by the primary coil is not changing. It is assumed that all of the magnetic field produced by I_1 is confined to the region inside the toroidal windings.

Suppose now that the resistance R is decreased at a constant rate so that I_1 increases. This increases the magnetic flux ψ_{m1} . Disregarding the negative sign, we have from Faraday's law that the magnitude of the emf v_2 induced in coil 2 and appearing at its terminals is

$$v_2 = N_2 \frac{d\psi_{m1}}{dt} \quad (1)$$

where ψ_{m1} is the magnetic flux produced by the primary coil. If a long solenoid is closed on itself, we obtain a toroid. Assuming that the radius r of the toroid is large compared with the radius s of the winding (Fig. 8-14a), the flux density B may be considered constant over the interior of the winding. Obtaining the magnitude of B from (5-11-5), we see that the total flux ψ_{m1} through the toroid is

$$\psi_{m1} = B\pi s^2 = \frac{\mu N_1 I_1 \pi s^2}{2\pi r} = \frac{\mu N_1 I_1 A}{l} \quad (\text{Wb}) \quad (2)$$

where A = area of winding cross section = πs^2 , m²

l = mean length of the toroidal coil = $2\pi r$, m

Substituting (2) in (1) gives

$$\mathbf{U}_2 = N_1 N_2 \frac{\mu A}{l} \frac{dI_1}{dt} \quad (3)$$

According to (3), the secondary emf \mathbf{U}_2 is proportional to the number of primary turns N_1 , the number of secondary turns N_2 , the permeability μ of the medium inside the winding, the cross-sectional area A of the winding, and the time rate of change of the primary current I_1 and is inversely proportional to the average length l of the winding. When we put

$$M = N_1 N_2 \frac{\mu A}{l} \quad (4)$$

(3) reduces to

$$\mathbf{U}_2 = M \frac{dI_1}{dt}$$

(5)

Dimensionally (5) is

$$\text{Emf} = M \frac{\text{current}}{\text{time}}$$

or $M = \frac{\text{emf}}{\text{current}} \times \text{time} = \text{resistance} \times \text{time}$

or $M = \text{ohm-seconds} = \text{henrys}$

Thus, M has the dimensions of inductance, and since M involves two coils, it is called the *mutual inductance* of the two coils.

The inductance L discussed in previous sections involves a single coil. Therefore, in contrast, L is called the *self-inductance*. The emf \mathcal{U}_1 applied to a coil of self-inductance L_1 is

$$\mathcal{U}_1 = L_1 \frac{dI_1}{dt} \quad (6)$$

where I_1 is the current in the coil. This relation involving the self-inductance of a coil is similar in form to (5), which involves the mutual inductance of two coils.

From (5-13-4) the self-inductance of a toroid is

$$L = N^2 \frac{\mu A}{l} = \frac{N^2}{l/\mu A} = \frac{N^2}{\mathcal{R}} \quad (H) \quad (7)$$

where N = number of turns of toroid, dimensionless

$\mathcal{R} = l/\mu A$ = reluctance of region enclosed by toroid winding, H^{-1}

From (4) the mutual inductance M of two coils (as in Fig. 8-14) is

$$M = N_1 N_2 \frac{\mu A}{l} = \frac{N_1 N_2}{l/\mu A} = \frac{N_1 N_2}{\mathcal{R}} \quad (H) \quad (8)$$

where N_1 = number of primary turns, dimensionless

N_2 = number of secondary turns, dimensionless

\mathcal{R} = reluctance of magnetic circuit linking primary and secondary windings, H^{-1}

Consider next the converse of the situation described above. That is, let the battery and resistance be connected across coil 2 (Fig. 8-14), and let the terminals of coil 1 be left open. Then the emf \mathcal{U}_1 at the terminals of coil 1 is

$$\mathcal{U}_1 = N_1 \frac{d\psi_{m2}}{dt} \quad (9)$$

where ψ_{m2} is the magnetic flux produced by the secondary coil. But

$$\psi_{m2} = \frac{\mu N_2 I_2 A}{l}$$

and so (9) becomes

$$\mathcal{U}_1 = N_1 N_2 \frac{\mu A}{l} \frac{dI_2}{dt} \quad (10)$$

$$\text{or} \quad \mathcal{U}_1 = M \frac{dI_2}{dt} \quad (11)$$

Thus, from (5) and (11),

$$M = \frac{\mathcal{U}_1}{dI_2/dt} = \frac{\mathcal{U}_2}{dI_1/dt} \quad (12)$$

Therefore, if a given time rate of change of current in the primary induces a certain voltage in the secondary, the same time rate of change of current applied to the secondary will induce the same voltage in the primary. In effect this is a statement of the *reciprocity theorem* as applied to a special case.

If the current I_1 varies harmonically with time (alternating current), we have

$$I_1 = I_0 e^{j\omega t} \quad (13)$$

For harmonic variation of I_1 and I_2 , (12) becomes

$$M = \frac{\mathcal{U}_1}{j\omega I_2} = \frac{\mathcal{U}_2}{j\omega I_1} \quad (14)$$

and

$$\frac{\mathcal{U}_1}{I_2} = \frac{\mathcal{U}_2}{I_1} = j\omega M = Z_m \quad (15)$$

where Z_m is the *mutual impedance* in ohms.

8-10 THE TRANSFORMER

Suppose that the two-coil arrangement of Fig. 8-15 has the secondary coil open, as shown, while the primary coil is connected to an alternating emf \mathcal{U}_1 . The emf \mathcal{U}_2 , appearing at the secondary terminals has a magnitude

$$\mathcal{U}_2 = N_2 \frac{d\psi_m}{dt} \quad (1)$$

where N_2 = number of turns of secondary coil

ψ_m = magnetic flux through transformer core

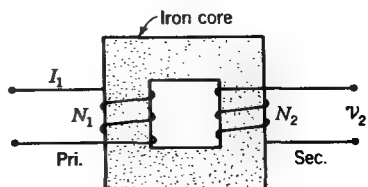


FIGURE 8-15
Transformer.

If the primary resistance is negligible, the counter emf across the primary terminals is equal in magnitude to the applied emf \mathcal{U}_1 , or

$$\mathcal{U}_1 = N_1 \frac{d\psi_m}{dt} \quad (2)$$

where N_1 is the number of turns of the primary coil. Dividing (1) by (2) yields

$$\frac{\mathcal{U}_2}{\mathcal{U}_1} = \frac{N_2}{N_1} \quad (3)$$

According to (3) the ratio of the secondary to the primary emf is equal to the ratio of the number of secondary turns N_2 to the number of the primary turns N_1 . The ratio is the same for effective (rms) voltages as for instantaneous.

Because the arrangement of Fig. 8-15 (or Fig. 8-14) can transform an emf or voltage from one value to another, it is called a *transformer*. In the present discussion the transformer is an ideal one in the sense that flux leakage is assumed to be zero so that ψ_m links all primary and secondary turns. It is further assumed that the resistance of the primary is very small and that negligible current is drawn from the secondary. This condition may be approached in practice where a transformer secondary is connected to a high-resistance circuit.

EXAMPLE An ideal transformer has a turns ratio of 2, that is, $N_2/N_1 = 2$. An ac emf of 10 V rms is applied to the primary. Find the emf or voltage appearing at the secondary terminals.

SOLUTION From (3) the secondary voltage is

$$\mathcal{U}_2 = \frac{N_2}{N_1} \mathcal{U}_1 = 2 \times 10 = 20 \text{ V (rms)}$$

8-11 ALTERNATING-CURRENT BEHAVIOR OF FERROMAGNETIC MATERIALS

We noted in Chap. 6 that the permeability of iron is not a constant. In spite of this, the permeability of the iron in an iron-cored coil carrying alternating current may be taken as a constant for certain applications, but its value, in this case, needs further explanation.

Where μ is not a constant, we have from (5-12-2) that the inductance L of a coil is given by

$$L = \frac{d\Lambda}{dI} \quad (\text{H}) \quad (1)$$

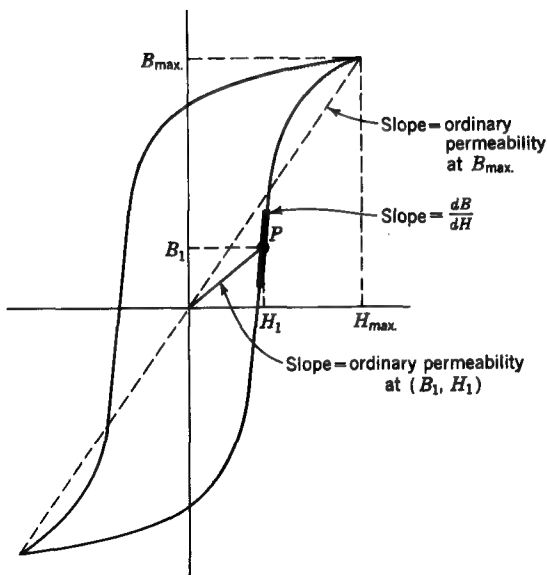


FIGURE 8-16
Hysteresis loop illustrating ordinary and differential permeabilities.

If there is no flux leakage, $\Lambda = N\psi_m$; so

$$L = N \frac{d\psi_m}{di} \quad (2)$$

For a toroidal type of coil, $d\psi_m = A dB$, and $di = l dH/N$, where A equals the area and l equals the mean length of the coil. Therefore (2) becomes

$$L = \frac{N^2 A}{l} \frac{dB}{dH} \quad (3)$$

In (3) dB/dH has the dimensions of permeability. It is equal to the slope of the hysteresis curve. At some point P , as in Fig. 8-16, this is different from the ordinary permeability, B_1/H_1 , which is equal to the slope of the line from the origin to the point P . Since dB/dH involves infinitesimals, it is sometimes called the *infinitesimal* or *differential permeability*.

If alternating current is applied to an iron-cored coil so that the condition of the iron moves around a hysteresis loop (Fig. 8-16) once per cycle, the slope dB/dH varies over a wide range and the instantaneous value of the inductance will, from (3), vary over a corresponding range. Under these conditions it is often convenient to consider the average inductance (over one cycle) as obtained from (3), using the average value

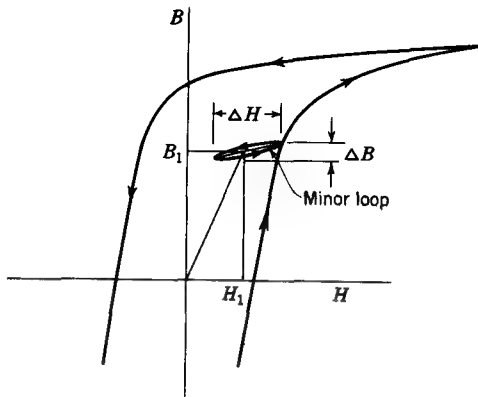


FIGURE 8-17
Minor hysteresis loop illustrating incremental permeability.

of the slope dB/dH . This is equal to the ordinary permeability at the maximum value of B attained in the cycle (see Fig. 8-16). Thus

$$L_{av} = \frac{N^2 A}{l} \left(\frac{dB}{dH} \right)_{av} = \frac{N^2 A}{l} \mu \quad (4)$$

where $\mu = B_{\max}/H_{\max}$ is the ordinary permeability at B_{\max} .

The above discussion is for alternating current only through the coil. If a small alternating current is superimposed on a relatively large steady, or direct, current through the coil, the situation is as suggested in Fig. 8-17. The magnetic condition of the iron then follows a minor hysteresis loop as indicated. In this case the average value of the slope dB/dH is given by the line passing through the tips of the minor hysteresis loop and is called the *incremental permeability* μ_{inc} . Referring to Fig. 8-17,

$$\mu_{inc} = \left(\frac{dB}{dH} \right)_{av} = \frac{\Delta B}{\Delta H} \quad (5)$$

The incremental permeability is much less than the ordinary permeability $B_1 H_1$ for a point at the center of the minor loop in Fig. 8-17.

In (8-9-7) the self-inductance L of a toroidal coil of N turns is given as

$$L = N^2 \frac{\mu A}{l} \quad (H) \quad (6)$$

and in (8-9-8) the mutual inductance M of two coils mounted, for example, on a ring-shaped core is given as

$$M = N_1 N_2 \frac{\mu A}{l} \quad (H) \quad (7)$$

where N_1 = number of primary turns

N_2 = number of secondary turns

For iron cores and ac operation these relations may be used to calculate the average L or average M provided the appropriate value of μ is used. As discussed above, this value of μ is equal to the average value of dB/dH over the operating range of the iron on a BH diagram.

Although the above discussion has concerned toroidal coils with uniform core cross section A , Eqs. (6) and (7) may be applied in the more general case, where the iron core is of nonuniform cross section and the magnetic circuit may include an air gap, by reexpressing them as

$$L = \frac{N^2}{\mathcal{R}} \quad (\text{H}) \quad (8)$$

where \mathcal{R} is the reluctance of the closed magnetic circuit through the coil,

$$\text{and} \quad M = \frac{N_1 N_2}{\mathcal{R}} \quad (\text{H}) \quad (9)$$

where \mathcal{R} is the reluctance of the closed magnetic circuit linking the primary and secondary coils. The above relations are applicable both to uniformly distributed coils and to concentrated coils (as in Fig. 8-16) provided that flux leakage is negligible. The reluctance of the magnetic circuit is calculated as discussed in Chap. 6.

8-12 EDDY CURRENTS

When large conducting specimens are subjected to transformer or motional induction, currents tend to be induced in the specimen. They flow in closed paths in the specimen and are called *eddy currents*. In accordance with Lenz's law, the eddy current tends to oppose the change in field inducing it.

Eddy currents result in joule heating in the conducting specimen. The energy loss due to eddy currents in the ferromagnetic cores of ac devices is in addition to the energy lost in the magnetization-demagnetization process (proportional to the area of the hysteresis loop), as discussed in Sec. 6-14. In order to reduce the eddy currents in iron-cored ac devices, the core is commonly made of thin sheets or laminations of iron insulated electrically from each other. Thus the eddy currents are confined to individual sheets, and the power loss is reduced. Each sheet is continuous in the direction of the magnetic flux through the core, but because of its thinness it has a relatively large reluctance. By stacking a sufficient number of sheets in parallel the total reluctance of the magnetic circuit can be reduced to the desired value. To reduce eddy currents to a minimum, iron wires are sometimes used in place of sheets, while at radio frequencies powdered-iron cores are commonly employed.

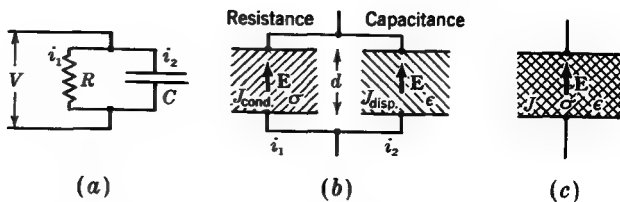


FIGURE 8-18
 (a) and (b) Conduction current through resistor and displacement current through capacitor. (c) Conduction and displacement currents through conducting dielectric medium.

8-13 DISPLACEMENT CURRENT

In this section a new concept is introduced, that of *displacement current*. Consider a voltage applied to a resistor and a capacitor in parallel, as in Fig. 8-18a. The nature of the current flow through the resistor is different from that through the capacitor. Thus a constant voltage across a resistor produces a continuous flow of current of constant value. On the other hand, there will be a current through the capacitor only while the voltage is changing.

For a voltage V across a resistor of resistance R and capacitor of capacitance C in parallel, as in Fig. 8-18a, we have a current through the resistor given by $i_1 = V/R$ and a current through the capacitor given by

$$i_2 = \frac{dQ}{dt} = C \frac{dV}{dt} \quad (1)$$

The instantaneous charge Q in the capacitor is given by $Q = CV$.

The current through the resistor is a *conduction current*, while the current "through" the capacitor may be called a *displacement current*. Although the current does not flow through the capacitor, the external effect is as though it did, since as much current flows out of one plate as flows into the opposite one. This circuit concept may be extended to three dimensions by supposing that the resistor and capacitor elements each occupies a volume as in Fig. 8-18b. Fringing of the field is neglected. Inside each element the electric field E equals the voltage V across the element divided by its length d . That is, $E = V/d$. From (4-9-4) the current density J_1 inside the resistor equals the product of the electric field E and the conductivity σ of the medium inside the resistor element; it is also equal to i_1 divided by the cross-sectional area A . Or

$$J_1 = E\sigma = \frac{i_1}{A} \quad (2)$$

The dimensional form of (2) in SI units is

$$\frac{\text{Amperes}}{\text{Meter}^2} = \frac{\text{volts}}{\text{meter}} \times \frac{\text{mhos}}{\text{meter}}$$

The capacitance of a parallel-plate capacitor is $C = \epsilon A/d$, where A is the area of the plates and d is the spacing between them. Substituting this value for C , and $V = Ed$, into (1) yields

$$i_2 = \frac{\epsilon Ad}{d} \frac{dE}{dt} = \epsilon A \frac{dE}{dt} \quad (3)$$

Dividing (3) by the area A gives the relation that the current density J_2 inside the capacitor equals the permittivity of the nonconducting medium filling the capacitor element multiplied by the time rate of change of the electric field. Thus

$$\frac{i_2}{A} = J_2 = \epsilon \frac{dE}{dt} \quad (4)$$

The dimensions of (4) in SI units are

$$\frac{\text{Amperes}}{\text{Meter}^2} = \frac{\text{farads}}{\text{meter}} \times \frac{\text{volts/meter}}{\text{second}}$$

Recalling that $D = \epsilon E$, (4) becomes

$$J_2 = \frac{dD}{dt} \quad (5)$$

In this example J_1 is a conduction current density J_{cond} , while J_2 is a displacement current density J_{disp} . Also, since the current density \mathbf{J} , the electric displacement \mathbf{D} , and the electric field intensity \mathbf{E} are actually space vectors, which all have the same direction in isotropic media, (2) and (5) may be expressed in more general form as

$$\mathbf{J}_{\text{cond}} = \sigma \mathbf{E} \quad (6)$$

and $\mathbf{J}_{\text{disp}} = \epsilon \frac{d\mathbf{E}}{dt} = \frac{d\mathbf{D}}{dt} \quad (7)$

As a final step suppose that instead of having two separate elements in parallel, one of which acts like a pure resistance and the other like a pure capacitance, we have only one, which has both capacitance and resistance. Thus, as in Fig. 8-18c, there is a single element filled with a conducting dielectric so that both conduction and displacement currents are present. Then the total current density $\mathbf{J}_{\text{total}}$ is

$$\mathbf{J}_{\text{total}} = \mathbf{J}_{\text{cond}} + \mathbf{J}_{\text{disp}} \quad (8)$$

The concept of displacement current, or displacement-current density, was introduced by James Clerk Maxwell to account for the production of magnetic fields in empty space. Here the conduction current is zero, and the magnetic fields are due entirely to displacement currents.

8-14 MAXWELL'S EQUATION FROM AMPÈRE'S LAW: COMPLETE EXPRESSION

According to Ampère's law, the line integral of \mathbf{H} around a closed contour is equal to the current enclosed. Where both conduction and displacement currents are present, this current is the *total current*. Thus (5-15-1), which applies only to conduction currents, may be extended as follows when both conduction and displacement currents are present:

$$\oint \mathbf{H} \cdot d\mathbf{l} = \int_s (\mathbf{J}_{\text{cond}} + \mathbf{J}_{\text{disp}}) \cdot d\mathbf{s} \quad (1)$$

or

$$\oint \mathbf{H} \cdot d\mathbf{l} = \int_s \left(\sigma \mathbf{E} + \epsilon \frac{\partial \mathbf{E}}{\partial t} \right) \cdot d\mathbf{s} \quad (2)$$

The line integral of \mathbf{H} on the left side of (2) is around the boundary of the surface s over which the surface integral is taken on the right side of (2). Each term in (2) has the dimensions of current. The conduction current through the surface s is given by

$$\int_s \sigma \mathbf{E} \cdot d\mathbf{s}$$

while the displacement current through the surface s is given by

$$\int_s \epsilon \frac{\partial \mathbf{E}}{\partial t} \cdot d\mathbf{s}$$

Equation (2) is the complete expression in integral form of Maxwell's equation derived from Ampère's law. It is also often written

$$\oint \mathbf{H} \cdot d\mathbf{l} = \int_s \left(\mathbf{J} + \frac{\partial \mathbf{D}}{\partial t} \right) \cdot d\mathbf{s} \quad (3)$$

where \mathbf{J} without a subscript is understood to refer only to conduction current density.

By an application of Stokes' theorem to (3) or by an extension of (5-21-12) to include displacement currents, the complete expression in *differential form of Maxwell's equation derived from Ampère's law is*

$$\boxed{\nabla \times \mathbf{H} = \mathbf{J} + \frac{\partial \mathbf{D}}{\partial t}} \quad (4)$$

or

$$\nabla \times \mathbf{H} = \sigma \mathbf{E} + \epsilon \frac{\partial \mathbf{E}}{\partial t} \quad (5)$$

It should be noted that when the electric field varies harmonically with time ($\mathbf{E} = \mathbf{E}_0 \sin \omega t$), the conduction and displacement currents are in time-phase quadrature. That is,

$$\mathbf{J} = \sigma \mathbf{E} = \sigma \mathbf{E}_0 \sin \omega t \quad (6)$$

and $\frac{\partial \mathbf{D}}{\partial t} = \epsilon \frac{\partial \mathbf{E}}{\partial t} = \omega \epsilon \mathbf{E}_0 \cos \omega t \quad (7)$

Thus, when $\omega t = 0$, the displacement current is a maximum and the conduction current is zero. On the other hand, when $\omega t = \pi/2$, the conduction current is a maximum and the displacement current is zero. Since the displacement current is a maximum one-quarter cycle ($\omega t = \pi/2$) before the conduction current, it is said that the displacement current leads the conduction current by 90° . This is similar to the situation in a circuit having a resistor and a capacitor in parallel (Fig. 8-18a) in which the current "through" the capacitor leads the current through the resistor by 90° .

This phase difference can also be readily shown by expressing the time variation of the field by† $\mathbf{E} = \mathbf{E}_0 e^{j\omega t}$. The displacement current is then

$$\epsilon \frac{\partial \mathbf{E}}{\partial t} = \epsilon j \omega \mathbf{E}_0 e^{j\omega t} = j \omega \epsilon \mathbf{E} \quad (8)$$

Maxwell's equation (5) then becomes

$$\boxed{\nabla \times \mathbf{H} = \sigma \mathbf{E} + j \omega \epsilon \mathbf{E} = (\sigma + j \omega \epsilon) \mathbf{E}} \quad (9)$$

†In using this notation it is understood that the instantaneous value of the field is given by the imaginary part of $E_0 e^{j\omega t}$. Thus

$$\mathbf{E} (\text{instantaneous}) = \mathbf{E}_0 \text{Im } e^{j\omega t} = \mathbf{E}_0 \sin \omega t$$

One might also use the real part of $e^{j\omega t}$, which is equal to $\cos \omega t$ (that is, $\text{Re } e^{j\omega t} = \cos \omega t$). However, in any given analysis one convention or the other should be adopted and used consistently. Here it is understood to be the imaginary part.

The operator j in the displacement-current term and its absence in the conduction-current term signifies that the displacement current is advanced in phase by 90° with respect to the conduction current.

8-15 DIELECTRIC HYSTERESIS

In dielectrics that are good insulators the dc conduction current may be negligible. However, an appreciable ac current in phase with the applied field may be present because of *dielectric hysteresis*. This phenomenon is analogous to magnetic hysteresis in ferromagnetic materials. Materials, such as glass or plastics, which are good insulators under static conditions may consume considerable energy in alternating fields. The heat generated in this way is sometimes applied in industrial radio-frequency heating processes.

As explained in Sec. 3-5, the electron cloud of an atom in a dielectric becomes slightly displaced or asymmetrical when an electric field is applied. This produces an electric dipole (moment Ql), and the atom is said to be polarized. When the electric field is removed, the atom returns to its normal, or unpolarized, state. If the electric field is again applied but in the opposite direction, the dipole will be reversed. Thus, when an alternating field is applied to a dielectric atom, the dipole goes through the successive stages suggested in Fig. 8-19a. An equivalent mechanical system is shown in Fig. 8-19b. The large sphere represents the large mass of the nucleus. The small sphere (attached by a spring and moving through a tunnel in the large sphere) represents the small mass of the electron cloud.

The atom constitutes an electromechanical system with mass m , damping (or friction) coefficient d , and tension (or spring) constant s . The behavior of the system is described by †

$$m \frac{d^2l}{dt^2} + d \frac{dl}{dt} + sl = qE_0 e^{j\omega t} \quad (1)$$

where l = dipole length, or separation

q = dipole charge

The first term involves mass times acceleration, the second term damping coefficient times velocity, and the third term spring constant times displacement. The right-hand side is the driving force (qE_0 = peak force) resulting from the harmonically varying applied electric field. Equation (1) is a second-order differential equation

† P. Debye, "Polar Molecules," chap. 5, Chemical Catalog Company, Inc., New York, 1929.

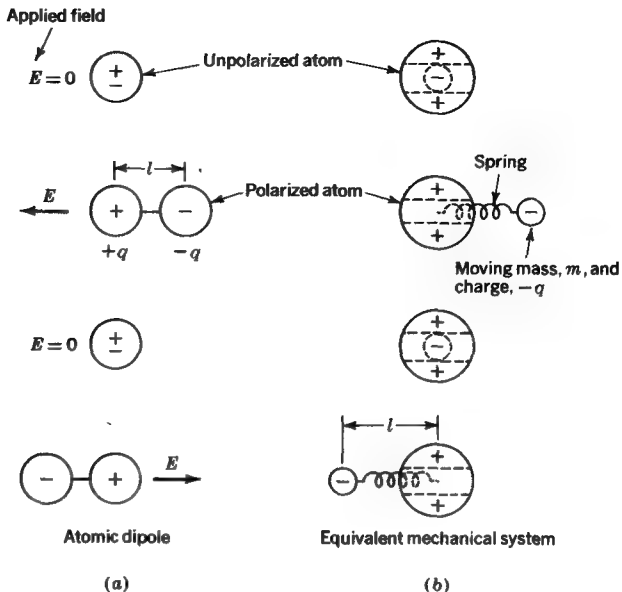


FIGURE 8-19

(a) Behavior of atomic dipole in alternating electric field and (b) equivalent mechanical system.

(of standard form) for a damped harmonic oscillation with a driving function. A solution is

$$l = l_0 e^{j\omega t} \quad (2)$$

where

$$l_0 = \frac{(q/m)E_0}{\omega_0^2 - \omega^2 + (j\omega d/m)} \quad (3)$$

where ω = driving radian frequency

ω_0 = resonant or natural radian frequency = $\sqrt{s/m}$ (for $d = 0$).

The resonant frequency ω_0 can be determined by solving (1) when $E_0 = 0$. From (3-6-1) the polarization or dipole moment per unit volume is

$$P = Nql = \frac{(Nq^2/m)E_0 e^{j\omega t}}{\omega_0^2 - \omega^2 + (j\omega d/m)} \quad (4)$$

where N is the number of polarized atoms per unit volume. Now $\epsilon = \epsilon_0 + P/E$. But $E = E_0 e^{j\omega t}$; so

$$\epsilon = \epsilon_0 + \frac{Nq^2/m}{\omega_0^2 - \omega^2 + (j\omega d/m)} \quad (5)$$

But writing

$$\epsilon = \epsilon' - j\epsilon''$$

we have

$$\epsilon' = \epsilon_0 \left[1 + \frac{(Nq^2/\epsilon_0 m)(\omega_0^2 - \omega^2)}{(\omega_0^2 - \omega^2)^2 + (wd/m)^2} \right] \quad (6)$$

$$\epsilon'' = \epsilon_0 \frac{(Nq^2/\epsilon_0 m)(wd/m)}{(\omega_0^2 - \omega^2)^2 + (wd/m)^2} \quad (7)$$

We observe that ϵ has real and imaginary parts which are both dependent on frequency.[†] Putting $\mathbf{J} = \sigma \mathbf{E}$ and $\epsilon = \epsilon' - j\epsilon''$ in Maxwell's equation $\nabla \times \mathbf{H} = \mathbf{J} + j\omega\epsilon\mathbf{E}$, we obtain

$$\boxed{\nabla \times \mathbf{H} = j\omega\epsilon'\mathbf{E} + (\sigma + \omega\epsilon'')\mathbf{E}} \quad (8)$$

It is apparent that ϵ'' (imaginary part of ϵ) is involved in a frequency-dependent term with the dimensions of conductance. At dc ($\omega = 0$ and therefore $\omega\epsilon'' = 0$) power loss is small in a good dielectric for which σ is small. However, at high frequencies (ω large) losses can become larger as $\omega\epsilon''$ becomes significant. The sum of σ and $\omega\epsilon''$ constitutes what may be called the *equivalent conductivity* σ' . Thus,

$$\sigma' = \sigma + \omega\epsilon'' \quad (9)$$

Now (8) can be expressed

$$\nabla \times \mathbf{H} = \mathbf{J}_{\text{total}} \quad (10)$$

It follows that

$$\mathbf{J}_{\text{total}} = \sigma' \mathbf{E} + j\omega\epsilon' \mathbf{E} \quad (11)$$

Referring to Fig. 8-20, we see that the total-current density $\mathbf{J}_{\text{total}}$ is the sum of a conduction-current density ($\sigma' \mathbf{E}$) and a displacement-current density $j\omega\epsilon' \mathbf{E}$ in time-phase quadrature. From Fig. 8-20 we have

$$\tan \delta = \frac{\sigma'}{\omega\epsilon'} \quad (12)$$

The quantity $\tan \delta$ is called the *loss tangent*. Also the cosine of the angle $\theta (= 90^\circ - \delta)$ is the *power factor* (PF). Thus (for small δ)

$$\text{PF} = \cos \theta \simeq \tan \delta = \frac{\sigma'}{\omega\epsilon'} \quad (13)$$

[†] Probs. 8-32 and 8-33 illustrate how ϵ' and ϵ'' change with frequency. Over very wide frequency ranges (radio to ultraviolet) materials may exhibit several such resonances and associated permittivity changes due to various vibrational modes.

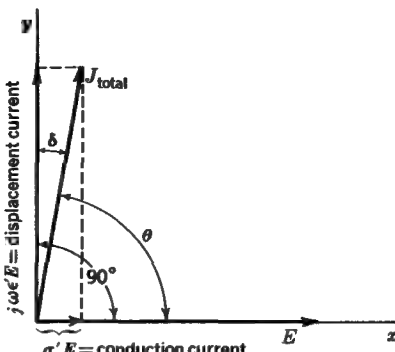


FIGURE 8-20
Time-phase diagram for dielectric with losses.

The power dissipated per unit volume is

$$p = \frac{\text{power}}{\text{volume}} = \frac{\text{current voltage}}{\text{area length}} = JE = \sigma'E^2 \quad (\text{W m}^{-3}) \quad (14)$$

EXAMPLE Find the average power dissipated per cubic meter in a nonconducting dielectric medium with relative permittivity of 4 and a loss tangent of 0.001 if $E = 1 \text{ kV m}^{-1}$ rms and the frequency is 10 MHz.

SOLUTION Since $\sigma = 0$, $\sigma' = \omega\epsilon''$ and $\tan \delta = \sigma'/\omega\epsilon' = \epsilon''/\epsilon'$, or $\epsilon'' = \epsilon' \tan \delta$ and since $\tan \delta$ is small, $\epsilon'' \ll \epsilon'$ and $\epsilon' \approx \epsilon$; so $\sigma' = \omega\epsilon' \tan \delta \approx \omega\epsilon \tan \delta$, or

$$\sigma' \approx 2\pi \times 10^7 \times 4 \times 8.85 \times 10^{-12} \times 10^{-3} = 2.22 \mu\text{S m}^{-1}$$

The power p dissipated per unit volume is then

$$p = E^2\sigma' = 10^6 \times 2.22 \times 10^{-6} = 2.22 \text{ W m}^{-3}$$

It is to be noted that the current density and the field intensity have the same space direction in isotropic media. Although both may have the same space direction, their scalar magnitudes may have different time phase. Thus, in the above discussion the space directions are the same and are fixed, but the scalar magnitude J_{total} of the total-current density leads the scalar magnitude E of the electric field intensity in time by the phase angle θ . Thus, on a time phase diagram, such as Fig. 8-20, J_{total} and E may be represented by vectors separated in direction by an angle θ . Such a pseudo vector used to represent the time phase of a scalar quantity is often called a *phasor*. A dot (·) is sometimes added when it is desired to indicate explicitly that the quantity is a complex function of time, i.e., a *phasor*.

Thus†

$$\mathbf{E} = \hat{\mathbf{a}} \dot{\mathbf{E}} = \hat{\mathbf{a}} E_0 e^{j\omega t} \quad (15)$$

where $\hat{\mathbf{a}}$ = unit (space) vector in direction of \mathbf{E}

$\dot{\mathbf{E}} = E_0 e^{j\omega t}$ = vector representation of time phase (phasor)

E_0 = amplitude of $\dot{\mathbf{E}}$

In (15) the quantity $E_0 e^{j\omega t}$ is a scalar function of the time. However, it may be represented on the complex plane by a vector (or phasor) of magnitude E_0 that rotates counterclockwise one revolution per cycle. This may be made more obvious by writing $\dot{\mathbf{E}}$ in its equivalent polar form. That is,

$$\dot{\mathbf{E}} = E_0 / \underline{\omega t} \quad (16)$$

which is interpreted to mean a vector (or phasor) of magnitude E_0 at an angle ωt with respect to some reference direction (usually the real or x axis). Hence, when $t = 0$, the phasor is in the positive x direction. One-quarter of a period later ($t = T/4$ and $\omega t = \pi/2$) the phasor has rotated 90° to the positive y direction. At $t = T/2$ the phasor has rotated a total of 180° to the negative x direction, etc.

It is understood that the instantaneous magnitude of the electric field intensity E is given by the real (Re) part or imaginary (Im) part of $\dot{\mathbf{E}}$. When it is taken equal to the imaginary part, the instantaneous value of the electric field intensity is

$$E = \hat{\mathbf{a}} \operatorname{Im} \dot{\mathbf{E}} = \hat{\mathbf{a}} \operatorname{Im} E_0 e^{j\omega t} = \hat{\mathbf{a}} E_0 \sin \omega t \quad (17)$$

Referring to (11), it is understood that E in this equation is a phasor as given by $E_0 e^{j\omega t}$ or $E_0 / \underline{\omega t}$. It follows that Fig. 8-20 shows the position of E and the other phasors at $t = 0$. As a function of time the entire diagram rotates counterclockwise one revolution per cycle, and the instantaneous value of any of the quantities is given by its projection on the y axis.

8-16 BOUNDARY RELATIONS

The boundary relations given in Tables 3-2 and 6-2 for the tangential and normal components of static electric and magnetic fields also hold for time-varying fields. This can be shown as follows. Consider first the tangential components E_t of the

† The quantity \mathbf{E} is not only a space vector but also a function of time (phasor). Thus, it may be called a vector-phasor and designated by \mathbf{E} (= $\hat{\mathbf{a}} \dot{\mathbf{E}}$). In general, we shall use the dot over a quantity only where we wish to indicate explicitly that it is a complex function of the time, i.e., a phasor. The fact that a quantity is a space vector is indicated by using boldface (heavy) type. In longhand notation a space vector may be designated by a bar placed above or below the letter.

electric field (see Fig. 3-5). Instead of using the relation that $\oint \mathbf{E} \cdot d\mathbf{l} = 0$ for a closed path, which is true for static fields due to charges, we should, in the time-varying case, use Maxwell's equation from Faraday's law

$$\oint \mathbf{E} \cdot d\mathbf{l} = - \int_s \frac{\partial \mathbf{B}}{\partial t} \cdot d\mathbf{s} \quad (1)$$

If there is a flux density \mathbf{B} normal to the rectangular path (half in each medium) and \mathbf{B} changes with time, then $\oint \mathbf{E} \cdot d\mathbf{l}$ is not zero if the path encloses a finite area. However, it is assumed that the dimension Δy approaches zero so that E_{t1} and E_{t2} are separated by only an infinitesimal distance. Therefore the area of the rectangle approaches zero, and the surface integral of $\partial \mathbf{B} / \partial t$ vanishes. Thus the work around the path is given by $E_{t1} \Delta x - E_{t2} \Delta x = 0$, as before, and it follows that $E_{t1} = E_{t2}$ holds for both static and time-varying situations.

Consider next the tangential components of the \mathbf{H} field (see Fig. 6-14). Instead of using the relation $\oint \mathbf{H} \cdot d\mathbf{l} = \iint \mathbf{J} \cdot d\mathbf{s}$ for steady fields, we should, in the time-varying case, use Maxwell's equation from Ampère's law in its complete form,

$$\oint \mathbf{H} \cdot d\mathbf{l} = \int_s \left(\mathbf{J} + \frac{\partial \mathbf{D}}{\partial t} \right) \cdot d\mathbf{s} \quad (2)$$

If there is a time-changing \mathbf{D} normal to the rectangular path (half in each medium), there will be a contribution due to \mathbf{D} . However, it is assumed that the dimension Δy approaches zero, so that the surface integral of $\partial \mathbf{D} / \partial t$ vanishes. In (2) the conduction-current density \mathbf{J} may also change with time. However, its surface integral also vanishes as Δy approaches zero unless the conduction current is assumed to exist in an infinitesimally thin layer at the conductor surface. Thus, for a sheet current of linear density K at the surface

$$H_{t1} - H_{t2} = K \quad (3)$$

as before, while in the absence of such a sheet

$$H_{t1} = H_{t2} \quad (4)$$

as before. Thus, the relations for the tangential \mathbf{H} field of Table 6-2 hold for both static and time-changing situations.

The formal approach in obtaining the continuity relations for the normal components of \mathbf{D} and \mathbf{B} is the same under time-varying conditions as for static conditions, and the relations given in Tables 3-2 and 6-2 apply under both conditions.

Table 8-1 summarizes the boundary relations developed for electric and magnetic fields. These relations apply under all situations, except as noted.

Table 8-1 BOUNDARY RELATIONS FOR ELECTRIC AND MAGNETIC FIELDS

Field component	Boundary relation	Condition
Tangential	$E_{t1} = E_{t2}$ (1)	Any two media
Tangential	$E_{t1} = 0$ (2)	Medium 2 is a perfect conductor ($\sigma_2 = \infty$)†
Tangential	$H_{t1} = H_{t2}$ (3)	Any two media
Tangential	$H_{t1} - H_{t2} = K$ (4)‡	Current sheet at boundary
Tangential	$H_{t1} = K$ (5)‡	Medium 2 is a perfect conductor ($\sigma_2 = \infty$) with current sheet at surface
Tangential	$H_{t1} = 0$ (6)	Medium 2 has infinite permeability ($\mu_2 = \infty$) (no currents)
Normal	$D_{n1} - D_{n2} = \rho_s$ (7)	Any two media with charge at boundary
Normal	$D_{n1} = D_{n2}$ (8)	Any two media with no charge at boundary
Normal	$D_{n1} = \rho_s$ (9)	Medium 2 is a perfect conductor with charge at surface
Normal	$B_{n1} = B_{n2}$ (10)	Any two media

† Under static conditions it suffices for medium 2 to be a conductor (σ_2 finite). However, for E_{t2} to be zero under time-varying conditions requires that $\sigma_2 = \infty$ (see Chap. 10).

‡ Note that although K and the components of H are measured parallel to the boundary, they are normal to each other. Thus, in vector notation (5) is expressed by $K = \hat{n} \times H$, where \hat{n} = unit vector normal to the boundary.

8-17 GENERAL FIELD RELATIONS

In Chap. 5 it was shown that the divergence of the curl of a vector function F is zero. Thus,

$$\nabla \cdot (\nabla \times F) = 0 \quad (1)$$

As a corollary, any vector function with no divergence must be the curl of some other vector function. Thus, if $\nabla \cdot G = 0$, we can write $G = \nabla \times F$, where F is some other vector function. As an example, $\nabla \cdot B = 0$, so that B can be expressed as the curl of a vector potential ($B = \nabla \times A$).

It was also shown in Chap. 5 that the curl of the gradient of a scalar function f is zero. Thus $\nabla \times (\nabla f) = 0$. As a corollary, any vector function with no curl is the gradient of some scalar function. Thus, if $\nabla \times \mathbf{F} = 0$, we can write $\mathbf{F} = \nabla g$, where g is a scalar function. As an example, the curl of the static electric field due to electric charges is zero ($\nabla \times \mathbf{E} = 0$). It follows that a static electric field due to charges may be expressed as the gradient of a scalar function. That is, $\mathbf{E} = -\nabla V$, where V is the electric scalar potential.

According to Maxwell's equation derived from Faraday's law, we note, however, that in time-changing situations the curl of the electric field is not zero but is equal to the time rate of decrease of \mathbf{B} . Thus

$$\nabla \times \mathbf{E} = -\frac{\partial \mathbf{B}}{\partial t} \quad (2)$$

Since $\nabla \times \mathbf{E}$ is not zero, the relation $\mathbf{E} = -\nabla V$ is not sufficient for time-varying fields. An additional term is required. This may be found as follows. Since $\mathbf{B} = \nabla \times \mathbf{A}$, (2) becomes

$$\nabla \times \mathbf{E} = -\frac{\partial(\nabla \times \mathbf{A})}{\partial t} \quad (3)$$

from which

$$\nabla \times \left(\mathbf{E} + \frac{\partial \mathbf{A}}{\partial t} \right) = 0 \quad (4)$$

Since the curl of the expression in parentheses in (4) equals zero, it must be equal to the gradient of a scalar function. Thus we can write

$$\mathbf{E} + \frac{\partial \mathbf{A}}{\partial t} = \nabla f \quad (5)$$

where f is a scalar function. If the electric scalar potential V is taken to be this scalar function, a relation is obtained that satisfies the requirements for both static and time-varying situations. Thus let $f = -V$, so that from (5) we have

$$\mathbf{E} = -\nabla V - \frac{\partial \mathbf{A}}{\partial t} \quad (6)$$

For static fields this reduces to $\mathbf{E} = -\nabla V$, as it should. In the general case, where the field may vary with time, \mathbf{E} is given by both a scalar potential V and a vector potential \mathbf{A} , as in (6). If the time variation is harmonic, (6) becomes

$$\mathbf{E} = -\nabla V - j\omega \mathbf{A} \quad (7)$$

When the vector potential \mathbf{A} and the scalar potential V are known, the electric and magnetic fields can be obtained under static or time-varying situations from the relations

$$\mathbf{E} = -\nabla V - \frac{\partial \mathbf{A}}{\partial t} \quad (\text{V m}^{-1}) \quad (8)$$

and

$$\mathbf{B} = \nabla \times \mathbf{A} \quad (\text{T}) \quad (9)$$

where

$$V = \frac{1}{4\pi\epsilon_0} \int_v \frac{\rho}{r} dv \quad (\text{V}) \quad (10)$$

and

$$\mathbf{A} = \frac{\mu}{4\pi} \int_v \frac{\mathbf{J}}{r} dv \quad (\text{Wb m}^{-1}) \quad (11)$$

It is assumed that the distance r in the expressions for V and \mathbf{A} is small compared with a wavelength, so that propagation-time effects can be neglected. If this is not the case, the propagation time must be considered and the more general retarded form used for ρ and \mathbf{J} , as explained in Chap. 14.

8-18 COMPARISON OF ELECTRIC AND MAGNETIC FIELD RELATIONS

In Table 5-2 a comparison is made of electric and magnetic field equations. All of these apply in static or slowly time-varying situations. Certain of the relations can be extended so as apply under rapidly time-varying conditions. These relations are listed in Table 8-2. It is to be noted that under static conditions the time derivatives

Table 8-2 COMPARISON OF THE ELECTRIC AND MAGNETIC FIELD RELATIONS FOR TIME-CHANGING SITUATIONS

Description of equation	Electric field	Magnetic field
Curl equations (point relations)	$\nabla \times \mathbf{E} = -\frac{\partial \mathbf{B}}{\partial t}$	$\nabla \times \mathbf{H} = \mathbf{J} + \frac{\partial \mathbf{D}}{\partial t}$
Closed path of integration	$\nabla \cdot \mathbf{E} = \oint \mathbf{E} \cdot d\mathbf{l} = - \int_s \frac{\partial \mathbf{B}}{\partial t} \cdot ds$	$\nabla \cdot \mathbf{H} = \oint \mathbf{H} \cdot d\mathbf{l} = \int_s \left(\mathbf{J} + \frac{\partial \mathbf{D}}{\partial t} \right) \cdot ds$
Derivation of fields from scalar and vector potentials†	$\mathbf{E} = -\nabla V - \frac{\partial \mathbf{A}}{\partial t}$	$\mathbf{B} = \nabla \times \mathbf{A}$

† V and \mathbf{A} are as indicated in (8-17-10) and (8-17-11).

are zero, and these relations reduce to the corresponding special cases given in Table 5-2. These static relations (Table 5-2) are also applicable in time-changing situations provided the variations are slow enough to permit the time derivatives to be neglected. In more rapidly time-varying situations, where the time derivatives cannot be neglected, the expressions of Table 8-2 must be employed.

PROBLEMS

- * 8-1 (a) A 3-turn loop with 0.5 m^2 area situated in air has a uniform magnetic field normal to the plane of the loop. If the flux density changes 5 mT s^{-1} , what is the emf appearing at the terminals of the loop? (b) If the emf at the loop terminals is 100 mV , what is the rate of change of the magnetic field?
- * 8-2 How many turns are required for a square loop 100 mm on a side to develop a maximum emf of 10 mV rms if the loop rotates 30 r s^{-1} in the earth's magnetic field? Take $B = 60 \mu\text{T}$.
- * 8-3 A uniform magnetic field $B = 100 \text{ mT}$ extends over a square area 100 mm on a side, as in Fig. P8-3, with zero field outside. A rectangular wire loop $40 \text{ by } 80 \text{ mm}$ is moved through the field with a velocity $v = 100 \text{ mm s}^{-1}$. Find the emf induced in the loop and plot the results on a graph of emf vs. the distance x for $-20 \leq x \leq 120 \text{ mm}$.
- * 8-4 Is the direction of the current I in the closed loop at the right of Fig. P8-4 clockwise (cw) or counterclockwise (ccw) when the switch is (a) closed and (b) opened?
- * 8-5 A wire pendulum with brush swings normal to a uniform magnetic field of 250 mT , as shown in Fig. P8-5. The velocity of any point on the pendulum at a distance r from its support point is given by $v = \omega d(r/R) \cos \omega t$, where d is the maximum horizontal displacement or half amplitude. If the length R of the pendulum is 4 m , its period T at the earth's surface will be about 4 s [$T(\text{s}) = 2\pi \sqrt{R(\text{m})/9.8 (\text{m s}^{-2})}$]. Using this value for the period, determine the peak emf appearing at the terminals if $d = 100 \text{ mm}$.

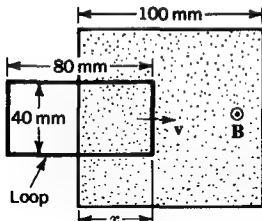


FIGURE P8-3
Moving loop.

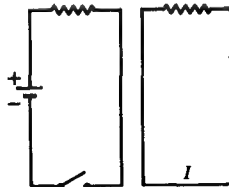


FIGURE P8-4
Stationary loops.

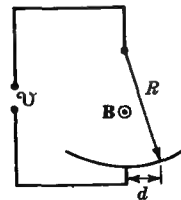


FIGURE P8-5
Pendulum.

* Answers to starred problems are given in Appendix C.

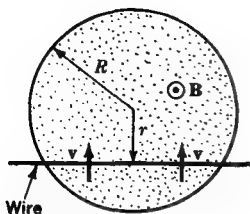


FIGURE P8-6
Moving wire.

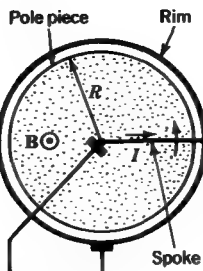


FIGURE P8-7
Moving spoke.

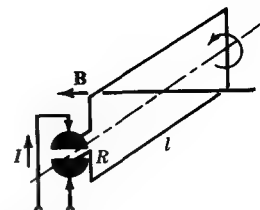


FIGURE P8-9
Dc machine.

- ★ 8-6 Find the emf induced in a straight wire moving perpendicular to a uniform magnetic field B with velocity v as in Fig. P8-6. The magnetic field is confined to the radius R of the pole pieces of a magnet.
- ★ 8-7 A conducting wheel of rim and single spoke rotates perpendicular to a uniform magnetic field B (Fig. P8-7). The magnetic field is confined to a radius R of the pole pieces of a magnet. An external circuit makes contact with the axle and rim through brushes. (a) If the wheel is rotated $N \text{ r s}^{-1}$, find the emf induced in the circuit. (b) If a current I is sent through the circuit, find the torque on the wheel. (c) If the current flows as shown, is the torque cw or ccw?

8-8 If the one-spoked wheel of Prob. 8-7 is replaced by a solid metal disk, what difference (if any) occurs in both generator and motor cases?

8-9 If a rectangular loop rotating in a uniform magnetic field B is equipped with a two-segment commutator, as in Fig. P8-9, the arrangement can function as either a dc generator or a motor. (a) If the loop rotates $N \text{ r s}^{-1}$, find the average dc voltage generated. (b) If a current I flows in the loop, find the average torque. (c) If the current flows as shown, find the rotation direction (cw or ccw). Assume commutator gap is negligible.

- ★ 8-10 A 5-turn wire loop of 0.5 m^2 area is situated in air in the presence of a 2-MHz radio wave. If the loop develops an emf of 10 mV rms when oriented for maximum response, find the rms magnetic field H of the wave.

- ★ 8-11 (a) A thin copper disk 300 mm in diameter is situated with its plane normal to a constant, uniform magnetic field $B = 600 \text{ mT}$. If the disk rotates 30 r s^{-1} , find the emf developed at the terminals connected to brushes as shown in Fig. P8-11. One brush contacts the periphery of the disk and the other contacts the axle or shaft. This arrangement is called a *Faraday disk generator*. (b) If the magnetic field varies with time, as given by $B = B_0 \sin \omega t$, where $B_0 = 600 \text{ mT}$ and $\omega = 2\pi \times 5 \text{ rad s}^{-1}$, find the emf developed at the terminals.

8-12 (a) A rectangular nonconducting trough 3 m wide carries a uniform flow of brackish water 250 mm deep with a velocity $v = 3 \text{ m s}^{-1}$. The water has a conductivity $\sigma = 1 \text{ S m}^{-1}$. If conducting plates 500 mm wide by 250 mm deep are placed at the sides of

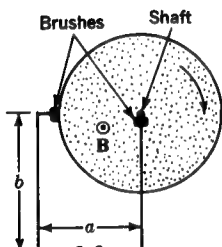


FIGURE P8-11
Faraday disk generator.

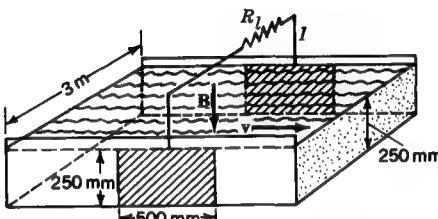


FIGURE P8-12
Water generator.

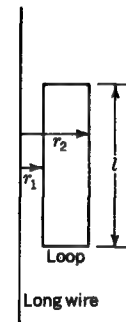


FIGURE P8-17
Wire and loop.

the trough and a magnetic field $B = 1 \text{ T}$ is impressed, as shown in Fig. P8-12, find the current I flowing in a load resistor $R_L = 10 \Omega$. Neglect resistance of plates and connecting wires. (b) Find the power delivered to the load. (c) Is this the maximum power which can be delivered to a load if R_L is variable? (d) Discuss the practical aspects of using a similar system to generate electric power directly from the flow of water in a large river using the earth's magnetic field. (e) Could the system be used to measure the velocity of flow of a river? If so, explain how such variables as depth and conductivity could be accommodated. (f) Can the arrangement of Fig. P8-12 be modified so that it can be used to pump a conducting liquid?

- * 8-13 A short bar magnet of 6 A m^2 magnetic moment rotates around its center point at 5 r s^{-1} . A 50-turn loop of 1 m^2 area is located 8 m from the bar magnet. Find the maximum rms emf induced in the loop by the magnet.

- 8-14 A toroid of 500 turns has a mean radius of 250 mm and a radius for the winding of 15 mm. Find the average inductance for (a) an air core and (b) an iron core with average relative incremental permeability of 750.

- * 8-15 What is the mutual inductance of an ideal transformer if a 60-Hz current of 2 A rms applied to the primary induces 6 V rms at the secondary terminals?

- 8-16 (a) Find the mutual inductance per unit length for two long straight parallel wires with separation s . (b) If the current in one wire is I , find the emf induced per unit length in the other wire if it is at a separation s and approaching at a velocity v .

- 8-17 Find the mutual inductance between a long straight wire and a rectangular wire loop as in Fig. P8-17.

- 8-18 Find the mutual inductance between two concentric circular wire loops of radius r_1 and r_2 (a) when the radius of the inner loop is much smaller than the outer loop and (b) without this restriction.

- * 8-19 A fixed square 8-turn wire loop has corners at (x,y) values of $(0,0)$, $(2,0)$, $(0,3)$, and $(2,3)$ m. If a magnetic field normal to the loop varies as a function of position, as given

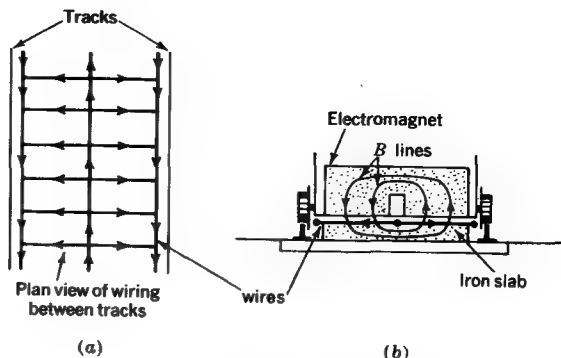


FIGURE P8-20
Linear motor for track-guided vehicle.

by $B = 5 \sin(\pi x/2) \cos(\pi y/3)$, find the rms emf induced in the loop if B also varies harmonically with time at 500 Hz.

8-20 (a) Design a linear dc motor for propelling and braking a track-guided vehicle. The wheels are not to be used for traction or braking except in emergency. The vehicle contains no power source other than that for magnetic field generation, and no power is supplied to the vehicle from any external source. Currents in the track region are controlled from the vehicle by radio command. Figure P8-20 shows a suggested scheme. (b) What current and magnetic field are required to accelerate a 50×10^3 kg vehicle from 0 to 100 km hr^{-1} in 60 s? The track width is 1.5 m. Neglect friction. [For other arrangements see E. R. Laithwaite, Linear Motion Electrical Machines, *Proc. IEEE*, 58:531–542 (April 1970).]

8-21 A copper conductor of diameter $d = 10$ mm is formed into a circular loop of radius $R = 215$ mm and connected to a parallel-plate capacitor, as in Fig. P8-21. The capacitor plates are square (side length $l = 100$ mm) and spaced a distance $s = 5$ mm apart. The medium is air. If the loop is placed in the field of a 40-MHz radio wave with $H = 4$ mA m^{-1} , and if the equivalent (series) resistance of the loop-capacitor circuit is 3Ω , find

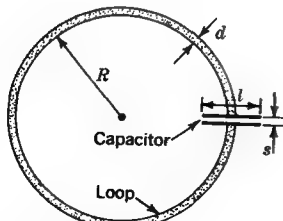


FIGURE P8-21
Radio loop.

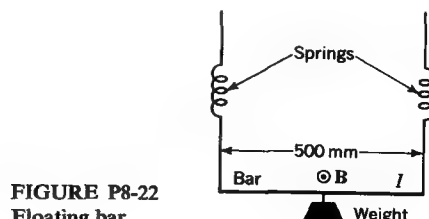


FIGURE P8-22
Floating bar.

(a) the rms displacement current density in the capacitor and (b) the rms voltage across the capacitor. (c) Repeat (a) and (b) if the frequency of the wave is adjusted to the resonant frequency of the circuit. Assume H is unchanged. Note: The dc resistance of the loop is only about 0.0002Ω , but its radiation resistance (see Chap. 14) is about 3Ω .

8-22 A straight conducting bar with weight attached is suspended by wire springs in a uniform magnetic field B as in Fig. P8-22. The length of the bar is 500 mm. Find the current I (magnitude and direction) required to "float" or balance the bar and weight if $B = 2 \text{ T}$ and the mass of the bar and weight is 5 kg.

* 8-23 Find the displacement-current density of a magnetic field in air given by (a) $H_y = H_0 \sin(\omega t - \beta x)$, (b) $\mathbf{H} = kH_x \sin 2x \sin(\omega t - \beta y) + 2H_z \sin 2x \cos(\omega t - \beta y)$.

8-24 A parallel-plate air capacitor has a $1,000-\Omega$ resistor connected between the centers of the plates. The plates are 100 mm square and separated by 1 mm. If 10 V rms is applied to the capacitor, find (a) rms displacement current through the capacitor, (b) rms conduction current, (c) total current, and (d) power dissipated in resistor at each of the following frequencies: (1) 1 Hz, (2) 1 kHz, (3) 1 MHz, and (4) 1 GHz. Make a table with four columns for the quantities (a), (b), (c), and (d) and four rows for the four different frequencies. Neglect fringing. Discuss the significance of the results.

8-25 Given that the average power dissipated per unit volume of a medium is $E(dD/dt) \cos \theta \text{ W m}^{-3}$, where θ is the time-phase angle between E and D , show that the total average power dissipated in a parallel-plate capacitor is $VI \cos \theta$ (W), where V = voltage across capacitor and I = current through capacitor. Neglect fringing. E , D , V , and I are rms values.

* 8-26 A parallel-plate capacitor is filled with a dielectric of 0.003 power factor and $\epsilon_r = 10$. The plates are 250 mm square, and the distance between is 10 mm. If 500 V rms at 2 MHz is applied to the capacitor, find the power dissipated as heat.

8-27 A coil of 60 turns and $1,000 \text{ mm}^2$ area has its plane normal to a magnetic field. If the charge flowing through the coil is measured to be 1 mC when the coil is flipped 180° , find B . The coil and attached measuring circuit have a resistance of 100Ω .

8-28 The average flux density inside the electron orbit of a betatron is given by $B = 60 \text{ mT}$, where $\omega = 2\pi \times 60 \text{ rad s}^{-1}$. If the radius of the electron orbit is 120 mm, find (a) velocity of electrons at $t = 1 \text{ ms}$ if $v \approx 0$ at $t = 0$, (b) energy per unit charge imparted to the electron per revolution, (c) number of revolutions in 1 ms, and (d) electron energy (in electron volts) after 1 ms. Neglect relativistic effects.

8-29 Is it true that any machine which functions satisfactorily as a generator will also work as a motor when a voltage is applied which is of the same type as that generated?

8-30 A bar magnet is attached perpendicular to an axle shaft which extends along the centerline of a cylindrical container of conducting fluid, as in Fig. P8-30. (a) If a current I is passed axially through the conducting fluid, will the device operate as a motor? (b) If the shaft with magnet is rotated, will the device operate as a generator?

8-31 A Faraday disk generator with superconducting solenoid is shown in cross section in Fig. P8-31. The disk has a radius of 100 mm, and it rotates at $3,600 \text{ r min}^{-1}$. If $B = 3 \text{ T}$, find (a) the required solenoid sheet-current density and (b) the emf generated. (See *Machine Design*, Nov. 11, 1971, p. 18.)

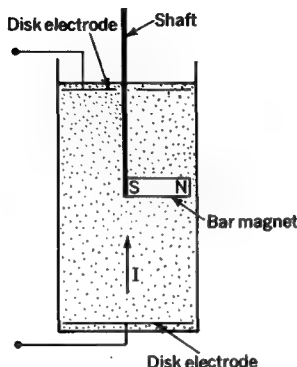


FIGURE P8-30
Magnet in conducting fluid.

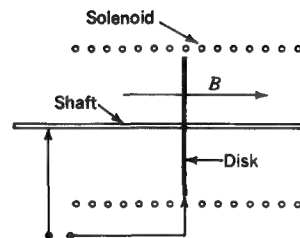


FIGURE P8-31
Faraday disk in superconducting solenoid.

8-32 (a) The permittivity of ice is a function of both temperature and frequency. In E. R. Pounder, "Physics of Ice," p. 129, Pergamon Press, New York, 1965, the complex relative permittivity is given by $\epsilon_r = \epsilon'_r - j\epsilon''_r$ and the Drude-Debye relations by

$$\epsilon'_r = \frac{\epsilon_1 + \epsilon_2 \alpha^2 f^2}{1 + \alpha^2 f^2} \quad \text{and} \quad \epsilon''_r = \frac{(\epsilon_1 - \epsilon_2)\alpha f}{1 + \alpha^2 f^2}$$

where T = temperature, °C

f = frequency, Hz

and where for pure water ice $\epsilon_1 = 75$, $\epsilon_2 = 3$, $\alpha = 1.2 \times 10^{-4} e^{-0.1T}$ (s). The relations are applicable from 0 to 10 GHz and from 0 to -70°C . The effect of impurities is not included, but they would probably increase the magnitude of the imaginary part (ϵ''_r). Calculate the complex relative permittivity of pure water ice at 0°C at 0, 1, 10, and 100 Hz; 1, 10, and 100 kHz; and 1, 10, and 100 MHz. (b) Calculate the equivalent conductivity σ' as a function of frequency (0 to 100 MHz). Take $\sigma = 0$. (c) Make a log-log graph of ϵ'_r , ϵ''_r , and σ' as a function of frequency; also a linear graph of ϵ'_r , ϵ''_r , and σ' vs. log frequency.

8-33 Setting the constants $Nq^2/\epsilon_0 m$ and d/m equal to unity, calculate the variation of ϵ'_r and ϵ''_r from (8-15-6) and (8-15-7) as a function of ω for $\omega_0 = 1$. Display results graphically in both log-log and linear-log form, as in Prob. 8-32.

8-34 A homogeneous 200-cc 200-g Idaho potato has a relative permittivity $\epsilon_r = 65 - j15$. If $E(\text{rms}) = 30 \text{ kV m}^{-1}$ at 2.45 GHz (alongside potato), how long will it take to bake the potato? Take $\sigma = 0$. [See N. E. Bengtsson and P. O. Risman, Dielectric Properties of Foods at 3 GHz, *J. Microwave Power*, 6(2): 107-123 (1972).]

8-35 Metal detectors operate on several principles. In one design a coil and capacitor form the resonant circuit of an oscillator at say 100 kHz. The introduction of a metal object into the field of the coil changes, or detunes, the oscillator frequency, and this change is noted. Another design operates on the null principle. Thus, two flat exciter coils are

placed side by side in the same plane. Both are connected to the oscillator (~ 100 kHz modulated at ~ 500 Hz), but the coils are so connected that the field between them is zero (balanced out). A third detector, or search coil, is situated at this point. Its rectified output is connected to an audio amplifier and transducer. When a metal object is introduced into the field, a voltage is induced in the search coil, producing an audible 500-Hz tone. (a) Design a device for detecting automobiles for traffic-light control at a highway intersection. (b) Design a device for locating buried pipes or coins. (c) Discuss the pros and cons of frequency-shift vs. null-principle designs for the above applications. (d) Can these detectors be used to locate dielectric bodies or anomalies?

9

THE RELATION BETWEEN FIELD AND CIRCUIT THEORY; MAXWELL'S EQUATIONS

9-1 INTRODUCTION

In circuit theory we deal with circuit elements, the voltage V across them, and the total current I through them. In field theory we deal with the field vectors (\mathbf{E} , \mathbf{D} , \mathbf{B} , \mathbf{H} , and \mathbf{J}) and their values as a function of position.

Consider, for instance, a short rod of length l and cross-sectional area A in Fig. 9-1. In low-frequency-circuit theory it is convenient to describe the rod in terms of one quantity, its resistance R . Its length, area, and shape are of secondary importance. Thus the voltage difference between the ends of the rod is, from Ohm's law,

$$V = IR \quad (1)$$

where I is the current through the rod.

From the field-theory point of view we consider the value of the electric field \mathbf{E} at a point in the rod. From Ohm's law at a point (see Sec. 4-9)

$$\mathbf{E} = \frac{\mathbf{J}}{\sigma} \quad (\text{V m}^{-1}) \quad (2)$$

where \mathbf{J} = conduction current density, A m^{-2}

σ = conductivity, $\Omega \text{ m}^{-1}$

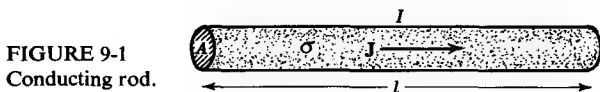


FIGURE 9-1
Conducting rod.

Now, integrating (2) over the length of the rod, we obtain the voltage difference V between the ends. That is,

$$V = \int \mathbf{E} \cdot d\mathbf{l} = \int \frac{\mathbf{J}}{\sigma} \cdot d\mathbf{l} \quad (3)$$

For a uniform rod with uniform current density this becomes

$$V = \frac{Jl}{\sigma} = JA \frac{l}{\sigma A} \quad (V) \quad (4)$$

where $JA = I$ = current through rod, A

$l/\sigma A = R$ = resistance of rod, Ω

A = cross-sectional area of rod, m^2

Thus, from (4) we have

$$V = IR \quad (5)$$

Starting with field theory, we have arrived at the circuit relation known as *Ohm's law*.

Historically, this and other circuit relations were postulated and verified first. Then, as a generalization, they were extended to apply to the more general field situation. It follows, therefore, that circuit relations are simply special cases of field equations and may be deduced from them. Although field relations are more general, it is usually much simpler to use circuit equations wherever they are applicable.

Equation (1) is a pure circuit relation. On the other hand, (2) is a pure field relation. Many equations are not purely one or the other but are a combination or mixture. Such mixed relations are necessary, for example, in order to provide a connection between field and circuit theory. Two important equations that provide such connecting links are

$$V = \int \mathbf{E} \cdot d\mathbf{l} \quad (V) \quad (6)$$

and

$$I = \oint \mathbf{H} \cdot d\mathbf{l} \quad (A) \quad (7)$$

Equation (6) relates V (a circuit quantity) between two points to the line integral of \mathbf{E} (a field quantity) between those points. Likewise (7), which is Ampère's law, relates I (a circuit quantity) to the line integral of \mathbf{H} (a field quantity) around a closed path.

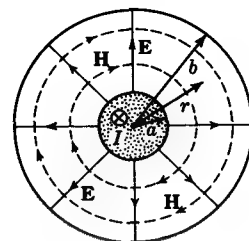


FIGURE 9-2

Coaxial transmission line with Transverse ElectroMagnetic (TEM) mode. E-lines are radial and solid. H-lines are circles and dashed.

9-2 APPLICATIONS OF CIRCUIT AND FIELD THEORY

While field relations are applicable in general, circuit relations are usually more convenient wherever V and I have a simple, well-defined significance.

Thus, in determining the capacitance of a capacitor of irregular shape with the aid of a graphical field map (see Fig. 3-19) we are in effect directing our attention to the field and its value as a function of position in the capacitor. However, once we have determined the capacitance, we may at low frequencies consider it as simply a two-terminal circuit element of capacitance C with a voltage difference V . The physical size and shape of the capacitor and the field configuration within it are then relegated to positions of secondary importance.

As another illustration let us consider the coaxial transmission line shown in cross section in Fig. 9-2 under two conditions, one where V and I are useful quantities and one where they are not. The coaxial line has an inner conductor of radius a and an outer conductor of inside radius b . With a steady potential difference between the conductors the electric field lines are radial, as shown. If a current I is flowing, the magnetic field lines \mathbf{H} are circles, as indicated. Now by (9-1-6) the potential difference between the inner and outer conductors is

$$V = \int_a^b \mathbf{E} \cdot d\mathbf{r} \quad (V) \quad (1)$$

Likewise from (9-1-7) the current I in the inner conductor is

$$I = \oint \mathbf{H} \cdot d\mathbf{l} = \int_0^{2\pi} H_r r d\theta \quad (A) \quad (2)$$

In (1) V is independent of the path between the conductors, while in (2) I is independent of the radius r provided it is between a and b . Hence, V and I have a simple, definite significance in this case and are useful quantities.

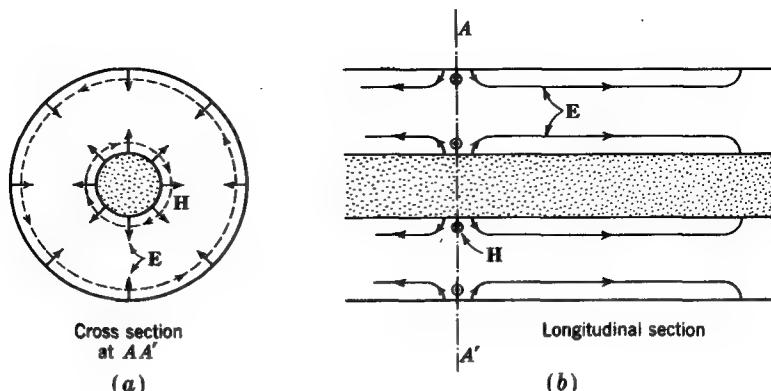


FIGURE 9-3
Coaxial transmission line with higher-order Transverse Magnetic (TM) mode.

The field configuration shown in Fig. 9-2 is called a *Transverse ElectroMagnetic* (TEM) *field* because the electric and magnetic field are entirely transverse (no component in the axial direction). This type of field is the only configuration or field mode possible under steady conditions and for time-varying situations where the wavelength is of the order of $4b$ or greater.[†] At higher frequencies (shorter wavelengths) more complex field configurations known as higher-order modes become possible. These modes are characterized by having some field components in the axial direction. Although coaxial lines are seldom used under such conditions, suppose that the frequency is sufficiently high for the mode or configuration shown in Fig. 9-3 to exist. Both a cross (or transverse) section and a longitudinal (or axial) section are needed to show the field configuration. This field is called a *Transverse Magnetic* (TM) *mode* because the magnetic field is entirely transverse, while the electric field has a longitudinal component. For this mode, the voltage V between the conductors as obtained by (1) may become negligible, while the current I obtained by (2) depends on the radius r at which \mathbf{H} is integrated. Hence V and I no longer have a simple significance and are not as useful as the field quantities themselves. The breakdown of the circuit concept occurred here when the transverse dimensions became comparable with the wavelength.

[†] That is, the frequency is so high that a disturbance traveling with the velocity of light can travel only about a distance equal to the diameter ($2b$) in one-half period. In free space a wave has a wavelength λ in meters that is related to the frequency f in hertz by the velocity of light c as follows: $\lambda = c/f$, where $c = 300 \text{ Mm s}^{-1}$. For a further discussion of field modes in lines and guides see Chap. 13.

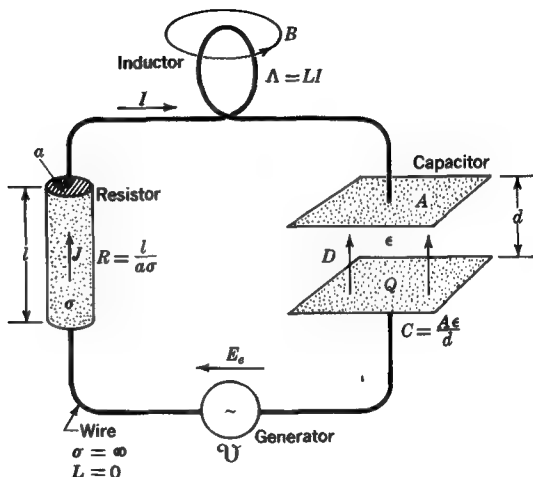


FIGURE 9-4

Series circuit with resistance, inductance, capacitance and ac generator used to illustrate equivalence of field and circuit theory.

9-3 THE SERIES CIRCUIT; COMPARISON OF FIELD AND CIRCUIT THEORY

From (4-10-1) we may express the total electric field $\mathbf{E}_{\text{total}}$ as the sum of a field \mathbf{E}_e related to emfs and a field \mathbf{E} induced by charges and currents. Thus,

$$\mathbf{E}_{\text{total}} = \mathbf{E}_e + \mathbf{E} \quad \text{or} \quad \mathbf{E}_e = \mathbf{E}_{\text{total}} - \mathbf{E} \quad (1)$$

From (4-9-4)

$$\mathbf{E}_{\text{total}} = \frac{\mathbf{J}}{\sigma} \quad (2)$$

and from (8-17-8)

$$\mathbf{E} = -\nabla V - \frac{\partial \mathbf{A}}{\partial t} \quad (3)$$

Consider now a series circuit of resistance, inductance, and capacitance connected to a generator as shown in Fig. 9-4. It is assumed that all resistance in the circuit is confined to the resistor, all inductance to the inductor, all capacitance to the capacitor, and all emf to the generator. Let us apply the above field relations to this circuit.

First substitute (2) and (3) in (1). Then to convert field into circuit quantities we integrate all terms completely around the circuit in a clockwise direction. This gives

$$\oint \mathbf{E}_e \cdot d\mathbf{l} = \oint \frac{\mathbf{J}}{\sigma} \cdot d\mathbf{l} + \oint \nabla V \cdot d\mathbf{l} + \oint \frac{\partial \mathbf{A}}{\partial t} \cdot d\mathbf{l} \quad (4)$$

Integrating the left side yields the emf \mathcal{V} of the generator. Also integrating the first two terms on the right and noting that $\nabla V = -\mathbf{E}$, we have

$$\mathcal{V} = \frac{Jl}{\sigma} + Ed + \frac{d}{dt} \oint \mathbf{A} \cdot d\mathbf{l} \quad (5)$$

But $J = I/a$ and $E = D/\epsilon$. The last term may be reexpressed as†

$$\frac{d}{dt} \oint \mathbf{A} \cdot d\mathbf{l} = \frac{dI}{dt} \oint \frac{\mathbf{A}}{I} \cdot d\mathbf{l} = L \frac{dI}{dt} \quad (6)$$

where $L = \oint \frac{\mathbf{A}}{I} \cdot d\mathbf{l}$ = inductance of circuit

$$\mathbf{A} = \frac{\mu_0}{4\pi} \int_v \frac{\mathbf{J}}{r} dv = \text{vector potential}$$

In this way (5) becomes

$$\mathcal{V} = I \frac{l}{a\sigma} + \frac{Dd}{\epsilon} + L \frac{dI}{dt} \quad (7)$$

Now $l/a\sigma = R$ and $D = Q/A$; so we have

$$\mathcal{V} = IR + \frac{Q}{A\epsilon/d} + L \frac{dI}{dt} \quad (8)$$

But $A\epsilon/d = C$ and the charge $Q = \int I dt$; so (8) takes the form

$$\mathcal{V} = IR + \frac{1}{C} \int I dt + L \frac{dI}{dt} \quad (9)$$

Thus, beginning with the field relations (1), (2), and (3) as applied to a series circuit, we have arrived at the familiar circuit relation (9) for a series circuit.

† The transformation of (6) may be also made with the aid of Stokes' theorem, recalling that $\mathbf{B} = \nabla \times \mathbf{A}$ and $\Delta = LI$, as follows:

$$\frac{d}{dt} \oint \mathbf{A} \cdot d\mathbf{l} = \frac{d}{dt} \int_s (\nabla \times \mathbf{A}) \cdot d\mathbf{s} = \frac{d}{dt} \int_s \mathbf{B} \cdot d\mathbf{s} = \frac{d\Delta}{dt} = L \frac{dI}{dt}$$

where L = inductance of loop

I = current through loop

For harmonic variation of the current with respect to time ($I = I_0 e^{j\omega t}$) we obtain

$$\mathfrak{U} = IR + \frac{I}{j\omega C} + j\omega LI \quad (10)$$

or

$$\boxed{\mathfrak{U} = IR + jI \left(\omega L - \frac{1}{\omega C} \right)} \quad (11)$$

In deriving (11) the assumption was made that at any instant the current is the same at all parts of the circuit. This implies that a disturbance is propagated around the circuit instantaneously. If the circuit length is small compared with the wavelength, this is a satisfactory assumption. However, if the circuit length is appreciable compared with the wavelength (say at least $\lambda/8$), the variation in current and phase around the circuit may become significant. Under these circumstances the simple circuit concepts tend to become inadequate and inaccurate. It is also to be noted that the above circuit treatment ignores the phenomenon of radiation, which is so important at high frequencies (see Chap. 14).

There are certain exceptions to the above statement that circuit concepts become inadequate when the circuit length is comparable with the wavelength. For example, circuit concepts are successfully applied to the long transmission line. In this case, the distributed inductance and capacitance are represented by suitable lumped elements (see Chap. 13). Although the length of the line can be many wavelengths, it is significant that even in this extension of circuit theory the treatment is adequate only for lines with transverse dimensions that are very small compared with the wavelength.

9-4 MAXWELL'S EQUATIONS AS GENERALIZATIONS OF CIRCUIT EQUATIONS†

In the remainder of this chapter a number of relations developed in the preceding chapters are brought together and considered as a group. These relations, known as *Maxwell's equations*, consist of four expressions: one derived from Ampère's law, one from Faraday's law, and two derived from Gauss' law. These equations are of profound importance and, together with boundary, continuity, and other auxiliary relations, form the basic tools for the analysis of most electromagnetic problems.

† James Clerk Maxwell, "A Treatise on Electricity and Magnetism," 2 vols., Oxford University Press, London, 1873; 3rd ed., 1904.

In Chap. 5 Ampère's law relating the line integral of \mathbf{H} around a closed path to the current I enclosed was given as

$$\oint \mathbf{H} \cdot d\mathbf{l} = I \quad (1)$$

Replacing the current I by the surface integral of the conduction-current density \mathbf{J} over an area bounded by the path of integration of \mathbf{H} , we have the more general relation

$$\oint \mathbf{H} \cdot d\mathbf{l} = \int_s \mathbf{J} \cdot ds \quad (2)$$

In Chap. 8 this relation was made even more general by adding a displacement-current density to the conduction-current density so that (2) becomes

$$\boxed{\oint \mathbf{H} \cdot d\mathbf{l} = \int_s \left(\mathbf{J} + \frac{\partial \mathbf{D}}{\partial t} \right) \cdot ds} \quad (3)$$

This relation is called *Maxwell's equation as derived from Ampère's law*. In (3) it is given in its integral form, the line integral of \mathbf{H} being taken over a closed path bounding the surface s . In circuit parlance a closed path or loop is often called a *mesh*. Hence, (3) is a *mesh relation*. Applying Stokes' theorem to (3), we obtain the corresponding *point relation*

$$\boxed{\nabla \times \mathbf{H} = \mathbf{J} + \frac{\partial \mathbf{D}}{\partial t}} \quad (4)$$

Equation (4) is a differential relation and relates the field quantities at a point. It is the differential form of Maxwell's equation as derived from Ampère's law.

In Chap. 8 Faraday's law relating the emf \mathcal{V} induced in a circuit to the time rate of decrease of the total magnetic flux linking the circuit was given as

$$\mathcal{V} = - \frac{d\Lambda}{dt} \quad (5)$$

Replacing the flux linkage Λ by the surface integral of \mathbf{B} over the area bounded by the circuit, we have the more general equation

$$\mathcal{V} = - \frac{d}{dt} \int_s \mathbf{B} \cdot ds \quad (6)$$

Replacing \mathcal{V} in (6) by the line integral of \mathbf{E} around the circuit, we have the still more general relation (for stationary circuits) that

$$\boxed{\oint \mathbf{E} \cdot d\mathbf{l} = - \int_s \frac{\partial \mathbf{B}}{\partial t} \cdot ds} \quad (7)$$

This field relation is a generalization of Faraday's circuit law (5). Equation (7) is called *Maxwell's equation as derived from Faraday's law*. It is given in (7) in integral form, i.e., it is a mesh equation. The corresponding point relation can be obtained from (7) by an application of Stokes' theorem, yielding

$$\boxed{\nabla \times \mathbf{E} = -\frac{\partial \mathbf{B}}{\partial t}} \quad (8)$$

Equation (8) is a differential relation and relates the field quantities at a point. It is the differential form of Maxwell's equation as derived from Faraday's law.

In Chap. 2 Gauss' law relating the surface integral of the electric flux density \mathbf{D} to the charge Q enclosed was given as

$$\oint_s \mathbf{D} \cdot d\mathbf{s} = Q \quad (9)$$

Replacing Q in (9) by the volume integral of the charge density ρ throughout the volume enclosed by the surface s , we can write (9) in a more general form as

$$\boxed{\oint_s \mathbf{D} \cdot d\mathbf{s} = \int \rho dv} \quad (10)$$

This field relation is a generalization of Gauss' law and is called *Maxwell's electric field equation as derived from Gauss' law*. In (10) it appears in integral form and applies to a finite volume v . Applying (10) to an infinitesimal volume, we can obtain the corresponding differential relation that relates the field quantities at a point as given by

$$\boxed{\nabla \cdot \mathbf{D} = \rho} \quad (11)$$

Equation (11) is Maxwell's electric field equation as derived from Gauss' law in differential form.

For magnetic fields the surface integral of \mathbf{B} over a closed surface s yields zero. Thus the magnetic counterpart of Gauss' electric field relation (9) is

$$\boxed{\oint_s \mathbf{B} \cdot d\mathbf{s} = 0} \quad (12)$$

The corresponding differential or point relation is

$$\boxed{\nabla \cdot \mathbf{B} = 0} \quad (13)$$

Equations (12) and (13) may be referred to as *Maxwell's magnetic field equations as derived from Gauss' law*, (12) being the integral and (13) the differential form.

The development of Maxwell's equations as generalizations of circuit relations involves both inductive and physical reasoning. It is not implied that the "derivation" is rigorous. Maxwell's equations are justified by the fact that conclusions based on them have been found in innumerable cases to be in excellent agreement with experiment, in the same way that the earlier circuit relations are justified within their more restricted domain by the excellent agreement of conclusions based on them with experiment. It is perhaps worth recalling that Maxwell's equations were *not* generally accepted for many years after they were postulated (1873). His curl equations (involving $\nabla \times \mathbf{E}$ and $\nabla \times \mathbf{H}$) implied that time-varying electric and magnetic fields in empty space were interdependent, a changing electric field being able to generate a magnetic field, and vice versa. The inference from this is that a time-changing electromagnetic field would propagate energy through empty space with the velocity of light (see Chap. 10) and, further, that light is electromagnetic in nature. Radio waves were unknown at the time, and it was 15 years (1888) before Hertz demonstrated that electromagnetic (or radio) waves were possible, as predicted by Maxwell.

There is no guarantee that Maxwell's equations are exact. However, insofar as the precision of experimental measurements allow, they appear to be, and therefore we may regard them as exact.

Along with Maxwell's equations certain other fundamental relations are of importance in dealing with electromagnetic problems. Among these may be mentioned Ohm's law at a point (4-9-4)

$$\boxed{\mathbf{J} = \sigma \mathbf{E}} \quad (14)$$

the continuity relation (4-13-3)

$$\boxed{\nabla \cdot \mathbf{J} = -\frac{\partial \rho}{\partial t}} \quad (15)$$

the force relations

$$\boxed{\begin{aligned} \mathbf{F} &= q\mathbf{E} \\ d\mathbf{F} &= (\mathbf{I} \times \mathbf{B}) dl \end{aligned}} \quad (16)$$

and the constitutive *relations* between \mathbf{E} and \mathbf{D} and between \mathbf{B} and \mathbf{H} as given by

$$\boxed{\mathbf{D} = \epsilon \mathbf{E} = \epsilon_0 \mathbf{E} + \mathbf{P}} \quad (17)$$

$$\boxed{\mathbf{B} = \mu \mathbf{H} = \mu_0 (\mathbf{H} + \mathbf{M})} \quad (18)$$

9-5 MAXWELL'S EQUATIONS IN FREE SPACE

In the preceding section, Maxwell's equations are stated in their general form. For the special case of free space, where the current density \mathbf{J} and the charge density ρ are zero, the equations reduce to a simpler form. In integral form the equations are

$$\oint_s \mathbf{H} \cdot d\mathbf{l} = \int_s \frac{\partial \mathbf{D}}{\partial t} \cdot d\mathbf{s} \quad (1)$$

$$\oint_s \mathbf{E} \cdot d\mathbf{l} = - \int_s \frac{\partial \mathbf{B}}{\partial t} \cdot d\mathbf{s} \quad (2)$$

$$\oint_s \mathbf{D} \cdot d\mathbf{s} = 0 \quad (3)$$

$$\oint_s \mathbf{B} \cdot d\mathbf{s} = 0 \quad (4)$$

In differential form the equations are

$$\nabla \times \mathbf{H} = \frac{\partial \mathbf{D}}{\partial t} \quad (5)$$

$$\nabla \times \mathbf{E} = - \frac{\partial \mathbf{B}}{\partial t} \quad (6)$$

$$\nabla \cdot \mathbf{D} = 0 \quad (7)$$

$$\nabla \cdot \mathbf{B} = 0 \quad (8)$$

9-6 MAXWELL'S EQUATIONS FOR HARMONICALLY VARYING FIELDS

If we assume that the fields vary harmonically with time, Maxwell's equations can be expressed in another special form. Thus, if \mathbf{D} varies with time as given by

$$\mathbf{D} = \mathbf{D}_0 e^{j\omega t} \quad (1)$$

then $\frac{\partial \mathbf{D}}{\partial t} = j\omega \mathbf{D}_0 e^{j\omega t} = j\omega \mathbf{D}$ (2)

When the same assumption is made for \mathbf{B} , Maxwell's equations in integral form reduce to

$$\oint_s \mathbf{H} \cdot d\mathbf{l} = (\sigma + j\omega\epsilon) \int_s \mathbf{E} \cdot d\mathbf{s} \quad (3)$$

$$\oint_s \mathbf{E} \cdot d\mathbf{l} = -j\omega\mu \int_s \mathbf{H} \cdot d\mathbf{s} \quad (4)$$

$$\oint_s \mathbf{D} \cdot d\mathbf{s} = \int_s \rho \, dv \quad (5)$$

$$\oint_s \mathbf{B} \cdot d\mathbf{s} = 0 \quad (6)$$

In differential form they are

$$\nabla \times \mathbf{H} = (\sigma + j\omega\epsilon)\mathbf{E} \quad (7)$$

$$\nabla \times \mathbf{E} = -j\omega\mu\mathbf{H} \quad (8)$$

$$\nabla \cdot \mathbf{D} = \rho \quad (9)$$

$$\nabla \cdot \mathbf{B} = 0 \quad (10)$$

9-7 TABLES OF MAXWELL'S EQUATIONS

Maxwell's equations are summarized in Tables 9-1 and 9-2. Table 9-1 gives Maxwell's equations in integral form and Table 9-2 in differential form. The equations are stated for the general case, free-space case, harmonic-variation case, steady case (static fields but with steady conduction currents), and static case (static fields with no currents). In Table 9-1 the equivalence is also indicated between the various field quantities and the electric potential V , the emf \mathcal{V} , the magnetic potential U , the mmf F , the total current I_{total} , the displacement current I_{disp} , the conduction current I_{cond} , the electric flux ψ , and the magnetic flux ψ_m . It should be noted that Maxwell's equations as tabulated here apply specifically to stationary systems or bodies at rest.

Table 9-1 MAXWELL'S EQUATIONS IN INTEGRAL FORM

Dimensions and SI Case units	From Ampère mmf, A		From Faraday		From Gauss	
	emf, V			Electric flux, C	Magnetic flux, Wb	
General	$F = \oint_s \mathbf{H} \cdot d\mathbf{l} = \int_s \left(\mathbf{J} + \frac{\partial \mathbf{D}}{\partial t} \right) \cdot d\mathbf{s} = I_{\text{total}}$	$\nabla U = \oint_s \mathbf{E} \cdot d\mathbf{l} = - \int_v \frac{\partial \mathbf{B}}{\partial t} \cdot d\mathbf{s}$	$\psi = \oint_s \mathbf{D} \cdot d\mathbf{s} = \int_v \rho \, dv$	$\psi_m = \oint_s \mathbf{B} \cdot d\mathbf{s} = 0$		
Free space	$F = \oint_s \mathbf{H} \cdot d\mathbf{l} = \int_s \frac{\partial \mathbf{D}}{\partial t} \cdot d\mathbf{s} = I_{\text{disp}}$	$\nabla U = \oint_s \mathbf{E} \cdot d\mathbf{l} = - \int_v \frac{\partial \mathbf{B}}{\partial t} \cdot d\mathbf{s}$	$\psi = \oint_s \mathbf{D} \cdot d\mathbf{s} = 0$	$\psi_m = \oint_s \mathbf{B} \cdot d\mathbf{s} = 0$		
Harmonic variation	$F = \oint_s \mathbf{H} \cdot d\mathbf{l} = (\sigma + j\omega\epsilon) \int_s \mathbf{E} \cdot d\mathbf{s} = I_{\text{total}}$	$\nabla U = \oint_s \mathbf{E} \cdot d\mathbf{l} = -j\omega\mu \int_s \mathbf{H} \cdot d\mathbf{s}$	$\psi = \oint_s \mathbf{D} \cdot d\mathbf{s} = \int_v \rho \, dv$	$\psi_m = \oint_s \mathbf{B} \cdot d\mathbf{s} = 0$		
Steady	$F = \oint_s \mathbf{H} \cdot d\mathbf{l} = \int_s \mathbf{J} \cdot d\mathbf{s} = I_{\text{cond}}$	$V = \oint_s \mathbf{E} \cdot d\mathbf{l} = 0$	$\psi = \oint_s \mathbf{D} \cdot d\mathbf{s} = \int_v \rho \, dv$	$\psi_m = \oint_s \mathbf{B} \cdot d\mathbf{s} = 0$		
Static	$U = \oint_s \mathbf{H} \cdot d\mathbf{l} = 0$	$V = \oint_s \mathbf{E} \cdot d\mathbf{l} = 0$	$\psi = \oint_s \mathbf{D} \cdot d\mathbf{s} = \int_v \rho \, dv$	$\psi_m = \oint_s \mathbf{B} \cdot d\mathbf{s} = 0$		

Table 9-2 MAXWELL'S EQUATIONS IN DIFFERENTIAL FORM

Case	Dimensions	From Ampère	From Faraday	From Gauss	
		Electric current area	Electric potential area	Electric flux volume	Magnetic flux volume
General		$\nabla \times \mathbf{H} = \mathbf{J} + \frac{\partial \mathbf{D}}{\partial t}$	$\nabla \times \mathbf{E} = -\frac{\partial \mathbf{B}}{\partial t}$	$\nabla \cdot \mathbf{D} = \rho$	$\nabla \cdot \mathbf{B} = 0$
Free space		$\nabla \times \mathbf{H} = \frac{\partial \mathbf{D}}{\partial t}$	$\nabla \times \mathbf{E} = -\frac{\partial \mathbf{B}}{\partial t}$	$\nabla \cdot \mathbf{D} = 0$	$\nabla \cdot \mathbf{B} = 0$
Harmonic variation		$\nabla \times \mathbf{H} = (\sigma + j\omega\epsilon)\mathbf{E}$	$\nabla \times \mathbf{E} = -j\omega\mu\mathbf{H}$	$\nabla \cdot \mathbf{D} = \rho$	$\nabla \cdot \mathbf{B} = 0$
Steady		$\nabla \times \mathbf{H} = \mathbf{J}$	$\nabla \times \mathbf{E} = 0$	$\nabla \cdot \mathbf{D} = \rho$	$\nabla \cdot \mathbf{B} = 0$
Static		$\nabla \times \mathbf{H} = 0$	$\nabla \times \mathbf{E} = 0$	$\nabla \cdot \mathbf{D} = \rho$	$\nabla \cdot \mathbf{B} = 0$

PROBLEMS

9-1 (a) Starting with Ampère's law, derive Maxwell's equation in integral form based on this law. (b) Obtain the corresponding differential or point relation by applying Stokes' theorem.

9-2 (a) Starting with Faraday's law, derive Maxwell's equation in integral form based on this law. (b) Obtain the corresponding differential or point relation by applying Stokes' theorem.

9-3 (a) Starting with Gauss' law for electric fields, derive Maxwell's equation in integral form based on this law. (b) Obtain the corresponding differential or point relation.

9-4 (a) Starting with Gauss' law applied to magnetic fields, derive Maxwell's equation in integral form based on this law. (b) Obtain the corresponding differential or point relation.

* 9-5 Why are Maxwell's equations not completely symmetrical?

9-6 (a) State Maxwell's equations in their general integral form. (b) Derive them for harmonically varying fields.

9-7 (a) State Maxwell's equations in their general differential form. (b) Derive them for harmonically varying fields.

* 9-8 A long cylindrical conductor of radius R and $\sigma = \infty$ carries a current $I = I_0 \sin \omega t$. As a function of radius r (for $r < R$ and $r > R$) find (a) the conduction-current density $J(r)$, (b) the displacement-current density $J_d(r)$, and (c) the magnetic flux density $B(r)$.

* Answers to starred problems are given in Appendix C.

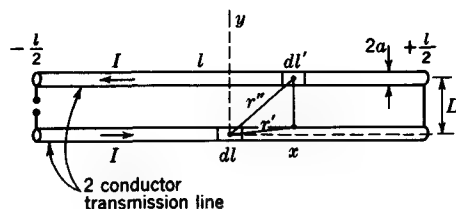


FIGURE P9-14
Two-conductor transmission line.

- * 9-9 A parallel-plate capacitor with plates of radius R and separation d has a voltage applied at the center as given by $V = V_0 \sin \omega t$. As a function of radius r (for $r < R$) find (a) the displacement-current density $J_d(r)$ and (b) the magnetic field $H(r)$. Take $d \ll R$.
- * 9-10 The magnetic field between two pole pieces of radius R varies as $B = B_0 [1 - \frac{1}{2}(\beta r)^2] \sin \omega t$. Assume $R \ll \lambda$. Find the displacement-current density as a function of radius r (for $r < R$).
- * 9-11 A long solenoid of radius R carries a sheet-current density $K = K_0 \sin \omega t$. Find the displacement-current density J_d as a function of radius r (for $r < R$).

9-12 Show that

$$\int_s \frac{\partial \mathbf{B}}{\partial t} \cdot d\mathbf{s} = \oint \frac{\partial \mathbf{A}}{\partial t} \cdot d\mathbf{l}$$

9-13 Show that the expression for the low-frequency inductance $L = \oint (A/I) \cdot dI$ reduces for a conducting circuit to Neumann's low-frequency inductance formula

$$L = \frac{\mu_0}{4\pi} \oint \oint \frac{dI'}{r} \cdot dI$$

9-14 A two-conductor transmission line of length l has a conductor (center-to-center) separation D and conductor radius a . The conductors are thin-walled tubes. Referring to Fig. P9-14, apply Neumann's low-frequency inductance formula (Prob. 9-13) to show that the inductance of the line is

$$L = \frac{\mu_0 l}{\pi} \ln \frac{D}{a} \quad (\text{H})$$

Compare with (5-13-12). Assume $l \gg D$, and neglect end effects.

9-15 Apply field theory to a circuit consisting of a resistor, inductor, and capacitor connected in parallel with an alternating-current source I . Proceeding in an analogous manner to that used for the series circuit in Sec. 9-3, show that

$$I = \frac{V}{R} + C \frac{dV}{dt} + \frac{1}{L} \int V dt$$

where V = voltage across parallel combination

R = resistance of resistor

C = capacitance of capacitor

L = inductance of inductor

PLANE WAVES IN DIELECTRIC AND CONDUCTING MEDIA

10-1 INTRODUCTION

The interdependence of electric and magnetic fields is demonstrated in a striking manner by an electromagnetic wave propagating through space. In such a wave the time-changing magnetic field may be regarded as generating a time-varying electric field, which in turn generates a magnetic field, and as the process repeats, energy is propagated through empty space at the velocity of light.

The first part of this chapter deals largely with a plane wave in free space (vacuum). This discussion also applies to any lossless† isotropic dielectric medium. In the last part of the chapter propagation through a conducting medium ($\sigma \neq 0$) is considered.

10-2 PLANE WAVES AND THE WAVE EQUATION

The field lines for a wave propagating toward the reader (out of the page) are indicated in Fig. 10-1. The directions of \mathbf{E} and \mathbf{H} are everywhere perpendicular. In a uniform plane wave \mathbf{E} and \mathbf{H} lie in a plane and have the same value everywhere in that plane.

† Referring to Sec. 8-15, lossless implies that $\epsilon'' = 0$, so that $\epsilon = \epsilon'$, and further that $\sigma = 0$.

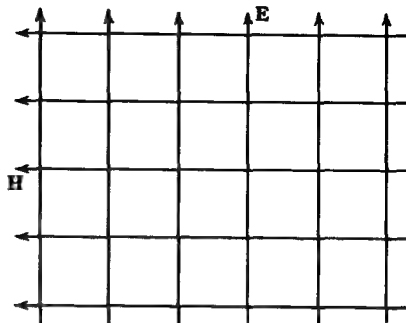


FIGURE 10-1
Plane traveling wave approaching reader (out of page).

A wave of this type with both \mathbf{E} and \mathbf{H} transverse to the direction of propagation is called a *Transverse ElectroMagnetic (TEM)* wave.

Referring to Fig. 10-2, assume that a plane wave is traveling in the direction of the x axis. The electric field \mathbf{E} has only a component E_y in the y direction and the magnetic field \mathbf{H} only a component H_z in the z direction. It is said that this wave is polarized in the y direction (vertically polarized) (see Chap. 11).

Since we are dealing with a nonconducting medium, the conduction-current density \mathbf{J} is zero. Thus Maxwell's equation from Ampère's law reduces to

$$\nabla \times \mathbf{H} = \frac{\partial \mathbf{D}}{\partial t} \quad (1)$$

or in rectangular coordinates

$$\hat{x} \left(\frac{\partial H_z}{\partial y} - \frac{\partial H_y}{\partial z} \right) + \hat{y} \left(\frac{\partial H_x}{\partial z} - \frac{\partial H_z}{\partial x} \right) + \hat{z} \left(\frac{\partial H_y}{\partial x} - \frac{\partial H_x}{\partial y} \right) = \frac{\partial}{\partial t} (\hat{x} D_x + \hat{y} D_y + \hat{z} D_z) \quad (2)$$

For a plane wave traveling in the x direction the only components of (2) that contribute are

$$-\hat{y} \frac{\partial H_z}{\partial x} = \hat{y} \frac{\partial D_y}{\partial t} \quad (3)$$

Therefore

$$\frac{\partial H_z}{\partial x} = -\epsilon \frac{\partial E_y}{\partial t} \quad (4)$$

Maxwell's equation from Faraday's law is

$$\nabla \times \mathbf{E} = -\frac{\partial \mathbf{B}}{\partial t} \quad (5)$$

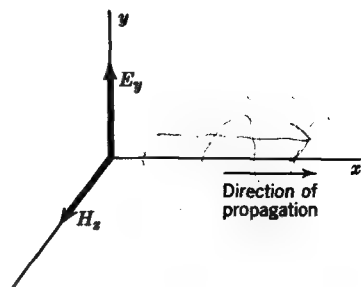


FIGURE 10-2
Field components of plane wave with relation to coordinate system.

or in rectangular coordinates

$$\hat{x}\left(\frac{\partial E_z}{\partial y} - \frac{\partial E_y}{\partial z}\right) + \hat{y}\left(\frac{\partial E_x}{\partial z} - \frac{\partial E_z}{\partial x}\right) + \hat{z}\left(\frac{\partial E_y}{\partial x} - \frac{\partial E_x}{\partial y}\right) = -\frac{\partial}{\partial t}(\hat{x}B_x + \hat{y}B_y + \hat{z}B_z) \quad (6)$$

For a plane wave traveling in the x direction the only components of (6) that contribute are†

$$\hat{z}\frac{\partial E_y}{\partial x} = -\hat{z}\frac{\partial B_x}{\partial t} \quad (7)$$

Therefore

$$\frac{\partial E_y}{\partial x} = -\mu \frac{\partial H_z}{\partial t} \quad (8)$$

Equation (4) relates the space derivative of H_z to the time derivative of E_y , while (8) relates the space derivative of E_y to the time derivative of H_z . By differentiating (4) with respect to time t and (8) with respect to distance x , H_z can be eliminated and an expression obtained for E_y in terms of t and x . Proceeding in this way, we obtain, from (4),

$$\frac{\partial}{\partial t} \left(\frac{\partial H_z}{\partial x} \right) = -\epsilon \frac{\partial^2 E_y}{\partial t^2} \quad (9)$$

and, from (8),

$$\frac{\partial^2 E_y}{\partial x^2} = -\mu \frac{\partial}{\partial x} \left(\frac{\partial H_z}{\partial t} \right) \quad (10)$$

† If we had specified only that the wave is linearly polarized with \mathbf{E} in the y direction and that the wave travels in the x direction, it follows from (6) and also from (7) that \mathbf{B} and hence \mathbf{H} must be in the z direction.

Dividing (10) by $-\mu$ yields

$$-\frac{1}{\mu} \frac{\partial^2 E_y}{\partial x^2} = \frac{\partial}{\partial x} \left(\frac{\partial H_z}{\partial t} \right) \quad (11)$$

Since in (9) it does not matter whether we differentiate first with respect to x and then with respect to t or vice versa, the left-hand side of (9) is equal to the right-hand side of (11) and it follows that

$$\frac{\partial^2 E_y}{\partial t^2} = \frac{1}{\mu\epsilon} \frac{\partial^2 E_y}{\partial x^2}$$

(12)

Equation (12) relates the space and time variation of the scalar magnitude E_y , of the electric field intensity and is called a *wave equation* in E_y . It is, in fact, a scalar wave equation of the simplest form.

Differentiating (4) and (8) in the reverse order, i.e., (4) with respect to x and (8) with respect to t , we can eliminate E_y and obtain a wave equation in H_z as

$$\frac{\partial^2 H_z}{\partial t^2} = \frac{1}{\mu\epsilon} \frac{\partial^2 H_z}{\partial x^2} \quad (13)$$

Both (12) and (13) are of the same form. A wave equation as given by (12) and (13) has many important physical applications and is sometimes called *D'Alembert's equation*, having been integrated by him in 1747. If E_y in (12) is a transverse displacement, the equation can represent the motion of a disturbance on a stretched string. This was D'Alembert's problem. If E_y is a mechanical compression, the equation can describe the motion of small oscillations of air in a narrow pipe. In our case E_y represents the scalar magnitude of the electric field intensity of a plane electromagnetic wave progressing in the x direction, and the equation is the most general way of describing the motion of this field as a function of time and space.

Let us now introduce a quantity v in (12) such that

$$v^2 = \frac{1}{\mu\epsilon}$$

(14)

Equation (12) then becomes

$$\frac{\partial^2 E_y}{\partial t^2} = v^2 \frac{\partial^2 E_y}{\partial x^2} \quad (15)$$

Dimensionally (15) is

$$\frac{\text{Volts}}{\text{Meter-second}^2} = v^2 \frac{\text{volts}}{\text{meter}^3}$$

so that

$$v = \frac{\text{meters}}{\text{second}}$$

Thus, it appears that v has the dimensions of velocity. This velocity is a characteristic of the medium, being dependent on the constants μ and ϵ for the medium. For free space (vacuum) v is approximately equal to 300 Mm s^{-1} .

10-3 SOLUTIONS OF THE WAVE EQUATION

The wave equation (10-2-15) is a linear partial differential equation of the second order. To apply the equation, a solution must be found for E_y . Methods of solving this type of equation are discussed in texts on differential equations. It will suffice here to say that if we take the following trial solution

$$E_y = \sin \beta(x + mt) \quad (1)$$

where $\beta = 2\pi/\lambda$

λ = wavelength

m = a constant (to be determined)

t = time

we find on substitution in (10-2-15) that (1) is a solution provided that

$$m = \pm v \quad (2)$$

where v is the velocity. Hence a general solution for (10-2-15) is

$$E_y = \sin \beta(x + vt) + \sin \beta(x - vt) \quad (3)$$

Either term alone is a solution, or the sum, as in (3), is a solution. This can be verified by taking the second derivatives of the solution in terms of t and x and substituting them in (10-2-15). Since $v = f\lambda$, it follows that

$$\beta v = \frac{2\pi}{\lambda} f \lambda = 2\pi f = \omega \quad (4)$$

Thus, (3) can also be expressed

$$E_y = \sin(\beta x + \omega t) + \sin(\beta x - \omega t)$$

(5)

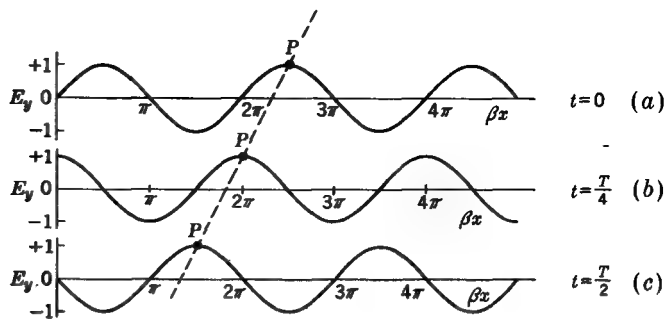


FIGURE 10-3
Curves for $E_y = \sin(\beta x + \omega t)$ at three instants of time: $t = 0$, $t = T/4$, and $t = T/2$. A constant-phase point P moves to the left as time progresses.

Suppose that the first term of (3) is considered by itself as a solution. That is,

$$E_y = \sin \beta(x + vt) \quad (6)$$

The significance of (6) can be illustrated by evaluating E_y as a function of x for several values of the time t . First let us take $t = 0$. Then $E_y = \sin \beta x$. The curve for this instant of time is shown by Fig. 10-3a. Next consider the situation one-quarter period later, i.e., when $t = T/4$, where T is the time of one period. Then

$$\beta vt = \omega t = (2\pi f)t = \frac{2\pi}{T}t = \frac{2\pi}{T}\frac{T}{4} = \frac{\pi}{2} \quad (7)$$

The curve for $t = T/4$ or $\omega t = \pi/2$ rad is shown in Fig. 10-3b. One-half period later, $t = T/2$, and $\omega t = \pi$, yielding the curve of Fig. 10-3c. Focusing our attention on the crest of one of the waves, as indicated by the point P , we note that as time progresses, P moves to the left. From Fig. 10-3 we can thus interpret (6) as representing a wave traveling to the left, or in the negative x direction. The maximum value of E_y for this wave is unity.

The point P is a point of constant phase and is characterized by the condition that

$$x + vt = \text{constant} \quad (8)$$

Taking the time derivative of (8) gives

$$\frac{dx}{dt} + v = 0 \quad (9)$$

and

$$\frac{dx}{dt} = -v \quad (10)$$

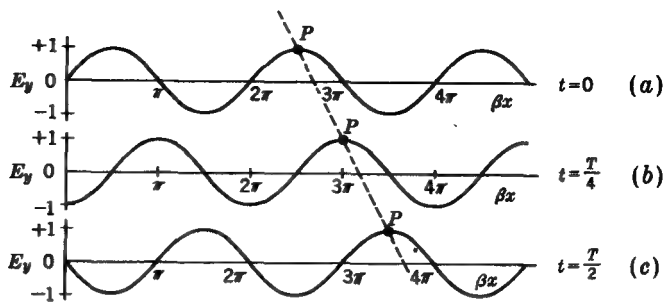


FIGURE 10-4

Curves for $E_y = \sin(\beta x - \omega t)$ at three instants of time $t = 0$, $t = T/4$, and $t = T/2$. A constant-phase point P moves to the right as time progresses.

In (10), dx/dt is the rate of change of distance with respect to time, or velocity, of a constant-phase point. Hence, v is the velocity of a constant-phase point and is called the *phase velocity*. We note also that v is negative, which means that the wave is traveling in the negative x direction.

Next consider the last term of (3) as a solution by itself. Then

$$E_y = \sin \beta(x - vt) = \sin(\beta x - \omega t) \quad (11)$$

Putting in values for $t = 0$, $T/4$, and $T/2$, we obtain from (11) the curves of Fig. 10-4. Here a constant-phase point P moves to the right as time progresses. Hence (11) represents a wave traveling in the positive x direction.

If we set $x - vt$ equal to a constant and proceed in the same manner as for (9) and (10), we find in this case that

$$\frac{dx}{dt} = +v \quad (12)$$

Thus, the wave travels with a velocity v in the positive x direction.

To summarize, a negative sign in $x \pm vt$ or in $\beta x \pm \omega t$ is associated with a wave to the right, while a positive sign is associated with a wave to the left. Accordingly, when solutions with both positive and negative signs are given, as in (3), two waves are represented, one to the left and one to the right, and the complete solution is equal to the sum of both waves.

Let us now treat in somewhat more detail the wave traveling in the positive x direction. A number of forms can be used which are equivalent except for a phase displacement. Four such forms are

$$\begin{aligned} E_y &= \sin(\beta x - \omega t) \\ E_y &= \sin(\omega t - \beta x) \\ E_y &= \cos(\beta x - \omega t) \\ E_y &= \cos(\omega t - \beta x) \end{aligned} \quad (13)$$

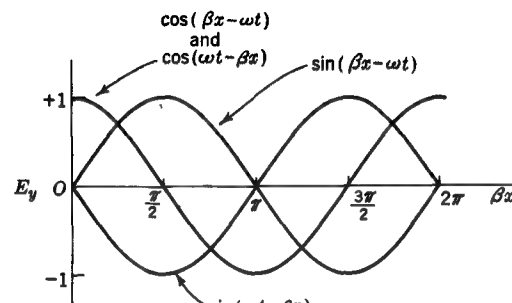


FIGURE 10-5
Four forms of wave expression at $t = 0$.

These can be rewritten so that their relation to the first is more apparent. Thus, recalling that $\sin(-u) = -\sin u = \sin(u + \pi)$ and $\cos(-u) = \cos u$, we have

$$E_y = \sin(\omega t - \beta x) = \sin(\beta x - \omega t + \pi)$$

$$E_y = \cos(\beta x - \omega t) = \sin\left(\beta x - \omega t + \frac{\pi}{2}\right) \quad (14)$$

$$E_y = \cos(\omega t - \beta x) = \sin\left(\beta x - \omega t + \frac{\pi}{2}\right)$$

The relation of the four forms of (13) is illustrated graphically in Fig. 10-5, where they are compared for $t = 0$. On substituting other values of t into the four equations, it is seen that in each case the equation represents a wave traveling to the right. The only difference between them is that in some cases there is a phase displacement of $\pi/2$ or π .

If the phase displacement is disregarded, any of the four forms given by (13) can be selected to represent a wave traveling in the positive x direction. Suppose, then, we choose the form

$$E_y = \sin(\omega t - \beta x) \quad (15)$$

This choice has the advantage that the term with the time t is positive for waves traveling in either the positive or the negative x direction.

Thus far, it has been assumed that the maximum amplitude of E_y is unity. If now we specify the maximum amplitude as E_0 , we have

$$E_y = E_0 \sin(\omega t - \beta x) \quad (16)$$

Since $f = 1/T$, (16) can be expressed in a form in which the period T appears explicitly. For the sake of symmetry, let us also put $\beta = 2\pi/\lambda$, obtaining

$$E_y = E_0 \sin\left(2\pi \frac{t}{T} - 2\pi \frac{x}{\lambda}\right) \quad (17)$$

These expressions, (16) and (17), represent a wave traveling in the positive x direction. The corresponding expressions for a wave traveling in the negative x direction are

$$E_y = E_0 \sin(\omega t + \beta x) \quad (18)$$

and

$$E_y = E_0 \sin\left(2\pi \frac{t}{T} + 2\pi \frac{x}{\lambda}\right) \quad (19)$$

The solutions of the wave equation given by (16) and (18) are *trigonometric* solutions. We can also express the solution in *exponential* form. Thus

$$E_y = E_0 e^{j(\omega t \pm \beta x)} \quad (20)$$

where it is understood that the instantaneous value of the field is given by either the imaginary or the real part of the exponential function. Thus, taking the imaginary part (Im), we have

$$E_y = E_0 \operatorname{Im} e^{j(\omega t - \beta x)} = E_0 \sin(\omega t - \beta x) \quad (21)$$

If the real part (Re) is taken, we obtain

$$E_y = E_0 \operatorname{Re} e^{j(\omega t - \beta x)} = E_0 \cos(\omega t - \beta x) \quad (22)$$

Taking the second derivatives of (20) with respect to t and x , it may be verified that (20) is indeed a solution.

10-4 TABLE OF SOLUTIONS OF THE WAVE EQUATION

In Table 10-1 both trigonometric and exponential solutions are given for a plane wave in a lossless medium. Solutions are listed for waves traveling to the left (negative x direction) and to the right (positive x direction). Solutions given by the sum of two such independent solutions are also included.

Table 10-1 SOLUTIONS OF WAVE EQUATION

	Trigonometric form	Exponential form
Wave to right	$E_y = E_1 \sin(\omega t - \beta x)$	$E_y = E_1 e^{j(\omega t - \beta x)}$
Wave to left	$E_y = E_0 \sin(\omega t + \beta x)$	$E_y = E_0 e^{j(\omega t + \beta x)}$
Two waves	$E_y = E_0 \sin(\omega t + \beta x) + E_1 \sin(\omega t - \beta x)$	$E_y = E_0 e^{j(\omega t + \beta x)} + E_1 e^{j(\omega t - \beta x)}$

10-5 PHASE VELOCITY

We have seen that $x - vt$ is a constant for a point of constant phase in a traveling wave. It follows that $\omega t - \beta x$ is a constant. That is, t and x must vary together, so that

$$\omega t - \beta x = \text{constant} \quad (1)$$

Differentiating (1) with respect to time to find the velocity of the constant-phase point, as done in (10-3-9), yields

$$\omega - \beta \frac{dx}{dt} = 0 \quad (2)$$

or

$$\frac{dx}{dt} = \frac{\omega}{\beta} \quad (3)$$

Thus, the *phase velocity*, or velocity of a constant-phase point, is given by ω/β . That ω/β has the dimensions of velocity is more apparent if it is reexpressed

$$\frac{\omega}{\beta} = \frac{2\pi f}{2\pi/\lambda} = \lambda f \quad (4)$$

where λ = wavelength

f = frequency

The product λf has the dimensions of wavelength (distance) times frequency (reciprocal of time). Thus, λf has the dimensions of distance per time, or velocity.

From (10-2-14) we have that the phase velocity is

$$\frac{\omega}{\beta} = v = \frac{1}{\sqrt{\mu\epsilon}} \quad (5)$$

Equation (5) gives the phase velocity of a wave in an unbounded medium of permeability μ and permittivity ϵ . For free space (vacuum) the velocity is a well-known constant (usually designated by c and usually called the *velocity of light*). Thus

$$c = \frac{1}{\sqrt{\mu_0 \epsilon_0}} = 300 \text{ Mm s}^{-1} \quad (6)$$

The SI unit for the permeability of vacuum is

$$\mu_0 = 400\pi \text{ nH m}^{-1} \quad (\text{exactly})$$

Therefore the permittivity of vacuum is

$$\epsilon_0 = \frac{1}{\mu_0 c^2} = 8.85 \text{ pF m}^{-1} \quad (7)$$

For other media the phase velocity relative to the velocity of light, or *relative phase velocity*, is

$$p = \frac{v}{c} = \frac{\sqrt{\mu_0 \epsilon_0}}{\sqrt{\mu\epsilon}} = \frac{1}{\sqrt{\mu_r \epsilon_r}} \quad (\text{dimensionless}) \quad (8)$$

where μ_r = relative permeability of medium

ϵ_r = relative permittivity of medium

The phase velocity of a plane wave in an unbounded lossless medium is equal to or less than the velocity of light ($p \leq 1$). In general, however, the phase velocity may have values both greater and less than the velocity of light. For example, in a hollow metal waveguide v is always equal to or greater than c (see Chap. 13).

If two waves of the same frequency travel with the same velocity in opposite directions or with different velocities in the same direction, the phase velocity of the resultant wave is not a constant but varies as a function of position. In measuring the velocity it is usually most convenient, at radio frequencies, to determine the electrical phase shift (by phase-comparison methods) between two points, one of which is taken as a reference.

For a wave traveling in the positive x direction there is an infinitesimal phase lag $d\phi$ or phase advancement $-d\phi$ in a positive distance dx . The time required for a constant-phase point to move this distance is then

$$dt = -\frac{T}{2\pi} d\phi \quad (\text{s}) \quad (9)$$

where T is the time for one period. Therefore the phase velocity as a function of position is given by

$$v = \frac{dx}{dt} = -\frac{dx}{(T/2\pi)d\phi} = -\frac{\omega}{d\phi/dx} \quad (10)$$

For a wave traveling in the positive x direction $d\phi/dx$ is negative, and hence v is positive.

As compared with (10), the phase velocity ω/β , as in (5), is an average phase velocity as averaged over an integral number of wavelengths. Thus, dividing (10) by ω/β , we obtain a relative phase velocity p which is a function of position as given by

$$p = -\frac{\beta}{d\phi/dx} \quad (11)$$

where $\beta = 2\pi/\lambda$, m⁻¹

λ = wavelength in free space, m

Both v in (10) and p in (11) are useful where the phase velocity is a function of position.

10-6 INDEX OF REFRACTION

In optics the *index of refraction* η is defined as the reciprocal of the relative phase velocity p . That is,

$$\boxed{\eta = \frac{1}{p} = \frac{1}{v/c} = \frac{c}{v} = \sqrt{\mu_r \epsilon_r}} \quad (1)$$

For nonferrous media μ_r is very nearly unity so that

$$\eta = \sqrt{\epsilon_r} \quad (2)$$

EXAMPLE 1 Paraffin has a relative permittivity $\epsilon_r = 2.1$. Find the index of refraction for paraffin and also the phase velocity of a wave in an unbounded medium of paraffin.

SOLUTION The index of refraction

$$\eta = \sqrt{2.1} = 1.45$$

The phase velocity

$$v = \frac{c}{\sqrt{2.1}} = 207 \text{ Mm s}^{-1}$$

EXAMPLE 2 Distilled water has the constants $\sigma \approx 0$, $\epsilon_r = 81$, $\mu_r = 1$. Find η and v .

SOLUTION

$$\eta = \sqrt{81} = 9$$

$$v = \frac{c}{\sqrt{81}} = 0.111c = 33.3 \text{ Mm s}^{-1}$$

The index of refraction given for water in the above example is the value at low frequencies ($f \rightarrow 0$). At light frequencies, say for sodium light ($\lambda = 5893 \text{ \AA}$), the index of refraction is observed to be about 1.33 instead of 9 as calculated on the basis of the relative permittivity. This difference was at one time cited as invalidating Maxwell's theory. The explanation for the difference is that the permittivity ϵ is not a constant but is a function of frequency. At zero frequency $\epsilon_r = 81$, but at light frequencies $\epsilon_r = 1.33^2 = 1.77$. The index of refraction and permittivity of many other substances also vary as a function of the frequency, as explained in Sec. 8-15.

10-7 GROUP VELOCITY†

Consider a plane wave traveling in the positive x direction, as in Fig. 10-2. Let the total electric field be given by

$$E_y = E_0 \cos(\omega t - \beta x) \quad (1)$$

Suppose now that the wave has not one but two frequencies of equal amplitude expressed by

$$\omega_0 + \Delta\omega$$

and

$$\omega_0 - \Delta\omega$$

It follows that the β values corresponding to these two frequencies are

$$\beta_0 + \Delta\beta \quad \text{corresponding to } \omega_0 + \Delta\omega$$

and $\beta_0 - \Delta\beta$ corresponding to $\omega_0 - \Delta\omega$

For frequency 1

$$E'_y = E_0 \cos[(\omega_0 + \Delta\omega)t - (\beta_0 + \Delta\beta)x] \quad (2)$$

and for frequency 2

$$E''_y = E_0 \cos[(\omega_0 - \Delta\omega)t - (\beta_0 - \Delta\beta)x] \quad (3)$$

Adding gives the total field

$$E_y = E'_y + E''_y \quad (4)$$

or

$$E_y = E_0 \{ \cos[(\omega_0 + \Delta\omega)t - (\beta_0 + \Delta\beta)x] + \cos[(\omega_0 - \Delta\omega)t - (\beta_0 - \Delta\beta)x] \} \quad (5)$$

Multiplying out (5) and by trigonometric transformation we get

$$E_y = 2E_0 \cos(\omega_0 t - \beta_0 x) \cos(\Delta\omega t - \Delta\beta x) \quad (6)$$

The two cosine factors indicate the presence of beats, i.e., a slow variation superimposed on a more rapid one.

For a *constant-phase* point

$$\omega_0 t - \beta_0 x = \text{constant}$$

and $\frac{dx}{dt} = \frac{\omega_0}{\beta_0} = v = f_0 \lambda_0$ (7)

† Leon Brillouin, "Wave Propagation in Periodic Structures," chap. 5, McGraw-Hill Book Company, New York, 1946; J. A. Stratton, "Electromagnetic Theory," p. 330, McGraw-Hill Book Company, New York, 1941.

where v is the *phase velocity*. Setting the argument of the second cosine factor equal to a constant, we have

$$\Delta\omega t - \Delta\beta x = \text{constant}$$

and

$$\frac{dx}{dt} = \frac{\Delta\omega}{\Delta\beta} = u = \Delta f \Delta\lambda \quad (8)$$

where u is the phase velocity of the wave envelope, which is usually called the *group velocity*. In the above development we can consider $\omega_0 + \Delta\omega$ and $\omega_0 - \Delta\omega$ as the two sideband frequencies due to the modulation of a carrier frequency ω_0 by a frequency $\Delta\omega$, the carrier frequency being suppressed.

In nondispersive media the group velocity is the same as the phase velocity. Free space is an example of a lossless, nondispersive medium, and in free space $u = v = c$. However, in dispersive media the phase and group velocities differ.

A *dispersive medium* is one in which the phase velocity is a function of the frequency (and hence of the free-space wavelength). Dispersive media are of two types:

- 1 *Normally dispersive*. In these media the change in phase velocity with wavelength is positive; that is, $dv/d\lambda > 0$. For these media $u < v$.
- 2 *Anomalously dispersive*. In these media the change in phase velocity with wavelength is negative; that is, $dv/d\lambda < 0$. For these media $u > v$.

The terms normal and anomalous are arbitrary, the significance being simply that anomalous dispersion is different from the type of dispersion described as normal.

For a particular frequency (bandwidth vanishingly small)

$$u = \lim_{\Delta\omega \rightarrow 0} \frac{\Delta\omega}{\Delta\beta} = \frac{d\omega}{d\beta} \quad (9)$$

But $\omega = 2\pi f = 2\pi f\lambda/\lambda = \beta v$; so

$$u = \frac{d\omega}{d\beta} = \frac{d(\beta v)}{d\beta} = \beta \frac{dv}{d\beta} + v \quad (10)$$

or

$$u = v + \beta \frac{dv}{d\beta} \quad (11)$$

It may also be shown that

$$u = v - \lambda \frac{dv}{d\lambda} \quad (12)$$

Equations (11) and (12) are useful in finding the group velocity for a given phase-velocity function.

EXAMPLE A 1-MHz (300 m wavelength) plane wave traveling in a normally dispersive, lossless medium has a phase velocity at this frequency of 300 Mm s⁻¹. The phase velocity as a function of wavelength is given by

$$v = k \sqrt{\lambda}$$

where k is a constant. Find the group velocity.

SOLUTION From (12) the group velocity is

$$u = v - \lambda \frac{dv}{d\lambda} = v - \frac{k}{2} \sqrt{\lambda}$$

or

$$u = v(1 - \frac{1}{2})$$

Hence

$$u = \frac{v}{2} = 150 \text{ Mm s}^{-1}$$

To illustrate graphically the difference between phase and group velocity, let us consider a wave of the same phase-velocity characteristics as in the above example and assume, further, that the wave has two frequencies, $f_0 + \Delta f$ and $f_0 - \Delta f$, of equal amplitude, where $f_0 = 1$ MHz and $\Delta f = 100$ kHz. This is equivalent to a 1-MHz carrier modulated at 100 kHz with the carrier suppressed. From (6) graphs of the instantaneous magnitude of E , as a function of distance (plotted in meters) are presented in Fig. 10-6 for three instants of time, $t = 0$, $t = T/4$, and $t = T/2$. The point P is a point of constant phase of the wave proper and moves with the phase velocity v . The point P' is a point of constant phase of the envelope enclosing the wave and moves with the group velocity u . It is apparent that in one-half period ($T/2$) the point P' has moved a distance d' which is one-half the distance d moved by the point P . That is to say, the group velocity u is one-half the phase velocity v . The intelligence conveyed by the modulation moves with the velocity of the envelope, i.e., at the group velocity.[†]

The difference between phase and group velocities is also illustrated by a crawling caterpillar. The humps on his back move forward with phase velocity, while the caterpillar as a whole progresses with group velocity.

For a single-frequency constant-amplitude (steady-state) wave the group velocity is not apparent. However, if the wave consists of two or more frequencies, or a frequency group, as in a modulated wave the group velocity may be observed because the wave amplitude is nonuniform and the individual waves appear to form groups that may be enclosed by an envelope, as in Fig. 10-6.

[†] In a lossless medium the energy is also conveyed at the group velocity.

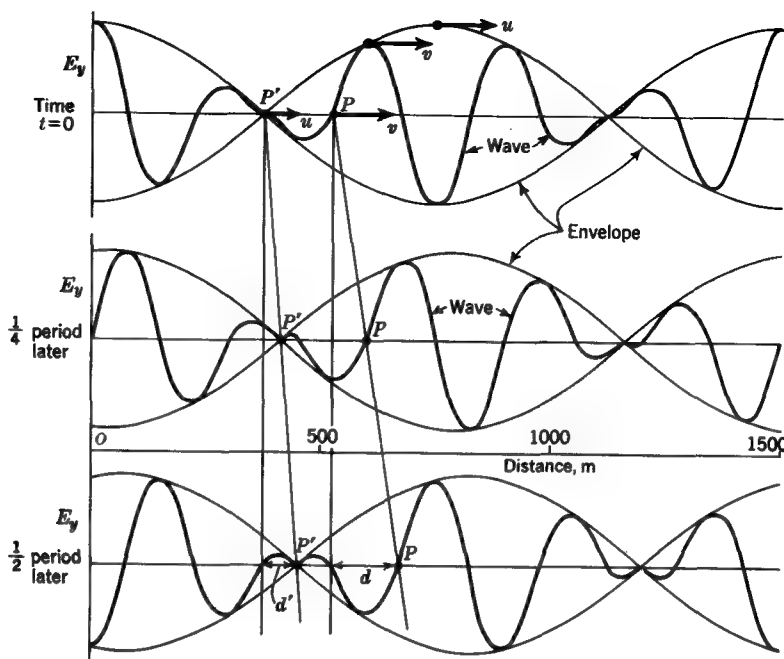


FIGURE 10-6

Constant-phase point P of the wave moves with phase velocity v , while point P' on the envelope moves with group velocity u . In this example the group velocity is one-half the phase velocity.

10-8 IMPEDANCE OF DIELECTRIC MEDIA

Thus far our attention has been focused on the electric field E_y . Let us now consider also the magnetic field H_z of the same plane wave (see Fig. 10-2) and, in particular, find how H_z is related in magnitude to E_y . A solution of the wave equation (10-2-13) in H_z is

$$H_z = H_0 \sin(\omega t - \beta x) \quad (1)$$

This solution represents a wave traveling in the positive x direction. A solution for E_y representing a wave in the positive x direction is given by (10-3-15) as

$$E_y = E_0 \sin(\omega t - \beta x) \quad (2)$$

To find how H_z in (2) is related to E_y , we recall from (10-2-8) that

$$\frac{\partial E_y}{\partial x} = -\mu \frac{\partial H_z}{\partial t} \quad (3)$$

Substituting (2) for E_y in (3), performing the indicated differentiation, and then integrating with respect to time yields

$$H_z = \frac{\beta}{\mu\omega} E_0 \sin(\omega t - \beta x) \quad (4)$$

Taking the ratio of E_y to H_z for a single traveling wave, as given by the ratio of (2) to (4), we obtain

$$\frac{E_y}{H_z} = \frac{\mu\omega}{\beta} = \frac{\mu}{\sqrt{\mu\epsilon}} = \sqrt{\frac{\mu}{\epsilon}} = \frac{E_0}{H_0} \quad (5)$$

or $E_y = \sqrt{\frac{\mu}{\epsilon}} H_z \quad (6)$

For comparison we can now write

$$E_y = E_0 \sin(\omega t - \beta x) \quad (\text{V m}^{-1}) \quad (7)$$

and $H_z = \sqrt{\frac{\epsilon}{\mu}} E_0 \sin(\omega t - \beta x) \quad (\text{A m}^{-1}) \quad (8)$

It is apparent that E_y and H_z are identical functions of x and t , but their magnitudes differ by a factor $\sqrt{\mu/\epsilon}$ or its reciprocal.

The dimensions of (5) expressed in SI units are

$$\frac{\text{Volts/meter}}{\text{Amperes/meter}} = \frac{\text{volts}}{\text{ampere}} = \text{ohms}$$

Thus, $\sqrt{\mu/\epsilon}$ has the dimensions of an impedance, and we can write

$$Z = \sqrt{\frac{\mu}{\epsilon}} \quad (9)$$

where Z is called the *intrinsic impedance* of the medium. For free space (vacuum)

$$Z = Z_0 = \sqrt{\frac{\mu_0}{\epsilon_0}} = 376.731 \approx 120\pi \Omega \quad (10)$$

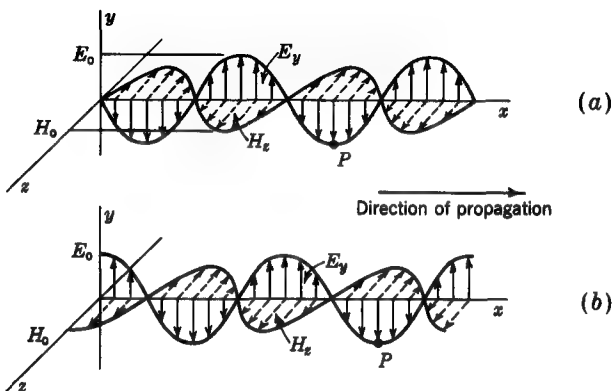


FIGURE 10-7

Instantaneous values of E_y and H_z along x axis (a) at time $t = 0$ and (b) $\frac{1}{4}$ period later. In this interval the point P has advanced $\lambda/4$ to the right.

If E and H are in time phase, Z is a pure resistance. This is the case for free space and all lossless dielectric media. To emphasize the fact that the impedance is a pure resistance, one can speak of the *intrinsic resistance* (instead of impedance) of free space and of lossless dielectric media. If E and H are not in time phase, as in conducting media, the ratio of E to H is complex, so that the more general term *intrinsic impedance* must be used in connection with such media.

Introducing (9) in (5), we have

$$\boxed{\frac{E_y}{H_z} = \frac{E_0}{H_0} = Z = \sqrt{\frac{\mu}{\epsilon}}} \quad (11)$$

EXAMPLE If the magnitude of \mathbf{H} in a plane wave is 1 A m^{-1} , find the magnitude of \mathbf{E} for a plane wave in free space.

SOLUTION From (11)

$$E = ZH = 376.7 \times 1 = 376.7 \text{ V m}^{-1}$$

The instantaneous values of E_y and H_z along the x axis for a plane wave progressing in the positive x direction are illustrated in Fig. 10-7. Figure 10-7a shows the condition at the time $t = 0$, while Fig. 10-7b shows the conditions one-quarter period later ($t = T/4$). The maximum values of E_y and H_z (E_0 and H_0) are shown to be equal. Hence, if the medium is free space, the scale in volts per meter along the y

axis should be 377 times the scale in amperes per meter along the z axis. The scales would be equal, however, if the medium had an intrinsic impedance of 1Ω . In Fig. 10-7 both the magnitudes and directions of E_y and H_z are shown for points along the x axis. Since we are considering a plane wave traveling in the direction of the x axis, the relations of E_y and H_z along all lines parallel to the x axis are the same as those shown.

10-9 IMPEDANCE OF TRANSMISSION-LINE CELL

Imagine a plane wave traveling out of the page (toward the reader) with space divided up by thin conducting strips into transmission-line cells, as suggested in Fig. 10-8. The strips are normal to \mathbf{E} , and they extend infinitely far normal to the page. The field \mathbf{H} is parallel to the strips. At the surface of each strip there is a current sheet of linear density K (normal to the page) that is equal in magnitude to H . The currents on opposite sides of one strip are opposed as shown. A plane (TEM) wave traveling through space divided up into line cells as in Fig. 10-8 has the same values of \mathbf{E} and \mathbf{H} everywhere as a wave in empty space (no strips present as in Fig. 10-2), it being assumed that the strips are of infinitesimal thickness. Assuming also that the strip width and spacing are equal (both equal to l), so that the cell cross section is square and the edges of the strips are infinitesimally close together, the voltage V between two strips of one cell is

$$V = El \quad (1)$$

The total current I flowing on the bottom surface of the top strip of a cell (or top surface of the bottom strip of a cell) is given by

$$I = Hl \quad (2)$$

Dividing (1) by (2) yields

$$\frac{E}{H} = \frac{V}{I} = Z \quad (3)$$

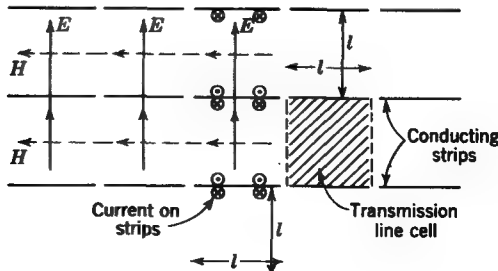


FIGURE 10-8

Plane wave traveling out of page with space divided by conducting strips into transmission-line cells.

Thus, for a single traveling wave the *intrinsic impedance* E/H of a wave is equal to the *characteristic impedance* V/I of a single transmission-line cell. Furthermore, from (10-8-11) we have

$$Z = \frac{E}{H} = \sqrt{\frac{\mu}{\epsilon}} \quad (4)$$

For a transmission-line cell we have from (5-17-2) that the inductance of the line per unit depth (normal to the page) is equal to the permeability of the medium, i.e.,

$$\frac{L}{d} = \mu \quad (5)$$

while we have from (3-22-3) that the capacitance of the line cell per unit depth equals the permittivity of the medium, or

$$\frac{C}{d} = \epsilon \quad (6)$$

Accordingly, we can write

$$Z = \sqrt{\frac{\mu}{\epsilon}} = \sqrt{\frac{L/d}{C/d}} \quad (7)$$

where Z = characteristic impedance of line cell, Ω

L/d = inductance per unit length of line cell, $H m^{-1}$

C/d = capacitance per unit length of line cell, $F m^{-1}$

To summarize, the *characteristic impedance of a transmission line cell is equal to the intrinsic impedance of the medium filling the cell*. If the medium is free space, $\mu = \mu_0$ and $\epsilon = \epsilon_0$; so the characteristic impedance of the line is

$$Z = \sqrt{\frac{\mu_0}{\epsilon_0}} = 376.7 \Omega \quad (8)$$

10-10 TWO PLANE WAVES TRAVELING IN OPPOSITE DIRECTIONS; STANDING WAVES

Thus far, we have considered only a single traveling wave, such as a wave moving in the positive or the negative x direction. Let us now examine the situation which exists when there are two waves traveling in opposite directions, such as the negative and

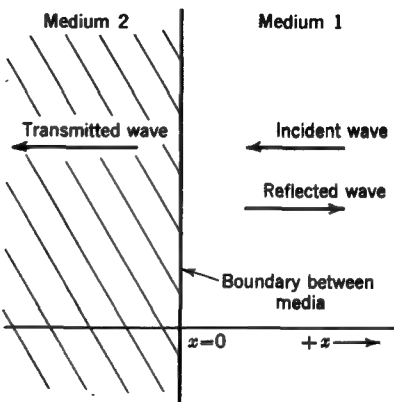


FIGURE 10-9
Relation of incident, reflected, and transmitted waves.

positive x directions. Assume that the two waves are of the same frequency and of sinusoidal form. The condition that the waves be of the same frequency and form is automatically fulfilled if one wave is a reflection of the other since both then originate from the same source.

Referring to Fig. 10-9, assume that space is divided into two media, 1 and 2, with a plane boundary between as shown. A wave originating in medium 1 and incident on the boundary is said to be the *incident wave*. The wave reflected from the boundary back into medium 1 is called the *reflected wave*. If the reflection of the incident wave at the boundary is not complete, some of the wave continues on into medium 2 and this wave is referred to as the *transmitted wave*.

In the solution of the wave equation for E_y as given by (10-3-5) there are two terms, the first representing a wave in the negative x direction (to the left) and the second a wave in the positive x direction (to the right). Referring now to the exponential solution in Table 10-1, let the incident wave (traveling to the left) be given by

$$\dot{E}_{y0} = E_0 e^{j(\omega t + \beta x)} \quad (1)$$

and the reflected wave (traveling to the right) by

$$\dot{E}_{y1} = E_1 e^{j(\omega t - \beta x + \delta)} \quad (2)$$

where δ = time-phase lead of \dot{E}_{y1} with respect to \dot{E}_{y0} at $x = 0$, that is, δ = phase shift at point of reflection

E_0 = amplitude of incident wave

E_1 = amplitude of reflected wave

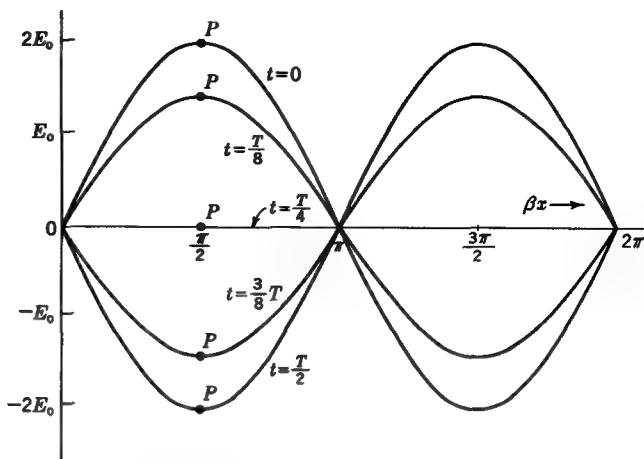


FIGURE 10-10
Pure standing wave showing E_y at various instants of time.

The dot is used here to indicate explicitly that \dot{E}_{y0} and \dot{E}_{y1} are complex functions of t , x , and δ .† The total electric field \dot{E}_y is

$$\dot{E}_y = \dot{E}_{y0} + \dot{E}_{y1} \quad (3)$$

The instantaneous magnitude of the fields is obtained by taking either the real (Re) or imaginary (Im) parts of (1) and (2). Thus, taking the imaginary parts, the total instantaneous electric field E_y is

$$E_y = \text{Im } \dot{E}_y = E_0 \sin(\omega t + \beta x) + E_1 \sin(\omega t - \beta x + \delta) \quad (4)$$

If $\delta = 0$ or 180° (4) can be expanded as follows:‡

$$E_y = E_0 \sin \omega t \cos \beta x + E_0 \cos \omega t \sin \beta x + E_1 \sin \omega t \cos \beta x - E_1 \cos \omega t \sin \beta x \quad (5)$$

Collecting terms, we have

$$E_y = (E_0 + E_1) \sin \omega t \cos \beta x + (E_0 - E_1) \cos \omega t \sin \beta x \quad (6)$$

If medium 2 is a perfect conductor, the reflected wave is equal in magnitude to the incident wave. If $x = 0$ is taken to be at the boundary between media 1 and 2, the

† However, both \dot{E}_{y0} and \dot{E}_{y1} are scalar space components of the total field vector \mathbf{E} . In the case being considered, \mathbf{E} has only one component. Thus $\mathbf{E} = \hat{y} \dot{E}_y$.

‡ $\sin(a \pm b) = \sin a \cos b \pm \cos a \sin b$.

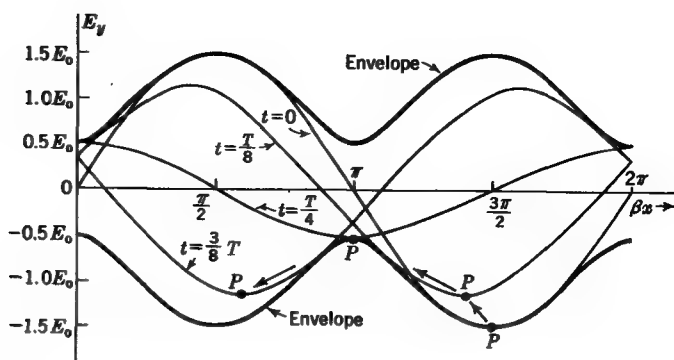


FIGURE 10-11

Standing-wave envelope for $E_1 = -0.5E_0$ with associated (traveling) wave at four instants of time: $t = 0$, $t = T/8$, $t = T/4$, and $t = 3T/8$.

boundary relation for the tangential component of \mathbf{E} requires that $E_y = 0$, so that $E_1 = -E_0$ at the boundary ($\delta = 180^\circ$). Thus (6) becomes

$$E_y = 2E_0 \cos \omega t \sin \beta x \quad (7)$$

This represents a wave which is stationary in space. The values of E_y at a particular instant are a sine function of x . The instantaneous values at a particular point are a cosine function of t . The peak value of the wave is the sum of the incident and reflected peak values or $2E_0$. A stationary wave of this type for which $|E_1| = |E_0|$ is a *pure standing wave*. This type of wave is associated with resonators.

The space and time variations of E_y for a pure standing wave are shown by the curves of Fig. 10-10. It is to be noted that a constant-phase point, such as P , does not move in the x direction but remains at a fixed position as time passes.

Now let us examine the conditions when the reflected wave is smaller than the incident wave, say one-half as large. Then, $E_1 = -0.5E_0$. Evaluating (6) for this case at four instants of time gives the curves of Fig. 10-11. The curves show the values of E_y as a function of βx at times equal to 0 , $\frac{1}{8}$, $\frac{1}{4}$, and $\frac{3}{8}$ period. The peak values of E_y range from $1.5E_0$ at $t = 0$ to $0.5E_0$ at $t = \frac{1}{4}$ period. The peak values as a function of x as observed over an interval of time greater than one cycle correspond to the envelope as indicated. This envelope remains stationary, but focusing our attention on a constant-phase point P of the wave, we note that the total instantaneous wave travels to the left. It will also be noted that the velocity with which P moves is not constant. Between time 0 and $\frac{1}{8}$ period P moves about 0.05λ (0.1π), while in the next $\frac{1}{8}$ period P moves about 4 times as far, or about 0.2λ (0.4π). Although the average

velocity of the constant-phase point is the same as for a pure traveling wave, its instantaneous magnitude varies between values which are greater and less.

To summarize, there are two E_y waves, one traveling in the negative x direction and another one-half as large traveling in the positive x direction. The waves reinforce each other at some points and subtract from each other at other points. The resultant wave travels in the negative x direction.

The envelope of the instantaneous curves in Fig. 10-11 can be called a *standing-wave curve*, or *envelope*. At any position βx the maximum value of the field at some time during the cycle is equal to the ordinate value of the envelope.

To calculate the value of the standing-wave envelope, we may proceed as follows. In (6) put

$$A = (E_0 + E_1)\cos \beta x \quad (8)$$

$$B = (E_0 - E_1)\sin \beta x \quad (9)$$

Expanding $\sin \omega t$ and $\cos \omega t$ in terms of exponentials, we can show that

$$A \sin \omega t + B \cos \omega t = \sqrt{A^2 + B^2} \sin(\omega t + \gamma) \quad (10)$$

Equation (6) can then be written

$$E_y = \sqrt{A^2 + B^2} \sin(\omega t + \beta x) \quad (11)$$

Expanding (11) by means of (8) and (9) yields

$$E_y = \sqrt{(E_0 + E_1)^2 \cos^2 \beta x + (E_0 - E_1)^2 \sin^2 \beta x} \sin(\omega t + \beta x) \quad (12)$$

The maximum value of E_y at some position βx as observed over an interval of at least one period occurs when $\sin(\omega t + \beta x) = 1$. Thus for the shape of the standing-wave envelope of E_y we have

$$E_y = \sqrt{(E_0 + E_1)^2 \cos^2 \beta x + (E_0 - E_1)^2 \sin^2 \beta x} \quad (13)$$

Ordinarily we are not so much interested in the shape of the standing-wave envelope as given by (13) as in the ratio of the maximum to minimum values for the envelope, which is called the *Standing-Wave Ratio* (SWR). The potential or voltage at any distance x will be proportional to the field,[†] and so the SWR in this case may be referred to as the *Voltage Standing-Wave Ratio* (VSWR). The maximum value of the envelope corresponds to the sum of the amplitudes of the incident and reflected waves ($E_0 + E_1$), while the minimum corresponds to the difference between the two ($E_0 - E_1$). With this information we can determine the fraction of the incident E_y wave which is reflected, forming the reflected wave, and also that which is transmitted (see Fig. 10-9).

[†] Provided E is integrated over equal paths I ($V = \int \mathbf{E} \cdot d\mathbf{l} = EI$).

As will be noted later, this knowledge is of value in determining the nature of the conditions at the point of reflection.

Thus, for the VSWR we can write

$$\boxed{\text{VSWR} = \frac{E_{\max}}{E_{\min}} = \frac{E_0 + E_1}{E_0 - E_1}} \quad (14)$$

When the reflected wave is zero ($E_1 = 0$), the VSWR is unity. When the reflected wave is equal to the incident wave ($E_1 = E_0$), the VSWR is infinite. Hence for all intermediate values of the reflected wave, the VSWR lies between 1 and infinity.

The ratio of the reflected wave to the incident wave is defined as the *reflection coefficient*. Thus, at the point of reflection ($x = 0$) and at the time $t = 0$, the ratio of (2) to (1) is

$$\dot{\rho} = \frac{\dot{E}_{y1}}{\dot{E}_{y0}} = \frac{E_1 e^{j\delta}}{E_0} = \frac{E_1 / \delta}{E_0} = \rho / \delta \quad (15)$$

The dot indicates that $\dot{\rho}$ is a complex function. Thus, in general, $\dot{\rho}$ expresses both the magnitude of the reflected wave with respect to the incident wave and also the phase shift δ at the point of reflection. The magnitude of $\dot{\rho}$ can range between 0 and 1 with phase angles between 0 and $\pm 180^\circ$.

In this discussion, we are dealing with the values of the electric field. Hence, more specifically $\dot{\rho}$ may be called the field *reflection coefficient*.

Rewriting (14) and substituting (15) gives

$$\boxed{\text{VSWR} = \frac{1 + (E_1/E_0)}{1 - (E_1/E_0)} = \frac{1 + |\dot{\rho}|}{1 - |\dot{\rho}|}} \quad (16)$$

Solving for $|\dot{\rho}|$ gives an expression for the magnitude of the reflection coefficient in terms of the VSWR:

$$|\dot{\rho}| = \rho = \frac{\text{VSWR} - 1}{\text{VSWR} + 1} \quad (17)$$

In Fig. 10-12, standing-wave envelopes are presented for three magnitudes of the reflected wave as given by reflection coefficients $\rho = 0, 0.5$, and 1 . The amplitude of the incident wave is taken as unity. The curves show E_y as a function of position in terms of both βx and wavelength. For complete reflection ($\rho = 1$) we have a pure standing wave with a VSWR of infinity. For zero reflection ($\rho = 0$), the VSWR is unity, and E_y is constant as a function of position. For a reflection coefficient of 0.5, the curve varies between 1.5 and 0.5 so that VSWR = 3. In general, the standing-wave envelope is *not* a sine curve, the minimum being sharper than the maximum.

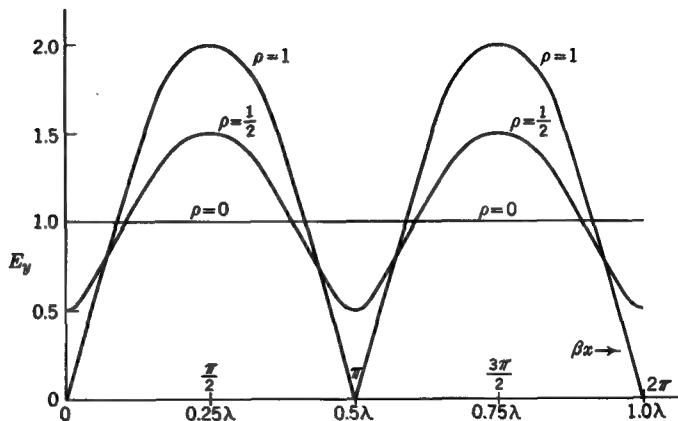


FIGURE 10-12

Standing-wave envelopes for three magnitudes of reflection coefficient, $\rho = 0$, 0.5, and 1.

This is illustrated by the curve for $\rho = 0.5$. However, in the limiting condition of $\rho = 1$ the curve does have the form of a rectified sine function ($|\sin \beta x|$). Also, as the condition $\rho = 0$ is approached, the curve approximates a sinusoidal variation.

10-11 ENERGY RELATIONS IN A TRAVELING WAVE

From (3-12-7) the energy density w_e at a point in an electric field is

$$w_e = \frac{1}{2}\epsilon E^2 \quad (\text{J m}^{-3}) \quad (1)$$

where ϵ = permittivity of medium, F m^{-1}

E = electric field intensity, V m^{-1}

From (5-19-2) the energy density w_m at a point in a magnetic field is

$$w_m = \frac{1}{2}\mu H^2 \quad (\text{J m}^{-3}) \quad (2)$$

where μ = permeability of medium, H m^{-1}

H = magnetic field, A m^{-1}

In a traveling wave in an unbounded, lossless medium

$$\frac{E}{H} = \sqrt{\frac{\mu}{\epsilon}} \quad (3)$$

Substituting for H from (3) in (2), we have

$$w_m = \frac{1}{2}\mu H^2 = \frac{1}{2}\epsilon E^2 = w_e \quad (4)$$

Thus the electric and magnetic energy densities in a plane traveling wave are equal, and the total energy density w is the sum of the electric and magnetic energies. Thus

$$w = w_e + w_m = \frac{1}{2}\epsilon E^2 + \frac{1}{2}\mu H^2 \quad (5)$$

or

$$w = \epsilon E^2 = \mu H^2 \quad (\text{J m}^{-3}) \quad (6)$$

10-12 THE POYNTING VECTOR

Continuing the discussion of the preceding section, any increase in the energy per unit volume must be produced by an inflow of energy. Likewise any decrease must be equal to an outflow (principle of conservation of energy). Thus, for a small volume Δv the decrease in energy as a function of time may be expressed as†

$$-\frac{\partial}{\partial t} (\frac{1}{2}\epsilon E^2 + \frac{1}{2}\mu H^2) \Delta v = \int_s \mathbf{S} \cdot d\mathbf{s} \quad (\text{W}) \quad (1)$$

where \mathbf{S} is the energy per unit area passing per unit time through the surface of the volume Δv in watts per square meter.

Dividing (1) by Δv and taking the limit as Δv approaches zero, we obtain

$$\nabla \cdot \mathbf{S} = -\frac{\partial}{\partial t} (\frac{1}{2}\epsilon E^2 + \frac{1}{2}\mu H^2) \quad (2)$$

The quantity \mathbf{S} has the dimensions of power per unit area and is expressed in watts per square meter. It is a vector since it indicates not only the magnitude of the energy flow but also its direction. It is usually called the *Poynting vector*.‡

Returning to Maxwell's equations for nonconducting media, we have

$$\nabla \times \mathbf{H} = \frac{\partial \mathbf{D}}{\partial t} \quad \text{and} \quad \nabla \times \mathbf{E} = -\frac{\partial \mathbf{B}}{\partial t} \quad (3)$$

Writing the scalar product of the first equation with \mathbf{E} and of the second with \mathbf{H} gives

$$\mathbf{E} \cdot (\nabla \times \mathbf{H}) = \mathbf{E} \cdot \frac{\partial \mathbf{D}}{\partial t} \quad \text{and} \quad \mathbf{H} \cdot (\nabla \times \mathbf{E}) = -\mathbf{H} \cdot \frac{\partial \mathbf{B}}{\partial t} \quad (4)$$

† We assume no loss or generation of energy within the volume.

‡ J. H. Poynting, On the Transfer of Energy in the Electromagnetic Field, *Phil. Trans.*, 174:343 (1883); Oliver Heaviside, "Electromagnetic Theory," vol. 1, p. 78, Ernest Benn, Ltd., London, 1893.

Subtracting the first from the second, we have

$$\mathbf{H} \cdot (\nabla \times \mathbf{E}) - \mathbf{E} \cdot (\nabla \times \mathbf{H}) = - \left(\mathbf{E} \cdot \frac{\partial \mathbf{D}}{\partial t} + \mathbf{H} \cdot \frac{\partial \mathbf{B}}{\partial t} \right) \quad (5)$$

By means of the conversion formula

$$\mathbf{G} \cdot (\nabla \times \mathbf{F}) - \mathbf{F} \cdot (\nabla \times \mathbf{G}) = \nabla \cdot (\mathbf{F} \times \mathbf{G}) \quad (6)$$

the two terms on the left side of (5) can be expressed as one:

$$\nabla \cdot (\mathbf{E} \times \mathbf{H}) = - \left(\mathbf{E} \cdot \frac{\partial \mathbf{D}}{\partial t} + \mathbf{H} \cdot \frac{\partial \mathbf{B}}{\partial t} \right) \quad (7)$$

For isotropic media, $\mathbf{D} = \epsilon \mathbf{E}$ and $\mathbf{B} = \mu \mathbf{H}$, and (7) takes the form

$$\nabla \cdot (\mathbf{E} \times \mathbf{H}) = - \left[\mathbf{E} \cdot \frac{\partial(\epsilon \mathbf{E})}{\partial t} + \mathbf{H} \cdot \frac{\partial(\mu \mathbf{H})}{\partial t} \right] \quad (8)$$

Recalling from calculus that

$$w \frac{\partial w}{\partial t} = \frac{1}{2} \frac{\partial w^2}{\partial t} \quad (9)$$

we see that (8) can be written

$$\nabla \cdot (\mathbf{E} \times \mathbf{H}) = - \left[\frac{\partial}{\partial t} \left(\frac{\epsilon E^2}{2} \right) + \frac{\partial}{\partial t} \left(\frac{\mu H^2}{2} \right) \right] \quad (10)$$

Taking the time-derivative operator outside the brackets, we have

$$\nabla \cdot (\mathbf{E} \times \mathbf{H}) = - \frac{\partial}{\partial t} \left(\frac{1}{2} \epsilon E^2 + \frac{1}{2} \mu H^2 \right) \quad (11)$$

Comparing (11) with (2) shows that

$$\mathbf{E} \times \mathbf{H} = \mathbf{S}$$

(12)

where \mathbf{E} = electric field intensity, V m^{-1}

\mathbf{H} = magnetic field, A m^{-1}

\mathbf{S} = instantaneous Poynting vector, W m^{-2}

The dimensional form of (12) in SI units is

$$\frac{\text{Volts}}{\text{Meter}} \times \frac{\text{amperes}}{\text{meter}} = \frac{\text{watts}}{\text{meter}^2}$$

In words, this important relation indicates that the rate of energy flow per unit area in a wave is directed normal to the plane containing \mathbf{E} and \mathbf{H} and has a magnitude in

watts per square meter equal to $EH \sin \theta$, where θ is the angle between \mathbf{E} and \mathbf{H} . It is often helpful to regard the Poynting vector as a *surface power density*.

For a plane wave traveling in the positive x direction, as in Fig. 10-2, (12) becomes

$$\hat{\mathbf{y}}\mathbf{E}_y \times \hat{\mathbf{x}}\mathbf{H}_z = \hat{\mathbf{x}}\mathbf{S}_x = \mathbf{S} \quad (13)$$

It should be mentioned that in some situations $\mathbf{E} \times \mathbf{H}$ does not represent energy flow, e.g., in a static magnetic field superimposed on a static electric field. However, the integral of the normal component of $\mathbf{E} \times \mathbf{H}$ over a closed surface always gives the total power through the surface. That is,

$$\oint_s \mathbf{S} \cdot d\mathbf{s} = P \quad (\text{W}) \quad (14)$$

where P is the power flowing out of closed surface s . The Poynting vector \mathbf{S} in the above relation is the instantaneous power density, and P in (14) is the instantaneous power.

When \mathbf{E} and \mathbf{H} are changing with time, we are often interested in the average power. This is obtained by integrating the instantaneous Poynting vector over one period and dividing by one period. It is also readily obtained using complex notation as follows. In complex notation the *complex Poynting vector* is given by†

$$\boxed{\mathbf{S} = \frac{1}{2}\mathbf{E} \times \mathbf{H}^*} \quad (15)$$

where $\mathbf{E} = \hat{\mathbf{a}}_E \dot{\mathbf{E}} = \hat{\mathbf{a}}_E E_0 e^{j\omega t}$

$\hat{\mathbf{a}}_E$ = unit vector in \mathbf{E} direction

$\mathbf{H}^* = \hat{\mathbf{a}}_H \dot{\mathbf{H}}^* = \hat{\mathbf{a}}_H H_0 e^{-j(\omega t - \xi)}$

$\hat{\mathbf{a}}_H$ = unit vector in \mathbf{H} direction

ξ = phase angle between $\dot{\mathbf{E}}$ and $\dot{\mathbf{H}}^*$

In (15) \mathbf{H}^* is called the *complex conjugate* of \mathbf{H} , where

$$\mathbf{H} = \hat{\mathbf{a}}_H H_0 e^{+j(\omega t - \xi)} \quad (16)$$

The quantity \mathbf{H} and its complex conjugate \mathbf{H}^* have the same space direction and the same amplitude H_0 , but they differ in sign in their phase factors. Assuming that the space directions of \mathbf{E} and \mathbf{H} (or \mathbf{H}^*) are normal to each other, the complex Poynting vector is normal to the plane containing \mathbf{E} and \mathbf{H}^* and is

$$\mathbf{S} = \frac{1}{2}\hat{\mathbf{n}}\mathbf{E}_0 H_0 e^{j\xi} \quad (17)$$

where $\hat{\mathbf{n}}$ is the unit vector normal to \mathbf{E} and \mathbf{H}^* .

† Although no distinction in notation is made in the symbol \mathbf{S} for the Poynting vector between instantaneous and complex values, the meaning should be clear from the context.

Now the *average Poynting vector* \mathbf{S}_{av} is given by the real part of the complex Poynting vector, or

$$\boxed{\mathbf{S}_{av} = \operatorname{Re} \mathbf{S} = \frac{1}{2} \hbar E_0 H_0 \cos \xi \quad (\text{W m}^{-2})} \quad (18)$$

where ξ is the time-phase angle between electric and magnetic fields. It is understood that E_0 and H_0 are the amplitudes or peak magnitudes of the fields. If, instead, one uses the rms values, the factor $\frac{1}{2}$ in (18) is omitted.

The average power P_{av} flowing outward through a closed surface can now be expressed as

$$\boxed{P_{av} = \oint_s \operatorname{Re} \mathbf{S} \cdot d\mathbf{s} = \frac{1}{2} \oint_s \operatorname{Re}(\mathbf{E} \times \mathbf{H}^*) \cdot d\mathbf{s} \quad (\text{W})} \quad (19)$$

Dividing the Poynting vector by the energy density, we obtain a quantity with the dimensions of velocity. Thus

$$\frac{\text{Poynting vector}}{\text{Energy density}} = \text{velocity} \quad (20)$$

or in dimensional symbols

$$\frac{MT^{-3}}{ML^{-1}T^{-2}} = \frac{L}{T}$$

This is the *energy velocity* v_{en} . In nondispersive media the energy velocity is equal to the phase velocity v . In a nondispersive lossless medium we have

$$v_{en} = \frac{EH}{\epsilon E^2} = \frac{1}{\sqrt{\mu\epsilon}} = v$$

In dispersive media that are also lossless the energy velocity is equal to the group velocity. In absorbing media (not lossless) where the absorption is not small the group velocity tends to lose its simple significance. However, the energy velocity still has a simple, definite meaning.

Whereas the phase velocity (and also the group velocity) may assume values greater or less than the velocity of light, the energy velocity never exceeds the velocity of light (300 Mm s^{-1}).

EXAMPLE 1 A plane traveling wave in free space has an average Poynting vector of 1 W m^{-2} . Find the average energy density.

SOLUTION The average energy density

$$w_{av} = \frac{S_{av}}{\text{velocity}} = 3.33 \text{ nJ m}^{-3}$$

The energy density w_{av} is an average value. The instantaneous value may be any value between zero and twice the average value. The difference between the average and instantaneous values is discussed in more detail in the following paragraphs.

Returning now to a further consideration of a plane wave traveling in the positive x direction in a lossless medium, let us substitute (10-8-7) and (10-8-8) in the Poynting vector equation (13). This yields

$$S_x = \sqrt{\frac{\epsilon}{\mu}} E_0^2 \sin^2(\omega t - \beta x) \quad (\text{W m}^{-2}) \quad (21)$$

This is the *instantaneous power per unit area*. At a fixed position, $\beta x = \text{constant}$, and this power pulsates with the passage of time as a sine-squared function. The *peak power per unit area* occurs when

$$\sin^2(\omega t - \beta x) = 1 \quad (22)$$

giving

$$\text{Peak } S_x = \sqrt{\frac{\epsilon}{\mu}} E_0^2 = \frac{E_0^2}{R} \quad (23)$$

where R is the *intrinsic resistance* of the medium. To find the *average power per unit area*, the instantaneous value given by (21) is integrated over one period and divided by the length of one period, which yields†

$$\text{Average } S_x = \frac{1}{2} \sqrt{\frac{\epsilon}{\mu}} E_0^2 = \frac{E_0^2}{2R} \quad (24)$$

Comparing (24) and (23) shows that

$$\text{Peak } S_x = 2(\text{average } S_x) \quad (25)$$

The energy flow per unit time per unit area, or power surface density, of a plane wave traveling in the positive x direction is illustrated in Fig. 10-13. Here the instantaneous values of S_x are shown at two instants of time, $t = 0$ and $t = T/8$. The values of the instantaneous power per unit area are given over a distance of 1λ in the x direction. Confining our attention to one of the curves, say for $t = 0$, we note that the power surface density is a pulsating quantity, with two pulses per wavelength.

† The same result may be obtained from (18) by noting that in a lossless medium $\xi = 0$.

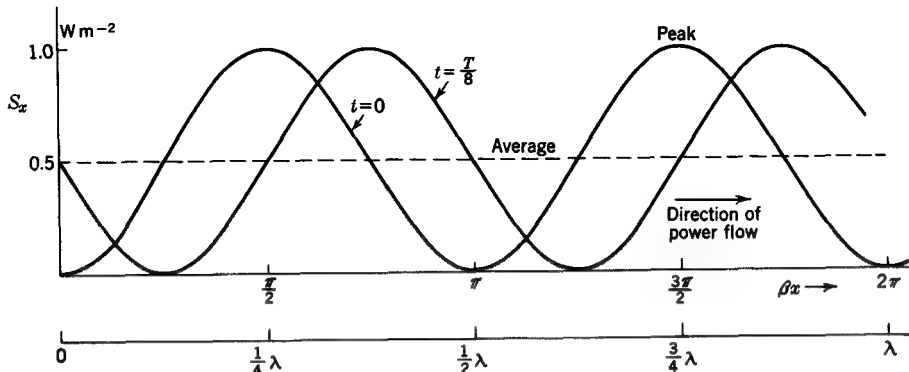


FIGURE 10-13

Instantaneous Poynting vector magnitude for plane wave traveling in positive x direction at two instants of time: $t = 0$ and $\frac{1}{8}$ period later.

Hence, at a fixed position there are two pulses per period or cycle. Comparing the curves for $t = 0$ and $t = T/8$, we note that the pulses move to the right a distance of $\lambda/8$ in the interval of $\frac{1}{8}$ period, indicating a power flow in the positive x direction.

To obtain the instantaneous energy density of the wave, the instantaneous Poynting vector is divided by the velocity of the wave. Thus, the *instantaneous energy density* is given by

$$w = \frac{S}{v} = \frac{1}{v} \sqrt{\frac{\epsilon}{\mu}} E_0^2 \sin^2(\omega t - \beta x) \quad (26)$$

Since $1/v = \sqrt{\epsilon\mu}$, (26) becomes

$$w = \epsilon E_0^2 \sin^2(\omega t - \beta x) \quad (\text{J m}^{-3}) \quad (27)$$

By steps similar to those for (23) and (24) the *peak* and *average energy densities* are

$$\text{Peak } w = \epsilon E_0^2 \quad (\text{J m}^{-3}) \quad (28)$$

$$\text{Average } w = \frac{1}{2} \epsilon E_0^2 \quad (\text{J m}^{-3}) \quad (29)$$

Table 10-2 summarizes the relations developed above for the Poynting vector and energy density of a single plane traveling wave.

The instantaneous energy-density distribution of the plane wave traveling in the positive x direction has the same form as the Poynting vector curves shown in Fig. 10-13. The ordinate, however, for energy-density curves is expressed in joules per cubic meter.

From the energy point of view, it is interesting to consider the *energy per pulse* of the wave. Here we consider that one pulse is $\lambda/2$ long. Its boundaries are defined by the positions where the energy density is zero. Since we are dealing with a plane wave of infinite extent, let us confine our attention to a volume 1 m^2 (parallel to the wavefront) by one pulse length (in the x direction). Since one pulse length is $\lambda/2$ long, the energy in this volume (one pulse long) is obtained by multiplying the average energy density by $\lambda/2$ expressed in meters. Thus

$$\text{Energy} = (\text{average } w) \frac{\lambda}{2} \quad (\text{J}) \quad (30)$$

where λ is the wavelength.[†]

EXAMPLE 2 The average energy density of a plane traveling wave is 1 J m^{-3} . If the wavelength is 500 mm, find the energy in a volume one pulse length by 1 m^2 .

SOLUTION From (30)

$$\text{Energy} = \frac{1}{2} \text{ J}$$

This is the energy in a volume 1 m^2 by one pulse length long, or the energy in a volume of 0.25 m^3 .

Table 10-2 POYNITING VECTOR AND ENERGY-DENSITY RELATIONS FOR A PLANE TRAVELING WAVE IN A DIELECTRIC MEDIUM

Condition	Poynting vector \mathbf{S} , W m^{-2}	Total energy density w , J m^{-2}
Instantaneous	$\sqrt{\frac{\epsilon}{\mu}} E_0^2 \sin^2(\omega t - \beta x)$	$\epsilon E_0^2 \sin^2(\omega t - \beta x)$
Peak	$\sqrt{\frac{\epsilon}{\mu}} E_0^2 = \sqrt{\frac{\mu}{\epsilon}} H_0^2$	$\epsilon E_0^2 = \mu H_0^2$
Average	$\frac{1}{2} \sqrt{\frac{\epsilon}{\mu}} E_0^2 = \frac{1}{2} \sqrt{\frac{\mu}{\epsilon}} H_0^2$	$\frac{1}{2} \epsilon E_0^2 = \frac{1}{2} \mu H_0^2$

[†] Each pulse contains w_p/hf quanta, where w_p = energy per pulse in joules, h = Planck's constant = $6.63 \times 10^{-34} \text{ J s}$, and f = frequency in hertz.

It is to be noted that the instantaneous values of E_x and H_z have a sine distribution as a function of x . The Poynting vector \mathbf{S} and the energy density w , however, have a sine-squared distribution.

The energy density w which we have been discussing is the total energy density of the plane electromagnetic wave. This energy density in the case of the plane traveling wave is equally divided at all times between the electric energy density and the magnetic energy density. This relationship is given by (10-11-5).

Equation (21) for the magnitude of the Poynting vector of a plane traveling wave is written in terms of E . Since the power is equally divided between electric and magnetic forms, we can write

$$S'_e = \frac{1}{2} \sqrt{\frac{\epsilon}{\mu}} E_0^2 \sin^2(\omega t - \beta x) \quad (31)$$

and

$$S'_m = \frac{1}{2} \sqrt{\frac{\mu}{\epsilon}} H_0^2 \sin^2(\omega t - \beta x) \quad (32)$$

where S'_e = electric power per unit area

S'_m = magnetic power per unit area

The phase factors for both S'_e and S'_m are identical. Since $S'_e = S'_m$ for the plane traveling wave, the total power can be expressed as twice the value of S'_e . Thus

$$S = S'_e + S'_m = 2S'_e \quad (33)$$

where the Poynting vector magnitude S is equal to the total power per unit area.

Likewise, the energy density is equally divided between the electric w_e and magnetic w_m , so that

$$w_e = \frac{1}{2} \epsilon E_0^2 \sin^2(\omega t - \beta x) \quad (34)$$

and

$$w_m = \frac{1}{2} \mu H_0^2 \sin^2(\omega t - \beta x) \quad (35)$$

Since $w_e = w_m$ for a plane traveling wave, the total w is twice w_e . Thus

$$w = w_e + w_m = 2w_e = 2w_m \quad (36)$$

10-13 ENERGY RELATIONS IN A STANDING WAVE

Next let us consider the energy and power relations for two plane waves traveling in opposite directions. Assume that both waves are polarized with \mathbf{E} in the y direction. Assume further that one wave travels in the negative x direction and has an amplitude E_0 , while the other wave travels in the positive x direction and has an amplitude E_1 . In this case the instantaneous value of E_y , resulting from the two waves, is given by

$$E_y = E_0 \sin(\omega t + \beta x) + E_1 \sin(\omega t - \beta x) \quad (1)$$

We may find a corresponding relation for H_z as follows. Let us start with (10-2-8), i.e.,

$$\frac{\partial E_y}{\partial x} = -\mu \frac{\partial H_z}{\partial t} \quad (2)$$

Substituting E_y from (1) into (2), differentiating with respect to x , and integrating with respect to t , we obtain

$$H_z = -\sqrt{\frac{\epsilon}{\mu}} E_0 \sin(\omega t + \beta x) + \sqrt{\frac{\epsilon}{\mu}} E_1 \sin(\omega t - \beta x) \quad (3)$$

The magnitude of the Poynting vector is

$$S_x = E_y H_z \quad (4)$$

Substituting (1) and (3) in (4) yields

$$S_x = -\sqrt{\frac{\epsilon}{\mu}} [E_0^2 \sin^2(\omega t + \beta x) - E_1^2 \sin^2(\omega t - \beta x)] \quad (5)$$

According to (5), the net Poynting vector is in the negative x direction provided $E_0 > E_1$. Furthermore, the net Poynting vector is equal to the difference of the Poynting vectors for the two traveling waves. Suppose that the wave to the left is incident on a plane boundary at $x = 0$ (as in Fig. 10-9). The wave to the right then becomes a reflected wave. If the medium to the left of the boundary is a perfect conductor, we have the condition at the boundary that $E_1 = -E_0$, resulting in a pure standing wave to the right of the boundary. We note that for this condition the net Poynting vector is zero, and hence no power is transmitted.

It is interesting to examine the condition of a pure standing wave ($E_1 = -E_0$) in more detail, particularly from the standpoint of concentrations of energy. Accordingly, let us find the values of the electric and magnetic energy densities separately. Substituting (10-10-7) into (10-11-1), we obtain, for the electric energy density of a pure standing wave,

$$w_e = 2\epsilon E_0^2 \cos^2 \omega t \sin^2 \beta x \quad (6)$$

Taking (3), expanding, collecting terms, and putting $E_1 \sqrt{\epsilon/\mu} = H_0$, we get

$$H_z = -2H_0 \sin \omega t \cos \beta x \quad (7)$$

Substituting this in (10-11-2) yields the value of the magnetic energy density of a pure standing wave,

$$w_m = 2\mu H_0^2 \sin^2 \omega t \cos^2 \beta x \quad (8)$$

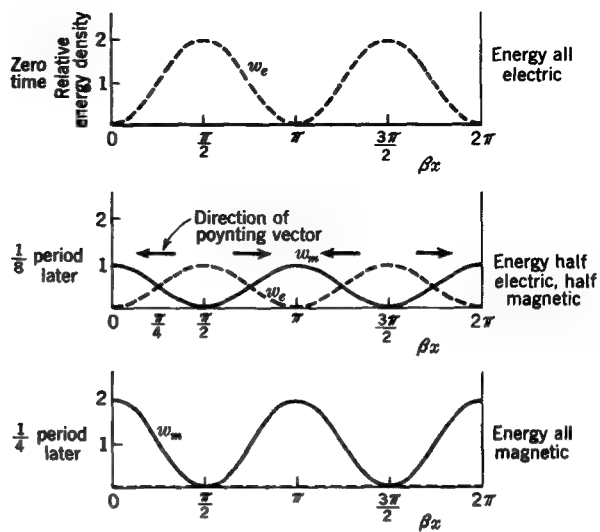


FIGURE 10-14

Total electric and magnetic energy densities at three instants of time for a pure standing wave. Conditions are shown over a distance of 1λ ($\beta x = 2\pi$). There is no net transmission of energy in a pure standing wave.

Comparing (6) and (8), we see that the electric energy density is a maximum when the magnetic is zero, and vice versa. Furthermore, the points where they are maximum are $\lambda/4$ apart. In other words, the electric and magnetic energy densities of a pure standing wave are in space and time quadrature. This condition is typical of a pure resonator (see Sec. 13-25). The energy oscillates back and forth from the electric form to the magnetic. Energy in this condition is often spoken of as reactive or stored energy. It is not transmitted but circulates from one form to the other. Simultaneously with the change from the electric to the magnetic form of energy there is a space motion of the energy back and forth over a distance of $\lambda/4$. These relations are shown graphically in Fig. 10-14. Here the energy densities are shown at three instants of time, $t = 0$, $T/8$, and $T/4$. The dashed curves show the instantaneous electric energy density w_e as evaluated from (6), and the solid curves show the instantaneous magnetic energy density w_m as evaluated from (8).

Finally, let us find an expression for the magnitude of the Poynting vector of a pure standing wave. To do this, we substitute (7) and (10-10-7) in (10-12-13), obtaining

$$S_x = -4E_0 H_0 \cos \omega t \sin \omega t \cos \beta x \sin \beta x \quad (9)$$

Putting H_0 in terms of E_0 gives

$$S_x = -4 \sqrt{\frac{\epsilon}{\mu}} E_0^2 \cos \omega t \sin \omega t \cos \beta x \sin \beta x \quad (10)$$

and the peak value of the Poynting vector is

$$\text{Peak } S_x = \sqrt{\frac{\epsilon}{\mu}} E_0^2 \quad (11)$$

From an inspection of (10) it is clear that S_x is a maximum at $\omega t = \pi/4$ ($\frac{1}{8}$ period). At this instant the position of one maximum is at $\beta x = \pi/4 (\lambda/8)$ and is directed to the left as shown by the arrow in Fig. 10-14. The other arrows indicate other Poynting vector maxima and illustrate that at $t = T/8$ the energy is flowing from the regions of electric energy density to those of magnetic energy density.

Referring to Fig. 10-11, we note that in a standing wave, a constant-phase point does not move with uniform velocity. As a result, the energy tends to bunch up, or localize. This condition becomes extreme with a pure standing wave for which a constant-phase point is stationary. Hence, localized concentrations of energy are associated with a nonuniform or stationary phase velocity.

10-14 CONDUCTORS AND DIELECTRICS

In the preceding sections of this chapter the discussion was confined to waves in nonconducting or lossless media. Let us now consider the case of conducting media. Assume that a plane traveling wave strikes the boundary of a conducting medium at normal incidence, as shown in Fig. 10-15. A portion of the incident energy is reflected,

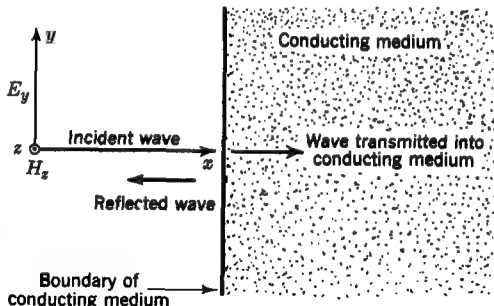


FIGURE 10-15

Plane wave entering conducting medium at normal incidence.

while the remainder enters the conducting medium. Let us disregard the reflected wave and focus our attention on the transmitted wave.

According to Maxwell's first curl equation,

$$\nabla \times \mathbf{H} = \mathbf{J} + \frac{\partial \mathbf{D}}{\partial t} \quad (1)$$

In nonconducting media $\mathbf{J} = 0$, but in conducting media \mathbf{J} may not be negligible. Recalling that $\mathbf{J} = \sigma \mathbf{E}$, we see that (1) becomes

$$\nabla \times \mathbf{H} = \sigma \mathbf{E} + \frac{\partial \mathbf{D}}{\partial t} \quad (2)$$

For a linearly polarized plane wave traveling in the x direction with \mathbf{E} in the y direction, the vector equation (2) reduces to the following scalar equation involving the field components E_y and H_z :

$$-\frac{\partial H_z}{\partial x} = \sigma E_y + \epsilon \frac{\partial E_y}{\partial t} \quad (3)$$

This equation has two terms in E_y . Assuming that E_y is a harmonic function of time, that is, $E_y = E_0 e^{j\omega t}$, (3) becomes

$$-\frac{\partial H_z}{\partial x} = \sigma E_y + j\omega \epsilon E_y \quad (4)$$

The terms in (4) each have the dimensions of current density, which is expressed in amperes per square meter. The term σE_y represents the *conduction-current density*, while the term $j\omega \epsilon E_y$ represents the *displacement-current density*. Thus, according to (4) the space rate of change of H_z equals the sum of the conduction- and displacement-current densities. If the conductivity is zero, the conduction-current term vanishes and we have the condition considered in previous sections. If σ is not equal to zero, one may arbitrarily define three conditions as follows:[†]

- (1) $\omega \epsilon \gg \sigma$
- (2) $\omega \epsilon \sim \sigma$
- (3) $\omega \epsilon \ll \sigma$

When the displacement current is much greater than the conduction current, as in condition (1), the medium behaves like a dielectric. If $\sigma = 0$, the medium is

[†] Referring to Sec. 8-15, condition (1) would be modified in the case of a lossy dielectric to $\omega \epsilon' \gg \sigma'$ and condition (2) to $\omega \epsilon' \sim \sigma'$, but for condition (3) we have $\omega \epsilon' \approx \omega \epsilon$ and $\sigma' = \sigma$, and hence we can write $\omega \epsilon \ll \sigma$, as indicated.

a perfect, or lossless, dielectric. For σ not equal to zero the medium is a lossy, or imperfect, dielectric. However, if $\omega\epsilon \gg \sigma$, it behaves more like a dielectric than anything else and may, for practical purposes, be classified as a *dielectric*. On the other hand, when the conduction current is much greater than the displacement current, as in condition (3), the medium may be classified as a *conductor*. Under conditions midway between these two, when the conduction current is of the same order of magnitude as the displacement current, the medium may be classified as a *quasi conductor*.

We can be even more specific and arbitrarily classify media as belonging to one of three types according to the value of the ratio $\sigma/\omega\epsilon$ as follows:

Dielectrics:

$$\frac{\sigma}{\omega\epsilon} < \frac{1}{100}$$

Quasi conductors:

$$\frac{1}{100} < \frac{\sigma}{\omega\epsilon} < 100$$

Conductors:

$$100 < \frac{\sigma}{\omega\epsilon}$$

where σ = conductivity of medium, Ωm^{-1}

ϵ = permittivity of medium, $F m^{-1}$

ω = radian frequency = $2\pi f$, where f is the frequency, Hz

The ratio $\sigma/\omega\epsilon$ is dimensionless.

It is to be noted that frequency is an important factor in determining whether a medium acts like a dielectric or a conductor. For example, take the case of average rural ground (Ohio) for which $\epsilon_r = 14$ (at low frequencies) and $\sigma = 10^{-2} \Omega m^{-1}$. Assuming no change in these values as a function of frequency, the ratio $\sigma/\omega\epsilon$ at three different frequencies is as tabulated.

Frequency, Hz	Ratio $\sigma/\omega\epsilon$
10^3	1.3×10^4
10^7	1.3
3×10^{10} ($\lambda = 10$ mm)	4.3×10^{-4}

At 1 kHz rural ground behaves like a conductor, while at the microwave frequency of 30 GHz it acts like a dielectric. At 10 MHz its behavior is that of a quasi conductor.

In Fig. 10-16 the ratio $\sigma/\omega\epsilon$ is plotted as a function of frequency for a number of common media. In preparing Fig. 10-16 the constants were assumed to maintain their low-frequency values at all frequencies. The curves in Fig. 10-16 should therefore not be regarded as accurate above the microwave region since the constants of media may vary with frequency, particularly at frequencies of the order of 1 GHz and higher.

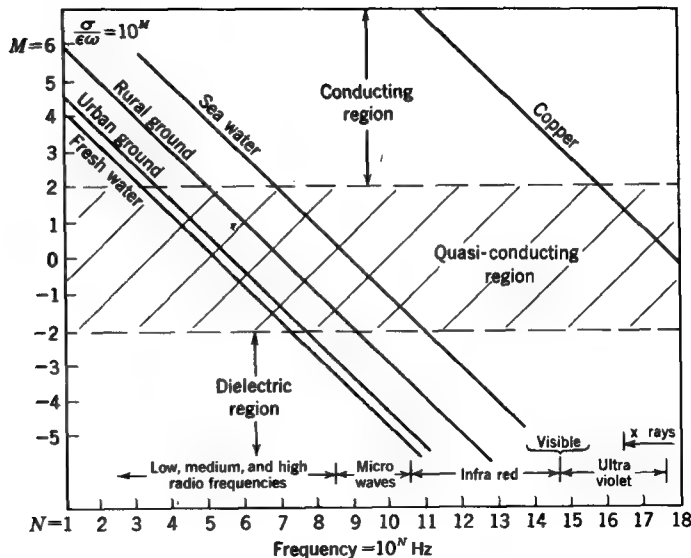


FIGURE 10-16
Ratio $\sigma/\omega\epsilon$ as a function of frequency for some common media (log-log plot).

A list of the low-frequency constants for the media of Fig. 10-16 is presented in Table 10-3.

Referring to Fig. 10-16, we note that copper behaves like a conductor at frequencies far above the microwave region. On the other hand, fresh water acts like a dielectric at frequencies above about 10 MHz. The $\sigma/\omega\epsilon$ ratios for seawater, rural ground, and urban ground are between the extremes of copper and fresh water.

Table 10-3 TABLE OF CONSTANTS FOR SOME COMMON MEDIA

Medium	Relative permittivity ϵ_r , dimensionless	Conductivity σ , S m^{-1}
Copper	1	5.8×10^7
Seawater	80	4
Rural ground (Ohio)	14	10^{-2}
Urban ground	3	10^{-4}
Fresh water	80	10^{-3}

10-15 WAVE EQUATION FOR CONDUCTING MEDIA

An electromagnetic wave is rapidly attenuated in a conducting medium. In fact, in a good conductor the attenuation is so rapid that at high radio frequencies the wave penetrates the conductor only to a very small depth.

This depth of the penetration is a matter of considerable interest. To calculate it, let us first develop a wave equation in E_y for a plane wave in a conducting medium. From a solution of this equation, an expression for the depth of penetration is then obtained.

From Maxwell's curl equations we have for a linearly polarized wave traveling in the x direction with \mathbf{E} in the y direction

$$-\frac{\partial H_z}{\partial x} = \sigma E_y + \epsilon \frac{\partial E_y}{\partial t} \quad (1)$$

and
$$\frac{\partial E_y}{\partial x} = -\mu \frac{\partial H_z}{\partial t} \quad (2)$$

Differentiating (1) with respect to t and (2) with respect to x , we obtain

$$\frac{\partial}{\partial t} \frac{\partial H_z}{\partial x} = -\sigma \frac{\partial E_y}{\partial t} - \epsilon \frac{\partial^2 E_y}{\partial t^2} \quad (3)$$

and
$$-\frac{1}{\mu} \frac{\partial^2 E_y}{\partial x^2} = \frac{\partial}{\partial x} \frac{\partial H_z}{\partial t} \quad (4)$$

Since the order of differentiation is immaterial, the left side of (3) is equal to the right side of (4) so that

$$\frac{1}{\mu} \frac{\partial^2 E_y}{\partial x^2} - \epsilon \frac{\partial^2 E_y}{\partial t^2} - \sigma \frac{\partial E_y}{\partial t} = 0 \quad (5)$$

This is the wave equation in E_y for a plane wave in a conducting medium. It is more general than the wave equation (10-2-12), developed for the case of a nonconducting medium. Whereas (10-2-12) has two terms, (5) has three, the third one involving the conductivity.

Assuming harmonic variation of E_y with respect to t , we may write

$$E_y = E_0 e^{j\omega t} \quad (6)$$

Taking the first and second derivatives of (6) with respect to t and substituting these values in (5) gives

$$\frac{1}{\mu} \frac{\partial^2 E_y}{\partial x^2} + \omega^2 \epsilon E_y - j\omega \sigma E_y = 0 \quad (7)$$

which, upon rearranging terms, becomes

$$\frac{\partial^2 E_y}{\partial x^2} - (j\omega \mu \sigma - \omega^2 \mu \epsilon) E_y = 0 \quad (8)$$

Let

$$\gamma^2 = j\omega \mu \sigma - \omega^2 \mu \epsilon \quad (9)$$

Then (8) reduces to

$$\frac{\partial^2 E_y}{\partial x^2} - \gamma^2 E_y = 0 \quad (10)$$

This equation is a simplified form of (5). The time t does not appear explicitly, harmonic variation with time being assumed. γ is called the *propagation constant*.

A solution of (10) for a wave traveling in the positive x direction is

$$E_y = E_0 e^{-\gamma x} \quad (11)$$

For conductors, $\sigma \gg \omega \epsilon$, so that (9) reduces to

$$\gamma^2 \approx j\omega \mu \sigma \quad (12)$$

and†

$$\gamma \approx \sqrt{j\omega \mu \sigma} = (1 + j) \sqrt{\frac{\omega \mu \sigma}{2}} \quad (13)$$

Thus, γ has a real and imaginary part. Putting $\gamma = \alpha + j\beta$, we see that α , the real part, is associated with attenuation and β , the imaginary part, is associated with phase.

Substituting the value of γ from (13) in (11) gives

$$E_y = E_0 \exp\left[-(1 + j) \sqrt{\frac{\omega \mu \sigma}{2}} x\right] = E_0 \exp\left(-\sqrt{\frac{\omega \mu \sigma}{2}} x\right) \exp\left(-j \sqrt{\frac{\omega \mu \sigma}{2}} x\right) \quad (14)$$

$$\dagger \text{Note: } \sqrt{j} = \sqrt{\frac{2j}{2}} = \sqrt{\frac{1+2j-1}{2}} = \sqrt{\frac{(1+j)^2}{2}}$$

$$= \frac{1+j}{\sqrt{2}} = 1 \angle 45^\circ$$

In (14) the *attenuation factor* is given by

$$\exp\left(-\sqrt{\frac{\omega\mu\sigma}{2}}x\right) \quad (15)$$

and the *phase factor* by

$$\exp\left(-j\sqrt{\frac{\omega\mu\sigma}{2}}x\right) \quad (16)$$

where ω = radian frequency $= 2\pi f$, rad s⁻¹

μ = permeability of medium, H m⁻¹

σ = conductivity of medium, S m⁻¹

x = distance, m

j = complex operator, dimensionless

Equation (14) is a solution of the wave equation for a plane wave traveling in the positive x direction in a conducting medium. It gives the variation of E_y in both magnitude and phase as a function of x . The field attenuates exponentially and is retarded linearly in phase with increasing x .

10-16 DEPTH OF PENETRATION

Continuing the discussion of the preceding section, let us now obtain a quantitative measure of the penetration of a wave in a conducting medium. Referring to Fig. 10-15, consider the wave that penetrates the conducting medium, i.e., the transmitted wave. Let $x = 0$ at the boundary of the conducting medium, so that x increases positively into the conducting medium.

Let (10-15-14) be written in the form

$$E_y = E_0 e^{-x/\delta} e^{-j(x/\delta)} \quad (1)$$

where $\delta = \sqrt{2/\omega\mu\sigma}$. At $x = 0$, $E_y = E_0$. This is the amplitude of the field at the surface on the conducting medium. Now δ in (1) has the dimension of distance. At a distance $x = \delta$ the amplitude of the field is

$$|E_y| = E_0 e^{-1} = E_0 \frac{1}{e} \quad (2)$$

Thus, E_y decreases to $1/e$ (36.8 percent) of its initial value, while the wave penetrates to a distance δ . Hence δ is called the $1/e$ depth of penetration.

As an example, consider the depth of penetration of a plane electromagnetic wave incident normally on a good conductor, such as copper. Since $\omega = 2\pi f$, the $1/e$ depth becomes

$$\boxed{\delta = \frac{1}{\sqrt{f\pi\mu\sigma}}} \quad (3)$$

For copper $\mu_r = 1$, so that $\mu = 1.26 \text{ }\mu\text{H m}^{-1}$. The conductivity $\sigma = 58 \text{ MU m}^{-1}$. Putting these values in (3), we obtain for copper

$$\delta = \frac{6.6 \times 10^{-2}}{\sqrt{f}} \quad (4)$$

where $\delta = 1/e$ depth of penetration, m

f = frequency, Hz

Evaluating (4) at specific frequencies, we find that

At 60 Hz: $\delta = 8.5 \times 10^{-3} \text{ m}$

At 1 MHz: $\delta = 6.6 \times 10^{-5} \text{ m}$

At 30 GHz: $\delta = 3.8 \times 10^{-7} \text{ m}$

Thus, while at 60 Hz the $1/e$ depth of penetration is 8.5 mm, the penetration decreases in inverse proportion to the square root of the frequency. At 10 mm wavelength (30 GHz) the penetration is only 0.00038 mm, or less than $\frac{1}{2} \mu\text{m}$. This phenomenon is often called *skin effect*.

Thus, a high-frequency field is damped out as it penetrates a conductor in a shorter distance than a low-frequency field.[†]

In addition to the $1/e$ depth of penetration, we can speak of other depths for which the electric field decreases to an arbitrary fraction of its original value. For example, consider the depth at which the field is 0.01 (1 percent) of its original value. This depth is obtained by multiplying the $1/e$ depth by 4.6 and may be called the *1 percent depth of penetration*.

[†] This is analogous to the way in which a rapid temperature variation at the surface of a thermal conductor penetrates a shorter distance than a slow temperature variation.

Phase velocity is given by the ratio ω/β . In the present case, $\beta = 1/\delta$ so that the phase velocity in the conductor is

$$v_c = \omega\delta = \sqrt{\frac{2\omega}{\sigma\mu}} \quad (5)$$

Since the $1/e$ depth is small, the phase velocity in conductors is small. It is apparent from (5) that the velocity is a function of the frequency and hence of the wavelength. In this case, $dv/d\lambda$ is negative, where λ is the free-space wavelength. Hence, conductors are anomalously dispersive media (Sec. 10-7).

The ratio of the velocity of a wave in free space to that in the conducting medium is the index of refraction for the conducting medium. At low frequencies the index for conductors is very large.

To find the wavelength λ_c in the conductor, we have from (5) that $f\lambda_c = \omega\delta$, or

$$\lambda_c = 2\pi\delta \quad (6)$$

In (6), both λ_c and δ are in the same units of length. Hence the wavelength in the conductor is 2π times the $1/e$ depth. Since the $1/e$ depth is small for conductors, the wavelength in conductors is small.

Values of the $1/e$ depth, 1 percent depth, wavelength, velocity, and refractive index for a medium of copper are given in Table 10-4 for three frequencies.

It is interesting to note that the electric field is damped to 1 percent of its initial amplitude in about $\frac{1}{4}\lambda$ in the metal.

Since the penetration depth is inversely proportional to the square root of the frequency, a thin sheet of conducting material can act as a low-pass filter for electromagnetic waves.

Table 10-4 PENETRATION DEPTHS, WAVELENGTH, VELOCITY, AND REFRACTIVE INDEX FOR COPPER

	Frequency		
	60 Hz	1 MHz	30 GHz
Wavelength in free space λ (m)	5 mm	300 m	10 mm
$1/e$ depth, m	8.5×10^{-3}	6.6×10^{-5}	3.8×10^{-7}
1 percent depth, m	3.9×10^{-2}	3×10^{-4}	1.7×10^{-6}
Wavelength in conductor λ_c , m	5.3×10^{-2}	4.1×10^{-4}	2.4×10^{-6}
Velocity in conductor v_c , m s ⁻¹	3.2	4.1×10^2	7.1×10^4
Index of refraction, dimensionless	9.5×10^7	7.3×10^5	4.2×10^3

10-17 RELAXATION TIME

Thus far, the behavior of electromagnetic waves in conducting media has been discussed from the standpoint of depth of penetration, velocity, and so forth. It is instructive to consider the problem from another point of view, namely, from that of the behavior of a charge configuration placed in the conducting medium.

Consider a conducting medium of infinite extent, in which is placed a charge of arbitrary shape and density. Imagine that the charge is released and, because of the mutual repulsion of the like charges of which it is composed, spreads out through the conducting medium. Now let us determine how long it takes for such a charge of density ρ to decrease in density to $1/e$ of its original value.

According to (4-13-3), the continuity relation between current density and charge density is

$$\nabla \cdot \mathbf{J} = -\frac{\partial \rho}{\partial t} \quad (1)$$

From Maxwell's equation $\nabla \cdot \mathbf{D} = \rho$, and from $\mathbf{D} = \epsilon \mathbf{E}$

$$\nabla \cdot \mathbf{E} = \frac{\rho}{\epsilon} \quad (2)$$

But $\mathbf{J} = \sigma \mathbf{E}$, so that (2) becomes

$$\nabla \cdot \mathbf{J} = \frac{\rho \sigma}{\epsilon} \quad (3)$$

From (1) and (3) it follows that

$$\frac{\partial \rho}{\partial t} + \frac{\sigma}{\epsilon} \rho = 0 \quad (4)$$

A solution of this equation is

$$\rho = \rho_0 e^{-(\sigma/\epsilon)t} \quad (5)$$

as may be readily verified by taking the first derivative with respect to time and substituting in (4). Let us put

$$T_r = \frac{\epsilon}{\sigma} \quad (6)$$

T_r has the dimension of time. At $t = 0$, $\rho = \rho_0$, which is the initial charge density. When $t = T_r$,

$$\rho = \rho_0 e^{-1} = \rho_0 \frac{1}{e} \quad (7)$$

Thus, T_r is the time required for the charge density to decrease to $1/e$ of its initial value. The quantity T_r is called the *relaxation time*.

In a lossless dielectric $\sigma = 0$, so that T_r is infinite. Hence the charge maintains its original density indefinitely. On the other hand, for a conductor such as copper, for which $\sigma = 58 \text{ M}\Omega \text{ m}^{-1}$ and $\epsilon = 8.85 \text{ pF m}^{-1}$, we find that

$$T_r = 1.5 \times 10^{-19} \text{ s}$$

This very short interval corresponds to the length of one period for x-rays. Thus, at radio and microwave frequencies the relaxation time is much less than the period. The result of the short relaxation time is that the conductor cannot maintain a charge configuration long enough to permit propagation of a wave more than a very short distance into the conductor. When the frequency is sufficiently high, of the order of 10^{19} Hz , the relaxation time is about the same length as the period and propagation is possible.

10-18 IMPEDANCE OF CONDUCTING MEDIA

The behavior of conducting media toward plane electromagnetic waves can be considered from yet another point of view, the standpoint of impedance.

A solution of the wave equation for the electric field of a linearly polarized plane wave traveling in the x direction in a conducting medium with \mathbf{E} in the y direction is of the form

$$\dot{\mathbf{E}}_y = E_0 e^{j(\omega t - \gamma x)} \quad (1)$$

while for the magnetic field a solution is

$$\dot{\mathbf{H}}_z = H_0 e^{j(\omega t - \xi - \gamma x)} \quad (2)$$

where ξ is the lag in time phase of $\dot{\mathbf{H}}_z$ with respect to $\dot{\mathbf{E}}_y$, or the lead of $\dot{\mathbf{E}}_y$ with respect to $\dot{\mathbf{H}}_z$.

Taking the ratio of (1) to (2) yields the intrinsic impedance \dot{Z}_c of the conducting medium. Thus

$$\dot{Z}_c = \frac{\dot{\mathbf{E}}_y}{\dot{\mathbf{H}}_z} = \frac{E_0}{H_0 e^{-j\xi}} = \frac{E_0}{H_0 / -\xi} = \frac{E_0 / \xi}{H_0} = Z_c / \xi \quad (3)$$

According to (3), the magnitude or modulus of the intrinsic impedance is equal to the ratio of the electric to the magnetic field, and the phase angle of the impedance is equal to ξ .†

† The dot on Z_c indicates explicitly that the impedance is also a complex quantity. It is a complex function of the phase angle ξ .

To evaluate \dot{Z}_c in terms of the constants of the conducting medium, we proceed as follows. Maxwell's equation from Faraday's law for a plane wave with components \dot{E}_y and \dot{H}_z is

$$\frac{\partial \dot{E}_y}{\partial x} = -\mu \frac{\partial \dot{H}_z}{\partial t} \quad (4)$$

Taking the x derivative of (1) and the t derivative of (2) and substituting in (4) yields

$$\gamma \dot{E}_y = j\mu\omega \dot{H}_z \quad (5)$$

The intrinsic impedance \dot{Z}_c is then given by

$$\dot{Z}_c = \frac{\dot{E}_y}{\dot{H}_z} = \frac{j\omega\mu}{\gamma} \quad (6)$$

When we recall from (10-15-13) that for a good conductor

$$\gamma \approx (1 + j) \sqrt{\frac{\omega\mu\sigma}{2}}$$

Eq. (6) becomes

$$\dot{Z}_c = \frac{\dot{E}_y}{\dot{H}_z} = \frac{1 + j}{\sqrt{2}} \sqrt{\frac{\mu\omega}{\sigma}} = (1 + j) \frac{1}{\sigma\delta} \quad (7)$$

Since

$$\frac{1 + j}{\sqrt{2}} = 1/45^\circ$$

the intrinsic impedance can also be expressed as

$$\dot{Z}_c = Z_c / \xi = \sqrt{\frac{\mu\omega}{\sigma}} / 45^\circ$$

(8)

It follows that the magnitude of the intrinsic impedance of a conductor is given by

$$Z_c = \sqrt{\frac{\mu\omega}{\sigma}} = \frac{E_0}{H_0} \quad (9)$$

and the phase angle by

$$\xi = 45^\circ \quad (10)$$

Whereas the intrinsic impedance of a perfect dielectric medium is a pure resistance (\dot{E}_y and \dot{H}_z in time phase), we note from (8) that the intrinsic impedance of a conductor is a complex quantity, \dot{H}_z lagging \dot{E}_y in time phase by very nearly 45° .

This is analogous to the situation in a circuit having resistance and inductance in series where the current lags the applied voltage. Therefore the conducting medium behaves like an inductive impedance. This can be expressed explicitly by writing \dot{Z}_c in terms of its resistive, or real, part R and its reactive, or imaginary, part X . That is,

$$\dot{Z}_c = R + jX = \sqrt{\frac{\mu\omega}{2\sigma}} + j\sqrt{\frac{\mu\omega}{2\sigma}} \quad (11)$$

The intrinsic impedance may be expressed in yet another form, as follows. Multiplying and dividing in (7) by ϵ , ϵ_0 , and μ_0 gives

$$\dot{Z}_c = \frac{1+j}{\sqrt{2}} \sqrt{\frac{\mu_0 \epsilon_0 \mu}{\epsilon \cdot \mu_0 \sigma}} \quad (12)$$

Substituting ϵ_r and μ_r for the ratios in (12), we have

$$\dot{Z}_c = \frac{1+j}{\sqrt{2}} \sqrt{\frac{\mu_0}{\epsilon_0}} \sqrt{\frac{\mu_r}{\epsilon_r}} \sqrt{\frac{\omega\epsilon}{\sigma}} \quad (13)$$

But $\sqrt{\mu_0/\epsilon_0}$ is the intrinsic resistance of free space, which equals 376.7Ω , so that

$$\dot{Z}_c = \frac{1+j}{\sqrt{2}} \times 376.7 \sqrt{\frac{\mu_r}{\epsilon_r}} \sqrt{\frac{\omega\epsilon}{\sigma}} \quad (\Omega) \quad (14)$$

where μ_r = relative permeability of medium, dimensionless

ϵ_r = relative permittivity of medium, dimensionless

ω = radian frequency = $2\pi f$, rad s⁻¹

ϵ = permittivity of medium, F m⁻¹

σ = conductivity of medium, S m⁻¹

The magnitude or modulus of \dot{Z}_c is

$$Z_c = |\dot{Z}_c| = 376.7 \sqrt{\frac{\mu_r}{\epsilon_r}} \sqrt{\frac{\omega\epsilon}{\sigma}} \quad (15)$$

The ratio $\omega\epsilon/\sigma$ or its reciprocal was discussed in Sec. 10-14. For good conductors $\omega\epsilon/\sigma$ is very small ($\sigma/\omega\epsilon$ very large). Take, for instance, copper. At a frequency of 3 GHz (wavelength 100 mm), $\omega\epsilon/\sigma = 2.9 \times 10^{-9}$. Taking μ_r and ϵ_r as unity, we find the intrinsic impedance of copper at 100 mm to be

$$\dot{Z}_c = \frac{1+j}{\sqrt{2}} \times 376.7 \times 5.4 \times 10^{-5}$$

or $\dot{Z}_c = \frac{1+j}{\sqrt{2}} \times 0.02 = 0.02/45^\circ \Omega$

The magnitude of the intrinsic impedance of copper is $Z_c = |\dot{Z}_c| = 0.02 \Omega$. These results indicate that for a conducting medium such as copper the ratio of E_y to H_z is much less than for free space. If σ is infinite (perfect conductor), $Z_c = 0$ and \mathbf{E} vanishes. The small value of Z_c for copper suggests that the conducting medium behaves like a short circuit to the electromagnetic field.

In the above discussion on the impedance of conducting media, we introduced a value of γ into (6) based on the assumption that $\sigma \gg \omega\epsilon$. However, in the case of a dielectric medium $\omega\epsilon \gg \sigma$, and $\gamma = j\beta = j\omega\sqrt{\mu\epsilon}$. Substituting this value of γ into (6) gives the intrinsic impedance for a dielectric medium equal to $\sqrt{\mu/\epsilon}$.

Some of the important relations for conductors developed in this and preceding sections are summarized in Table 10-5.

Table 10-5 PENETRATION DEPTHS, VELOCITY, WAVELENGTH, INDEX OF REFRACTION, IMPEDANCE, AND RELAXATION TIME IN CONDUCTING MEDIA ($\sigma \gg \omega\epsilon$)[†]

$$\frac{1}{e} \text{ depth} = \delta = \frac{1}{\sqrt{\pi f \mu \sigma}} = \sqrt{\frac{2}{\omega \mu \sigma}} \quad (\text{m})$$

$$1 \text{ percent depth} = 4.6 \delta \quad (\text{m})$$

$$\text{Phase velocity} = v_c = \omega \delta = \sqrt{\frac{2\omega}{\sigma\mu}} \quad (\text{m s}^{-1})$$

$$\text{Wavelength} = \lambda_c = 2\pi\delta \quad (\text{m})$$

$$\text{Index of refraction} = \eta = \frac{c}{v_c} = \frac{c}{\omega\delta} = \sqrt{\frac{\sigma}{2\omega\epsilon_0}} \quad (\text{dimensionless})$$

$$\text{Relaxation time} = T_r = \frac{\epsilon}{\sigma} \quad (\text{s})$$

$$\text{Impedance} = \dot{Z}_c = \sqrt{\frac{\mu\omega}{\sigma}} / 45^\circ \quad (\Omega)$$

[†] where $\omega = 2\pi f$ = radian frequency, rad s⁻¹

f = frequency, Hz

μ = permeability $\approx 1.26 \mu\text{H m}^{-1}$ if no ferromagnetic material is present

ϵ = permittivity, F m⁻¹

σ = conductivity, S m⁻¹

10-19 THE POYNTING VECTOR IN CONDUCTING MEDIA

Assume that a plane wave is traveling in a uniform conducting medium. Let us find the value of the Poynting vector \mathbf{S} for the wave. Suppose that the wave is linearly polarized and traveling in the positive x direction with \mathbf{E} in the y direction and \mathbf{H} in the z direction, as in Fig. 10-17. Let the boundary of the conducting medium be at $x = 0$, and let

$$\dot{E}_y = E_0 e^{j\omega t} \quad (1)$$

and $\dot{H}_z = H_0 e^{j(\omega t - \xi)}$ (2)

From (10-12-18) the scalar magnitude of the average Poynting vector is

$$S_{av} = \operatorname{Re} \dot{\mathbf{S}} = \frac{1}{2} \operatorname{Re} \dot{E}_y \dot{H}_z^* = \frac{1}{2} E_0 H_0 \operatorname{Re} e^{j\xi} \quad (3)$$

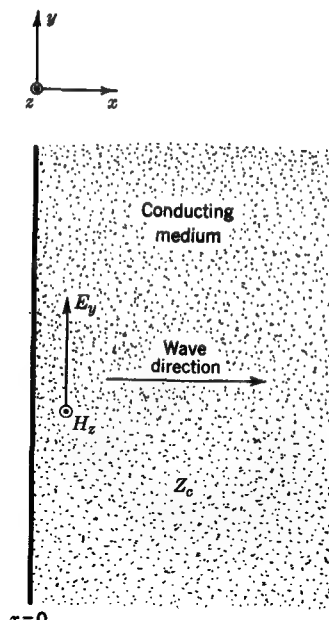
or $S_{av} = \frac{1}{2} E_0 H_0 \cos \xi \quad (\text{W m}^{-2})$ (4)

where E_0 = amplitude of electric field, V m^{-1}

H_0 = amplitude of magnetic field, A m^{-1}

ξ = phase difference between electric and magnetic fields, rad or deg

FIGURE 10-17
Field components of wave in conducting medium.



The Poynting vector is entirely in the x direction in this case. If E_0 and H_0 are rms values, the factor $\frac{1}{2}$ in (4) is omitted. For a conducting medium, ξ is very nearly 45° . Returning to a further consideration of the average Poynting vector, we see that the intrinsic impedance \dot{Z}_c is equal to \dot{E}_y/\dot{H}_z so that (3) can be expressed

$$S_{av} = \frac{1}{2} \operatorname{Re} \dot{H}_z \dot{H}_z^* \dot{Z}_c = \frac{1}{2} |\dot{H}_z|^2 \operatorname{Re} \dot{Z}_c = \frac{1}{2} H_0^2 \operatorname{Re} \dot{Z}_c \quad (\text{W m}^{-2}) \quad (5)$$

This is a very useful relation since if the intrinsic impedance \dot{Z}_c of a conducting medium and also the magnetic field H_0 at the surface are known, it gives the average Poynting vector (or average power per unit area) into the conducting medium.

EXAMPLE A plane 1-GHz traveling wave in air with peak electric field intensity of 1 V m^{-1} is incident normally on a large copper sheet. Find the average power absorbed by the sheet per square meter of area.

SOLUTION First let the intrinsic impedance of copper be calculated at 1 GHz. From (10-18-14)

$$\dot{Z}_c = \frac{1+j}{\sqrt{2}} 376.7 \sqrt{\frac{\mu_r}{\epsilon_r}} \sqrt{\frac{\omega \epsilon}{\sigma}}$$

For copper $\mu_r = \epsilon_r = 1$ and $\sigma = 58 \text{ MU m}^{-1}$. Hence the real part of \dot{Z}_c is

$$\operatorname{Re} \dot{Z}_c = (\cos 45^\circ)(376.7) \sqrt{\frac{2\pi \times 10^9 \times 8.85 \times 10^{-12}}{5.8 \times 10^7}} = 8.2 \text{ m}\Omega$$

Next we find the value of H_0 at the sheet (tangent to the surface). This is very nearly double H for the incident wave. Thus

$$H_0 = 2 \frac{E}{Z} = \frac{2 \times 1}{376.7} \text{ A m}^{-1}$$

From (5) the average power per square meter into the sheet is

$$S_{av} = \frac{1}{2} \left(\frac{2}{376.7} \right)^2 8.2 \times 10^{-3} = 116 \text{ nW m}^{-2}$$

The power from a wave absorbed by a conducting medium may also be conveniently regarded in terms of the current induced in the medium. Since $J = \sigma E$, the current density J in the medium varies in the same manner as the electric field E . Thus for a plane wave incident normally on a conducting medium, as in Fig. 10-17, the current-density variation is expressed by

$$J = J_0 e^{-x/\delta} e^{-j(x/\delta)} \quad (\text{A m}^{-2}) \quad (6)$$

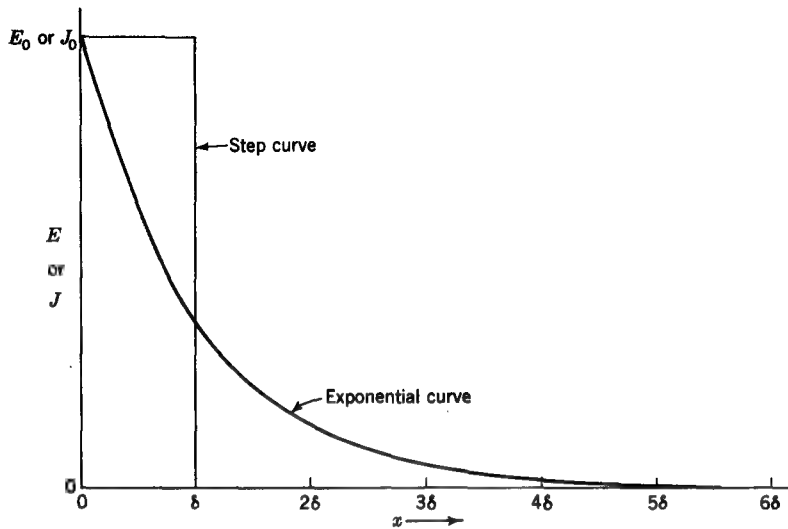


FIGURE 10-18

Relative magnitude of electric field E or current density J as a function of depth of penetration δ for a plane wave traveling in x direction into conducting medium. The abscissa gives the penetration distance x and is expressed in $1/e$ depths (δ). The wavelength in the conductor equals $2\pi\delta$.

where J_0 is the current density at the surface of the medium ($x = 0$). The variation of the magnitude of J (or E) as a function of the distance x is portrayed by the exponential curve in Fig. 10-18. Assuming that the conducting medium extends infinitely far in the positive x direction, the total current per unit width (in z direction) induced in the conducting medium by the wave is given by the integral of the magnitude of J from the surface of the medium ($x = 0$) to infinity. That is,

$$K = \int_0^{\infty} |J| dx = J_0 \int_0^{\infty} e^{-x/\delta} dx = J_0 \delta \quad (7)$$

where K = current per unit width (sheet-current density), $A m^{-1}$

J_0 = current density at surface, $A m^{-2}$

$\delta = 1/e$ depth of penetration, m

Thus the area under the exponential curve in Fig. 10-18 is equal to the area under the step curve. It follows that the total current K per unit width is equal to what would be obtained if J maintained the constant amplitude J_0 from the surface to a depth δ and were zero elsewhere. This gives added significance to the $1/e$ depth of penetration δ .

The average power absorbed per unit area of the conducting medium is, from (5),

$$S_{av} = \frac{1}{2} H_0^2 \operatorname{Re} \dot{Z}_c \quad (8)$$

or since $H_0 = K$ and $\operatorname{Re} \dot{Z}_c = R$,

$$S_{av} = \frac{1}{2} K^2 R \quad (\text{W m}^{-2}) \quad (9)\dagger$$

where $K = J_0 \delta$ = current per unit width, as in (7), A m^{-1}

$R = 1/\sigma\delta$ = resistance of square sheet of conducting medium of thickness δ , Ω per square

The resistance R in (9) is sometimes referred to as the *skin resistance*, since at high frequencies the current may be confined to a very thin layer. Referring to Fig. 12-3, R is the resistance of a square sheet of the medium of thickness $\delta = h$ as measured between two opposite edges.

10-20 CIRCUIT APPLICATION OF THE POYNTING VECTOR

In field theory we deal with point functions such as \mathbf{E} , \mathbf{H} , and \mathbf{S} . Thus, \mathbf{E} and \mathbf{H} give the electric and magnetic fields at a point and \mathbf{S} the power density at a point. In dealing with waves in space it is convenient to use such point functions. On the other hand, in dealing with circuits it is usually more convenient to employ integrated quantities such as V , I , and P . That is, V is the voltage between two points and is equal to the line integral of \mathbf{E} between the points, or

$$V = \int_1^2 \mathbf{E} \cdot d\mathbf{l} \quad (1)$$

The quantity I is the current through a conductor, which is equal to the integral of \mathbf{H} around the conductor or

$$I = \oint \mathbf{H} \cdot d\mathbf{l} \quad (2)$$

The quantity P is, for example, the power dissipated in a load and is equal to the integral of the Poynting vector over a surface enclosing the load, or

$$P = \oint_s \mathbf{S} \cdot d\mathbf{s} \quad (3)$$

[†] Note the similarity between (9) and the circuit relation for the power dissipated in an impedance with a real part (resistance) R as given by $P = \frac{1}{2} I_0^2 R(\text{W})$.

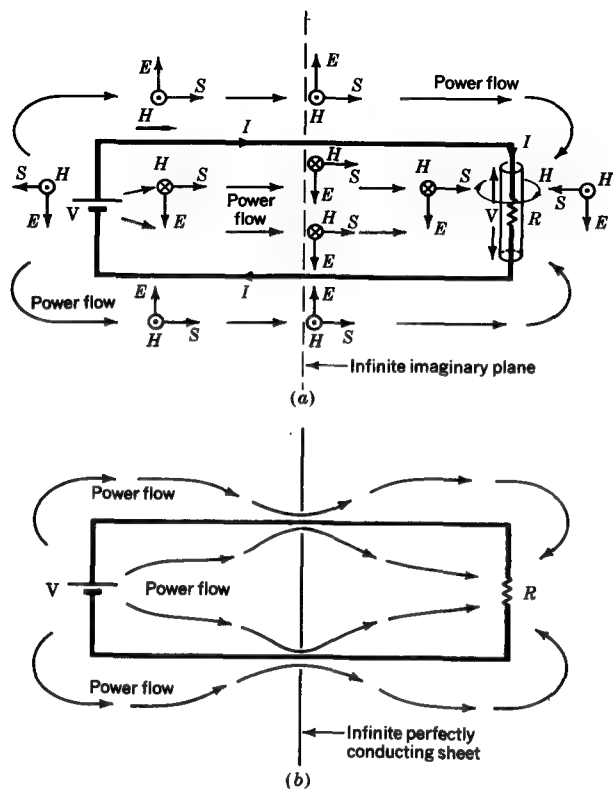


FIGURE 10-19
Simple circuit showing Poynting vector or power flow lines from battery (source) to resistor (load) (a) without and (b) with intervening conducting sheet.

Consider as an illustration the simple circuit of Fig. 10-19a, consisting of a battery connected by a conductor with current I to a load of resistance R . All the emf of the circuit is confined to the battery and all resistance to the load (conductivity of the conductor is infinite).

There exists an electric field \mathbf{E} extending between the conductors ($\oint \mathbf{E} \cdot d\mathbf{l} = V$, where \mathbf{E} is integrated from the upper to the lower conductor) and a magnetic field \mathbf{H} around the conductors ($\oint \mathbf{H} \cdot d\mathbf{l} = I$), as suggested in Fig. 10-19a. At any point the Poynting vector \mathbf{S} (in watts per square meter) is given by the cross product of \mathbf{E} and \mathbf{H} ($\mathbf{S} = \mathbf{E} \times \mathbf{H}$). The direction of the Poynting vector is suggested at several points in Fig. 10-19a. Around the battery (power source) the Poynting vector is outward (positive). Around the resistor (load) the Poynting vector is inward (negative).

Over an imaginary plane through the middle of the circuit the Poynting vector is to the right (from battery to load). The total power leaving the battery or entering the load is given by the integral of the Poynting vector over a surface enclosing the battery (positive power), over a surface enclosing the load (negative power), or over an infinite plane dividing the circuit as suggested.

The total power into the load is given by

$$P = \oint_s (\mathbf{E} \times \mathbf{H}) \cdot d\mathbf{s} \quad (4)$$

where the integration is over a surface enclosing the load, such as the cylindrical surface shown in Fig. 10-19a. The fields \mathbf{E} and \mathbf{H} are everywhere normal to each other. They are also both tangent to the cylindrical surface enclosing the resistor or load. Thus, from the geometry in this case (4) reduces to

$$P = - \int \mathbf{E} \cdot d\mathbf{l} \oint \mathbf{H} \cdot d\mathbf{l} \quad (5)$$

or

$$P = -VI \quad (6)$$

where $V = \int \mathbf{E} \cdot d\mathbf{l}$ = voltage between ends of the cylinder (or load), V

$I = \oint \mathbf{H} \cdot d\mathbf{l}$ = current through load, A

Thus, integrating the Poynting vector over the resistor† yields the same power VI as given by circuit theory. However, from the field point of view the power entering the load is negative power since \mathbf{S} is inward, or negative, over the surface enclosing the load.

In Fig. 10-19a flow lines of the Poynting vector (power flow lines) are shown. It is evident that the power flow is through the empty space surrounding the circuit, the conductors of the circuit acting as guiding elements. From the circuit point of view we usually think of the power as flowing *through* the wires but this is an oversimplification and does not represent the actual situation.

Suppose now that a perfectly conducting infinite sheet is placed across the middle of the circuit, as in Fig. 10-19b. The sheet is continuous except for two small openings through which the circuit conductors pass. The power flow through the sheet is zero (\mathbf{E} in sheet is zero), and all power flow from the battery to the load is through the two holes containing the circuit conductors. However, \mathbf{E} is very large in these openings, and \mathbf{S} is also large. The integral of \mathbf{S} over these openings again equals the total power flowing from the battery to the load. The flow lines of the Poynting vector (power flow lines) for this case are as suggested in Fig. 10-19b.

† We have neglected the contribution of power flowing through the flat end surfaces of the cylinder. However, this can be made negligibly small if the cylinder diameter is very small compared to its length.

Consider now that the battery in Fig. 10-19a and b is replaced by an alternator whose emf varies harmonically with time. The average (or total power) is now given by

$$\begin{aligned} P_{av} &= \oint_s \operatorname{Re} \mathbf{S} \cdot d\mathbf{s} = \frac{1}{2} \oint_s \operatorname{Re} (\mathbf{E} \times \mathbf{H}^*) \cdot d\mathbf{s} \\ &= \frac{1}{2} \operatorname{Re} \int \mathbf{E} \cdot dl \oint \mathbf{H}^* \cdot dl \end{aligned} \quad (7)$$

Integrating over the alternator gives†

$$P_{av} = \frac{1}{2} \operatorname{Re} VI^* = \frac{1}{2} V_0 I_0 \operatorname{Re} e^{j\xi} = \frac{1}{2} V_0 I_0 \cos \xi \quad (8)$$

where $V = V_0 e^{j\omega t}$

$$I^* = I_0 e^{-j(\omega t - \xi)}$$

V_0 = amplitude or peak value of V

I_0 = amplitude or peak value of I

ξ = time-phase angle between current and voltage

$\cos \xi$ = power factor

Integrating (7) over the load, we obtain

$$P_{av} = -\frac{1}{2} V_0 I_0 \cos \xi \quad (9)$$

which is equal in magnitude but opposite in sign to (8).

Since the load impedance $Z = V/I$, we also have (omitting the negative sign) that

$$P_{av} = \frac{1}{2} I_0^2 \operatorname{Re} Z = \frac{1}{2} I_0^2 R \quad (10)$$

where R is the resistance of the load (real part of Z) in ohms.

10-21 GENERAL DEVELOPMENT OF THE WAVE EQUATION

In this chapter we have dealt with plane waves (traveling in the x direction). The wave equation was developed for this special case, and appropriate solutions were obtained. A more general development of the wave equation will now be given, and it will be shown that for a plane wave it reduces to the expressions obtained previously.

Maxwell's curl equations are

$$\nabla \times \mathbf{H} = \mathbf{J} + \frac{\partial \mathbf{D}}{\partial t} = \sigma \mathbf{E} + \epsilon \frac{\partial \mathbf{E}}{\partial t} \quad (1)$$

$$\text{and } \nabla \times \mathbf{E} = - \frac{\partial \mathbf{B}}{\partial t} = -\mu \frac{\partial \mathbf{H}}{\partial t} \quad (2)$$

† \mathbf{E} , \mathbf{H}^* , V , and I^* are complex quantities (phasors). For simplicity the dot is omitted.

Taking the curl of (2) and introducing the value of $\nabla \times \mathbf{H}$ from (1) gives

$$\nabla \times (\nabla \times \mathbf{E}) = -\mu \frac{\partial(\nabla \times \mathbf{H})}{\partial t} = -\mu \frac{\partial}{\partial t} \left(\sigma \mathbf{E} + \epsilon \frac{\partial \mathbf{E}}{\partial t} \right) \quad (3)$$

But by a vector identity, meaningful only in rectangular coordinates, the left-hand side of (3) can be expressed

$$\nabla \times (\nabla \times \mathbf{E}) = \nabla(\nabla \cdot \mathbf{E}) - \nabla^2 \mathbf{E} \quad (4)$$

Equating (4) and (3), and noting that in space having no free charge $\nabla \cdot \mathbf{E} = 0$, we get

$$\nabla^2 \mathbf{E} = \mu\epsilon \frac{\partial^2 \mathbf{E}}{\partial t^2} + \mu\sigma \frac{\partial \mathbf{E}}{\partial t} \quad (5)$$

With the assumption of harmonic variation of the field with time, (5) reduces to

$$\nabla^2 \mathbf{E} = (-\omega^2 \mu\epsilon + j\omega \mu\sigma) \mathbf{E} = \gamma^2 \mathbf{E} \quad (6)$$

or

$$\nabla^2 \mathbf{E} - \gamma^2 \mathbf{E} = 0 \quad (7)$$

From (4) we can also write

$$\boxed{\nabla \times \nabla \times \mathbf{E} + \gamma^2 \mathbf{E} = 0} \quad (8)$$

Equations (5) to (8) are vector wave equations in \mathbf{E} . In (5) the time is explicit, while in the other three it is implicit, harmonic variation with time being assumed. These wave equations incorporate all four of Maxwell's equations. Maxwell's two curl equations are the starting point for the wave equation, and (5) to (8) satisfy them. Maxwell's two divergence equations are also satisfied.

For a plane wave traveling in the x direction with \mathbf{E} in the y direction ($\mathbf{E} = \hat{y} E_y$), Eq. (5) reduces to

$$\frac{\partial^2 E_y}{\partial x^2} = \mu\epsilon \frac{\partial^2 E_y}{\partial t^2} + \mu\sigma \frac{\partial E_y}{\partial t} \quad (9)$$

which is the same as (10-15-5). If $\sigma = 0$,

$$\frac{\partial^2 E_y}{\partial x^2} = \mu\epsilon \frac{\partial^2 E_y}{\partial t^2} \quad (10)$$

which is the same as obtained for a lossless medium in (10-2-12). These are scalar wave equations.

If \mathbf{E} does not change with time (\mathbf{E} static),

$$\nabla^2 \mathbf{E} = 0 \quad (11)$$

If \mathbf{E} is a harmonic function of time, (9) becomes

$$\frac{\partial^2 E_y}{\partial x^2} = -\omega^2 \mu \epsilon E_y + j\omega \mu \sigma E_y, \quad (12)$$

or

$$\frac{\partial^2 E_y}{\partial x^2} - \gamma^2 E_y = 0 \quad (13)$$

which is the same as (10-15-10).

PROBLEMS

- * 10-1 A plane traveling wave has a peak electric field $E_0 = 6 \text{ V m}^{-1}$. If the medium is lossless with $\mu_r = 1$ and $\epsilon_r = 3$, find (a) velocity of wave, (b) peak Poynting vector, (c) average Poynting vector, (d) impedance of medium, and (e) peak value of the magnetic field H .
- * 10-2 A plane traveling 100-MHz wave has an average Poynting vector of 5 W m^{-2} . If the medium is lossless with $\mu_r = 2$ and $\epsilon_r = 2$, find (a) velocity of wave, (b) wavelength, (c) impedance of medium, (d) rms electric field E , and (e) rms magnetic field H .
- 10-3 Does the term perfect vacuum (or free space) imply the absence of everything?
- * 10-4 For a 10-MHz traveling wave with $E_0 = 6 \text{ V m}^{-1}$ find (a) average Poynting vector, (b) peak energy density, and (c) mass equivalent per unit volume. The medium is free space.
- 10-5 Show that for a traveling wave the peak energy density stored in the electric field equals that stored in the magnetic field.
- 10-6 (a) From Maxwell's curl equations derive the wave equation in H for a plane wave traveling in the positive x direction in a medium with constants $\mu = \mu_0$, $\epsilon = \epsilon_0$, and $\sigma = 0$. The electric field is in the y direction. (b) Obtain a solution for the case of harmonic variation and prove that it is a solution.
- * 10-7 A plane 3-GHz wave is incident normally on a large sheet of polystyrene ($\epsilon_r = 2.7$). How thick must the sheet be to retard the wave in phase by 180° with respect to a wave which travels through a large hole in the sheet?
- * 10-8 The earth receives $2.0 \text{ g cal min}^{-1} \text{ cm}^{-2}$ of sunlight. (a) What is the Poynting vector in watts per square meter? (b) What is the power output of the sun in sunlight assuming that the sun radiates isotropically? (c) What is the rms electric field E at the earth assuming that the sunlight is all at a single frequency? (d) How long does it take the sunlight to reach the earth? Take the earth-sun distance as 150 Gm. ($1 \text{ W} = 14.3 \text{ g cal min}^{-1}$.)
- 10-9 A 1.4-GHz radio wave received from an extragalactic radio source has an average Poynting vector per unit bandwidth (or flux density) of $10^{-26} \text{ W m}^{-2} \text{ Hz}^{-1}$. (a) How much power is intercepted by an area of $1,000 \text{ m}^2$ over a bandwidth of 1 MHz? The area is normal to the wave direction. (b) If the radio source is at a distance of 10^9 light-years and radiates isotropically, what is the power radiated by the source in a 1-MHz bandwidth?

* Answers to starred problems are given in Appendix C.

One light-year equals the distance light or radio waves travel in 1 year. Assume that the medium is free space. (c) How does this power compare with the earth's *total* power requirements for electricity, heating, industry, transportation, etc.?

- * 10-10 3-GHz radio waves from the sun have a flux density of $10^{-20} \text{ W m}^{-2} \text{ Hz}^{-1}$. (a) What is the Poynting vector for a 1-GHz bandwidth assuming the flux density is constant over this bandwidth? (b) What is the rms electric field E assuming that the power in the 1-GHz bandwidth is at a single frequency? (c) What is the radio power output of the sun for the 1-GHz bandwidth assuming that the sun radiates isotropically? Take earth-sun distance as 150 Gm.

10-11 (a) Referring to Prob. 10-8, what is the Poynting vector per unit bandwidth of sunlight at the earth? Take the sunlight band as 400 to 800 nm (4000 to 8000 Å). (b) What is the ratio of this Poynting vector to that given in Prob. 10-10 for 3-GHz radio waves? (c) According to Planck's radiation law, the radiation brightness \mathcal{B} from a blackbody is given by

$$\mathcal{B} = \frac{2hf^3}{c^2} \frac{1}{e^{hf/kT} - 1} \quad (\text{W m}^{-2} \text{ Hz}^{-1} \text{ rad}^{-2})$$

where h = Planck's constant = $6.63 \times 10^{-34} \text{ J s}$

f = frequency, Hz

c = velocity of light or radio waves = 300 Mm s^{-1}

k = Boltzmann's constant = $1.38 \times 10^{-23} \text{ J K}^{-1}$

T = blackbody temperature, K

Taking $T = 6 \text{ kK}$ for the sun, would you say that the sun behaves as a blackbody (or Planck) radiator over the above optical-radio range?

10-12 According to quantum theory, electromagnetic waves are transmitted by photons of energy hf , where h = Planck's constant = $6.63 \times 10^{-34} \text{ J s}$ and f = frequency in hertz. Find the number of photons per second which are intercepted by an area 1 m square for a wave with average Poynting vector of $10^{-20} \text{ W m}^{-2}$ for two cases: (a) frequency = 2 GHz and (b) wavelength = 600 nm. The area is normal to the wave direction. (c) What advantage do radio waves have over optical waves for transmission of information if the wave is so weak that the number of photons is small?

- * 10-13 The earth receives about 1.5 kW m^{-2} of power from the sun (integrated over all frequencies). (a) What is the sun's total power output assuming it radiates isotropically? Take the earth-sun distance as 150 Gm. (b) What is the total power received by the earth? Take the earth's radius as 6.4 Mm. (c) If the sun's mass is $2 \times 10^{30} \text{ kg}$ and its mass is converted to radiant energy according to Einstein's relation (energy = mc^2) at 1 percent efficiency, how long can the sun radiate at its present level?

10-14 A spaceship at lunar distance from the earth transmits 2-GHz waves. If a power of 10 W is radiated isotropically, find (a) average Poynting vector at the earth, (b) rms electric field E at the earth, (c) the time it takes for the radio waves to travel from the spaceship to the earth. (Take the earth-moon distance as 380 Mm.) (d) How many photons per unit area per second fall on the earth from the spaceship transmitter?

- * 10-15 At 100 kHz a lossless medium has constants $\mu_r = 1$ and $\epsilon_r = 81$. These constants are approximated by distilled water. Find (a) Z/Z_0 , the ratio of the impedance of the medium to that of free space, (b) λ/λ_0 , the ratio of the wavelength in the medium to

that in free space, (c) v/v_0 , the ratio of the wave velocity in the medium to that in free space, and (d) the index of refraction.

10-16 Compute and plot curves for the amplitude of the resultant electric field due to two plane waves traveling in the positive and negative x direction at three instants of time $t = 0$, $T/8$, and $T/4$, where T = period. The waves have only E_x components. The wave in the positive x direction has an amplitude $E_0 = 1 \text{ V m}^{-1}$ and the other wave an amplitude $E_1 = 0.4 \text{ V m}^{-1}$. Extend the plot over a distance of at least 1λ in the x direction. (a) In which direction does a constant-phase point move? (b) What is the standing-wave ratio? (c) Assuming that the smaller wave is a reflection of the larger, what is the magnitude of the reflection coefficient?

10-17 A plane wave in free space is reflected at normal incidence from an infinite perfectly conducting sheet, producing a standing wave. The amplitude of E of the incident wave is 12 mV m^{-1} . (a) How far from the sheet is the Poynting vector a maximum? (b) What is the average value of the Poynting vector? (c) What is the maximum value of the Poynting vector?

* **10-18** A plane wave is reflected at normal incidence from a boundary surface. The amplitude of the electric field E of the incident wave is 10 mV m^{-1} and of the reflected wave is E_r . Find the VSWR when (a) $E_r = 2 \text{ mV m}^{-1}$, (b) $E_r = 5 \text{ mV m}^{-1}$, and (c) $E_r = 8 \text{ mV m}^{-1}$. (d) Under what conditions is there a pure standing wave?

* **10-19** A 50-mW 11-GHz transmitter radiates isotropically. At a distance of 5 km find (a) rms electric field E , (b) rms magnetic field H , (c) average power per unit area (Poynting vector), (d) average energy density, and (e) energy contained in a volume of unit area (1 m^2) perpendicular to the wave direction by 10λ in the direction of propagation. The medium is air.

10-20 A cylindrical resistor of length l , radius a , and conductivity σ carries an rms current I . (a) Show that the Poynting vector is directed normally *inward* with respect to the surface of the resistor. (b) Show that the integral of the Poynting vector over the surface of the resistor equals $I^2 R$, where R is the resistance of the resistor.

10-21 A parallel-plate capacitor which is being charged consists of two flat circular disks of radius a and separation distance d . (a) Show that the Poynting vector is directed normally *inward* with respect to a surface enclosing the capacitor. (b) Show that the integral of the Poynting vector over this surface equals $\frac{1}{2}da^2\epsilon_0 dE^2/dt$. The medium filling the capacitor is air. Neglect fringing. (c) Under what circumstances would the integral of the Poynting vector over the surface enclosing the capacitor be zero, even though the charge on the capacitor is not zero?

10-22 (a) Referring to part (a) of Prob. 10-21, what circumstances are required for the Poynting vector to be directed normally *outward* with respect to the surface bounding the capacitor? (b) Referring to part (a) of Prob. 10-20, what circumstances are required for the Poynting vector, if not zero, to be everywhere directed normally *outward* with respect to the surface of the resistor?

10-23 Show that in a standing wave the average phase velocity of the resultant field is equal to the geometric mean of the maximum and minimum velocities; that is, $v_{av} = \sqrt{v_{max} v_{min}}$.

10-24 Show that when the incident-wave amplitude E_0 is much greater than the reflected-wave amplitude E_1 , the standing-wave-envelope expression of (10-10-13) becomes approximately $E_y = E_0 + E_1 \cos 2\beta x$.

10-25 Given a plane wave for which $E = E_0 \operatorname{Re} e^{j(\omega t - \beta x)}$. Show that the resultant of two waves of this type of equal amplitude and of two frequencies $\omega_0 + \omega_1$ and $\omega_0 - \omega_1$ (and two corresponding phase constants given by $\beta_0 + \beta_1$ and $\beta_0 - \beta_1$) may be expressed as $E = 2E_0 \cos(\omega_0 t - \beta_0 x) \cos(\omega_1 t - \beta_1 x)$.

10-26 The group velocity $u = dw/d\beta$. Show that u can be expressed also in the following forms: $u = v + \beta (dv/d\beta) = v - \lambda (dv/d\lambda) = df/d\lambda^{-1}$, where v = phase velocity.

10-27 Find the group velocity for a 100-MHz wave in a normally dispersive, lossless medium for which the phase velocity $v = 2 \times 10^7 \lambda^{2/3} \text{ m s}^{-1}$.

10-28 For a plane wave in a dielectric medium show that the energy velocity can be expressed as $1/\epsilon Z$ or Z/μ , where Z is the intrinsic impedance of the medium.

* **10-29** A medium has constants $\sigma = 0.1 \text{ U m}^{-1}$, $\mu_r = 1$, $\epsilon_r = 40$. Assuming that these values do not change with frequency, does the medium behave like a conductor or a dielectric at (a) 50 KHz and (b) 10 GHz?

10-30 A plane 1.59-GHz wave with rms electric field $E = 3 \text{ V m}^{-1}$ is traveling in a medium with constants $\sigma = 0.01 \text{ U m}^{-1}$, $\mu_r = \epsilon_r = 1$. Find the rms values of (a) conduction-current density, (b) displacement-current density, and (c) total-current density. (d) What is the average power flow per unit area in the direction of the wave propagation?

* **10-31** A medium has constants $\sigma = 10^2 \text{ U m}^{-1}$, $\mu_r = 2$, $\epsilon_r = 3$. If the constants do not change with frequency, find the $1/e$ and 1 percent depths of penetration at (a) 60 Hz, (b) 2 MHz, (c) 3 GHz.

10-32 At 500 MHz a medium has constants $\mu_r = 5$, $\epsilon_r = 7$, $\sigma = 1 \text{ U m}^{-1}$. Find (a) Z/Z_0 , the ratio of the intrinsic impedance of the medium to that of free space, (b) λ/λ_0 , the ratio of the wavelength in the medium to that in free space, (c) v/v_0 , the ratio of the wave velocity in the medium to that in free space, (d) $1/e$ depth of penetration, (e) wave attenuation in decibels for a 5-mm thickness, and (f) reflection coefficient ρ for a wave in air incident normally on a large flat surface of a half-space filled with the medium.

* **10-33** At 200 MHz a solid ferrite-titanate medium has complex constants $\mu_r = 15(1-j3)$ and $\epsilon_r = 50(1-j1)$. Find (a) Z/Z_0 , (b) λ/λ_0 , (c) v/v_0 , (d) $1/e$ depth, (e) attenuation for a 5-mm thickness, and (f) ρ , where the symbols and circumstances are as explained in Prob. 10-32.

10-34 (a) A medium of large extent with constants $\sigma = 10^{-3} \text{ U m}^{-1}$, $\mu_r = \epsilon_r = 1$ is terminated by an infinitely conducting sheet situated at $x = 0$. A plane 1.59-GHz wave in the medium is incident normally on the sheet. If the electric field of the incident wave is 1 V m^{-1} at the sheet, draw a graph of E from $x = 0$ (at the sheet) to $x = 4 \text{ m}$ for (a) incident wave, (b) reflected wave, and (c) total wave.

10-35 In Prob. 10-34 at what distance from the sheet is the reflected wave (a) down 20 dB and (b) down 40 dB with respect to the incident wave at the same distance?

10-36 Antarctica and Greenland are covered with ice of great thickness. Radio-equipped surface vehicles are used to measure the thickness of the ice by sending radio waves down through the ice and obtaining a reflection from the ground under the ice. It is assumed

that the ice is homogeneous and of uniform thickness over a flat perfectly conducting earth. Take the constants for the ice at 30 MHz as $\mu_r = 1$ and $\epsilon_r = 3 - j0.01$. (a) Find the ratio of the power received per unit area to the power radiated at 30 MHz for a 2-km thickness of ice. Express in decibels. (b) Compare this value with the ratio in decibels if the ice were replaced by air. The difference is the attenuation due to the presence of the ice. In (a) and (b) assume that the vehicle transmitter radiates isotropically and that there is no loss (mismatch) at the air-ice interface. (c) What is the travel time for the wave down and back through the ice? (d) Would it be more accurate to determine the ice thickness by pulsing the transmitter and measuring the delay time of the reflected pulse, as in a radar system, or by measuring the wave attenuation? (e) Which scheme would be more practical?

10-37 By a technique like that in Prob. 10-36 discuss the possibilities of using radio waves for exploring the interior of the moon.

* 10-38 If distilled water has constants $\mu_r = 1$, $\epsilon_r = 81$ and power factor = 0.05 at 1 GHz, calculate (a) the $1/e$ depth of penetration and (b) the 1 percent depth of penetration at this frequency.

10-39 (a) A 1-GHz traveling wave in air has an electric field $E = 100 \text{ MV m}^{-1}$. If the wave is incident normally on a flat copper sheet, how thick must the sheet be to reduce the wave transmitted through the sheet to the nonhazardous level of 100 W m^{-2} ? Hint: Consider the copper sheet as a short section of lossy transmission line connected between two lossless lines of characteristic impedance $Z_0 = 376.7 \Omega$. [Regarding hazardous radiation levels see W. W. Mumford, Some Technical Aspects of Microwave Radiation Hazards, *Proc. IRE*, 49:427-447 (February 1961)]. (b) What power is dissipated per square meter in the sheet? (c) Will dissipation of this power be a problem, and if so, how can it be accomplished?

11

WAVE POLARIZATION

11-1 INTRODUCTION†

In this chapter the polarization of electromagnetic waves is discussed. Linear, elliptical, and circular polarization are considered, and their relation on the Poincaré sphere is explained. These concepts are first developed for coherent, completely polarized waves and then extended to the case of partially and completely unpolarized or incoherent radiation. Finally Stokes parameters and coherency matrices are introduced for handling waves of this kind.

11-2 LINEAR, ELLIPTICAL, AND CIRCULAR POLARIZATION

Consider a plane wave traveling out of the page (positive z direction), as in Fig. 11-1a, with the electric field at all times in the y direction. This wave is said to be *linearly polarized* (in the y direction). As a function of time and position the electric field of a

† A more detailed discussion of wave polarization is given in J. D. Kraus, "Radio Astronomy," McGraw-Hill Book Company, New York, 1966.

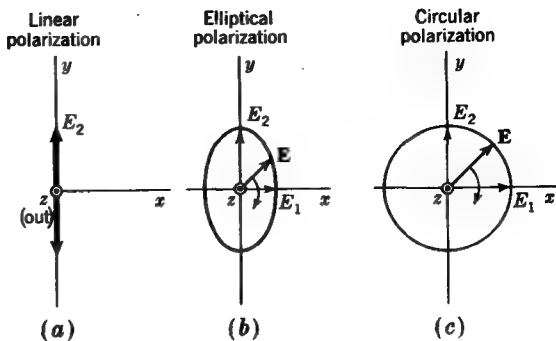


FIGURE 11-1
Linear, elliptical, and circular polarization.

linearly polarized wave (as in Fig. 11-1a) traveling in the positive z direction (out of page) is given by

$$E_y = E_2 \sin(\omega t - \beta z) \quad (1)$$

In general the electric field of a wave traveling in the z direction may have both a y component and an x component, as suggested in Fig. 11-1b. In this more general situation the wave is said to be *elliptically polarized*. At a fixed value of z the electric vector \mathbf{E} rotates as a function of time, the tip of the vector describing an ellipse called the *polarization ellipse*. The ratio of the major to minor axes of the polarization ellipse is called the *axial ratio (AR)*. Thus, for the wave in Fig. 11-1b, $\text{AR} = E_2/E_1$. Two extreme cases of elliptical polarization correspond to *circular polarization*, as in Fig. 11-1c, and *linear polarization*, as in Fig. 11-1a. For circular polarization $E_1 = E_2$ and $\text{AR} = 1$, while for linear polarization $E_1 = 0$ and $\text{AR} = \infty$.

In the most general case of elliptical polarization the polarization ellipse may have any orientation, as suggested in Fig. 11-2. The elliptically polarized wave may be expressed in terms of two linearly polarized components, one in the x direction and one in the y direction. Thus, if the wave is traveling in the positive z direction (out of the page), the electric field components in the x and y directions are

$$E_x = E_1 \sin(\omega t - \beta z) \quad (2)$$

$$E_y = E_2 \sin(\omega t - \beta z + \delta) \quad (3)$$

where E_1 = amplitude of wave linearly polarized in x direction

E_2 = amplitude of wave linearly polarized in y direction

δ = time-phase angle by which E_y leads E_x

Combining (2) and (3) gives the instantaneous total vector field \mathbf{E} :

$$\mathbf{E} = \hat{\mathbf{x}}E_1 \sin(\omega t - \beta z) + \hat{\mathbf{y}}E_2 \sin(\omega t - \beta z + \delta) \quad (4)$$

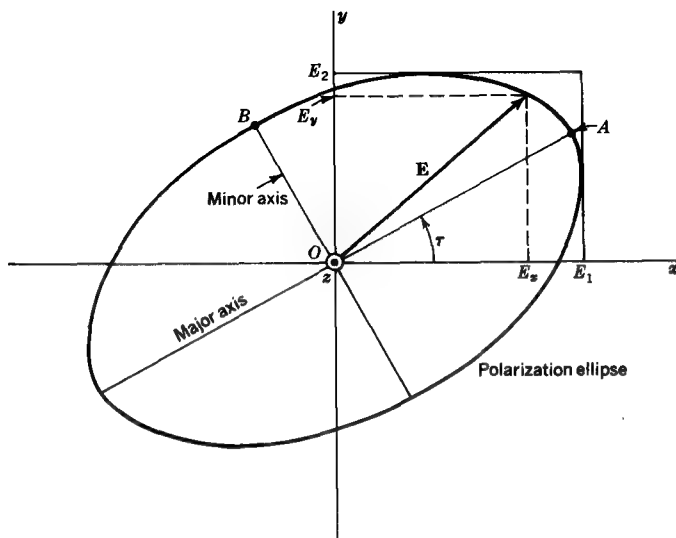


FIGURE 11-2

Polarization ellipse at tilt angle τ showing instantaneous components E_x and E_y , and amplitudes (or peak values) E_1 and E_2 .

At $z = 0$, $E_x = E_1 \sin \omega t$ and $E_y = E_2 \sin(\omega t + \delta)$. Expanding E_y yields

$$E_y = E_2 (\sin \omega t \cos \delta + \cos \omega t \sin \delta) \quad (5)$$

From the relation for E_x we have $\sin \omega t = E_x/E_1$ and $\cos \omega t = \sqrt{1 - (E_x/E_1)^2}$. Introducing these in (5) eliminates ωt , and on rearranging we obtain

$$\frac{E_x^2}{E_1^2} - \frac{2E_x E_y \cos \delta}{E_1 E_2} + \frac{E_y^2}{E_2^2} = \sin^2 \delta \quad (6)$$

or

$$aE_x^2 - bE_x E_y + cE_y^2 = 1 \quad (7)$$

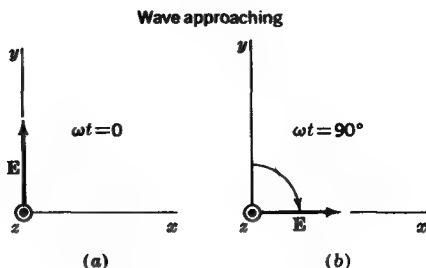
where $a = \frac{1}{E_1^2 \sin^2 \delta}$ $b = \frac{2 \cos \delta}{E_1 E_2 \sin^2 \delta}$ $c = \frac{1}{E_2^2 \sin^2 \delta}$

Equation (7) describes a (polarization) ellipse, as in Fig. 11-2. The line segment OA is the semimajor axis, and the line segment OB is the semiminor axis. The tilt angle of the ellipse is τ . The axial ratio is

$$AR = \frac{OA}{OB} \quad (1 \leq AR \leq \infty) \quad (8)$$

FIGURE 11-3

Instantaneous orientation of electric field vector \mathbf{E} at two instants of time for a left circularly polarized wave which is approaching (out of page).



If $E_1 = 0$, the wave is linearly polarized in the y direction. If $E_2 = 0$, the wave is linearly polarized in the x direction. If $\delta = 0$ and $E_1 = E_2$, the wave is also linearly polarized but in a plane at an angle of 45° with respect to the x axis ($\tau = 45^\circ$).

If $E_1 = E_2$ and $\delta = \pm 90^\circ$, the wave is circularly polarized. When $\delta = +90^\circ$, the wave is *left circularly polarized*, and when $\delta = -90^\circ$, the wave is *right circularly polarized*. For the case $\delta = +90^\circ$ and for $z = 0$ and $\tau = 0$ we have from (2) and (3) that $\mathbf{E} = \hat{\mathbf{y}} E_2$, as in Fig. 11-3a. One-quarter cycle later ($\omega t = 90^\circ$) $\mathbf{E} = \hat{\mathbf{x}} E_1$, as in Fig. 11-3b. Thus, at a fixed position ($z = 0$) the electric field vector rotates clockwise (viewing the wave approaching). According to the IEEE definition, this corresponds to left circular polarization.[†] The opposite rotation direction ($\delta = -90^\circ$) corresponds to right circular polarization.

If the wave is viewed receding (from negative z axis in Fig. 11-3), the electric vector appears to rotate in the opposite direction. Hence, clockwise rotation of \mathbf{E} with the wave approaching is the same as counterclockwise rotation with the wave receding. Thus, unless the wave direction is specified, there is a possibility of ambiguity as to whether the wave is left- or right-handed. This can be avoided by defining the polarization with the aid of helical-beam antennas (see Chap. 14). Thus, a right-handed helical-beam antenna radiates (or receives) right circular (IEEE) polarization.[‡] A right-handed helix, like a right-handed screw, is right-handed regardless of the position from which it is viewed. There is no possibility here of ambiguity.

11-3 POYNTING VECTOR FOR ELLIPTICALLY OR CIRCULARLY POLARIZED WAVES

In complex notation with all complex quantities (phasors) indicated explicitly by a dot, the complex Poynting vector is

$$\dot{\mathbf{S}} = \frac{1}{2} \dot{\mathbf{E}} \times \dot{\mathbf{H}}^* \quad (1)$$

[†] This IEEE definition is opposite to the classical optics definition.

[‡] A left-handed helical-beam antenna radiates (or receives) left circular (IEEE) polarization.

The average Poynting vector is the real part of (1), or

$$\mathbf{S}_{av} = \operatorname{Re} \dot{\mathbf{S}} = \frac{1}{2} \operatorname{Re} \dot{\mathbf{E}} \times \dot{\mathbf{H}}^* \quad (2)$$

Referring to Fig. 11-2, let the elliptically polarized wave have x and y components with a phase difference δ as given by

$$\dot{E}_x = E_1 e^{j(\omega t - \beta z)} \quad (3)$$

$$\dot{E}_y = E_2 e^{j(\omega t - \beta z + \delta)} \quad (4)$$

At $z = 0$ the total electric field (vector) is then

$$\dot{\mathbf{E}} = \hat{x}\dot{E}_x + \hat{y}\dot{E}_y = \hat{x}E_1 e^{j\omega t} + \hat{y}E_2 e^{j(\omega t + \delta)} \quad (5)$$

where \hat{x} = unit vector in x direction

\hat{y} = unit vector in y direction

Note that $\dot{\mathbf{E}}$ is a complex vector (phasor-vector) which is resolvable into two component complex vectors $\hat{x}\dot{E}_x$ and $\hat{y}\dot{E}_y$, where each component has a vector part (indicating space direction) and a complex part or phasor (indicating time phase). Thus, in $\hat{x}\dot{E}_x$, \hat{x} is the vector and \dot{E}_x is the phasor.

The \mathbf{H} -field component associated with \dot{E}_x is

$$\dot{H}_y = H_1 e^{j(\omega t - \beta z - \xi)} \quad (6)$$

where ξ is the phase lag of \dot{H}_y with respect to \dot{E}_x . The \mathbf{H} -field component associated with \dot{E}_y is

$$\dot{H}_x = H_2 e^{j(\omega t - \beta z + \delta - \xi)} \quad (7)$$

The total \mathbf{H} field (vector) at $z = 0$ for a wave traveling in the positive z direction is then

$$\dot{\mathbf{H}} = \hat{y}\dot{H}_y - \hat{x}\dot{H}_x = \hat{y}H_1 e^{j(\omega t - \xi)} - \hat{x}H_2 e^{j(\omega t + \delta - \xi)} \quad (8)$$

The complex conjugate of $\dot{\mathbf{H}}$ is equal to (8) except for the sign of the exponents. That is,

$$\dot{\mathbf{H}}^* = \hat{y}H_1 e^{-j(\omega t - \xi)} - \hat{x}H_2 e^{-j(\omega t + \delta - \xi)} \quad (9)$$

Substituting (5) and (9) in (2) gives the average Poynting vector at $z = 0$ as

$$\begin{aligned} \mathbf{S}_{av} &= \frac{1}{2} \operatorname{Re}[(\hat{x} \times \hat{y})\dot{E}_x \dot{H}_y^* - (\hat{y} \times \hat{x})\dot{E}_y \dot{H}_x^*] \\ &= \frac{1}{2} \hat{z} \operatorname{Re}(\dot{E}_x \dot{H}_y^* + \dot{E}_y \dot{H}_x^*) \end{aligned} \quad (10)$$

where \hat{z} is the unit vector in the z direction (direction of propagation of wave). It follows that

$$\begin{aligned} \mathbf{S}_{av} &= \frac{1}{2}(E_1 H_1 \operatorname{Re} e^{j\xi} + E_2 H_2 \operatorname{Re} e^{j\xi}) \\ &= \frac{1}{2}(E_1 H_1 + E_2 H_2) \cos \xi \end{aligned} \quad (11)$$

It is to be noted that \mathbf{S}_{av} is independent of δ .

In a lossless medium $\xi = 0$ (electric and magnetic fields in time phase) and $E_1/H_1 = E_2/H_2 = Z$, where Z , the intrinsic impedance of the medium, is real; so

$$\begin{aligned} \mathbf{S}_{av} &= \frac{1}{2}(E_1 H_1 + E_2 H_2) \\ &= \frac{1}{2}(H_1^2 + H_2^2)Z = \frac{1}{2}H^2Z \end{aligned} \quad (12)$$

where $H = \sqrt{H_1^2 + H_2^2}$ is the amplitude of the total \mathbf{H} field. We can also write

$$\mathbf{S}_{av} = \frac{1}{2} \frac{E_1^2 + E_2^2}{Z} = \frac{1}{2} \frac{E^2}{Z}$$

(13)

where $E = \sqrt{E_1^2 + E_2^2}$ is the amplitude of the total \mathbf{E} field.

EXAMPLE An elliptically polarized wave traveling in the positive z direction in air has x and y components

$$\begin{aligned} E_x &= 3 \sin(\omega t - \beta z) \quad (\text{V m}^{-1}) \\ E_y &= 6 \sin(\omega t - \beta z + 75^\circ) \quad (\text{V m}^{-1}) \end{aligned}$$

Find the average power unit per area conveyed by the wave.

SOLUTION The average power per unit area is equal to the average Poynting vector, which from (13) has a magnitude

$$S_{av} = \frac{1}{2} \frac{E^2}{Z} = \frac{1}{2} \frac{E_1^2 + E_2^2}{Z}$$

From the stated conditions the amplitude $E_1 = 3 \text{ V m}^{-1}$, and the amplitude $E_2 = 6 \text{ V m}^{-1}$. Also for air $Z = 376.7 \Omega$. Hence

$$S_{av} = \frac{1}{2} \frac{3^2 + 6^2}{376.7} = \frac{1}{2} \frac{45}{376.7} \approx 60 \text{ mW m}^{-2}$$

11-4 THE POLARIZATION ELLIPSE AND THE POINCARÉ SPHERE

In the Poincaré sphere† representation of wave polarization, the *polarization state* is described by a point on a sphere where the longitude and latitude of the point are related to parameters of the polarization ellipse (see Fig. 11-4) as follows:

$$\begin{aligned} \text{Longitude} &= 2\tau \\ \text{Latitude} &= 2\epsilon \end{aligned} \quad (1)$$

† H. Poincaré, "Théorie mathématique de la lumière," G. Carré, Paris, 1892; G. A. Deschamps, Geometrical Representation of the Polarization of a Plane Electromagnetic Wave, Proc. IRE, 39: 540 (May 1951).

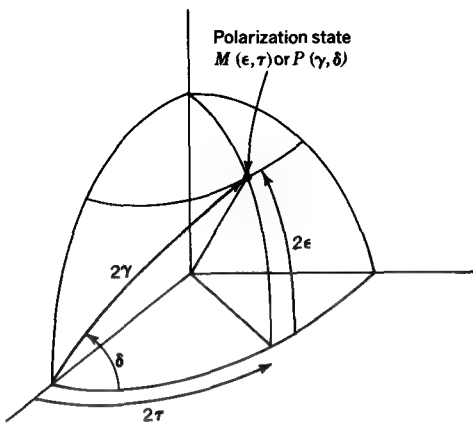


FIGURE 11-4
Poincaré sphere showing relation of angles ϵ , τ , γ , and δ .

where τ = tilt angle, $0^\circ \leq \tau \leq 180^\circ$

$$\epsilon = \cot^{-1}(\mp \text{AR}), -45^\circ \leq \epsilon \leq +45^\circ$$

The axial ratio (AR) is negative for right-handed and positive for left-handed (IEEE) polarization.

The polarization state described by a point on a sphere can also be expressed in terms of the angle subtended by the great circle drawn from a reference point on the equator and the angle between the great circle and the equator (see Fig. 11-4) as follows:

$$\text{Great-circle angle} = 2\gamma \quad (2)$$

$$\text{Equator-to-great-circle angle} = \delta$$

where $\gamma = \tan^{-1}(E_2/E_1)$, $0^\circ \leq \gamma \leq 90^\circ$

δ = phase difference between E_y and E_x , $-180^\circ \leq \delta \leq +180^\circ$

The geometric relation of τ , ϵ , and γ to the polarization ellipse is illustrated in Fig. 11-5. The trigonometric interrelations of τ , ϵ , γ , and δ are as follows:[†]

$\cos 2\gamma = \cos 2\epsilon \cos 2\tau$ $\tan \delta = \frac{\tan 2\epsilon}{\sin 2\tau}$ $\tan 2\tau = \tan 2\gamma \cos \delta$ $\sin 2\epsilon = \sin 2\gamma \sin \delta$	(3)
---	-----

Knowing ϵ and τ , one can determine γ and δ or vice versa. It is convenient to describe the *polarization state* by either of the two sets of angles (ϵ, τ) or (γ, δ) which

[†]These relations involve spherical trigonometry. See M. Born and E. Wolf, "Principles of Optics," pp. 24-27, The Macmillan Co., New York, 1964.

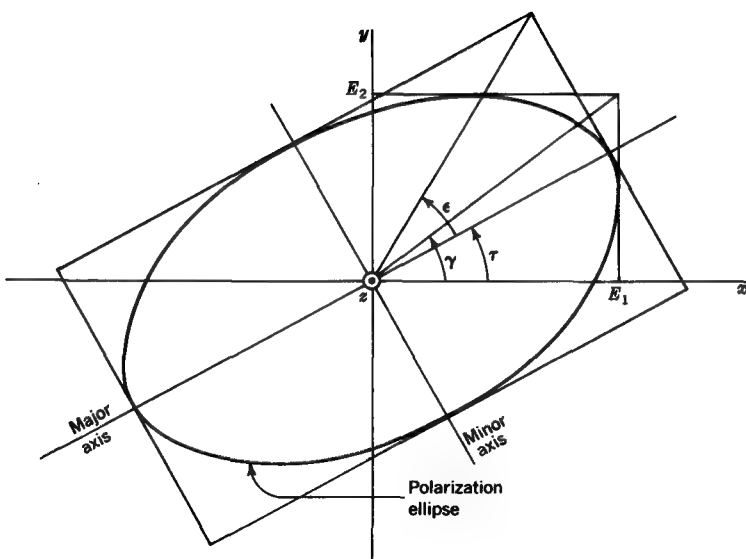


FIGURE 11-5
Polarization ellipse showing relation of angles ϵ , γ , and τ .

describe a point on the Poincaré sphere (Fig. 11-4). Let the polarization state as a function of ϵ and τ be designated by $M(\epsilon, \tau)$ or simply M and the polarization state as a function of γ and δ be designated by $P(\gamma, \delta)$ or simply P , as in Fig. 11-4. Two special cases are of interest.

Case 1 For $\delta = 0$ or $\delta = \pm 180^\circ$, E_x and E_y are exactly in phase or out of phase, so that any point on the equator represents a state of linear polarization. At the origin ($\epsilon = \tau = 0$) the polarization is linear and in the x direction ($\tau = 0$), as suggested in Fig. 11-6a. On the equator 90° to the right the polarization is linear with a tilt angle $\tau = 45^\circ$, while 180° from the origin the polarization is linear and in the y direction ($\tau = 90^\circ$). See Fig. 11-6a and b. One octant of the Poincaré sphere is shown in Fig. 11-6a and the full sphere is shown in Fig. 11-6b in rectangular projection.

Case 2 For $\delta = \pm 90^\circ$ and $E_2 = E_1$ ($2\gamma = 90^\circ$ and $2\epsilon = \pm 90^\circ$) E_x and E_y have equal amplitudes but are in phase quadrature, which is the condition for circular polarization. Thus, the poles represent a state of circular polarization, the upper pole representing left circular polarization and the lower pole right circular (IEEE) polarization, as suggested in Fig. 11-6a and b.

Cases 1 and 2 represent limiting conditions. In the general case any point on the upper hemisphere describes a left elliptically polarized wave ranging from pure left circular at the pole to linear at the equator. Likewise, any point on the lower

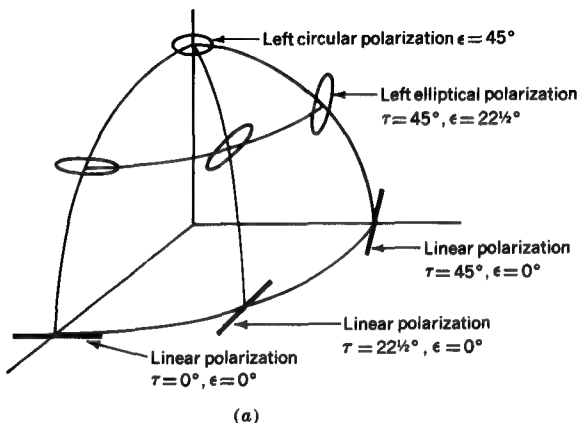


FIGURE 11-6 a
One octant of Poincaré sphere with polarization states.

hemisphere describes a right elliptically polarized wave ranging from pure right circular at the pole to linear at the equator. Several elliptical states of polarization are shown by ellipses with appropriate tilt angles τ and axial ratios AR at points on the Poincaré sphere in Fig. 11-6 a and b.

As an application of the Poincaré sphere representation it may be shown that the voltage response V of an antenna to a wave of arbitrary polarization is given by†

$$V = k \cos \frac{MM_a}{2} \quad (4)$$

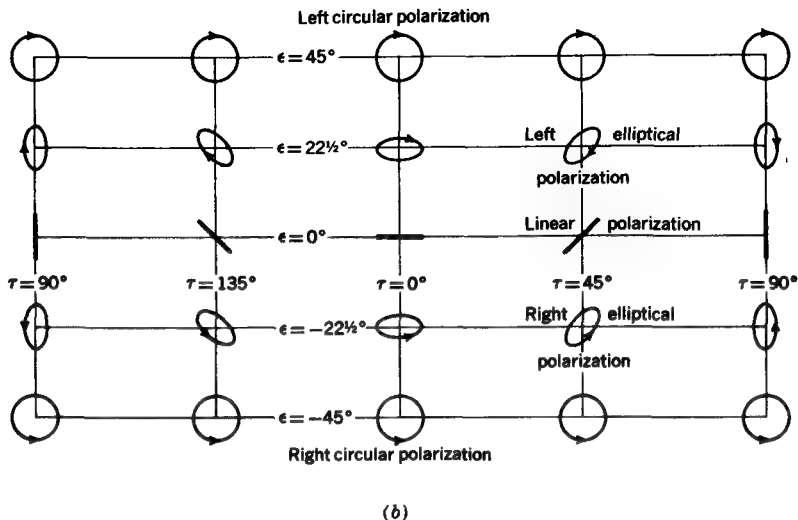
where MM_a = angle subtended by great-circle line from polarization state M to M_a

M = polarization state of wave

M_a = polarization state of antenna

k = constant

The polarization state of the antenna is defined as the polarization state of the wave radiated by the antenna when it is transmitting. The factor k in (4) involves the field strength of the wave and the size of the antenna. An important result to note is that if $MM_a = 0^\circ$, the antenna is matched to the wave (polarization state of wave same as for antenna) and the response is maximized. However, if $MM_a = 180^\circ$, the response is zero. This can occur, for example, if the wave is linearly polarized in the y direction while the antenna is linearly polarized in the x direction; or if the wave

FIGURE 11-6 *b*

Rectangular projection of Poincaré sphere showing full range of polarization states.

is left circularly polarized while the antenna is right circularly polarized. More generally we may say that *an antenna is blind to a wave of opposite (or antipodal) polarization state.*

11-5 PARTIAL POLARIZATION AND THE STOKES PARAMETERS

The previous sections deal with completely polarized waves, i.e., waves for which E_1 , E_2 , and δ are constants (or at least slowly varying functions of time). The radiation from a single-frequency (monochromatic) radio transmitter is of this type. However, the radiation from many celestial radio sources extends over a wide frequency range and within any bandwidth Δf consists of the superposition of a large number of statistically independent waves of a variety of polarizations. The resultant wave is said to be *incoherent* or *unpolarized*. For such a wave we can write

$$E_x = E_1(t) \sin \omega t \quad (1)$$

$$E_y = E_2(t) \sin[\omega t + \delta(t)] \quad (2)$$

† G. Sinclair, The Transmission and Reception of Elliptically Polarized Waves, *Proc. IRE*, 38: 151 (1950).

where all the time functions are independent. The variations of $E_1(t)$, $E_2(t)$, and $\delta(t)$ with time are slow compared with that of the mean frequency $f(\omega = 2\pi f)$ and are of the order of the bandwidth Δf . A wave of this type could be generated by connecting one noise generator to an antenna which is linearly polarized in the y direction and another noise generator to an adjacent antenna which is linearly polarized in the x direction. If the waves from both antennas have the same average power at an observing point, the total wave at this point will be completely unpolarized.

The most general situation of wave polarization occurs when a wave is *partially polarized*; i.e., it may be considered to be of two parts, one completely polarized and the other completely unpolarized.

To deal with partial polarization it is convenient to use the *Stokes parameters*, introduced in 1852 by Sir George Stokes.[†] The Stokes parameters I , Q , U , and V are defined as follows:

$$I = S = S_x + S_y = \frac{\langle E_1^2 \rangle}{Z} + \frac{\langle E_2^2 \rangle}{Z} \quad (3)$$

$$Q = S_x - S_y = \frac{\langle E_1^2 \rangle}{Z} - \frac{\langle E_2^2 \rangle}{Z} \quad (4)$$

$$U = \frac{2}{Z} \langle E_1 E_2 \cos \delta \rangle = S \langle \cos 2\epsilon \sin 2\tau \rangle \quad (5)$$

$$V = \frac{2}{Z} \langle E_1 E_2 \sin \delta \rangle = S \langle \sin 2\epsilon \rangle \quad (6)$$

where S = total Poynting vector magnitude for the wave

S_x = Poynting vector component of wave polarized in x direction

S_y = Poynting vector component of wave polarized in y direction

E_1 = amplitude of electric field component of wave polarized in x direction

E_2 = amplitude of electric field component of wave polarized in y direction

Z = intrinsic impedance of medium

The angles δ , ϵ , and τ are as defined in the previous section. The angle brackets indicate the time average. It is understood that in general E_1 , E_2 , δ , ϵ , and τ are functions of time. Thus, for example,

$$\langle E_1^2 \rangle = \frac{1}{T} \int_0^T [E_1(t)]^2 dt \quad (7)$$

[†] G. Stokes, On the Composition Resolution of Streams of Polarized Light from Different Sources, *Trans. Camb. Phil. Soc.*, 9(3): 399–416 (1852).

For a *completely unpolarized wave* $S_x = S_y$, and E_1 and E_2 are uncorrelated. It may be shown that under these conditions

$$\langle E_1 E_2 \cos \delta \rangle = \langle E_1 E_2 \sin \delta \rangle = 0$$

and we have

$$I = S$$

$$Q = 0$$

$$U = 0$$

$$V = 0$$

where S is the total Poynting vector of the wave. The condition $Q = U = V = 0$ is a requirement for a completely unpolarized wave.

For a *completely polarized wave* E_1 , E_2 , δ , ϵ , and τ may be considered to be constant, so that the Stokes parameters as in (3) to (6) do not require time averages. Thus, for example, we would have $\langle E_1^2 \rangle = E_1^2$.

For a *linearly (completely) polarized wave with E in the x direction* ($E_2 = 0$, and $\tau = \epsilon = 0$) the Stokes parameters are

$$I = S$$

$$Q = S$$

$$U = 0$$

$$V = 0$$

For a *linearly (completely) polarized wave with E in the y direction* ($E_1 = 0$, $\tau = 90^\circ$, $\epsilon = 0$) the Stokes parameters are

$$I = S$$

$$Q = -S$$

$$U = 0$$

$$V = 0$$

For a *left circularly (completely) polarized wave* ($E_1 = E_2$, $\delta = 90^\circ$)

$$I = S$$

$$Q = 0$$

$$U = 0$$

$$V = S$$

By consideration of other polarization states it is possible to show that the Stokes parameter I is always equal to the total power (density) of the wave, Q is equal to the power in the linearly polarized components (in x or y directions), U is equal to the power in the linearly polarized components at tilt angles $\tau = 45$ or 135° , and V is equal to the power in the circularly polarized components (left- or right-handed).

It is often convenient to normalize the Stokes parameters by dividing each parameter by S , obtaining the *normalized Stokes parameters* s_0 , s_1 , s_2 , and s_3 , where $s_0 = I/S = 1$, $s_1 = Q/S$, $s_2 = U/S$, and $s_3 = V/S$. The normalized Stokes parameters for the cases discussed above are summarized in Table 11-1.

If any of the parameters Q , U , or V (or s_1 , s_2 , or s_3) has a nonzero value, it indicates the presence of a polarized component in the wave. The *degree of polarization* d is defined as the ratio of completely polarized power to the total power, or

$$d = \frac{\text{polarized power}}{\text{total power}} \quad 0 \leq d \leq 1$$

or

$$d = \frac{\sqrt{Q^2 + U^2 + V^2}}{I} = \frac{\sqrt{s_1^2 + s_2^2 + s_3^2}}{1} \quad (8)$$

The condition $Q^2 + U^2 + V^2 = I^2$ or $s_1^2 + s_2^2 + s_3^2 = 1$ indicates a completely polarized wave. A partially polarized wave may be regarded as the sum of a completely unpolarized wave and a completely polarized wave. Thus, we may write for a partially polarized wave

$$\begin{bmatrix} s_0 \\ s_1 \\ s_2 \\ s_3 \end{bmatrix} = \begin{bmatrix} 1 - d \\ 0 \\ 0 \\ 0 \end{bmatrix} + \begin{bmatrix} d \\ d \cos 2\epsilon \cos 2\tau \\ d \cos 2\epsilon \sin 2\tau \\ d \sin 2\epsilon \end{bmatrix} \quad (9)$$

Table 11-1 NORMALIZED STOKES PARAMETERS FOR SEVEN WAVE-POLARIZATION STATES

Normalized Stokes parameter	Completely unpolarized wave	Completely polarized waves					
		Linearly polarized				Circularly polarized	
		$\tau = 0^\circ$	$\tau = 90^\circ$	$\tau = 45^\circ$	$\tau = 135^\circ$	Left-hand	Right-hand
s_0	1	1	1	1	1	1	1
s_1	0	1	-1	0	0	0	0
s_2	0	0	0	1	-1	0	0
s_3	0	0	0	0	0	1	-1

where the first term on the right of (9) represents the unpolarized part and the second term the polarized part of the wave.

Consider now a wave with Stokes parameters s_0, s_1, s_2, s_3 incident on an antenna with Stokes parameters a_0, a_1, a_2, a_3 .[†] The parameters a_0, a_1, a_2, a_3 are those for a wave radiated by the antenna when it is transmitting. It follows that the total power P available (to a receiver) from the antenna due to the incident wave is given by

$$P = \frac{1}{2} A_e S [a_0 \quad a_1 \quad a_2 \quad a_3] \begin{bmatrix} s_0 \\ s_1 \\ s_2 \\ s_3 \end{bmatrix} \quad (10)$$

or

$$P = \frac{1}{2} A_e S (a_0 s_0 + a_1 s_1 + a_2 s_2 + a_3 s_3) \quad (\text{W}) \quad (11)$$

where A_e = effective aperture of antenna (see Chap. 14), m^2

S = Poynting vector of incident wave, W m^{-2}

This result may also be expressed as

$$P = \frac{1}{2} A_e S (1 + d \cos MM_a) \quad (12)$$

or

$$P = \frac{1}{2} A_e S (1 - d) + d S A_e \cos^2 \frac{MM_a}{2} \quad (13)$$

where MM_a is the angle subtended by the great-circle line between the wave- and antenna-polarization states on the Poincaré sphere. In (13) the first term on the right side represents the unpolarized power and the second term the polarized power. This form emphasizes the fact that only one-half the incident unpolarized power is available to a receiver but all the completely polarized power is available.

By arrangement of (13) we have

$$P = \left(\frac{1 - d}{2} + d \cos^2 \frac{MM_a}{2} \right) A_e S = F A_e S \quad (\text{W}) \quad (14)$$

where F is the factor in parentheses, which may be called the *wave-to-antenna coupling factor*. This factor is a function of the degree of polarization and the angle MM_a and gives the fraction of the power $A_e S$ which is received. It is dimensionless with values between 0 and 1. Its possible range of values as a function of the degree of

[†] H. C. Ko, On the Reception of Quasi-monochromatic Partially Polarized Radio Waves, Proc. IRE, 50: 1950 (September 1962).

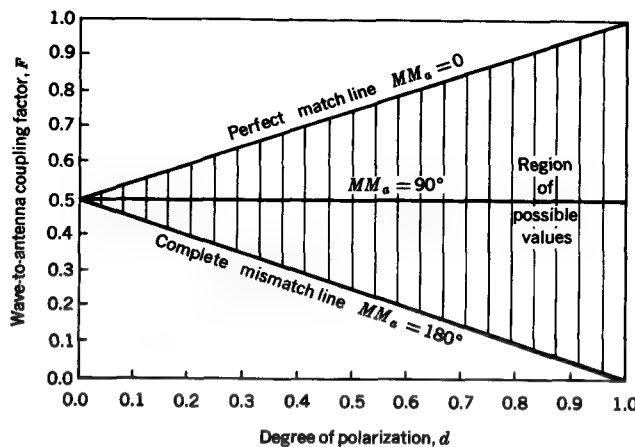


FIGURE 11-7

Chart showing wave-to-antenna coupling factor F vs. the degree of polarization d for various values of the wave-to-antenna angle MM_a . The region of possible values is shaded. These values range from a perfect match ($MM_a = 0$) to a complete mismatch ($MM_a = 180^\circ$). No values are possible outside this region. Note that for completely polarized waves ($d = 1$) matching is important but for a completely unpolarized wave ($d = 0$) the condition of match makes no difference. (After H. C. Ko.)

polarization is shown by the shaded area in Fig. 11-7. Thus, for a perfect match ($MM_a = 0$) F ranges from $\frac{1}{2}$ to 1 as d goes from 0 to 1, while for a complete mismatch ($MM_a = 180^\circ$) F ranges from $\frac{1}{2}$ to 0 as d goes from 0 to 1. Between these extremes ($MM_a = 0$ and $MM_a = 180^\circ$) we have conditions of partial mismatching between antenna and wave, for example, $MM_a = 90^\circ$.

Equation (14) may be interpreted as signifying that the response P of the system is given by the maximum available power $A_e S$ times the factor F which characterizes the receiving antenna. The relation (14) is typical of all observing or measuring systems in that the response (or observed result) may be modified from the optimum or ideal result by a quantity characterizing the observing or measuring system.

If we define four new parameters

$$\begin{aligned} s_{11} &= \frac{1}{2}(s_0 + s_1) & s_{12} &= \frac{1}{2}(s_2 + js_3) \\ s_{21} &= \frac{1}{2}(s_2 - js_3) & s_{22} &= \frac{1}{2}(s_0 - s_1) \end{aligned} \quad (15)$$

and four similar parameters ($a_{11}, a_{12}, a_{21}, a_{22}$) for the antenna, we can express the available power with 2×2 matrices as

$$P = A_e S \operatorname{Tr} \left\{ \begin{bmatrix} a_{11} & a_{12} \\ a_{21} & a_{22} \end{bmatrix} \begin{bmatrix} s_{11} & s_{12} \\ s_{21} & s_{22} \end{bmatrix} \right\} \quad (16)$$

where Tr signifies the *trace*, i.e., the sum of the diagonal elements of a square matrix or

$$P = A_e S(a_{11}s_{11} + a_{12}s_{21} + a_{21}s_{12} + a_{22}s_{22}) \quad (17)$$

More concisely

$$P = A_e S \text{ Tr } \{[a_{ij}][s_{ij}]\} = A_e S F \quad (\text{W}) \quad (18)$$

where F is the wave-to-antenna coupling factor, as in (14). The above matrix relations are similar to ones used in optics, which is appropriate if we regard the antenna-receiver as a detector of radio photons. In optics the matrices are called *coherency matrices*.† A further discussion of the response of an antenna to waves of arbitrary polarization is given in Sec. 14-28.

11-6 CROSS FIELD

The preceding sections have dealt with the polarization of waves in which the directions of the electric field vector at a given point are entirely perpendicular to the direction of propagation.

Another situation can occur in which the electric vector rotates in a plane parallel to the propagation direction. This condition, called *cross field*,‡ never exists in the case of a single plane wave in free space since such a wave has no field component in the direction of propagation. However, in the near field of an antenna there are electric field components in both the direction of propagation and normal to this direction, so that cross field is present (see Chap. 14). Also cross field may be present near the surface of a conducting medium with a plane wave traveling parallel to the surface. If the medium is not perfectly conducting, the direction of \mathbf{E} is tilted forward near the surface, so that \mathbf{E} has a component E_n normal to the surface and a component E_t tangent to the surface (in the direction of propagation) (see Chap. 13). In general, cross field may be present wherever two waves of the same frequency traveling in different directions cross, e.g., when a wave is reflected from a conducting surface at an oblique angle (see Chap. 12).

† M. Born and E. Wolf, "Principles of Optics," The Macmillan Company, New York, 1964.

‡ A. Alford, J. D. Kraus, and E. C. Barkofsky, chap. 9, p. 200, in Radio Research Laboratory Staff, H. J. Reich (ed.), "Very High Frequency Techniques," McGraw-Hill Book Company, New York, 1947; see also J. D. Kraus, "Electromagnetics," 1st ed., sec. 9-15, McGraw-Hill Book Company, New York, 1953.

PROBLEMS

- * 11-1 A wave traveling normally out of the page (toward the reader) is the resultant of two linearly polarized components $E_x = 3 \cos \omega t$ and $E_y = 2 \cos(\omega t + 90^\circ)$. For the resultant wave: (a) What is the axial ratio? (b) What is the angle between the major axis of the polarization ellipse and the positive x axis? (c) Does E rotate clockwise or counterclockwise? (d) Is the wave left- or right-handed?
- 11-2 A wave traveling normally out of the page is the resultant of two circularly polarized components $E_r = 2e^{j\omega t}$ and $E_t = 4e^{-j(\omega t + 45^\circ)}$. For the resultant wave: (a) What is the axial ratio? (b) What is the angle between the major axis of the polarization ellipse and the positive x axis? (c) Does E rotate clockwise or counterclockwise? (d) Is the wave left- or right-handed?
- * 11-3 A wave traveling normally out of the page is the resultant of two elliptically polarized waves, one with components $E_x = 5 \cos \omega t$ and $E_y = 3 \sin \omega t$ and another with components $E_r = 3e^{j\omega t}$ and $E_t = 4e^{-j\omega t}$. For the resultant wave: (a) What is the axial ratio? (b) What is the angle between the major axis of the polarization ellipse and the positive x axis? (c) Does E rotate clockwise or counterclockwise? (d) Is the wave left- or right-handed?
- 11-4 Show that the instantaneous Poynting vector of a plane circularly polarized traveling wave is a constant.
- 11-5 Show that the average Poynting vector of a circularly polarized wave is twice that of a linearly polarized wave if the maximum electric field E is the same for both waves.
- * 11-6 An elliptically polarized wave in a medium with constants $\sigma = 0$, $\mu_r = 2$, $\epsilon_r = 5$ has H -field components (normal to the direction of propagation and normal to each other) of amplitude 3 and 4 A m^{-1} . Find the average power conveyed through an area of 5 m^2 normal to the direction of propagation.
- 11-7 An elliptically polarized ($\text{AR} = 2$) 3-GHz wave in air is incident normally on a flat conducting sheet with intrinsic-impedance magnitude of $10 \text{ m}\Omega$. If the wave has an instantaneous peak electric field $E = 100 \text{ mV m}^{-1}$, find the average Poynting vector into the sheet.
- * 11-8 Three waves have the following characteristics: (a) unpolarized, (b) left elliptically polarized with $d = \frac{1}{2}$, $\text{AR} = 3$, $\tau = 135^\circ$, (c) left circularly polarized. Three antennas produce the following types of waves when transmitting: (1) linear horizontal polarization, (2) right elliptical polarization with $\text{AR} = 3$, $\tau = 45^\circ$, (3) right circular polarization. If all the antennas have unit effective aperture and all waves have unit Poynting vector, find the received power for the nine wave-antenna combinations $a1, a2, a3, b1, b2, \text{etc.}$ Arrange answers in 3×3 row-column display with top row $a1, a2, a3$, second row $b1, b2, \text{etc.}$
- 11-9 Ten waves have the following characteristics:
- | | |
|--|---|
| (a) $d = 0$ | (b) $d = \frac{1}{2}$, $\text{AR} = \infty$, $\tau = 0^\circ$ |
| (c) $d = \frac{1}{2}$, $\text{AR} = \infty$, $\tau = 45^\circ$ | (d) $d = \frac{1}{2}$, $\text{AR} = -1$ |

* Answers to starred problems are given in Appendix C.

- (e) $d = 1, \text{AR} = +1$
 (g) $d = 1, \text{AR} = \infty, \tau = 135^\circ$
 (i) $d = \frac{1}{2}, \text{AR} = 4, \tau = 30^\circ$

- (f) $d = 1, \text{AR} = \infty, \tau = 90^\circ$
 (h) $d = \frac{1}{2}, \text{AR} = 10, \tau = 0^\circ$
 (j) $d = \frac{1}{2}, \text{AR} = 3, \tau = 120^\circ$

Find the normalized Stokes parameters and the coherency matrices for these waves.

11-10 (a) A wave for which $d = 0.4, \text{AR} = 3, \tau = 45^\circ$ is received by six antennas of unit effective aperture with polarization as follows: (1) linear horizontal, (2) linear vertical, (3) linear slant (45°), (4) linear slant (135°), (5) left circular, and (6) right circular. If the wave has unit Poynting vector, find the six power responses. (b) Is there a wave to which all six antennas of part (a) respond equally? If so what are the wave parameters? (See Sec. 14-28.)

* 11-11 What is the percentage of polarized wave power in each of five waves characterized by the following Stokes parameters: (a) $1, 0, 0, 0$, (b) $1, 1, 0, 0$, (c) $1, 0, -\frac{1}{2}, 0$, (d) $1, \frac{1}{2}, \frac{1}{2}, 0$, (e) $1, 0, 1/\sqrt{2}, 1/\sqrt{2}$.

11-12 (a) What are the wave characteristics (τ and AR) for a completely polarized wave for which $Q^2 = U^2 = V^2$? (b) Draw the polarization ellipse.

* 11-13 A wave of unit Poynting vector with coherency matrix

$$\begin{bmatrix} \frac{1}{2} & \frac{1}{2} \\ \frac{1}{2} & \frac{1}{2} \end{bmatrix}$$

is incident on a right circularly polarized receiving antenna of unit effective aperture. Find the received power.

11-14 The degree of polarization d of a wave can be resolved into a *linearly polarized* component $d_l = \sqrt{s_1^2 + s_2^2}$ and a *circularly polarized* component $d_c = \sqrt{s_3^2}$, with $d = \sqrt{d_l^2 + d_c^2}$. What are the Stokes parameters for a completely polarized wave for which $d_l = d_c$ and for which $s_1 = s_2$?

11-15 (a) Draw a graph as in Fig. 11-7 and plot points on the graph for each of the nine wave-antenna combinations of Prob. 11-8. (b) Add points to the graph for the six combinations of Prob. 11-10a. (c) Add another point for the combination of Prob. 11-13. (d) Do all points fall inside the inner triangular region (shaded) of Fig. 11-7?

11-16 (a) A plane traveling wave is incident at an angle of 45° to an infinite, perfectly conducting flat sheet. The electric field is everywhere contained in a plane normal to the sheet and parallel to the direction of wave propagation. Plot the axial ratio of the cross-field ellipse as a function of distance from the sheet for a distance of 1λ . (b) Draw the cross-field ellipses at distances of $0\lambda, \frac{1}{2}\lambda, \frac{1}{4}\lambda, \frac{3}{4}\lambda$, and 1λ from the sheet.

11-17 Two waves of equal magnitude intersect at the origin. One (y wave) is traveling in the positive y direction and is right circularly polarized. The other (x wave) is traveling in the positive x direction and is left circularly polarized. At the origin, \mathbf{E} for the y wave is in the positive z direction at the same instant that \mathbf{E} for the x wave is in the negative z direction. What is the locus of the resulting \mathbf{E} at the origin?

11-18 Draw the polarization ellipse and the antenna response pattern of a linearly polarized antenna for waves with axial ratios as follows: (a) $\text{AR} = 1$, (b) $\text{AR} = 4$, (c) $\text{AR} = 12$, and (d) $\text{AR} = \infty$.

* 11-19 Describe the characteristics (AR, left- or right-handed, tilt angle) of waves having Stokes parameters as follows:

- | | |
|----------------------------|--|
| (1) 1,0,0,1 | (2) 1,0,0,-1 |
| (3) 1,1,0,0 | (4) 1,-1,0,0 |
| (5) 1,0,1,0 | (6) 1,0,-1,0 |
| (7) 1,0.577,0.577,0.577 | (8) 1,0,0,0 |
| (9) 1,0,0,- $\frac{1}{2}$ | (10) 1, $\frac{1}{2}$,0,0 |
| (11) 1,0, $\frac{1}{2}$,0 | (12) 1,- $\frac{1}{2}$,0, $\frac{1}{2}$ |

11-20 Demonstrate the validity of Eqs. (11-4-3).

WAVE REFLECTION, REFRACTION, AND DIFFRACTION

12-1 INTRODUCTION

In this chapter, consideration is given to wave reflection from and refraction into dielectric and metallic surfaces. The plane wave normally incident on a boundary between two media is first discussed, with the treatment then extended to include plane waves obliquely incident on boundaries. The difference between physical-optics (wavefront) and geometrical-optics (ray-path) methods is illustrated. The geometrical theory of diffraction is discussed and applied to a simple example.

12-2 PLANE WAVE, NORMAL INCIDENCE

Consider a linearly polarized wave traveling in the positive x direction with \mathbf{E} in the y direction and \mathbf{H} in the z direction. The wave is incident normally on the boundary between two media, as in Fig. 12-1a. Assume that the incident traveling wave has field components $\hat{\mathbf{E}}_i$ and $\hat{\mathbf{H}}_i$ at the boundary. Part of the incident wave is, in general, reflected while another part is transmitted into the second medium. The reflected traveling wave has field components $\hat{\mathbf{E}}_r$ and $\hat{\mathbf{H}}_r$ at the boundary. The transmitted wave has field components $\hat{\mathbf{E}}_t$ and $\hat{\mathbf{H}}_t$ at the boundary.

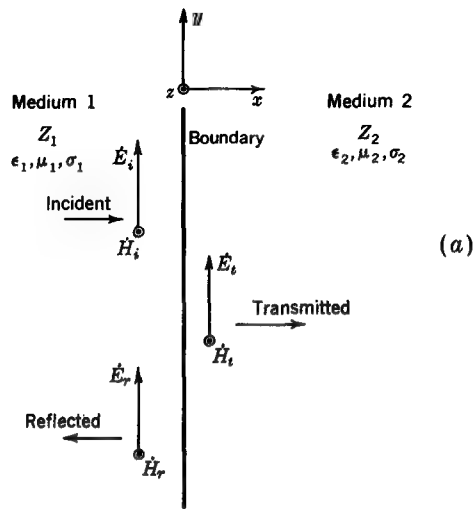
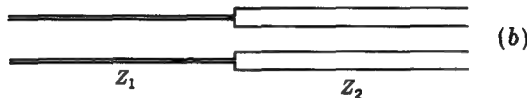


FIGURE 12-1

(a) Plane wave incident normally on boundary between two media and (b) analogous transmission line.



From the continuity of the tangential field components at a boundary

$$\dot{E}_t + \dot{E}_r = \dot{E}_t \quad (1)$$

and

$$\dot{H}_i + \dot{H}_r = \dot{H}_t \quad (2)$$

The electric and magnetic fields of a plane wave are related by the intrinsic impedance of the medium. Thus

$$\frac{\dot{E}_i}{\dot{H}_i} = \dot{Z}_1 \quad \frac{\dot{E}_r}{\dot{H}_r} = -\dot{Z}_1 \quad \frac{\dot{E}_t}{\dot{H}_t} = \dot{Z}_2 \quad (3)$$

The impedance of the reflected wave (traveling in the negative x direction) is taken to be negative \dot{Z}_1 and of the incident wave, positive \dot{Z}_1 . From (2) and (3)

$$\dot{H}_t = \frac{\dot{E}_t}{\dot{Z}_2} = \frac{\dot{E}_i}{\dot{Z}_1} - \frac{\dot{E}_r}{\dot{Z}_1} \quad (4)$$

$$\text{or} \quad \dot{E}_t = \frac{\dot{Z}_2}{\dot{Z}_1} \dot{E}_i - \frac{\dot{Z}_2}{\dot{Z}_1} \dot{E}_r \quad (5)$$

Multiplying (1) by \dot{Z}_2/\dot{Z}_1 gives

$$\frac{\dot{Z}_2}{\dot{Z}_1} \dot{E}_t = \frac{\dot{Z}_2}{\dot{Z}_1} \dot{E}_i + \frac{\dot{Z}_2}{\dot{Z}_1} \dot{E}_r \quad (6)$$

Adding (5) and (6), we get

$$\dot{E}_t \left(1 + \frac{\dot{Z}_2}{\dot{Z}_1} \right) = \frac{2\dot{Z}_2}{\dot{Z}_1} \dot{E}_i \quad (7)$$

or

$$\dot{E}_t = \frac{2\dot{Z}_2}{\dot{Z}_2 + \dot{Z}_1} \dot{E}_i = t \dot{E}_i \quad (8)$$

where t is called the *transmission coefficient*. It follows that

$$\boxed{t = \frac{\dot{E}_t}{\dot{E}_i} = \frac{2\dot{Z}_2}{\dot{Z}_2 + \dot{Z}_1}} \quad (9)$$

Subtracting (5) from (6) gives

$$\dot{E}_t \left(\frac{\dot{Z}_2}{\dot{Z}_1} - 1 \right) = \frac{2\dot{Z}_2}{\dot{Z}_1} \dot{E}_r \quad (10)$$

Substituting \dot{E}_t from (8) into (10) and solving for \dot{E}_r , we have

$$\dot{E}_r = \frac{\dot{Z}_2 - \dot{Z}_1}{\dot{Z}_2 + \dot{Z}_1} \dot{E}_i = \rho \dot{E}_i \quad (11)$$

where ρ is called the *reflection coefficient*.† It follows that

$$\boxed{\rho = \frac{\dot{E}_r}{\dot{E}_i} = \frac{\dot{Z}_2 - \dot{Z}_1}{\dot{Z}_2 + \dot{Z}_1}} \quad (12)$$

From (9) and (12)

$$\boxed{t = \rho + 1} \quad (12a)$$

The situation (Fig. 12-1) of a plane wave incident normally on a boundary between two different media of infinite extent, with intrinsic impedances Z_1 and Z_2 , is analogous to the situation of a guided wave on an infinite transmission line having an abrupt change in impedance from Z_1 to Z_2 (Fig. 12-1b). The transmission and reflection coefficients for voltage across the transmission line are identical to those given

† This is the same as the reflection coefficient discussed in Sec. 10-10.

in (9) and (12) if the intrinsic impedance Z_1 of medium 1 is taken to be the characteristic impedance of the line to the left of the junction (Fig. 12-1b) and the intrinsic impedance Z_2 of medium 2 is taken to be the characteristic impedance of the line to the right of the junction. This is discussed further in Chap. 13.

Returning now to the case of a plane wave incident normally on the boundary between two media of infinite extent as in Fig. 12-1a, let us consider several special cases.

Case 1 Assume that medium 1 is air and medium 2 is a conductor, so that $Z_1 \gg Z_2$. Then, from (8) we have the approximate relation

$$\dot{E}_t \approx \frac{2\dot{Z}_2}{\dot{Z}_1} \dot{E}_i \quad (13)$$

But from (3) this becomes

$$\dot{H}_r \dot{Z}_2 \approx \frac{2\dot{Z}_2}{\dot{Z}_1} \dot{H}_i \dot{Z}_1 \quad (14)$$

from which

$$\dot{H}_r \approx 2\dot{H}_i \quad (15)$$

Thus, for a plane wave in air incident normally on a conducting medium, the magnetic field is, to a good approximation, doubled in intensity at the boundary. It also follows that $\dot{H}_r \approx \dot{H}_i$, so that there is a nearly pure standing wave to the left of the boundary (in medium 1).

Case 2 Consider now the opposite situation, where medium 1 is a conductor and medium 2 is air so that $Z_1 \ll Z_2$. Then, from (8) we have approximately

$$\dot{E}_r \approx 2\dot{E}_i \quad (16)$$

Thus, for a wave leaving a conducting medium, the electric field is nearly doubled at the boundary. It follows that $\dot{E}_r \approx \dot{E}_i$, so that there is a nearly pure standing wave ($VSWR = \infty$) immediately to the left of the boundary (in medium 1). However, owing to the attenuation of waves in medium 1, the VSWR decreases rapidly as one moves away from the boundary (to the left).

Case 3 In case 1 it is assumed that $Z_1 \gg Z_2$. Consider now that $Z_2 = 0$ (medium 2 a perfect conductor). Then from (12) the reflection coefficient $\rho = -1$, and from (9) the transmission coefficient $\tau = 0$. Thus, the wave is completely reflected, and no field is transmitted into medium 2. Further $\dot{E}_r = -\dot{E}_i$, and $\dot{H}_r = \dot{H}_i$, so that the magnetic field intensity exactly doubles at the boundary. This situation is analogous to a short-circuited transmission line.[†]

[†] Although ρ , τ , \dot{Z}_1 , and \dot{Z}_2 , are, in general, complex and, hence, should be written with a dot, the dot will frequently be omitted for simplicity.

Case 4 In case 2 it is assumed that $Z_1 \ll Z_2$. Consider now the hypothetical situation where Z_2 is infinite.[†] Then from (12) $\rho = +1$ and from (9) $\tau = 2$. Thus the wave is completely reflected, but $E_r = +E_i$, so that the electric field intensity at the boundary is exactly doubled. This situation is analogous to an open-circuited transmission line.

Case 5 Assume that both medium 1 and medium 2 are lossless nonferromagnetic dielectrics ($\mu_1 = \mu_2 = \mu_0$). Then it follows from (12) that

$$\rho = \frac{\sqrt{\epsilon_1/\epsilon_2} - 1}{\sqrt{\epsilon_1/\epsilon_2} + 1} \quad (17)$$

and from (9) that

$$\tau = \frac{2}{1 + \sqrt{\epsilon_2/\epsilon_1}} \quad (18)$$

Case 6 Take now the case where $Z_2 = Z_1$. Then $\rho = 0$ and $\tau = 1$, so that the wave propagates into medium 2 without any reflection. This situation is similar to that on a continuous transmission line of uniform characteristic impedance.

12-3 THE TERMINATED WAVE

In the preceding section we considered various reflection and transmission situations at a boundary. In all cases there was a reflected wave except where the two media were of the same impedance, and in this case the wave was entirely transmitted. No case was considered in which the incident wave is terminated so that no wave will be transmitted or reflected. This case deserves special mention and is considered in this section.

The intrinsic impedance of free space is 376.7Ω . This concept of an impedance for free space takes on more physical significance if we consider the properties of a resistive sheet having a resistance of 376.7Ω per square. Material so treated is often called *space paper* or *space cloth*. It should be noted that the resistance is not per square centimeter or per square meter but simply *per square*. This is equivalent to saying that the resistance between the edges of any square section of the material is the same.[‡] Hence the resistance between the opposite edges of the small square of

[†] It is to be noted that for free space the intrinsic impedance is only 376.7Ω . To obtain a higher impedance would require that $\mu_r > 1$ such as in ferromagnetic media.

[‡] If the large square in Fig. 12-2 is 4 times the area of the small, it is equivalent to two small squares in series connected in parallel with two more small squares in series. Thus, the resistance of this large square is the same as that of the small square.

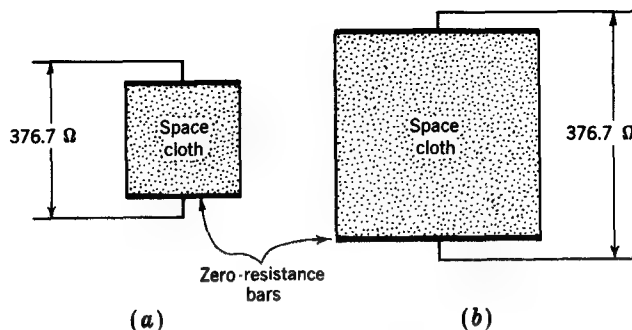


FIGURE 12-2
Space cloth has a resistance of 376.7Ω per square.

space cloth in Fig. 12-2a is 376.7Ω , as is also the resistance between the edges of the large square in Fig. 12-2b. In this illustration it is assumed that the edges are clamped with zero-resistance bars and that the impedance of the leads is negligible.

The conductivity of the material required for a sheet of the space cloth depends on the thickness of the sheet. Thus the resistance R of a square section as in Fig. 12-3 is expressed by

$$R = \frac{l}{\sigma a} = \frac{l}{\sigma h l} = \frac{1}{\sigma h} \quad (\Omega) \quad (1)$$

where l = length of side, m

a = area of edge, m^2

h = thickness of sheet, m

σ = conductivity of sheet, O m^{-1}

It follows that the required conductivity is

$$\sigma = \frac{1}{Rh} = \frac{1}{376.7h} \quad (\text{O m}^{-1}) \quad (2)$$

Consider now the behavior of a sheet of space cloth placed in the path of a plane wave. Suppose, as shown in Fig. 12-4a, that a plane wave in free space traveling to the right is incident normally on a sheet of space cloth of infinite extent.

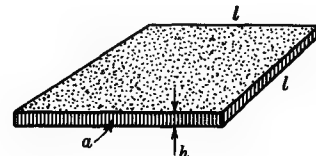


FIGURE 12-3
Square of space cloth of thickness h .

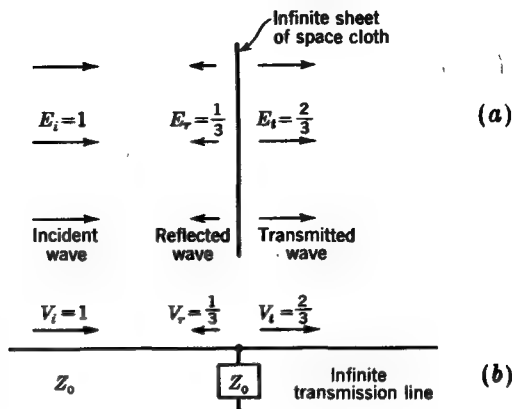


FIGURE 12-4

(a) Plane wave traveling to right incident normally on sheet of space cloth and (b) analogous transmission-line arrangement.

Taking the amplitude of the incident wave as 1 V m^{-1} , we have from (12-2-9) that there is a transmitted wave continuing to the right of the sheet of amplitude

$$E_t = \tau E_i = \frac{2 \times 188.3}{188.3 + 376.7} = \frac{2}{3} \text{ V m}^{-1}$$

and from (12-2-12) that there is a reflected wave to the left of the sheet of amplitude

$$E_r = \rho E_i = \frac{188.3 - 376.7}{188.3 + 376.7} = -\frac{1}{3} \text{ V m}^{-1}$$

It is to be noted that the impedance presented to the incident wave at the sheet is the resultant of the space cloth in parallel with the impedance of the space behind it. This is one-half of 376.7, or 188.3Ω .

It is apparent that a sheet of space cloth by itself is insufficient to terminate a wave. This may also be seen by considering the analogous transmission arrangement shown in Fig. 12-4b.

In order completely to absorb or terminate the incident wave without reflection or transmission, let an infinite, perfectly conducting sheet be placed parallel to the space cloth and $\lambda/4$ behind it, as portrayed in Fig. 12-5a. Now the impedance presented to the incident wave at the sheet of space cloth is 376.7Ω , being the impedance of the sheet in parallel with an infinite impedance. As a consequence, this arrangement results in the total absorption of the wave by the space cloth, with no reflection to the left of the space cloth. There is, however, a standing-wave and energy circulation between the cloth and the conducting sheet. The analogous transmission-line arrangement is illustrated in Fig. 12-5b.

In the case of the plane wave, the perfectly conducting sheet effectively isolates the region of space behind it from the effects of the wave. In a roughly analogous

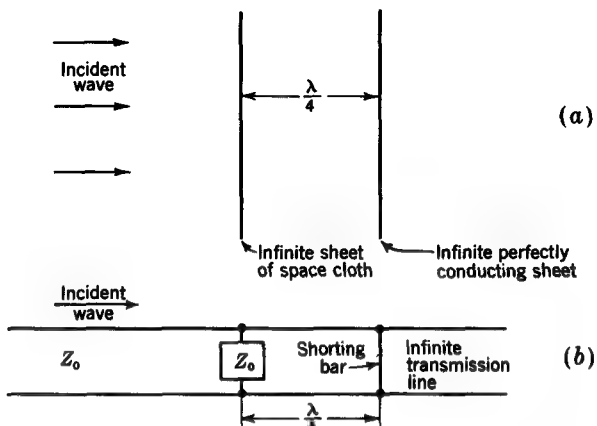


FIGURE 12-5

(a) Plane wave traveling to right incident normally on sheet of space cloth backed by conducting sheet is absorbed without reflection. (b) Wave traveling to right on transmission line is absorbed without reflection by analogous arrangement.

manner, the shorting bar on the transmission line reduces the wave beyond it to a small value.

A transmission line may also be terminated by placing an impedance across the line which is equal to the characteristic impedance of the line, as in Fig. 12-4b, and disconnecting the line beyond it. Although this provides a practical method of terminating a transmission line, there is no analogous counterpart in the case of a wave in space because it is not possible to "disconnect" the space to the right of the termination. A region of space may only be isolated or shielded, as by a perfectly conducting sheet.

A lossy mixture of a high- μ (ferrite) material and a high- ϵ (barium titanate) material can be used effectively for wave absorption if the ratio μ/ϵ is equal to that for free space ($\mu_r/\epsilon_r = 1$). The mixture constitutes a physical discontinuity, but the wave enters it without reflection. The velocity of the wave is reduced and large attenuation can occur in a short distance.

12-4 LINEARLY POLARIZED PLANE WAVE, OBLIQUE INCIDENCE

We have previously considered a linearly polarized plane wave normally incident on an interface between two media. In this section, attention is given to a linearly polarized plane wave obliquely incident on a boundary between two media, as shown in Fig.

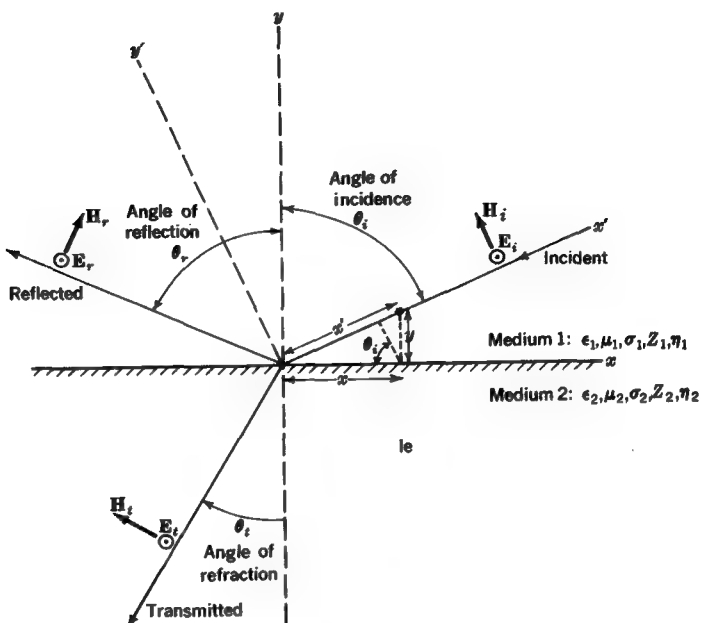


FIGURE 12-6

Geometry in the plane of incidence (xy plane) for linearly polarized wave at oblique incidence and for perpendicular polarization.

12-6. The incident wave (from medium 1) makes an angle of θ_i with the y axis, the reflected wave (medium 1) makes an angle of θ_r with the y axis, and the transmitted wave† makes an angle of θ_t with the negative y axis.

Consider two cases: (1) the electric field perpendicular to the *plane of incidence* (xy plane) and (2) the electric field parallel to the plane of incidence. These waves are said to be *perpendicularly-polarized* and *parallel-polarized*, respectively. The field vectors shown in Fig. 12-6 are for the case of *perpendicular polarization*. It is clear that any arbitrary plane wave can be resolved into perpendicular and parallel components.

Referring to Fig. 12-6, the $x'y'$ axes are orthogonal, with the x' axis oriented along the direction of the incident wave. It is seen that

$$x' = x \sin \theta_i + y \cos \theta_i \quad (1)$$

† The transmitted wave is also called the *refracted wave*. Hence, θ_t is called the *angle of refraction*.

and that a unit vector in the y' direction can be expressed as

$$\hat{y}' = -\hat{x} \cos \theta_i + \hat{y} \sin \theta_i \quad (2)$$

Perpendicular Case

Consider an incident *perpendicularly (\perp) polarized wave* propagating in the negative x' direction, i.e.,

$$\mathbf{E}_i = 2E_0 e^{j\beta_1 x'} \quad (3)$$

$$\mathbf{H}_i = \hat{y}' \frac{E_0}{Z_1} e^{j\beta_1 x'} \quad (4)$$

Substituting (1) and (2) into (3) and (4) gives

$$\mathbf{E}_i = 2E_0 \exp[j\beta_1(x \sin \theta_i + y \cos \theta_i)] \quad (5)$$

$$\mathbf{H}_i = (-\hat{x} \cos \theta_i + \hat{y} \sin \theta_i) \frac{E_0}{Z_1} \exp[j\beta_1(x \sin \theta_i + y \cos \theta_i)] \quad (6)$$

The reflected fields are denoted by $(\mathbf{E}_r, \mathbf{H}_r)$ and the transmitted fields by $(\mathbf{E}_t, \mathbf{H}_t)$. From (12-2-12) and (12-2-9) the reflection and transmission coefficients for a perpendicularly (\perp) polarized wave are (at origin)

$$\rho_{\perp} = \frac{E_r}{E_i} \quad (7)$$

$$\tau_{\perp} = \frac{E_t}{E_i} \quad (8)$$

By developing relations similar to (1) and (2) for the reflected and transmitted waves, it follows that

$$\mathbf{E}_r = 2\rho_{\perp} E_0 \exp[j\beta_1(x \sin \theta_r - y \cos \theta_r)] \quad (9)$$

$$\mathbf{H}_r = (\hat{x} \cos \theta_r + \hat{y} \sin \theta_r) \rho_{\perp} \frac{E_0}{Z_1} \exp[j\beta_1(x \sin \theta_r - y \cos \theta_r)] \quad (10)$$

$$\mathbf{E}_t = 2\tau_{\perp} E_0 \exp[j\beta_2(x \sin \theta_t + y \cos \theta_t)] \quad (11)$$

$$\mathbf{H}_t = (-\hat{x} \cos \theta_t + \hat{y} \sin \theta_t) \tau_{\perp} \frac{E_0}{Z_2} \exp[j\beta_2(x \sin \theta_t + y \cos \theta_t)] \quad (12)$$

The boundary conditions are as follows: (1) the tangential components of the electric fields in both media must be equal at $y = 0$, and (2) the tangential components

of the magnetic fields in both media must be equal at $y = 0$. Condition (1) can be written using (5), (9), and (11), to yield

$$\exp(j\beta_1 x \sin \theta_i) + \rho_\perp \exp(j\beta_1 x \sin \theta_r) = \tau_\perp \exp(j\beta_2 x \sin \theta_t) \quad (13)$$

From (12-2-12a), $1 + \rho_\perp = \tau_\perp$. It follows that the exponential arguments are all equal, i.e.,

$$\beta_1 \sin \theta_i = \beta_1 \sin \theta_r = \beta_2 \sin \theta_t \quad (14)$$

From the first equality,

$$\boxed{\theta_r = \theta_i} \quad (15)$$

i.e., the angle of reflection is equal to the angle of incidence.† From the second equality and using (15),

$$\boxed{\sin \theta_t = \frac{\eta_1}{\eta_2} \sin \theta_i} \quad (16)$$

where η_1 and η_2 are the indexes of refraction of medium 1 and medium 2, respectively. Equation (16) is known as *Snell's law*‡ and is a relation of fundamental importance in geometrical optics. For a lossless medium the index of refraction η can be written as equal to $\sqrt{\mu_r \epsilon_r}$, and Snell's law becomes

$$\boxed{\sin \theta_t = \sqrt{\frac{\mu_1 \epsilon_1}{\mu_2 \epsilon_2}} \sin \theta_i} \quad (17)$$

EXAMPLE 1 Polystyrene has a relative permittivity of 2.7. If a wave is incident at an angle of $\theta_i = 30^\circ$ from air onto polystyrene, calculate the angle of transmission θ_t . Interchange polystyrene and air and repeat the calculation.

SOLUTION From air onto polystyrene, $\epsilon_1 = \epsilon_0$, $\mu_1 = \mu_0$, $\epsilon_2 = 2.7\epsilon_0$, $\mu_2 = \mu_0$. From (16)

$$\sin \theta_t = \sqrt{\frac{1}{2.7}} (0.5) = 0.304$$

$$\theta_t = 17.7^\circ$$

From polystyrene onto air, $\epsilon_1 = 2.7\epsilon_0$, $\mu_1 = \mu_0$, $\epsilon_2 = \epsilon_0$, $\mu_2 = \mu_0$.

$$\sin \theta_t = \sqrt{2.7} (0.5) = 0.822$$

$$\theta_t = 55.2^\circ$$

† This is sometimes called *Snell's law of reflection*.

‡ This is sometimes called *Snell's law of refraction*.

Boundary condition (2) can be written using (6), (10), (12), and (14) with $y = 0$, to yield

$$-\cos \theta_i + \rho_{\perp} \cos \theta_i = -\tau_{\perp} \frac{Z_1}{Z_2} \cos \theta_i \quad (18)$$

but from (12-2-12a)

$$1 + \rho_{\perp} = \tau_{\perp} \quad (19)$$

and we have on substituting (19) into (18) and solving for ρ_{\perp} that

$$\rho_{\perp} = \frac{Z_2 \cos \theta_i - Z_1 \cos \theta_i}{Z_2 \cos \theta_i + Z_1 \cos \theta_i} \quad (20)$$

where Z_1 and Z_2 are the impedances of medium 1 and medium 2, respectively. It is seen that the previously derived reflection coefficient for normal incidence, (12-2-12), is obtained as a special case of (20) when $\theta_i = 0$.

If medium 2 is a perfect conductor, $Z_2 = 0$ and $\rho_{\perp} = -1$. If both media are lossless nonmagnetic dielectrics, (20) becomes

$$\rho_{\perp} = \frac{\cos \theta_i - \sqrt{(\epsilon_2/\epsilon_1) - \sin^2 \theta_i}}{\cos \theta_i + \sqrt{(\epsilon_2/\epsilon_1) - \sin^2 \theta_i}}$$

(21)

Provided medium 2 is a more dense dielectric than medium 1 ($\epsilon_2 > \epsilon_1$), the quantity under the square root will be positive and ρ_{\perp} will be real. If, however, the wave is incident from the more dense medium onto the less dense medium ($\epsilon_1 > \epsilon_2$), and if $\sin^2 \theta_i \geq \epsilon_2/\epsilon_1$, then ρ_{\perp} becomes complex and $|\rho_{\perp}| = 1$. Under these conditions, the incident wave is *totally internally reflected* back into the more dense medium.[†] The incident angle for which $\rho_{\perp} = 1/0^\circ$ is called the *critical angle* θ_{ic} . From (21) it is seen that this happens when the radical is zero; i.e.,

$$\theta_{ic} = \sin^{-1} \sqrt{\frac{\epsilon_2}{\epsilon_1}} \quad (22)$$

defines the critical angle. For all angles greater than the critical angle, $|\rho_{\perp}| = 1$. Using Snell's law, it is seen that when $\theta_i > \theta_{ic}$, then $\sin \theta_i > 1$,[‡] and $\cos \theta_i$ must be imaginary, i.e.,

$$\cos \theta_i = \sqrt{1 - \sin^2 \theta_i} = jA \quad (23)$$

[†] It can be shown that this is true for either perpendicular or parallel polarization.

[‡] Although the sine is greater than unity and the cosine is imaginary, there is a simple interpretation of the resulting field in such a case. See Example 2.

where $A = \sqrt{(\epsilon_1/\epsilon_2) \sin^2 \theta_i - 1}$ is a real number. The electric field in the less dense medium can now be written, from (11), as

$$\mathbf{E}_t = 2\tau_{\perp} E_0 \exp(-\alpha y) \exp(j\beta_2 x \sin \theta_i) \quad (24)$$

where

$$\alpha = \beta_2 A = \omega \sqrt{\mu_2 \epsilon_2} \sqrt{\frac{\epsilon_1}{\epsilon_2} \sin^2 \theta_i - 1} \quad (25)$$

Thus, E_{\perp} in the less dense medium has a magnitude $\tau_{\perp} E_0$, decaying exponentially away from the surface (y direction) and propagating without loss in the $-x$ direction. Waves whose fields are of the form of (24) are called *surface waves*. These results can be summarized by the *Principle of Total Internal Reflection* as follows. *When a wave is incident from the more dense onto the less dense medium at an angle equal to or exceeding the critical angle, the wave will be totally internally reflected and will also be accompanied by a surface wave in the less dense medium.*

EXAMPLE 2 Distilled water is a dielectric having the constants $\epsilon_r = 81$, $\mu_r = 1$. If a wave is incident from water onto a water-air interface, calculate the critical angle. If the incident $E_{\perp} = 1 \text{ V m}^{-1}$ and the incident angle is 45° , calculate the magnitude of the field strength in the air (a) at the interface and (b) $\lambda/4$ away from the interface.

SOLUTION From (22),

$$\theta_{ic} = \sin^{-1} \sqrt{\frac{1}{81}} = 6.38^\circ$$

For $\theta_i = 45^\circ$,

$$\sin \theta_t = \sqrt{81} (0.707) = 6.36$$

$$\cos \theta_t = \sqrt{1 - 6.36^2} = j6.28$$

so that

$$\alpha = \frac{2\pi}{\lambda_0} 6.28 = \frac{39.49}{\lambda_0} \quad (\text{Np m}^{-1})$$

$$\tau_{\perp} = 1 + \rho_{\perp} = 1 + \frac{0.707 - \sqrt{\frac{1}{81} - 0.5}}{0.707 + \sqrt{\frac{1}{81} - 0.5}} = 1.42 / -44.64^\circ$$

Therefore, the magnitude of the field strength is:

(a) at the interface: $|E_t| = 1.42 \text{ V m}^{-1}$

(b) $\lambda/4$ away from the interface:

$$|E_t| = 1.42 \exp\left(-\frac{39.49 \lambda_0}{4}\right) = 73.2 \mu\text{V m}^{-1}$$

indicating that the surface wave is very tightly bound to the water surface.

Parallel Case

Consider now the case of *parallel* (||) *polarization*. The geometry is the same as in Fig. 12-6 but with \mathbf{E}_i , \mathbf{E}_r , and \mathbf{E}_t parallel to the plane of incidence as would be obtained by replacing \mathbf{H}_i by \mathbf{E}_i , \mathbf{H}_r by \mathbf{E}_r , and \mathbf{H}_t by \mathbf{E}_t . It can be shown that the fields are given by

$$\mathbf{E}_i = (-\hat{\mathbf{x}} \cos \theta_i + \hat{\mathbf{y}} \sin \theta_i) E_0 \exp[j\beta_1(x \sin \theta_i + y \cos \theta_i)] \quad (26)$$

$$\mathbf{H}_i = -\frac{\mathbf{E}_0}{Z_1} \exp[j\beta_1(x \sin \theta_i + y \cos \theta_i)] \quad (27)$$

$$\mathbf{E}_r = (-\hat{\mathbf{x}} \cos \theta_r - \hat{\mathbf{y}} \sin \theta_r) \rho_{||} E_0 \exp[j\beta_1(x \sin \theta_r - y \cos \theta_r)] \quad (28)$$

$$\mathbf{H}_r = \frac{\mathbf{E}_0}{Z_1} \exp[j\beta_1(x \sin \theta_r - y \cos \theta_r)] \quad (29)$$

$$\mathbf{E}_t = (-\hat{\mathbf{x}} \cos \theta_t + \hat{\mathbf{y}} \sin \theta_t) \tau_{||} E_0 \exp[j\beta_2(x \sin \theta_t + y \cos \theta_t)] \quad (30)$$

$$\mathbf{H}_t = -\frac{\mathbf{E}_0}{Z_1} \exp[j\beta_2(x \sin \theta_t + y \cos \theta_t)] \quad (31)$$

By matching boundary conditions, as before, it is found that the angle of incidence equals the angle of reflection and that Snell's law (16) holds. It can also be shown that

$$1 + \rho_{||} = \frac{\cos \theta_t}{\cos \theta_i} \tau_{||} \quad (32)$$

The reflection coefficient is found to be

$$\rho_{||} = \frac{Z_2 \cos \theta_t - Z_1 \cos \theta_i}{Z_1 \cos \theta_i + Z_2 \cos \theta_t} \quad (33)$$

which for lossless nonmagnetic dielectrics becomes

$$\rho_{||} = \frac{-(\epsilon_2/\epsilon_1) \cos \theta_i + \sqrt{(\epsilon_2/\epsilon_1) - \sin^2 \theta_i}}{(\epsilon_2/\epsilon_1) \cos \theta_i + \sqrt{(\epsilon_2/\epsilon_1) - \sin^2 \theta_i}} \quad (34)$$

and to be $\rho_{||} = -1$ if medium 2 is a perfect conductor.

It is of especial interest that, for parallel polarization, it is possible to find an incident angle so that $\rho_{||} = 0$ and the wave is *totally transmitted* into medium 2. This angle, called the *Brewster angle* θ_{iB} , can be found by setting the numerator of (34) equal to zero, giving

$$\theta_{iB} = \sin^{-1} \sqrt{\frac{\epsilon_2/\epsilon_1}{1 + (\epsilon_2/\epsilon_1)}} = \tan^{-1} \sqrt{\frac{\epsilon_2}{\epsilon_1}} \quad (35)$$

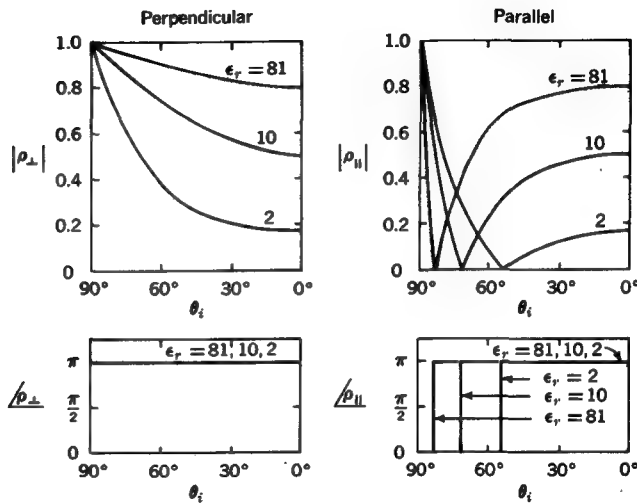


FIGURE 12-7

Reflection coefficient for perpendicular and parallel polarization vs. angle of incidence θ_i for distilled water ($\epsilon_r = 81$), flint glass ($\epsilon_r = 10$), and paraffin ($\epsilon_r = 2$). $|\rho_{\parallel}| = 0$ at the Brewster angle (see Example 3).

The Brewster angle is also sometimes called the *polarizing angle* since a wave composed of both perpendicular and parallel components and incident at the Brewster angle produces a reflected wave with only a perpendicular component. Thus, a circularly polarized wave incident at the Brewster angle becomes linearly polarized on reflection.

EXAMPLE 3 A parallel-polarized wave is incident from air onto (a) distilled water ($\epsilon_r = 81$), (b) flint glass ($\epsilon_r = 10$), and (c) paraffin ($\epsilon_r = 2$). Find the Brewster angle for each of these cases.

SOLUTION

$$(a) \quad \theta_{iB} = \tan^{-1} \sqrt{81} = 83.7^\circ$$

$$(b) \quad \theta_{iB} = \sin^{-1} \tan^{-1} \sqrt{10} = 72.4^\circ$$

$$(c) \quad \theta_{iB} = \sin^{-1} \tan^{-1} \sqrt{2} = 54.7^\circ$$

The magnitude and phase angle of the reflection coefficients ρ_{\perp} and ρ_{\parallel} are shown in Fig. 12-7 for waves incident from air onto distilled water ($\epsilon_r = 81$), flint glass ($\epsilon_r = 10$), and paraffin ($\epsilon_r = 2$). Note that the phase angle for ρ_{\perp} is always π , whereas for ρ_{\parallel} the

phase angle jumps from 0 to π at the Brewster angle. Furthermore, the reflection coefficient has unit magnitude at grazing incidence ($\theta_i = 90^\circ$).

The quantities ρ_{\parallel} and ρ_{\perp} as given in (21) and (34) are sometimes called the *Fresnel (fray-nel') reflection coefficients*.

12-5 ELLIPTICALLY POLARIZED PLANE WAVE, OBLIQUE INCIDENCE

We now consider an elliptically polarized plane wave obliquely incident on a boundary. The problem is to find the magnitude and polarization of the reflected and transmitted waves.

The incident electric field is composed of both parallel ($E_{i\parallel}$) and perpendicular ($E_{i\perp}$) components, as shown in inset A of Fig. 12-8. As viewed from the origin, the orthogonal field components are

$$E_z = E_{i\perp} e^{j\omega t} \quad (1)$$

$$E_y' = E_{i\parallel} e^{j(\omega t + \delta_i)} \quad (2)$$

where δ_i is the angle by which E_y' leads E_z and $E_{i\perp}$ and $E_{i\parallel}$ are the component amplitudes. Thus, as in Sec. 11-4, the incident wave has a polarization ellipse specified by (γ_i, δ_i) , where

$$\gamma_i = \tan^{-1} \frac{E_{i\parallel}}{E_{i\perp}} \quad (3)$$

The polarization ellipse can also be specified in terms of its axial ratio AR_i and tilt angle τ_i . From (11-4-3) we can relate (AR_i, τ_i) to (γ_i, δ_i) :

$$\tan 2\tau_i = \tan 2\gamma_i \cos \delta_i \quad (4)$$

$$\sin 2\epsilon_i = \sin 2\gamma_i \sin \delta_i \quad (5)$$

$$\cos 2\gamma_i = \cos 2\epsilon_i \cos 2\tau_i \quad (6)$$

$$\tan \delta_i = \frac{\tan 2\epsilon_i}{\sin 2\tau_i} \quad (7)$$

where

$$\epsilon_i = \cot^{-1} (\mp AR_i) \quad (8)$$

If the wave is right elliptically polarized, the minus sign is used; if it is left elliptically polarized, the plus sign is used.

Considering the reflected wave as viewed from point P (see inset B), the orthogonal field components are

$$E_z = E_{r\perp} e^{j\omega t} = |\rho_{\perp}| E_{i\perp} \exp[j(\omega t + \phi_{\perp})] \quad (9)$$

$$E_{y''} = -E_{r\parallel} e^{j\omega t} = |\rho_{\parallel}| E_{i\parallel} \exp[j(\omega t + \phi_{\parallel} + \delta_i + \pi)] \quad (10)$$

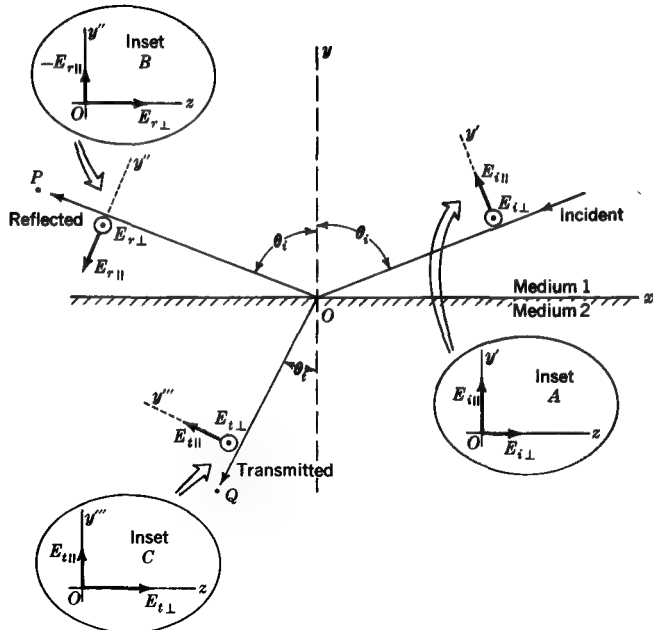


FIGURE 12-8

Geometry in the plane of incidence (xy plane) for elliptically polarized wave incident obliquely on a plane surface. The incident electric field has parallel ($E_{i\parallel}$) and perpendicular ($E_{i\perp}$) components which appear as in inset A when viewed from the origin O . The reflected and transmitted fields shown in insets B and C are viewed looking toward the origin from points P and Q , respectively.

where ϕ_{\parallel} and ϕ_{\perp} are the phase angles of the parallel and perpendicular reflection coefficients ρ_{\parallel} and ρ_{\perp} , respectively. The phase angle by which $E_{y''}$ leads E_z is thus given by

$$\delta_r = \delta_i + \pi + (\phi_{\perp} - \phi_{\parallel}) \quad (11)$$

and similarly [see (3)],

$$\gamma_r = \tan^{-1} \left(\frac{|\rho_{\parallel}|}{|\rho_{\perp}|} \tan \gamma_i \right) \quad (12)$$

The relations (11) and (12) specify the polarization state of the reflected wave, as seen by an observer at point P . To find the axial ratio and tilt angle of the polarization ellipse of the reflected wave, the relations (4), (5), and (8) are used with the subscript i replaced by the subscript r .

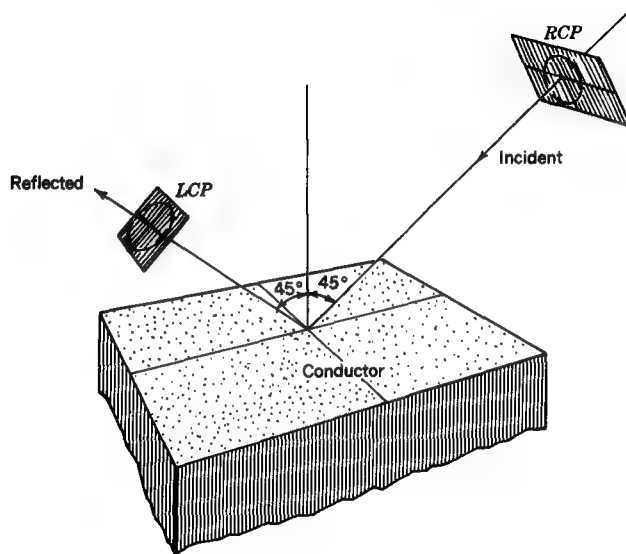


FIGURE 12-9a [Example 1(a)]

Right circularly polarized (RCP) wave incident on a perfect conductor. The reflected wave is left circularly polarized (LCP). No wave is transmitted.

In similar fashion, it can be shown that an observer at point Q (see inset C) will see a transmitted wave with polarization ellipse given by

$$\delta_t = \delta_i + (\xi_{\perp} - \xi_{\parallel}) \quad (13)$$

$$\gamma_t = \tan^{-1}\left(\frac{|\tau_{\parallel}|}{|\tau_{\perp}|} \tan \gamma_i\right) \quad (14)$$

where ξ_{\parallel} and ξ_{\perp} are the phase angles of the parallel and perpendicular transmission coefficients τ_{\parallel} and τ_{\perp} , respectively.[†]

EXAMPLE 1 A right circularly polarized wave (RCP) is incident at an angle of 45° from air onto (a) a perfect conductor and (b) polystyrene ($\epsilon_r = 2.7$). What is the polarization state of the reflected wave for these two cases?

SOLUTION (a) When medium 1 is air and medium 2 is a perfect conductor,

$$\rho_{\parallel} = 1/180^\circ \quad \rho_{\perp} = 1/180^\circ$$

For a right circularly polarized wave, $\gamma_i = 45^\circ$, $\delta_i = -90^\circ$, so that from (11), $\delta_r = -90^\circ + 180^\circ + (180^\circ - 180^\circ) = 90^\circ$ and from (12), $\gamma_r = \tan^{-1}(1 \times 1) = 45^\circ$. Therefore the

[†] Note that when τ is used in this section to denote the *tilt angle* it is associated with the incident, reflected, or transmitted wave (that is, τ_i , τ_r , or τ_p) but when it is used to denote the *transmission coefficient* it is associated with either a parallel or perpendicular case (that is, τ_{\parallel} or τ_{\perp}).

reflected wave is *left circularly polarized* (LCP), as shown in Fig. 12-9a. Conversely, if the incident wave had been LCP, the reflected wave would be RCP.

(b) When medium 1 is air and medium 2 is polystyrene, then from (12-4-34)

$$\rho_{\parallel} = \frac{-2.7(0.707) + \sqrt{2.7 - 0.5}}{2.7(0.707) + \sqrt{2.7 - 0.5}} = 0.126/180^\circ$$

and from (12-4-21)

$$\rho_{\perp} = \frac{0.707 - \sqrt{2.7 - 0.5}}{0.707 + \sqrt{2.7 - 0.5}} = 0.354/180^\circ$$

Therefore,

$$\delta_r = -90^\circ + 180^\circ + (180^\circ - 180^\circ) = 90^\circ$$

$$\gamma_r = \tan^{-1} \frac{0.126}{0.354} = 19.6^\circ$$

Substituting these values into (4), (5), and (8) (with subscripts *i* replaced by *r*), we find $\tau_r = 0^\circ$ and $AR_r = 2.81$. Thus the reflected wave is left elliptically polarized (LEP), as shown in Fig. 12-9b.

EXAMPLE 2 A linearly polarized wave whose electric field vector bisects the zy' axis (see Fig. 12-8, inset *A*) is incident at an angle of 45° from air onto (a) a perfect conductor, and (b) polystyrene ($\epsilon_r = 2.7$). What is the polarization state of the reflected wave for these two cases? (c) If the angle of incidence onto polystyrene is 58.7° (Brewster angle), what is the polarization state of the reflected wave?

SOLUTION (a) Since $\rho_{\parallel} = 1/180^\circ$ and $\rho_{\perp} = 1/180^\circ$,

$$\delta_r = 0^\circ + 180^\circ + (180^\circ - 180^\circ) = 180^\circ$$

$$\gamma_r = \tan^{-1}(\frac{1}{1} \times 1) = 45^\circ$$

From (4), $\tan 2\tau_r = -\infty$, so that $\tau_r = 135^\circ$; and from (5) and (8), $AR_r = \infty$. Therefore the reflected wave is *linearly polarized* with the electric field vector bisecting the $-z$ and y' axes.

(b) From Example 1,

$$\rho_{\parallel} = 0.126/180^\circ \quad \text{and} \quad \rho_{\perp} = 0.354/180^\circ$$

so that $\gamma_r = \tan^{-1}(0.126/0.354) = 19.6^\circ$ and $\delta_r = 180^\circ$. From (4), $\tan 2\tau_r = \tan 39.2^\circ$ $\cos \pi = -0.815$, so that $\tau_r = 70.4^\circ$. From (5) and (8), $AR_r = \infty$. Therefore the reflected wave is *linearly polarized* with the electric field vector making an angle of 70.4° with the z axis.

(c) When $\theta_i = \theta_{rs} = 58.7^\circ$,

$$\rho_{\parallel} = 0$$

$$\rho_{\perp} = \frac{0.520 - 1.40}{0.520 + 1.40} = 0.46/180^\circ$$

Therefore the reflected wave is perpendicularly polarized.

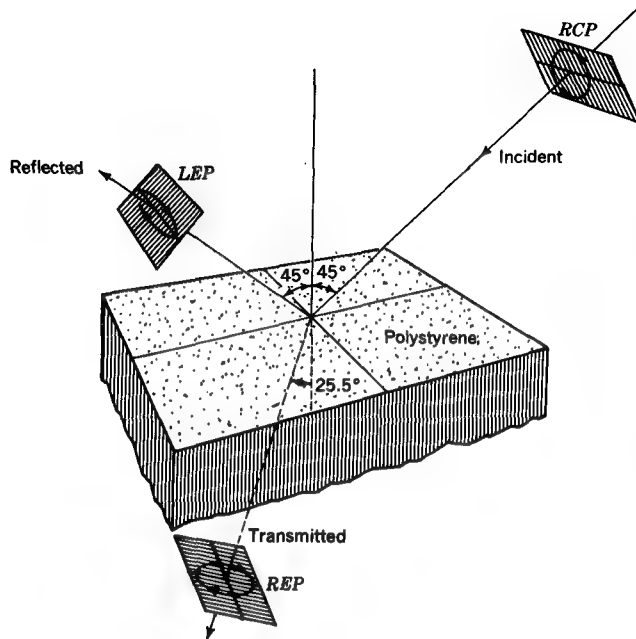


FIGURE 12-9b [Example 1(b)]

Right circularly polarized (RCP) wave incident on dielectric slab of polystyrene. The reflected wave is left elliptically polarized (LEP) with major axis of the polarization ellipse horizontal and the transmitted wave right elliptically polarized (REP) with major axis of the polarization ellipse in the (vertical) plane of incidence. (See Prob. 12-15.) If the angle of incidence is increased to 58.7° (=Brewster angle) the angle of reflection increases to 58.7° and the angle of refraction increases from 25.5° to 31.3° . Also the polarization ellipse of the reflected wave collapses to a straight horizontal line (linear \perp polarization).

12-6 HUYGENS' PRINCIPLE AND PHYSICAL OPTICS

Huygens' principle† states that *each point on a primary wavefront can be considered to be a new source of a secondary spherical wave and that a secondary wavefront can be constructed as the envelope of these secondary spherical waves*, as suggested in Fig. 12-10. This fundamental principle of physical optics can be used to explain the apparent bending of radio waves around obstacles, i.e., the diffraction of waves. A

† C. Huygens, "Traité de la lumière," Leyden, 1690. English translation by S. P. Thompson, London, 1912, reprinted by The University of Chicago Press.

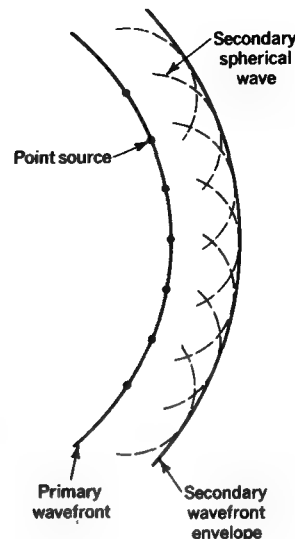


FIGURE 12-10
Illustrating Huygens' principle of physical optics (point-to-wave correspondence.)

diffracted ray is one that follows a path that cannot be interpreted as either reflection or refraction.

As an example, consider a uniform plane wave incident on a conducting half-plane, as in Fig. 12-11a.[†] We want to calculate the electric field at point P by using Huygens' principle, i.e.,

$$E = \int_{\text{over } x \text{ axis}} dE \quad (1)$$

where dE is the electric field at P due to a point source at a distance x from the origin O , as in Fig. 12-11b, i.e.,

$$dE = \frac{E_0}{r} e^{-j\beta(r+\delta)} dx \quad (2)$$

so that

$$E = \frac{E_0}{r} e^{-j\beta r} \int_a^\infty e^{-j\beta \delta} dx \quad (3)$$

If $\delta \ll r$, it follows that

$$\delta = \frac{x^2}{2r} \quad (4)$$

[†]J. D. Kraus, "Radio Astronomy," pp. 194-198, McGraw-Hill Book Company, New York, 1966.

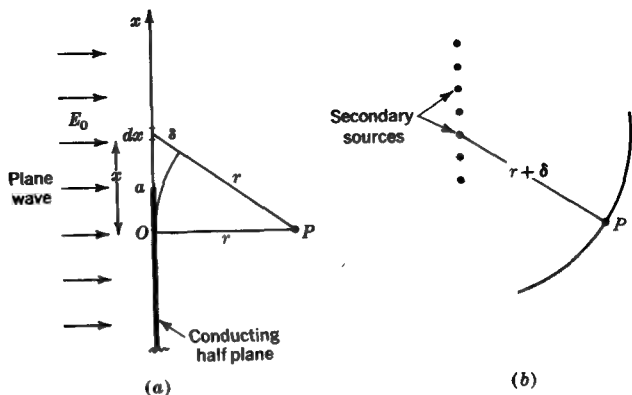


FIGURE 12-11
Diffraction of a plane wave by a conducting half-plane.

When we let $\kappa^2 = 2/r\lambda$ and $u = \kappa x$, (3) becomes

$$E = \frac{E_0}{\kappa r} e^{-j\beta r} \int_{\kappa a}^{\infty} e^{-j\kappa u^2/2} du \quad (5)$$

which can be rewritten as

$$E = \frac{E_0}{\kappa r} e^{-j\beta r} \left(\int_0^{\infty} e^{-j\kappa u^2/2} du - \int_0^{\kappa a} e^{-j\kappa u^2/2} du \right) \quad (6)$$

The integrals in (6) have the form of Fresnel integrals† and can be written

$$E = \frac{E_0}{\kappa r} e^{-j\beta r} \left(\frac{1}{2} - j \frac{1}{2} - [C(\kappa a) - jS(\kappa a)] \right) \quad (7)$$

where $C(\kappa a) = \int_0^{\kappa a} \cos \frac{\pi u^2}{2} du \quad \text{Fresnel cosine integral}$ (8)

$$S(\kappa a) = \int_0^{\kappa a} \sin \frac{\pi u^2}{2} du \quad \text{Fresnel sine integral} \quad (9)$$

† See M. Abramowitz and I. A. Stegun, "Handbook of Mathematical Functions," pp. 295-329, National Bureau of Standards, U.S. Government Printing Office, 1964. E. Jahnke and F. Emde, "Tables of Functions," pp. 35-38, Dover Publications, New York, 1943.

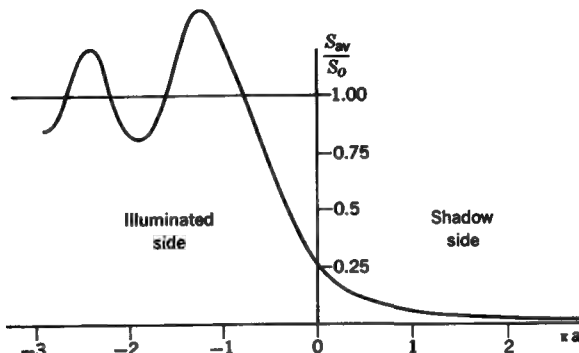


FIGURE 12-12
Physical-optics solution to half-plane diffraction pattern.

The power density at P is then

$$S_{av} = \frac{EE^*}{2Z} = S_0 \frac{1}{2} \{ [\frac{1}{2} - C(\kappa a)]^2 + [\frac{1}{2} - S(\kappa a)]^2 \} \quad (\text{W m}^{-2}) \quad (10)$$

where†

$$S_0 = \frac{E_0^2 \lambda}{2Zr} \quad (11)$$

The half-plane diffraction curve, (10), is shown in Fig. 12-12. Note that when $\kappa a = -\infty$, which corresponds to no edge present, $S_{av} = S_0$; when $\kappa a = 0$, $S_{av} = S_0/4$; and when $\kappa a = +\infty$, which corresponds to complete obscuration of the plane wave by the half-plane, $S_{av} = 0$. Furthermore, the power density does not abruptly go to zero as the point of observation goes from the illuminated side ($\kappa a < 0$) to the shadow side ($\kappa a > 0$); rather, there are fluctuations followed by a gradual decrease in power density.

Another illustration of Huygens' principle occurs in *holography*. In an ordinary photograph only amplitude information is recorded. In a *hologram* both amplitude information and phase information are recorded. Thus, when the hologram is illuminated with coherent light, it generates waves (in both amplitude and phase) which, in accord with Huygens' principle, produce a three-dimensional picture.‡

† Since this is a cylindrical (rather than spherical) wave, the field must diminish as $1/\sqrt{r}$ (see Sec. 12-7), and the power density must diminish as $1/r$.

‡ D. Gabor, A New Microscopic Principle, *Nature*, 161: 777 (May 15, 1948); E. N. Leith and J. Upatnieks, Progress in Holography, *Phys. Today*, 25(3): 28-34 (March 1972).

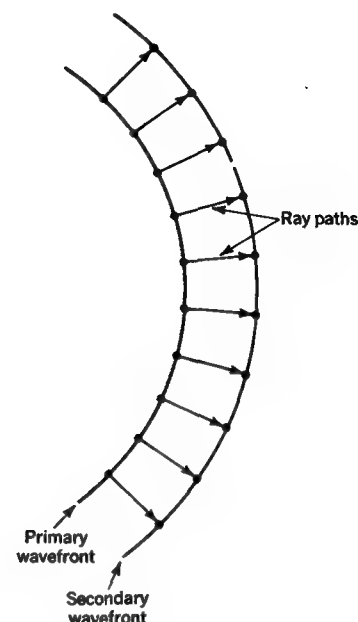


FIGURE 12-13
The principle of geometrical optics
(ray paths).

12-7 GEOMETRICAL-OPTICS CONCEPTS†

Imagine that a family of ray paths is drawn from each point on a primary wavefront to corresponding points on a secondary wavefront, as in Fig. 12-13. The ray paths are perpendicular to the wavefronts and are in the direction of the Poynting vector at each point. Geometrical-optics theory uses a *point-to-point ray correspondence* between two successive positions of a wavefront, in contrast to the physical-optics theory of Sec. 12-6, which postulates a *point-to-spherical-wave correspondence*. Put simply, physical optics involves *wavefronts* while geometrical optics involves *ray paths*.

To illustrate this, let us reconsider the example of Sec. 12-6, where a plane wave is incident on a straight edge, as in Fig. 12-14. According to the theory of geometrical optics, the power density on the right side of the edge will drop abruptly to zero (solid line) as an observer goes from the illuminated region to the shadow region, in contrast to the physical-optics solution (dashed line), which predicts fluctuations followed by a gradual decrease. The geometrical-optics approximation can be considered as the high-frequency limit of the physical optics approximation.

† The material in this section is based on lecture notes by Prof. Leon Peters, Jr., Ohio State University.

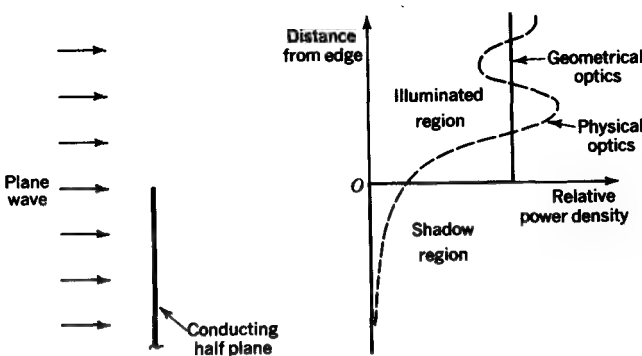


FIGURE 12-14
Comparison of geometrical- and physical-optics solutions to diffraction of plane wave by a half-plane.

In geometrical optics it is assumed that the power flow between a set of rays remains constant. In Fig. 12-15, for example, four rays from a point source are shown passing through small concentric spherically shaped wavefronts of areas A_1 and A_2 . According to geometrical optics, the power passing through areas A_1 and A_2 must remain constant (conservation of power), i.e.,

$$S_1 A_1 = S_2 A_2 \quad (1)$$

where $S_1 = \frac{|E_1|^2}{2Z} = \text{power density at area } A_1$ (2)

and $S_2 = \frac{|E_2|^2}{2Z} = \text{power density at area } A_2$ (3)

where E_1 and E_2 are the electric fields at A_1 and A_2 , respectively, and Z is the impedance of the medium. Taking the ratio S_2/S_1 from (1) and substituting (2) and (3), we have

$$\frac{|E_2|^2}{|E_1|^2} = \frac{A_1}{A_2} \quad (4)$$

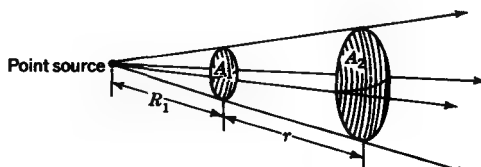


FIGURE 12-15
Tube of rays from a point source.

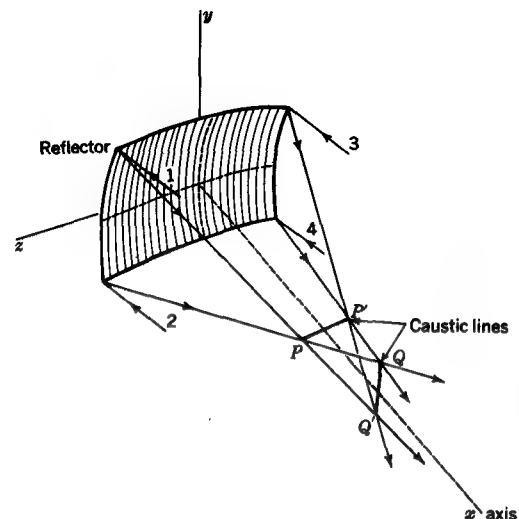


FIGURE 12-16

Astigmatic tube of rays from non-spherical reflector.

Also we note that the ratio of areas is

$$\frac{A_1}{A_2} = \frac{R_1^2}{(R_1 + r)^2} \quad (5)$$

Combining (5) and (4), we obtain

$$|E_2| = |E_1| \frac{R_1}{R_1 + r} \quad (6)$$

Taking into account the phase-delay factor, we have

$$E_2 = |E_1| \frac{R_1}{R_1 + r} e^{-j\beta(R_1 + r)} \quad (7)$$

or $E_2 = E_1 \frac{R_1}{R_1 + r} e^{-j\beta r} \quad (8)$

where

$$E_1 = |E_1| e^{-j\beta R_1} \quad (9)$$

We now consider a more general situation in which the wavefronts are not necessarily spherical. In Fig. 12-16, a curved reflecting surface is shown with a radius of curvature in the xy plane which is unequal to the radius of curvature in the xz plane. The incident rays 1, 2, 3, and 4 are all parallel to the x axis. After reflection, rays 1 and 2 then cross (focus) at P , rays 3 and 4 focus at P' , rays 1 and 3 focus at Q' , and rays 2 and 4 focus at Q . The tube of rays is then said to be *astigmatic*,

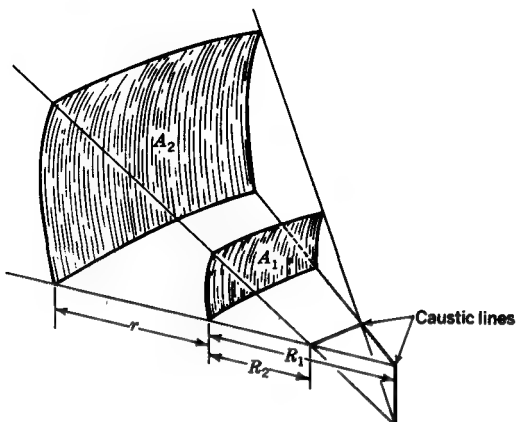


FIGURE 12-17
Geometry for astigmatic tube of rays
with caustic lines.

and lines PP' and QQ' are called *caustics*. An astigmatic tube of rays is shown in Fig. 12-17 along with two wavefronts of areas A_1 and A_2 , respectively. It follows that

$$\frac{A_1}{A_2} = \frac{R_1 R_2}{(R_1 + r)(R_2 + r)} \quad (10)$$

Substituting (10) into (4) gives

$$|E_2| = |E_1| \left[\frac{R_1 R_2}{(R_1 + r)(R_2 + r)} \right]^{1/2} \quad (11)$$

Introducing the phase-delay term, we have

$$E_2 = E_1 \left[\frac{R_1 R_2}{(R_1 + r)(R_2 + r)} \right]^{1/2} e^{-j\beta r} \quad (12)$$

where E_1 is the complex electric field at the reference wavefront A_1 .† Note that (8) is a special case of (12) when $R_2 = R_1$.

For cylindrical curved surfaces with axes parallel to the z axis, the radius of curvature in the xz plane becomes infinite, so that $R_1 = \infty$. For this case, (12) becomes

$$E_2 = E_1 \left(\frac{R_2}{R_2 + r} \right)^{1/2} e^{-j\beta r} \quad (13)$$

† The phase term in (12) assumes $r > 0$. If $0 > r > -R_2$, a constant-phase factor of -90° is added to the exponential term of (12). If $-R_2 > r > -R_1$, a phase shift of 180° is added. If $r = -R_1$ or $r = -R_2$ (caustic points), the value of E_2 cannot be found by geometrical-optics methods.

In general, a geometrical-optics expression for the field can be written as

$$\mathbf{E} = E_0 e^{j\phi_0} F(r) e^{-j\beta r} \quad (14)$$

where E = rectangular component of electric field, V m^{-1}

E_0 = amplitude of field component at reference point, $r = 0$, V m^{-1}

ϕ_0 = phase of field component at reference point, $r = 0$, rad

$F(r)$ = spatial attenuation factor, dimensionless

$\beta = 2\pi/\lambda$, m^{-1}

r = distance from reference point, m

That is,

$$E(r) = \text{reference field} \times \text{attenuation factor} \times \text{phase-delay factor}$$

12-8 SCATTERING FROM A CONDUCTING STRIP

To illustrate the geometrical-optics concept, let us consider an infinite perfectly conducting strip of width D . A line source is located a distance d from the center of the strip, as shown in Fig. 12-18, so that the electric field is perpendicular to the page. If $D \gg \lambda$, the geometrical-optics expression (12-7-13) can be used to find the field at a point P . The point P is assumed to be sufficiently far from the strip and line source for the reflected and direct rays to be essentially parallel. From (12-7-13) the *direct field* is

$$E_d = E_1 \sqrt{\frac{R}{R + r_0}} e^{-j\beta r_0} \quad (1)$$

where $R = \overline{OQ}$ and $r_0 = \overline{QP}$, as shown in Fig. 12-18a, and where E_1 is equal to the field at point Q . It is convenient to relate the amplitude $|E_1|$ to a reference amplitude $|E_0|$ at a fixed point such as the center of the strip. According to geometrical optics,

$$|E_0|^2 A_0 = |E_1|^2 A_1 \quad (2)$$

where for cylindrical wavefronts originating at O and of length l perpendicular to the page, $A_0 = ld$ and $A_1 = lR$. Therefore

$$|E_1| = \sqrt{\frac{d}{R}} |E_0| \quad (3)$$

Also $E_0 = |E_0| e^{-j\beta R}$. Substituting this and (3) into (1) gives

$$E_d = |E_0| \sqrt{\frac{d}{R + r_0}} e^{-j\beta(r_0 + R)} \quad (4)$$

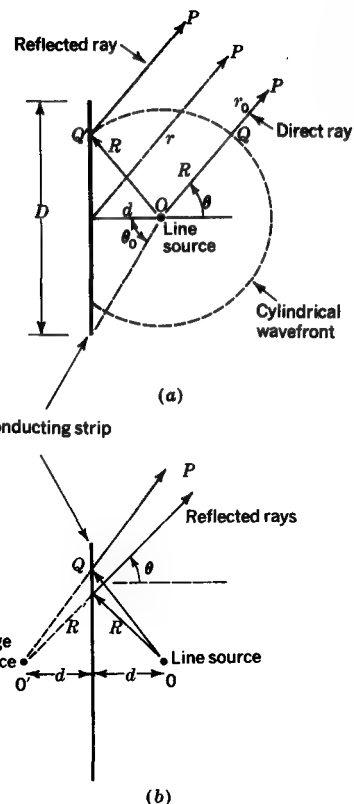


FIGURE 12-18

(a) Infinite conducting strip of width D perpendicular to page with infinite line source parallel to it at distance d . (b) Line source and image line source.

It is also convenient to refer the phase to the center of the strip by defining the length r as shown in Fig. 12-18a, where $r = r_0 + R + d \cos \theta$. Substituting this into (4) gives

$$E_d = |E_0| \sqrt{\frac{d}{R + r_0}} \exp(-j\beta r) \exp(j\beta d \cos \theta) \quad (5)$$

Furthermore, if r_0 is large in comparison with R , the substitution $R + r_0 \approx r$ can be made in the denominator, so that (5) becomes

$$E_d = |E_0| \sqrt{\frac{d}{r}} \exp(-j\beta r) \exp(j\beta d \cos \theta) \quad (6)$$

which holds for all angles θ except those in the shadow of the strip. Thus (6) is valid for $-(\pi - \theta_0) \leq \theta \leq \pi - \theta_0$, where

$$\theta_0 = \tan^{-1} \frac{D/2}{d} \quad (7)$$

For θ outside this range (behind strip), $E_d = 0$.

The cylindrical wavefront passing through Q also intersects the reflected ray at Q' . By the method of images (Secs. 7-15 and 7-16) the reflected ray can be viewed as coming from an image line source at O' (Fig. 12-18b) which is 180° out of phase with the line source at O . Thus, the *reflected field* is given by

$$E_r = -|E_0| \sqrt{\frac{d}{r}} \exp(-j\beta r) \exp(-j\beta d \cos \theta) \quad (8)$$

which holds over the range $-\theta_0 \leq \theta \leq \theta_0$. When $|\theta| > \theta_0$, $E_r = 0$. Thus in the range $|\theta| < \theta_0$, the total geometrical-optics field is given by the sum of (6) and (8):

$$\begin{aligned} E_G = E_d + E_r &= |E_0| \sqrt{\frac{d}{r}} \exp(-j\beta r) [\exp(j\beta d \cos \theta) - \exp(-j\beta d \cos \theta)] \\ &= 2j|E_0| \sqrt{\frac{d}{r}} e^{-j\beta r} \sin(\beta d \cos \theta) \end{aligned} \quad (9)$$

In the range $\pi - \theta_0 > |\theta| > \theta_0$ the reflected field is zero, so that E_G is given by (6) alone. When $\pi \geq |\theta| > \pi - \theta_0$ (incident- and reflected-ray shadow zone), the total field is zero.

12-9 GEOMETRICAL THEORY OF DIFFRACTION

In recent years, a very powerful extension of geometrical optics has been developed, known as the *geometrical theory of diffraction*. Its basis lies in the fact that the interaction of electromagnetic energy with a material body is essentially a localized phenomenon provided the body is not too small in terms of a wavelength. Thus, the geometrical-optics field (Sec. 12-7) represents an important contribution to the fields set up by such an interaction. However, this must be supplemented by various other contributions. The two most prominent supplementary contributors are those of *edge diffraction* and *creeping-wave diffraction*. The latter represents the mechanism by which energy is diffracted to the shadow region of a curved metallic surface such as a cylinder.[†]

In this section, attention is confined to edge diffraction. Although this appears to be a very special case, it has been found to be applicable to a wide variety of geom-

[†] L. Peters, Jr., and C. E. Ryan, Jr., Empirical Formulas for E-plane Creeping Waves on General Smooth Conducting Bodies, *IEEE Trans. Antennas Propag.*, AP-18: 432-434 (May, 1970).

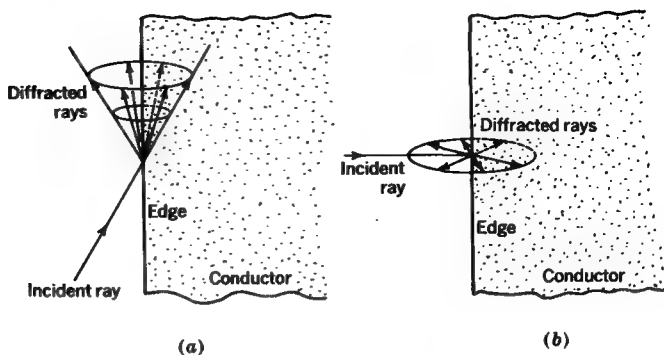


FIGURE 12-19
 (a) Cone of diffracted rays from edge of a conductor ; (b) plane of diffracted rays when edge is hit by normally incident ray. [After J. B. Keller, *J. Opt. Soc. Am.*, 52 (2): 116-130 February 1962].

tries because of the local nature of the diffracted fields. The *Law of Edge Diffraction* states that in a homogeneous medium a diffracted ray and the corresponding incident ray make equal angles with the edge at the point of diffraction. They lie on opposite sides of the plane normal to the edge at the point of diffraction, as suggested in Fig. 12-19 for a conducting half-plane.[†]

The diffracted field E'_D of a conducting half-plane can be found by slightly modifying (12-7-14), i.e.,

$$E'_D = \mathcal{D} |E_1| e^{j\phi} r^{-1/2} e^{-j\beta r} \quad (1)$$

where \mathcal{D} = diffraction coefficient, $\text{m}^{1/2}$

$|E_1|$ = amplitude of incident field at $r = 0$, V m^{-1}

ϕ = phase of incident field at $r = 0$, rad

r = distance from the edge, m

$\beta = 2\pi/\lambda$, m^{-1}

If βr is large and a plane wave is incident normally on the edge, the diffraction coefficient is given approximately by

$$\mathcal{D} = \frac{e^{-j\pi/4}}{2\sqrt{2\pi\beta}} \left(\sec \frac{\theta - \alpha}{2} \pm \csc \frac{\theta + \alpha}{2} \right) \quad (2)$$

[†] J. B. Keller, Geometrical Theory of Diffraction, *J. Opt. Soc. Am.*, 52: 116-130 (February 1962).

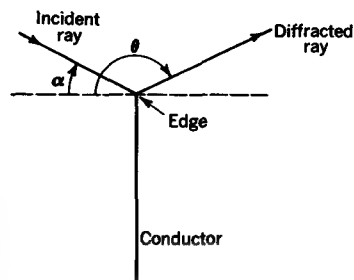


FIGURE 12-20

Edge-on view of plane conducting obstacle showing incident and diffracted ray.

where θ and α are the angles shown in Fig. 12-20. In (2) the plus sign is used if the electric field is parallel to the edge, and the minus sign is used if the magnetic field is parallel to the edge. The approximation (2) is not valid near the shadow boundaries, where more complex expressions for the diffracted field must be used.[†]

In order to illustrate the procedure for calculating the diffracted field, let us return to the example of a conducting strip illuminated by a line source, as discussed in Sec. 12-8. The total diffracted field is the sum of the diffracted fields from edges 1 and 2, as shown in Fig. 12-21. From (1) it follows, therefore, that the total diffracted field is

$$E_D = |E_1| e^{-j\beta R} \left(\mathcal{D}_1 \frac{e^{-j\beta r_1}}{\sqrt{r_1}} + \mathcal{D}_2 \frac{e^{-j\beta r_2}}{\sqrt{r_2}} \right) \quad (3)$$

where \mathcal{D}_1 , \mathcal{D}_2 = diffraction coefficients associated with edges 1 and 2

$$R = \sqrt{(D/2)^2 + d^2}$$

$|E_1|$ = amplitude of electric field at edges

It follows from the geometry of Fig. 12-21 that $r_1 = r + (D/2) \sin \theta$ and $r_2 = r - (D/2) \sin \theta$. Furthermore, from (12-8-3),

$$|E_1| = \sqrt{\frac{d}{R}} |E_0| \quad (4)$$

[†] A. Sommerfeld, "Optics," pp. 258-262, Academic Press Inc., New York, 1954. See also P. M. Russo, R. C. Rudduck, and L. Peters, Jr., A Method for Computing E-plane Patterns of Horn Antennas, *IEEE Trans. Antennas Propag.*, AP-13: 219-224 (March 1965).

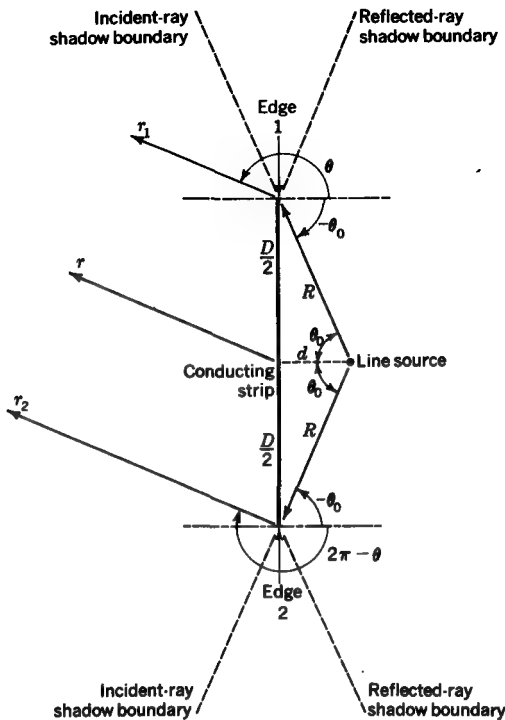


FIGURE 12-21

Geometry for calculation of edge-diffracted field from a conducting strip illuminated by a line source.

When we note from Figs. 12-20 and 12-21 that†

$$\alpha_1 - \theta_1 = \theta + \theta_0 \quad (5)$$

$$\alpha_1 + \theta_1 = \theta - \theta_0 \quad (6)$$

$$\alpha_2 - \theta_2 = \theta - \theta_0 - 2\pi \quad (7)$$

$$\alpha_2 + \theta_2 = \theta + \theta_0 - 2\pi \quad (8)$$

and using (2), the diffraction coefficients become

$$\mathcal{D}_1 = \frac{e^{-j\pi/4}\sqrt{\lambda}}{4\pi} \left(+ \sec \frac{\theta + \theta_0}{2} - \csc \frac{\theta_0 - \theta}{2} \right) \quad (9)$$

and

$$\mathcal{D}_2 = \frac{e^{-j\pi/4}\sqrt{\lambda}}{4\pi} \left(- \sec \frac{\theta_0 - \theta}{2} - \csc \frac{\theta_0 + \theta}{2} \right) \quad (10)$$

† The subscripts 1 and 2 on α and θ refer to these angles as measured with respect to edges 1 and 2, that is, α_1 is the same as α and θ_1 is the same as θ in Fig. 12-20 (edge 1 in Fig. 12-21), while α_2 and θ_2 are related to the corresponding geometry for edge 2.

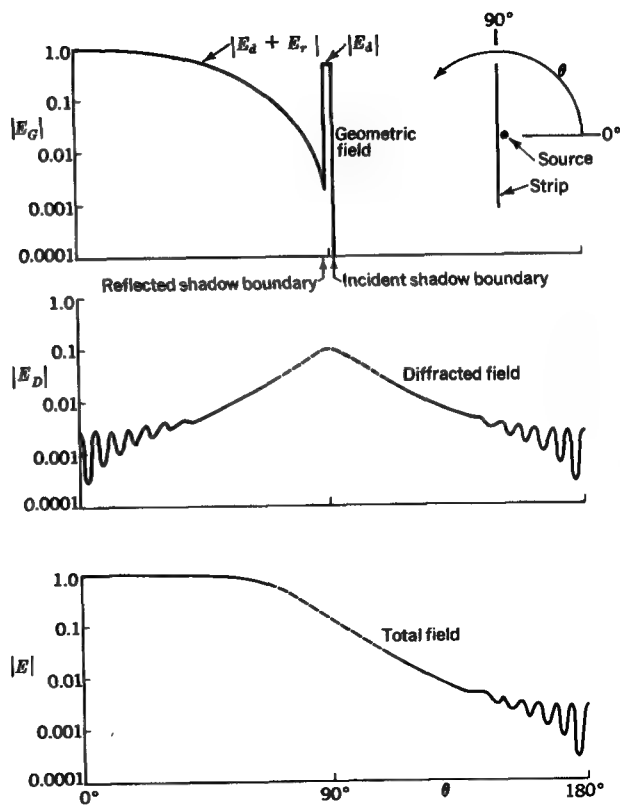


FIGURE 12-22

Magnitudes of geometrical field (E_G), diffracted field (E_D), and total field (E) for line source and conducting strip of Fig. 12-21 for the case where $D = 10\lambda$ and $d = \lambda/4$. Dashed lines are for region in which the approximation (12-9-12) is not valid.

If $r \gg D$, the square-root terms in (3) become $\sqrt{r_1} \approx \sqrt{r_2} \approx \sqrt{r}$. Substituting r_1 and r_2 [given before (4)] and (4), (9), and (10) into (3), we get

$$\begin{aligned}
 E_D = & \frac{|E_0|}{4\pi} \sqrt{\frac{d}{R}} \sqrt{\frac{\lambda}{r}} e^{-j(\pi/4 + \beta R)} e^{-j\beta r} \\
 & \times \left[\left(\sec \frac{\theta + \theta_0}{2} - \csc \frac{\theta_0 - \theta}{2} \right) \exp \left(-j\beta \frac{D}{2} \sin \theta \right) \right. \\
 & \left. - \left(\sec \frac{\theta_0 - \theta}{2} + \csc \frac{\theta_0 + \theta}{2} \right) \exp \left(+j\beta \frac{D}{2} \sin \theta \right) \right] \quad (11)
 \end{aligned}$$

which is accurate except for angles near the shadow boundaries. On the shadow boundary, the field from (12-6-10) is one-half the value of the field in the absence of the conducting strip. The total electric field is the sum of the geometric field and the diffracted field, i.e.,

$$E = E_G + E_D \quad (12)$$

where E_G is given by (12-8-9) or (12-8-6) and E_D by (11), as shown in Fig. 12-22. See also Fig. 14-48.

PROBLEMS

- * 12-1 A plane traveling wave in air with rms electric field $E = 100 \text{ mV m}^{-1}$ is incident normally on a large body of saltwater with constants $\sigma = 3 \text{ S m}^{-1}$, $\mu_r = 1$, $\epsilon_r = 80$. If the constants are independent of frequency, find the depths at which $E = 1 \mu\text{V m}^{-1}$ for frequencies of (a) 10 kHz, (b) 1 MHz, and (c) 100 MHz.
- * 12-2 A plane traveling wave in air (medium 1) with magnetic field H_1 is incident normally on the plane boundary of a large conducting medium (medium 2) with intrinsic impedance $10 + j10 \text{ m}\Omega$. (a) Calculate without approximation the magnitude of the magnetic field H_2 at the boundary in medium 2. (b) Compare this result with the approximation that $H_2 = 2H_1$ and determine the error involved in the approximation.
- * 12-3 Calculate the conductivity required for a sheet of space cloth ($Z_0 = 377 \Omega$ per square) which is 1 mm thick.
- * 12-4 A half-space of air (medium 1) and a half-space of dielectric (medium 2) are separated by a sheet of copper. A plane linearly polarized 2-GHz traveling wave in medium 1 (air) with electric field $E = 10 \text{ V m}^{-1}$ rms is incident normally on the copper sheet. The copper sheet has constants $\sigma = 58 \text{ M}\Omega \text{ m}^{-1}$ and $\mu_r = \epsilon_r = 1$, and it is $10 \mu\text{m}$ thick. The constants for medium 2 (dielectric) are $\sigma = 0$, $\mu_r = 1$, $\epsilon_r = 5$. Determine the rms value of (a) E just inside the copper sheet adjacent to medium 1 (air), (b) E just inside the copper sheet adjacent to medium 2 (dielectric), (c) E in medium 2 at a distance of 2 m from the copper sheet, and (d) H at same point as in (c).
- * 12-5 A large flat sheet of ferrous-dielectric material is backed by aluminum foil. At 500 MHz the constants of the ferrous-dielectric medium are $\mu_r = \epsilon_r = 6 - j6$. How thick must the sheet be for a 500-MHz wave (in air) incident on the sheet to be reduced upon reflection by 30 dB if the wave is incident normally. Take $\sigma = 0$.
- * 12-6 A linearly polarized plane traveling wave in air is incident at an angle θ_i on the flat surface of a dielectric medium of large extent. The constants of the dielectric medium are $\sigma = 0$, $\mu_r = 1$, $\epsilon_r = 8$. Calculate the magnitude of the reflected field E_r and the transmitted field E_t , relative to the incident field E_i as a function of θ_i when E_i is (a) parallel and (b) perpendicular to the plane of incidence. (c) Prepare graphs showing E_r/E_i and E_t/E_i as ordinates vs. θ_i as abscissa. (d) What value of θ_i is the Brewster angle?

* Answers to starred problems are given in Appendix C.

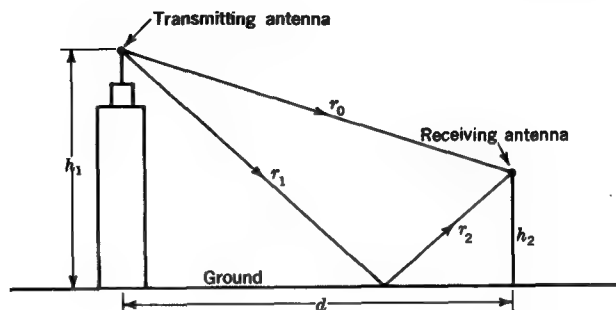


Fig. P12-10
Microwave circuit

12-7 (a) An *unpolarized* plane traveling wave in air is incident at an angle θ_i on the flat surface of a dielectric medium of large extent. The constants of the dielectric medium are $\sigma = 0$, $\mu_r = 1$, $\epsilon_r = 8$. Calculate the ratio of the transmitted Poynting vector S_t and the reflected Poynting vector S_r , relative to the incident Poynting vector S_i , as a function of θ_i . Prepare graphs showing S_t/S_i and S_r/S_i as ordinates vs. θ_i as abscissa. (b) Is there any angle for which the reflected or transmitted wave becomes (linearly) polarized?

12-8 (a) Repeat Prob. 12-7a with circumstances reversed, i.e., with the unpolarized wave originating in the dielectric medium. (b) Is there an angle or angles for which there is no transmitted wave?

12-9 (a) A 60-MHz radio transmitter which radiates isotropically is situated 20 m below the surface of a deep freshwater lake with constants $\mu_r = 1$, $\epsilon_r = 80 - j4$. If the power radiated is 100 W and the polarization is circular, what is the ratio of the power received per unit area at a radius of 1 km as a function of the zenith angle from 0 to 90° ? The radial distance is measured from a point on the water surface directly above the transmitter. Express the power ratio in decibels and plot this ratio as ordinate vs. zenith angle as abscissa. (b) Discuss the practical aspects of radio communication over such paths. (c) Compare the situation of this problem with transmission from the earth to an extraterrestrial point above the ionosphere (see Chap. 15).

12-10 (a) A typical microwave communication circuit for AM, FM, or TV between a transmitter on a tall building and a distant receiver involves two paths of transmission, one a direct path (length r_0) and one an indirect path with ground reflection (length $r_1 + r_2$), as suggested in Fig. P12-10. Let $h_1 = 300$ m and $d = 5$ km. For a frequency of 100 MHz calculate the ratio of the power received per unit area to the transmitted power as a function of the height h_2 of the receiving antenna. Plot these results in decibels as abscissa vs. h_2 as ordinate for three cases with transmitting and receiving antennas both (a) vertically polarized, (b) horizontally polarized, and (c) right circularly polarized for h_2 values from 0 to 100 m. Assume that the transmitting antenna is isotropic and that the receiving antennas are also isotropic and all have the same effective aperture. Consider that the ground is flat and perfectly conducting. (b) Compare the results for the three types of polarization and show

that circular polarization is best from the standpoint of both the noncriticalness of the height h_2 and of the absence of echo or ghost signals. Thus, for horizontal polarization the direct and ground-reflected waves may reinforce at a certain height h_2 (path-length difference equals an odd number of half wavelengths), but if this path-length difference yields delays of the order of microseconds, objectionable ghost images can appear on a TV screen. (c) Extend the comparison of (b) to consider the effect of other buildings or structures which may produce additional paths of transmission.

12-11 (a) Repeat Prob. 12-10 for the case where the ground has constants $\sigma = 0.0001 \text{ } \Omega \text{ m}^{-1}$, $\mu_r = 1$, $\epsilon_r = 5$. (b) What difference in effect does the ground have in the two cases?

12-12 When a radio wave of frequency f and wavelength λ traveling in air enters a denser medium, why does the wavelength change but not the frequency?

12-13 (a) Calculate the geometrical, diffraction, and total field of an infinite conducting strip of width $D = 5\lambda$ illuminated by an infinite line source at a spacing $d = 1\lambda$. See Figs. 12-21 and 12-22. (b) Repeat for $d = 5\lambda$.

12-14 When the moon occults (passes in front of) a distant celestial radio source, a Fresnel type of diffraction pattern is obtained, as in Fig. 12-12. (a) Calculate and plot the occultation pattern if the source subtends an angle of 8 seconds of arc. The wavelength is 1 m. Take the earth-moon distance as 380 Mm. (b) Repeat (a) for the case of a point source (zero subtended angle) and compare with the pattern for (a). Part (a) may be done as a convolution (see Kraus, "Radio Astronomy," pp. 194-198) or by superimposing the patterns of several point sources situated within an angle of 8 seconds of arc.

12-15 In Example 1 of Sec. 12-5 determine the axial ratio AR and the tilt angle τ of the polarization ellipse of the transmitted wave (a) for the conditions of the problem and (b) for the case where the angle of incidence is increased to the Brewster angle. (c) If the power density of the incident wave is 5 W m^{-2} what are the power densities of the reflected and transmitted waves for cases *a* and *b*?

12-16 A right circularly polarized wave of 10 W m^{-2} in air is incident at an angle of 50° from the normal to a flat dielectric slab of large extent. If $\epsilon_r = 5$ for the dielectric find the axial ratio AR, tilt angle τ , and power density for (a) the reflected wave and (b) the wave transmitted into the dielectric slab. (c) Repeat parts (a) and (b) if the angle of incidence is adjusted to the Brewster angle. (d) In parts (a) and (b), is the wave left- or right-handed?

12-17 Referring to the steps leading to (12-8-5) show that $r = r_0 + R + d \cos \theta$.

13

TRANSMISSION LINES, WAVEGUIDES, AND RESONATORS

13-1 INTRODUCTION

As discussed earlier, there is a close analogy between plane waves in unbounded media and guided waves on transmission lines. The subject of transmission lines is considered further in this chapter, and additional comparisons are made between waves in space and waves on transmission lines.

A *transmission line* may be defined as a device for transmitting or guiding energy from one point to another. Usually it is desired that the energy be conveyed with maximum efficiency, losses in heat or radiation being as small as possible.

Transmission lines may be of many forms and shapes. It will be convenient to classify transmission lines on the basis of the field configurations, or *modes*, which they can transmit. Thus transmission lines may be divided into two main groups: (1) those capable of transmitting transverse electromagnetic (TEM) modes and (2) those able to transmit only higher-order modes. In a TEM mode both the electric and the magnetic fields are entirely transverse to the direction of propagation. There is no component of either \mathbf{E} or \mathbf{H} in the direction of transmission. Higher-order modes, on the other hand, always have at least one field component in the direction of transmission. All two-conductor lines such as coaxial or two-wire transmission lines

are examples of TEM-mode types, while hollow single-conductor waveguides or dielectric rods are examples of higher mode types.

To summarize, transmission lines may be classified as follows:

- 1 TEM-mode type: \mathbf{E} and \mathbf{H} entirely transverse, e.g., all two-conductor types such as coaxial and two-wire lines
- 2 Higher mode type: \mathbf{E} or \mathbf{H} or both have components in the direction of transmission, e.g., hollow single-conductor waveguides and dielectric rods

In the above discussion we have used "transmission line" as a general, all-inclusive expression. In common present-day usage, however, "line" or "transmission line" is usually restricted to those devices which can transmit TEM modes, while "guide" or "waveguide" is employed for those devices which can transmit *only* higher-order modes.

13-2 COAXIAL, TWO-WIRE, AND INFINITE-PLANE TRANSMISSION LINES

The most common forms of TEM-mode transmission lines are the coaxial and two-wire types. Many other forms, in fact an infinite variety of them, are also possible. However, all may be regarded as derived from a basic or parent form. Thus let us consider the infinite-parallel-plane transmission line as the basic two-conductor type. This type consists of two parallel-plane conducting sheets of infinite extent. A cross section through such a line is shown in Fig. 13-1a. Considering only a TEM wave, \mathbf{E} is everywhere normal and \mathbf{H} everywhere parallel to the sheets.

An approximation to the infinite-parallel-plane transmission line is provided by the parallel-strip line shown in perspective in Fig. 13-1b. Here the sheets have been reduced to form long parallel strips of width b . A cross section of this line is portrayed by Fig. 13-1c. In the region between the strips \mathbf{E} and \mathbf{H} are oriented the same as for the infinite-sheet line. However, \mathbf{E} and \mathbf{H} also extend outside the region between the strips, the \mathbf{H} lines forming loops that enclose each strip.

Now let the strips of the line of Fig. 13-1c be curved away from each other at the edges, as suggested by Fig. 13-1d. Continuing this process, we end up with the two-conductor transmission line shown in Fig. 13-1e.

As another variation, let the strips of the line of Fig. 13-1c be bent in the same direction, as suggested in Fig. 13-1f. Continuing this process, we arrive at the coaxial transmission line portrayed in Fig. 13-1g.

Thus we may regard both the two-wire transmission line (Fig. 13-1e) and the coaxial line (Fig. 13-1g) as forms that can be derived from the parallel-plane type.

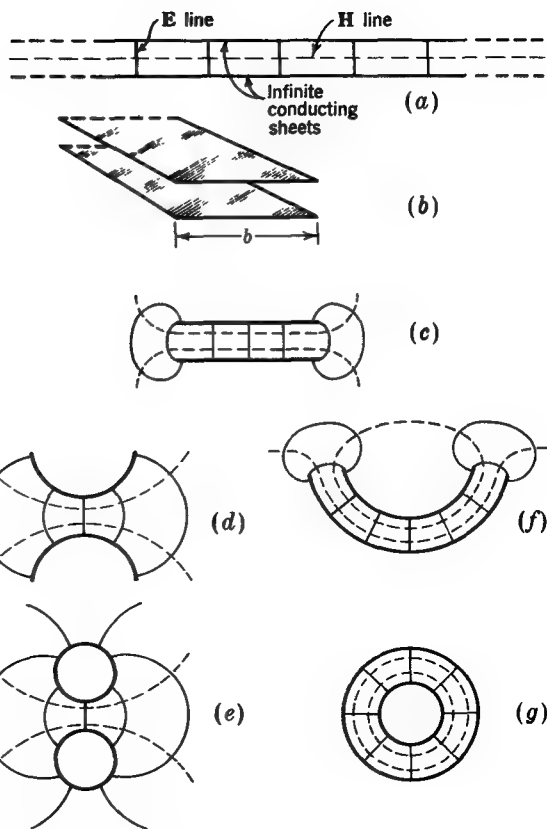


FIGURE 13-1
Evolution of two-wire and coaxial transmission lines from infinite-parallel-plane type by means of transitional forms.

In the first part of this chapter the properties of two-conductor transmission lines are developed by an extension of ordinary circuit theory to take into account the finite velocity of propagation along the line, and comparisons are made with corresponding relations for plane waves in space. The development applies to *coaxial*, *two-wire*, or any *two-conductor type* of transmission line carrying only TEM waves. Next higher-order mode transmission is considered on a *two-conductor infinite parallel-plane transmission line*. This leads logically to wave transmission in a *closed rectangular pipe*, or *waveguide*. Closed hollow guides of circular and other cross section are also discussed. Guiding waves by *open surfaces* is then considered. The remainder of the chapter deals with resonators, in particular the *cavity resonator*.

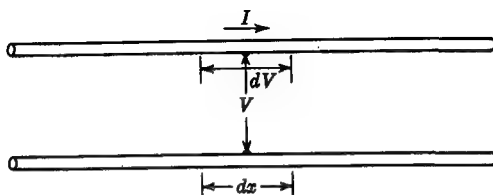


FIGURE 13-2
Two-wire transmission line.

13-3 THE INFINITE UNIFORM TRANSMISSION LINE

Consider the uniform two-wire transmission line shown in Fig. 13-2. In earlier chapters expressions were developed for the capacitance and inductance per unit length of such a line. If the line is not lossless, it will also have a series resistance and a shunt conductance that may need to be considered. The net effect of the series resistance and inductance can be expressed by the *series impedance* Z per unit length. Thus†

$$Z = R + j\omega L = R + jX \quad (\Omega \text{ m}^{-1}) \quad (1)$$

where R = series resistance, $\Omega \text{ m}^{-1}$

L = series inductance, H m^{-1}

ω = radian frequency $= 2\pi f$, s^{-1}

X = series reactance, $\Omega \text{ m}^{-1}$

The net effect of the shunt conductance and capacitance is expressed by the *shunt admittance* Y per unit length. Thus

$$Y = G + j\omega C = G + jB \quad (\text{S m}^{-1}) \quad (2)$$

where G = shunt conductance, S m^{-1}

C = shunt capacitance, F m^{-1}

ω = radian frequency $= 2\pi f$, s^{-1}

B = shunt susceptance, S m^{-1}

Consider now an infinitesimal section dx of the line, and let a harmonically varying wave be present on the line. Let the voltage across the line be V and the current through the line be I (Fig. 13-2). The voltage change dV over the length of the section dx is equal to the IZ change per unit length multiplied by the length of the section, or $dV = IZ dx$ where I is the line current. Thus

$$\frac{dV}{dx} = IZ \quad (3)$$

The change in current dI between the ends of the section dx is equal to the shunt current YY flowing across the line from one wire to the other, multiplied by the length of the section, or $dI = YY dx$ where V is the voltage across the line. Thus

$$\frac{dI}{dx} = YY \quad (4)$$

† Note that here R , G , X , B , L , C , Z , and Y are *distributed quantities*, i.e., per unit length.

Differentiating (3) and (4) with respect to x , we obtain

$$\frac{d^2V}{dx^2} = I \frac{dZ}{dx} + Z \frac{dI}{dx} = I \frac{dZ}{dx} + ZVY \quad (5)$$

$$\frac{d^2I}{dx^2} = V \frac{dY}{dx} + Y \frac{dV}{dx} = V \frac{dY}{dx} + YIZ \quad (6)$$

On a uniform line Z and Y are independent of x (do not vary along the line), and so dZ/dx and dY/dx are zero.[†] Thus, for a *uniform* line (5) and (6) reduce to

$$\boxed{\frac{d^2V}{dx^2} - ZVY = 0} \quad (7)$$

and

$$\boxed{\frac{d^2I}{dx^2} - ZVI = 0} \quad (8)$$

Equations (7) and (8) are the basic differential equations, or wave equations, for a uniform transmission line. In mathematical terminology they are linear differential equations of the second order with constant coefficients. They are the most general way of expressing the natural law relating the variation of voltage and current with distance along a uniform transmission line. However, they tell us nothing specifically about the voltage or current distribution on a particular transmission line. For this we must first obtain a solution appropriate to the imposed conditions. As a trial solution of (7) let us substitute

$$V = e^{rx} \quad (9)$$

[†] For a nonuniform (tapered) transmission line the terms with dZ/dx and dY/dx must be retained. From (3)

$$I = \frac{1}{Z} \frac{dV}{dx} \quad (6a)$$

so that the first term on the right side of (5) can be written

$$I \frac{dZ}{dx} = \frac{1}{Z} \frac{dZ}{dx} \frac{dV}{dx} = \frac{d(\ln Z)}{dx} \frac{dV}{dx} \quad (6b)$$

Substituting (6b) in (5) gives

$$\frac{d^2V}{dx^2} - \frac{d(\ln Z)}{dx} \frac{dV}{dx} - ZVY = 0 \quad (6c)$$

In a like manner (6) becomes

$$\frac{d^2I}{dx^2} - \frac{d(\ln Y)}{dx} \frac{dI}{dx} - ZVI = 0 \quad (6d)$$

Equations (6c) and (6d) are basic differential equations for a *nonuniform* transmission line. For a uniform line they reduce to (7) and (8).

from which

$$\frac{d^2V}{dx^2} = \gamma^2 e^{\gamma x} = \gamma^2 V \quad (10)$$

Thus, (7) becomes

$$(\gamma^2 - ZY)e^{\gamma x} = 0 \quad (11)$$

and $\gamma^2 - ZY = 0 \quad (12)$

Equation (12), known as the *auxiliary equation*, has two unequal roots $+\sqrt{ZY}$ and $-\sqrt{ZY}$, so that the general solution for (7) is

$$V = C_1 \exp(\sqrt{ZY}x) + C_2 \exp(-\sqrt{ZY}x) \quad (13)$$

where C_1 and C_2 are constants. Thus (9) is a solution provided $\gamma = \pm\sqrt{YZ}$.

If (8) is solved in the same fashion as (7), we obtain a solution for I similar in form to (13) but having two more constants. Instead of solving for I in this manner, let us proceed along another avenue of approach and obtain a solution for I from (13). To do this, let (13) be differentiated with respect to x . Recalling also (3), we obtain

$$\frac{dV}{dx} = C_1 \sqrt{ZY} \exp(\sqrt{ZY}x) - C_2 \sqrt{ZY} \exp(-\sqrt{ZY}x) = IZ \quad (14)$$

from which it follows that

$$I = \frac{C_1}{\sqrt{ZY}} \exp(\sqrt{ZY}x) - \frac{C_2}{\sqrt{ZY}} \exp(-\sqrt{ZY}x) \quad (15)$$

This is a solution for the current. To evaluate the constants, we note from (13) that when $x = 0$,

$$V = C_1 + C_2 \quad (16)$$

where V is the instantaneous voltage at the point $x = 0$ on the line. We may regard this voltage as the sum of two voltages which, in general, are unequal in amplitude and vary harmonically with time. Let V_1 and V_2 be the amplitudes of the voltages. The quantities C_1 and C_2 are constants with respect to x but may be regarded as variables with respect to time. Thus we can put $C_1 = V_1 e^{j\omega t}$ and $C_2 = V_2 e^{j\omega t}$. Substituting these into (13) and (15) yields

$$V = V_1 e^{j\omega t} \exp(\sqrt{ZY}x) + V_2 e^{j\omega t} \exp(-\sqrt{ZY}x) \quad (17)$$

and $I = \frac{V_1 e^{j\omega t}}{\sqrt{ZY}} \exp(\sqrt{ZY}x) - \frac{V_2 e^{j\omega t}}{\sqrt{ZY}} \exp(-\sqrt{ZY}x) \quad (18)$

The quantity $\sqrt{ZY} = \gamma$ is called the *propagation constant*. In general it is complex, with a real part α called the *attenuation constant* and an imaginary part β called the *phase constant*. Thus

$$\gamma = \sqrt{ZY} = \alpha + j\beta \quad (19)$$

or

$$\alpha = \operatorname{Re} \sqrt{ZY} \quad (20)$$

and

$$\beta = \operatorname{Im} \sqrt{ZY} \quad (21)$$

Introducing (19) into (17) and (18) and rearranging, we obtain

$$V = V_1 e^{\alpha x} e^{j(\omega t + \beta x)} + V_2 e^{-\alpha x} e^{j(\omega t - \beta x)} \quad (22)$$

and

$$I = \frac{V_1}{\sqrt{ZY}} e^{\alpha x} e^{j(\omega t + \beta x)} - \frac{V_2}{\sqrt{ZY}} e^{-\alpha x} e^{j(\omega t - \beta x)} \quad (23)$$

Equation (22) is the solution for the voltage on the transmission line. The solution has two terms. The first term, involving $\omega t + \beta x$, represents a wave traveling in the *negative x* direction along the line. The magnitude of this wave at $x = 0$ and $t = 0$ is V_1 , and the factor $e^{\alpha x}$ indicates that this wave decreases in magnitude as it proceeds in the negative x direction. The second term, involving $\omega t - \beta x$, represents a wave traveling in the *positive x* direction along the line. The magnitude of this wave at $x = 0$ and $t = 0$ is V_2 , and the factor $e^{-\alpha x}$ indicates that this wave decreases in magnitude as it proceeds in the positive x direction. The factors $e^{\alpha x}$ and $e^{-\alpha x}$ are *attenuation factors*, α being the *attenuation constant*. The factors $e^{j(\omega t + \beta x)}$ and $e^{j(\omega t - \beta x)}$ are *phase factors*, β being the *phase constant*.

The solution for I in (23) also has two terms, the first term representing a current wave traveling in the negative x direction and the second term a current wave traveling in the positive x direction. The total current at any point is the resultant of the two traveling-wave components.

Confining our attention now to a single wave traveling in the negative x direction as represented by the first terms of (22) and (23), we note that V and I are identical functions of x and t . The amplitudes differ. Taking the ratio of the voltage V across the line to the current I through the line for a single traveling wave, we obtain the impedance Z_0 , which is called the *characteristic, or surge, impedance* of the line.

That is,

$$\frac{V}{I} = \sqrt{\frac{Z}{Y}} = Z_0 \quad (\Omega) \quad (24)$$

This impedance is a function of the series impedance Z per unit length and shunt admittance Y per unit length. Expanding Z and Y as in (1) and (2), we obtain, from (24),

$$Z_0 = \sqrt{\frac{R + j\omega L}{G + j\omega C}} \quad (\Omega) \quad (25)$$

When R and G are small or when the frequency is large, so that $\omega L \gg R$ and $\omega C \gg G$, (25) reduces to

$$Z_0 = \sqrt{\frac{L}{C}} \quad (\Omega) \quad (26)$$

where Z_0 = characteristic impedance, Ω

L = series inductance, $H m^{-1}$

C = shunt capacitance, $F m^{-1}$

In (26) Z_0 is entirely real, or resistive, so that in this case we may, to be explicit, speak of the *characteristic resistance* R_0 of the line. That is, for this case

$$Z_0 = \sqrt{\frac{L}{C}} = R_0 \quad (\Omega) \quad (27)$$

In general, when R and G cannot be neglected, Z_0 is complex and the term characteristic impedance, should be used. However, if R and G are negligible, Z_0 is real ($= R_0$) and the term characteristic resistance may be used.

When R and G are small, but not negligible, (25) may be reexpressed approximately in the following form:

$$Z_0 = \sqrt{\frac{L}{C}} \left[1 + j \left(\frac{G}{2\omega C} - \frac{R}{2\omega L} \right) \right] \quad (28)$$

Thus Z_0 for this case is, in general, complex. However, if

$$\frac{G}{C} = \frac{R}{L} \quad (29)$$

Z_0 is real. This situation is *Heaviside's condition* for a distortionless line.

Table 13-1 CHARACTERISTIC IMPEDANCE OF TRANSMISSION LINES

Condition	Characteristic impedance, Ω
General case	$Z_0 = \sqrt{\frac{Z}{Y}} = \sqrt{\frac{R + j\omega L}{G + j\omega C}}$
Small losses	$Z_0 = \sqrt{\frac{L}{C}} \left[1 + j \left(\frac{G}{2\omega C} - \frac{R}{2\omega L} \right) \right]$
Lossless case, $R = 0, G = 0$	$Z_0 = \sqrt{\frac{L}{C}} = R_0$

The relations developed above for the characteristic impedance of a uniform transmission line are summarized in Table 13-1.

The phase velocity v of a wave traveling on the line is given by ω/β . That is,

$$v = \frac{\omega}{\beta} = \frac{\omega}{\text{Im } \gamma} = \frac{\omega}{\text{Im } \sqrt{ZY}} \quad (30)$$

If the line is lossless or $R \ll \omega L$ and $G \ll \omega C$,

$$v = \frac{\omega}{\omega \sqrt{LC}} = \frac{1}{\sqrt{LC}} \quad (\text{m s}^{-1}) \quad (31)$$

where L = series inductance, H m^{-1}

C = shunt capacitance, F m^{-1}

13-4 COMPARISON OF CIRCUIT AND FIELD QUANTITIES

It is interesting to compare some of the relations for transmission lines developed in the preceding section with corresponding relations for waves developed in earlier chapters. For example, consider the transmission-line equations

$$\frac{dV}{dx} = ZI = (R + j\omega L)I \quad (\text{V m}^{-1}) \quad (1)$$

and $\frac{dI}{dx} = YV = (G + j\omega C)V \quad (\text{A m}^{-1}) \quad (2)$

The corresponding relations for a plane wave traveling in the x direction with \mathbf{E} in the y direction, as obtained from Maxwell's two curl equations, are

$$\frac{dE_y}{dx} = -j\omega\mu H_z \quad (\text{V m}^{-2}) \quad (3)$$

and

$$\frac{dH_z}{dx} = -(\sigma + j\omega\epsilon)E_y \quad (\text{A m}^{-2}) \quad (4)$$

In these relations harmonic variation with time is assumed, and the differentiations with respect to time have been performed,

Comparing (1) with (3), we note that $j\omega\mu$ in the wave case corresponds to $Z = R + j\omega L$ for the line. Comparing (2) with (4), we see that $\sigma + j\omega\epsilon$ for the wave corresponds to $Y = G + j\omega C$ for the line.

Further comparisons of the circuit relations used for lines and the field relations employed for waves are made in Table 13-2. The first column gives the circuit quantity and the last column the corresponding field quantity. The center column indicates the SI units, which are the same for corresponding circuit and field relations.

Table 13-2 COMPARISON OF CIRCUIT AND FIELD RELATIONS

Circuit relation for transmission line	SI units	Field relation for space wave
$Z = R + j\omega L$	$\Omega \text{ m}^{-1}$	$j\omega\mu$
$Y = G + j\omega C$	S m^{-1}	$\sigma + j\omega\epsilon$
Characteristic impedance = $\sqrt{\frac{L}{C}}$	Ω	Intrinsic impedance = $\sqrt{\frac{\mu}{\epsilon}}$
Velocity = $\frac{1}{\sqrt{LC}}$	m s^{-1}	Velocity = $\frac{1}{\sqrt{\mu\epsilon}}$
Series inductance = L	H m^{-1}	Permeability = μ
Shunt capacitance = C	F m^{-1}	Permittivity = ϵ
Voltage = $\frac{V}{x}$	V m^{-1}	Electric field = \mathbf{E}
Current = $\frac{I}{x}$	A m^{-1}	Magnetic field = \mathbf{H}

13-5 CHARACTERISTIC-IMPEDANCE DETERMINATIONS

The correspondence of L to μ and C to ϵ (see Table 13-2) is of particular interest. Thus, if space is divided up into transmission-line cells, μ is the series inductance per unit length (or depth) of a cell, while ϵ is the shunt capacitance per unit length (or depth) of a cell.

The transmission-line-cell concept (see Secs. 5-17 and 10-9) is of considerable value in connection with the determination of the characteristic impedance of lossless transmission lines operating in the TEM mode. For instance, consider the transmission line portrayed in Fig. 13-3. Let the space between the conductors be divided into curvilinear squares by graphical field-mapping methods. Each square represents the end of a transmission-line cell of characteristic impedance $Z'_0 = \sqrt{\mu/\epsilon}$. Then, the characteristic impedance of the line is given by

$$Z_0 = \frac{N}{n} Z'_0 \quad (\Omega) \quad (1)$$

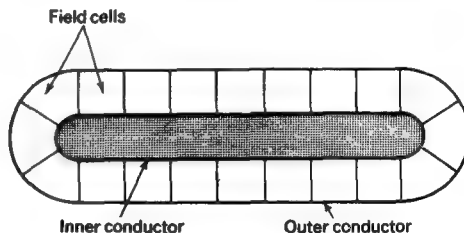
where N = number of cells in series

n = number of cells in parallel

Z'_0 = characteristic impedance of one cell ($= \sqrt{\mu/\epsilon}$, where μ is permeability and ϵ is permittivity of medium filling line)

This method may be applied to two-conductor transmission lines of any shape. The characteristics of lossless high-frequency lines of any shape can also be obtained by a simple dc measurement. For example, if we wish to find the inductance or capacitance per unit length or the characteristic impedance (or resistance) of the line shown in Fig. 13-3 by this method, the conductor cross section is drawn to scale† with conducting paint (such as silver paint) on a sheet of resistance (Teledeltos) paper of uniform resistance R_s per square, as suggested in Fig. 13-4. Then by connecting the

FIGURE 13-3
Coaxial transmission line of noncircular cross section divided into curvilinear squares.



† Since only the shape is important, the cross section may be scaled to any convenient size.

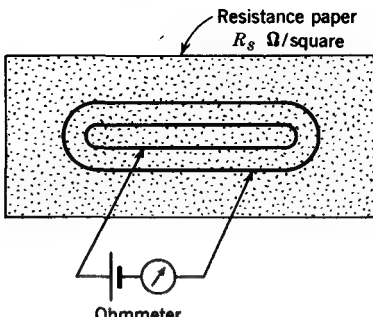


FIGURE 13-4
Determination of characteristic impedance of transmission line by simple dc measurement.

terminals of an ohmmeter to the inner and outer conductors, as indicated, a dc resistance R_m is measured.[†]

Since $R_m = (N/n) R_s$ and $R_m/R_s = N/n$ it follows that

$$L = \mu \frac{R_m}{R_s} \quad (\text{H m}^{-1}) \quad (2a)$$

$$C = \epsilon \frac{R_s}{R_m} \quad (\text{F m}^{-1}) \quad (2b)$$

$$Z_0 = \sqrt{\frac{\mu}{\epsilon}} \frac{R_m}{R_s} \quad (\Omega) \quad (2c)$$

Thus, if the line is air-filled, $\sqrt{\mu/\epsilon} = \sqrt{\mu_0/\epsilon_0} = 376.7 \Omega$ and (2c) becomes

$$Z_0 = \frac{376.7}{R_s} R_m \quad (\Omega) \quad (3)$$

Hence, if "space paper" ($R_s = 376.7 \Omega$ per square) is used

$$Z_0 = R_m \quad (\Omega) \quad (4)$$

and the ohmmeter reads directly the characteristic impedance of the line.

EXAMPLE 1 Find the characteristic impedance (or resistance) of the lossless coaxial line shown in Fig. 13-5. The line is air-filled.

SOLUTION Dividing the space between the conductors into curvilinear squares or cells by graphical field mapping, we obtain a total of 18.3 squares in parallel and 2 in series.

[†] Supposing that the resistance paper between the conductors were marked off in curvilinear squares, R_m would be given by $R_m = (N/n)R_s$, where N = number of squares in series, n = number of squares in parallel, and R_s = resistance per square, i.e., resistance of one square.

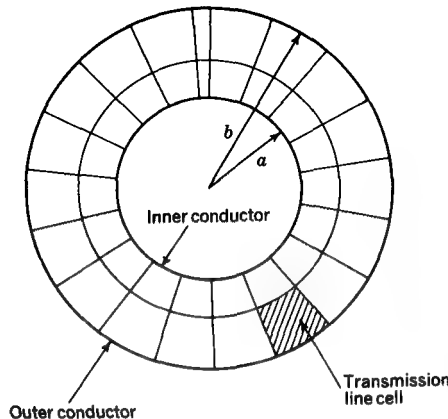


FIGURE 13-5
Coaxial transmission line with 18.3 transmission-line cells in parallel and 2 in series.

The characteristic impedance of each cell is 376.7Ω . Hence, from (1), the characteristic impedance of the line of Fig. 13-5 is

$$Z_0 = \frac{N}{n} Z'_0 = \frac{2}{18.3} 376.7 = 41.2 \Omega$$

If a cross section of this line is drawn to scale with conducting paint on a sheet of space paper 41.2Ω would be measured directly on an ohmmeter connected between the inner and outer conductors.

When this resistance-measurement method is applied to open types of line such as a two-wire line, the sheet of resistance material should extend out to a distance that is large compared with the line cross section if accurate results are to be obtained.

Although graphical, analog-computer, and digital-computer methods can be applied to two-conductor lines of any shape, some configurations yield to a simple calculation. Thus, for the case under consideration, where the characteristic impedance

$$Z_0 = \sqrt{\frac{L}{C}} \quad (\Omega) \quad (5)$$

the value of Z_0 can be determined by a knowledge of L and C for the line. Thus, obtaining L from (5-13-8) and C from (3-18-2), the characteristic impedance of a coaxial line (as in Fig. 13-5) is given by

$$Z_0 = \frac{1}{2\pi} \sqrt{\frac{\mu}{\epsilon} \ln \frac{b}{a}} = 0.367 \sqrt{\frac{\mu}{\epsilon} \log \frac{b}{a}} \quad (\Omega) \quad (6)$$

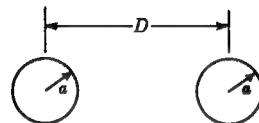


FIGURE 13-6
Two-wire transmission line.

If there is no ferromagnetic material present, $\mu = \mu_0$ and (6) reduces to

$$Z_0 = \frac{138}{\sqrt{\epsilon_r}} \log \frac{b}{a} \quad (\Omega) \quad (7)$$

where ϵ_r = relative permittivity of medium filling line

a = outside radius of inner conductor

b = inside radius of outer conductor

For an air-filled line $\epsilon_r = 1$, and (7) becomes

$$Z_0 = 138 \log \frac{b}{a} \quad (\Omega) \quad (8)$$

EXAMPLE 2 The air-filled coaxial line in Fig. 13-5 has a radius ratio $b/a = 2$. Find its characteristic impedance.

SOLUTION From (8)

$$Z_0 = 138 \log 2 = 41.4 \Omega$$

The value obtained previously by graphical methods agrees well with this exact value.

In a similar way, the characteristic impedance can be obtained for a *two-wire line*, as in Fig. 13-6. Thus, if $D \gg a$, we have

$$Z_0 = \frac{1}{\pi} \sqrt{\frac{\mu}{\epsilon}} \ln \frac{D}{a} = 0.73 \sqrt{\frac{\mu}{\epsilon}} \log \frac{D}{a} \quad (\Omega) \quad (9)$$

If there is no ferromagnetic material present, $\mu = \mu_0$ and (9) reduces to

$$Z_0 = \frac{276}{\sqrt{\epsilon_r}} \log \frac{D}{a} \quad (\Omega) \quad (10)$$

where ϵ_r = relative permittivity of medium

D = center-to-center spacing (see Fig. 13-6)

a = radius of conductor (in same units as D)

If the medium is air, $\epsilon_r = 1$ and (10) becomes

$$Z_0 = 276 \log \frac{D}{a} \quad (\Omega) \quad (11)$$

The characteristic impedances obtained above are summarized in Table 13-3.

Table 13-3 CHARACTERISTIC IMPEDANCE OF COAXIAL AND TWO-WIRE LINES

Type of line	Characteristic impedance, Ω
Coaxial (filled with medium of relative permittivity ϵ_r)	$Z_0 = \frac{138}{\sqrt{\epsilon_r}} \log \frac{b}{a}$ (see Fig. 13-5)
Coaxial (air-filled)	$Z_0 = 138 \log \frac{b}{a}$ (see Fig. 13-5)
Two-wire (in medium of relative permittivity ϵ_r) ($D \gg a$)	$Z_0 = \frac{276}{\sqrt{\epsilon_r}} \log \frac{D}{a}$ (see Fig. 13-6)
Two-wire (in air) ($D \gg a$)	$Z_0 = 276 \log \frac{D}{a}$ (see Fig. 13-6)

It is assumed throughout this section that the line is lossless (or $R \ll \omega L$ and $G \ll \omega C$) and also that the currents are confined to the conductor surfaces to which the radii refer. This condition is approximated at high frequencies owing to the small depth of penetration. This condition may also be approximated at low frequencies by the use of thin-walled tubes. It is also assumed that the lines are operating in the TEM mode.

13-6 THE TERMINATED UNIFORM TRANSMISSION LINE

In Sec. 13-3 the line was considered to be of infinite length. Let us now analyze the situation where a line of characteristic impedance Z_0 is terminated in a load impedance Z_L , as in Fig. 13-7. The load is at $x = 0$, and positive distance x is measured to the left along the line. The total voltage and total current are expressed as the resultant of two traveling waves moving in opposite directions as on an infinite transmission line. However, on the terminated line the wave to the right may be regarded as the incident wave and the wave to the left as the reflected wave, with the reflected wave related to the incident wave by the load impedance Z_L .

At a point on the line at a distance x from the load let the voltage between the wires and the current through one wire due to the incident wave traveling to the right be designated \dot{V}_0 and \dot{I}_0 , respectively. Let \dot{V}_1 and \dot{I}_1 be the voltage and current due to the wave traveling to the left that is reflected from the load. The resultant voltage

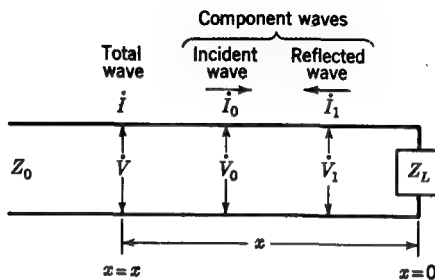


FIGURE 13-7
Terminated transmission line.

\dot{V} at a point on the line is equal to the sum of the voltages \dot{V}_0 and \dot{V}_1 at the point. That is,

$$\dot{V} = \dot{V}_0 + \dot{V}_1 \quad (1)$$

where $\dot{V}_0 = V_0 e^{j\omega t}$ (the factor $e^{j\omega t}$ is understood to be present)

$\dot{V}_1 = V_1 e^{-jx+j\xi}$ (the factor $e^{j\omega t}$ is understood to be present)

γ = propagation constant $= \alpha + j\beta$

ξ = phase shift at load

At the load ($x = 0$) we have $\dot{V}_0 = V_0$ and $\dot{V}_1 = V_1 e^{j\xi} = V_1 \angle \xi$, so that *at the load*

$$\boxed{\frac{\dot{V}_1}{\dot{V}_0} = \frac{V_1}{V_0} \angle \xi = \rho_v} \quad (2)$$

where ρ_v is the *reflection coefficient for voltage* (dimensionless). It follows that

$$\dot{V} = V_0 (e^{jx} + \rho_v e^{-jx}) \quad (3)$$

The resultant current \dot{I} at a point on the line is equal to the sum of the currents \dot{I}_0 and \dot{I}_1 at the point. That is,

$$\dot{I} = \dot{I}_0 + \dot{I}_1 \quad (4)$$

where $\dot{I}_0 = I_0 e^{jx-j\delta}$

$\dot{I}_1 = I_1 e^{-jx+j(\xi-\delta)}$

δ = phase difference between current and voltage

At the load

$$\boxed{\frac{\dot{I}_1}{\dot{I}_0} = \frac{I_1}{I_0} \angle \xi = \rho_i} \quad (5)$$

where ρ_i is the *reflection coefficient for current* (dimensionless). It follows that

$$\dot{I} = I_0 e^{-j\delta} (e^{jx} + \rho_i e^{-jx}) \quad (6)$$

Now $\dot{\rho}_v$ and $\dot{\rho}_i$ may be expressed in terms of the characteristic impedance Z_0 and the load impedance Z_L .[†] Thus we note that at any point on the line

$$Z_0 = \frac{\dot{V}_0}{\dot{I}_0} = \frac{V_0}{I_0} / \underline{\delta} = - \frac{\dot{V}_1}{\dot{I}_1} = - \frac{V_1}{I_1} / \underline{\delta} \quad (7)$$

while at the load ($x = 0$)

$$Z_L = \frac{\dot{V}}{\dot{I}} \quad (8)$$

It follows from (4) that at the load

$$\frac{\dot{V}}{Z_L} = \frac{\dot{V}_0}{Z_0} - \frac{\dot{V}_1}{Z_0} = \frac{\dot{V}_0 - \dot{V}_1}{Z_0} \quad (9)$$

But $\dot{V} = \dot{V}_0 + \dot{V}_1$; so we have

$$\frac{\dot{V}_0 + \dot{V}_1}{Z_L} = \frac{\dot{V}_0 - \dot{V}_1}{Z_0} \quad (10)$$

Solving for \dot{V}_1/\dot{V}_0 yields

$$\boxed{\frac{\dot{V}_1}{\dot{V}_0} = \frac{Z_L - Z_0}{Z_L + Z_0} = \dot{\rho}_v} \quad (11)$$

For real load impedances Z_L ranging from 0 to ∞ , $\dot{\rho}_v$ ranges from -1 to +1 in value.

In a similar way it can be shown that

$$\dot{\rho}_i = - \frac{Z_L - Z_0}{Z_L + Z_0} = - \dot{\rho}_v \quad (12)$$

The ratio \dot{V}/\dot{I} at any point x on the line gives the impedance Z_x at the point looking toward the load. Taking this ratio and introducing the relation (12) in (6) for \dot{I} , we obtain

$$Z_x = \frac{\dot{V}}{\dot{I}} = \frac{V_0}{I_0} / \underline{\delta} \frac{\frac{e^{\gamma x} + \dot{\rho}_v e^{-\gamma x}}{e^{\gamma x} - \dot{\rho}_v e^{-\gamma x}}}{\underline{\delta}} \quad (13)$$

Noting (7) and (11), we can reexpress this as

$$\boxed{Z_x = Z_0 \frac{Z_L + Z_0 \tanh \gamma x}{Z_0 + Z_L \tanh \gamma x} \quad (\Omega)} \quad (14)$$

[†] Although the impedances Z_L and Z_0 are (in general) also complex quantities, the dot over the letter will, for simplicity, be omitted. If it becomes necessary to indicate the absolute value, or modulus, of Z_L , this will be done by the use of bars (thus the absolute value of Z_L equals $|Z_L| = \sqrt{R_L^2 + X_L^2}$).

where Z_x = impedance at distance x looking toward load, Ω

Z_0 = characteristic impedance of line, Ω

Z_L = load impedance, Ω

γ = propagation constant $= \alpha + j\beta$, m^{-1}

x = distance from load, m

This is the general expression for the impedance Z_x at a distance x from the load.

If the line is open-circuited, $Z_L = \infty$ and (14) reduces to

$$Z_x = \frac{Z_0}{\tanh \gamma x} = Z_0 \coth \gamma x \quad (15)$$

If the line is short-circuited, $Z_L = 0$ and (14) reduces to

$$Z_x = Z_0 \tanh \gamma x \quad (16)$$

It is to be noted that, in general, γ is complex ($= \alpha + j\beta$). Thus

$$\tanh \gamma x = \frac{\sinh \alpha x \cos \beta x + j \cosh \alpha x \sin \beta x}{\cosh \alpha x \cos \beta x + j \sinh \alpha x \sin \beta x} \quad (17)$$

or

$$\tanh \gamma x = \frac{\tanh \alpha x + j \tan \beta x}{1 + j \tanh \alpha x \tan \beta x} \quad (18)$$

Note that the product of the impedance of the line when it is open-circuited and when it is short-circuited equals the square of the characteristic impedance, i.e.,

$$Z_0^2 = Z_{oc} Z_{sc} \quad (19)$$

where $Z_{oc} = Z_x$ for open-circuited line ($Z_L = \infty$)

$Z_{sc} = Z_x$ for short-circuited line ($Z_L = 0$)

If the line is *lossless* ($\alpha = 0$), the above relations reduce to the following:
In general,

$$Z_x = Z_0 \frac{Z_L + jZ_0 \tan \beta x}{Z_0 + jZ_L \tan \beta x} \quad (20)$$

When the line is *open-circuited* ($Z_L = \infty$),

$$Z_x = \frac{Z_0}{j \tan \beta x} = -jZ_0 \cot \beta x \quad (21)$$

When the line is *short-circuited* ($Z_L = 0$),

$$Z_x = jZ_0 \tan \beta x \quad (22)$$

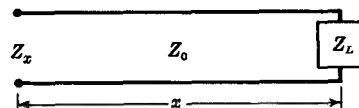


FIGURE 13-8
Terminated transmission line.

We note that (19) is also fulfilled on the lossless line. Furthermore, the impedance for an open- or short-circuited lossless line is a pure reactance.

The impedance relations developed above apply to all uniform two-conductor lines, such as coaxial and two-wire lines. They give the input impedance Z_x of a uniform transmission line of length x and characteristic impedance Z_0 terminated in a load Z_L (see Fig. 13-8). These relations are summarized in Table 13-4.

On a lossless line the *voltage standing-wave ratio* (VSWR) is given by

$$\boxed{\text{VSWR} = \frac{V_{\max}}{V_{\min}} = \frac{I_{\max}}{I_{\min}}} \quad (23)$$

It follows that

$$\text{VSWR} = \frac{V_0 + V_1}{V_0 - V_1} = \frac{1 + (V_1/V_0)}{1 - (V_1/V_0)} \quad (24)$$

But

$$\frac{V_1}{V_0} = |\dot{\rho}_v| \quad (25)$$

and so

$$\boxed{\text{VSWR} = \frac{1 + |\dot{\rho}_v|}{1 - |\dot{\rho}_v|}} \quad (26)$$

Table 13-4 INPUT IMPEDANCE OF TERMINATED TRANSMISSION LINE†

Load condition	General case ($\alpha \neq 0$)	Lossless case ($\alpha = 0$)
Any value of load Z_L	$Z_x = Z_0 \frac{Z_L + Z_0 \tan \gamma x}{Z_0 + Z_L \tanh \gamma x}$	$Z_x = Z_0 \frac{Z_L + jZ_0 \tan \beta x}{Z_0 + jZ_L \tan \beta x}$
Open-circuited line ($Z_L = \infty$)	$Z_x = Z_0 \coth \gamma x$	$Z_x = -jZ_0 \cot \beta x$
Short-circuited line ($Z_L = 0$)	$Z_x = Z_0 \tanh \gamma x$	$Z_x = jZ_0 \tan \beta x$

† $\gamma = \alpha + j\beta$, where α = attenuation constant in nepers per meter and $\beta = 2\pi/\lambda$ = phase constant in radians per meter, where λ is the wavelength.

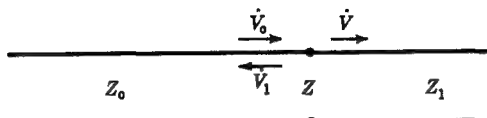


FIGURE 13-9

Junction of transmission lines of different characteristic impedance.

where ρ_v is the reflection coefficient for voltage. This relation is identical with that given by (10-10-16) for the VSWR of plane waves. Solving (26) for the magnitude of the reflection coefficient gives

$$|\rho_v| = \frac{\text{VSWR} - 1}{\text{VSWR} + 1} \quad (27)$$

It is often of interest to know the voltage \dot{V} at the load in terms of the voltage \dot{V}_0 of the incident wave. This is given by the *transmission coefficient for voltage* t_v . That is, at the load

$$\dot{V} = t_v \dot{V}_0 \quad \text{or} \quad t_v = \frac{\dot{V}}{\dot{V}_0} \quad (28)$$

The load impedance may be a lumped element, as suggested in Fig. 13-7 or Fig. 13-8, or it may be the impedance presented by another line of characteristic impedance Z_1 , as suggested in Fig. 13-9. In the latter case (28) gives the voltage \dot{V} of the wave transmitted beyond the junction.

It may be shown that the coefficient t_v is related to Z_L and Z_0 by

$$t_v = \frac{2Z_L}{Z_L + Z_0} = 1 + \rho_v \quad (29)$$

where Z_L = load impedance presented to line of characteristic impedance Z_0

ρ_v = reflection coefficient for voltage

As Z_L ranges from 0 to ∞ , t_v ranges from 0 to 2.

It also follows that the *transmission coefficient for current* t_i is given by

$$t_i = \frac{\dot{I}}{\dot{I}_0} = \frac{2Z_0}{Z_0 + Z_L} = 1 + \rho_i \quad (30)$$

As Z_L ranges from 0 to ∞ , t_i varies from 2 to 0.

The relations for reflection and transmission coefficients developed in this section are summarized in Table 13-5.

Table 13-5 RELATIONS FOR REFLECTION AND TRANSMISSION COEFFICIENTS

Reflection coefficient for voltage	$\hat{\rho}_v = \frac{Z_L - Z_0}{Z_L + Z_0}$
Reflection coefficient for current	$\hat{\rho}_i = \frac{Z_0 - Z_L}{Z_0 + Z_L} = -\hat{\rho}_v$
Transmission coefficient for voltage	$t_v = \frac{2Z_L}{Z_0 + Z_L} = 1 + \hat{\rho}_v$
Transmission coefficient for current	$t_i = \frac{2Z_0}{Z_0 + Z_L} = 1 + \hat{\rho}_i$
Voltage standing-wave ratio (VSWR)	$\frac{1 + \hat{\rho}_v }{1 - \hat{\rho}_v } = \frac{1 + \hat{\rho}_i }{1 - \hat{\rho}_i }$
Magnitude of reflection coefficient	$ \hat{\rho}_v = \hat{\rho}_i = \frac{\text{VSWR} - 1}{\text{VSWR} + 1}$

13-7 TRANSMISSION-LINE CHARTS

Transmission-line calculations are often tremendously facilitated by the use of transmission-line charts. In particular, the rectangular and the Smith impedance charts are extremely useful in making calculations on uniform lossless transmission lines.

A rectangular impedance chart is illustrated in Fig. 13-10.† The rectangular coordinates on this chart give the normalized resistance R_n as abscissa and the normalized reactance X_n as ordinate for points on the transmission line, while the closed circles indicate the VSWR on the line and the partial circles the distance in wavelengths from the load. The normalized resistance R_n is equal to the actual resistance R divided by the characteristic resistance R_0 of the line. That is,

$$R_n = \frac{R}{R_0} \quad (\text{dimensionless}) \quad (1)$$

The normalized reactance X_n is equal to the actual reactance X divided by R_0 , or

$$X_n = \frac{X}{R_0} \quad (\text{dimensionless}) \quad (2)$$

† For methods of constructing this chart see, for example, M.I.T. Radar School Staff, J. F. Reintjes (ed.), "Principles of Radar," pp. 8-64, McGraw-Hill Book Company, New York, 1946.

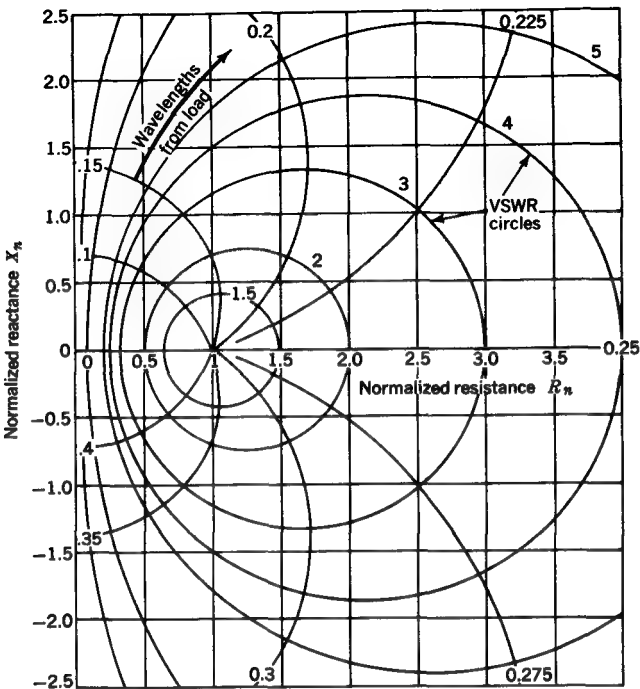


FIGURE 13-10
Rectangular impedance chart.

Thus, the normalized impedance Z_n is related to the actual impedance Z by

$$Z_n = \frac{Z}{R_0} = \frac{R}{R_0} + j \frac{X}{R_0} \quad (\text{dimensionless}) \quad (3)$$

The chart can also be used for admittances, the normalized admittance Y_n being given by

$$Y_n = G_n + jB_n = YR_0 = \frac{R_0}{Z} \quad (\text{dimensionless}) \quad (4)$$

An example will be given to illustrate the use of the rectangular chart.

EXAMPLE 1 Referring to the terminated transmission line with short-circuited stub shown in Fig. 13-11, the load $Z_L = 150 + j50 \Omega$. The line and stubs have a characteristic impedance $Z_0 = R_0 = 100 \Omega$. Find the shortest values of d_1 and d_2 for which there is no reflected wave at A (VSWR = 1).

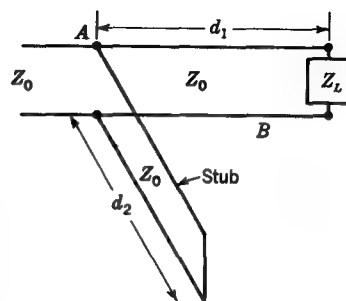


FIGURE 13-11

Terminated transmission line with single matching stub. Both the stub position d_1 and its length d_2 are adjustable.

SOLUTION The normalized impedance of the load is

$$Z_n = \frac{Z_L}{R_0} = \frac{150 + j50}{100} = 1.5 + j0.5$$

The chart is now entered at the point $1.5 + j0.5$, as indicated by P_1 in Fig. 13-12. For clarity most of the rectangular and circular coordinate lines are omitted in this figure. Point P_1 is on the VSWR circle for which $\text{VSWR} = 1.77$. Hence, the VSWR at B is 1.77. Since the

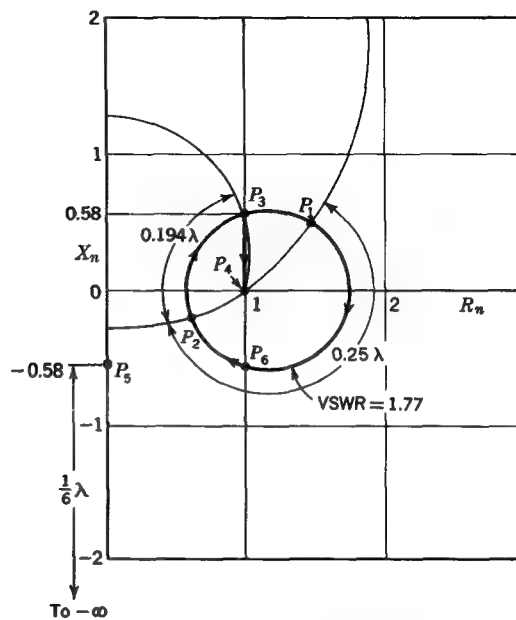


FIGURE 13-12

Worked example of single-stub tuner (Fig. 13-11) using rectangular impedance chart.

stub is connected in parallel with the line, it will be advantageous to work in admittances; so moving from P_1 $\lambda/4$ (90 electrical degrees) to P_2 (see Fig. 13-10 for distance scale) converts Z_n to a normalized admittance $Y_n = 0.6 - j0.2$ at the load.[†] Next, moving a distance $d_1 = 0.194\lambda$ to the point A (or from P_2 to P_3 on the chart), the normalized admittance is $Y_n = 1.0 + j0.58$. If the stub length is now adjusted so that the stub presents a normalized admittance of $-j0.58$ at A , the total admittance at A is $1.0 + j0.58 - j0.58 = 1.0 + j0$ and the line is matched ($VSWR = 1$). This corresponds to a move from P_3 to P_4 on the chart. A normalized admittance $Y_n = -j0.58$ (pure susceptance) is indicated at P_5 , and we note that the distance required from a short circuit ($Y_n = \pm j\infty$) to obtain this value is 0.167λ . Thus the required stub length is

$$d_2 = 0.167\lambda$$

The required distance of the stub from the load as obtained above is

$$d_1 = 0.194\lambda$$

We note that matching with the stub can be accomplished from any point on the vertical line containing P_4 . Thus, we might have moved beyond P_3 all the way to P_6 . However, both d_1 and d_2 would be larger.

A Smith chart[‡] is illustrated in Fig. 13-13. In this chart the rectangular diagram has been transformed (see Prob. 13-14) so that all impedance values fall within the circular periphery. The chart coordinates give the normalized resistance and reactance. The VSWR circles are usually not included but can be constructed as needed with a compass centered on the center point of the chart. For example, the $VSWR = 2$ circle is shown in Fig. 13-13. The VSWR is unity at the center of the chart and infinity at the periphery. Intercepts of the VSWR circle with the $X_n = 0$ line are $R_n = 1/VSWR$ and $R_n = VSWR$. The distance from the load is indicated around the periphery of the chart. For instance, at a distance of $\lambda/10$ from a load for which $R_n < 1$ and $X_n = 0$ the impedance must correspond to some value on the straight line constructed from the center of the chart to the peripheral point marked 0.1 wavelength in Fig. 13-13. The fact that distance is proportional to angular position around the periphery is one of the principal advantages of this type of chart.

EXAMPLE 2 Repeat Example 1 using a Smith chart.

SOLUTION The points P_1 , P_2 , etc., on the rectangular impedance chart of Fig. 13-12 have been transferred to the Smith chart of Fig. 13-13. Thus, for $Z_n = 1.5 + j0.5$ we enter at P_1 . Transforming to admittances, we proceed to P_2 , obtaining $Y_n = 0.6 - j0.2$ at the

[†] Moving $\lambda/4$ on the chart transforms an impedance to an admittance (or vice versa) at the same location on the line.

[‡] P. H. Smith, Transmission Line Calculator, *Electronics*, 12: 29-31 (January 1939).

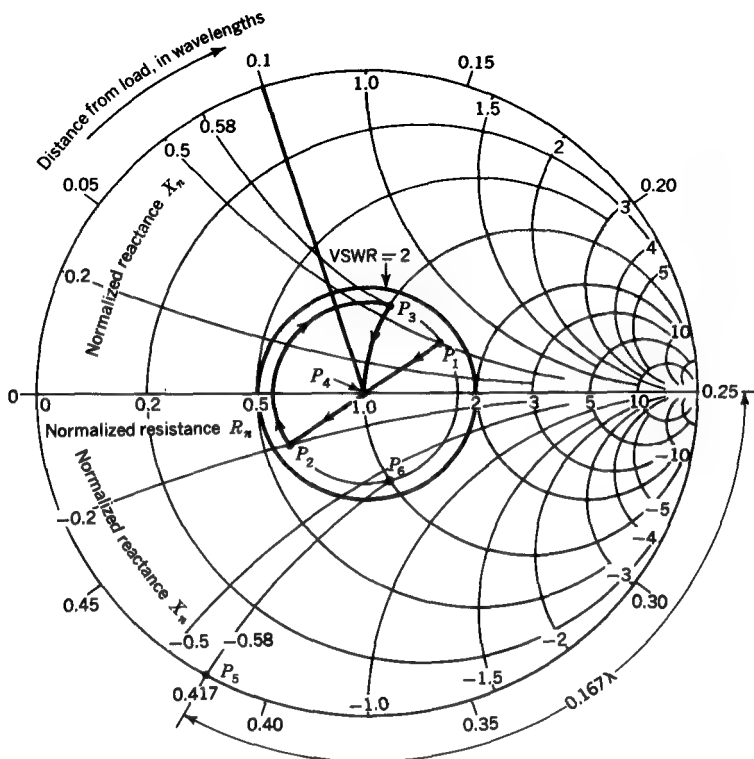


FIGURE 13-13
Smith impedance chart and worked Example 2. (Same problem as in Fig. 13-12).

load. We then move 0.194λ along the line to A or to P_3 on the chart or to $Y_n = 1.0 + j0.58$. Connecting the stub brings us to P_4 . The stub length (0.167λ) is obtained by noting the position of P_5 ($Y_n = -j0.58$) and reading off the distance between it and 0.25λ (at right end of the real axis).

EXAMPLE 3 Consider the terminated line with the two short-circuited stubs portrayed in Fig. 13-14. The position at which the stubs connect to the line is fixed, as shown, but the stub lengths, d_1 and d_2 , are adjustable. This kind of arrangement is called a *double-stub tuner*. The load $Z_L = 50 + j100 \Omega$. The line and stubs have a characteristic impedance $Z_0 = R_0 = 100 \Omega$. Find the shortest values of d_1 and d_2 such that there is no reflected wave at A (VSWR = 1).

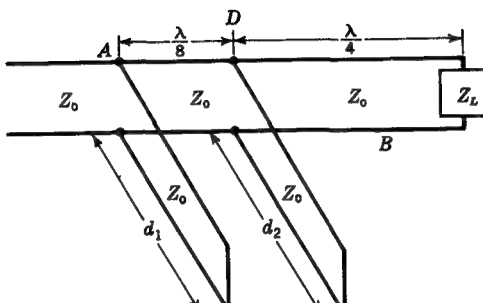


FIGURE 13-14
Double-stub tuner with short-circuited
stubs.

SOLUTION The normalized value of the load impedance is

$$Z_n = \frac{50 + j100}{100} = 0.5 + j1.0$$

The chart (Fig. 13-15) is entered at this normalized impedance, as indicated by the point P_1 . Constructing a VSWR curve through P_1 , we note that the VSWR at B (Fig. 13-14) is 4.6. Next, constructing the diametric line through P_1 , we locate P_2 halfway around the constant VSWR circle from P_1 . Thus, the normalized load admittance is $0.4 - j0.8$. Now, moving clockwise along the constant VSWR circle from P_2 a distance $\lambda/4$ away from the load (toward the generator), we arrive back at P_1 .† Thus at the point D on the line the normalized admittance of the main line (looking toward the load) is $0.5 + j1.0$. Since the reflection at A must be zero, we may anticipate the fact that the admittance of the main line at A (without the stub of length d_1 connected) must fall on the circle marked C_1 (Fig. 13-15). Therefore, at the junction of the stub of length d_2 the admittance must fall on this circle rotated back (counterclockwise) $\lambda/8$ to the position indicated by the circle marked C_2 .

The admittance added by the stub of length d_2 will cause the total admittance to move from P_1 along a constant-conductance line. In order to end up on the circle C_2 , we can move either to the left, arriving at P_3 , or to the right, arriving at P_4 . Moving to P_3 results in shorter stubs; so we will make the stub of such length as to bring the total admittance to P_3 . This requires a stub admittance (pure susceptance) of

$$Y_n = -j(1.0 - 0.14) = -j0.86$$

A short-circuited stub has an infinite VSWR so that the admittance at points along the stub are on the circle at the periphery of the chart. At the short circuit the admittance is infinite (point P_5). Therefore, in order to present a value

$$Y_n = -j0.86 \text{ (point } P_6\text{)}$$

(noting that the outside scale on the chart reads 0.25 at P_5) the stub length must be given by

$$d_2 = 0.388 - 0.25 = 0.138\lambda$$

† We arrive back at P_1 because the point D on the line is $\lambda/4$ from the load. For other line lengths, we would arrive at some other point on the chart.

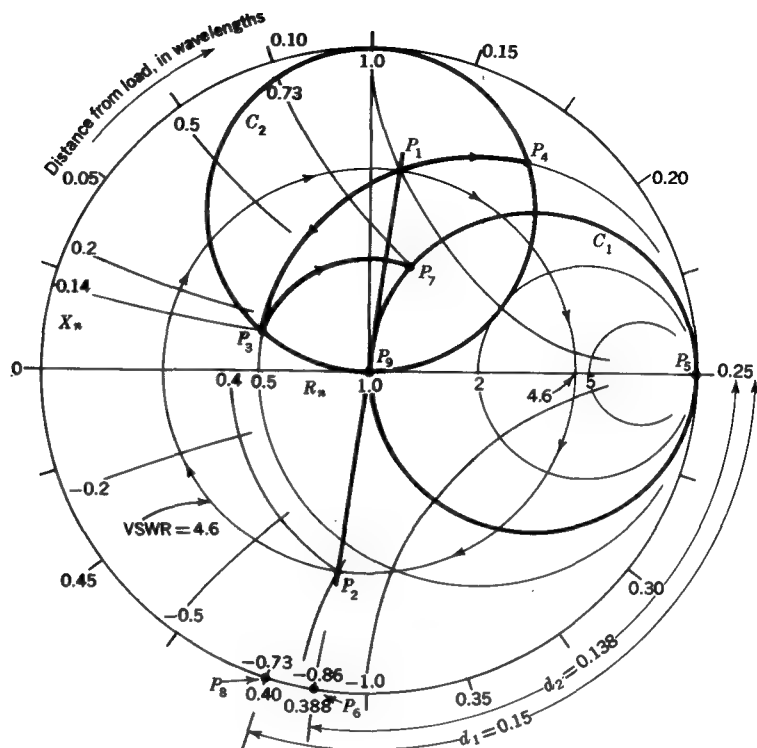


FIGURE 13-15

Worked Example 3. Double stub tuner of Fig. 13-14 using Smith chart.

Next, moving along the constant VSWR curve from P_3 to P_7 , we find that the line admittance at A is $Y_n = 1.0 + j0.73$. Hence a stub admittance of $Y_s = -j0.73$ is required in order to make the total normalized admittance at A equal to $1.0 + j0$, and therefore the actual impedance at A equal to $100 + j0 \Omega$. A value $Y_s = -j0.73$ falls at point P_8 . Therefore the length of the stub is given by

$$d_1 = 0.40 - 0.25 = 0.15\lambda$$

Connecting this stub brings the total admittance (or impedance) to the center of the chart (point P_9) and the line is matched ($VSWR = 1$).

To summarize, the required stub lengths are

$$d_1 = 0.15\lambda$$

$$d_2 = 0.138\lambda$$

We note from Figs. 13-14 and 13-15 that

$$\text{VSWR} = \begin{cases} 4.6 & \text{at } B \text{ (points } P_1 \text{ and } P_2\text{)} \\ 2.05 & \text{between } D \text{ and } A \text{ (points } P_3 \text{ and } P_7\text{)} \\ 1 & \text{at } A \text{ (point } P_9\text{)} \\ \infty & \text{on stubs (points } P_6 \text{ and } P_8\text{)} \end{cases}$$

If we had moved to P_4 instead of to P_3 , we would have ended up with longer stubs, namely,

$$d_1 = 0.443\lambda \quad \text{and} \quad d_2 = 0.364\lambda$$

and also a larger VSWR between D and A .

13-8 $\lambda/4$ TRANSFORMER

There are many situations where a $\lambda/4$ section of transmission line of suitable impedance may be useful. Suppose that we wish to connect a transmission line of 100Ω characteristic impedance to a load of $400 + j0 \Omega$, as in Fig. 13-16. This can be done with a $\lambda/4$ transformer of proper characteristic impedance Z_1 . From (13-6-20) we note that when $x = \lambda/4$ ($\beta x = \pi/2$) (line assumed lossless),

$$Z_x = \frac{(Z_1)^2}{Z_L} \quad \text{or} \quad Z_1 = \sqrt{Z_L Z_x} \quad (1)$$

Here Z_1 is the *geometric mean* of Z_L and Z_x . In the present example $Z_L = 400 + j0 \Omega$, while Z_x must be equal to $100 + j0 \Omega$. It follows that

$$Z_1 = \sqrt{400 (100)} = 200 \Omega$$

Therefore, a $\lambda/4$ section of line of characteristic impedance $Z_1 = R_1 = 200 \Omega$ provides the desired transformation, eliminating a reflected wave on the $100-\Omega$ line.

An interesting application of the $\lambda/4$ -transformer principle is to the $\lambda/4$ plate, which can be used to eliminate plane-wave reflection. Thus, for example, a plane

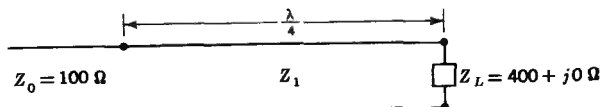


FIGURE 13-16
 $\lambda/4$ transformer.

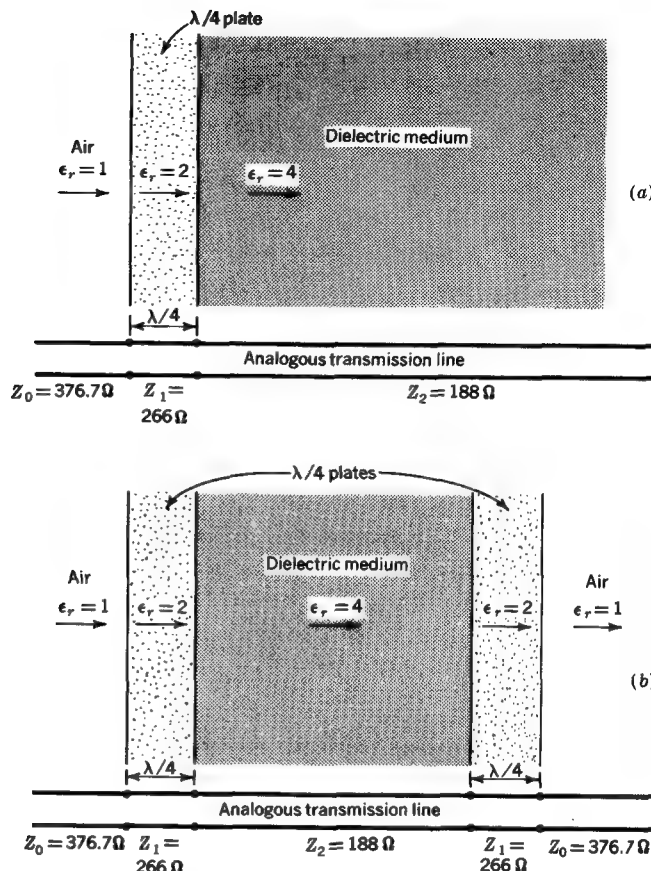


FIGURE 13-17

(a) $\lambda/4$ plate at interface of air and dielectric medium and (b) two $\lambda/4$ plates for transmission through a dielectric medium.

wave in air incident normally on a half-space filled with a lossless dielectric medium of relative permittivity $\epsilon_r = 4$ will be partly reflected and partly transmitted. The reflection can be eliminated, as shown in Fig. 13-17a, by placing a $\lambda/4$ plate between the air and the dielectric medium provided the plate has an intrinsic impedance

$$Z_1 = \sqrt{Z_0 Z_2}$$

where Z_0 = intrinsic impedance of air

Z_2 = intrinsic impedance of dielectric medium

In the present example,

$$Z_0 = \sqrt{\frac{\mu_0}{\epsilon_0}} = 376.7 \Omega$$

$$Z_2 = \frac{Z_0}{\sqrt{\epsilon_r}} = \frac{376.7}{\sqrt{4}} = 188 \Omega$$

Therefore the intrinsic impedance of the plate must be

$$Z_1 = \sqrt{Z_0 Z_2} = 266 \Omega$$

and its relative permittivity must be

$$\epsilon_r = \left(\frac{Z_0}{Z_2} \right)^2 = 2$$

The analogous transmission-line equivalent is also shown in Fig. 13-17a. It is assumed that no ferromagnetic material is present, and so $\mu = \mu_0$. It is to be noted that the plate is $\lambda/4$ thick as measured in terms of the wavelength *in the plate*.

For reflectionless transmission of a plane wave *through* a dielectric medium of finite thickness, a $\lambda/4$ plate is required on both sides to prevent reflection at each dielectric-air interface. The arrangement is suggested in Fig. 13-17b, where the analogous transmission-line equivalent is also shown.

13-9 TRANSFORMER BANDWIDTH

With the $\lambda/4$ transformer discussed in the preceding section (see Fig. 13-16) the reflected wave is eliminated at the design frequency (or wavelength). However, there will be reflection at adjacent frequencies. In other words, the transformer is a frequency-sensitive device. Referring to Sec. 13-8 and Fig. 13-16 we have $Z_L = 400 + j0 \Omega$, $Z_1 = 200 \Omega$, and $Z_0 = 100 \Omega$.

Suppose that this system is operating at ultrahigh frequency (UHF) with 300 MHz as the design frequency for which reflection is to be zero (line assumed lossless). At 300 MHz, $\lambda = 1$ m, and a $\lambda/4$ section is 250 mm long. Using a Smith chart, as in Fig. 13-18, we enter at the normalized impedance of the load, i.e., normalized with respect to the characteristic impedance of the $\lambda/4$ section, which is equal to $2 + j0 [= (400 + j0)/200]$. This is the point *P* on the chart. At 300 MHz the $\lambda/4$ section is 0.25λ long, so that to find the impedance at the input (or left) end of the transformer section we move clockwise from *P* along the VSWR = 2 circle $\lambda/4$, which is halfway around. This point, marked 300 MHz in Fig. 13-18, gives the normalized impedance at the input, which is $0.5 + j0$. The actual impedance is this value multiplied by the characteristic impedance of the transformer section ($= 200 \Omega$) or $100 + j0 \Omega$.

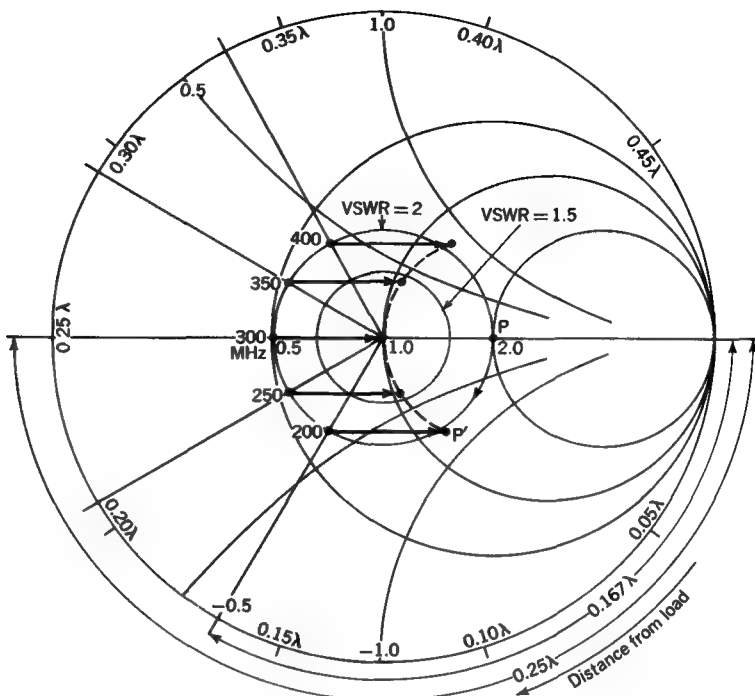


FIGURE 13-18
Smith chart analysis of performance of $\lambda/4$ transformer over a band of frequencies.

On the Smith chart the normalized impedance with respect to the $100\text{-}\Omega$ line is then $1 + j0$, which is at the center of the chart. Thus, the system is matched and the VSWR = 1 on the $100\text{-}\Omega$ line.

Suppose we wish to find the VSWR of this $\lambda/4$ transformer at adjacent frequencies in the range between 200 and 400 MHz. Consider first the situation at 200 MHz. At this frequency the wavelength is longer, and the transformer section is now less than $\lambda/4$ long. Its length at 200 MHz is 0.167λ [$= 0.25/(300/200)$], so that again entering the Smith chart at P , we move only 0.167λ along the VSWR = 2 circle to the point marked 200 in Fig. 13-18. To refer this normalized impedance to the $100\text{-}\Omega$ line we multiply by 2 (as before), which moves us to the point P' . The resulting VSWR on the $100\text{-}\Omega$ line is thus about 2.1. Calculating the VSWR at other frequencies in the range 200 to 400 MHz, as shown on the Smith chart of Fig. 13-18, we can draw a VSWR-vs.-frequency curve as in Fig. 13-19 (solid line). We note that the VSWR = 1 (zero reflection) at 300 MHz but that the VSWR rises to more than 2 at

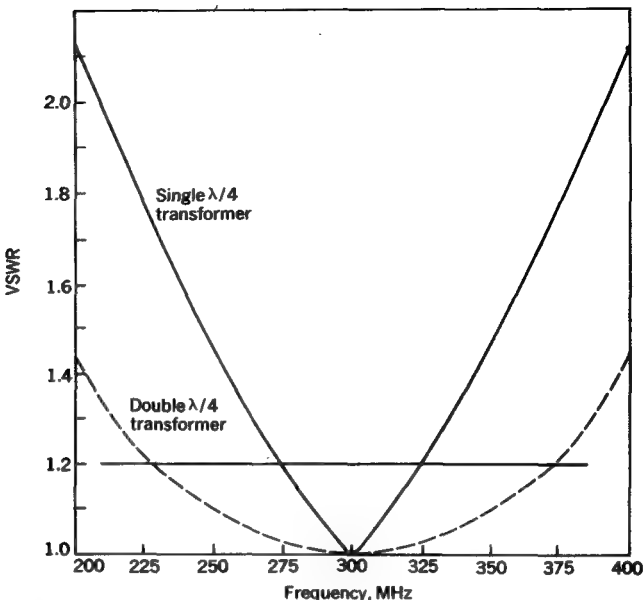


FIGURE 13-19
Comparison of VSWR with single and double $\lambda/4$ transformers over a 2 to 1 bandwidth. The double $\lambda/4$ transformer has a much wider bandwidth.

200 and 400 MHz. As indicated in the figure, the bandwidth for which the $VSWR \leq 1.2$ is about 50 MHz. This yields a bandwidth with respect to the design frequency of

$$\frac{50}{300} \times 100 = 16.7\%$$

One method of increasing the bandwidth of the transformer is to connect two $\lambda/4$ transformers in series, as in Fig. 13-20a. The impedances chosen satisfy the requirement of the geometric mean. Thus, $\sqrt{400(100)} = 200 \Omega$, which should be the impedance seen looking either way at the midpoint *A*. Then, $141.4 \Omega [= \sqrt{100(200)}]$ and $283 \Omega [= \sqrt{200(400)}]$ are the impedances required for the two sections. The VSWR for this double (or two-section) $\lambda/4$ transformer is shown by the dashed line in Fig. 13-19.[†] It is evident that this combination possesses considerably greater

[†] The VSWR can be found with a Smith chart by entering at $1.41 + j0 [= (400 + j0)/283]$ and moving clockwise the length of the transformer on a constant-VSWR circle to get the impedance at *A* (Fig. 13-20a), as above for the single $\lambda/4$ section. The process is then repeated for the second $\lambda/4$ section to get the impedance at the input.

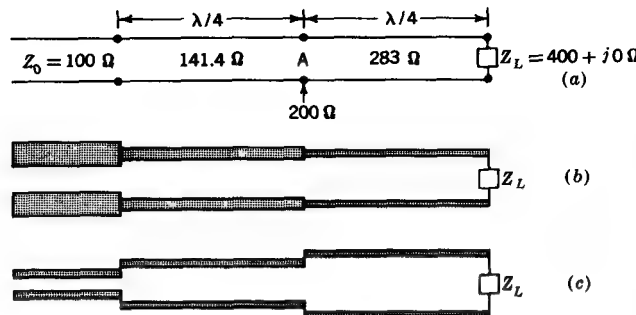


FIGURE 13-20

(a) Double $\lambda/4$ transformer dimensions and impedances, (b) constant conductor spacing but different conductor diameter, and (c) constant conductor diameter but different spacing.

bandwidth. The bandwidth for which the $VSWR \leq 1.2$ is about 150 MHz ($= 375 - 225$), or

$$\frac{150}{300} \times 100 = 50\%$$

compared to 16.7 percent for the single section. Over the 200- to 400-MHz range the VSWR does not exceed about 1.5 for the two-section type. With a two-wire transmission line, shown schematically in Fig. 13-20a, the different impedances might be achieved in practice with a constant spacing but different conductor diameter, as in Fig. 13-20b, or with a constant conductor diameter and different spacing, as in Fig. 13-20c, or by using dielectrics of different permittivity between the conductors, or some combination of these methods.

With a transformer consisting of three $\lambda/4$ sections connected in series the bandwidth could be increased further.[†] As we add still more sections, the discontinuity (impedance step) between sections becomes less, until in the limit we would approach an infinitely long, smooth, gradually tapered transmission line with no reflection over an infinite bandwidth. (We are assuming, of course, that the load impedance remains

[†] To justify the geometric-mean requirement the impedances Z_1 , Z_2 , and Z_3 , of the three sections would be 119, 200, and 336 Ω , i.e., the logarithms of the impedance ratios are related as the coefficients of the binomial series (1, 2, 1 for two sections; 1, 3, 3, 1 for three sections; 1, 4, 6, 4, 1 for four sections, etc.). Thus, we have the requirement that

$$3 \log \frac{Z_1}{100} = \log \frac{Z_2}{Z_1} = \log \frac{Z_3}{Z_2} = 3 \log \frac{400}{Z_3}$$

from which $Z_1 = 119$, $Z_2 = 200$, and $Z_3 = 336 \Omega$. See J. C. Slater, "Microwave Transmission," pp. 57-61, McGraw-Hill Book Company, New York.

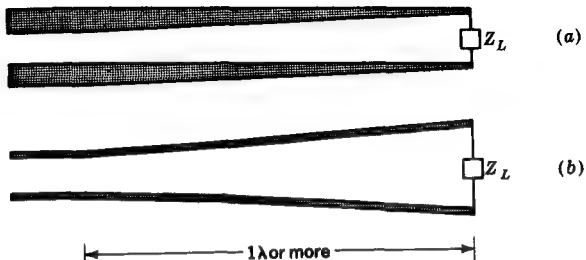


FIGURE 13-21
Transformers with gradual taper for wide bandwidth.

constant with frequency.) In practice we must deal with lines of finite length and hence finite bandwidth. However, if the transition is made smoothly and gradually by changing the conductor diameter or the spacing, as suggested in Fig. 13-21a and Fig. 13-21b, it may be possible to achieve a very wide bandwidth in practice. The characteristic impedance of the line can be made to follow an exponential taper. It is necessary, however, that the transition be at least 1λ long at the lowest frequency of operation (see Prob. 13-12). We may conclude that spreading out a discontinuity into a long gradual transition will provide broadband matching.

13-10 WAVE REFLECTIONS ON A $\lambda/4$ TRANSFORMER

The reflectionless property of the $\lambda/4$ transformer is achieved by adjusting reflections from two points (one at each end of the transformer) so that they balance out at the design frequency. Let us investigate this in more detail using the wave-reflection method.

Consider again the $\lambda/4$ transformer of Sec. 13-8 but with a short section of 400Ω line inserted between the $\lambda/4$ transformer and the load, as suggested in Fig. 13-22. This permits us to discuss waves to the right of junction 2 without altering the problem. We need to consider three waves: *A* approaching junction 1 from the left, *B* approaching junction 1 from the right, and *C* approaching junction 2 from the left. In a general situation we would also need to consider a wave *D* approaching junction 2 from the right, but here this wave is absent since the load and line are matched (no reflection at load). The reflection and transmission coefficients (ρ and τ) for each wave are as indicated in Fig. 13-22.

Assume that the initial incoming wave from the left is equal to 1 V and that the lines are lossless. Then at junction 1, $\frac{1}{3}$ V will be transmitted and $\frac{1}{3}$ V reflected.

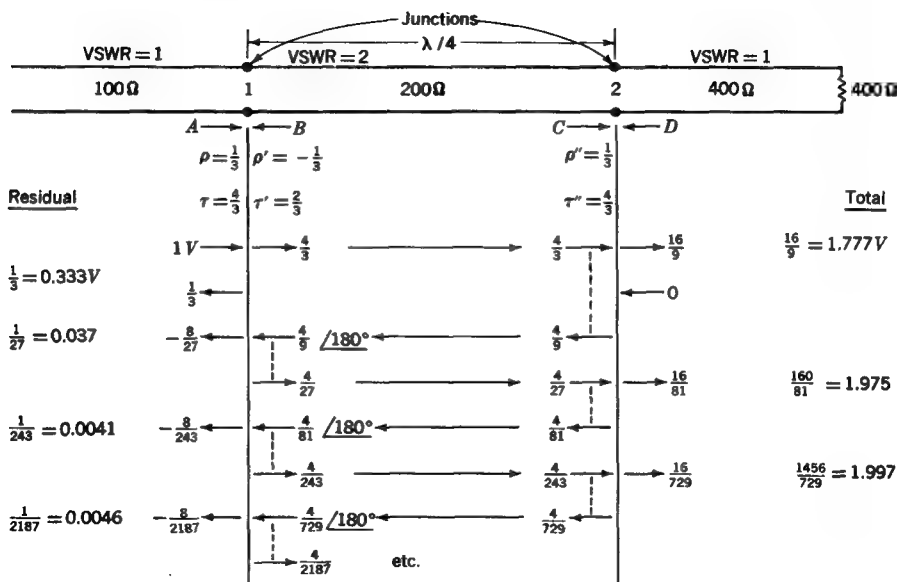


FIGURE 13-22
Wave reflections on a $\lambda/4$ transformer.

When the $\frac{4}{3}$ -V wave arrives at junction 2, four-thirds of it will be transmitted and one-third reflected, giving rise to a $\frac{16}{9}$ -V wave proceeding to the load and a $\frac{4}{9}$ -V wave traveling back to the left from junction 2, as in Fig. 13-22. When this $\frac{4}{9}$ -V wave arrives back at junction 1, it will be reversed in phase (having traveled $\lambda/2$, or 180°) and two-thirds of it will be transmitted and one-third reflected (with sign change) resulting in a $-\frac{8}{27}$ -V wave traveling to the left from junction 1 and a $+\frac{4}{27}$ -V wave to the right, as indicated in Fig. 13-22. This $\frac{4}{27}$ -V wave will travel to junction 2 and be partly transmitted and partly reflected, and the process will continue indefinitely.

Values of the voltages transmitted and reflected at each junction for several reflections are shown in Fig. 13-22 (proceeding from top to bottom). The left-hand column lists the residual voltage of the wave traveling to the left from junction 1. Except for the $\frac{1}{3}$ -V reflected wave (due to the incident 1-V wave) all waves traveling to the left have negative voltage and after each round trip of the waves on the $\lambda/4$ section the residual wave becomes less. It is $1/27$ V after the first round trip, $1/243$ V after the second, and $1/2187$ V after the third. It is evident that, in principle at least, we must wait an infinitely long time before the reflected wave on the 100Ω line is reduced to exactly zero. But as a practical matter it will be reduced to 0.00046 V ($= 1/2187$) after three round trips of the wave on the transformer. At 300 MHz ($\lambda = 1$ m) the

$\lambda/4$ transformer is 250 mm long, and for a lossless line ($v = c = 300 \text{ Mm s}^{-1}$) the time for one round trip is $16.7 \times 10^{-10} \text{ s} (= 0.5/3 \times 10^8)$, or 1.67 ns; and for three round trips is 5 ns. Still lower levels of reflected wave will be achieved after longer time intervals, and after a sufficient time we may assume that steady-state conditions have been achieved and the reflection is substantially zero.[†]

The action of the $\lambda/4$ transformer is like that of a *resonator* (see Sec. 13-25). Waves are reflected back and forth between the junctions, the wave traveling to the right being equal to 1.5 V and the one traveling to the left being equal to 0.5 V. The student can confirm these values by adding up the wave fractions in Fig. 13-22. The resulting $VSWR = 2$ on the $\lambda/4$ section.

As indicated in Fig. 13-22, the wave to the right of junction 2 (traveling into the load) will add up to 2 V after a sufficient number of wave reflections on the transformer. Thus, the $\lambda/4$ transformer transforms the 1-V input wave to a 2-V wave into the load. It may also be said that the transformer makes the 400Ω load appear as 100Ω at its input (junction 1).

13-11 FURTHER TIME-DOMAIN STUDIES OF A $\lambda/4$ TRANSFORMER

The behavior of the $\lambda/4$ transformer as a function of time, discussed in the preceding section, can be investigated further with the aid of time-distance diagrams, as in Fig. 13-23. Assume an incident wave of frequency f which is a step function of magnitude 1 V arriving at junction 1 at time $t = 0$. This unit step function is given by

$$V(t) = \begin{cases} 1 & \text{for } t \geq 0 \\ 0 & \text{for } t < 0 \end{cases}$$

Proceeding from top to bottom in Fig. 13-23, we can follow the progress of the transmitted and reflected traveling waves at successive instants of time leading ultimately to the steady-state condition shown at the bottom of the figure. The ordinate gives the voltage magnitude of the traveling waves except for the lowest graph, where it gives the magnitude of the total voltage. Note the standing wave on the transformer.

Consider next that a square pulse of duration t_1 and magnitude 1 V is applied.[‡] Proceeding from top to bottom in Fig. 13-24, we can follow the progress of this pulse at successive instants of time until it has disappeared. It is clear that the transformer

[†] The time for two round trips is the same as for one cycle. Thus, the steady-state condition is substantially achieved within a few cycles.

[‡] The pulse is given by

$$V(t) = \begin{cases} 1 & \text{for } 0 \leq t \leq t_1 \\ 0 & \text{for } t < 0 \text{ and } t > t_1 \end{cases}$$

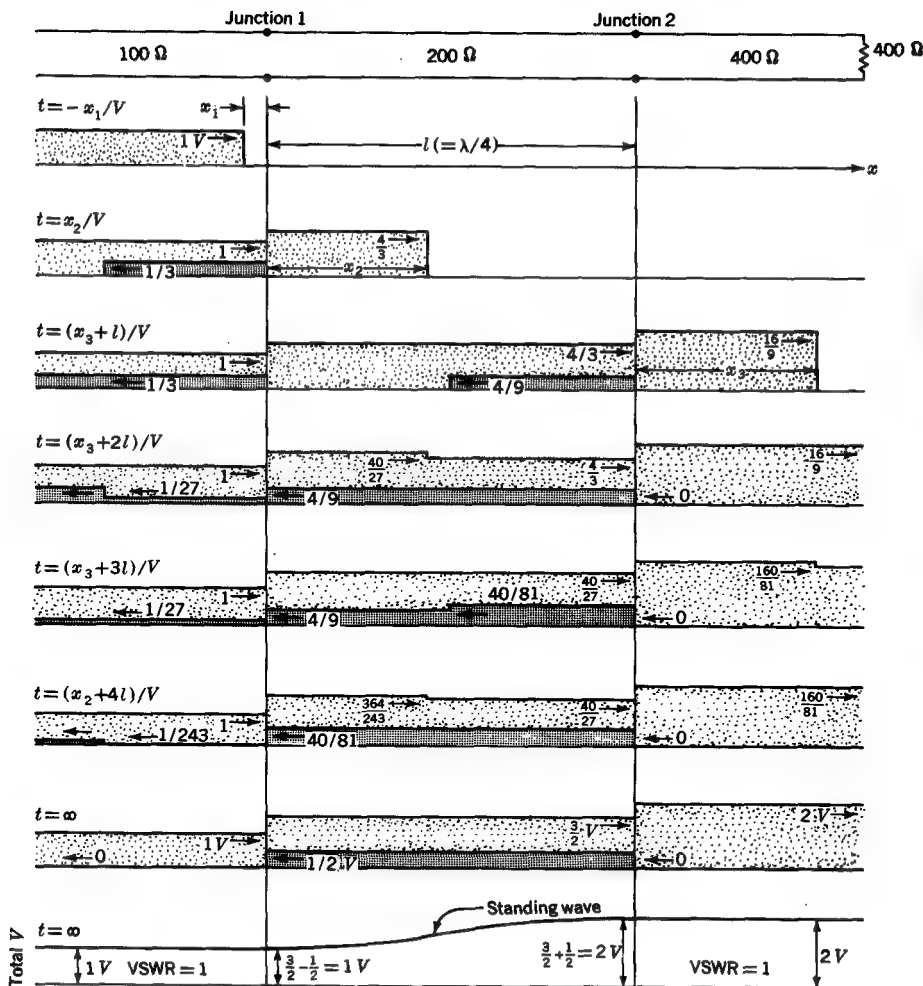


FIGURE 13-23

Time-domain analysis of $\lambda/4$ transformer showing progress of wave along transmission line and effect of two junctions. Waves traveling to right are shaded light and those to left dark. Time increases by successive intervals except for lowest graph which gives total voltage (sum of both traveling waves).

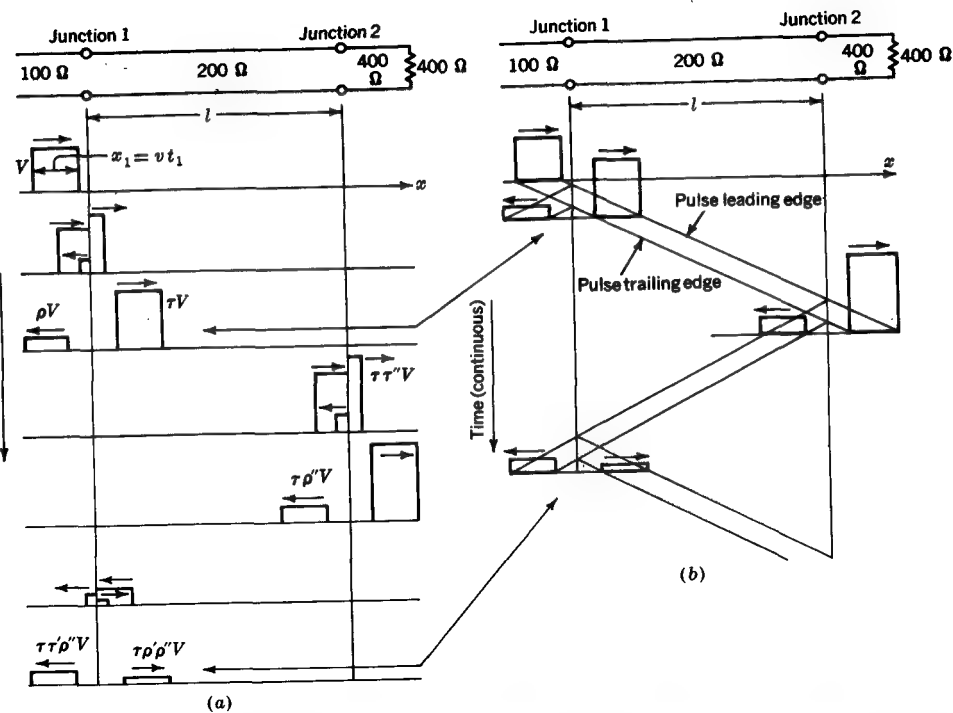
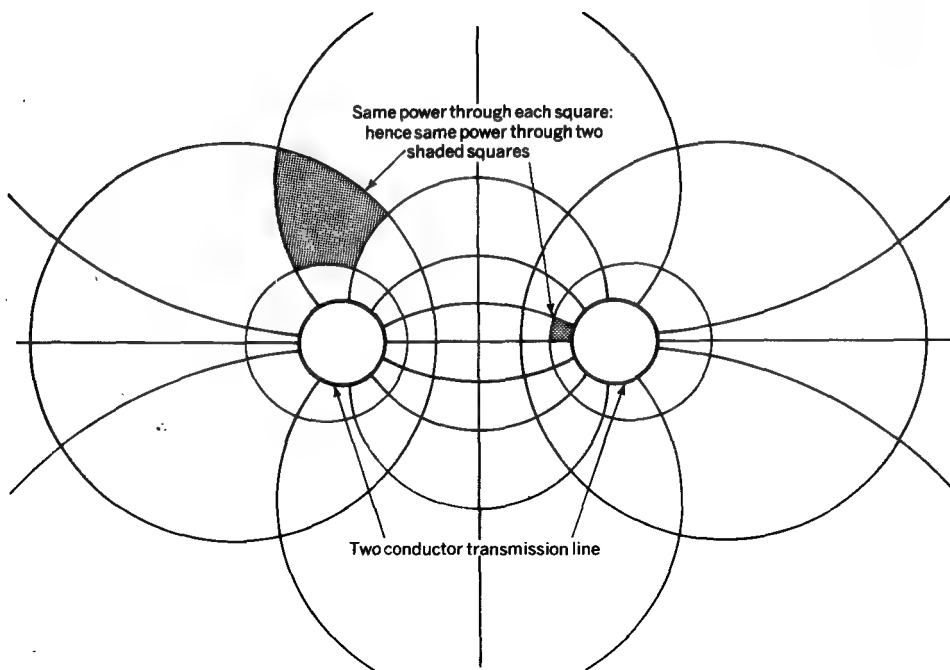


FIGURE 13-24

Progress of short pulse along transmission line with resulting pulses reflected and transmitted at junctions. (a) Situation at successive instants. (b) Situation on continuous basis. Note that an incident pulse splits into a reflected and transmitted pulse at each junction. A CRT display connected to the line at the left would show a series of echo pulses of decreasing magnitude: The first echo from junction 1, the second from junction 2, the third from 2, 1, and 2, the fourth from 2, 1, 2, 1, and 2, etc. The magnitude of the pulses after each encounter with a junction is indicated in (a) by the τ , ρ values. For example, the pulse traveling through junction 1, reflected from junction 2 and then reflected from junction 1, has a magnitude $\tau\rho'\rho''V$ where τ is the transmission coefficient through junction 1 (left to right), ρ' is the reflection coefficient at junction 2, and ρ'' is the reflection coefficient at junction 1 (right to left) [see bottom of (a) and (b)].

fails to function as a reflectionless device for a pulse as short as indicated in Fig. 13-24 ($t_1 \ll l/v$, where l is the length of the transformer and v is the wave velocity). There is no way for the pulse reflected from junction 2 to catch up with the one reflected from junction 1 and reduce its magnitude.[†] Only for the steady-state condition or for a

[†] Hence, a Smith chart analysis of a line is of no value if the line is to be used with very short pulses.



(Figure 13-25a)

very long pulse ($t_1 \gg l/v$) can the multiple reflections reduce the wave reflected to the left from junction 1 to its desired low value. To avoid reflections with short pulses one must construct lines without discontinuities. Conversely, one can use short pulses to locate and measure the magnitude of discontinuities on transmission lines. To obtain short enough pulses for such diagnostic measurements, it may be desirable to use frequencies which are much higher than the design frequency.

13-12 POWER FLOW ON A TRANSMISSION LINE

The electric and magnetic fields around a two-conductor transmission line are shown in Fig. 13-25a (see also Fig. 3-16). At any point the power flow parallel to the line (perpendicular to page) is given by the Poynting vector. But $E/H = Z_0$ ($= \sqrt{\mu_0/\epsilon_0} = 376.7 \Omega$ for air or vacuum), so that the Poynting vector ($= E^2/Z_0$) is proportional to the square of the electric field E . Calculating the Poynting vector for the transmission line of Fig. 13-25a, we can obtain the power-flow map of Fig. 13-25b. The contours

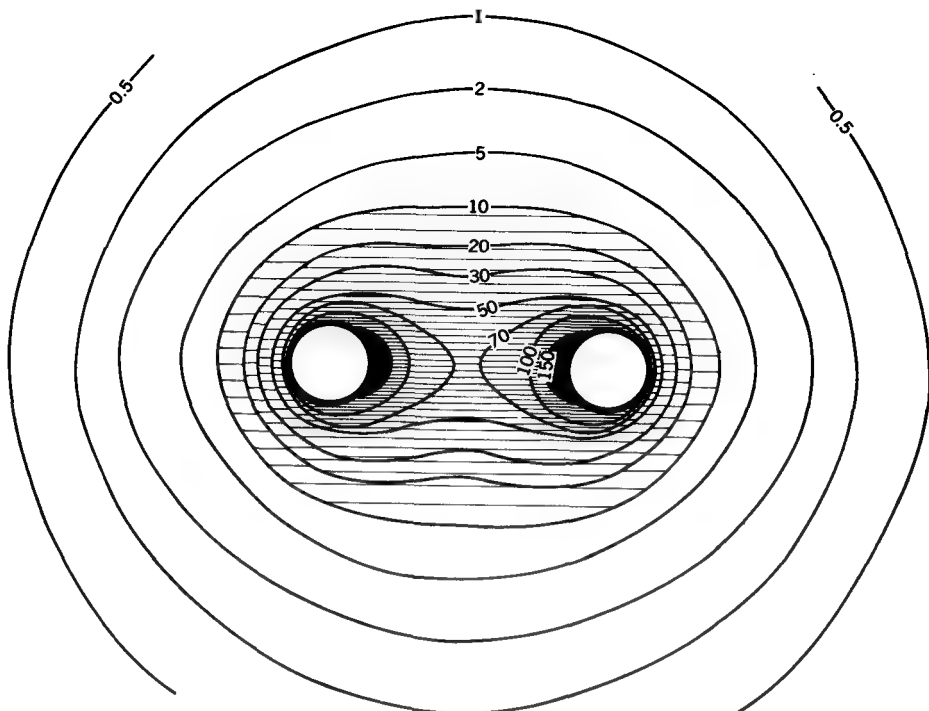


(Figure 13-25b)

FIGURE 13-25

(a) Electric field map for infinite 2-conductor lossless transmission line with potential difference of 10 V rms. (b) Power-flow map; the contours give the power density (Poynting vector) in watts per square meter. The same power is transmitted through each curvilinear square in (a). The two conductors are 25.4 mm in diameter and are spaced 76.2 mm between centers. The maximum power density is between the conductors and close to each one as shown by the contours in (b) and by the fact that the smallest curvilinear squares are so located in (a).

indicate power flow in watts per square meter for the case where each conductor is 25.4 mm in diameter with spacing between centers of 76.2 mm and a potential difference between conductors of 10 V rms. It is interesting to note that the maximum power flow is concentrated between the two conductors and close to each one. Integrating the Poynting vector over an infinite plane perpendicular to the conductors yields the total power transmitted. The total power can also be obtained from the interconductor voltage V and the characteristic impedance Z_c of the line, or in this case 465 mW ($= V^2/Z_c = 10^2/215$).

The field map of Fig. 13-25a has been drawn with true curvilinear squares (see Sec. 3-22). An important property of this map is that *the same power is transmitted through each curvilinear square*. Thus, if we know the power through any square and the number of squares, we can obtain the total power transmitted. Or conversely, from a knowledge of the total power and the number of squares we can obtain the power per square. In the present case there are $3 \times 5\frac{1}{2} = 15\frac{1}{2}$ squares in each quadrant, or a total of 63 squares. (Note that all squares, including those which extend to infinity, appear at least partially in Fig. 13-25a.) The total power is 465 mW, and the power per square is 7.4 mW ($= 465/63$).

13-13 CIRCUITS, LINES, AND GUIDES: A COMPARISON

At low frequencies a concept of currents, voltages, and lumped circuit elements is practical. Thus, for the simple circuit of Fig. 13-26a, consisting of a generator G and resistor R , circuit theory involving lumped elements can be used.

At somewhat higher frequencies these ideas can be extended satisfactorily to lines of considerable length provided that the velocity of propagation and the distributed constants of the line are considered. Thus, the behavior of the transmission line of Fig. 13-26b can be handled by an extension of circuit theory involving distributed elements, as in the preceding sections.

Consider now another type of transmission system, as shown in Fig. 13-26c, consisting of a hollow cylindrical or rectangular pipe or tube of metal. Suppose we ask: can such a pipe convey electromagnetic energy? If our experience were restricted to simple circuits or transmission lines, as in Fig. 13-26a and b, our answer would be

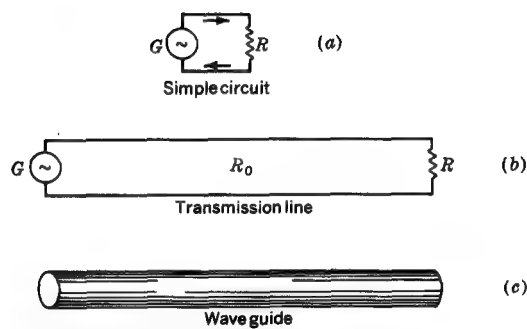


FIGURE 13-26

Comparison of (a) circuit, (b) two-conductor transmission line, and (c) hollow single-conductor waveguide.

no, since there is only a single conductor and no return circuit for the current. However, if our experience were restricted to optics, our answer would be *yes*, since light will pass through a straight metal pipe and light consists of electromagnetic waves of extremely high frequency (10^{16} Hz).

The complete answer is *yes* and *no*, depending on the frequency. Carrying our reasoning further, we might deduce that if the metal pipe will not transmit low frequencies but will transmit extremely high frequencies, there must be some intermediate frequency at which there is a transition from one condition to the other. In the following sections on waveguides we shall find that this transition, or low-frequency cutoff, occurs when the wavelength is of the same order of magnitude as the diameter of the pipe.

In explaining the transmission of electromagnetic energy through the pipe of Fig. 13-26c it is found that the circuit theory which worked for lumped circuits and two-conductor transmission lines is inadequate. For the hollow metal pipe or tube it is necessary to direct our attention to the empty space inside the tube and to the electric and magnetic fields \mathbf{E} and \mathbf{H} inside the tube. From the field-theory point of view we realize that the energy is actually conveyed through the empty space inside the tube and that the currents or voltages are merely associated effects.

13-14 TE MODE WAVE IN THE INFINITE-PARALLEL-PLANE TRANSMISSION LINE

As an introduction to waveguides let us consider an infinite-parallel-plane transmission line, as in Fig. 13-27. This is a two-conductor line which is capable of guiding energy in a TEM mode with \mathbf{E} in the z direction. However, at sufficiently high frequencies it

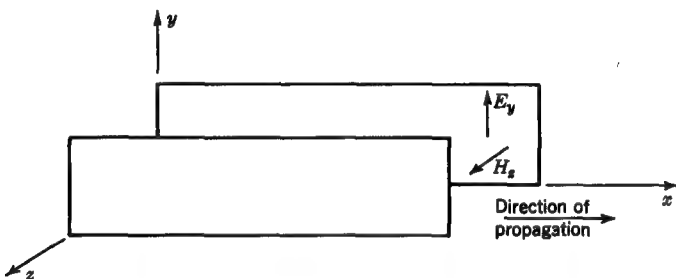


FIGURE 13-27

Transmission system consisting of two conducting planes parallel to the xy plane. The planes are assumed to be infinite in extent (infinite parallel-plane transmission line).

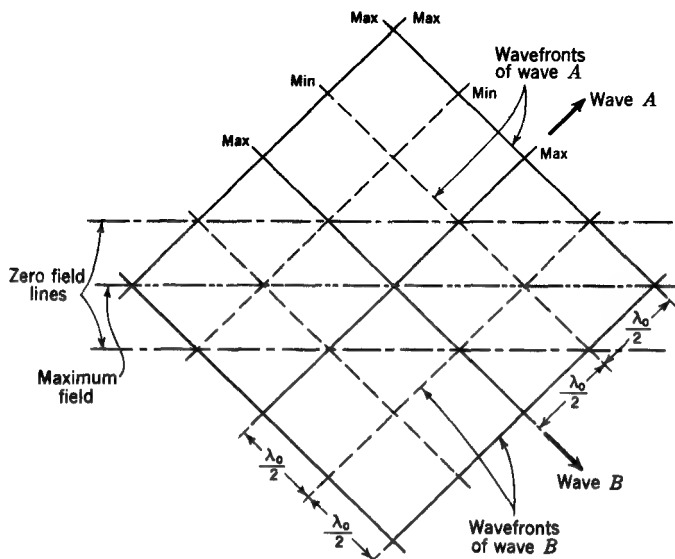


FIGURE 13-28
Two plane TEM waves traveling in free space in different directions.

can also transmit high-order modes, and this type of transmission between the parallel planes serves as a good starting point for our discussion of higher-order modes. Devices which can transmit energy *only* in higher-order modes are usually called *waveguides*.

Consider the higher-order mode where the electric field is everywhere in the y direction, with transmission in the x direction; i.e., the electric field has only an E_y component. Since E_y is transverse to the direction of transmission, this mode is designated a *transverse electric* (TE) mode. Although \mathbf{E} is everywhere transverse, \mathbf{H} has longitudinal, as well as transverse, components. Assuming perfectly conducting sheets, boundary conditions require that E_y vanish *at* the sheets. However, E_y need not be zero at points removed from the sheets. It is possible to determine the properties of a TE wave of the type under discussion by regarding it as being made up of two plane TEM waves reflected obliquely back and forth between the sheets.

First, however, consider the situation that exists when two plane TEM waves of the same frequency traveling in free space intersect at an angle, as suggested in Fig. 13-28. It is assumed that the waves are linearly polarized with \mathbf{E} normal to the page. Wavefronts, or surfaces of constant phase, are indicated for the two waves.

The solid lines (marked "max") show where the field is a maximum with \mathbf{E} directed out from the page. These lines may be regarded as representing the crests of

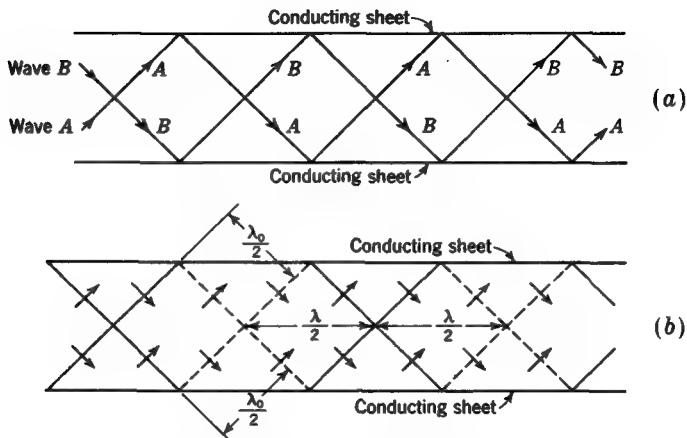


FIGURE 13-29

(a) Wave paths and (b) wavefronts between infinite parallel conducting sheets acting as a waveguide.

the waves. The dashed lines (marked "min") show where the field is a minimum, i.e., where \mathbf{E} is of maximum absolute magnitude but directed into the page. These lines may be regarded as representing the troughs of the waves. Wherever the crest of one wave coincides with the trough of the other wave there is cancellation, and the resultant \mathbf{E} at that point is zero. Wherever crest coincides with crest or trough with trough there is reinforcement, and the resultant \mathbf{E} at that point doubles. Referring to Fig. 13-28, it is therefore apparent that at all points along the dash-dot lines the field is always zero, while along the line indicated by dash and double dots the field will be reinforced and will have its maximum value.

Since \mathbf{E} is zero along the dash-dot lines, boundary conditions will be satisfied at plane, perfectly conducting sheets placed along these lines normal to the page. The waves, however, will now be reflected at the sheets with an angle of reflection equal to the angle of incidence, and waves incident from the outside will not penetrate to the region between the sheets. But if two plane waves (A and B) are launched between the sheets from the left end, they will travel to the right via multiple reflections between the sheets, as suggested by the wave paths in Fig. 13-29a (see also Sec. 12-4). The wavefronts (normal to the wave paths) for these waves are as indicated in Fig. 13-29b. Here the field between the sheets is the same as in Fig. 13-28, with solid lines indicating that \mathbf{E} is outward (a maximum) and dashed lines that \mathbf{E} is inward (a minimum). At the sheets the resultant \mathbf{E} is always zero.

Although the two component waves we have been considering are plane TEM-mode waves, the *resultant wave* belongs to a higher-order TE mode. It is an

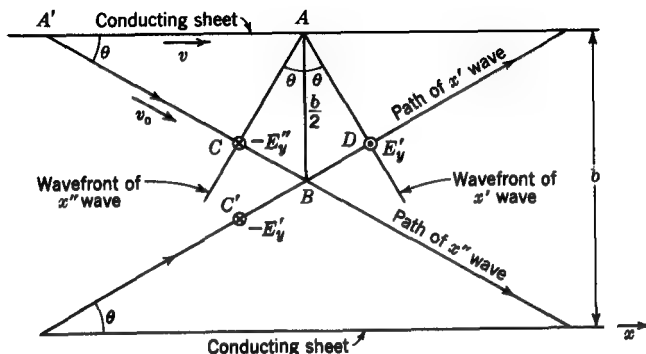


FIGURE 13-30

Component waves between infinite-parallel-plane conducting sheets acting as a waveguide.

important property of the TE-mode wave that it will not be transmitted unless the wavelength is sufficiently short. The critical wavelength at which transmission is no longer possible is called the *cutoff wavelength*. It is possible by a very simple analysis, which will now be given, to calculate the cutoff wavelength as a function of the sheet spacing.

Referring to Fig. 13-30, let the TE wave be resolved into two component TEM waves traveling in the x' and x'' directions. These directions make an angle θ with the conducting sheets (and the x axis). The electric field is in the y direction (normal to the page). The spacing between the sheets is b . From Fig. 13-30 we note that E'_y of the x' wave and E''_y of the x'' wave cancel at a point such as A at the conducting sheet and reinforce at point B midway between the sheets provided that the distance

$$CB = BD = C'B = \frac{\lambda_0}{4} \quad (1)$$

where λ_0 is the wavelength of the TEM wave in unbounded space filled with the same medium as between the sheets. Thus, if E''_y is into the page (negative) at the point C and E'_y is out of the page (positive) at the point D , the two waves will cancel at A . They will also reinforce at B since by the time the field $-E''_y$ moves from C to B the field $-E'_y$ will have moved from C' to B . More generally we can write

$$CB = \frac{n\lambda_0}{4} \quad (2)$$

where n is an integer (1, 2, 3, ...).† It follows that

$$AB \sin \theta = \frac{b}{2} \sin \theta = \frac{n\lambda_0}{4} \quad (3)$$

or

$$\lambda_0 = \frac{2b}{n} \sin \theta \quad (4)$$

where λ_0 = wavelength, m

b = spacing of conducting sheets, m

$n = 1, 2, 3, \dots$

θ = angle between component wave direction and conducting sheets

According to (4), we note that for a given sheet separation b , the longest wavelength that can be transmitted in a higher-order mode occurs when $\theta = 90^\circ$. This wavelength is the cutoff wavelength λ_{oc} of the higher order mode. Thus, for $\theta = 90^\circ$,

$$\lambda_{oc} = \frac{2b}{n} \quad (5)$$

Each value of n corresponds to a particular higher-order mode. When $n = 1$, we find that

$\lambda_{oc} = 2b$

(6)

This is the longest wavelength which can be transmitted between the sheets in a higher-order mode. That is, the spacing b must be at least $\lambda/2$ for a higher-order mode to be transmitted.

When $n = 1$, the wave is said to be the lowest of the higher-order types. When $n = 2$, we have the next higher-order mode and for this case

$$\lambda_{oc} = b \quad (7)$$

Thus the spacing b must be at least 1λ for the $n = 2$ mode to be transmitted. For $n = 3$, $\lambda_{oc} = \frac{2}{3}b$, etc.

Introducing (5) in (4) yields $\sin \theta = \lambda_0/\lambda_{oc}$, or

$$\theta = \sin^{-1} \frac{\lambda_0}{\lambda_{oc}} \quad (8)$$

† For n even, the field halfway between the sheets is zero, with maximum fields either side of the centerline.

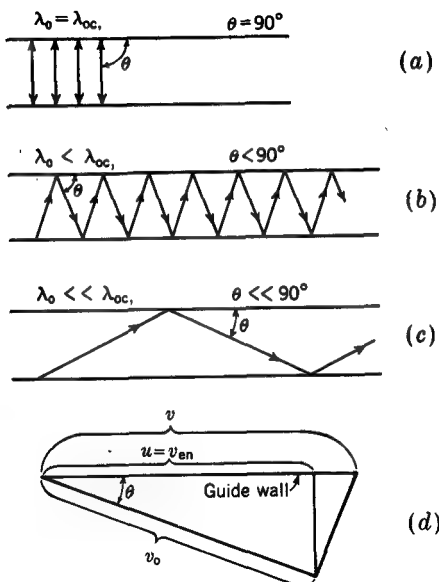


FIGURE 13-31

(a) to (c) Reflection of waves between walls of waveguide. (d) Triangle showing relative magnitude of phase velocity v , group velocity u , and energy velocity v_{en} in the guide, to phase velocity v_0 of the component wave (equal to phase velocity of wave in an unbounded medium).

Hence, at cutoff for any mode ($\lambda_0 = \lambda_{0c}$) the angle $\theta = 90^\circ$. Under these conditions the component waves for this mode are reflected back and forth between the sheets, as in Fig. 13-31a, and do not progress in the x direction. Hence there is a standing wave between the sheets, and no energy is propagated. If the wavelength λ_0 is slightly less than λ_{0c} , θ is less than 90° and the wave progresses in the x direction although making many reflections from the sheets, as in Fig. 13-31b. As the wavelength is further reduced, θ becomes less, as in Fig. 13-31c, until at very short wavelengths the transmission for this mode approaches the conditions in an unbounded medium.

It is apparent from Fig. 13-30 that a constant-phase point of the TE wave moves in the x direction with a velocity v that is greater than that of the component waves. The phase velocity v_0 of the component TEM waves is the same as for a wave in an unbounded medium of the same kind as fills the space between the conducting sheets. That is,

$$v_0 = \frac{I}{\sqrt{\mu\epsilon}} \quad (\text{m s}^{-1}) \quad (9)$$

where μ = permeability of medium, H m^{-1}
 ϵ = permittivity of medium, F m^{-1}

From Fig. 13-30 it follows that

$$\frac{v_0}{v} = \frac{A'C}{A'A} = \cos \theta \quad (10)$$

or

$$v = \frac{v_0}{\cos \theta} = \frac{1}{\sqrt{\mu\epsilon}} \cos \theta \quad (\text{ms}^{-1}) \quad (11)$$

According to (11), the phase velocity v of a TE wave approaches an infinite value as the wavelength is increased toward the cutoff value. On the other hand, v approaches the phase velocity v_0 in an unbounded medium as the wavelength becomes very short. Thus, the phase velocity of a higher-order mode wave in the guide formed by the sheets is always equal to or greater than the velocity in an unbounded medium. The energy, however, is propagated with the velocity of the zigzag component wave. Thus $v_{en} = v_0 \cos \theta$. Accordingly, the energy velocity v_{en} is always equal to or less than the velocity in an unbounded medium.[†] When, for instance, the wavelength approaches cutoff, the phase velocity becomes infinite while the energy velocity approaches zero. This is another way of saying that the wave degenerates into a standing wave and does not propagate energy at the cutoff wavelength or longer wavelengths. The relative magnitudes of the various velocities are shown by the triangle in Fig. 13-31d.

Since the wavelength is proportional to the phase velocity, the wavelength λ of the higher-order mode in the guide is given in terms of the wavelength λ_0 in an unbounded medium by

$$\lambda = \frac{\lambda_0}{\cos \theta} \quad (12)$$

The phase velocity and group (or energy) velocity in the guide as a function of θ are shown in Fig. 13-32. As θ approaches 90° , the phase velocity becomes infinite while the energy velocity goes to zero. The velocities are expressed in terms of the phase velocity v_0 of the wave in an unbounded medium. The situation here is analogous to the action of water waves at a breakwater. Thus, as suggested in Fig. 13-33, a water plume moves along the breakwater where a wave crest (constant-

[†] The waveguide behaves like a lossless dispersive medium. It follows that

$$u = v_{en} = \frac{v_0^2}{v}$$

where u = group velocity

v_{en} = energy velocity

v_0 = phase velocity in unbounded medium

v = phase velocity in guide

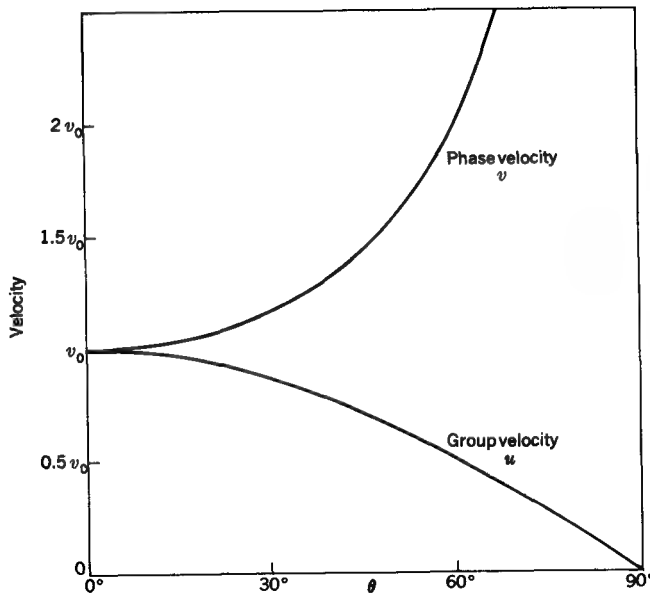


FIGURE 13-32

Phase and group velocity as a function of wave angle. The ordinate gives v and u in terms of the velocity v_0 for a wave in an unbounded medium of the same type as fills the waveguide.

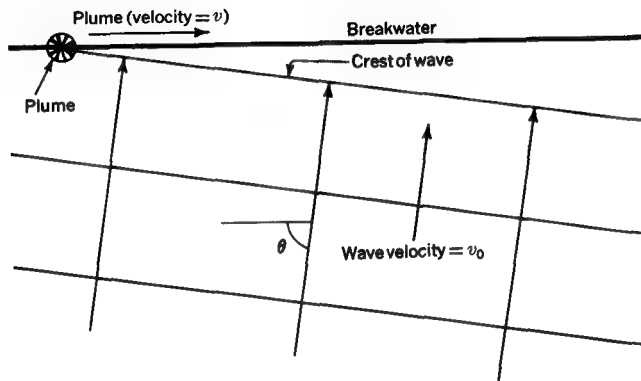


FIGURE 13-33

A plume of water moves along a breakwater with a phase velocity v that is greater than the wave velocity v_0 .

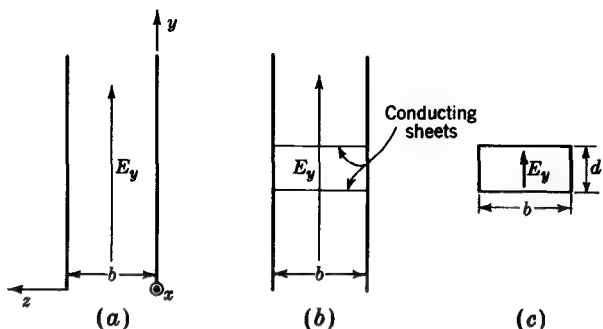


FIGURE 13-34

(a) Infinite-parallel-plane transmission line acting as a waveguide for TE wave. \mathbf{E} is in y direction with wave in x direction (out of page). The guide consists of two parallel conducting sheets separated by a distance b . (b) Additional sheets introduced normal to E_y . (c) Hollow rectangular waveguide.

phase point) strikes the breakwater. The velocity v of the plume is greater than the wave velocity v_0 . The plume velocity can become infinite if θ becomes 90° .

The infinite-parallel-plane transmission line we have been considering is an idealization and not a type to be applied in practice. Actual waveguides for higher-order modes usually take the form of a single hollow conductor. The hollow rectangular guide is a common form. The above analysis for the infinite-parallel-plane transmission line is of practical value, however, because the properties of TE-mode waves, such as are discussed above, are the same in a rectangular guide of width b as between two infinite parallel planes separated by a distance b . This follows from the fact that if infinitely conducting sheets are introduced normal to \mathbf{E} between the parallel planes, the field is not disturbed. Thus, if a TE-mode wave with electric field in the y direction is traveling in the x direction, as indicated in Fig. 13-34a, the introduction of sheets normal to E_y , as in Fig. 13-34b, does not disturb the field. The conducting sheets now form a complete enclosure of rectangular shape. Proceeding a step further, let the sheets beyond the rectangular enclosure be removed, leaving the hollow rectangular waveguide shown in Fig. 13-34c. The cutoff wavelengths for the TE modes as given by (5) for the infinite-parallel-plane line also apply for this rectangular guide of width b . For the type of TE modes we have thus far considered (E_y component only) the dimension d (Fig. 13-34c) is not critical.

Although the above simple analysis yields information about cutoff wavelength, phase velocity, etc., it gives little information concerning the field configuration and fails to consider more complex higher-order modes of wave transmission in which, for example, \mathbf{E} is transverse but with both y and z components. To obtain complete

information concerning the waves in a hollow waveguide, we shall solve the wave equation subject to the boundary conditions for the guide. This is done for the hollow rectangular guide in the next section.

13-15 THE HOLLOW RECTANGULAR WAVEGUIDE†

In Sec. 13-14 certain properties of an infinite-parallel-plane transmission line and of a hollow rectangular guide were obtained by considering that the higher-mode wave consists of two plane TEM component waves and then applying the boundary condition that the tangential component of the resultant \mathbf{E} must vanish at the perfectly conducting walls of the guide. This method could be extended to provide more complete information about the waves in a hollow waveguide. However, in this section we shall use another approach, which involves the solution of the wave equation subject to the above-mentioned boundary condition for the tangential component of \mathbf{E} .

In this method we start with Maxwell's equations and develop a wave equation in rectangular coordinates. This choice of coordinates is made in order that the boundary conditions for the rectangular guide can be easily applied later. The restrictions are then introduced of harmonic variation with respect to time and a wave traveling in the x direction (direction of guide). Next a choice is made of the type of higher-order mode of transmission to be analyzed. Thus we may consider a transverse electric (TE) wave for which $E_x = 0$ or a transverse magnetic (TM) wave for which $H_x = 0$. If, for example, we select the TE type, we know that there must be an H_x component, since a higher-mode wave always has a longitudinal field component and E_x being zero means that H_x must have a value. It is then convenient to write the remaining field components in terms of H_x . Next a solution of a scalar-wave equation in H_x is obtained that fits the boundary conditions of the rectangular guide. This solution is substituted back into the equations for the other field components (E_y , E_z , H_y , and H_z). In this way we end up with a set of equations giving the variation of each field component with respect to space and time. This method of solution is very general and can be applied to many problems.

† Rayleigh, Lord, On the Passage of Electric Waves through Tubes, *Phil. Mag.*, 43: 125-132 (February 1897); L. J. Chu and W. L. Barrow, Electromagnetic Waves in Hollow Metal Tubes of Rectangular Cross Section, *Proc. IRE*, 26: 1520-1555 (December 1938). A general dyadic Green's function method for solving transmission line and waveguide problems is developed by C-T Tai, "Dyadic Green's Functions in Electromagnetic Theory," International Textbook Company, Scranton, Pa., 1971.

We shall develop the method in detail for TE waves in a hollow rectangular waveguide. First, however, the procedure will be outlined in step form as follows:

- 1 Start with Maxwell's equations.
- 2 Apply restriction of harmonic variation with respect to time.
- 3 Apply restriction of harmonic variation and attenuation with respect to x .
- 4 Select the type or mode of wave transmission (TE in this case; so $E_x = 0$ and $H_x \neq 0$).
- 5 Find equations for other four field components (E_y , E_z , H_y , and H_z) in terms of H_x .
- 6 Develop scalar wave equation for H_x .
- 7 Solve this wave equation for H_x subject to boundary conditions of waveguide.
- 8 Substitute H_x back into equations of step 5, giving a set of equations expressing each field component as a function of space and time. This constitutes the complete solution of the problem.

Beginning now with step 1 of the procedure, we have from Maxwell's curl equations in rectangular coordinates the following set of six scalar equations:

$$\frac{\partial H_z}{\partial y} - \frac{\partial H_y}{\partial z} - \sigma E_x - \epsilon \frac{\partial E_x}{\partial t} = 0 \quad (1)$$

$$\frac{\partial H_x}{\partial z} - \frac{\partial H_z}{\partial x} - \sigma E_y - \epsilon \frac{\partial E_y}{\partial t} = 0 \quad (2)$$

$$\frac{\partial H_y}{\partial x} - \frac{\partial H_x}{\partial y} - \sigma E_z - \epsilon \frac{\partial E_z}{\partial t} = 0 \quad (3)$$

$$\frac{\partial E_z}{\partial y} - \frac{\partial E_y}{\partial z} + \mu \frac{\partial H_x}{\partial t} = 0 \quad (4)$$

$$\frac{\partial E_x}{\partial z} - \frac{\partial E_z}{\partial x} + \mu \frac{\partial H_y}{\partial t} = 0 \quad (5)$$

$$\frac{\partial E_y}{\partial x} - \frac{\partial E_x}{\partial y} + \mu \frac{\partial H_z}{\partial t} = 0 \quad (6)$$

From Maxwell's divergence equations in rectangular coordinates we have in space free from charge the following two scalar equations:

$$\frac{\partial E_x}{\partial x} + \frac{\partial E_y}{\partial y} + \frac{\partial E_z}{\partial z} = 0 \quad (7)$$

$$\frac{\partial H_x}{\partial x} + \frac{\partial H_y}{\partial y} + \frac{\partial H_z}{\partial z} = 0 \quad (8)$$

Let us assume now that any field component varies harmonically with time and distance and also may attenuate with distance (steps 2 and 3). Thus, confining our attention to waves traveling in the positive x direction, we have, for instance, that the field component E_y is expressed by

$$E_y = E_1 e^{j\omega t - \gamma x} \quad (9)$$

where γ = propagation constant $= \alpha + j\beta$

α = attenuation constant

β = phase constant

When the restriction of (9) is introduced into the equations, (1) to (8) reduce to

$$\frac{\partial H_z}{\partial y} - \frac{\partial H_y}{\partial z} - (\sigma + j\omega\epsilon)E_x = 0 \quad (10)$$

$$\frac{\partial H_x}{\partial z} + \gamma H_z - (\sigma + j\omega\epsilon)E_y = 0 \quad (11)$$

$$-\gamma H_y - \frac{\partial H_x}{\partial y} - (\sigma + j\omega\epsilon)E_z = 0 \quad (12)$$

$$\frac{\partial E_z}{\partial y} - \frac{\partial E_y}{\partial z} + j\omega\mu H_x = 0 \quad (13)$$

$$\frac{\partial E_x}{\partial z} + \gamma E_z + j\omega\mu H_y = 0 \quad (14)$$

$$-\gamma E_y - \frac{\partial E_x}{\partial y} + j\omega\mu H_z = 0 \quad (15)$$

$$-\gamma E_x + \frac{\partial E_y}{\partial y} + \frac{\partial E_z}{\partial z} = 0 \quad (16)$$

$$-\gamma H_x + \frac{\partial H_y}{\partial y} + \frac{\partial H_z}{\partial z} = 0 \quad (17)$$

The above eight equations can be simplified by introducing a series impedance Z and shunt admittance Y , analogous to a transmission line (see Table 13-2), where

$$Z = -j\omega\mu \quad (\Omega \text{ m}^{-1}) \quad (18)$$

$$Y = \sigma + j\omega\epsilon \quad (\text{S m}^{-1}) \quad (19)$$

Substituting these relations in (10) to (17) yields

$$\frac{\partial H_z}{\partial y} - \frac{\partial H_y}{\partial z} - YE_x = 0 \quad (20)$$

$$\frac{\partial H_x}{\partial z} + \gamma H_z - YE_y = 0 \quad (21)$$

$$-\gamma H_y - \frac{\partial H_x}{\partial y} - YE_z = 0 \quad (22)$$

$$\frac{\partial E_z}{\partial y} - \frac{\partial E_y}{\partial z} - ZH_x = 0 \quad (23)$$

$$\frac{\partial E_x}{\partial z} + \gamma E_z - ZH_y = 0 \quad (24)$$

$$-\gamma E_y - \frac{\partial E_x}{\partial y} - ZH_z = 0 \quad (25)$$

$$-\gamma E_x + \frac{\partial E_y}{\partial z} + \frac{\partial E_z}{\partial z} = 0 \quad (26)$$

$$-\gamma H_x + \frac{\partial H_y}{\partial y} + \frac{\partial H_z}{\partial z} = 0 \quad (27)$$

These are the general equations for the steady-state field of a wave traveling in the x direction. No restrictions have as yet been made on the mode of the wave or the shape of the guide. We are now ready to proceed with **step 4** and introduce the condition for a TE wave that $E_x = 0$. The equations then reduce to

$$\frac{\partial H_z}{\partial y} - \frac{\partial H_y}{\partial z} = 0 \quad (28)$$

$$\frac{\partial H_x}{\partial z} + \gamma H_z - YE_y = 0 \quad (29)$$

$$-\gamma H_y - \frac{\partial H_x}{\partial y} - YE_z = 0 \quad (30)$$

$$\frac{\partial E_z}{\partial y} - \frac{\partial E_y}{\partial z} - ZH_x = 0 \quad (31)$$

$$\gamma E_z - ZH_y = 0 \quad (32)$$

$$-\gamma E_y - ZH_z = 0 \quad (33)$$

$$\frac{\partial E_y}{\partial z} + \frac{\partial E_z}{\partial z} = 0 \quad (34)$$

$$-\gamma H_x + \frac{\partial H_y}{\partial y} + \frac{\partial H_z}{\partial z} = 0 \quad (35)$$

Proceeding to **step 5**, let us rewrite these equations so that each field component is expressed in terms of H_x . To do this, we note from (32) and (33) that

$$\frac{E_z}{H_y} = -\frac{E_y}{H_z} = \frac{Z}{\gamma} \quad (\Omega) \quad (36)$$

The ratio E_z/H_y or E_y/H_z is a quantity which corresponds, in the case of a waveguide, to the characteristic impedance of a transmission line. Since (36) involves only transverse field components, it may be called the *transverse-wave impedance* Z_{yz} of the waveguide. Thus

$$Z_{yz} = \frac{E_y}{H_z} = -\frac{E_z}{H_y} = -\frac{Z}{\gamma} = \frac{j\omega\mu}{\gamma} \quad (\Omega) \quad (37)$$

Introducing (37) into (30) and solving for H_y yields

$$H_y = \frac{-1}{\gamma - YZ_{yz}} \frac{\partial H_x}{\partial y} \quad (38)$$

In a like manner we have, from (29),

$$H_z = \frac{-1}{\gamma - YZ_{yz}} \frac{\partial H_x}{\partial z} \quad (39)$$

Now, substituting (39) into (37), we obtain

$$E_y = \frac{Z_{yz}}{\gamma - YZ_{yz}} \frac{\partial H_x}{\partial z} \quad (40)$$

and substituting (38) into (37) gives

$$E_z = \frac{-Z_{yz}}{\gamma - YZ_{yz}} \frac{\partial H_x}{\partial y} \quad (41)$$

Equations (38) to (41) express the four transverse field components in terms of H_x . This completes step 5.

Proceeding now to step 6, we can obtain a wave equation in H_x by taking the y derivative of (38) and the z derivative of (39) and substituting both in (35). This yields

$$-\gamma H_x - \frac{1}{\gamma - YZ_{yz}} \left(\frac{\partial^2 H_x}{\partial y^2} + \frac{\partial^2 H_x}{\partial z^2} \right) = 0 \quad (42)$$

or $\frac{\partial^2 H_x}{\partial y^2} + \frac{\partial^2 H_x}{\partial z^2} + \gamma(\gamma - YZ_{yz})H_x = 0 \quad (43)$

Putting $k^2 = \gamma(\gamma - YZ_{yz})$ reduces (43) to

$$\frac{\partial^2 H_x}{\partial y^2} + \frac{\partial^2 H_x}{\partial z^2} + k^2 H_x = 0 \quad (44)$$

This is a partial differential equation of the second order and first degree. It is a scalar wave equation in H_x . It applies to a TE wave in a guide of any cross-sectional shape. This completes step 6.

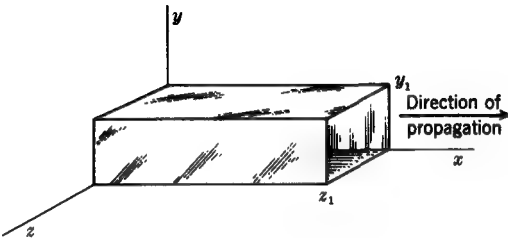


FIGURE 13-35
Coordinates for hollow rectangular waveguide.

Step 7 is to find a solution of (44) that satisfies the boundary conditions for the waveguide under consideration, which is a hollow rectangular type, as shown in Fig. 13-35. The width of the guide is z_1 , and the height is y_1 . Assuming that the walls are perfectly conducting, the tangential component of \mathbf{E} must vanish at the guide surface. Thus, at the sidewalls E_y must be zero, and at the top and bottom surfaces E_z must be zero. The problem now is to find a solution of (44) subject to these boundary conditions. The method of separation of variables can be used in obtaining the solution. Thus, H_x in (44) is a function of y and z . Hence we may seek a solution of the form

$$H_x = YZ \quad (45)$$

where Y = a function of y only, that is, $Y = f(y)$

Z = a function of z only†

Substituting (45) in (44) gives

$$Z \frac{d^2 Y}{dy^2} + Y \frac{d^2 Z}{dz^2} + k^2 YZ = 0 \quad (46)$$

Dividing by YZ to separate variables gives

$$\frac{1}{Y} \frac{d^2 Y}{dy^2} + \frac{1}{Z} \frac{d^2 Z}{dz^2} = -k^2 \quad (47)$$

The first term is a function of y alone, the second term is a function of z alone, while k^2 is a constant. For the two terms (each involving a different independent variable) to equal a constant requires that each term be a constant. Thus we can write

$$\frac{1}{Y} \frac{d^2 Y}{dy^2} = -A_1 \quad (48)$$

† Sometimes the notation $f(y)$ or $Y(y)$ is used to represent a function of y only and $f(z)$ or $Z(z)$ a function of z only. However, to simplify notation, the symbols Y and Z are used in Eqs. (45) to (55), inclusive, to indicate functions only of y or z , respectively. Y and Z in these equations should not be confused with admittance and impedance, for which these symbols are also used.

and

$$\frac{1}{Z} \frac{d^2 Z}{dz^2} = -A_2 \quad (49)$$

where A_1 and A_2 are constants. It follows that

$$A_1 + A_2 = k^2 \quad (50)$$

Equations (48) and (49) each involve but one independent variable. A solution of (48) is

$$Y = c_1 \sin b_1 y \quad (51)$$

Substituting (51) in (48) yields

$$b_1 = \sqrt{A_1} \quad (52)$$

Hence (51) is a solution provided (52) is fulfilled. Another solution is

$$Y = c_2 \cos b_1 y \quad (53)$$

If (51) and (53) are each a solution for Y , their sum is also a solution, or

$$Y = c_1 \sin \sqrt{A_1} y + c_2 \cos \sqrt{A_1} y \quad (54)$$

In the same manner a solution may be written for Z as

$$Z = c_3 \sin \sqrt{A_2} z + c_4 \cos \sqrt{A_2} z \quad (55)$$

Substituting (54) and (55) into (45), we obtain the solution for H_x as

$$H_x = c_1 c_3 \sin \sqrt{A_1} y \sin \sqrt{A_2} z + c_2 c_3 \cos \sqrt{A_1} y \sin \sqrt{A_2} z \\ + c_1 c_4 \sin \sqrt{A_1} y \cos \sqrt{A_2} z + c_2 c_4 \cos \sqrt{A_1} y \cos \sqrt{A_2} z \quad (56)$$

Substituting (56) in (40) and (41) and introducing the boundary conditions that $E_y = 0$ at $z = 0$ and $z = z_1$ and $E_z = 0$ at $y = 0$ and $y = y_1$, we find that only the last term of (56) can satisfy the boundary conditions and then only provided that

$$\sqrt{A_1} = \frac{n\pi}{y_1} \quad (57)$$

and

$$\sqrt{A_2} = \frac{m\pi}{z_1} \quad (58)$$

where m and n are integers ($0, 1, 2, 3, \dots$). They may be equal to the same integer or to different integers. The solution for H_x now assumes the form

$$H_x(y,z) = H_0 \cos \frac{n\pi y}{y_1} \cos \frac{m\pi z}{z_1} \quad (59)$$

where $H_0 = c_2 c_4$ = a constant. If (59) is multiplied by a constant factor, it is still a solution. That is, the factor should not involve y or z although it may involve x and the time t . Accordingly, (59) may be multiplied by the exponential factor in (9) since this gives the variation assumed for the fields with respect to x and t . The complete solution for H_x then becomes

$$H_x(y,z,x,t) = H_0 \cos \frac{n\pi y}{y_1} \cos \frac{m\pi z}{z_1} e^{j\omega t - \gamma x} \quad (60)$$

This completes step 7. To perform step 8, Eq. (60) is substituted into (38) through (41), giving the solutions for the transverse field components as

$$H_y = \frac{\gamma H_0}{k^2} \frac{n\pi}{y_1} \sin \frac{n\pi y}{y_1} \cos \frac{m\pi z}{z_1} e^{j\omega t - \gamma x} \quad (61)$$

$$H_z = \frac{\gamma H_0}{k^2} \frac{m\pi}{z_1} \cos \frac{n\pi y}{y_1} \sin \frac{m\pi z}{z_1} e^{j\omega t - \gamma x} \quad (62)$$

$$E_y = \frac{\gamma Z_{yz} H_0}{k^2} \frac{m\pi}{z_1} \cos \frac{n\pi y}{y_1} \sin \frac{m\pi z}{z_1} e^{j\omega t - \gamma x} \quad (63)$$

$$E_z = -\frac{\gamma Z_{yz} H_0}{k^2} \frac{n\pi}{y_1} \sin \frac{n\pi y}{y_1} \cos \frac{m\pi z}{z_1} e^{j\omega t - \gamma x} \quad (64)$$

Equations (60) to (64), to which may be added $E_x = 0$, are the solutions we have sought for the field components of a TE mode in a hollow rectangular guide of width z_1 and height y_1 . This completes step 8†.

Turning our attention now to an interpretation of the solutions for the field components, let us consider the significance of the integers m and n . It is apparent that for $m = 1$ and $n = 0$ we have only three field components H_x , H_z , and E_y and, further, that each of these components has no variation with respect to y but each has a half-cycle variation with respect to z . For example, E_y has a sinusoidal variation across the guide (in the z direction), being a maximum in the center and zero at the walls, and has no variation as a function of y .

† Note that to be explicit in (61) to (64) we could write $H_y(y,z,x,t)$ instead of H_y , $H_z(y,z,x,t)$ instead of H_z , etc., but for simplicity we do not.

If $m = 2$, there is a variation of two half-cycles (full-cycle variation) of each field component as a function of z . When $n = 1$, there is a half-cycle variation of each field component with respect to y . Hence we may conclude that the value of m or n indicates the number of half-cycle variations of each field component with respect to z and y , respectively. Each combination of m and n values represents a different field configuration or mode in the guide. Since we are dealing here with TE modes, it is convenient to designate them by adding the subscript mn so that, in general, any TE mode can be designated by the notation TE_{mn} , where m is the number of half-cycle variations in the z direction (usually taken as the larger transverse dimension of the guide) and n is the number of half-cycle variations in the y direction (usually taken as the smaller transverse dimension of the guide).

Case 1: TE_{10} mode For this mode $m = 1$ and $n = 0$, and we have, as mentioned above, only three components E_y , H_x , and H_z that are not zero. The six field components for the TE_{10} mode are

$$E_x = 0 \quad \text{TE mode condition}$$

$$E_y = \frac{\gamma Z_{yz} H_0}{k^2} \frac{\pi}{z_1} \sin \frac{\pi z}{z_1} e^{j\omega t - \gamma x} \quad (65)$$

$$E_z = 0$$

$$H_x = H_0 \cos \frac{\pi z}{z_1} e^{j\omega t - \gamma x}$$

$$H_y = 0$$

$$H_z = \frac{\gamma H_0}{k^2} \frac{\pi}{z_1} \sin \frac{\pi z}{z_1} e^{j\omega t - \gamma x}$$

The variation of these components as a function of z is portrayed in Fig. 13-36a. There is no variation with respect to y . This mode has the longest cutoff wavelength of any higher-order mode, and hence the lowest frequency of transmission in a hollow rectangular waveguide must be in the TE_{10} mode. In Fig. 13-37a the field configuration of the TE_{10} mode is illustrated for a guide cross section and in Fig. 13-37b for a longitudinal section of the guide (top view).

Case 2: TE_{20} mode The variation of the field components as a function of z for the TE_{20} mode ($m = 2, n = 0$) is shown in Fig. 13-36b. The field configuration for a TE_{20} mode is shown in cross section in Fig. 13-37c and in longitudinal section (top view) in Fig. 13-37d.

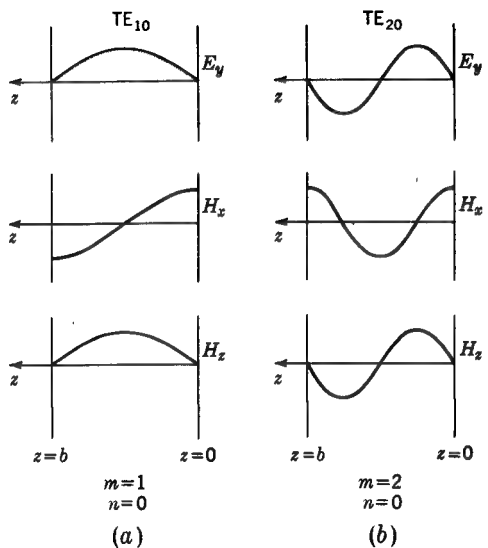


FIGURE 13-36

Variation of field components for TE_{10} and TE_{20} modes in a hollow rectangular waveguide. (Wave traveling out of page.)

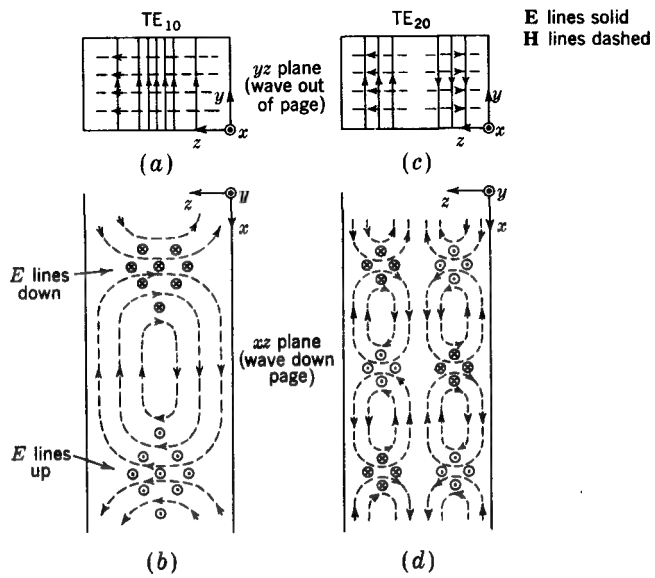


FIGURE 13-37

Field configurations for TE_{10} and TE_{20} modes in a hollow rectangular waveguide.

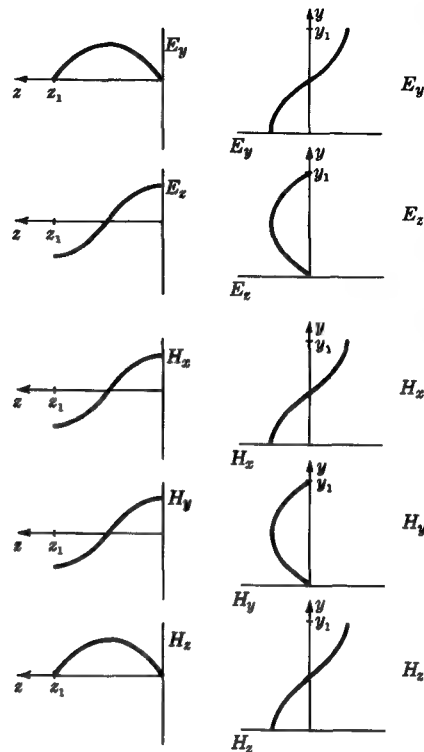


FIGURE 13-38
Variation of field components for TE_{11} mode in a square waveguide. (Wave traveling out of page.)

Case 3: TE_{11} mode For this mode $m = 1, n = 1$, and the field components are given by

$$E_x = 0 \quad \text{TE mode condition}$$

$$E_y = \frac{\gamma Z_{yz} H_0}{k^2} \frac{\pi}{z_1} \cos \frac{\pi y}{y_1} \sin \frac{\pi z}{z_1} e^{j\omega t - \gamma x}$$

$$E_z = -\frac{\gamma Z_{yz} H_0}{k^2} \frac{\pi}{y_1} \sin \frac{\pi y}{y_1} \cos \frac{\pi z}{z_1} e^{j\omega t - \gamma x}$$

$$H_x = H_0 \cos \frac{\pi y}{y_1} \cos \frac{\pi z}{z_1} e^{j\omega t - \gamma x} \quad (66)$$

$$H_y = \frac{\gamma H_0}{k^2} \frac{\pi}{y_1} \sin \frac{\pi y}{y_1} \cos \frac{\pi z}{z_1} e^{j\omega t - \gamma x}$$

$$H_z = \frac{\gamma H_0}{k^2} \frac{\pi}{z_1} \cos \frac{\pi y}{y_1} \sin \frac{\pi z}{z_1} e^{j\omega t - \gamma x}$$

For this mode five field components have a value, only E_x being everywhere and always zero. The variation of the five field components with respect to z and y is shown in Fig. 13-38. It is assumed that the guide has a square cross section ($y_1 = z_1$). The field configuration for the TE₁₁ mode in a square guide is illustrated in cross section (end view) in Fig. 13-39a and in longitudinal section (side view) in Fig. 13-39b.

The solution we have obtained tells us what modes are possible in the hollow rectangular waveguide. However, the particular mode or modes that are actually present in any case depend on the guide dimensions, the method of exciting the guide, and the irregularities or discontinuities in the guide. The resultant field in the guide is equal to the sum of the fields of all modes present.

Returning now to a consideration of the general significance of the solution, we have from (50), (57), and (58) that

$$\left(\frac{n\pi}{y_1}\right)^2 + \left(\frac{m\pi}{z_1}\right)^2 = k^2 \quad (67)$$

From (43), (18), and (19), k^2 is given by

$$k^2 = \gamma^2 - j\omega\mu(\sigma + j\omega\epsilon) \quad (68)$$

Assuming a lossless dielectric medium in the guide, we can put $\sigma = 0$. Then equating (67) and (68) and solving for γ yields

$$\gamma = \sqrt{\left(\frac{n\pi}{y_1}\right)^2 + \left(\frac{m\pi}{z_1}\right)^2 - \omega^2\mu\epsilon} \quad (69)$$

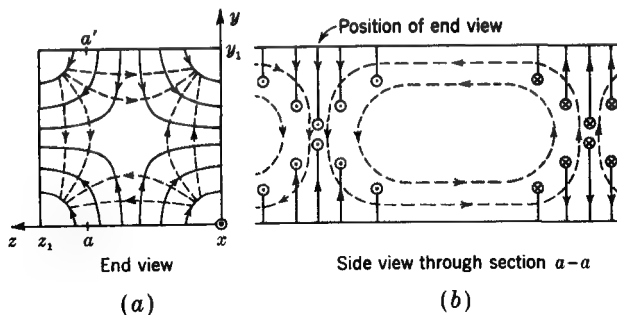


FIGURE 13-39

Field configurations for TE₁₁ mode in a square waveguide. E lines are solid, and H lines are dashed.

At sufficiently low frequencies the last term in (69) is smaller than the sum of the first two terms under the square-root sign. It follows that for this condition γ is real and therefore that the wave is attenuated. Under this condition it is said that the wave (or mode) is not propagated.

At sufficiently high frequencies the last term in (69) is larger than the sum of the first two terms under the square-root sign. Under this condition γ is imaginary, and therefore the wave is propagated without attenuation.

At some intermediate frequency the right-hand side of (69) is zero, and hence $\gamma = 0$. This frequency is called the *cutoff frequency* for the mode under consideration. At frequencies higher than cutoff this mode propagates without attenuation, while at frequencies lower than cutoff the mode is attenuated.

To summarize the three cases:

- 1 At low frequencies, ω small, γ real, guide opaque, wave does not propagate
- 2 At an intermediate frequency, ω intermediate, $\gamma = 0$, transition condition, cutoff
- 3 At high frequencies, ω large, γ imaginary, guide transparent, wave propagates

Referring to (69), it is to be noted that $\sqrt{\omega^2 \mu \epsilon}$ is equal to the phase constant β_0 for a wave traveling in an unbounded medium of the same dielectric material as fills the guide. Thus we can write

$$\gamma = \sqrt{k^2 - \beta_0^2} \quad (\text{m}^{-1}) \quad (70)$$

where $\beta_0 = \sqrt{\omega^2 \mu \epsilon} = 2\pi/\lambda_0$ = phase constant in unbounded medium

λ_0 = wavelength in unbounded medium

$$k = \sqrt{(n\pi/y_1)^2 + (m\pi/z_1)^2}$$

Thus, at frequencies higher than cutoff $\beta_0 > k$, and

$$\gamma = \sqrt{k^2 - \beta_0^2} = j\beta \quad (71)$$

where $\beta = 2\pi/\lambda$ = phase constant in guide, m^{-1}

λ = wavelength in guide, m

At sufficiently high frequencies ($\beta_0 \gg k$) we note that the phase constant β in the guide approaches the phase constant β_0 in an unbounded medium. On the other hand, at frequencies less than cutoff $\beta_0 < k$, and

$$\gamma = \sqrt{k^2 - \beta_0^2} = \alpha \quad (72)$$

where α is the attenuation constant.

At sufficiently low frequencies ($\beta_0 \ll k$) we note that the attenuation constant α approaches a constant value k .

At the cutoff frequency, $\beta_0 = k$, and $\gamma = 0$. Thus, at cutoff

$$\omega^2 \mu \epsilon = \left(\frac{n\pi}{y_1} \right)^2 + \left(\frac{m\pi}{z_1} \right)^2 \quad (73)$$

It follows that the *cutoff frequency* is

$$f_c = \frac{1}{2\sqrt{\mu \epsilon}} \sqrt{\left(\frac{n}{y_1} \right)^2 + \left(\frac{m}{z_1} \right)^2} \quad (\text{Hz}) \quad (74)$$

and the *cutoff wavelength* is

$$\lambda_{oc} = \frac{2\pi}{\sqrt{(n\pi/y_1)^2 + (m\pi/z_1)^2}} = \frac{2}{\sqrt{(n/y_1)^2 + (m/z_1)^2}} \quad (\text{m}) \quad (75)$$

where λ_{oc} is the wavelength in an unbounded medium at the cutoff frequency (or, more concisely, the *cutoff wavelength*).† Equations (74) and (75) give the *cutoff frequency and cutoff wavelength for any TE_{mn} mode in a hollow rectangular guide*. For instance, the cutoff wavelength of a TE₁₀ mode is

$$\lambda_{oc} = 2z_1 \quad (76)$$

This is identical with the value found in Sec. 13-14 since $z_1 = b$.

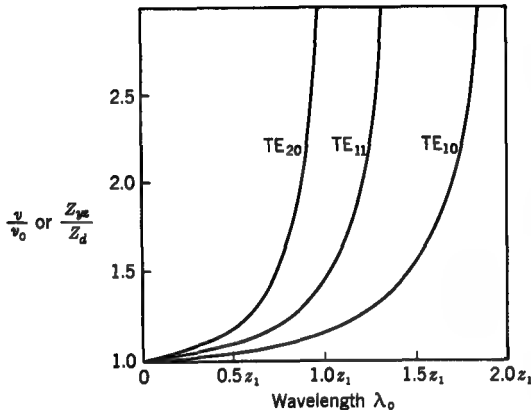
At frequencies above cutoff ($\beta_0 > k$)

$$\beta = \sqrt{\beta_0^2 - k^2} = \sqrt{\omega^2 \mu \epsilon - \left(\frac{n\pi}{y_1} \right)^2 - \left(\frac{m\pi}{z_1} \right)^2} \quad (77)$$

It follows that the *phase velocity* v_p in the guide is equal to

$$v_p = \frac{\omega}{\beta} = \frac{v_0}{\sqrt{1 - (n\lambda_0/2y_1)^2 - (m\lambda_0/2z_1)^2}} \quad (\text{m s}^{-1}) \quad (78)$$

† Note that $k = 2\pi/\lambda_{oc}$. If this value of k is introduced, (71) can be used to relate λ , λ_0 , and λ_{oc} when $\lambda_0 < \lambda_{oc}$.

**FIGURE 13-40**

Relative phase velocity v/v_0 or relative transverse impedance Z_{ys}/Z_d as a function of the wavelength λ_0 for TE modes in a hollow square guide (height y_1 equal to width z_1).

or

$$v_p = \frac{v_0}{\sqrt{1 - (\lambda_0/\lambda_{oc})^2}} \quad (79)$$

where $v_0 = 1/\sqrt{\mu\epsilon}$ = phase velocity in unbounded medium ($= 300 \text{ Mm s}^{-1}$ for air)

λ_0 = wavelength in unbounded medium

λ_{oc} = cutoff wavelength

The ratio v/v_0 as a function of the wavelength λ_0 is shown in Fig. 13-40 for several TE modes in a hollow waveguide of square cross section ($y_1 = z_1$).

In the above analysis there is no attenuation whatsoever at frequencies above cutoff. This results from the assumption of perfectly conducting guide walls and a lossless dielectric medium filling the guide. However, if the walls are not perfectly conducting or the medium is not lossless, or both, there is attenuation.[†]

If the guide is filled with air, the dielectric loss is usually negligible compared with losses in the guide walls, so that the attenuation at frequencies greater than cutoff is mainly determined by the conductivity of the guide walls. The fact that the guide walls are not perfectly conducting means that the tangential component E_t of the electric field is not zero at the walls but has a finite value. However, for walls made of a good conductor, such as copper, E_t will generally be so small that the above analysis (based on $E_t = 0$) is not affected to any appreciable extent. However, as a result of the finite wall conductivity α is not zero. Thus, in most practical problems where the wall conductivity is high (but not infinite) the field configuration in the guide, the

[†] That γ may have both a real and an imaginary part at frequencies greater than cutoff can be shown by solving (68) for γ under these conditions, with σ not equal to zero.

wavelength λ , the phase constant β , the phase velocity v , etc., can all be calculated with high accuracy on the assumption that the walls have infinite conductivity, as done earlier in this section. The small (but not zero) attenuation may then be calculated separately, using (10-19-5) to find the power lost per unit area in the guide wall, it being assumed that the **H**-field distribution is the same as with perfectly conducting walls.

Finally, let us determine the value of the transverse-wave impedance Z_{yz} for TE modes in a rectangular hollow guide. Thus, from (37)

$$Z_{yz} = \frac{j\omega\mu}{\gamma} \quad (80)$$

At frequencies higher than cutoff $\gamma = j\beta$; so

$$Z_{yz} = \frac{\omega\mu}{\beta} = \frac{Z_d}{\sqrt{1 - (\lambda_0/\lambda_{oc})^2}} \quad (\Omega) \quad (81)$$

where Z_d = intrinsic impedance of dielectric medium filling guide

$$= \sqrt{\mu/\epsilon} = 376.7 \Omega \text{ for air}$$

λ_0 = wavelength in unbounded medium

λ_{oc} = cutoff wavelength

The ratio of Z_{yz} (transverse-wave impedance) to Z_d (intrinsic impedance) as a function of the wavelength λ_0 is shown in Fig. 13-40 for several TE modes in a hollow waveguide of square cross section ($y_1 = z_1$).

Thus far only TE-mode waves have been considered. To find the field relations for transverse magnetic (TM) mode waves we proceed precisely as in the eight-step list given earlier in this section except that where TE appears we substitute TM and where E_x appears we substitute H_x , and vice versa. In the TM wave $H_x = 0$, and the longitudinal field component is E_x . This analysis will not be carried through here (see Prob. 13-39). However, it may be mentioned that (75) for the cutoff wavelength applies to both TE and TM waves, as does (78) for the phase velocity, but this is not the case with (81) for the transverse impedance (see Prob. 13-42). The notation for any TM mode, in general, is TM_{mn} , where m and n are integers (1, 2, 3, ...). It is to be noted that neither m nor n may be equal to zero for TM waves. Thus, the lowest-frequency TM wave that will be transmitted by a rectangular waveguide is the TM_{11} mode.

We have seen that each mode of transmission in a waveguide has a particular cutoff wavelength, velocity, and impedance. When the frequency is high enough to

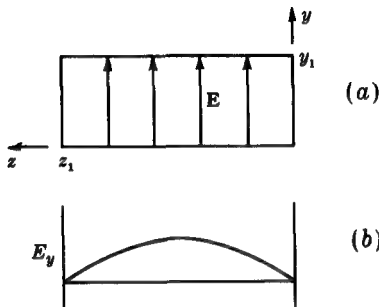


FIGURE 13-41
Rectangular waveguide with TE_{10} mode only.

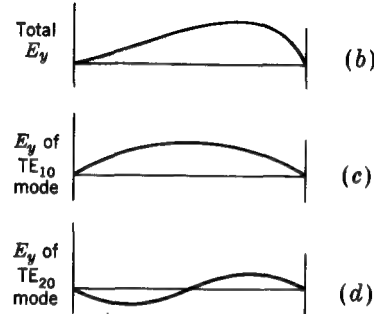
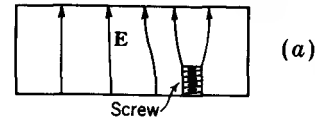


FIGURE 13-42
Rectangular waveguide with TE_{20} mode induced from TE_{10} mode by asymmetrically placed projection (screw).

permit transmission in more than one mode, the resultant field is the sum of the fields of the individual mode fields in the guide.

For example, suppose that a rectangular waveguide, as shown in cross section in Fig. 13-41a, is excited in the TE_{10} mode. The variation of E_y across the guide is sinusoidal, as shown in Fig. 13-41b. Suppose now that z_1 exceeds 1λ , so that the TE_{20} mode can also be transmitted.[†] If only the TE_{10} mode is excited, no TE_{20} will appear provided that the guide is perfectly regular. However, in practice certain asymmetries and irregularities will be present, and these will tend to convert some of the TE_{10} -mode energy into TE_{20} -mode energy. Thus, if an asymmetrically located screw projects into the guide as in Fig. 13-42a, the total E_y field will tend to become asymmetrical, as suggested in Fig. 13-42b. This total field may be resolved into TE_{10} and TE_{20} components as shown in Fig. 13-42c and d. If both TE_{10} and TE_{20} modes can be transmitted, the field in the guide beyond the screw location will have energy in both modes. In effect the screw is a receiving antenna that extracts energy from the incident TE_{10} -mode wave and reradiates it so as to excite the TE_{20} mode. However, if the frequency is decreased so that only the TE_{10} wave can be transmitted, the asymmetric field (Fig. 13-42b) will exist only in the vicinity of the screw and farther down the

[†] But $y_1 < \lambda_0/2$, so that no TE_{01} mode (E in z direction) is transmitted.

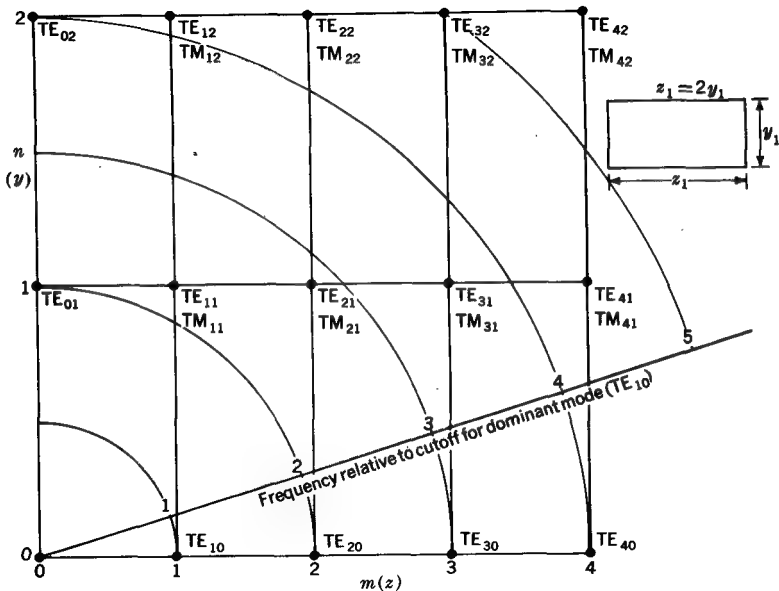


FIGURE 13-43

Possible TE and TM modes in a hollow rectangular waveguide as a function of frequency. At three times the cutoff frequency for the TE_{10} mode there are seven modes which will pass (see text at end of Sec. 13-15) and one mode (TE_{30}) at cutoff.

guide the field will be entirely in the TE_{10} mode. To avoid the problems of multiple-mode transmission, a waveguide is usually operated so that only one mode is capable of transmission.[†] For instance, to ensure transmission only in the TE_{10} mode, z_1 must be less than 1λ and y_1 less than $\lambda/2$. But to allow transmission of the TE_{10} mode, z_1 must exceed $\lambda/2$. Hence z_1 must be between $\lambda/2$ and 1λ , and a value of 0.7λ is often used since this is well below 1λ and yet enough more than $\lambda/2$ so that the velocity and transverse impedance values are not too critical a function of frequency. We recall that at cutoff ($z_1 = \lambda/2$) the velocity and impedance approach infinite values. The height y_1 may be as small as desired without preventing transmission of the TE_{10} mode. Too small a value of y_1 , however, increases attenuation (because of power lost in the guide walls) and also reduces the power-handling capabilities of the guide. It is often the practice to make $y_1 = z_1/2$. Many TE_{mn} and TM_{mn} modes of a rectangular guide for which $y_1 = z_1/2$ are shown in Fig. 13-43. The slant scale gives the frequency

[†] The lowest-frequency mode that a guide can transmit is called the *dominant mode*.

relative to the cutoff frequency for the dominant mode (TE_{10}). Thus, if the frequency is 3 times this value, we note from Fig. 13-43 that the following modes will be transmitted: TE_{10} , TE_{01} , TE_{20} , TE_{11} , TM_{11} , TE_{21} , and TM_{21} . An additional mode (TE_{30}) is at its cutoff frequency.

The relations derived in this section for a hollow rectangular waveguide (see Fig. 13-35) are summarized in Table 13-6.

Table 13-6 RELATIONS FOR TE_{mn} MODES IN HOLLOW RECTANGULAR WAVEGUIDES†

Name of relation	Relation
Cutoff frequency	$f_c = \frac{1}{2\sqrt{\mu\epsilon}} \sqrt{\left(\frac{n}{y_1}\right)^2 + \left(\frac{m}{z_1}\right)^2}$ (Hz)
Cutoff wavelength	$\lambda_{oc} = \frac{2}{\sqrt{(n/y_1)^2 + (m/z_1)^2}}$ (m)
Wavelength in guide	$\lambda_g = \frac{\lambda_0}{\sqrt{1 - (\lambda_0/\lambda_{oc})^2}}$ (m)
Phase velocity	$v_p = \frac{v_0}{\sqrt{1 - (n\lambda_0/2y_1)^2 - (m\lambda_0/2z_1)^2}}$ $= \frac{v_0}{\sqrt{1 - (\lambda_0/\lambda_{oc})^2}}$ $= \frac{v_0}{\sqrt{1 - (f_c/f)^2}}$ (m s ⁻¹) where $v_0 = 1/\sqrt{\mu\epsilon}$
Transverse-wave impedance	$Z_{yx} = \frac{Z_d}{\sqrt{1 - (n\lambda_0/2y_1)^2 - (m\lambda_0/2z_1)^2}}$ $= \frac{Z_d}{\sqrt{1 - (\lambda_0/\lambda_{oc})^2}}$ $= \frac{Z_d}{\sqrt{1 - (f_c/f)^2}}$ (Ω) where $Z_d = \sqrt{\mu/\epsilon}$

† All the relations also apply to TM_{mn} modes except for the transverse-wave impedance relation. The velocity and impedance relations involving $(\lambda_0/\lambda_{oc})^2$ apply not only to rectangular guides but also to TE modes in hollow single-conductor guides of any shape.

13-16 THE HOLLOW CYLINDRICAL WAVEGUIDE†

Consider the problem of describing wave propagation in a hollow (circular) cylindrical waveguide of radius r_0 . This problem is most easily handled with a cylindrical coordinate system, as shown in Fig. 13-44. The procedure is similar to that used in the preceding section for the rectangular waveguide. We assume time-harmonic variation, perfectly conducting walls, and a lossless interior medium ($\sigma = 0$) containing no charge ($\rho = 0$).

Maxwell's two curl equations yield six scalar equations, and Maxwell's two divergence equations yield two scalar equations. In cylindrical coordinates these are as follows:

$$\frac{1}{r} \frac{\partial E_z}{\partial \phi} + \gamma E_\phi - ZH_r = 0 \quad (1)$$

$$-\gamma E_r - \frac{\partial E_z}{\partial r} - ZH_\phi = 0 \quad (2)$$

$$\frac{\partial E_\phi}{\partial r} + \frac{1}{r} E_\phi - \frac{1}{r} \frac{\partial E_r}{\partial \phi} - ZH_z = 0 \quad (3)$$

$$\frac{1}{r} \frac{\partial H_z}{\partial \phi} + \gamma H_\phi - YE_r = 0 \quad (4)$$

$$-\gamma H_r - \frac{\partial H_z}{\partial r} - YE_\phi = 0 \quad (5)$$

$$\frac{\partial H_\phi}{\partial r} + \frac{1}{r} H_\phi - \frac{1}{r} \frac{\partial H_r}{\partial \phi} - YE_z = 0 \quad (6)$$

$$\frac{\partial E_r}{\partial r} + \frac{E_r}{r} + \frac{1}{r} \frac{\partial E_\phi}{\partial \phi} - \gamma E_z = 0 \quad (7)$$

$$\frac{\partial H_r}{\partial r} + \frac{H_r}{r} + \frac{1}{r} \frac{\partial H_\phi}{\partial \phi} - \gamma H_z = 0 \quad (8)$$

where Z = series impedance = $-j\omega\mu$, $\Omega \text{ m}^{-1}$

Y = shunt admittance = $j\omega\epsilon$, $\Omega \text{ m}^{-1}$

$E_\phi = E_1 e^{j\omega t - \gamma z}$, etc.

$\gamma = \alpha + j\beta$ = propagation constant

These eight relations are the general equations for the steady-state field of a wave traveling in the z direction as expressed in cylindrical coordinates. At this point

† W. L. Barrow, Transmission of Electromagnetic Waves in Hollow Tubes of Metal, *Proc. IRE*, 24: 1298-1328 (October 1936); G. C. Southworth, Some Fundamental Experiments with Wave Guides, *ibid.*, 25: 807-822 (July 1937).

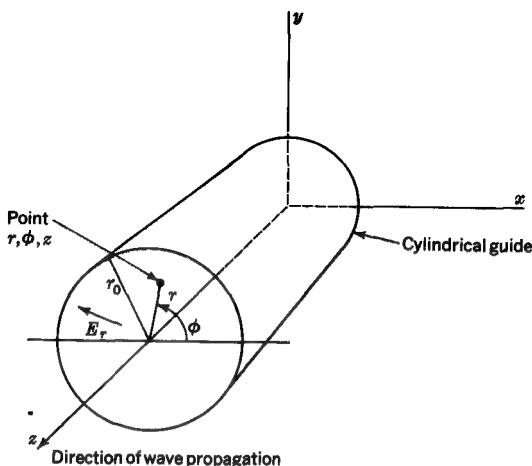


FIGURE 13-44
Coordinates for hollow cylindrical waveguide.

we can limit the problem to either a TE wave or a TM wave. Selecting the TE wave and proceeding in the same manner as for a rectangular waveguide following (13-15-27), we find the solution for the H_z component to be

$$H_z = c_1 c_3 \sin n\phi J_n(kr) + c_2 c_3 \cos n\phi J_n(kr) \\ + c_1 c_4 \sin n\phi N_n(kr) + c_2 c_4 \cos n\phi N_n(kr) \quad (9)$$

where $k = \sqrt{\gamma^2 + ZY} = \sqrt{\gamma^2 + \omega^2 \mu \epsilon}$

n = integer

Equation (9) is a solution for H_z , but any term or combination of terms is also a solution. The appropriate solution must satisfy the boundary conditions, which are that $E_\phi = 0$ at $r = r_0$ and that the fields in the guide are finite.† The Neumann function becomes infinite at $r = 0$ and so is not a suitable solution. Thus, (9) can be reduced to

$$H_z = H_0 (\cos n\phi + j \sin n\phi) J_n(kr) \quad (10)$$

where

$$H_0 = c_2 c_3 = \frac{c_1 c_3}{j}$$

† The boundary condition $E_\phi = 0$ at $r = r_0$ can also be expressed

$$\hat{n} \times \mathbf{E} = 0 \quad \text{at } r = r_0$$

When the sine term is dropped, (10) simplifies to

$$H_z = H_0 \cos n\phi J_n(kr) \quad (11)$$

This choice means that H_z is a maximum where $\phi = 0$ and $\phi = \pi$ and is zero where $\phi = \pi/2$ and $3\pi/2$ provided $n \neq 0$. If we had dropped the cosine term instead of the sine term, the conditions for H_z would be rotated 90° in the guide. Assuming that the field orientation is arbitrary, either solution would suffice (but both would be required for a circularly polarized wave in the guide). The six components are†

$$E_r = \frac{n\gamma H_0 Z_{r\phi}}{k^2 r} \sin n\phi J_n(kr) e^{j\omega t - \gamma z} = Z_{r\phi} H_\phi \quad (12)$$

$$E_\phi = \frac{\gamma H_0 Z_{r\phi}}{k^2} \cos n\phi \frac{dJ_n(kr)}{dr} e^{j\omega t - \gamma z} = -Z_{r\phi} H_r \quad (13)$$

$$E_z = 0 \quad \text{TE-mode condition} \quad (14)$$

$$H_r = \frac{-\gamma H_0}{k^2} \cos n\phi \frac{dJ_n(kr)}{dr} e^{j\omega t - \gamma z} \quad (15)$$

$$H_\phi = \frac{n\gamma H_0}{k^2 r} \sin n\phi J_n(kr) e^{j\omega t - \gamma z} \quad (16)$$

$$H_z = H_0 \cos n\phi J_n(kr) e^{j\omega t - \gamma z} \quad (17)$$

The variation of the fields with time and distance has also been expressed explicitly (proportional to $e^{j\omega t - \gamma z}$). Alternative expressions for E_ϕ and H_r can be written using the recurrence relations (see Appendix, Sec. A-10):

$$\frac{dJ_n(kr)}{dr} = k \left[\frac{n}{kr} J_n(kr) - J_{n+1}(kr) \right] \quad (18)$$

Equations (12) to (17) are general expressions for a TE-mode wave in a cylindrical guide. However, the boundary condition $E_\phi = 0$ at $r = r_0$ has not been imposed. Applying this condition requires that

$$\frac{dJ_n(kr)}{dr} = 0 \quad \text{at } r = r_0 \quad (18a)$$

and hence that

$$k = \frac{k'_{nr}}{r_0} \quad (19)$$

† In (12) and (13)

$$Z_{r\phi} = \frac{E_r}{H_\phi} = -\frac{E_\phi}{H_r} = -\frac{Z}{\gamma} = \frac{j\omega\mu}{\gamma} \quad (\Omega)$$

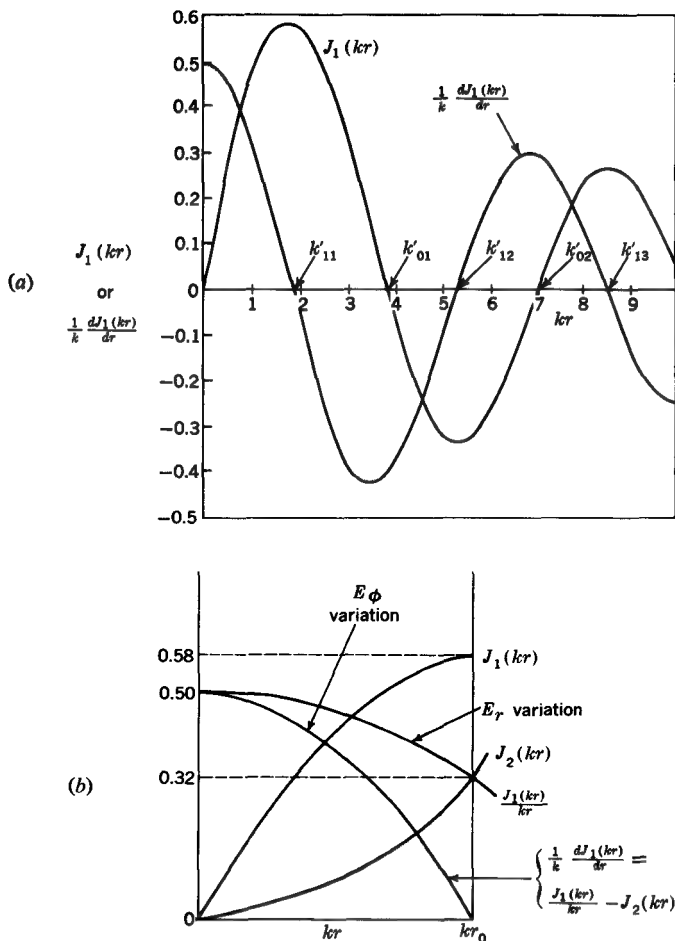


FIGURE 13-45

(a) First-order Bessel function and its derivative as a function of kr . (b) Bessel function relations involved in determining E_r and E_ϕ variation for TE_{11} mode.

where k'_{nr} is the r th root of the derivative of the n th-order Bessel function. The situation is illustrated in Fig. 13-45a for $n = 1$. The first three roots of the derivative of the first-order Bessel function occur at $kr_0 = k'_n = 1.84, 5.33$, and 8.54 . Thus, the roots are $k'_{11} = 1.84$, $k'_{12} = 5.33$, and $k'_{13} = 8.54$, corresponding to wave modes TE_{11} , TE_{12} , and TE_{13} in the guide. In general, a TE mode in a cylindrical guide is designated TE_{nr} , where the subscript n indicates the order of the Bessel function and r indicates the rank of the root. For TE_{01} and TE_{02} modes, $n = 0$ and the roots of (18) for this

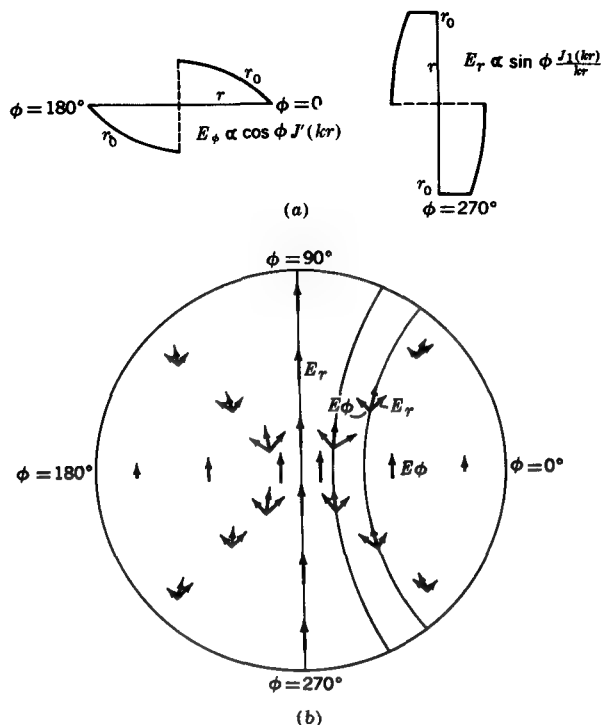


FIGURE 13-46

(a) Variation of electric field components E_r and E_ϕ with radial distance r for TE_{11} mode in cylindrical waveguide. (b) Electric field vectors for TE_{11} mode in cylindrical waveguide with component fields E_r and E_ϕ .

case are $k'_{nr} = 3.832$ and 7.016 . These are the same as the zeros of $J_1(kr)$. See Fig. 13-45a.

Referring to (13), the variation of E_ϕ with r (at $\phi = 0$) for the TE_{11} mode is as shown in Fig. 13-45b. From (13) the variation of E_r with r (at $\phi = 90^\circ$) is as given by the curve for $J_1(kr)/kr$. The amplitudes of the two field components, E_r and E_ϕ , can thus be represented by curves, as in Fig. 13-46a, or by arrows, as in Fig. 13-46b. Note that E_ϕ is a maximum at $\phi = 0^\circ$ and 180° and zero at $\phi = 90^\circ$ and 270° while E_r is a maximum at $\phi = 90^\circ$ and 270° and zero at $\phi = 0^\circ$ and 180° . Note also that at the center of the guide ($r = 0$) E_r and E_ϕ both have the same direction and amplitude. When the E_r and E_ϕ components are added, the total electric field for the TE_{11} in the cylindrical guide is as suggested by the heavy arrows in Fig. 13-46b with the direction of the total electric field as indicated by the curved lines (see also Fig. 13-47a). In a

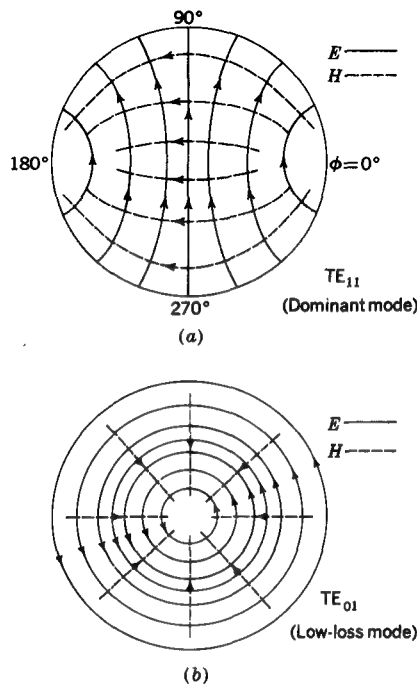


FIGURE 13-47
 Electric field lines (solid) and magnetic field lines (dashed) in hollow cylindrical waveguide for (a) TE₁₁ (dominant mode) and (b) TE₀₁ (low-loss mode).

similar manner the transverse magnetic field configuration for the TE₁₁ mode can be deduced from the variation of H_r and H_ϕ with r [from (15) and (16)], with the result shown in Fig. 13-47a.

The solution we have obtained for the TE₁₁ mode is but one of an infinite number of possible wave modes in a cylindrical guide. The particular mode or modes that are actually present in any case depend on the guide dimensions, the method of exciting the guide, and discontinuities in the guide. The resultant field in the guide is equal to the sum of the fields of all modes present. The field configuration for the TE₀₁ mode is illustrated in Fig. 13-47b.

Thus far only TE modes in a cylindrical guide have been considered. To find the field relations for TM-mode waves we let $H_z = 0$ in (1) to (8) and express the remaining field components in terms of the longitudinal field E_z . A wave equation in E_z is developed and solved to satisfy the boundary condition, which requires that $J_n(kr) = 0$ at $r = r_0$. The first three roots k_{nr} ($= kr_0$) for the case $n = 1$ are $k_{11} = 3.832$, $k_{12} = 7.016$, and $k_{13} = 10.173$. The fields for TM modes are given in Prob. 13-40.

The roots (or eigenvalues) for the TM modes written k_{nr} (unprimed) correspond to zero values of the Bessel function $J_n(kr)$, whereas the roots for the TE modes written

k'_{nr} (primed) correspond to zero values of the derivative (with respect to r) of the Bessel function. The relations for TE and TM modes are displayed in Fig. 13-48 and their numerical values listed in Table 13-7.

As seen in Fig. 13-48, the TE_{01} mode should logically be designated the TE_{02} mode since it refers to the *second* root of the derivative of the Bessel function. Likewise the TE_{02} mode should properly be designated TE_{03} . The first root is $k'_{nr} = 0$, corresponding to a trivial (nonexistent) mode. This inconsistency in the nomenclature for cylindrical guides has been pointed out by C-T Tai,[†] but the common and incorrect designations persist and Table 13-7 and Fig. 13-48 conform to this common usage.

Let us now examine the conditions necessary for propagation inside a cylindrical waveguide. Substituting (19) into $k = \sqrt{\gamma^2 + \omega^2 \mu \epsilon}$ and solving for the propagation constant, we obtain

$$\boxed{\gamma = \pm \sqrt{\left(\frac{k'_{nr}}{r_0}\right)^2 - \omega^2 \mu \epsilon} = \alpha + j\beta} \quad (20)$$

Table 13-7 CYLINDRICAL WAVEGUIDE MODES

Mode designation	Eigenvalues		Cutoff wavelength, λ_{oc}
	k'_{nr}	k_{nr}	
TM_{01}		2.405	$2.61r_0$
TE_{01} (low loss)	3.832		$1.64r_0$
TM_{02}		5.520	$1.14r_0$
TE_{02}	7.016		$0.89r_0$
TE_{11} (dominant)	1.840		$3.41r_0$
TM_{11}		3.832	$1.64r_0$
TE_{12}	5.330		$1.18r_0$
TM_{12}		7.016	$0.89r_0$
TE_{21}	3.054		$2.06r_0$
TM_{21}		5.135	$1.22r_0$
TE_{22}	6.706		$0.94r_0$
TE_{31}	4.201		$1.49r_0$
TM_{31}		6.379	$0.98r_0$
TE_{41}	5.318		$1.18r_0$
TM_{41}		7.588	$0.83r_0$
TE_{51}	6.416		$0.98r_0$

[†] C-T Tai, On the Nomenclature of TE_{01} modes in a Cylindrical Waveguide, *Proc. IRE*, 49: 1442-1443 (September 1961).

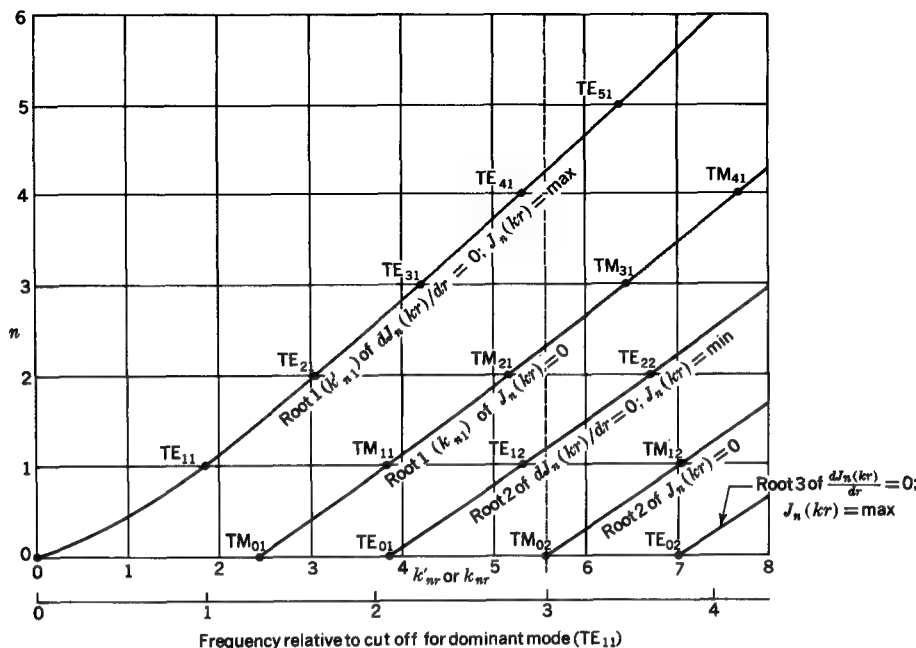


FIGURE 13-48

Possible TE and TM modes in a hollow cylindrical waveguide as a function of frequency. (After C-T Tai.) At 3 times the cutoff frequency for the TE_{11} mode there are 9 modes which will pass (see text paragraph preceding Sec. 13-17) and one mode (TM_{02}) at cutoff.

As in the rectangular guide, there are three conditions:

- 1 At low frequencies, ω small, γ real, guide opaque (wave does not propagate).
- 2 At an intermediate frequency, ω intermediate, $\gamma = 0$, transition condition (cutoff).
- 3 At high frequencies, ω large, γ imaginary, guide transparent (wave propagates).

Putting $\gamma = 0$ in (20), we find for the *cutoff frequency* and *cutoff wavelength*

$$f_c = \frac{1}{2\pi\sqrt{\mu\epsilon}} \frac{k'_{nr}}{r_0} \quad (\text{Hz}) \quad (21)$$

$$\lambda_{oc} = \frac{2\pi r_0}{k'_{nr}} \quad (\text{m})$$

(22)

For the TE_{11} mode $k'_{nr} = k'_{11} = 1.84$, so that $\lambda_{oc} = 2\pi r_0/1.84 = 3.41r_0$. Thus, the cutoff wavelength for the TE_{11} mode corresponds to a wavelength 3.41 times the radius of the guide. The cutoff wavelengths for various modes in a cylindrical guide are listed in Table 13-7.

At frequencies above cutoff

$$\beta = \sqrt{\omega^2 \mu \epsilon - \left(\frac{k'_{nr}}{r_0}\right)^2} \quad (\text{rad m}^{-1}) \quad (23)$$

From (23) and (22) we get for the *wavelength in the guide* (in z direction)

$$\lambda_g = \frac{\lambda_0}{\sqrt{1 - (\lambda_0/\lambda_{oc})^2}} \quad (\text{m})$$

(24)

where λ_0 = wavelength in unbounded medium of same type that fills guide, m

λ_{oc} = cutoff wavelength, m

For the *phase velocity in the guide* ($v_p = f\lambda_g$) we obtain

$$v_p = \frac{\omega}{\beta} = \frac{v_0}{\sqrt{1 - (\lambda_0/\lambda_{oc})^2}} \quad (\text{m s}^{-1})$$

(25)

where $v_0 = 1/\sqrt{\mu \epsilon}$

Equations (24) and (25) are identical to those derived earlier for the rectangular waveguide (see Table 13-6). They also apply to waves in hollow guides of any cross section.

It will be noted that the roots k'_{nr} (also called *eigenvalues*) are not regularly spaced, in contrast to the case for the rectangular guide. Table 13-7 gives the roots and cutoff wavelengths for some TE and TM modes in a cylindrical guide. These modes are also illustrated in Fig. 13-48. The TE_{11} mode will propagate at a lower frequency than any other mode (including TM modes) and hence is called the *dominant mode* for a cylindrical guide. The TE_{01} mode is of interest because of its low attenuation characteristics in practical guides having finite wall conductivity. For this mode the attenuation decreases monotonically with increasing frequency (see Sec. 13-19).

Referring to Fig. 13-48, we note that if the frequency is 3 times that required to pass the dominant mode (TE_{11}), the guide will pass the following modes (to the left of the dashed line in Fig. 13-48): TE_{11} , TM_{01} , TE_{21} , TM_{11} , TE_{01} , TE_{31} , TM_{21} , TE_{12} , and TE_{41} . An additional mode (TM_{02}) is at its cutoff frequency.

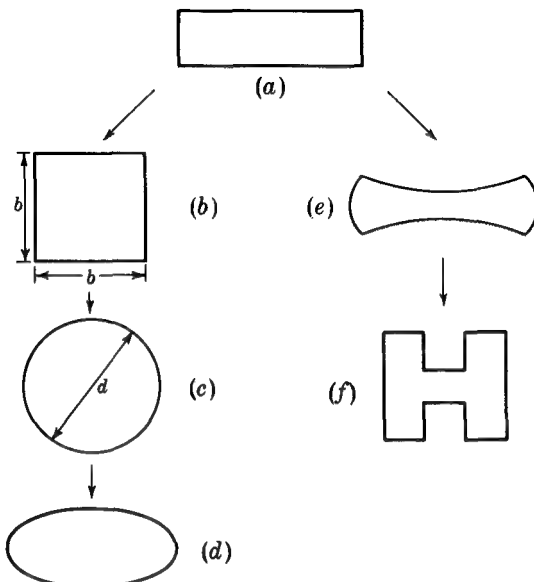


FIGURE 13-49

Forms of hollow single-conductor waveguides showing how square (b), cylindrical (c), and elliptical (d) shaped waveguides may be derived from rectangular type at (a). Types (e) and (f) may also be derived from (a).

13-17 HOLLOW WAVEGUIDES OF OTHER CROSS SECTION

In earlier sections we considered rectangular and cylindrical waveguides. These are only two of an infinite variety of forms in which single-conductor hollow waveguides may be made. For example, the waveguide could have an elliptical[†] cross section, as in Fig. 13-49d, or a reentrant[‡] cross section, as in 13-49e.

All these forms and many others may be regarded as derivable from the rectangular type (Fig. 13-49a). Thus the square cross section (Fig. 13-49b) is a special case of the rectangular guide. By bending out the walls the square guide can be transformed to the circular shape (Fig. 13-49c). By flattening the circular guide the elliptical form of Fig. 13-49d is obtained. On the other hand, by bending the top and bottom surfaces of the rectangular waveguide inward the form shown in Fig. 13-49e is obtained. A still further modification is the reentrant form in Fig. 13-49f. The value of regarding these as related forms is that often certain properties of a guide of a

[†] L. J. Chu, Electromagnetic Waves in Hollow Elliptic Pipes of Metal, *J. Appl. Phys.*, 9 (September 1938).

[‡] S. B. Cohn, Properties of Ridge Wave Guide, *Proc. IRE*, 35: 783-789 (August 1947).

particular shape can be interpolated approximately from the known properties of waveguides of closely related shape.

For example, the longest wavelength that the square guide (Fig. 13-49b) will transmit is equal to $2b$. This is for the TE_{10} mode. This information can be used to predict with fair accuracy the longest wavelength that a circular guide can transmit. Thus, if the cross-sectional area of the square guide is taken equal to the area of the circular guide,

$$b^2 = \pi \left(\frac{d}{2}\right)^2 \quad (1)$$

where d is the diameter of the circular guide. Now $\lambda_{oc} = 2b$ for the square waveguide or $b = \lambda_{oc}/2$, and so we have

$$\left(\frac{\lambda_{oc}}{2}\right)^2 = \left(\frac{d}{2}\right)^2 \quad (2)$$

or

$$\lambda_{oc} = \sqrt{\pi} d = 1.77d = 3.54r \quad (3)$$

as the cutoff wavelength for a circular waveguide of diameter d or radius r . This approximate value is only 4 percent greater than the exact value of $3.41r$ (see Table 13-7).

The procedure for carrying out a complete analysis of the properties of a waveguide of any shape is formally the same as in the preceding sections for the rectangular and circular waveguides. It is usually most convenient, however, to set up the equations in a coordinate system such that the waveguide surfaces can be specified by a fixed value of a coordinate. Thus, as we have seen, a rectangular guide is conveniently handled with rectangular coordinates, the guide surfaces being specified by $y = 0$, $y = y_1$, $z = 0$, and $z = z_1$. Likewise, a circular waveguide is readily analyzed using cylindrical coordinates, the guide surface being specified by $r = r_0$. Referring to Fig. 13-49d and e, these shapes can be analyzed using elliptical-hyperbolic coordinates. However, if the guide surface cannot be specified in a simple manner, the application of the boundary condition ($E_t = 0$) may be very difficult.

13-18 ATTENUATION AT FREQUENCIES LESS THAN CUTOFF

It has been shown that at frequencies less than cutoff, waves are not transmitted through hollow single-conductor guides but are attenuated. Let us now calculate the magnitude of this attenuation. From (13-15-72) the attenuation constant for a rectangular guide at frequencies less than cutoff is

$$\alpha = \sqrt{\left(\frac{n\pi}{y_1}\right)^2 + \left(\frac{m\pi}{z_1}\right)^2 - \left(\frac{2\pi}{\lambda_0}\right)^2} \quad (1)$$

Noting (13-15-75), we can reexpress this as

$$\alpha = \frac{2\pi}{\lambda_0} \sqrt{\left(\frac{\lambda_0}{\lambda_{oc}}\right)^2 - 1} = \beta_0 \sqrt{\left(\frac{\lambda_0}{\lambda_{oc}}\right)^2 - 1} \quad (\text{Np m}^{-1}) \quad (2)$$

where λ_0 = wavelength in unbounded medium, m

λ_{oc} = cutoff wavelength, m

The attenuation constant α as given in (2) applies not only to rectangular guides but to hollow single-conductor guides of any cross-sectional shape.

If the frequency is much less than cutoff ($\lambda_0 \gg \lambda_{oc}$), Eq. (2) reduces to the approximate relation

$$\alpha \approx \frac{2\pi}{\lambda_{oc}} \quad (\text{Np m}^{-1}) \quad (3)$$

where λ_{oc} is the cutoff wavelength in meters. Since, in dealing with voltage, 1 Np = 8.68 dB,†

$$\alpha \approx \frac{2\pi \times 8.69}{\lambda_{oc}} = \frac{54.6}{\lambda_{oc}} \quad (\text{dB m}^{-1}) \quad (4)$$

EXAMPLE A certain waveguide has a cutoff wavelength λ_{oc} of 100 mm. Find the attenuation per meter along the guide for an applied wavelength λ_0 of 1 m.

SOLUTION Since $\lambda_0 \gg \lambda_{oc}$, Eq. (3) or (4) can be used, yielding

$$\alpha = 20\pi \text{ Np m}^{-1}, \text{ or } 546 \text{ dB m}^{-1}$$

This is a very high rate of attenuation, the applied field falling to a negligible value in a very short distance.

A simple attenuator operating at frequencies less than cutoff is illustrated in longitudinal section in Fig. 13-50. A metal tube, acting as a waveguide, has loops arranged at each end, as shown, to couple from coaxial transmission lines into and out of the waveguide. One of the loops is mounted on a movable plunger so that the distance between the loops is variable. If the applied wavelength λ_0 is much longer than the cutoff wavelength λ_{oc} of the guide and the loops are not in too close proximity, the attenuation is as given by (3) or (4). For instance, if $\lambda_{oc} = 100$ mm and λ_0 is much greater (1 m or more), the attenuation increases 5.45 dB per centimeter of outward movement of the plunger. This type of attenuator is very useful but has the

† Note that a 1 neper (1 Np) attenuation means a reduction to $1/e$ of the original value. Conversely, an increase of 1 Np means an increase to $e (= 2.7183)$ times the original value. Hence, for voltages 1 Np is equal to $20 \log e = 8.69$ dB.

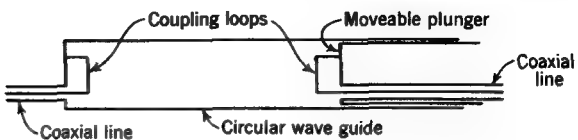


FIGURE 13-50

Attenuator for use at frequencies less than cutoff.

disadvantage of a high insertion loss, i.e., a large initial attenuation when inserted in a coaxial line. Since $\beta = 0$, there is no change in phase with change in plunger position.

13-19 ATTENUATION AT FREQUENCIES GREATER THAN CUTOFF

If the waveguide has perfectly conducting walls and the medium filling the guide is lossless, there is no attenuation at frequencies greater than cutoff. Thus, $\alpha = 0$, and from (13-15-71) we have for a rectangular guide that

$$\gamma = j\beta = \sqrt{\left(\frac{n\pi}{y_1}\right)^2 + \left(\frac{m\pi}{z_1}\right)^2 - \left(\frac{2\pi}{\lambda_0}\right)^2} \quad (1)$$

or

$$\beta = \frac{2\pi}{\lambda_0} \sqrt{1 - \left(\frac{\lambda_0}{\lambda_{oc}}\right)^2} = \beta_0 \sqrt{1 - \left(\frac{\lambda_0}{\lambda_{oc}}\right)^2} \quad (2)$$

The phase constant β as given in (2) applies not only to rectangular guides but to hollow single-conductor guides of any cross-sectional shape.

The behavior of the phase constant β for this case and for the case discussed in Sec. 13-18 is compared on the composite graph in Fig. 13-51. Here the propagation constant γ is shown as ordinate vs. λ_0 in an unbounded medium as abscissa. The real part of $\gamma (= \alpha)$ is plotted as the solid curve above the x axis and the imaginary part ($= \beta$) as the dashed curve below the axis. At very short wavelengths ($\lambda_0 \rightarrow 0$), α is zero, and β approaches an infinite value that is equal to β_0 for an unbounded medium. As λ_0 increases, β decreases until at cutoff ($\lambda_0 = \lambda_{oc}$) β is zero. At still longer wavelengths, β remains zero, but α does not. At sufficiently long wavelengths ($\lambda_0 \gg \lambda_{oc}$), α approaches a value of $2\pi/\lambda_{oc}$ as indicated. This diagram applies to lossless hollow single-conductor guides with cross sections of any shape.

Actual guides are not lossless, so that α is not zero for $\lambda_0 < \lambda_{oc}$, as indicated in Fig. 13-51. However, for air-filled guides of a good conducting material, such as copper, β is substantially as indicated for $\lambda_0 < \lambda_{oc}$, while α is small but not necessarily

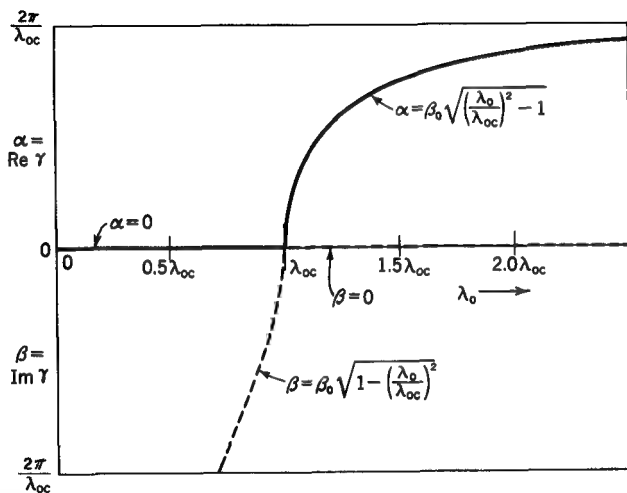


FIGURE 13-51

Composite graph showing attenuation constant α and phase constant β for a lossless hollow single-conductor waveguide as a function of the wavelength λ_0 in an unbounded medium. At wavelengths less than the cutoff wavelength (λ_{oc}) there is no attenuation ($\alpha = 0$) but a phase shift β . At wavelengths longer than cutoff there is no phase shift ($\beta = 0$) but an attenuation α .

negligible. To calculate α for this case, we note (see Fig. 13-52) that the average power in the guide varies with the distance x in the direction of transmission as given by

$$P = P_0 e^{-2\alpha x} \quad (W) \quad (3)$$

where P_0 = average power at reference point ($x = 0$), W

x = distance in direction of transmission through guide, m

The factor 2 in the exponent is present because power is proportional to field squared. It follows that

$$\alpha = \frac{1}{2} \frac{-dP/dx}{P} \quad (\text{Np m}^{-1}) \quad (4)$$

In (4), $-dP/dx$ represents the decrease in power per unit distance along the guide at a particular location, while P is the power transmitted through the guide at that location.[†]

Thus, in words the attenuation constant in nepers per unit distance is expressed by

$$\alpha = \frac{\text{power lost per unit distance}}{\text{twice the power transmitted}}$$

[†] It is to be noted that the attenuation in this case is due to an actual power loss (joule heating of guide walls), whereas at frequencies less than cutoff no joule-heating effect is involved, the attenuation being due to the inability of the guide to transmit the higher-order mode (wave reflected).

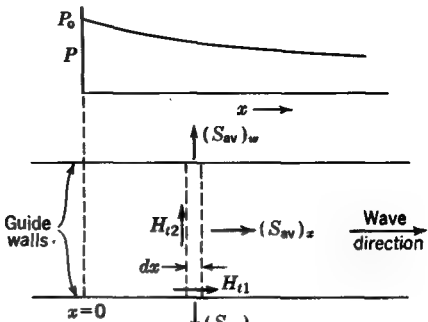


FIGURE 13-52

Power lost in walls of waveguide results in attenuation.

If the medium filling the guide is lossless, the decrease in power per unit distance is equal to the power lost per unit distance in the walls of the guide. This is

$$-\frac{dP}{dx} = \frac{1}{dx} \iint (S_{av})_w ds = \int (S_{av})_w dl \quad (5)$$

where $(S_{av})_w$ is the average Poynting vector into the wall (average with respect to time). The surface integral in (5) is taken over a strip of length dx of the interior surface of the waveguide (Fig. 13-52). The line integral in (5) is taken around the inside of the guide (same path as that for strip). In general, the average Poynting vector is

$$\mathbf{S}_{av} = \frac{1}{2} \operatorname{Re} \mathbf{E} \times \mathbf{H}^* \quad (6)$$

Since \mathbf{E} and \mathbf{H} are normal, the magnitude of the average Poynting vector into the conducting wall medium is (see Fig. 13-52)

$$(S_{av})_w = \frac{1}{2} \operatorname{Re} H_{t1} H_{t1}^* Z_c = \frac{1}{2} |H_{t1}|^2 \operatorname{Re} Z_c \quad (7)$$

where $|H_{t1}|$ = absolute value (or magnitude) of component of \mathbf{H} tangent to conducting surface of guide walls

$\operatorname{Re} Z_c$ = real part of intrinsic impedance of conducting wall medium = $\sqrt{\mu\omega/2\sigma}$
Introducing (7) in (5) yields

$$-\frac{dP}{dx} = \frac{\operatorname{Re} Z_c}{2} \int |H_{t1}|^2 dl \quad (8)$$

Now the power traveling through the guide (in x direction) is

$$P = \iint (S_{av})_x ds \quad (\text{W}) \quad (9)$$

where in this case the surface integral is taken over the guide cross section. It follows that

$$P = \frac{1}{2} \operatorname{Re} Z_{yz} \iint |H_{t2}|^2 ds \quad (10)$$

where $|H_{t2}|$ = absolute value of component of \mathbf{H} tangent to a cross-sectional plane through guide (Fig. 13-52)

$\text{Re } Z_{yz}$ = real part of transverse impedance of guide

Therefore, the attenuation constant α is, in general, given by

$$\boxed{\alpha = \frac{\text{Re } Z_c \int |H_{t1}|^2 dl}{2 \text{Re } Z_{yz} \iint |H_{t2}|^2 ds} \quad (\text{Np m}^{-1})} \quad (11)$$

where $\text{Re } Z_c$ = real part of intrinsic impedance of guide walls (conductor)

$\text{Re } Z_{yz}$ = real part of transverse impedance of guide

$|H_{t1}|$ = absolute value of component of \mathbf{H} tangent to conducting surface of guide walls (integrated around interior surface of guide)

$|H_{t2}|$ = absolute value of component of \mathbf{H} tangent to plane of cross section through guide (integrated over cross-sectional area) (Fig. 13-52)

Equation (11) applies to any mode in any guide. For each mode the attenuation constant must be calculated using (11), with values of $|H_{t1}|$ and $|H_{t2}|$ corresponding to the field distribution for that mode. If the guide walls are of good conducting material, we may assume, with but little error, that the \mathbf{H} -field distribution used in (11) is the same as for perfectly conducting walls. The following example illustrates an application of (11) to a simple problem.

EXAMPLE 1 Find the attenuation constant for a 300-MHz TEM wave in an infinite-parallel-plane transmission line with a spacing between planes of 100 mm. The planes or walls are made of copper, and the medium between the planes is air.

SOLUTION For a TEM wave the transverse impedance equals the intrinsic impedance; so (11) becomes

$$\alpha = \frac{2 \text{Re } Z_c \int_0^{y_1} |H_{t1}|^2 dy}{2 \text{Re } Z_d \int_0^{y_1} \int_0^{z_1} |H_{t2}|^2 dz dy} \quad (12)$$

where y_1 = arbitrary distance along conducting wall (see Fig. 13-27)

z_1 = spacing between walls, m

$\text{Re } Z_c$ = real part of intrinsic impedance of conducting walls, Ω

$\text{Re } Z_d$ = real part of intrinsic impedance of dielectric medium between walls (Z_d is entirely real for lossless medium)

The integral with H_{t1} involves the power lost in one wall of the line. The total power lost in both walls is twice this; hence the factor 2 in the numerator. For a TEM wave \mathbf{H} is everywhere parallel to the walls and normal to the direction of propagation, so that both

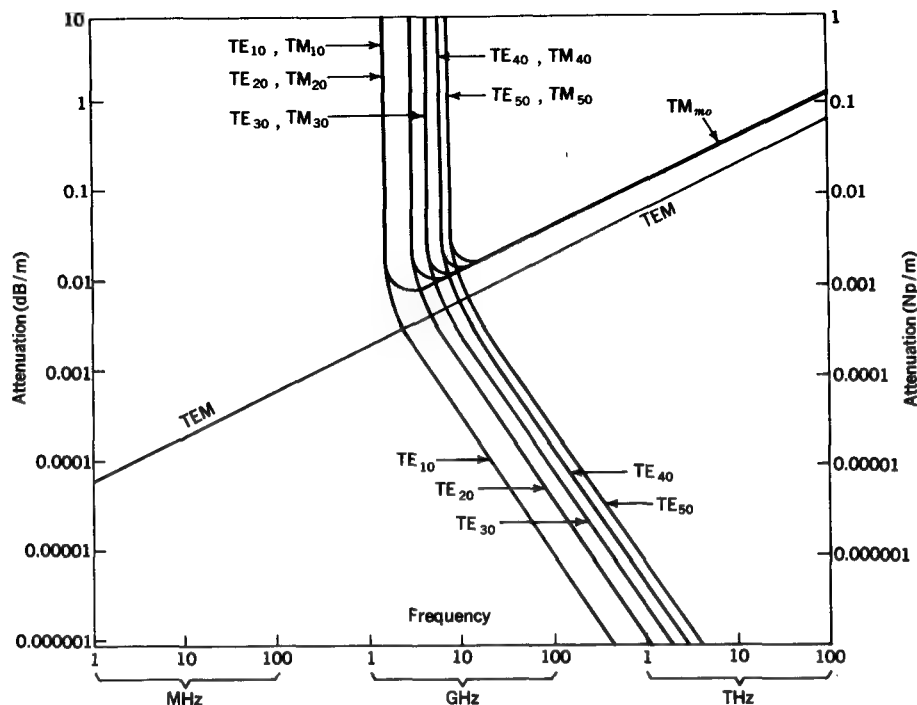


FIGURE 13-53

Attenuation α in decibels and nepers per meter as a function of frequency for various modes in an air-filled infinite-parallel-plane waveguide of copper with 100-mm spacing between planes. Note that the TEM mode and the TM_{m0} modes shown cannot occur in a single hollow rectangular guide but the TE_{mo} modes can. At frequencies below cutoff for the TE_{10} mode (1.5 GHz) only the TEM mode is transmitted but many TE and TM modes can be transmitted above and at sufficiently high frequencies the TE modes have the lowest attenuation.

H_{t1} and H_{t2} are perpendicular to the page instead of as suggested in Fig. 13-52. It follows that $|H_{t1}| = |H_{t2}| = \text{a constant}$. Hence, (12) reduces to

$$\alpha = \frac{\operatorname{Re} Z_c y_1}{\operatorname{Re} Z_d y_1 z_1} = \frac{\operatorname{Re} Z_c}{z_1 \operatorname{Re} Z_d} \quad (13)$$

For copper at 300 MHz, $\operatorname{Re} Z_c = 4.55 \text{ m}\Omega$, while for air $\operatorname{Re} Z_d = 376.7 \Omega$. Therefore

$$\alpha = 1.2 \times 10^{-4} \text{ Np m}^{-1}$$

or

$$\alpha = 1.04 \times 10^{-3} \text{ dB m}^{-1}$$

Thus, the attenuation amounts to about 1 dB km⁻¹.

The attenuation in decibels per meter (and in nepers per meter) as a function of frequency for a number of modes in an air-filled infinite-parallel-plane guide of copper is shown in Fig. 13-53. The spacing between planes is 100 mm. We note that

there is no cutoff for the TEM mode and attenuation decreases for this mode with decreasing frequency. However, at 100 GHz the TE₁₀ mode has the lowest attenuation although the TE₂₀ and higher-order modes can also be transmitted. The TE₂₀ and higher-order modes all have higher attenuation than the TE₁₀ mode.

EXAMPLE 2 Find the attenuation constant for the TE_{nr} mode in a circular cylindrical waveguide of radius a at frequencies above cutoff. Determine this attenuation in decibels per meter for the TE₀₁ and TE₁₁ modes in a 50.8-mm-diameter copper pipe.

SOLUTION From (13-16-16) and (13-16-17) for a TE_{nr} mode

$$\begin{aligned} |H_{t1}|^2 &= |H_z(r=a)|^2 + |H_\phi(r=a)|^2 \\ &= |H_0|^2 J_n^2(ka) \left(\cos^2 n\phi + \frac{|\gamma|^2 n^2}{k^4 a^2} \sin^2 n\phi \right) \end{aligned} \quad (14)$$

and from (13-16-15) and (13-16-16),

$$\begin{aligned} |H_{t2}|^2 &= |H_r|^2 + |H_\phi|^2 \\ &= \frac{|H_0|^2 |\gamma|^2}{k^4} \left\{ \cos^2 n\phi \left[\frac{dJ_n(kr)}{dr} \right]^2 + \frac{n^2}{r^2} \sin^2 n\phi J_n^2(kr) \right\} \end{aligned} \quad (15)$$

Substituting (14) and (15) into (11) gives

$$\alpha = \frac{k^4 \operatorname{Re} Z_c}{2\beta^2 \operatorname{Re} Z_{r\phi}} \frac{J_n^2(ka) \left[\int_{\phi=0}^{2\pi} \cos^2 n\phi (a d\phi) + \frac{\beta^2 n^2}{k^4 a^2} \int_{\phi=0}^{2\pi} \sin^2 n\phi (a d\phi) \right]}{\left\{ \int_{\phi=0}^{2\pi} \int_{r=0}^a \left[\cos^2 n\phi \left(\frac{dJ_n(kr)}{dr} \right)^2 + \frac{n^2}{r^2} \sin^2 n\phi J_n^2(kr) \right] \right\} r dr d\phi} \quad (16)$$

We note that

$$\int_0^{2\pi} \cos^2 n\phi d\phi = \begin{cases} 2\pi & n = 0 \\ \pi & n \neq 0 \end{cases}$$

and

$$\int_0^{2\pi} \sin^2 n\phi d\phi = \begin{cases} 0 & n = 0 \\ \pi & n \neq 0 \end{cases}$$

Thus for TE_{nr} modes ($n = 0, 1, 2, 3, \dots$)

$$\alpha = \frac{k^4 \operatorname{Re} Z_c a}{2\beta^2 \operatorname{Re} Z_{r\phi}} \frac{J_n^2(ka)\pi[1+(\beta^2 n^2/k^4 a^2)]}{\pi \int_0^a \left\{ \left[\frac{dJ_n(kr)}{dr} \right]^2 + \frac{n^2}{r^2} J_n^2(kr) \right\} r dr} \quad (17)^\dagger$$

† The integral in the denominator of (18) is evaluated in E. V. Bohn, "Introduction to Electromagnetic Fields and Waves," p. 446, Addison-Wesley Publishing Company, Inc., Reading, Mass., 1968.

Evaluating (17) and referring to Tables 13-6 and 13-8 for $\operatorname{Re} Z_{r\phi}$ gives

$$\alpha = \frac{\operatorname{Re} Z_c}{a \operatorname{Re} Z_d \sqrt{1 - (f_c/f)^2}} \left[\left(\frac{f_c}{f} \right)^2 + \frac{n^2}{(k'_{nr})^2 - n^2} \right] \quad (\text{Np m}^{-1}) \quad (18)$$

where $\operatorname{Re} Z_c = \sqrt{\pi\mu/\sigma} \sqrt{f} = 2.63 \times 10^{-7} \sqrt{f} \text{ } (\Omega)$ for copper and $\operatorname{Re} Z_d = 377 \Omega$ for an air-filled waveguide. The value of k'_{nr} can be found from Table 13-7.

Evaluating (18) for TE_{01} and TE_{11} modes yields the attenuation curves of Fig. 13-54. Note that for the TE_{01} (low-loss) mode the attenuation decreases monotonically as the frequency increases. This trend also occurs for any TE_{or} mode. The TE_{11} (dominant) mode has a minimum at $f/f_c = 3.1$. A minimum at this f/f_c ratio also occurs with all TE_{nr} modes for which $n \neq 0$.

Parameters of rectangular and cylindrical waveguides are summarized in Table 13-8.

Table 13-8 RECTANGULAR AND CIRCULAR CYLINDRICAL WAVEGUIDE PARAMETERS

Symbol	Name	Equation (rectangular or cylindrical)	
α^\dagger	Attenuation constant:		
	Below cutoff frequency	$\alpha = \frac{2\pi}{\lambda_0} \sqrt{\left(\frac{\lambda_0}{\lambda_{oc}}\right)^2 - 1} \quad (\text{Np m}^{-1})$	
β^\dagger	Above cutoff frequency	$\alpha = \frac{\operatorname{Re} Z_c \int H_{11} ^2 dl}{2 \operatorname{Re} Z_{yz} \iint H_{12} ^2 ds} \quad (\text{Np m}^{-1})$	
	Phase constant	$\beta = \sqrt{\left(\frac{2\pi}{\lambda_0}\right)^2 - k^2} \quad (\text{rad m}^{-1})$	
v_p	Phase velocity	$v_p = \frac{\omega}{\beta} = \frac{v_0}{\sqrt{1 - (\lambda_0/\lambda_{oc})^2}} \quad (\text{m s}^{-1})$	
		Rectangular	Cylindrical
$Z_{yz}, Z_{r\phi}$	Transverse-wave impedance	$Z_{yz} = \frac{Z_d}{\sqrt{1 - (\lambda_0/\lambda_{oc})^2}}$ TE _{mn} mode only	$Z_{r\phi} = \frac{Z_d}{\sqrt{1 - (\lambda_0/\lambda_{oc})^2}} \quad (\Omega)$ TE _{nr} mode
λ_{oc}	Cutoff wavelength	$\lambda_{oc} = \frac{2}{\sqrt{(n/y_1)^2 + (m/z_1)^2}}$ TE _{mn} or TM _{mn} mode	$\lambda_{oc} = \frac{2\pi r_0}{k'_{nr}}$ or $\frac{2\pi r_0}{k_{nr}} \quad (\text{m})$ TE _{nr} mode (k'_{nr}), TM _{nr} mode (k_{nr})

$\dagger \gamma = \text{propagation constant} = \alpha + j\beta$.

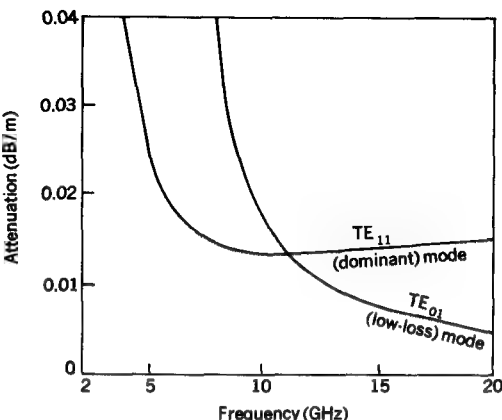


FIGURE 13-54

Attenuation α in decibels per meter as a function of frequency for TE_{01} (low-loss) and TE_{11} (dominant) modes in a circular copper waveguide of 50.8 mm inside diameter (see Example 2).

13-20 WAVEGUIDE DEVICES

Several basic waveguide devices are discussed in this section, namely, *terminations*, *power dividers*, and *guide-to-line transitions*. Reference should be made to more specialized books for detailed treatments of these and other waveguide devices.[†]

A matched *termination* for a rectangular or circular waveguide is shown in cross section in Fig. 13-55a. A card of resistance material is placed transversely in the guide $\lambda/4$ from a metal plate capping the end of the guide. The situation here is similar to that discussed in Sec. 12-3 for the terminated wave. For zero reflection it is necessary only that the card have a resistance per square equal to the transverse-wave impedance of the guide. The termination of Fig. 13-55a will be matched at the design frequency for which the card-to-end-plate distance is $\lambda/4$ but not at adjacent frequencies. This termination is a narrowband device. To provide a broadband termination a wedge of resistance material can be used, as suggested in Fig. 13-55b. The length of the wedge should be of the order of a wavelength or more.

In applications where waveguides feed two or more antennas a *power divider* may be required to divide the power in a predetermined ratio. Figure 13-55c shows a power divider for a rectangular waveguide (with TE_{10} mode) delivering twice the power to the lower branch as compared to the upper. The division is achieved by inserting a thin septum which divides the guide cross-sectional area in the ratio 2 : 1. Note that the septum is perpendicular to the direction of the electric field vector \mathbf{E} so that it does not disturb the field configuration in the guide. The height of the guide to the right of the septum in each branch is increased gradually over a dis-

[†] N. Marcuvitz, "Waveguide Handbook," McGraw-Hill Book Company, New York, 1949; J. C. Slater, "Microwave Electronics," D. Van Nostrand Company, Inc., New York, 1950.

END VIEWS SIDE VIEWS

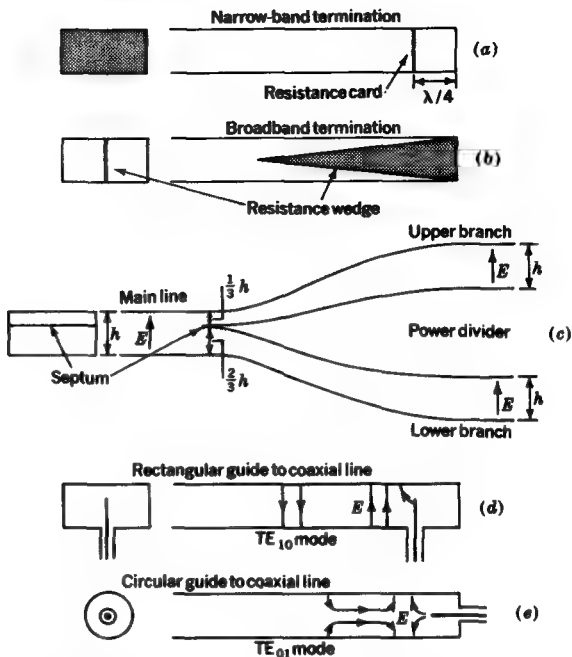


FIGURE 13-55

(a) and (b) Waveguide terminations, (c) power divider, and (d) and (e) waveguide-to-coaxial-line transitions. The arrows with E indicate the direction of the electric fields in the guides.

tance of several wavelengths back to the standard height h . If both branches are connected into nonreflecting loads or antennas, there will be no reflection from this power divider and the device can be used over a broad band of frequencies.

At some point in most waveguide systems it is necessary to convert to TEM-mode transmission on a coaxial line. Two *waveguide-to-coaxial-line transitions* are shown in Fig. 13-55d and e. The one in Fig. 13-55d provides a transition from a TE_{10} mode in a rectangular guide to a coaxial line, while the one in Fig. 13-55e provides a transition from a TM_{01} mode in a circular waveguide to a coaxial line.

13-21 WAVEGUIDE IRIS THEORY

A partial opening, or iris, in a waveguide presents a discontinuity which is analogous to placing a susceptance across a transmission line. If the iris is located the proper distance from a load or other discontinuity, and if the susceptance of the iris is correct, the iris can act as a matching device.

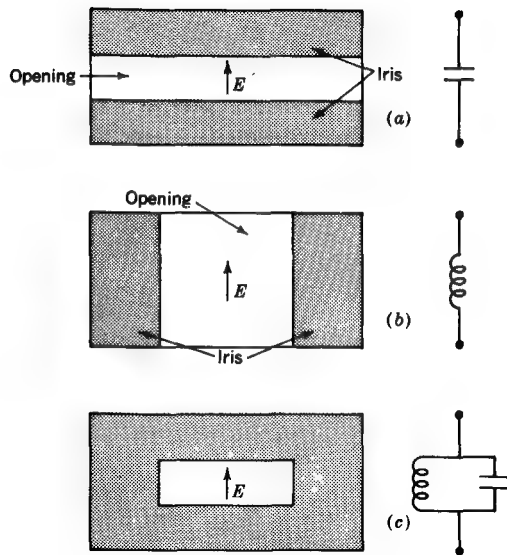


FIGURE 13-56

Rectangular waveguide with three types of iris openings equivalent to (a) shunt capacitance, (b) shunt inductance, and (c) a parallel-tuned circuit.

Consider the cross section of a rectangular guide (with TE_{10} mode) and iris or slot openings as in Fig. 13-56. It can be shown[†] that the normalized susceptance presented by the iris is given by

$$B = j2Z^2 \frac{\iint H_t \cdot H'_t ds}{\iint E_t \cdot E'_t ds} \quad (1)$$

where E_t, H_t = transverse field components of dominant mode in guide (without iris)

E'_t, H'_t = transverse components of the actual field at iris

The quantity Z is the characteristic impedance of the guide.[‡] The numerator is integrated over the metallic surface of the iris, and the denominator is integrated over the opening. The field components E_t and H_t can be calculated simply from the guide geometry, but the determination of the actual field components (E'_t and H'_t) is more difficult since they are the resultant of many higher-order modes which exist in the proximity of the iris.

[†] Slater, ibid., p. 118.

[‡] The term characteristic impedance usually implies a two-conductor transmission line but it can be extended to the dominant mode in a waveguide. For example, in a rectangular waveguide with TE_{10} mode it is equal to the ratio of the maximum voltage across the guide to the wall current.

If the opening is small compared to the metal area of the iris, the denominator in (1) is small and the susceptance B is large. As the opening is reduced to zero, B approaches infinity. Conversely, a large opening gives a small B , and as the opening becomes complete (no iris at all), B goes to zero.

For the iris of Fig. 13-56a with full horizontal slot the susceptance is capacitive (positive), and the effect is like a capacitor across a transmission line. For the iris of Fig. 13-56b with full vertical slot the susceptance is inductive (negative), and the slot acts like an inductance across a transmission line. For the iris of Fig. 13-56c there are both capacitive and inductive susceptances, and if the dimensions are chosen properly, the total, or net, susceptance can be made zero. In this case the effect is like a parallel-tuned circuit across a transmission line, and the device provides a bandpass-filtering action with no reflection (complete transmission) at the resonant or design frequency.

13-22 INTRINSIC, CHARACTERISTIC, AND WAVE IMPEDANCES

We have dealt with three types of impedances: intrinsic, characteristic, and wave impedance. The *intrinsic impedance* refers to the ratio of E to H for a plane (TEM) wave in an unbounded medium. Thus, for a lossless dielectric medium

$$\text{Intrinsic impedance} = Z_d = \frac{E}{H} = \sqrt{\frac{\mu}{\epsilon}} \quad (\Omega \text{ per square}) \quad (1)$$

For vacuum or air

$$\text{Intrinsic impedance} = Z_d = Z_0 = \sqrt{\frac{\mu_0}{\epsilon_0}} = 376.7 \quad (\Omega \text{ per square}) \quad (2)$$

For a good conductor the intrinsic impedance equals $Z_c = \sqrt{\mu\omega/\sigma} / 45^\circ$.

The *characteristic impedance* refers to the ratio of the voltage V to the current I on an infinite two-conductor transmission line. The voltage V is equal to the integral of the electric field \mathbf{E} along any path between the conductors, while the current I is equal to the integral of the magnetic field \mathbf{H} around one of the conductors (Ampère's law). The characteristic impedance of a two-conductor line can also be expressed in terms of the series resistance R , series inductance L , the shunt conductance G , and shunt capacitance C . Thus, for a two-conductor line

$$\text{Characteristic impedance} = Z_0 = \frac{V}{I} = \frac{\int \mathbf{E} \cdot d\mathbf{l}}{\oint \mathbf{H} \cdot d\mathbf{l}} = \sqrt{\frac{R + j\omega L}{G + j\omega C}} \quad (\Omega) \quad (3)$$

For a transmission-line cell the characteristic impedance V/I equals the intrinsic impedance E/H .

The *wave impedance* refers to the ratio of an electric field component to a magnetic field component at the same point of the same wave. For a TEM wave the wave impedance is the same as the intrinsic impedance, but for higher-order modes, as in a hollow single-conductor waveguide, there can be as many wave impedances as there are combinations of electric and magnetic field components. In the preceding sections we have confined our attention to the *transverse-wave impedance*, e.g., the ratio of E_y to H_z for a TE mode in a rectangular guide (both E_y and H_z are transverse to the direction of wave propagation x). Thus,

$$\text{Transverse-wave impedance} = Z_{yz} = \frac{E_y}{H_z} \quad (\Omega) \quad (4)$$

In a cylindrical waveguide the transverse-wave impedance equals $Z_{r\phi}$ ($= E_r/H_\phi$). The transverse-wave impedance of a waveguide is a function of the intrinsic impedance of the medium filling the guide and the guide dimensions as given in Tables 13-6 and 13-8. As the transverse guide dimensions become very large compared to the wavelength, the transverse-wave impedance of the guide approaches the intrinsic impedance of the medium.

Whereas the characteristic impedance is basically a circuit quantity ($= V/I$), the intrinsic impedance and the wave impedance are field or wave quantities involving the ratio of electric to magnetic field components.

13-23 WAVES TRAVELING PARALLEL TO A PLANE BOUNDARY

In Sec. 13-19 we considered the attenuation due to the power lost in the walls of a waveguide. In this section some of the phenomena associated with this power loss or power flow are discussed in more detail.

Consider the plane boundary between two media shown in Fig. 13-57a, assuming that medium 1 is air and medium 2 is a perfect conductor. From the boundary condition that the tangential component of the electric field vanishes at the surface of a perfect conductor, the electric field of a TEM wave traveling parallel to the boundary must be exactly normal to the boundary, as portrayed in the figure. However, if medium 2 has a finite conductivity σ , there will be a tangential electric field E_x at the boundary, and, as a result, the electric field of a wave traveling along the boundary has a *forward tilt*, as suggested in Fig. 13-57b. From the continuity relation for tangential electric fields, the field on both sides of the boundary is E_x .

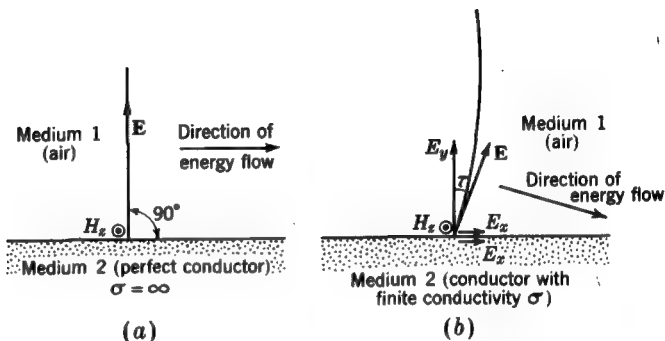


FIGURE 13-57
TEM wave traveling to right (a) along surface of perfectly conducting medium and (b) along surface of medium with finite conductivity.

The direction and magnitude of the power flow per unit area are given by the Poynting vector. The average value of the Poynting vector is

$$S_{av} = \frac{1}{2} \operatorname{Re} \mathbf{E} \times \mathbf{H}^* \quad (\text{W m}^{-2}) \quad (1)$$

At the surface of the conducting medium (Fig. 13-57b) the power into the conductor is in the negative y direction, and from (1) its average value per unit area is†

$$S_y = -\frac{1}{2} \operatorname{Re} E_x H_z^* \quad (2)$$

The space relation of E_x , H_z (or H_z^*), and S_y is shown in Fig. 13-58a. But

$$\frac{E_x}{H_z} = Z_c \quad (3)$$

where Z_c is the intrinsic impedance of the conducting medium, so that (2) can be written

$$S_y = -\frac{1}{2} H_z H_z^* \operatorname{Re} Z_c = -\frac{1}{2} H_{z0}^2 \operatorname{Re} Z_c \quad (4)$$

where $H_z = H_{z0} e^{j(\omega t - \xi) - \gamma x}$

$H_z^* = H_{z0} e^{-[j(\omega t - \xi) - \gamma x]}$ = complex conjugate of H_z

ξ = phase lag of H_z with respect to E_x

The relation for the Poynting vector in (4) is the same as given in (13-19-7).

At the surface of the conducting medium (Fig. 13-57b) the power per unit area flowing parallel to the surface (x direction) is

$$S_x = \frac{1}{2} \operatorname{Re} E_y H_z^* \quad (5)$$

† The component of the average Poynting vector in the y direction is $(S_{av})_y$, but to simplify notation we shall write S_y for $(S_{av})_y$.

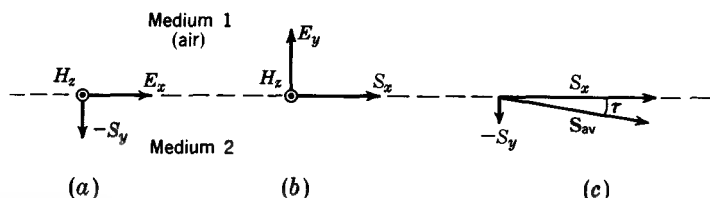


FIGURE 13-58

FIELDS AND POYNTING VECTOR AT SURFACE OF A CONDUCTING MEDIUM WITH WAVE TRAVELING PARALLEL TO SURFACE.

The space relation of E_y , H_z (or H_x^*), and S_x is illustrated by Fig. 13-58b. But

$$\frac{E_y}{H_z} = Z_d \quad (6)$$

where Z_d is the intrinsic impedance of the dielectric medium (air). It follows that

$$S_x = \frac{1}{2} H_{z0}^2 \operatorname{Re} Z_d \quad (7)$$

The total average Poynting vector is then

$$S_{av} = \hat{x}S_x + \hat{y}S_y = \frac{H_{z0}^2}{2} (\hat{x} \operatorname{Re} Z_d - \hat{y} \operatorname{Re} Z_c) \quad (8)$$

The relation of S_{av} to its x and y components is illustrated in Fig. 13-58c. It is to be noted that the average power flow (per unit area) is not parallel to the surface but inward at an angle τ . This angle is also the same as the angle of forward tilt of the average electric field (see Fig. 13-57b). If medium 2 were perfectly conducting, τ would be zero.

It is of interest to evaluate the tilt angle τ for a couple of practical situations. This is done in the following examples.

EXAMPLE 1 Find the forward tilt angle τ for a vertically polarized 3-GHz wave traveling in air along a sheet of copper.

SOLUTION From (8) the tilt angle τ is given by

$$\tau = \tan^{-1} \frac{\operatorname{Re} Z_c}{\operatorname{Re} Z_d} \quad (9)$$

At 3 GHz, we have for copper that $\operatorname{Re} Z_c = 14.4 \text{ m}\Omega$. The intrinsic impedance of air is independent of frequency. ($\operatorname{Re} Z_d = 376.7 \Omega$) Thus

$$\tau = \tan^{-1} \frac{1.44 \times 10^{-2}}{376.7} = 0.0022^\circ$$

Although τ is not zero in the above example, it is very small, so that \mathbf{E} is nearly normal to the copper surface and \mathbf{S} nearly parallel to it. This small value of tilt is typical at most air-conductor boundaries but accounts for the power flow into the conducting medium. If the conductivity of medium 2 is very low, or if it is a dielectric medium, τ may amount to a few degrees. Thus the forward tilt of a vertically polarized radio wave propagating along poor ground is sufficient to produce an appreciable horizontal electric field component. In the Beverage, or wave, antenna this horizontal component is utilized to induce emfs along a horizontal wire oriented parallel to the direction of transmission of the wave.

In contrast to Example 1, in which medium 2 is copper, the following example considers the case of fresh water as medium 2.

EXAMPLE 2 Find the forward tilt angle τ for a vertically polarized 3-GHz wave traveling in air along the surface of a smooth freshwater lake.

SOLUTION At 3 GHz the conduction current in fresh water is negligible compared with the displacement current, so that the lake may be regarded as a dielectric medium of relative permittivity $\epsilon_r = 80$. Thus

$$\tau = \tan^{-1} \frac{1}{\sqrt{80}} = 6.4^\circ$$

In this case the forward tilt of 6.4° is sufficient to be readily detected by a direct measurement of the direction of the electric field.

The angle τ discussed above is an average value. In general, the instantaneous direction of the electric field varies as a function of time. In the case of a wave in air traveling along a copper sheet, E_y and E_x are in phase octature (45° phase difference), so that at one instant of time the total field \mathbf{E} may be in the x direction and $\frac{1}{2}$ period later it will be in the y direction. (See Fig. 13-59a.) With time the locus of the tip of \mathbf{E} describes a cross-field ellipse (see Sec. 11-6), as portrayed in Fig. 13-59b for a 3-GHz wave in air traveling along a copper sheet (in the x direction) as in Example 1. The ellipse is not to scale, the abscissa values being magnified 5,000 times. The positions of \mathbf{E} for various values of ωt are indicated. The variation of the instantaneous Poynting vector for this case is shown in Fig. 13-60. Here the ordinate values are magnified 5,000 times. It is to be noted that the tip of the Poynting vector travels around the ellipse twice per cycle.

Whereas copper has a complex intrinsic impedance, fresh water, at the frequency considered in Example 2, has a real intrinsic impedance. It follows that the E_x and E_y components of the total field \mathbf{E} are in time phase so that the cross-field ellipse in this case collapses to a straight line (linear cross field) with a forward tilt of 6.4° .

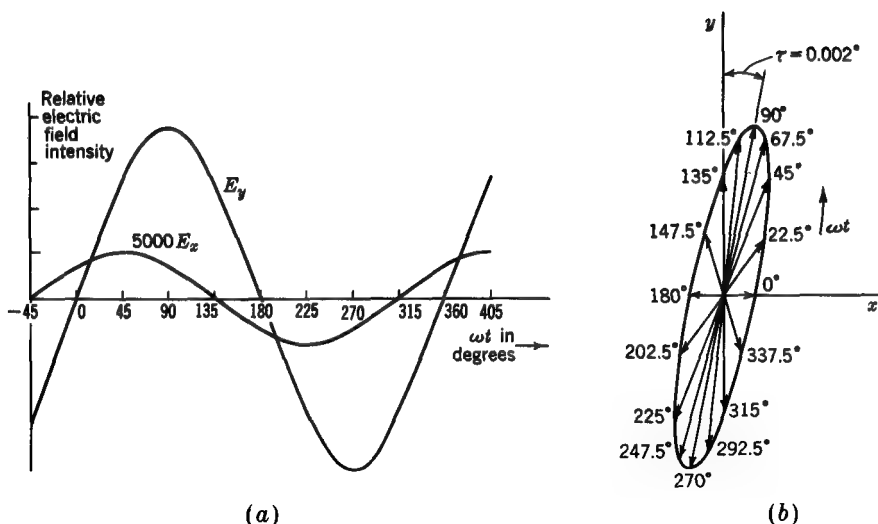
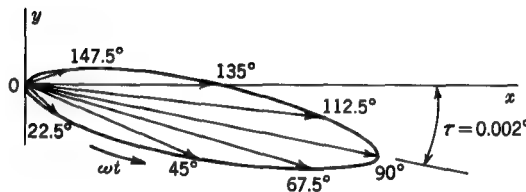


FIGURE 13-59

(a) Magnitude variation with time of E_y and E_x components of \mathbf{E} in air at the surface of a copper region for a 3,000-MHz TEM wave traveling parallel to the surface. (b) Resultant values of \mathbf{E} (space vector) at 22.5° intervals over one cycle, illustrating elliptical cross field at the surface of the copper region. The wave is traveling to the right. Abscissa values are magnified 5,000 times compared with the ordinate values.

FIGURE 13-60

Poynting vector in air at a point on the surface of a copper region for a 3,000-MHz TEM wave traveling along the surface (to right). The Poynting vector is shown at 22.5° intervals over one-half cycle. The ordinate values are magnified 5,000 times compared with the abscissa values.



13-24 OPEN WAVEGUIDES

In the previous section we have seen that a wave traveling along an air-conductor or air-dielectric boundary has a longitudinal (E_x) component of the electric field, resulting in a forward tilt of the total electric field. Hence the Poynting vector is not entirely

parallel to the boundary but has a component directed from the air into the adjacent medium, as suggested in Fig. 13-58c. This tends to keep the energy in the wave from spreading out and to concentrate it near the surface, resulting in a *bound wave*, or *surface wave*. The phase velocity of such a bound wave is always less than the velocity in free space. Although the field of this guided wave extends to infinity, such a large proportion of the energy may be confined within a few wavelengths of the surface that the surface can be regarded as an open type of waveguide. It should be noted, however, that even though the forward-tilt effect is present along all finitely conducting surfaces, the bound wave may be of negligible importance without a launching device of relatively large dimensions (several wavelengths across) to initiate the wave. If the surface is perfectly smooth and perfectly conducting, the tangential component of the electric field vanishes, there is no forward tilt of the electric field, and no tendency whatever for the wave to be bound to the surface.

In 1899 Sommerfeld† showed that a wave could be guided along a round wire of finite conductivity. Zenneck‡ pointed out that for similar reasons a wave traveling along the earth's surface would tend to be guided by the surface.

The guiding action of a flat conducting surface can be enhanced by adding corrugations or a dielectric coating or slab. If the dielectric slab is sufficiently thick, it can act alone as an effective *nonmetallic guide*. The characteristics of a number of these open waveguides are discussed in this section.

Consider a perfectly conducting flat surface of infinite extent with transverse conducting corrugations, as in Fig. 13-61a. The corrugations have many teeth per wavelength ($s \ll \lambda$). The slots between the teeth can support a TEM wave traveling vertically with electric field component E_x . Thus, each slot acts like a short-circuited section of a parallel-plane two-conductor transmission line of length d . Assuming lossless materials, the impedance Z presented to a wave traveling vertically downward onto the corrugated surface is a pure reactance, or

$$Z = jZ_d \tan \frac{2\pi\sqrt{\epsilon_r} d}{\lambda_0} \quad (\Omega) \quad (1)$$

where Z_d = intrinsic impedance of medium filling the slots, Ω

ϵ_r = relative permittivity of the medium, dimensionless

λ_0 = free-space wavelength, m

d = depth of the slots, m

The slots may be regarded as storing energy from the passing wave. When $2\pi\sqrt{\epsilon_r} d/\lambda_0 < 90^\circ$ the surface is inductively reactive.

† A. Sommerfeld, Fortpflanzung elektrodynamischer Wellen an einem zylindrischen Leiter, *Ann. Phys. u. Chem.*, 67: 233 (December 1899).

‡ J. Zenneck, Über die Fortpflanzung ebener elektromagnetischer Wellen langs einer ebenen Leiterfläche und ihre Beziehung zur drahtlosen Telegraphie, *Ann. Phys.*, (4), 23: 846-866 (Sept. 20, 1907).

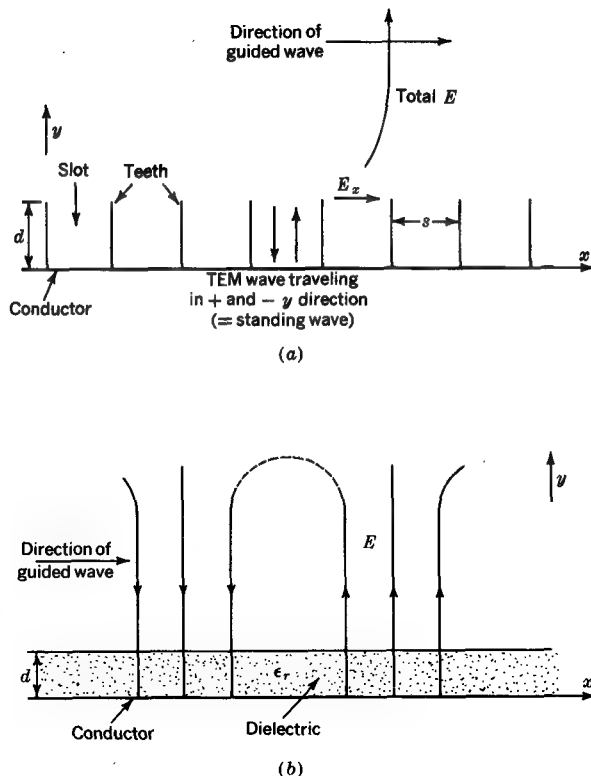


FIGURE 13-61
(a) Wave guided by corrugated surface. (b) Wave guided by conductor with dielectric coating of thickness d .

Consider next a flat perfectly conducting surface with coating of lossless dielectric of thickness d , as in Fig. 13-61b.[†] The electric field configuration for a TM_0 (dominant) mode wave launched parallel to the surface is shown. For a sufficiently thick coating d the fields attenuate perpendicular to the surface (in the y direction) as $e^{-\alpha y}$, where

$$\alpha = \frac{2\pi}{\lambda_0} \sqrt{\epsilon_r - 1} \quad (\text{Np m}^{-1}) \quad (2)$$

[†] S. A. Schelkunoff, Anatomy of "Surface Waves," *IRE Trans. Antennas Propag.*, AP-7: S133-139 (December 1959); R. F. Harrington, "Time-Harmonic Electromagnetic Fields," p. 168, McGraw-Hill Book Company, New York, 1961.

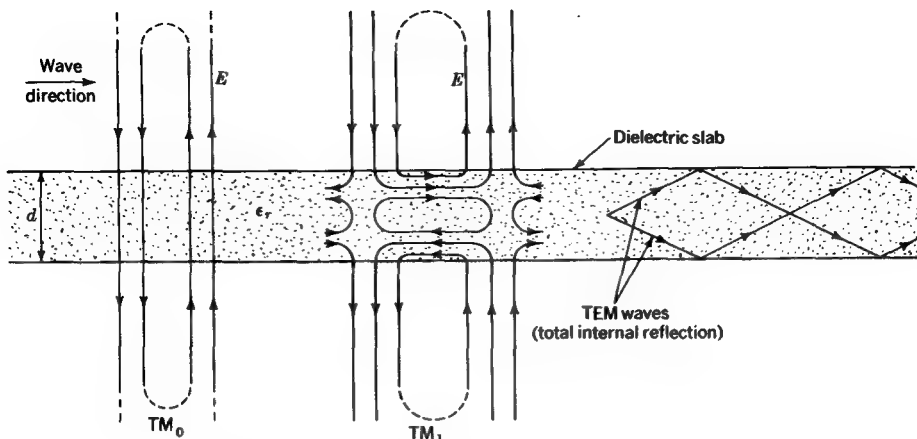


FIGURE 13-62
Dielectric-slab waveguide showing electric field configuration for dominant mode (TM_0) and higher-order mode (TM_1). The higher mode is equivalent to TEM waves which have total internal reflection as suggested at right.

For $\epsilon_r = 2$ this gives over 50 dB attenuation per wavelength. Thus, the field is effectively confined close to the surface. Assuming a lossless dielectric, the attenuation in the x direction will be due entirely to radiation.

Consider now a completely nonmetallic guide consisting of a lossless dielectric slab of thickness d , as in Fig. 13-62. The situation here is the same as in Fig. 13-61b but with the conducting surface removed from the lower side of the dielectric slab. The electric field configuration for a TM_0 (dominant) mode wave launched parallel to the surface is shown at the left in Fig. 13-62. This TM_0 mode has no cutoff; i.e., it can be propagated at all frequencies down to zero frequency. Higher-order modes (with low-frequency cutoffs) are possible at sufficiently high frequencies. As an example, the electric field configuration for the TM_1 (higher-order) mode is shown at the right in Fig. 13-62. These higher modes may be regarded as the resultant of total internal reflection (see Sec. 12-4) of two plane TEM waves, as suggested in Fig. 13-62. The situation is analogous to that discussed in Sec. 13-14 for higher-order modes in an infinite-parallel-plane transmission line. For modes higher than TM_1 , there are more closed electric field loops inside the dielectric slab, but the field outside is the same. Higher-order modes are also possible for the flat conducting surface with dielectric coating (Fig. 13-61b). Above the cutoff frequency for the higher-order modes in these open guides, there is unattenuated propagation for a lossless dielectric. Below the cutoff frequency the mode can still propagate, but there is attenuation even for a lossless dielectric. This implies losses due to radiation.

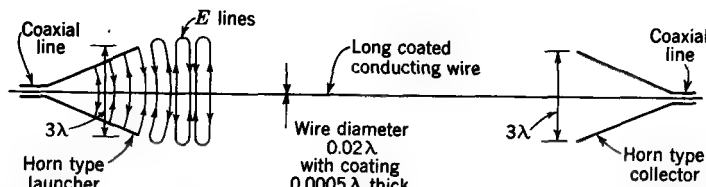


FIGURE 13-63
Single coated-wire open waveguide or "G-string." (After Goubau.)

In the preceding paragraphs we have discussed guiding by open flat structures of infinite extent in the z direction (perpendicular to the page). Guiding can also occur along round wires of metal, of dielectric, or a combination of both. As an example, let us consider the guiding action of a single round conducting wire with dielectric coating. As shown by Goubau,[†] this arrangement forms a relatively efficient open type of waveguide. However, to initiate the guided wave along the wire with good efficiency requires a relatively large launching device, its function being to excite a mode, closely related in form to the guided mode, over a diameter of perhaps several wavelengths. Hence this type of guide is practical only at very high frequencies.

A dielectric-coated single-wire waveguide with typical dimensions is illustrated in Fig. 13-63. The dielectric coat consists of a layer of enamel of relative permittivity $\epsilon_r = 3$ having a thickness of only 0.0005λ . The wire diameter is 0.02λ . The configuration of the electric field lines in the launcher and along the wire guide is suggested in the figure. The mode on the wire is a TM type, but it is like a plane TEM wave to a considerable distance from the wire.

Wires wound in the form of long helices are also effective single-conductor open-type waveguides (see Sec. 14-14). Helix diameters as large as 0.4λ can be used successfully.

A linear wire made of a nonconducting dielectric material also forms an effective open type of waveguide.[‡] The wave modes in this case may be of the TM_0 or the TM_1 type like in Fig. 13-62 for a dielectric slab. If the dielectric wire is of sufficiently small diameter (in terms of wavelengths), most of the energy is guided in the air outside the wire. However, if the wire or rod is sufficiently large in diameter, most of the energy may be conveyed inside the rod. For rods of moderate permittivity (say $\epsilon_r = 2.5$) diameters of the order of 1λ or more are required to confine most of the

[†] G. Goubau, Surface Waves and Their Application to Transmission Lines, *J. Appl. Phys.*, 21: 1119-1128 (November 1950).

[‡] D. Hondros and P. Debye, Elektromagnetische Wellen an dielektrischen Drahten, *Ann. Phys.*, 32: 465-476 (1910); R. M. Whitmer, Fields in Non-metallic Guides, *Proc. IRE*, 36: 1105-1109 (September 1948).

energy to the inside of the rod. Hollow dielectric wires or tubes are also feasible as waveguides, but larger diameters may be required for effective guiding action.

For efficient transmission of energy by a guiding system the attenuation should be small. With two-conductor transmission lines this requires that the series resistance R and the shunt conductance G be small. The conductor separation must also be small compared to the wavelength in order that radiation losses be negligible. Under these conditions the fields vary as $1/r^2$, where r is the distance perpendicular to the line and the power density varies as $1/r^4$. Thus, most of the power flow is close to the line (see Fig. 13-25b). Waves carried in a single hollow conducting waveguide will be unattenuated if the guide walls are perfectly conducting and the material filling the guide is lossless. Perfectly conducting walls also prevent any radiation from the guide. With open guides losses due to radiation tend to become significant, and modes which confine the power flow close to the guiding surface are desirable for efficient transmission. High attenuation of the fields perpendicular to guides is also important to reduce coupling or cross talk between adjacent transmission systems.

13-25 CAVITY RESONATORS

The purpose of transmission lines and waveguides is to transmit electromagnetic energy efficiently from one point to another. A *resonator*, on the other hand, is an energy storage device. As such it is equivalent to a resonant circuit element. At low frequencies a parallel capacitor and inductor, as in Fig. 13-64a, are used to provide a resonant circuit. To make this combination resonate at shorter wavelengths the inductance and capacitance can be reduced, as in Fig. 13-64b. Parallel straps reduce the inductance still further, as in Fig. 13-64c. The limiting case is the completely enclosed rectangular box or *cavity resonator* shown in Fig. 13-64d. In this cavity resonator the maximum voltage is developed between points 1 and 2 at the center of the top and bottom plates.

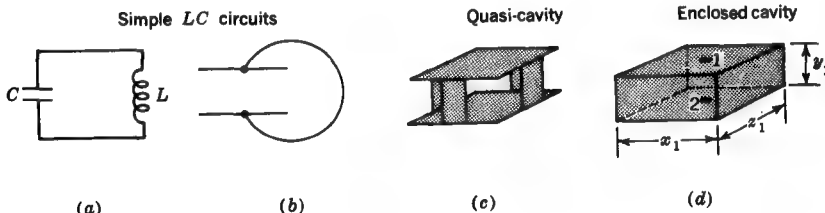


FIGURE 13-64
Evolution of (enclosed) cavity resonator from simple *LC* circuit.

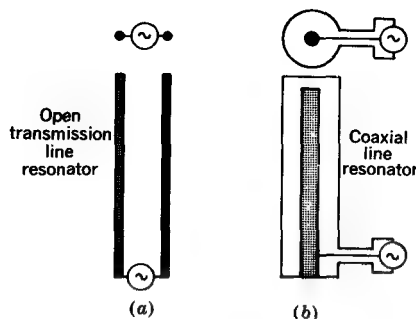


FIGURE 13-65
Resonator consisting of (a) 2-conductor open transmission line and (b) enclosed coaxial line.

Resonators can also be constructed using sections of open- or short-circuited transmission lines, as in Fig. 13-65. The type at (a) uses a two-conductor transmission line, while that at (b) uses a coaxial line. The disadvantage of the two-conductor (open) type is that there can be a small but significant loss due to radiation. In the resonators of Fig. 13-65 the fields are in the TEM mode, whereas in the cavity resonator of Fig. 13-64d the fields must be in higher-order modes.

The basic principle of a cavity resonator was described in connection with the pure standing wave of Sec. 10-13. Here the energy oscillates back and forth from entirely electric to entirely magnetic twice per cycle. Let us now consider the case of a rectangular cavity resonator in more detail and determine the *resonant frequency* and Q . It is convenient to begin by recalling the situation for a TE_{m0} -mode wave in a hollow rectangular waveguide. Referring to Fig. 13-66, let a TE_{m0} -mode wave traveling in the $-x$ direction be incident on a conducting plate across the guide at $x = 0$, producing a pure standing wave in the guide. This standing wave is the resultant of two traveling waves of equal amplitude traveling in the negative x direction (incident wave) and in the positive x direction (reflected wave). The fields of these traveling waves are given by

$$E_y = \frac{j\beta Z_{yz}}{k_z} H_0 \sin k_z z e^{j(\omega t \pm \beta x)} \quad (1)$$

$$H_x = H_0 \cos k_z z e^{j(\omega t \pm \beta x)} \quad (2)$$

$$H_z = \frac{j\beta}{k_z} H_0 \sin k_z z e^{j(\omega t \pm \beta x)} \quad (3)$$

where $k_z = m\pi/z_1$. The plus sign in the exponential refers to a wave traveling in the $-x$ direction and the minus sign to one traveling in the $+x$ direction. Adding the fields of the two traveling waves to obtain the fields of the standing wave, we obtain

$$E_y = \frac{-j\beta Z_{yz}}{k_z} H_0 \sin k_z z (e^{j\beta x} - e^{-j\beta x}) e^{j\omega t} \quad (4)$$

$$= \frac{2\beta Z_{yz}}{k_z} H_0 \sin k_z z \sin \beta x e^{j\omega t} \quad (5)$$

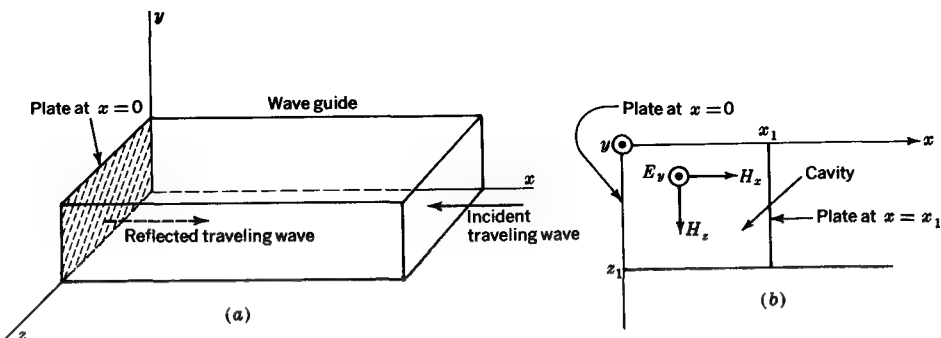


FIGURE 13-66

(a) Perspective view of rectangular waveguide closed with plate at $x = 0$ and (b) cross-sectional top view with additional plate at $x = x_1$ trapping wave inside the cavity.

Inserting another conducting plate across the guide at $x = x_1$ requires that $\beta = k_x = l\pi/x_1$. Noting that the transverse-wave impedance $Z_{yz} = \omega\mu/\beta = \omega\mu/k_x$, we get

$$E_y = \frac{2\omega\mu}{k_z} H_0 \sin k_x x \sin k_z z e^{j\omega t} \quad (6)$$

Proceeding in like manner for the magnetic field components, we get

$$H_x = -2H_0 \sin k_x x \cos k_z z e^{j[\omega t + (\pi/2)]} \quad (7)$$

$$H_z = \frac{2k_x}{k_z} H_0 \cos k_x x \sin k_z z e^{j[\omega t + (\pi/2)]} \quad (8)$$

With conducting plates across the waveguide at $x = 0$ and $x = x_1$ the wave is trapped in the rectangular cavity. We note that the electric and magnetic fields are in time-phase quadrature ($\pi/2$ in exponent for H_x and H_z but not for E_y), as is typical of a standing wave.

The mode of a TE wave in a rectangular cavity would in general be designated as a TE_{lmn} mode, where l refers to variations of the fields in the x direction, m in the z direction, and n in the y direction. Since we assumed $n = 0$ in the above discussion, the designation appropriate to our example would be TE_{lm0} . Now $k^2 = k_z^2 = \gamma^2 + \omega^2\mu\epsilon$, but $\gamma^2 = -\beta^2$ ($\alpha = 0$) and $\beta = k_x$. Thus,

$$k_z^2 = -k_x^2 + \omega^2\mu\epsilon = -k_x^2 + (2\pi f)^2 \frac{1}{(f\lambda)^2}$$

so

$$\boxed{\lambda = \frac{2}{\sqrt{(l/x_1)^2 + (m/z_1)^2}}} \quad (9)$$

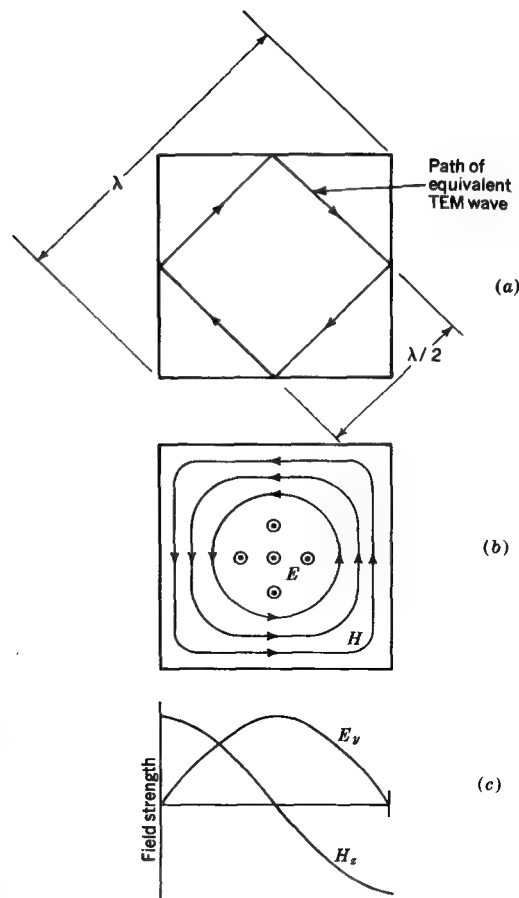


FIGURE 13-67

(a) The resonant wavelength of a square cavity is equal to the diagonal distance. The path of the equivalent TEM wave is also shown. (b) Electric and magnetic field configuration in square cavity resonator with TE_{110} mode. (c) Variation of E_y and H_z field components across centerline of cavity.

where λ is the *resonant wavelength*. For example, the resonant wavelength for a TE_{110} mode in a square-box resonator ($x_1 = z_1$) is given by

$$\lambda = \frac{2}{\sqrt{2/x_1^2}} = 1.41x_1 \quad (\text{m}) \quad (10)$$

Thus, the resonant wavelength is equal to the diagonal of the square box, as suggested in Fig. 13-67a. The resonant frequency is given by $f = c/\lambda = (3 \times 10^8)/\lambda \text{ Hz}$. The electric and magnetic field configuration in the resonator is as indicated in Fig. 13-67b and c. There is no variation in the y direction ($n = 0$). The wave inside the cavity is equivalent to a TEM-mode wave reflected at 45° angles, as in Fig. 13-67a, assuming that the box is infinitely long in the y direction (perpendicular to the page in Fig. 13-67a).

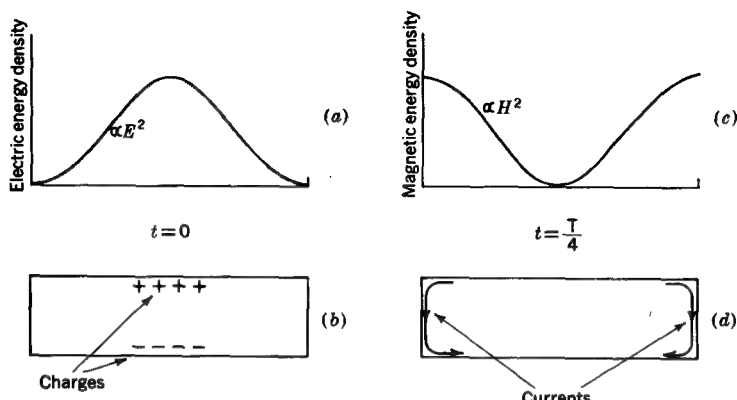


FIGURE 13-68

Electric and magnetic energy along centerline of cavity resonator. At time $t = 0$ all the energy is in the electric form, (a) and (b), while one-quarter period later ($t = T/4$) all the energy is in the magnetic form (c) and (d).

In principle the y dimension is noncritical for the mode being considered ($n = 0$), but in practice too large a value of y could permit modes with field variations in the y direction ($n \neq 0$).

At one instant of time ($t = 0$) the energy is all in electric form, as suggested in Fig. 13-68a, with accumulation of positive and negative charges on the top and bottom surfaces of the cavity, as in Fig. 13-68b. One-quarter cycle later ($t = T/4$) the energy is all in magnetic form (Fig. 13-68c) with electric currents flowing down the sidewalls, as in Fig. 13-68d.

To find the Q of the cavity resonator we note that by definition

$$Q = 2\pi \frac{\text{total energy stored}}{\text{decrease in energy in 1 cycle}}$$

The energy situation as a function of time is presented in Fig. 13-69. To get the total energy stored we can integrate the electric energy density w_e ($= \frac{1}{2}\epsilon_0 E_y^2$) over the interior volume of the cavity when E_y is a maximum, and to get the decrease in energy we can integrate the average power into the walls of the cavity and multiply this by the period $T(= 1/f)$. It is assumed that the medium filling the cavity is air or vacuum. Thus, we have

$$Q = \frac{2\pi W}{T(-dW/dt)} = \frac{2\pi \iiint w_e dv}{T \frac{1}{2} \operatorname{Re} Z_c \iint |H_t|^2 ds} \quad (11)$$

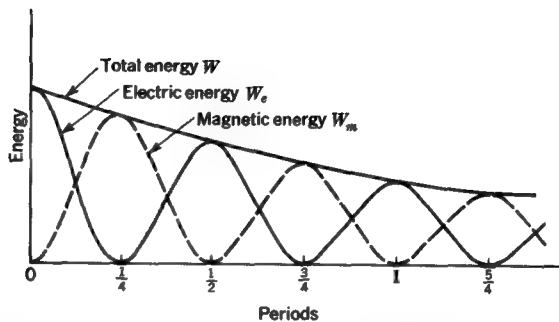


FIGURE 13-69

Decrease of stored energy with time in a resonator. The energy oscillates from all electric energy at one instant to all magnetic energy $\frac{1}{4}$ period later.

where H_t is the magnetic field component tangent to the cavity wall. Noting (6) and performing the integration for the total energy stored gives

$$\begin{aligned} W = W_e &= \frac{1}{2}\epsilon_0 \left(\frac{2\omega\mu_0 H_0}{k_z}\right)^2 \int_0^{x_1} \int_0^{y_1} \int_0^{z_1} \sin^2 k_x x \sin^2 k_z z \, dx \, dy \, dz \\ &= \frac{1}{8}\epsilon_0 x_1 y_1 z_1 \left(\frac{2\omega\mu_0 H_0}{k_z}\right)^2 = \frac{\mu_0 H_0^2 x_1 y_1 z_1}{2} \left[\left(\frac{lz_1}{mx_1}\right)^2 + 1 \right] \quad (\text{J}) \end{aligned} \quad (12)$$

The factor $-dW/dt$ in (11) is the power lost in the walls. It is convenient to calculate this as the power lost in three pairs of faces: two perpendicular to the x direction, two perpendicular to the y direction (top and bottom), and two perpendicular to the z direction. Thus,

$$P_x = 2 \times \frac{1}{2} \operatorname{Re} Z_c \int_0^{y_1} \int_0^{z_1} H_z^2 \, dy \, dz = 2H_0^2 y_1 z_1 \operatorname{Re} Z_c \left(\frac{lz_1}{mx_1}\right)^2 \quad (13)$$

$$P_y = H_0^2 x_1 z_1 \operatorname{Re} Z_c \left[\left(\frac{lz_1}{mx_1}\right)^2 + 1\right] \quad (14)$$

$$P_z = 2H_0^2 x_1 y_1 \operatorname{Re} Z_c \quad (15)$$

where Z_c is the intrinsic impedance of the conducting material forming the walls of the cavity.

Substituting these results in (11), we have for the Q of a rectangular cavity with a TE_{lm0} mode

$$Q = \frac{\mu_0 \pi f}{\operatorname{Re} Z_c} x_1 y_1 z_1 \frac{(lz_1/mx_1)^2 + 1}{2(lz_1/mx_1)^2 y_1 z_1 + [(lz_1/mx_1)^2 + 1]x_1 z_1 + 2x_1 y_1} \quad (16)$$

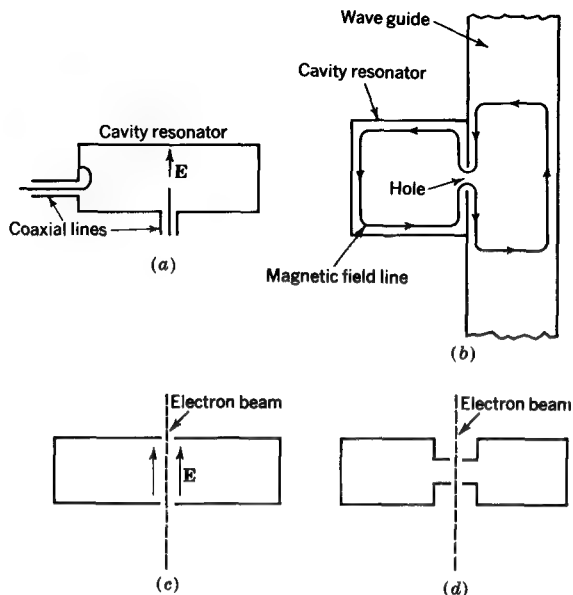


FIGURE 13-70

Cross sections through rectangular cavity resonators showing coupling to (a) coaxial lines, (b) to a hollow rectangular waveguide, and (c) and (d) to electron beams.

For a square cavity ($x_1 = z_1$) and a TE_{110} mode

$$Q = \frac{2\mu_0 \pi f}{\text{Re } Z_c} \frac{x_1 y_1 z_1}{2(y_1 z_1 + x_1 z_1 + x_1 y_1)} \\ = \frac{2\mu_0 \pi f}{\text{Re } Z_c} \frac{\text{volume of cavity}}{\text{interior surface area of cavity}} \quad (17)$$

$$\text{or} \quad Q = \frac{2}{\delta} \frac{\text{volume of cavity}}{\text{interior surface area of cavity}} \quad (18)$$

where $\delta = 2 \text{ Re } Z_c / \omega \mu_0 = 1/e$ depth of penetration. For copper $\delta = 6.6 \times 10^{-2} / \sqrt{f}$. If $x_1 = z_1 = 100 \text{ mm}$ and $y_1 = 50 \text{ mm}$, we have that the resonant wavelength $\lambda = 141 \text{ mm}$ and $Q = 17,500$ (dimensionless).

Methods for coupling are illustrated in Fig. 13-70 for a square cavity with TE_{110} mode. Couplings to coaxial lines are shown in Fig. 13-70a. These involve an electric probe at the center of the cavity ($E = \text{max}$) and a current loop at the wall ($H = \text{max}$). Coupling to a hollow rectangular waveguide can be via a hole in the cavity wall, as in Fig. 13-70b. Coupling to an electron beam can be accomplished with holes in the

top and bottom surfaces of the cavity, as in Fig. 13-70c. Here the electrons move parallel to the electric field where it is a maximum. To reduce the transit time for the electrons the cavity may be modified as in Fig. 13-70d.

PROBLEMS

- * 13-1 A transmission line of 50Ω characteristic impedance is terminated in an impedance of $100 + j100 \Omega$. (a) Calculate the impedance at a point $\frac{1}{4}\lambda$ from the load. (b) Calculate the VSWR on the line. Check this calculation and the one in (a) using a Smith chart. (c) Find the reflection and transmission coefficients for voltage.
- 13-2 Show that a transmission line having no attenuation must also have a nonreactive characteristic impedance.
- * 13-3 A uniform transmission line has constants $R = 10 \text{ m}\Omega \text{ m}^{-1}$, $G = 1 \mu\text{V m}^{-1}$, $L = 1 \mu\text{H m}^{-1}$, and $C = 1 \text{ nF m}^{-1}$. At 3.18 kHz find (a) the characteristic impedance of the line; (b) the phase velocity of wave propagation on the line; (c) the percentage to which the voltage of a traveling wave decreases in 10 km.
- 13-4 Find the high-frequency characteristic impedance Z_0 of an air-filled coaxial transmission line having a radius ratio $b/a = 3$, where b is the inside radius of the outer conductor and a is the outside radius of the inner conductor.
- * 13-5 (a) Find the characteristic impedance Z_0 for a two-conductor transmission line in air with center-to-center conductor spacing of 50 mm and conductor diameter of 6 mm. (b) What is the upper frequency limit at which this line should be used if losses due to radiation are to be minimized?
- * 13-6 A strip transmission line consists of a thin conducting strip 5 mm wide mounted on a 1-mm-thick dielectric substrate of the same width placed against a large flat conducting ground plane. If $\epsilon_r = 2.7$ for the dielectric material, (a) what is the characteristic impedance of the line? (b) What is the ratio of the wave velocity to that of light?
- 13-7 A coaxial transmission line consists of a cylindrical inner conductor of diameter d and a symmetrically situated outer conductor of square cross section with side dimension $3d$. Find the characteristic impedance if the line is (a) air-filled and (b) filled with polyfoam ($\epsilon_r = 1.13$). (c) What is the ratio of the wave velocity to that of light for the case in (b)?
- * 13-8 A transmission line of characteristic impedance $Z_0 = R_0 = 150 \Omega$ is connected through a section of length d and characteristic impedance Z_1 to a load of $250 + j100 \Omega$. Find d and Z_1 which match the load to the 150Ω line.
- * 13-9 A double-stub tuner, shown in Fig. P13-9, is constructed of 200Ω line ($Z_0 = R_0 = 200 \Omega$). Find the shortest lengths d_1 and d_2 which match the load $Z_L = 400 + j200 \Omega$ to the 200Ω line.
- * 13-10 A 150Ω transmission line is connected to two loads as shown in Fig. P13-10. Find d_1 , d_2 , R_1 , and R_2 such that the loads receive equal powers but with voltages of opposite phase.

* Answers to starred problems are given in Appendix C.

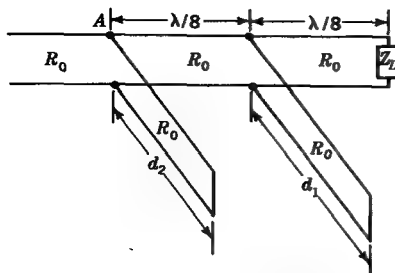


FIGURE P13-9
Double-stub tuner.

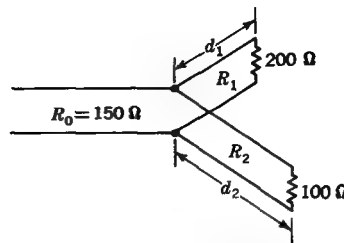


FIGURE P13-10
Line with two loads.

* 13-11 The arrangement for a three-port lossless circulator is suggested in Fig. P13-11. All three segments of the circulator have equal lengths l and characteristic resistance R_0 . Port 1 is connected to a transmission line of characteristic resistance R_0 , and ports 2 and 3 are terminated in R_0 . If a wave of unit voltage is incident at port 1, find the value of the reflected voltage r at port 1 when (a) $l = \lambda/2$ and (b) $l = \lambda/4$. (c) Is there a length l for which $r = 0$?

13-12 Show that the input impedance to a lossless exponential line of length y connected as in Fig. P13-12 to a load Z_L is given by

$$Z(y) = Z_0(0)e^{-ky} \frac{Z_L + jZ_0(0) \tan \beta y}{Z_0(0) + jZ_L \tan \beta y}$$

where $Z_0(0)$ is the characteristic impedance of the line at the load.

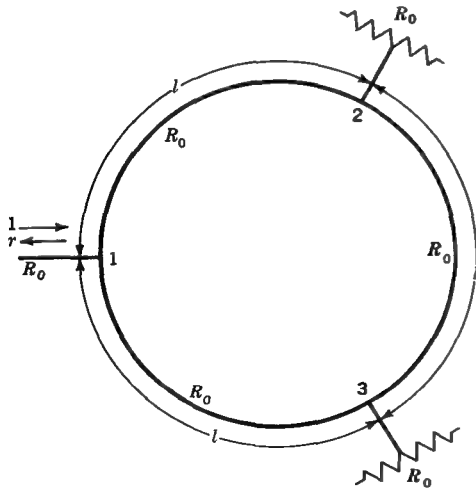


FIGURE P13-11
Three-port circulator.

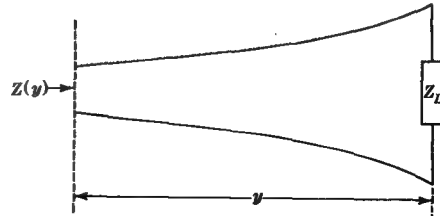


FIGURE P13-12
Exponential line.

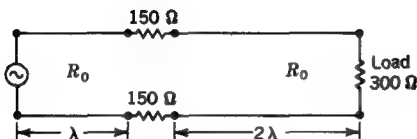


FIGURE P13-13
Line with series resistances.

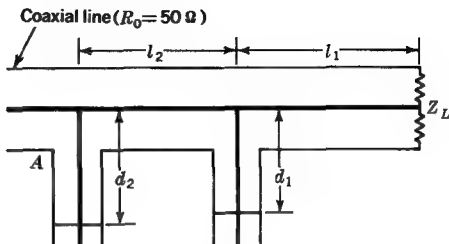


FIGURE P13-17
Coaxial double-stub tuner.

- * 13-13 Referring to Fig. P13-13, find (a) the power in the load and (b) the maximum and minimum voltages on the 2λ section for two cases: (1) R_0 (both sections) = 300Ω , and (2) R_0 (both sections) = 150Ω .

13-14 The reflection coefficient for voltage on a line of characteristic impedance Z_0 is

$$\dot{\rho}_v = \frac{Z - Z_0}{Z + Z_0} = \frac{(Z/Z_0) - 1}{(Z/Z_0) + 1} = \frac{Z_n - 1}{Z_n + 1}$$

where Z = load impedance, Ω

Z_n = normalized impedance = $R_n + jX_n$, dimensionless

It follows that

$$Z_n = \frac{1 + \dot{\rho}_v}{1 - \dot{\rho}_v}$$

Show that if R_n and X_n are obtained as functions of the real and imaginary parts of $\dot{\rho}_v$, a map of R_n and X_n in the $\dot{\rho}_v$ plane yields the Smith impedance chart (see Sec. 13-7).

- 13-15 Find the characteristic impedance Z_0 and ratio of the wave velocity to the velocity of light v/v_0 for the transmission line of (a) Prob. 7-1, (b) Prob. 7-2, (c) Prob. 7-3, (d) Prob. 7-24, (e) Prob. 7-25, (f) Prob. 7-26, (g) Prob. 7-30 (four cases), take $\epsilon = 3\epsilon_0$, (h) Prob. 7-31, (i) Prob. 7-32, take $\epsilon = 3\epsilon_0$, and (j) Prob. 7-33.

- 13-16 (a) Find the characteristic resistances for a binomial three-section $\lambda/4$ transformer for matching a 500Ω load to a 50Ω line. (b) Plot the impedance presented to the 50Ω line (normalized to 50Ω) on a Smith chart over the frequency range $0.5f_0 \leq f \leq 1.5f_0$ in steps of $0.1f_0$, where f_0 is the center frequency. (c) Plot the VSWR on the 50Ω line as ordinate vs. the above frequency range as abscissa. (d) For comparison also plot the VSWR over the same frequency range for the case where only a single $\lambda/4$ section is used.

- 13-17 (a) A double-stub tuner (Fig. P13-17) is constructed of air-filled 50Ω coaxial transmission line. If the load impedance $Z_L = 40 + j80 \Omega$, $l_1 = 200$ mm, and $l_2 = 150$ mm, find the two sets of stub lengths, d_1 and d_2 , which will match the load to the line at 300 MHz (VSWR = 1 at A). (b) Find the VSWR at A at 20-MHz intervals over the bandwidth 200

to 400 MHz for both sets of stub lengths. Assume that the load impedance is constant with respect to frequency. Draw a graph of the VSWR as ordinate (log scale) vs. frequency (linear scale) as abscissa for both sets of stub lengths. Each curve should have VSWR values at 11 frequencies. (c) Discuss the significance of the VSWR curves of part (b). Which combination of stub lengths results in the wider bandwidth for $VSWR < 2$? One of the curves has a $VSWR = \infty$ point close to the $VSWR = 1$ point at 300 MHz. Might this have a practical application?

- * 13-18 A two-conductor 300- Ω transmission line is connected to a load of $450 + j450 \Omega$. A short-circuited single-stub tuner of the same type of line is connected across the main line at a distance d_1 from the load. The stub length is d_2 . Find the shortest values of d_1 and d_2 to match the load to the line.

- * 13-19 A plane 1-GHz wave is incident normally on the plane surface of a half-space of material having constants $\mu_r = 1$ and $\epsilon_r = 3.5$. Find (a) the thickness in millimeters and (b) the relative permittivity required for a matching plate which will eliminate reflection of the incident wave.

- 13-20 A quartz window ($\epsilon_r = 5$) is used to pass a linearly polarized laser beam from a vacuum chamber into the air. For adequate mechanical strength the window must be at least 3 mm thick. Design an arrangement that will allow transmission of the laser beam through the window without reflection. A $\lambda/4$ coating can be applied to the air side of the window but not to the vacuum side. The wavelength is 700 nm. Hint: Utilize the Brewster angle.

- 13-21 Prove that the power through each curvilinear square in Fig. 13-25a is the same.

- 13-22 Overhead long-distance high-power transmission lines radiate electromagnetic interference, generate poisonous ozone, and otherwise disrupt the ecology. Design a transmission line for handling terawatt power levels over megameter distances which avoids the above effects. Assume that a 25-K superconductor is available. Hint: Consider a buried thermally insulated liquid-hydrogen-cooled dc line operating at levels of a few volts. Alternatively consider a liquid-hydrogen-cooled cylindrical waveguide operating at 100 GHz in a higher order mode or modes (see Sec. 4-7).

- 13-23 In Prob. 13-22 superconductors are considered for low-loss power transmission. Another advantage is that superconductive cables can provide faster response (wider bandwidth) for transmission of information. Design a superconductive two-conductor cable with nanosecond response. See, for example, H. J. Jensen, Nuclear Test Instrumentation with Miniature Superconductive Cables, *IEEE Spectrum*, 5:91-99 (September 1968).

- 13-24 Show that when the series resistance R and the shunt conductance G of a transmission line are small but not negligible, the attenuation constant may be written as

$$\alpha \approx \frac{R}{2} \sqrt{\frac{C}{L}} + \frac{G}{2} \sqrt{\frac{L}{C}}$$

and the phase constant as $\beta \approx \omega \sqrt{LC}$.

- * 13-25 An air-filled hollow rectangular waveguide has cross-sectional dimensions $y_1 = 40$ mm and $z_1 = 80$ mm. (a) Find the cutoff frequencies for the following modes: TEM, TE₁₀, TE₂₀, TE₀₁, TE₀₂, TE₁₁, TE₂₁, and TE₁₂. (b) Find the ratio of the wave

velocity in the guide to the velocity in free space for each of the modes if $f = 1.5 f_c$. (c) If the waveguide is of copper find the attenuation in decibels per meter for each of the higher order modes at $1.5 f_c$.

- * 13-26 An air-filled hollow rectangular waveguide has cross-sectional dimensions $y_1 = 40$ mm and $z_1 = 50$ mm. (a) At frequencies below 8 GHz what modes will this guide transmit of the TE and TM type? (b) Find the ratio of the wave velocity in the guide to the velocity in free space for each of the modes if $f = 1.7 f_c$.

13-27 The wavelength region around 10 mm is commonly referred to as K band, 30 mm as X band, and 100 mm as S band. Design a rectangular waveguide for transmitting TE_{10} mode K-band waves with minimum attenuation and with minimum change in velocity over the wavelength range 9 to 11 mm. The guide should be incapable of passing any modes other than the TE_{10} (such as TE_{01}) in this wavelength range and any waves at all at wavelengths greater than 15 mm. Your result should be in the form of a drawing with dimensions.

- * 13-28 An air-filled cylindrical waveguide has a diameter $d = 50$ mm. (a) Find the cutoff frequencies for the following modes: TM_{01} , TM_{02} , TM_{11} , TM_{12} , TE_{01} , TE_{02} , TE_{11} , and TE_{12} . (b) Find the ratio of the wave velocity in the guide to the velocity in free space for each of the modes if $f = 1.3 f_c$. (c) If the waveguide is of copper find the attenuation in decibels per meter for each of the modes at $1.3 f_c$.

- * 13-29 An air-filled cylindrical waveguide has a diameter $d = 75$ mm. At frequencies below 5 GHz what modes will this guide transmit of the TE and TM type? (b) Find the ratio of the wave velocity in the guide to the velocity in free space for each of the modes if $f = 1.2 f_c$.

- * 13-30 A perfectly conducting flat sheet of large extent has a dielectric coating ($\epsilon_r = 3$) of thickness $d = 5$ mm. Find the cutoff frequency for the TM_0 (dominant) mode and its attenuation per unit distance.

13-31 Find the reflection angle θ of the TE_{10} rectangular-waveguide mode in Prob. 13-25 at a frequency (a) 1.1 times the cutoff frequency and (b) 2.5 times the cutoff frequency.

13-32 (a) A communications service using mobile units wants communication to be maintained even when their radio-equipped automobiles and trucks are in a vehicular tunnel. If the smallest tunnel diameter encountered is 5 m, what is the lowest frequency which can be employed? (b) What could be installed in the tunnel to permit communication at lower frequencies? No frequency converters are permitted.

- * 13-33 A metal-clad building has window openings 1.5 by 0.5 m. What is the longest wavelength which can readily penetrate into the interior of the building?

- * 13-34 A plane 3-GHz wave in air is traveling parallel to the boundary of a conducting medium with \mathbf{H} parallel to the boundary. The constants for the conducting medium are $\sigma = 10^7 \text{ S m}^{-1}$ and $\mu_r = \epsilon_r = 1$. If the traveling-wave rms electric field $E = 75 \text{ mV m}^{-1}$, find the average power per unit area lost in the conducting medium.

13-35 Design a waveguide for handling gigawatt power levels with minimum attenuation over a 20-km distance at 1 GHz. Consider using a cylindrical guide in a mode or modes which are of much higher order number than the dominant mode.

13-36 Identify the type of device and explain the function for as many of the microwave components in Fig. P13-36 as possible.

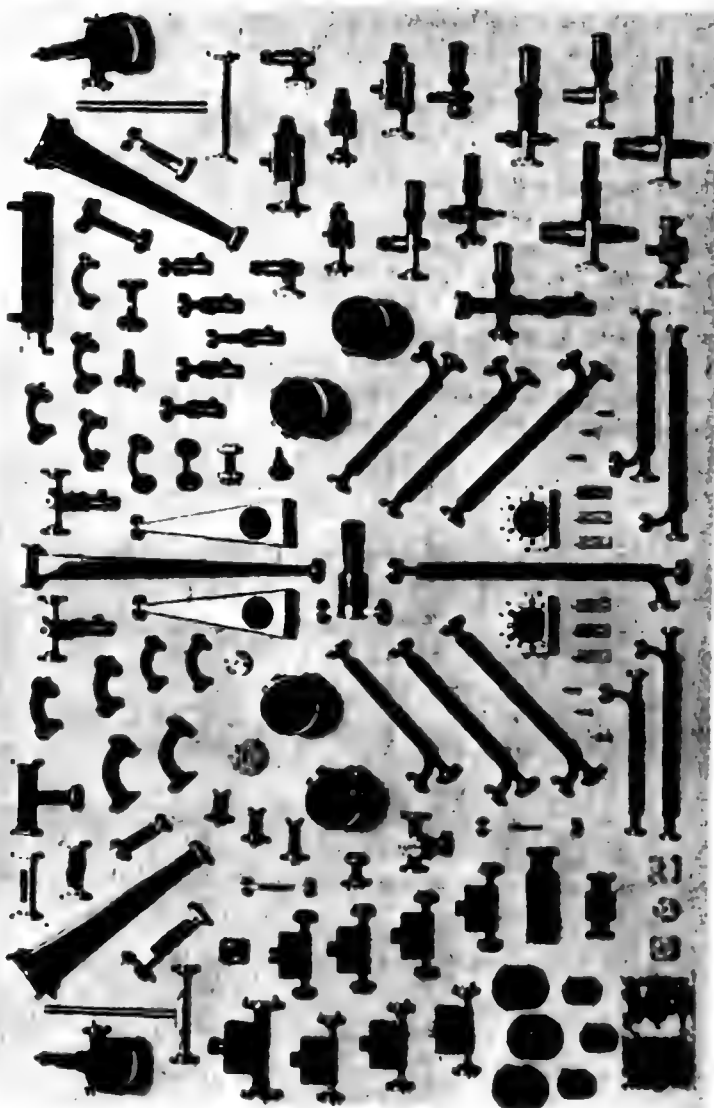


FIGURE P13-36
Microwave components. (Baytron Co., Inc., Medford, Mass.)

13-37 Show that for a dielectric-coated conductor, as in Fig. 13-61b, the ratio of the power transmitted in the dielectric P_d to the power transmitted in the air P_a is given by

$$\frac{P_d}{P_a} = \frac{\cos \beta d}{\sin^3 \beta d} (\sin 2\beta d - 2\beta d)$$

where d is the thickness of the dielectric coating.

13-38 Discuss the possibilities of using dielectric-slab surface-wave modes for radio communication on the moon over long distances (1,000 km or more). Note that the moon has no ionosphere. See, for example, W. W. Salisbury and D. L. Fernald, Post-occultation Reception of Lunar Ship Endeavour Radio Transmission, *Nature*, 234:95 (Nov. 12, 1971); also A. F. Wickersham, Jr., Generation, Detection and Propagation on the Earth of HF and VHF Radio Surface Waves, *Nature*, 230:125-130 (Apr. 5, 1971).

13-39 Show that the field components for a TM wave in a hollow rectangular single-conductor waveguide (see Fig. 13-35) are given by

$$E_x = E_0 \sin \frac{n\pi y}{y_1} \sin \frac{m\pi z}{z_1} e^{j\omega t - \gamma x}$$

$$E_y = -\frac{\gamma E_0 n\pi}{k^2 y_1} \cos \frac{n\pi y}{y_1} \sin \frac{m\pi z}{z_1} e^{j\omega t - \gamma x}$$

$$E_z = -\frac{\gamma E_0 m\pi}{k^2 z_1} \sin \frac{n\pi y}{y_1} \cos \frac{m\pi z}{z_1} e^{j\omega t - \gamma x}$$

$$H_x = 0 \quad \text{TM mode condition}$$

$$H_y = -\frac{\gamma Y_{yz} E_0 m\pi}{k^2 z_1} \sin \frac{n\pi y}{y_1} \cos \frac{m\pi z}{z_1} e^{j\omega t - \gamma x}$$

$$H_z = \frac{\gamma Y_{yz} E_0}{k^2} \frac{n\pi}{y_1} \cos \frac{n\pi y}{y_1} \sin \frac{m\pi z}{z_1} e^{j\omega t - \gamma x}$$

13-40 Show that the field components for a TM wave in a hollow cylindrical waveguide (see Fig. 13-44) are given by

$$E_r = -\frac{\gamma E_0}{k^2} \cos n\phi \frac{dJ_n(kr)}{dr} e^{j\omega t - \gamma z}$$

$$E_\phi = -\frac{n\gamma E_0}{k^2 r} \sin n\phi J_n(kr) e^{j\omega t - \gamma z}$$

$$E_z = E_0 \cos n\phi J_n(kr) e^{j\omega t - \gamma z}$$

$$H_z = 0 \quad \text{TM mode condition}$$

$$H_\phi = \frac{n\gamma E_0 Y_{r\phi}}{k^2 r} \sin n\phi J_n(kr) e^{j\omega t - \gamma z}$$

$$H_r = -\frac{n\gamma E_0}{k^2} \cos n\phi \frac{dJ_n(kr)}{dr} e^{j\omega t - \gamma z}$$

13-41 Show that the transverse impedance of a TE wave in a rectangular guide is equal to $Z_{yz} = Z_d(\lambda/\lambda_0)$, where Z_d is the intrinsic impedance of the medium, λ the wavelength in the guide, and λ_0 the wavelength in an unbounded medium of the same material that fills the guide.

13-42 Show that the transverse impedance of a TM wave in a rectangular guide is equal to

$$Z_{yz} = Z_d \sqrt{1 - \left(\frac{n\lambda_0}{2y_1}\right)^2 - \left(\frac{m\lambda_0}{2z_1}\right)^2} = Z_d \sqrt{1 - \left(\frac{\lambda_0}{\lambda_{oc}}\right)^2}$$

13-43 Show that the attenuation constant for a TE_{10} wave at frequencies above cutoff in an infinite-plane transmission line or guide is

$$\alpha = \frac{2 \operatorname{Re} Z_c}{d \operatorname{Re} Z_d} \frac{(\lambda_0/2d)^2}{\sqrt{1 - (\lambda_0/2d)^2}} \quad (\text{Np m}^{-1})$$

where $\operatorname{Re} Z_c$ = real part of intrinsic impedance of wall medium (conductor), Ω

$\operatorname{Re} Z_d$ = real part of intrinsic impedance of medium filling guide (dielectric), Ω

d = wall spacing, m

λ_0 = wavelength in unbounded medium, m

13-44 Show that the attenuation constant for a TE_{m0} wave at frequencies above cutoff in an infinite-parallel-plane transmission line of spacing d is

$$\alpha = \frac{\operatorname{Re} Z_c}{d \operatorname{Re} Z_d} \frac{2(\lambda_0/\lambda_{oc})^2}{\sqrt{1 - (\lambda_0/\lambda_{oc})^2}}$$

where λ_{oc} is the cutoff wavelength.

13-45 A TEM wave is traveling in air parallel to the plane boundary of a conducting medium. Show that if $K = \rho_s v$, where K is the sheet-current density in amperes per meter, ρ_s is the surface charge density in coulombs per square meter, and v the velocity of the wave in meters per second, it follows that $K = H$, where H is the magnitude of the \mathbf{H} field of the wave.

13-46 Show that the average power transmitted by a perfectly conducting rectangular guide operating in the TE_{10} mode is given by

$$P_{av} = \frac{\omega \mu \beta |H_0|^2 y_1 z_1^3}{4\pi^2}$$

13-47 Show that the average power transmitted by a perfectly conducting cylindrical guide operating in the TE_{11} mode is given by

$$P_{av} = \frac{\omega \mu \beta |H_0|^2 r_0^4}{82}$$

13-48 Write the field equations and sketch the variation of each field component with y and z for a TE_{12} wave in a square conducting guide ($y_1 = z_1$).

13-49 Write the field equations and sketch the variation of each field component with r and ϕ for a TE_{12} wave in a cylindrical conducting guide of radius r_0 .

13-50 Write the field equations and sketch the variation of each field component with y for a TE₁ wave in a dielectric slab-on-conductor guide, where y is distance from the conductor. The dielectric-slab thickness $d = \lambda_0/2$, and its relative permittivity is $\epsilon_r = 5$.

* 13-51 In an infinite-parallel-plane air-filled transmission line of 15 mm spacing find the attenuation constant α for a TEM wave and a TE₁₀ wave at 12 GHz. The planes are made of copper.

* 13-52 What is the attenuation constant α in decibels per meter for a hollow single-conductor waveguide at an applied frequency 0.85 times the lowest cutoff frequency for the guide?

13-53 In an infinite-parallel-plane transmission line show that at a wavelength λ_0 , less than cutoff, the attenuation constant for a TM₁₀ wave is

$$\alpha' = \frac{2\alpha}{\sqrt{1 - (\lambda_0/2b)^2}}$$

where α = attenuation constant for TEM wave

b = parallel-plane spacing

* 13-54 A 500-MHz TEM traveling wave in a strip transmission line has an electric field $E = 500 \text{ mV m}^{-1}$ rms. The line consists of a copper strip 10 mm wide separated 1 mm from a flat copper ground plane by a 1-mm-thick ribbon of polystyrene ($\epsilon_r = 2.7$). (a) Find the average power in the direction of transmission. (b) Find the average power into the guide walls per meter of length. (c) What is the attenuation constant in decibels per meter? (d) What is the characteristic impedance? (e) What is the wave velocity?

13-55 In a hollow rectangular guide with TE₁₀ mode show that the ratio of the voltage V between the top and bottom of the guide (at the middle) to the longitudinal current I on the upper or lower inside surface is an impedance given by

$$Z = \frac{V}{I} = \frac{\pi y_1}{2z_1} Z_{yz}$$

where y_1 = height of guide

z_1 = width of guide

Z_{yz} = transverse impedance

13-56 Show that the attenuation constant for a TE_{m0} wave at frequencies above cutoff in a hollow rectangular waveguide of height y_1 and width z_1 is

$$\alpha = \frac{2 \operatorname{Re} Z_d [(\lambda_0/\lambda_{oc})^2 + z_1/2y_1]}{z_1 \operatorname{Re} Z_d \sqrt{1 - (\lambda_0/\lambda_{oc})^2}}$$

13-57 Show that the group velocity u in a hollow rectangular single-conductor waveguide (equal to the velocity of energy transport) is given by

$$\begin{aligned} u &= v_0 \sqrt{1 - \left(\frac{m\lambda_0}{2y_1}\right)^2 - \left(\frac{m\lambda_0}{2z_1}\right)^2} \\ &= v_0 \sqrt{1 - \left(\frac{\lambda_0}{\lambda_{oc}}\right)^2} \end{aligned}$$

where λ_0 = wavelength in unbounded medium

λ_{oc} = cutoff wavelength

Both λ_0 and λ_{oc} should be distinguished from λ , the wavelength in the guide. Note that it follows that $uv = v_0^2$, where v is the phase velocity in the guide and v_0 is the phase velocity in an unbounded medium.

13-58 Compare the Q values attainable with a parallel inductor-capacitor circuit, a short-circuited section of two-conductor line, a short-circuited section of coaxial line, a cavity resonator, a quartz crystal, an ammonia molecule, and a cesium atom (hyperfine transition of ground state of cesium 133).

* 13-59 An air-filled cavity resonator operates in the TE_{110} mode. The cavity is square, $x_1 = z_1 = 80$ mm, with height $y_1 = 35$ mm. The cavity is made of copper and is gold-plated inside. Find (a) resonant frequency, (b) resonant wavelength, and (c) Q .

* 13-60 A cavity resonator is constructed of a short section of cylindrical tubing of diameter d closed at both ends by flat plates separated by $d/2$. The cavity is made of brass and is silver-plated inside. (a) What is the required value of d if the cavity is to operate in its dominant mode at K band (10 mm)? (b) What is the Q ?

13-61 (a) Radio-frequency dielectric heaters are widely used in many industrial processes, particularly for injection molding of plastics. The heating results from the dielectric hysteresis (see Sec. 8-15). Another application of this heating effect is for cooking using microwave ovens. The oven consists of a cavity resonator connected to a microwave power source. Design such a microwave oven operating at 2,450 MHz with 750 W radio-frequency power and an oven volume of 200 by 400 by 400 mm. (a) What maximum rate of temperature rise will be possible for 3 kg of dielectric material with complex permittivity $\epsilon_r = 4 + j1$ if its specific heat is $5 \text{ J g}^{-1} \text{ }^\circ\text{C}^{-1}$? (b) If the oven has a window covered by a metal screen, give the screen specifications, material, wire size, and hole size required to keep radiation loss through the screen to less than 10 mW cm^{-2} . (See Prob 10-39.) Also is it important that the screen wires be bonded at all contact points? (c) Describe the standing-wave mode or modes in the oven and what means (such as fan or paddles) are used to "stir" the standing-wave pattern. (d) How will the edges of the oven door be sealed to prevent radio-frequency leakage?

13-62 Select a suitable type of transmission line or waveguide for frequencies, applications, and line lengths as follows: (a) dc low-voltage measurement, length 5 m, (b) dc 1-MV buried power line, length 10 km, (c) 60-Hz low-voltage flexible power (~ 10 -kW) line, 50 m, (d) 500-Hz to 5-kHz bandwidth audio circuit, ordinary telephone application over 50 km distance with 100 such circuits placed in compact bundle with minimum cross talk, (e) 100-kHz two-conductor 600- Ω line from 100-kW transmitter to antenna, distance 1 km, (f) 2-MHz buried 50- Ω line from 50-kW transmitter to antenna, distance 500 m, (g) 5- to 25-MHz 50- Ω line from shortwave antenna to receiver, distance 500 m, (h) 54- to 890-MHz 300- Ω line from receiving antenna to TV set through low electromagnetic noise, distance 50 m, (i) same as (h) but through high noise, distance 200 m, (j) 1.42-GHz line or guide with 6-MHz bandwidth between radio-telescope antenna and receiver, distance 10 m, lowest possible loss, (k) 3-GHz (S band) line or guide with 10-MHz bandwidth from 100-kW radar transmitter to antenna, distance 10 m, (l) 30-GHz (K band) line or guide with 10-GHz bandwidth between radio-telescope antenna and receiver, distance 10 m, (m) 100-GHz line or guide with 10-GHz bandwidth for data transmission, between amplifiers, distance 5 km. Some of the types to choose from are as follows: two-conductor parallel or twisted pair, two conductors in shield,

coaxial line (dielectric-filled), coaxial line (air-filled), strip line, waveguide (rectangular or circular) in dominant or higher-order modes. Specify conductor or guide dimensions and material in all cases. Also explain reasons for selection, including attenuation, cost, etc.

13-63 A uniform transmission line is connected to a load. Let the load be at $x = 0$ and the line extend to positive values of x . An incident wave has voltage V_i , and the wave reflected from the load has voltage V_r . Use a computer to calculate and plot the magnitude and phase of the total voltage $V = V_i + V_r$ at 100-mm intervals to a distance of 5 m from the load (50 points) for

$$V_i = V_0 e^{\alpha x} e^{j(\omega t + \beta x)}$$

$$V_r = -\frac{1}{2} V_0 e^{-\alpha x} e^{j(\omega t - \beta x)}$$

$$V_0 = 10 \text{ V}$$

$$f = 300 \text{ MHz } (\lambda = 1 \text{ m})$$

$$\alpha = 0.3 \text{ Np m}^{-1}$$

Plot results with magnitude of V as ordinate vs. x as abscissa for one graph and phase angle (from -180° through 0° to $+180^\circ$) as ordinate vs. x as abscissa for second graph. Use same scale for x in both graphs and display both graphs together with magnitude graph below the phase graph.

- 13-64** (a) Make a power-flow contour map like that in Fig. 13-25b using a computer.
 (b) Repeat using a conductor spacing twice that in Fig. 13-25b but with the same conductor diameter and the same total power.

13-65 Demonstrate the equivalence of (12-4-21) and (12-4-34) for a normally incident wave to (13-6-11) for a transmission line.

13-66 Hold your hand between your eye and a lamp or bright area with your forefinger close to but not quite touching your thumb. Explain the phenomenon you observe when you look at the finger-thumb gap. *Hints:* Consider higher order modes between two parallel boundaries. Consider diffraction.

ANTENNAS AND RADIATION

14-1 INTRODUCTION

In discussing transmission lines and waveguides in Chap. 13 our attention was focused on guiding energy along the system. Little consideration was given to *radiation*, i.e., the loss of energy from the system into free space. While transmission lines or waveguides are usually made so as to minimize radiation, antennas are designed to radiate (or receive) energy as effectively as possible.

A two-wire transmission line is shown in Fig. 14-1a, connected to a radio-frequency generator (or transmitter). Along the uniform part of the line, energy is guided as a plane TEM-mode wave with little loss. The spacing between wires is assumed to be a small fraction of a wavelength. At the right the transmission line is opened out. As the separation approaches the order of a wavelength or more, the wave tends to be radiated so that the opened-out line acts like an antenna which launches a free-space wave. To be more explicit, *the region of transition between a guided wave and a free-space wave may be defined as the antenna*. We have described the antenna as a transmitting device. As a receiving device the definition is turned around, and the antenna is defined as the region of transition between a free-space wave and a guided wave.

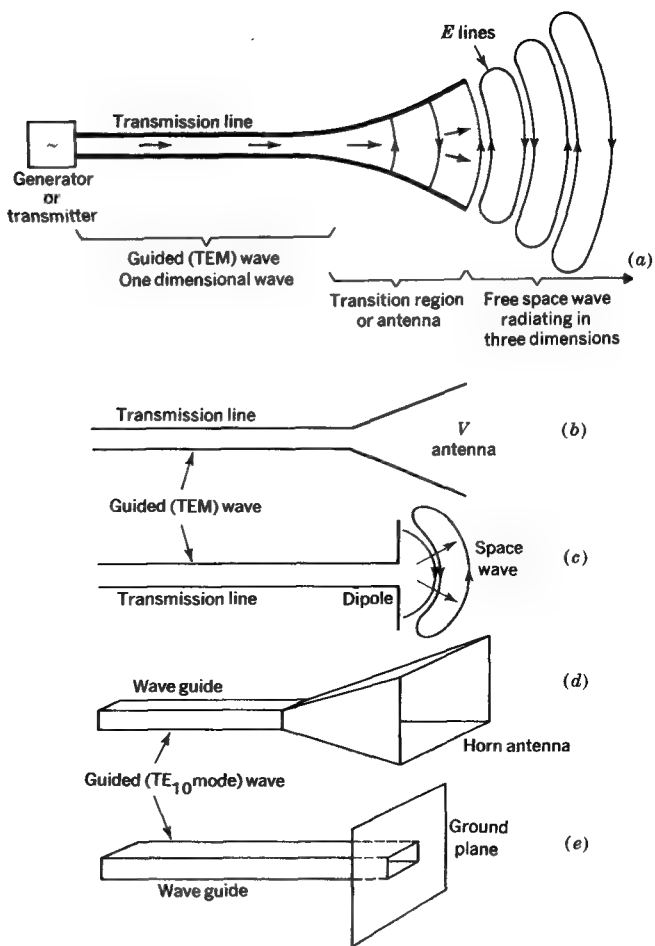


FIGURE 14-1

The antenna as a region of transition between a guided wave and a free-space wave or vice versa.

If the wires separate gradually, as in Fig. 14-1a, to a maximum separation of 1λ or more, the arrangement will be an efficient radiator with maximum power beamed to the right, as suggested. Modifying this antenna to one with straight wires yields the V antenna of Fig. 14-1b. Folding the wires perpendicular to the transmission line, we arrive at the simple dipole antenna of Fig. 14-1c. The transition from a guided wave to a space wave is more abrupt with the dipole antenna (Fig. 14-1c) than for the antenna of Fig. 14-1a, and there is more reactive or stored energy in the vicinity of the dipole antenna.

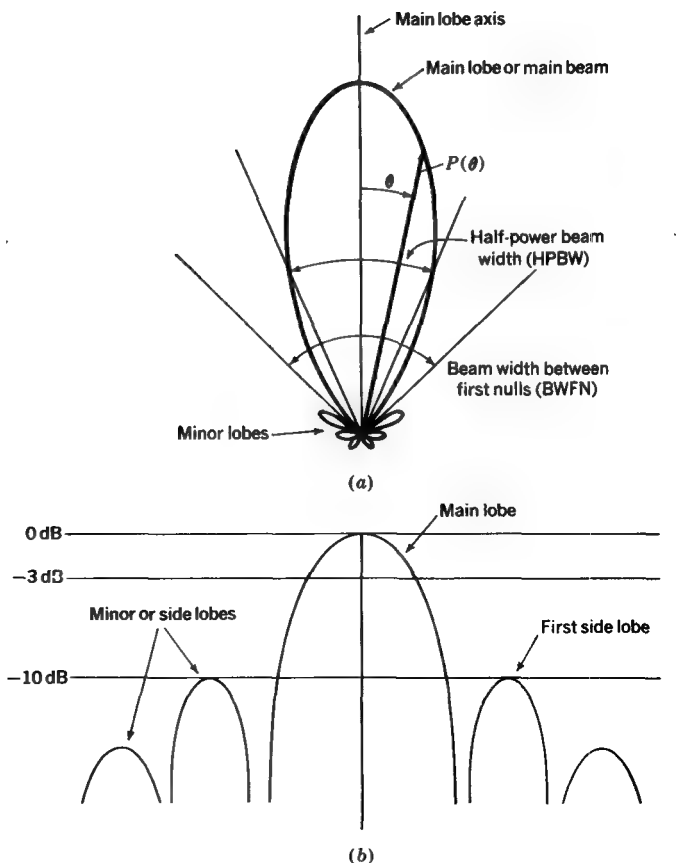


FIGURE 14-2
 (a) Antenna power pattern in polar coordinates and linear scale; (b) antenna pattern in rectangular coordinates and decibel (logarithmic scale). Both patterns are the same.

An opened-out section of hollow rectangular waveguide or horn (Fig. 14-1*d*) is also an effective radiator or antenna. Bending the horn sides back into a flat plane, we arrive at the more abrupt transition shown in Fig. 14-1*e*, where the waveguide opens into the center of a flat conducting plane.[†]

The response of an antenna as a function of direction is given by the antenna pattern. By reciprocity (see Sec. 14-18) this pattern is the same for both transmitting and receiving conditions.

[†] For a more complete discussion of antennas and their basic properties see, for example, J. D. Kraus, "Antennas," McGraw-Hill Book Company, New York, 1950.

The pattern commonly consists of a number of lobes, as suggested in Fig. 14-2a. The lobe with the largest maximum is called the *main lobe*, while the smaller lobes are referred to as the minor lobes or side and back lobes.

If the pattern is measured sufficiently far from the antenna for there to be no change in pattern with distance, the pattern is the *far-field pattern*. Measurements at lesser distances yield *near-field patterns*, which are a function of both angle and distance. The pattern may be expressed in terms of the field intensity (*field pattern*) or in terms of the Poynting vector or radiation intensity (*power patterns*). Figure 14-2a is a power pattern in polar coordinates. To show the minor-lobe structure in more detail the pattern can be plotted on a logarithmic or decibel scale (decibels below main-lobe maximum). Figure 14-2b is an example of a pattern on a decibel scale in rectangular coordinates. The pattern in Fig. 14-2b is the same as the one in Fig. 14-2a.

A single pattern, as in Fig. 14-2, would be sufficient to completely specify the variation of radiation with angle provided the pattern is symmetrical. This would mean, in the case of Fig. 14-2a, that the three-dimensional pattern is a figure of revolution of the one shown around the pattern axis. If the pattern is not symmetrical, a three-dimensional diagram or a contour map is required to show the pattern in its entirety. However, in practice two patterns perpendicular to each other and perpendicular to the main-lobe axis may suffice. These mutually perpendicular patterns through the main-lobe axis are called the *principal-plane patterns*, one in the *E* plane (containing *E*) and one in the *H* plane (containing *H*). This assumes that the antenna is linearly polarized in one of the principal planes. If this is not the case, more patterns may be required. As an example, the dominant radiation from an antenna might be linearly polarized in one principal plane, but the radiation from some minor lobes might be linearly polarized in the principal plane at right angles. Or the antenna might be elliptically polarized.

In this chapter the most important parameters of an antenna are considered. These include the *gain* (or *directivity*), the *terminal impedance* (real part equals the *radiation resistance*), the *pattern*, *beam width*, *beam area*, *effective aperture*, *bandwidth*, and *antenna temperature*. A variety of antenna types are also discussed. These include the dipole, loop, helix, reflector antennas, arrays, and the interferometer. The short dipole is important theoretically and is considered first (in Sec. 14-3).

14-2 RETARDED POTENTIALS

In dealing with antennas or radiating systems the propagation time is a matter of great importance. Thus, if an alternating current is flowing in the short element in Fig. 14-3, the effect of the current is not felt instantaneously at the point *P* but only

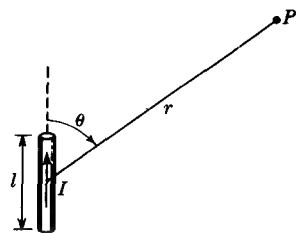


FIGURE 14-3
Short current-carrying element.

after an interval equal to the time required for the disturbance to propagate over the distance r .

Accordingly, instead of writing the current I as

$$I = I_0 \sin \omega t \quad (1)$$

which implies instantaneous propagation of the effect of the current, we can introduce the time of propagation (or retardation time†), as done by Lorentz, and write

$$[I] = I_0 \sin \omega \left(t - \frac{r}{c} \right) \quad (2)$$

where $[I]$ is called the *retarded current*. The brackets $[]$ may be added, as here, to indicate explicitly that the current is retarded.

Equation (2) is a statement of the fact that the disturbance at a time t and at a distance r from the element is caused by a current $[I]$ that occurred at an earlier time $t - (r/c)$. The time difference r/c is the interval required for the disturbance to travel the distance r , where c is the velocity of light (300 Mm s^{-1}).

It is to be noted that we dealt with retarded quantities in Chap. 10 in connection with wave propagation, although the term retarded was not used. For example, in Chap. 10 a solution of the wave equation is given that involves $\sin(\omega t - \beta x)$, which is similar in form to the trigonometric function in (2) since‡

$$\sin \omega \left(t - \frac{r}{c} \right) = \sin (\omega t - \beta r) \quad (3)$$

where $\beta (= \omega/c = 2\pi/\lambda)$ is the phase constant.

† Called *retardation time* because the phase of the wave at P is retarded with respect to the phase of the current in the element by an angle $\omega r/c$.

‡ The expression $\sin(\omega t - \beta x)$ in Chap. 10 refers to a plane wave traveling in the x direction. The relation $\sin \omega [t - (r/c)]$ or $\sin(\omega t - \beta r)$ refers to a spherical wave traveling in the radial direction. An important point of difference between a plane and a spherical wave is that a plane wave suffers no attenuation (in a lossless medium) but a spherical wave does because it expands over a larger and larger region as it propagates.

In complex form (2) is†

$$[I] = I_0 e^{j\omega[t - (r/c)]} = I_0 e^{j(\omega t - \beta r)} \quad (\text{A}) \quad (4)$$

In the more general situation where the current is distributed we may write for the retarded-current density

$$[\mathbf{J}] = \mathbf{J}_0 e^{j\omega[t - (r/c)]} = \mathbf{J}_0 e^{j(\omega t - \beta r)} \quad (\text{A m}^{-2}) \quad (5)$$

Introducing this value of current density in (5-25-10) for the vector potential, we obtain a *retarded vector potential* that is applicable in time-varying situations where the distances involved are significant in terms of the wavelength. That is, the retarded vector potential is

$$[\mathbf{A}] = \frac{\mu_0}{4\pi} \int_v \frac{[\mathbf{J}]}{r} dv = \frac{\mu_0}{4\pi} \int_v \frac{\mathbf{J}_0 e^{j\omega[t - (r/c)]}}{r} dv \quad (\text{Wb m}^{-1}) \quad (6)$$

Likewise the *scalar potential* V can be put in the retarded form

$$[V] = \frac{1}{4\pi\epsilon_0} \int_v \frac{[\rho]}{r} dv \quad (7)$$

where $[V]$ = retarded scalar potential, V

$[\rho] = \rho_0 e^{j\omega[t - (r/c)]}$ = retarded charge density, C m⁻³

14-3 THE SHORT DIPOLE ANTENNA

A short linear conductor is often called a short *dipole*. In the following discussion, a short dipole is always of finite length even though it may be very short. If the dipole is vanishingly short, it is an infinitesimal dipole.

Any linear antenna may be regarded as being composed of a large number of short dipoles connected in series. Thus, a knowledge of the properties of the short dipole is useful in determining the properties of longer dipoles or conductors of more complex shape such as are commonly used in practice.

Let us consider a short dipole like that shown in Fig. 14-4a. The length l is very short compared with the wavelength ($l \ll \lambda$). Plates at the ends of the dipole provide capacitive loading. The short length and the presence of these plates result in a uniform current I along the entire length l of the dipole. The dipole may be energized by a balanced transmission line, as shown. It is assumed that the transmis-

† It is understood that the instantaneous value of current is given either by the imaginary (Im) or the real (Re) part of the exponential expression in (4).

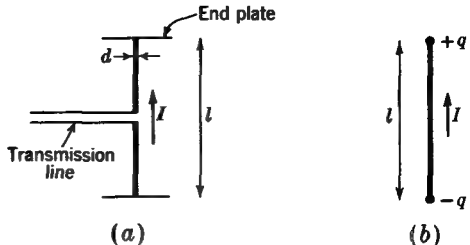


FIGURE 14-4

(a) Short-dipole antenna fed by 2-conductor transmission line and (b) its equivalent.

sion line does not radiate, and its presence will therefore be disregarded. Radiation from the end plates is also considered to be negligible. The diameter d of the dipole is small compared with its length ($d \ll l$). Thus, for purposes of analysis we may consider that the short dipole appears as in Fig. 14-4b. Here it consists simply of a thin conductor of length l with a uniform current I and point charges q at the ends. According to (4-13-6), the current and charge are related by

$$\frac{dq}{dt} = I \quad (1)$$

Let us now proceed to find the fields everywhere around a short dipole. Let the dipole of length l be placed coincident with the z axis and with its center at the origin, as in Fig. 14-5. At any point P the electric field has, in general, three components, E_θ , E_ϕ , and E_r , as shown. It is assumed that the medium surrounding the dipole is air or vacuum.

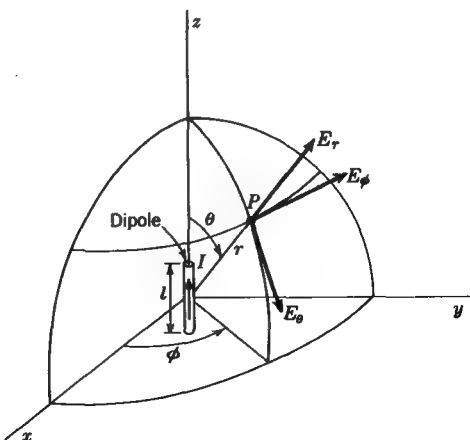


FIGURE 14-5

Relation of dipole antenna to coordinates.

From (8-17-11) the electric field intensity \mathbf{E} at any point P is expressed by

$$\mathbf{E} = -\nabla V - \frac{\partial \mathbf{A}}{\partial t} \quad (\text{V m}^{-1}) \quad (2)$$

where V = electric scalar potential at point P , V

\mathbf{A} = vector potential at point P , Wb m⁻¹

From (5-25-2) the magnetic field \mathbf{H} at any point P is

$$\mathbf{H} = \frac{1}{\mu_0} \nabla \times \mathbf{A} \quad (\text{A m}^{-1}) \quad (3)$$

where μ_0 = permeability of air (400π nH m⁻¹)

\mathbf{A} = vector potential at point P , Wb m⁻¹

If the scalar potential V and the vector potential \mathbf{A} at the point P are known, the electric and magnetic fields \mathbf{E} and \mathbf{H} at P can be determined by means of (2) and (3). Since we are interested in the fields not only at points near the dipole but also at distances that are comparable to and larger than the wavelength, we must use the retarded potentials given in (14-2-6) and (14-2-7). Thus we have

$$\boxed{\mathbf{E} = -\nabla[V] - \frac{\partial[\mathbf{A}]}{\partial t} = -\nabla[V] - j\omega[\mathbf{A}] \quad (\text{V m}^{-1})} \quad (4)$$

and

$$\boxed{\mathbf{H} = \frac{1}{\mu_0} \nabla \times [\mathbf{A}] \quad (\text{A m}^{-1})} \quad (5)$$

where†

$$\boxed{[V] = \frac{1}{4\pi\epsilon_0} \int_v \frac{\rho_0 e^{j\omega[t-(r/c)]}}{r} dv \quad (\text{V})} \quad (5a)$$

$$\boxed{[\mathbf{A}] = \frac{\mu_0}{4\pi} \int_v \frac{\mathbf{J}_0 e^{j\omega[t-(r/c)]}}{r} dv \quad (\text{Wb m}^{-1})} \quad (5b)$$

The electric and magnetic fields due to any configuration of currents and charges are given by (4) and (5), where the retarded scalar potential $[V]$ is a quantity that depends only on the charges (stationary) and the retarded vector potential $[\mathbf{A}]$ is a quantity that depends only on the currents. Equation (5) indicates that the magnetic field \mathbf{H} depends only on the currents, while (4) indicates that the electric field \mathbf{E} depends on both the currents and the charges. However, it will be shown later that in determining the radiation field (at large distances from a current and charge distribution) only the currents need be considered. Since the retarded potentials will be used exclusively in the following development, the brackets will be omitted for the sake of simplicity, it being understood that the potentials are retarded.

† More concisely $\mathbf{A} = \mu_0 \int_v \mathbf{J}_0 G e^{j\omega t} dv$, where G = free space Green's function = $e^{-j\theta r}/4\pi r$.

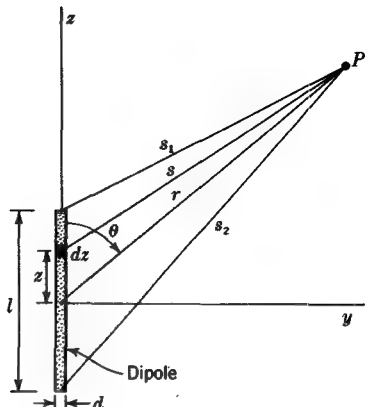


FIGURE 14-6
Geometry for short dipole.

We shall now proceed to find the electric and magnetic fields everywhere from a short dipole by first determining the retarded vector and scalar potentials and then substituting these values in (4) and (5) and performing the indicated operations.

Referring to Fig. 14-5 or 14-6, the current is entirely in the z direction. Hence, it follows that the retarded vector potential has only a z component. Its value is

$$A_z = |\mathbf{A}| = \frac{\mu_0 I_0}{4\pi} \int_{-l/2}^{l/2} \frac{e^{j(\omega t - \beta s)}}{s} dz \quad (6)$$

where I_0 = amplitude (peak value in time) of current (same at all points along dipole), \mathbf{A}

μ_0 = permeability of free space = $400 \pi \text{ nH m}^{-1}$

dz = element of length of conductor, m

ω = radian frequency ($= 2\pi f$, where f = frequency, Hz)

t = time, s

s = distance from dz to point P (see Fig. 14-6), m

β = phase constant, rad m^{-1} ($= 2\pi/\lambda$)

If the distance from the dipole is large compared with its length ($r \gg l$), and if the wavelength is large compared with the length ($\lambda \gg l$), we can put $s = r$ and neglect the magnitude and phase differences of the contributions from the different parts of the wire.[†] Thus (6) becomes

$$A_z = \frac{\mu_0 I_0 l e^{j(\omega t - \beta r)}}{4\pi r} \quad (7)$$

[†] If r is large compared with l but λ is not large compared with l , we may put $s = r$ in the denominator in (6) and neglect the differences in magnitude. However, in such cases we should retain s in the exponential expression since the difference in phase of the contributions may be significant.

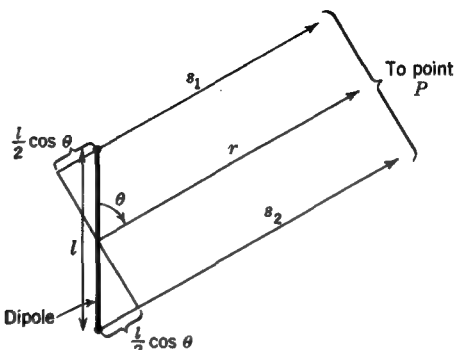


FIGURE 14-7
Relations for short dipole when $r \gg l$.

The electric charge is confined to the ends of the dipole; so turning our attention to the retarded scalar potential, we find its value to be

$$V = \frac{q_0}{4\pi\epsilon_0} \left(\frac{e^{j(\omega t - \beta s_1)}}{s_1} - \frac{e^{j(\omega t - \beta s_2)}}{s_2} \right) \quad (\text{V}) \quad (8)$$

where q_0 = amplitude (peak value in time) of charge at ends of dipole, C

s_1 = distance from upper end of dipole to P , m

s_2 = distance from lower end of dipole to P , m

From (1)

$$q = \int I dt = \frac{I}{j\omega} \quad (9)$$

where $q = q_0 e^{j(\omega t - \beta s)}$ = retarded charge, C

$I = I_0 e^{j(\omega t - \beta s)}$ = retarded current, A

It follows that $q_0 = I_0/j\omega$ so that (8) can be reexpressed

$$V = \frac{I_0}{4\pi\epsilon_0 j\omega} \left(\frac{e^{j(\omega t - \beta s_1)}}{s_1} - \frac{e^{j(\omega t - \beta s_2)}}{s_2} \right) \quad (10)$$

When $r \gg l$, the lines of length s_1 and s_2 from the ends of the dipole to the point P may be considered parallel, as shown in Fig. 14-7, so that $s_1 = r - (l/2) \cos \theta$ and $s_2 = r + (l/2) \cos \theta$. Substituting these into (10) and clearing fractions yields

$$V = \frac{I_0 e^{j(\omega t - \beta r)}}{4\pi\epsilon_0 j\omega} \frac{[r + (l/2) \cos \theta] \exp(j \frac{1}{2} \beta l \cos \theta) - [r - (l/2) \cos \theta] \exp(-j \frac{1}{2} \beta l \cos \theta)}{r^2} \quad (11)$$

where the term $(l^2 \cos^2 \theta)/4$ in the denominator has been neglected in comparison with r^2 since $r \gg l$. By de Moivre's theorem, (11) becomes

$$V = \frac{I_0 e^{j(\omega t - \beta r)}}{4\pi\epsilon_0 j\omega r^2} \left[\left(\cos \frac{\beta l \cos \theta}{2} + j \sin \frac{\beta l \cos \theta}{2} \right) \left(r + \frac{l}{2} \cos \theta \right) \right. \\ \left. - \left(\cos \frac{\beta l \cos \theta}{2} - j \sin \frac{\beta l \cos \theta}{2} \right) \left(r - \frac{l}{2} \cos \theta \right) \right] \quad (12)$$

Since it is assumed that the wavelength is much greater than the length of the dipole ($\lambda \gg l$),

$$\cos \frac{\beta l \cos \theta}{2} = \cos \frac{\pi l \cos \theta}{\lambda} \approx 1 \quad (13)$$

and $\sin \frac{\beta l \cos \theta}{2} \approx \frac{\beta l \cos \theta}{2}$ (14)

Introducing (13) and (14) into (12) reduces the expression for the scalar potential to

$$V = \frac{I_0 l e^{j(\omega t - \beta r)} \cos \theta}{4\pi\epsilon_0 c} \left(\frac{1}{r} + \frac{c}{j\omega} \frac{1}{r^2} \right) \quad (V) \quad (15)\dagger$$

where I_0 = amplitude (peak value in time) of current, A

l = length of dipole, m

ω = radian frequency ($= 2\pi f$, where f = frequency, Hz)

β = phase constant, rad m $^{-1}$ ($= 2\pi/\lambda$)

t = time, s

θ = angle between dipole and radius vector of length r to point P , dimensionless

ϵ_0 = permittivity of free space = 8.85 pF m $^{-1}$

c = velocity of light = 300 Mm s $^{-1}$

j = complex operator = $\sqrt{-1}$

r = distance from center of dipole to point P , m

Equation (15) gives the retarded scalar potential and (7) the retarded vector potential at a distance r and at an angle θ from a short dipole. The only restrictions are that $r \gg l$ and $\lambda \gg l$. Before substituting these values in (4) and (5), let us express \mathbf{E} in polar coordinates. Thus, in polar coordinates (see Fig. 14-5),

$$\mathbf{E} = \hat{r} E_r + \hat{\theta} E_\theta + \hat{\phi} E_\phi \quad (16)$$

Now in polar coordinates

$$\mathbf{A} = \hat{r} A_r + \hat{\theta} A_\theta + \hat{\phi} A_\phi \quad (17)$$

\dagger Note that $1/\epsilon_0 c = \mu_0 c = \sqrt{\mu_0/\epsilon_0} = 376.7 \Omega$.



FIGURE 14-8
Resolution of vector potential into A_r and A_θ components.

In our case \mathbf{A} has only a z component, so that $A_\phi = 0$, and from Fig. 14-8

$$A_r = A_z \cos \theta \quad (17a)$$

$$A_\theta = -A_z \sin \theta \quad (17b)$$

In polar coordinates we also have for the gradient of the scalar potential

$$\nabla V = \hat{\mathbf{r}} \frac{\partial V}{\partial r} + \hat{\theta} \frac{1}{r} \frac{\partial V}{\partial \theta} + \hat{\phi} \frac{1}{r \sin \theta} \frac{\partial V}{\partial \phi} \quad (18)$$

It follows from (4) and the above relations that the components of \mathbf{E} are

$$E_r = -j\omega A_r - \frac{\partial V}{\partial r} = -j\omega A_z \cos \theta - \frac{\partial V}{\partial r} \quad (19)$$

$$E_\theta = -j\omega A_\theta - \frac{1}{r} \frac{\partial V}{\partial \theta} = j\omega A_z \sin \theta - \frac{1}{r} \frac{\partial V}{\partial \theta} \quad (20)$$

$$E_\phi = -j\omega A_\phi - \frac{1}{r \sin \theta} \frac{\partial V}{\partial \phi} = - \frac{1}{r \sin \theta} \frac{\partial V}{\partial \phi} \quad (21)$$

Now introducing the value of A_z from (7) and V from (15) into these equations, we find that $E_\phi = 0$ (since V is independent of ϕ , so that $\partial V / \partial \phi = 0$) and also that

$$E_r = \frac{I_0 le^{j(\omega t - \beta r)} \cos \theta}{2\pi\epsilon_0} \left(\frac{1}{cr^2} + \frac{1}{j\omega r^3} \right) \quad (22)$$

and

$$E_\theta = \frac{I_0 le^{j(\omega t - \beta r)} \sin \theta}{4\pi\epsilon_0} \left(\frac{j\omega}{c^2 r} + \frac{1}{cr^2} + \frac{1}{j\omega r^3} \right) \quad (23)$$

Turning our attention now to the magnetic field, we can calculate it by (5). In polar coordinates the curl of \mathbf{A} is

$$\begin{aligned} \nabla \times \mathbf{A} &= \frac{\hat{\mathbf{r}}}{r \sin \theta} \left[\frac{\partial (\sin \theta A_\phi)}{\partial \theta} - \frac{\partial (A_\theta)}{\partial \phi} \right] \\ &\quad + \frac{\hat{\theta}}{r \sin \theta} \left[\frac{\partial A_r}{\partial \phi} - \frac{\partial (r \sin \theta A_\phi)}{\partial r} \right] + \frac{\hat{\phi}}{r} \left[\frac{\partial (r A_\theta)}{\partial r} - \frac{\partial A_r}{\partial \theta} \right] \end{aligned} \quad (24)$$

Since $A_\phi = 0$, the first and fourth terms of (24) are zero. From (7), (17a), and (17b) we note that A_r and A_θ are independent of ϕ , so that the second and third terms of (24) are also zero. Thus, since only the last two terms in (24) contribute, $\nabla \times \mathbf{A}$ has only a ϕ component. Introducing A_r and A_θ into (24), performing the indicated operations, and substituting this result into (5), we find that $H_r = H_\theta = 0$ and that

$$H_\phi = |\mathbf{H}| = \frac{I_0 le^{j(\omega t - \beta r)} \sin \theta}{4\pi} \left(\frac{j\omega}{cr} + \frac{1}{r^2} \right) \quad (25)$$

Thus the electric and magnetic fields from the dipole have only three components E_r , E_θ , and H_ϕ . The components E_ϕ , H_r , and H_θ are everywhere zero.

When r is very large, the terms involving $1/r^2$ and $1/r^3$ in (22), (23), and (25) can be neglected in comparison with terms in $1/r$. Thus, in the far field E_r is negligible, and we have effectively only two field components, E_θ and H_ϕ , given by

$$E_\theta = \frac{j\omega I_0 le^{j(\omega t - \beta r)} \sin \theta}{4\pi\epsilon_0 c^2 r} = j \frac{30I_0 \beta l}{r} e^{j(\omega t - \beta r)} \sin \theta \quad (26)$$

$$H_\phi = \frac{j\omega I_0 le^{j(\omega t - \beta r)} \sin \theta}{4\pi cr} = j \frac{I_0 \beta l}{4\pi r} e^{j(\omega t - \beta r)} \sin \theta \quad (27)$$

Taking the ratio of E_θ to H_ϕ as given by (26) and (27), we obtain for air or vacuum

$$\frac{E_\theta}{H_\phi} = \frac{1}{\epsilon_0 c} = \sqrt{\frac{\mu_0}{\epsilon_0}} = 376.7 \Omega \quad (28)$$

This is the intrinsic impedance of free space.

It is to be noted that E_θ and H_ϕ are in time phase in the far field. Thus, \mathbf{E} and \mathbf{H} in the far field of the spherical wave from the dipole are related in the same manner as in a plane traveling wave. Both are also proportional to $\sin \theta$. That is, both are a maximum when $\theta = 90^\circ$ and a minimum when $\theta = 0$ (in the direction of the dipole axis). This variation of E_θ (or H_ϕ) with angle can be portrayed by a *field pattern* as in Fig. 14-9, the length ρ of the radius vector being proportional to the value of the far field (E_θ or H_ϕ) in that direction from the dipole. The pattern in Fig. 14-9a is one-half of a three-dimensional pattern and illustrates that the fields are a function of θ but are independent of ϕ . The pattern in Fig. 14-9b is two-dimensional and represents a cross section through the three-dimensional pattern. The three-dimensional far-field pattern of the short dipole is doughnut-shaped, while the two-dimensional pattern has the shape of a figure of eight.

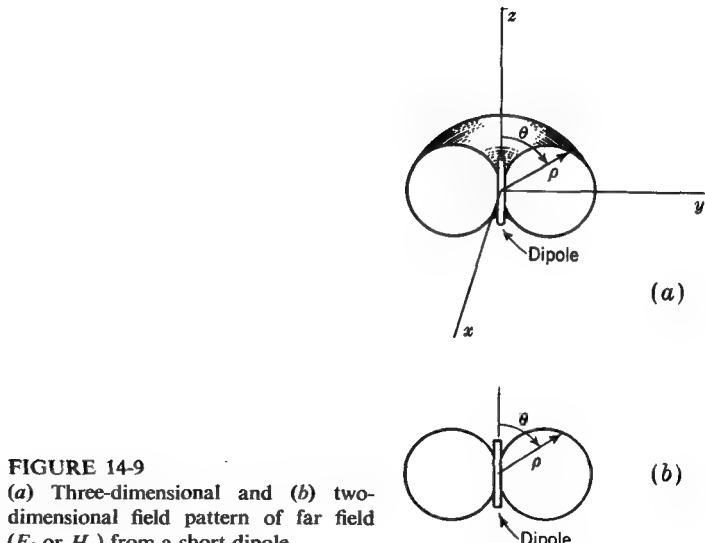


FIGURE 14-9

(a) Three-dimensional and (b) two-dimensional field pattern of far field (E_θ or H_ϕ) from a short dipole.

From (22), (23), and (25) we note that for a small value of r the electric field has two components, E_r and E_θ , both of which are in time-phase quadrature with the magnetic field H_ϕ . Thus, in the *near field*, \mathbf{E} and \mathbf{H} are related as in a standing wave. At intermediate distances, E_θ and E_r can approach time-phase quadrature with each other so that the total electric field vector rotates in a plane parallel to the direction of propagation and containing the dipole, exhibiting the phenomenon of cross field (see Sec. 11-6).

In the far field the energy flow is real. That is, the energy flow is always radially outward. This energy is radiated. As a function of angle it is maximum at the equator ($\theta = 90^\circ$). In the near field the energy flow is largely reactive. That is, energy flows out and back twice per cycle without being radiated. There is also angular energy flow (in the θ direction). This energy picture is suggested by Fig. 14-10, where the arrows represent the direction of energy flow at successive instants.[†]

Let us now consider the situation at very low frequencies. This will be referred to as the *quasi-stationary* case. Noting that $I_0 = j\omega q_0$, we can express the field components as

$$E_r = \frac{q_0 le^{j(\omega t - \beta r)} \cos \theta}{2\pi\epsilon_0} \left(\frac{j\omega}{cr^2} + \frac{1}{r^3} \right) \quad (29)$$

[†] The instantaneous direction and time rate of energy flow per unit area is given by the instantaneous Poynting vector ($= \mathbf{E} \times \mathbf{H}$).

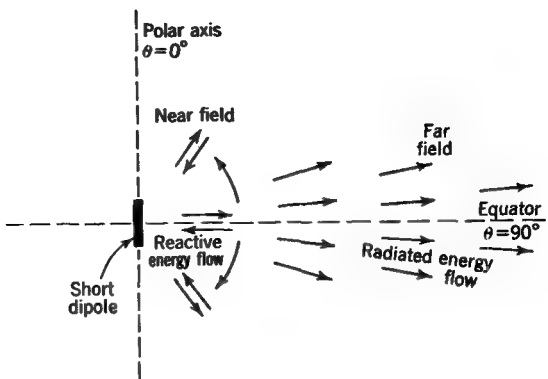


FIGURE 14-10
Energy flow in near and far regions of short dipole.

$$E_\theta = \frac{q_0 l e^{j(\omega t - \beta r)} \sin \theta}{4\pi\epsilon_0} \left(-\frac{\omega^2}{c^2 r} + \frac{j\omega}{cr^2} + \frac{1}{r^3} \right) \quad (30)$$

$$H_\phi = \frac{I_0 l e^{j(\omega t - \beta r)} \sin \theta}{4\pi} \left(\frac{j\omega}{cr} + \frac{1}{r^2} \right) \quad (31)$$

As the frequency approaches zero ($\omega \rightarrow 0$), the terms with ω in the numerator can be neglected. Also $e^{j(\omega t - \beta r)}$ approaches unity. Thus, for the quasi-stationary (or dc) case† the field components become

$$E_r = \frac{q_0 l \cos \theta}{2\pi\epsilon_0 r^3} \quad (32)$$

$$E_\theta = \frac{q_0 l \sin \theta}{4\pi\epsilon_0 r^3} \quad (33)$$

$$H_\phi = \frac{I_0 l \sin \theta}{4\pi r^2} \quad (34)$$

The electric field components, (32) and (33), are the same as (2-15-4) and (2-15-5) for a static electric dipole, while the magnetic field component H_ϕ in (34) is equivalent to (5-3-3) for a current element. Since these fields vary as $1/r^2$ or $1/r^3$, they are effectively confined to the vicinity of the dipole and radiation is negligible. At high frequencies in the far field, however, we note from (26) and (27) that the fields (E_θ and H_ϕ) vary as $1/r$. These fields are radiated and hence are often called the *radiation fields* of the dipole.

† For this case the wavelength is very large ($\lambda \rightarrow \infty$) so that $\lambda \gg l$. We also have $r \gg l$ and hence in this case $\lambda \gg r$.

The expressions for the fields from a short dipole, developed above, are summarized in Table 14-1. In the table the restriction applies that $r \gg l$ and $\lambda \gg l$. The three field components not listed are everywhere zero, that is, $E_\phi = H_r = H_\theta = 0$.

If we had been interested only in the far field, the development following (7) could have been much simplified. The scalar potential V does not contribute to the far field, so that both \mathbf{E} and \mathbf{H} can be determined from \mathbf{A} alone. Thus, from (4), E_θ and H_ϕ of the far field can be obtained very simply from $E_\theta = |\mathbf{E}| = -j\omega A_\theta$ and $H_\phi = |\mathbf{H}| = E_\theta/Z_0 = -(j\omega/Z_0)A_\theta$, where $Z_0 = \sqrt{\mu_0/\epsilon_0} = 376.7 \Omega$. Or H_ϕ may be obtained directly from (5) and E_θ from this. Thus

$$H_\phi = |\mathbf{H}| = \frac{1}{\mu_0} |\nabla \times \mathbf{A}| \quad (35)$$

and, neglecting terms in $1/r^2$,

$$E_\theta = |\mathbf{E}| = ZH_\phi = \frac{Z}{\mu_0} |\nabla \times \mathbf{A}| \quad (36)$$

Referring to (26) for the far E_θ field of a short dipole, it is instructive to separate the expression into its six basic factors. Thus,

$$E_\theta = 60\pi I_0 \frac{l}{\lambda} \frac{1}{r} j e^{j(\omega t - \beta r)} \sin \theta \quad (37)$$

Magni- Current Length Distance Phase Pattern
tude

where 60π is a constant (*magnitude*) factor, I_0 is the dipole *current*, l/λ is the dipole *length* in terms of wavelengths, $1/r$ is the *distance* factor, $j e^{j(\omega t - \beta r)}$ is the *phase* factor, and $\sin \theta$ is the *pattern* factor giving the variation of the field with angle. In general, the expression for the field of any antenna will involve these six factors.

Table 14-1 FIELDS OF A SHORT DIPOLE

Com- ponent	General expression	Far field	Quasi-stationary
E_r	$\frac{I_0 l e^{j(\omega t - \beta r)} \cos \theta}{2\pi\epsilon_0} \left(\frac{1}{cr^2} + \frac{1}{j\omega r^3} \right)$	0	$\frac{q_0 l \cos \theta}{2\pi\epsilon_0 r^3}$
E_θ	$\frac{I_0 l e^{j(\omega t - \beta r)} \sin \theta}{4\pi\epsilon_0} \left(\frac{j\omega}{c^2 r} + \frac{1}{cr^2} + \frac{1}{j\omega r^3} \right)$	$\frac{j60\pi I_0 e^{j(\omega t - \beta r)} \sin \theta}{r} \frac{l}{\lambda}$	$\frac{q_0 l \sin \theta}{4\pi\epsilon_0 r^3}$
H_ϕ	$\frac{I_0 l e^{j(\omega t - \beta r)} \sin \theta}{4\pi} \left(\frac{j\omega}{cr} + \frac{1}{r^2} \right)$	$\frac{jI_0 e^{j(\omega t - \beta r)} \sin \theta}{2r} \frac{l}{\lambda}$	$\frac{I_0 l \sin \theta}{4\pi r^2}$

The field relations in Table 14-1 are those for a short dipole. Longer linear antennas or large antennas of other shape may be regarded as being made up of many such short dipoles. Hence the fields of these larger antennas can be obtained by integrating the field contributions from all the small dipoles making up the antenna (see Sec. 14-9).

14-4 RADIATION RESISTANCE OF A SHORT DIPOLE

By taking the surface integral of the average Poynting vector over any surface enclosing an antenna the total power radiated by the antenna is obtained. Thus

$$P = \int_s \mathbf{S}_{av} \cdot d\mathbf{s} \quad (W) \quad (1)$$

where P = power radiated, W

\mathbf{S}_{av} = average Poynting vector, $W m^{-2}$

The simplest surface we might choose is a sphere with the antenna at the center. Since the far-field equations for an antenna are simpler than the near-field relations, it will be to our advantage to make the radius of the sphere large compared with the dimensions of the antenna. In this way the surface of the sphere lies in the far field, and only the far-field components need be considered.

Assuming no losses, the power radiated by the antenna is equal to the average power delivered to the antenna terminals. This is equal to $\frac{1}{2}I_0^2R$, where I_0 is the amplitude (peak value in time) of the current at the terminals and R is the *radiation resistance* appearing at the terminals. Thus $P = \frac{1}{2}I_0^2R$, and the radiation resistance is

$$R = \frac{2P}{I_0^2} \quad (\Omega) \quad (2)$$

where P is the radiated power in watts.

Let us now carry through the calculation, as outlined above, in order to find the radiation resistance of a short dipole. The power radiated is

$$P = \int_s \mathbf{S}_{av} \cdot d\mathbf{s} = \frac{1}{2} \int_s \text{Re}(\mathbf{E} \times \mathbf{H}^*) \cdot d\mathbf{s} \quad (3)$$

In the far field only E_θ and H_ϕ are not zero, so that (3) reduces to

$$P = \frac{1}{2} \int_s \text{Re} E_\theta H_\phi^* \hat{\mathbf{f}} \cdot d\mathbf{s} \quad (4)$$

where \hat{r} is the unit vector in the radial direction. Thus the power flow in the far field is entirely radial (normal to surface of sphere of integration). But $\hat{r} \cdot d\mathbf{s} = ds$; so

$$P = \frac{1}{2} \int_s \operatorname{Re} E_\theta H_\phi^* ds \quad (5)$$

where E_θ and H_ϕ^* are complex, H_ϕ^* being the complex conjugate of H_ϕ . Now $E_\theta = H_\phi Z$; so (5) becomes

$$P = \frac{1}{2} \int_s \operatorname{Re} H_\phi H_\phi^* Z ds = \frac{1}{2} \int_s |H_\phi|^2 \operatorname{Re} Z ds \quad (6)$$

Since $\operatorname{Re} Z = \sqrt{\mu_0/\epsilon_0}$ and $ds = r^2 \sin \theta d\theta d\phi$,†

$$P = \frac{1}{2} \sqrt{\frac{\mu_0}{\epsilon_0}} \int_0^{2\pi} \int_0^\pi |H_\phi|^2 r^2 \sin \theta d\theta d\phi \quad (7)$$

where the angles θ and ϕ are as shown in Fig. 14-5 and $|H_\phi|$ is the absolute value (or amplitude) of the H field. From (14-3-27) this is

$$|H_\phi| = \frac{\omega I_0 l \sin \theta}{4\pi c r} \quad (8)$$

Substituting this into (7), we have

$$P = \frac{1}{32} \sqrt{\frac{\mu_0}{\epsilon_0}} \left(\frac{\beta I_0 l}{\pi} \right)^2 \int_0^{2\pi} \int_0^\pi \sin^3 \theta d\theta d\phi \quad (9)$$

Upon integration (9) becomes

$$P = \sqrt{\frac{\mu_0}{\epsilon_0}} \frac{(\beta I_0 l)^2}{12\pi} \quad (\text{W}) \quad (10)$$

This is the power radiated by the short dipole.

Substituting the power P from (10) into (2) yields for the *radiation resistance of the short dipole*

$$R = \sqrt{\frac{\mu_0}{\epsilon_0}} \frac{(\beta l)^2}{6\pi} \quad (\Omega) \quad (11)$$

Since $\sqrt{\mu_0/\epsilon_0} = 376.7 \approx 120\pi \Omega$, (11) reduces to

$$R = 20(\beta l)^2 = 80\pi^2 \left(\frac{l}{\lambda} \right)^2 \quad (\Omega) \quad (12)$$

† Since $\sqrt{\mu_0/\epsilon_0} \approx 120\pi \approx E_\theta/H_\phi$, we may also write

$$P = \frac{1}{240\pi} \int_0^{2\pi} \int_0^\pi |E_\theta|^2 r^2 \sin \theta d\theta d\phi$$

EXAMPLE Find the radiation resistance of a dipole antenna $\lambda/10$ long.

SOLUTION From (12)

$$R = 80\pi^2 \left(\frac{1}{10}\right)^2 = 7.9 \Omega$$

If there is any heat loss in the antenna due to finite conductivity of the dipole or to losses in the associated dielectric structure, an equivalent *loss resistance* R_{loss} will appear such that the terminal resistance is given by

$$R = R_{\text{loss}} + R_r \quad (\Omega) \quad (13)$$

where R_{loss} = loss resistance, Ω

R_r = radiation resistance, Ω

Suppose, for instance, that $R_{\text{loss}} = 1 \Omega$ for the $\lambda/10$ dipole of the above example. The terminal resistance is then $8.9 \Omega (= 1.0 + 7.9)$. The *antenna efficiency* k is

$$\begin{aligned} k &= \frac{\text{Power radiated}}{\text{Power input}} = \frac{R_r}{R_r + R_{\text{loss}}} \\ &= \frac{7.9}{8.9} = 89 \text{ percent.} \end{aligned} \quad (13a)$$

A longer dipole with larger radiation resistance would be more efficient provided R_{loss} remained small.

The radiation resistance of antennas other than the short dipole can be calculated as above provided the far field is known as a function of angle. Thus, from (2) and (6) the *radiation resistance at the terminals of an antenna* is given by

$$R_r = \frac{120\pi}{I_0^2} \int_s |H|^2 ds \quad (\Omega) \quad (14)$$

where $|H|$ = amplitude of far H field, A m^{-1}

I_0 = amplitude of terminal current, A

If we integrate the complex Poynting vector ($= \frac{1}{2} \mathbf{E} \times \mathbf{H}^*$) over a surface enclosing an antenna, we shall obtain, in general, both a real part equal to the power radiated and an imaginary part equal to the reactive power. Whereas the real part, or radiated power, is the same for *any* surface enclosing the antenna, the imaginary, or reactive, power obtained depends on the size and shape of the surface enclosing the antenna. For a large surface lying only in the far field the reactive power is zero, but for a surface lying in the near field it may be of considerable magnitude. In the case of a very thin linear antenna, it turns out that if the surface of integration is collapsed so as to coincide with the surface of the antenna, the complex power so obtained divided by the square of the terminal current yields the terminal impedance $R + jX$, where R is the radiation resistance.

14-5 DIRECTIVITY, GAIN, AND EFFECTIVE APERTURE

A useful way of describing the pattern of an antenna is in terms of the angular width of the main lobe at a particular level. Referring to Fig. 14-2a, the angle at the half-power level or *half-power beam width* (HPBW)[†] is usually the one given. The *beam width between first nulls* (BWFN) or beam widths 10 or 20 dB below the pattern maximum are also sometimes used.

The antenna power pattern as a function of angle can be expressed as the radial component of the average Poynting vector multiplied by the square of the distance r at which it is measured. Thus, regardless of the wave polarization we have from (11-3-12) and (11-3-13) that

$$P(\theta, \phi) = S_r r^2 = \frac{1}{2} \frac{E^2(\theta, \phi)}{Z} r^2 = \frac{1}{2} H^2(\theta, \phi) Z r^2 \quad (\text{W sr}^{-1}) \quad (1)$$

where S_r = radial component of Poynting vector (time-average value), W m^{-2}

$E(\theta, \phi)$ = total transverse electric field as a function of angle, V m^{-1}

$H(\theta, \phi)$ = total transverse magnetic field as a function of angle, A m^{-1}

r = distance from antenna to point of measurement, m

Z = intrinsic impedance of medium, Ω per square

It is assumed that the medium is lossless. In the far field the Poynting vector is entirely radial (fields entirely transverse), and E and H vary as $1/r$, so that $P(\theta, \phi)$ is independent of distance. The quantity $P(\theta, \phi)$ is often called the *radiation intensity* (W sr^{-1} or W rad^{-2}). Dividing $P(\theta, \phi)$ by its maximum value [$P(\theta, \phi)_{\max}$], we obtain the *normalized antenna power pattern*,

$$P_n(\theta, \phi) = \frac{P(\theta, \phi)}{P(\theta, \phi)_{\max}} \quad (\text{dimensionless}) \quad (2)$$

A normalized antenna power pattern is shown in Fig. 14-11 with pattern maximum coinciding with the direction $\theta = 0$. A highly significant way of describing an antenna pattern is to integrate the normalized power pattern with respect to angle and obtain a *solid angle*. Thus, integrating $P_n(\theta, \phi)$ over $4\pi \text{ sr (rad}^2)$ we get the total pattern solid angle or *beam solid angle*

$$\Omega_A = \int_{\phi=0}^{\phi=2\pi} \int_{\theta=0}^{\theta=\pi} P_n(\theta, \phi) \sin \theta \, d\theta \, d\phi = \iint_{4\pi} P_n(\theta, \phi) \, d\Omega \quad (\text{sr}) \quad (3)$$

[†] Also called the 3-dB beamwidth.

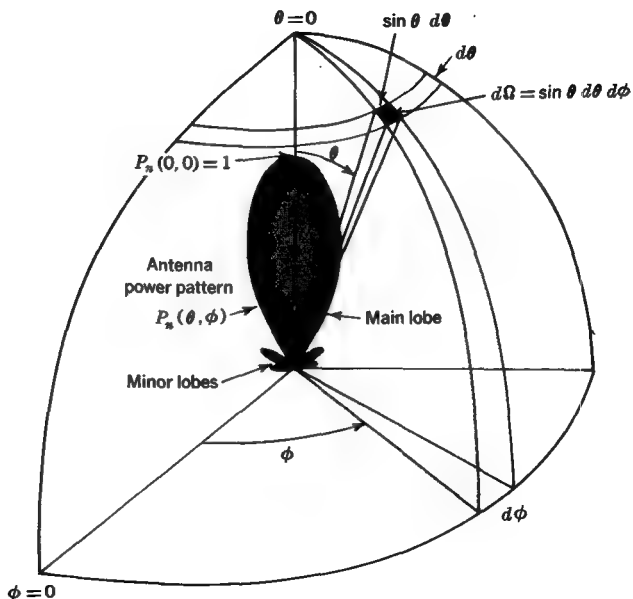


FIGURE 14-11

Antenna power pattern with maximum aligned with the $\theta = 0$ direction (zenith).

Although the term total pattern solid angle would be explicit, the term *beam solid angle* is customarily used for Ω_A .

The *beam solid angle* Ω_A is the angle through which all the power from a transmitting antenna would stream if the power (per unit solid angle) were constant over this angle and equal to the maximum value. It turns out that for typical patterns this angle is approximately equal to the half-power beam width (HPBW), as suggested in Fig. 14-12.

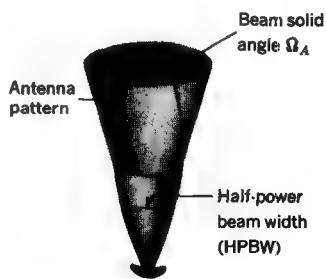


FIGURE 14-12

Antenna power pattern and its relation to the beam solid angle.

Integrating over the main lobe gives the *main-lobe solid angle*[†]

$$\Omega_M = \iint_{\substack{\text{main} \\ \text{lobe}}} P_n(\theta, \phi) d\Omega \quad (\text{sr}) \quad (4)$$

It follows that the *minor-lobe solid angle* Ω_m is given by the difference of the beam (total pattern) solid angle and the main-beam solid angle. That is,

$$\Omega_m = \Omega_A - \Omega_M \quad (\text{sr}) \quad (5)$$

If the antenna has no minor lobes ($\Omega_m = 0$), then $\Omega_A = \Omega_M$. For an isotropic antenna (radiation same in all directions) $P_n(\theta, \phi) = 1$ for all θ and ϕ , and $\Omega_A = 4\pi$.‡

Another important antenna parameter is the *directivity* D , which may be defined as the ratio of the maximum radiation intensity (antenna transmitting) to the average radiation intensity, or

$$D = \frac{\text{maximum radiation intensity}}{\text{average radiation intensity}} = \frac{P(\theta, \phi)_{\max}}{P_{av}} \quad (\text{dimensionless}) \quad (6)$$

The average radiation intensity is given by the total power radiated W divided by 4π sr. The total power radiated is equal to the radiation intensity $P(\theta, \phi)$ integrated over 4π sr. Hence,

$$\begin{aligned} D &= \frac{P(\theta, \phi)_{\max}}{W/4\pi} = \frac{4\pi P(\theta, \phi)_{\max}}{\iint_{4\pi} P(\theta, \phi) d\Omega} \\ &= \frac{4\pi}{\iint_{4\pi} [P(\theta, \phi)/P(\theta, \phi)_{\max}] d\Omega} = \frac{4\pi}{\iint_{4\pi} P_n(\theta, \phi) d\Omega} \end{aligned} \quad (7)$$

We note that the denominator of the last member of (7) is the beam solid angle as given by (3); so

$$D = \frac{4\pi}{\Omega_A} \quad (\text{dimensionless}) \quad (8)$$

Thus, the *directivity* of an antenna is equal to the solid angle of a sphere (4π sr) divided by the antenna beam solid angle Ω_A . In this relation, directivity is derived from the pattern. The directivity is a unique dimensionless quantity. It indicates

† In patterns for which no clearly defined minimum exists the extent of the main lobe may be somewhat indefinite, and an arbitrary level such as -20 dB can be used to delineate it.

‡ The *beam efficiency* ϵ_M may be defined as $\epsilon_M = \Omega_M/\Omega_A$.

how well the antenna concentrates power into a limited solid angle; the smaller the angle the larger the directivity.

EXAMPLE 1 Calculate the directivity of an isotropic antenna (uniform radiation intensity in all directions).

SOLUTION For an isotropic antenna $P_n(\theta, \phi) = 1$ and $\Omega_A = 4\pi$; so

$$D = \frac{4\pi}{\Omega_A} = 1 \quad (9)$$

Thus, the directivity of an isotropic antenna is unity. This is the smallest value the directivity can attain.

EXAMPLE 2 Calculate the directivity of a short dipole.

SOLUTION The short dipole has only an H_ϕ component of the magnetic field as given by (14-3-27). Thus, its normalized power pattern is

$$P_n(\theta, \phi) = \frac{H_\phi^2(\theta, \phi)}{H_\phi^2(\theta, \phi)_{\max}} = \sin^2 \theta \quad (10)$$

and noting (3) and (8),

$$D = \frac{4\pi}{\int_0^{2\pi} \int_0^\pi \sin^3 \theta \, d\theta \, d\phi} = \frac{3}{2} \quad (11)$$

Hence, the directivity of a short dipole is $\frac{3}{2}$. That is, the maximum radiation intensity is 1.5 times as much as if the power were radiated uniformly in all directions.

Directivity is based entirely on the shape of the far- (or radiated-) field pattern. The antenna efficiency is not involved. However, the power gain, or simply the *gain*, of an antenna does involve the efficiency. It is defined as follows:

$$\text{Gain} = G = \frac{\text{maximum radiation intensity}}{\text{maximum radiation intensity from a reference antenna with the same power input}} \quad (12)$$

Any convenient type of antenna may be taken as the reference. If the reference antenna is a lossless isotropic type (radiation intensity uniform in all directions), the gain (designated G_0) is given by

$$G_0 = \frac{P'_m}{P_0} \quad (13)$$

where P'_m = maximum radiation intensity from antenna under consideration

P_0 = radiation intensity from a lossless (100 percent efficient) isotropic antenna with same power input

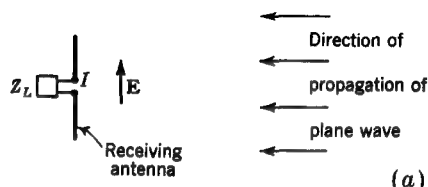
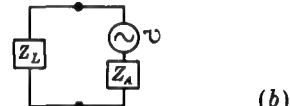


FIGURE 14-13
(a) Terminated receiving antenna immersed in field of plane traveling wave and (b) equivalent circuit.



Since P'_m is related to the radiation intensity P_m of a 100 percent efficient antenna by the antenna efficiency factor k , same as k in (14-4-13a),

$$G_0 = \frac{kP_m}{P_0} = kD \quad (14)$$

Thus, the gain of an antenna over a lossless isotropic type equals the directivity if the antenna is 100 percent efficient ($k = 1$) but is less than the directivity if any losses are present in the antenna ($k < 1$).

The gain G_0 (over an isotropic source) when expressed in decibels can be written dB_i (*decibels over isotropic*) to distinguish it from the gain over a reference $\lambda/2$ antenna, as discussed in Sec. 14-20. The gain (in dB_i) equals the directivity D if the antenna is lossless.

The directivity D is never less than unity. Its value must lie between 1 and infinity ($1 \leq D \leq \infty$). On the other hand, the gain (G or G_0) may lie between 0 and infinity.

A transmitting antenna radiates energy. A receiving antenna, on the other hand, collects energy. In this connection it is often useful to consider that the receiving antenna possesses an aperture or equivalent area A over which it extracts energy from a passing radio wave.

Thus, suppose that a receiving antenna is immersed in the field of a plane traveling wave, as suggested in Fig. 14-13a. The antenna is terminated in a load of impedance $Z_L = R_L + jX_L$. Let the aperture A of the antenna be defined as the ratio of the received power to the power density (or Poynting vector) of the incident wave. The received power is equal to $I^2 R_L$, where I is the terminal current. Therefore

$$A = \frac{I^2 R_L}{S} = \frac{\text{received power}}{\text{power density of incident wave}} \quad (15)$$

where A = aperture, m^2

I = rms terminal current, A

S = Poynting vector (or power density) of incident wave, W m^{-2}

R_L = load resistance, Ω

Replacing the antenna by its equivalent, or Thévenin, generator having an equivalent emf \mathcal{U} and impedance $Z_A (= R_A + jX_A)$, we may draw the equivalent circuit shown in Fig. 14-13b. The terminal current I is

$$I = \frac{\mathcal{U}}{Z_L + Z_A} \quad (\text{A}) \quad (16)$$

where \mathcal{U} = rms emf induced by passing wave, V

Z_L = load impedance, Ω

Z_A = antenna impedance Ω

When (16) is substituted into (15), it follows that

$$A = \frac{\mathcal{U}^2 R_L}{S[(R_A + R_L)^2 + (X_A + X_L)^2]} \quad (17)$$

where R_A = antenna resistance, Ω

X_A = antenna reactance, Ω

R_L = load resistance, Ω

X_L = load reactance, Ω

The emf \mathcal{U} will be greatest when the antenna is oriented for maximum response. Under these conditions the maximum power will be transferred to the load when $X_L = -X_A$ and $R_L = R_r$. It is assumed that the antenna is lossless, so that R_A is entirely radiation resistance ($R_A = R_r$). Under these conditions we obtain the maximum aperture, known as the *effective aperture* A_e , as given by

$$A_e = \frac{\mathcal{U}^2 R_L}{4SR_r^2} = \frac{\mathcal{U}^2}{4SR_r} \quad (\text{m}^2) \quad (18)$$

The *effective aperture* A_e has a unique, simply defined value for all antennas.

EXAMPLE 3 Find the effective aperture of a short dipole antenna.

SOLUTION Referring to (18), we need to know \mathcal{U} , S , and R_r . The emf induced in the short dipole is a maximum when the dipole is parallel to the incident electric field \mathbf{E} . Hence

$$\mathcal{U} = El \quad (\text{V}) \quad (19)$$

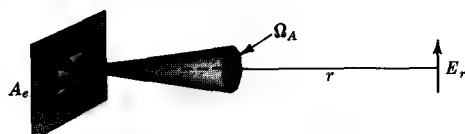


FIGURE 14-14
Radiation from aperture A_e with uniform field E_a .

The Poynting vector is

$$S = \frac{E^2}{Z_0} \quad (\text{W m}^{-2}) \quad (20)$$

where Z_0 is the intrinsic impedance of medium (air or vacuum) ($= \sqrt{\mu_0/\epsilon_0}$). From (14-4-11) the radiation resistance is

$$R_r = \sqrt{\frac{\mu_0}{\epsilon_0}} \frac{(\beta l)^2}{6\pi} \quad (\Omega) \quad (21)$$

Substituting these values for U , S , and R_r into (18) gives the effective aperture of a short dipole:

$$A_e = \frac{3}{8\pi} \lambda^2 = 0.119\lambda^2 \quad (22)$$

Thus, regardless of how small the dipole is, it can collect power over an aperture of $0.119\lambda^2$ and deliver it to its terminal impedance or load. It is assumed here that the dipole is lossless. However, in practice, losses are present due to the finite conductivity of the dipole conductor, so that the actual effective aperture is less ($R_d = R_r + R_{loss}$).

Consider next that an antenna with effective aperture A_e has the beam solid angle Ω_A , as suggested in Fig. 14-14. If the field E_a is constant over the aperture, the power radiated is

$$P = \frac{E_a^2}{Z} A_e \quad (\text{W}) \quad (23)$$

where Z is the intrinsic impedance of the medium. Let the field at a radius r be E_r . Then the power radiated is given by

$$P = \frac{E_r^2}{Z} r^2 \Omega_A \quad (\text{W}) \quad (24)$$

Equating (23) and (24) and substituting $E_r = E_a A_e / r \lambda$ [see (14-7-5)] yields the important relation

$\lambda^2 = A_e \Omega_A \quad (\text{m}^2)$

(25)

where λ = wavelength, m

A_e = effective aperture, m^2

Ω_A = beam solid angle, sr

According to (25), the product of the effective aperture and the beam solid angle is equal to the wavelength squared. If A_e is known, we can determine Ω_A (or vice versa) at a given wavelength.

From (25) and (8) it follows that

$$D = \frac{4\pi}{\lambda^2} A_e \quad (26)$$

Here the directivity is based on the aperture. Aperture is discussed further in Sec. 14-23. Three expressions have now been given for the directivity D . They are

$$D = \frac{P(\theta, \phi)_{\max}}{P_{av}} \quad \text{from pattern} \quad (27)$$

$$D = \frac{4\pi}{\Omega_A} \quad \text{from pattern} \quad (28)$$

$$D = \frac{4\pi}{\lambda^2} A_e \quad \text{from aperture} \dagger \quad (29)$$

14-6 ARRAY THEORY

Much of antenna theory (and almost all of array theory) involves little more than the proper addition of the field contributions from all parts of an antenna. We must deal with the field (not power) since we must include both magnitude *and* phase.

14-6.1 Two Isotropic Point Sources

Consider two isotropic point sources separated by a distance d , as in Fig. 14-15a. A point source is an idealization representing here an isotropic radiator occupying zero volume. By reciprocity (see Sec. 14-18) the pattern of arrays of such sources (transmitting case) will be identical with the pattern when the array is used as a receiving antenna. Let the two point sources be identical (in amplitude) and in the same phase. Assume also that both sources have the same polarization; i.e., let both be linearly polarized with \mathbf{E} perpendicular to the page. When the reference point for phase is taken halfway between the sources, the far field in the direction θ is given by

$$\mathbf{E} = E_2 e^{j\psi/2} + E_1 e^{-j\psi/2} \quad (1)$$

[†] Here A_e is independent of ohmic losses. Thus, the gain G of the antenna is the same as given by (29) for a lossless antenna but is less if losses are present.

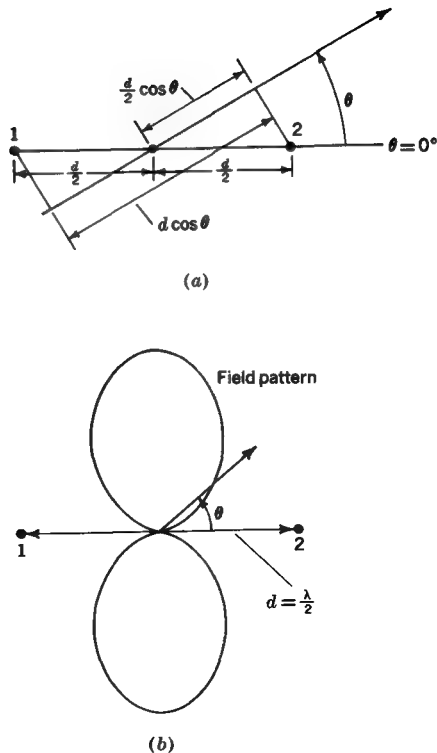


FIGURE 14-15
(a) Two isotropic point sources separated by a distance d and (b) field pattern when sources are of equal amplitude and in phase with $\lambda/2$ separation.

where E_1 = far electric field at distance r due to source 1

E_2 = far electric field at distance r due to source 2

$$\psi = \beta d \cos \theta = (2\pi d/\lambda) \cos \theta$$

The quantity ψ is the phase-angle difference between the fields of the two sources as measured along the radius-vector line at the angle θ (see Fig. 14-15a). When $E_1 = E_2$ we have

$$E = 2E_1 \frac{e^{j\psi/2} + e^{-j\psi/2}}{2} = 2E_1 \cos \frac{\psi}{2} \quad (2)$$

For a spacing of $\lambda/2$ the field pattern is as shown in Fig. 14-15b.

If the reference for phase for the two sources in Fig. 14-15 had been taken at source 1 (instead of midway between the sources), the resultant far field pattern would be

$$E = E_1 + E_2 e^{j\psi} \quad (3)$$

and for $E_1 = E_2$

$$E = 2E_1 \cos \frac{\psi}{2} e^{j\psi/2} = 2E_1 \cos \frac{\psi}{2} \angle \psi/2 \quad (4)$$

The field (amplitude) pattern is the same as before, but the phase pattern is not. This is because the reference was taken at the *phase center* (midpoint of array) in developing (2) but at one end of the array in developing (4).

14-6.2 Pattern Multiplication

We assumed above that each point source was isotropic (completely nondirectional). If the individual point sources have directional patterns which are identical, the resultant pattern is given by (14-6.1-2) [or (14-6.1-4)], where E_1 is now also a function of angle [$E_1 = E(\theta)$]. The pattern $E(\theta)$ may be called the *primary pattern* and $\cos \psi/2$ the *secondary pattern* or *array factor*. This is an example of the *Principle of Pattern Multiplication*, which may be stated more generally as follows: *The total field pattern of an array of nonisotropic but similar sources is the product of the individual source pattern and the pattern of an array of isotropic point sources each located at the phase center of the individual source and having the same relative amplitude and phase, while the total phase pattern is the sum of the phase patterns of the individual sources and the array of isotropic point sources.*†

14-6.3 Binomial Array

From (14-6.1-2) the relative far-field pattern of two identical in-phase isotropic point sources spaced $\lambda/2$ apart is given by

$$E = \cos\left(\frac{\pi}{2} \cos \theta\right) \quad (1)$$

For convenience we have set $E_1 = \frac{1}{2}$ in (14-6.1-2) so that the pattern is normalized. This pattern, as shown in Fig. 14-15b, has no minor lobes. If a second identical array of two sources is placed $\lambda/2$ from the first, the arrangement shown in Fig. 14-16a is obtained. The two sources at the center should be superimposed but are shown separated for clarity. By the principle of pattern multiplication, the resultant pattern is given by

$$E = \cos^2\left(\frac{\pi}{2} \cos \theta\right) \quad (2)$$

† It is assumed that the pattern of the individual source is the same when it is in the array as when it is isolated.

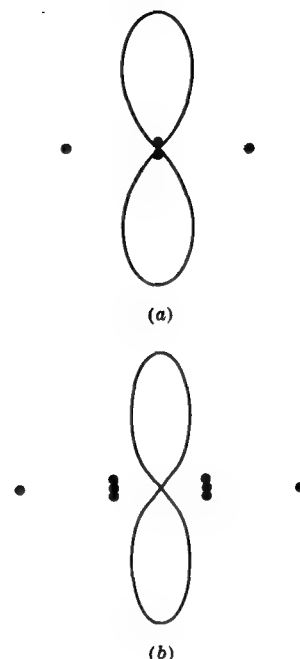


FIGURE 14-16
 (a) Binomial array with source amplitudes 1:2:1: and (b) binomial array with source amplitudes 1:3:3:1:. The spacing between sources is $\lambda/2$.

as shown in Fig. 14-16a. If this three-source array with amplitudes 1:2:1 is arrayed with an identical one at a spacing $\lambda/2$, the arrangement of Fig. 14-16b is obtained with the pattern

$$E = \cos^3\left(\frac{\pi}{2} \cos \theta\right) \quad (3)$$

as shown in Fig. 14-16b. This array has effectively four sources with amplitudes 1:3:3:1, and it also has no minor lobes. Continuing this process, it is possible to obtain a pattern with arbitrarily high directivity and no minor lobes if the amplitudes

Table 14-2 PASCAL'S TRIANGLE

							1					
							1	1	1	1	1	
							1	3	3	3	1	
							1	4	6	4	1	
							1	5	10	10	5	1
							1	6	15	20	15	6

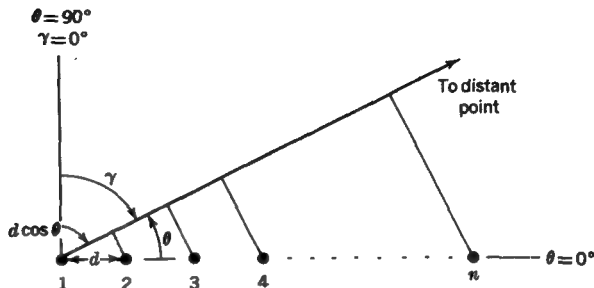


FIGURE 14-17
Array of n isotropic point sources of equal amplitude and spacing.

of the sources in the array correspond to the coefficients of a binomial series.[†] These coefficients are conveniently displayed by Pascal's triangle (Table 14-2). Each internal integer is the sum of the adjacent ones above. The pattern of the array is then

$$E = \cos^{-1} \left(\frac{\pi}{2} \cos \theta \right) \quad (4)$$

where n is the total number of sources.

Although the above array has no minor lobes, its directivity is less than that of an array of the same size with equal-amplitude sources. In practice most arrays are designed as a compromise between these extreme cases (binomial and uniform).

14-6.4 Array with n Sources of Equal Amplitude and Spacing

The binomial array is a nonuniform array. For a uniform array, as in Fig. 14-17, with n isotropic sources of equal amplitude and spacing, the far field is

$$E = E_0 (1 + e^{j\psi} + e^{j2\psi} + \cdots + e^{j(n-1)\psi}) \quad (1)$$

or

$$E = E_0 \sum_{n=1}^N e^{j(n-1)\psi} \quad (2)$$

where $\psi = \beta d \cos \theta + \delta$

d = spacing between sources

δ = progressive phase difference between sources

[†] J. S. Stone, U.S. Pats. 1,643,323 and 1,715,433.

[‡] This is a polynomial of degree $n - 1$, as can be seen by putting $e^{j\psi}$ equal to a unit phasor \hat{r} . Thus (1) becomes

$$\frac{E}{E_0} = 1 + \hat{r} + \hat{r}^2 + \cdots + \hat{r}^{n-1}$$

Multiplying (1) by $e^{j\psi}$ yields

$$Ee^{j\psi} = E_0(e^{j\psi} + e^{j2\psi} + e^{j3\psi} + \dots + e^{jn\psi}) \quad (3)$$

Subtracting (3) from (1), we have

$$E = E_0 \frac{1 - e^{jn\psi}}{1 - e^{j\psi}} = E_0 \frac{\sin(n\psi/2)}{\sin(\psi/2)} \angle (n-1)\frac{\psi}{2} \quad (4)$$

If the center of the array is chosen as the reference for phase, instead of source 1, the phase angle, $(n-1)\psi/2$, is eliminated. If the sources are nonisotropic but similar, E_0 represents the primary or individual source pattern, while $\sin(n\psi/2)/\sin(\psi/2)$ is the array factor.

For isotropic sources and the center of the array as reference for phase the pattern is

$$E = E_0 \frac{\sin(n\psi/2)}{\sin(\psi/2)} \quad (5)$$

As $\psi \rightarrow 0$, (5) reduces to

$$E = nE_0 \quad (6)$$

This is the maximum value of the field. It is n times the field from a single source. In the direction of the maximum the condition $\psi = 0$ or $\beta d \cos \theta = -\delta$ is satisfied. Dividing (5) by (6) yields the normalized field pattern

$$E_n = \frac{E}{nE_0} = \frac{1}{n} \frac{\sin(n\psi/2)}{\sin(\psi/2)}$$

(7)

Referring to (4), the null directions of the pattern occur for $e^{jn\psi} = 1$ provided $e^{j\psi} \neq 1$. This requires that $n\psi = \pm 2k\pi$ or

$$\pm \frac{2k\pi}{n} = \beta d \cos \theta_0 + \delta \quad (8)$$

or

$$\theta_0 = \cos^{-1} \left[\left(\pm \frac{2k\pi}{n} - \delta \right) \frac{\lambda}{2\pi d} \right] \quad (9)$$

where θ_0 = null angle

$k = 1, 2, 3, \dots$ (but $k \neq mn$, where $m = 1, 2, 3, \dots$)

14-6.5 Array with n Sources of Equal Amplitude and Spacing: Broadside Case

In the direction of the pattern maximum the condition $\beta d \cos \theta = -\delta$ must be satisfied. For a broadside array (maximum at $\theta = 90^\circ$) the sources must be in phase ($\delta = 0$). When θ is replaced by its complementary angle γ (see Fig. 14-17) the null angles are given by

$$\gamma_0 = \sin^{-1} \left(\pm \frac{k\lambda}{nd} \right) \quad (1)$$

If the array is large, so that $nd \gg k\lambda$ (and γ_0 is small),

$$\gamma_0 = \frac{k}{nd/\lambda} \approx \frac{k}{L/\lambda} \quad (2)$$

where L = length of array, m

$$L = (n - 1)d \approx nd \text{ if } n \text{ is large}$$

The first nulls (γ_{01}) occur when $k = 1$. Hence, the beam width between first nulls (BWFN) is

$$\text{BWFN} = 2\gamma_{01} \approx \frac{2}{L/\lambda} \text{ rad} = \frac{114.6^\circ}{L/\lambda} \quad (3)$$

The more commonly used parameter is the half-power beam width (HPBW), which is about one-half (more nearly 0.44) the BWFN of a long uniform broadside array. Thus,

$$\text{HPBW} \approx \frac{\text{BWFN}}{2} = \frac{1}{L/\lambda} \text{ rad} = \frac{57.3^\circ}{L/\lambda} \quad (4)$$

The field pattern of a broadside array of 20 sources of equal amplitude spaced $\lambda/2$ apart is shown in Fig. 14-18a. The BWFN is 11.5° , and the HPBW is 5.1° . The three-dimensional pattern is a (disk-shaped) figure of revolution obtained by rotating the pattern of Fig. 14-18a around the array axis.

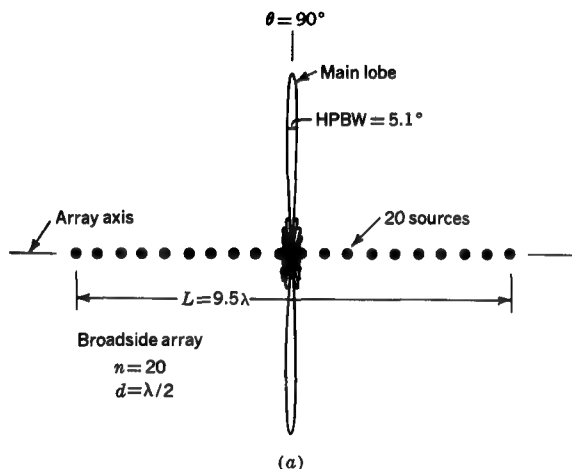
14-6.6 Array with n Sources of Equal Amplitude and Spacing: End-fire Case

For an end-fire array (maximum at $\theta = 0^\circ$) the condition $\beta d \cos \theta = -\delta$ requires that the progressive phase difference δ between sources be $-\beta d$. From (14-6.4-8)

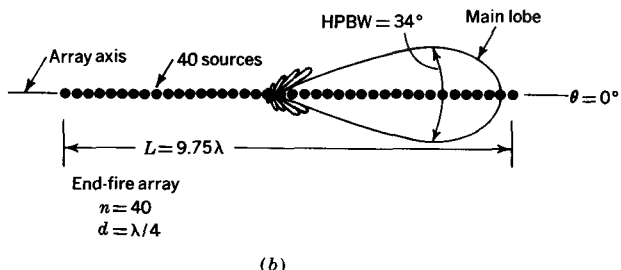
$$\cos \theta_0 - 1 = \pm \frac{k}{nd/\lambda} \quad (1)$$

or

$$\frac{\theta_0}{2} = \sin^{-1} \left(\pm \sqrt{\frac{k}{2nd/\lambda}} \right) \quad (2)$$



(a)



(b)

FIGURE 14-18

(a) Broadside array of 20 point sources of equal amplitude and $\lambda/2$ spacing with field pattern; (b) (ordinary) end-fire array of 40 point sources of equal amplitude and $\lambda/4$ spacing with field pattern. Note that both arrays are of approximately the same length (9.5 vs. 9.75λ).

For a long array ($nd \gg k\lambda$)

$$\theta_0 = \pm \sqrt{\frac{2k}{nd/\lambda}} \approx \sqrt{\frac{2k}{L/\lambda}} \quad (3)$$

where $L = (n - 1)d \approx nd$ if n is large. The first nulls (θ_{01}) occur when $k = 1$. Hence,

$$\text{BWFN} = 2\theta_{01} \approx \pm 2 \sqrt{\frac{2}{L/\lambda}} \text{ rad} = \pm 114.6 \sqrt{\frac{2}{L/\lambda}} \text{ deg} \quad (4)$$

The field pattern of an end-fire array of 40 sources spaced $\lambda/4$ apart is shown in Fig. 14-18b. The BWFN is 52° , and the HPBW† is 34° . The three-dimensional pattern is a (cigar-shaped) figure of revolution obtained by rotating the pattern of Fig. 14-18b around the array axis.

Although the two arrays in Fig. 14-18 are approximately the same length (broadside array 9.5λ , end-fire array 9.75λ) we note that the beam width is much smaller for the broadside array (5° as compared to 34°) but only in the plane shown in the figure. The pattern of the broadside array is disk-shaped with a small beam width in the plane of the figure, but the beam width is 360° in a plane perpendicular to the page. On the other hand, the pattern of the end-fire array is ellipsoidal, or cigar-shaped, with the same pattern in both principal planes (in plane of page and perpendicular to page through array axis), and, as will be shown below (compare Examples 1 and 2), the directivity of the end-fire array is greater.

From (14-5-28) the directivity of an antenna is given by

$$D = \frac{4\pi}{\Omega_A} \quad (5)$$

An exact evaluation of the beam solid angle Ω_A requires an integration as in (14-5-3). However, a very simple *approximation*‡ can be made using the HPBWs in the two principal planes as follows:

$$D \approx \frac{4\pi}{\theta_{HP}^\circ \phi_{HP}^\circ} = \frac{41,253}{\theta_{HP}^\circ \phi_{HP}^\circ}$$

(6)

where θ_{HP} = HPBW in θ plane, rad

ϕ_{HP} = HPBW in ϕ plane, rad

θ_{HP}° = HPBW in θ plane, deg

ϕ_{HP}° = HPBW in ϕ plane, deg

In connection with (6) note that

$$4\pi \text{ sr} = 4\pi \text{ rad}^2 = 4\pi(57.3^2) \text{ deg}^2 = 41,253 \text{ deg}^2 \quad (7)$$

EXAMPLE 1 For the 9.5λ broadside array discussed above, with $\theta_{HP}^\circ = 5.1^\circ$ and $\phi_{HP}^\circ = 360^\circ$, calculate the approximate directivity.

† This HPBW is calculated exactly from (14-6-4-7). For a long uniform end-fire array $\text{HPBW} \approx \frac{3}{2} \text{ BWFN}$, while for a long uniform broadside array $\text{HPBW} \approx \frac{1}{2} \text{ BWFN}$, as given in (14-6-5-4).

‡ Minor lobes are ignored, and $\theta_{HP} \phi_{HP}$ is only approximately equal to the beam solid angle. Hence (6) may be in error by ± 1 dB or so.

SOLUTION From (6)

$$D \approx \frac{41,253}{5.1^\circ \times 360^\circ} = 22.5 \text{ (or } 13.5 \text{ dB}) \quad (8)$$

EXAMPLE 2 For the 9.75λ end-fire array discussed above, with $\theta_{HP}^0 = \phi_{HP}^0 = 34^\circ$, calculate the approximate directivity.

SOLUTION From (6)

$$D \approx \frac{41,253}{34^\circ \times 34^\circ} = 35.7 \text{ (or } 15.5 \text{ dB}) \quad (9)$$

This directivity is 2 dB more than for the broadside array of approximately the same length.

14-6.7 Graphical Representation of Phasor Addition of Fields

At the beginning of Sec. 14-6 it was stated that much of array theory is basically little more than the proper addition of the field contributions from all parts of an antenna. This can be emphasized by analyzing several simple antenna arrays using only graphical methods.

Consider the array of two isotropic in-phase sources, 1 and 2, of equal amplitude spaced a distance $d = \lambda/2$ ($\beta d = 180^\circ$), as shown in Fig. 14-19a. We assume that both sources have the same polarization, e.g., linear polarization with the electric field vector perpendicular to the page. The field pattern of the array can be determined by the addition of these fields with proper account taken of their relative phase. This is done with phasors. Thus, let the phasors shown by arrows E_1 and E_2 represent the magnitude and phase of the two sources or of the fields radiated by the sources. We have the condition given that $E_2 = E_1 \angle 0^\circ$ at the sources. The arrows (phasors) rotate counterclockwise (ccw) on the complex plane once per cycle (360° per cycle). In the direction $\theta = 90^\circ$ (broadside), E_1 and E_2 are received without phase change, so that the total field $E = 2E_1$ in this direction. In the direction $\theta = 45^\circ$, source 2 is $(\lambda/2) \sin 45^\circ = 0.35\lambda$ closer to the distant observer than source 1. When E_1 is taken as reference for phase, E_1 and E_2 add as suggested, with an internal angle between them of 127° ($= 180^\circ \sin 45^\circ$), giving a total $E = 0.9 E_1$. In the direction $\theta = 0^\circ$, the total field $E = 0$. This can be seen graphically from Fig. 14-19b. At time $t = 0$, E_1 and E_2 are as shown at the sources. Let E_1 be taken as reference for phase. Then one-quarter cycle later ($t = T/4$) the radiated field E_1 has traveled $\lambda/4$ (with no phase change), but during this interval E_2 has advanced 90° . By the time $t = T/2$, the radiated field E_1 has traveled $\lambda/2$ and reached source 2. In the meantime the phase of E_2 at source 2 has advanced a total of 180° and is in phase opposition to E_1 . Hence, the

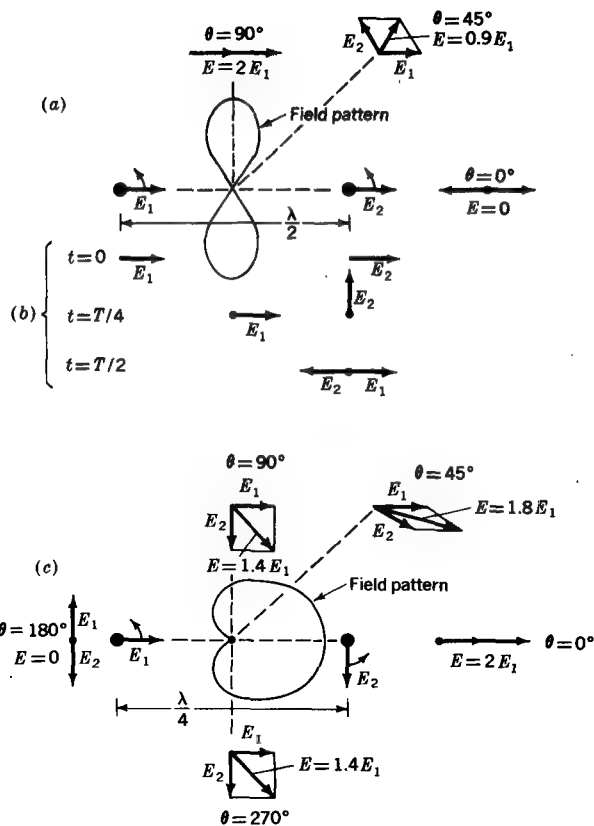


FIGURE 14-19

(a) and (b) Graphical addition of fields for array of two isotropic point sources of equal amplitude and same phase and (c) for end-fire array of two isotropic point sources of equal amplitude and phase quadrature.

total field E radiated in the direction $\theta = 0^\circ$ is zero, as suggested. Adding phasors for other directions, we obtain the field pattern shown in Fig. 14-19a.^f

Using this method, we find that the fields radiated from an array of two isotropic sources of equal amplitude spaced $\lambda/4$ apart with source 2 lagging source 1 by 90° are as suggested in Fig. 14-19c. In the direction $\theta = 0^\circ$, E_2 and E_1 add in the same

^f The magnitude of the arrows (phasors) is considered constant as a function of distance (even though fields do attenuate with distance) because we are interested in the difference of the field components at a distant point. Thus, when observing at a distance of thousands of wavelengths there is a negligible difference in magnitude from sources separated $\lambda/2$, as above, and this effect can be ignored. However, the phase difference cannot be neglected.

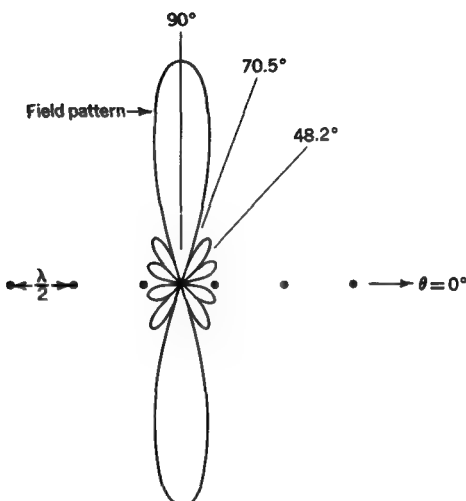


FIGURE 14-20

Field pattern of array of six isotropic in-phase point sources of equal amplitude with $\lambda/2$ spacing (see Table 14-3 for graphical addition of fields in different directions).

phase as shown (we take source 1 as reference for phase). In the direction $\theta = 180^\circ$, E_2 and E_1 add in phase opposition (we take E_2 as reference for phase). Thus, the total field $E = 2E_1$ to the right ($\theta = 0^\circ$) and is zero to the left. The complete pattern is a cardioid, as indicated.

EXAMPLE Calculate the pattern of a broadside array of six isotropic point sources with $d = \lambda/2$ and draw the phasor (addition) diagram for the pattern maxima and nulls.

SOLUTION The pattern is given by (14-6.4-5) with $\delta = 0^\circ$. From (14-6.4-8) the nulls (roots) occur when

$$\pm \frac{2k\pi}{6} = \frac{2\pi}{\lambda} \frac{\lambda}{2} \cos \theta = \pi \cos \theta \quad (1)$$

$$\text{or} \quad \cos \theta = \pm \frac{k}{3} \quad (2)$$

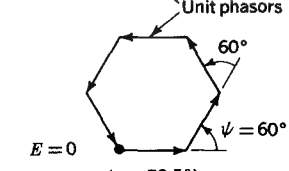
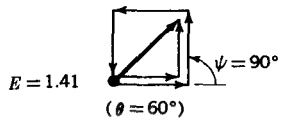
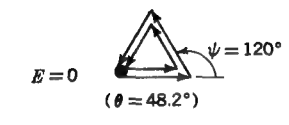
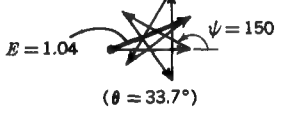
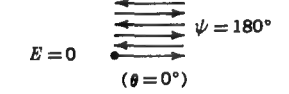
The minor-lobe maxima occur *approximately* when

$$\psi = \pm \frac{(2k+1)\pi}{n} \quad (3)$$

where $k = 1, 2, 3, \dots$. The values of k , θ , and ψ are related as in Table 14-3, and the column "Phasor addition" in the table illustrates how the unit phasors from each source add for the various conditions (see also Sec. 14-6.7). Note that in the null directions the phasors close on themselves. The field pattern of the array is shown in Fig. 14-20.

In this example and also in other cases considered in this section the total field is n times the field from a single source ($E = nE_1$) in the direction of the maximum radiation. This is the ordinary situation. However, it should be noted that it is possible to have a total $E < nE_1$ in the direction of maximum radiation. This condition is sometimes used to obtain increased directivity.

Table 14-3 PARAMETERS FOR LINEAR ARRAY OF SIX ISOTROPIC IN-PHASE POINT SOURCES OF EQUAL AMPLITUDE AND SPACING $d = \lambda/2$. FIELD PATTERN IS IN FIG. 14-20

Condition	k	θ	ψ	Phasor addition
Maximum	0	$\pm 90^\circ$	0	
Null	1	$\pm 70.5^\circ$	$\pm \frac{\pi}{3}$ ($\pm 60^\circ$)	
Maximum of minor lobe	—	$\pm 60^\circ$	$\pm \frac{\pi}{2}$ ($\pm 90^\circ$)	
Null	2	$\pm 48.2^\circ$	$\pm \frac{2}{3}\pi$ ($\pm 120^\circ$)	
Maximum of minor lobe	—	$\pm 33.7^\circ$	$\pm \frac{5}{6}\pi$ ($\pm 150^\circ$)	
Null	3	$0^\circ, 180^\circ$	$\pm \pi$ ($\pm 180^\circ$)	

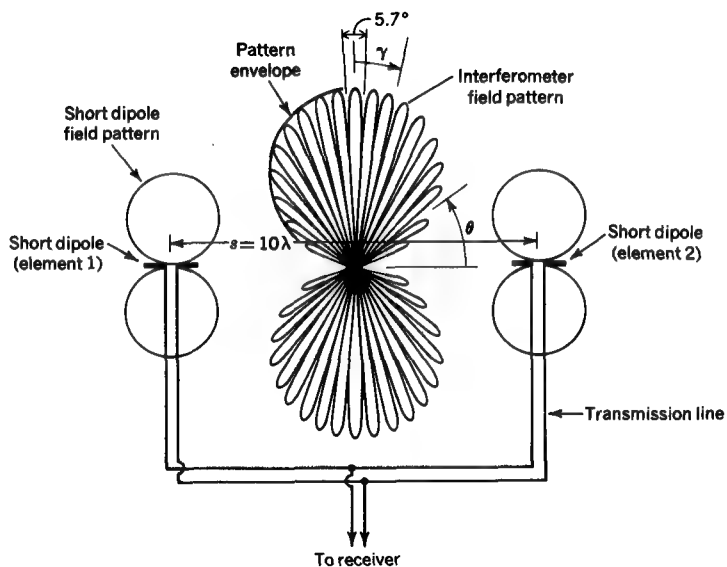


FIGURE 14-21

Simple two-element interferometer using short dipoles spaced 10λ showing patterns of the individual (short-dipole) elements and of the interferometer.

14-6.8 Simple Two-element Interferometer

The interferometer is a specialized type of antenna used widely for radio-astronomy observations. It provides a good example of pattern multiplication and array theory.

Consider two short-dipole antennas with spacing s connected in phase, as in Fig. 14-21. From (14-6.1-2) the field pattern is given by

$$E = 2E_1 \cos \frac{\psi}{2} \quad (1)$$

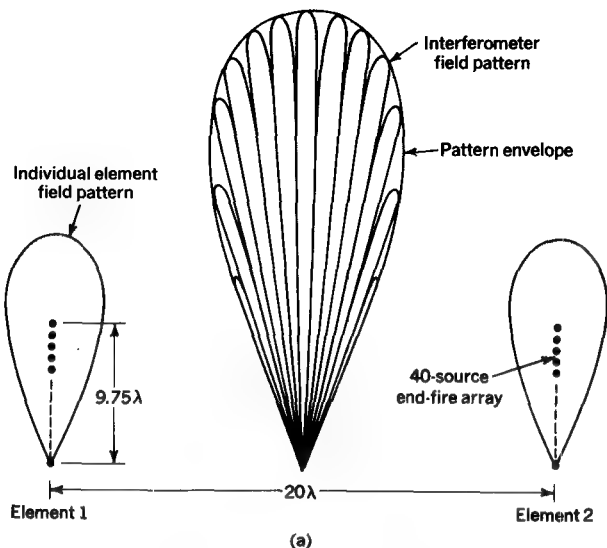
where $\psi = \beta s \cos \theta$

By pattern multiplication E_1 is the field pattern of the short dipole [= $\sin \theta$, see (14-3-37)], and $\cos(\psi/2)$ is the array factor. Hence, the complete interferometer pattern is

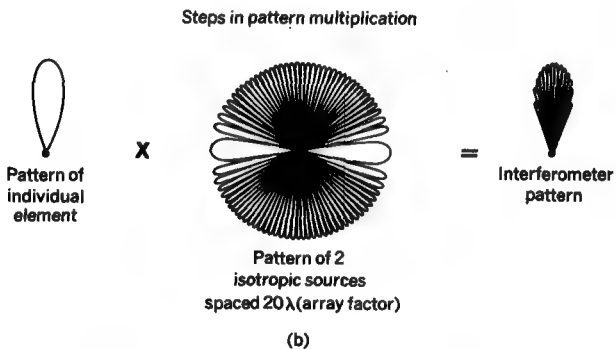
$$E = 2 \sin \theta \cos \left(\frac{\pi s}{\lambda} \cos \theta \right) \quad (2)$$

When θ is replaced by its complementary angle γ , the first null occurs when $(\pi s/\lambda) \sin \gamma_{01} = \pi/2$ or

$$\gamma_{01} = \sin^{-1} \frac{1}{2s/\lambda} \quad (3)$$



(a)



(b)

FIGURE 14-22

(a) Two-element interferometer using 40-point-source end-fire arrays spaced 20λ showing patterns of the individual (end-fire array) elements and of the interferometer. (b) Steps in pattern multiplication to obtain interferometer pattern. Individual element pattern (at left) multiplied by array pattern (center) yields interferometer pattern (at right).

If we assume that the spacing s is many wavelengths, the BWFN is then

$$\boxed{\text{BWFN} = 2y_{01} = \frac{1}{s/\lambda} \text{ rad} = \frac{57.3}{s/\lambda} \text{ deg}} \quad (4)$$

This BWFN is one-half the value for a uniform array of n sources as given by (14-6.5-3). The interferometer field pattern is illustrated in Fig. 14-21 for $s = 10\lambda$. The

BWFN of this interferometer pattern is, from (4), equal to 5.7° . The envelope of the multilobed pattern is the same shape as the short-dipole pattern ($= \sin \theta$). In most applications more directional individual element patterns would be desirable. An interferometer array of this type is shown in Fig. 14-22a. Here two 40-source end-fire arrays (like the one described in Sec. 14-6.6) are arrayed with a spacing of 20λ . Each 40-source array has a field pattern as shown (see also Fig. 14-18b). When connected as a two-element broadside array (or interferometer), as in Fig. 14-22a, the result is a multilobed pattern with $\text{BWFN} = 2.9^\circ$ ($= 57.3/20$). The steps in the pattern multiplication are illustrated in Fig. 14-22b.

In radio-astronomy applications an interferometer is used for receiving radiation from celestial radio sources as they drift across the sky through the antenna pattern. The detection and location of the source are facilitated by the small beam widths of the lobes of the patterns.[†]

14-7 CONTINUOUS APERTURE DISTRIBUTION

In the preceding pages we have dealt with arrays of point sources, i.e., arrays of a finite number of sources separated by finite distances. Now let us consider a *continuous* array of point sources, i.e., an array of an infinite number of point sources separated by infinitesimal distances. By Huygens' principle (Sec. 12-6) a continuous array of point sources is equivalent to a continuous field (or current-sheet distribution). In this way we can extend array analysis to include the radiation patterns of field distributions across apertures of electromagnetic horns or parabolic dish antennas.

Consider the aperture distribution of length a in the y direction and width x_1 in the x direction (perpendicular to page), as suggested in Fig. 14-23. The magnitude of the field over the aperture is a function of y but is independent of x . The field is in the same phase over the entire aperture. The infinitesimal field at a distance from an elemental aperture area $dx dy$ is, from $E = -j\omega A$ and (14-3-7),[‡]

$$dE = -j\omega [dA_x] = \frac{-j\omega \mu E(y)}{4\pi r Z} e^{-j\beta r} e^{j\omega t} dx dy \quad (\text{V m}^{-1}) \quad (1)$$

where $[A_x] = x$ component of retarded vector potential [see (14-2-6)], Wb m^{-1}

$E(y) =$ electric field distribution as function of y across aperture, V m^{-1}

$Z =$ intrinsic impedance of medium, Ω

The total field in the θ direction at a distance r_0 from the center of the aperture

[†] This discussion is much simplified. For a more detailed discussion see, for example, J. D. Kraus, "Radio Astronomy," chap. 6, McGraw-Hill Book Company, New York, 1966.

[‡] Note that $E(y)/Z = E_x(y)/Z = H_y = J_x z_1$, where z_1 is the thickness of the equivalent current sheet in the aperture. Thus, in (14-3-7) let $I_0 = J_x z_1 dy$ and $l = dx$.

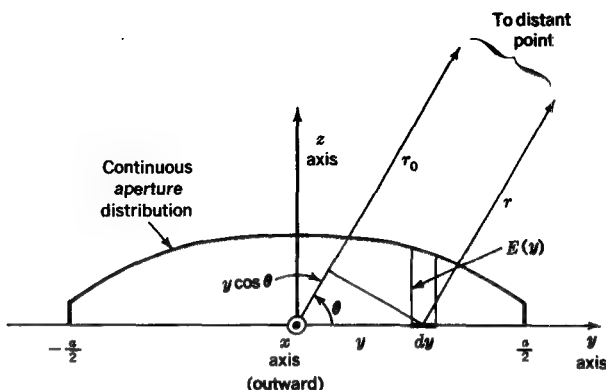


FIGURE 14-23
Aperture of width a and amplitude distribution $E(y)$.

is obtained by integrating (1) over the aperture (extent a by x_1). If $r \gg a$, then $r = r_0 - y \cos \theta$ and

$$E(\theta) = \frac{-j\omega\mu x_1 e^{j(\omega t - \beta r_0)}}{4\pi r_0 Z} \int_{-a/2}^{+a/2} E(y) \exp(j\beta y \cos \theta) dy \quad (2)$$

The magnitude of $E(\theta)$ is then†

$$E(\theta) = \frac{x_1}{2r_0 \lambda} \int_{-a/2}^{+a/2} E(y) \exp(j\beta y \cos \theta) dy \quad (3)$$

For a uniform aperture distribution [$E(y) = E_a$] (3) reduces to

$$E(\theta) = \frac{x_1 E_a}{2r_0 \lambda} \int_{-a/2}^{+a/2} \exp(j\beta y \cos \theta) dy \quad (4)$$

On axis ($\theta = 90^\circ$) we have

$$E(\theta) = \frac{E_a a x_1}{2r_0 \lambda} = \frac{E_a A}{2r_0 \lambda} \quad (5)$$

where $A = ax_1$ is the aperture area in square meters. If the aperture is unidirectional (maximum radiation at $\theta = 90^\circ$ but none at $\theta = 270^\circ$), the value of $E(\theta)$ should be doubled. This is the value which was used in deriving (14-5-25). Integrating (4) gives

$$E(\theta) = \frac{E_a A}{2r_0 \lambda} \frac{\sin[(\beta a/2)\cos \theta]}{(\beta a/2)\cos \theta} \quad (6)$$

This gives the far-field pattern as a function of θ for a continuous, uniform distribution of field intensity E_a over a rectangular aperture of area A and length a (in the y direction).

† Note that $\omega\mu/4\pi Z = 1/2\lambda$.

Referring to the array of n isotropic sources of equal amplitude and spacing discussed earlier in Sec. 14-6.4, we recall that the field pattern was given in (14-6.4-5) as

$$E(\theta) = E_0 \frac{\sin n\psi/2}{\sin \psi/2} \quad (7)$$

where $\psi = \beta d \cos \theta + \delta$

E_0 = field from individual source

For the broadside case, $\delta = 0$, and (7) becomes

$$E(\theta) = E_0 \frac{\sin[(n\beta d/2)\cos \theta]}{\sin[(\beta d/2)\cos \theta]} \quad (8)$$

Let a' = length of array. Then if a' is large, $a' = (n - 1)d \approx nd$. Restricting our attention to angles near 90° (main beam direction), we can rewrite (8) as

$$E(\theta) = nE_0 \frac{\sin[(\beta a'/2)\cos \theta]}{(\beta a'/2)\cos \theta} \quad (9)$$

Comparing this expression with (6), we see that for a large aperture and at angles near the main beam, the field pattern of a continuous aperture is identical with the pattern of an n source broadside array of same length ($a = a'$). Also the fields have the same absolute value provided $nE_0 = E_a A / 2r_0 \lambda$.

14-8 FOURIER TRANSFORM RELATIONS BETWEEN THE FAR-FIELD PATTERN AND THE APERTURE DISTRIBUTION†

A one-dimensional aperture distribution $E(y)$ and its far-field pattern $E(\theta)$ are reciprocal *Fourier transforms*. For a finite aperture one of these transforms may be written

$$E(\theta) = \int_{-a/2}^{+a/2} E(y) \exp(j\beta y \cos \theta) dy \quad (1)$$

This is identical with (14-7-3) except for a constant factor.‡ Examples of the far-field patterns $E(\theta)$ of several field distributions $E(y)$ are presented in Fig. 14-24.

† Dividing by n , we get

$$E_0 = \frac{A}{n} \frac{E_a}{2r_0 \lambda} = \frac{A_0 E_a}{2r_0 \lambda}$$

where E_0 is the field at a distance r_0 from a source of effective aperture A_0 and field E_a in the aperture. This is equivalent to (14-7-5).

‡ H. G. Booker and P. C. Clemmow, The Concept of an Angular Spectrum of Plane Waves and Its Relation to That of Polar Diagram and Aperture Distribution, *Proc. IEE London*, (3) 97:11-17 (January 1950); C. H. Walter, "Traveling Wave Antennas," McGraw-Hill Book Company, New York, 1965.

§ Equation (14-7-3) is an absolute relation, whereas (1) is relative.

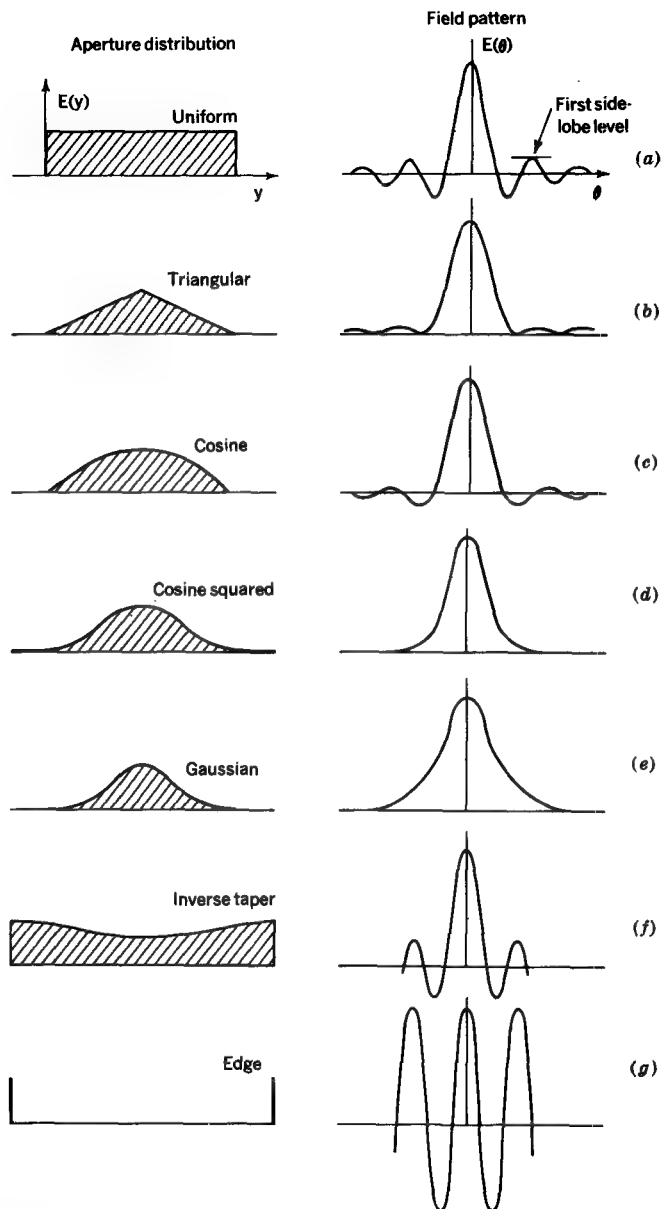


FIGURE 14-24

Seven different antenna aperture distributions with associated far-field patterns.

Taking the uniform aperture distribution and its pattern (Fig. 14-24a) as reference, we find that the tapered distributions (triangular and cosine) have larger beam widths but smaller minor lobes, while the most gradually tapered distributions (cosine squared and gaussian) have still larger beam widths but no minor lobes. On the other hand, an inverse taper, as in Fig. 14-24f, yields a smaller beam width but larger minor lobes than for the uniform distribution. Carrying the inverse taper to its extreme limit results in the edge distribution of Fig. 14-24g, which is equivalent to that of a two-element interferometer. The pattern in this case has a beam width one-half that of the uniform distribution but side lobes equal in amplitude to the main (central) lobe.

A useful property of (1) is that an aperture distribution can be taken as the sum of two or more component distributions with the resulting pattern equal to the sum of the transforms of these distributions.

14-9 LINEAR ANTENNAS

In Sec. 14-3 the dipole antenna was analyzed for the case where its length was small compared to the wavelength (say $\lambda/10$ or less). Let us now consider linear dipole antennas of any length L . It is assumed that the current distribution is sinusoidal. This is a satisfactory approximation provided the conductor diameter is small, say $\lambda/200$ or less.

Referring to Fig. 14-25, we shall calculate the far-field pattern for a symmetrical thin linear center-fed dipole antenna of length L . It will be done by regarding the antenna as being made up of a series of elemental short dipoles of length dy and current I and integrating their contribution at a large distance. The form of the current distribution on the antenna is found from experimental measurements to be given approximately by

$$I = I_0 \sin \left[\frac{2\pi}{\lambda} \left(\frac{L}{2} \pm y \right) \right] \quad (A)$$

where I_0 is the value of the current at the current maximum point, and where $(L/2) + y$ is used when $y < 0$ and $(L/2) - y$ is used when $y > 0$. Referring to Table 14-1 for the fields of a short dipole, we find the far (electric) field of an antenna of length L to be

$$E_\theta = k \sin \theta \int_{-L/2}^{L/2} I \exp(j\beta y \cos \theta) dy \quad (2)$$

where $k = \{j60\pi \exp[j(\omega t - \beta r_0)]\}/r_0 \lambda$. Substituting (1) for I in (2) and integrating yields

$$E_\theta = \frac{j60[I_0]}{r_0} \left\{ \frac{\cos[(\beta L \cos \theta)/2] - \cos(\beta L/2)}{\sin \theta} \right\} \quad (3)$$

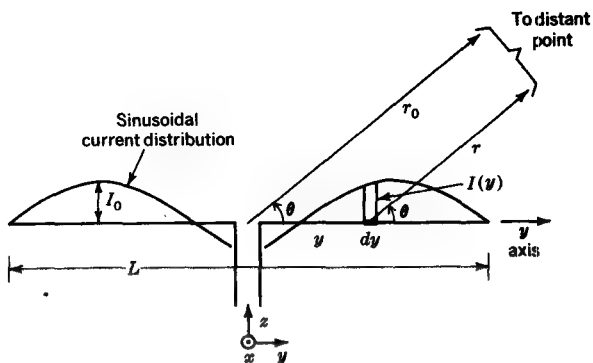


FIGURE 14-25

Geometry for linear center-fed dipole antenna of length L with sinusoidal current distribution.

where $[I_0] = I_0 \exp[j\omega(t - (r_0/c))]$ is the retarded current. The shape of the far-field pattern is given by the factor in braces in (3). For a $\lambda/2$ dipole antenna this factor reduces to

$$E_\theta(\theta) = \frac{\cos[(\pi/2) \cos \theta]}{\sin \theta} \quad (4)$$

with the shape shown in Fig. 14-26a. This pattern is only slightly more directional than the $\sin \theta$ pattern of an infinitesimal or short dipole (shown dashed). The HPBW of the $\lambda/2$ antenna is 78° , compared with 90° for a short dipole.

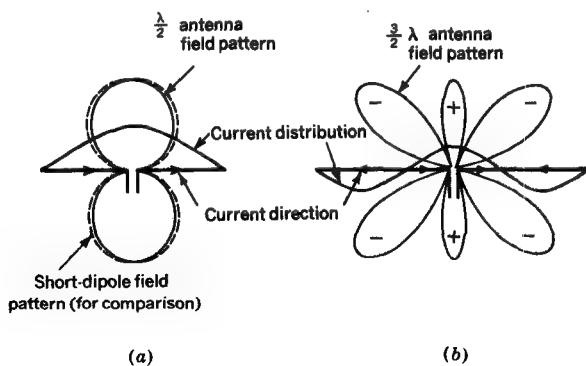


FIGURE 14-26

(a) Far-field pattern of $\lambda/2$ center-fed dipole antenna and (b) far-field pattern of 1.5λ center-fed dipole antenna.

For a 1.5λ dipole the pattern factor is

$$E_\theta(\theta) = \frac{\cos(\frac{3}{2}\pi \cos \theta)}{\sin \theta} \quad (5)$$

as shown in Fig. 14-26b. With the midpoint of the antenna as phase center, the phase of the far field (at a constant r_0) shifts 180° at each null, the relative phase of the lobes being indicated by the plus and minus signs. In Fig. 14-26a and b the three-dimensional pattern is a figure of revolution of the one shown with the dipole as axis (y axis in Fig. 14-25).

EXAMPLE Find the directivity of a $\lambda/2$ linear dipole.

SOLUTION For the $\lambda/2$ dipole we have from (4) and (14-5-7) that

$$D = \frac{4\pi}{\iint P_n(\theta, \phi) d\Omega} = \frac{4\pi}{2\pi \int_0^\pi \frac{\cos^2[(\pi/2)\cos \theta]}{\sin^2 \theta} \sin \theta d\theta} = 1.64 (= 2.15 \text{ dB}) \quad (6)$$

This is $1.64/1.5 = 1.09$ ($= 0.4$ dB) greater than the directivity of an infinitesimal or short dipole. Note: The integration of (6) involves sine (Si) and cosine (Ci) integrals.

To find the radiation resistance R of the $\lambda/2$ dipole the average Poynting vector is integrated over a large sphere, yielding the power radiated. This power is then equated to $I^2 R$, where I is the rms terminal current. Performing this calculation for the $\lambda/2$ dipole yields

$$R = 30 \text{ Cin } 2\pi = 30 \times 2.44 = 73 \Omega \quad (7)$$

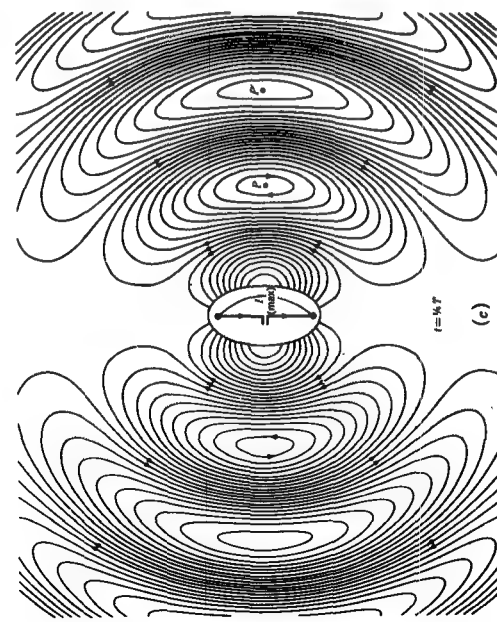
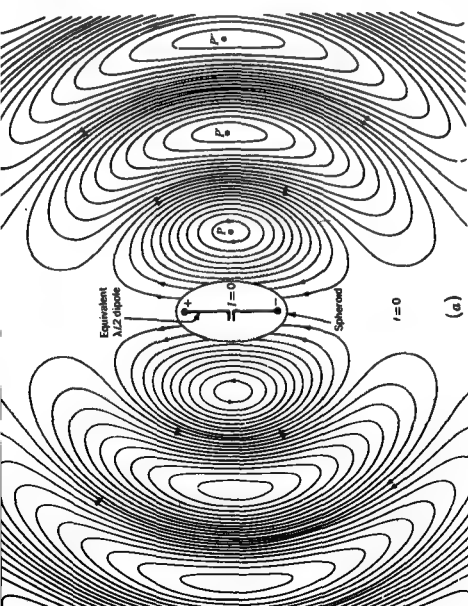
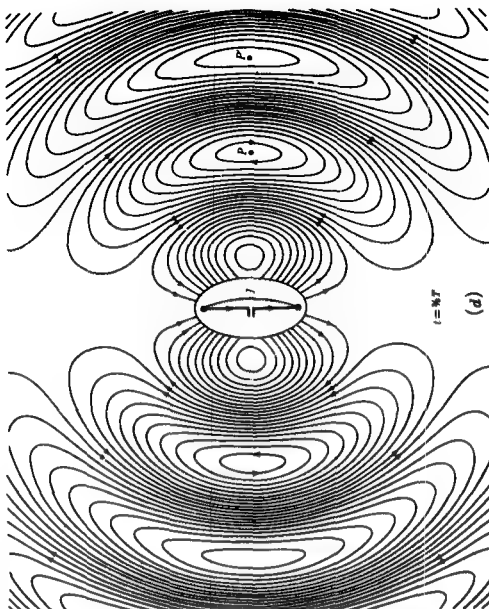
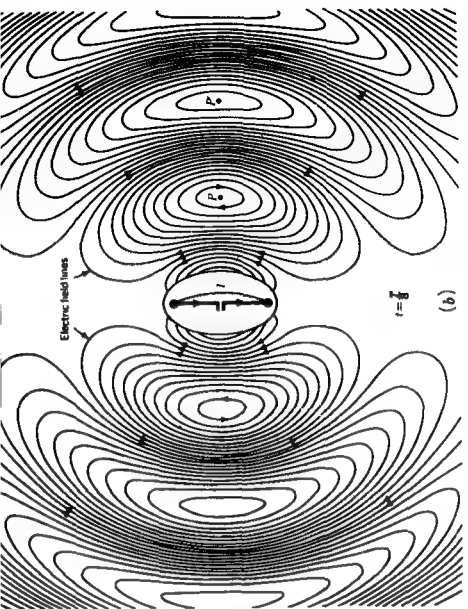
where Cin is the modified cosine integral. This is the resistance presented by a $\lambda/2$ dipole to the transmission-line terminals (Fig. 14-26a). The antenna impedance Z also contains a positive reactance of 42.5Ω ($Z = 73 + j42.5 \Omega$). To make the antenna resonant ($X = 0$) the length can be shortened a few percent. However, this also results in a slight reduction of the radiation resistance (to approximately 70Ω). The radiation resistance for the 1.5λ linear dipole is about 100Ω .

14-10 FIELDS OF $\lambda/2$ DIPOLE ANTENNA

To illustrate the configuration of the fields radiated by an antenna, the electric field lines of a $\lambda/2$ antenna are shown in Fig. 14-27 at four successive instants of time.

FIGURE 14-27

Electric field configuration for a $\lambda/2$ antenna at four instants of time (a) $t = 0$, (b) $t = T/8$, (c) $t = T/4$, and (d) $t = \frac{3}{8}T$ where $T = \text{period}$. Note outward movement of constant-phase points P , P' , and P'' as time advances. The strength of the electric field is proportional to the density of the lines. The field at $t = T/4$ is also shown on the book cover. (From "A Resonant Spheroid Radiator," produced at the Ohio State University for the National Committee for Electrical Engineering Films; Project Initiator, Prof. Edward M. Kennaugh; diagrams courtesy of Prof. John D. Cowan, Jr.)



Although the fields were computer-generated (and plotted) for a prolate spheroid with $\lambda/2$ interfocal distance, they are substantially the same as for a thin $\lambda/2$ center-fed dipole[†] except in the immediate proximity of the antenna. At time $t = 0$ (Fig. 14-27a) the antenna current is zero, and the charge at the ends of the dipole is a maximum. One-eighth of a period later ($t = T/8$) the current has started to flow, as suggested in Fig. 14-27b. At $t = T/4$ (Fig. 14-27c) the current has reached its peak value, and the charge at the ends is zero. At $t = \frac{3}{8}T$ (Fig. 14-27d) the current continues to flow in the same direction but with reduced magnitude. At $t = T/2$ the current is again zero, and the charge is a maximum at the ends. The field configuration at $t = T/2$ is identical with that shown in Fig. 14-27a except that the arrows and signs are reversed. At $t = \frac{5}{8}T$ the current has started to flow in the reverse direction (up), and the field is identical to that shown in Fig. 14-27b except that all arrows are reversed. Note that the lines in Fig. 14-27 are the actual field lines, not the field pattern (field intensity vs. angle). Compare with Fig. 14-26a with the dipole turned vertical.

Referring to all parts of Fig. 14-27, we note that a constant-phase point, such as P , moves radially outward approximately $\lambda/2$ in $\frac{1}{2}$ period (traveling approximately at the velocity of light, c). However, careful measurements show that P moves faster than c close to the antenna, like a higher-order-mode wave confined between the parallel plates of a waveguide, but farther out the velocity becomes exactly equal to c .[‡] Figure 14-27 is incomplete in that the magnetic field lines are not shown. They consist of circular loops concentric with the antenna and perpendicular to the plane of the figure. From the standpoint of power flow the situation is similar to that shown by the arrows in Fig. 14-10 for the short dipole with maximum power radiated outward in the equatorial plane ($\theta = 90^\circ$). This is real power flow. There is also reactive (nonradiating) power flow, oscillating back and forth close to the antenna, as suggested in Fig. 14-10.

14-11 TRAVELING-WAVE ANTENNAS[§]

In Sec. 14-9 on the linear antenna a sinusoidal current distribution was assumed. This type of current distribution is closely approximated if the antenna is thin (conductor diameter $<\lambda/200$) and provided the antenna is *unterminated*.

[†] For the thin $\lambda/2$ dipole the E_θ component would be as obtained from an equation like (14-9-2) but one which holds at small distances (see General expression in Table 14-1). Similarly calculating an E_r component makes it possible to determine the total field at any point.

[‡] This may be inferred from the fact that the distances between similar phase points (P, P', P'') are more than $\lambda/2$ apart near the antenna but are exactly $\lambda/2$ apart farther out.

[§] For a more detailed discussion of traveling-wave antennas, see, for example, Walter, op. cit.

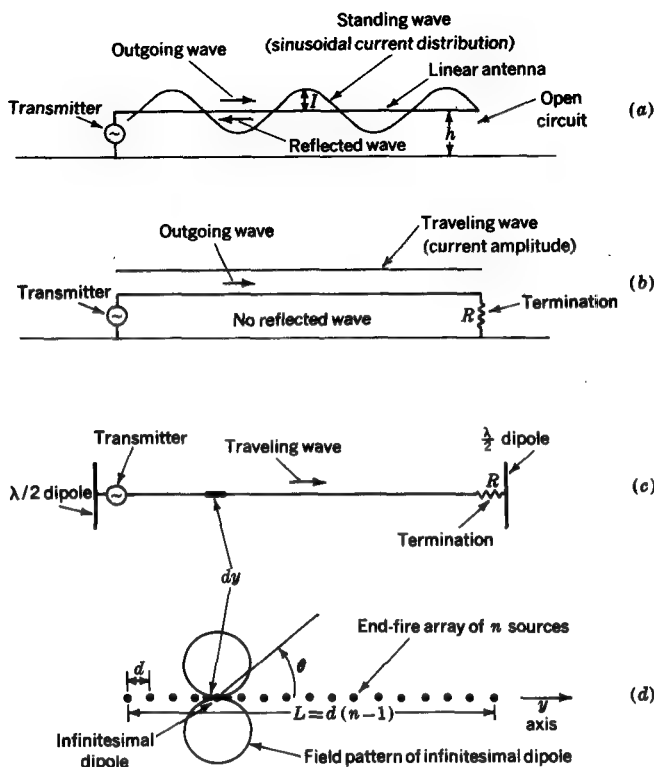


FIGURE 14-28

Long linear antennas (a) without and (b) and (c) with termination; (d) equivalent end-fire array of isotropic point sources.

Consider a thin linear antenna several wavelengths long situated a distance h above a perfectly conducting ground plane, as in Fig. 14-28a, with a transmitter connected at the left end. The antenna-ground-plane combination acts like an open-circuited transmission line. The transmitter sends a traveling wave down the line (to the right), which is reflected at the open end, causing an equal-amplitude wave to travel back (to the left). As a result a standing wave is set up on the line with a sinusoidal current distribution. The current is zero at the open end and is a maximum $\lambda/4$ from the open end, as suggested in Fig. 14-28a (see also Sec. 13-6). This is the situation assumed in Sec. 14-9 on the linear dipole antenna.

Let us now connect a resistance R equal to the characteristic resistance of the antenna-ground-plane transmission line between the open end of the antenna and the ground, as in Fig. 14-28b. This converts the antenna to a terminated type. There is

an outgoing traveling wave (to the right) but (ideally) no reflected wave. The current amplitude is constant over the length of the antenna provided losses are negligible and there is a progressive uniform phase change along the antenna. An arrangement for establishing a traveling wave on a long linear antenna remote from the ground is suggested in Fig. 14-28c. The midpoint of a $\lambda/2$ antenna is used as a ground equivalent.

The pattern of a linear antenna with traveling wave can be readily determined if we regard the antenna as being made up of an array of a large number of series-connected infinitesimal dipoles operating as an end-fire array, as in Fig. 14-28d. Thus, from Secs. 14-6.6 and 14-6.4 the far electric field pattern of such an array is given by

$$E_\theta(\theta) = E_0 \frac{\sin(n\psi/2)}{n \sin(\psi/2)} \quad (1)$$

where $\psi = \beta d \cos \theta - \beta d = \beta d(\cos \theta - 1)$. The first factor (E_0) represents the pattern of the infinitesimal elements of the array, which have the same pattern as a short dipole ($E_0 = \sin \theta$). The second factor is the normalized pattern of an array of n isotropic sources. By the principle of pattern multiplication the resultant pattern [$E_\theta(\theta)$] is the product of these two factors. For large $L [=d(n-1) \approx nd]$, resulting from a large n and small d , (1) can be expressed approximately as

$$E_\theta(\theta) = \sin \theta \frac{\sin[(\beta L/2)(1 - \cos \theta)]}{(\beta L/2)(1 - \cos \theta)} \quad (2)$$

For example, the pattern of a 9.75λ linear antenna with traveling wave is shown in Fig. 14-29a as the product of the pattern of an infinitesimal dipole and the pattern of an end-fire array of 40 isotropic sources with $\lambda/4$ spacing and uniform progressive phase shift $\delta = -\beta d = -\pi/2$. This is the same array as in Sec. 14-6.6 (see also Fig. 14-18b). The pattern of the array of 40 isotropic sources has a maximum at $\theta = 0^\circ$ (end-fire direction). However, the infinitesimal dipoles making up the array have a null at $\theta = 0^\circ$ and a maximum at $\theta = 90^\circ$. The resulting (product) pattern is of conical shape with cross section as shown in Fig. 14-29a (pattern at right). The first minor lobe is only 4.7 dB down. The large minor lobes are characteristic of long linear antennas. By contrast, the first minor lobe of the isotropic-source array is 13.5 dB down (see Fig. 14-29a, center pattern).

The maximum radiation for the 9.75λ linear antenna is at $\theta \approx 15^\circ$. By arranging two such linear antennas in the form of a V with about 30° included angle, as in Fig. 14-29b, a unidirectional antenna is obtained which can be conveniently fed by a balanced two-conductor transmission line. The resulting pattern of this terminated V antenna is suggested in Fig. 14-29b (pattern at right).

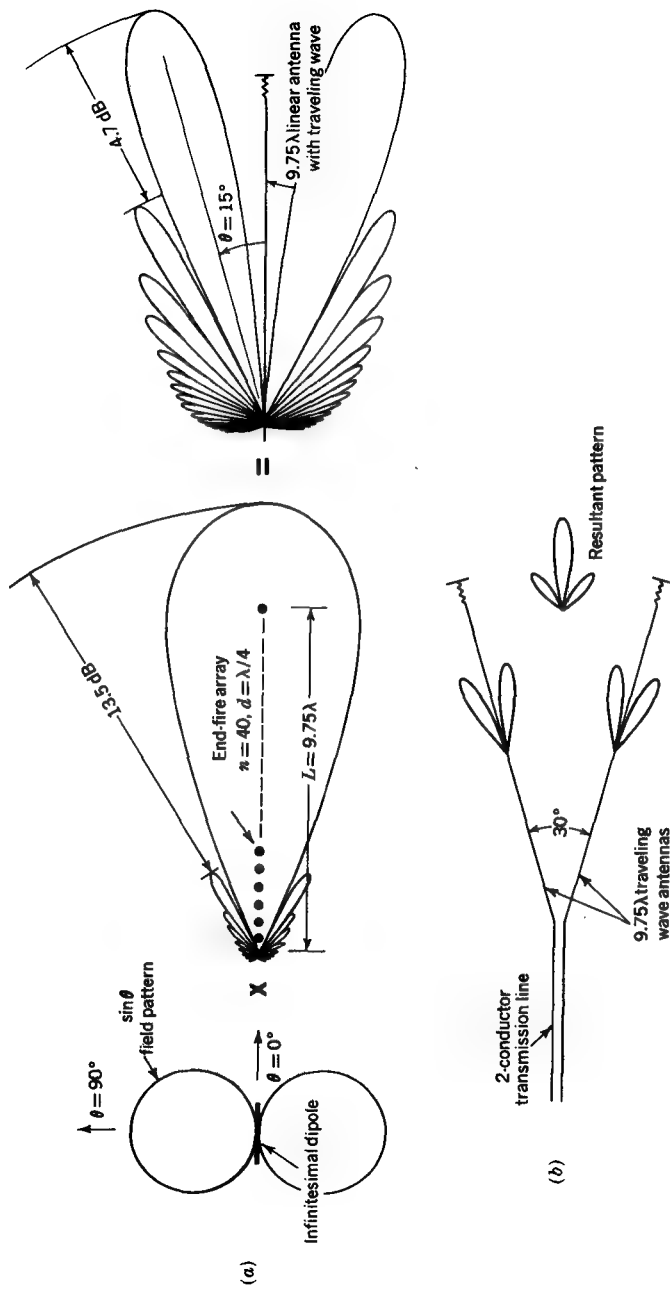


FIGURE 14-29
 (a) Far-field pattern of 9.75λ linear (terminated) antenna as obtained by pattern multiplication of short-dipole pattern with pattern of end-fire array of isotropic point sources. (b) Combination of two antennas of (a) to form a V antenna.

The vertical patterns of these antennas when operated parallel to a ground plane, as in Fig. 14-28b, can be obtained by multiplying the patterns of the isolated antenna by that of a pair of isotropic sources, one at the center of the antenna and the other (as its image) an equal distance below the ground plane (see Sec. 14-20.1).

14-12 THE SMALL LOOP ANTENNA

Consider a small circular loop antenna of diameter d , as in Fig. 14-30a. Its dimensions are assumed small compared with the wavelength ($d \ll \lambda$), so that the current is of constant amplitude and phase around the loop. This small circular loop may be approximated by a square loop of equal area [$s^2 = \pi(d/2)^2$], as suggested in Fig. 14-30b. In this way the loop can be analyzed as four short dipoles whose properties we considered in Sec. 14-3. Let the square loop be oriented with respect to the coordinates as in Fig. 14-30b and c. The field in the yz plane is produced by the radiation from the two short dipoles 2 and 4. Short dipoles 1 and 3 do not contribute since their fields are *exactly* equal and in opposite phase at all angles in the yz plane. Since the short dipoles (2 and 4) are nondirectional in the yz plane, the field pattern in this plane is the same as for two isotropic point sources in opposite phase. Thus, the electric field pattern is given by

$$E(\theta) = E_2 e^{-j\psi/2} - E_4 e^{j\psi/2} \quad (1)$$

where $E_2 = E_4$ is the electric field from the individual short dipole. Assuming $s \ll \lambda$, it follows that

$$E(\theta) = -jE_2 \beta s \sin \theta \quad (2)$$

Introducing the value of the far field E_2 of a short dipole from Table 14-1, we get

$$E(\theta) = \frac{60\pi I l}{r\lambda} \beta s \sin \theta \quad (3)$$

where l is the length of the short dipole. But in our case $l = s$ and $s^2 = A$ (=area of loop); so

$$E(\theta) = \frac{120\pi^2 I A}{r \lambda^2} \sin \theta \quad (\text{V m}^{-1}) \quad (4)$$

This is the value of the electric field from a small loop antenna of area A (square or circular†). It is the same in any plane perpendicular to the plane of the loop. The approximation (square for circular loop) becomes exact as the loop dimensions become very small.

† Or any other shape.

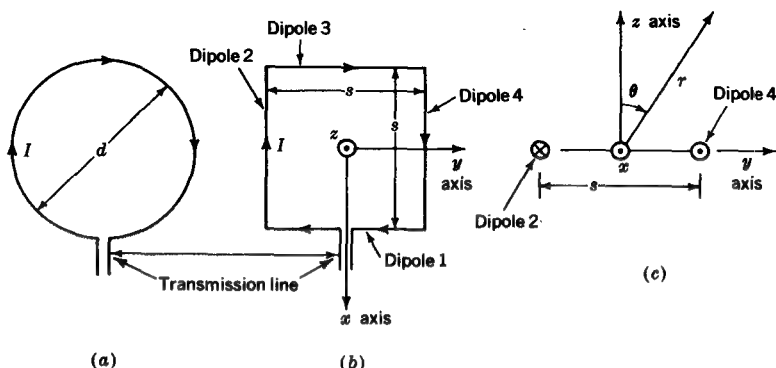


FIGURE 14-30

(a) Circular and (b) square loop antennas; (c) geometry for calculating far field

14-13 THE SMALL HELICAL ANTENNA

A wire wound in a helical coil is shown in Fig. 14-31a. Assuming that the diameter is small compared with the wavelength ($d \ll \lambda$), the radiated field can be readily determined by regarding the helix as a series of short linear dipoles and small loops connected in series, as in Fig. 14-31b. The field from one turn of the helix is then the sum of the fields from a short dipole and a small loop with equal in-phase currents. From Table 14-1 the field of the short dipole is

$$E_\theta(\theta) = j \frac{60\pi I}{r} \frac{l}{\lambda} \sin \theta \quad (1)$$

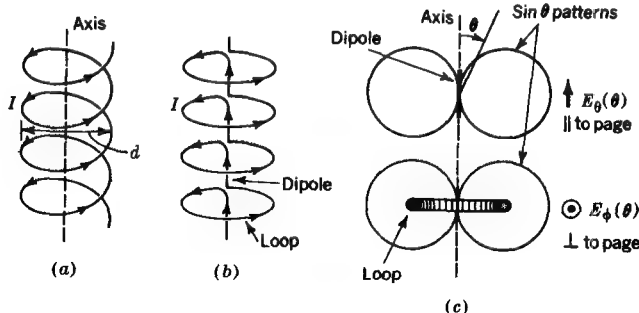


FIGURE 14-31

(a) Small-helix antenna with (b) equivalent arrangement of small loops and short dipoles and (c) associated far-field patterns

while from (14-12-4) the field of a small loop oriented as in Fig. 14-31c is

$$E_\phi(\theta) = \frac{120\pi^2 I}{r} \frac{A}{\lambda^2} \sin \theta \quad (2)$$

The electric field $E_\theta(\theta)$ of the short dipole lies in the plane of the page (Fig. 14-31c), while the electric field $E_\phi(\theta)$ of the small loop is perpendicular to the page. Both patterns are independent of ϕ ; that is, they are figures of revolution of the ones shown about the vertical axis. We note also that (1) contains a j while (2) does not. Thus, in general, the field of the helix will have two orthogonal components which are in time-phase quadrature. Dividing (1) by (2), we obtain for the axial ratio

$$AR = \frac{|E_\theta|}{|E_\phi|} = \frac{l\lambda}{2\pi A} \quad (3)$$

If the condition $l\lambda = 2\pi A$ is fulfilled, the radiation is circularly polarized. Then the magnitude of the field varies as $\sin \theta$ but is circularly polarized in all directions (except on axis, where the field is zero).† This is for a small helix of one turn. However, if the axial length of the helix is small, the field pattern and polarization of a number of turns will be substantially the same as for one turn. This can be seen from the principle of pattern multiplication where the multturn helix is represented by a row of point sources each with the pattern of one turn. If the row of point sources is short compared with the wavelength, there will be but little difference between its pattern and the pattern of one source.

14-14 THE HELICAL-BEAM ANTENNA‡

In the preceding section we discussed the radiation properties of a small helix. The maximum radiation of a small helix is broadside (perpendicular to helix axis). If the helix diameter is larger, such that the circumference is approximately 1λ , an entirely different mode of radiation occurs. In this case the helix acts as an end-fire beam antenna with maximum radiation in the axial direction. The radiation is circularly polarized on axis, and the directivity of the helix increases linearly with the length of the helix; i.e., doubling the length doubles the directivity. To distinguish

† H. A. Wheeler, A Helical Antenna for Circular Polarization, *Proc. IRE*, 35: 1484-1488 (December 1947).

‡ J. D. Kraus, Helical Beam Antenna, *Electronics*, 20: 109-111 (April 1947); also J. D. Kraus, Helical Beam Antennas for Wide Band Applications, *Proc. IRE*, 36: 1236-1242 (October 1948). For extensive treatment see J. D. Kraus, "Antennas," chap. 7, McGraw-Hill Book Company, New York, 1950.

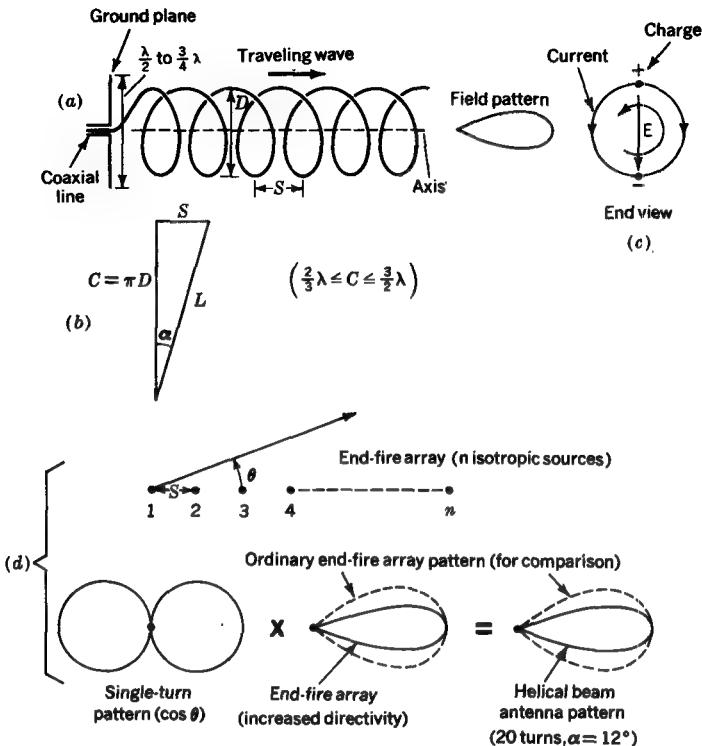


FIGURE 14-32

(a) and (b) Dimensions for helical-beam antenna. (c) End view of helix with instantaneous direction of rotating electric field (E). (d) Far-field pattern of helical-beam antenna obtained by pattern multiplication of single-turn pattern with end-fire array of isotropic sources with increased directivity. The pattern for an ordinary end-fire array of the same length is shown for comparison.

this end-fire mode of helix operation from the broadside mode of the small helix, we refer to the end-fire helix as a *helical-beam antenna*.

The helical-beam antenna is conveniently fed with a coaxial transmission line and square or circular ground, as suggested in Fig. 14-32a. The important dimensions of the helix are its diameter D , circumference C , spacing between turns S , turn length L , and pitch angle α . These are related as in Fig. 14-32b. When the helix circumference ($C = \pi D$) is approximately 1λ , the instantaneous charge and current distribution on a single turn will be as suggested in the end view of Fig. 14-32c, with the resultant E field as indicated. As the wave travels outward on the helix, the electric field vector rotates, producing circular polarization on axis. The helical-beam

antenna acts as a traveling-wave antenna without requiring a termination. The current distribution is essentially that of a single outward-traveling wave of uniform amplitude; the wave reflected back toward the feed from the open end of the helix is very small.

The pattern of a helical-beam antenna can be readily calculated if it is regarded as an end-fire array of n isotropic sources, each source representing one turn. By the principle of pattern multiplication the actual helix pattern is then the product of this array pattern and the pattern of one turn. The single-turn pattern may be approximated as a cosine function, $E(\theta) = \cos \theta$. This is an oversimplification, but the single-turn pattern has little effect, especially for long helices, because the array pattern is so much sharper than the single-turn pattern. Thus, we may write for the field pattern

$$E(\theta) = \cos \theta \frac{\sin(n\psi/2)}{\sin(\psi/2)} \quad (1)$$

where $\psi = \beta S \cos \theta - \frac{\beta L}{p}$ (2)

We note that (1) differs from the linear traveling-wave antenna pattern as given in (14-11-2) in that the single-turn helix pattern ($\cos \theta$) has a maximum on the axis (in the same direction as the array maximum) while for the linear antenna the infinitesimal dipole pattern has a *null* on the axis (in the direction of the array maximum), resulting in the conical pattern of Fig. 14-29a and less directivity.

Since the radiation is circularly polarized on axis and symmetrical, (1) is the pattern for both components, that is, $E_\theta(\theta)$ and $E_\phi(\theta)$.

If all fields added in phase on axis, we would have the ordinary end-fire condition, which requires $\psi = 0, \pm 2\pi, \pm 4\pi$, etc. In our case $\psi = -2\pi$. Comparing a pattern calculated using this value of ψ with the actual measured pattern shows that the actual pattern is much sharper or more directional (see Fig. 14-32d). To obtain a calculated pattern which agrees with the actual one, approximately π/n additional phase change per turn is required, so that the total phase change per turn is†

$$\psi = -2\pi - \frac{\pi}{n} \quad (3)$$

The fulfillment of this requirement implies that the wave on the helix travels with a velocity which automatically satisfies (3). Thus, we have from (2) and (3)

$$-2\pi - \frac{\pi}{n} = \beta S - \frac{\beta L}{p} \quad (4)$$

† Hansen and Woodyard have shown that the additional π/n phase change results in increased directivity; W. W. Hansen and J. R. Woodyard, A New Principle in Directional Antenna Design, *Proc. IRE*, 26: 333-345 (March 1938).

where $p = v/c$ = relative phase velocity of wave on helix, dimensionless

v = velocity of wave on helix, m s^{-1}

c = velocity of light or radio waves = 300 Mm s^{-1}

L = length of turn, m

S = spacing between helix turns, m

Solving (4) for p , we get

$$p = \frac{L/\lambda}{(S/\lambda) + (2n + 1)/2n} \quad (5)$$

In a typical case where the helix dimensions are $C = \lambda$, $\alpha = 12^\circ$, and $n = 20$, we obtain a phase velocity $p = 0.82$. This calculated value agrees with the actual measured value. It is a remarkable property of the helical-beam antenna that the relative phase velocity p of the wave traveling out on the helix adjusts automatically, so that increased directivity is obtained over a considerable range of pitch angles ($5^\circ < \alpha < 20^\circ$) and over a 2 to 1 bandwidth ($\frac{1}{4}\lambda < C < \frac{1}{2}\lambda$) provided $n > 3$. The directivity can be made higher by increasing the number of turns. The practical limit here is that the dielectric structure holding the helix should not support other modes to any appreciable extent. The patterns shown in Fig. 14-32d are those of a 20-turn helix with $\alpha = 12^\circ$ and an ordinary end-fire array of the same length with 20 sources each with a $\cos \theta$ pattern.

The approximate directivity of a helical-beam antenna is given by†

$$D = 15 \left(\frac{C}{\lambda} \right)^2 \frac{nS}{\lambda} \quad (6)$$

For a 20-turn helix with typical parameters $C = \lambda$ and $\alpha = 12^\circ$ the directivity $D = 63$ (or 18 dB).

With a pitch angle $\alpha = 12^\circ$, $S = 0.213\lambda$; so there are nearly 5 turns per wavelength, and the 20-turn helix is 4.3λ long ($= nS = 20 \times 0.213\lambda$). An ordinary end-fire array of this length has less than one-fourth of this directivity. Because of this four-fold directivity, or gain, improvement of a helical-beam antenna over an ordinary end-fire antenna of the same length, the helical-beam antenna can be called a *super-gain* antenna.

The high gain, large bandwidth, simplicity, and circular polarization‡ of the helical-beam antenna have made it indispensable for space-communication applications. For example, helical-beam antennas are used on the moon for transmitting

† Kraus, "Antennas," p. 197.

‡ With linearly polarized antennas, the plane of polarization of the wave from the transmitting antenna should be aligned with the receiving antenna [$MM_a = 0$ in (11-4-4)]. When the planes are perpendicular, the received power goes to zero ($MM_a = 180^\circ$). Due to rotation of a space vehicle or to Faraday rotation in the ionosphere (Chap. 15), the plane of polarization may rotate and cause signal fading and dropouts. This fading is overcome with circularly polarized antennas.

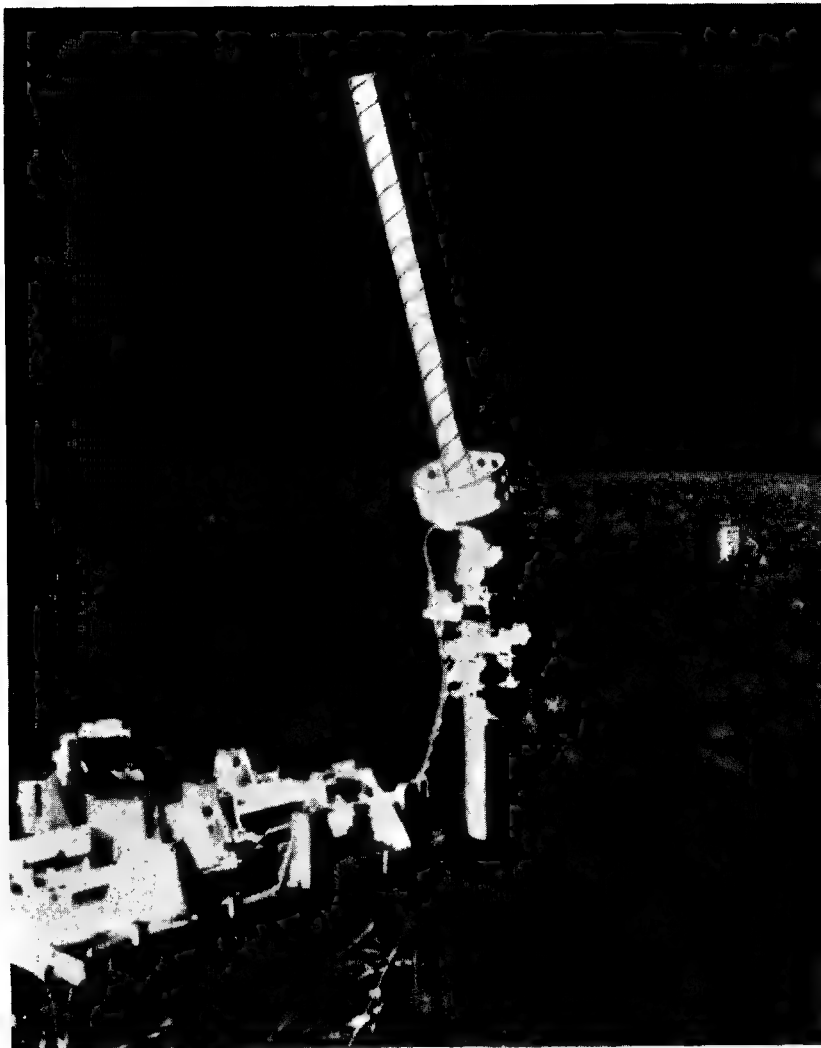


FIGURE 14-33a

Helical-beam antenna with 18 dBi gain placed on Fra Mauro highlands of the moon by Apollo 14 astronauts for continuous transmission of telemetry data back to earth from the ALSEP experiment. The helix conductor is supported by a thin plastic tube. (*National Aeronautics and Space Administration.*)

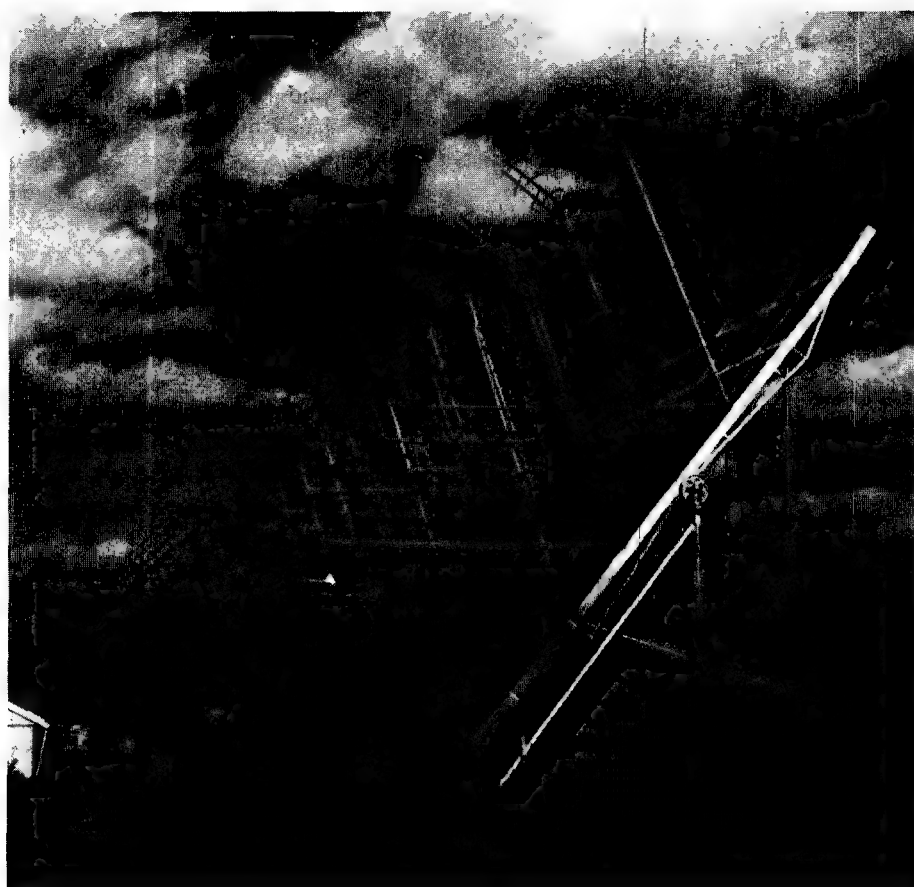


FIGURE 14-33b

Broadside array of 96 helical-beam antennas at Ohio State University Radio Observatory.

telemetry data back to earth from the ALSEP' (Apollo Lunar Surface Experiment Package) equipment. A photograph of one of these helical-beam antennas placed on the moon by the Apollo 14 astronauts, Alan Shepard, Jr., and Edgar Mitchell, is shown in Fig. 14-33a. Other helical-beam antennas have been set up on the moon by later Apollo groups. The helical-beam antenna also has found many other applications, as in radio astronomy. The original 200- to 300-MHz Ohio State University radio telescope (in 1952) consisted of a broadside array of 96 helical-beam antennas, as shown in Fig. 14-33b, with each helix of 11 turns and 1.5 m long. The 300- to 400-MHz radio telescope of the University of Texas has a number of helical-beam antenna arrays in an interferometer arrangement. Each array consists of 100 helices each of 40 turns.

14-15 BEAM WIDTH AND DIRECTIVITY OF ARRAYS

In the preceding sections we have discussed the directional properties of a number of types of uniform arrays, both broadside and end-fire. Table 14-4 summarizes relations for the BWFN, the HPBW, and directivity for a uniform linear broadside array and an ordinary end-fire array of isotropic sources and for a helical-beam antenna (end fire with increased directivity). In addition the beam widths and directivity are listed for a unidirectional square-aperture broadside array with uniform distribution.

Table 14-4 ARRAY BEAM WIDTHS AND DIRECTIVITIES†

Type of array	BWFN	HPBW	Directivity
Broadside	$\frac{115^\circ}{L/\lambda}$	$\frac{51^\circ}{L/\lambda}$	$2.2L/\lambda$
End fire (ordinary)	$\frac{162^\circ}{\sqrt{L/\lambda}}$	$\frac{108^\circ}{\sqrt{L/\lambda}}$	$3.5L/\lambda$
Helical-beam antenna (end fire with in- creased directivity)	$\frac{78^\circ}{(C/\lambda)^2 \sqrt{L/\lambda}}$	$\frac{52^\circ}{(C/\lambda)^2 \sqrt{L/\lambda}}$	$15 \left(\frac{C}{\lambda}\right)^2 \frac{L}{\lambda}$
Square-aperture broadside array (unidirectional)	$\frac{115^\circ}{L/\lambda}$	$\frac{51^\circ}{L/\lambda}$	$13(L/\lambda)^2$

† L = array length for end-fire arrays or side length for broadside array

C = circumference of helix

λ = wavelength

14-16 SCANNING ARRAYS

In Secs. 14-6.5 and 14-6.6 we considered broadside and end-fire arrays. In the broadside array all sources are in phase ($\delta = 0$), while in the (ordinary) end-fire array the progressive phase difference between sources is $-\beta d$, where d is the spacing between sources. Actually the beam maximum can be tilted in any arbitrary direction θ_{\max} if the phase difference δ satisfies the relation

$$\delta = -\beta d \cos \theta_{\max} \quad (1)$$

For a broadside array $\theta_{\max} = 90^\circ$ and $\delta = 0$. For an end-fire array $\theta_{\max} = 0^\circ$ and $\delta = -\beta d$. To direct the maximum radiation at 45° ($\theta_{\max} = 45^\circ$) requires that $\delta = -0.707\beta d$. By controlling the phase difference between elements of an array the beam angle can be adjusted or scanned without turning the antenna. Such arrays are sometimes called *scanning arrays* or antennas.

An interesting example of the scanning antenna is the slow-wave backward angle-fire grid-structure array shown in Fig. 14-34,[†] in which the beam scanning action is accomplished by shifting the frequency. The array shown in Fig. 14-34a has 7×4 meshes. Each mesh has dimensions l by s . The arrows indicate the approximate instantaneous current directions. The array may be placed a distance h above a ground plane and fed from one end, as suggested in Fig. 14-34a and b. Typical parameters are $l = 2.75s$, $h = 0.3s$, and $s \approx 0.35\lambda$. The approximate *E*-plane pattern can be calculated assuming each mesh to be represented by a point source with a short dipole ($\sin \theta$) pattern. Thus, from (14-6.4-5) the *E*-plane pattern is

$$E_\theta(\theta) = \sin \theta \frac{\sin(n\psi/2)}{\sin(\psi/2)} \quad (2)$$

where

$$\psi = \beta s \cos \theta + \delta \quad (3)$$

Assuming a traveling wave moving along the wires with velocity c , the phase difference between successive elements such as 1 and 2 (Fig. 14-34a, b, and c) is

$$\delta = -\beta \frac{l}{2} - \beta s \quad (4)$$

For the direction of maximum radiation θ_{\max} it is required that $\psi = 0, \pm 2\pi, \pm 4\pi$, etc. In our case $\psi = -2\pi$, so (3) becomes

$$-2\pi = \frac{2\pi}{\lambda} \left(s \cos \theta_{\max} - \frac{l}{2} - s \right) \quad (5)$$

[†] J. D. Kraus, A Backward Angle-fire Array, *IEEE Trans. Antennas Propag.*, AP-12: 48-50 (January 1964); J. D. Kraus, U.S. Patent 3,290,688 Dec. 6, 1966; J. D. Kraus and K. R. Carver, Wave Velocities on the Grid-structure Backward Angle-fire Antenna, *ibid.*, 509-510 (July 1964).

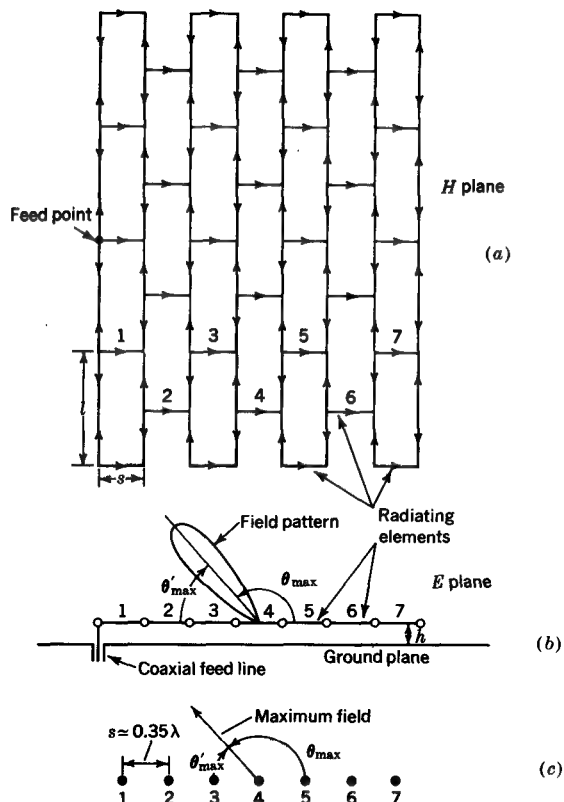


FIGURE 14-34
Backward angle-fire grid array; (a) plan and (b) and (c) side views.

or typically ($l = 2.75s$)

$$\cos \theta_{\max} = 2.37 - \frac{1}{s/\lambda} \quad (6)$$

As shown in Fig. 14-35, the beam direction θ'_{\max} (complementary angle to θ_{\max}) varies from about 15° to 83° for changes in s from 0.3 to 0.4λ . Thus, a wavelength change of ± 14 percent ($= (0.05/0.35) \times 100$) swings the beam through nearly 70° .

The above analysis is oversimplified, but values calculated as above are in good agreement with measurements. When the antenna structure is regarded as a transmission line, the extra path length $l/2$ has the effect of slowing down the phase velocity (left to right in Fig. 14-34) in the ratio $s/[s + (l/2)]$. Typically ($l = 2.75s$) the effective

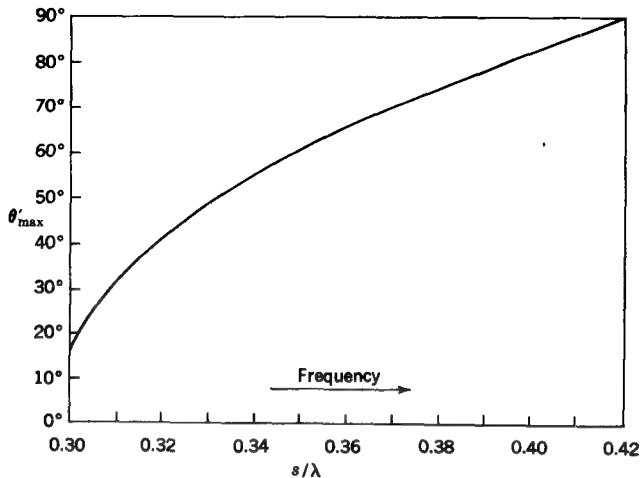


FIGURE 14-35

Angle of maximum radiation θ'_{\max} from backward angle-fire grid antenna as a function of frequency (expressed in terms of the wavelengths of the mesh spacing s/λ). A wave velocity equal to c is assumed on the structure.

phase velocity is only about $0.4c$, so that the antenna can be considered as a *slow-wave structure*. Since the phase change between successive elements (such as 1 and 2) is less than 360° {typically around $300^\circ = (360^\circ/\lambda)[(l/2) + s]$ }, radiation occurs at a backward angle (toward feed).

14-17 FREQUENCY-INDEPENDENT ANTENNAS

A frequency-independent antenna may be defined as one for which the impedance and pattern (and hence directivity) remain constant as a function of the frequency.

Consider the arrangement in Fig. 14-36, which consists of an adjustable $\lambda/2$ dipole made with two drum-type pocket rulers. If L is adjusted to approximately $\lambda/2$

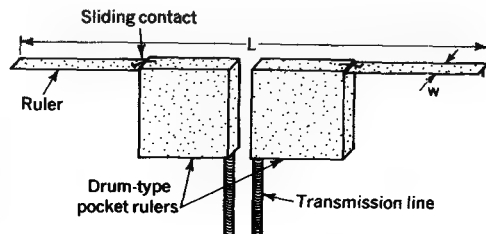


FIGURE 14-36

A frequency-independent antenna made of adjustable roll-up pocket rulers set so that L equals $\lambda/2$ at the operating frequency.

at the frequency of operation, the impedance and pattern remain the same. Strictly speaking, the element thickness or width w should also be adjusted, but this effect is small and for many purposes may be negligible. This simple antenna illustrates the requirement that *the antenna should expand or contract in proportion to the wavelength in order to be frequency-independent*, or if the antenna structure is not mechanically adjustable as above, the size of the active or radiating region should be proportional to the wavelength.

Rumsey† proposed that an antenna which is defined only in terms of angles would be frequency-independent.‡ This requirement can be met with a variety of physical structures such as a pair of concentric equiangular spirals.

The log-periodic antenna§ is another example of a frequency-independent antenna, and one employing dipoles¶ is shown in Fig. 14-37. The dipole lengths increase along the antenna so that the included angle α is a constant, and the lengths and spacings of adjacent elements are scaled so that

$$\boxed{\frac{l_{n+1}}{l_n} = \frac{s_{n+1}}{s_n} = k} \quad (1)$$

where k is a constant. At a wavelength near the middle of the operating range, radiation occurs primarily from the central region of the antenna, as suggested in Fig. 14-37. The elements in this active region are about $\lambda/2$ long, and the phasing is (as indicated by the arrows) below the elements. By the time the field radiated to the left from element 8 arrives at element 7, the phase of 7 has advanced 90° and its field adds in phase to that from element 8. When these fields from elements 8 and 7 arrive at element 6, its phase has advanced so that the fields from all three elements add in phase, producing a large resultant field radiating to the left, as suggested at the bottom of Fig. 14-37. Examining the field radiated to the right from element 6, we find that it combines with the fields from elements 7 and 8 to produce only a small resultant field radiating to the right. Thus, maximum radiation is to the left or in the backward direction from the wave entering the antenna on the transmission, or feed, line. Elements 9, 10, and 11 are in the neighborhood of 1λ long and carry only small currents (they present a large impedance to the line). The small currents in elements 9, 10, and 11 mean that the antenna is effectively truncated at the right of the active region.

† V. H. Rumsey, "Frequency Independent Antennas," Academic Press Inc., New York, 1966.

‡ Such antennas possess a wide instantaneous bandwidth, whereas the antenna of Fig. 14-36 has a narrow bandwidth but is tunable.

§ So called because the logarithm of (1) yields a constant logarithmic increment for each step or period in the structure.

¶ D. E. Isbell, *IRE Trans. Antennas Propag.*, AP-8: 260-267 (1960).

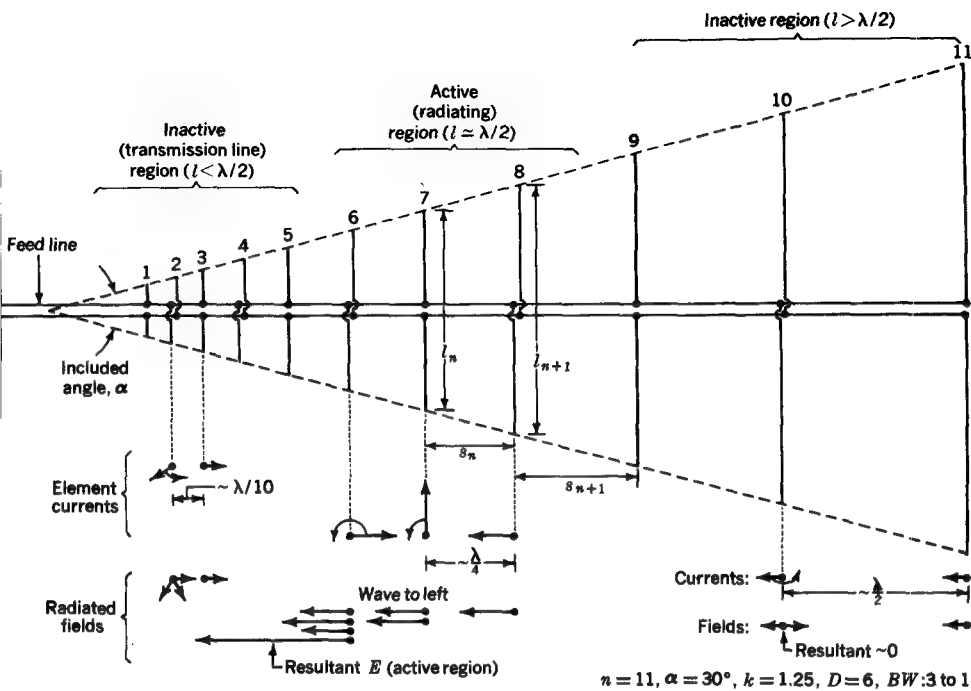


FIGURE 14-37
Log-periodic frequency-independent antenna of 8 dBi gain with 11 dipoles showing active (central) region and inactive regions (left and right ends).

Any small fields from elements 9, 10, and 11 also tend to cancel in both forward and backward directions. However, some radiation may occur broadside since the currents are approximately in phase. The elements at the left (1, 2, 3, etc.) are less than $\lambda/2$ long and present a large capacitative reactance to the line. Hence, currents in these elements are small and radiation is small. Thus, under the condition assumed above that the wavelength is near the center of the operating range, only the middle portion of the antenna is active, while the left and right ends are relatively inactive. If the wavelength is increased, the active region moves to the right, and if the wavelength is decreased, the active region moves to the left. Thus, we see that at any given frequency only a fraction of the antenna is used (where the dipoles are about $\lambda/2$ long). At the short-wavelength limit of the bandwidth only 15 percent of the length may be used, while at the long wavelength limit a larger fraction is used but still less than 50 percent. For the log-periodic antenna of Fig. 14-37 the included angle $\alpha = 30^\circ$, $k = 1.25$, the directivity is about 6 (= 8 dB), and the bandwidth about 3 to 1.

14-18 RECIPROCITY

By reciprocity it follows that the *pattern, directivity, aperture, and terminal impedance of an antenna are the same transmitting or receiving*. In general, however, the current distribution on an antenna is not the same for transmission as for reception.

To show that reciprocity applies to antennas consider the two antennas 1 and 2 (Fig. 14-38a) with media everywhere that are linear, passive, and isotropic. Let a zero-impedance transmitter of frequency f be connected to the terminals of antenna 1 (Fig. 14-38a), producing a current I_1 and inducing a voltage V_{21} at the (open) terminals of antenna 2. Now let the transmitter be transferred to the terminals of antenna 2 (Fig. 14-38b), producing a current I_2 and inducing a voltage V_{12} at the open terminals of antenna 1. Since any four-terminal network can be reduced to an equivalent T section, the antenna arrangement of Fig. 14-38a and b can be replaced by the network of Fig. 14-38c. Since reciprocity is easily demonstrated for this network, it follows that

$$\frac{V_{21}}{I_1} = \frac{V_{12}}{I_2} \quad (1)$$

and that reciprocity applies to antennas. In words, the reciprocity theorem for antennas states that if a current I_1 at the terminals of antenna 1 induces a voltage V_{21} at the (open) terminals of antenna 2 and a current I_2 at the terminals of antenna 2 induces a voltage V_{12} at the (open) terminals of antenna 1, then if $I_2 = I_1$, $V_{12} = V_{21}$. In Fig.

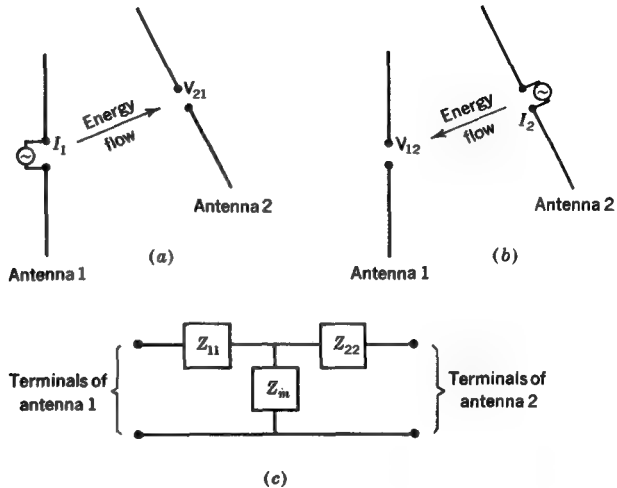


FIGURE 14-38
(a) and (b) Reciprocity between two antennas. (c) Equivalent circuit.

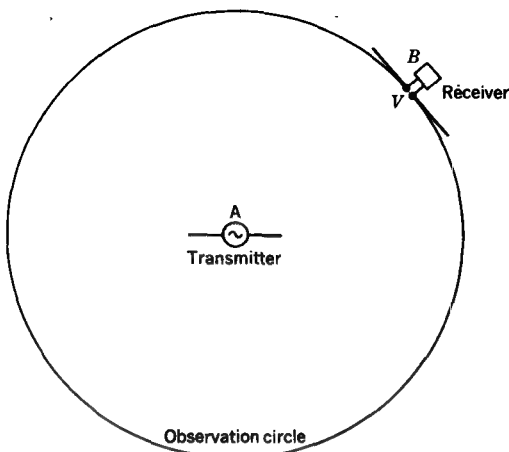


FIGURE 14-39

Pattern measurement on observation circle illustrating reciprocity for antenna patterns.

14-38c Z_{11} is the self-impedance of antenna 1, Z_{22} is the self-impedance of antenna 2, and Z_m is the mutual impedance of antennas 1 and 2 as given by

$$Z_m = Z_{12} = \frac{-V_{12}}{I_2} = \frac{-V_{21}}{I_1} = Z_{21} \quad (2)$$

Pattern If all media involved are linear, passive, and isotropic, reciprocity holds and it follows that *the transmitting and receiving patterns of an antenna are identical*. Referring to Fig. 14-39, let the pattern of antenna A (transmitting) be measured by observing its field with a receiving antenna B at points around an observation circle having A at its center.[†] The voltage at the terminals of antenna B is a measure of the field at the observation circle. If the measurement procedure is reversed by interchanging transmitter and receiver so that antenna B transmits and antenna A receives, it follows from reciprocity that the pattern of antenna A , observed by moving antenna B , will be identical to that obtained when antenna A is transmitting.

Directivity and aperture Directivity was discussed in Sec. 14-5 for a transmitting antenna. In general, the directivity is equal to

$$D = \frac{4\pi}{\iint P_n(\theta, \phi) d\Omega} \quad (3)$$

where $P_n(\theta, \phi)$ is the normalized power pattern.

[†] The same result is obtained by keeping antenna B fixed and rotating antenna A about its center point.

Thus, D depends only on the shape of the power pattern. As shown in the preceding subsection, an antenna has the same pattern for both transmission and reception. Hence, the directivity determined with an antenna's transmitting pattern is identical with the directivity determined with the antenna's receiving pattern. Accordingly, the term directivity can be applied to both transmitting and receiving antennas, the directivity of an antenna being the same for both situations.

According to (14-5-29), the effective aperture A_e of an antenna is equal to the directivity of the antenna times a constant. Hence, the term effective aperture may be applied to both transmitting and receiving antennas, it being understood that the effective aperture of a transmitting antenna is the same as its effective aperture when receiving.

Impedance When an antenna is transmitting, it may be excited at only one point. However, when used for reception, the antenna is excited over its entire extent by the received wave.[†] As a consequence the current distribution on the antenna is, in general, not the same for transmission and reception. However, the antenna always behaves as the same circuit regardless of the mode of excitation, so that the impedance of an antenna is the same for transmission and reception. This means that if the terminal impedance of a transmitting antenna is Z_T , the load impedance required for maximum power transfer when the antenna is receiving is equal to its complex conjugate Z_T^* .

That Z_T must be the same for transmission and reception can also be seen by considering a circuit or network of many meshes. Although the currents in the network are dependent on the location or locations of the emfs, the circuit impedances are independent of the distribution of the emfs.

14-19 SELF AND MUTUAL IMPEDANCE AND ARRAYS OF DIPOLES

The impedance presented by an antenna to a transmission line can be represented by a two-terminal network. This is illustrated in Fig. 14-40, in which the antenna is replaced by its equivalent impedance connected to the transmission-line terminals. This impedance to which the transmission line connects is called the *terminal* or *driving-point impedance* Z_T . If the antenna is isolated, i.e., remote from other objects, and is lossless, its terminal impedance is the same as the *self-impedance* of the antenna ($Z_T = Z_{11}$). This impedance has a real part equal to the *radiation resistance* R_{11} and

[†] Furthermore, the manner in which the receiving antenna is excited depends on the direction of the incident wave.

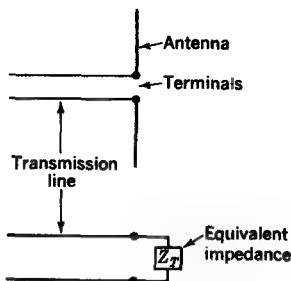


FIGURE 14-40

Transmission line with antenna and with equivalent lumped (terminal) impedance Z_T .

an imaginary part called the *self-reactance* X_{11} . If there are nearby objects, such as other active antennas, the terminal impedance will be modified to include contributions involving the mutual impedance between the antennas and currents flowing in them.

In Sec. 14-9 the radiation resistance of a thin $\lambda/2$ dipole was calculated and found to be equal to 73Ω . The method used involved a calculation of the (real) power radiated by integrating the Poynting vector over a large sphere (in far field). No reactance term resulted from this calculation. To include the antenna reactance requires integration (in effect) of the Poynting vector over a closed surface collapsed down so that it just fits over the antenna conductors. In this way the reactive (non-radiating) power circulating back and forth near the antenna enters into the integration, and, in general, this will result in a reactance term. Such calculations are tedious and will be omitted here.[†] As stated following (14-9-7) the self-impedance of a thin linear $\lambda/2$ center-fed dipole is given by

$$Z_{11} = R_{11} + jX_{11} = 73 + j42.5 \Omega \quad (1)$$

The terminal impedance of a thin linear center-fed dipole antenna as a function of the frequency is shown by the spiral solid line in the impedance diagram of Fig. 14-41.[‡] The length-to-diameter ratio (l/d ratio) for this antenna (solid curve) is 2,000. With change in frequency the impedance varies over a wide range of values. At frequencies where $l/\lambda \approx 0.5$ the resistance is small, and the reactance changes rapidly from large negative to large positive values with increase in frequency (increase in l/λ). At resonance $l/\lambda = 0.48$ and $Z_{11} = 70 + j0 \Omega$. At higher frequencies where $l/\lambda \approx 1$ the resistance is several thousand ohms, and the reactance may also be of comparable magnitude. Another (second) resonance occurs when $l/\lambda = 0.93$, and for this condition $Z_{11} = 3,300 + j0 \Omega$. At still higher frequencies the impedance values again become small, and another (third) resonance occurs when $l/\lambda = 1.48$. For this

[†] For a detailed discussion see, for example, Kraus, "Antennas," chaps. 9 and 10.

[‡] Erik Hallén, Admittance Diagrams for Antennas and the Relation between Antenna Theories, *Harv. Univ., Crust Lab. Tech. Rep.* 46, June, 1, 1948.

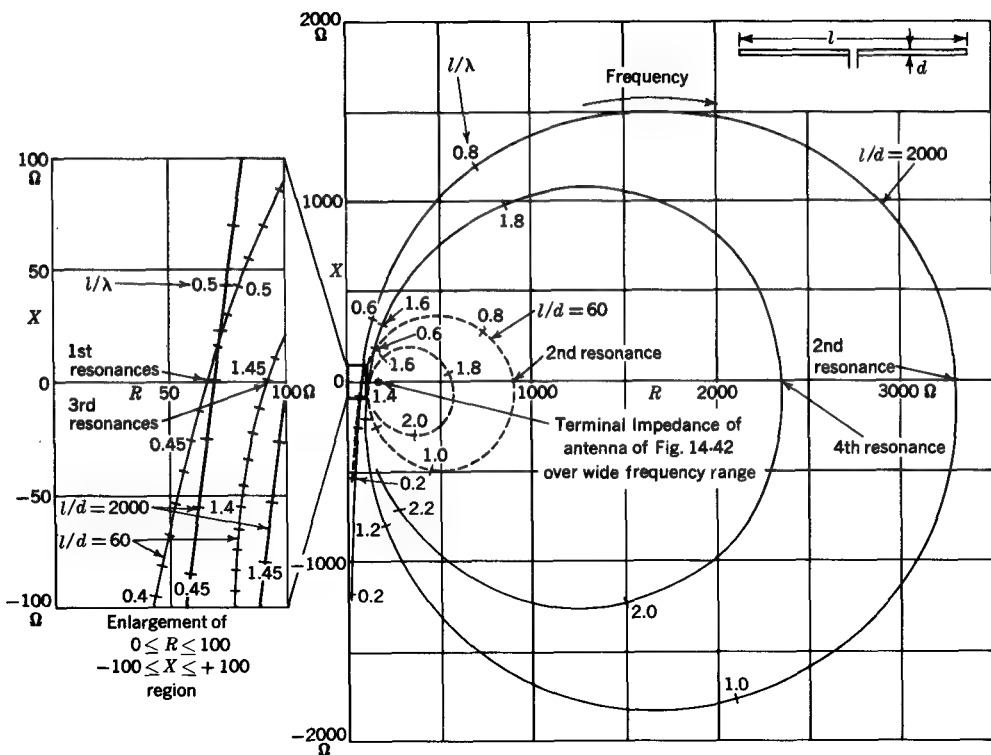


FIGURE 14-41

Self-impedance diagram (R, X) as a function of frequency (expressed in l/λ ratios indicated along curves) for linear antennas with length-diameter (l/d) ratios of 60 (dashed) and 2,000 (solid). The diagram at the left is an enlargement of the region of first and third resonances near the origin of the main diagram. (After Hallén.)

resonance $Z_{11} = 100 + j0 \Omega$. With further increase in frequency the antenna impedance goes through further resonances. At the odd-numbered resonances the resistance is small, and at the even-numbered it is high. If the antenna thickness is increased (l/d ratio smaller), the impedance variation with frequency is smaller. This is illustrated by the dashed spiral curve in Fig. 14-41, which is for a center-fed dipole with l/d ratio of 60. The resistance values of this dipole at its first and third resonances are not much different from those for the thinner dipole but the resistance values at the second and fourth resonances are greatly reduced. As the antenna thickness is increased further, the impedance variation becomes still less.

A simple explanation for this tendency follows from a consideration of the V-type antenna shown in Fig. 14-42. If a two-conductor transmission line is gradually

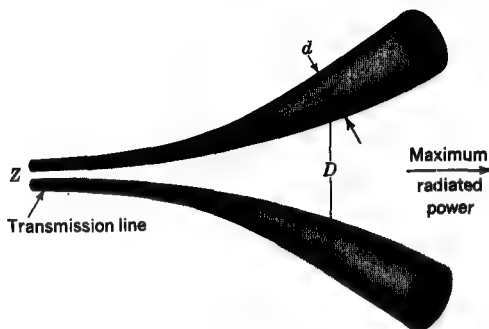


FIGURE 14-42

Two-conductor transmission line opened out into antenna. By keeping ratio D/d constant the arrangement presents a constant impedance Z over a wide frequency range.

opened out and the ratio of conductor spacing D to diameter d kept constant, the characteristic impedance of the line will also be constant. Hence, there will be no reflected wave on the line provided none occurs at the end, and this will be essentially the case if D is sufficiently large ($D > \lambda$) at the end of the structure. In the opened-out region of the thick conductors the transmission line acts as an antenna, and most of the power is radiated in a beam to the right. Accordingly, the antenna terminal impedance will be equal to the characteristic resistance of the transmission line, and this value will remain substantially constant at all frequencies for which the above conditions hold. Thus, for an antenna like that in Fig. 14-42, the impedance spiral reduces to a single point representing the characteristic impedance (all resistance) of the opened-out transmission line.

Let us now consider the mutual impedance of the two antennas of Fig. 14-43. The mutual impedance is given by

$$Z_m = Z_{12} = Z_{21} = \frac{-V_{21}}{I_1} = \frac{-1}{I_1 I_2} \int_0^L I_z E_z dz \quad (2)$$

where I_z, E_z = current and field at distance z along antenna 2 induced by current in antenna 1

I_1, I_2 = terminal currents of antennas 1 and 2, respectively

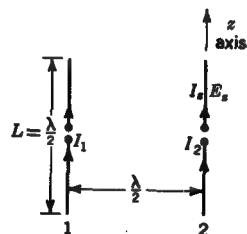


FIGURE 14-43

Two parallel linear $\lambda/2$ center-fed dipole antennas with $\lambda/2$ spacing.

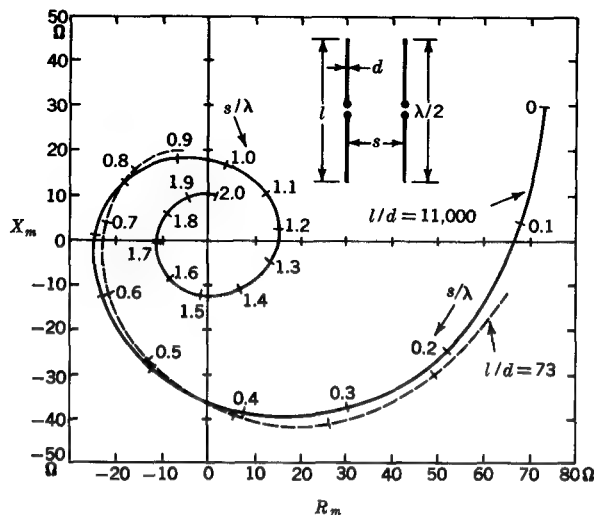


FIGURE 14-44

Mutual-impedance diagram (R_m , X_m) as a function of element spacing s/λ for two parallel $\lambda/2$ center-fed dipoles with length-diameter (l/d) ratios of 73 (dashed) and 11,000 (solid). (After Tai and Carter.)

The integration is over the length L of antenna 2. The evaluation of (2) will be omitted here. However, for the case of two parallel thin linear $\lambda/2$ center-fed antennas spaced $\lambda/2$, as in Fig. 14-43,

$$Z_m = Z_{12} = Z_{21} = -13 - j29 \Omega \quad (3)$$

The mutual impedance of two parallel linear $\lambda/2$ antennas as a function of spacing is shown by the spiral curves of Fig. 14-44.[†] The solid spiral curve is for antenna elements with an l/d ratio of 11,000. The dashed spiral curve is for an l/d ratio of 73. As the spacing s between the antennas increases, the mutual impedance rapidly spirals in around the origin ($R_m = X_m = 0$). It is to be noted that whereas the self-resistance of an antenna is always positive, the mutual resistance may be either positive or negative.

The mutual impedance Z_m of two antennas is usually a complicated function of the size, separation, and orientation of the antennas. However, in the case of two short-dipole antennas the relation is relatively simple and illustrates clearly the effect

[†] C-T Tai, Coupled Antennas, *Proc. IRE*, **36**: 487-500 (April 1948); P. S. Carter, Circuit Relations in Radiating Systems and Applications to Antenna Problems, *ibid.*, **20**: 1004-1041 (June 1932).

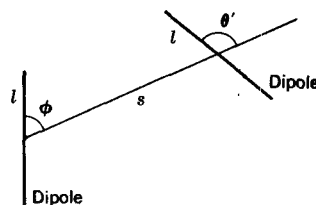


FIGURE 14-45

Two short dipoles of length l , separation s , and orientation angles θ and θ' for mutual-impedance equation.

of these parameters. Referring to Fig. 14-45, the mutual impedance of the two dipoles is given by

$$Z_m = \frac{60\pi l^2}{s\lambda} (\sin \theta \sin \theta') (\sin \beta s + j \cos \beta s) \quad (4)$$

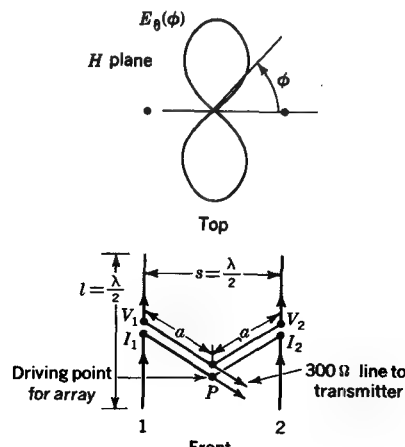
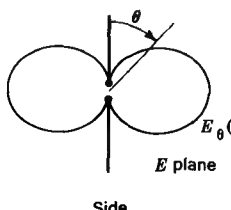
Note that the first factor is a *magnitude factor*, the second an *orientation factor*, and the third a *periodic, or complex, factor* with real and imaginary parts. Note also that when the separation distance $s = n\lambda/4$ and n is odd, Z_m is real; but if n is even, Z_m is imaginary. Both dipoles are in the same plane and it is assumed that $l \ll \lambda$ and $l \ll s$ and also that the current is of uniform magnitude and constant phase on each dipole.

Consider now an array of two identical parallel thin linear center-fed dipole antenna elements to be driven with equal in-phase currents and fed by a two-conductor 300Ω transmission line. This can be accomplished by the arrangement of Fig. 14-46. The voltage at the terminals of element 1 is

$$V_1 = I_1 Z_{11} + I_2 Z_{12} \quad (5)$$

FIGURE 14-46

Broadside array of two thin $\lambda/2$ center-fed dipoles with $\lambda/2$ spacing showing field patterns in both principal planes.



where I_1 = terminal current in element 1

I_2 = terminal current in element 2

Z_{11} = self impedance of element 1

Z_{12} = mutual impedance between elements

Likewise, we have for the terminal voltage of element 2

$$V_2 = I_2 Z_{22} + I_1 Z_{21} \quad (6)$$

where Z_{22} is the self-impedance of element 2. We require $I_1 = I_2$, and we also know that $Z_{11} = Z_{22}$ and $Z_{12} = Z_{21}$. Therefore,

$$V_1 = I_1(Z_{11} + Z_{12}) = V_2 \quad (7)$$

and the terminal impedance Z_1 of element 1 and Z_2 of element 2 are equal and given by

$$Z_1 = \frac{V_1}{I_1} = Z_{11} + Z_{12} = Z_2 \quad (8)$$

For the case where $l = \lambda/2$ and $s = \lambda/2$

$$Z_{11} = 73 + j43 \Omega \quad (9)$$

$$Z_{12} = -13 - j29 \Omega \quad (10)$$

Therefore,

$$Z_2 = Z_{11} + Z_{12} = 73 - 13 + j(43 - 29) = 60 + j14 \Omega \quad (11)$$

If each element is shortened slightly, the self-reactance (43Ω) may be reduced more than the mutual reactance so as to yield a total reactance of zero. In so doing the self-resistance and terminal resistance will be reduced, so that

$$Z_1 = 57 + j0 \Omega \quad (12)$$

In order that the array will present a resistive load of 300Ω at the driving point of the array (point P in Fig. 14-46) the transmission-line sections between P and the element terminals can be constructed so that their length $a = \lambda/4$ and their characteristic impedance $Z_0 = \sqrt{57 \times 600} = 185 \Omega$. Thus, each $\lambda/4$ section transforms the element terminal resistance of 57Ω to 600Ω and the two lines in parallel yield a driving-point impedance $Z = 300 + j0 \Omega$.

The above array consisting of two parallel thin $\lambda/2$ antenna elements fed with equal in-phase currents has maximum radiation broadside. The principal-plane patterns are as shown in Fig. 14-46 and are given by:

$$\text{E plane: } E_\theta(\theta) = 2kI_1 \frac{\cos[(\pi/2)\cos\theta]}{\sin\theta} \quad (13)$$

$$\text{H plane: } E_\phi(\phi) = 2kI_1 \cos \frac{\pi \cos\phi}{2} \quad (14)$$

The shape of the E -plane pattern is the same as for a $\lambda/2$ linear antenna, as given by (14-9-4), while the shape of the H -plane pattern is the same as for two equal isotropic in-phase point sources spaced $\lambda/2$ apart, as given by (14-6.1-2) with $d = \lambda/2$.

The directivity of the above array can be calculated from (14-5-7) by integrating the power pattern over 4π sr. An alternative method of calculating the directivity will now be described which employs the self- and mutual resistances of the antenna elements.

Assuming no heat losses, the power input to the array (Fig. 14-46) is given by

$$P = 2I_1^2(R_{11} + R_{12}) \quad (15)$$

Hence, the individual element currents are

$$I_1 = I_2 = \sqrt{\frac{P}{2(R_{11} + R_{12})}} \quad (16)$$

If the same power is supplied to a single isolated $\lambda/2$ antenna, its current is

$$I_0 = \sqrt{\frac{P}{R_{11}}} \quad (17)$$

In the H plane the pattern of the single $\lambda/2$ antenna is nondirectional and is given by†

$$E_{HW}(\phi) = kI_0 = k\sqrt{\frac{P}{R_{11}}} \quad (18)$$

The maximum radiation from the array occurs in the direction $\phi = 90^\circ$ (Fig. 14-46). Hence, the gain of the array over the single $\lambda/2$ antenna as reference is given by the ratio of (14) to (18) with $\phi = 90^\circ$, or

$$\text{Array gain} = \frac{2kI_1}{kI_0} = \sqrt{\frac{2R_{11}}{R_{11} + R_{12}}} \quad (19)$$

Now $R_{11} = 73 \Omega$ and $R_{12} = -13 \Omega$. Therefore,

$$\text{Array gain} = \sqrt{\frac{2 \times 73}{73 - 13}} = 1.56 \quad (= 1.9 \text{ dB})$$

This gain is with respect to a $\lambda/2$ antenna (with same power input) as reference. The directivity of a linear $\lambda/2$ (dipole) antenna has been calculated earlier as 1.64 (=gain of $\lambda/2$ antenna over isotropic source). Therefore, the directivity of the array of Fig. 14-46 is

$$D = 1.56 \times 1.64 = 2.56 \quad (= 4.1 \text{ dB})\ddagger$$

This is the same directivity that would be obtained by integrating the power pattern of the array over 4π sr, yet we have carried out no such integration, at least *explicitly*. However, such an integration or its equivalent is *implicit* in the self- and mutual resistances.

† The subscript HW on E in (18) stands for *half wavelength antenna*.

‡ When expressing the gain over an isotropic source (or directivity) in decibels, it can be given in *decibels over isotropic* (dBi), or in this case 4.1 dBi.

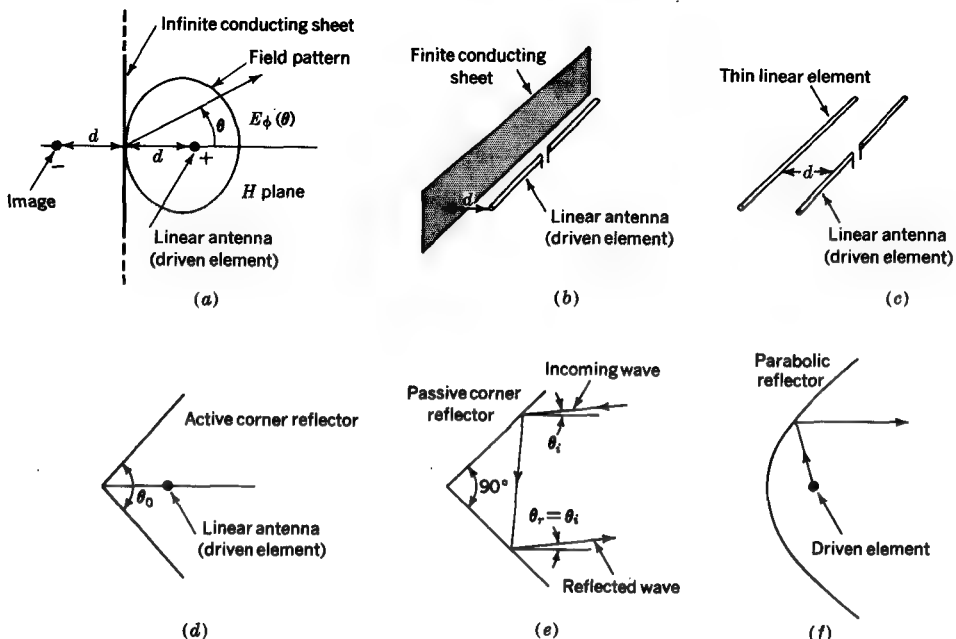


FIGURE 14-47

Linear antenna (a) with infinite reflecting sheet and (b) with sheet of finite extent. In (c) the reflecting sheet has degenerated to a thin linear element. (d) Corner reflector with (active) driven element and (e) passive corner reflector (no driven element). (f) Driven element and parabolic reflector.

14-20 REFLECTOR AND LENS ANTENNAS

In this section a variety of reflector antennas are considered. The lens-type antenna is also discussed. It is convenient to treat both reflector and lens types together since the design of both involves the principle of equality of path length.

Figure 14-47 displays six types of reflector antennas. In Fig. 14-47a the reflector is an infinite flat sheet, but in (b) the sheet is of finite extent. The infinite flat sheet can be analyzed by simple image theory, but the finite one requires the addition of diffraction theory. In Fig. 14-47c the reflector has degenerated to a thin linear element, and this arrangement is analyzed by simple array and circuit theory. Corner reflector antennas are shown in Fig. 14-47d and e. In one case the antenna is active (contains driven element), and in the other case the corner reflector is passive. A parabolic reflector antenna is shown in Fig. 14-47f.

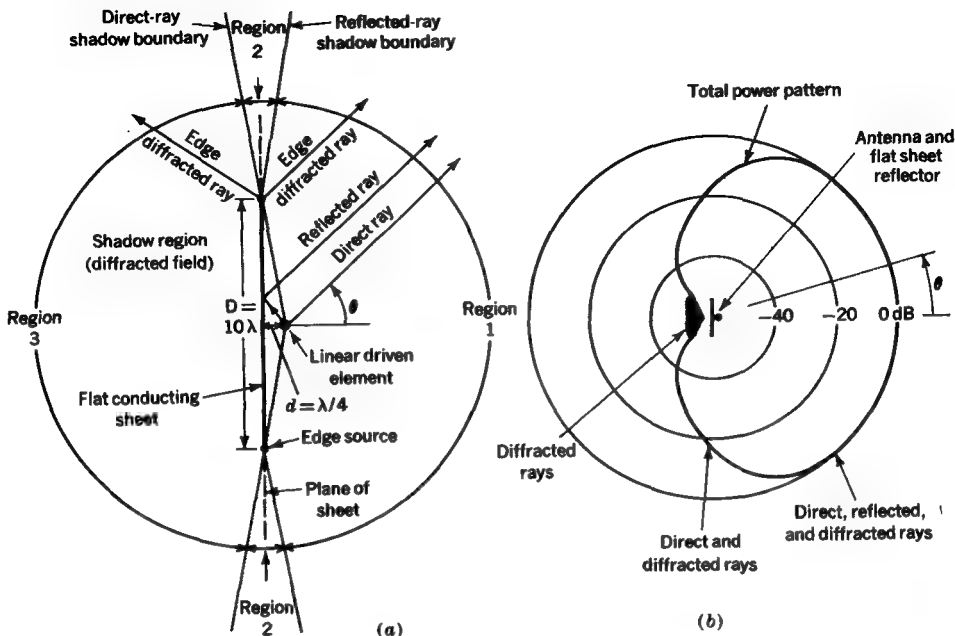


FIGURE 14-48

(a) Linear element with finite reflecting sheet analyzed by diffraction theory and (b) power pattern. Note that this pattern is on a logarithmic (decibel) scale in order to cover the wide range in power.

14-20.1 Infinite-flat-sheet Reflector

In Fig. 14-47a a linear antenna is situated a distance d from an infinite flat perfectly conducting metal sheet, or ground plane. This combination can be analyzed simply by replacing the ground plane by an image of the antenna at a distance $2d$ from the antenna (see Fig. 7-16). The pattern in the θ plane (H plane)[†] is that of two equal isotropic point sources spaced a distance $2d$ apart and in opposite phase, or

$$E_\phi(\theta) = \sin(\beta d \cos \theta) \quad (1)$$

If $d = \lambda/4$, the pattern is as suggested in Fig. 14-47a with maximum at $\theta = 0$.

14-20.2 Finite-flat-sheet Reflector

When the reflecting sheet or ground plane is reduced in size, the analysis is less simple. The situation is illustrated in Fig. 14-48a. There are three principal angular regions: (1) region of direct and reflected rays (in front of sheet or to right side); (2) region of

[†] In the E plane the pattern is that of an isolated antenna in this plane multiplied by (1).

direct but no reflected ray (contains plane of sheet); (3) shadow region (no direct or reflected ray behind sheet or to left; i.e., only diffracted rays are present).

If the ground plane is extensive (say several wavelengths in size) and the antenna is close to the ground plane, image theory accounts adequately for the pattern in region 1. In region 2, the distant field is dominated by the direct ray from the antenna. In the shadow region behind the sheet (region 3) the geometrical theory of diffraction (Sec. 12-9) must be used. The pattern in this region is effectively that of two cardioid-pattern sources (see Fig. 14-19c), one at each edge of the sheet. The beam maximum of the upper-edge pattern is directed upward in the figure, and the beam maximum of the lower edge is directed downward. Calculating the fields for the three regions as outlined above results in the $E_\phi(\theta)$ (H -plane) pattern shown in Fig. 14-48b for the case where the sheet dimension $D = 10\lambda$ and the antenna spacing $d = \lambda/4$. It is assumed that the antenna is a linear element and that the sheet is infinite (or very large) perpendicular to the page. Note that this pattern is on a logarithmic (decibel) scale in order to show the wide range of fields involved. The pattern in Fig. 14-48b is similar to that in Fig. 12-22 except that the *power* pattern [P (dB) = $20 \log|E|$] is in polar coordinates here and that the *field* pattern $|E|$ is in rectangular coordinates in Fig. 12-22. In the shadow region the power is down 40 to 50 dB.

14-20.3 Thin Reflectors and Directors

When the reflecting sheet degenerates into a thin linear conductor, as in Fig. 14-47c, the arrangement can be analyzed by circuit and array theory as follows.[†] Let the active (driven) element be designated element 1 and the passive (degenerate flat sheet) element be designated element 2, as in Fig. 14-49a. The circuit relations for this arrangement are

$$\boxed{\begin{aligned} V_1 &= I_1 Z_{11} + I_2 Z_{12} \\ 0 &= I_2 Z_{22} + I_1 Z_{21} \end{aligned}} \quad (1)$$

where V_1 = terminal voltage of element 1

I_1 = terminal current of element 1

I_2 = terminal current of element 2

Z_{11} = self-impedance of element 1

Z_{22} = self-impedance of element 2 (if it were opened at center and measured in isolated situation)

$Z_{12} = Z_{21}$ = mutual impedance of elements 1 and 2

[†] G. H. Brown, Directional Antennas, *Proc. IRE*, **25**: 78-145 (January 1937).

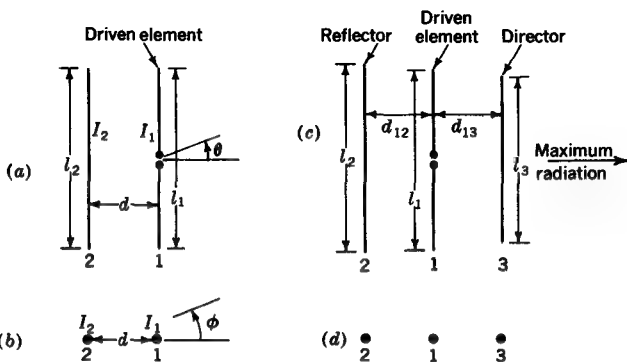


FIGURE 14-49

(a) and (b) Driven element with single parasitic element and (c) and (d) driven element with reflector and director.

From (1)

$$I_2 = -I_1 \frac{Z_{12}}{Z_{22}} = -I_1 \frac{|Z_{12}|}{|Z_{22}|} \frac{\angle \tan^{-1}(X_{12}/R_{12})}{\angle \tan^{-1}(X_{22}/R_{22})} \quad (2)$$

The field pattern $E_\theta(\phi)$ (H plane) is then

$$E_\theta(\phi) = k(I_1 + I_2 / \beta d \cos \phi) \quad (3)$$

where I_2 is as given in (2) and k is a constant. In general, I_1 and I_2 will be of different magnitude, so that the pattern cannot be reduced to the simple forms used in Sec. 14-6.1. Also note that, in general, $Z_{22} \neq Z_{11}$. Suppose that the driven element 1 is approximately $\lambda/2$ long ($l_1 \approx \lambda/2$) and that l_2 is about the same length but not necessarily exactly the same. Referring to Fig. 14-41, we note that the reactance of a thin linear element varies rapidly as a function of frequency when $l/\lambda \approx 0.5$, going from positive to negative reactance values as the length is reduced. Thus, if the length of element 2 is more than $\lambda/2$ ($l_2/\lambda > 0.5$), it has a positive self-reactance; while if it is somewhat shorter (say $l_2/\lambda < 0.48$), it has a negative reactance. Calculating the pattern $E_\theta(\phi)$ as above shows that in the former case (element 2 reactance positive) element 2 acts as a *reflector* and maximum radiation from the array is to the right ($\theta = \phi = 0$, Fig. 14-49a and b). On the other hand, if l_2 is shorter, so that its self-reactance is negative, the maximum radiation is to the left ($\theta = \phi = 180^\circ$) and element 2 acts as a *director*. It is assumed that the interelement spacing is small, say 0.1 to 0.2 λ .

An extension of the arrangement of Fig. 14-49a and b is to add a third (passive) element as in Fig. 14-49c and d. Let element 2 be made inductively reactive (X_{22} positive) and element 3 capacitively reactive (X_{33} negative). In this way element 2 acts as a reflector and element 3 as a director. For thin linear elements typical dimensions are as follows: driven-element length $l_1 = 0.48\lambda$ (to make $X_{11} = 0$),

reflector-element length $l_2 = 0.50\lambda$, director-element length $l_3 = 0.46\lambda$, and interelement spacings $d_{12} \approx d_{13} \approx 0.1\lambda$.[†] The gain of such an array is about 5 (=7 dB) as compared with a reference $\lambda/2$ dipole and the directivity $D = 5 \times 1.64 = 8.2$ (=9 dB = gain over isotropic source). With a single reflector (or director) element as in Fig. 14-49a and b the maximum possible gain is about 5 dB with respect to a $\lambda/2$ dipole ($D = 7$ dB).

In arrays like those discussed above, where one element is driven and the others are passive, it is customary to refer to the passive elements as *parasitic* elements. Thus, the above reflector and director elements are parasitic elements. Arrays may be constructed with larger numbers of parasitic elements. For example, Yagi[‡] has built arrays with many parasitic director elements, and arrays with a number of parasitic elements are commonly referred to as *Yagi* or *Yagi-Uda antennas*.[§]

14-20.4 Corner Reflectors

A corner reflector consists of two flat reflecting sheets intersecting at an angle, as in Fig. 14-47d. When the corner angle is 90° , the sheets meet at right angles, forming a square-corner reflector. With a driven element placed as shown, the arrangement is an effective (active) directional antenna for a wide range of corner angles ($0 < \theta_0 < 180^\circ$).[¶] Without a driven element a square corner is an effective (passive) wave reflector over a wide range of angles of incidence ($0 < \theta_i < \pm 45^\circ$). The reflected wave is directed along the path direction of the incoming wave, as illustrated in Fig. 14-47e.

The active corner reflector (with driven element) can be readily analyzed using the method of images for corner angles equal to $180^\circ/n$, where $n = 1, 2, 3, \dots$. It will be convenient to illustrate the method for a *square corner*, as in Fig. 14-50. For this case there are three images, as indicated. The driven element and all images carry equal currents. Driven element 1 and image element 4 are in phase, while image elements 2 and 3 are in opposite phase (with respect to 1 and 4). The field pattern $E_\phi(\theta)$ (H plane) is given by

$$E_\phi(\theta) = 2kI_1 |\cos(\beta s \cos \theta) - \cos(\beta s \sin \theta)| \quad (1)$$

where s is the corner-to-driven-element spacing. The maximum radiation is in the direction $\theta = 0^\circ$ (along corner bisector) for all values of $s < \lambda$.

[†] The exact lengths are a weak function of the element thickness. Thus, compare solid and dashed curves in the RX diagrams of Figs. 14-41 and 14-44.

[‡] H. Yagi, Beam Transmission of Ultra-short Waves, *Proc. IRE*, 16: 715-740 (June 1928).

[§] S. Uda and Y. Mushiake, "Yagi-Uda Antenna," Research Institute of Electrical Communication, Tohoku University, Sendai, Japan, 1954.

[¶] J. D. Kraus, The Corner Reflector Antenna, *Proc. IRE*, 28: 513-519 (November 1940); J. D. Kraus, U.S. Patent 2,270,314, Jan. 20, 1942.

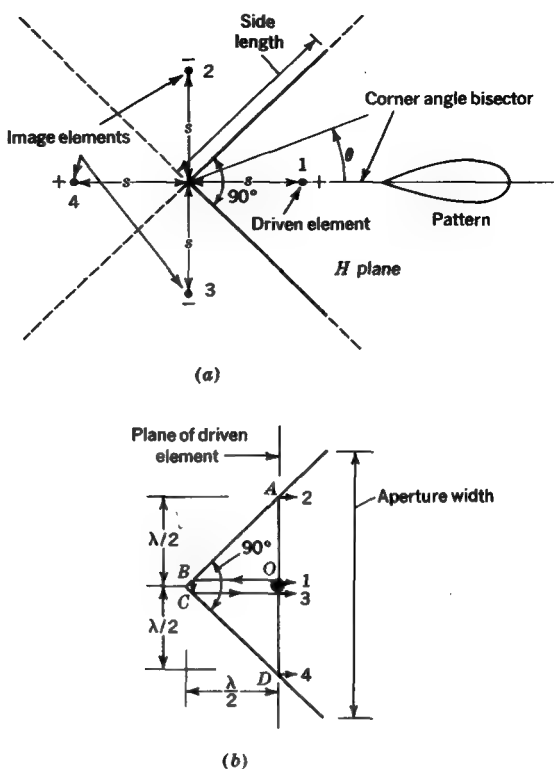


FIGURE 14-50
(a) Square-corner reflector with driven element analyzed as driven element with three image elements. **(b)** Path lengths in corner reflector.

The terminal voltage for the driven element is

$$V_1 = I_1 Z_{11} + I_1 Z_{14} - 2I_1 Z_{12} \quad (2)$$

where Z_{11} = self-impedance of element 1 (driven element)

Z_{12} = mutual impedance between elements 1 and 2 or between 1 and 3

Z_{14} = mutual impedance between elements 1 and 4

Similar expressions can be written for the voltage at the terminals of each of the image elements. Then for a power P to the driven element (power to each image is also P)† we have

$$I_1 = \sqrt{\frac{P}{R_{11} + R_{14} - 2R_{12}}} \quad (3)$$

† But the actual total power supplied to the corner-reflector antenna is that supplied to the driven element ($= P$).

The pattern for the isolated driven element (no reflector present) is

$$E_1(\theta) = \sqrt{\frac{P}{R_{11}}} \quad (4)$$

Substituting (3) in (1) and taking the ratio of (1) to (4) yields the gain over the reference (driven) element (in direction $\theta = 0$) as

$$\text{Gain over reference} = \sqrt{\frac{R_{11}}{R_{11} + R_{14} - 2R_{12}}} (\cos \beta s - 1) \quad (5)$$

If the driven linear element is $\lambda/2$ long, the image elements are also $\lambda/2$ long and for a typical driven-element-to-corner spacing $s = 0.25\lambda$ the gain of the square corner-reflector antenna over a $\lambda/2$ dipole antenna is 10.2 dB (directivity $D = 12.35$ dB). The above analysis assumes reflecting sheets of infinite size. In practice it is found that if the side length (in plane of page, Fig. 14-50a) is at least twice the driven-element-to-corner spacing, the reduction in gain is small. The reflector length perpendicular to the page should equal or somewhat exceed that of the driven element.[†] The corner reflector is very widely used in many television, point-to-point communication, and radio-astronomy applications.

14-20.5 Parabolic Reflectors and Lens Antennas

Parabolic reflectors and lens antennas may be considered together since the design of both involves the principle of equality of path length. Consider, for example, the parabolic reflector shown in Fig. 14-51a. We wish to convert the circular wavefront from the driven element or source at the point O (focus) to a plane wavefront.[‡] From geometric optics the *Principle of Equality of Path Length* requires that the electrical length along all ray paths between a pair of wavefronts be equal.[§] This means here that the electrical distance $AO = OBC$ or that $2L = R + R \cos \theta$, from which[¶]

$$R = \frac{2L}{1 + \cos \theta} \quad (2)$$

[†] For a detailed discussion of corner-reflector parameters see Kraus, "Antennas," pp. 328-336.

[‡] A wavefront is an equiphasic surface; i.e., the phase is the same at all points on the surface.

[§] For more detailed discussion see, for example, S. Silver, "Microwave Antenna Theory and Design," McGraw-Hill Book Company, New York, 1949.

[¶] More explicitly we should write

$$2L + \frac{1}{2} = R + R \cos \theta + \frac{1}{2} \quad (1)$$

where the distances are expressed in wavelengths. Waves reflected at the parabolic surface undergo a phase reversal (180° phase change) which is equivalent to a path length of $\lambda/2$. Hence the terms with $1/2$ in (1).

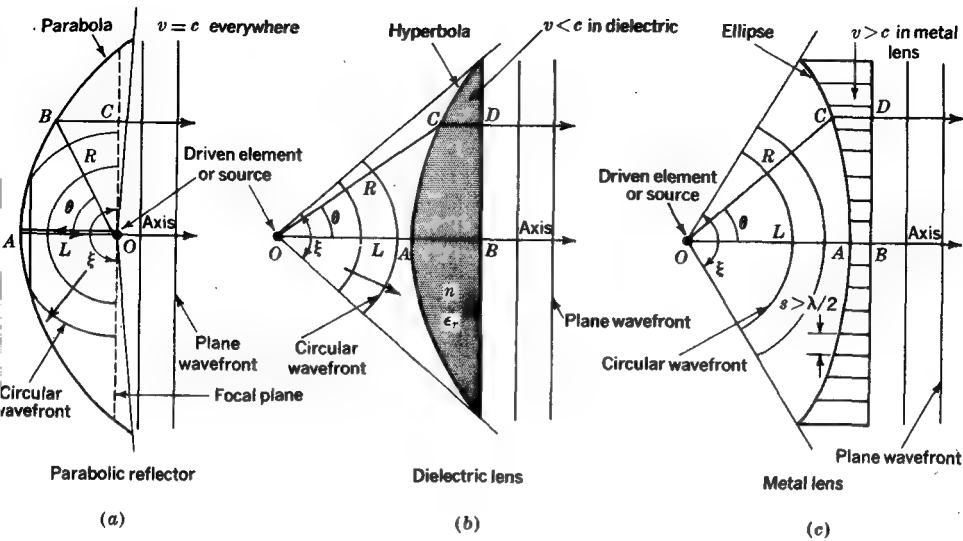


FIGURE 14-51
(a) Parabolic-reflector, **(b)** dielectric-lens, and **(c)** metal-lens antennas with path lengths used in analysis.

This is the equation of the required surface. It is a *parabola* with focus at *O*.

Consider next the dielectric lens of Fig. 14-51b with driven element or source at *O*. The principle of equality of path length requires that $OAB = OCD$ or that $R = \eta(R \cos \theta - L) + L$, from which

$$R = \frac{(\eta - 1)L}{\eta \cos \theta - 1} \quad (3)$$

where η is the index of refraction ($\eta = \sqrt{\epsilon_r}$ for nonmagnetic media). Equation (3) gives the required shape of the curved lens surface. It is a *hyperbola*.

We note that with the parabolic reflector, $\eta = 1$ everywhere and the wave velocity $v = c$. For the dielectric lens, however, $\eta > 1$ in the lens, and hence $v < c$. Therefore, the electrical distance, or phase change, is greater per unit distance in the lens than in the air outside, and this is accounted for in (3). A general expression for the electrical length is

$$\text{Electrical length} = \beta_0 \int \eta dl = \frac{2\pi}{\lambda_0} \int \eta dl \quad (4)$$

where λ_0 is the free-space wavelength and the integration is over the physical path length. In (2) and (3) we have applied (4) in incremental form with $\eta = 1$ in air and $\eta = \sqrt{\epsilon_r}$ in the dielectric lens. The integral form of (4) is required only if η is a continuously variable function of distance.

Finally, let us analyze the metal-plate lens of Fig. 14-51c. The lens consists of a stack of parallel metal sheets spaced somewhat more than $\lambda/2$ and hence capable of transmitting a higher-mode wave (E perpendicular to page), as in a waveguide (see Sec. 13-14).† For equality of electrical path length we must have $OAB = OCD$ or $R + (L - R \cos \theta)\eta = L$, from which

$$R = \frac{(1 - \eta)L}{1 - \eta \cos \theta} \quad (5)$$

This relation is identical with (3) for the dielectric lens. However, in the metal-plate lens $v > c$ and $\eta < 1$, and so the form of (5) is used in order to keep both numerator and denominator positive. For this case ($\eta < 1$) (5) is the equation of an *ellipse*. Metal-plate lens antennas with E parallel to the page (and metal plate parallel to the page) are also possible. They are analyzed in the same way as the lens of Fig. 14-51c.

This discussion of the antennas of Fig. 14-51 applies both to cylindrical geometry (uniform surfaces and line source perpendicular to page) and to spherical geometry (surfaces given by figure of revolution around axes) with point sources. As a generalization, all the antennas of Fig. 14-51 may be regarded as *wave transformers* which convert a cylindrical or spherical wavefront to a plane wave or vice versa.

14-20.6 Some Comments on Corner Reflectors vs. Parabolic Reflectors

The driven element or source for the parabola (and also lens) antennas should be directional, and for greatest operating efficiency most of its pattern angle should be included within the angle ξ subtended by the reflector (or lens) (Fig. 14-51). This puts an additional requirement on the primary or feed antenna used at the focus of a parabolic reflector. This requirement is not present in the corner reflector, where the driven element is a simple linear antenna with omnidirectional pattern (in plane of page, Fig. 14-50).

It should be noted that the principal advantages of the corner reflector are for small apertures. When the aperture width (Fig. 14-50b) is less than 2λ , a corner reflector may be simpler and more practical than a parabolic reflector, but for larger apertures the parabola is better. For small apertures the actual shape of the reflector becomes of secondary importance since the ray-path differences involved are small.

† W. E. Kock, Metal Lens Antennas, *Proc. IRE*, 34: 828-836 (November 1946).

It is instructive to apply the principle of equality of path length to the corner reflector. Referring to the square-corner reflector of Fig. 14-50b with driven-element-to-corner spacing of $\lambda/2$, the path lengths of the four principal rays to a point at an infinitesimal distance to the right of the plane of the driven element are

$$\text{Length (ray 1)} = 0\lambda$$

$$\text{Length (ray 2)} = OA + \frac{1}{2} = \frac{1}{2} + \frac{1}{2} = 1\lambda$$

$$\text{Length (ray 3)} = OB + CO + \frac{1}{2} - \frac{1}{2} = \frac{1}{2} + \frac{1}{2} + \frac{1}{2} - \frac{1}{2} = 1\lambda$$

$$\text{Length (ray 4)} = OD + \frac{1}{2} = \frac{1}{2} + \frac{1}{2} = 1\lambda$$

Thus, all four rays are in the same phase.

14-21 SLOT AND COMPLEMENTARY ANTENNAS

If a $\lambda/2$ slot is cut in a large flat metal sheet and a transmission line connected to the points *FF*, as in Fig. 14-52a, the arrangement will radiate effectively due to currents flowing on the sheet. The analysis of such a *slot antenna* is greatly facilitated by considering the slot's *complementary antenna*.† Thus, the antenna which is complementary to the slot of Fig. 14-52a is the dipole of Fig. 14-52b. The metal and air regions of the slot are interchanged for the dipole. According to Booker's theory,† the pattern of the slot of Fig. 14-52a is identical in shape to that of the dipole of Fig. 14-52b except that the electric field will be vertically polarized for the slot and horizontally

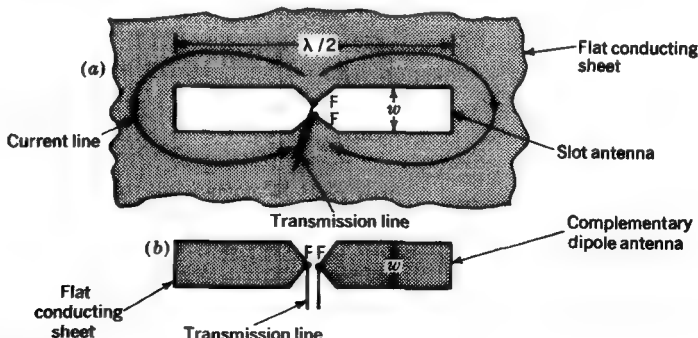


FIGURE 14-52

(a) Slot antenna and (b) complementary dipole antenna. Both are $\lambda/2$ long and have a width *w*. They are fed at the points *FF*.

† H. G. Booker, *Slot Aerials and Their Relation to Complementary Wire Aerials*, *J. IEE (London)*, 93, part IIIA, no. 4 (1946).

polarized for the dipole. Further, the terminal impedance Z_s of the slot is related to the terminal impedance Z_d of the dipole by the intrinsic impedance Z_0 ($= 376.7\Omega$) of free space as follows:

$$Z_s = \frac{Z_0^2}{4Z_d} = \frac{35,481}{Z_d} \quad (\Omega) \quad (1)$$

Thus, knowing the properties of the dipole enables us to predict the properties of the complementary slot. For example, let the width of the dipole and slot of Fig. 14-52 be reduced to a very small fraction of a wavelength so that the dipole qualifies as a thin $\lambda/2$ linear dipole with $Z_d = 73 + j42.5$ (see Sec. 14-19). According to (1), the terminal impedance of the complementary slot antenna will be

$$Z_s = \frac{35,481}{73 + j42.5} = 363 - j211 \Omega$$

14-22 HORN ANTENNAS

A horn antenna may be regarded as a flared-out (or opened-out) waveguide. A pyramidal horn fed by a rectangular waveguide is shown in Fig. 14-53a. The function of the horn is to produce a uniform phase front with a larger aperture than that of the waveguide and hence greater directivity. The principle of equality of path length is applicable to the horn design but with a different emphasis. Instead of specifying that the wave over the plane of the horn mouth be *exactly* in phase, this requirement is relaxed to one where the phase may deviate but by less than a specified amount.[†] From the geometry of Fig. 14-53b we have $\cos \theta = l/(l + \delta)$, $\sin \theta = h/[2(l + \delta)]$, $\tan \theta = h/2l$, from which

$$l = \frac{h^2}{8\delta} \quad \delta \text{ small} \quad (1)$$

$$\theta = \tan^{-1} \frac{h}{2l} = \cos^{-1} \frac{l}{l + \delta} \quad (2)$$

In the *E* plane of the horn, it is customary to allow no more than 72° phase difference ($\delta < \lambda/5$) (deviation $\pm 36^\circ$). However, in the *H* plane the difference can be larger, say 135° ($\delta < 3\lambda/8$), without undesirable effects since *E* goes to zero at the horn edges (boundary condition $E_t = 0$ satisfied).

[†] This could be stated as the *principle of inequality of path length*, where the inequality does not exceed a specified amount.

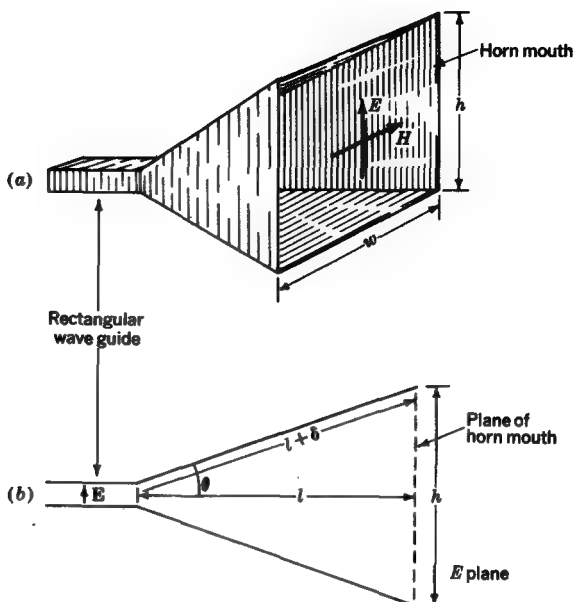


FIGURE 14-53

(a) Horn antenna showing field orientation in mouth and (b) dimensions used in analysis.

EXAMPLE Determine the length l , width w , and half-angles θ and ϕ (in E and H planes, respectively) of a pyramidal electromagnetic horn as in Fig. 14-53a for which the mouth height $h = 10\lambda$. The horn is fed by a rectangular waveguide with TE_{10} mode as in the figure.

SOLUTION Taking $\delta = \lambda/5$ in the E plane, we have from (1) that $l = h^2/8\delta = 100\lambda/(8) = 62.5\lambda$ and half the flare angle θ (in the E plane) is

$$\theta = \tan^{-1} \frac{h}{2l} = \tan^{-1} \frac{10}{125} = 4.6^\circ$$

Taking $\delta = 3\lambda/8$ in the H plane gives

$$\phi = \cos^{-1} \frac{62.5}{62.5 + 0.375} = 6.3^\circ$$

and the width w of the horn in the H plane is

$$w = 2l \tan \phi = 2 \times 62.5 \times \tan 6.3^\circ = 13.7\lambda$$

14-23 APERTURE CONCEPT

According to (14-5-29), the *effective aperture* A_e of an antenna is related to its directivity D by

$$D = \frac{4\pi}{\lambda^2} A_e \quad (1)$$

The effective aperture is a unique quantity for any antenna. For a short-dipole antenna it may be larger than its physical cross section or aperture. However, for antennas like horns or parabolic reflectors which have large aperture dimensions in terms of wavelength, the effective aperture is always less than the physical aperture. Ideally if the field is exactly uniform and in phase over the aperture and there are no thermal losses, the *effective aperture* A_e is equal to the *physical aperture* A_p . Under these conditions the maximum directivity D_m is achieved, or

$$D_m = \frac{4\pi}{\lambda^2} A_p \quad (2)$$

The ratio of (1) to (2) gives the *aperture efficiency*

$$\boxed{\epsilon_{ap} = \frac{A_e}{A_p}} \quad (3)$$

A uniform field distribution has the disadvantage that minor lobes are large (see Fig. 14-24). Although minor lobes are less for a tapered field distribution (zero minor lobes for cosine-squared or gaussian distributions), the effective aperture and directivity are less. One of the problems of antenna design is to achieve a suitable compromise, so that the aperture efficiency is as large as possible for a given side-lobe level. An empirical approach to the problem is to postulate a number of aperture field distributions and to select the best efficiency and side-lobe combination. The pattern with side lobes can be calculated from (14-8-1), while the aperture efficiency can be evaluated from

$$\boxed{\epsilon_{ap} = \frac{E_{av}^2}{(E^2)_{av}}} \quad (4)$$

where E = field at any point in aperture

E_{av} = average of E over aperture

$(E^2)_{av}$ = average of E^2 over aperture

It is assumed that E is exactly in phase over the aperture and that there are no thermal losses.†

† This discussion is highly simplified. For a more complete treatment see Kraus, "Radio Astronomy," pp. 212-223.

EXAMPLE 1 Calculate the aperture efficiency of a rectangular aperture antenna (x_0 by y_0) with a uniform field in the y direction and a linearly tapered field in the x direction going from E_0 at the centerline ($x = x_0/2$) to 0 at both edges (triangular taper as in Fig. 14-24b).

SOLUTION We have $E(x) = E_0 [x/(x_0/2)]$, and $E(x)_{av} = E_0/2$. Also

$$[E^2(x)]_{av} = \frac{1}{x_0/2} \int_0^{x_0/2} E^2(x) dx = \frac{E_0^2}{(x_0/2)^3} \int_0^{x_0/2} x^2 dx = \frac{E_0^2}{3}$$

Hence the aperture efficiency is

$$\epsilon_{ap} = \frac{[E(x)_{av}]^2}{[E^2(x)]_{av}} = \frac{\frac{1}{4}}{\frac{1}{3}} = \frac{3}{4}$$

A cosine rather than a linear type of taper is common in practice for large apertures, the field going from a maximum at the center to about 0.3 times the center value at the edges (down about 10 dB).

The aperture concept is useful in other ways. For example, it can be used to help decide between a very long end-fire antenna or a broadside array of several shorter end-fire antennas and, for the latter, to determine what spacing should be used between the antennas. This will be illustrated in the following problem.

EXAMPLE 2 Design a circularly polarized antenna using one or more end-fire elements so as to produce a directivity of 100 (= 20 dB) for operation at a given wavelength λ .

SOLUTION From Table 14-4 the highest directivity per unit length for an end-fire array is obtained with the increased-directivity condition as with the helical-beam antenna. For this antenna with $C = \lambda$, the required length is

$$L = \frac{D}{15} = \frac{100}{15} = 6.7\lambda$$

or about 31 turns for a helix with a pitch angle $\alpha = 12^\circ$, as shown in Fig. 14-54a. A more compact design results with four shorter helical-beam antennas (quad-helix array). From (2) the physical aperture required (with uniform distribution) to produce a directivity $D = 100$ is

$$A_p = \frac{D}{4\pi} = \frac{100}{4\pi} = 8\lambda^2$$

Dividing A_p in quarters, we get $2\lambda^2$ as the required effective aperture for each helix, and so the directivity for each helix must be

$$D = \frac{4\pi}{\lambda^2} 2\lambda^2 = 25$$

and its length

$$L = \frac{2.5}{1.7} = 1.7\lambda$$

or about 8 turns for a helix with a pitch angle $\alpha = 12^\circ$, as shown in Fig. 14-54b. Putting each helix at the center of its aperture area, we see from Fig. 14-54d that the spacing between helices should be 1.4λ .

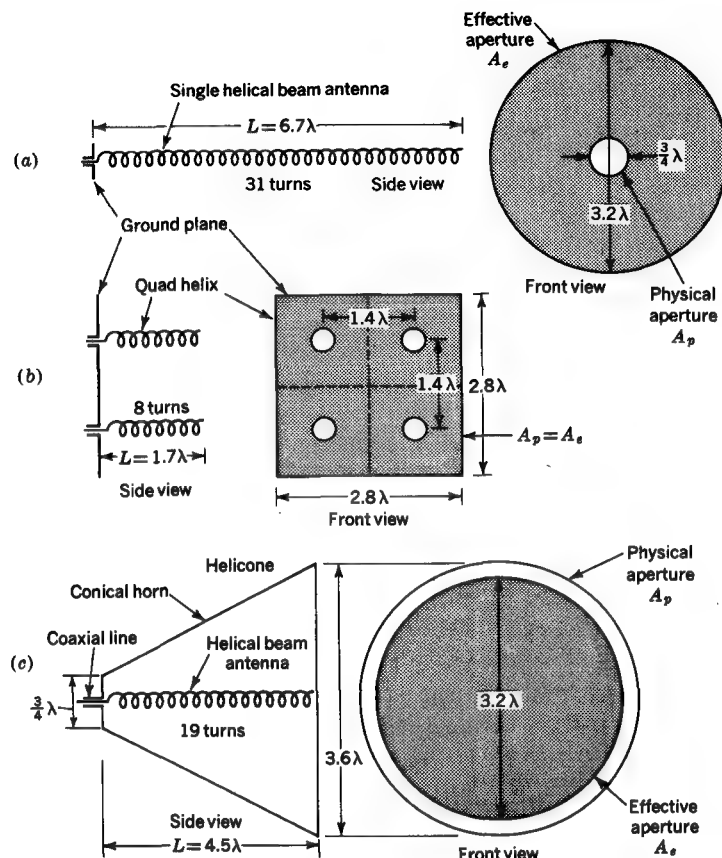


FIGURE 14-54

(a) Single helical-beam antenna, (b) quad-helix array, and (c) helicone antenna compared on basis of effective apertures A_e . All three antennas have equivalent directivity.

The antennas of Fig. 14-54a and b have equivalent directivity, but the quad helix array is more compact. On the other hand, the single long helix is simpler to feed. Other choices are also available to the designer. For example, a *helicone* antenna,[†] as shown in Fig. 14-54c, is a likely candidate. This antenna consists of a helical-beam antenna (fed by coaxial cable) enclosed in a truncated conical horn. A directivity $D = 100$ requires a length $L = 4.5\lambda$ and horn-mouth diameter of 3.6λ . Note that the

[†] K. R. Carver, The Helicone: A Circularly Polarized Antenna with Low Side Lobe Level, Proc. IEEE, 55: 559 (April 1967).

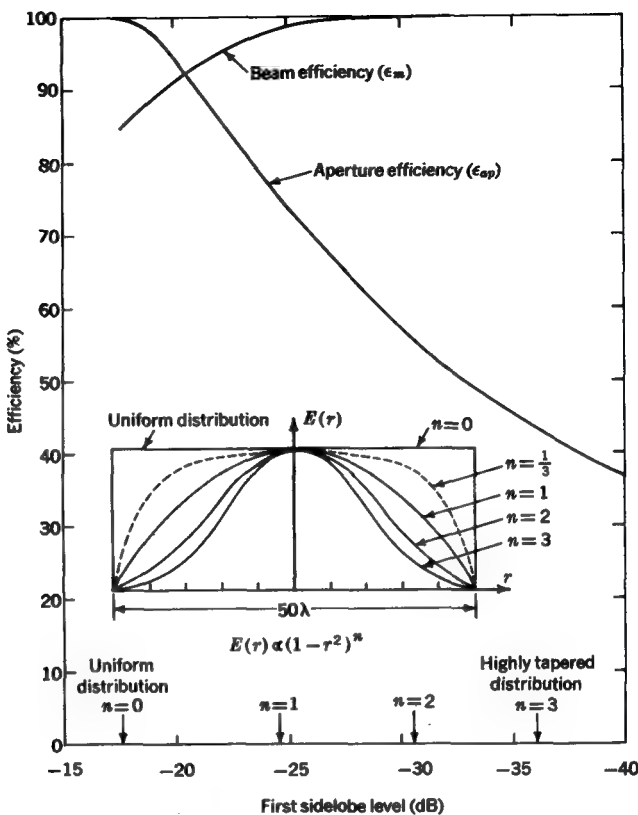


FIGURE 14-55
Aperture and beam efficiencies as a function of side-lobe level (and aperture distribution) for a circular aperture of 50λ diameter.

physical aperture for this antenna is about $10\lambda^2$. This is more than the $8\lambda^2$ needed for a uniform aperture distribution because the aperture distribution over the mouth of the helicone antenna is highly tapered (resulting in reduced side lobes).

EXAMPLE 3 Determine the aperture efficiency and the beam efficiency $\epsilon_m = \Omega_M/\Omega_A$ for a 50λ -diameter circular aperture with aperture distribution of the form $(1 - r^2)^n$, where $r = 0$ at the center and $r = 1$ at the rim ($n = \text{constant}$). What distribution provides high efficiency and low side-lobe level?

SOLUTION The aperture efficiency is obtained from (4). The beam efficiency is obtained by integrating the pattern over 4π for Ω_A and over the main beam for Ω_M using numerical methods. The results are shown in Fig. 14-55 with efficiency as ordinate vs. the first side-lobe

level as abscissa. We note that a highly tapered distribution ($n = 3$) gives a very low side-lobe level (-36 dB) but a low aperture efficiency. However, at a side-lobe level of -20 dB ($n \approx \frac{1}{2}$) both aperture *and* beam efficiencies are large. Hence, at this side-lobe level and corresponding aperture distribution (see dashed curve) we have a satisfactory compromise.[†]

14-24 COHERENCE

In Chap. 11 coherence was discussed in connection with wave polarization. Thus, if the E_x and E_y components of a wave (as in Fig. 14-56a) are given by

$$E_x = E_1(t) \sin \omega t \quad (1)$$

$$E_y = E_2(t) \sin[\omega t + \delta(t)] \quad (2)$$

where all the time functions are independent, the resultant wave is said to be completely *unpolarized* or *incoherent*. [It is assumed that $\langle E_1^2(t) \rangle = \langle E_2^2(t) \rangle$.]

Coherence in another sense will now be discussed. Consider a plane wave traveling to the right, as in Fig. 14-56b. As the wave travels from point 1 to point 2,

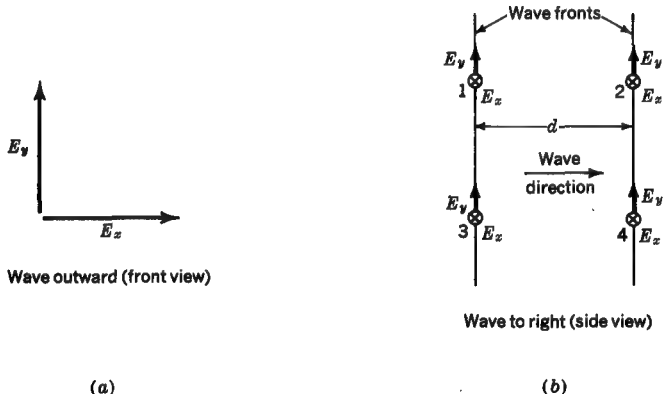


FIGURE 14-56
(a) Electric fields of wave traveling out of page illustrating polarization coherence and (b) wavefronts with electric fields at four points illustrating wavefront (or phase) coherence.

[†] K. R. Carver, B. Potts, and R. Widner, Beam and Aperture Efficiencies vs. Sidelobe Level, *IEEE/G-AP Symp. Los Angeles, 1971*. See also R. T. Nash, Beam Efficiency Limitations of Large Antennas, *IEEE Trans. Antennas Propag., AP-12*: 918-923 (December 1964).

we expect that the phase at point 2 will be retarded by βd . Likewise, we expect the phase of point 3 to be identical with that at point 1 (phase difference zero). Also the phase difference of points 2 and 4 should be zero. The conditions just described may be characterized as providing *wavefront coherence*, in contrast with the situation involving polarization. In homogeneous media, wavefront coherence prevails, but the wave need not be coherent with respect to polarization. However, in inhomogeneous media it is possible that wavefront incoherence exists, which means that we can no longer define a wavefront, i.e., an equal-phase surface. Thus, for example, the E_x components of the field at points 1 and 3 (Fig. 14-56b) will be time-independent.

Wavefront incoherence may be apparent at wavelengths of 10 to 20 m for waves received through the earth's ionosphere from celestial radio sources when comparing phase at points (such as 1 and 3 in Fig. 14-56b) separated by several kilometers. This means that an interferometer antenna with elements separated by such distances will not produce fringes (multilobed pattern, as in Fig. 14-22). The ionosphere has less effect at shorter wavelengths, and at 100- to 200-mm wavelengths fringes are obtained with interferometer base lines (element separation) of thousands of kilometers, thus demonstrating wavefront coherence over large distances. This is remarkable since the energy of a radio photon is very small (one quantum contains hf J of energy, where h = Planck's constant = 6.6×10^{-34} J s and f = frequency in Hz; at $\lambda = 200$ mm, $hf = 10^{-24}$ J). Hence, it means either that a photon spreads its energy over a very wide front or that all the photons in a wavefront are phase-locked.

Although wavefront coherence usually prevails, it is instructive to consider the behavior of receiving devices which are completely incoherent. For example, consider the cosmic-ray telescope planned by Grote Reber at the Ohio State University Radio Observatory. The basic element of this telescope is a pair of disk-shaped cosmic-ray sensors arranged as coincidence counters (A and B), as in Fig. 14-57. Thus, a particle passing through both sensors (A and B) will be counted, but one passing through only one sensor will not. As a result the pair of sensors has a cone of reception (or beam width) defined by the ray-path geometry (geometrical optics). By increasing the sensor-separation distance d the cone angle can be decreased. The sensitivity of the telescope can be increased by adding more units (C and D) as in Fig. 14-57. In general, particles passing through the sensors (A and B) of the left unit will be independent or incoherent with respect to those passing through the sensors (C and D) of the right unit, so that adding the right unit doubles the telescope sensitivity but the beam width (cone of reception) is unchanged.[†] This is in contrast

[†] However, if a shower of particles forming a flat disk (transverse to their direction of travel) impinges on the telescope, the difference in arrival time at the two units (left and right) could be used to determine the direction of arrival, hence providing quasi coherence.

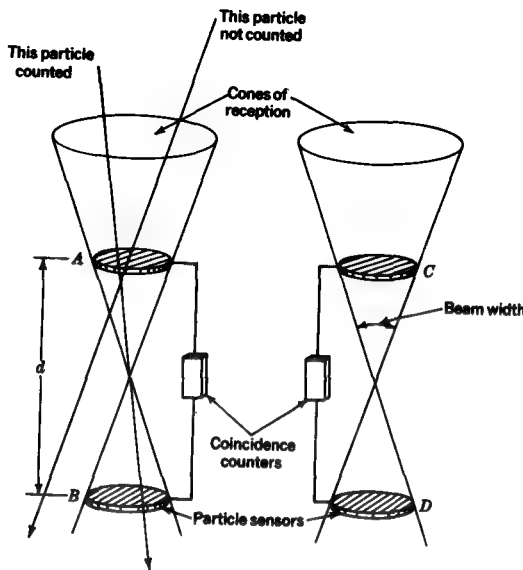


FIGURE 14-57

Cosmic-ray telescope, illustrating lack of coherence between left and right units for individual particles (*After Reber.*)

to an antenna, where adding another element or unit in a broadside array would both increase the effective aperture (and directivity) and make the response pattern (beam width) narrower.

14-25 FRIIS FORMULA AND RADAR EQUATION

Consider the communication circuit of Fig. 14-58a, consisting of a transmitter T with antenna of effective aperture A_{et} , and receiver R with antenna of effective aperture A_{er} . The distance between transmitting and receiving antennas is r . If the transmitter power P_t were radiated by an isotropic source, the power received per unit area at the receiving antenna would be

$$S = \frac{P_t}{4\pi r^2} \quad (1)$$

and the power available to the receiver would be

$$P'_r = S A_{er} \quad (2)$$

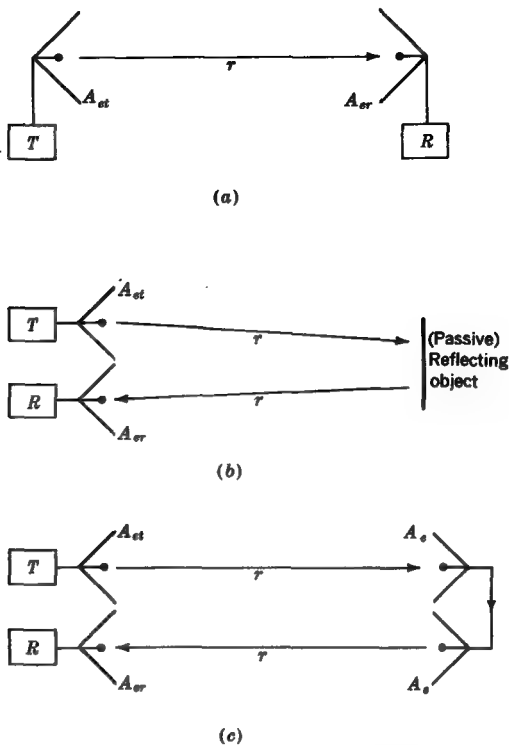


FIGURE 14-58

(a) Single transmission path with parameters used in Friis transmission formula.
 (b) and (c) Double-path geometry used in obtaining radar equation.

The transmitting antenna has an effective aperture A_{et} and hence a directivity $D = 4\pi A_{et}/\lambda^2$, so that with the antenna connected the power available at the receiver is

$$P_r = \frac{P_t' 4\pi A_{et}}{\lambda^2} \quad (3)$$

Substituting (1) in (2) and (2) in (3) gives

$$P_r = \frac{P_t A_{er} 4\pi A_{et}}{4\pi r^2 \lambda^2}$$

or

$$\frac{P_r}{P_t} = \frac{A_{er} A_{et}}{r^2 \lambda^2} \quad (\text{dimensionless}) \quad (4)$$

where P_r = received power, W

P_t = transmitted power, W

A_{er} = effective aperture of receiving antenna, m^2

A_{et} = effective aperture of transmitting antenna, m^2

r = distance between receiving and transmitter antennas, m

λ = wavelength, m

This is the *Friis transmission formula*, which gives the ratio of the received to transmitted power for a direct path.

Let the problem now be modified, as in Fig. 14-58b, so that a passive reflecting object, such as a flat sheet or a single passive corner reflector, constitutes part of the transmission path. For convenience let the reflecting object be regarded as a pair of antennas connected as in Fig. 14-58c. Applying the Friis formula in two steps, we obtain

$$\frac{P_r}{P_t} = \frac{A_{et} A_{er} A_e^2}{r^4 \lambda^4} \quad (\text{dimensionless}) \quad (5)$$

where A_e = effective aperture of reflecting object, m^2

r = distance from transmitting (or receiving) antenna to reflecting object, m.

The remainder of the symbols in (5) are the same as for (4). This is a radar equation for the ratio of the received to transmitted power. If the receiving and transmitting antennas are identical so $A_{et} = A_{er} = A$ we have

$$\frac{P_r}{P_t} = \frac{A^2 A_e^2}{r^4 \lambda^4} \quad (6)$$

The aperture A_e is the *effective scattering aperture* of the reflecting object.[†] If the reflecting object is a large, flat, conducting sheet oriented for specular reflection, $A_e = A_p$, where A_p is the physical aperture.

For most objects the scattering aperture is much less than the cross-sectional area because the objects tend to scatter or reradiate isotropically. Making this change (i.e., assuming isotropic scattering) we get the *radar equation*

$$\frac{P_r}{P_t} = \frac{A^2 \sigma}{4\pi \lambda^2 r^4}$$

(7)

where σ is the *radar cross section* (m^2).[‡] The radar cross section (σ) is equal to the ratio of the scattered power (assumed isotropic) to the incident Poynting vector (or power density). Thus

$$\sigma = \frac{\text{scattered power}}{\text{incident power density}} = \frac{4\pi r^2 S_r}{S_{inc}} \quad (8)$$

[†] It is assumed that the angle subtended by the reflecting object is small compared to the antenna beam width.

[‡] We have

$$\begin{aligned} P_r &= (\text{scattered power}) \times (\text{fraction of sphere subtended by receiving antenna}) \\ &= (\text{power density incident on object}) \times \sigma \times (\text{fraction of sphere subtended by receiving antenna}) \\ &= (P_t (4\pi A / 4\pi r^2 \lambda^2)) \times \sigma \times (A / 4\pi r^2) \\ &= P_t A^2 \sigma / 4\pi \lambda^2 r^4 \end{aligned}$$

We can also derive (7) from (6) as follows: Referring to (6) the aperture of the object is set equal to the radar cross section as regards incident power [$A_e(\text{inc}) = \sigma$], but it is set equal to the aperture of an isotropic antenna as regards scattered power [$A_e(\text{sc}) = \lambda^2 / 4\pi$]. Hence, we can put $A_e^2 = A_e(\text{inc}) A_e(\text{sc}) = \sigma \lambda^2 / 4\pi$ in (6), which gives (7).

where S_s = scattered power density at distance r , W m^{-2}

S_{inc} = power density incident on object, W m^{-2}

For a large perfectly reflecting metal sphere of radius a , the radar cross section is equal to the physical cross section (πa^2). For imperfectly reflecting spheres, the radar cross section is smaller. For example, at meter wavelengths, the radar cross section of the moon is about 0.1 times the physical cross section.

14-26 RADIO TELESCOPES, NOISE POWER, AND ANTENNA TEMPERATURE†

The noise power per unit bandwidth available at the terminals of a resistor of resistance R and temperature T (Fig. 14-59a) is given by‡

$$w = kT \quad (1)$$

where w = power per unit bandwidth, W Hz^{-1}

k = Boltzmann's constant = $1.38 \times 10^{-23} \text{ J K}^{-1}$

T = absolute temperature of resistor, K

The temperature T in (1) may be called the *noise temperature*.

If the resistor is replaced by a lossless resonant antenna of radiation resistance R (Fig. 14-59b), the impedance presented at the terminals is unchanged. However, the noise power will not be the same unless the antenna is receiving from a region at the temperature T .

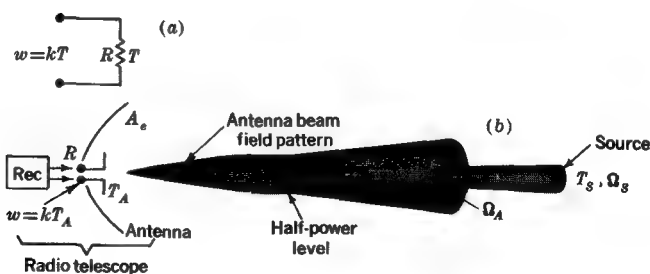


FIGURE 14-59

(a) Noise power of resistance R at temperature T and (b) noise power of antenna radiation resistance R at temperature T_A due to distant regions in antenna beam.

† For a more complete treatment see Kraus, "Radio Astronomy," pp. 97-104.

‡ H. Nyquist, Thermal Agitation of Electric Charge in Conductors, *Phys. Rev.*, 32: 110-113 (1928).

In a radio-telescope antenna operating at centimeter wavelengths, the beam may be directed at regions of the sky which are at effective temperatures close to absolute zero (0 K, or -273°C). The noise temperature T_A of the antenna is equal to this sky temperature and *not* to the physical temperature of the antenna structure. Thus, for a radio-telescope antenna the noise power is given by

$$w = kT_A \quad (\text{W Hz}^{-1}) \quad (2)$$

where T_A is the antenna (noise) temperature, or temperature of the antenna radiation resistance, determined by the sky temperature at which the antenna beam is directed. Thus, a radio-telescope antenna (and receiver) may be regarded as a radiometer (or temperature-measuring device) for determining the temperature of distant regions of space coupled to the system through the radiation resistance of the antenna. It has been assumed that the antenna has no thermal losses and that all of the antenna pattern is directed at the sky (negligible side and back lobes).

In receiving with a radio telescope it is convenient to express the received power as a (power) *flux density*. Thus, dividing the received power per unit bandwidth by the effective aperture A_e of the antenna (Fig. 14-59b) yields the flux density S , or

$$S = \frac{w}{A_e} = \frac{kT_A}{A_e} \quad (\text{W m}^{-2} \text{ Hz}^{-1}) \quad (3)$$

Note that the units for the flux density ($\text{W m}^{-2} \text{ Hz}^{-1}$) are the same as for the Poynting vector per unit bandwidth, so that we may regard the flux density as a measure of the Poynting vector (per unit bandwidth) received from distant celestial sources of radio emission.[†] Most such sources radiate waves which are completely unpolarized; i.e. they have polarization incoherence. Since any antenna (regardless of its polarization characteristics) can receive only half the incident power of an unpolarized wave (see Fig. 11-7), the actual flux density should be twice that given in (3), or

$$S = \frac{2kT_A}{A_e} \quad (4)$$

where S = flux density, $\text{W m}^{-2} \text{ Hz}^{-1}$

k = Boltzmann's constant = $1.38 \times 10^{-23} \text{ J K}^{-1}$

T_A = antenna (noise) temperature, K

A_e = effective aperture of telescope antenna, m^2

The value S in (4) results from power received over the entire antenna pattern. If the celestial source extent Ω_s is small compared to the antenna-beam solid angle Ω_A and

[†] The common unit of flux density in radio-astronomy measurements is the *flux unit* (*fu*) = $10^{-26} \text{ W m}^{-2} \text{ Hz}^{-1}$.

the antenna beam is aligned with the source, the observed flux density is as given in (3). Hence, it is said that this relation applies to *point sources*.

If the angular size of the source is small (compared to Ω_A) and its magnitude is known, it is possible to determine the source temperature T_s very simply from the relation

$$T_A = \frac{\Omega_s}{\Omega_A} T_s \quad \text{or} \quad T_s = \frac{\Omega_A}{\Omega_s} T_A \quad (5)$$

where Ω_A = antenna beam solid angle, sr (see Fig. 14-59b)

Ω_s = source solid angle, sr (see Fig. 14-59b)

T_A = antenna (noise) temperature, K

T_s = source temperature, K

EXAMPLE 1 The antenna temperature for the planet Mars measured with the U.S. Naval Research Laboratory† 15-m radio telescope at 31.5 mm wavelength was 0.24 K. Mars subtended an angle of 0.005° at the time of measurement, and the antenna HPBW = 0.116° . Find the temperature of Mars.

SOLUTION From (5) the temperature of Mars is given by

$$T_s = \frac{\Omega_A}{\Omega_s} T_A \approx \frac{0.116^2}{\pi(0.005^2/4)} 0.24 = 164 \text{ K}$$

This temperature is less than the infrared temperature of the sunlit side (250 K), implying that the radio emission may originate further below the Martian surface than the infrared radiation.

The sensitivity of a radio-telescope receiver must be sufficient to measure very small antenna (noise) temperatures T_A . The *minimum detectable temperature* of a radio-telescope receiver is given by

$$T_{\min} = \frac{kT_{\text{sys}}}{\sqrt{\Delta f t}} \quad (\text{K}) \quad (6)$$

where k = system constant (order of unity), dimensionless

T_{sys} = system temperature (sum of antenna and receiver equivalent temperatures), K

Δf = predetection bandwidth of receiver, Hz

t = postdetection time constant of receiver, s

† C. H. Mayer, T. P. McCullough, and R. M. Sloanaker, Observations of Mars and Jupiter at a Wavelength of 3.15 cm, *Astrophys. J.*, 127: 11-16 (January 1958).

EXAMPLE 2 The Ohio State University 110 by 21 m radio telescope has an effective aperture of $1,200 \text{ m}^2$ and a system temperature of 90 K at 1,415 MHz. The radio-frequency bandwidth is 6 MHz, the output time constant is 10 s, and the system constant is 2.2. Find the minimum detectable flux density.

SOLUTION From (6) the minimum detectable temperature is given by

$$T_{\min} = \frac{T_{sys}}{\sqrt{\Delta f t}} = \frac{2.2 \times 90}{\sqrt{6 \times 10^6 \times 10}} = 0.026 \text{ K}$$

From (4) the minimum detectable flux density is

$$S_{\min} = \frac{2kT_{\min}}{A_e} = \frac{2 \times 1.38 \times 10^{-23} \times 0.026}{1,200} = 5.9 \times 10^{-28} \text{ W m}^{-2} \text{ Hz}^{-1}$$

or $S_{\min} = 59 \text{ mJy}$

By repeating observations and averaging, the minimum can be further reduced ($\propto \sqrt{1/n}$, where n = number of observations). In an all-sky survey at 1,415 MHz with the Ohio State University radio telescope it is expected that about 20,000 radio sources will be detected at flux densities above 0.18 Jy.

14-27 ROTATING BAR MAGNET AS A VERY-LOW-FREQUENCY RADIATOR (PULSAR)[†]

One of the most remarkable objects discovered with radio telescopes is the *pulsar*. These radio sources emit short pulses of radio energy at rates up to about 30 s^{-1} . The pulse repetition rate for a given pulsar is astonishingly constant. It is thought that these pulsars are rapidly rotating superdense[‡] neutron stars within our own galaxy. A pulsar is believed to result from the explosion and subsequent gravitational collapse of a burned-out star. Typically a pulsar may consist of a dense spherical core perhaps 10 to 20 km in diameter with a co-rotating disk of plasma extending out to a distance at which the peripheral velocity equals the velocity of light. It is implied that a pulsar emitting 30 pulses per second is rotating 30 r s^{-1} ($= 1,800 \text{ r min}^{-1}$). For such a pulsar this means a radius ($r = c/\omega$) of 1,600 km. An idealized simplified model of such a pulsar is shown in Fig. 14-60. The magnetic field of the star is also very intense (millions of gauss or hundreds of teslas), and this field locks the

[†] Anthony Hewish, Pulsars, *Sci. Am.*, **219**(4): 25 (October 1968); J. P. Ostriker, The Nature of Pulsars, *ibid.*, **224**(1): 48 (January 1971).

[‡] Mass of 1 cm³ of star is approximately equal to the mass of 1 km³ of rock.

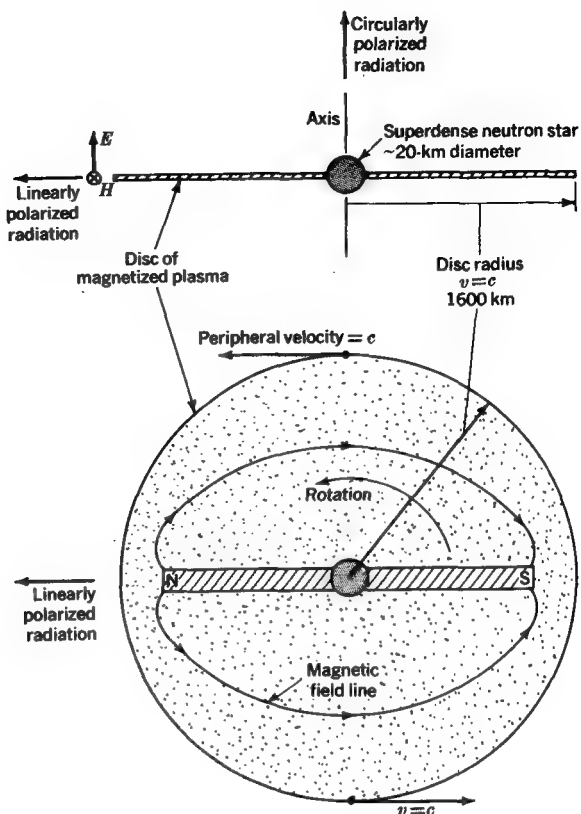


FIGURE 14-60

Idealized model of pulsar, a superdense neutron star with co-rotating disk of magnetized plasma, which attains the velocity of light at its perimeter. Very-low-frequency radio waves of enormous power are radiated by the mechanical rotation of the star (and disk). The radiation is linearly polarized in the equatorial plane (plane of disk) and circularly polarized in the direction of the axis.

surrounding plasma region to the star (Fig. 14-60). The magnetized plasma (Sec. 15-10) rotates with the neutron star at the center.

It has been suggested that the pulsar is a huge rotating machine which acts like an antenna to radiate extremely powerful very-low-frequency radio waves (order of 30 Hz or less).† Usually an antenna structure is stationary, and electric currents oscillate back and forth along the antenna conductor. However, in the pulsar we

† M. J. Rees, New Interpretation of Extragalactic Radio Sources, *Nature*, **229**: 312-317 (Jan. 29, 1971). Discusses pulsars and galactic nuclei.

appear to have a huge bar magnet (several thousand kilometers long) rotating about its center and producing a changing magnetic field, which generates an electromagnetic wave radiating in all directions. In the equatorial plane (perpendicular to the axis) the pulsar radiates with linear polarization (E parallel to axis), while in the axial (or polar) direction it radiates with circular polarization (E rotating in plane perpendicular to axis). In Sec. 14-3 on the short dipole we noted that the radiation resistance of a small antenna is very low. Hence, systems which are small (compared to the wavelength) may not be effective radiators. In the case of a 30 r s^{-1} pulsar, 1λ is $10,000 \text{ km}$ ($\lambda = c/f$). Thus, the diameter ($3,200 \text{ km}$) of the rotating magnetized disk is about $\lambda/3$, which is sufficient for the structure to have significant radiation resistance. According to Rees, a pulsar loses its energy through the very-low-frequency radio waves as it gradually spins down over millions of years. Radio powers of the order of 10^{22} W are probably involved. Assuming that the power is radiated isotropically, the Poynting vector at 1 Gm distance is given by

$$S = \frac{P}{4\pi r^2} = \frac{10^{22}}{4\pi 10^{18}} \approx 800 \text{ W m}^{-2}$$

and this implies an electric field intensity

$$E = \sqrt{SZ} = \sqrt{800 \times 377} \approx 550 \text{ V m}^{-1}$$

An electric field of this intensity lasting for the order of $\frac{1}{2}$ period ($1/60 \text{ s}$ for a 30 r s^{-1} pulsar) can accelerate electrons to relativistic velocities ($v \lesssim c$) (see Chap. 15).† This is at a distance of 1 Gm. The magnetic field associated with this E will deflect the charged particles in the direction of the wave, so that the particles will tend to be swept along by the waves (like surfers) producing a shell of relativistic particles at a large distance from the pulsar. These relativistic particles in turn produce synchrotron radiation at much higher radio frequencies, and this is the radiation detected by radio telescopes.

14-28 ANTENNAS FOR POLARIZATION MEASUREMENTS‡

In this section we describe an antenna system suitable for measuring the polarization of a received wave of unknown characteristics. The measurements will be made without measurement of phase.

† In a relatively short (1-km) distance an electron would fall through a potential difference of 550 kV . From (15-1-11) this is sufficient to attain a velocity $v \rightarrow c$.

‡ Kraus, "Radio Astronomy," pp. 126-128.

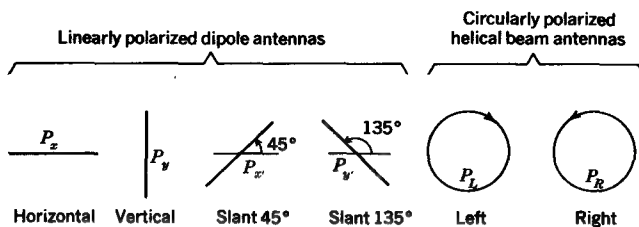


FIGURE 14-61

Arrangement of six antennas for measurement of polarization parameters of wave of unknown characteristics. Four linearly polarized and two circularly polarized antennas are used.

Let the antenna system consist of four linearly polarized dipole antennas and two helical-beam antennas (one left- and one right-handed)[†] deployed as in Fig. 14-61.[‡] The linearly polarized antennas are oriented for horizontal, vertical, and two perpendicular slant polarizations. The received wave is incident from a direction normal to the page. Let a separate receiver be connected to each antenna (or a single receiver to each in turn). The power received from the incoming wave by each antenna may then be designated by

- P_x for horizontal dipole
- P_y for vertical dipole
- P'_x for slant 45° dipole
- P'_y for slant 135° dipole
- P_L for left circular helix
- P_R for right circular helix

It is assumed that all six antennas have equal effective aperture. This means that all should give identical power response to a completely unpolarized (incoherent) wave. Then from (11-5-3) to (11-5-6) we have that the normalized Stokes parameters are

$$s_0 = \frac{I}{I} = \frac{P_x + P_y}{P_x + P_y} = \frac{P_x' + P_y'}{P_x' + P_y'} = \frac{P_L + P_R}{P_L + P_R} = 1 \quad (1)$$

$$s_1 = \frac{Q}{I} = \frac{P_x - P_y}{P_x + P_y} \quad (2)$$

[†] A left-handed helical-beam antenna receives (or transmits) left circular polarization (IEEE definition), and a right-handed one receives (or transmits) right circular polarization.

[‡] S. Suzuki and A. Tsuchiya used three pairs of antennas similar to this arrangement for measuring the polarization characteristics of radio waves emitted by the sun [A Time Sharing Polarimeter, *Proc. IRE*, 46: 190-194 (January 1958)].

$$s_2 = \frac{U}{I} = \frac{P_{x'} - P_y}{P_x + P_y} \quad (3)$$

$$s_3 = \frac{V}{I} = \frac{P_L - P_R}{P_x + P_y} \quad (4)$$

These results are summarized in Table 14-5. Assuming that the sums of each of the power pairs ($P_x + P_y$, $P_{x'} + P_y$, $P_L + P_R$) are unity, the normalized Stokes parameters s_1 , s_2 , s_3 are then given by the difference of the vertical and horizontal dipoles, the difference of the two slant dipoles, and the difference of the two helices, respectively, as suggested by the table.

There is some redundancy in the above system, i.e., the Stokes parameters can be measured with fewer antennas. A minimum of four is required in the most general case. For example, we can use a horizontal dipole (P_x), a slant 45° dipole ($P_{x'}$), and a left- and right-handed helical-beam antenna (P_L and P_R). Then the normalized Stokes parameters are given by

$$s_0 = \frac{P_L + P_R}{P_L + P_R} \quad (5)$$

$$s_1 = \frac{2P_x - P_L - P_R}{P_L + P_R} \quad (6)$$

$$s_2 = \frac{2P_{x'} - P_L - P_R}{P_L + P_R} \quad (7)$$

$$s_3 = \frac{P_L - P_R}{P_L + P_R} \quad (8)$$

Table 14-5 RELATION OF NORMALIZED STOKES PARAMETERS TO ANTENNA PAIRS

Stokes parameters	Vertical and horizontal dipoles	Two slant dipoles	Two helical-beam antennas
s_0	Sum	Sum	Sum
s_1	Difference		
s_2		Difference	
s_3			Difference

PROBLEMS

- * 14-1 A thin-dipole antenna is $\lambda/15$ long. If it has a loss resistance of 1.5Ω , find (a) directivity D , (b) gain G , (c) effective aperture A_e , (d) beam solid angle Ω_A , (e) radiation resistance R_r , and (f) terminal resistance.
- * 14-2 The radiated field of a short-dipole antenna is given by $|E| = 30\beta l(I/r)\sin\theta$, where l = length, I = current, r = distance, and θ = orientation angle. Find the radiation resistance by integrating the Poynting vector over a large sphere and equating to $I^2 R_r$, where R_r = radiation resistance.
- * 14-3 Two equal isotropic in-phase point sources are spaced 1λ apart. (a) Calculate and plot the field pattern and find the directivity. (b) Repeat for two sources in opposite phase.
- 14-4 Find the point near a short dipole where circular cross field (or elliptical cross field which is the most nearly circular) occurs. Make a drawing showing the distance in wavelengths and the angle from the dipole to the point.
- 14-5 A linear broadside array consists of four equal isotropic in-phase point sources with $\lambda/3$ spacing (overall length of array = 1λ). (a) Calculate and plot the field pattern. (b) Find the directivity.
- 14-6 Repeat Prob. 14-5 for the ordinary end-fire situation, i.e., where the progressive phase shift between sources is 120° .
- 14-7 (a) An AM broadcasting station is to be located south of the area it is to serve. Design an antenna for this station which gives a broad coverage to the north (from NW through N to NE) with reduced field intensity in other directions. However, to obtain Federal Communications Commission approval the pattern must have a null SE (135° from N) in order to protect another station on the same frequency in that direction. The antenna is to consist of an in-line array of $\lambda/4$ vertical elements oriented along a north-south line with equal spacing between elements. The minimum number of elements should be used.
Hint: In plan view the problem reduces to a linear array of isotropic point sources. (b) Repeat part (a) with the additional requirement of another null to the west (90° from N).
Hint: Apply pattern multiplication.
- 14-8 Show that the HPBW of a long uniform broadside array is given (without approximation) by $50.8^\circ/L_\lambda$, where $L_\lambda = L/\lambda$ = length of array in wavelengths.
- * 14-9 An antenna with rectangular aperture x_1, y_1 has a uniform field in the y direction and a cosine field distribution in the x direction (zero at edges, maximum at center). If $x_1 = 16\lambda$ and $y_1 = 8\lambda$, calculate (a) aperture efficiency and (b) directivity.
- 14-10 Repeat Prob. 14-9 for the case where the aperture field has a cosine distribution in both x and y directions.
- 14-11 Assume that the current is of uniform magnitude and in phase along the entire length of a thin center-fed $\lambda/2$ dipole antenna. (a) Calculate and plot the far-field pattern. (b) Find the radiation resistance. (c) Compare the resistance value of (b) with that for a thin center-fed $\lambda/2$ dipole with sinusoidal in-phase current distribution and with the radiation

* Answers to starred problems are given in Appendix C.

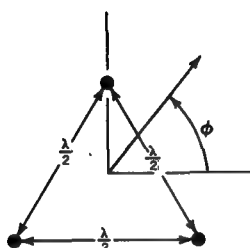


FIGURE P14-16
Three sources in triangle.

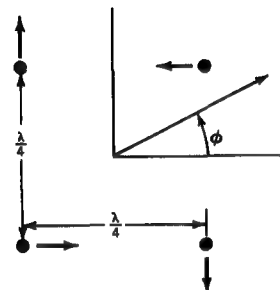


FIGURE P14-17
Four sources in square.

resistance of a $\lambda/2$ dipole calculated by means of the short-dipole formula. (b) Explain the reasons for the three different resistance values.

14-12 (a) Calculate and plot the far-field pattern of a thin center-fed 2.5λ dipole antenna. Assume a sinusoidal current distribution. (b) Find the radiation resistance.

14-13 An antenna array consists of three collinear thin $\lambda/2$ dipole antennas each with sinusoidal current distribution and spaced $\lambda/2$ apart. The current in the center dipole is twice the current in the end dipoles (binomial array). (a) Calculate and plot the far-field pattern. (b) What is the HPBW? (c) How does this HPBW value compare with the HPBW for a binomial array of three isotropic point sources spaced $\lambda/2$ apart?

* 14-14 A uniform linear array consists of 12 isotropic in-phase point sources spaced $\lambda/2$ apart. Calculate exactly (a) HPBW, (b) level of first side lobe, (c) beam solid angle Ω_A , (d) beam efficiency, (e) directivity, and (f) effective aperture.

* 14-15 A uniform linear array consists of 16 isotropic point sources with a spacing of $\lambda/4$. If the phase difference $\delta = -90^\circ$ (ordinary end-fire condition), calculate exactly the six quantities listed in Prob. 14-14.

14-16 Three isotropic point sources of equal amplitude are arranged at the corners of an equilateral triangle, as in Fig. P14-16. If all sources are in phase, determine and plot the far-field pattern.

14-17 Four isotropic point sources of equal amplitude are arranged at the corners of a square, as in Fig. P14-17. If the phases are as indicated by the arrows, determine and plot the far-field pattern. A graphical solution may be used for this problem and Prob. 14-16 (see Fig. 14-19 and Table 14-3).

14-18 Apply the Fourier transform method to obtain the far-field pattern of an array of two equal in-phase isotropic point sources with a separation d . Reduce the expression to its simplest trigonometric form.

14-19 An interferometer antenna consists of two square broadside in-phase apertures with uniform field distribution. (a) If the apertures are 10λ square and are separated 60λ on centers, calculate and plot the far-field pattern to the first null of the aperture pattern.

(b) How many lobes are contained between first nulls of the aperture pattern? (c) What is the effective aperture? (d) What is the HPBW of the central interferometer lobe? (e) How does this HPBW compare with the HPBW for the central lobe of two isotropic in-phase point sources separated 60λ ?

* 14-20 (a) Calculate and plot the far-field pattern of a continuous in-phase aperture 20λ long with cosine-squared field distribution. (b) What is the HPBW?

14-21 (a) Calculate and plot the far-field pattern of a terminated V antenna with 5λ legs and 45° included angle. (b) What is the HPBW?

14-22 A square loop antenna is 1λ on a side. If the current is uniform and in phase around the loop, calculate and plot the far-field pattern in a plane normal to the plane of the loop and parallel to one side.

* 14-23 A circular loop antenna with uniform in-phase current has a diameter D . Find (a) far-field pattern (calculate and plot), (b) radiation resistance, and (c) directivity for the following three cases: (1) $D = \lambda/3$, (2) $D = 0.75\lambda$, and (3) $D = 2\lambda$.

14-24 (a) Using a Poynting vector integration, show that the radiation resistance of a small loop is equal to $320\pi^4(A/\lambda)^2 \Omega$, where A = area of loop. (b) Show that the effective aperture of an isotropic antenna equals $\lambda^2/4\pi$.

14-25 A conductor is wound into a right-handed helix of 10 turns with diameter of 100 mm and turn spacing of 20 mm. Calculate and plot the far-field pattern and describe the polarization state if the helix is fed with radio-frequency power at a frequency of (a) 3 MHz and (b) 1 GHz.

* 14-26 A helical-beam antenna has 30 turns, $\lambda/3$ diameter, and $\lambda/5$ turn spacing. The helix is right-handed. (a) Calculate and plot the far-field pattern. (b) What is the HPBW? (c) What is the directivity? (d) What is the polarization state?

* 14-27 Two $\lambda/2$ dipoles are crossed at 90° . If the two dipoles are fed with equal currents, what is the polarization of the radiation perpendicular to the plane of the dipoles if the currents are (a) in phase, (b) phase quadrature (90° difference in phase), and (c) phase octature (45° difference in phase)?

14-28 Two identical helical-beam antennas, one left-handed and the other right-handed, are arranged as in Fig. P14-28. What is the polarization of the radiation to the right if the two helices are fed (a) in phase and (b) in opposite phase?

14-29 A linear array consists of an in-line configuration of 24 $\lambda/2$ dipoles spaced $\lambda/2$. The dipoles are fed with equal currents but with an arbitrary progressive phase shift δ between dipoles. What value of δ is required to put the main-lobe maximum (a) perpendicular to the line of the array (broadside condition), (b) 25° from broadside, (c) 50° from broadside, and (d) 75° from broadside? (e) Calculate and plot the four field patterns in polar coordinates. (f) Discuss the feasibility of this arrangement for a scanning array by changing feed-line lengths to change δ or by keeping the array physically unchanged but changing the frequency. What practical limits occur in both cases?

14-30 Three identical right-handed helical-beam antennas spaced 1.5λ apart are arranged in a broadside array, as in Fig. P14-30. (a) If the outer two helices rotate on their axes in opposite directions while the center helix is fixed, determine the angle ϕ of the main lobe with respect to the broadside direction and describe how ϕ varies as the helices

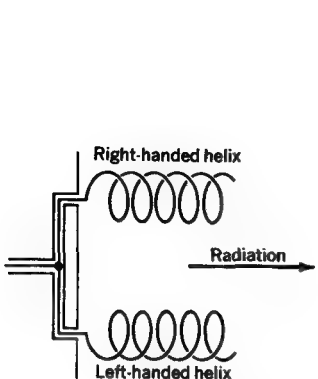


FIGURE P14-28
Two helices.

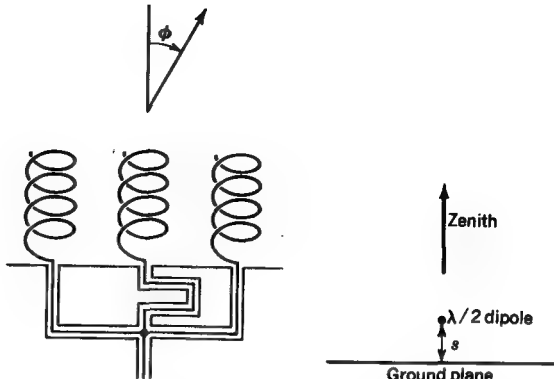


FIGURE P14-30
Three-helix array.

FIGURE P14-37
Dipole above ground.

rotate. (b) What is the maximum scan angle ϕ ? (c) What is the main-lobe HPBW as a function of ϕ ?

14-31 Design a log-periodic antenna of the type in Fig. 14-37 to operate at frequencies between 50 and 250 MHz. Make a drawing with dimensions in meters.

* 14-32 Two short-dipole antennas $\lambda/10$ long with $1\ \Omega$ loss resistance are oriented parallel to each other (side by side) and situated 1λ apart. Find (a) the mutual impedance and (b) the terminal impedance.

14-33 Explain why the mutual *resistance* of two antennas can be both positive and negative but the self-resistance of a single antenna can only be positive.

14-34 (a) Calculate the mutual impedance of two parallel $\lambda/15$ dipoles as a function of their separation from zero distance to 2λ . (b) Plot the mutual resistance RM as abscissa vs. the mutual reactance $\pm X_m$ as ordinate and put marks on the resulting impedance spiral at dipole separation intervals of 0.1λ . Compare with Fig. 14-44 for two $\lambda/2$ dipoles.

14-35 Two $\lambda/2$ dipoles are spaced $\lambda/8$ apart and fed with equal currents in opposite phase, producing an end-fire antenna. The dipoles are oriented parallel to each other and perpendicular to the line connecting their centers (as in Fig. 14-46). The dipole length-to-diameter ratio is 2,000. (a) Calculate and plot the two principal-plane far-field patterns. (b) What are the HPBWs in the two principal planes? (c) What is the gain in decibels over a single $\lambda/2$ dipole (assuming zero losses)? (d) What is the directivity in decibels? (e) What is the gain over an isotropic source if each dipole has a loss resistance $R_L = 1\ \Omega$? (f) Design a two-conductor feed system for this antenna with a terminal or driving-point impedance of $400\ \Omega$. For self- and mutual-impedance values needed in this problem interpolate from Figs. 14-41 and 14-44.

14-36 A broadside array consists of four in-phase $\lambda/2$ dipoles spaced $\lambda/2$ and fed with equal currents. The dipoles are oriented parallel to each other and perpendicular to

the line connecting their centers. The dipole length-to-diameter ratio is 2,000. (a) Calculate and plot the two principal-plane far-field patterns. (b) What are the HPBWs in the two principal planes? (c) Find the gain in decibels over a single $\lambda/2$ dipole (assuming zero losses). (d) What is the gain in decibels over an isotropic source (assuming zero losses)? (e) What is the directivity? (f) What is the gain in decibels over an isotropic source if each dipole has a loss resistance $R_L = 1 \Omega$? (g) Design a two-conductor feed system for this antenna with a terminal or driving-point impedance of 500Ω . Note that this feed system must supply equal currents to the four dipoles in spite of unequal dipole feed-point impedances.

* 14-37 A thin $\lambda/2$ dipole is parallel to an infinite flat ground plane and a distance s above it, as in Fig. P14-37. (a) Calculate and plot the gain of the dipole with ground plane with respect to a single $\lambda/2$ dipole in free space for s values from zero to $\lambda/2$. Confine consideration to the zenith direction (perpendicular to ground plane). Assume zero losses. (b) Repeat (a) for dipole loss resistance $R_L = 1 \Omega$.

14-38 Calculate and plot the far-field pattern of a thin $\lambda/2$ dipole spaced $\lambda/2$ from an infinite conducting strip 8λ wide (as in Fig. 14-48a). Plot the pattern in polar coordinates with field in decibels vs. angle, as in Fig. 14-48b.

14-39 Show that the maximum mutual impedance Z_m of two antennas separated by a large distance is $Z_m = (\sqrt{D_1 D_2} \sqrt{R_1 R_2}) / 2\pi r_1$, where D_1 = directivity of antenna 1, D_2 = directivity of antenna 2, R_1 = radiation resistance of antenna 1, R_2 = radiation resistance of antenna 2, and $r_1 = r/\lambda$ = separation of antennas (wavelengths) (see Fig. 14-38). It is assumed that the receiving antenna is terminated for maximum power transfer.

14-40 (a) Show by means of an equivalent network that at the terminals of a receiving antenna (see Fig. 14-38) the equivalent, or Thévenin, generator has an impedance $Z_{22} - (Z_m^2/Z_{11})$ and an emf $\mathcal{U}_1 Z_m/Z_{11}$, where Z_{11} = self-impedance of transmitting antenna, Z_{22} = self-impedance of receiving antenna, Z_m = mutual impedance, and \mathcal{U}_1 = emf applied to terminals of transmitting antenna. (b) What load impedance connected to the terminals of the receiving antenna results in the maximum power transfer?

14-41 A square-corner reflector has a spacing of $\lambda/4$ between the driven $\lambda/2$ element and the corner. Show that the directivity $D = 12.5$ dB.

14-42 A square-corner reflector has a driven $\lambda/2$ dipole $\lambda/2$ from the corner. (a) Calculate and plot the far-field pattern in both principal planes. (b) What are the HPBWs in the two principal planes? (c) What is the terminal impedance of the driven element? (d) Calculate the directivity two ways: (1) from impedances of driven and image dipoles and (2) from HPBWs, and compare. Assume perfectly conducting sheet reflectors of infinite extent.

14-43 (a) Show that the variation of field across the aperture of a paraboloidal reflector with isotropic source is proportional to $1/[1 + (r/2L)^2]$, where r = radial distance from axis of paraboloid and L = focal distance. (b) If the parabola extends to the focal plane and the feed is isotropic over the hemisphere subtended by the parabola, calculate the aperture efficiency.

14-44 The Schmidt telescope employs a spherical reflector with a correcting plate, as in Fig. P14-44. Use the principle of equality of path length to determine the required thickness of the plate as a function of radius.

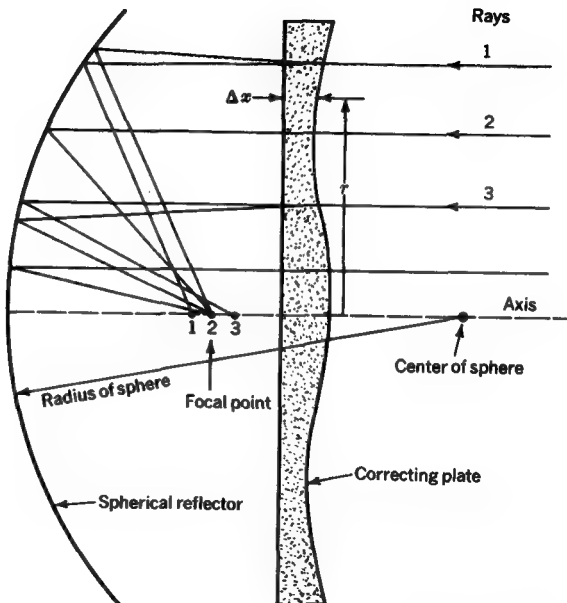


FIGURE P14-44
Schmidt telescope.

14-45 Two $\lambda/2$ -slot antennas, as in Fig. 14-52a, are arranged end to end in a large conducting sheet with a spacing of 1λ between centers. If the slots are fed with equal in-phase voltages, calculate and plot the far-field pattern in the two principal planes. Note that the H plane coincides with the line of the slots.

- * **14-46** The complementary dipole of a slot antenna has a terminal impedance $Z = 90 + j10 \Omega$. If the slot antenna is boxed in so that it radiates only in one half-space, what is the terminal impedance of the slot antenna? The box adds no shunt susceptance at the terminals.
- * **14-47** (a) Determine the length l , width w , and half angles in E and H planes for a pyramidal electromagnetic horn for which the mouth height $h = 8\lambda$. The horn is fed with a rectangular waveguide with TE_{10} mode, as in Fig. 14-53. Take $\delta = \lambda/10$ in the E plane and $\delta = \lambda/4$ in the H plane. (b) What are the HPBWs in both E and H planes? (c) What is the directivity? (d) What is the aperture efficiency?

- * **14-48** A radio link from the moon to the earth has a moon-based 5λ -long right-handed helical-beam antenna (as in Fig. 14-33a) and a 2-W transmitter operating at 1.5 GHz. What should the polarization state and effective aperture be for the earth-based antenna in order to deliver 10^{-14} W to the receiver? Take the earth-moon distance as 1.27 light-seconds.

14-49 (a) Design an earth-based radar system capable of delivering 10^{-15} W of peak echo power from Venus to a receiver. The radar is to operate at 2 GHz, and the same antenna is to be used for both transmitting and receiving. Specify the effective aperture of the antenna and the peak transmitter power. Take the earth-Venus distance as 3 light-minutes, the diameter of Venus as 12.6 Mm, and the radar cross section of Venus as 10 percent of the physical cross section. (b) If the system of (a) is used to observe the moon, what will the received power be? Take the moon diameter as 3.5 Mm and the moon radar cross section as 10 percent of the physical cross section.

14-50 (a) Design a two-way radio link to operate over earth-Mars distances for data transmission at 2.5 GHz with 5 MHz bandwidth. A power of 10^{-19} W Hz $^{-1}$ is to be delivered to the earth receiver and 10^{-17} W Hz $^{-1}$ to the Mars receiver. The Mars antenna must be no larger than 3 m in diameter. Specify effective aperture of Mars and earth antennas and transmitter power (total over entire bandwidth) at each end. Take earth-Mars distance as 6 light-minutes. (b) Repeat (a) for an earth-Jupiter link. Take the earth-Jupiter distance as 40 light-minutes.

14-51 Design a CW doppler radar operating at 30 GHz for measuring the velocity of automobiles at distances up to 1.5 km. The transmitter power is limited to 500 mW, and the receiver requires 10^{-10} W. Specify antenna size and the precision with which frequency shift must be measured in order to achieve velocity measurements accurate to 1 km hr $^{-1}$. Take the radar cross section of an automobile as 30 percent of the physical cross section.

14-52 Consider the three mutually perpendicular rectangular coordinate planes for which $x = 0$, $y = 0$, and $z = 0$ and their intersection at the origin. If three flat conducting sheets are made to intersect in this manner, a three-dimensional square-corner reflector is formed. To distinguish this reflector from a corner reflector with driven element it may be called a *passive square-corner reflector*. (a) Show that a plane wave incident on this passive reflector from any direction within the octant bounded by the planes is reflected back in the same direction (producing retroreflection). (b) Show that if the dimensions of this *retro-reflector* are large compared to the wavelength, the effective scattering aperture equals the physical aperture. (c) Discuss how such a reflector might be used to assist in radar navigation. (d) If an isotropic source were placed on an axis which makes equal angles with the x , y , and z axes of a passive square-corner reflector, could it function effectively as an active antenna? What limitations would there be?

14-53 Consider a collinear array of eight $\lambda/2$ dipole antennas with spacing between dipole centers of $\lambda/2$. Let the dipoles be numbered consecutively 1 through 8. (a) If each dipole pair 1 and 8, 2 and 7, 3 and 6, and 4 and 5 is connected together by an identical transmission line of the same length, show that a plane wave incident on this array will be reflected back in the same direction. This passive retroreflecting antenna is called a *van Atta array*. (b) What limitation is there on the angle of incidence θ of the wave? Measure θ from the broadside direction. (c) What is the effective scattering aperture of this antenna? (d) What is its radar cross section? (e) Discuss how such an antenna might be used to assist in radar navigation. (f) Compare with the passive square-corner reflector of Prob. 14-52. (g) Can elements other than $\lambda/2$ dipoles be used? (h) Can more than eight elements or fewer than eight be used?

- * 14-54 The Ohio State University radio telescope operates at 2,650 MHz with the following parameters: system temperature 150 K, predetection bandwidth 100 MHz, postdetection time constant 5 s, system constant 2.2, and effective aperture of antenna 800 m^2 . Find (a) minimum detectable temperature and (b) minimum detectable flux density. (c) If four records are averaged, what change results in (a) and (b)?

14-55 Design a 30-GHz antenna for an earth-resources observation satellite to measure earth-surface temperatures with 1 km^2 resolution from a 300-km orbital height. Make a drawing of the antenna with dimensions.

14-56 Flux densities of $10^{-20} \text{ W m}^{-2} \text{ Hz}^{-1}$ are commonly received from Jupiter at 20 MHz. What is the power per unit bandwidth radiated at the source? Take the earth-Jupiter distance as 40 light-minutes and assume that the source radiates isotropically.

- * 14-57 Some radio sources have been identified with optical objects and the doppler, or red, shift $z (= \Delta\lambda/\lambda = v/c)$ measured from an optical spectrum. Assume that the objects with larger red shift are more distant, according to the Hubble relation $R = v/H_0$, where R = distance in megaparsecs (1 megaparsec = 1 Mpc = 3.26×10^6 light-years), v = velocity of recession of object in meters per second, and H_0 = Hubble constant = $75 \text{ km s}^{-1} \text{ Mpc}^{-1}$. Determine the distance R to the following radio sources: (a) Cygnus A (prototype radio galaxy), $z = 0.06$, (b) OQ208 (Seyfert galaxy with peaked radio spectrum), $z = 0.08$, and (c) 3C273 (quasi-stellar radio source, or quasar), $z = 0.16$. (d) The above sources have flux densities as follows at 3 GHz: Cygnus A, 600 fu; OQ208, 2 fu; and 3C273, 30 fu ($1 \text{ fu} = 1 \text{ flux unit} = 10^{-26} \text{ W m}^{-2} \text{ Hz}^{-1}$). Determine the power per unit bandwidth radiated at the source. Assume that radiation is isotropic.

- * 14-58 The peak flux density of a pulsar is 25 fu at 150 MHz. The pulsar rate is 30 s^{-1} with pulse duration one-fourth the pulse period. (a) What is the energy density per pulse ($\text{J m}^{-2} \text{ Hz}^{-1}$)? (b) If the pulsar is at a distance of 100 light-years, what is the energy radiated per pulse in a 20-MHz bandwidth? Assume that the source radiates isotropically and that 25 fu is the average flux density over the bandwidth. (c) Assuming that the above radio-frequency radiation is the only energy lost by the pulsar, how long can it radiate at the above rate if it has one solar mass ($= 2 \times 10^{30} \text{ kg}$)? Assume that the pulsar diameter is 25 km and that its kinetic energy of rotation is transformed to radio frequency power with 5 percent efficiency.

14-59 Consider the following four antennas: horizontal $\lambda/2$ dipole, vertical $\lambda/2$ dipole, left-handed 8-turn helical-beam antenna, and right-handed 8-turn helical-beam antenna with four power response P_x , P_y , P_L , and P_R , respectively. All antennas are oriented for maximum response to waves from a distant source. Each antenna can be switched in

	Case							
	1	2	3	4	5	6	7	8
P_x	1	1	0.5	0.5	0.6	0.3	0.5	0.4
P_y	1	0.5	0	0.5	0.4	0.1	0.5	0.5
P_L	20	10	10	20	9	2	15	1
P_R	20	10	10	0	6	8	15	18

turn to a power-measuring unit to which it is properly matched. (a) Determine the Stokes parameters and also the parameters d , AR, and r for eight different cases if the measured power responses to the eight waves are as tabulated above. Take the directivity of each $\lambda/2$ dipole as 1.6 and of each helical-beam antenna as 32. (b) What type of transmitting systems are required to produce waves of these types?

- * 14-60 A center-fed dipole is 150 mm long. The dipole is made of copper wire 1 mm in diameter. How efficient would this dipole be as transmitting antenna at (a) 10 kHz, (b) 1 MHz, (c) 100 MHz, (d) 1 GHz, and (e) 100 GHz? (f) For efficient operation as an antenna how large should a dipole be (measured in wavelengths)? (g) What other factors, aside from efficiency, could restrict its usefulness?

14-61 Prove (14-23-4).

14-62 Show that the terminal impedance of a center-fed linear dipole is twice that for half of the dipole oriented as a stub perpendicular to a ground plane.

- * 14-63 (a) What is the effective aperture of a pocket transistor-radio receiver at 1 MHz? Assume isotropic pattern. (b) At 1 km from a 10-kW 1-MHz broadcast station what power would be available in this aperture? (c) What power is actually required by the receiver (approximately 1 μ V in 300Ω)? (d) What is the antenna efficiency? (e) Would the pocket unit be effective for transmitting at 1 MHz? (f) Would the above considerations be altered appreciably if one used the actual patterns instead of assuming isotropic patterns?

14-64 (a) Use a computer to calculate the field patterns of the following arrays of equal-amplitude isotropic point sources: (1) 10 sources broadside ($\lambda/2$ spacing), (2) 100 sources broadside ($\lambda/2$ spacing), (3) 10 sources ordinary end fire ($\lambda/4$ spacing), and (4) 100 sources end fire ($\lambda/4$ spacing). Plot field patterns through 180° for parts (1) and (2) and through 360° for parts (3) and (4). Use linear scale for field vs. polar (or linear) scale for angle. Also plot one graph in decibel scale for field (in addition to linear scale). A total of five graphs required. (b) Tabulate HPBW, BWFN, directivity D , beam solid angle Ω_A , and effective aperture A_e for all four cases.

- * 14-65 A radio-telescope antenna of 500 m^2 effective aperture is directed at the zenith. Calculate the antenna temperature assuming that the sky temperature is uniform and equal to 10 K. Take the ground temperature equal to 300 K and assume that half the minor-lobe beam area is in the back direction. The wavelength is 200 mm and the beam efficiency is 0.7.

15

PARTICLES AND PLASMAS

15-1 INTRODUCTION

The first part of this chapter treats the motion of nonrelativistic particles in the presence of electric and magnetic fields in vacuum. The effect of a plasma (a cloud of equal positively and negatively charged particles; total charge zero) on the propagation of electromagnetic waves in the presence of a static magnetic field is then considered, and the phenomenon of Faraday rotation is discussed. Finally, a brief treatment is given on magnetohydrodynamic waves (mechanical waves in a dense magnetized plasma).

15-2 CHARGED PARTICLE IN A STATIC ELECTRIC FIELD

Let a particle of charge $e\ddagger$ be placed in a uniform electric field \mathbf{E} . Since \mathbf{E} is the force per unit charge (newtons per coulomb), the force \mathbf{F} on the particle is

$$\mathbf{F} = e\mathbf{E} \quad (1)$$

[†] The symbol e is used in this chapter to designate the charge of a particle (instead of q) since e is usually employed for the charge of a particle, commonly an electron.

The force is in the same direction as the field if the charge is positive and opposite to the field if the charge is negative. If the particle is at rest and the field is applied, the particle is accelerated uniformly in the direction of the field. According to Newton's second law, the force on a particle is related to its mass and acceleration by

$$\mathbf{F} = m\mathbf{a} \quad (2)$$

where \mathbf{F} = force, N

m = mass, kg

\mathbf{a} = acceleration, m s^{-2}

Therefore the acceleration of the particle is

$$\mathbf{a} = \frac{e}{m} \mathbf{E} \quad (3)$$

The velocity v of the particle after a time t is then

$$\mathbf{v} = \mathbf{a}t = \frac{e}{m} \mathbf{E}t \quad (4)$$

where \mathbf{v} = velocity of particle, m s^{-1}

e = charge of particle, C

m = mass of particle, kg

\mathbf{E} = electric field intensity, V m^{-1} or N C^{-1}

t = time, s

The field imparts energy to the charged particle. If (4) is reexpressed as

$$m\mathbf{a} = e\mathbf{E} \quad (5)$$

it has the dimensions of force. Integrating this force over the distance moved yields the energy W acquired. Thus

$$W = m \int_1^2 \mathbf{a} \cdot d\mathbf{l} = -e \int_1^2 \mathbf{E} \cdot d\mathbf{l} \quad (6)$$

The line integral of \mathbf{E} between two points, 1 and 2, may be recognized as the potential difference V between the points. When $\mathbf{a} = dv/dt$ and $d\mathbf{l} = v dt$ are substituted, (6) becomes

$$W = m \int_1^2 \mathbf{v} \cdot d\mathbf{v} = eV \quad (7)$$

or

$$W = \frac{1}{2}m(v_2^2 - v_1^2) = eV \quad (8)$$

where W = energy acquired, J

v_2 = velocity at point 2, or final velocity, m s^{-1}

v_1 = velocity at point 1, or initial velocity, m s^{-1}

e = charge on particle, C

V = potential difference between points 1 and 2, V or J C^{-1}

If the particle starts from rest, the initial velocity is zero; so

$$W = eV = \frac{1}{2}mv^2 \quad (9)$$

where v is the final velocity. Equation (9) has the dimensions of energy. The dimensional relation in SI units is

$$\text{Joules} = \text{coulombs} \times \text{volts} = \text{kilograms} \frac{\text{meters}^2}{\text{seconds}^2}$$

Thus the energy acquired by a particle of charge e starting from rest and passing through a potential drop V is given either by the product of the charge and the potential difference or by one-half the product of the mass of the particle and the square of the final velocity.

Solving (9) for the velocity gives

$$v = \sqrt{\frac{2eV}{m}} \quad (\text{m s}^{-1}) \quad (10)$$

The energy acquired by an electron ($e = 1.6 \times 10^{-19}$ C) in falling through a potential difference of 1 V is 1.6×10^{-19} J. This amount of energy is a convenient unit for designating the energies of particles and is called one *electron volt* (eV).

For an electron $e = 1.6 \times 10^{-19}$ C and $m = 0.91 \times 10^{-30}$ kg, so that (10) becomes

$$v = 5.93 \times 10^5 \sqrt{V} \quad (\text{m s}^{-1}) \quad (11)$$

Thus, if $V = 1$ V, the velocity of the electron is 59 Mm s $^{-1}$, or 590 km s $^{-1}$. It is apparent that a relatively small voltage imparts a very large velocity to an electron. If $V = 2.5$ kV, the velocity is 30 Mm s $^{-1}$, or about one-tenth the velocity of light. The above relations are based on the assumption that the particle velocity is small compared with that of light. The mass of a particle approaches an infinite value as the velocity approaches that of light (relativistic effect), whereas the above relations are based on a constant mass. Actually, however, the mass increase is of negligible consequence for most applications unless the velocity is at least 10 percent that of light. The relation between the mass m of the particle and its mass m_0 at low velocities (rest mass) is given by

$$m = \frac{m_0}{\sqrt{1 - (v/c)^2}} \quad (12)$$

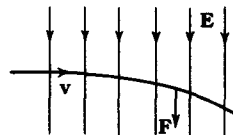


FIGURE 15-1
Path of positively charged particle in electric field.

where v = velocity of particle, m s^{-1}

c = velocity of light = 300 Mm s^{-1}

If the velocity is one-tenth that of light, the mass is only one-half of 1 percent greater than the rest mass.

If the particle has an initial velocity which is not parallel to the field direction, as assumed above, the particle describes a parabolic path (Fig. 15-1). The deflection of an electron by a transverse electric field is discussed in Sec. 15-4.

15-3 CHARGED PARTICLE IN A STATIC MAGNETIC FIELD

From (5-9-3) the force F on a current element of length dl in a magnetic field is

$$d\mathbf{F} = (\mathbf{I} \times \mathbf{B}) dl \quad (\text{N}) \quad (1)$$

where I = current (vector indicating magnitude and direction of current), A

B = magnetic flux density, T

dl = element length, m

This is the fundamental motor equation of electrical machinery. It also applies to moving charged particles in the absence of any metallic conductor.

The current I in a conductor or in a beam of ions or electrons can be expressed in terms of the current density J , the charge (volume) density ρ , the beam area A , and the velocity v by

$$\mathbf{I} = \mathbf{J}A = \rho v A \quad (2)$$

Substituting (2) for I in (1) gives

$$d\mathbf{F} = \rho A dl (\mathbf{v} \times \mathbf{B}) \quad (3)$$

But $\rho A dl = dq$, the charge in a length dl of the beam. Thus

$$d\mathbf{F} = dq (\mathbf{v} \times \mathbf{B}) \quad (4)$$

For a single particle of charge e , we have for the (Lorentz) force

$$\mathbf{F} = e(\mathbf{v} \times \mathbf{B}) \quad (5)$$

Consider now the motion of a particle of charge e in a uniform magnetic field of flux density B . The velocity of the particle is v . From Newton's second law the

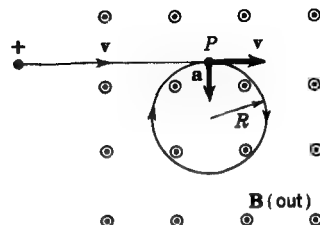


FIGURE 15-2
Path of positively charged particle in magnetic field.

force on the particle is equal to the product of its mass m and its acceleration \mathbf{a} ($= d\mathbf{v}/dt$). Thus

$$m\mathbf{a} = e(\mathbf{v} \times \mathbf{B}) \quad (6)$$

or $\mathbf{a} = \frac{e}{m}(\mathbf{v} \times \mathbf{B}) \quad (7)$

According to (7), the acceleration is normal to the plane containing the particle path and \mathbf{B} . If the direction of the particle path (indicated by \mathbf{v}) is normal to \mathbf{B} , the acceleration is a maximum. If the particle is at rest, the field has no effect. Likewise, if the particle path is in the same direction as \mathbf{B} , there is no effect, the particle continuing undeflected. Only when the path or the velocity \mathbf{v} has a component normal to \mathbf{B} does the field have an effect.

If a magnetic field of large extent is at right angles to the direction of motion of a charged particle, the particle is deflected into a circular path. Suppose that in a field-free region a positively charged particle is moving to the right, as indicated in Fig. 15-2, and that when it reaches the point P a magnetic field is applied. The direction of \mathbf{B} is normal to the page (outward). According to the cross product of \mathbf{v} into \mathbf{B} in (7), the acceleration \mathbf{a} is downward, so that the particle describes a circle in the clockwise direction in the plane of the page.

Radius Let us determine the radius R of the circle. The magnitude of the force \mathbf{F} (radially inward) on the particle is, by (7),

$$\mathbf{F} = m\mathbf{a} = ev\mathbf{B} \quad (8)$$

This force is also given by

$$\mathbf{F} = \frac{mv^2}{R}\mathbf{n} \quad (9)$$

Equating (8) and (9) yields

$$\frac{mv^2}{R} = evB \quad (10)$$

or

$$R = \frac{mv}{eB} \quad (11)$$

where R = radius of particle path, m

m = mass of particle, kg

v = velocity of particle, m s⁻¹

e = charge of particle, C

B = flux density, T

Thus, the larger the velocity of the particle or the larger its mass, the greater the radius. On the other hand, the larger the charge or the flux density, the smaller the radius.

Frequency The number of revolutions per second of the particle in the circular path is called the frequency f [†] of the particle. This frequency is

$$f = \frac{v}{2\pi R} = \frac{eB}{2\pi m} \quad (\text{r s}^{-1}) \quad (12)$$

EXAMPLE An electron has a velocity of 10 km s⁻¹ normal to a magnetic field of 0.1 T flux density. Find the radius of the electron path and also its frequency. (See Table 15-1 or Appendix A-2 for charge and mass of electron.)

SOLUTION From (11) the radius is

$$R = \frac{9.1 \times 10^{-31} \times 10^4}{1.6 \times 10^{-19} \times 10^{-1}} = 569 \text{ nm}$$

This is a very small circle. The frequency is

$$f = \frac{10^4}{2\pi \times 5.7 \times 10^{-7}} = 2.8 \times 10^9 \text{ r s}^{-1}$$

If the particle in the above example had an initial velocity component parallel to \mathbf{B} as well as perpendicular to \mathbf{B} , the particle would move in a helical path with the axis of the helix parallel to \mathbf{B} .

15-4 THE CATHODE-RAY TUBE

A cathode-ray tube (CRT) is a device for observing rapid voltage variations. In a cathode-ray tube (Fig. 15-3) a beam of electrons is emitted from a cathode and accelerated by an electrode A and impinges on a fluorescent screen. By means of either a transverse electric or a transverse magnetic field the beam can be deflected so that it strikes the screen at a distance y from the undeflected position. The spot on the screen is visible, and the particular usefulness of the cathode-ray tube is that, because of the small inertia of the electron beam, it can follow very rapid changes in the applied deflecting field. This is a somewhat oversimplified description of a cathode-ray tube but will suffice for the following brief analysis of some of its characteristics.

[†] This is the same as gyro, or cyclotron, frequency (see Secs. 15-5 and 15-8).

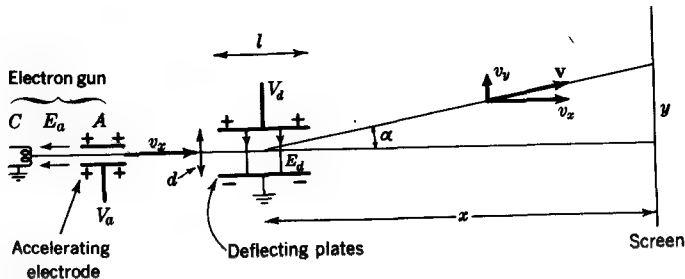


FIGURE 15-3

Cathode-ray tube with electrostatic deflection. Electron fired by electron gun is deflected by electrostatic field between parallel plates.

The positive accelerating potential V_a is applied to the electrode A . This produces an accelerating field E_a that imparts a velocity v_x to the electrons. From (15-2-10)

$$v_x = \sqrt{\frac{2eV_a}{m}} \quad (1)$$

After an electron leaves the accelerating electrode, it maintains this velocity v_x .

Electrostatic deflection For this case let us consider two plates at a potential difference V_d as in Fig. 15-3. The path of an electron in the transverse deflecting field is a parabola. When fringing of the field at the edges of the plates is neglected, the electron is subjected to the deflecting field E_d for a distance l or for a time $t = l/v_x$. The field E_d produces an acceleration a_y in the y direction, which, from (15-2-3), is

$$a_y = \frac{eV_d}{md} \quad (2)$$

Thus, the electron acquires a velocity component v_y in the y direction given by

$$v_y = a_y t = \frac{eV_d}{md} \frac{l}{v_x} \quad (3)$$

The deflection angle α (Fig. 15-3) is then

$$\alpha = \tan^{-1} \frac{v_y}{v_x} = \tan^{-1} \frac{eV_d l}{md v_x^2} \quad (4)$$

or
$$\alpha = \tan^{-1} \frac{V_d l}{2V_a d} \quad (5)$$

But from the tube geometry, assuming $x \gg l$, the angle α is also given by $\alpha = \tan^{-1}(y/x)$; so from this and (5)

$$y = \frac{V_d l x}{2V_a d} \quad (\text{m}) \quad (6)$$

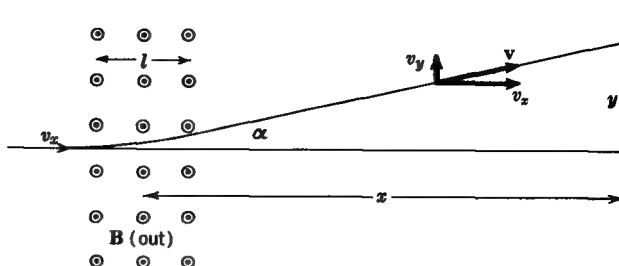


FIGURE 15-4
Cathode-ray tube with magnetic deflection.

where $y = \text{deflection distance at screen, m}$

V_d = deflecting potential, V

l = length of deflecting plates, m

x = distance from deflecting plates to screen, m

V_a = accelerating potential, V

d = spacing of deflecting plates, m

Solving for the volts per meter of deflection (ratio V_d/y), we have

$$\frac{V_d}{y} = \frac{2V_a d}{lx} \quad (\text{V m}^{-1}) \quad (7)$$

EXAMPLE 1 A cathode-ray tube with electrostatic deflection has an accelerating voltage $V_a = 1.5$ kV, a deflecting-plate spacing $d = 10$ mm, a deflecting-plate length $l = 10$ mm, and a distance $x = 300$ mm from deflecting plates to the screen. Find the voltage V_d required to deflect the spot by 10 mm on the screen. Neglect fringing of the field.

SOLUTION From (7)

$$\frac{V_d}{y} = \frac{2 \times 1,500 \times 10^{-2}}{10^{-2} \times 30 \times 10^{-2}} = 10 \text{ kV m}^{-1}$$

or

$$\frac{V_d}{y} = 10 \text{ V mm}^{-1}$$

To increase the sensitivity, i.e., to decrease the number of volts per meter of deflection, V_a or d should be decreased or an increase made in l or x .

Magnetic deflection For this case let the deflecting plates and electric field E_d of Fig. 15-3 be replaced by a magnetic field of flux density \mathbf{B} normal to the page as in Fig. 15-4. The direction of \mathbf{B} is outward from the page.

Now for this case the acceleration due to the magnetic field is not in the y direction but is normal to the circular path of the electron. Assume, however, that l is so

small that as an approximation the acceleration can be taken in the y direction. Then the velocity component in the y direction is

$$v_y = a_y t = a_y \frac{l}{v_x} \quad (8)$$

Thus from (15-3-7)

$$v_y = \frac{ev_x B}{m} \frac{l}{v_x} = \frac{eBl}{m} \quad (9)$$

The deflection angle α (Fig. 15-4) is

$$\alpha = \tan^{-1} \frac{v_y}{v_x} = \tan^{-1} \frac{eBl}{v_x m} = \tan^{-1} \left(Bl \sqrt{\frac{e}{2mV_a}} \right) \quad (10)$$

But we have also $\alpha = \tan^{-1}(y/x)$, and so

$$y = xBl \sqrt{\frac{e}{2mV_a}} \quad (\text{m}) \quad (11)$$

where y = deflection distance at screen, m

x = distance from magnetic deflecting field to screen, m

B = flux density of deflecting field, T

e = charge on particle, C

m = mass of particle, kg

V_a = accelerating voltage, V

l = axial length of deflecting field, m

Solving for the flux density per meter of deflection (ratio B/y), we have

$$\frac{B}{y} = \frac{1}{xl} \sqrt{\frac{2mV_a}{e}} \quad (12)$$

where the ratio B/y is in teslas per meter of deflection. For an electron (12) becomes

$$\frac{B}{y} = \frac{3.38 \times 10^{-6}}{xl} \sqrt{V_a} \quad (13)$$

where x = distance from deflecting field to screen, m

l = axial length of deflecting field, m

V_a = accelerating voltage, V

EXAMPLE 2 A cathode-ray tube with magnetic deflection has an accelerating voltage $V_a = 1.5$ kV, a magnetic deflecting field axial length $l = 20$ mm, and a distance $x = 300$ mm

from the deflecting field to the screen. Find the magnetic field flux density B required to deflect the spot of an electron beam 1 mm on the screen.

SOLUTION From (13)

$$\frac{B}{y} = \frac{3.38 \times 10^{-6} \times 1,500^{1/2}}{3.0 \times 10^{-1} \times 2 \times 10^{-2}} = 21.8 \text{ mT m}^{-1}$$

15-5 THE CYCLOTRON

The cyclotron is a heavy-particle accelerator, invented in 1929 by Ernest O. Lawrence, for obtaining a beam of high-energy ions. Particles such as protons, deuterons, or alpha particles are given multiple accelerations in a resonance chamber. Referring to Fig. 15-5, two hollow D-shaped copper electrodes, or *dees*, are between the pole

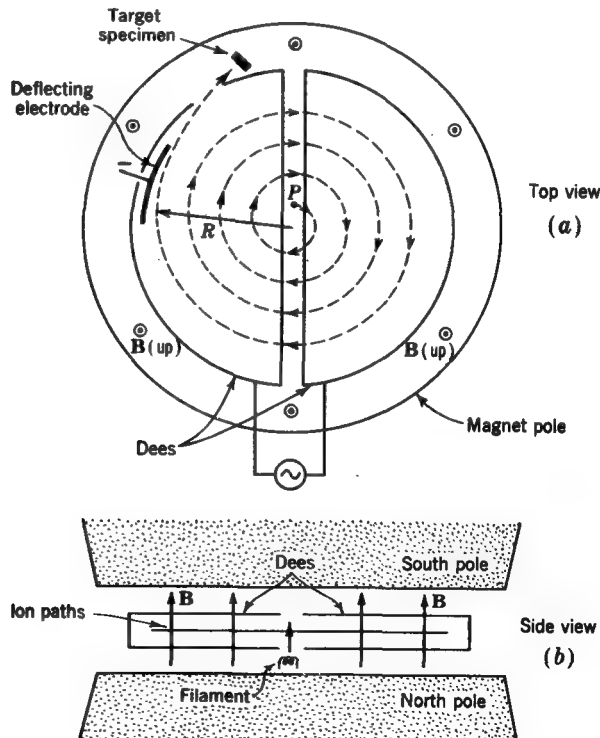


FIGURE 15-5
Cyclotron.

pieces of a large electromagnet. The region between the pole pieces is evacuated. In Fig. 15-5 the walls of the vacuum chamber are omitted. The two dees are connected to a high-frequency source of alternating voltage. In the case of deuteron operation, ions in heavy-hydrogen gas at low pressure are produced at the center of the chamber by electrons emitted from a filament.

Starting with a deuteron at the point *P*, a negative potential on the right-hand dee accelerates the deuteron to the right. Entering the dee, the deuteron is in a region free of electric field but still in the magnetic field between the pole pieces. Suppose that the lower pole is a north pole so that *B* is upward. The deuteron then moves in a circle in a clockwise direction. If the timing is proper, so that when the deuteron again reaches the gap between the dees the electric field has reversed, it will be accelerated to the left. Having acquired additional energy, it moves in a circle of larger radius. By repetition of this process the energy of the deuteron is increased in steps until it reaches the periphery of the dees. Here a deflecting electrode at a high negative potential pulls the deuteron through an opening in the dee so that it can impinge on a specimen placed outside the dee.

The frequency in revolutions per second of a particle moving normal to the magnetic field in a cyclotron is given by (15-3-12), i.e.,

$$f = \frac{eB}{2\pi m} \quad (1)$$

Provided the particle velocity is small compared with light, *m* is substantially constant. Since *e* and *B* are also constant, *f* is a constant regardless of the velocity of the particle. However, from (15-3-11) the radius of the circular path is proportional to the particle velocity.

EXAMPLE 1 Find the frequency for a deuteron ($e = 1.6 \times 10^{-19}$ C, $m = 3.34 \times 10^{-27}$ kg) in a cyclotron with a flux density $B = 1.5$ T.

SOLUTION From (1) the frequency is

$$f = \frac{1.6 \times 10^{-19} \times 1.5}{2\pi \times 3.34 \times 10^{-27}} = 1.14 \times 10^7 \text{ r s}^{-1}$$

This is the frequency required of the oscillator connected to the dees. Accordingly, the oscillator frequency must be 11.4 MHz for accelerating deuterons.

The final energy of a particle is determined by the radius *R* and the flux density *B*. From (15-3-11)

$$R = \frac{mv}{eB} \quad \text{or} \quad v = \frac{ReB}{m} \quad (2)$$

The energy W of the particle is

$$W = \frac{1}{2}mv^2 \quad \text{or} \quad v = \sqrt{\frac{2W}{m}} \quad (3)$$

Equating these relations for v and solving for the energy W of the particle yields

$$W = \frac{1}{2} \frac{(ReB)^2}{m} \quad (4)$$

EXAMPLE 2 A cyclotron has a maximum working radius $R = 500$ mm and a flux density $B = 1.5$ T. Find the energy which can be imparted to deuterons.

SOLUTION From (4) the final energy is

$$W = \frac{(0.5 \times 1.6 \times 10^{-19} \times 1.5)^2}{2 \times 3.34 \times 10^{-27}} = 2.16 \text{ pJ}$$

Since

$$\text{Energy in electron volts} = \frac{\text{energy in joules}}{1.6 \times 10^{-19}}$$

this result in electron volts is

$$W_{\text{eV}} = \frac{2.16 \times 10^{-12}}{1.6 \times 10^{-19}} = 1.35 \times 10^7 \text{ eV}$$

or an energy of 13.5 MeV.

If the voltage V applied between the gap of the dees is small, a large number n of revolutions is required before the particle reaches the periphery. However, to reduce the dispersion of the beam it is desirable to make n small and hence V as large as possible. The total energy W acquired in n revolutions is $W = 2nVe$. Thus, for a given energy W as determined by (4) and for a particular voltage V , the number of revolutions is

$$n = \frac{W}{2eV} \quad (r) \quad (5)$$

where W is in joules. If the energy is expressed in electron volts W_{eV} ,

$$n = \frac{W_{\text{eV}}}{2eV} \times 1.6 \times 10^{-19} \quad (r) \quad (6)$$

where e = charge of particle, C

V = dee voltage, V

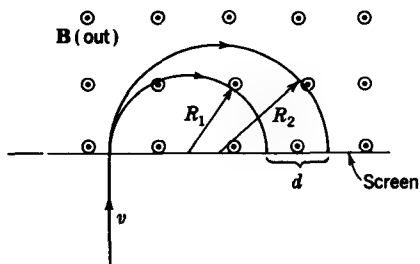


FIGURE 15-6
Mass spectrograph.

15-6 THE MASS SPECTROGRAPH

A mass spectrograph is a device for separating particles of the same charge but different mass. Referring to Fig. 15-6, the particles are injected with a known velocity v into a uniform magnetic field of flux density B . Particles with larger mass strike the fluorescent screen or photographic plate at a greater distance from the point of entry, as suggested. It can be shown that two particles of the same charge e and of masses m_1 and m_2 injected with the same velocity v are separated at the screen by a distance d given by

$$d = \frac{2v/Be}{m_2 - m_1} \quad (1)$$

where $m_2 > m_1$.

15-7 TABLE OF CHARGE AND MASS FOR COMMON PARTICLES

The charge and mass for a number of common particles are listed in Table 15-1. The mass given is the rest mass, or mass at zero velocity.

Table 15-1 CHARGE AND MASS OF PARTICLES

Particle	Charge e , C	Mass m , kg	Ratio e/m , C kg $^{-1}$
Electron	-1.602×10^{-19}	9.11×10^{-31}	-1.76×10^{11}
Positron	$+1.602 \times 10^{-19}$	9.11×10^{-31}	$+1.76 \times 10^{11}$
Neutron	0	1.6747×10^{-27}	0
Proton (hydrogen nucleus)	$+1.602 \times 10^{-19}$	1.6725×10^{-27}	$+9.6 \times 10^7$
Deuteron (heavy-hydrogen nucleus)	$+1.6 \times 10^{-19}$	3.34×10^{-27}	$+4.8 \times 10^7$
Alpha particle (helium nucleus)	$+3.2 \times 10^{-19}$	6.644×10^{-27}	$+4.81 \times 10^7$

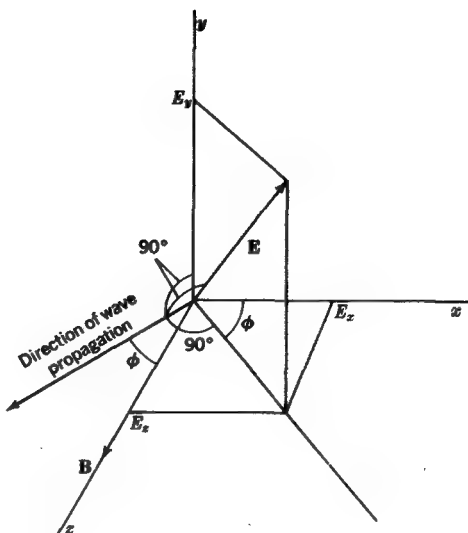


FIGURE 15-7

Relation of direction of wave propagation to coordinate system. The direction of wave propagation is in the xz plane at an angle ϕ with respect to the z axis. The electric field E of the wave lies in a plane perpendicular to the direction of wave propagation. A steady magnetic field B is in the z direction.

15-8 PLANE WAVES IN AN IONIZED MEDIUM IN THE PRESENCE OF A MAGNETIC FIELD†

In Chap. 10 wave propagation in lossless and conducting media was discussed. Although an ionized medium may be classified as a conducting medium, the condition $\sigma \gg \omega\epsilon$ assumed in Chap. 10 may not apply. Furthermore, an ionized medium becomes anisotropic (propagation variable as a function of direction) in the presence of a steady magnetic field. This greatly complicates the situation compared with that considered in Chap. 10, where the medium was assumed to be isotropic (propagation same in all directions). Consequently, a more general development will now be made for a plane wave in an ionized medium in the presence of a steady magnetic field.

The medium to be considered is a *plasma*; i.e., it consists of equal positive and negative charges (total charge zero) but would be described as *cool* (thermal energies small) and *tenuous* (collisions unimportant). In such a plasma only the interaction of the negative charges (electrons) with the wave will be considered, the positive ions being too massive to interact appreciably.

Referring to Fig. 15-7, it will be assumed that the steady magnetic flux density B is in the z direction; that is, $|B| = B_z$. This simplifies the analysis without any loss

† This section and Secs. 15-9 and 15-10 are adapted from sec. 5-4 of J. D. Kraus, "Radio Astronomy," McGraw-Hill Book Company, New York, 1966. The straightforwardness of the development of this section is due to Prof. R. G. Kouyoumjian, Lecture Notes for Electromagnetics Course, Ohio State University.

of generality. The direction of propagation of the wave is taken in the xz plane with the angle between this direction and the z axis equal to ϕ . The electric field \mathbf{E} associated with the wave may have any orientation perpendicular to the direction of propagation, i.e., may be polarized in any manner.

The force equations involving a charged particle of charge e and mass m in the presence of a wave and magnetic flux density \mathbf{B} are

$$\boxed{\mathbf{F}_m = e(\mathbf{v} \times \mathbf{B})} \quad (1)$$

$$\boxed{\mathbf{F}_e = e\mathbf{E}} \quad (2)$$

$$\boxed{\mathbf{F} = m\mathbf{a} = m \frac{d\mathbf{v}}{dt}} \quad (3)$$

where \mathbf{F} = total force, N

\mathbf{F}_m = magnetic force, N

\mathbf{F}_e = electric force, N

e = charge of particle, C

m = mass of particle, kg

\mathbf{v} = velocity of particle due to the wave, m s⁻¹

\mathbf{B} = steady magnetic field, T

\mathbf{E} = electric field of wave, V m⁻¹

\mathbf{a} = acceleration of particle, m s⁻²

t = time, s

In (3) (Newton's second law) it is assumed that the velocity is small compared to the velocity of light; i.e., relativistic effects are neglected.†

Combining the force relations [(3) equals (1) plus (2)] gives

$$\mathbf{F} = e(\mathbf{E} + \mathbf{v} \times \mathbf{B}) = m \frac{d\mathbf{v}}{dt} \quad (4)$$

Dividing by e to obtain the force per unit charge yields

$$\frac{\mathbf{F}}{e} = \mathbf{E} + \mathbf{v} \times \mathbf{B} = \frac{m}{e} \frac{d\mathbf{v}}{dt} \quad (5)$$

† A more general statement of (3) is

$$\mathbf{F} = \frac{d(m\mathbf{v})}{dt} = m \frac{d\mathbf{v}}{dt} + \mathbf{v} \frac{dm}{dt} \quad (3a)$$

where $m\mathbf{v}$ is the momentum of the particle. For $v \ll c$, $dm/dt = 0$; so (3a) reduces to (3).

Expressing this vector equation in terms of its three (rectangular) scalar components, we have

$$\frac{F_x}{e} = E_x + v_y B_z = \frac{m}{e} \frac{dv_x}{dt} \quad (6)$$

$$\frac{F_y}{e} = E_y - v_x B_z = \frac{m}{e} \frac{dv_y}{dt} \quad (7)$$

$$\frac{F_z}{e} = E_z = \frac{m}{e} \frac{dv_z}{dt} \quad (8)$$

Assuming harmonic motion of the wave and charged particle and solving for its component velocities, we have

$$v_x = \frac{j(m\omega/e)E_x + B_z E_y}{B_z^2 - (m^2\omega^2/e^2)} \quad (9)$$

$$v_y = \frac{j(m\omega/e)E_y - E_x B_z}{B_z^2 - (m^2\omega^2/e^2)} \quad (10)$$

$$v_z = \frac{-jeE_z}{m\omega} \quad (11)$$

where ω = radian or angular frequency = $2\pi f$, rad s⁻¹

f = frequency, Hz

From these relations it can be inferred that the wave will cause the charged particle to move in a helical path with axis coincident with the magnetic field (z direction). For the condition

$$B_z^2 = \frac{m^2\omega^2}{e^2} \quad (12)$$

v_x and v_y become infinite, indicating a strong interaction of the wave with the particles at this frequency.[†] This corresponds to *gyro resonance*. Calling the radian frequency at which this occurs ω_g , we have

$$\omega_g = \frac{e}{m} B_z \quad (13)$$

where ω_g is the (radian) gyro frequency (= $2\pi f$, rad s⁻¹).

[†] The effect of collisions between particles is neglected.

This is the resonance condition in a cyclotron (Sec. 15-5), and for this reason ω_g is also called the *cyclotron (radian) frequency*. Introducing (13) into (9) and (10) yields

$$v_x = \frac{e}{m} \frac{\omega_g E_y + j\omega E_x}{\omega_g^2 - \omega^2} \quad (14)$$

$$v_y = \frac{e}{m} \frac{-\omega_g E_x + j\omega E_y}{\omega_g^2 - \omega^2} \quad (15)$$

From Maxwell's equation we have

$$\nabla \times \mathbf{H} = \mathbf{J} + j\omega \mathbf{D} = N e v + j\omega \epsilon_0 \mathbf{E} \quad (16)$$

where N is the number of charged particles per unit volume. It is assumed that a movement of the charged particles constitutes a conduction current. Expressing (16) in terms of its three rectangular components, we have

$$(\nabla \times \mathbf{H})_x = j\omega \epsilon_0 E_x + N e v_x \quad (17)$$

$$(\nabla \times \mathbf{H})_y = j\omega \epsilon_0 E_y + N e v_y \quad (18)$$

$$(\nabla \times \mathbf{H})_z = j\omega \epsilon_0 E_z + N e v_z \quad (19)$$

Introducing the values of v_x , v_y , and v_z from (14), (15), and (11) into these relations, we obtain

$$(\nabla \times \mathbf{H})_x = j\omega \epsilon_0 E_x \left[1 + \frac{N e^2}{\epsilon_0 m (\omega_g^2 - \omega^2)} \right] + \frac{N e^2 \omega_g E_y}{m (\omega_g^2 - \omega^2)} \quad (20)$$

$$(\nabla \times \mathbf{H})_y = -\frac{N e^2 \omega_g E_x}{m (\omega_g^2 - \omega^2)} + j\omega \epsilon_0 E_y \left[1 + \frac{N e^2}{\epsilon_0 m (\omega_g^2 - \omega^2)} \right] \quad (21)$$

$$(\nabla \times \mathbf{H})_z = j\omega \epsilon_0 E_z \left(1 - \frac{N e^2}{\epsilon_0 m \omega^2} \right) \quad (22)$$

If the frequency is much greater than the gyro frequency ($\omega \gg \omega_g$), all three relations become identical in form. Further, if

$$\frac{N e^2}{\epsilon_0 m \omega^2} = 1 \quad (23)$$

a *critical, or plasma, frequency* occurs, for which the permittivity and the index of refraction of the medium become zero. Designating the critical frequency as ω_0 ($= 2\pi f_0$), we have

$$\omega_0^2 = \frac{N e^2}{\epsilon_0 m} \quad (24)$$

or

$$f_0 = \frac{e}{2\pi} \sqrt{\frac{N}{\epsilon_0 m}} \quad (25)$$

where ω_0 = critical radian frequency = $2\pi f_0$, rad s⁻¹

f_0 = critical frequency, Hz

N = density of charged particles, number m⁻³

e = charge of particle, C

m = mass of particle, kg

ϵ_0 = permittivity of medium = 8.85 pF m⁻¹

For an electron (25) becomes

$$f_0 = 9\sqrt{N} \quad (26)$$

where f_0 = critical frequency, Hz

N = electron density, number m⁻³

At or below the critical frequency the wave is totally reflected by the medium. A typical value of N for the earth's ionosphere is about 10^{12} electrons per cubic meter, which from (26) corresponds to a critical frequency of 9 MHz.

Introducing (24) into (20) to (22), we may write in general, that†

$$\nabla \times \mathbf{H} = j\omega\bar{\epsilon} \cdot \mathbf{E} \quad (27)$$

where $\bar{\epsilon}$ is the tensor permittivity, or

$$\bar{\epsilon} = \begin{bmatrix} \epsilon_{11} & -j\epsilon_{12} & \epsilon_{13} \\ j\epsilon_{21} & \epsilon_{22} & \epsilon_{23} \\ \epsilon_{31} & \epsilon_{32} & \epsilon_{33} \end{bmatrix} \quad (28)$$

$$\text{or } \bar{\epsilon} = \begin{bmatrix} \left(1 + \frac{\omega_0^2}{\omega_g^2 - \omega^2}\right)\epsilon_0 & \frac{-j\omega_0^2\omega_g\epsilon_0}{\omega(\omega_g^2 - \omega^2)} & 0 \\ \frac{j\omega_0^2\omega_g\epsilon_0}{\omega(\omega_g^2 - \omega^2)} & \left(1 + \frac{\omega_0^2}{\omega_g^2 - \omega^2}\right)\epsilon_0 & 0 \\ 0 & 0 & \left(1 - \frac{\omega_0^2}{\omega^2}\right)\epsilon_0 \end{bmatrix} \quad (29)$$

† From $\nabla \times \mathbf{H} = \sigma\mathbf{E} + j\omega\epsilon_0\mathbf{E}$ we could write $\nabla \times \mathbf{H} = \bar{\sigma} \cdot \mathbf{E}$, describing the medium in terms of an effective tensor conductivity $\bar{\sigma}$, or we can write $\nabla \times \mathbf{H} = j\omega\bar{\epsilon} \cdot \mathbf{E}$, describing the medium in terms of an effective tensor permittivity $\bar{\epsilon}$. In the present instance, the latter procedure has been chosen, as given by (27).

Equation (29) has the form of a skew-symmetric tensor (elements symmetrical about main diagonal, upper left to lower right, but signs reversed). In the absence of a magnetic field ($\mathbf{B} = 0$) or where $\omega \gg \omega_0$, (29) reduces to

$$\bar{\epsilon} = \begin{bmatrix} \left(1 - \frac{\omega_0^2}{\omega^2}\right)\epsilon_0 & 0 & 0 \\ 0 & \left(1 - \frac{\omega_0^2}{\omega^2}\right)\epsilon_0 & 0 \\ 0 & 0 & \left(1 - \frac{\omega_0^2}{\omega^2}\right)\epsilon_0 \end{bmatrix} = \epsilon \quad (30)$$

where

$$\epsilon = \left(1 - \frac{\omega_0^2}{\omega^2}\right)\epsilon_0 = \epsilon_r \epsilon_0 \quad (31)$$

and

$$\nabla \times \mathbf{H} = j\omega \left(1 - \frac{\omega_0^2}{\omega^2}\right)\epsilon_0 \mathbf{E} \quad (32)$$

The quantity $1 - (\omega_0^2/\omega^2)$ is equivalent to the relative permittivity ϵ_r of the medium. The index of refraction is then

$$\eta = \sqrt{\epsilon_r} = \sqrt{1 - \left(\frac{\omega_0}{\omega}\right)^2} = \sqrt{1 - \left(\frac{f_0}{f}\right)^2} \quad (33)$$

When $f > f_0$, the index of refraction is real and the wave is propagated. However, η is less than unity, so that refraction is opposite to that which occurs when waves enter a denser medium. When $f < f_0$, the index of refraction is imaginary and the wave is not propagated but reflected.

When a cloud of charged particles is perturbed, it may tend to oscillate at the plasma frequency. Certain types of radiation from the solar atmosphere or corona are believed to be due to such plasma oscillations. The electron density in the solar corona decreases with height, and from (26) the plasma frequency will also decrease. Hence, at a given frequency f , radiation is received on the earth only from the corona at heights above the height for which $f = f_0$. Actually the radiation appears to come mostly from a relatively thin layer just above the height for which $f = f_0$.

These comments apply to the quiet sun. When disturbances on the sun, such as flares, occur, more dynamic phenomena may be involved, in which high-velocity jets or shock waves rise into the solar corona. Plasma oscillations of electron clouds excited by such mechanisms appear to be responsible for relatively narrow-band radiation, which drifts downward in frequency as the disturbance rises through the corona into regions of lower electron density.

Returning to the general situation (with $\mathbf{B} \neq 0$), let us take the curl of

$$\nabla \times \mathbf{E} = -j\omega\mu\mathbf{H} \quad (34)$$

for the case $\mu = \mu_0$ (ferromagnetic effects assumed negligible) and introduce $\nabla \times \mathbf{H}$ from (27) so that we have

$$\nabla \times \nabla \times \mathbf{E} = \omega^2 \mu_0 \bar{\epsilon} \cdot \mathbf{E} \quad (35)$$

This is a wave equation in \mathbf{E} . Neglecting the effect of collisions (attenuation assumed zero), let a solution be assumed of the form

$$\mathbf{E} = \mathbf{E}_0 e^{j(\omega t - \beta r)} \quad (36)$$

where β = phase constant (in r direction)

r = distance measured in direction of wave propagation (see Fig. 15-7)

It is left as an exercise (straightforward but tedious) to show that (36) is a solution provided

$$\beta^2 = \omega^2 \mu_0 \{ (\epsilon_{11}^2 - \epsilon_{12}^2 - \epsilon_{11}\epsilon_{33}) \sin^2 \phi + 2\epsilon_{11}\epsilon_{33} \pm [(\epsilon_{11}^2 - \epsilon_{12}^2 - \epsilon_{11}\epsilon_{33})^2 \sin^4 \phi + 4\epsilon_{12}^2 \epsilon_{33}^2 \cos^2 \phi]^{1/2} \} / 2[(\epsilon_{11} - \epsilon_{33}) \sin^2 \phi + \epsilon_{33}] \quad (37)$$

where ϕ is the angle between \mathbf{B} (or z) and wave direction (see Fig. 15-7), and where ϵ_{11} , ϵ_{12} , etc., are as given by comparing (28) and (29). When ω is much larger than ω_g , so that $\epsilon_{11} \approx \epsilon_{33}$, but not so large that ϵ_{12} (or ϵ_{21}) can be neglected, (37) reduces to

$$\beta^2 = \omega^2 \mu_0 \epsilon_{11} \left\{ 1 - \frac{\epsilon_{12}^2}{2\epsilon_{11}^2} \left[\sin^2 \phi \pm \sqrt{\sin^4 \phi + \left(\frac{2\epsilon_{11} \cos \phi}{\epsilon_{12}} \right)^2} \right] \right\} \quad (38)$$

When the wave propagates parallel to the magnetic field ($\phi = 0$), the condition is called *longitudinal propagation* and (38) reduces for this case to

$$\boxed{\beta = \omega \sqrt{\mu_0 (\epsilon_{11} \pm \epsilon_{12})}} \quad (39)$$

From (39) it can be shown that the wave may consist of two circularly polarized components of opposite sense of rotation.

When the wave propagates perpendicular to \mathbf{B} ($\phi = 90^\circ$), the condition is called *transverse propagation* and (38) reduces for this case to

$$\boxed{\beta = \omega \sqrt{\mu_0 \left(\epsilon_{12} - \frac{\epsilon_{12}^2}{\epsilon_{11}} \right)}} \quad (40)$$

when the electric field \mathbf{E} of the wave is linearly polarized *perpendicular to \mathbf{B}* and to

$$\boxed{\beta = \omega \sqrt{\mu_0 \epsilon_{33}}} \quad (41)$$

when \mathbf{E} is *parallel to \mathbf{B}* . In this latter case propagation is the same as though no magnetic field were present. This wave is sometimes referred to as the *ordinary ray*, while in the case described by (40), where \mathbf{E} is perpendicular to \mathbf{B} , the wave is referred to as the *extraordinary ray*.

More general relations than the above can be deduced for *quasi-longitudinal* and *quasi-transverse* conditions of propagation. For the former case, ϕ is considered small enough to permit $\sin^2 \phi$ and $\sin^4 \phi$ terms to be neglected although $\cos \phi$ is not unity. For the latter case ϕ is considered to be sufficiently near 90° to allow $\cos \phi$ terms to be neglected. We then have for the *quasi-longitudinal* case that

$$\boxed{\beta = \omega \sqrt{\mu_0(\epsilon_{11} \pm \epsilon_{12} \cos \phi)}} \quad (42)$$

and for the *quasi-transverse* case that

$$\boxed{\beta = \omega \sqrt{\mu_0 \left[\epsilon_{11} - (1 \pm 1) \frac{\epsilon_{12}^2}{2\epsilon_{11}} \sin \phi \right]}} \quad (43)$$

These propagation relations are summarized in Table 15-2.

Table 15-2 PROPAGATION RELATIONS†

Quasi-longitudinal propagation (ϕ small)	$\beta = \omega \sqrt{\mu_0(\epsilon_{11} \pm \epsilon_{12} \cos \phi)}$
Quasi-transverse propagation (ϕ near 90°)	$\beta = \omega \sqrt{\mu_0 \left[\epsilon_{11} - (1 \pm 1) \frac{\epsilon_{12}^2}{2\epsilon_{11}} \sin \phi \right]}$
Longitudinal propagation (\parallel to \mathbf{B} ; $\phi = 0$)	$\beta = \omega \sqrt{\mu_0(\epsilon_{11} \pm \epsilon_{12})}$
Transverse propagation (\perp to \mathbf{B} ; $\phi = 90^\circ$)	
Ordinary ray: $\mathbf{E} \parallel \mathbf{B}$	$\beta = \omega \sqrt{\mu_0 \epsilon_{11}}$
Extraordinary ray: $\mathbf{E} \perp \mathbf{B}$	$\beta = \omega \sqrt{\mu_0 \left(\epsilon_{11} - \frac{\epsilon_{12}^2}{\epsilon_{11}} \right)}$

† See text for assumptions involved.

Note: $\epsilon_{11} = \{1 + [\omega_0^2 / (\omega_g^2 - \omega^2)]\} \epsilon_0$

$\epsilon_{12} = \omega_0 \omega_g^2 \epsilon_0 / (\omega(\omega_g^2 - \omega^2))$

ω = radian frequency of wave = $2\pi f$, rad s⁻¹, where f = frequency of wave, Hz

ω_g = radian gyro frequency = $(e/m)/B$

ω_0 = radian plasma frequency = $e\sqrt{N/\epsilon_0 m}$

B = magnetic flux density, T

e = charge on particle, C

m = mass of particle, kg

ϵ_0 = permittivity of vacuum = 8.85 pF m⁻¹

β = phase constant = $2\pi/\lambda$

λ = wavelength, m

μ_0 = permeability of vacuum = 400π nH m⁻¹

ϕ = angle between wave direction and magnetic field \mathbf{B}

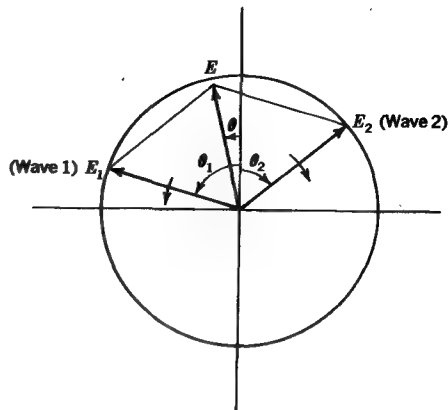


FIGURE 15-8

Resolution of linearly polarized wave into two circularly polarized waves (1 and 2) of opposite rotation direction.

15-9 FARADAY ROTATION†

A linearly polarized wave may be regarded as the resultant of two circularly polarized waves of equal amplitude and opposite sense of rotation (see Chap. 11). If the two circularly polarized waves have different phase constants, the plane of polarization of the resultant linearly polarized wave rotates as the wave propagates. Thus, consider two circularly polarized waves traveling out of the page, as in Fig. 15-8 for the quasi-longitudinal case (ϕ small). The elemental angular rotation of one wave is given by

$$d\theta_1 = \beta^- dr \quad (1)$$

and of the other wave by

$$d\theta_2 = \beta^+ dr \quad (2)$$

where dr is the elemental propagation distance perpendicular to the page, and where β^- and β^+ are as given by (15-8-42) for the cases where the sign in the parentheses is $-$ and $+$, respectively.

Now from Fig. 15-8

$$\tan \theta = \frac{E_1 \sin \theta_1 - E_2 \sin \theta_2}{E_1 \cos \theta_1 + E_2 \cos \theta_2} \quad (3)$$

Now assuming $E_1 = E_2$ we have

$$\tan \theta = \frac{\sin \theta_1 - \sin \theta_2}{\cos \theta_1 + \cos \theta_2} \quad (4)$$

† The name derives from Faraday's early investigations of the phenomenon, in which he observed the rotation of the plane of polarization of light passing through a crystal with an applied magnetic field.

from which

$$\tan \theta = \tan \frac{\theta_1 - \theta_2}{2} \quad (5)$$

and the resultant rotation angle is then

$$\theta = \frac{\theta_1 - \theta_2}{2} \quad (6)$$

and from (1) and (2)

$$d\theta = \frac{\beta^- - \beta^+}{2} dr \quad (7)$$

Introducing (15-8-42) and the values of ϵ_{11} and ϵ_{12} from (15-8-28) and (15-8-29) for $\omega \gg \omega_g$, $\omega \gg \omega_0$, and small ϕ , we obtain approximately that

$$d\theta = \frac{Ne^3 B \lambda^2 \cos \phi dr}{8\pi^2 c^3 \epsilon_0 m^2} \quad (\text{rad}) \quad (8)$$

The total *Faraday rotation* for the *quasi-longitudinal case* (ϕ small) is then

$$\theta = \frac{e^3 \lambda^2}{8\pi^2 c^3 \epsilon_0 m^2} \int_0^r N B \cos \phi dr \quad (\text{rad}) \quad (9)$$

where e = charge of particle, C

m = mass of particle, kg

$\omega = 2\pi f$ = radian frequency, rad s⁻¹

ϵ_0 = permittivity of vacuum = 8.85 pF m⁻¹

c = velocity of light = 300 Mm s⁻¹

N = particle density, number m⁻³

B = magnetic flux density, T

ϕ = angle between \mathbf{B} and direction of wave propagation, rad or deg

r = distance in direction of propagation, m

If B and ϕ are constant, (9) becomes

$$\theta = \frac{e^3 B \lambda^2 \cos \phi}{8\pi^2 c^3 \epsilon_0 m^2} \int_0^r N dr \quad (\text{rad}) \quad (10)$$

If B and ϕ are known, a measurement of ϕ at a wavelength λ permits a determination of the total number of charged particles in a column 1 m² between the source and observer given by

$$N_t = \int_0^r N dr \quad (11)$$

where N_t is total number of particles in a column of length r and cross section of 1 m².

For the *quasi-transverse case* (ϕ near 90°) we have

$$d\theta = \frac{Ne^4\lambda^3 B^2 \sin^2 \phi dr}{32\pi^3 c^4 m^3 \epsilon_0} \quad (\text{rad}) \quad (12)$$

and for the *total Faraday rotation*

$$\theta = \frac{e^4 \lambda^3}{32\pi^3 c^4 m^3 \epsilon_0} \int_0^r NB^2 \sin^2 \phi dr \quad (\text{rad}) \quad (13)$$

where the symbols are as listed following (9).

Equations (9) and (13) give the angle by which a linearly-polarized wave is rotated during its passage through a magnetized plasma for the two cases, ϕ small and ϕ near 90° .

In radio-astronomy observations of the polarization of radio sources, the *position angle* θ of the electric field vector of the linearly polarized component of the radiation is usually measured relative to north with θ increasing counterclockwise, or to the east. Since the position angle of the electric field vector varies as the square of the wavelength [see (9)], a θ -vs.- λ^2 graph should show a straight-line relationship over a range of wavelengths. By extrapolating the straight line to zero wavelength the *polarization angle at the source*, or *intrinsic polarization*, can be determined. The slope of the line ($=\theta/\lambda^2$) has been called the *rotation measure*. The rotation measure is positive when the magnetic field direction is toward the observer. There is an ambiguity of $n\pi$ (n = integer) in the position angle, which is resolved if measurements are made sufficiently close in frequency to ensure that θ changes less than $\pi/2$ between measurements.

With the assumption of a constant electron density and angle ϕ the total Faraday rotation $\Delta\theta$ for the quasi-longitudinal magnetic case (9) reduces for electrons to†

$$\Delta\theta = 2.6 \times 10^{-13} NB\lambda^2 \cos \theta \Delta r \quad (\text{rad}) \quad (14)$$

where N = electron density, number m^{-3}

B = magnetic flux density, T

λ = wavelength, m

ϕ = angle between wave direction and \mathbf{B} , rad or deg

Δr = path length, m

† For a transmitter in an artificial earth satellite traveling toward or away from the observer along a line nearly parallel to \mathbf{B} it is convenient to replace $\Delta\theta$ by π and Δr by $v \Delta T$, where v is the satellite velocity in meters per second and ΔT the time in seconds between nulls in the signal as measured with a linearly polarized receiving antenna. Assuming that B is known, the average N can then be determined. It is assumed that the fading (nulls) is entirely due to Faraday rotation effects and not to rotation of the satellite (with a linearly polarized antenna).

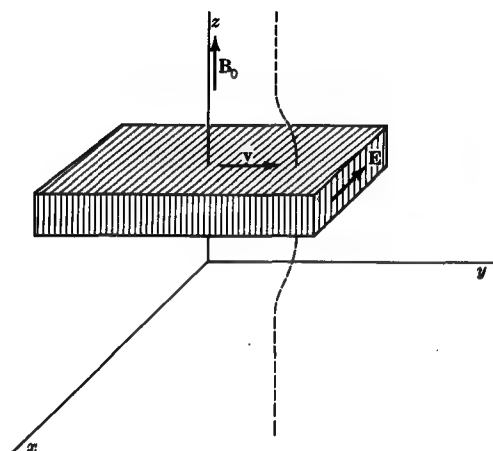


FIGURE 15-9

Geometry for rectangular slab in a medium of conducting fluid. Motion of the slab to the right pulls the magnetic field with it as suggested by the dashed field line. (See footnote, p. 741.)

15-10 MAGNETOHYDRODYNAMIC WAVES

In Sec. 15-8 no motion of the medium other than a harmonic motion of the charged particles was considered. Suppose now that a layer or column in a conducting medium with applied magnetic field is mechanically moved or displaced. No incident waves are considered, but let us study the effect of this motion of the medium in generating a disturbance, or wave. This situation has been investigated by Alfvén.[†] The waves produced by the motion are referred to as *magnetohydrodynamic waves (MHD waves)* or *Alfvén waves*.

It should be noted that the medium being considered here differs significantly from that considered in Secs. 15-8 and 15-9, because it is much denser, so that collisions are important. It might consist of a conducting fluid, such as mercury; or it might consist of a very dense, hot plasma.

Let a slab in a conducting fluid, as in Fig. 15-9, be moved with a velocity v in the y direction. The slab is infinite in extent in this $\pm y$ directions. A steady magnetic field \mathbf{B}_0 is applied in the z direction. Since \mathbf{v} is in the y direction and \mathbf{B}_0 in the z direction, we have from

$$\mathbf{E} = \mathbf{v} \times \mathbf{B} \quad (1)$$

that an electric field \mathbf{E} will be induced by the motion in the x direction, as suggested in Fig. 15-9. This field produces a current in the slab in the x direction which has its return paths through the medium above and below the slab. This current, in turn, produces forces which tend to impede the motion of the slab but which impart an

[†] H. Alfvén, "Cosmical Electrodynamics," Oxford University Press, 1950.

acceleration to the fluid above and below the slab in the y direction. Thus, the original motion initiates motion of the fluid, which propagates as a wave in the direction of the magnetic field.[†] The pertinent equations are

$$\nabla \times \mathbf{H} = \mathbf{J} + \frac{\partial \mathbf{D}}{\partial t} \quad (2)$$

$$\nabla \times \mathbf{E} = - \frac{\partial \mathbf{B}}{\partial t} \quad (3)$$

$$\mathbf{J} = \sigma(\mathbf{E} + \mathbf{v} \times \mathbf{B}) \quad (4)$$

$$\mathbf{B} = \mu \mathbf{H} \quad (5)$$

$$\frac{d\mathbf{v}}{dt} = \mathbf{G} + \frac{1}{\rho} (\mathbf{J} \times \mathbf{B} - \nabla p) \quad (6)$$

where \mathbf{v} = velocity of displacement, m s^{-1}

\mathbf{J} = current density, A m^{-2}

ρ = mass density, kg m^{-3}

p = pressure, $\text{kg m}^{-1} \text{s}^{-2}$

\mathbf{G} = parameter involving nonelectromagnetic forces, m s^{-2}

Equations (2) and (3) are Maxwell curl equations, (4) is a current equation, (5) is an equation characterizing the medium (constitutive equation), and (6) is a hydrodynamic equation with the dimensions of acceleration (Navier-Stokes equation).

Consider the case of plane waves in an incompressible fluid (density constant). From (4) we have that

$$\frac{\mathbf{J}}{\sigma} = \mathbf{E} + \mathbf{v} \times \mathbf{B} \quad (7)$$

From the geometry $J_y = J_z = 0$; so

$$E_x = \frac{J_x}{\sigma} - v_y B_0 \quad (8)$$

and $E_y = E_z = 0$. From (3) and (5)

$$\frac{\partial E_x}{\partial z} = -\mu \frac{\partial H_y}{\partial t} \quad (9)$$

Introducing (8) for E_x in (9) yields

$$\mu \frac{\partial H_y}{\partial t} = B_0 \frac{\partial v_y}{\partial z} - \frac{1}{\sigma} \frac{\partial J_x}{\partial z} \quad (10)$$

[†] The net result is as though the magnetic field is frozen into the slab and its motion to the right pulls the magnetic field \mathbf{B} with it as suggested by the dashed field line in Fig. 15-9. This displacement of \mathbf{B} then propagates vertically (in z direction).

Neglecting G , we have from (6)

$$\frac{\partial v_y}{\partial t} = -\frac{1}{\rho} J_x B_0 \quad (11)$$

It is assumed that ∇p can have no component perpendicular to z . Introducing (2) in (11), we have (neglecting $\partial D/\partial t$ in comparison with J)

$$\frac{\partial v_y}{\partial t} = \frac{B_0}{\rho} \frac{\partial H_y}{\partial z} \quad (12)$$

Eliminating v_y between (10) and (12), we obtain a wave equation in H_y for a wave propagating in the z direction, or

$$\frac{\partial^2 H_y}{\partial t^2} = \frac{B_0^2}{\mu\rho} \frac{\partial^2 H_y}{\partial z^2} + \frac{1}{\mu\sigma} \frac{\partial^3 H_y}{\partial t \partial z^2} \quad (13)$$

For sufficiently large conductivity the last term may be neglected. The velocity of the wave, or *Alfvén velocity*, is then given by

$$v = \frac{B_0}{\sqrt{\mu\rho}}$$

(14)

where v = velocity of wave, m s^{-1}

B_0 = magnetic flux density, T

μ = permeability of medium, H m^{-1}

ρ = density of medium, kg m^{-3}

It is of interest to evaluate (14) for the case of the solar photosphere, where appropriate values are $\rho = 200 \text{ mg m}^{-3}$ and $B_0 = 100 \text{ mT}$. Taking $\mu = \mu_0 = 400\pi \text{ nH m}^{-1}$ yields a velocity of 6.3 km s^{-1} for a magnetohydrodynamic wave in the photosphere (visible surface of sun). In the solar corona at about one solar radius above the photosphere the value of B is less but ρ is much less, and a magnetohydrodynamic wave velocity approaching the velocity of light is obtained.

PROBLEMS

- * 15-1 A particle with a negative charge of 10^{-17} C and a mass of 10^{-26} kg is at rest in a field-free space. If a uniform electric field $E = 1 \text{ kV m}^{-1}$ is applied for $1 \mu\text{s}$, find (a) the velocity of the particle and (b) the radius of curvature of the particle path if the particle enters a magnetic field $B = 2 \text{ mT}$ with this velocity moving normal to \mathbf{B} .
- * 15-2 A cathode-ray tube has electrostatic-deflection plates as in Fig. 15-3 plus a magnetic field between these plates. The magnetic field is oriented parallel to the electrostatic-deflection field. The tube has an accelerating voltage $V = 7 \text{ kV}$, a plate spacing $d = 20 \text{ mm}$, and a plate length (and magnetic field length) $l = 20 \text{ mm}$. Find (a) the deflec-

tion-plate voltage and (b) the magnetic flux density B required to deflect the electron beam 50 mm in the y direction and 100 mm in the z direction (perpendicular to page) at a screen placed at a distance $x = 500$ mm from the deflecting plates.

- * 15-3 The cathode-ray-tube screen of a television receiver measures 400 mm (horizontally) by 300 mm (vertically). The electron-beam spot scans 525 lines per frame and 30 frames per second. Find (a) the horizontal spot velocity in millimeters per microsecond and (b) the total distance traveled by the spot per second. (c) What is the rate of change of magnetic flux density B required if the tube parameters are as in Prob. 15-2?

15-4 (a) A deuteron accelerated through a potential difference V enters a region of uniform magnetic flux density B moving normal to \mathbf{B} . If the radius of the deuteron path is 120 mm, what is the required relation between B and V ? (b) If V and B are the same as in (a) but the particle is a proton, find the radius of its path. (c) Repeat for an alpha particle. (d) Compare the kinetic energies of the three particles.

- * 15-5 (a) Find the maximum energy (in MeV) for alpha particles in a cyclotron with maximum usable radius of 450 mm. The flux density $B = 1.2$ T in the air gap. (b) Repeat (a) if protons are used. (c) Repeat (a) if deuterons are used. (d) How many revolutions does each particle make if the peak potential between the dees is 9 kV?

15-6 (a) What is the ratio of the path radius of a proton to that of a deuteron if both enter a magnetic field \mathbf{B} normally with the same kinetic energy? (b) What is the ratio of the path radius of an alpha particle to that of a deuteron?

- * 15-7 Find the radius of curvature for the path of a proton with velocity $v = 10 \text{ Mm s}^{-1}$ moving perpendicular to a magnetic field with (a) $B = 5 \text{ mT}$ (solar-corona magnetic field), (b) $B = 100 \mu\text{T}$ (earth's magnetic field), (c) $B = 10 \text{ nT}$ (interstellar magnetic field).

15-8 A 5-keV proton is injected into a magnetic field $B = 500 \text{ mT}$ at an angle of 85° with respect to \mathbf{B} . Find the following parameters of the resulting helical path: (a) radius, (b) distance between turns of helix, (c) circular velocity in radians per second and meters per second, (d) axial velocity in meters per second, and (e) period.

15-9 (a) The chimney flue of an industrial factory has a rectangular (interior) cross section of 1 by 0.5 m. Flat electrodes 1 m square are placed against the long sides of the flue to precipitate solid particles in the smoke electrostatically. If a typical particle has a mass of $1 \mu\text{g}$ and a charge of 10^{-14} C , what voltage between the electrodes is required to precipitate the particle against an electrode? Take the smoke velocity $v = 1 \text{ m s}^{-1}$ and assume that when the particle enters the electrode space it is at the greatest possible distance (0.25 m) from the electrode to which it will move. (b) Design a precipitator for a 1-m-diameter cylindrical steel chimney flue capable of precipitating solid particulate wastes being exhausted at the rate of 10 kg min^{-1} with a velocity of 3 m s^{-1} . Assume that the particles have masses of $1 \mu\text{g}$ each. The flue is 20 m tall. See, for example, A. D. Moore, Electrostatics, *Sci. Am.*, **226**(3):47 (March 1972).

15-10 (a) In Millikan's oil-drop experiment a tiny droplet of oil of mass m is suspended in equilibrium in the gravitational field (of acceleration g) by an electric field E between two horizontal capacitor plates. If the droplet has N electron charges, show that the magnitude of the charge e of an electron is given by $e = mg/NE$. (b) How can the polarity of the droplet be determined by the experiment?

15-11 The alternating electric field of a passing electromagnetic wave causes an electron (initially at rest) to oscillate. This oscillation of the electron makes it equivalent to a dipole radiator. Show that the ratio of the power scattered per steradian to the incident Poynting vector is given by $(\mu_0 e^2 \sin \theta / 4\pi m)^2$, where e and m are the charge and mass of the electron and θ is the angle of the scattered radiation with respect to the direction of the electric field E of the incident wave. This ratio times 4π is the radar cross section of the electron. Such reradiation is called *Thompson scatter*.

15-12 A ground-based vertical-looking radar can be used to determine electron densities in the earth's ionosphere by means of *Thompson scatter* (see Prob. 15-11). The scattered-power radar return is proportional to the electron density. If a short pulse is transmitted by the radar, the backscattered power as a function of time is a measure of the electron density as a function of height. Design a Thompson scatter radar operating at 430 MHz capable of measuring ionospheric electron densities with 1-km resolution in height and horizontal position to heights of 1 Mm. The radar should also be capable of detecting a minimum of 100 electrons at a height of 1 Mm. The design should specify radar peak power, pulse length, antenna size, and receiver sensitivity. See W. E. Gordon, Radar Backscatter from the Earth's Ionosphere, *IEEE Trans. Antennas Propag.*, AP-12:873-876 (December 1964).

* **15-13** Right-handed helical-beam antennas are used for communication between an earth base and a space vehicle to eliminate fading due to vehicle spin and Faraday rotation in the earth's ionosphere. If the space vehicle is transmitting at 150 MHz and traveling without spin toward the earth base at 7 km s^{-1} , what change in frequency results? The transmission path is substantially parallel to the earth's magnetic field. Take $B = 100 \mu\text{T}$ and the electron density $N = 10^{11} \text{ m}^{-3}$.

* **15-14** Layers are said to exist in the earth's ionosphere where the ionization gradient is sufficient to refract radio waves back to the earth. [Although the wave actually may be bent gradually along a curved path in an ionized region of considerable thickness, a useful simplification for some situations is to assume that the wave is reflected as though from a horizontal perfectly conducting surface situated at a (virtual) height h .] The highest frequency at which this layer reflects a vertically incident wave back to the earth is called the *critical frequency* f_0 . Higher frequencies at vertical incidence pass through. For waves at oblique incidence ($\phi > 0$ in Fig. P15-14) the *maximum usable frequency* (MUF) for point-to-point communication on the earth is given by $\text{MUF} = f_0 / \cos \phi$, where ϕ = angle of incidence. The critical frequency f_0 is a function of the electron density, which in turn is a function of solar irradiation and other factors. Both f_0 and h vary with time of day, season, latitude, and phase of the 11-year sunspot cycle. Find the MUF for (a) a distance $d = 1.3 \text{ Mm}$ by F₂ layer ($h = 325 \text{ km}$) reflection with F₂ layer electron density $N = 6 \times 10^{11} \text{ m}^{-3}$, (b) a distance $d = 1.5 \text{ Mm}$ by F₂ layer ($h = 275 \text{ km}$) reflection with $N = 10^{12} \text{ m}^{-3}$, and (c) a distance $d = 1 \text{ Mm}$ by sporadic E layer ($h = 100 \text{ km}$) reflection with $N = 8 \times 10^{11} \text{ m}^{-3}$. Neglect earth curvature.

15-15 Referring to Prob. 15-14, show that due to earth curvature the maximum angle of incidence ϕ for the F₂ layer ($h = 300 \text{ km}$) is about 74° . If the F₂ layer height $h = 300 \text{ km}$ and the electron density $N = 10^{12} \text{ m}^{-3}$ all along a great-circle path around the

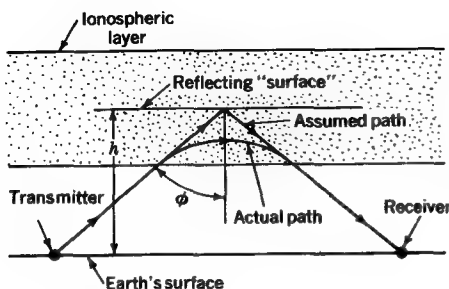


FIGURE P15-14

Communication path via reflection from ionospheric layer.

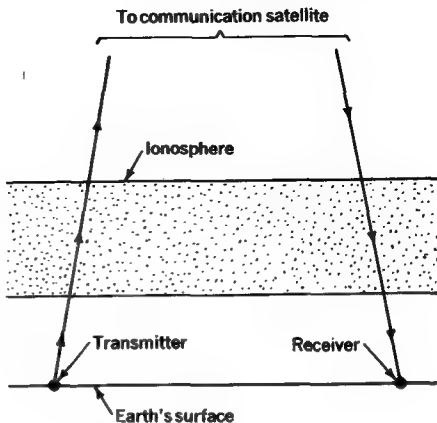


FIGURE P15-16

Communication path via stationary relay satellite.

world, find (a) the MUF and (b) the number of hops required for an around-the-world signal. (c) What is the percent delay of the round-the-world signal with respect to a circular path at the earth's surface? (d) What is the transmission time for the round-the-world signal (in milliseconds)?

* 15-16 Stationary communication (relay) satellites are placed at heights of about 40 Mm. This is far above the ionosphere, so that the transmission path passes completely through the ionosphere twice, as in Fig. P15-16. Since frequencies of 2 GHz and above are usually used, the ionosphere has little effect. The high frequency also permits wide bandwidths. If the ionosphere consists of a layer 200 km thick between heights of 200 and 400 km with a uniform electron density $N = 10^{12} \text{ m}^{-3}$, find the lowest frequency (or *minimum usable frequency, MUF*) which can be used with a communication satellite (a) for vertical incidence and (b) for paths 30° from the zenith. (c) Discuss the relation of answers to (a) and (b) to the minimum usable frequency for a ground-based radio telescope.

15-17 In Prob. 15-14 we were interested in the *maximum usable frequency* and in Prob. 15-16 in the *minimum usable frequency*. Does the maximum usable frequency of one case equal the minimum usable frequency of the other case?

15-18 A 7-MHz radio station in San Francisco transmits with vertical polarization. Must a receiving station in Tokyo use vertical polarization for best results? Explain reasons for your answer.

15-19 Compare communication between two points on the earth using ionospheric reflection (frequencies between 3 and 30 MHz) and using transmission through the ionosphere via relay satellite (frequencies of 2 GHz and up) at distances of (a) 50 km, (b) 1 Mm, (c) 5 Mm, (d) 10 Mm, and (e) 20 Mm. Compare reliability, fading, bandwidth, power, signal delay time, cost, etc.

* 15-20 Assume the ionosphere consists of a 200-km thick layer with uniform electron density $N = 10^{12} \text{ m}^{-3}$ at heights between 200 and 400 km. Assume further that the earth's magnetic field is vertical and that $B = 100 \mu\text{T}$. (a) What is the electrical-path length (in wavelengths) for a 14-MHz wave (a) traveling through the layer at vertical incidence and (b) traveling horizontally in the layer for 200 km? Consider both modes of propagation for each case. (c) Calculate the ratios of the above values to the path length (in wavelengths) over 200 km in free space. (d) How can a path length (in wavelengths) be less in the denser medium? (e) What is the Faraday rotation in turns over each path (1 turn = 2π rad).

* 15-21 Calculate the velocity of an Alfvén wave for the following cases: (a) the earth's ionosphere, $B = 100 \mu\text{T}$, $N = 10^{12} \text{ m}^{-3}$, medium is fully ionized nitrogen; (b) the solar corona, $B = 5 \text{ mT}$, $N = 10^{12} \text{ m}^{-3}$, medium is fully ionized hydrogen; (c) earth's core, $\rho = 10^4 \text{ kg m}^{-3}$, $B = 10 \text{ mT}$; and (d) liquid mercury, $\rho = 1.4 \times 10^4 \text{ kg m}^{-3}$, $B = 1 \text{ T}$.

15-22 Prove (15-8-9), (15-8-10), and (15-8-11).

15-23 Prove (15-8-29).

15-24 Prove (15-8-37).

15-25 Prove (15-9-8). Note that $\sqrt{1 + \delta} = 1 + (\delta/2)$, when $\delta \ll 1$.

15-26 Design a pump for liquid mercury using no moving parts which can move 1 liter of mercury per second against a head of 2 m of mercury.

* 15-27 A plasma travels through a square tube of 100 by 100 mm cross section at a velocity $v = 30 \text{ Mm s}^{-1}$. The plasma has an electron density $N = 10^{17} \text{ m}^{-3}$. If a magnetic field $B = 1 \text{ mT}$ is applied transversely to the tube, what emf is generated across the tube? The tube is curved to correspond to the radius of gyration of the plasma.

15-28 If an electron is injected into a magnetic field traveling nearly parallel to \mathbf{B} , it will move in a helical path with large distance between turns. If \mathbf{B} gradually increases, the distance between turns will decrease until a point is reached where the distance between turns becomes zero and the electron then reverses its direction with respect to \mathbf{B} and returns toward its starting point (see Fig. P15-28). It is as though the electron were reflected by a mirror. What relation must be satisfied between the electron energy and the magnetic field at such a *mirror point*?

15-29 A charged particle can be contained between two mirror points forming a magnetic "bottle." The magnetosphere of the earth forms such a bottle for particles which travel between northern and southern hemispheres (see Fig. P15-29). The maximum value of the earth's magnetic field $B \approx 100 \mu\text{T}$. What energy-field conditions are required for particles to be contained if the particles are (a) electrons and (b) protons? Higher-energy particles will be dumped, producing an auroral display.

15-30 How can a magnetic "bottle" be employed to contain a plasma?

15-31 Discuss similarities and differences between plasma and gyro resonances.

15-32 Consider a horizontal ionized layer (such as in the ionosphere) which is 100 km thick with uniform electron density $N = 10^{12} \text{ m}^{-3}$ and above it another layer of equal thickness but with $N = 4 \times 10^{12} \text{ m}^{-3}$. The magnetic field is vertical and of magnitude $B = 100 \mu\text{T}$. A circularly polarized 16-MHz wave is incident on the bottom layer from below at an angle of incidence $\phi = 40^\circ$. Trace the paths of the wave transmitted through or reflected from the layers. Consider all modes of propagation.

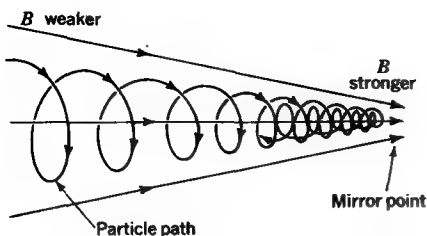


FIGURE P15-28
Magnetic mirror.

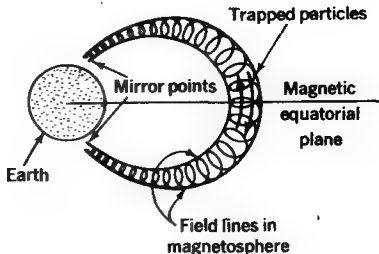


FIGURE P15-29
Magnetic bottle in magnetosphere.

15-33 (a) Show that under conditions where electron collisions with gas molecules are significant but the magnetic field can be neglected, the complex relative permittivity of an ionized medium can be expressed as $\epsilon_r = \epsilon'_r - j\epsilon''_r$, where

$$\epsilon'_r = 1 - \frac{Ne^2}{\epsilon_0 m(f_c^2 + \omega^2)} \quad \text{and} \quad \epsilon''_r = \frac{Ne^2 f_c}{\epsilon_0 m \omega (f_c^2 + \omega^2)}$$

where f_c = collision frequency

$\omega = 2\pi \times$ wave frequency

It is assumed that the wave power lost as heat in the medium is equal to f_c times the momentum mv of the electron. (b) Demonstrate that attenuation due to collisions is greatest when $f_c = \omega$.

15-34 Calculate the attenuation (in decibels) for a 3-MHz wave which has traveled 100 m through a nonmagnetized ionized region with electron density $N = 6 \times 10^{10} \text{ m}^{-3}$ when $f_c = \omega$.

15-35 Find the radius of curvature of a proton with velocity $v = 2 \times 10^8 \text{ m s}^{-1}$ traveling normally to the following magnetic fields: (a) synchrotron, $B = 1 \text{ T}$, (b) earth's magnetosphere, $B = 50 \mu\text{T}$, (c) solar corona, $B = 5 \text{ mT}$, and (d) interstellar medium, $B = 10 \text{ nT}$. The particle is relativistic; i.e., its mass is significantly larger than its rest mass [see (15-2-12)]. Such a particle in space could be called a *cosmic ray*.

15-36 A *synchrotron* is a particle accelerator similar to a cyclotron but with the following modifications. The magnetic field B and gyro frequency f are both varied in such a way that the particle radius is a constant ($= R_0$), so that an annular, or ring-shaped, magnet can be used, at a substantial cost reduction. Show that the two conditions which must be satisfied in a synchrotron are that $B = 2\pi fm/e$ and $f = v/2\pi R_0$. Thus, increasing the frequency increases the particle velocity (and energy) while B must be increased with the frequency (and particle mass) to keep the particle radius constant.

15-37 (a) Design an electron gun for propulsion of a space vehicle. Specify electron beam current and energy required to produce a thrust of 1 N. (b) Design a proton gun for the same purpose. Specify proton beam current and energy required to produce a thrust of 1 N.

15-38 Explain why a charged particle is "swept along like a surfer" by the very-low-frequency wave from a pulsar, using $\mathbf{F}_e = e\mathbf{E}$ and $\mathbf{F}_m = e(\mathbf{v} \times \mathbf{B})$. (See Sec. 14-27.)

15-39 Prove (15-6-1).

15-40 Why is the deflection of an electron by an electrostatic field as given by (15-4-6) and (15-4-7) independent of its charge and mass but its deflection by a magnetic field as given by (15-4-11) and (15-4-12) is dependent on its charge and mass?

MOVING SYSTEMS AND SPACE-TIME

16-1 INTRODUCTION†

Early thinkers believed a given instant of time had the same meaning for all observers, moving or stationary. However, a critical analysis by Einstein in 1905 resulted in a new formulation of ideas about space and time.‡ The concept of simultaneity, discussed in the next section, is fundamental to this formulation. Space-time relationships based on the concept of simultaneity are developed in subsequent sections. These are followed by the Lorentz transformation of coordinates, a four-dimensional field formulation, fields of moving systems, and the interrelation of electric and magnetic fields. These topics culminate in the development of the Maxwell stress tensor.

16-2 SIMULTANEITY

Is it possible to say that an event on the earth and an event of Mars are simultaneous? At first glance it might appear to be a simple matter to do so. Mars and the earth,

† An equally good title for this chapter is *Moving Systems and Relativity*.

‡ Albert Einstein, *Zur Elektrodynamik bewegter Korper* (The Electrodynamics of Moving Bodies), *Ann. Phys.*, 17: 89 (1905); reprinted in English in "The Principle of Relativity," Methuen and Co., Ltd., London, 1923.

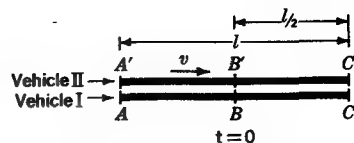


FIGURE 16-1

Two space ships or vehicles. Vehicle II is passing vehicle I with a relative velocity v to the right.

however, are in motion with respect to each other, and for bodies having such relative motion it is not possible to state that an event is simultaneous on both. According to Einstein's hypothesis, *simultaneity can be invoked only if there is no relative motion*. Thus, consider two points A and C on the earth's surface, say 120 km apart, and a third point B midway between, or 60 km from A and C . A radio signal transmitted from B will arrive at both A and C simultaneously so that clocks at A and C can be set to run in synchronism. In this way the simultaneity of events at A and C can be compared. Since the time required for the radio signal to reach A and C from B is $200 \mu\text{s}$ [$= 60 \text{ km}/(3 \times 10^5 \text{ km s}^{-1})$], advancing the clocks at A and C by $200 \mu\text{s}$ will synchronize all three clocks and the simultaneity of events at all three points can be compared. Likewise the simultaneity of events at two points on the surface of Mars can be ascertained by sending a radio signal from a third point midway between them. But the simultaneity of events at points on the earth relative to points on Mars cannot be determined except in an approximate manner.

To illustrate this let us consider two long spaceships, or vehicles, as in Fig. 16-1. Both vehicles have been constructed in the same factory to identical dimensions and specifications. The length of each is l . Each vehicle is equipped with three clocks, one located at the center and one at each end. Consider that we are aboard vehicle I (lower one in Fig. 16-1) and that vehicle II is passing us from left to right with a velocity v relative to our vehicle. Assume that we are far out in space and remote from the earth or other celestial bodies, so that the only motion of which we are aware is the relative motion of the two vehicles. At the instant shown in Fig. 16-1 vehicle II is directly alongside our vehicle, and at this instant ($t = 0$ on clock at B) a radio signal is emitted from the center of our vehicle. Neglecting the transverse separation of the vehicles, the signal is received at the same instant at point B' at the center of vehicle II. For convenience we shall say that this also is at $t = 0$ on the clock at B' .

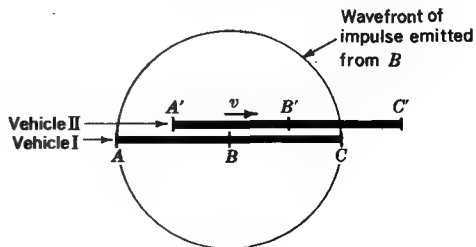


FIGURE 16-2

Space vehicles in Fig. 16-1 after a time $t = l/2c$.

All three clocks on vehicle I were previously synchronized with the clock at B , and all three clocks on vehicle II were previously synchronized with the clock at B' . When the impulse emitted from B reaches the ends of our vehicle (points A and C), the clocks on our vehicle will read $t = t_1 = l/2c$, where c is the velocity of the radio waves. However, as suggested in Fig. 16-2, it will appear to us on vehicle I that the impulse will have arrived at point A' on vehicle II at an earlier time t_2 and will arrive at point C' at the other end of vehicle II at a later time t_3 . Thus

$$t_2 = \frac{l/2}{c+v} \leq t_1 \quad (1)$$

and

$$t_3 = \frac{l/2}{c-v} \geq t_1 \quad (2)$$

On the other hand, an observer on vehicle II can regard our vehicle as passing his vehicle from right to left in Fig. 16-1, in which case the impulse from B (or B') arrives at the same time t_1 at the end points A' and C' of his vehicle but at an earlier time ($\leq t_1$) at the right end C of our vehicle and at a later time ($\geq t_1$) at the left end A of our vehicle. It is evident that what is simultaneous on one vehicle is not simultaneous on the other (unless $v = 0$).

A convenient way of illustrating these space-time relationships is by means of a Minkowski diagram.[†] Consider, for example, the expansion of the radio waves from point B on our space vehicle I. As shown in Fig. 16-3a, the radio impulse is transmitted at $t = 0$ and radiates in a spherical manner like an expanding soap bubble. The wavefront reaches points A and C at the time $t = t_1 = l/2c$. In the Minkowski diagram corresponding to this situation (Fig. 16-3b) distance along the axis of vehicle I is represented by the x coordinate (abscissa) while the distance that the radio waves travel is represented by the y coordinate (ordinate). The medium is vacuum ($\mu_r = \epsilon_r = 1$), and the radio waves travel with the velocity c ($= 300 \text{ Mm s}^{-1}$), the same as for light. Thus, the ordinate can be expressed in terms of ct , the distance traveled by the waves in the time t . The position of the wavefront at any time t is given by the two slant lines making a 45° angle with the x axis. When the wavefront reaches the points A and C at the two ends of our vehicle I, $ct = l/2$, as shown in Fig. 16-3b, and the slant lines intersect perpendiculars to the x axis at A ($x = 0$) and at C ($x = l$). These perpendiculars are called *world lines* for the points A and C , while the slant lines are called *light lines*. In our case they might more appropriately be called *radio lines* since our signaling is being done by radio instead of light.

[†] H. Minkowski, Die Grundgleichungen für die elektromagnetischen Vorgänge in bewegten Körpern, *Goettingen Nachr.* 1908, 53; Space and Time, address given at Cologne, Germany, 1908, reprinted in "The Principle of Relativity," Methuen and Co., Ltd., London, 1923.

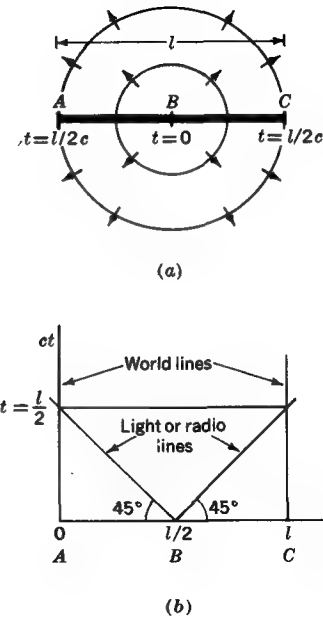


FIGURE 16-3

(a) Space vehicle I with expanding radio wave emitted from point B at the center of the vehicle; (b) Minkowski diagram for this situation.

16-3 SPACE-TIME CONCEPT

Consider now the representation by a Minkowski diagram of the situation for the two space vehicles I and II which we have been discussing. As illustrated in Fig. 16-4, the world lines for the points A and C of vehicle I will be perpendiculars to the x axis, the same as before, while the world lines for the points A' and C' of vehicle II are slant lines making an angle θ with respect to the ct axis, where $\tan \theta = v/c$, and where v is the velocity of vehicle II with respect to vehicle I and c is the velocity of light. The intersection of these world lines for A' and C' with the light lines occurs at P ($ct = ct_2$) and P' ($ct = ct_3$), as shown in Fig. 16-4, where $t_2 \leq t_1$ and $t_3 \geq t_1$, as we have previously deduced. The slant line connecting these intersection points (PP' in Fig. 16-4) makes an angle θ with the x axis. Taking a slant line parallel to PP' as one axis and the world line for the point A' as the other axis for an observer on vehicle II, we can construct the Minkowski diagram of Fig. 16-5. Here the space-time axes for an observer on vehicle I are x and ct , as before, while for an observer on vehicle II the space-time axes are x' and ct' . For convenience in Fig. 16-5 we also consider that the radio pulse is emitted at $t = 0$ (or $t' = 0$) from the point A (or A') at the left-hand end of the vehicles (see Fig. 16-1) instead of from the center point B (or B') as in Fig. 16-4. We shall call the coordinates for the unprimed axes (for vehicle I) system S and the

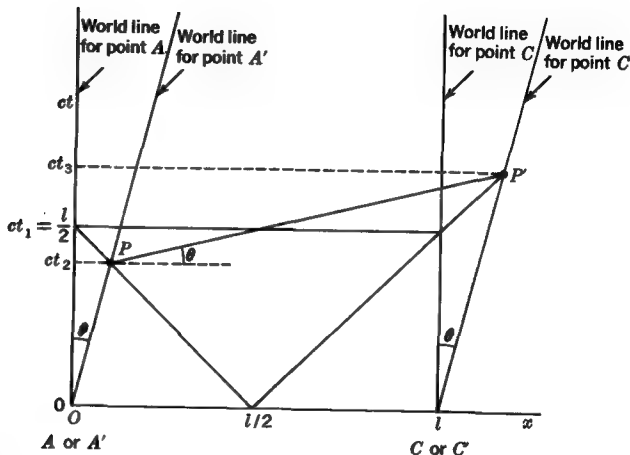


FIGURE 16-4

Space-time, or Minkowski, diagram for both space vehicles of Figs. 16-1 and 16-2 with midpoint as reference. The world lines for vehicle I are vertical, and those for vehicle II are slanting.

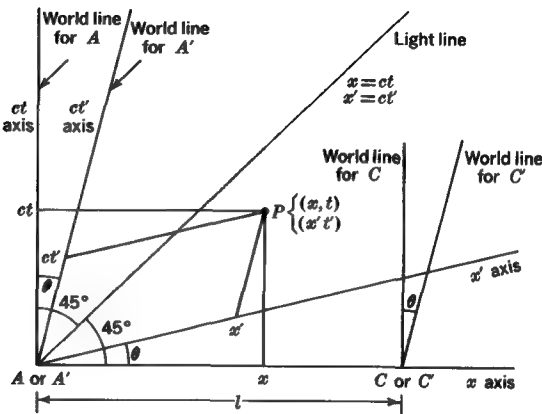


FIGURE 16-5

Space-time, or Minkowski, diagram for both space vehicles of Fig. 16-1 and 16-2 with point A as reference.

coordinates for the primed axes (for vehicle II) system S' . The system S' axes form an oblique (nonorthogonal) coordinate system. The S' axes make an angle θ with respect to the corresponding system S axes as given by

$$\theta = \tan^{-1} \frac{v}{c} \quad (1)$$

where v = velocity of vehicle II with respect to vehicle I

c = velocity of light

As indicated in Fig. 16-5, the light line of both systems is identical (bisects both sets of axes). This line is defined by the relations

$$x = ct \quad (2)$$

$$x' = ct' \quad (3)$$

It is said that these light lines are *invariant*; i.e., they are the same in both systems. To us on vehicle I all events on the x axis ($t = 0$) appear simultaneous. To an observer on vehicle II all events on the x' axis ($t' = 0$) appear simultaneous while to us they appear progressive with increasing x' .

The projection of a general event P on both the (x, ct) and the (x', ct') axes is also shown in Fig. 16-5.

Let us now determine the relation between the unprimed coordinates for vehicle I (ours) and the primed coordinates for vehicle II. Following Einstein, we make three assumptions:

- 1 The two systems are at rest or in uniform linear motion with respect to each other.
- 2 The velocity of the radio waves (or light) is c as measured in any system.
- 3 Measurements cannot disclose any fundamental difference between the two systems.

The coordinates for vehicle I are given by the system S (unprimed) and those for vehicle II by the system S' (primed). Each system moves with its respective vehicle, so that the vehicle appears at rest in its own coordinate system. The length of vehicle I (in system S) is l and the length of vehicle II (in system S') is l' . When the vehicles are stationary with respect to each other ($v = 0$), the lengths are equal ($l = l'$). But when there is relative motion ($v \neq 0$), the length of vehicle II will appear to us on vehicle I to be less than l ($= l - \Delta l$) while the length of our vehicle will appear to an observer on vehicle II to be less than l' ($= l' - \Delta l'$). This is illustrated in Fig. 16-6.

To fulfill assumption 3 above requires a reciprocal relationship between the two systems such that

$$\frac{l'}{l' - \Delta l'} = \frac{l}{l - \Delta l} \quad (4)$$

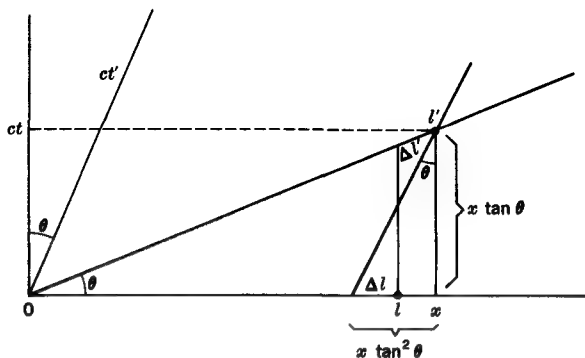


FIGURE 16-6

Space-time relations between the two space vehicles illustrating the *length-contraction* effect.

From the geometry of Fig. 16-6 we have the relations

$$(l' - \Delta l')^2 = l^2(1 + \tan^2 \theta) \quad (5)$$

$$l'^2 = x^2(1 + \tan^2 \theta) \quad (6)$$

$$l - \Delta l = x(1 - \tan^2 \theta) \quad (7)$$

Combining (6) and (7) gives

$$l' = (l - \Delta l) \frac{\sqrt{1 + \tan^2 \theta}}{1 - \tan^2 \theta} \quad (8)$$

Substituting (8) and the square root of (5) into (4), we have

$$\frac{l - \Delta l}{l} = \sqrt{1 - \tan^2 \theta} = \sqrt{1 - (v/c)^2} \quad (9)$$

In (9) the quantity $l - \Delta l$ is the length l' of vehicle II as observed from vehicle I. It is less than the length l of vehicle I as observed from itself by the factor $\sqrt{1 - (v/c)^2}$. The factor $\sqrt{1 - (v/c)^2}$ lies in the range between 0 and 1 and is called a *contraction factor*. It is the factor by which the length l' of vehicle II appears to be shortened as observed from vehicle I.

It also follows that

$$\frac{l' - \Delta l'}{l'} = \sqrt{1 - (v/c)^2} \quad (10)$$

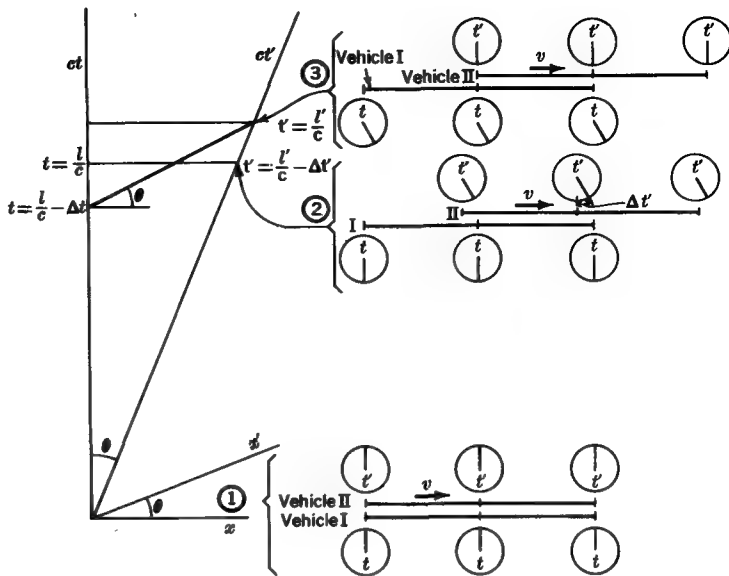


FIGURE 16-7
Space-time relations between the two space vehicles illustrating the *time-retardation effect*.

In (10) the quantity $l' - \Delta l'$ is the length l of vehicle I as observed from vehicle II. It is less than the length l' of vehicle II as observed from itself by the same contraction factor.

From (8) and (9)

$$\boxed{\frac{l'}{l} = \frac{\sqrt{1 + (v/c)^2}}{\sqrt{1 - (v/c)^2}}} \quad (11)$$

Thus, although l' is the same length at rest on vehicle II as l is on vehicle I, the length contraction requires that l' be longer than l on the Minkowski diagram by the factor given in (11). This is illustrated in Fig. 16-6.

In the unprimed system of vehicle I and the primed system of vehicle II the times will be related as illustrated in Fig. 16-7. We set the clocks at zero on both vehicles ($t = t' = 0$) when the two vehicles are opposite each other [(1) in Fig. 16-7]. At this instant a radio signal is transmitted from the left end of both vehicles. After the two vehicles have begun to separate and the radio waves have traveled the length l of vehicle I, the time $t = l/c$ and the hands on the clocks of vehicle I will have moved, for example, one-half turn [lower clocks at (2) in Fig. 16-7]. To an observer on vehicle

I the clocks on vehicle II at this instant will appear to read $t' = (l'/c) - \Delta t'$ [upper clocks at (2) in Fig. 16-7]. Thus, the clocks on vehicle II appear to an observer on vehicle I to run slow, or be *retarded*. The retardation is seen from the geometry to be

$$\frac{(l'/c) - \Delta t'}{l'/c} = \sqrt{1 - \left(\frac{v}{c}\right)^2} \quad (12)$$

After the radio waves have traveled the length l' of vehicle II, the time $t' = l'/c$ and the hands on the clocks of vehicle II will have moved one-half turn [upper clocks at (3) in Fig. 16-7]. To an observer on vehicle II the clocks on vehicle I at this instant will appear to read $t = (l/c) - \Delta t$ [lower clocks at (3) in Fig. 16-7]. Thus, the clocks on vehicle I appear to an observer on vehicle II to run slow, or be retarded, in the amount

$$\frac{(l/c) - \Delta t}{l/c} = \sqrt{1 - \left(\frac{v}{c}\right)^2} \quad (13)$$

This is the same retardation factor by which the clocks on vehicle II appear to run slow to an observer on vehicle I. It is also the same factor by which the lengths appear to be shortened. The length contraction and time retardation are necessary consequences of the theory of relativity.

It is clear that the appearance of the space vehicle depends on the viewpoint of the observer. To describe how it will appear to all observers requires a formulation involving both space and time.†

16-4 COORDINATE TRANSFORMATION

Let us now consider the transformation of coordinates between a system S (unprimed system) which is at rest with respect to us and a system S' (primed system) which is moving in the z direction with a velocity v , as in Fig. 16-8. The motion produces no effect on the transformation in the x and y directions, so that we have

$$x' = x \quad (1)$$

$$y' = y \quad (2)$$

The length of a meterstick in the stationary or unprimed system is z_0 . However, the length z'_0 of a meterstick moving in the primed system will appear altered in the unprimed or stationary system like the lengths of the space vehicles discussed in the preceding section.

† How the vehicle appears is *relative* to the viewpoint of the observer. Hence, the term *relativity*.

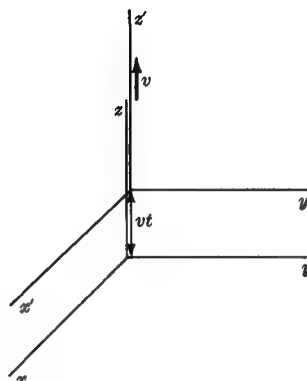


FIGURE 16-8

Rectangular coordinate system x' , y' , z' moving with a velocity v in the z direction with respect to stationary system x , y , z .

The fourth coordinate involving time must also be considered in the transformation. Thus, a *moving* meterstick involves space (three dimensions) and time (fourth dimension); so a four-dimensional transformation is required.

Let a point P be expressed by the coordinates x , y , z , ut in the unprimed, or stationary, system and by x' , y' , z' , ut' in the primed, or moving, system. The factor u has the dimensions of velocity, so that the product ut (velocity times time) has the dimensions of distance, like the other three coordinates x , y , z . Later we take $u = jc$, where c is the velocity of light. The time $t = t' = 0$ is taken as the instant when the origins of the moving and stationary coordinate frames are coincident.

EXAMPLE Draw the Minkowski diagram for the case where the above moving system has a velocity $v = 0.53c$.

SOLUTION A Minkowski diagram for this case is shown in Fig. 16-9 with rectangular grid for reference. Here $\tan \theta = v/c = 0.53$, and so the primed axis z' makes an angle $\theta = 28^\circ$ with respect to the unprimed axis z . In Fig. 16-9 we have arbitrarily made $z_0 = 3$ grid units. Now from (16-3-11) we have

$$z'_0 = z_0 \frac{\sqrt{1 + (v/c)^2}}{\sqrt{1 - (v/c)^2}} = 1.33z_0 \quad (3)$$

Therefore, $z'_0 = 1.33z_0 = 4$ grid units, as indicated.

It is necessary to distinguish between the length of a line in millimeters on the Minkowski diagram and the units of length the line represents in a given system. Thus, z'_0 is longer than z_0 on the diagram but z'_0 and z_0 represent the *same* length in each system.

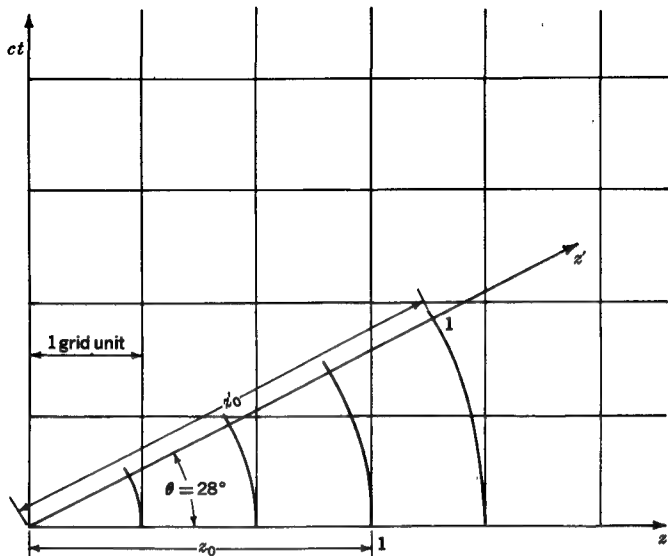


FIGURE 16-9
Space-time diagram illustrating calibration of axes for case where moving system has a velocity $v = 0.53c$ in z direction. (See worked example.)

The relation of a general event P to the coordinates is illustrated in Fig. 16-10. Comparing Fig. 16-10 with Fig. 16-6 and noting (16-3-8), we can write

$$\frac{z'}{z - vt} = \frac{l'}{l - \Delta l} = \frac{\sqrt{1 + (v/c)^2}}{\sqrt{1 - (v/c)^2}} \quad (4)$$

or

$$z' = \frac{\sqrt{1 + (v/c)^2}}{\sqrt{1 - (v/c)^2}} \frac{z - vt}{\sqrt{1 - (v/c)^2}} = \frac{z'_0}{z_0} \frac{z - vt}{\sqrt{1 - (v/c)^2}} \quad (5)$$

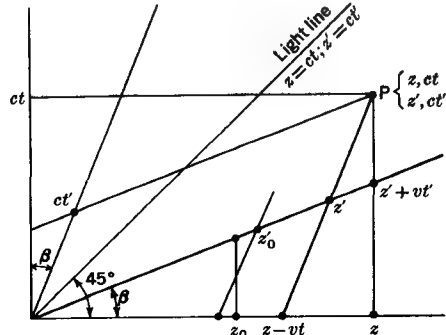


FIGURE 16-10
Space-time diagram for moving (primed) and stationary (unprimed) coordinate systems.

The units for z'_0 and z_0 differ on the Minkowski diagram (Fig. 16-9), but they each represent the same length in their own system; therefore if we put $z'_0 = z_0$,

$$z' = \frac{z - vt}{\sqrt{1 - (v/c)^2}} \quad (6)$$

which is a relation for the transformation of the coordinate z from the unprimed (stationary) to the primed (moving) system.

In like manner from Figs. 16-10 and 16-6 we obtain

$$\frac{z' + vt'}{z} = \frac{l'}{x} = \sqrt{1 + \left(\frac{v}{c}\right)^2} \quad (7)$$

or $\frac{z' + vt}{\sqrt{1 + (v/c)^2}} = \frac{\sqrt{1 - (v/c)^2}}{\sqrt{1 + (v/c)^2}} \frac{z' + vt'}{\sqrt{1 - (v/c)^2}}$ (8)

and $z = \frac{z_0}{z'_0} \frac{z' + vt'}{\sqrt{1 - (v/c)^2}}$ (9)

Putting $z'_0 = z_0$, as before, gives

$$z = \frac{z' + vt'}{\sqrt{1 - (v/c)^2}} \quad (10)$$

which is the relation for the transformation from z' to z .

Eliminating z from (6) and (10) yields

$$t = \frac{t' + (v/c)^2 z'}{\sqrt{1 - (v/c)^2}} \quad (11)$$

Eliminating z' from (6) and (10) yields

$$t' = \frac{t - (v/c^2)z}{\sqrt{1 - (v/c)^2}} \quad (12)$$

Equations (11) and (12) indicate how the time t transforms from the moving to the stationary system and vice versa.

In summary, the transformations from the primed to the unprimed coordinates and vice versa are

$x = x'$	$x' = x$
----------	----------

(13)

$y = y'$	$y' = y$
----------	----------

(14)

$$z = \frac{z' + vt'}{\sqrt{1 - (v/c)^2}} \quad z' = \frac{z - vt}{\sqrt{1 - (v/c)^2}} \quad (15)$$

$$t = \frac{t' + (v/c^2)z'}{\sqrt{1 - (v/c)^2}} \quad t' = \frac{t - (v/c^2)z}{\sqrt{1 - (v/c)^2}} \quad (16)$$

Taken as a group, these constitute the *Lorentz transformation*.† If the wave velocity is assumed infinite instead of equal to the velocity of light, so that c in the above equations is replaced by ∞ , we obtain the *Galilean transformation*

$$x = x' \quad x' = x \quad (17)$$

$$y = y' \quad y' = y \quad (18)$$

$$z = z' + vt' \quad z' = z - vt \quad (19)$$

$$t = t' \quad t' = t \quad (20)$$

The Galilean transformation implies instantaneous transmission of information. If $v = 0$, both transformations reduce to the same form

$$\begin{aligned} x &= x' \\ y &= y' \\ z &= z' \\ t &= t' \end{aligned} \quad (21)$$

An alternative (nongeometrical) derivation of the Lorentz transformation is as follows. Referring to Fig. 16-8, suppose that a radio wave is emitted from the origin of the stationary (unprimed) system of coordinates at the instant $t = 0$ when the moving (primed) system is coincident with the unprimed system. An observer at a point (x, y, z) in the stationary system will detect the passage of the wave after a time t such that

$$x^2 + y^2 + z^2 - c^2 t^2 = 0 \quad (22)$$

An observer moving in the primed system will detect the wave after a time t' such that

$$x'^2 + y'^2 + z'^2 - c^2 t'^2 = 0 \quad (23)$$

† H. A. Lorentz, Electromagnetic Phenomena in a System Moving with Any Velocity Less than That of Light, *Proc. Acad. Sci. Amsterdam*, **6**: 809 (1904); reprinted in "The Principle of Relativity," Methuen and Co., Ltd., London, 1923.

The desired transformation must be linear and also must not alter the quadratic form of the equations. Thus, the transformation must be of the form

$$x' = x \quad (24a)$$

$$y' = y \quad (24b)$$

$$z' = a_1 z + a_2 t \quad (24c)$$

$$t' = a_3 z + a_4 t \quad (24d)$$

where a_1, a_2, a_3, a_4 are constants to be determined. Taking the time derivative of (24c) yields

$$\frac{dz'}{dt} = a_1 \frac{dz}{dt} + a_2 \quad (25)$$

Now $dz/dt = v$, the velocity of the primed system as seen by a stationary observer. However, $dz'/dt = 0$, since an observer moving with the primed system is at rest with respect to it. Thus, $a_2 = -a_1 v$ and $z' = a_1(z - vt)$. Substituting this value of z' and the values of x', y', t' from (24a), (24b), and (24d) into (23) yields

$$x^2 + y^2 + (a_1^2 - c^2 a_3^2)z^2 - 2zt(a_1^2 v + c^2 a_3 a_4) = (c^2 a_4^2 - a_1^2 v^2)t^2 \quad (26)$$

When this is compared with (22), it follows that

$$\begin{aligned} a_1^2 - c^2 a_3^2 &= 1 \\ a_4^2 c^2 - a_1^2 v^2 &= c^2 \\ a_1^2 v + c^2 a_3 a_4 &= 0 \end{aligned} \quad (27)$$

Solving these three equations for a_1, a_3, a_4 , we obtain

$$a_1 = a_4 = \frac{1}{\sqrt{1 - (v/c)^2}} \quad (28)$$

$$a_3 = \frac{-v}{c^2 \sqrt{1 - (v/c)^2}} \quad (29)$$

Substituting these values back in (24c) and (24d), we obtain for the Lorentz transformation

$$\begin{aligned} x' &= x \\ y' &= y \\ z' &= a_1(z - vt) = \frac{z - vt}{\sqrt{1 - (v/c)^2}} \\ t' &= a_3 z + a_4 t = \frac{t - (v/c^2)z}{\sqrt{1 - (v/c)^2}} \end{aligned} \quad (30)$$

the same as in (13) to (16).

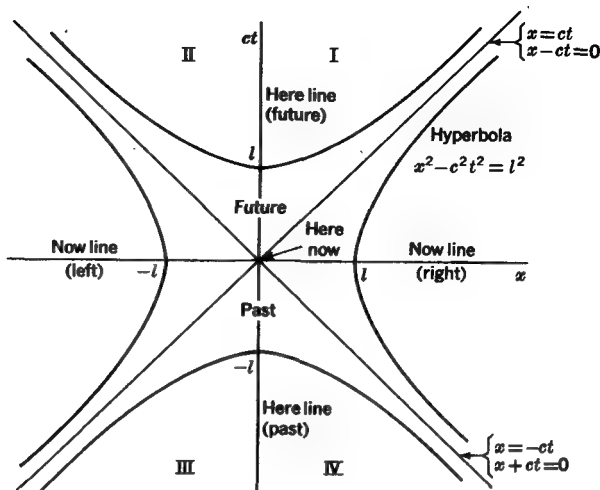


FIGURE 16-11

General space-time (Minkowski) diagram, relating position and time for different systems and epochs.

16-5 INVARIANCE IN SPACE-TIME

It has already been shown that the light lines defined by $x = ct$ (or $x' = ct'$) are invariant with respect to a stationary coordinate system or one moving in the x direction. The Minkowski diagram of Fig. 16-5 represents but one quadrant of the more general situation of four quadrants shown in Fig. 16-11. Here the light lines are given by

$$x - ct = 0 \quad (1)$$

and $x + ct = 0 \quad (2)$

More generally we may write

$$p = x - ct \quad (3)$$

$$q = x + ct \quad (4)$$

where $p = q = 0$ in (1) and (2). Taking the product of p and q , we have

$$pq = (x - ct)(x + ct) = x^2 - c^2 t^2 \quad (5)$$

Equation (5) is the equation of a hyperbola for which the product pq is a constant equal to $\pm l^2$, where $\pm l$ is the intercept of the four branches of the hyperbola with the x and ct axes. This is illustrated in Fig. 16-11.

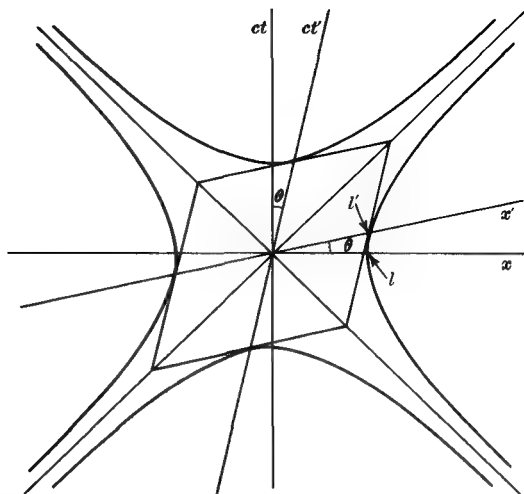


FIGURE 16-12
Diagrams illustrating the invariance of the space-time hyperbolae.

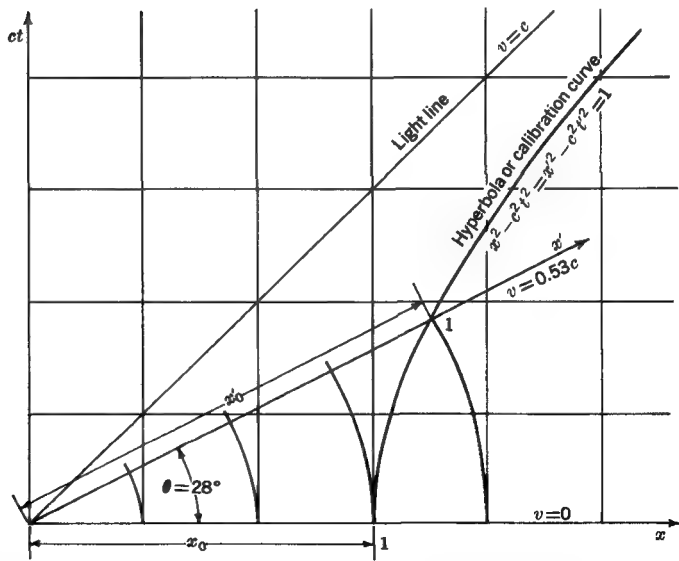


FIGURE 16-13
Space-time diagram showing hyperbola as invariant calibration curve for case where $v = 0.53c$ in x direction. On the diagram x'_0 is four-thirds the length of x_0 , but the observer in each system sees his own length as equal to unity.

From the Lorentz transformation

$$\begin{aligned}x^2 - c^2 t^2 &= \left[\frac{x' + vt'}{\sqrt{1 - (v/c)^2}} \right]^2 - c^2 \left[\frac{t' + (v/c)^2 z'}{\sqrt{1 - (v/c)^2}} \right]^2 \\&= x'^2 - c^2 t'^2\end{aligned}\quad (6)$$

It follows that

$$pq = x^2 - c^2 t^2 = x'^2 - c^2 t'^2 \quad (7)$$

Thus, as illustrated in Fig. 16-12, the hyperbolas are the same whether defined in the stationary (unprimed) coordinates ($x^2 - c^2 t^2 = pq = l^2$) or in the moving (primed) coordinates ($x'^2 - c^2 t'^2 = pq = l'^2$). The intercept of the hyperbola with the x and ct axes is l , whereas the intercept of the hyperbola with the x' and ct' axes is l' . From the example illustrated in Fig. 16-9, where $v = 0.53c$, the lengths are related to a hyperbola for which $x_0^2 = l^2 = 1$ and $x'_0^2 = l'^2 = 1$. This is illustrated in Fig. 16-13.

Returning to Fig. 16-11, we note that the origin represents the point "here-now" ($x = t = 0$), while points above the x axis represent the future and points below the past. For an observer in the primed system points above the x' axis (see Fig. 16-12) represent the future, and points below represent the past.

It is now clear that the light lines are invariant axes on the world diagram while the hyperbola is an invariant calibration curve.

16-6 FOUR-DIMENSIONAL FIELD FORMULATION†

In this section Maxwell's equations are given a four-dimensional (or 4-space) formulation. This prepares the way in the next section for the development of fields of moving systems by incorporating the Lorentz transformation in the four-dimensional formulation using tensors.

Maxwell's curl equation from Ampère's law is given by

$$\nabla \times \mathbf{H} = \mathbf{J} + \frac{\partial \mathbf{D}}{\partial t} \quad (1)$$

Expanding this in rectangular coordinates, we have

$$\begin{aligned}\hat{x} \left(\frac{\partial H_z}{\partial y} - \frac{\partial H_y}{\partial z} \right) + \hat{y} \left(\frac{\partial H_x}{\partial z} - \frac{\partial H_z}{\partial x} \right) + \hat{z} \left(\frac{\partial H_y}{\partial x} - \frac{\partial H_x}{\partial y} \right) \\= \hat{x} \left(J_x + \frac{\partial D_x}{\partial t} \right) + \hat{y} \left(J_y + \frac{\partial D_y}{\partial t} \right) + \hat{z} \left(J_z + \frac{\partial D_z}{\partial t} \right)\end{aligned}\quad (2)$$

† P. Moon and D. E. Spencer, "Foundations of Electrodynamics," p. 263, D. Van Nostrand Company, Inc., Princeton, N.J., 1960.

This vector equation yields three scalar equations; adding to this the expansion of Maxwell's divergence equation from Gauss' law ($\nabla \cdot \mathbf{D} = \rho$) yields a set of four equations:

$$0 + \frac{\partial H_z}{\partial y} - \frac{\partial H_y}{\partial z} - \frac{\partial D_x}{\partial t} = J_x \quad (3)$$

$$-\frac{\partial H_z}{\partial x} + 0 + \frac{\partial H_x}{\partial z} - \frac{\partial D_y}{\partial t} = J_y \quad (4)$$

$$\frac{\partial H_y}{\partial x} - \frac{\partial H_x}{\partial y} + 0 - \frac{\partial D_z}{\partial t} = J_z \quad (5)$$

$$\frac{\partial D_x}{\partial x} + \frac{\partial D_y}{\partial y} + \frac{\partial D_z}{\partial z} + 0 = \rho \quad (6)$$

The terms on the left of the above equations have been arranged so that the first three are derivatives with respect to x , y , and z , while the fourth is a derivative with respect to time. If any term is absent, a zero is introduced to indicate this explicitly. The right side of the above equations involves current density J or charge density ρ .

Recalling (16-4-22), we have

$$x^2 + y^2 + z^2 - c^2 t^2 = 0 \quad (7)$$

The equivalent equation in four-dimensional notation is

$$x_1^2 + x_2^2 + x_3^2 + x_4^2 = 0 \quad (8)$$

so that

$$x_1 = x \quad x_2 = y \quad x_3 = z \quad x_4 = jct \quad (9)$$

where j is the complex operator ($=\sqrt{-1}$). All four of these quantities have the dimensions of distance since c (velocity) multiplied by t (time) yields distance. Substituting and multiplying the fourth equation by jc to achieve symmetry gives†

$$\begin{aligned} 0 + \frac{\partial H_3}{\partial x_2} - \frac{\partial H_2}{\partial x_3} - jc \frac{\partial D_1}{\partial x_4} &= J_1 \\ -\frac{\partial H_3}{\partial x_1} + 0 + \frac{\partial H_1}{\partial x_3} - jc \frac{\partial D_2}{\partial x_4} &= J_2 \\ \frac{\partial H_2}{\partial x_1} - \frac{\partial H_1}{\partial x_2} + 0 - jc \frac{\partial D_3}{\partial x_4} &= J_3 \\ jc \frac{\partial D_1}{\partial x_1} + jc \frac{\partial D_2}{\partial x_2} + jc \frac{\partial D_3}{\partial x_3} + 0 &= jc\rho \end{aligned} \quad (10)$$

† Note that

$$-jc \frac{\partial D_1}{\partial x_4} = -jc \frac{\partial D_1}{\partial t} \frac{dt}{dx_4} = -\frac{jc}{c} \frac{\partial D_x}{\partial t} = -\frac{\partial D_x}{\partial t}$$

Now let

$$G_{mn} = \begin{bmatrix} 0 & H_3 & -H_2 & -jcD_1 \\ -H_3 & 0 & H_1 & -jcD_2 \\ H_2 & -H_1 & 0 & -jcD_3 \\ jcD_1 & jcD_2 & jcD_3 & 0 \end{bmatrix} \quad (11)$$

Here G_{mn} is a skew-symmetric or antisymmetric matrix ($G_{mn} = -G_{nm}$; $G_{mm} = 0$ when $m = n$). We note that G_{mn} contains only six independent quantities. We can now write the four scalar equations in concise summation form as

$$\boxed{\sum_{n=1}^4 \frac{\partial G_{mn}}{\partial x_n} = J_m \quad m = 1, 2, 3, 4} \quad (12)$$

where G_{mn} = matrix as in (11)

$$J_4 = jcp$$

Equation (12) is a four-dimensional formulation of two of Maxwell's equations ($\nabla \times \mathbf{H} = \mathbf{J} + \partial \mathbf{D} / \partial t$ and $\nabla \cdot \mathbf{D} = \rho$) in which the fourth dimension involves time. For each value of m we have a scalar equation, and for each value of n we have one term of that equation.

In a like manner we can express Maxwell's curl equation from Faraday's law ($\nabla \times \mathbf{E} = -\partial \mathbf{B} / \partial t$) and Maxwell's divergence equation from Gauss' law ($\nabla \cdot \mathbf{B} = 0$) in four-dimensional form as follows:

$$\boxed{\sum_{n=1}^4 \frac{\partial F_{mn}}{\partial x_n} = 0 \quad m = 1, 2, 3, 4} \quad (13)$$

where

$$F_{mn} = \begin{bmatrix} 0 & E_3 & -E_2 & jcB_1 \\ -E_3 & 0 & E_1 & jcB_2 \\ E_2 & -E_1 & 0 & jcB_3 \\ -jcB_1 & -jcB_2 & -jcB_3 & 0 \end{bmatrix} \quad (13a)$$

The quantities G_{mn} and F_{mn} are sometimes called the Ampère-Maxwell vector and the Faraday-Maxwell vector, respectively.

Expanding the continuity relation

$$\nabla \cdot \mathbf{J} = -\frac{\partial \rho}{\partial t} \quad (14)$$

we have

$$\frac{\partial J_x}{\partial x} + \frac{\partial J_y}{\partial y} + \frac{\partial J_z}{\partial z} + \frac{\partial \rho}{\partial t} = 0 \quad (15)$$

Let $x_1 = x$, $x_2 = y$, $x_3 = z$, $x_4 = jct$, as before, and $J_1 = J_x$, $J_2 = J_y$, $J_3 = J_z$, $J_4 = jc\rho$, so that

$$\frac{\partial J_1}{\partial x_1} + \frac{\partial J_2}{\partial x_2} + \frac{\partial J_3}{\partial x_3} + \frac{\partial J_4}{\partial x_4} = \square \cdot \mathbf{J} = 0 \quad (16)$$

or

$$\square \cdot \mathbf{J} = \sum_{m=1}^4 \frac{\partial J_m}{\partial x_m} = 0 \quad (17)$$

where $\square \cdot \mathbf{J}$ is the four-dimensional divergence of \mathbf{J} . Likewise from the relation between the scalar and vector potential

$$\nabla \cdot \mathbf{A} = -\frac{1}{c^2} \frac{\partial V}{\partial t} \quad (18)$$

we can write

$$\sum_{m=1}^4 \frac{\partial V_m}{\partial x_m} = 0 \quad (19)$$

where

$$V_1 = A_x \quad V_2 = A_y \quad V_3 = A_z \quad V_4 = \frac{jV}{c}$$

$$x_1 = x \quad x_2 = y \quad x_3 = z \quad x_4 = jct$$

The above four four-dimensional equations in summary are

$$\sum_{m=1}^4 \frac{\partial G_{mn}}{\partial x_n} = J_m \quad m = 1, 2, 3, 4 \quad (20a)$$

$$\sum_{n=1}^4 \frac{\partial F_{mn}}{\partial x_n} = 0 \quad m = 1, 2, 3, 4 \quad (20b)$$

$$\sum_{m=1}^4 \frac{\partial J_m}{\partial x_m} = 0 \quad \text{or} \quad \square \cdot \mathbf{J} = 0 \quad (20c)$$

$$\sum_{m=1}^4 \frac{\partial V_m}{\partial x_m} = 0 \quad (20d)$$

By *Einstein's summation convention* these four-dimensional relations can be abbreviated as follows:

$$\frac{\partial G_{mn}}{\partial x_n} = J_m \quad (21a)$$

Maxwell's equations:

$$\frac{\partial F_{mn}}{\partial x_n} = 0 \quad (21b)$$

**Continuity relation or equation
of conservation of charge:**

$$\frac{\partial J_m}{\partial x_m} = 0 \quad (21c)$$

Potential relation:

$$\frac{\partial V_m}{\partial x_m} = 0 \quad (21d)$$

According to the Einstein summation convention, the above equations are understood to have summation signs as in the equations of (20a) to (20d). These four equations of (20a) to (20d) or (21a) to (21d) contain the essence of electromagnetic theory in highly concise form. The four-dimensional formulation is especially useful in coordinate transformations, as demonstrated in the next section.

16-7 FIELDS OF A MOVING SYSTEM

We have discussed moving systems and four-dimensional field formulations. Let us now apply this information to the problem of the electromagnetic fields associated with a moving system. The first full solution of this problem was made by Minkowski in 1908.

Consider two coordinate systems x_1, x_2, x_3, x_4 and x'_1, x'_2, x'_3, x'_4 . The use of the four-dimensional formulation means that we can specify not just a point in space but a point in both space and time. Let the first (unprimed) system be at rest with respect to us and the second (primed) system in motion with a velocity v . Without loss of generality let the x_3 (or z axis) coincide with the direction of v (see Fig. 16-8). Also assume v to be linear and uniform (no acceleration).

According to the Lorentz transformation (16-4-30), we have

$$\begin{aligned} x' &= x \\ y' &= y \\ z' &= \frac{z - vt}{\sqrt{1 - (v/c)^2}} \\ t' &= \frac{t - (v/c^2)z}{\sqrt{1 - (v/c)^2}} \end{aligned} \quad (1)$$

But in the four-dimensional formulation

$$\begin{aligned} x &= x_1 & x' &= x'_1 \\ y &= x_2 & y' &= x'_2 \\ z &= x_3 & z' &= x'_3 \\ t &= \frac{x_4}{jc} & t' &= \frac{x'_4}{jc} \end{aligned} \quad (2)$$

Hence, in the four-dimensional formulation the Lorentz transformation becomes

$$\begin{aligned} x'_1 &= x_1 \\ x'_2 &= x_2 \\ x'_3 &= \frac{1}{\sqrt{1 - (v/c)^2}} \left(x_3 + j \frac{v}{c} x_4 \right) \\ x'_4 &= \frac{1}{\sqrt{1 - (v/c)^2}} \left(x_4 - j \frac{v}{c} x_3 \right) \end{aligned} \quad (3)$$

In tabular or matrix form the transformation is

$$\begin{array}{l} \begin{matrix} x_1 & x_2 & x_3 & x_4 \end{matrix} \\ \begin{matrix} x'_1 \\ x'_2 \\ x'_3 \\ x'_4 \end{matrix} \left[\begin{matrix} 1 & 0 & 0 & 0 \\ 0 & 1 & 0 & 0 \\ 0 & 0 & \gamma & j\gamma \frac{v}{c} \\ 0 & 0 & -j\gamma \frac{v}{c} & \gamma \end{matrix} \right] \end{array} \quad (3a)$$

where

$$\gamma = \frac{1}{\sqrt{1 - (v/c)^2}}$$

In general this transformation may be expressed as

$$\begin{aligned} x'_1 &= \frac{\partial x'_1}{\partial x_1} x_1 + \frac{\partial x'_1}{\partial x_2} x_2 + \frac{\partial x'_1}{\partial x_3} x_3 + \frac{\partial x'_1}{\partial x_4} x_4 \\ x'_2 &= \frac{\partial x'_2}{\partial x_1} x_1 + \frac{\partial x'_2}{\partial x_2} x_2 + \frac{\partial x'_2}{\partial x_3} x_3 + \frac{\partial x'_2}{\partial x_4} x_4 \\ x'_3 &= \frac{\partial x'_3}{\partial x_1} x_1 + \frac{\partial x'_3}{\partial x_2} x_2 + \frac{\partial x'_3}{\partial x_3} x_3 + \frac{\partial x'_3}{\partial x_4} x_4 \\ x'_4 &= \frac{\partial x'_4}{\partial x_1} x_1 + \frac{\partial x'_4}{\partial x_2} x_2 + \frac{\partial x'_4}{\partial x_3} x_3 + \frac{\partial x'_4}{\partial x_4} x_4 \end{aligned} \quad (4)$$

or more concisely as

$$x'_m = \sum_{n=1}^4 \frac{\partial x'_m}{\partial x_n} x_n \quad m = 1, 2, 3, 4 \quad (4a)$$

where $\frac{\partial x_m}{\partial x_n} = \begin{bmatrix} \frac{\partial x'_1}{\partial x_1} & \frac{\partial x'_1}{\partial x_2} & \frac{\partial x'_1}{\partial x_3} & \frac{\partial x'_1}{\partial x_4} \\ \frac{\partial x'_2}{\partial x_1} & \frac{\partial x'_2}{\partial x_2} & \frac{\partial x'_2}{\partial x_3} & \frac{\partial x'_2}{\partial x_4} \\ \frac{\partial x'_3}{\partial x_1} & \frac{\partial x'_3}{\partial x_2} & \frac{\partial x'_3}{\partial x_3} & \frac{\partial x'_3}{\partial x_4} \\ \frac{\partial x'_4}{\partial x_1} & \frac{\partial x'_4}{\partial x_2} & \frac{\partial x'_4}{\partial x_3} & \frac{\partial x'_4}{\partial x_4} \end{bmatrix} = \begin{bmatrix} a_{11} & a_{12} & a_{13} & a_{14} \\ a_{21} & a_{22} & a_{23} & a_{24} \\ a_{31} & a_{32} & a_{33} & a_{34} \\ a_{41} & a_{42} & a_{43} & a_{44} \end{bmatrix} = a_{mn}$ (5)

or $a_{mn} = \begin{bmatrix} 1 & 0 & 0 & 0 \\ 0 & 1 & 0 & 0 \\ 0 & 0 & \gamma & j\gamma \frac{v}{c} \\ 0 & 0 & -j\gamma \frac{v}{c} & \gamma \end{bmatrix}$ (6)

where $\gamma = \frac{1}{\sqrt{1 - (v/c)^2}}$

A quantity transforming as in (4) is a *tensor of rank 1*. Commonly superscripts are employed instead of subscripts as here. The coefficient $\partial x_m / \partial x_n$ is the transformation matrix. It describes how a dimension in the unprimed system transforms into a dimension in the primed system.

The four-dimensional equation incorporating Maxwell's equations $\nabla \times \mathbf{E} = -\partial \mathbf{B} / \partial t$ and $\nabla \cdot \mathbf{B} = 0$ from (16-6-13) is

$$\sum_{n=1}^4 \frac{\partial F_{mn}}{\partial x_n} = 0 \quad m = 1, 2, 3, 4 \quad (7)$$

To transform the fields given by F_{mn} in the stationary or unprimed system to the moving or primed system we write

$$F'_{kl} = \sum_{m=1}^4 \sum_{n=1}^4 a_{km} a_{ln} F_{mn} \quad k, l = 1, 2, 3, 4 \quad (8)$$

where F'_{kl} represents the transformed fields in the moving system and the coefficients a_{km} and a_{ln} are as given by a_{mn} in (6). The field quantities F_{mn} and F'_{kl} which transform as in (8) are *tensors of rank 2*. Each component F'_{kl} of the transformed field is, from (5), given by the sum of 16 terms. We note, however, that many elements of the matrix for

the coefficients are zero. Thus, $a_{12} = a_{13} = a_{14} = a_{21} = a_{23} = a_{24} = a_{31} = a_{32} = a_{41} = a_{42} = 0$. Also the components of the untransformed field $F_{11} = F_{22} = F_{33} = F_{44} = 0$.

Thus, for the transformed or primed field components we find

$$F'_{11} = 0 \quad (9)$$

$$F'_{12} = a_{11}a_{22}F_{12} = F_{12} \quad (10)$$

$$F'_{13} = a_{11}a_{33}F_{13} + a_{11}a_{34}F_{14} = \gamma \left(F_{13} + j\frac{v}{c}F_{14} \right) \quad (11)$$

$$F'_{14} = a_{11}a_{43}F_{13} + a_{11}a_{44}F_{14} = \gamma \left(F_{14} - j\frac{v}{c}F_{13} \right) \quad (12)$$

$$F'_{21} = F_{21} = -F_{12} = -F'_{12} \quad (13)$$

$$F'_{22} = 0 \quad (14)$$

$$F'_{23} = a_{22}a_{33}F_{23} + a_{22}a_{34}F_{24} = \gamma \left(F_{23} + j\frac{v}{c}F_{24} \right) \quad (15)$$

$$F'_{24} = a_{22}a_{43}F_{23} + a_{22}a_{44}F_{24} = \gamma \left(F_{24} - j\frac{v}{c}F_{23} \right) \quad (16)$$

$$F'_{31} = -F'_{13} \quad (17)$$

$$F'_{32} = -F'_{23} \quad (18)$$

$$F'_{33} = 0 \quad (19)$$

$$F'_{34} = a_{33}a_{44}F_{34} + a_{34}a_{43}F_{43} = \gamma^2 \left(F_{34} + \frac{v^2}{c^2}F_{43} \right) \quad (20)$$

$$= \gamma^2 \left(1 - \frac{v^2}{c^2} \right) F_{34} = F_{34} \quad (20)$$

$$F'_{41} = -F'_{14} \quad (21)$$

$$F'_{42} = -F'_{24} \quad (22)$$

$$F'_{43} = -F'_{34} \quad (23)$$

$$F'_{44} = 0 \quad (24)$$

Writing these in matrix form and, from (16-6-13a), putting $F_{12} = E_3$, $F_{13} = -E_2$, $F_{14} = jcB_1$, etc., we get

$$F'_{kl} = \begin{bmatrix} 0 & E_3 & -\gamma(E_2 + vB_1) & jc\gamma \left(B_1 + \frac{v}{c^2}E_2 \right) \\ -E_3 & 0 & \gamma(E_1 - vB_2) & jc\gamma \left(B_2 - \frac{v}{c^2}E_1 \right) \\ \gamma(E_2 + vB_1) & -\gamma(E_1 - vB_2) & 0 & jcB_3 \\ -jc\gamma \left(B_1 + \frac{v}{c^2}E_2 \right) & -jc\gamma \left(B_2 - \frac{v}{c^2}E_1 \right) & -jcB_3 & 0 \end{bmatrix} \quad (25)$$

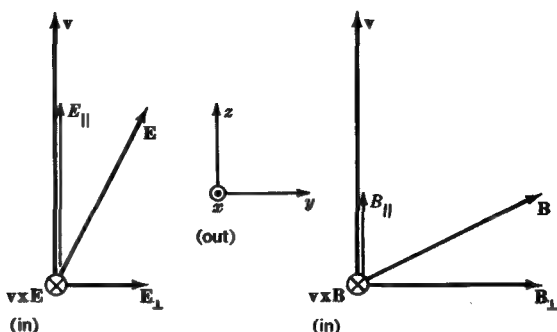


FIGURE 16-14

Components of fields \mathbf{E} and \mathbf{B} and their cross products with v . In the figure we have arbitrarily set $E_x = B_x = 0$, and so $|E_{\perp}| = E_y$, $|B_{\perp}| = B_y$, $|v \times E| = (v \times E)_z$, and $|v \times B| = (v \times B)_z$. (Note that $v \times E$ and $v \times B$ are always perpendicular to v .)

Comparing (25) with (16-6-13a) element by element and putting $E_x = E_1$, $E_y = E_2$, etc., it follows that

$$\begin{aligned} E'_x &= \gamma(E_x - vB_y) & B'_x &= \gamma\left(B_x + \frac{v}{c^2}E_y\right) \\ E'_y &= \gamma(E_y + vB_x) & B'_y &= \gamma\left(B_y - \frac{v}{c^2}E_x\right) \\ E'_z &= E_z & B'_z &= B_z \end{aligned} \quad (26)$$

The choice of the z direction for v is arbitrary. Referring to Fig. 16-14, the above relations can be expressed more generally by

$E'_{\parallel} = E_{\parallel} (= E_z)$	$B'_{\parallel} = B_{\parallel} (= B_z)$
$E'_{\perp} = \gamma E_{\perp} + (v \times B) $	$B'_{\perp} = \gamma \left B_{\perp} - \left(\frac{1}{c^2} v \times E \right) \right $

(27)

where the subscript \parallel indicates the field component parallel to the motion and the subscript \perp indicates the field component perpendicular to the motion. The interdependence of electric and magnetic fields is illustrated by the equations for the perpendicular field components. Thus, to a stationary observer the electric field \mathbf{E} and magnetic field \mathbf{B} appear to be independent quantities. However, to the moving observer the electric field has parts involving both the electric field \mathbf{E} and the magnetic

field \mathbf{B} of the stationary observer, while the magnetic field has parts involving both the magnetic field \mathbf{B} and the electric field \mathbf{E} of the stationary observer. It is clear that the appearance of a field depends on the viewpoint of the observer and that there is no such thing as a pure electric field or a pure magnetic field which retains its identity for all observers. For small velocities ($v \ll c$), $(v/c)^2$ approaches zero and

$$\gamma = \frac{1}{\sqrt{1 - (v/c)^2}} \approx 1 \quad (28)$$

These equations then reduce to

$E'_\parallel = E_\parallel$	$B'_\parallel = B_\parallel$
$E'_\perp = \mathbf{E}_\perp + (\mathbf{v} \times \mathbf{B}) $	$B'_\perp = B_\perp$

(29)

Integration of the relation $E'_\perp = |\mathbf{E}_\perp + (\mathbf{v} \times \mathbf{B})|$ around a closed circuit yields an emf

$$\nabla U = \oint \mathbf{E} \cdot d\mathbf{l} + \oint (\mathbf{v} \times \mathbf{B}) \cdot d\mathbf{l} \quad (30)$$

By Stokes' theorem [$\oint \mathbf{E} \cdot d\mathbf{l} = \iint (\nabla \times \mathbf{E}) \cdot d\mathbf{s}$] and Maxwell's equation $\nabla \times \mathbf{E} = -\partial \mathbf{B} / \partial t$ it follows that

$$\oint \mathbf{E} \cdot d\mathbf{l} = - \iint \frac{\partial \mathbf{B}}{\partial t} \cdot d\mathbf{s} \quad (31)$$

so that (30) becomes

$U = - \iint \frac{\partial \mathbf{B}}{\partial t} \cdot d\mathbf{s} + \oint (\mathbf{v} \times \mathbf{B}) \cdot d\mathbf{l}$

(32)

This is the same equation as appears in (8-5-1). As discussed in Chap. 8, the first term represents transformer emf and the second term motional emf.

The four-dimensional divergence of \mathbf{J} is, from (16-6-17),

$$\square \cdot \mathbf{J} = \sum_{n=1}^4 \frac{\partial J_n}{\partial x_n} = 0 \quad (33)$$

To transform the current densities given by J_m in the stationary or unprimed system to the moving or primed system we write

$$J'_m = \sum_{n=1}^4 a_{mn} J_n \quad m = 1, 2, 3, 4 \quad (34)$$

where a_{mn} is as given in (6). It follows that

$$\begin{aligned} J'_x &= J_x \\ J'_y &= J_y \\ J'_z &= \gamma(J_z - v\rho) \\ \rho' &= \gamma\left(\rho - \frac{v}{c^2} J_z\right) \end{aligned} \quad (35)$$

The interdependence of current and charge is illustrated by this result. To a stationary observer the current density \mathbf{J} and charge density ρ appear to be independent quantities. However, to the moving observer the current density involves both the current density \mathbf{J} and the charge density ρ of the stationary observer. Also to the moving observer the charge density involves both the charge density ρ and the current density \mathbf{J} of the stationary observer. *It is clear that the appearance of the current and charge density depends on the viewpoint of the observer and that there is no such thing as a pure electric current or a pure charge which retains its identity for all observers.*

16-8 MAXWELL'S STRESS TENSOR

Stress is defined as the force acting on a unit area in a material medium. In this section a four-dimensional force-energy relation is derived which describes the stress produced by the electromagnetic field on a body.

Maxwell's equation from Ampère's law is

$$\nabla \times \mathbf{H} = \mathbf{J} + \frac{\partial \mathbf{D}}{\partial t} \quad (1)$$

Assuming harmonic variation and taking the cross product with \mathbf{B} yields

$$(\nabla \times \mathbf{H}) \times \mathbf{B} = \mathbf{J} \times \mathbf{B} + \frac{1}{2} \frac{\partial}{\partial t} (\mathbf{D} \times \mathbf{B}) \quad (2)$$

Maxwell's equation from Faraday's law is

$$\nabla \times \mathbf{E} = - \frac{\partial \mathbf{B}}{\partial t} \quad (3)$$

Taking the cross product with \mathbf{D} yields

$$(\nabla \times \mathbf{E}) \times \mathbf{D} = - \frac{1}{2} \frac{\partial}{\partial t} (\mathbf{B} \times \mathbf{D}) = \frac{1}{2} \frac{\partial}{\partial t} (\mathbf{D} \times \mathbf{B}) \quad (4)$$

Adding (2) and (4) gives

$$(\nabla \times \mathbf{E}) \times \mathbf{D} + (\nabla \times \mathbf{H}) \times \mathbf{B} = \mathbf{J} \times \mathbf{B} + \frac{\partial}{\partial t} (\mathbf{D} \times \mathbf{B}) \quad (5)$$

Each term of this equation has the dimensions of force per unit volume ($M/L^2 T^2$). We can expand and regroup $(\nabla \times \mathbf{E}) \times \mathbf{D}$ so that it takes the form

$$(\nabla \times \mathbf{E}) \times \mathbf{D} = \nabla \cdot (\mathbf{T}_{kl})_e - \mathbf{E}(\nabla \cdot \mathbf{D}) \quad (6)$$

In like manner we have

$$(\nabla \times \mathbf{H}) \times \mathbf{B} = \nabla \cdot (\mathbf{T}_{kl})_m - \mathbf{H}(\nabla \cdot \mathbf{B}) \quad (7)$$

Adding (6) and (7) yields

$$(\nabla \times \mathbf{E}) \times \mathbf{D} + (\nabla \times \mathbf{H}) \times \mathbf{B} = \nabla \cdot \mathbf{T}_{kl} - \mathbf{E}(\nabla \cdot \mathbf{D}) - \mathbf{H}(\nabla \cdot \mathbf{B}) \quad (8)$$

where $\mathbf{T}_{kl} = (\mathbf{T}_{kl})_e + (\mathbf{T}_{kl})_m$ = Maxwell stress tensor, $N m^{-2}$

$(\mathbf{T}_{kl})_e$ = stress tensor due to electric field, $N m^{-2}$

$(\mathbf{T}_{kl})_m$ = stress tensor due to magnetic field, $N m^{-2}$

The subscripts k, l assume values 1 to 3, and the matrix for the stress tensor is

$$\mathbf{T}_{kl} = \begin{bmatrix} \epsilon E_x^2 + \mu H_x^2 - \frac{1}{2}(\epsilon E^2 + \mu H^2) & \epsilon E_x E_y + \mu H_x H_y & \epsilon E_x E_z + \mu H_x H_z \\ \epsilon E_x E_y + \mu H_x H_y & \epsilon E_y^2 + \mu H_y^2 - \frac{1}{2}(\epsilon E^2 + \mu H^2) & \epsilon E_y E_z + \mu H_y H_z \\ \epsilon E_x E_z + \mu H_x H_z & \epsilon E_y E_z + \mu H_y H_z & \epsilon E_z^2 + \mu H_z^2 - \frac{1}{2}(\epsilon E^2 + \mu H^2) \end{bmatrix} \quad (9)$$

Each term of the stress tensor (9) has the dimensions of force per unit area,^f and may be a pressure, a tension, or a shear. We note that $\nabla \cdot \mathbf{B} = 0$ and $\nabla \cdot \mathbf{D} = \rho$. Substituting (8) in (5) then yields[‡]

$$\nabla \cdot \mathbf{T}_{kl} = \rho \mathbf{E} + \mathbf{J} \times \mathbf{B} + \frac{\partial}{\partial t} (\mathbf{D} \times \mathbf{B})$$

(10)

Each term of this equation has the dimensions of force per unit volume. Thus, $\rho \mathbf{E}$ represents the electric force per unit volume and $\mathbf{J} \times \mathbf{B}$ the magnetic force per unit volume. When the sum of these two force terms is called \mathbf{f} , (10) becomes

$$\mathbf{f} = \nabla \cdot \mathbf{T}_{kl} - \frac{\partial}{\partial t} (\mathbf{D} \times \mathbf{B}) \quad (N m^{-3}) \quad (11)$$

^f For example, the force dF_x in the x direction is given by

$$dF_x = T_{xx} dy dz + T_{xy} dz dx + T_{xz} dx dy \quad (N)$$

[‡] See note with Prob. 16-4 regarding the significance of the divergence of a tensor.

and assuming $\epsilon = \epsilon_0$ and $\mu = \mu_0$,

$$\mathbf{f} = \nabla \cdot \bar{\mathbf{T}}_{kl} - \frac{1}{c^2} \frac{\partial}{\partial t} (\mathbf{E} \times \mathbf{H}) \quad (12)$$

If we let $x_1 = x$, $x_2 = y$, $x_3 = z$, $x_4 = jct$, this relation can be expressed in four dimensional formulation as

$$\mathbf{f} = \nabla \cdot \bar{\mathbf{T}}_{kl} - \frac{j}{c} \frac{\partial}{\partial x_4} (\mathbf{E} \times \mathbf{H}) \quad k, l = 1, 2, 3 \quad (13)$$

or

$$\boxed{\mathbf{f} = \square \cdot \bar{\mathbf{T}}_{mn} \quad m, n = 1, 2, 3, 4} \quad (14)$$

where $\square \cdot$ is the four-dimensional divergence and $\bar{\mathbf{T}}_{mn}$ is the four-dimensional Maxwell stress tensor whose matrix is given by

$$\bar{\mathbf{T}}_{mn} =$$

$$\begin{bmatrix} \epsilon E_1^2 + \mu H_1^2 - \frac{1}{2}(\epsilon E^2 + \mu H^2) & \epsilon E_1 E_2 + \mu H_1 H_2 & \epsilon E_1 E_3 + \mu H_1 H_3 & -\frac{j}{c}(\mathbf{E} \times \mathbf{H})_1 \\ \epsilon E_1 E_2 + \mu H_1 H_2 & \epsilon E_2^2 + \mu H_2^2 - \frac{1}{2}(\epsilon E^2 + \mu H^2) & \epsilon E_2 E_3 + \mu H_2 H_3 & -\frac{j}{c}(\mathbf{E} \times \mathbf{H})_2 \\ \epsilon E_1 E_3 + \mu H_1 H_3 & \epsilon E_2 E_3 + \mu H_2 H_3 & \epsilon E_3^2 + \mu H_3^2 - \frac{1}{2}(\epsilon E^2 + \mu H^2) & -\frac{j}{c}(\mathbf{E} \times \mathbf{H})_3 \\ -\frac{j}{c}(\mathbf{E} \times \mathbf{H})_1 & -\frac{j}{c}(\mathbf{E} \times \mathbf{H})_2 & -\frac{j}{c}(\mathbf{E} \times \mathbf{H})_3 & \frac{1}{2}(\epsilon E^2 + \mu H^2) \end{bmatrix} \quad (15)$$

The concise equation of (14) incorporates all of Maxwell's equations. Integrating (14) over a volume yields the total force on the volume due to electric and magnetic forces. It is to be noted that the top three elements of the first three columns of $\bar{\mathbf{T}}_{mn}$ are equal to $\bar{\mathbf{T}}_{kl}$. Thus, the components for the matrix of $\bar{\mathbf{T}}_{mn}$ can be grouped as follows:

$$\bar{\mathbf{T}}_{mn} = \left[\begin{array}{c|c} T_{kl} & S_2 \\ \hline S_1 & W \end{array} \right] \quad (16)$$

Although the elements of all zones have the dimensions of force per unit area, we note that element W [$= \frac{1}{2}(\epsilon E^2 + \mu H^2)$] may be regarded as representing energy per unit volume, while the elements of groups S_1 and S_2 involve the Poynting vector ($= \mathbf{E} \times \mathbf{H}$), or power per unit area.

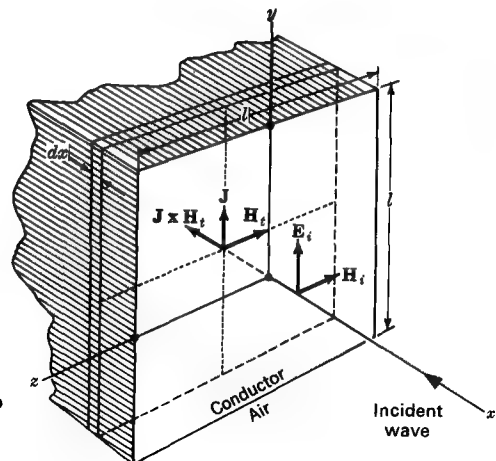


FIGURE 16-15

Plane wave incident on conducting slab for calculation of the radiation pressure.
(See worked example.)

EXAMPLE A plane wave is normally incident from air onto the plane surface of an infinitely thick perfect conductor. Calculate each element of the stress tensor \bar{T}_{mn} at a point inside the conductor to find the radiation pressure on the conductor.

SOLUTION Referring to Fig. 16-15, let the incident complex electric field be given by the equation

$$\hat{E}_i = \hat{y} E_0 e^{j(\omega t + \beta x)} \quad (17)$$

The transmitted electric field is

$$\hat{E}_t = \hat{y} \tau E_0 e^{x/\delta} e^{jx/\delta} e^{j\omega t} \quad (18)$$

where $\tau = \frac{2Z_1}{Z_0 + Z_1}$ = transmission coefficient

Z_1 = impedance of conductor

Z_0 = impedance of air

$\delta = 1/e$ depth of penetration

Similarly, the transmitted magnetic field is

$$\hat{H}_t = -2\alpha\tau H_0 e^{x/\delta} e^{jx/\delta} e^{j\omega t} \quad (19)$$

where $a = Z_0/Z_1$. The instantaneous fields are given by

$$\mathbf{E}_t = \operatorname{Re} \dot{\mathbf{E}}_t = \frac{y}{\tau} |E_0 e^{x/\delta} \cos(\omega t + \frac{x}{\delta} + \theta)| \quad (20)$$

$$\mathbf{H}_t = \operatorname{Re} \dot{\mathbf{H}}_t = -\frac{z}{\tau} |H_0 e^{x/\delta} \cos(\omega t + \frac{x}{\delta})| \quad (21)$$

Thus, in (15),

$$E_1 = E_3 = H_1 = H_2 = 0 \quad (22)$$

$$E_2 = E_t \quad (23)$$

$$H_3 = H_t \quad (24)$$

so that the stress tensor is given by

$$\bar{\mathbf{T}}_{mn} = \begin{bmatrix} -\frac{1}{2}(\epsilon_0 E_t^2 + \mu_0 H_t^2) & 0 & 0 & \frac{j}{c} E_t H_t \\ 0 & \frac{1}{2}(\epsilon_0 E_t^2 - \mu_0 H_t^2) & 0 & 0 \\ 0 & 0 & -\frac{1}{2}(\epsilon_0 E_t^2 - \mu_0 H_t^2) & 0 \\ \frac{j}{c} E_t H_t & 0 & 0 & \frac{1}{2}(\epsilon_0 E_t^2 + \mu_0 H_t^2) \end{bmatrix} \quad (25)$$

where E_t and H_t are given in (20) and (21). The volume force density \mathbf{f} has a component in the x direction which can be found from (14) as

$$\begin{aligned} f_x &= (\nabla \cdot \bar{\mathbf{T}}_{mn})_x \\ &= \frac{\partial T_{11}}{\partial x} + \frac{\partial T_{12}}{\partial y} + \frac{\partial T_{13}}{\partial z} - \frac{j}{c} \frac{\partial T_{14}}{\partial t} \\ &= -\frac{1}{2} \frac{\partial}{\partial x} (\epsilon_0 E_t^2 + \mu_0 H_t^2) + \frac{1}{c^2} \frac{\partial}{\partial t} (E_t H_t) \end{aligned} \quad (26)$$

The force-density components f_y and f_z are zero since T_{22} is not a function of y and T_{33} is not a function of z . The time average of f_x is given by

$$(f_x)_{av} = \frac{1}{T} \int_0^T f_x(x, t) dt \quad (27)$$

Carrying out the operations indicated in (26) and (27) gives

$$(f_x)_{av} = -\left(\epsilon_0 \frac{|\tau|^2}{2} E_0^2 + \frac{|a\tau|^2}{2} \mu_0 H_0^2 \right) \frac{e^{2x/\delta}}{\delta} \quad (\text{N m}^{-3}) \quad (28)$$

where $(f_x)_{av}$ is the average force per unit volume in the negative x direction or the stress on a unit area (l by l) of conductor of thickness dx , as shown in Fig. 16-15. Thus the total

average stress in the x direction on the conductor is found by integrating over all such infinitesimal slices dx , that is,

$$(T_x)_{av} = \int_0^{-\infty} (f_x)_{av} dx \\ = - \left(\frac{|\tau|^2}{4} \epsilon_0 E_0^2 + \frac{1}{4} \left| \frac{Z_0 \tau}{Z_1} \right|^2 \mu_0 H_0^2 \right) \quad (29)$$

If we now assume a *perfect conductor* ($Z_1 \rightarrow 0; \tau \rightarrow 0$), the *stress* is given by

$$(T_x)_{av} = -\mu_0 H_0^2 \quad (\text{N m}^{-2}) \quad (30)$$

Thus the *radiation pressure* is given by

$$\mathcal{P}_{av} = -(T_x)_{av} = \mu_0 H_0^2 \quad (\text{N m}^{-2}) \quad (31)$$

Physically, this pressure is due to the interaction of the conduction-current density \mathbf{J} (in the y direction) with the magnetic field H , inside the conductor (in the $-z$ direction) so that a magnetic force of volume density $\mathbf{J} \times \mathbf{H}_i$ is produced. This force density in turn causes the conduction electrons to move in the $-x$ direction, colliding with stationary atoms of the conductor, thus producing a net pressure on the conductor. The force on a square element l by l of thickness dx is given by $(\mathbf{J} \times \mathbf{H}_i)l^2 dx$ and thus the total force on the conductor is

$$\mathbf{F} = l^2 \int_0^{-\infty} (\mathbf{J} \times \mathbf{H}_i) dx \quad (32)$$

(End of worked example.)

See also Probs. 16-30 and 16-31.

PROBLEMS

16-1 Show that $\nabla \times \mathbf{E} = -\partial \mathbf{B}/\partial t$ and $\nabla \cdot \mathbf{B} = 0$ can both be expressed in four-dimensional form as

$$\sum_{m=1}^4 \frac{\partial F_{mn}}{\partial x_m} = 0 \quad m = 1, 2, 3, 4$$

16-2 Show that

$$\nabla \cdot \mathbf{A} = -\frac{1}{c^2} \frac{\partial V}{\partial t}$$

can be expressed as

$$\sum_{m=1}^4 \frac{\partial V_m}{\partial x_m} = 0$$

where $V_1 = A_x$, $V_2 = A_y$, $V_3 = A_z$, $V_4 = jV/c$.

16-3 Show that the force \mathbf{F}' on a point charge q moving in a stationary electric field \mathbf{E} and magnetic field \mathbf{B} is given by the components

$$\begin{aligned}\mathbf{F}'_z &= q\gamma[\mathbf{E}_z + (\mathbf{v} \times \mathbf{B})] \\ \mathbf{F}'_x &= qE_x\end{aligned}$$

16-4 Show that $(\nabla \times \mathbf{E}) \times \mathbf{D}$ can be expressed as $\nabla \cdot (\bar{\mathbf{T}}_{kl})_z - \mathbf{E}(\nabla \cdot \mathbf{D})$. Hint: After expanding $(\nabla \times \mathbf{E}) \times \mathbf{D}$ add and subtract terms like $E_x \partial E_x / \partial x$, $E_x \partial E_y / \partial y$, $E_x \partial E_z / \partial z$ from each component and regroup. Note further that the divergence of a nine-component tensor such as $\bar{\mathbf{T}}_{kl}$ is defined as

$$\begin{aligned}\nabla \cdot \bar{\mathbf{T}}_{kl} &= \mathfrak{x} \left(\frac{\partial T_{xx}}{\partial x} + \frac{\partial T_{xy}}{\partial y} + \frac{\partial T_{xz}}{\partial z} \right) \\ &\quad + \mathfrak{y} \left(\frac{\partial T_{yx}}{\partial x} + \frac{\partial T_{yy}}{\partial y} + \frac{\partial T_{yz}}{\partial z} \right) \\ &\quad + \mathfrak{z} \left(\frac{\partial T_{zx}}{\partial x} + \frac{\partial T_{zy}}{\partial y} + \frac{\partial T_{zz}}{\partial z} \right)\end{aligned}$$

Thus, the divergence of a nine-component tensor is a vector.

16-5 Show that each element of the Maxwell stress tensor $\bar{\mathbf{T}}_{mn}$ has the dimensions of force per unit area or energy per unit volume.

16-6 Show that the electric field \mathbf{E} of a charge e moving with a uniform velocity \mathbf{v} is given by

$$\mathbf{E} = \mathfrak{k} \frac{e}{4\pi\epsilon_0 r^2} \frac{1 - \beta^2}{(1 - \beta^2 \sin^2 \phi)^{3/2}}$$

where \mathbf{r} = radius vector from charge to point for which \mathbf{E} is given

ϕ = angle between \mathbf{r} and \mathbf{v}

$\beta = v/c$

Note that when $v = 0$, this reduces to $\mathbf{E} = \mathfrak{k}e/4\pi\epsilon_0 r^2$, as given in Chap. 2 for a static charge.

16-7 Show that the magnetic field \mathbf{B} of a charge e moving with a uniform velocity \mathbf{v} is given by

$$\mathbf{B} = \frac{\mu}{4\pi} \frac{e(\mathbf{v} \times \mathbf{r})}{r^3} \frac{1 - \beta^2}{(1 - \beta^2 \cos^2 \phi)^3}$$

where \mathbf{r} = radius vector from charge to point for which \mathbf{B} is given

ϕ = angle between \mathbf{r} and \mathbf{v}

$\beta = v/c$

Note that for $v \ll c$ this reduces to

$$d\mathbf{B} = \frac{\mu}{4\pi} \frac{\mathbf{J} \times \mathbf{r}}{r^3} dv$$

as given in Chap. 5 for a steady current of density \mathbf{J} . (dv is a volume element.)

16-8 Show that $a_1 = a_4 = \gamma$ and $a_3 = -v\gamma/c^2$ in (16-4-28), where $\gamma = 1/\sqrt{1 - (v/c)^2}$.

16-9 Prove (16-2-1) and (16-2-2).

16-10 A stationary observer determines that a certain region of space contains a static electric field $E_z = 10 \text{ V m}^{-1}$. How does this field appear to an observer moving through the region in the positive y direction with a velocity of (a) 10 m s^{-1} , (b) 10^4 m s^{-1} , (c) 10^7 m s^{-1} , (d) 10^8 m s^{-1} , and (e) $3 \times 10^8 \text{ m s}^{-1}$?

16-11 Repeat Prob. 10-10 for the case where the stationary observer determines that the region contains a time-varying electric field as given by $E_z = 10 \sin 20\pi t (\text{V m}^{-1})$, where t = time in seconds.

* **16-12** A stationary observer determines that a certain region of space contains a static magnetic field $B_x = \mu_0/12\pi (\text{T})$. How does this field appear to an observer moving through the region in the positive y direction with a velocity of (a) 10 m s^{-1} , (b) 10^4 m s^{-1} , (c) 10^7 m s^{-1} , (d) 10^8 m s^{-1} , and (e) $3 \times 10^8 \text{ m s}^{-1}$?

16-13 Repeat Prob. 16-12 for the case where the stationary observer determines that the region contains a time-varying magnetic field as given by $B_x = (\mu_0/12\pi) \sin 20\pi t (\text{T})$, where t = time in seconds.

* **16-14** A stationary observer determines that a certain region of space contains a static electric field $E_z = 10 \text{ V m}^{-1}$ and a static magnetic field $B_x = \mu_0/12\pi (\text{T})$. How do these field components appear to an observer moving through the region in the positive y direction with a velocity of (a) 10 m s^{-1} , (b) 10^4 m s^{-1} , (c) 10^7 m s^{-1} , (d) 10^8 m s^{-1} , and (e) $3 \times 10^8 \text{ m s}^{-1}$?

16-15 (a) A plane linearly polarized wave is traveling in the positive y direction. A stationary observer determines that its peak electric and magnetic fields are $E_z = 10 \text{ V m}^{-1}$ and $B_z = \mu_0/12\pi (\text{T})$, respectively. How does this wave appear to an observer traveling in the positive y direction at the same velocity ($v = c$, that is, riding along with the wave)? (b) What difference would it make to the observer if the wave were circularly polarized?

16-16 A point charge of 1 C is situated at the origin. How does this point charge appear to a moving observer traveling in the positive y direction at a constant distance $z = 10 \text{ m}$ if the observer velocity is (a) 10 m s^{-1} , (b) 10^4 m s^{-1} , (c) 10^7 m s^{-1} , (d) 10^8 m s^{-1} , and (e) $3 \times 10^8 \text{ m s}^{-1}$?

16-17 An electric current of 10 A is flowing in the positive y direction. How does this current appear to a moving observer traveling in the positive y direction at a constant distance $z = 10 \text{ m}$ from the current if the observer velocity is (a) 10 m s^{-1} , (b) 10^4 m s^{-1} , (c) 10^7 m s^{-1} , (d) 10^8 m s^{-1} , and (e) $3 \times 10^8 \text{ m s}^{-1}$?

* **16-18** A plane wave in free space is incident normally on a perfectly conducting flat sheet. If the Poynting vector of the wave is 1 kW m^{-2} , what is the pressure (in kilograms per square meter) exerted by the wave on the sheet?

16-19 (a) Can an antenna be used for propulsion of a space vehicle? (b) If so what power must be radiated to produce a thrust of 1 N ?

16-20 (a) If radio sources all have the same power output and are distributed uniformly throughout space, show that the number N observed by a radio telescope at a flux density equal to or greater than S should conform to the $\frac{1}{2}$ power relation $N \propto S^{-3/2}$. (b)

* Answers to starred problems are given in Appendix C.

Discuss the effect of the following factors in producing a reduction in the observed number N at low values of flux density S : (1) radio-telescope resolution, (2) radio-telescope sensitivity, (3) velocity of recession of sources, (4) absorption by the medium, and (5) actual reduction in source density at large distances. In factor 3 assume that the velocity of recession of a source increases in proportion to its distance.

16-21 At the earth's distance from the sun the sun's electromagnetic radiation amounts to about 1.5 kW m^{-2} (mostly in optical and infrared regions) while the solar wind consists mainly of protons with velocities of about 1 Mm s^{-1} and densities of about 2×10^7 protons per cubic meter. (a) Compare the radiation pressure in newtons per square meter of the electromagnetic radiation with that of the solar wind on a flat uncharged conducting sheet normal to the radiation and wind direction. (b) Can either the radiation or the wind be used to propel an interplanetary vehicle? (c) If so how much sail (square meters) is required to develop 100 N thrust downwind, and (d) how much is required cross wind (traveling perpendicular to wind direction)?

16-22 A plane 5-GHz wave with power flux (Poynting vector) of 10 W m^{-2} is traveling in the positive y direction. The wave is incident normally on a large flat perfectly conducting sheet (sheet is parallel to the xz plane). Find the pressure on the sheet if the sheet is (a) stationary and (b) moving in the positive y direction with a velocity $v = c/5$. (c) What is the Poynting vector of the reflected wave for the two cases? (d) What is the frequency of the reflected wave for the two cases?

* 16-23 A spacecraft leaves the earth and travels directly away from the earth at a velocity $v = 0.8c$. After it reaches a distance 8 light-years from the earth, a radio signal is transmitted from the craft back to the earth. (a) How long after the craft departs is the signal received on earth? (b) How much time has elapsed on the spacecraft since departure when the signal is sent from it? (c) From the spacecraft point of view how much time appears to have elapsed on the earth when the signal is sent, and (d) when the signal is received there? (e) Draw a space-time diagram with appropriate lines to illustrate the problem and its solution.

16-24 A spacecraft receding from an observer at a velocity v emits a radio signal with Poynting vector S_{em} measured in the rest frame of the craft. Show that the observed Poynting vector is given by

$$S_{obs} = S_{em} \frac{[1 - (v/c)]^2}{1 - (v/c)^2} = S_{em} \frac{1 - (v/c)}{1 + (v/c)} \quad (\text{W m}^{-2})$$

16-25 If the craft of Prob. 16-24 emits the signal at a frequency f_e as measured on the craft, show that the observed frequency is given by

$$f_o = f_e \frac{\sqrt{1 - (v/c)^2}}{1 + (v/c)} \quad \text{or} \quad \frac{f_e}{f_o} = \frac{1 + (v/c)}{1 - (v/c)^2} = 1 + z$$

where z is the doppler, or red, shift. Thus, the red shift is

$$z = \frac{1 + (v/c)}{\sqrt{1 - (v/c)^2}} - 1$$

16-26 From Probs. 16-24 and 16-25 show that

$$S_{\text{em}} = S_{\text{obs}}(1+z)^2 \quad (\text{W m}^{-2})$$

16-27 From Probs. 16-24 and 16-25 show that

$$S'_{\text{em}} = S'_{\text{obs}}(1+z) \quad (\text{W m}^{-2} \text{ Hz}^{-1})$$

16-28 If the radiation from the craft is emitted over a continuous spectrum (not monochromatic) with spectral index α defined by $S \propto f^{-\alpha}$, show that the Poynting vector per unit bandwidth ($\text{W m}^{-2} \text{ Hz}^{-1}$) in the rest frame of the craft at the emitted frequency f_e is

$$S'_{e0} = S'_{\text{obs}}(1+z)^{\alpha+1} \quad (\text{W m}^{-2} \text{ Hz}^{-1})$$

* *16-29* Two spaceships traveling in opposite directions away from the earth have a velocity of $0.7c$ as measured by an earth observer. What is the velocity of one spaceship as observed from the other?

16-30 Show that the radiation pressure ($= \mu H^2$) of a wave incident on a perfect conductor is equal to the force on a unit area caused by the reversal in momentum when the wave is reflected. *Hint:* Consider the mass equivalent of a wave column using Einstein's relation: energy $= mc^2$.

16-31 What is the radiation pressure of a wave incident on a medium with intrinsic impedance $Z = Z_0$ so that the wave is entirely absorbed?

APPENDIX A

UNITS, CONSTANTS, AND A FEW MATHEMATICAL RELATIONS

A-1 UNITS

Multiples and submultiples of the basic units are designated by the prefixes listed in Table 1. Note that in the SI system, multiples and submultiples are in steps of 10^3 or 10^{-3} . Larger or smaller quantities are designated by the exponential form. For a discussion of dimensions and units see Secs. 1-2 to 1-4.

Table 1

Prefix	Abbreviation	Magnitude	Derivation
tera (tēr'ā)	T	10^{12}	Greek <i>teras</i> , "monster"
giga (jī'gā)	G	10^9	Latin <i>gigas</i> , "giant"
mega (mēg'ā)	M	10^6	Greek <i>megas</i> , "great"
kilo (kil'ō)	k	10^3	Greek <i>chilioi</i> , "a thousand"
milli (mīl'ī)	m	10^{-3}	Latin <i>mille</i> , "a thousand"
micro (mī' krō)	μ	10^{-6}	Greek <i>mikros</i> , "small"
nano (nān'ō)	n	10^{-9}	Greek <i>nanos</i> , "dwarf"
pico (pē' kō)	p	10^{-12}	Spanish <i>pico</i> , "small quantity"
femto (fēm' tō)	f	10^{-15}	Danish <i>femten</i> , "fifteen"
atto (āt' tō)	a	10^{-18}	Danish <i>atten</i> , "eighteen"

In Table 2 dimensions or quantities commonly used in electromagnetics are listed alphabetically under the headings Fundamental, Mechanical, Electrical, and Magnetic. In the *first* column the name of the dimension or quantity is given and in the *second* column the common symbol for designating it. In the *third* column (Description) the dimension is described in terms of the fundamental dimensions (mass, length, time, and electric current) or other secondary dimensions. In the *fourth* column (SI unit) lists the SI unit and abbreviation, and the *fifth* column gives equivalent units. The *last* column indicates the fundamental dimensions by means of the symbols *M* (mass), *L* (length), *T* (time), and *I* (electric current).

Table 2

Fundamental units					
Name of dimension or quantity	Symbol	Description	SI unit and abbreviation	Equivalent units	Dimension
Current	<i>I</i>	charge time	ampere (A)	6.25 electron charges per second = $\frac{C}{s}$	<i>I</i>
Length	<i>L, l</i>		meter (m)	1,000 mm = 100 cm	<i>L</i>
Mass	<i>M, m</i>		kilogram (kg)	1,000 g	<i>M</i>
Time	<i>T, t</i>		second (s)	$\frac{1}{60}$ min = $\frac{1}{3,600}$ hr $= \frac{1}{86,400}$ day	<i>T</i>

Table 2—(Continued)

Mechanical units

Name of dimension or quantity	Symbol	Description	SI unit and abbreviation	Equivalent units	Dimension
Acceleration	a	$\frac{\text{velocity}}{\text{time}} = \frac{\text{length}}{\text{time}^2}$	meter second ⁻² (m s^{-2})	N kg	$\frac{L}{T^2}$
Area	A, a, s	length ²	meter ² (m^2)		L^2
Energy or work	W	force \times length = power \times time	joule (J)	$\text{N m} = \text{W s} = \text{V C}$ $= 10^7 \text{ ergs}$ $= 10^8 \text{ dynes mm}$	$\frac{ML^2}{T^2}$
Energy density	w	energy volume	joule meter ⁻³ (J m^{-3})	$\frac{1}{100} \text{ erg mm}^3$	$\frac{M}{LT^2}$
Force	F	mass \times acceleration	newton (N)	$\frac{\text{kg m}}{\text{s}^2} = \frac{\text{J}}{\text{m}}$ $= 10^5 \text{ dynes}$	$\frac{ML}{T^2}$
Frequency	f	cycles time	hertz (Hz)	cycles s	$\frac{1}{T}$
Length	L, l		meter (m)	1,000 mm $= 100 \text{ cm}$	L
Mass	M, m		kilogram (kg)	1,000 g	M
Moment (torque)		force \times length	newton-meter (N m)	$\frac{\text{kg m}^2}{\text{s}} = \text{J}$	$\frac{ML^2}{T^2}$
Momentum	mv	mass \times velocity = force \times time = energy velocity	newton-second (N s)	$\frac{\text{kg m}}{\text{s}} = \frac{\text{J s}}{\text{m}}$	$\frac{ML}{T}$
Period	T	1 frequency	second (s)		T
Power	P	force \times length time = energy time	watt (W)	$\frac{\text{J}}{\text{s}} = \frac{\text{N m}}{\text{s}}$ $= \frac{\text{kg m}^2}{\text{s}^3}$	$\frac{ML^2}{T^3}$

Table 2 Mechanical units—(Continued)

Name of dimension or quantity	Symbol	Description	SI unit and abbreviation	Equivalent units	Dimension
Time	T, t		second (s)	$\frac{1}{60} \text{ min} = \frac{1}{3,600} \text{ hr}$ $= \frac{1}{86,400} \text{ day}$	T
Velocity (velocity of light in vacuum = 300 Mm s ⁻¹)	v	length / time	meter second (m s ⁻¹)		$\frac{L}{T}$
Volume	v	length ³	meter ³ (m ³)		L^3

Electrical units

Admittance	Y	1 impedance	mho (Ω)	$\frac{A}{V} = \frac{C^2}{J s} = S \dagger$	$\frac{I^2 T^3}{ML^2}$
Capacitance	C	charge potential	farad (F)	$\frac{C}{V} = \frac{C^2}{J} = \frac{As}{V}$ $= 9 \times 10^{11} \text{ cm}$ (cgs esu)	$\frac{I^2 T^4}{ML^2}$
Charge	Q, q	current × time	coulomb (C)	$6.25 \times 10^{18} \text{ electron charges}$ $= A s$ $= 3 \times 10^9$ cgs esu $= 0.1 \text{ cgs emu}$	IT
Charge (volume) density	ρ	charge volume = $\nabla \cdot D$	coulomb meter ³ (C m ⁻³)	$\frac{A s}{m^3}$	$\frac{IT}{L^3}$
Conductance	G	1 resistance	mho (Ω)	$\frac{A}{V} = \frac{C^2}{J s}$	$\frac{IT^3}{ML^2}$
Conductivity	σ	1 resistivity	mho meter (Ω m ⁻¹)	$\frac{1}{\Omega m}$	$\frac{I^2 T^4}{ML^3}$
Current	I, i	charge time	ampere (A)	$\frac{C}{s} = 3 \times 10^9$ cgs esu $= 0.1 \text{ cgs emu}$	I

[†] S is the SI abbreviation for siemens, used outside the United States for mho.

Table 2 Electrical units—(Continued)

Name of dimension or quantity	Symbol	Description	SI unit and abbreviation	Equivalent units	Dimension
Current density	J	$\frac{\text{current}}{\text{area}}$	ampere meter ² (A m ⁻²)	$\frac{\text{C}}{\text{s m}^2}$	$\frac{I}{L^2}$
Dipole moment	$p (= ql)$	charge \times length	coulomb-meter (C m)	A s m	$LI T$
Emf	ψ	$\int \mathbf{E}_e \cdot d\mathbf{l}$	volt (V)	$\frac{\text{Wb}}{\text{s}} = \frac{\text{J}}{\text{C}}$	$\frac{ML^2}{IT^3}$
Energy density (electric)	w_e	$\frac{\text{energy}}{\text{volume}}$	joule meter ³ (J m ⁻³)	$\frac{1}{100} \frac{\text{erg}}{\text{mm}^3}$	$\frac{M}{LT^2}$
Field intensity (E vector)	\mathbf{E}	$\frac{\text{potential}}{\text{length}} = \frac{\text{force}}{\text{charge}}$	volt meter (V m ⁻¹)	$\frac{\text{N}}{\text{C}} = \frac{\text{J}}{\text{C m}}$ $= \frac{1}{2} \times 10^{-4}$ cgs esu $= 10^6$ cgs emu	$\frac{ML}{IT^3}$
Flux	ψ	charge $= \iint \mathbf{D} \cdot d\mathbf{s}$	coulomb (C)	A s	IT
Flux density (displacement) (D vector)	\mathbf{D}	$\frac{\text{charge}}{\text{area}}$	coulomb meter ² (C m ⁻²)	$\frac{\text{A s}}{\text{m}^2} = \frac{\text{A}}{\text{m}^2 \text{s}^{-1}}$	$\frac{IT}{L^2}$
Impedance	Z	$\frac{\text{potential}}{\text{current}}$	ohm (Ω)	$\frac{\text{V}}{\text{A}}$	$\frac{ML^2}{I^2 T^3}$
Linear charge density	ρ_L	$\frac{\text{charge}}{\text{length}}$	coulomb meter (C m ⁻¹)	$\frac{\text{A s}^{-1}}{\text{m}}$	$\frac{IT}{L}$
Permittivity (dielectric constant) (for vacuum, $\epsilon_0 = 8.85 \text{ pF} \approx 10^{-9}/36\pi \text{ F m}^{-1}$)	ϵ	capacitance length	farad meter (F m ⁻¹)	$\frac{\text{C}}{\text{V m}}$	$\frac{I^2 T^4}{ML^3}$

Table 2 Electrical units—(Continued)

Name of dimension or quantity	Symbol	Description	SI unit and abbreviation	Equivalent units	Dimension
Polarization	P	dipole moment volume	coulomb meter ² (C m ⁻²)	A s m ²	$\frac{IT}{L^2}$
Potential	V	work charge	volt (V)	$\frac{J}{C} = \frac{N\ m}{C} = \frac{W\ s}{C}$ $= \frac{W}{A} = \frac{Wb}{s}$ $= \frac{1}{300} \text{ cgs esu}$ $= 10^8 \text{ cgs emu}$	$\frac{ML^2}{IT^3}$
Poynting vector	S	power area	watt meter ² (W m ⁻²)	J s m ²	$\frac{M}{T^3}$
Radiation intensity	P	power unit solid angle	watt steradian (W sr ⁻¹)		$\frac{ML^2}{T^3}$
Reactance	X	potential current	ohm (Ω)	V A	$\frac{ML^2}{I^2 T^3}$
Relative permittivity	ϵ_r	ratio $\frac{\epsilon}{\epsilon_0}$			dimensionless
Resistance	R	potential current	ohm (Ω)	$\frac{V}{A} = \frac{Js}{C^2}$ $= \frac{1}{4\pi} \times 10^{-11}$ cgs esu $= 10^{-9}$ cgs emu	$\frac{ML^2}{I^2 T^3}$
Resistivity	s	resistance \times length $= \frac{1}{conductivity}$	ohm-meter, (Ω m)	V m A	$\frac{ML^3}{I^2 T^3}$
Sheet-current density	K	current length	ampere meter (A m ⁻¹)	$\frac{A}{m^2} \times m$	$\frac{I}{L}$

Table 2 Electrical units—(Continued)

Name of dimension or quantity	Symbol	Description	SI unit and abbreviation	Equivalent units	Dimension
Susceptance	B	$\frac{1}{\text{reactance}}$	mho (Ω)	$\frac{\text{A}}{\text{V}}$	$\frac{I^2 T^3}{ML^2}$
Wavelength	λ	length	meter (m)		L

Magnetic units

Dipole moment (magnetic)	m (= $Q_m l$)	pole strength \times length = current \times area $= \frac{\text{torque}}{\text{magnetic flux density}}$	ampere-meter ² ($A m^2$)	$\frac{C m^2}{s}$	IL^2
Energy density (magnetic)	w_m	$\frac{\text{energy}}{\text{volume}}$	joule meter ³ ($J m^{-3}$)	$\frac{1}{100} \frac{\text{erg}}{\text{mm}^3}$	$\frac{M}{LT^2}$
Flux (magnetic)	ψ_m	$\iint \mathbf{B} \cdot d\mathbf{s}$	weber (Wb)	$V s = \frac{n m}{A}$ $= 10^8 \text{ Mx} \ddagger$ (cgs emu)	$\frac{ML^2}{IT^2}$
Flux density (B vector)	\mathbf{B}	$\frac{\text{force}}{\text{pole}} = \frac{\text{force}}{\text{current moment}}$ $= \frac{\text{magnetic flux}}{\text{area}}$	telsa (T) $= \frac{\text{weber}}{\text{meter}^2}$ ($Wb m^{-2}$)	$\frac{Vs}{m^2} = \frac{N}{Am}$ $= 10^4 \text{ G} \ddagger$ (cgs emu)	$\frac{M}{IT^2}$
Flux linkage	Λ	flux \times turns	weber-turn (Wb turn)		$\frac{ML^2}{IT^2}$
H field (H vector)	\mathbf{H}	mmf length	ampere meter ($A m^{-1}$)	$\frac{N}{Wb} = \frac{W}{Vm}$ $= 4\pi \times 10^{-3}$ $Oe \ddagger$ (cgs emu) $= 400\pi$ gammas	$\frac{I}{L}$

 \ddagger Mx, G, and Oe are SI abbreviations for maxwell, gauss, and oersted.

Table 2 Magnetic units—(Continued)

Name of dimension or quantity	Symbol	Description	SI unit and abbreviation	Equivalent units	Dimension
Inductance	L	<u>magnetic flux linkage</u> current	henry (H)	$\frac{\text{Wb}}{\text{A}} = \frac{\text{J}}{\text{A}^2}$ $= \Omega \text{ s}$ $= \frac{1}{2} \times 10^{-11} \text{ cgs esu}$ $= 10^9 \text{ cm}$ (cgs emu)	$\frac{ML^2}{I^2T^2}$
Magnetization (magnetic polarization)	M	<u>magnetic moment</u> volume	ampere meter (A m^{-1})	$\frac{\text{A m}^2}{\text{m}^3} = \frac{\text{A m}}{\text{m}^2}$	$\frac{I}{L}$
Mmf	F	$\int \mathbf{H} \cdot d\mathbf{l}$	ampere-turn (A turn)	$\frac{\text{C}}{\text{s}}$	
Permeability (for vacuum $\mu_0 = 400\pi \text{ nH m}^{-1}$)	μ	<u>inductance</u> length	henry meter (H m^{-1})	$\frac{\text{Wb}}{\text{A m}} = \frac{\text{V s}}{\text{A m}}$	$\frac{ML}{I^2T^2}$
Permeance	ϕ	<u>magnetic flux</u> mmf $= \frac{1}{\text{reluctance}}$	henry (H)	$\frac{\text{Wb}}{\text{A}}$	$\frac{ML^2}{I^2T^2}$
Pole density	ρ_m	<u>pole strength</u> volume $= \frac{\text{current}}{\text{area}}$ $= \nabla \cdot \mathbf{H} = -\nabla \cdot \mathbf{M}$	ampere meter ² (A m^{-2})		$\frac{I}{L^2}$
Pole strength	Q_m, q_m	current \times length $= \iiint \rho_m dv$	ampere-meter (A m)	$\frac{\text{C m}}{\text{s}}$	IL
Potential (magnetic) (for \mathbf{H})	U	$\int \mathbf{H} \cdot d\mathbf{l}$	ampere (A)	$\frac{\text{J}}{\text{Wb}} = \frac{\text{W}}{\text{V}} = \frac{\text{C}}{\text{s}}$ $= \frac{4\pi}{10} \text{ Gb} \S$ (cgs emu)	I

\S Gb is the SI abbreviation for gilbert.

Table 2 Magnetic units—(Continued)

Name of dimension or quantity	Symbol	Description	SI unit and abbreviation	Equivalent units	Dimension
Relative permeability	μ_r	ratio $\frac{\mu}{\mu_0}$			Dimensionless
Reluctance	\mathcal{R}	$\frac{\text{mmf}}{\text{magnetic flux}}$ $= \frac{1}{\text{permeance}}$	$\frac{1}{\text{henry}}$ (H^{-1})	$\frac{\text{A}}{\text{Wb}}$	$\frac{I^2 T^2}{ML^2}$
Vector potential	\mathbf{A}	current \times permeability	$\frac{\text{Weber}}{\text{meter}}$ (Wb m^{-1})	$\frac{\text{H A}}{\text{m}} = \frac{\text{N}}{\text{A}}$	$\frac{ML}{IT^2}$

A-2 CONSTANTS AND CONVERSIONS

Quantity	Symbol or abbreviation	Nominal value	More accurate value†
Astronomical unit	AU	1.5×10^8 km	1.496
Boltzmann's constant	k	1.38×10^{-23} J K ⁻¹	1.38062×10^{-23}
Earth mass		6.0×10^{24} kg	5.98×10^{24}
Earth radius (average)		6.37 Mm	
Electron charge	e	-1.60×10^{-19} C	-1.602
Electron rest mass	m	9.11×10^{-31} kg	9.10956×10^{-31}
Electron charge-to-mass ratio	e/m	1.76×10^{11} C kg ⁻¹	1.758803×10^{11}
Flux unit	fu	10^{-26} W m ⁻² Hz ⁻¹	10^{-26} (by definition)
Foot	ft	0.30 m (1 m = 3.281 ft)	0.3048
Foot squared	ft ²	9.3×10^{-2} m ² (1 m ² = 10.76 ft ²)	9.290×10^{-2}
Light-second		300 Mm (≈ 1 Gft)	
Light, velocity of	c	300 Mm s ⁻¹ (≈ 1 Gft s ⁻¹)	299.7925
Light-year	LY	9.46×10^{12} km	9.4605×10^{12}
Logarithm (natural) base	e	2.72	2.71828
Logarithm, reciprocal of base	$1/e$	0.368	0.36788
Logarithm conversion		$\ln x = 2.3 \log x$ $\log x = 0.43 \ln x$	$\ln x = 2.3026 \log x$ $\log x = 0.4343 \ln x$
Mile (statute)	mi	1.61 km (1 km = 0.6214 mi)	1.60935
Moon distance (average)		380 Mm	
Moon mass		6.7×10^{22} kg	
Moon radius (average)		1.738 Mm	
Permeability of vacuum	μ_0	1,260 nH m ⁻¹	400π (exact value)
Permittivity of vacuum	ϵ_0	8.85 pF m ⁻¹	$8.854185 = 1/\mu_0 c^2$
Pi	π	3.14	3.1415927
Pi squared	π^2	9.87	9.8696044
Planck's constant	h	6.63×10^{-34} J s	6.62620×10^{-34}
Proton rest mass		1.67×10^{-27} kg	1.67261×10^{-27}
Radian	rad	57.3°	57.2958°
Space, impedance of	Z	376.7 ($\approx 120\pi$) Ω	$376.7304 = \mu_0 c$
Sphere, solid angle		12.6 sr	$4\pi = 12.5664$
Square degree	deg ²	$41,253$ deg ²	41,252.96
		3.05×10^{-4} sr	3.04617×10^4
Steradian (square radian)	sr	3,283 deg ²	$(180/\pi)^2 = 3,282.81$
Sun, distance	AU	1.5×10^8 km	1.496×10^8
Sun mass	M_\odot	2.0×10^{30} kg	1.99×10^{30}
Sun radius (average)	R_\odot	700 Mm	695.3
	$\sqrt{2}$	1.414	1.41421
	$\sqrt{3}$	1.73	1.73205
	$\sqrt{10}$	3.16	3.16228

† Same units as nominal value. Regarding permittivity ϵ_0 and space impedance Z note that the values for these quantities are determined by the exact (definition) value of μ_0 and the measured value of c (velocity of light).

A-3 TRIGONOMETRIC RELATIONS

$$\sin(x \pm y) = \sin x \cos y \pm \cos x \sin y$$

$$\cos(x \pm y) = \cos x \cos y \mp \sin x \sin y$$

$$\sin(x + y) + \sin(x - y) = 2 \sin x \cos y$$

$$\cos(x + y) + \cos(x - y) = 2 \cos x \cos y$$

$$\sin(x + y) - \sin(x - y) = 2 \cos x \sin y$$

$$\cos(x + y) - \cos(x - y) = -2 \sin x \sin y$$

$$\sin 2x = 2 \sin x \cos x$$

$$\cos 2x = \cos^2 x - \sin^2 x = 2 \cos^2 x - 1 = 1 - 2 \sin^2 x$$

$$\cos x = 2 \cos^2 \frac{1}{2}x - 1 = 1 - 2 \sin^2 \frac{1}{2}x$$

$$\sin x = 2 \sin \frac{1}{2}x \cos \frac{1}{2}x$$

$$\sin^2 x + \cos^2 x = 1$$

$$\tan(x + y) = \frac{\tan x + \tan y}{1 - \tan x \tan y}$$

$$\tan(x - y) = \frac{\tan x - \tan y}{1 + \tan x \tan y}$$

$$\tan 2x = \frac{2 \tan x}{1 - \tan^2 x}$$

$$\sin x = x - \frac{x^3}{3!} + \frac{x^5}{5!} - \frac{x^7}{7!} + \dots$$

$$\cos x = 1 - \frac{x^2}{2!} + \frac{x^4}{4!} - \frac{x^6}{6!} + \dots$$

$$\tan x = x + \frac{x^3}{3} + \frac{2x^5}{15} + \frac{17x^7}{315} + \frac{62x^9}{2,835} + \dots$$

A-4 HYPERBOLIC RELATIONS

$$\sinh x = \frac{e^x - e^{-x}}{2} = x + \frac{x^3}{3!} + \frac{x^5}{5!} + \frac{x^7}{7!} + \dots$$

$$\cosh x = \frac{e^x + e^{-x}}{2} = 1 + \frac{x^2}{2!} + \frac{x^4}{4!} + \frac{x^6}{6!} + \dots$$

$$\tanh x = \frac{\sinh x}{\cosh x}$$

$$\coth x = \frac{\cosh x}{\sinh x} = \frac{1}{\tanh x}$$

$$\sinh(x \pm iy) = \sinh x \cos y \pm j \cosh x \sin y$$

$$\cosh(x \pm iy) = \cosh x \cos y \pm j \sinh x \sin y$$

$$\cosh(jx) = \frac{1}{2}(e^{+jx} + e^{-jx}) = \cos x \quad \text{de Moivre's theorem}$$

$$\sinh(jx) = \frac{j}{2}(e^{+jx} - e^{-jx}) = j \sin x$$

$$e^{\pm jx} = \cos x \pm j \sin x$$

$$e^{\pm jx} = 1 \pm jx - \frac{x^2}{2!} \mp j \frac{x^3}{3!} + \frac{x^4}{4!} \pm j \frac{x^5}{5} - \dots$$

$$e^x = \cosh x + \sinh x$$

$$e^{-x} = \cosh x - \sinh x$$

$$e^x = 1 + x + \frac{x^2}{2!} + \frac{x^3}{3!} + \frac{x^4}{4!} + \dots$$

$$\cosh x = \cos jx$$

$$j \sinh x = \sin jx$$

$$\tanh(x \pm jy) = \frac{\sinh 2x}{\cosh 2x + \cos 2y} \pm j \frac{\sin 2y}{\cosh 2x + \cos 2y}$$

$$\coth(x \pm jy) = \frac{\sinh 2x}{\cosh 2x - \cos 2y} \pm j \frac{\sin 2y}{\cosh 2x - \cos 2y}$$

A-5 LOGARITHMIC RELATIONS

$$\log_{10} x = \log x \quad \text{common logarithm}$$

$$\log_e x = \ln x \quad \text{natural logarithm}$$

$$\log_{10} x = 0.4343 \log_e x = 0.4343 \ln x$$

$$\ln x = \log_e x = 2.3026 \log_{10} x$$

$$e = 2.71828$$

A-6 APPROXIMATION FORMULAS FOR SMALL QUANTITIES

(δ is a small quantity compared with unity)

$$(1 \pm \delta)^2 = 1 \pm 2\delta$$

$$(1 \pm \delta)^n = 1 \pm n\delta$$

$$\sqrt{1 + \delta} = 1 + \frac{1}{2}\delta$$

$$\frac{1}{\sqrt{1 + \delta}} = 1 - \frac{1}{2}\delta$$

$$e^\delta = 1 + \delta$$

$$\ln(1 + \delta) = \delta$$

$$J_n(\delta) = \frac{\delta^n}{n! 2^n} \quad \text{for } |\delta| \ll 1$$

where J_n is Bessel function of order n . Thus

$$J_1(\delta) = \frac{\delta}{2}$$

A-7 SERIES

Binomial:

$$(x+y)^n = x^n + nx^{n-1}y + \frac{n(n-1)}{2!} x^{n-2}y^2 + \frac{n(n-1)(n-2)}{3!} x^{n-3}y^3 + \dots$$

$$\text{Taylor's: } f(x+y) = f(x) + \frac{df(x)}{dx} \frac{y}{1} + \frac{d^2f(x)}{dx^2} \frac{y^2}{2!} + \frac{d^3f(x)}{dx^3} \frac{y^3}{3!} + \dots$$

A-8 SOLUTION OF QUADRATIC EQUATION

If $ax^2 + bx + c = 0$, then

$$x = \frac{-b \pm \sqrt{b^2 - 4ac}}{2a}$$

A-9 VECTOR IDENTITIES

(F , f , G , and g are scalar functions; \mathbf{F} , \mathbf{G} , and \mathbf{H} are vector functions.)

$$\mathbf{F} \cdot \mathbf{G} = FG \cos \theta \quad \text{scalar (or dot) product}$$

where $\theta = \cos^{-1}(\mathbf{F} \cdot \mathbf{G})/FG$

$$\mathbf{F} \times \mathbf{G} = \mathbf{\hat{n}}FG \sin \theta \quad \text{vector (or cross) product}$$

where $\theta = \sin^{-1}(\mathbf{F} \times \mathbf{G})/\mathbf{\hat{n}}FG$

$\mathbf{\hat{n}}$ = unit vector normal to plane containing \mathbf{F} and \mathbf{G}

$$\nabla \cdot (\nabla \times \mathbf{F}) = 0 \quad (1)$$

$$\nabla \cdot \nabla f = \nabla^2 f \quad (2)$$

$$\nabla \times \nabla f = 0 \quad (3)$$

$$\nabla(f+g) = \nabla f + \nabla g \quad (4)$$

$$\nabla \cdot (\mathbf{F} + \mathbf{G}) = \nabla \cdot \mathbf{F} + \nabla \cdot \mathbf{G} \quad (5)$$

$$\nabla \times (\mathbf{F} + \mathbf{G}) = \nabla \times \mathbf{F} + \nabla \times \mathbf{G} \quad (6)$$

$$\nabla(fg) = g \nabla f + f \nabla g \quad (7)$$

$$\nabla \cdot (f\mathbf{G}) = \mathbf{G} \cdot (\nabla f) + f(\nabla \cdot \mathbf{G}) \quad (8)$$

$$\nabla \times (f\mathbf{G}) = (\nabla f) \times \mathbf{G} + f(\nabla \times \mathbf{G}) \quad (9)$$

$$\nabla \times (\nabla \times \mathbf{F}) = \nabla(\nabla \cdot \mathbf{F}) - \nabla^2 \mathbf{F} \quad (10)$$

$$\Delta \mathbf{F} = \nabla^2 \mathbf{F} = \hat{x} \nabla^2 F_x + \hat{y} \nabla^2 F_y + \hat{z} \nabla^2 F_z \quad (11)$$

$$\nabla \cdot (\mathbf{F} \times \mathbf{G}) = \mathbf{G} \cdot (\nabla \times \mathbf{F}) - \mathbf{F} \cdot (\nabla \times \mathbf{G}) \quad (12)$$

$$\mathbf{F} \cdot (\mathbf{G} \times \mathbf{H}) = \mathbf{G} \cdot (\mathbf{H} \times \mathbf{F}) = \mathbf{H} \cdot (\mathbf{F} \times \mathbf{G}) \quad (13)$$

$$\nabla \times (\mathbf{F} \times \mathbf{G}) = \mathbf{F}(\nabla \cdot \mathbf{G}) - \mathbf{G}(\nabla \cdot \mathbf{F}) + (\mathbf{G} \cdot \nabla) \mathbf{F} - (\mathbf{F} \cdot \nabla) \mathbf{G} \quad (14)$$

$$\nabla(\mathbf{F} \cdot \mathbf{G}) = (\mathbf{F} \cdot \nabla) \mathbf{G} + (\mathbf{G} \cdot \nabla) \mathbf{F} + \mathbf{F} \times (\nabla \times \mathbf{G}) + \mathbf{G} \times (\nabla \times \mathbf{F}) \quad (15)$$

In the following three relations the surface (left side of equation) encloses the volume (right side of equation)

$$\oint_s f \, ds = \int_v \nabla f \, dv \quad (16)$$

$$\oint_s \mathbf{F} \cdot d\mathbf{s} = \int_v \nabla \cdot \mathbf{F} \, dv \quad \text{divergence theorem} \quad (17)$$

$$\oint_s \hat{n} \times \mathbf{F} \, ds = \int_v \nabla \times \mathbf{F} \, dv \quad (18)$$

In the following two formulas the line integral (left-side of equation) is along a closed path which bounds an unclosed surface (right side of equation)

$$\oint_s f \, dl = \int_s \hat{n} \times \nabla f \, ds \quad (19)$$

$$\oint_s \mathbf{F} \cdot d\mathbf{l} = \int_s (\nabla \times \mathbf{F}) \cdot d\mathbf{s} \quad \text{Stokes' theorem} \quad (20)$$

A-10 RECURRENCE RELATIONS FOR BESSSEL FUNCTIONS

Equations expressing Bessel functions or their derivatives in terms of Bessel functions of the same or different order are called *recurrence formulas* or *relations*. A few of these formulas are listed below for reference.

$$\frac{dJ_\nu(u)}{du} = \frac{\nu}{u} J_\nu(u) - J_{\nu+1}(u) \quad (1)$$

$$\frac{dJ_\nu(u)}{du} = -\frac{\nu}{u} J_\nu(u) + J_{\nu-1}(u) \quad (2)$$

$$\frac{dJ_\nu(u)}{du} = \frac{1}{2} [J_{\nu-1}(u) - J_{\nu+1}(u)] \quad (3)$$

$$J_\nu(u) = \frac{u}{2\nu} [J_{\nu+1}(u) + J_{\nu-1}(u)] \quad (4)$$

$$J_{\nu+1}(u) = \frac{2\nu}{u} J_\nu(u) - J_{\nu-1}(u) \quad (5)$$

From (1) we have for $\nu = n = 0$,

$$\frac{dJ_0(u)}{du} = -J_1(u) \quad (6)$$

That is, the slope of the $J_0(u)$ curve is equal to $-J_1(u)$.

A-11 COORDINATE DIAGRAMS

Diagrams for rectangular, cylindrical, and spherical coordinates are shown in Fig. A-1. The construction for elemental volumes and lengths in the three systems are shown in Fig. A-2. See inside back cover for gradient, divergence, curl, and laplacian in rectangular, cylindrical, spherical, and general curvilinear coordinates.

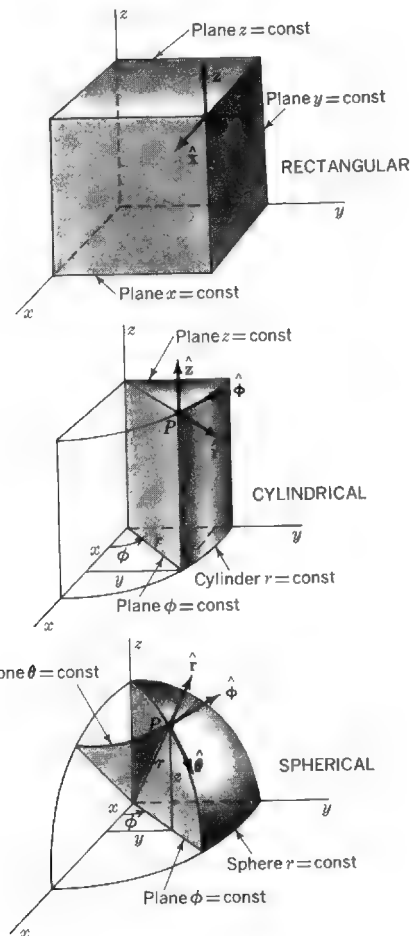
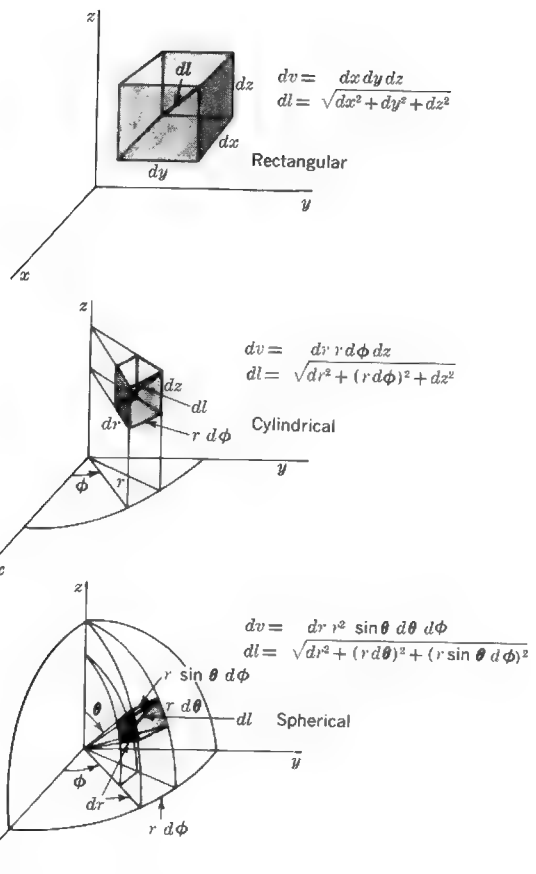


FIGURE A-1
Rectangular, cylindrical, and spherical coordinate systems.

**FIGURE A-2**

Elemental volumes and lengths in rectangular, cylindrical, and spherical coordinate systems.

APPENDIX B

BIBLIOGRAPHY

Footnotes throughout the text include many references to important articles or books on specific topics. The following list provides a few selected general references for supplemental reading.

- BILLINGHAM, J. (ed.): "Project Cyclops: A Design Study of a System for Detecting Extraterrestrial Life," NASA/Ames Research Center (Code LT), Moffett Field, Calif., 1972.
- BOZORTH, R. M.: "Ferromagnetism," D. Van Nostrand Company, Inc., Princeton, N.J., 1951.
- CURY, R., and E. D. ISAAC: "Magnetic Domains and Techniques for Their Observation," Academic Press Inc., New York, 1966.
- ELLIOT, R. S.: "Electromagnetics," McGraw-Hill Book Company, New York, 1966. Provides excellent historical insight.
- FEYNMAN, R. P., R. B. LEIGHTON, and M. SANDS: "Feynman Lectures on Physics," Addison-Wesley Publishing Company, Reading, Mass., 1964.
- HALLIDAY, D., and R. RESNICK: "Physics," John Wiley & Sons, Inc., New York, 1962.
- HARRINGTON, R. F.: "Time-harmonic Electromagnetic Fields," McGraw-Hill Book Company, New York, 1961.
- HAYT, W. H., JR.: "Engineering Electromagnetics," 2d ed., McGraw-Hill Book Company, New York, 1967.
- JASIK, H. (ed.): "Antenna Engineering Handbook," McGraw-Hill Book Company, New York, 1961.

- JORDAN, E. C., and K. D. BALMAIN: "Electromagnetic Waves and Radiative Systems," 2d ed., Prentice-Hall, Inc., Englewood Cliffs, N.J., 1966.
- KING, R. W. P.: "The Theory of Linear Antennas," Harvard University Press, Cambridge, Mass., 1956.
- MAGNUSSON, P. C.: "Transmission Lines and Wave Propagation," 2d ed., Allyn and Bacon, Inc., Boston, 1970.
- MOON, P., and D. E. SPENCER: "Foundations of Electrodynamics," D. Van Nostrand, Company, Inc., Princeton, N.J., 1960.
- MOORE, A. D.: "Fundamentals of Electrical Design," McGraw-Hill Book Co., New York, 1927.
- PLONSEY, R., and R. E. COLLIN: "Principles and Applications of Electromagnetic Fields," McGraw-Hill Book Company, New York, 1961.
- PURCELL, E. M.: "Berkeley Physics Course," vol. 2, "Electricity and Magnetism," McGraw-Hill Book Company, New York, 1965.
- RAMO, S., J. R. WHINNERY, and R. VANDUZER: "Fields and Waves in Communication Electronics," 3d ed., John Wiley & Sons, Inc., New York, 1965.
- SCHELKUNOFF, S. A.: "Applied Mathematics for Engineers and Scientists," D. Van Nostrand Company, Inc., Princeton, N.J., 1948.
- : "Electromagnetic Waves," D. Van Nostrand Company, Inc., Princeton, N.J., 1943.
- SOMMERFELD, A.: "Partial Differential Equations in Physics," Academic Press Inc., New York, 1949.
- SMYTHE, W. R.: "Static and Dynamic Electricity," 2d ed., McGraw-Hill Book Company, New York, 1950.
- STRATTON, J. A.: "Electromagnetic Theory," McGraw-Hill Book Company, New York, 1941.
- WATSON, G. N.: "Theory of Bessel Functions," Cambridge University Press, London, 1944.

APPENDIX

C

ANSWERS TO STARRED PROBLEMS

CHAPTER 1

1-1 velocity, $\frac{L}{T}$, meters second; work, $\frac{ML^2}{T^2}$, joules; ratio, dimensionless

1-2 charge, IT , coulombs; potential, $\frac{ML^2}{T^3I}$, volts; electric field intensity, $\frac{ML}{T^3I}$,
volts meter; potential, $\frac{ML^2}{T^3I}$, volts; constant, $\frac{ML^3}{T^4I^2}$, meters farad; force,
 $\frac{ML}{T^2}$, newtons; current density, $\frac{I}{L^2}$, amperes meter²; force, $\frac{ML}{T^2}$, newtons

CHAPTER 2

2-1 $F = 900 \text{ nN}$ (repulsive)

2-2 $|F| = 14.3 \text{ nN}$; $\theta = 4.0^\circ$ (angle with x axis)

2-3 $E = 9 \text{ kV m}^{-1}$; $V = 900 \text{ V}$

2-4 $E = 0$; $V = 1/2\pi\epsilon_0 a$

2-7 $E = -\hat{x}12 \text{ V m}^{-1}$; $V = 0$

2-8 $\mathbf{f} = \hat{x}0.424 + \hat{y}0.566 + \hat{z}0.707$

- 2-10 at (0,0), $\mathbf{E} = -\hat{\mathbf{y}}\infty$; (4,0), $\mathbf{E} = -\hat{\mathbf{y}}\infty$; (0,4), $\mathbf{E} = -\hat{\mathbf{y}}(0.75) \text{ V m}^{-1}$
- 2-11 at (0,0), $\mathbf{E} = -\hat{\mathbf{x}}12$; (0,3), $\mathbf{E} = -\hat{\mathbf{x}}12 - \hat{\mathbf{y}}42$; (5,0), $\mathbf{E} = -\hat{\mathbf{x}}12$; (5,3), $\mathbf{E} = -\hat{\mathbf{x}}12 - \hat{\mathbf{y}}42 \text{ V m}^{-1}$
- 2-14 (a) $y = 303 \text{ mm}$; (b) $Q_y = 0$
- 2-20 when $r \leq R$, $\mathbf{E} = \frac{90r}{\pi} \text{ kV m}^{-1}$, $V = 900 + 45,000(0.01 - r^2) \text{ V}$
when $r \geq R$, $\mathbf{E} = \frac{90}{\pi}(90/r^2) \text{ V m}^{-1}$, $V = (90/r) \text{ V}$
- 2-25 $\psi = 4\pi\epsilon_0 R^3$
- 2-29 (a) $Q = 32 \text{ C}$; (b) $Q = 8 \text{ C}$; (c) $Q = 24 \text{ C}$; (d) $Q = 164 \text{ C}$
- 2-34 (a) $Q_e = 518 \text{ TC}$, $Q_m = 6.04 \text{ TC}$; (b) $Ql = \sqrt{Q_e Q_m} l = 2.23 \times 10^{22} \text{ C m}$
- 2-38 (a) $E = 0$ ($r \leq r_1$), $E = \frac{Q_1}{4\pi\epsilon_0 r^2}$ ($r_1 \leq r \leq r_2$),

$$E = \frac{Q_1 + Q_2}{4\pi\epsilon_0 r^2} \quad r \geq r_2;$$
(b) $V = \frac{1}{4\pi\epsilon_0} \left(\frac{Q_2}{r_2} + \frac{Q_1}{r_1} \right) \quad r \leq r_1,$

$$V = \frac{1}{4\pi\epsilon_0} \left(\frac{Q_2}{r_2} + \frac{Q_1}{r} \right) \quad r_1 \leq r \leq r_2,$$

$$V = \frac{1}{4\pi\epsilon_0} \left(\frac{Q_2 + Q_1}{r} \right) \quad r \geq r_2$$
- 2-40 $V = 3.22 \times 10^{15} \text{ V}$

CHAPTER 3

- 3-1 (a) $P = 800 \text{ mC m}^{-2}$; (b) $Ql = 80 \text{ mC m}$
- 3-2 (a) $P = 500 \text{ mC m}^{-2}$; (b) $D = 670 \text{ mC m}^{-2}$; (c) $D = 670 \text{ mC m}^{-2}$;
(d) $E = 18.8 \text{ GV m}^{-1}$; (e) $E = 75.4 \text{ GV m}^{-1}$
- 3-3 left half: $E = 10 \text{ kV m}^{-1}$, $D = 265 \text{ nC m}^{-2}$, $P = 177 \text{ nC m}^{-2}$;
right half: $E = 10 \text{ kV m}^{-1}$, $D = 88.5 \text{ nC m}^{-2}$, $P = 0$
- 3-4 (a) $E_a = 15 \text{ kV m}^{-1}$, $E_d = 5 \text{ kV m}^{-1}$, $P_a = 0$,
 $P_d = 88.5 \text{ nC m}^{-2}$, $D_a = D_d = 133 \text{ nC m}^{-2}$,
(b) $V_a = 25 + 15,000(y - 0.005) \text{ (V)}$, $V_d = 5y \text{ (kV)}$
- 3-5 (a) $E_1 = 1.13 \text{ kV m}^{-1}$; (b) $E_2 = 226 \text{ V m}^{-1}$
- 3-6 $F = 111 \text{ N}$
- 3-10 $\epsilon_r = 2.57$
- 3-12 in the slab, $D = \frac{\epsilon_0 \epsilon_r V}{t(1 - \epsilon_r) + d\epsilon_r}$, $E = \frac{V}{t(1 - \epsilon_r) + d\epsilon_r}$, $P = \frac{\epsilon_0(\epsilon_r - 1)V}{t(1 - \epsilon_r) + d\epsilon_r}$;
in air, $D = \frac{\epsilon_0 \epsilon_r V}{t(1 - \epsilon_r) + d\epsilon_r}$, $E = \frac{\epsilon_r V}{t(1 - \epsilon_r) + d\epsilon_r}$, $P = 0$
- 3-16 $C =$ (a) 39.3 pF , (b) 44.2 pF , (c) 58.7 pF , (d) 87.4 pF , (e) 171.0 pF ,
(f) 4.02 nF

- 3-20 (a) W (before) = $500Q$ J, W (after) = $1,000Q$ J;
 (b) a mechanical energy of $500Q$ J was supplied

$$3-24 E = 0, V = \frac{Q}{4\pi\epsilon_0 l} \ln \left(\frac{\sqrt{2} + 1}{\sqrt{2} - 1} \right)$$

$$3-26 V = \frac{Q}{4\pi\epsilon_0 l} \ln \frac{x_1}{x_1 - l}$$

- 3-33 (b) ratio = 2.67; (c) $V = 15$ V; (d) $C/l = 70.8$ pF m⁻¹

- 3-34 (a) $L = 155$ mm; (b) $L = 150$ mm; (c) $V_a = 51.78$ kV,
 $V_b = 52.62$ kV; (d) $V = 45.97$ kV; (e) $V = 59.95$ kV

- 3-39 (a) $\nabla \cdot \mathbf{F} = 0$; (b) $\nabla \cdot \mathbf{G} = -a \cos az$

- 3-44 (a) $3 + 12y^2 + 10z$; (b) $2y^2z$; (c) $14x^2yz^2 + z^{-2}$; (d) 0;
 (e) $2z$; (f) $3r^{-1/2} - r^{-1} \cos 2\phi$; (g) $r^{-2} + r^{-1}2 \sin \phi \cos \theta - r^{-1} \cos \phi$
 (h) $3z + r^{-1} \sin^{-1} \theta \sin \phi \cos 2\theta$

$$3-49 (a) V_a = \frac{Q}{4\pi\epsilon_0 r}, V_d = \frac{Q}{4\pi\epsilon_0 R} + \frac{Q}{4\pi\epsilon} \left(\frac{1}{r} - \frac{1}{R} \right), \mathbf{E}_a = \hat{r} \frac{Q}{4\pi\epsilon_0 r^2}, \mathbf{E}_d = \hat{r} \frac{Q}{4\pi\epsilon r^2}; \\ \rho_s = -\frac{Q}{4\pi\epsilon_r R^2}$$

CHAPTER 4

- 4-1 (a) $R = 21.93$ $\mu\Omega$; (b) $G = 45.61$ $\text{k}\Omega$; (c) $I = 2.28$ kA;
 (d) $J = 1.43$ MA m⁻²; (e) $E = 25.0$ mV m⁻¹; (f) $P = 114$ W;
 (g) 35.6 kW m⁻³; (h) $W = 410$ kJ; (i) $v = 71.3$ $\mu\text{m s}^{-1}$

4-3 $I = 12$ A

- 4-4 (a) $R_{12} = 3.51$ $\mu\Omega$, $G_{12} = 285$ k Ω ; (b) $R_{34} = 219$ $\mu\Omega$, $G_{34} = 4.64$ M Ω ;
 (c) $R_{bf} = 110$ n Ω , $G_{bf} = 9.12$ M Ω
 (d) $J_2 = 178$ kA m⁻², $E_2 = 3.13$ mV m⁻¹, $J_1 = 509$ kA m⁻², $E_1 = 8.93$ mV m⁻¹;
 (e) ratio = 2.86

- 4-5 (a) $R = 3.95$ $\mu\Omega$; (b) ratio = 1.13;

(c) average current path longer in L-shaped bar

- 4-6 (a) $R = 13.2$ $\mu\Omega$; (b) $R = 12.8$ $\mu\Omega$; (c) $R = 14.3$ $\mu\Omega$;
 (d) average current path longer for (a) than (b) but shorter than (c)

4-8 $I_4 = 4$ A (flowing toward junction)

- 4-9 (a) $R = 107$ $\mu\Omega$; (b) $R = 63$ $\mu\Omega$; (c) $l = 171$ mm

- 4-16 (a) $E = 100$ mV m⁻¹; (b) $|E| = 910$ V m⁻¹, $\theta = 6.3^\circ$ (from normal)

4-19 $R/l = 17.6$ k Ω m⁻¹

$$4-20 (a) R = \frac{1}{2\pi\sigma t} \ln \frac{r_2}{r_1}; (b) R = \frac{t}{\sigma\pi(r_2^2 - r_1^2)}; (c) R = \frac{2\pi}{\sigma t \ln(r_2/r_1)}$$

- 4-24 (a) $\sigma = 2.4$ Ω m⁻¹; (b) $v_e = 4$ and $v_b = 2$ m s⁻¹

CHAPTER 5

- 5-1 (a) $F = 100 \text{ mN}$ (repulsive); (b) $F = 100 \text{ mN}$ (attractive)
- 5-2 $\mathbf{F}/l = -\hat{\mathbf{x}}40 + \hat{\mathbf{y}}30 \text{ N m}^{-1}$
- 5-4 $\mathbf{F} = -\hat{\mathbf{y}}800 \mu\text{N}$
- 5-5 (a) $\psi_m = 9.73 \text{ Wb}$; (b) $\psi_m = 2\pi kr_0 \text{ Wb}$
- 5-7 (a) $B = 62.5 \mu\text{T}$; (b) $B = 31.4 \mu\text{T}$; (c) $B = 62.1 \mu\text{T}$
- 5-10 (a) 0; (b) $T = 3.53 \text{ N m}$; (c) $m = 0.884 \text{ A m}^2$
- 5-11 (a) $B = 12.6 \text{ mT}$; (b) $H = 10 \text{ kA m}^{-1}$; (c) $w_m = 62.8 \text{ J m}^{-3}$;
(d) $K = 10 \text{ kA m}^{-1}$; (e) $W_m = 11.1 \text{ mJ}$; (f) $L = 5.6 \text{ mH}$
- 5-13 $B = 1.7 \mu\text{T}$
- 5-14 $B = \mu_0 I/4r_0$ (r_0 = focal length)
- 5-17 (a) $T = 144 \text{ N m}$; (b) $m = 36 \text{ A m}^2$
- 5-18 $T = 3.77 \mu\text{N m}$
- 5-22 $L = 40 \text{ mH}$
- 5-27 (a) $H = 0$; (b) $H = 41.8 \text{ A m}^{-1}$; (c) $H = 159.0 \text{ A m}^{-1}$
- 5-32 $\nabla \times \mathbf{F} = -\hat{\mathbf{x}}2y + \hat{\mathbf{y}}2x$; circle with center at origin

CHAPTER 6

- 6-1 $T = 1 \text{ mN m}$
- 6-3 $H = -10 \text{ kA m}^{-1}$
- 6-5 (a) $H_1 = 1.59 \text{ MA m}^{-1}$; (b) $H_2 = 7.96 \text{ kA m}^{-1}$
- 6-8 $\theta = 0.92^\circ$
- 6-10 $5.1 \pm 0.5 \text{ m south}; 6.7 \pm 1.7 \text{ m deep}$
- 6-11 $\mathcal{P} = \frac{(\mu_1 - \mu_0)A}{x_1 \ln(\mu_1/\mu_0)}$
- 6-20 $m = 2.83 \text{ mA m}^2$
- 6-21 $K' = 326 \text{ MA m}^{-1}$
- 6-25 $NI = 2.4 \text{ kA turns}$
- 6-27 (a) $\mathcal{P} = 4.29 \text{ mH}, \mathcal{R} = 233 \text{ H}^{-1}$; (b) $\mathcal{P} = 31.5 \mu\text{H}, \mathcal{R} = 31,746 \text{ H}^{-1}$
- 6-30 1217.5 kg weight
- 6-33 $F = 78.3 \text{ kN}$

CHAPTER 7

- 7-1 (a) $E = 1 \text{ kV m}^{-1}$; (b) $D = 885 \text{ nC m}^{-2}$; (c) $C/l = 7.08 \text{ nF m}^{-1}$
- 7-2 (a) $E_1 = 227.5 \text{ V m}^{-1}, E_2 = 75.8 \text{ V m}^{-1}$;
(b) $D_1 = 2.01 \text{ nC m}^{-2}, D_2 = 671 \text{ pC m}^{-2}$; (c) $B_1 = 50 \text{ nT}, B_2 = 16.7 \text{ nT}$;
(d) $H_1 = 39.8 \text{ mA m}^{-1}, H_2 = 13.3 \text{ mA m}^{-1}$; (e) $C/l = 50.6 \text{ pF m}^{-1}$;
(f) $L/l = 219.7 \text{ nH m}^{-1}$; (g) $\psi/l = 505 \text{ pC m}^{-1}$; (h) $\psi_m/l = 2.2 \text{ nWB m}^{-1}$

7-4 (a) $E_1 = 197.8 \text{ V m}^{-1}$, $D_1 = 1.17 \text{ nC m}^{-2}$, $H_1 = 10 \text{ A m}^{-1}$, $B_1 = 12.56 \mu\text{T}$,

$$E_2 = 83.2 \text{ V m}^{-1}, D_2 = 736 \text{ pC m}^{-2}, H_2 = 6.67 \text{ A m}^{-1}, B_2 = 8.38 \mu\text{T},$$

$$E_3 = 35.8 \text{ V m}^{-1}, D_3 = 316 \text{ pC m}^{-2}, H_3 = 3.33 \text{ A m}^{-1}, B_3 = 4.19 \mu\text{T}$$

7-11 (a) sheet current $K_\phi \propto \sin \theta$, where $\theta = \text{angle from axis}$; (b) turns per meter (of continuous winding) should be proportional to $\sin \theta$

7-12 $C_1 = -\frac{1}{2}\mu_0 k_0$; $C_2 = \mu_0 k_0 R^3/3$

7-16 (a) $V = C_1 \ln \tan(\theta_i/2) + C_2$, where $C_1 = V_1/\ln[\tan(\theta_i/2)/\tan(\theta_0/2)]$ and
 $C_2 = -V_1/(\{\ln \tan(\theta_i/2)/\ln \tan(\theta_0/2)\} - 1)$; (b) $C_1 = V_1/\ln \tan(\theta_i/2)$, $C_2 = 0$

7-22 $V = V_1 \sin(\pi\alpha/2\theta)$ (α is the angle made with the $V=0$ sheet)

7-23 $V = \frac{Q}{4\pi\epsilon_0 r} \quad r_3 \leq r < \infty$

$$V = \frac{Q}{4\pi\epsilon_0} \frac{(\epsilon_r - 1)r + r_3}{\epsilon_r r r_3} \quad r_2 \leq r \leq r_3$$

$$V = \frac{Q}{4\pi\epsilon_0} \left[\frac{(\epsilon_r - 1)r_2 + r_3}{\epsilon_r r_2 r_3} + \frac{r_2 - r}{rr_2} \right] \quad r_1 \leq r \leq r_2$$

$$V = \frac{Q}{4\pi\epsilon_0} \left[\frac{(\epsilon_r - 1)r_2 + r_3}{\epsilon_r r_2 r_3} + \frac{r_2 - r_1}{r_1 r_2} \right] \quad 0 \leq r \leq r_1$$

7-27 $V_0 = \frac{-E_0 \cos \theta (\epsilon(b^2 + a^2)(r^2 - b^2) + \epsilon_0(b^2 - a^2)(r^2 + b^2))}{r(\epsilon(b^2 + a^2) + \epsilon_0(b^2 - a^2))}$

$$V_1 = \frac{-2E_0 b^2 \epsilon_0 \cos \theta (r^2 - a^2)}{r[\epsilon(b^2 + a^2) + \epsilon_0(b^2 - a^2)]}$$

7-29 (a) $V = -[1 - (a/r)^3]E_0 r \cos \theta$; (b) $\rho_s = 3\epsilon_0 E_0 \cos \theta$ (on sphere),
 $\rho_s = \epsilon_0 E_0 [1 - (a/r)^3]$ (on sheet)

7-34 (a) $V = (V_1 + V_2) \frac{r_1}{2r} + (V_1 - V_2) \left[\frac{3}{4} \left(\frac{r_1}{r} \right)^2 \cos \theta - \frac{7}{16} \left(\frac{r_1}{r} \right)^4 P_3(\cos \theta) + \frac{11}{32} \left(\frac{r_1}{r} \right)^6 P_5(\cos \theta) - \dots \right]$

7-35 (b) $d = 6.24s$

7-42 $v = (\rho_0/6\epsilon x_1)(x_1^3 - x^3)$

CHAPTER 8

8-1 (a) $\mathcal{U} = 7.5 \text{ mV}$; (b) $dB/dt = 66.6 \text{ mT s}^{-1}$

8-2 $N = 125$ turns

8-3 $x \leq 0, \mathcal{U} = 0$; $0 \leq x \leq 80, \mathcal{U} = 400 \mu\text{V}$; $80 \leq x \leq 100, \mathcal{U} = 0$;
 $100 \leq x \leq 120, \mathcal{U} = -400 \mu\text{V}$

8-4 (a) clockwise; (b) counterclockwise

8-5 $\mathcal{U} = 78.5 \text{ mV}$

8-6 $\mathcal{U} = 2vB\sqrt{R^2 - r^2}$

8-7 (a) $\mathcal{U} = \pi NBR^2$; (b) $T = \frac{1}{2}IBR^2$; (c) clockwise

8-10 $H = 1.27 \text{ mA m}^{-1}$

8-11 (a) $\mathcal{V} = 1.27 \text{ V}$; (b) $\mathcal{V} = 1.27 \sin(10\pi t) - 18.8 ab \cos(10\pi t) \text{ V}$

8-13 $\mathcal{V} = 3.68 \mu\text{V}$

8-15 $M = 7.96 \text{ mH}$

8-19 $\mathcal{V} = 0$

8-23 (a) $\mathbf{J}_t = -2\beta H_0 \cos(\omega t - \beta x)$; (b) $\mathbf{J}_t = \frac{1}{2}[\beta H_x \sin 2x \sin(\omega t - \beta y)] - \frac{1}{2}[2H_x \cos 2x \cos(\omega t - \beta y)] + 2[\beta H_x \sin 2x \cos(\omega t - \beta y)]$

8-26 $P = 5.22 \text{ W}$

CHAPTER 9

9-5 because isolated magnetic charges do not exist

9-8 (a) $J = (I_0/\pi R^2) \sin \omega t$ for $0 \leq r \leq R$, $J = 0$ for $r \geq R$;

(b) $J_t = 0$ for all r ; (c) $B = \mu_0 I/2\pi r$ for $r \geq R$, $B = \mu_0 Ir/2\pi R^2$ for $0 < r \leq R$

9-9 (a) $J_t = \frac{\epsilon_0 \omega V_0}{d} \cos \omega t$; (b) $H_\phi = r \frac{\epsilon_0 \omega V_0}{2d} \cos \omega t$

9-10 $J_t = C_1 r$, where $C_1 = \frac{1}{2} \epsilon_0 \omega^2 B_0 \sin \omega t$ and $r < R$

9-11 $J_t = C_2 r$, where $C_2 = \frac{1}{2} \mu_0 \epsilon_0 \omega^2 K_0 \sin \omega t$ and $r < R$

CHAPTER 10

10-1 (a) $v = 173.2 \text{ Mm s}^{-1}$; (b) $S_{\text{peak}} = 165.4 \text{ mW m}^{-2}$; (c) $S_{\text{av}} = 82.7 \text{ mW m}^{-2}$;

(d) $Z = 217.7 \Omega$; (e) $H_{\text{peak}} = 27.6 \text{ mA m}^{-1}$

10-2 (a) $v = 150 \text{ Mm s}^{-1}$; (b) $\lambda = 1.5 \text{ m}$; (c) $Z = 377 \Omega$;

(d) $E = 43.4 \text{ V m}^{-1}$; (e) $H = 115.1 \text{ mA m}^{-1}$

10-4 (a) $S_{\text{av}} = 47.7 \text{ mW m}^{-2}$; (b) $w = 319 \text{ pJ m}^{-3}$;

(c) $m/v = 1.77 \times 10^{-27} \text{ kg m}^{-3}$

10-7 $t = 77.7 \text{ mm}$

10-8 (a) $S = 1.4 \text{ kW m}^{-2}$; (b) $P = 3.96 \times 10^{26} \text{ W}$; (c) $E = 726.5 \text{ V m}^{-1}$;

(d) $t = 8.33 \text{ min}$

10-10 (a) $S = 10 \text{ pW m}^{-2}$; (b) $E = 61.4 \mu\text{V m}^{-1}$; (c) $P = 2.83 \text{ TW}$

10-13 (a) $P = 4.24 \times 10^{26} \text{ W}$; (b) $P_e = 1.93 \times 10^{17} \text{ W}$; (c) $t = 1.35 \times 10^{11} \text{ years}$

10-15 (a) $Z/Z_0 = 0.111$; (b) $\lambda/\lambda_0 = 0.111$; (c) $v/v_0 = 0.111$; (d) $\eta = 9.0$

10-18 (a) $\text{VSWR} = 1.5$; (b) $\text{VSWR} = 3.0$; (c) $\text{VSWR} = 3.6$;

(d) when $E_r = 10 \text{ mV m}^{-1}$

10-19 (a) $E = 245 \mu\text{V m}^{-1}$; (b) $H = 650 \text{ nA m}^{-1}$; (c) $S = 159 \text{ pW m}^{-2}$;

(d) $w = 2.66 \times 10^{-19} \text{ J m}^{-3}$; (e) $W = 7.25 \times 10^{-20} \text{ J}$

10-29 (a) conductor; (b) dielectric

10-31 (a) $\delta(1/e) = 4.59 \text{ m}$, $\delta(1\%) = 21.1 \text{ m}$; (b) $\delta(1/e) = 25.2 \text{ mm}$,

$\delta(1\%) = 115.8 \text{ mm}$; (c) $\delta(1/e) = 650 \mu\text{m}$, $\delta(1\%) = 2.99 \text{ mm}$

10-33 (a) $Z/Z_0 = 0.80 - j0.19$; (b) $\lambda/\lambda_0 = 0.033$; (c) $v/v_0 = 0.033$;

(d) $\delta(1/e) = 4.86 \text{ mm}$; (e) $\alpha = 1.03 \text{ Np}$; (f) $\rho = 0.153 \angle -130.5^\circ$

10-38 (a) $\delta(1/e) = 212 \text{ mm}$; (b) $\delta(1\%) = 977 \text{ mm}$

CHAPTER 1111-1 (a) AR = 1.5; (b) $\tau = 0^\circ$; (c) clockwise; (d) left-handed11-3 (a) AR = 6.0; (b) $\tau = 0^\circ$; (c) counterclockwise; (d) right-handed11-6 $P = 14.9 \text{ kW}$

11-8

		Antenna		
		1	2	3
Wave	a	0.50	0.50	0.50
	b	0.50	0.25	0.35
	c	0.50	0.20	0

11-11 $d = (a) 0\%; (b) 100\%; (c) 50\%; (d) 70.7\%; (e) 100\%$ 11-13 $P = 500 \text{ mW}$

11-19 (1) AR = 1, LCP; (2) AR = 1, RCP; (3) AR = ∞ , horizontally polarized, $\tau = 0^\circ$; (4) AR = ∞ , vertically polarized, $\tau = 90^\circ$; (5) AR = ∞ , linear, $\tau = 45^\circ$; (6) AR = ∞ , linear, $\tau = 135^\circ$; (7) AR = 3.13, LEP, $\tau = 22.5^\circ$; (8) unpolarized; (9) $d = \frac{1}{2}$, AR = 1, RCP; (10) $d = \frac{1}{2}$, AR = ∞ , linear, $\tau = 0^\circ$; (11) $d = \frac{1}{2}$, AR = ∞ , linear, $\tau = 45^\circ$; (12) $d = 0.47$, AR = 2.41, LEP, $\tau = 90^\circ$. (Note: LCP = left circularly polarized, RCP = right circularly polarized, LEP = left elliptically polarized)

CHAPTER 1212-1 (a) $x = 12.96 \text{ m}$; (b) $x = 1.97 \text{ m}$; (c) $x = 263 \text{ mm}$ 12-2 (a) $H_2/H_1 = 1.99995$; (b) 0.0026% error12-3 $\sigma = 2.65 \text{ } \Omega \text{ m}^{-1}$ 12-4 (a) $E = 903 \mu\text{V m}^{-1}$; (b) $E = 1.05 \mu\text{V m}^{-1}$ (c) $E = 2.10 \mu\text{V m}^{-1}$;(c) $H = 12.5 \text{ nA m}^{-1}$ 12-5 $t = 27.5 \text{ mm}$

$$12-6 (a) \tau_{\parallel} = \frac{\cos \theta_i}{\cos \theta_t} \left(1 + \frac{-8 \cos \theta_i + \sqrt{8 - \sin^2 \theta_i}}{8 \cos \theta_i + \sqrt{8 - \sin^2 \theta_i}} \right)$$

$$(b) \tau_{\perp} = 1 + \frac{\cos \theta_i - \sqrt{8 - \sin^2 \theta_i}}{\cos \theta_i + \sqrt{8 - \sin^2 \theta_i}}; (d) \theta_{iB} = 70.5^\circ$$

CHAPTER 1313-1 (a) $Z = 15.4 + j26.9 \Omega$; (b) VSWR = 4.26; (c) $\rho = 0.62 \angle 29.7^\circ$, $\tau = 1.568 \angle 11.3^\circ$ 13-3 (a) $Z_0 = 32.3 - j6.8 \Omega$; (b) $v = 31.3 \text{ Mm s}^{-1}$; (c) 18.6%13-5 (a) $Z_0 = 337 \Omega$; (b) $f = 60 \text{ MHz}$ 13-6 (a) $Z_0 = 45.9 \Omega$; (b) $v/c = 0.61$ 13-8 $d = 0.342\lambda$, $Z_1 = 229 \Omega$ 13-9 $d_1 = 0.195\lambda$, $d_2 = 0.150\lambda$

- 13-10 $d_1 = 0.75\lambda$, $d_2 = 0.25\lambda$, $R_1 = 245.0 \Omega$, $R_2 = 173.2 \Omega$
- 13-11 (a) $r = -0.715$; (b) $r = 0.244 \angle 76^\circ$; (c) no
- 13-13 (1) $V_{\max} = V_{\min} = 500 \text{ mV}$; (2) $V_{\max} = 500 \text{ mV}$, $V_{\min} = 250 \text{ mV}$
- 13-18 $d_1 = 0.226\lambda$, $d_2 = 0.104\lambda$
- 13-19 (a) $t = 54.8 \text{ mm}$; (b) $\epsilon_r = 1.87$
- 13-25 (a) TEM not passed, TE_{10} 1.87 GHz, TE_{20} 3.75, TE_{01} 3.75, TE_{02} 7.50, TE_{11} 4.19, TE_{21} 5.30, TE_{12} 7.73 GHz; (b) $v/v_0 = 1.342$ for all modes passed
- 13-26 (a) TE_{10} 3.0 GHz, TE_{20} 6.0, TE_{11} 4.8, TE_{21} 7.1, TE_{01} 3.7, TE_{02} 7.5, TM_{11} 4.8, TM_{21} 7.1 GHz; (b) $v/v_0 = 1.237$ for all modes
- 13-28 (a) TM_{01} 2.3 GHz, TM_{02} 5.3, TM_{11} 3.7, TM_{12} 6.7, TE_{01} 3.7, TE_{02} 6.7, TE_{11} 1.8, TE_{12} 5.1 GHz; (b) $v/v_0 = 1.565$ for all modes
- 13-29 (a) TE_{11} 1.17 GHz, TE_{21} 1.97, TE_{31} 2.67, TE_{41} 3.37, TE_{51} 4.01, TE_{01} 2.45, TE_{02} 4.46, TE_{12} 3.39, TE_{22} 4.27, TM_{01} 1.52, TM_{11} 2.45, TM_{21} 3.28, TM_{31} 4.05, TM_{41} 4.82, TM_{02} 3.51, TM_{12} 4.46 GHz; (b) $v/v_0 = 1.809$ for all modes
- 13-30 $f_c = 0$, $\alpha = 8.89/\lambda_0 \text{ Np m}^{-1}$
- 13-33 $\lambda = 3 \text{ m}$
- 13-34 $S = 1.33 \text{ nW m}^{-2}$
- 13-51 TEM: $\alpha = 5.09 \text{ mNp m}^{-1}$, TE_{10} : $\alpha = 12.79 \text{ mNp m}^{-1}$
- 13-52 $\alpha = 8.42/r_0 \text{ dB m}^{-1}$, where $r_0 = \text{radius}$
- 13-54 (a) $P = 10.9 \text{ nW}$
- 13-59 (a) $f = 2.65 \text{ GHz}$, (b) $\lambda = 113 \text{ mm}$, (c) $Q = 12,413$
- 13-60 (a) $d = 7.7 \text{ mm}$, (b) $Q = 5,178$

CHAPTER 14

- 14-1 (a) $D = 1.5$; (b) $G = 1.05$; (c) $A_e = 0.083 \lambda^2$; (d) $\Omega_A = 8.38 \text{ sr}$;
 (e) $R_r = 3.5 \Omega$; (f) $R_T = 5.0 \Omega$
- 14-2 $R_r = 790(l/\lambda)^2 \Omega$
- 14-3 (a) $E = \cos(\pi \cos \theta)$, $D = 2.0$; (b) $E = \sin(\pi \cos \theta)$, $D = 2.0$
- 14-9 (a) $\epsilon_{ap} = 81.1\%$; (b) $D = 1,304$ (31.2 dB)
- 14-14 (a) HPBW = 8.4°; (b) -13.0 dB; (c) $\Omega_A = 1.15 \text{ sr}$; (d) $\epsilon_M = 91\%$;
 (e) $D = 10.8$ (10.3 dB); (f) $A_e = 0.86\lambda^2$
- 14-15 (a) HPBW = 53.6°; (b) -13.2 dB; (c) $\Omega_A = 0.87 \text{ sr}$; (d) $\epsilon_M = 83\%$;
 (e) $D = 14.4$ (11.6 dB); (f) $A_e = 1.14\lambda^2$
- 14-20 (a) $E(\theta) = \frac{\sin(20\pi \cos \theta)}{2\pi \cos \theta} \frac{-0.01}{4 \cos^2 \theta - 0.01}$; (b) HPBW = 4.2°
- 14-23 (a) $E_1 = J_1(1.05 \sin \theta)$, $E_2 = J_1(2.36 \sin \theta)$, $E_3 = J_1(6.28 \sin \theta)$;
 (b) $R_1 = 691 \Omega$, $R_2 = 1,836 \Omega$, $R_3 = 2,573 \Omega$; (c) $D_1 = 1.5$, $D_2 = 1.2$, $D_3 = 3.6$
- 14-26 (a) $E(\theta) = \cos \theta \frac{\sin 30(\psi/2)}{\sin(\psi/2)}$, where $\frac{\psi}{2} = 90^\circ (0.2 \cos \theta - 1.217)$
 (b) HPBW = 23.2°; (c) $D = 98.7$ (19.9 dB); (d) REP, AR = 1.02
- 14-27 (a) linear, $\tau = 45^\circ$; (b) CP; (c) elliptically polarized, AR = 2.41, $\tau = 45^\circ$
- 14-32 (a) $Z_m = -6.4 + j1.8 \Omega$; (b) $Z_T = 2.5 + j1.8 \Omega$

14-37 (a) gain = $2 \sqrt{\frac{R_{11}}{R_{11} - R_{12}}} \left| \sin \frac{2\pi s}{\lambda} \right|$

(b) gain = $2 \sqrt{\frac{R_{11} + R_0}{R_{11} + R_0 - R_{12}}} \left| \sin \frac{2\pi s}{\lambda} \right|$

14-46 $Z = 778 - j86 \Omega$

14-47 (a) $l = 80\lambda$, $w = 12.7\lambda$, $\theta_E = 2.86^\circ$, $\theta_H = 4.52^\circ$;

(b) HPBW_E = 7.0°, HPBW_H = 5.3°; (c) $D = 762$ (28.8 dB);

(d) $\epsilon_{ap} = 59.7\%$

14-48 $A_{er} = 121.6 \text{ m}^2$ (RCP)

14-54 (a) $\Delta T_{\min} = 0.015 \text{ K}$; (b) $\Delta S_{\min} = 518 \text{ fu}$; (c) $\Delta S_{\min} = 259 \text{ fu}$

14-57 (a) $R = 240 \text{ Mpc}$; (b) $R = 320 \text{ Mpc}$; (c) $R = 640 \text{ Mpc}$;

(d) $P_s/\Delta f = 3.99 \times 10^{27} \text{ W Hz}^{-1}$, $P_b/\Delta f = 2.36 \times 10^{25} \text{ W Hz}^{-1}$,

$P_c/\Delta f = 1.42 \times 10^{27} \text{ W Hz}^{-1}$

14-58 (a) $w = 2.08 \times 10^{-27} \text{ J m}^{-2} \text{ Hz}^{-1}$; (b) $W = 4.68 \times 10^{17} \text{ J}$;

(c) $t = 5.2 \times 10^{13} \text{ years}$

14-60 $\eta = (a) 0.0006\%$; (b) 5.5%; (c) 99.8%; (d) 100%; (e) 100%;

(f) $l \geq 0.01\lambda$ for better than 90% efficiency; (g) polarization mismatch, insufficient gain

14-63 (a) $A_e = 7,162 \text{ m}^2$; (b) $P_r = 5.7 \text{ W}$; (c) $P_{reqd} = 8.3 \mu\text{W}$;

(d) $> 10^{-4}\%$; (e) no; (f) parts (a) and (b) by a few dB but (d) and (e) not significantly

14-65 53.5 K

CHAPTER 15

15-1 (a) $v = 1 \text{ Mm s}^{-1}$; (b) $R = 500 \text{ mm}$

15-2 (a) $V_d = 1.4 \text{ kV}$; (b) $B = 2.82 \text{ mT}$

15-3 (a) $v = 6.3 \text{ mm } \mu\text{s}^{-1}$; (b) $d = 6.3 \text{ km}$; (c) $dB/dt = 177.7 \text{ T s}^{-1}$

15-5 (a) $W = 14 \text{ MeV}$; (b) $W = 14 \text{ MeV}$; (c) $W = 7 \text{ MeV}$;

(d) $n_e = 388 \text{ r}$, $n_p = 777 \text{ r}$, $n_d = 388 \text{ r}$

15-7 (a) $R = 20.8 \text{ m}$; (b) $R = 1.04 \text{ mm}$; (c) $R = 10.4 \text{ Mm}$

15-13 $\Delta f = 3.5 \text{ kHz}$

15-14 (a) MUF = 15.6 MHz; (b) MUF = 26.1 MHz; (c) MUF = 12.7 THz

15-16 (a) $f_0 = 9 \text{ MHz}$; (b) $f_0 = 10.4 \text{ MHz}$; (c) $\text{MUF} = \frac{f_0(\phi = 0^\circ)}{\cos \phi_{\max}}$,

where ϕ_{\max} is the maximum pointing angle from the zenith

15-20 (a) $(\beta r)^+ = 2,659.8\lambda_0$, $(\beta r)^- = 2,687.8\lambda_0$; (b) $\beta r = 2,603.6\lambda_0$;

(c) $(\beta r)^+ / (\beta r)^0 = 0.972$, $(\beta r)^- / (\beta r)^0 = 0.982$, $(\beta r)/(\beta r)^0 = 0.952$;

(d) if $\omega \gg \omega_0$ but $\omega < \omega_0$; (e) for horizontal travel, $\Delta\theta = 0$, for vertical incidence, $\Delta\theta = 380$ turns

15-21 (a) $v = 824.7 \text{ km s}^{-1}$; (b) $v = 109.1 \text{ Mm s}^{-1}$; (c) $v = 89.2 \text{ mm s}^{-1}$;

(d) $v = 7.54 \text{ m s}^{-1}$

15-27 $\mathfrak{U} = 3 \text{ kV}$

CHAPTER 16

- 16-10** (a) $E'_\perp = 10.0 \text{ V m}^{-1}$, $B'_\perp = 1.1 \text{ fT}$; (b) $E'_\perp = 10.0 \text{ V m}^{-1}$, $B'_\perp = 1.1 \text{ pT}$;
 (c) $E'_\perp = 10.0 \text{ V m}^{-1}$, $B'_\perp = 1.1 \text{ nT}$; (d) $E'_\perp = 10.6 \text{ V m}^{-1}$, $B'_\perp = 11.7 \text{ nT}$;
 (e) $E'_\perp = \infty$, $B'_\perp = \infty$
- 16-12** (a) $E'_\perp = 333.3 \text{ nV m}^{-1}$, $B'_\perp = 33.3 \text{ nT}$; (b) $E'_\perp = 333.3 \mu\text{V m}^{-1}$, $B'_\perp = 33.3 \text{ nT}$;
 (c) $E'_\perp = 333.3 \text{ mV m}^{-1}$, $B'_\perp = 33.3 \text{ nT}$; (d) $E'_\perp = 3.5 \text{ V m}^{-1}$, $B'_\perp = 35.3 \text{ nT}$;
 (e) $E'_\perp = \infty$, $B'_\perp = \infty$
- 16-14** (a) $E'_\perp = 10 \text{ V m}^{-1}$, $B'_\perp = 33.3 \text{ nT}$; (b) $E'_\perp = 10 \text{ V m}^{-1}$, $B'_\perp = 33.3 \text{ nT}$;
 (c) $E'_\perp = 9.7 \text{ V m}^{-1}$, $B'_\perp = 32.2 \text{ nT}$; (d) $E'_\perp = 7.1 \text{ V m}^{-1}$, $B'_\perp = 23.5 \text{ nT}$;
 (e) $E'_\perp = \infty$, $B'_\perp = \infty$
- 16-18** $\mathcal{P} = 3.33 \text{ mg m}^{-2}$
- 16-23** (a) 18 years; (b) 6 years; (c) 3.6 years; (d) 6.5 years
- 16-29** $v = 0.94c$

INDEX

- Abramowitz, M., 466n.
Absolute potential, 22
Absorption of wave, 451
Ac generator, 315
Aerial (*see* Antennas)
Alford, A., 441n.
Alfvén, H., 740n.
Alfvén velocity, 742
Alfvén waves, 740
Algorithm, 273
ALSEP experiment, 660, 662
Alternator, 419
AM, 480 (Prob. 12-10)
AM broadcasting station, 707 (Prob. 14-7)
Ammonia molecule, Q for, 599 (Prob. 13-58)
Ampere, definition, 3, 147
Ampère-Maxwell vector, 767
Ampère's law, 7
and H, 163-165
Maxwell's equation from, 166
Analog computer, 276-278
Angle of refraction, 453n.
Anisotropic materials, 57
Anisotropic medium, 729
Anode, 289
Anomalously dispersive medium, 376
Antarctica, 424 (Prob. 10-36)
Antenna array (*see* Arrays)
Antenna efficiency, 619
Antenna fields, computer-calculated, 648-649
Antenna impedance, self- and mutual, 670-675
Antenna pattern, 602
Antenna reactance, 625
Antenna resistance, 625
Antenna temperature (*see* Temperature, noise)
Antenna voltage response, 435
Antennas:
circularly-polarized, 691-692
complementary, 687-688
current distribution on, 646
dipole, 602
directivity of, 622
effective aperture of, 625
Fourier transform relation for, 644-646
frequency-independent, 665-667
active region, 666
equiangular spiral, 666
log-periodic, 666-667
gain of, 623
half-wave dipole (*see* Half-wave dipole)
helical-beam, 656-662
(*See also* Helical-beam antennas)
helicone, 692-693
horn, 688-689
pyramidal, 689
interferometer (*see* Interferometer)
isotropic, 623
lens (*see* Lens antenna)
linear, 646-648
loop, 654-655
mutual impedance of, 673-675
parabolic dish, 642
phase center of, 648
pocket ruler, 665-666
polarization state, 435
prolate spheroid, 648-649
radio telescope, 700
(*See also* Radio telescope)
receiving, 601, 624
reflector, 678-687
corner, 682-684
finite-flat-sheet, 679
infinite-flat-sheet, 679
nonspherical, 470
parabolic, 684-685
spherical, 711 (Prob. 14-44)
thin, 680-682
resonance of, 648
retroreflector, 713 (Prob. 14-52)
self-impedance of, 670-673
short dipole (*see* Short dipole)
shortwave, 599 (Prob. 13-62)
slot, 687-688
small helical, 655-656
stored energy of, 602
supergain, 659
transmitting, 601, 624
traveling wave, 650-654
V, 602, 672
Yagi-Uda, 682
Antipodal state, 435
Antisymmetric matrix (*see* Skew-symmetric matrix)
Aperture, 624
effective, 690
physical, 690
scattering, 698
Aperture concept, 690-694
Aperture distribution, 646
continuous, 642-644

- Aperture efficiency, 690
 of large circular aperture, 693-694
 Apollo 14 astronauts, 660
 Appearance of field, 773-775
 Applied field, 46
 Approximation formulas, 796
 Array factor, 629
 Array gain, 677
 Array theory, 627-642
 Arrays:
 beam width of, 662
 binomial, 629-631
 directivity of, 662
 collinear, 708 (Prob. 14-13)
 continuous, 642
 grid structure, 663-665
 of helical beam antennas, 661
 with n sources, 631-636
 broadside case, 633
 end-fire case, 633-635
 null directions of, 632
 phase center of, 629
 scanning, 663-665
 of six-point sources, 638
 two isotropic point sources as, 627-629
 uniform, 631
 van Atta, 713 (Prob. 14-53)
 Artificial dielectrics, 63-66
 Associated Legendre function, 284
 Astigmatic tube, 470
 Astronauts, Apollo 14, 660
 Atomic current loop, 198
 Atomic dipole:
 electric, 59, 333
 magnetic, 199
 Attenuation, 546
 at frequencies above cutoff, 563
 at frequencies below cutoff, 561
 Attenuation constant, 488, 564, 566
 for cylindrical guide, 568-569
 for infinite-parallel-plane line, 566-567
 Attenuation factor, 404, 488
 Automobiles, detection of, 347 (Prob. 8-35)
 Auxiliary equation, 487
 Axial ratio (AR), 427, 428

 Backlobe, antenna, 604
 Balanced transmission line, 606
 Balmain, K. D., 801
 Bandwidth, 376, 436, 513
 of helical beam antenna, 659
 predetection, 701
 of transformer, 511-515
 Barium titanate material, 452
 Barkofsky, E. C., 441
 Barrow, W. L., 532n., 551n.
 Base units, 2
 Battery, energy of, 105 (Prob. 3-18),
 108 (Prob. 3-50)
 Baytron Co., Inc., figure, 595
 Beam of ions, 719
 Beam direction, 664
 Beam efficiency, 622n.
 of large circular aperture, 693-694

 Beam solid angle, 620-621
 Beam width between first nulls (BWFN), 620
 Bengtsson, N. E., 346 (Prob. 8-34)
 Bessel function, 284, 554
 recurrence relations for, 798
 root of, 554
 Betatron, 345 (Prob. 8-28)
 Beverage antenna, 577
 Binomial array, 629-631
 Binomial series, 514n., 631
 Biot-Savart law, 144
 Blackbody, 422 (Prob. 10-11)
 Bohn, E. V., 568n.
 Boltzmann's constant, 422 (Prob. 10-11), 700
 Booker, H. G., 644n., 687n.
 Born, M., 432n., 441n.
 Bound charge (*see* Charge polarization)
 Bound wave (*see* Surface wave)
 Boundary relations:
 at conducting surface, 50-51
 at conductor-conductor boundary, 130
 at conductor-insulator boundary, 127-128
 electric field, 67-69
 magnetic field, 216-221
 tables of, 71, 221
 for time-varying fields, 336-337
 Boundary-value problems, 262
 Bozorth, R. M., 801
 Breakdown (*see* Dielectric strength)
 Brewster angle, 458, 593 (Prob. 13-20)
 Brightness, 422 (Prob. 10-11)
 Brillouin, Leon, 375
 Broadband matching, 515
 Broadside array, 633
 Brown, G. H., 680n.
 Bushing, capacitor, 106 (Prob. 3-34)
 BWFN, 620

 Candela, definition, 3
 Capacitance, 49
 of coaxial line, 81
 of earth, 55 (Probs. 2-36, 2-39)
 of isolated metal sphere, 55 (Prob. 2-35)
 of stripline, 296 (Prob. 7-1)
 of two concentric shells, 55 (Prob. 2-41)
 units of, 49
 Capacitor, 49
 analogy to storm cloud, 105 (Prob. 3-21)
 dielectric strength of, 73
 divergence of \mathbf{D} and \mathbf{P} in, 99
 energy in, 74
 energy density in, 75
 field cell, 89
 parallel-plate, 49, 61-62, 71-73, 99-100
 (*See also* Parallel-plate capacitor)
 two conductor line as, 85
 Capacitor bushing, 106 (Prob. 3-34)
 Cardioid-pattern antenna, 680
 Carrier modulated wave, 377
 Carter, P. S., 674
 Carver, Keith R., 663n., 692n., 694n.
 Cathode, 289
 Cathode-ray oscilloscope, 303 (Prob. 7-39)

- Cathode-ray tube (CRT), 721-725
 electrostatic deflection in, 722
 magnetic deflection in, 723
- Caustics, 471
- Cavity resonator, 583
- Cell:
 conductor, 131
 field, 89, 90
- Center-fed dipole antenna, 646
- Cesium atom, Q for, 599 (Prob. 13-58)
- Characteristic impedance, 382, 488, 573
 of coaxial line, 493-495
 determination by dc measurement, 493
 of two-wire line, 495
- Characteristic resistance, 489
- Charge:
 electric, 13
 induced, 46
 point, 13
 polarization, 99, 110
 single shell of, 43
- Charge density:
 linear, 30
 polarization, 60-62
 surface, 30
 volume, 29
- Charged particle:
 in static electric field, 716-719
 in static magnetic field, 719-721
- Chart:
 rectangular impedance, 502
 Smith, 505
 SPEMP, 11
 transmission-line, 502
- Chawla, B. R., 303 (Prob. 7-40)
- Child, D. C., 292
- Child-Langmuir law, 292
- Chimney flue, 743 (Prob. 15-9)
- Chu, L. J., 532n.
- Circularly polarized antenna, 691-692
- Circularly polarized wave, 427
 left-handed, 429
 right-handed, 429
- Circulator, three-port, 591 (Prob. 13-11)
- Clemmow, P. C., 644n.
- Closed rectangular pipe, 485
- Coaxial line, 284-288
 with asymmetrically located inner conductor, 195 (Prob. 5-24)
 capacitance of, 81
 characteristic impedance of, 495
 cylindrical, 297 (Prob. 7-2)
 elliptical, 297 (Prob. 7-3)
 field cells, 172-173
 fields in, 128
 inductance of, 161
 square, 304 (Prob. 7-41)
- Coercive force, 229
- Coercivity, 230
- Coherence, 694-696
 polarization, 695
 waveform, 695
- Coherency matrices, 441, 443
- Coherent light, 467
- Coil (see Inductor)
- Collector, 289
- Collin, R. E., 802
- Collisions, effect of, 735
 with gas molecules, 747 (Prob. 15-33)
- Communication:
 between earth and space vehicle, 744 (Prob. 15-13)
 on moon, 596 (Prob. 13-38)
- Communications service, 594 (Prob. 13-32)
- Compass needle, 140
- Complementary antennas, 687-688
- Complementary solution, 288
- Complete solution, 282
- Completely polarized wave, 437
- Completely unpolarized wave, 437
- Complex conjugate, 391
- Complex power, 619
- Complex vector, 430
- Components, microwave, 594-595 (Prob. 13-36)
- Computer:
 analog, 276-278
 digital: desk-top, 276
 programmable, 276
 vest-pocket, 276
- Computer calculation of antenna pattern, 715 (Prob. 14-64)
- Computer methods:
 for field of charges, 107 (Prob. 3-38)
 relation to field mapping, 92
- Computer program:
 for electric charge distribution, 53-54 (Probs. 2-30, 2-31)
 Fortran IV, 273, 275
- Condenser (see Capacitor)
- Conductance, 116
- Conducting bar with notch, figure, 134
- Conducting block, rectangular, 301 (Prob. 7-20)
- Conducting fluid, 740
- Conducting half-plane, 465
- Conducting hemisphere, 302 (Prob. 7-29)
- Conducting media, 399
- Conducting paint, 277
- Conducting rod, 349
- Conducting sheet:
 with slot, 302 (Probs. 7-28, 7-34)
 between two conducting planes, 278-283
- Conducting wheel, 342 (Prob. 8-7)
- Conduction current, 328
- Conduction-current density, 400
- Conductivity, 116
 equivalent, 334
 table of, 117
 tensor, 733n.
- Conductor, 45, 57, 401
 electron motion in, 110
 over ground plane, 295
 with right-angle bend, 303 (Prob. 7-40)
- Conductor cell, 131
- Conservation of charge relation, 126n.
- Conservation of energy, principle of, 389
- Constant-phase point, 368
- Constants, fundamental, 794
- Constitutive relations, 358
- Continuity relation, 126, 357, 767

- Continuous aperture distribution, 642–644
field of, 644
- Continuous array, 642
- Contour map, 604
- Contraction factor, 755
- Convergence, 283
- Conversion factors, table of, 794
- Cool plasma, 729
- Coordinate diagrams, 799
- Coordinate transformation, 757–763
Galilean, 761
Lorentz, 761
- Corona, 73n., 734
- Cosine integrals, 648
- Cosmic ray, 747 (Prob. 15-35)
- Cosmic-ray telescope, 695
- Coulomb, Charles A. de, 13n.
- Coulomb's law, 13
- Coulomb's Law Committee, 59n.
- Counter emf, 324
- Coupling factor, wave-to-antenna, 439
- Cowan, John D., Jr., 648
- Crawling caterpillar, 377
- Creeping-wave diffraction, 474
- Critical angle, 456
- Critical frequency, 732, 744 (Prob. 15-14)
- Cross field, 441
- Cross product, 152
- Cross section, radar, 698
- Crossfield ellipse, 577
- CRT (*see* Cathode-ray tube)
- CRT display, 519
- Crystals, 58n.
- Curie point, 222
- Curl, 175–179
compared with divergence, 184
examples of, 179–182
- Curl meter, 180–181
- Current, 109–110
continuity relation for, 126
density of, 118
induced, 306
mapping of, 131–134
retarded, 605, 647
solenoidal, 124
- Current density, 118
- Current distribution on antenna, 646
- Current mapping, 131–134
- Current moment, 142
- Current reflection coefficient, 497
- Current sheet, 338
- Curvilinear square, 88, 132
power through, 522
- Cury, R., 801
- Cutoff frequency, 544
for cylindrical guide, 558
for rectangular guide, 545
- Cutoff wavelength, 526
for cylindrical guide, 558
for rectangular guide, 545
- CW doppler radar, 713 (Prob. 14-51)
- Cyclotron, 725–727
- Cyclotron frequency, 732
- Cyclotron magnet, 260 (Prob. 6-29)
- Cygnus A, 714 (Prob. 14-57)
- Cylindrical conductor, charged, 293
- Cylindrical guide, low-loss mode in, 556
(*See also* Waveguide, cylindrical)
- D'Alembert's equation, 366
- Damped harmonic oscillation, 333
- Damping coefficient, 332
- dBi, 624
- Debye, P., 332, 582n.
- Decibel, relation to neper, 562n.
- Dees, 725
- Deflection distance, 723, 724
- Degree of polarization, 438
- Del, operations involving, 183
- Del operator, 33
- Demagnetization, 236–237
- Demagnetization curve, 234
- de Moivre's theorem, 281, 611
- Deperming, 237
- Depth of penetration, 406
- Derived units, 3
- Deschamps, G. A., 431
- Deuteron, 726
- Diamagnetic materials, 199
- Dielectric, 57, 110, 401
artificial, 63–66
Class A, 57n.
lossy, 334
nonmagnetic, 456
- Dielectric coated conductor guide, 580
- Dielectric constant, 13n., 57n.
- Dielectric hysteresis, 332, 599 (Prob. 13-61)
- Dielectric rod line, 483
- Dielectric strength, 73
- Differential permeability (*see* Infinitesimal permeability)
- Diffracted field, total, 476
- Diffracted ray, 465
- Diffraction of plane wave, 466
- Diffraction coefficient, 475
- Diffraction curve, half-plane, 467
- Digital computer solution to Laplace's equation, 273–276
- Digital computer techniques compared with
manual techniques, 276
- Digital voltmeter (DVM), 277
- Dimensional analysis, 5–6
- Dimensions, 2, 786
- Diode, 289
- Diode current, 292
- Dipole:
atomic, 59
electric (*see* Electric dipole)
magnetic, 201
short (*see* Short dipole)
- Dipole antenna, 602
center-fed, 646
- Dipole moment, 60
- Directivity, 622, 627
approximate formula for, 635
of isotropic antenna, 623
relation to gain, 624
of short dipole, 623
- Dish antenna, parabolic, 642

- Dispersive medium, 376
 waveguide as, 529n.
- Displacement current, 328
- Displacement-current density, 330, 400
- Distortionless line, 489
- Distributed quantities, 485
- Divergence, 94
 compared with curl, 184
 of \mathbf{D} and \mathbf{P} in a capacitor, 99–101
 example of, 97–98
 of \mathbf{H} in toroid, 214
 of \mathbf{J} , 125–126
 of tensor, 776n.
- Divergence operator, 96
- Divergence theorem, 98
- Dixon, Robert S., 273
- Domain, magnetic, 221
- Dominant mode, 549n.
 for cylindrical guide, 559
- Doppler shift, 714 (Prob. 14–57)
- Double-stub tuner, 506, 590 (Prob. 13–9), 592 (Prob. 13–17)
- Driving force, 332
- Drude-Debye relations, 346 (Prob. 8–32)
- Dyadic Green's function, 532n.
- Earth, magnetic field of, 261 (Prob. 6–36)
- Earth-Jupiter radio link, 713 (Prob. 14–50)
- Earth-Mars radio link, 713 (Prob. 14–50)
- Earth-moon radio link, 712 (Prob. 14–48)
- Earth resources satellite, 714 (Prob. 14–55)
- Easy magnetization, 222, 226
- Echo signals (*see* Ghost signals)
- Ecology, 593 (Prob. 13–22)
- Eddy currents, 315, 327
- Edge diffraction, 474
- Effective aperture, 625, 690
- Efficiency:
 antenna, 619
 aperture, 690
 beam, 622n.
- Eigenvalues, 556, 559
- Einstein, Albert, 749
- Einstein's energy relation, 784 (Prob. 16–30)
- Einstein's relation, 422 (Prob. 10–13)
- Einstein's summation convention, 769
- Electric and magnetic field relations compared, 340
- Electric circuit, 113
- Electric dipole, 36
 electric field of, 38
 figure, 27, 37
 potential of, 37
 table for, 38
- Electric-dipole moment, 36, 60
- Electric field intensity:
 boundary relations for, 67
 at center of circular ring, 105 (Prob. 3–23)
 at center of square ring, 105 (Prob. 3–24)
 of charged dielectric sphere, 108 (Prob. 3–49)
 of charged spherical shell, 43–44
 due to charges, 307
 of dipole, 38
 of a finite line of charge, 78–79
- of an infinite cylinder of charge, 80
- of an infinite line of charge, 79
- of moving charge, 781 (Prob. 16–6)
- of octopole, 53 (Prob. 2–16)
- of quadrupole, 52–53 (Prob. 2–13)
- relation to electric flux density, 40–41, 62
- relation to electric potential, 33–36
- relation to polarization, 62
- of several point charges, 18–20
- of two equal point charges, 27–29
 opposite sign, 27
 same sign, 28
- Electric field strength (*see* Electric field intensity)
- Electric flux, 39–43
 over closed surface, 41–43
 tubes of, 39
 figure, 40
- Electric flux density, 39–41, 62
 boundary relations for, 51, 68
 definition, 40
 divergence in capacitor, 99–101
 relation to electric field intensity, 40–41, 62
- Electric potential, 20–22
 (*See also* Potential)
- Electric scalar potential (*see* Electric potential)
- Electric susceptibility, 63
- Electromagnet, 260–261 (Prob. 6–30)
- Electromagnetic interference, 593 (Prob. 13–22)
- Electromagnetic theory in concise form, 769
- Electromechanical analogy, 332
- Electromotance, 120n.
- Electromotive force (emf), 120
- Electron, 116
- Electron cloud, 332
- Electron current, 289
- Electron density, 733
- Electrostatic precipitator, 743 (Prob. 15–9)
- Electrostatic press, 104 (Prob. 3–15)
- Element pattern (*see* Primary pattern)
- Elliott, R. S., 801
- Ellipse, 686
 crossfield, 577
 polarization, 431
- Elliptical conducting loop, magnetic flux density of, 193 (Prob. 5–16)
- Elliptically polarized wave, 427
- Emde, F., 466n.
- Emf, 306
 total induced, 312
- Emf-producing field, 119, 307
- Emitter, 289
- Endfire array, 633–635
- Energy:
 in capacitor, 74
 conservation of, 389
 in inductor, 173–174
 in magnet, 232–234
 per pulse, 395
 stored, 398
- Energy density, 388
 average, 394
 electric, 74–76
 instantaneous, 394
 magnetic, 174

- peak, 394
- total, 389
- Energy product, 235
- Energy relations:
 - in standing wave, 396
 - in traveling wave, 388
- Energy velocity, 392, 529
- Equality of path lengths, principle of, 684
- Equation numbering, 5
- Equator-to-great-circle angle, 432
- Equiangular spiral antenna, 666
- Equipotential contour, 25
- Equipotential line, 22
- Equipotential surface, 29, 294
- Equipotentials, magnetic, 170
- Equivalence of magnetized rod and solenoid, 203–205, 215
- Equivalent conductivity, 334
- Equivalent surface charge distribution, 292
- Equivalent units, 786
- Exponential line, 591 (Prob. 13-12)
- Exponential taper, 515
- Extraordinary ray, 735

- Fading, polarization, 659n.
due to Faraday rotation, 744 (Prob. 15-13)
- Far field, 613
- Far-field pattern, 604
- Farad (unit), 49
- Faraday, Michael, 305, 307
- Faraday disk generator, 314, 342 (Prob. 8-11)
- Faraday-Maxwell vector, 767
- Faraday rotation, 659n., 737–739
 - position angle, relation to, 739
 - for quasi-longitudinal case, 738
 - for quasi-transverse case, 739
 - total, 739
- Faraday's ice pail experiment, 46n.
- Faraday's law, 307
- Federal Communications Commission, 707 (Prob. 14-7)
- Fernald, D. L., 596 (Prob. 13-38)
- Ferrite material, 452
- Ferrite-titanate medium, 424 (Prob. 10-33)
- Ferromagnetic materials, 199–200
- Ferrous-dielectric material, 479 (Prob. 12-5)
- Field cell, 89
 - capacitor, 89, 90
 - magnetic, 243
 - transmission line, 171
- Field components, transformed, 772
- Field distributions, 76–77
- Field intensity:
 - electric (*see* Electric field intensity)
 - magnetic (*see* Magnetic field)
- Field lines, 87n.
- Field mapping, 86–93, 242–250
- Field maps:
 - comparison, 247–248
 - properties of, 91–92
- Field pattern, 613
- Field relations, general, 338–340
- Fields of moving system, 769–775
- Filamentary conductor, 295

- Filter, low-pass, 407
- Flow chart, 273
- Fluid, incompressible, 741
- Fluorescent screen, 721
- Flux:
 - electric (*see* Electric flux)
 - magnetic (*see* Magnetic flux)
- Flux-cutting law (*see* Motional-induction law)
- Flux density:
 - electric, 39–41, 62
 - magnetic, 142, 149
 - of radio source, 700
- Flux leakage, 324
- Flux linkage, magnetic, 159
- Flux tubes, electric, 39–40, 87
- Flux unit (fu), 700n.
- Fluxmeter, 224
- FM, 480 (Prob. 12-10)
- Force:
 - aligning, 140
 - per charge, 16
 - coercive, 229
 - on current-carrying conductor, 152
 - driving, 332
 - electric, 14
 - gravitational, 15
 - magnetic, 140–142
 - magnetic gap, 254
 - on parallel-plates of capacitor, 104 (Prob. 3-6)
 - between two parallel conductors, 146–147
 - per unit volume, 776
- Force relations, 357
- Fortran IV program, 273, 275
- Forward tilt of wave, 574
- Four-conductor transmission line, 301 (Prob. 7-25)
- Four-dimensional divergence, 768
- Four-dimensional field formulation, 765
- Fourier sine expansion, 282
- Fourier transform method, 708 (Prob. 14-18)
- Fourier transform relations, 644–646
- Fra Mauro highlands of moon, 660
- Frequency-independent antennas, 665–667
- Freshwater lake, 480 (Prob. 12-9)
- Fresnel cosine integral, 466
- Fresnel diffraction pattern, 481 (Prob. 12-14)
- Fresnel integrals, 466
- Fresnel reflection coefficients, 460
- Fresnel sine integral, 466
- Friis transmission formula, 698
- Fringing field, magnetic, 141
- Frozen magnetic field, 741n.
- Fundamental dimensions, 2, 786
- Fundamental units, 2–4

- G-string guide, 582
- Gabor, D., 467n.
- Gain:
 - antenna, 623
 - array, 677
 - relation to directivity, 624
- Gallilean transformation, 761
- Gapless circuit, 250–252

- Gauss, Karl Friedrich, 43
 Gauss' law, 43-44, 47
 Gauss' theorem (*see* Divergence theorem)
 Geometric mean, 509
 Geometrical optics, principle of, 468
 Geometrical-optics approximation, 468
 Geometrical optics concepts, 468
 Geometrical theory of diffraction (GTD), 474, 680
 Germanium semiconductor, 139 (Probs. 4-24, 4-25)
 Ghost signals, 481 (Prob. 12-10)
 Glass envelope, 289
 Gordon, W. E., 744 (Prob. 15-12)
 Goubau, G., 582n.
 Gradient, 33-36
 ionization, 744 (Prob. 15-44)
 in rectangular coordinates, 34-36
 Graphical field mapping (*see* Mapping, graphical)
 Gravitational attraction, 55 (Prob. 2-34)
 Gravitational field of earth, 55 (Prob. 2-33)
 Great-circle angle on Poincare sphere, 432
 Greenland, 424 (Prob. 10-36)
 Green's function:
 dyadic, 532n.
 electrostatic, 32
 free-space, 608n.
 Grid structure array, 663-665
 Group velocity, 376
 Guide (*see* Waveguide)
 Gyro frequency, 731
 Gyro resonance, 731
- Half-cylindrical metal tube, 303 (Prob. 7-38)
 Half-cylindrical trough transmission line, 300 (Prob. 7-10)
 Half-plane, conducting, 465
 Half-plane diffraction curve, 467
 Half-power beamwidth (HPBW), 620
 Half-wave dipole:
 directivity of, 648
 fields of, 648-650
 radiation resistance of, 648
 Hall effect, 197 (Prob. 5-34)
 Hall voltage, 197 (Prob. 5-34)
 Hallén, Erik, 671n.
 Halliday, D., 801
 Hansen-Woodyard increased directivity condition, 658n.
 Hard magnetization, 226
 Harmonics, 283
 Harrington, R. F., 580n., 801
 Hayt, W. H., Jr., 801
 Heaters, RF, 599 (Prob. 13-61)
 Heaviside, Oliver, 389
 Heaviside's condition, 489
 Helical-beam antennas, 429, 656-662
 array of, 661-662
 bandwidth of, 659
 directivity of, 659
 pattern of, 658
 phase velocity on, 659
 use in space communication, 659
- Helical coil (*see* Solenoid)
 Helicone antenna, 692-693
 Helmholtz formula, 312
 Helmholtz pair of coils, 195 (Prob. 5-23)
 Henry, Joseph, 305
 Henry (unit), 159
 Hertz, H., 357
 High-resistance voltmeter, 277
 Higher-order mode, 482, 600 (Prob. 13-66)
 wavelength of, 529
 Holes in semiconductors, 116
 Hologram, 467
 Holography, 467
 Homogeneous equation, 288
 Homogeneous medium, 56
 Hondros, D., 582n.
 Horn antenna, 642, 688-689
 HPBW, 620
 Hubble constant, 714 (Prob. 14-57)
 Hubble relation, 714 (Prob. 14-57)
 Huygens, C., 464n.
 Huygen's principle, 464, 642
 Hydraulic analogue, 122
 Hyperbola, 685
 Hyperbolic relations, 795
 Hyperbolic wire, magnetic flux density of, 193 (Prob. 5-15)
 Hyperfine transition, 599 (Prob. 13-58)
 Hysteresis, 229-231
 Hysteresis loop, 230, 325
 major, 230
 minor, 326
- Ice:
 permittivity of, 346 (Prob. 8-32)
 thickness of, 425 (Prob. 10-36)
 Idaho potato, 346 (Prob. 8-34)
 Idealness, 15
 Image of conductor, 296
 Image charges, 292
 Image current, 296
 Images, theory of, 85
 Imaginary part of ϵ , 334
 Impedance:
 antenna, 670-675
 characteristic, 382, 488, 573
 intrinsic (*see* Intrinsic impedance)
 mutual, 323
 self-, 670-673
 wave, 574
 Incident wave, 383
 Incoherent wave, 435
 Incompressible fluid, 741
 Increased directivity condition, Hansen-Woodyard, 658n.
 Incremental permeability, 326
 Index of refraction, 374
 for conducting medium, 407
 for plasma, 734
 Induced charges, 46
 Induced current, 306
 Induced emf, 310
 Induced field, 46
 Induced magnetization, 222

- Inductance, 159
 average, 325
 of coaxial line, 161
 general case, 311
 of solenoid, 160
 of toroid, 161
 of two-wire line, 162
- Inductor, 158
 coaxial line, 161
 energy in, 173-174
 solenoidal, 159-160
 toroidal, 161
 two-conductor line, 162
- Industrial RF heating, 332
- Infinite-parallel-plane line, 483
- Infinite square trough, 269-272
- Infinitesimal dipole (*see* Short dipole)
- Infinitesimal permeability, 325
- Initial magnetization curve, 226
- Injection molding, 599 (Prob. 13-61)
- Insulator, 110
- Interference, electromagnetic, 593 (Prob. 13-22)
- Interferometer:
 as radio telescope antenna, 640
 two-element, 640-642
- Interferometer pattern, 642
- International System of Units (SI), 2-3
- Interplanetary vehicle, 783 (Prob. 16-21)
- Intrinsic impedance, 379, 380, 382, 511, 573
 of conducting medium, 409, 410
 of copper, 412
- Intrinsic polarization, 739
- Intrinsic resistance, 379
- Invariance in space-time, 763-765
- Invariant axes, 765
- Invariant hyperbola, 763
- Invariant lines, 753
- Inverse-square law, 13
- Ion beam, 719
- Ionization gradient, 744 (Prob. 15-14)
- Ionized medium, plane waves in, 729
- Ionosphere of earth, 55 (Prob. 2-36)
- Iris, waveguide, 571-573
- Iron ring, 210-213
- Isaac, E. D., 801
- Isbell, D. E., 666n.
- Isotropic antenna, 623
- Isotropic material, 56
- Isotropic source (*see* Isotropic antenna)
- Iterative method (*see* Point-by-point method)
- Jahnke, E., 466n.
- Jasik, H., 801
- Jensen, H. J., 593 (Prob. 13-23)
- Jordan, E. C., 801
- Joule heating, 327, 564
- Joule's law, 112
- Keeper, 237
- Keller, J. B., 475n.
- Kelvin, Lord, 2
- Kelvin, definition, 3
- Kennaugh, Edward M., 648
- Kilogram, definition, 3
- Kinetic energy, 290
- King, R. W. P., 801
- Kirchoff's current law, 124-125
- Kirchoff's voltage law, 120
- Ko, H. C., 439n.
- Kock, W. E., 63n., 686n.
- Kouyoumjian, R. G., 729n.
- Kraus, John D., 63n., 441n., 465n., 603n., 642n., 656n., 659n., 663n., 671n., 682n., 690n., 699n., 704n., 729n.
- Laithwaite, E. R., 344 (Prob. 8-20)
- Lamellar field, 167, 186
- Laminations, 327
- Langmuir, I., 292
- Laplace's equation, 103, 262
 for conducting media, 133-135
 in cylindrical coordinates, 283
 for parallel-plate capacitor, 264-266
 in rectangular coordinates, 263
 in spherical coordinates, 284
- Laser beam, 593 (Prob. 13-20)
- Latitude on Poincaré sphere, 431
- Launching device, 579
- Law:
 Ampère's, 7
 Biot-Savart, 144
 Child-Langmuir, 292
 Coulomb's, 13
 of edge diffraction, 475
 Faraday's, 307
 Lenz's, 306, 327
- Lawrence, Ernest O., 725
- Left circular polarization, 429
- Lens antenna:
 dielectric, 685-686
 metal plate, 686
- Lenz's law, 306, 327
- Light lines, 751
- Light pen, 303 (Prob. 7-39)
- Line integral, 23
 around closed path, 24
- Linear antenna, 646-648
- Linear charge density, 30
- Linear medium, 56
- Linear motor for vehicle, 344 (Prob. 8-20)
- Linearly independent solution, 288
- Linearly polarized wave, 426
- Linkage, magnetic flux, 159
- Load impedance, 496
- Log-periodic antenna, 666-667
- Logarithmic pattern, 604
- Logarithmic relations, 796
- Longitude on Poincaré sphere, 431
- Longitudinal propagation, 735
- Loop:
 atomic current, 198
 static: electric field of, 105 (Prob. 3-23)
 magnetic field of, 147-148
 torque on, 154-155
- Loop antenna, small, 654-655
- Lorentz, H. A., 761n.
- Lorentz transformation, 761

- Loss resistance, 619
 Loss tangent, 334
 Lossless line, 496
 Low-pass filter, 407
 Lunar communication, 596 (Prob. 13-38)
 Lunar Fra Mauro highlands, 660
- McCullough, T. P.**, 701
Magic pencil (*see* Light pen)
Magnet:
 bar, 201
 force on, 257 (Prob. 6-4)
 magnetic flux density of, 259 (Prob. 6-17)
 rotating (*see* Pulsar)
 domains in, 223
 effect on current-carrying wire, 141-142
 energy in, 232-234
 iron ring, 261 (Prob. 6-33)
 materials for, 236
 permanent (*see* Permanent magnet)
 U-shaped, 260-261 (Prob. 6-30)
Magnetic bottle, 746 (Prob. 15-29)
Magnetic circuit, 238
 with air gap, 252-254
Magnetic dipoles, 201
Magnetic field:
 in air gap, 252
 figure, 244
 boundary relations for, 218
 definition, 163-164
 of earth, 261 (Prob. 6-36)
 energy density in, 174-175
 frozen, 741n.
 of moving charge, 781 (Prob. 16-7)
 relation to magnetic flux density, 163-164, 206
 of solid cylindrical conductor, 164-165
Magnetic field intensity (*see* Magnetic field)
Magnetic flux, 149, 308
 over closed surface, 150
 tubes of, 150
Magnetic flux density:
 of bar magnet, 259 (Prob. 6-17)
 boundary relations for, 217
 of coaxial line, 161
 of current carrying loop, 147-148
 single-turn, 259 (Prob. 6-18)
 square, 193 (Prob. 5-13)
 due to current distribution, 149
 definition, 149
 of elliptical loop, 193 (Prob. 5-16)
 of hyperbolic wire, 193 (Prob. 5-15)
 of infinite linear conductor, 145-146
 of iron ring, 210-212
 of parabolic wire, 193 (Prob. 5-14)
 relation to magnetic field, 163-164, 206
 relation to magnetization, 206
 of solenoid, 155-157, 214-216
 of toroid, 160, 208-209
 of two-conductor line, 162
Magnetic flux linkage, 159
Magnetic gap forces, 254
Magnetic levitation system, 258 (Prob. 6-9)
Magnetic moment, 154, 201
- Magnetic poles**, 175
Magnetic potential function (*see* Magnetostatic potential)
Magnetic saturation, 222, 226
Magnetic sheet current density, 204-205
Magnetic susceptibility, 207
Magnetic vector potential, 186
Magnetization, 202
 induced, 212
 permanent, 212
Magnetization curve, 223
Magnetizing force, 223
Magnetohydrodynamic (MHD) waves, 740-742
Magnetomotance (*see* Magnetomotive force)
Magnetomotive force (mmf), 168
Magnetostatic potential, 167
Magnusson, P. C., 802
Main lobe, 604
Main-lobe solid angle, 622
Major lobe (*see* Main lobe)
Mapping, graphical: current, 131-134
 electric field, 86-93
 magnetic field, 242-250
Marcuvitz, N., 570n.
Mars, temperature of, 701
Mass, 332
 relativistic, 718
 rest, 718
Mass spectrograph, 728
Matching:
 broadband, 515
 polarization, 435
Matching stub, 504
Matrix, 777
 coherency, 441
Matthias, B. T., 116n.
Maximum usable frequency (MUF), 744 (Prob. 15-14)
Maxwell, James Clerk, 354
Maxwell's equations, 354
 from Ampère's law, 330, 355
 from Faraday's law, 356
 differential form, 319
 integral form, 309-310
 in free space, 354
 from Gauss' law, 356, 357
 for harmonically varying fields, 358
 involving curl, 182
 involving divergence, 97, 150
 symmetry of, 361 (Prob. 9-5)
Maxwell's stress tensor, 775-780
Mayer, C. H., 701
Measurable quantity, 59
Mechanical moment (*see* Torque)
Mechanical system, equivalent, 332
Megaparsec, 714 (Prob. 14-57)
Mesh, 355
Metal detectors, 346 (Prob. 8-35)
Metal plate lens, 686
Metal trough with partition, 301 (Prob. 7-17)
Meter, definition, 2
MHD (*see* Magnetohydrodynamics)
Microwave communication circuit, 480 (Prob. 12-10)
Microwave components, 594-595 (Prob. 13-36)

- Microwave ovens, 599 (Prob. 13-61)
 Microwave radiation hazard, 425 (Prob. 10-39)
 Millikan's oil-drop experiment, 743 (Prob. 15-10)
 Minimum detectable flux density, 702
 Minimum detectable temperature, 701
 Minimum usable frequency, 745 (Prob. 15-16)
 Minkowski, H., 751n.
 Minkowski diagram, 751
 Minor lobe, 604
 Minor-lobe solid angle, 622
 Mirror point, 746 (Prob. 15-28)
 Mitchell, Edgar, 662
 MKSA system, 3
 Mobile units, 594 (Prob. 13-32)
 Mobility, 116, 139 (Probs. 4-24, 4-25)
 Mode, 482
 higher-order, 482
Moment:
 current, 142
 electric-dipole (*see* Electric-dipole moment)
 magnetic, 154
 mechanical (*see* Torque)
 Monochromatic transmitter, 435
 Moon, P., 765n., 802
 Moon, occultation of, 481 (Prob. 12-14)
 Moore, A. D., 86, 743 (Prob. 15-9), 802
 Motional induction, 312
 Motional-induction law, 311
 Motor, linear (*see* Linear motor for vehicle)
 Motor equations, 142, 719
Moving charge:
 electric field of, 781 (Prob. 16-6)
 magnetic field of, 781 (Prob. 16-7)
 Moving conductor, 310
 Moving meterstick, 758
 Moving system, fields of, 769-775
 MUf (*see* Maximum usable frequency)
 Multilobed pattern, 642
 Mumford, W. W., 425 (Prob. 10-39)
 Mushiaki, Y., 682n.
 Mutual impedance, 323
 of antenna, 673-675
 Mutual inductance, 321

 Nabla, 33
 Nash, R. T., 694n.
 National Aeronautics and Space Administration, 660
 Navier-Stokes equation, 741
 Near field, 614
 Near-field pattern, 604
 Negative magnetic pole (*see* South pole)
 Neumann function, 284, 552
 Neumann's law, 307
 Neumann's low-frequency inductance formula, 362 (Prob. 9-13)
 Neutron star, 703
 Newton, definition, 14n.
 Newton's second law, 6, 717, 730
 Noise power, 700
 Noise temperature, 699
 Nondispersive media, 376
 Nonisotropic (*see* Anisotropic materials)
 Nonlinear elements, 111

 Nonmagnetic materials, 200
 Nonmetallic guide, 579
 Nonspherical reflector, 470
 Nonuniform transmission line, 486
 Normal magnetization curve, 231
 Normalized admittance, 503
 Normalized impedance, 503
 Normalized power pattern, 620
 Normalized Stokes parameters, 438, 706
 Normally dispersive medium, 376
 North pole, magnetic, 140, 199
 Notation, longhand, 4n.
 Null directions of array, 632
 Null principle, 346 (Prob. 8-35)
 Numbering, equation, 5
 Nyquist, H., 699n.

Oblique incidence:
 of elliptically polarized wave, 460
 of linearly polarized wave, 452
 Observer, viewpoint of, 757
 Occultation of moon, 481 (Prob. 12-14)
 Octopole:
 distance factor for, 38
 electric field intensity of, 53 (Prob. 2-16)
 Ohio State University Radio Observatory, 661
 Ohm, Georg Simon, 111
 Ohmmeter, 493
 Ohm's law, 111, 349
 at a point, 118, 357
 Oil-drop experiment, Millikan's, 743 (Prob. 15-10)
 Onnes, H. Kamerlingh, 115
 Open-circuited line, 499
 Optical spectrum, 714 (Prob. 14-57)
 Ordinary permeability, 326
 Ordinary ray, 735
 Orthogonality, 25
 Outwardness, 18
 Oven, microwave, 599 (Prob. 13-61)
 Ozone, 593 (Prob. 13-22)

 Parabola, 685
 Parabolic dish antenna, 642
 Parabolic line of charge, 108 (Prob. 3-47)
 Parabolic wire, magnetic flux density of, 193 (Prob. 5-14)
 Parallel-plate capacitor, 49, 61-62, 71-73
 analogy with storm cloud, 105 (Prob. 3-21)
 charging, 423 (Prob. 10-21)
 divergence of \mathbf{D} and \mathbf{P} in, 99-101
 force squeezing plates together, 104 (Prob. 3-6)
 fringing field of, 303 (Prob. 7-37)
 Laplace's equation for, 264-266
 magnetic field in, 362 (Prob. 9-9)
 power dissipated in, 345 (Probs. 8-25, 8-26)
 problems involving, 103-104
 with space charge, 289-292
 Parallel polarization, 453, 458-460
 Paramagnetic materials, 199
 Partial differential equation, 367
 Partially polarized wave, 436

- Particle:**
 energy of, 718
 frequency of, 721
 velocity of, 718
- Particle accelerator**, 725
- Particular solution**, 288
- Particulate wastes**, 743 (Prob. 15-9)
- Pascal's triangle**, 631
- Pattern:**
 antenna, 603
 far-field, 604
 field, 613
 interferometer, 642
 multilobed, 642
 near-field, 604
 polar, 604
 power, 604
 principal-plane, 604
 rectangular, 604
- Pattern multiplication, principle of**, 629
- Pendulum, wire**, 341 (Prob. 8-5)
- Permanent magnet**, 141, 222
 with gap, 255-256
 materials for, table, 236
- Permeability:**
 incremental, 326
 infinitesimal, 325
 initial, 226
 maximum, 224
 ordinary, 326
 relative, 200
 table, 201
 of vacuum, 144, 200
- Permeance**, 239
- Permittivity:**
 of air, 14, 57
 of artificial dielectric, 64-66, 104 (Probs. 3-10, 3-11)
 of crystals, 58n.
 of ice, 346 (Prob. 8-32)
 relative, 57
 table, 58
 tensor, 733
 of titanates, 58n.
 of vacuum, 13, 57
- Perpendicular polarization**, 453-457
- Peters, Leon, Jr.**, 468n., 474n., 476n.
- Phase center of antenna**, 629, 648
- Phase constant**, 488
- Phase factor**, 404, 488
- Phase shift**, 383
- Phase velocity**, 369, 372
 in guide, 559
 rectangular, 545
 relative, 373
 of standing wave, 423 (Prob. 10-23)
 on transmission line, 490
- Phased array** (*see* Arrays, scanning)
- Phasor**, 335
- Phasor addition of fields**, 636-639
- Photon**, 695
- Photosphere**, 742
- Physical aperture**, 690
- Physical optics**, 465
- Physical optics approximation**, 468
- Pipe, closed rectangular**, 485
- Pipeline location**, 258 (Prob. 6-10)
- Pipelines, buried**, 138 (Prob. 4-19)
- Planck's constant**, 395, 422 (Prob. 10-11), 695
- Planck's radiation law**, 422 (Prob. 10-11)
- Plane of incidence**, 453
- Plane wave**, 364
 diffraction of, 466
- Plasma**, 729
- Plasma frequency**, 732
- Plasma oscillations**, 734
- Plessner, K. W.**, 58n.
- Plonsey, R.**, 802
- Plotter, computer-controlled**, 276
- Plume, water**, 529
- Plume velocity**, 531
- Pocket ruler antenna**, 665-666
- Pocket transistor radio**, 715 (Prob. 14-63)
- Poincaré, H.**, 431n.
- Poincaré sphere**, 431
- Point charge**, 13
- Point-by-point method**, 267-269
- Point-to-point correspondence**, 468
- Point relation**, 355
- Point source** (*see* Isotropic antenna)
- Point-to-wave correspondence**, 465
- Poisson's equation**, 103, 262, 288
- Polarization:**
 degree of, 438
 of dielectric, 59-63
 intrinsic, 739
 volume charge density, 101
 wave, 364
- Polarization fading**, 659n.
- Polarization matching**, 435
- Polarization measurements, antennas for**, 704-706
- Polarization state**, 431, 432
 antenna, 435, 439
 wave, 439
- Polarizing angle**, 459
- Pole strength**, 175
- Poles, magnetic**, 175
- Positive magnetic pole** (*see* North pole)
- Positiveness**, 17
- Potato, Idaho**, 346 (Prob. 8-34)
- Potential:**
 absolute, 22
 electric scalar: definition, 20n.
 of linear charge distribution, 31
 of octopole, 53 (Prob. 2-16)
 of quadrupole, 52 (Prob. 2-15)
 retarded, 604
 of surface charge distribution, 31
 of volume charge distribution, 32, 102
 magnetostatic, 167
 vector (*see* Vector potential)
- Potential difference**, 21
 rise in, 25
- Potts, Bing**, 694n.
- Pounder, E. R.**, 346 (Prob. 8-32)
- Powdered-iron cores**, 327
- Power:**
 complex, 619
 through curvilinear square, 522

- dissipated by dielectric, 335
 reactive, 619
- Power density, surface, 391
- Power divider, waveguide, 570
- Power factor, 334
- Power flow:
 reactive, 650
 real, 650
 on transmission line, 520
- Power flow lines, 417
- Power-flow-map, 521
- Power pattern, 604
 normalized, 620
 in polar coordinates, 604
 in rectangular coordinates, 604
 relation to Poynting vector, 620
- Power per unit area:
 average, 393
 instantaneous, 393
 peak, 393
- Poynting, J. H., 389
- Poynting vector, 389
 average, 392, 430
 circuit application of, 416
 complex, 391, 429
 in conducting media, 413
 flow lines of, 418
 instantaneous, 390
- Precipitator, electrostatic, 743 (Prob. 15-9)
- Prefixes for units, 4
- Press, electrostatic, 104 (Prob. 3-15)
- Pressure, 776
 radiation, 778-780
- Primary pattern, 629
- Primary winding, 320
- Principal-plane pattern, 604
- Principle of superposition:
 of electric fields, 18
 of electric potentials, 30
- Prolate spheroid antenna, 648-649
- Propagation, 363
 longitudinal, 735
 transverse, 735
- Propagation constant, 404, 488, 499
- Propulsion of space vehicle, 747 (Prob. 15-37),
 782 (Prob. 16-19)
- Pseudo-vector, 335
- Pulsar, 702-704, 714 (Prob. 14-58)
- Pulse, square, 517
- Q, 587-589**
- Quadratic equation, solution of, 797
- Quadrupole, distance factor for, 38
- Quanta, 395
- Quarter-wave plate, 509
- Quarter-wave transformer, 509-511
 double section, 513
 single section, 509
 three section, 514, 592 (Prob. 13-16)
 wave reflections on, 515
- Quartz crystal, Q for, 599 (Prob. 13-58)
- Quartz window, 593 (Prob. 13-20)
- Quasar, 714 (Prob. 14-57)
- Quasi conductor, 401
- Quasi-longitudinal conditions, 736
- Quasi-stationary field, 614
- Quasi-transverse conditions, 736
- Quiet sun, 734
- Radar, CW doppler, 713 (Prob. 14-51)
- Radar cross section, 698
 of automobile, 713 (Prob. 14-51)
 of electron, 744 (Prob. 15-11)
- Radar equation, 698
- Radar system, 425 (Prob. 10-36)
 design of, 713 (Prob. 14-49)
- Radiation field, 615
(See also Far field)
- Radiation hazard, microwave, 425 (Prob. 10-39)
- Radiation intensity, 620
- Radiation pressure, 778-780
 on conductor, 784 (Prob. 16-30)
- Radiation resistance, 617
- Radio, pocket transistor, 715 (Prob. 14-63)
- Radio communication, 480 (Prob. 12-9)
- Radio lines, 751
- Radio source, extragalactic, 421 (Prob. 10-9)
- Radio telescope:
 of Ohio State University, 661, 702
 of University of Texas, 661
- Radio-telescope antenna, 700
- Radio-telescope receiver, sensitivity of, 701
- Radiometer, 700
- Ramo, S., 802
- Rank of root, 554
- Ray paths, 468
- Rayleigh, Lord, 259 (Prob. 6-24), 532n.
- Reactive energy, 398
- Reactive power, 619
- Real part of ϵ , 334
- Reber, Grote, 695, 696
- Receiving antenna, 601, 624
- Reciprocity, 603, 668-670
 directivity, 669-670
 impedance, 670
 pattern, 669
- Reciprocity theorem, 323, 668
- Rectangular impedance chart, 502
- Rectangular loop, rotating, 342 (Prob. 8-9)
- Rectangular trough transmission line, 298
 (Prob. 7-7)
- Recurrence relations for Bessel functions, 798
- Red shift, 714 (Prob. 14-57), 783 (Prob. 16-25)
- Rees, M. J., 703
- Reflected wave, 383, 451, 453
- Reflection coefficient, 387, 447
 for current, 497
 for voltage, 497
- Reflection coefficients, Fresnel, 460
- Reflector (*see* Antennas, reflector)
- Refracted wave, 453n.
- Refraction, angle of, 453n.
- Relative motion, 750
- Relative phase velocity, 373
- Relativity, 757
- Relaxation time, 409
- Reluctance, 239, 327
- Remanence, 229
- Residual density (*see* Remanence)
- Resistance, 111

- antenna, 625
 loss, 619
 radiation, 617
 Resistance-measurement method, 494
 Resistance paper, 277, 492
 Resistivity, 114
 Resnick, R., 801
 Resonant frequency, 584
 of atomic dipole, 333
 Resonant wavelength, 584
 Resonator, 517, 583
 Response, system, 440
 Resultant wave, 525
 Retardation time, 605n.
 Retarded current, 605, 647
 Retarded potentials, 604
 Retarded scalar potential, 606
 Retarded time, 757
 Retarded vector potential, 606
 Retrotivity, 230
 Retroreflector antenna, 713 (Prob. 14-52)
 RF heaters, 599 (Prob. 13-61)
 RF heating, industrial, 332
 Right circular polarization, 429
 Right-hand rule, 140
 figure, 141
 Right-handedness, 17
 Risman, P. O., 346 (Prob. 8-34)
 Rotating bar magnet as pulsar, 702-704
 Rotation measure, 739
 Rowland ring, 224
 Rudduck, R. C., 476n.
 Rumsey, V. H., 666n.
 Rural ground, electrical behavior of, 402
 Russo, P. M., 476n.
 Ryan, C. E., Jr., 474n.
- Salisbury, W. W., 596 (Prob. 13-38)
 Saltwater, plane wave on, 479 (Prob. 12-1)
 Satellite:
 earth resources, 714 (Prob. 14-55)
 stationary, 745 (Prob. 15-16)
 Saturation, magnetic, 222, 226
 Scalar potential:
 electric, 20-22, 340
 (See also Potential, electric scalar)
 magnetic, 167
 (See also Potential, magnetostatic)
 Scalar wave equation, 366
 Scanning arrays, 663-665
 Scarborough, J. B., 267
 Scattering from strip, 472-474
 Scattering aperture, effective, 698
 Schelkunoff, S. A., 802
 Schmidt telescope, 711 (Prob. 14-44)
 Screen, fluorescent, 721
 Search coil, 347 (Prob. 8-35)
 Seawater, electrical behavior of, 402
 Second, definition, 3
 Secondary dimensions, 2, 786
 Secondary units, 2-4
 Secondary winding, 320
 Self-impedance of antenna, 670-673
 Self-inductance, 322
 Semiconductor junction, 304 (Prob. 7-43)
 Semiconductor rod, 304 (Prob. 7-43)
 Semiconductors, 109-110
 germanium, 139 (Probs. 4-24, 4-25)
 Sensitivity of receiver, 701
 Sensors, cosmic-ray, 695
 Separation of variables, 263, 278, 284, 286, 537
 Septum, waveguide, 570
 Series circuit, 352
 Series expansions, 797
 Series impedance, 485, 534
 Seyfert galaxy, 714 (Prob. 14-57)
 Shear, 776
 Shearing line, 256
 Sheet-current density, 415
 Shell:
 of charge, 43-45
 conducting, 46-48
 Shepard, Alan, Jr., 662
 Shock waves, 734
 Short-circuited line, 499
 Short dipole, 606-617
 effective aperture of, 625
 energy flow of, 614
 far fields of, 613
 fields of, 612-613
 near fields of, 614
 radiation resistance of, 617-619
 scalar potential for, 610
 vector potential for, 609
 Shortwave antenna, 599 (Prob. 13-62)
 Shunt admittance, 485, 534
 SI (International System of Units), 2-3, 786
 Sidelobe, 604
 Silver, S., 684n.
 Silver paint, 277
 Simultaneity, 747-751
 Sinclair, G., 435n.
 Sine integrals, 648
 Single-stub tuner, 504
 Single-wire line with ground return, 85-86
 Singular point, 29
 Skew-symmetric matrix, 767
 Skew-symmetric tensor, 734
 Skilling, H. H., 180n.
 Skin effect, 406
 Skin resistance, 416
 Sky survey, 702
 Sky temperature, 700
 Slater, J. C., 514n., 570n., 572n.
 Sloanaker, R. M., 701
 Slot antennas, 687-688
 Slow-wave structure, 665
 Small helical antenna, 655-656
 Smith, P. H., 505n.
 Smith chart, 505
 Smythe, W. R., 802
 Snell's law, 455
 of reflection, 455n.
 Soap bubble, expanding, 751
 Solar atmosphere, 734
 Solar corona, 742
 Solar disturbances, 734
 Solar power output, 422 (Prob. 10-13)
 Solar wind, 783 (Prob. 16-21)
 Solenoid, 155-158
 and equivalent rod, 203-205, 215

- inductance of, 160
 magnetic field of, 156
 magnetic flux density, 192 (Prob. 5-9)
Solenoidal currents, 124
Solenoidal field, 186
Solenoidal flux tubes, 150
Solid angle, 620
 beam, 620-621
 main-lobe, 622
 minor-lobe, 622
Solid zonal harmonic, 284
Sommerfeld, A., 476n., 579n., 802
Source temperature, 701
South pole, 199
Southworth, G. C., 551n.
Space and time quadrature, 398
Space charge, 288
Space-charge limitation, 289
Space cloth, 449
Space paper, 449, 493
Space-time concept, 752-757
Space-time diagram (*see* Minkowski diagram)
Space vehicle, propulsion of, 747 (Prob. 15-37)
Spaceship, 422 (Prob. 10-14)
Spangenberg, K. R., 289
Spectrograph, mass, 728
SPEMP chart, 10-11
Spencer, D. E., 765n., 802
Sphere, Poincaré, 431
Spherical conducting shell, thin, 302 (Prob. 7-34)
Spherical reflector, 711 (Prob. 14-44)
Spherical trigonometry, 432
Spherical wave, 613
Spheroid radiator, 648
Spring constant, 332
Square trough, infinite, 269-272
Square trough transmission line, 297 (Prob. 7-4)
Stabilized magnet, 256
Standing wave, 385
Standing-wave envelope, 385, 386
Standing-Wave Ratio (SWR), 386
(See also Voltage Standing-Wave Ratio)
State, polarization, 431
Static electric field, 24
Staticeless, 15
Stationary envelope, 385
Stationary observer, 773
Stationary satellites, 745 (Prob. 15-16)
Stegun, I. A., 466n.
Stokes, G., 436
Stokes parameters, 436
 normalized, 438
Stokes' theorem, 319
Stone, J. S., 631n.
Stored energy, 398
Storm cloud, energy in, 105 (Prob. 3-21)
Stratton, J. A., 375, 802
Stress tensor, Maxwell's, 775-780
Strip transmission line (*see* stripline)
Stripline, 296 (Prob. 7-1), 590 (Prob. 13-6),
 598 (Prob. 13-54)
Stub:
 matching, 504
 short circuited, 503
Substrate, dielectric, 590 (Prob. 13-6)
Superconducting solenoid, 345 (Prob. 8-31)
Superconductors, 115, 593 (Prob. 13-23)
Supergain antenna, 659
Suppressed carrier, 377
Surface wave, 457, 579
Surfers, analogy of particles to, 704
Surge impedance (*see* Characteristic impedance)
Susceptibility:
 electric, 63
 magnetic, 207
Suzuki, S., 705n.
Symbol, 786
Symbols, how to read, 4-5
Synchrotron, 747 (Prob. 15-36)
Synchrotron radiation, 704
System temperature, 701
- Tables:**
 array beam widths and directivities, 662
 boundary relations: electric fields, 71
 electric and magnetic fields, 338
 magnetic fields, 221
 characteristic impedance of lines, 490, 496
 charge and mass of particles, 728
 comparison of circuit and field quantities, 491
 comparison of field relations, 168
 comparison of time-varying electric and magnetic field relations, 340
 conductivities, 117
 cylindrical waveguide modes, 557
 dielectric strength, 73
 electric and magnetic fields compared, 191
 field-map quantities, 249
 fields of short dipole, 616
 input impedance of terminated line, 500
 Maxwell's equations: in differential form, 361
 in integral form, 360
 multiples and submultiples of basic units, 785
 normalized Stokes parameters, 438
 parameters for six-element array, 639
 Pascal's triangle, 630
 penetration depths, etc. for conducting media, 412
 permanent magnetic materials, 236
 permeability, 201
 permittivities, 58
 polarization and magnetization, 257
 potential and field of charge configurations, 39
 Poynting vector and energy density relations, 395
 propagation relations, 736
 rectangular guide, relations for, 550
 reflection and transmission coefficients, 502
 solutions of wave equation, 371
 Stokes parameters, relation to antenna pairs, 706
 units, fundamental, mechanical, electrical, and magnetic, 786-793
 waveguide parameters, 569
- Tai, C-T, 312, 532n., 557n., 674
 Tapered line, 486
 Teledeltos paper, 277, 492
Telescope:
 cosmic-ray, 695

- radio (*see Radio telescope*)
 Schmidt, 711 (Prob. 14-44)
 Television receiver, 743 (Prob. 15-3)
- Temperature:
 minimum detectable, 701
 noise, 699
 sky, 700
 source, 701
 system, 701
- Tension, 776
- Tensor:
 divergence of, 776n.
 of rank 1, 771
 skew-symmetric, 734
- Tensor conductivity, 733n.
- Tensor permittivity, 733
- Tenuous plasma, 729
- Terminated transmission line, 496
- Terminated wave, 499
- Terminations, waveguide, 570
- Theoretical quantity, 59
- Theory of images, 292
- Thevenin generator, 625
- Thompson scatter radar, 744 (Prob. 15-12)
- 3 dB beamwidth (*see Half-power beamwidth*)
- Three-halves relation, 292
- Three-port circulator, 591 (Prob. 13-11)
- Thumbnail electromagnetics, 6-10
- Tilt angle:
 of polarization ellipse, 432
 of wave, 576
- Time constant, postdetection, 701
- Time-domain analysis, 517
- Time-phase quadrature, 614
- Toroid, 206
 inductance of, 161
- Toroidal coil, 320
 with gap, 208-209
- Torque:
 aligning, 142
 on dipole, 53 (Prob. 2-19)
 on loop, 154-155, 195 (Prob. 5-20)
 magnetic, 140
- Total internal reflection, principle of, 457
- Total transmission, 458
- Trace, 441
- Transformer, 324
 bandwidth, 511-515
 quarter-wave, 509-511
 spherical-to-plane wave, 686
- Transformer core, 323
- Transformer induction, 312
- Transformer induction equation, 309
- Transitions, waveguide, 570
- Transmission coefficient, 447
 for current, 501
 for voltage, 501
- Transmission line, 482
 balanced, 606
 coaxial, 484
 dielectric rod, 483
 distortionless, 489
 exponential, 591 (Prob. 13-12)
 four-conductor, 301 (Prob. 7-25)
 half-cylindrical, 300 (Prob. 7-10)
 high power, 593 (Prob. 13-22)
- infinite-parallel-plane, 483
 TE mode in, 523
 infinite uniform, 486
 lossless, 496
 nonuniform, 486
 phase velocity on, 490
 power flow on, 520
 rectangular trough, 298 (Prob. 7-7)
 square trough, 297 (Prob. 7-4)
 strip (*see stripline*)
 terminated, 496
 triangular trough, 300 (Prob. 7-9)
 of two conducting strips, 303 (Prob. 7-36)
 two conductor, 495
- Transmission line cell, 171, 492
 impedance of, 381
- Transmission-line charts, 502
- Transmission-line equations, 490
- Transmitted wave, 383, 451, 453
- Transmitting antenna, 601, 624
- Transverse electric (TE) mode, 524
- Transverse ElectroMagnetic (TEM) mode, 351, 364
- Transverse field components, 539
- Transverse Magnetic (TM) mode, 351, 547
- Transverse propagation, 735
- Transverse-wave impedance, 574
- Traveling wave on antenna, 651
- Traveling-wave antenna, 650-654
 terminated, 651
 unterminated, 650
- Triangular trough transmission line, 300 (Prob. 7-9)
- Trigonometric relations, 795
- Trigonometry, spherical, 432
- Trough carrying brackish water, 342 (Prob. 8-12)
- Tsuchiya, A., 705n.
- Tube of rays, astigmatic, 470
- Tubes:
 of current, 123-124
 of electric flux, 39-40, 87
- Tuner:
 double-stub, 506, 590 (Prob. 13-9), 592 (Prob. 13-17)
 single-stub, 504
- Tunnel, vehicular, 594 (Prob. 13-32)
- TV, 480 (Prob. 12-10)
- Two-conductor line (*see Two-wire line*)
- Two-element interferometer, 640-642
- Two-element vacuum tube, 289
- Two metal cones, 300 (Prob. 7-16)
- Two metal sheets at angle, 301 (Prob. 7-22)
- Two-wire line:
 capacitance of, 85
 characteristic impedance of, 495
 inductance of, 162
 potential of, 82-83
- Uda, S., 682n.
- Uniform array, 631
- Uniform transmission line, 485
 wave equations for, 486
(See also Transmission line)
- Unique solution, 266, 267

- Uniqueness, 266-267
 Unit, 2
 U.S. Naval Research Laboratory, 701
 University of Texas, radio telescope of, 662
 Unpolarized wave, 435
 Upatnieks, J., 467n.
 Urban ground, electrical behavior of, 402
- V antenna, 602, 672
 Vacuum, perfect, 421 (Prob. 10-3)
 Vacuum chamber, 593 (Prob. 13-20)
 van Atta array, 713 (Prob. 14-53)
 Van Duzer, R., 802
 Vector, complex, 430
 Vector identities, 797
 Vector potential:
 magnetic, 186, 188, 340
 retarded, 606
 Vector product (*see* Cross product)
 Vehicles:
 linear motor for, 344 (Prob. 8-20)
 radio equipped, 424 (Prob. 10-36)
 relative motion of, 750
 Vehicular tunnel, 594 (Prob. 13-32)
 Velocity, 367
 electron, 116, 139 (Probs. 4-24, 4-25)
 energy, 392-329
 group, 376
 hole, 116, 139 (Probs. 4-24, 4-25)
 of light, 372
 phase (*see* Phase velocity)
 relativistic, 784 (Prob. 16-29)
 Venus, echo power from, 713 (Prob. 14-49)
 Vertically polarized wave, 364
 Vibrational modes, 334
 Viewpoint of observer, 757
 Voltage reflection coefficient, 497
 Voltage response of antenna, 435
 Voltage Standing-Wave Ratio (VSWR), 386, 500
 Voltmeter:
 digital (DVM), 277
 high-resistance, 277
 Von Hippel, A. R., 58n.
- Walter, C. H., 644n.
 Washer, conducting, magnetic flux density of, 193 (Prob. 5-12)
 Water, distilled, 425 (Prob. 10-38)
 Water plume, 529
 Watson, G. N., 802
 Wave:
 circularly polarized, 427
 elliptically polarized, 426
 linearly polarized, 426
 partially polarized, 436
 propagation of, 363
 reflected, 451
 resultant, 525
 spherical, 613
 surface, 457, 579
 transmitted, 451
 Wave absorption, 451
- Wave antenna (*see* Beverage antenna)
 Wave-to-antenna coupling factor, 439
 Wave equation, 536
 for conductors, 403
 for dielectrics, 366
 general development, 419
 for rectangular waveguide, 536
 scalar, 366
 for transmission line, 486
 Wave equation solutions:
 exponential, 371
 trigonometric, 371
 Wave impedance, 574
 Wave path, 525
 Wave polarization, 364
 Wave-reflection method, 515
 Wave reflections on quarter-wave transformer, 515
 Wave transformer, 686
 Wavefront, 525
 Wavefronts, 468
 Waveguide, 483, 524
 coated conductor, 580
 corrugated, 579
 cylindrical, 551
 dielectric slab, 581
 discontinuities in, 543
 elliptical, 560
 G-string, 582
 nonmetallic, 579
 open surface, 484
 phase velocity in, 559
 rectangular, 532-550
 reentrant, 560
 screw in, 548
 square, 561
 wavelength in, 559
 Waveguide devices, 570-571
 Waveguide iris, 571-573
 Waveguide power dividers, 570
 Waveguide terminations, 570
 Waveguide transitions, 570
 Wavelength, 367, 372
 Wavelength in guide, 559
 West, R., 58n.
 Wheeler, H. A., 656n.
 Whinnery, J. R., 802
 Whitmer, R. M., 582n.
 Wickersham, A. F., 596 (Prob. 13-38)
 Widner, Ronald, 694n.
 Windows in building, 594 (Prob. 13-33)
 Wolf, E., 432n., 441n.
 World lines, 751
- Xerographic machine, 55 (Prob. 2-42)
- Yagi, H., 682n.
 Yagi-Uda antenna, 682
- Zenneck, J., 579n.
 Zonal harmonics, solid, 284

GRADIENT, DIVERGENCE, CURL AND LAPLACIAN IN RECTANGULAR, CYLINDRICAL, SPHERICAL, AND GENERAL CURVILINEAR COORDINATES

Spherical Coordinates

$$\nabla f = \hat{r} \frac{\partial f}{\partial r} + \hat{\theta} \frac{1}{r} \frac{\partial f}{\partial \theta} + \hat{\phi} \frac{1}{r \sin \theta} \frac{\partial f}{\partial \phi}$$

$$\nabla \cdot \mathbf{A} = \frac{1}{r^2} \frac{\partial}{\partial r} r^2 A_r + \frac{1}{r \sin \theta} \frac{\partial}{\partial \theta} (A_\theta \sin \theta) + \frac{1}{r \sin \theta} \frac{\partial A_\phi}{\partial \phi}$$

$$\begin{aligned} \nabla \times \mathbf{A} &= \hat{r} \frac{1}{r \sin \theta} \left[\frac{\partial}{\partial \theta} (A_\phi \sin \theta) - \frac{\partial A_\theta}{\partial \phi} \right] + \hat{\theta} \frac{1}{r} \left(\frac{1}{\sin \theta} \frac{\partial A_r}{\partial \phi} - \frac{\partial}{\partial r} r A_\phi \right) \\ &\quad + \hat{\phi} \frac{1}{r} \left(\frac{\partial}{\partial r} r A_\theta - \frac{\partial A_r}{\partial \theta} \right) \end{aligned}$$

$$\nabla^2 f = \frac{1}{r^2} \frac{\partial}{\partial r} \left(r^2 \frac{\partial f}{\partial r} \right) + \frac{1}{r^2 \sin \theta} \frac{\partial}{\partial \theta} \left(\sin \theta \frac{\partial f}{\partial \theta} \right) + \frac{1}{r^2 \sin^2 \theta} \frac{\partial^2 f}{\partial \phi^2}$$

General Curvilinear Coordinates

$$\nabla f = \hat{x}_1 \frac{1}{h_1} \frac{\partial f}{\partial x_1} + \hat{x}_2 \frac{1}{h_2} \frac{\partial f}{\partial x_2} + \hat{x}_3 \frac{1}{h_3} \frac{\partial f}{\partial x_3}$$

$$\nabla \cdot \mathbf{A} = \frac{1}{h_1 h_2 h_3} \left(\frac{\partial}{\partial x_1} h_2 h_3 A_1 + \frac{\partial}{\partial x_2} h_3 h_1 A_2 + \frac{\partial}{\partial x_3} h_1 h_2 A_3 \right)$$

$$\begin{aligned} \nabla \times \mathbf{A} &= \hat{x}_1 \frac{1}{h_2 h_3} \left[\frac{\partial}{\partial x_2} h_3 A_3 - \frac{\partial}{\partial x_3} h_2 A_2 \right] + \hat{x}_2 \frac{1}{h_3 h_1} \left(\frac{\partial}{\partial x_3} h_1 A_1 - \frac{\partial}{\partial x_1} h_3 A_3 \right) \\ &\quad + \hat{x}_3 \frac{1}{h_1 h_2} \left(\frac{\partial}{\partial x_1} h_2 A_2 - \frac{\partial}{\partial x_2} h_1 A_1 \right) \end{aligned}$$

$$\nabla^2 f = \frac{1}{h_1 h_2 h_3} \left[\frac{\partial}{\partial x_1} \left(\frac{h_2 h_3}{h_1} \frac{\partial f}{\partial x_1} \right) + \frac{\partial}{\partial x_2} \left(\frac{h_3 h_1}{h_2} \frac{\partial f}{\partial x_2} \right) + \frac{\partial}{\partial x_3} \left(\frac{h_1 h_2}{h_3} \frac{\partial f}{\partial x_3} \right) \right]$$

	h_1	h_2	h_3	x_1	x_2	x_3
Rectangular	1	1	1	x	y	z
Cylindrical	1	r	1	r	ϕ	z
Spherical	1	r	$r \sin \theta$	r	θ	ϕ

Rectangular Coordinates

$$\nabla f = \hat{x} \frac{\partial f}{\partial x} + \hat{y} \frac{\partial f}{\partial y} + \hat{z} \frac{\partial f}{\partial z}$$

$$\nabla \cdot \mathbf{A} = \frac{\partial A_x}{\partial x} + \frac{\partial A_y}{\partial y} + \frac{\partial A_z}{\partial z}$$

$$\nabla \times \mathbf{A} = \hat{x} \left(\frac{\partial A_z}{\partial y} - \frac{\partial A_y}{\partial z} \right) + \hat{y} \left(\frac{\partial A_x}{\partial z} - \frac{\partial A_z}{\partial x} \right) + \hat{z} \left(\frac{\partial A_y}{\partial x} - \frac{\partial A_x}{\partial y} \right) = \begin{vmatrix} \hat{x} & \hat{y} & \hat{z} \\ \frac{\partial}{\partial x} & \frac{\partial}{\partial y} & \frac{\partial}{\partial z} \\ A_x & A_y & A_z \end{vmatrix}$$

$$\nabla^2 f = \frac{\partial^2 f}{\partial x^2} + \frac{\partial^2 f}{\partial y^2} + \frac{\partial^2 f}{\partial z^2}$$

Cylindrical Coordinates

$$\nabla f = \hat{r} \frac{\partial f}{\partial r} + \hat{\phi} \frac{1}{r} \frac{\partial f}{\partial \phi} + \hat{z} \frac{\partial f}{\partial z}$$

$$\nabla \cdot \mathbf{A} = \frac{1}{r} \frac{\partial}{\partial r} r A_r + \frac{1}{r} \frac{\partial A_\phi}{\partial \phi} + \frac{\partial A_z}{\partial z}$$

$$\nabla \times \mathbf{A} = \hat{r} \left(\frac{1}{r} \frac{\partial A_z}{\partial \phi} - \frac{\partial A_\phi}{\partial z} \right) + \hat{\phi} \left(\frac{\partial A_r}{\partial z} - \frac{\partial A_z}{\partial r} \right) + \hat{z} \frac{1}{r} \left(\frac{\partial}{\partial r} r A_\phi - \frac{\partial A_r}{\partial \phi} \right) = \begin{vmatrix} \hat{r} \frac{1}{r} & \hat{\phi} & \hat{z} \frac{1}{r} \\ \frac{\partial}{\partial r} & \frac{\partial}{\partial \phi} & \frac{\partial}{\partial z} \\ A_r & r A_\phi & A_z \end{vmatrix}$$

$$\nabla^2 f = \frac{1}{r} \frac{\partial}{\partial r} \left(r \frac{\partial f}{\partial r} \right) + \frac{1}{r^2} \frac{\partial^2 f}{\partial \phi^2} + \frac{\partial^2 f}{\partial z^2} = \frac{\partial^2 f}{\partial r^2} + \frac{1}{r} \frac{\partial f}{\partial r} + \frac{1}{r^2} \frac{\partial^2 f}{\partial \phi^2} + \frac{\partial^2 f}{\partial z^2}$$

Kraus
and
Carver

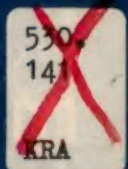


**OTHER McGRAW-HILL
INTERNATIONAL STUDENT EDITIONS
IN RELATED FIELDS**

- Angelo: ELECTRONICS-BJT's, FET's, and Microcircuits
Carlson: COMMUNICATION SYSTEMS-An Introduction to Signals and Noise in Electrical Communication, 2/e
D'Azzo: FEEDBACK CONTROL SYSTEM ANALYSIS AND SYNTHESIS, 2/e
Elgerd: CONTROL SYSTEMS THEORY
Fitzgerald: BASIC ELECTRICAL ENGINEERING, 4/e
Fitzgerald: ELECTRIC MACHINERY, 3/e
Hayt: ENGINEERING ELECTROMAGNETICS, 3/e
Hayt: ENGINEERING CIRCUIT ANALYSIS, 2/e
Johnson: TRANSMISSION LINES AND NETWORKS
Millman: INTEGRATED ELECTRONICS
Millman: PULSE, DIGITAL, AND SWITCHING WAVEFORMS
Ryder: ENGINEERING ELECTRONICS, 2/e
Schilling: ELECTRONIC CIRCUITS
Schwartz: INFORMATION, TRANSMISSION, MODULATION, AND NOISE
Taub: PRINCIPLES OF COMMUNICATION SYSTEMS
Terman: ELECTRONIC AND RADIO ENGINEERING, 4/e
Terman: ELECTRONIC MEASUREMENTS, 2/e

ELECTROMAGNETICS

**SECOND
EDITION**



McGRAW-HILL
KOGAKUSHYA